METHODS IN MOLECULAR BIOLOGY™ 384

Capillary Electrophoresis

Methods and Protocols

Edited by

Philippe Schmitt-Kopplin

Humana Press

Capillary Electrophoresis

METHODS IN MOLECULAR BIOLOGY™

John M. Walker, SERIES EDITOR

417. Tissue Engineering, Second Edition, edited by *Hannsjörg Hauser and Martin Fussenegger, 2007*
416. Gene Essentiality: *Protocols and Bioinformatics,* edited by *Andrei L. Osterman, 2008*
415. Innate Immunity, edited by *Jonathan Ewbank and Eric Vivier, 2007*
414. Apoptosis and Cancer: *Methods and Protocols*, edited by *Gil Mor and Ayesha B. Alvero, 2008*
413. Protein Structure Prediction, Second Edition, edited by *Mohammed Zaki and Chris Bystroff, 2008*
412. Neutrophil Methods and Protocols, edited by *Mark T. Quinn, Frank R. DeLeo, and Gary M. Bokoch, 2007*
411. Reporter Genes for Mammalian Systems, edited by *Don Anson, 2007*
410. Environmental Genomics, edited by *Cristofre C. Martin, 2007*
409. Immunoinformatics: *Predicting Immunogenicity In Silico*, edited by *Darren R. Flower, 2007*
408. Gene Function Analysis, edited by *Michael Ochs, 2007*
407. Stem Cell Assays, edited by *Vemuri C. Mohan, 2007*
406. Plant Bioinformatics: *Methods and Protocols,* edited by *David Edwards, 2007*
405. Telomerase Inhibition: *Strategies and Protocols,* edited by *Lucy Andrews and Trygve O. Tollefsbol, 2007*
404. Topics in Biostatistics, edited by *Walter T. Ambrosius, 2007*
403. Patch-Clamp Methods and Protocols, edited by *Peter Molnar and James J. Hickman, 2007*
402. PCR Primer Design, edited by *Anton Yuryev, 2007*
401. Neuroinformatics, edited by *Chiquito J. Crasto, 2007*
400. Methods in Lipid Membranes, edited by *Alex Dopico, 2007*
399. Neuroprotection Methods and Protocols, edited by *Tiziana Borsello, 2007*
398. Lipid Rafts, edited by *Thomas J. McIntosh, 2007*
397. Hedgehog Signaling Protocols, edited by *Jamila I. Horabin, 2007*
396. Comparative Genomics, *Volume 2*, edited by *Nicholas H. Bergman, 2007*
395. Comparative Genomics, *Volume 1*, edited by *Nicholas H. Bergman, 2007*
394. Salmonella: *Methods and Protocols,* edited by *Heide Schatten and Abe Eisenstark, 2007*
393. Plant Secondary Metabolites, edited by *Harinder P. S. Makkar, P. Siddhuraju, and Klaus Becker, 2007*
392. Molecular Motors: *Methods and Protocols*, edited by *Ann O. Sperry, 2007*
391. MRSA Protocols, edited by *Yinduo Ji, 2007*
390. Protein Targeting Protocols, Second Edition, edited by *Mark van der Giezen, 2007*
389. *Pichia* Protocols, Second Edition, edited by *James M. Cregg, 2007*
388. Baculovirus and Insect Cell Expression Protocols, Second Edition, edited by *David W. Murhammer, 2007*
387. Serial Analysis of Gene Expression (SAGE): *Digital Gene Expression Profiling,* edited by *Kare Lehmann Nielsen, 2007*
386. Peptide Characterization and Application Protocols, edited by *Gregg B. Fields, 2007*
385. Microchip-Based Assay Systems: *Methods and Applications,* edited by *Pierre N. Floriano, 2007*
384. Capillary Electrophoresis: *Methods and Protocols,* edited by *Philippe Schmitt-Kopplin, 2008*
383. Cancer Genomics and Proteomics: *Methods and Protocols,* edited by *Paul B. Fisher, 2007*
382. Microarrays, Second Edition: *Volume 2, Applications and Data Analysis,* edited by *Jang B. Rampal, 2007*
381. Microarrays, Second Edition: *Volume 1, Synthesis Methods,* edited by *Jang B. Rampal, 2007*
380. Immunological Tolerance: *Methods and Protocols,* edited by *Paul J. Fairchild, 2007*
379. Glycovirology Protocols, edited by *Richard J. Sugrue, 2007*
378. Monoclonal Antibodies: *Methods and Protocols,* edited by *Maher Albitar, 2007*
377. Microarray Data Analysis: *Methods and Applications,* edited by *Michael J. Korenberg, 2007*
376. Linkage Disequilibrium and Association Mapping: *Analysis and Application,* edited by *Andrew R. Collins, 2007*
375. In Vitro Transcription and Translation Protocols: *Second Edition,* edited by *Guido Grandi, 2007*
374. Quantum Dots: *Applications in Biology*, edited by *Marcel Bruchez and Charles Z. Hotz, 2007*
373. Pyrosequencing® Protocols, edited by *Sharon Marsh, 2007*
372. Mitochondria: Practical Protocols, edited by *Dario Leister and Johannes Herrmann, 2007*
371. Biological Aging: *Methods and Protocols*, edited by *Trygve O. Tollefsbol, 2007*
370. Adhesion Protein Protocols, *Second Edition*, edited by *Amanda S. Coutts, 2007*
369. Electron Microscopy: *Methods and Protocols*, *Second Edition,* edited by *John Kuo, 2007*
368. Cryopreservation and Freeze-Drying Protocols, *Second Edition,* edited by *John G. Day and Glyn Stacey, 2007*
367. Mass Spectrometry Data Analysis in Proteomics, edited by *Rune Matthiesen, 2007*
366. Cardiac Gene Expression: *Methods and Protocols*, edited by *Jun Zhang and Gregg Rokosh, 2007*
365. Protein Phosphatase Protocols: edited by *Greg Moorhead, 2007*
364. Macromolecular Crystallography Protocols: *Volume 2, Structure Determination,* edited by *Sylvie Doublié, 2007*
363. Macromolecular Crystallography Protocols: *Volume 1, Preparation and Crystallization of Macromolecules,* edited by *Sylvie Doublié, 2007*
362. Circadian Rhythms: *Methods and Protocols*, edited by *Ezio Rosato, 2007*
361. Target Discovery and Validation Reviews and Protocols: *Emerging Molecular Targets and Treatment Options, Volume 2,* edited by *Mouldy Sioud, 2007*
360. Target Discovery and Validation Reviews and Protocols: *Emerging Strategies for Targets and Biomarker Discovery, Volume 1,* edited by *Mouldy Sioud, 2007*

METHODS IN MOLECULAR BIOLOGY™

Capillary Electrophoresis

Methods and Protocols

Edited by

Philippe Schmitt-Kopplin

HelmholtzZentrum München
German Research Center for Environmental Health
Neuherberg, Germany

Humana Press

Editor
Philippe Schmitt-Kopplin
HelmholtzZentrum München
German Research Center for Environmental Health
Neuherberg, Germany

Series Editor
John M. Walker, Professor Emeritus
School of Life Sciences,
University of Hertfordshire
Hatfield
Hertfordshire AL10 9AB, UK.

ISBN: 978-1-58829-539-2 e-ISBN: 978-1-59745-376-9

Library of Congress Control Number: 2007933469

©2008 Humana Press, a part of Springer Science+Business Media, LLC
All rights reserved. This work may not be translated or copied in whole or in part without the written permission of the publisher (Humana Press, 999 Riverview Drive, Suite 208, Totowa, NJ 07512 USA), except for brief excerpts in connection with reviews or scholarly analysis. Use in connection with any form of information storage and retrieval, electronic adaptation, computer software, or by similar or dissimilar methodology now known or hereafter developed is forbidden.
The use in this publication of trade names, trademarks, service marks, and similar terms, even if they are not identified as such, is not to be taken as an expression of opinion as to whether or not they are subject to proprietary rights.
While the advice and information in this book are believed to be true and accurate at the date of going to press, neither the authors nor the editors nor the publisher can accept any legal responsibility for any errors or omissions that may be made. The publisher makes no warranty, express or implied, with respect to the material contained herein.

Cover illustration: Electron microscopy of zone electrophoretic-enriched yeast mitochondria (Fig. 8B, Chapter 28; *see* complete figure on p. 714 and discussion on p. 715)

Printed on acid-free paper

9 8 7 6 5 4 3 2 1

springer.com

For Tina, Leïla-Felice, and Cedric-Félicien

Preface

Capillary electrophoresis techniques have become an important component of the "-omic" analytical toolset; they are orthogonal and complementary to many other analytical approaches critical to system-based modern biology. Capillary electrophoresis formed the basis of the *genomic* era with the optimization of multiplex-CGE with multifluorescence detection to ideal sequencing tools; and in *proteomics* not only peptide mixtures but also native proteins can now be resolved on miniaturized or multidimensional platforms.

"*Another book on capillary electrophoresis?*" Our goal was certainly not to give a complete overview of capillary electrophoresis, nor to present the detailed theory of electrokinetics. Instead, our challenge was to present in few chapters—a picture of the moment—a select group of capillary electrophoresis methods, zone electrophoresis [CZE], gel electrophoresis [CGE], electrokinetic chromatography [MEKC/MECC], electrochromatography [CEC]), all within different applications that separate representative types of molecules and particles (organic/inorganic, charged/uncharged, small to macromolecules), in combination with different detection techniques (conductivity, UV/Vis, indirect-UV/Vis, laser-induced fluorescence [LIF], and mass spectrometry [MS]).

In the first, *Analyte-Oriented,* part of the book (Chapters 1–22) *methods and protocols* are presented based on the sample type and size: inorganic and organic small ions, anionic, cationic and neutral pollutants and pharmaceuticals, sugars, sugar acids and polysaccharides, amino acids, peptides and proteins, nucleotides and DNA, and synthetic copolymers up to entire microorganisms.

In the second, more *Methods-Oriented,* part (Chapters 23–32) *methods and protocols* are focused more on methodological descriptions of particular and new CE techniques, such as basic principles and applications of CZE, MEKC/MECC, CEC, affinity CE, coating and online concentration techniques, and single-cell analysis or multidimensional techniques.

Capillary Electrophoresis: Methods and Protocols is particularly valuable for the beginner in the field of capillary electrophoresis. The panoply of techniques we present is an overview of the current state of the field and the select references the authors supply are an entrée to the literature on many applications. Each technique is spelled out in a straightforward way that assumes only a modicum of previous exposure to the method. Each chapter stands on its own as a complete description that allows the technique to be

duplicated in another lab. All chapters present first a mini-review of the topic that enables further precise literature research. This is followed by very specific (and representative) examples of separations used by the authors in their daily lab work. Finally, a Notes section in most chapters reveals tips for avoiding or overcoming problems and pitfalls that may occur, and describes alternative procedures as well, i.e., the sort of important, practical detail that never seems to appear in other publications.

Many existing publications nicely describe CE methods and techniques in greater detail. While our aim was not to give a comprehensive synopsis of capillary electrophoresis, but to present highlights in the possibilities of combinations of analyte/matrix/separation/detection, some of the themes treated here are also available in detailed single volumes in the Methods in Molecular Biology series. For deeper insights the reader is encouraged to have a closer look at:

Clinical Applications of Capillary Electrophoresis (Palfrey, Stephen M., 1999),
Clinical and Forensic Applications of Capillary Electrophoresis (Mohammad, Amin A. and Petersen, John R. 2001),
Capillary Electrophoresis of Nucleic Acids, Volume II: Practical Applications of Capillary Electrophoresis (Mitchelson, Keith R. and Cheng, Jing, 2001),
Capillary Electrophoresis of Nucleic Acids, Volume I: Introduction to the Capillary Electrophoresis of Nucleic Acids (Mitchelson, Keith R. and Cheng, Jing, 2000),
Capillary Electrophoresis of Carbohydrates (Thibault, Pierre and Honda, Susumu, 2003),
Capillary Electrophoresis of Proteins and Peptides (Strege, Mark A. and Lagu, Avinash L., 2004),
Chiral Separations: Methods and Protocols (Gübitz, Gerald and Schmid, Martin G., 2003),
Microchip Capillary Electrophoresis: Methods and Protocols (Henry, Charles, 2006).

Eighty participants from governmental research institutes, industry, and universities in more than sixteen countries participated in this project, *Capillary Electrophoresis: Methods and Protocols,* and present their methods, tricks, and tips for a range of separations, from small ions to macromolecules. I would like to express my thanks to all of them for their enthusiastic participation and motivation. My thanks certainly also go to my family for their support and to all the members of my team who followed me in the CE adventure over the

last decade; especially to Heidi Neumeier, who always managed to motivate her "*old Lady,*" a 15-year-old CE system that still runs and does a very good job, and to A. Wayne Garrison, remembering our first CE steps and runs with that same instrument.

Philippe Schmitt-Kopplin

Contents

Preface ..... *vii*
Contributors ..... *xv*

PART I: ANALYTE-ORIENTED

1 Determination of Small Ions With Capillary Electrophoresis and Contactless Conductivity Detection
Andreas Zemann, Irene Rohregger, and Roland Zitturi..... ***3***

2 Metal Analysis With Capillary Zone Electrophoresis
Ashok Kumar Malik..... ***21***

3 Measurement of Low-Molecular-Weight Carboxylic Acids in Ambient Air and Vehicle Emission by Capillary Electrophoresis
Ewa Dabek-Zlotorzynska and Valbona Celo..... ***43***

4 Determination of Aliphatic Low-Molecular-Weight and Biogenic Amines by Capillary Zone Electrophoresis
Agnes Fekete, Majlinda Lahaniatis, Jutta Lintelmann and Philippe Schmitt-Kopplin..... ***65***

5 Capillary Electrophoretic Analysis of Organic Pollutants
Ashok Kumar Malik, Jatinder Singh Aulakh, and Varinder Kaur..... ***93***

6 Capillary Electrophoresis With Laser-Induced Fluorescence: *Environmental Applications*
Lee Riddick and William C. Brumley..... ***119***

7 Practical Considerations for the Analysis of Ionic and Neutral Organic Molecules With Capillary Electrophoresis/Mass Spectrometry
Moritz Frommberger, Matthias Englmann, and Philippe Schmitt-Kopplin..... ***135***

8 Analysis of the Enantiomers of Chiral Pesticides and Other Pollutants in Environmental Samples by Capillary Electrophoresis
Arthur W. Garrison, Philippe Schmitt-Kopplin, and Jimmy K. Avants..... ***157***

9 Capillary Electrophoresis of Tropane Alkaloids and Glycoalkaloids Occurring in *Solanaceae* Plants
Tommaso R. I. Cataldi and Giuliana Bianco ***171***

10 Capillary Electrophoresis for Pharmaceutical Analysis
Alex Marsh, Margo Broderick, Kevin Altria, Joe Power, Sheila Donegan, and Brian Clark ***205***

11 Capillary Electrophoresis of Neutral Carbohydrates: *Mono-, Oligosaccharides, and Glucosides*
Cristiana Campa and Marco Rossi ***247***

12 Capillary Electrophoresis of Sugar Acids
Cristiana Campa, Edi Baiutti, and Anna Flamigni ***307***

13 Use of Capillary Electrophoresis for Polysaccharide Studies and Applications
Amelia Gamini, Anna Coslovi, Isabella Rustighi, Cristiana Campa, Amedeo Vetere, and Sergio Paoletti ***357***

14 Analysis of Oligonucleotides Using Capillary Zone Electrophoresis and Electrospray Mass Spectrometry
An Willems, Dieter L. Deforce, and Jan Van Bocxlaer ***401***

15 Separation of DNA by Capillary Electrophoresis
Bruce McCord, Brittany Hartzell-Baguley, and Stephanie King ***415***

16 Capillary Electrophoresis of Oxidative DNA Damage
Guowang Xu, Xianzhe Shi, Surong Mei, Qinghong Yao, Qianfeng Weng, and Caiying Wu ***431***

17 Capillary Electrophoresis of Gene Mutation
Guowang Xu, Xianzhe Shi, Chunxia Zhao, Kailong Yuan, Qianfeng Weng, Peng Gao, and Jing Tian ***441***

18 Biomedical Applications of Amino Acid Detection by Capillary Electrophoresis
Giuseppe E. De Benedetto ***457***

19 Separation of Peptides by Capillary Electrophoresis
Gerhard K. E. Scriba and Arndt Psurek ***483***

20 Analysis of Proteins by Capillary Electrophoresis
Christian W. Huck and Günther K. Bonn ***507***

21 Separation of Synthetic (Co)Polymers by Capillary Electrophoresis Techniques
Hervé Cottet and Pierre Gareil ***541***

22 Capillary Electrophoresis Separation of Microorganisms
Bartolomé M. Simonet, Angel Ríos, and Miguel Valcárcel ***569***

PART II: METHODS-ORIENTED

23 A Semi-Empirical Approach for a Rapid Comprehensive Evaluation of the Electrophoretic Behaviors of Small Molecules in Free-Zone Electrophoresis
Philippe Schmitt-Kopplin and Agnes Fekete ***593***

24 The CE Way of Thinking: *All is Relative!*
Philippe Schmitt-Kopplin and Agnes Fekete ***611***

25 Adsorbed Cationic Polymer Coatings for Enhanced Capillary Electrophoresis/Mass Spectrometry of Proteins
Sara Ullsten, Aida Zuberovic, and Jonas Bergquist ***631***

26 On-Column Ligand/Receptor Derivatization Coupled to Affinity Capillary Electrophoresis
Jose Zavaleta, Dinora Chinchilla, Alvaro Gomez, Catherine Silverio, Maryam Azad, and Frank A. Gomez ***647***

27 On-Line Concentration of Environmental Pollutant Samples by Using Capillary Electrophoresis
Janpen Intaraprasert and Philip J. Marriott ***661***

28 Free-Flow Electrophoresis System for Proteomics Applications
Gerhard Weber and Robert Wildgruber ***703***

29 Microemulsion Electrokinetic Chromatography
Wolfgang W. Buchberger ***717***

30 Micellar Electrokinetic Chromatography of Aminoglycosides
Ulrike Holzgrabe, Stefanie Laug, and Frank Wienen ***735***

31 Capillary Electrochromatography and On-Line Concentration
Guichen Ping, Philippe Schmitt-Kopplin, Yukui Zhang, and Yoshinobu Baba ***751***

32 Analysis of Alkaloids in Single Plant Cells by Capillary Electrophoresis
Katrin Wieland, Björn Thiele, and Uli Schurr 771

33 Multi-Dimensional Capillary Electrophoresis and Chromatography for Proteomic Analysis
Mingxia Gao and Xiangmin Zhang 783

Index ***803***

Contributors

Kevin Altria • *GlaxoSmithKline Research & Development, Harlow, Essex, UK*

Jatinder Singh Aulakh • *Department of Chemistry, G.N.D. University, Punjab, India*

Jimmy K. Avants • *US Environmental Protection Agency, National Exposure Research Laboratory, Athens, GA*

Maryam Azad • *California State University, Los Angeles, Los Angeles, CA*

Yoshinobu Baba • *Department of Molecular and Pharmaceutical Biotechnology, Graduate School of Pharmaceutical Sciences, The University of Tokushima, Japan*

Edi Baiutti • *Bracco Imaging SpA-CRM Trieste, AREA Science Park, Trieste, Italy*

Jonas Bergquist • *Department of Analytical Chemistry, Biomedical Centre, Uppsala University, Uppsala, Sweden*

Giuliana Bianco • *Dipartimento di Chimica, Università degli Studi della Basilicata, Potenza, Italy*

Jan Van Bocxlaer • *Laboratory of Medical Biochemisty and Clinical Analysis, Ghent University, Ghent, Belgium*

Günther K. Bonn • *Institute of Analytical Chemistry and Radiochemistry, Leopold-Franzens University, Innsbrück, Austria*

Margo Broderick • *Waterford Institute of Technology, Department of Chemical and Life Sciences, Waterford, Ireland*

William C. Brumley • *US Environmental Protection Agency, Office of Research and Development, National Exposure Research Laboratory, Environmental Sciences Division, Las Vegas, NV*

Wolfgang Buchberger • *Department of Analytical Chemistry, Johannes Kepler University, Linz, Austria*

Cristiana Campa • *Novartis Vaccines and Diagnostics, Siena, Italy*

Tommaso R. I. Cataldi • *Dipartimento di Chimica, Università degli Studi della Basilicata, Potenza, Italy*

Valbona Celo • *Analysis and Air Quality Division, Environmental Technology Centre, Environment Canada, Ottawa, Ontario, Canada*

Dinora Chinchilla • *California State University, Los Angeles, Los Angeles, CA*

Brian Clark • *Univeristy of Bradford, School of Pharmacy, Bradford, UK*

Anna Coslovi • *Department of Biochemistry, Biophysics and Macromolecular Chemistry, University of Trieste, Trieste, Italy*
Hervé Cottet • *Laboratoire Organisation Moléculaire, Évolution et Matériaux Fluorés, Université de Montpellier II, Montpellier, France*
Ewa Dabek-Zlotorzynska • *Analysis and Air Quality Division, Environmental Technology Centre, Environment Canada, Ottawa, Ontario, Canada*
Giuseppe E. De Benedetto • *Dipartimento dei Beni delle Arti e della Storia, Università degli Studi di Lecce, Lecce, Italy*
Dieter L. Deforce • *Laboratory for Pharmaceutical Biotechnology, Ghent University, Ghent, Belgium*
Sheila Donegan • *Waterford Institute of Technology, Department of Chemical & Life Sciences, Waterford, Ireland*
Matthias Englmann • *HelmholtzZentrum München, German Research Center for Environmental Health, Institute of Ecological Chemistry/Chemical BioGeoAnalysis, BioGeomics, Neuherberg, Germany*
Agnes Fekete • *HelmholtzZentrum München, German Research Center for Environmental Health, Institute of Ecological Chemistry/Chemical BioGeoAnalysis, BioGeomics, Neuherberg, Germany*
Anna Flamigni • *Bracco Imaging SpA-CRM Trieste, AREA Science Park, Trieste, Italy*
Moritz Frommberger • *HelmholtzZentrum München, German Research Center for Environmental Health, Institute of Ecological Chemistry/Chemical BioGeoAnalysis, BioGeomics, Neuherberg, Germany*
Amelia Gamini • *Department of Biochemistry, Biophysics and Macromolecular Chemistry, University of Trieste, Trieste, Italy*
Mingxia Gao • *Department of Chemistry & Research Center for Proteome, Fudan University, Shanghai, China*
Peng Gao • *Dalian Institute of Chemical Physics, Chinese Academy of Sciences, Dalian, China*
Pierre Gareil • *Laboratoire d'Électrochimie et de Chimie Analytique, École Nationale Supérieure de Chimie de Paris, Paris, France*
Arthur W. Garrison • *US Environmental Protection Agency, National Exposure Research Laboratory, Athens, GA*
Alvaro Gomez • *California State University, Los Angeles, Los Angeles, CA*
Frank A. Gomez • *California State University, Los Angeles, Los Angeles, CA*
Brittany Hartzell-Baguley • *Department of Chemistry and Biochemistry, University of South Carolina, Columbia, SC*
Ulrike Holzgrabe • *Institut für Pharmazie und Lebensmittelchemie, Universität Würzburg, Würzburg, Germany*

Christian W. Huck • *Institute of Analytical Chemistry and Radiochemistry, Leopold-Franzens University, Innsbruck, Austria*
Janpen Intaraprasert • *Department of Chemistry, Ubon Ratchathani University, Ubon Ratchathani, Thailand*
Varinder Kaur • *Department of Chemistry, Punjab University, Patiala, Punjab, India*
Stephanie King • *Department of Chemistry and Biochemistry, Ohio University, Athens, OH*
Majlinda Lahaniatis • *European Commission-Joint Research Centre, Institute for Health and Consumer Protection Unit "Physical and Chemical Exposure," Ispra, Italy*
Stefanie Laug • *Institut für Pharmazie und Lebensmittelchemie, Universität Würzburg, Würzburg, Germany*
Jutta Lintelmann • *HelmholtzZentrum München, German Research Center for Environmental Health, Neuherberg, Germany*
Ashok Kumar Malik • *Department of Chemistry, Punjab University, Patiala, Punjab, India*
Philip J. Marriott • *School of Applied Sciences, RMIT University, Melbourne, Victoria, Australia*
Alex Marsh • *GlaxoSmithKline Research & Development, Harlow, Essex, UK*
Bruce McCord • *Department of Chemistry, Florida International University, University Park, Miami, FL*
Sergio Paoletti • *Department of Biochemistry, Biophysics and Macromolecular Chemistry, University of Trieste, Trieste, Italy*
Guichen Ping • *Department of Molecular and Pharmaceutical Biotechnology, Graduate School of Pharmaceutical Sciences, The University of Tokushima, Tokushima, Japan*
Joe Power • *Waterford Institute of Technology, Department of Chemical & Life Sciences, Waterford, Ireland*
Arndt Psurek • *University of Jena, Department of Pharmaceutical Chemistry, Jena, Germany*
Lee Riddick • *US Environmental Protection Agency, Office of Research and Development, National Exposure Research Laboratory, Environmental Sciences Division, Las Vegas, NV*
Angel Ríos • *Department of Analytical Chemistry and Food Technology, University of Castilla-La Mancha, Spain*
Irene Rohregger • *Papierfabrik Wattens GmbH&CoKG, Wattens, Austria*
Marco Rossi • *Bracco Imaging SpA-CRM Trieste, AREA Science Park, Trieste, Italy*

Isabella Rustighi • *Department of Biochemistry, Biophysics and Macromolecular Chemistry, University of Trieste, Trieste, Italy*
Philippe Schmitt-Kopplin • *HelmholtzZentrum München, German Research Center for Environmental Health, Neuherberg, Germany*
Uli Schurr • *HGF/FZJ-Research Centre Jülich, Phytosphere, Jülich, Germany*
Gerhard K. E. Scriba • *University of Jena, Department of Pharmaceutical Chemistry, Jena, Germany*
Xianzhe Shi • *Dalian Institute of Chemical Physics, Chinese Academy of Sciences, Dalian, China*
Catherine Silverio • *California State University, Los Angeles, Los Angeles, CA*
Bartolomé M. Simonet • *Department of Analytical Chemistry, University of Córdoba, Campus de Rabanales, Spain*
Björn Thiele • *HGF/FZJ-Research Centre Jülich, Phytosphere, Jülich, Germany*
Jing Tian • *Dalian Institute of Chemical Physics, Chinese Academy of Sciences, Dalian, China*
Sara Ullsten • *Department of Analytical Chemistry, Biomedical Centre, Uppsala University, Uppsala, Sweden*
Miguel Valcárcel • *Department of Analytical Chemistry, University of Córdoba, Córdoba, Spain*
Amedeo Vetere • *Department of Biochemistry, Biophysics and Macromolecular Chemistry, University of Trieste, Trieste, Italy*
Gerhard Weber • *FFE Weber GmbH, Planegg, Germany*
Qianfeng Weng • *Dalian Institute of Chemical Physics, Chinese Academy of Sciences, Dalian, China*
Katrin Wieland • *HGF/FZJ-Research Centre Jülich, Phytosphere, Jülich, Germany*
Frank Wienen • *Institut für Pharmazie und Lebensmittelchemie, Universität Würzburg, Würzburg, Germany*
Robert Wildgruber • *FFE Weber GmbH, Planegg, Germany*
An Willems • *Laboratory of Medical Biochemisty and Clinical Analysis, Ghent University, Ghent, Belgium*
Guowang Xu • *Dalian Institute of Chemical Physics, Chinese Academy of Sciences, Dalian, China*
Kailong Yuan • *Dalian Institute of Chemical Physics, Chinese Academy of Sciences, Dalian, China*
Jose Zavaleta • *California State University, Los Angeles, Los Angeles, CA*
Andreas Zemann • *Papierfabrik Wattens GmbH&CoKG, Wattens, Austria*

Xiangmin Zhang • *Department of Chemistry & Research Center for Proteome, Fudan University, Shanghai, China*
Yukui Zhang • *Dalian Institute of Chemical Physics, Chinese Academy of Sciences, Dalian, China*
Chunxia Zhao • *Dalian Institute of Chemical Physics, Chinese Academy of Sciences, Dalian, China*
Roland Zitturi • *Papierfabrik Wattens GmbH & Co KG, Wattens, Austria*
Aida Zuberovic • *Department of Analytical Chemistry, Biomedical Centre, Uppsala University, Uppsala, Sweden*

I

Analyte-Oriented

1

Determination of Small Ions With Capillary Electrophoresis and Contactless Conductivity Detection

Andreas Zemann, Irene Rohregger, and Roland Zitturi

Summary

Capillary Electrophoresis (CE) has become an accepted method for the separation of inorganic and organic ions. Usually, direct and indirect optical detection methods are used in conventional CE. However, with contactless conductivity detection, much better detection limits in the low ppb range are obtained compared to optical detection modes. Besides offering great flexibility in capillary handling, this detection technique can be performed on-capillary also with capillaries made of other materials than fused silica (PEEK®, Teflon®) and with capillaries having very small inner diameters.

Key Words: Capillary electrophoresis; contactless conductivity detection; inorganic ions; organic ions; organic acids.

1. Introduction

Recent review articles specifically describe the various aspects of conductivity detection in capillary electrophoresis (CE) ***(1–5)***, including contactless conductivity detection schemes.

Commercial CE instruments are usually equipped with ultraviolet (UV) absorption detectors. However, indirect optical detection strategies must be employed for non-UV-absorbing analytes, such as inorganic ions, and this usually reduces sensitivity.

Commercial CE instruments with conductivity detectors are rarely found ***(6–8)***, and other ambitious attempts, such as suppressed conductivity detection for CE, unfortunately never reached a commercial status ***(9,10)***. A few years ago, contactless conductivity detectors for CE were successfully presented.

From: *Methods in Molecular Biology, vol. 384: Capillary Electrophoresis*
Edited by: P. Schmitt-Kopplin © Humana Press Inc., Totowa, NJ

2. Basic Principles of Conductivity Detection in Capillary Electrophoresis

Several aspects characterize conductivity detection in CE.

Electrophoretic mobility and signal response in conductivity detection are related to, as well as arise from, the equivalent conductivity of an analyte. Solute ions displace background co-ions equivalent to their charge. As a consequence, the recorded response is a result of the difference in conductivity between analytes and background electrolyte co-ions. For optimum S/N ratio, a difference of the conductance of analyte and electrolyte is required.

Two situations are now important to consider:

1. The sample ion zone has a conductivity higher than the background electrolyte. As a consequence, positive analytical response signals are obtained even at equal concentrations of analyte and electrolyte co-ions. However, this gain in response is paid by peak asymmetry.
2. The equivalent conductivities of the sample ions and background electrolyte co-ions match. A higher ionic strength of the sample zone compared to the electrolyte is required to obtain a positive analytical response. However, this counteracts general principles of CE which require the use of electrolytes with a higher ionic strength than the sample zone in order to take advantage of the respective electrostacking effects.

3. Contactless Conductivity Detection

Contactless conductivity detection (CCD) for electrokinetic separations dates back into the seventies when capillary isotachophoretic (CITP) separations of inorganic species were monitored using high-frequency inductively coupled detectors ***(11–13)***. This detection technique used four electrodes, which were placed around the capillary.

Detection techniques of this kind were applied for the detection of inorganic anions in aqueous soil extracts ***(14)*** or in milk samples ***(15)***. Especially for samples with a high matrix contents, this detection technique offers several advantages as a result of the larger inner capillary diameters.

4. Capacitively Coupled Contactless Conductivity Detection

In 1998, two groups presented quite similar, however independently developed, contactless conductivity detectors for CE ***(16,17)***. The detection principle was later termed as *capacitively coupled contactless conductivity detection* (C^4D) ***(16,18)***.

The detection signal is obtained in a longitudinal dimension along the capillary. One major advantage of this technique is that very narrow inner diameter (ID) capillaries can be used. Thus, it can be used in capillaries with small IDs and miniaturized instrumentation such as in chip based separation systems.

Figure 1A shows a scheme of a capacitively coupled contactless conductivity detector. Two cylindrical stainless steel electrodes are placed around the capillary. After applying a frequency in the range of 20–900 kHz, a capacitive transition between the actuator electrode and the liquid inside the capillary as well as between the electrolyte and the pick-up electrode occurs. This setup enables recording of the conductivity changes of the electrolyte in the detection gap between the electrodes inside the capillary. The electrodes are placed on an insulated socket to ensure a mechanically stable construction and a constant electrode distance. A grounded shielding, usually made of a thin metal sheet or foil, can be placed between the electrodes in order to reduce noise and capacitive leakage (**Fig. 1C**). The shielded socket is placed in a grounded metal housing.

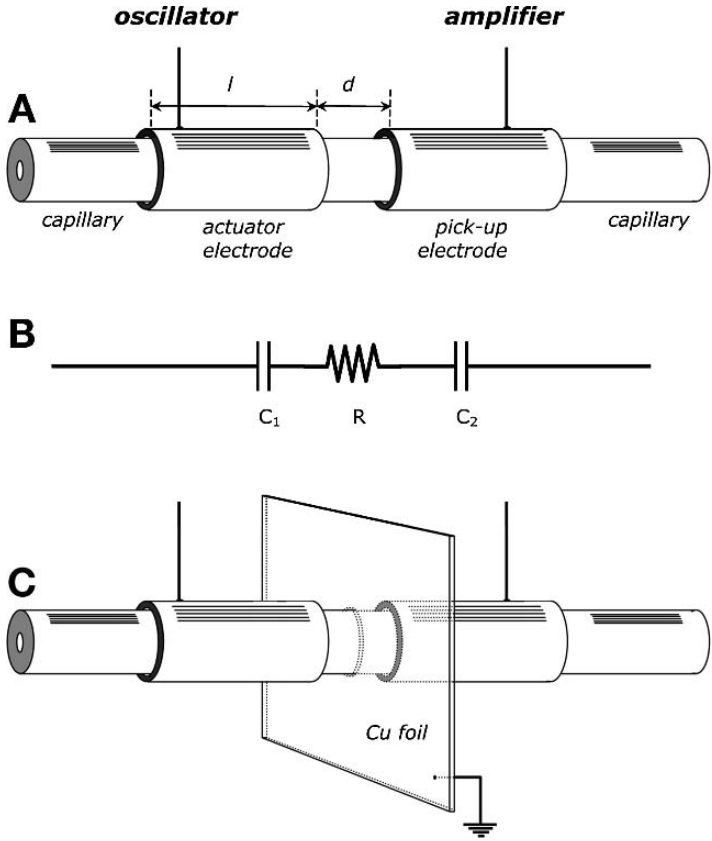


Fig. 1. Principle of a capacitively coupled contactless conductivity detection (C^4D) system. (Reprinted from **ref. *5***.) **A**, schematic drawing of the sensing electrodes (as first described in **ref. *16***); **B**, simplified circuitry for C^4D; **C**, electrode arrangement with shielding (as first described in **ref. *17***).

Initially, the groups working with contactless conductivity detection ***(16,17)*** used a conducting silver varnish painted on the capillary, which allows a direct contact of the electrode material with the outer capillary wall. This prevents build-up of an additional capacitance as a result of the air gap, which is the case in the syringe needle design ***(16,18)***. Despite the fact that a higher sensitivity can be achieved with the painted electrodes, flexible handling of the capillaries is limited when changing the separation capillaries.

A C^4D cell where all the pieces (electrodes, metal sheet, and spacers) required for the detection cell were assembled on a capillary has also been proposed ***(19)***. The capillary is impregnated with silicon grease in order to prevent adhesion to the finished cell and the parts were held in position and covered with epoxy resin. After hardening, a conducting silver varnish and finally a common nail polish for mechanical protection is used.

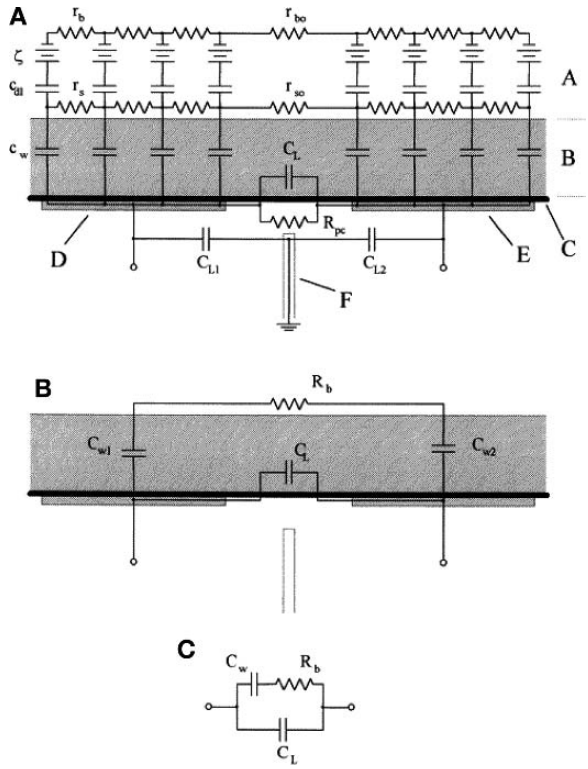


Fig. 2. Equivalent circuits for a C^4D cell. (Reprinted from **ref. *17***.)

C^4D is not limited to fused silica capillaries. Tanyanyiwa et al. ***(20)*** found polyether ether ketone (PEEK) capillaries to be compatible with C^4D and could achieve fairly good detection limits for inorganic ions in the range of 10^{-7} *M*.

Meanwhile, a commercially available detector (TraceDec® from Innovative Sensor Technologies [IST] GmbH) using this principle is available for CE as well as for liquid chromatography ***(21)***. The instrument exhibits excellent detection limits and sensitivity for the analysis of inorganic and small organic ions.

Instrumental parameters, such as design, length (l), and distance of the electrodes (d), outer and ID of the capillary, and electric properties, such as oscillation frequency, voltage, wave form, and detector electronics, can be varied in order to optimize sensitivity.

In order to minimize peak dispersion effects and to achieve good sensitivity at the same time, amphoteric buffer electrolytes with a low equivalent conductivity ***(22–24)*** at considerably high concentrations are commonly used when using electrokinetic separation systems and conductivity detection. As a consequence, the ionic strength increases and electrostacking effects can take place. **Figure 2** shows equivalent circuits for a C^4D cell.

4.1. Separation and Detection of Cations

In the first report of capacitively coupled contactless conductivity detection in CE, lactic acid and 4-methylbenzylamine at pH 4.9 ***(16)*** have been used as background electrolyte components for cations. These compounds enable the simultaneous indirect photometric and direct conductivity detection of inorganic cations (*see* summary of applications for cations in **Table 1**).

2-[*N*-morpholino]ethanesulfonic acid (MES) and histidine (His) have later become widely used buffer components in the C^4D for the separation and direct conductivity detection of both inorganic cations ***(16–18,25,26,35)*** and inorganic anions ***(16,34)***. The ampholyte (His) keeps background conductivity low, and at the same provides a sufficiently high ionic strength for current transport. Transition earth metal ions can be separated in MES/His and detected using C^4D ***(18,25)***, whereas higher conducting cations, such as Mn^{2+}, Pb^{2+}, Cd^{2+}, Fe^{3+} show positive peaks, and other metal ions, such as Cu^{2+}, Zn^{2+}, Co^{2+}, Ni^{2+}, are monitored by indirect conductivity detection. Hydroxyl-iso-butyric acid alters selectivity and sensitivity of some cations as a result of complexation and helps improving the detection of Fe^{3+} by preventing its precipitation as a result of the lower pH value ***(25)***.

18-crown-6 is a suitable selector for the separation of potassium and ammonium, as it does not increase the background electrolyte conductivity ***(18)***.

Table 1
Capillary Electrophoresis and Contactless Conductivity Detection of Cations

Analytes	Electrolyte	Capillary ID	Mode of detection	Ref.
Li^+, Na^+, K^+, Rb^+, Mg^{2+}, Ca^{2+}, Mn^{2+}, Cd^{2+}	10 m*M* lactic acid, 8 m*M* 4-methylbenzylamine, 15% methanol, pH 4.9	50 μm	Direct C^4D; indirect UV	***16***
Li^+, Na^+, K^+, Rb^+, Mg^{2+}, Ca^{2+}, Mn^{2+}	20 m*M* MES, 20 m*M* His, pH 6.0	50 μm	Direct C^4D	***16***
Li^+, Na^+, K^+, Mg^{2+}, Ca^{2+}, Ba^{2+}	10 m*M* MES, 10 m*M* His, pH 6.0	75 μm	Direct C^4D	***17***
TMA^+, TEA^+, $BTEA^+$, TBA^+	5 m*M* KOAc, pH 5.2	75 μm	Indirect C^4D	***17***
Li^+, Na^+, K^+, Rb^+, NH_4^+, Mg^{2+}, Ca^{2+}, Mn^{2+}	20 m*M* MES, 20 m*M* His, 1 m*M* 18 crown-6, pH 6.0	50 μm	Direct C^4D	***18***
Li^+, Na^+, K^+	20 m*M* MES, 20 m*M* His, 1 m*M* 18-crown-6, pH 6.0	10, 25, 50, 75, 100 μm	Direct C^4D	***18***
Me_4N^+, $PrNH_3^+$, $Pr_2NH_2^+$, Pr_4N^+, Me-CH-NH_2^+, Bu_4N^+, $C_{12}NH_3^+$, $Me_2(C_{12})_2N^+$	10 m*M* acetic acid, 10 m*M* Tris acetate, pH 4.75	50 μm	Direct C^4D	***39***
Li^+, Na^+, K^+, Mg^{2+}, Ca^{2+}, Ba^{2+}, Mn^{2+}	20 m*M* MES, 20 m*M* His, pH 6.0	50 μm	Direct C^4D	***26***
Me_4N^+, $PrNH_3^+$, $Pr_2NH_2^+$, Pr_4N^+, Me-CH-NH_2^+, Bu_4N^+, $C_{12}NH_3^+$, $Me_2(C_{12})_2N^+$	10 m*M* 2,6-dihydroxybenzoic acid, 10 m*M* tetraethylammonium 2,6-dihydroxybenzoate; NACE in various organic solvents (DMF, DMAc, PC)	50 μm	Direct C^4D	***39***
Li^+, Na^+, K^+, Rb^+, Cs^+, NH_4^+, Mg^{2+}, Ca^{2+}, Sr^{2+}, Ba^{2+}	10 m*M* MES, 10 m*M* His, 2.5 m*M* 18crown6, pH 6.0	75 μm	Direct C^4D	***25***
Li^+, Na^+, K^+, NH_4^+, Mg^{2+}	10 m*M* MES, 10 m*M* His, 1 m*M* 18 crown 6, pH 6.0	PEEK; 50, 75 μm	Direct C^4D	***20***

Li^+, Na^+, K^+, Ca^{2+}, Mg^{2+}, Mn^{2+}	20 m*M* MES, 20 m*M* His, pH 6.1	50 μm	Direct C^4D	***35***
Na^+, K^+, Mg^{2+}, Ca^{2+}, tyramine, ephedrine, codeine	20 m*M* citric acid, 10 m*M* LiOH, pH 2.95	75 μm	Direct/Indirect C^4D; direct UV	***28***
Vishnevski infusion solution: Na^+, K^+, Ca^{2+}, procaine	20 m*M* citric acid, 10 m*M* LiOH, pH 2.95	75 μm	Direct/Indirect C^4D; direct UV	***28***
Pb^{2+}, Cu^{2+}, Zn^{2+}, Cd^{2+}, Mn^{2+}, Fe^{3+}, Co^{2+}, Ni^{2+}	10 m*M* MES, 10 m*M* His, 2.5 m*M* 18crown6, pH 6.0	75 μm	Direct/Indirect C^4D	***25***
Li^+, Na^+, K^+, Cs^+, (NH_4^+), Mg^{2+}, Ca^{2+}, Sr^{2+}, Ba^{2+}, Pb^{2+}, Cu^{2+}, Zn^{2+}, Cd^{2+}, Mn^{2+}, Fe^{3+}, Co^{2+}, Ni^{2+}	10 m*M* MES, 10 m*M* His, (2.5 m*M* 18crown6), pH 6.0	75 μm	Direct/Indirect C^4D	***25***
Pb^{2+}, Cu^{2+}, Zn^{2+}, Cd^{2+}, Mn^{2+}, Fe^{3+}, Co^{2+}, Ni^{2+}	5 m*M* MES, 5 m*M* His, 3 m*M* HIBA, pH 5.2	75 μm	Direct/Indirect C^4D	***25***
Me_4N^+, $BuNH_3^+$, Bu_4N^+	6 m*M* NH_4OAc, pH 6.8	50 μm	Indirect C^4D	***35***
Catecholamines (HMBA, dopamine, normetanephedrine, metanephrine)	10 m*M* ammonium acetate, pH 4	50 μm	Indirect C^4D	***26***
Lys, Arg, His, Gly, Ala, Val, Ile, Leu, Ser, Thr, Asn, Met, Gln, Trp, Glu, Phe, Pro, Tyr, Cys, Asp	2.3 m*M* acetic acid, 0.1% (w/w) HEC, pH 2.1	50 μm	Indirect C^4D	***29***

Even smaller IDs compared to the standard 50-μm ID capillaries are suitable separation media in combination with C^4D and have been demonstrated with capillary IDs as low as 5 μm ***(18,27)***. The use of even smaller IDs is also conceivable. For the indirect conductometric detection of alkylammonium surfactants, a potassium acetate background electrolyte at acidic pH was used ***(17)***.

Other electrolyte constituents for use with C^4D of cations are acetic acid for alkylammonium cations ***(28)*** and underivatized amino acids ***(29)***. as well as citric acid and lactic acid for inorganic cations ***(28)***. For the separation of catecholamines, ammonium acetate was used as a suitable background electrolyte ***(26)***.

4.2. Separation and Detection of Anions

The electrophoretic separation of anions usually requires alkaline or slightly acidic background electrolytes (*see* **Table 2**). Sorbate/arginine buffers are suitable for the sensitive direct conductivity detection of inorganic anions ***(18)***. Indirect conductivity detection schemes can be used for organic anions. Although the sensitivity of inorganic anions is reduced when compared to direct detection, organic anions can be detected at low concentrations. As an example, haloacetic acids can be at least partly separated and detected by indirect conductometric detection using electrolyte containing phosphate, citrate, or borate ***(30)***.

C^4D is also suitable for capillary chromatography (CEC) in packed capillaries ***(31)***. Although it is highly selective, CEC was long hampered by the fragility of the packed capillaries as a results of the detection window. With C^4D, no optical detection window is necessary, as the detection can be performed in the packed region of the capillary. In addition, limitations with respect to the concentration range of UV absorbing eluants are reduced.

4.3. Simultaneous Separation and Detection of Anions and Cations

A summary of methods for the simultaneous separation of anions and cations in one electrophoretic run and contactless conductivity detection is given in **Table 3**.

A dual detection (photometric and contactless conductivity) scheme was used employing optical fibres between the conductivity electrodes to simultaneously monitor the conductivity as well as the optical response ***(28)***. Thus, identical migration times for both detection tracks are obtained. For UV-absorbing analytes with a low equivalent conductivity, non-UV-absorbing solutes with high equivalent conductivities, and sample components with intermediate absorbing and conducting properties, a sensitive detection is observed

Table 2
Capillary Electrophoresis and Contactless Conductivity Detection of Anions

Analytes	Electrolyte	Capillary ID	Mode of detection	Ref.
Cl^-, Br^-, NO_2^-, NO_3^-, SO_4^{2-}, $C_2O_4^{2-}$	20 m*M* MES, 20 m*M* His, 0.001% HDB, pH 6.0	50 μm	Direct C^4D	***16***
F^-, Cl^-, NO_3^-, SO_4^{2-}, PO_4^{2-}, CO_3^{2-}, OAc^-, Lac^-, But^-	7.5 m*M* sorbate, 15 m*M* Arg, 0.0007% HDOH, pH 8.9	50 μm	Direct C^4D; indirect UV	***18***
Cl^-, SO_4^{2-}, picrate, benezenesulfonate, 2-bromobenzoate	20 m*M* citric acid, 10 m*M* LiOH, pH 2.95	75 μm	Direct C^4D; direct UV	***28***
F^-, Cl^-, Br^-, I^-, NO_2^-, NO_3^-, PO_4^{3-}, SO_4^{2-}	10 m*M* *p*-toluenesulfonic acid, 20 m*M* Tris, pH 8.05	75 μm; packed with Dionex AS9-SC	Direct C^4D	***31***
F^-, Cl^-, Br, NO_3^-, SO_4^{2-}, PO_4^{3-}, $C_2O_4^{2-}$	10 m*M* MES, 10 m*M* His, 1 m*M* 18 crown 6, pH 6.0	PEEK; 50, 75 μm	Direct C^4D	***20***
F^-, citrate, succinate, acetate	10 m*M* MES, 10 m*M* His, 1 m*M* 18 crown 6, pH 6.0	PEEK; 50, 75 μm	Direct C^4D	***20***
F^-, Cl^-, Br^-, NO_2^-, NO_3^-, PO_4^{3-}	20 m*M* MES, 20 m*M* His, 0.03 m*M* CTAB, pH 6.0	50 μm	Direct C^4D	***35***
Cl^-, NO_3^-, SO_4^{2-}, $Form^-$, CO_3^{2-}, OAc^-, Lac^-, But^-	2.5 m*M* chromate, 0.0007% HDOH, pH 8.2	50 μm	Indirect C^4D	***18***
Haloacetic acids	12.5 m*M* phosphate, 5 m*M* DETA, pH 9.4	50—75 μm	Indirect C^4D	***30***
Haloacetic acids	100 m*M* borate, 80 m*M* Tris, 3 m*M* DETA, 8.6	50–75 μm	Indirect C^4D	***30***

Table 3
Simultaneous Capillary Electrophoretic Separation of Anions and Cations With Contactless Conductivity Detection

Analytes	Electrolyte	Capillary ID	Mode of detection	Ref.
K^+, Na^+, acetylsalicylate, benzoate, salicylate	20 m*M* boric acid, 10 m*M* LiOH, pH 9.2	75 μm	Direct/Indirect C^4D; direct UV	***28***
Li^+, Na^+, K^+, NH_4^+, Mg^{2+}, Cl^-, Br^-, NO_2^-, NO_3^-, SO_4^{2-}	50 m*M* MES, 50 m*M* His, 1 m*M* 18 crown 6, 0.001% SPAS, pH 6.0	50 μm	Direct C^4D	***34***
Li^+, Na^+, K^+, NH_4^+, Mg^{2+}, Ca^{2+}, Mn^{2+}, F^-, Cl^-, Br^-, NO_2^-, NO_3^-, PO_4^{3-}	20 m*M* MES, 20 m*M* His, 1.5 m*M* 18crown6, 0.01 m*M* CTAB, pH 6.0	50 μm	Direct C^4D	***35***
Li^+, Na^+, K^+, NH_4^+, Mg^{2+}, Cl^-, NO_3^-, SO_4^{2-}, $C_2O_4^{2-}$, tartrate, citrate, succinate	10 m*M* MES, 10 m*M* His, 1 m*M* 18 crown6, pH 6.0	PEEK; 50 μm	Direct C^4D	***20***
Li^+, Na^+, K^+, NH_4^+, Mg^{2+}, Ca^{2+}, Sr^{2+}, Ba^{2+}, Zn^{2+}, Cd^{2+}, Cr^{3+}, Mn^{2+}, Fe^{3+}, Co^{2+}, F^-, Cl^-, Br^-, NO_2^-, NO_3^-, SO_4^{2-}, formate, fumarate	8 m*M* His, 2.8 m*M* HIBA, 0.32 m*M* 18crown6, pH 4.25 (adjusted with acetic acid)	50 μm	Direct C^4D	***36***
Li^+, Na^+, K^+, NH_4^+, Mg^{2+}, Ca^{2+}, Sr^{2+}, Ba^{2+}, Zn^{2+}, Cd^{2+}, Cr^{3+}, Mn^{2+}, Fe^{3+}, Co^{2+}, F^-, Cl^-, Br^-, NO_2^-, NO_3^-, SO_4^{2-}, formate, fumarate	9 m*M* His, 4.6 m*M* lactic acid, 0.38 m*M* 18crown6, pH 4.25 (adjusted with acetic acid)	50 μm	Direct C^4D	***36***

for mixtures of inorganic cations and aromatic acids. Inorganic cations were monitored using the C^4D, whereas the organic acids produced an indirect and a direct signal in the C^4D and UV track, respectively. Medical infusion solutions can thus be analyzed.

The simultaneous separation of anions and cations in one analytical run often is a wishful task which, however, can be easily performed by CE ***(32,33)***. This technique is, however, limited because of the requirement of a UV-transparent detection window in optical detection. Thus, flexibility in terms of the effective separation length is reduced. With C^4D, the effective separation length can be flexibly adjusted, which significantly facilitates method development. With dual-end injection of anions and cations in combination with C^4D, the selectivity of anions and cations can be effectively altered and optimized between runs. Thus, the selectivity between anionic and cationic analytes no longer solely depends on the buffer composition but also on the position of the detector. For this effect, the term "apparent selectivity" has been introduced ***(34,19)***. These separation and detection techniques have been applied for the simultaneous separation of anions and cations in standard solutions as well as for real samples, such as water samples ***(34,19,20,35,36)***, with excellent reproducibility in terms of migration times and peak areas of 0.4% and 5.9%, respectively ***(36)***.

4.4. Other Analytes

Electrokinetic capillary chromatography for neutral compounds is also reported with C^4D ***(37)***. The determination of aliphatic alcohols by using sodium dodecyl sulfate (SDS) as selector and indirect contactless conductivity detection can be performed with limits of detection in the range of 1–5 m*M* (**Table 4**).

Contactless conductivity detection for the indirect conductivity detection of neutrals and other analytes has rarely been used in the past. High concentrations of either hydronium or hydroxide ions are suitable to serve as high-conductivity background electrolyte co-ions: they both carry a single charge, which enables good transfer ratios for the charged solute ions, and they exhibit high equivalent conductivities. Thus, C^4D is no longer restricted to pH values near neutrality between pH 5.0 and 9.0, and strongly acidic or alkaline electrolytes become useful background electrolyte components, such as in the separation and detection of carbohydrates ***(38)***.

C^4D extends the application range of UV-absorbing organic solvents ***(38)***. This is specifically interesting, as the cut-off wavelengths of many organic solvents often limit their use in the UV region below 260 nm. The use of organic solvents has generally proven to be advantageous in terms of selectivity ***(40–43)***, thus these method development strategies were also made

Table 4
Capillary Electrophoresis and Contactless Conductivity Detection of Neutral Compounds and Proteins

Analytes	Electrolyte	Capillary ID	Mode of detection	Ref.
2-PrOH, 1-PrOH, 2-Me-2-PrOH, 2-BuOH, 2-Me-1-PrOH, 1-BuOH, 2-Me-2-BuOH, 3-Me-1-BuOH, 1-PeOH, 1-HeOH	50 m*M* Na_3PO_4, 50 m*M* SDS, (10% methanol), pH 6.9	50 μm	Indirect C^4D	***37***
sucrose, fructose	100 m*M* phosphate, pH 2.5	50 μm	Indirect C^4D	***38***

use of with contactless conductivity detection. An interesting fundamental study employed C^4D to prove the theory of lower theoretical plate numbers in nonaqueous compared to aqueous electrolytes ***(44)***. Additional theoretical investigations include the development of a mathematical and computational model for the optimization of background electrolytes ***(45)*** and the determination of electroosmotic flow mobilities in organic solvents ***(46)***.

5. Materials

5.1. CZE-Conductivity Detection of Inorganic Cations in Cigarette Paper (Fig. 3)

1. Samples: aqueous extract of a cigarette paper (*see* **Notes 1–3**).
2. CE buffer: 20 m*M* MES, 20 m*M* L-histidine, 1 m*M* 18-crown-6 (Fluka-Sigma-Aldrich, Vienna, Austria), pH 6.1; capillary: 60 cm ID 50 μm; detection: conductivity; injection: 15 m bar 10 s; voltage: 30 kV; temperature: 20 °C; peak identification: 1, ammonium; 2, potassium; 3, calcium; 4, sodium; 5, magnesium.

5.2. CZE-Conductivity Detection of Inorganic Anions in Tobacco (Fig. 4)

1. Samples: aqueous extract of an American blend tobacco.
2. CE buffer: 15 m*M* arginine, 7.5 m*M* sorbate, 0.001% HDB, pH 9.1; capillary: 70 cm ID 50 μm; detection: conductivity; injection: 30 m.bar 10 s; voltage: –30 kV; temperature: 25 °C; peak identification: 1, chloride; 2, sulfate; 3, oxalate; 4, formiate; 5, malate; 6, carbonate; 7, acetate.

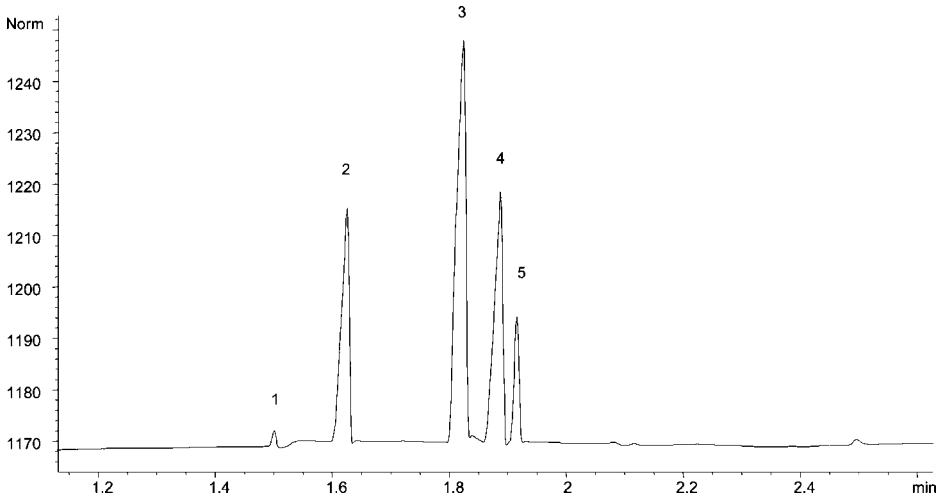


Fig. 3. Capillary electropherogram of an aqueous extract of cigarette paper.

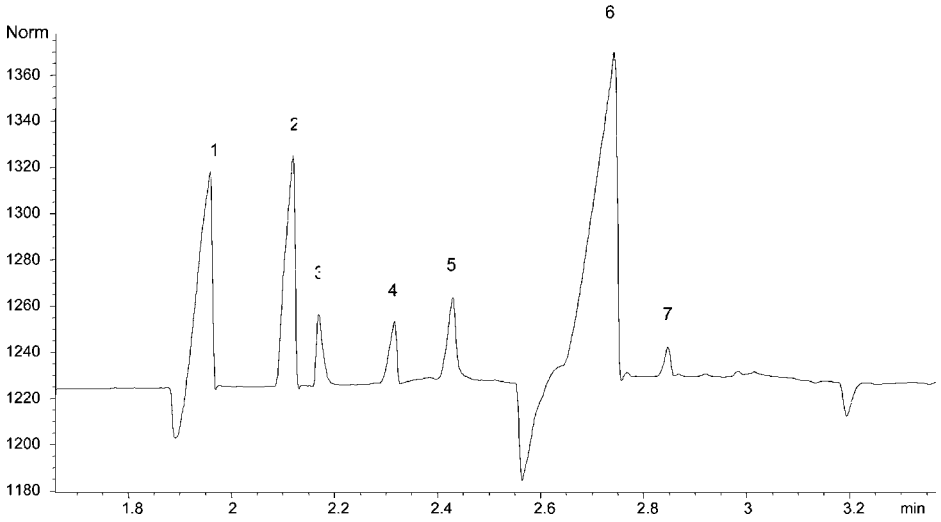


Fig. 4. Capillary electropherogram of an aqueous extract of an American blend tobacco.

6. Equipment

1. High-performance CE system from Agilent Technologies (Palo Alto, CA), with ChemStation software.
2. Fused silica column (Polymicro Technologies, Phoenix, AZ); total length: 70 cm; effective length: 58 cm; ID: 50 μm.
3. Contactless Conductivity Detection, TraceDec (IST, Strasshof, Austria).

7. Notes

1. Paper and tobacco samples were extracted with distilled water (500mg dry sample in 25 mL water) using sonication for 15 minutes.
2. Dilute extraction solution.
3. Use sample solution for CE analysis.

References

1. Swinney, K. and Bornhop, D. J. (2000) Detection in Capillary Electrophoresis. *Electrophoresis* **21,** 1239–1250.
2. Zemann, A. J. (2001) Conductivity detection in capillary electrophoresis. *Trends Anal. Chem.* **20,** 346–354.
3. Tanyanyiwa, J., Leuthardt, S., and Hauser, P. C. (2002) Conductimetric and potentiometric detection in conventional and microchip capillary electrophoresis. *Electrophoresis* **23,** 3659–3666.
4. Gujt, R. M., Evenhuis, C. J., Macka, M., and Haddad, P. R. (2004) Conductivity detection for conventional and miniaturised capillary electrophoresis systems. *Electrophoresis* **25,** 4032–4057.
5. Zemann, A. J. (2003) Capacitively coupled contactless conductivity detection in capillary electrophoresis. *Electrophoresis* **24,** 2125–2137.
6. Jones, W. R., Soglia, J., Mcglynn, M., Haber, C., Reineck, J., and Krstanovic, C. (1996) Capillary ion electrophoresis with conductivity detection. *American Laboratory* **28,** 25–33.
7. Haber, C., Jones, W. R., Soglia, J., et al. (1996) Conductivity detection in capillary electrophoresis. *J. Cap. Elec.* **3,** 1–11.
8. Haber, C., VanSaun, R. J., and Jones, W. R. (1998) Quantitative analysis of anions at ppb/ppt levels with capillary electrophoresis and conductivity detection: enhancement of system linearity and precision using an internal standard. *Anal. Chem.* **70,** 2261–2267.
9. Dasgupta, P. K. and Bao, L. Y. (1993) Suppressed conductometric capillary electrophoresis separation systems. *Anal. Chem.* **65,** 1003–1011.
10. Avdalovic, N., Pohl, C. A., Rocklin, R. D., and Stillian, J. R. (1993) Determination of cations and anions by capillary electrophoresis combined with suppressed conductivity detection. *Anal. Chem.* **65,** 1470–1475.
11. Gas, B., Demjanenko, M., and Vacik, J. (1980) High-frequency contactless conductivity detection. *J. Chromatogr.* **192,** 253.

12. Reijenga J. C., Slaats H. J. L. A., and Everaerts, F. M. (1983) Determination of conjugated bile acids in human bile by isotachophoresis in a non-aqueous solvent using a.c. conductivity and UV detection. *J. Chromatogr*. **267,** 85–89.
13. Vacik, J., Zuska, J., and Muselasova, I. (1985) Improvement of the performance of a high-frequency contactless conductivity detector for isotachophoresis. *J. Chromatogr*. **320,** 233–240.
14. Kaniansky, D., Zelenska, V., Masar, M., Ivanyi, F., and Gazdikova, S. (1999) Contactless conductivity deteciton in capillary zone electrophoresis. *J. Chromatogr. A* **844,** 349–359.
15. Masar, M., Bodor, R., and Kaniansky, D. (1999) Separations of inorganic anions based on their compexations with α-cyclodextrin by capillary zone electrophoresis with contactless conductivity detection. *J. Chromatogr. A* **834,** 179–188.
16. Zemann, A. J., Schnell, E., Volgger, D., and Bonn, G. K. (1998) Contactless conductivity detection for capillary electrophoresis. *Anal. Chem*. **70,** 563–567.
17. Fracassi da Silva, J. A., and do Lago, C. L. (1998) An oscillometric detector for capillary electrophoresis. *Anal. Chem*. **70,** 4339–4343.
18. Mayrhofer, K., Zemann, A. J., Schnell, E., and Bonn, G. K. (1999) Capillary electrophoresis and contactless conductivity detection of ions in narrow inner diameter capillaries. *Anal. Chem*. **71,** 3828–3833.
19. Macka, M., Hutchinson, J., Zemann, A., Shusheng, Z., and Haddad, P.R. (2003) Miniaturized movable contactless conductivity detection cell for capillary electrophoresis. *Electrophoresis* **24,** 2144–2149.
20. Tanyanyiwa, J., Leuthardt, S., and Hauser, P. C. (2002) Electrophoretic separations with polyether ether ketone capillaries and capacitevely copuled contactless conductivity detection. *J. Chromatogr. A* **978,** 205–211.
21. www.istech.at
22. Good, N. E., Winget, G. D., Winter, W., Connolly, T. N., Izawa, S., and Singh, R. M. M. (1966) Hydrogen ion buffers for biological research. *Biochemistry* **5,** 467–477.
23. Good, N. E. and Izawa, S. (1972) Hydrogen ion buffers, in: *Methods in Enzymology* (Colowick, S. P. and Kaplan, N. O., eds.). Academic, New York: pp. 53–68.
24. Beckers, J. L. (2003) Ampholytes as backgruond electrolytes in capillary zone electrophoresis: sense or nonsense? Histidine as a model ampholyte. *Electrophoresis* **23,** 548–556.
25. Tanyanyiwa, J. and Hauser, P. C. (2002) High-voltage contactless conductivity detection of metal ions in capillary electrophoresis. *Electrophoresis* **23,** 3781–3786.
26. Vuorinen, P. S., Jussila, M., Siren, H., Palonen, S., and Riekkola, M.-L. (2003) Integration of a contactless conductivity detector into a commercial capillary cassette: Detection of inorganic cations and catecholamines. *J. Chromatogr. A* **990,** 45–52.
27. Unterholzner, V. (2004) Analytik von sensorisch relevanten Verbindungen in Zellstoffen und Papieren mit Kapillarelektrophorese und Ionenchromtographie, Doctoral Thesis University of Innsbruck.

28. Chvojka, T., Jelinek, I., Opekar, F., and Stulik, K. (2001) Dual photometric-contactless conductometric detector for capillary electrophoresis. *Anal. Chim. Acta* **433,** 13–21.
29. Coufal, P., Zuska, J., van de Goor, T., Smith, V., and Gas, B. (2003) Separation of twenty underivatized essential amino acids by capillary zone electorphoresis with contactless conductivity detection. *Electrophoresis* **24,** 671–677.
30. Lopez-Avila, V., van de Goor, T., Gas, B., and Coufal, P. (2003) Separation of haloacetic acids in water by capillary zone electrophoresis with direct UV detection and contactless conductivity detection. *J. Chromatogr. A* **993,** 143–152.
31. Hilder, E. F., Zemann, A. J., Macka, M., and Haddad, P. R. (2001) Anion-exchange capillary electrochromatography with indirect UV and direct contactless conductivity detection. *Electrophoresis* **22,** 1273–1281.
32. Kuban, P. and Karlberg, B. (1998) Simultaneous determination of small cations and anions by capillary electrophoresis. *Anal. Chem.* **70,** 360–365.
33. Padarauskas, A., Olsauskaite, V., and Schwedt, G. (1998) Simultaneous separation of inorganic anions and cations by capillary zone electrophoresis. *J. Chromatogr. A* **800,** 369–375.
34. Unterholzner, V., Macka, M., Haddad, P. R., and Zemann, A. (2002) Simultaneous separation of inorganic anions and cations unsing capillary electrophoresis with a movable contactless conductivity detector. *Analyst* **127,** 715–718.
35. Kuban, P., Karlberg, B., Kuban, P., and Kuban, V. (2002) Application of a contactless conductometric detector for the simultaneous determination of small anions and cations by capillary electrophoresis with dual-opposite end injection. *J. Chromatogr. A* **964,** 227–241.
36. Kuban, P., Kuban, P., and Kuban, V. (2002) Simultaneous determination of inorganic and organic anions, alkali, alkaline earth and transition metal cations by capillary electrophoresis with contactless conductometric detection. *Electrophoresis* **23,** 3725–3734.
37. da Silva, J. A. F. and do Lago, C. L. (2000) Conductivity detection of aliphatic alcohols in micellar electrokinetic chromatography using an oscillometric detector. *Electrophoresis* **21,** 1405–1408.
38. Carvalho, A. Z., da Silva, J. A. F, and do Lago, C. L. (2003) Determination of mono- and disaccharides by capillary electrophoresis with contactless conductivity detection. *Electrophoresis* **24,** 2138–2143.
39. Muzikar, J., van de Goor, T., Gas, B., and Kenndler, E. (2001) Extension of the application range of UV-absorbing organic solvents in capillary electrophoresis by the use of a contactless conductivity detector. *J. Chromatogr. A* **924,** 147–154.
40. Okada, T. J. (1999) Polyethers in inorganic capillary electrophoresis. *Chromatogr. A* **834,** 73–87.
41. Sarmini, K. and Kenndler, E. (1997) Influence of organic solvents on the separation selectivity in capillary electrophoresis. *J. Chromatogr. A* **792,** 3–11.
42. Lucy, C. A. (1999) Factors affecting selectivity of inorganic anions in capillary electrophoresis. *J. Chromatogr. A* **850,** 319–337.

43. Riekkola, M. L., Jussila, M., Porras, S. P., and Valko, I. E. (2000) Non-aqueous capillary electrophoresis. *J. Chromatogr. A* **892,** 155–170.
44. Muzikar, J., van de Goor, T., and Kenndler, E. (2002) The principle cause for lower plate numbers in capillary zone electorphoresis with most organic solvents. *Anal. Chem*. **74,** 434–439.
45. Gas, B., Coufal, P., Jaros, M., Muzikar, J., and Jelinek, I. (2001) Optimization of background electrolytes for capillary electrophoresis I. Methematical and computational model. *J. Chromatogr. A* **905,** 269–279.
46. Muzikar, J., van de Goor, T., Gas, B., and Kenndler, E. (2002) Determination fo electroosmotic flow mobility with a pressuremediated dual-ion technique for capillary electrophoresis with conductivity detection using organic solvents. *J. Chromatogr. A* **960,** 199–208.

2

Metal Analysis With Capillary Zone Electrophoresis

Ashok Kumar Malik

Summary

Capillary electrophoresis has recently attracted considerable attention as a promising analytical technique for metal ion separations. Significant advances in various auxiliary separation principles have opened new application areas for capillary electrophoresis in the analysis of metal species. These advances are mainly due to complexation, ion pairing, solvation and micellization interactions between metal analytes and electrolyte additives, which alter the separation selectivity in a broad range. Likewise, many separation studies on metal ions have been concentrated on the use of pre-electrophoresis derivatization methodology. Approaches suitable for improvement of selectivity for different metal species including metal cations, metal complexes, metal oxoanions and organometallic compounds are discussed, with special attention paid to the related electrophoretic system variables using illustrative examples.

Key Words: Capillary zone electrophoresis; metal ions; transition metal ions; complexing agents; metal ligand interactions; lanthanides; actinides; speciation.

1. Introduction

Most of the electrophoretic methods developed for the separation and quantification of macromolecules of biological origin are in the field of biochemistry and molecular biology. Only a few applications of electrophoretic technique are reported for inorganic metal analysis ***(1–4)***. Nowadays, capillary electrophoresis (CE) is considered a powerful method for inorganic ion separations as a result of extensive research in this field. Furthermore, in many cases, the methods are known to be superior to the conventional high-performance liquid chromatography (HPLC) methods for ionic multispecies analysis. Some advantages of CE over HPLC are (a) high separation efficiency,

From: *Methods in Molecular Biology, vol. 384: Capillary Electrophoresis*
Edited by: P. Schmitt-Kopplin © Humana Press Inc., Totowa, NJ

Table 1
Some Separation of Metal Cations With Organic Acids as the Complexing Agents

Cations (number of cations)	Separation conditions	Separation time (min)	Reference
K^+, Na^+, Mg^{+2}, Li^+, Lanthanides (18)	4 m*M* HIBA, 30 m*M* creatinine (pH 4.8)	5	***6***
Alkali, alkaline earth, transition metals, lanthanides (19)	4 m*M* HIBA, 10 m*M* Waters UVCat-1 (pH 4.4)	2	***7***
Alkali, alkaline earth, transition metals, lanthanides (26)	4.2 m*M* HIBA, 0.2 m*M* Triton X-100, 6 m*M* *N*, *N*-dimethylbenzylamine (pH 4.25)	10	***8***
Alkali, alkaline earth, transition metals, lanthanides, Pb^{2+} (27)	15 mm lactic acid, 5% methanol, 8 mm 4-methylbenzylamine (pH 4.25)	7	***9***
Alkali, alkaline earth and transition metals (12)	2.5 m*M* tartaric acid, 20% methanol, 6 m*M* *p*-toluidine (pH 4.8)	9	***9***
Alkali, alkaline earth and transition metals (14)	12 m*M* HIBA, 6 m*M* imidazole (pH 3.95)	For	***10***
Alkali, alkaline earth, transition metals, Pb^{2+}, NH_4^+, (16)	11 mm lactic acid-2.6 m*M* 18-crown-6, 8% methanol, 7.5 m*M* 4-methylbenzyl amine (pH 4.3)	6	***11***
Alkali, alkaline earth, transition metals, Pb^{2+}(17)	13 mm glycolic acid, 10 m*M* imidazole (pH 4.0)	14	***12***
Alkali, alkaline earth, NH_4^+, Mn^{2+}, Cd^{2+} (12)	6 mm glycine-2 m*M* 18-crown-6, 2% methanol, 5 m*M* 1,1′-diphenylbipyri-dinium (pH 6.5)	5	***13***
Alkali, alkaline earth, transition metals, Pb^{2+}, NH_4^+, (17)	5 m*M* lactic acid-0.5 m*M* 18-crown-6, 10 m*M* imidazole (pH 6.5)	5	***14***
Alkali, alkaline earth, transition metals, Pb^{2+} (17)	1 mm oxalic acid–100 m*M* acetic acid (pH 2.84)	15	***15***

(b) low material and sample consumption, (c) relatively short analysis, (d) low instrument and operational costs and (e) tolerance of complex matrices which can be processed without extensive pretreatment. Various published reviews cover different aspects of the inorganic metal analysis ***(1–4)***. A complete and optimized separation of REEs in geological samples (rock, mineral, or fluids) at trace levels (μg/g or ng/g) by CE techniques is a challenging analytical problem.

An up-to-date survey of the literature is given by Timerbaev ***(4)***. A large number of complexing agents are employed for the separation and to increase the selectivity and sensitivity for inorganic metal analysis ***(1–4)***. Various organic reagents have already been examined for the CE separation of metal cations. Among these are 4-(2-pyridylazo)resorcinol, 8-hydroxyquinoline-5-sulfonic acid and various polyaminocarboxylic acids such as EDTA, CDTA and others ***(1–4)***. Inorganic ligands like chloride and cyanide are less applicable, as these require more rigid control of complexation conditions. A brief summary of various organic acids used as reagents is presented in **Table 1**. The different parameters affecting the separation of metal ions using CZE involve (a) the nature of the complexing reagent, (b) the concentration of the free ligand and (c) pH of the electrolyte.

2. Materials and Equipment

2.1. Analysis of Rare Earth Elements (Lanthanides) (16)

1. Analytes: 1000 mg/L of all lanthanides (La-Lu).
2. Sample: synthetic geochemical standards (SPV-1 and SPV-4).
3. Sample should be prepared from high-purity oxides in deionized water by mixing the analytes as given in **Tables 2** and **3**. Take 100 μL of each of these metal ions and evaporate and dilute to 500 μL and inject 20 μL of this solution to get the electropherogram.
4. CE instrument and capillary: a Quanta 4000 CE instruments (Waters, Miliford, MA) equipped with positive power supply; variable wavelength ultraviolet (UV) detection system (Waters 820 Workstation for collecting electrographic data); Millennium 2000 software; fused silica capillary (36.5 cm length × 75 μm inner diameter [ID]). The applied voltage was +30 kV. The UV detection was set at a wavelength of 214 nm using a zinc lamp. Hydrostatic injection mode was used for elevating the sample at a constant height of 10 cm for 20 s. A temperature control system was employed for fixing the working capillary column temperature.
5. CE buffer: 100 m*M* α-hydroxyisobutyric acid (HIBA) solution, further diluted to 4 m*M* HIBA; UV Cat-1 solution or electrolyte modifier (Waters) with a complexing agent solution of 4 m*M* HIBA. Adjust the pH of the solutions to 4.4 with dilute acetic acid and filter through a 0.22-μm membrane filter.

Table 2
Chemical Composition Pattern of the REE Synthetic Geochemical Standards (SPV-1 and SPV-4)

REE	Chemical symbol	SPV-1 (mg/mL)	Quantity injected	SPV-4 (mg/mL)	Quantity injected (ng)
Lanthanum	La	34.627	138.508	78.525	314.100
Cerium	Ce	69.400	277.600	141.029	564.116
Praseodymium	Pr	10.784	43.136	14.531	58.124
Neodymium	Nd	42.334	169.336	69.945	279.780
Samarium	Sm	9.882	39.528	15.695	62.780
Europium	Eu	2.720	10.880	3.524	14.096
Gadolinium	Gd	10.251	41.004	11.144	44.576
Terbium	Tb	21.840	87.360	2.345	9.380
Dysprosium	Dy	10.669	42.676	7.267	29.068
Holmium	Ho	2.387	9.548	2.000	8.000
Erbium	Er	5.706	22.824	4.934	19.736
Thulium	Tm	1.084	4.336	0.756	3.024
Ytterbium	Yb	5.420	21.680	3.708	14.832
Lutetium	Lu	1.015	4.060	0.708	2.832

Table 3
Reproducibility Tests Based on Six Injections of Standard Solution SPV-1

REE height[a]	Chemical Symbol	Quantity Injected (ng)	Migration Time[a] (%)	Peak area[a] (%)	Peak (%)
Lanthanum	La	138.508	0.12	0.30	0.18
Cerium	Ce	277.600	0.15	0.15	0.21
Praseodymium	Pr	43.136	0.12	0.88	0.93
Neodymium	Nd	169.336	0.10	0.17	0.74
Samarium	Sm	39.528	0.07	1.77	1.20
Europium	*Eu*	10.880	0.14	4.61	2.77
Gadolinium	*Gd*	41.004	0.06	2.63	2.81
Terbium	Tb	87.360	0.10	2.64	1.61
Dysprosium	Dy	42.676	0.11	1.54	0.48
Holmium	Ho	9.548	0.09	3.23	3.93
Erbium	Er	22.824	0.14	1.30	1.38
Thulium	Tm	4.336	0.18	9.30	5.36
Ytterbium	Yb	21.680	0.24	2.12	1.52
Lutetium	Lu	4.060	0.30	4.73	7.48

[a] The numbers refer to the relative standard deviation (RSD) values expressed in %.

2.2. Analysis of Alkali and Alkaline Earth Metal Ion (17)

1. Analytes: K, Na, Ba, Li, Sr, Mg and Ca 1000 μg/mL. Dilute these solutions as desired in the ppm range.
2. Sample: river water, urine and a solid sample of calcium carbonate.
3. Sample preparation: dilute the water and urine samples with deionized water and then mix with buffer to ensure that the differences in ionic strength, conductivity and pH between samples and running buffer are negligible and peak heights are in the linear range of the calibration curve. Weigh 0.15 g calcium carbonate and add a few drops of the deionized water to it. Add perchloric acid (60%) (*see* **Note 1**) until calcium carbonate is completely dissolved. Transfer the sample into a 10-mL volumetric flask and dilute with water as desired.
4. CE instrument and capillary: CE system equipped with a positive power supply (Spellman, Plainview, NY); linear UV-VIS 200 detector (linear Instruments Corp., Reno, NV); polyimide–coated fused silica capillaries 39.5 cm long, ID 75 μm.
5. CE buffer: EDTA disodium salt (EDTA) 0.8 m*M* as the complexing agent and 10 m*M* pyridine as carrier electrolyte and background absorber for indirect UV detection.

2.3. Multi-Element Separation and Detection of Metal Ions by Capillary Electrophoresis Using Precapillary Complexation (18)

1. Analytes: Ag(I), Al(III), Ba(II), Bi(III), Ca(II), Cd(II), Ce(II), Cu(II), Co(II), Cr(III), Fe(II), Fe(III), Hg(II), La(III), Mg(II), Mn(II), Mo(V), Ni(II), Pb(II), Pd(II), Sb(III), Sn(IV), Sr(II), Tl(I), U(VI), V(IV), V(V), W(VI), Zn(II), Zr(IV).
2. Sample preparation: 5×10^{-3} *M* solution of metals in 20 m*M* sodium borate.
3. CE instrument and capillary: Waters Quanta 4000 CE system (Millipore Waters, Miliford, MA) equipped with negative power supply; polyimide-coated fused-silica capillaries (Polymicro Technology, Phoenix, AZ) 50 cm in length with a 75-μm ID. Condition the new capillaries by rinsing with 0.1 *M* NaOH for 1 min, followed by a 20-min rinse with water. Then rinse with 0.005 *M* NaOH and then with water to wash the capillary between runs with different electrolyte solutions. Also, purge the capillary with electrolyte solution for 2 min before each run.
4. CE buffer: for the metal complexes, add 5×10^{-3} *M* solution of reagent in 0.01 *M* sodium tetraborate to give 1×10^{-3} *M* CDTA solution and to give a 2.5-fold molar excess in the final solution in 5% ethylene glycol.

2.4. Determination of Pd(II) as a Chloro Complex in the Presence of Rhodium(III), Ruthenium(III), Osmium(VI) and Iridium(III) (19)

1. Analytes: Pd(II), Rh(III), Ru(III), Os(VI) and Ir(III).
2. Sample: *see* **Note 2**.
3. Sample preparation:

   a. Palladium(II) stock solution (1.0 mg/mL) (dissolve 0.1 g of the Pd metal in aqua-regia, fume the solution to dryness with hydrochloric acid and dilute to

100 mL with 1 *M* hydrochloric acid). Further dilute the standard stock solution to 10.00 μg/mL Pd with deionized water. Further dilute the solutions to have a 200-fold stoichiometric excess of Cl^- so that there is complete formation of Pd(II) chloro complex.

b. Prepare Rh(III), Ru(III), Os(III) and Ir(III) stock solution (100 μg/mL) from $(NH_4)_2 \cdot OsCl_6$ in the presence of 5.0 g of ascorbic acid as reducing agent for dissolution, $(NH_4)_2.Rh(H_2O)Cl_5$, $(NH_4)_2Ru(H_2O)Cl_5$ and $(NH_4)_3IrCl_6.H_2O$ by dissolving these 20 mL of 6 *M* HCl and finally diluting to 100 mL with deionized water.

4. CE instrument and capillary: Waters Quanta 4000 CE system (Millipore Waters, Milford, MA) equipped with negative power supply. UV detector with Zn lamp and 214-nm optical filter. Waters AccSep fused silica capillaries (52.2 cm × 75 μm ID).
5. CE buffer: prepare carrier electrolyte of 50 m*M* HCl-KCl (50 m*M* Cl^-; pH: 3.0) containing 0.2 m*M* cetyltrimethylammonium bromide (CTAB) by mixing 50 m*M* HCl containing 0.2 m*M* CTAB. Adjust the pH of the solution with the addition of KOH solution to get the desired pH. Degas the electrolyte and filter through a 0.45-μm membrane prior to use.

2.5. Determination of Cr(III), Fe(III), Cu(II) and Pb(II) (20)

1. Analytes: use 1000 mg/L $CrCl_3$, $FeCl_3$, $CuCl_2$ and $Pb(NO_3)_2$; $ZnCl_2$ and $AlCl_3$; and EDTA (solid) to prepare dilute metal-chelate solutions.
2. Sample: waste water from tanning industry.
3. Sample preparation: transfer a suitable volume of the unknown sample into a 100-mL Erlenmeyer flask and adjust the pH of the solution to 5.5 by adding 15 mL of 0.1 *M* acetate buffer; then, add 0.2 g of EDTA and boil the mixture for 10 min. A violet-colored $[Cr\text{-}EDTA]^-$ complex will form—dilute this with 0.1 *M* acetate buffer. Filter the solution through a 0.45-μm filter. Degas and inject directly into the CZE system.
4. CE instrument and capillary: analyte ISCO (Lincoln, NE) Model 3850 integrated CE system equipped with high voltage (up to 30 kV) and reversible polarity. Sample injection can be done by applying a 3.4-kPa vacuum at the detector end of the capillary. Perform the separation with unmodified fused silica capillary column of length 46.5 cm (30.5 cm to the UV detector) and 80 cm (60 cm to the UV detector) with 50 μm ID.
5. CE buffer: Prepare standard stock solution of 0.2 M sodium acetate and acetic acid and dilute it as desired with Millipore Milli-Q water (18 MΩ). Filter all the solutions through a 0.45 μm membrane filter and degas by ultrasound.

2.6. Determination of Cu, Fe Zn, Co and Ni using 4-(2-pyridylazo)resorcinol (21)

1. Analytes: prepare a stock solution of (Co^{2+}, Fe^{3+}, Cu^{2+}) from nitrates and (Ni^{2+} and Zn^{2+}) from sulfates with pH value 1.0. Prepare stock solution of 4-(2-pyridylazo)resorcinol (PAR) (Aldrich) of pH 8.5.

2. Sample: tea
3. Sample preparation: weigh 1.0 g of tea sample into a 200-mL beaker and add 50 mL HNO_3. After 10 min of reaction, place the tea sample on a hot plate and evaporate to dryness. Cool the tea sample, add 25 mL HNO_3 and 5 mL $HClO_4$ and heat again to dryness. Transfer the residue into a 100-mL calibrated flask and dilute to volume with water. Prepare a reagent blank by following the same procedure as discussed above.
4. CE instrument and capillary: a CE-L1 CE system (CE Resources Pvt. Ltd., Singapore) with a SPD-10A UV-vis detector of Shimadzu Co. (Kyoto, Japan) (detection made at 505 nm; fused silica capillaries (50 μm ID) of 80 cm length and effective length from the injection end to the detection window 66 cm (from Polymicro Technologies Phoenix, AZ).
5. CE buffer: the separation electrolyte consists of *N*-tris[hydroxymethyl]methyl-3 aminopropanesulfonic acid (TAPS) (Sigma) and it is mixed with PAR and ion additive to a final concentration of 10 m*M* for TAPS, 0.1 m*M* for PAR. Adjust the pH value to 8.5 with NaOH. Use only analytical reagent-grade chemicals and 18 MΩ water for the experiments.

2.7. Determination of Uranium(VI) and Transition Metal Ions With 4-(2- thiazolylazo)resorcinol (22)

1. Analytes: prepare dilute solutions of cobalt, copper, cadmium, nickel, titanium and uranium from their stock solutions in water. Prepare the metal complex by reacting the appropriate metal ion with 1 m*M* 4-(2- thiazolylazo)resorcinol (TAR) solution and use NaOH or HCl to adjust the pH to 8.3.
2. Sample preparation: filter the solutions through a 2-μm membrane filter and keep them for 5 min before injecting.
3. CE instrument and capillary: BioFocus 3000 CE system (Bio-Rad, Hercules, CA) equipped with a 72 cm effective length × 50 μm ID fused silica capillary (Alltech, Deerfield, IL). Inject the samples hydrostatically into the capillary for 2 s and perform the separation in the normal polarity mode at +25 kV. Perform the detection at the cathodic end with a photo-diode array detector functioning in either the single wavelength (530 nm) or scanning mode (370–600 nm).
4. CE buffer: the carrier electrolyte consists of 5×10^{-3} stock solution of TAR in 15 m*M* NaH_2PO_4-$Na_2B_4O_7$ buffer, pH 8.3.

2.8. Determination of Na^+, K^+, Mg^{2+} and Ca^{2+} by Indirect Detection (23)

1. Analytes: prepare standard stock solution of Na^+, K^+, Mg^{2+} and Ca^{2+} and further dilute as desired.
2. Sample: sea water from Drøbak from a depth of 40 m and the formation water from a oil company. A certified reference material is BCR CRM 399 (Brussels, Belgium).
3. Sample preparation: dilute the samples to 1:1000 with distilled water.

4. CE instrument and capillary: Waters Quanta 4000 capillary electroporesis system, equipped with a positive power supply and fused-silica capillary (60 cm total length, 75 μm ID). The distance from the point of sample introduction to the detector window is 52 cm. Indirect UV detection is at 185 and 254 nm with a mercury lamp and optical filters. Use polyethylene vials as containers for the carrier electrolyte and for all the standards and samples.
5. CE buffer: the running electrolyte consists of 6.5 m*M* HIBA (Fluka, puriss), 5.0 m*M* UV CAT-1 (4-methylbenzylamine), 6.2 m*M* 18-crown-6 (1,4,7,10,13,16-hexaoxacyclooctadecane; Merck) and 25% (v/v) methanol. Maintain the pH of the solution at 4.8.

3. Methods

The methods described here in outline the methods for the analysis of lanthandes, alkali metal ions and some transition metal ions using CE. This method involves the complexation with the carrier electrolytes HIBA, EDTA and CDTA. The developed reported methods involve very good separation of all the elements with a wide range of applications. Any of the particular metal ions can be analyzed by these methods.

3.1. Analysis of Rare Earth Elements Lanthanides

1. Flush the capillary with deionized water and with working electrolyte for 10 min.
2. Use the hydrostatic mode for injecting the sample in to the capillary. Immerse the capillary in the sample at a height of 10 cm above the running electrolyte level for 20 s.
3. Lower the capillary into the electrolyte and apply the voltage of +30 kV.
4. **Fig. 1** presents an electropherogram showing partial separation of the REEs at 25 °C. These separations are possible in less than 2 min (~1.6), a considerably reduced analysis time. La, Ce, Pr, Nd, Sm, Tb, Dy and Er are baseline-separated. These elements can be easily detected, as they easily show optimal peak shape. The following problems were observed: (1) the co-elution of Eu and Gd, (2) tailing problem in the Ho and Yb peaks and (3) a poor sensitivity of the Tm and Lu peaks. The linearity response of the individual lanthanides are given in **Table 4**.
5. **Fig. 2** shows the separation of the lanthanides using lactic and 4-methyl-benzylamine at pH 4.3. Europium is not resolved in the REEs standard mixture.
6. Temperature plays an important role in the separation of the lanthanides. For this study, the separations were performed at 35 °C and at 15 °C. The separation at 35 °C did not involve the resolution of Eu and Gd **(Fig. 3)**, whereas these are completely resolved at 15 °C. A slightly longer time (~1.6 min) is required for the efficient separation of Eu and Gd at 15 °C.

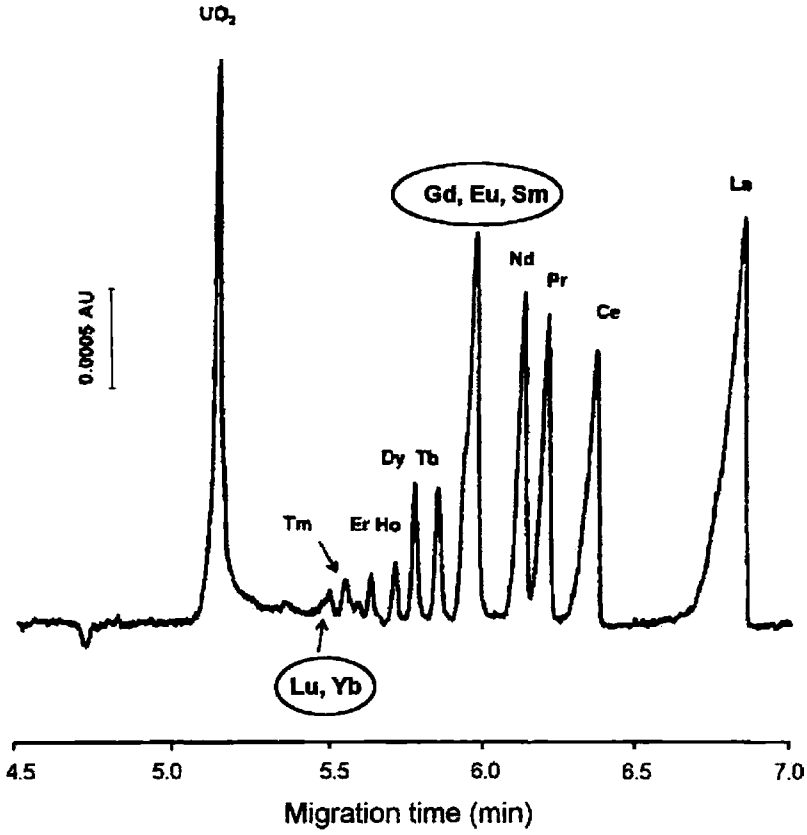


Fig. 1. Electropherogram of a typical separation pattern of 14 lanthanides. Background electrolyte 0.025 m*M* All in 15 m*M* citric acid and 20 m*M* Tris (pH 4.3); temperature 25 °C; separation voltage, −30 kV (30 μA); injection of a standard solution containing 10 μ*M* of each metal [except 20 m*M* for Tm(III), Yb(III) and Lu(III)] in 10 m*M* HNO_3. (From **ref. *16***.)

3.2. Analysis of Alkali and Alkaline Earth Metal Ion

1. Place the sample solution in the sample vial.
2. Use 0.8 m*M* EDTA solution containing 10 m*M* pyridine solution as running electrolyte.
3. Inject the sample solution by hydrostatic injection for 15 s with 4.0 cm height difference.
4. Repeat the injections and prepare the calibration curve upto 1.00 μg/mL. **Fig. 4** indicates the standard capillary electropherogram for the determination of alkali and alkaline earth metal ions.

Table 4
Linearity of Response for the Individual REEs by CE (Inferred From Calibration Curves With Four Data Points)

REE coefficients	Chemical Symbol	Quantity injected min–max (ng)	Correlation
Lanthanum	La	0–415.5	0.9994
Cerium	Ce	0–832.8	0.9998
Praseodymium	Pr	0–129.4	0.9998
Neodymium	Nd	0–508.0	0.9998
Samarium	Sm	0–118.5	0.9972
Europium	*Eu*	0–32.6	0.9985
Gadolinium	*Gd*	0–123.0	0.9951
Terbium	Tb	0–262.1	0.9994
Dysprosium	Dy	0–128.0	0.9969
Holmium	Ho	0–28.6	0.9946
Erbium	Er	0–68.5	0.9996
Thulium	Tm	0–13.0	0.8840
Ytterbium	Yb	0–65.0	0.9971
Lutetium	Lu	0–12.2	0.6561

5. Apply the method for the determination of magnesium in calcium carbonate sample, river water and urine. **Fig. 5** shows the determination of magnesium in real samples.

3.3. Multi-Element Separation and Detection of Metal Ions by Capillary Zone Electrophoresis Using Precapillary Complexation

1. Prepare the electrolyte solution containing 20 m*M* sodium borate and 5% ethylene glycol.
2. Inject the solution of the metal ions in to the capillary by hydrostatic injection at at 100 mm for 20 s.
3. Apply 12.5 kV and record the capillary electropherogram.
4. Separation of the metal complexes with nonmodified borate electrolyte is shown in **Fig. 5**. The carrier electrolyte consists of 10 m*M* sodium borate containing 1 mM CDTA (pH 9.0).
5. A standard capillary electropherogram is shown in **Fig. 6**. The separation of 23 cations is reported under these conditions.
6. The detection limits as reported (three times the signal to noise ratio) range from $1\times10^{-7}\,M$ (Fe(III) to 4×10^{-6} M (Ca(II), Hg(II) and on average are $10^{-6}\,M$.

3.4. Determination of Pd(II) as a Chloro Complex in the Presence of Rhodium(III), Ruthenium(III), Osmium(III) and Iridium(III)

1. Purge the electrolyte prior to injection of the samples for 3 min by employing a vacuum of 12–15 psi at the receiving electrolyte vial.
2. Inject the samples by gravity at the cathode.
3. Place the detector at 7.25 cm from the receiving electrolyte.
4. Determine the electroosmotic flow (μ_{eo}) from the migration time of formamide.
5. $PdCl_4^{2-}$ can be separated **(Fig. 7)** in the presence of 20 ppm of Ir(III), Os(III), Rh(III) and Ru(III), 100 ppm of Cu(II), Ni(II), Fe(II) and Co(II) and a large amount of Cl^-. The cations Cu(II), Ni(II), Fe(II) and Co(II) do not influence the determination of Pd because they travel in the opposite direction to the cathode and therefore the peaks; as a result, Cu(II), Ni(II), Fe(II) and Co(II) do not appear in the chromatogram.

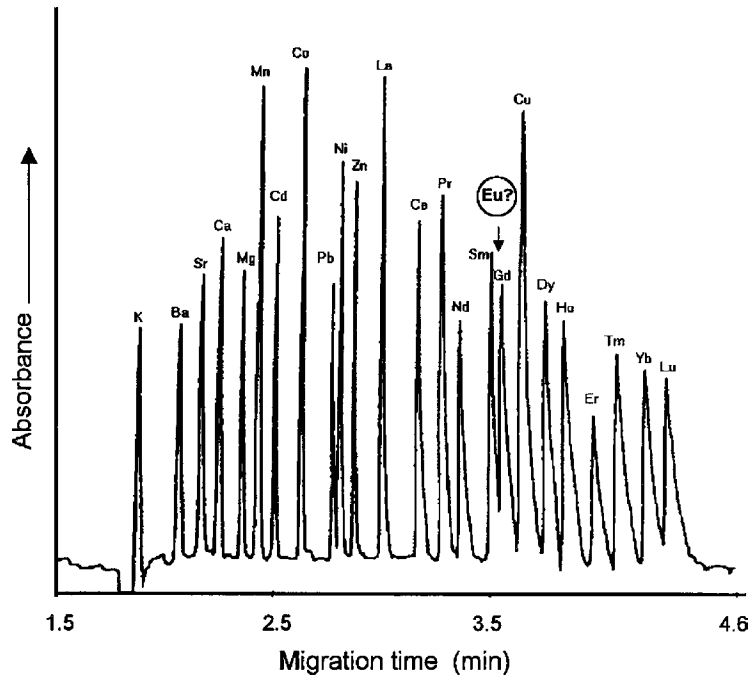


Fig. 2. **(A)** Separation of some cations and lanthanide elements by co-EQF capillary electrophoresis with indirect spectrophotometric detection. The electrolyte was 15 m*M* lactic acid and 10 m*M* 4-methylbenzylamine at pH 4.3. Europium was not included in the REE standard mixture. (From **ref. *16***.) **(B)** Electropherogram of typical separation pattern of 14 lanthanides. Background electrolyte, 4 m*M* HIBA and 10 m*M* UV Cat-1 (pH 4.4 with acetic acid); temperature 15 °C; separation voltage +30 kV; injection of SPV-1 standard solution. (From **ref. *16***.)

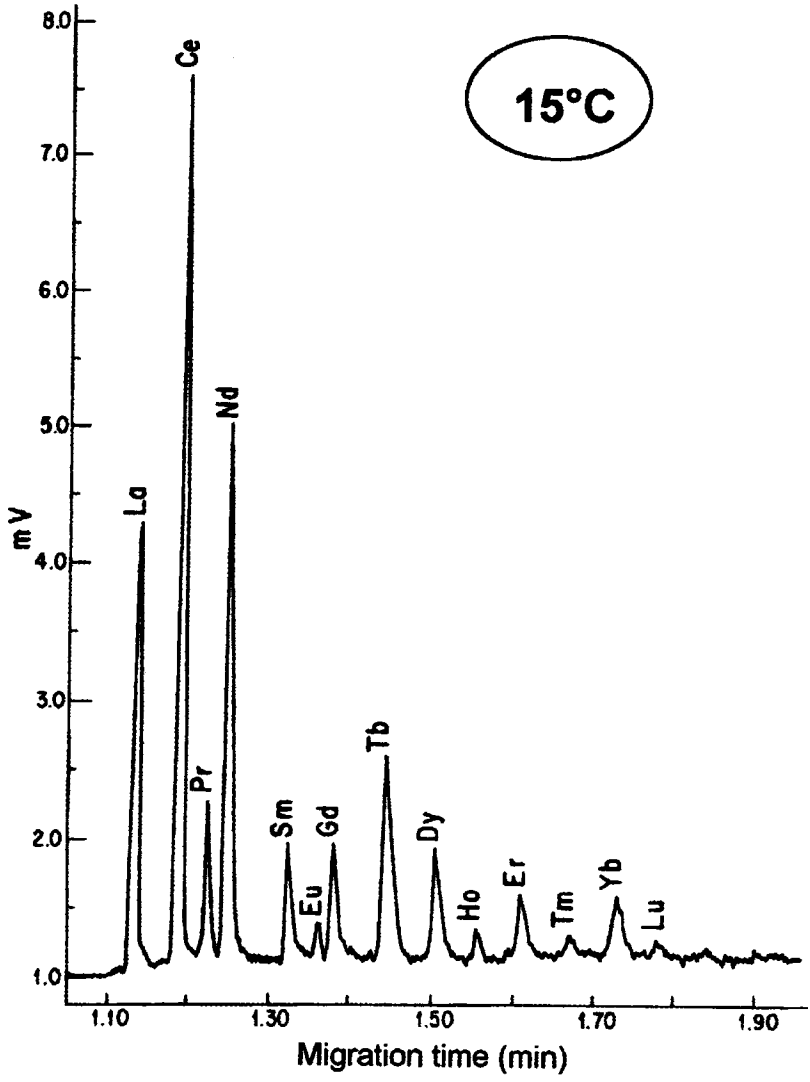


Fig. 2. ***(Continued)***

6. The detection limit for $PdCl_4^{2-}$ is 20 ppb for 50 m*M* KCl-HCl carrier electrolyte containing 0.2 m*M* CTAB.

3.5. Analysis of Cr(III), Fe(III), Cu(II) and Pb(II)

1. Rinse the capillary with deionised water for several hours.
2. Equilibrate the capillary with carrier solution for 40 min before the first run.

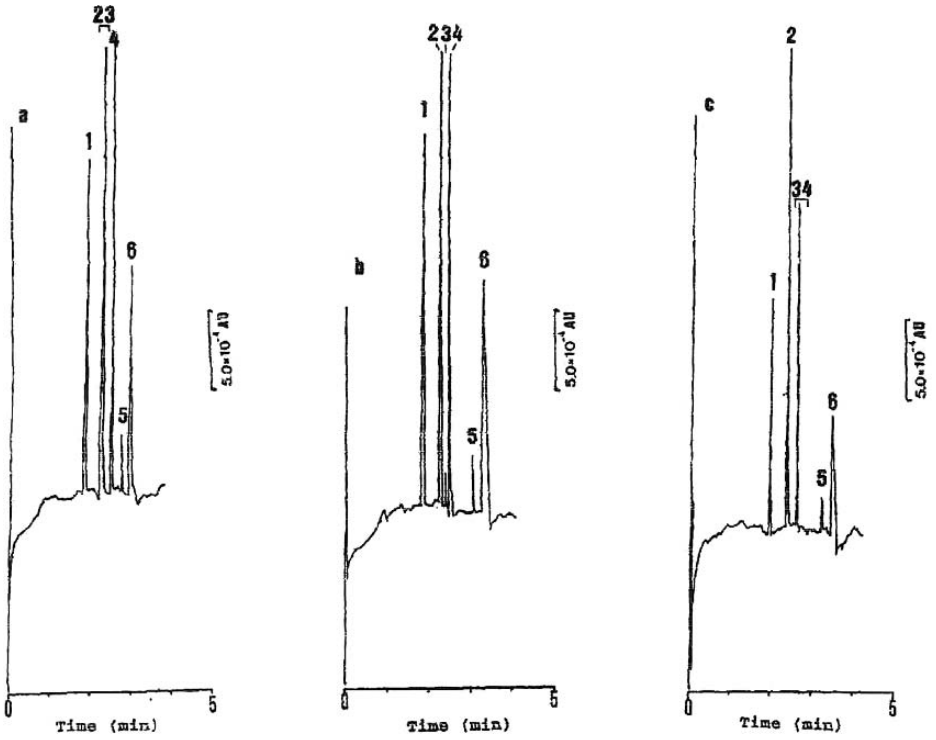


Fig. 3. Effect of concentration of EDTA on the separation of metal ions. Conditions: $L_{total} = 39.5$ cm, $L_{effective} = 30.0$ cm, pH = 5.0; 10 m*M* pyridine; hydrostatic injection for 15 s with 4.0 cm height difference **(a)** 0.6 m*M* EDTA; **(b)** 0.8 m*M* EDTA; **(c)** 1.0 m*M* EDTA. Peaks 1 = K, 2 = Na, 3 = Ba, 4 = Li, 5 = Sr, 6 = Mg and 7 = Ca. Sample concentration: K, Na, Ba, Li, Sr, Mg and Ca 1 μg/mL each in deionized water. (From **ref. *17***.)

3. Fill the capillary with carrier solution using a syringe purge.
4. Dip both ends into two separate beakers filled with the same carrier solution.
5. Introduce the sample through cathodic or anodic end of the capillary by vacuum injection.
6. Apply a high voltage of −30kV.
7. **Fig. 8** shows the separation of Cr(III), Fe(III), Cu(II) and Pb(II) as EDTA complexes.
8. Prepare the standard calibration curve for these ions and carry out the analysis.
9. The detection limit of the metal complexes is in the range of 6–27 μ*M*.
10. Apply the same procedure for the analysis of Cr(III) in waste water from tanning industry. **Fig. 9** indicates the capillary electropherogram of waste water from tannery effluent.

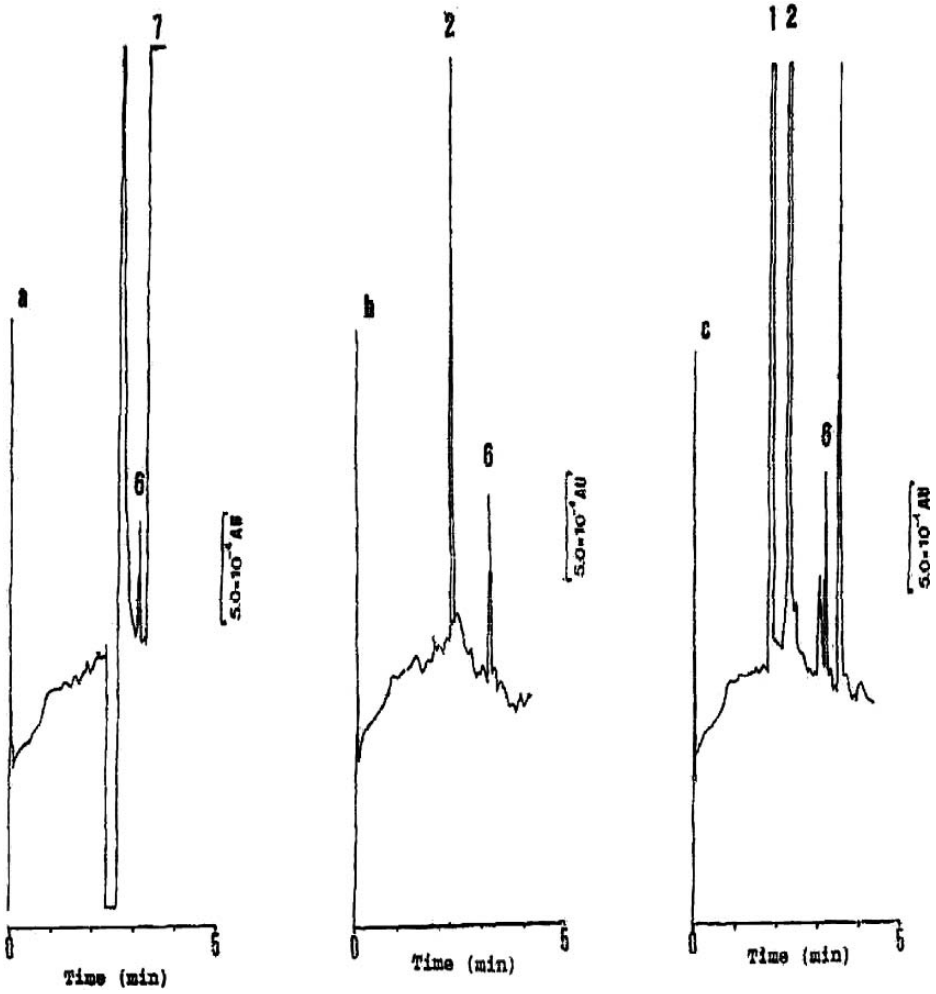


Fig. 4. Electropherograms obtained with some real samples **(a)** calcium carbonate sample **(b)** river water **(c)** urine. Other conditions and peak identifications are the same as those in Fig. 5. (From **ref.** ***17***.)

3.6. Determination of Cu, Fe, Zn, Co and Ni Using PAR

1. Rinse the capillary with 1 *M* NaOH for 15 min, followed by a rinse with water for 15 min and a 15-min rinse with appropriate electrolyte solution.
2. Repeat the rinsing procedures after every 10 runs.
3. Prepare the separation electrolytes daily.
4. Prepare the PAR metal chelate complexes by mixing with 1 m*M* PAR and adjust the pH to 9.2 for better stability of the complexes.

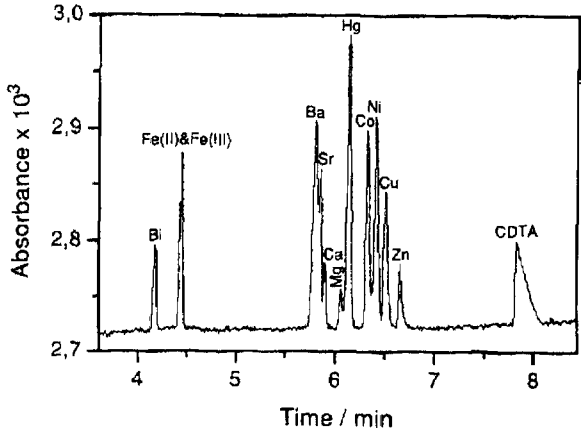


Fig. 5. Separation of metal complexes with nonmodified borate electrolyte. Carrier electrolyte sodium borate: containing 1 m*M* CDTA (pH 9.0). Metal ion concentration: 5×10^{-5} *M* Fe(II), Fe(III) and 1.0×10^{-4} *M* other metals. (From **ref.** ***18***.)

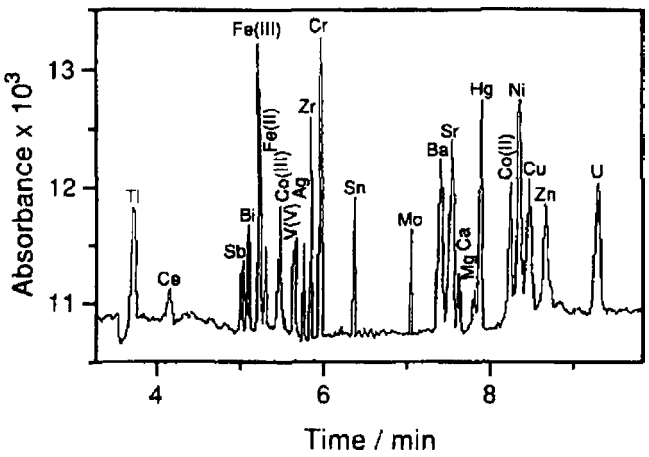


Fig. 6. Separation of metal–CDTA complexes using ethylene glycol as an electrolyte additive. Electrolyte: 20 m*M* sodium borate, 1 m*M* CDTA and 5% ethylene glycol, voltage: 12.5 kV. (From **ref.** ***18***.)

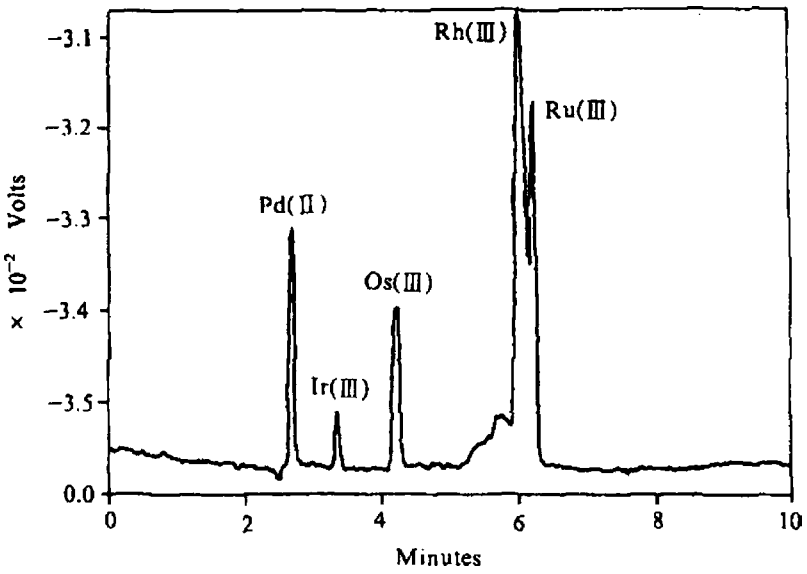


Fig. 7. Electropherogram for the determination of Pd(II) in the presence of 20 ppm each of Ir(III), Os(III), Rh(III) and Ru(III) chloride complexes and 100 ppm each of Cu(II), Ni(II), Fe(II) and Co(II). Carrier electrolyte, 50 m*M* HCl-KCl containing 0.2 m*M* CTAB at pH 3.0 applied voltage 17 kV, untreated fused-silica capillary, 52.2 cm×75 μm ID; applied voltage, 15 kV. (From **ref. *19***.)

5. Introduce the samples into the capillary by applying pressure.
6. Apply a voltage of 30 kV.
7. Prepare the standard calibration curve for the determination of these metal ions.
8. **Fig. 10** indicates the separation of Co, Cu, Fe, Zn and Ni under the optimum conditions. The detection limits calculates for Co, Cu, Fe, Zn and Ni are 17, 6, 30, 24 and 22 μg/L.
9. Apply the method for the determination of these metal ions in the tea sample. **Fig. 11** indicates the capillary electropherogram of Cui Ming green tea. The concentration of these metal ions reported for Cui Ming green tea is, for Co, Cu, Fe, Zn and Ni, 21.8, 74.0, 48.8 and 7.5 mg/kg, respectively.

3.7. Determination of Uranium(VI) and Transition Metal Ions With TAR

1. Rinse the capillary with 15 m*M* $Na_2B_4O_7$ (pH 12.0) for 30 min, followed by a 30-min rinse with deionized water.
2. Perform all the experiments at 20 °C and make all the runs in triplicate. Before each run, rinse the capillary for 1 min with 15 m*M* $Na_2B_4O_7$ (pH 12.0 buffer) followed by a 2-min rinse with deionized water and finally rinse with the run buffer for 2 min.

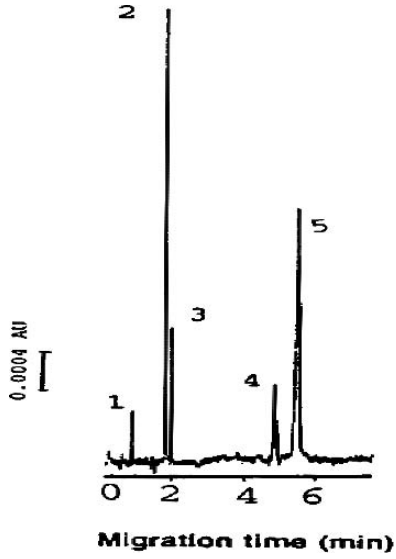


Fig. 8. Electropherogram for a standard metal solutions in excess of EDTA at −30 kV; 0.1 M acetate and 0.1 m*M* TTAB in carrier solution; 20 μg/mL of each metal ions. Peaks 1 = NO_3^-, 2 = EDTA; 3 = Cu-EDTA, Pb-EDTA, 4 = Cr-EDTA; 5 = Fe-EDTA. (From **ref. *20***.)

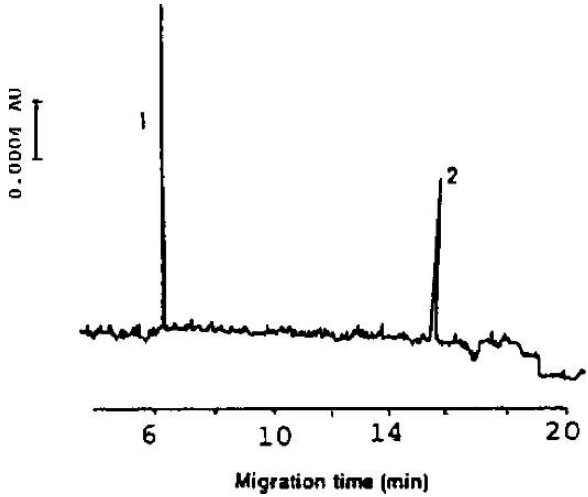


Fig. 9. Electropherogram of a tannery sample at −30 kV; 0.1 M acetate and 0.1 m*M* TTAB in carrier solution (pH 5.5). Fused silica capillary (80 cm × 50 μm ID). Sample preparation: diluted, pH 5.5 M-EDTA formed by boiling for 10 min in excess of EDTA, filtered, degassed and injected. Peaks: 1 = EDTA; 2 = Cr-EDTA, 26.14 μg/ml Cr(III) (From **ref. *20***.)

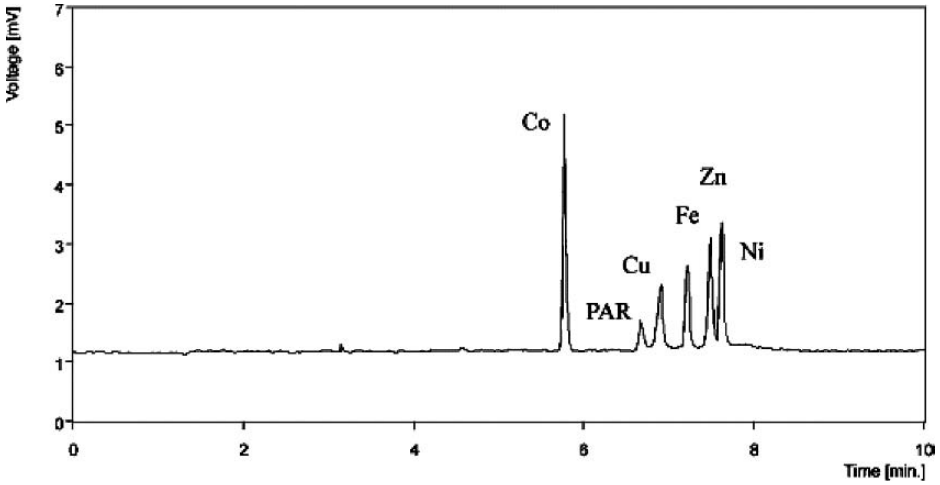


Fig. 10. Electropherogram of five metal ions under optimal conditions. The separation electrolyte, 10 m*M* TAPS, 0.1 m*M* PAR, 5 m*M* TBA, 5 m*M* TMA, pH value 8.75. Applied voltage, 30 kV. Sample introduction, pressure 10 s at 0.29 psi. (From **ref. *21***.)

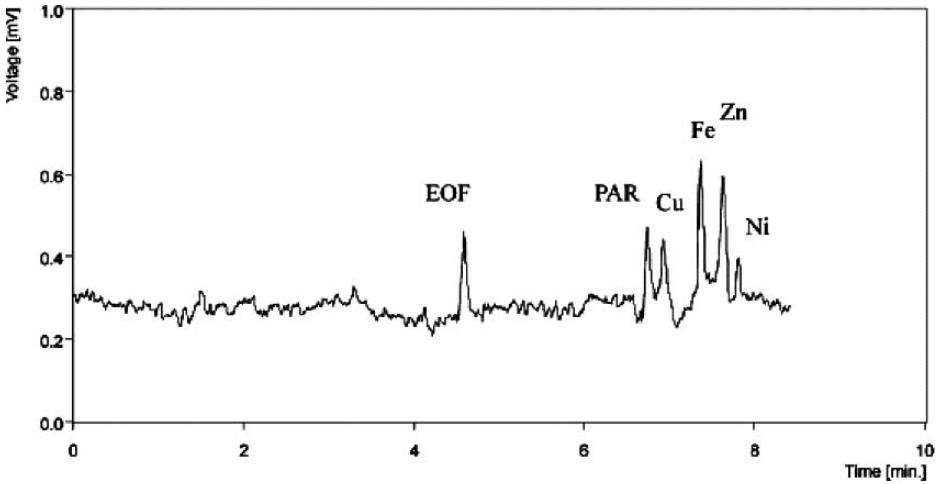


Fig. 11. Determination of metal ions in Cui Ming green tea. Running conditions were the same as Fig. 10. (From **ref. *21***.)

3. Use Rhodamine B (Lambda Physik, Bedford, MA) as the neutral marker to measure the electroosmotic flow (EOF).
4. Inject the TAR–metal complexes into the capillary and carry out the separation.

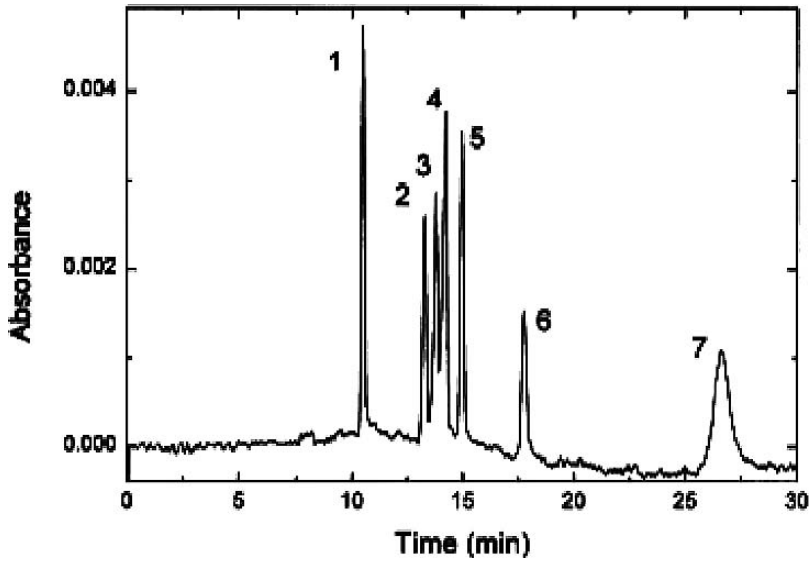


Fig. 12. Separation of TAR complexes in 15 m*M* NaH_2PO_4–$Na_2B_4O_7$, pH 8.3, 1×10^{-4} TAR (optimum conditions). 1 = cobalt (5 ppm), 2 = free TAR,3 = copper (5 ppm), 4 = cadmium (5 ppm), 5 = nickel (2.5 ppm) 6 = titanium (15 ppm) and 7 uranium (30 ppm). (From **ref. *22***.)

5. **Fig. 12** indicates the separation of metal–TAR complexes. Prepare the standard calibration curves for the determination of these metal ions.
6. The detection limits are found to be 88, 114, 59, 144, 733 and 1.7 ppm for cobalt, cadmium, nickel, copper, titanium and uranium, respectively.

3.8. Determination of Na^+, K^+, Mg^{2+} *and* Ca^{2+} *by Indirect Detection*

1. Rinse the capillary with 0.1 *M* NaOH for 15 min, followed by a rinse with water for 15 min and a 15 min rinse with appropriate electrolyte solution.
2. Filter the carrier electrolyte and sample with 0.45-μm filter prior to analysis.
3. Inject the samples into the capillary using 20 s hydrostatic injection from a height of 9.8 cm.
4. Apply a voltage of 20 kV and set the temperature at 13 °C.
5. Purge the capillary for 2.0 min between the runs.
6. Perform the indirect UV detection at 185 nm.
7. **Fig. 13** shows the standard capillary electropherogram of K^+, Ba^{+2}, Sr^{2+}, Ca^{2+}, Na^+ and Mg^{+2} and **Fig. 14** shows their separation in sea water.

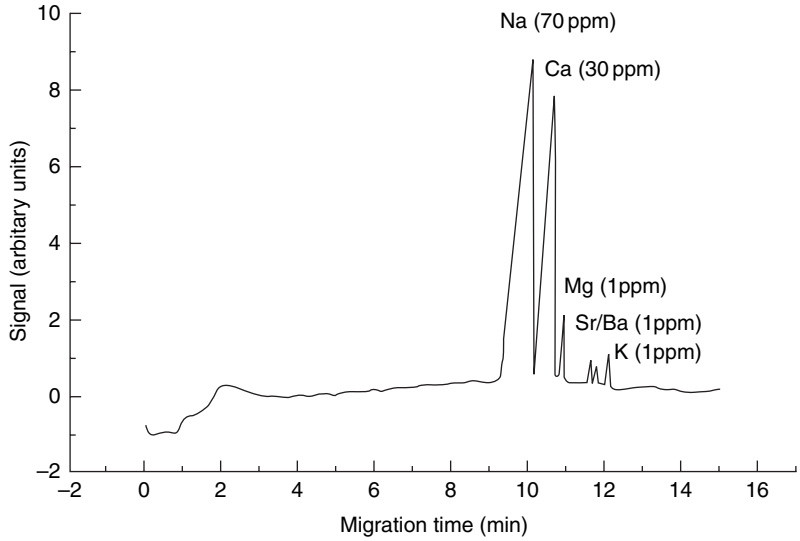


Fig. 13. Electropherogram of 70 ppm Na^+, 30 ppm Ca^{2+}, 1 ppm Mg^{2+}, Sr^{2+}, Ba^{2+} and K^+. Electrolyte: 6.5 m*M* HIBA, 5.0 m*M* UVCAT-I, 6.2 m*M* 18-crown-6 and 25.00% (v/v) methanol (From **ref. *23***.)

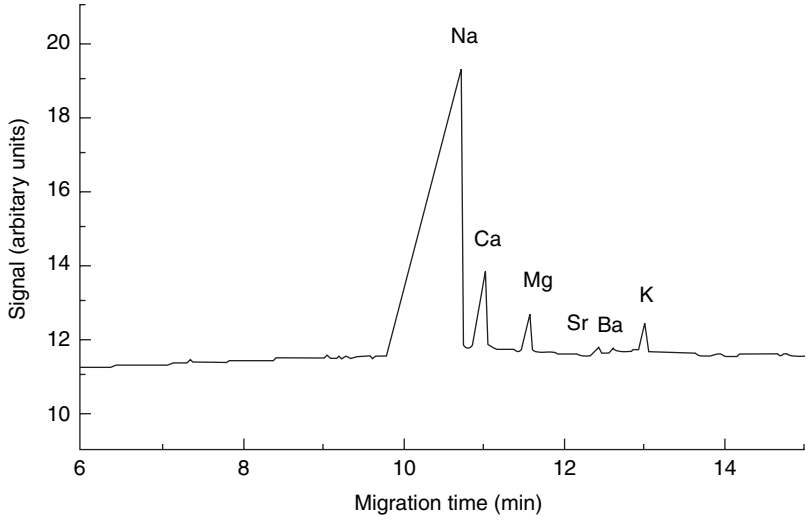


Fig. 14. Electropherogram of a mixture of seawater and formation water diluted by a factor of 125. Electrolyte: 6.5 m*M* HIBA, 5.0 m*M* UVCAT-I, 6.2 m*M* 18-crown-6 and 25.00% (v/v) methanol. (From **ref. *23***.)

4. Notes

1. In order to avoid vigorous or explosive reactions, ensure that there is no oxidizable matter in the samples before adding perchloric acid.
2. This method is recommended for the analysis of Pd(II) and Pt(II) as chloro complexes in the metal refining industry and in the control of waste water from synthetic rubber plants.

References

1. Timerbaev, A. R. (1997) Strategies for selectivity control in capillary electrophoresis of metal species. *J. Chromatogr. A*. **792,** 495–518.
2. Timerbaev, A. R. (2002) Recent advances and tends in capillary electrophoresis of inorganic ions. *Electrophoresis* **23,** 3884–3906.
3. Boyce, M. C., and Haddad, P. R. (2003) Tailoring the separation of metal complexes and organometallic compounds resolved by capillary electrophoresis using auxillary separation processes. *Electrophoresis* **24,** 2013–2022.
4. Timerbaev, A. R. (2004) Capillary electrophoresis of inorganic ions: an update. *Electrophoresis* **25,** 4008–4031.
5. Shaw, M. J., and Haddad P. R. (2004) The determination of trace metal pollutants in environmental matrices using ion chromatography. *Environ. Int*. **30,** 403–431.
6. Foret, F., Fanali S., Nardi, A., and Bocek, P. (1990) Capillary zone electrophoresis of rare earth metals with indirect UV absorbance detection. *Electrophoresis* **11,** 780–783.
7. Weston, A., Brown, P. R., Jandik, P., Jones, W. R., and Heckenberg, A. L. (1992) Optimization of detection sensitivity in the analysis of inorganic cations by capillary ion electrophoresis using indirect photometric detection. *J. Chromatogr*. **593,** 289.
8. Chen, M., and Cassidy, R. M. (1993) Separation of metal ions by capillary electrophoresis. *J. Chromatogr*. **640,** 425–431.
9. Shi, Y., and Fritz, J. S. (1993) Separation of metal ions by capillary electrophoresis with a complexing electrolyte. *J. Chromatogr*. **640,** 473–479.
10. Quang, C., and Khaledi, M. G. (1994) A Prediction and optimization of the separation of metal cations by capillary electrophoresis with indirect UV detection. *J. Chromatogr*. **659,** 459–466.
11. Shi, Y., and Fritz, J. S. (1994) New electrolyte systems for the determination of metal cations by capillary zone electrophoresis. *J. Chromatogr. A*. **671,** 429–435.
12. Lee, Y. H., and Lin, T. I. (1994) Determination of metal cations by capillary electrophoresis effect of background carrier and complexing agents. *J. Chromatogr. A*. **675,** 227–236.
13. Dabek-Zlotorzynska, E., and Dlouhy J. F. (1995) Application of capillary electrophoresis in atmospheric aerosol analysis: determination of cations. *J. Chromatogr. A*. **706,** 527–534.
14. Francois, C., Morin, Ph., and Dreux, M. (1995) Separation of transition metal cations by capillary electrophoresis optimization of complexing agent concentrations (lactic acid and 18-crown-6). *J. Chromatogr. A*. **717,** 393–408.

15. Haber, C., Jones, W. R., Soglia, J., *et al*. (1996) Conductivity detection in capillary electrophoresis—a powerful tool in ion analysis. *J. Cap. Electrophor*. **3,** 11.
16. Verma, S. P., Roberto, G., Santoyoa, E., and Apariciob, A. (2000) Improved capillary electrophoresis method for measuring rare-earth elements in synthetic geochemical standards, *J. Chromatogr. A*. **884,** 317–328.
17. Wang, T., and Li, S. F. Y. (I995) Migration behaviour of alkali and alkaline-earth metal ion-EDTA complexes and quantitative analysis of magnesium in real samples by capillary electrophoresis with indirect ultraviolet detection. *J. Chromatogr. A*. **707,** 343–353.
18. Timerbaev, A. R., Semenova, O. E., and Fritz, J. S. (1996) Advanced possibilities on multi-element separation and detection of metal ions by capillary zone electrophoresis using precapillary complexation I. Separation aspects. *J. Chromatogr. A*. **756,** 300–306.
19. Zhang, H. W., Jia, L., and Hu, Z. D. (1995) Determination of palladium(II) as a chloro complex by capillary zone electrophoresis, *J. of Chromatogr. A*. **704,** 242–246.
20. Baraj, B., Martinez, M., Sastre, A., and Manuel, A. (1995) Simultaneous determination of Cr(III), Fe(III), Cu(II) and Pb(II) as UV-absorbing EDTA complexes by capillary zone electrophoresis, *J. of Chromatogr. A*., ***695,*** 103–111.
21. Feng, H., Wang, T., Fong, S., and Li, Y. (2003) Sensitive determination of trace-metal elements in tea with capillary electrophoresis by using chelating agent 4-(2-pyridylazo) resorcinol (PAR). *Food Chem*. **81,** 607–611.
22. Evans L., and Collins, G. E. (2001) Separation of uranium (VI) and transition metal ions with 4-(2-thiazolylazo)resorcinol by capillary electrophoresis. *J. of Chromatogr. A*. **911,** 127–133.
23. Tangen, A., Lund, W., and Frederiksen, R. B. (1997) Determination of $Na^{+,}$ $K^{+,}$ Mg^{2+} and Ca^{2+} in mixtures of seawater and formation water by capillary electrophoresis *J. of Chromatogr. A*. **767,** 311–317.

3

Measurement of Low-Molecular-Weight Carboxylic Acids in Ambient Air and Vehicle Emission by Capillary Electrophoresis

Ewa Dabek-Zlotorzynska and Valbona Celo

Summary

Within the last few years, capillary electrophoresis (CE), especially with indirect ultraviolet detection, has successfully been utilized for the analysis of low-molecular-weight (LMW) organic acids in a wide variety of matrices (e.g., food, pharmaceutical, environmental, industrial, clinical). The speed, resolution, and simplicity of CE, combined with low operating costs, make the technique an attractive option for the development of improved methods in this field. Hence, CE is becoming increasingly accepted for routine analytical work. In this chapter, the unique capability and applicability of the five selected CE methods used in the analysis of LMW carboxylic acids in ambient air and/or vehicle-emitted samples are described.

Key Words: Capillary electrophoresis; low-molecular weight carboxylic acids; environmental samples; ambient air; vehicle emission.

1. Introduction

Low-molecular-weight (LMW) carboxylic acids have received considerable attention as a result of their role in environmental and biological processes. They are widely used in pharmaceutical, food and other industries. In the pharmaceutical industry, for example, they are used as antioxidants, acidifiers, and drug adsorption modifiers. Their characterization in biological fluids has been used to diagnose numerous inborn errors of metabolism. They are monitored in wastewater from sewage treatment plants, as these compounds destroy methane-producing bacteria. Numerous studies have shown that carboxylic acids are considered to be one of the dominant classes of

From: *Methods in Molecular Biology, vol. 384: Capillary Electrophoresis*
Edited by: P. Schmitt-Kopplin © Humana Press Inc., Totowa, NJ

water-soluble organic compounds found in urban and global air sheds, and hence have been a recent target of interest in the chemical characterization of the atmosphere ***(1,2)***. Thus, development of simple, inexpensive, sensitive, and rapid methods is of great importance in determining LMW carboxylic acids in various matrices. The analysis of LMW carboxylic acids is generally performed by chromatographic methods such as gas chromatography (GC), high-performance liquid chromatography (HPLC), and ion chromatography (IC). GC and HPLC methods can achieve the necessary sensitivities but typically involve time-consuming sample preparation steps such as extraction and/or derivatization. Recently, capillary electrophoresis (CE) has become an attractive alternative as a result of its greater efficiency and resolution, speed, simplicity, and economy compared to more conventional chromatographic techniques. For these reasons, CE is becoming increasingly accepted for routine analytical work, although its introduction into regulated methods might still take some time. Several reviews have been published demonstrating successful CE applications for the measurement of LMW organic acids in specific fields (e.g., food, pharmaceutical, environmental, industrial, clinical) ***(3–6)***. For example, **Table 1** provides a number of pertinent environmental applications dealing with the CE analysis of LMW organic acids in real-world samples. A number of studies have directly compared CE analysis with IC, HPLC, or GC method.

As can been seen in **Table 1**, various detection schemes were utilized to determine LMW organic acids. However, the growing use of CE for the analysis of small ions, such as LMW organic acids, many of which are ultraviolet (UV)-transparent or absorb weakly, resulting in poor detection, is in part due to a breakthrough in the use of indirect UV detection. In indirect UV detection, analytes without chromophores are detected by recording the decreases of the absorption of the sample zones, which are caused by the displacement of the chromophoric background electrolyte (BGE) ions by the sample ions. Both theoretical and practical aspects addressed by many research groups have shown that for high sensitivity and good peak shape, the matching of mobility between absorbing BGE ion (probe, carrier ion) and analyte is necessary. Thus, the proper choice of the BGE, its concentration and pH are of great importance, especially when solutes such as LMW carboxylic acids with acid-base properties are analyzed. Because indirect UV detection relies on displacement of a chromophore, the carrier ion should have a large molar absorptivity to maximize the decrease in signal. With an increasing concentration of carrier ion in the BGE, the separation efficiency for the separated ions is normally enhanced but at the same time the sensitivity is reduced. Regarding the detection sensitivity, it is held that the lower the concentration of the operational electrolyte, the higher the relative concentration of the detected

Table 1
Determination of Low-Molecular-Weight Carboxylic Acids in Environmental Samples by Capillary Electrophoresis

Matrix	Analytes	BGE	Capillary	Injection mode	Detection Mode	Detection limits	Ref.
Atmospheric aerosols	Inorganic anions, oxalic, malonic, formic, succinic, acetic	6 m*M* chromate, 2.5% Anion BT, pH 8.0	52/60 cm × 75 μm ID	Hydrostatic (10 cm, 30 s)	Indirect UV, 254 nm	88–100 μg/L	***10***,***11***
Atmospheric aerosols, vehicle exhaust	Oxalic, malonic, fumaric, formic, malic, succinic, glutaric, pimelic, phthalic, hydroxymethanesulfonic, pyruvic, suberic, acetic, glyoxylic, sebacic, propionic, hydroxybutyric, butyric/benzoic,	4 m*M* NDC, 0.2 m*M* TTAB, 14.4 m*M* Bis-Tris, pH 6.2	50/57 cm × 75 μm ID	Pressure (10 s 0.5 psi) Electrokinetic (−10 kV, 15 s)	Indirect UV, 214 nm	50–180 μg/L; 2–10 μg/L	***13***,***14***
Atmospheric aerosols, vehicular emission	Formic, glycolic, acetic, lactic, propionic, β-hydroxybutyric, butyric	10 m*M* DNB, 0.1 m*M* CTAB, pH 5.0 (adjusted with 0.1 m*M* NaOH)	50/70 cm × 50 or 75 μm ID	Hydrodynamic (5 in-Hg, 10 s)	Indirect UV, 254 nm	50–360 μg/L	***15–17***
Atmospheric aerosol particles	Oxalic, malonic, succinic, glutaric, adipic, pimelic, suberic, azelaic, sebacic	4 m*M* PDA, 0.5 m*M* TTAB, pH 11.0 (adjusted with 1.0 *M* NaOH)	58.5/50 cm × 50 μm ID	Pressure (6 s, 2 psi)	Indirect UV, 266 nm	1–8 mg/L	***18***

(Continued)

Table 1
(Continued)

Matrix	Analytes	BGE	Capillary	Injection mode	Detection Mode	Detection limits	Ref.
Ambient air (gas phase)	Acetic, propionic, butyric, valeric, capronic, oenanthic, caprylic and pelargonic acids	50 m*M* lithium borate, pH 10, 15% (v/v) methanol	79/55 cm × 75 μm ID	Hydrostatic (15 cm, 30 s)	LIF, ext. 442 nm, em. 470 nm	3–150 nM	***19***
Atmospheric aerosols	Inorganic and organic acids (malonic, citric, formic, succinic, phthalic, C_1–C_8 alkyl sulfonic acids)	4 m*M* Orange G, 0.05% HPMC, pH 7.7 (buffered with 10.0 m*M* histidine)	PEI-coated 64.5/56 cm × 50 μm ID 60/52 cm × 75 μm ID	Hydrodynamic (50 mbar, 10 s) Hydrostatic (10 cm, 40 s)	Indirect UV, 248 nm Indirect Vis, 476 nm	0.2–0.9 μM 0.2–0.8 μM	***21***
Rain water	Inorganic anions, acetic, formic	5 m*M* molybdate, 0.15 m*M* CTAH, 0.01% PVA at pH 7.9 (adjusted with 5 m*M* Tris).	65 cm × 75 μm ID	Hydrodynamic (8 cm, 20 s) Electrokinetic (−3 kV, 20 s)	Indirect UV, 230 nm	75–98 μg/L 16–20 μg/L	***22***
Rain water	Chloride, nitrate, sulphate, formic, acetic	20 m*M* MES, 20 m*M* His, pH 6.2, 0.2 m*M* CTAB;	60/50 cm × 75 μm ID	Hydrostatic (10 cm, 30 s)	CCD, 600 kHz	Not reported	***23***
Ice crystals	Inorganic anions, formic, acetic, propionic	8.5 m*M* SA, 0.001% HDB, 21 m*M*Tris, 2% methanol, pH 8.25 (adjusted with 2 m*M* NaOH)	60/66 cm × 50 μm ID	Hydrostatic (10 cm, 60 s)	Indirect UV, 232 nm	0.3–0.8 μM	***24***

Forensic environmental samples	Inorganic anions, oxalic, citric, malic, tartric, formic, acetic, propionic, butyric, valeric	3 mM SSA, 21 mM Tris; pH 8.2; flushing buffer 0.001% HDB	70/77 cm × 50 μm ID	Pressure (70 mbar or 0.5 psi, 22 s) Electrokinetic (−2 kV, 16s)	Indirect UV, 210 nm	9–82 μg/L 0.1–7 μg/L	***25***
Chlorine tap water	Monochloro-, monobromo-, dichloro-, dibromo-, bromochloro- and trichloroacetic	12 m*M* KHP, 0.5 m*M* CTAB; pH 6.0 (adjusted with NaOH)	56/64.5 cm × 75 μm ID	Pressure (40 mbar, 20 s)	Indirect UV, 254 nm	2–5 mg/L	***26***
Chlorine tap water	Monochloro-, monobromo-, dichloro-, dibromo-, bromochloro- and trichloroacetic	4 m*M* NDC, 0.5 m*M* CTAB; pH 7.5 (adjusted with NaOH)	56/64.5 cm × 75 μm ID	Pressure (40 mbar, 20 s)	Indirect UV, 235 nm	150–900 μg/L	***26***
Model standards	12 haloacetatic acids (fluoro-, chloro-, bromo-, chloro-bromo acetatic)	2 m*M* NDC, 0.2 m*M* TTAB, pH 6.2, 7.2 m*M* Bis-Tris	50/57 cm × 75 μm ID	Pressure (0.5 psi, 10 s)	Indirect UV, 214 nm	17–70 μg/L	***27***
Water	Monochloro-, monobromo-, dichloro-, bromochloro-, dibromo-, trichloro-, bromodichloro-, dibromo-, tribromoacetic	(a) 12.5 m*M* NaH_2PO_4—12.5 m*M* Na_2HPO_4, 5 m*M* HDB, pH 7.21; (b) 50 m*M* citric acid—70 m*M* LiOH, 5 m*M* HDB, pH 4.61	80.5/72 cm × 50 μm ID	Electrokinetic (−5 kV, 10 s)	Direct UV, 200 nm	0.1 mg/L level	***28***

(Continued)

Table 1
(Continued)

Matrix	Analytes	BGE	Capillary	Injection mode	Detection Mode	Detection limits	Ref.
Water	Monochloro-, monobromo-, dichloro-, bromochloro-, dibromo-, trichloro-, bromodichloro-, dibromo-, tribromoacetic	6.25 m*M* NaH_2PO_4—6.25 m*M* Na_2HPO_4, 5 m*M* DETA, pH 9.40	80.5/63.5 cm × 50 μm ID	Electrokinetic (−5 kV, 10 s)	CCD, 625 kHz	0.1 mg/L level	***28***
Model standards	Malonic, succinic, malic, glutaric	4 m*M* PMA, 4 m*M* NDS, 2 m*M* DETA, 20% methanol	100 cm × 100 μm ID	Pneumatically (~60 nL)	Electrospray MS	1–10 mg/L	***29***
Soil, plants, water	Formic, tartric, malic, citric, succinic, acetic, lactic	15 m*M* KHP, 0.5 m*M* TTAB, pH 5.6, 5% methanol (v/v)	57/50 cm × 50 μm or 75 μm ID	Electrokinetic (−5 kV, 5 s)	Indirect UV, 254 nm	0.5–6 μ*M*	***30***
Model solutions	Fumaric, citric, succinic, pyruvic, acetic and lactic	20 m*M* MES/His, pH 5.8, 0.2 m*M* TTAB	Chip	Electrokinetic (ramping from 0 to −1000 V and back to 0 V in 800 ms)	Four electrodes CCD	100 μ*M*	***31***

Model solutions	Inorganic ions and acetic, lactic, butyric	7.5 m*M* sorbic acid, 15 m*M* Arginine, 0.0007% HDOH, pH 8.9	70/57 cm × 75 μm ID 70/62.5 × 75 μm ID	Hydrostatic (10 cm, 30 s) Hydrostatic (10 cm, 30 s)	CCD, 100 kHz Indirect UV, 254 nm	10–520 μg/L 47–212 μg/L	***32***
Bayer liquor	Inorganic anions and formic, malonic, succinic and acetic	5.0 m*M* MoO_3, 1.3 m*M* CTAB, ca. 20 m*M* DEA to pH 9.2	80.0/72.3 cm × 75 μm ID	Hydrostatic (100 mm, 30 s)	Indirect UV, 214 nm	0.17–0.51 mg/L	***33***
Diamide (used in nuclear fuel reprocessing plants) degradation products	C_4 to C_{14}linear saturated carboxylic acids	0.01 *M* p-aminobenzoate, 27 m*M* TEA, pH 8.0, 70% methanol (v/v)	40.5/34.5 cm × 50 μm ID	Hydrodynamic (0.8 psi, 5 s)	Indirect UV, 264 nm	3 μ*M*	***34***

BGE, background electrolyte; NDC, 2,6-naphthalenedicarboxylic acid; TTAB, tetradecylmethylammonium bromide; CTAB, cetyltrimethylammonium bromide; PDA, 2,6-pyridinedicarboxylic acid; PEI, poly(ethylenimine), ;CTAH, cetyltrimethylammonium hydroxide; PVA, polyvinyl alcohol; MES, 2-[morphine]ethanesulfonic acid; CCD, contactless conductivity detection; SA, salicylic acid; HDB, hexadimethrine bromide; SSA, 5-sulfosalicylic acid; KHP, potassium hydrogenphthalate; DETA, diethylenetriamine; HDOH, hexadimethrine hydroxide; DEA, diethanolamine; TEA, triethanolamine.

analytes in their zones. At the same time, some disturbing effects such as noise and baseline drift are more pronounced at lower concentrations of the BGE. Also, the wavelength at which the carrier ion absorbs should be well away from any wavelength at which analytes may absorb. This is to prevent a direct UV absorbance form the analyte which will result in a counteraction of the indirect absorbance mechanism. Because the best separation of weak acids is achieved at pH values near their pKa values, this pH range provides the best conditions for the selectivity enhancement.

Usually, LMW carboxylic acids are separated in a co-electroosmotic mode. For this purpose, the direction of electroosmotic flow (EOF) has to be reversed and directed to the anode by adding an EOF modifier to the BGE. EOF modifiers commonly used for dynamic modification of the fused-silica surface are long-chain alkyl trimethylammonium salts, such as cetyltrimethylammonium bromide (CTAB), tetradecyltrimethylammonium bromide (TTAB), or hexyldiquaternary ammonium salts such as hexadimethrine bromide (HDB). Thus, the combination of anodic EOF and indirect UV detection is the most favorable for the fast and complete CE analysis of LMW carboxylic acids. In addition, the following specific factors such as buffering of BGEs, separation conditions (capillary, use voltage or current mode), conditioning and rinsing of capillaries, sample injection method (type and amount of injection), sample characteristics (solubility and matrix composition), and data analysis should be taken into account. The influence of these factors on the selection of experimental parameters of CE with indirect UV detection is overviewed in more details in specific articles ***(5,7–9)***.

This chapter is dedicated to the use of CE in the environmental field focusing on the description of methods used in the analysis of various airborne and vehicle emitted LMW organic acids ***(2,10–20)***. Emphasis is placed on describing the unique capability and applicability of the selected methods. The scope and applicability of the described methods are presented below.

1.1. Chromate-Based BGE Method (10,11)

1. This method is applicable for the simultaneous determination of inorganic anions and some organic acids using CE with chromate-based BGE and indirect UV detection (*see* **Note 1**).
2. This method provides precise measurements with the relative standard deviation (RSD) for the migration times and corrected peak area at 2 mg/L below 0.5% and 2%, respectively. The precision of this method was 5–10% at the detection limit of 100–200 μg/L (ppb).
3. This method is used to analyze organic acids (oxalate, malonate, formate, succinate, and acetate) in atmospheric aerosol samples collected by a Berner-type cascade impactor (*see* **Note 2**).

1.2. NCD-Based BGE Method (13,14)

1. This method pertains to the determination of a large number of LMW mono- and dicarboxylic acids in atmospheric aerosol and vehicle emission samples. It uses 2,6-naphthalenedicarboxylic acid (NDC) as the carrier electrolyte for indirect UV detection. (*see* **Notes 3** and **4**).
2. This method is robust as a result of buffered BGE, proper rinse steps, and constant current mode with migration time variations less than 3% RSD on a day-to-day basis, using different capillaries and performed by different analysts. Detection limits are in tens of μg/L (ppb) level using a pressure injection, which is suitable to the analysis of organic acids in vehicle emission collected on KOH-coated filters. Use of electrokinetic injection mode allows for detection at low μg/L (ppb) levels, which are relevant when analyzing LMW organic samples in atmospheric aerosols (*see* **Note 5**).
3. This method is routinely used for monitoring of LMW carboxylic acids in atmospheric aerosol and vehicle emission samples (**Figs. 1** and **2**).

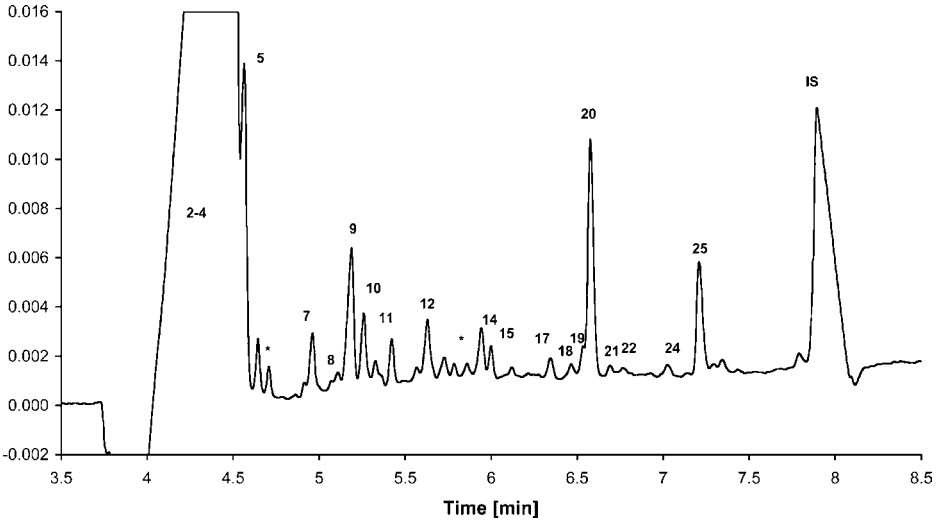


Fig. 1. A representative electropherogram of fine airborne particulate matter extract using naphthalenedicarboxylic acid (NDC)-based background electrolyte (BGE). Conditions: BGE, 4 m*M* NDC-14.5 m*M* Bis-Tris-0.2 m*M* tetradecylmethylammonium bromide (pH = 6.2); injection, electrokinetic injection (−10 kV, 10 s) with a 2-s pressure co-injection of BGE plug; separation mode, constant current at 6.6 μA; detection, indirect ultraviolet at 214 nm. Peaks: 2–4, inorganic anions; 7, malonate; 8, fumarate; 9, formate; 10, malate; 11, succinate; 12, glutarate; 14, methanesulphonate; 15, adipate; 17, pyruvate; 18, suberate; 19, glycolate; 20, acetate; 21, azeliate; 22, glyoxylate; 24, phosphate; 25, lactate. IS, internal standard (pentasulphonate); *, unidentified peaks.(Reproduced from **ref. *13***, with permission of Elsevier Science.)

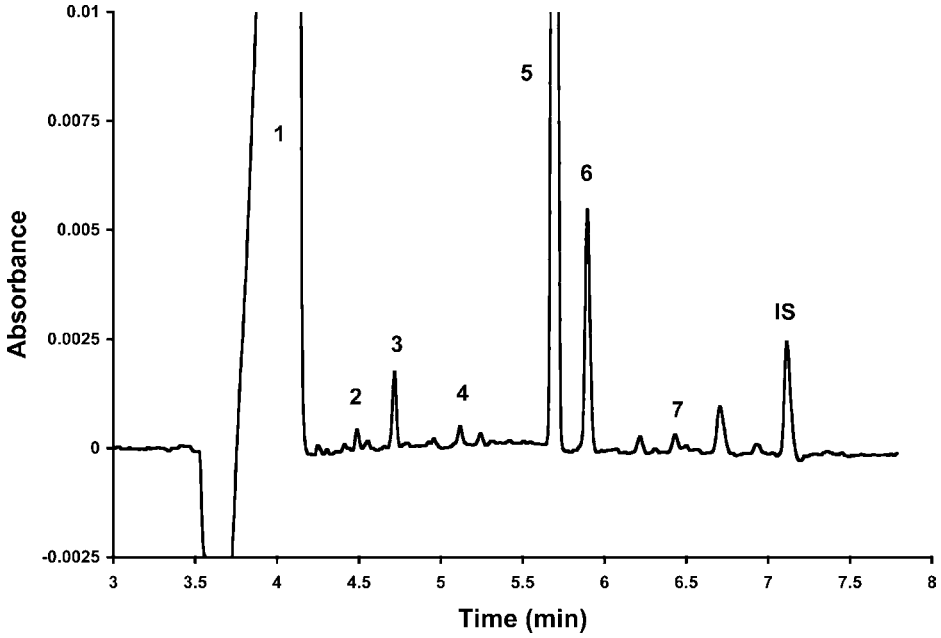


Fig. 2. A representative electropherogram of an aqueous extract of vehicle emission sample collected on a KOH-coated quartz filter using a pressure injection (0.5 psi for 10 s) with a 2-s pressure co-injection of background electrolyte plug. Peaks: 1, inorganic anions; 2, malonate; 3, formate; 4, sulfite; 5, HMSA; 6, acetate; 7, lactate. Conditions are the same as in **Fig. 1**. (Reproduced from **ref. *14***, with permission of Wiley-VCH Verlag GmbH & Co. KGaA.)

1.3. DNB-Based BGE Method (15)

1. This method is applicable for the simultaneous determination of mono- and hydroxycarboxylic acids. It uses 3,5-dinitrobenzoic acid (DNB) as the carrier electrolyte for UV indirect detection (*see* **Note 6**).
2. This method is routinely used for measuring the diurnal and nocturnal atmospheric gas and particle-phase LMW carboxylic acids (formic, acetic, pyruvic, β-hydroxybutyric, glycolic, and oxalic) in urban atmosphere at the detection limits ranged from 50 to 360 μg/L (ppb) ***(16)***.
3. This method with few modifications is also capable for the determination of major LMW organic acids in the condensed aqueous-phase vapor of vehicle exhaust **(Fig. 3)**.

1.4. PDA-Based BGE Method (18)

1. This method is applicable for the determination of C_2–C_{10} dicarboxylic acids (DCAs). It utilizes 2,6-pyridinedicarboxylic acid (PDA) as a carrier electrolyte for indirect UV detection.

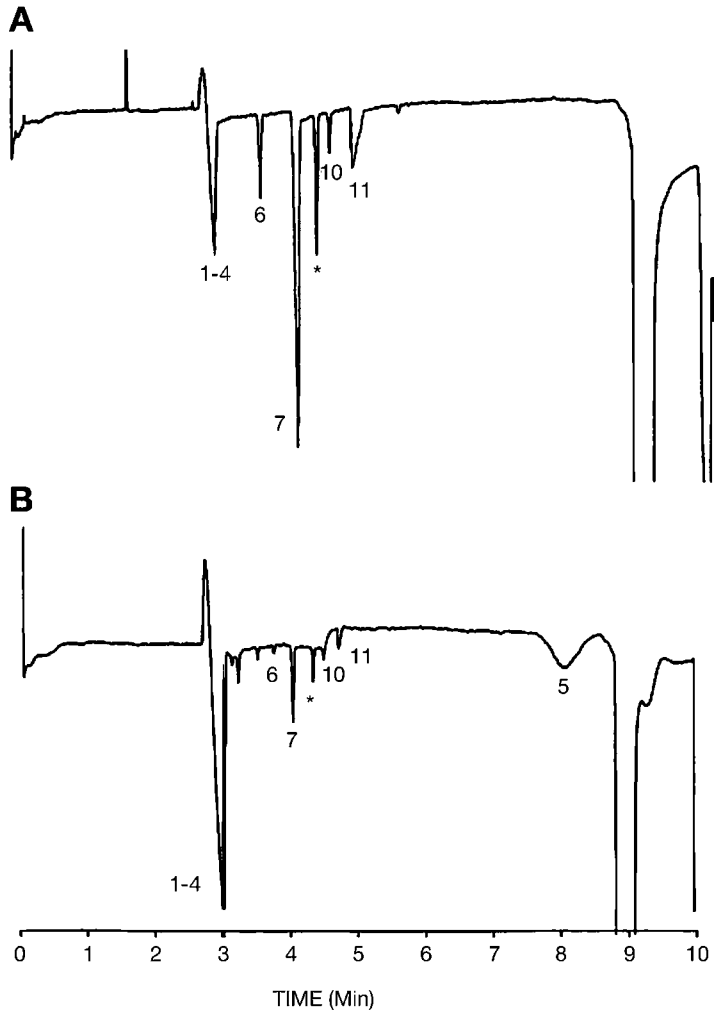


Fig. 3. Analysis of organic anions in the aqueous-phase vapor collected from the pipe tail exhaust of passenger cars without **(A)** and with **(B)** catalytic converters. Conditions: background electrolyte (BGE), 7.5 m*M* 3,5-dinitrobenzoic acid (DNB)/0.115 m*M* cetyltrimethylammonium bromide (pH 5.0); injection, 5 in-Hg pressure for 1 s; separation mode, constant voltage, −20 kV; detection, indirect ultraviolet at 254 nm. Peaks: 1–4, inorganic anions; 5, carbonate; 6, formate; 7, pyruvate; 10, lactate; 11, acetate; *- unidentified peaks. (Reproduced from **ref. *17***, with permission of Elsevier Science.)

2. This method provides precise measurements with RSDs for the migration times of DCAs below 1% for within-day and 2% to 4% for day-to-day analysis. RSDs for peak height and area were lower then 10%.
3. This method is capable for the analysis of aerosol samples at the detection limits ranged between 1 and 5 mg/L (ppm). An example of the results produced is shown in **Fig. 4**.

1.5. LIF Method (19)

1. This method is applicable for the determination of C_2–C_9 monocarboxylic acids. It uses a precapillary derivatization utilizing 4-aminofluorescein as flourophore and dicyclohexylcarbodiimide (DCC) as activating agent for laser-induced fluorescence (LIF) detection (*see* **Note 6**).

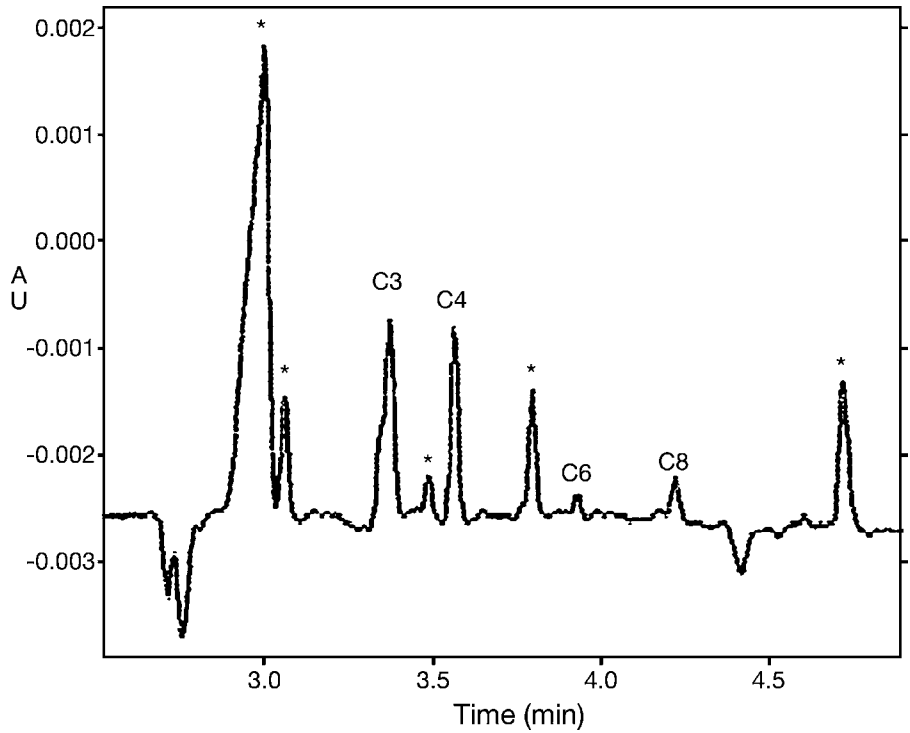


Fig. 4. A representative electropherogram of an aerosol particle sample. Conditions: background electrolyte (BGE), 4 m*M* PDA, 0.5 m*M* TTAB, pH 11.0; injection, 2 psi pressure for 6 s; separation, constant voltage at −24 kV; detection, indirect ultraviolet at 266 nm. Peaks: *unidentified peaks; C3, malonic acid; C4, succinic acid; C6, adipic acid; and C8, suberic. (Reproduced from **ref. *18***, with permission of Elsevier Science.)

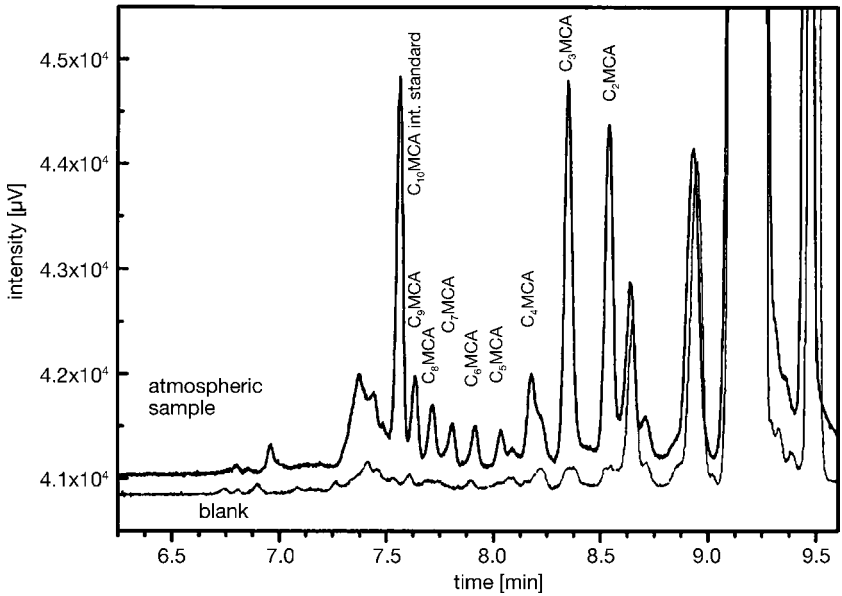


Fig. 5. Representative electropherograms of an atmospheric air sample and a reaction blank analysed by capillary electrophoresis–laser-induced fluorescence. Conditions: background electrolyte (BGE), 50 mmol/L lithium borate; pH 10.0; 15% (v/v) methanol; injection, hydrostatically at 15 cm for 30 s; separation mode, +30 kV (26 µA). Peaks: C_{10}MCA, caprinic acid; C_9MCA, pelargonic acid; C_8MCA, caprylic acid; C_7MCA, oenathic acid; C_6MCA, capronic acid; C_5MCA, valeric acid; C_4MCA, butyric acid; C_3MCA, propionic acid; C_2MCA, acetic acid. (Reproduced from **ref. *19***, with permission of Elsevier Science.)

2. This method provides precise measurements with RSDs for the migration times <1% and for the peak area between 6 and 16%.
3. This method in combination with the scrubber technique of sampling is capable for the measurements of diurnal profiles of monocarboxylic acids (C_5–C_9) in ambient air with time resolution of 1 h, and detection limits ranged from 3–150 n*M* (0.4–9.6 µg/L). A representative electropherogram is shown in **Fig. 5**.

2. Materials

2.1. Chromate-Based BGE Method (10,11)

1. Capillary: fused silica capillary (Polymicro Technologies, Phoenix, AZ); 75 µm inner diameter (ID) × 60 cm total length (52 cm to detector).
2. Capillary rinsing solution: 0.5 *M* KOH; BGE.
3. BGE: 6 m*M* chromate (pH 8.0–8.1) with 2.5 mL of Anion BT (Waters) in 100 mL (*see* **Notes 7** and **8**).

4. Samples: aerosol samples collected on glass fiber filters (Whatman, Maidstone, UK), for about 60 h, providing about 120 m^3 of air volume.

2.2. NDC-Based BGE Method (13)

1. Capillary: fused silica capillary (Polymicro Technologies, Phoenix, AZ, USA); 75 μm ID × 57 cm total length (50 cm to detector).
2. Capillary rinsing solutions: methanol; 0.5 *M* NaOH; 0.1 *M* NaOH; deionized water; BGE.
3. BGE: 4 m*M* NDC; 14.4 m*M* Bis-Tris; 0.2 m*M* TTAB (pH 6.2) (*see* **Notes 8** and **9**).
4. Standards: prepare the stock solutions of carboxylic and other acids (1000 mg/L) by dissolving appropriate amount of acids or their sodium salts in degassed water. Obtain the mixed standards by appropriate dilution of stock solutions and store them at 4 °C. Prepare all diluted standards daily from the stock standard solutions.
5. Samples: aerosol fine particles (aerodynamic diameter <2.5 μm) were collected on 47-mm Teflon filters using a Partisol air sampler at a flow rate of 16.7 L/min for 24 h. Gaseous LMW carboxylic acids in vehicle emissions were collected on KOH-coated quartz fiber filters using the air sampler at a constant flow rate of 16.7 L/min for 23 min.

2.3. DNB-Based BGE Method (15)

1. Capillary: fused silica capillary (Polymicro Technologies, Phoenix, AZ); 50 μm ID × 72 cm total length (50 cm to detector).
2. Capillary rinsing solutions: 1 *M* NaOH; deionized water; BGE
3. BGEs: (ambient air analysis): 10 m*M* DNB; 0.1 m*M* CTAB adjusted to pH 5.0 with 0.1 m*M* NaOH; (vehicle exhaust analysis): 7.5 m*M* DNB; 0.115 m*M* CTAB (pH 5.0) (*see* **Note 8**).
4. Stock standard solutions of individual analytes, prepared at 100-mg/L concentrations, can be stored in refrigerator for up to 2 mo with the exception of formic acid, which should be prepared fresh at the day of analysis because of its decomposition problems.
5. Samples: airborne particulate matter samples were collected on 47-mm diameter polytetrafluoroethylene (PTFE)-coated quartz-fiber filters (TX40H120WW, Pallflex, Puttnam, CT) at a 10 L/min flow rate for approx 12 h. Atmospheric gaseous acids were collected using gas diffusion denuders, 6 mm ID × 50 cm, coated with a solution of 5% Na_2CO_3 at 2.0 L/min air flow rate. The vehicle emission gaseous acids were collected at 1.0 L/min for 20 min using impigner flasks filled with 10 mL deionized water and cooled by ice baths.

2.4. PDA-Based BGE Method (18)

1. Capillary: fused silica capillary (Composite Metal Services, The Chase, UK); 50 μm ID × 58.5 cm total length (50 cm to detector).
2. Capillary rinsing solution: 0.1 *M* NaOH; water; BGE.

3. BGE: 4 m*M* PDA; 0.5 m*M* TTAB (pH 11.0) (*see* **Note 8**).
4. Standards: prepare the stock solutions (1000 mg/L) of each DCA separately and a mixture of all nine (9000 mg/L) by dissolving the appropriate amounts in methanol. Store these solutions at −20 °C. Just prior to use, prepare the working solutions (1 to 100 mg/L) by diluting the appropriate aliquots with methanol.
5. Samples: aerosol samples were collected on 47-mm Whatman QM-A quartz microfiber filters (Whatman, Maidstone, UK) at a flow rate of 20.5 L/min for 48–72 h.

2.5. CE-LIF Method (19)

1. Capillary: fused silica capillary (Chromatographie Service, Lanternwheel, Germany); 50 μm ID × 63 cm total length (55 cm to detector).
2. Capillary rinsing solution: not described.
3. BGE: 50 m*M* lithium borate buffer (pH 10.0) containing 15% (v/v) methanol (*see* **Notes 8** and **10**).
4. Derivatization solutions: 250 m*M* DCC in diethyl ether; 50 m*M* 4-aminofluorscein; 1 m*M* NaOH. A solution of 100 μ*M* of caprinic acid is used as internal standard during derivatization.
5. Standards: prepare carboxylic acids standards in 1 m*M* NaOH.
6. Samples: ambient atmospheric air samples were collected using a misting chamber (scrubber) containing 1 m*M* NaOH solution for 1 h, giving an air volume of approx 400 L.

3. Methods

The methods described herein outline the use of four CE techniques with indirect UV detection and one CE method with laser induced fluorescence (LIF) detection to determine LMW carboxylic acids in ambient air and/or vehicle emitted samples. Numerous useful and inexpensive strongly absorbing carrier electrolytes, including chromate ***(10,11)***, NDC ***(12–14)***, DNB ***(15–17)***, and PDA ***(18)*** have been utilized for the analysis of LMW organic acids with indirect UV detection in such matrices. CE-LIF method with precapillary derivatization was developed to analyze carboxylic acids collected in the scrubber solution (1 m*M* NaOH) ***(19)***.

3.1. Chromate-Based BGE Method (10,11)

1. This method assumes the use of a Quanta 4000 CE system (Waters, Milford, MA) equipped with a mercury lamp set at 254 nm and a capillary temperature control device maintained at 25.0 °C.
2. Capillary treatment: flush the capillary with 0.5 *M* KOH for 15 min and then with the BGE for 30–60 min prior to analysis. Between runs, purge the capillary with the BGE for 2 min.

3. To prepare the BGE solution, weigh 0.0972 g of Na_2CrO_4, add 2.5 mL Anion BT solution and dilute it to 100 mL with water (*see* **Note 7**).
4. Extract the samples in ultrasonic bath with 10 mL Mill-Q water for 30 min. Filter the extracts with Millex GV membrane filter of 0.22-μm pore size (Millipore, Bedford, MA).
5. Introduce samples into the capillary using hydrostatic injection by lifting the sample vial 10 cm above the electrolyte level for 30 s.
6. Run samples using reversed polarity and constant current mode at 25 μA (*see* **Note 11**).

3.2. NDC-Based BGE Method (13)

1. This instruction assumes the use of a P/ACE 2100 CE system (Beckman Instruments, Fullerton, CA) equipped with a mercury lamp set at 214 nm, and a capillary temperature control device maintained at 25.0 ± 0.1 °C by means of a fluorocarbon liquid being continuously circulated through the cartridge.
2. Prepare BGE as follows: for 100 mL of BGE, weigh 0.0908 g of 95% NDC in a 20-mL polystyrene disposable beaker and wet with 100 μL methanol. Add 10.0 mL of 144 m*M* Bis-Tris, transfer to a 100-mL volumetric flask via a glass funnel and dilute to approx 90 mL with deionized, degassed water (*see* **Note 12**). Sonicate flask for 20–30 min (or until solution is clear). Add 2.0 mL of 10 m*M* TTAB and make up to the mark (*see* **Note 13**). Filter solution slowly through a 0.45-μm filter and store in the refrigerator up to 1 wk.
3. Capillary treatment:

    a. New capillary: activate a new capillary by rinsing with methanol (10 min) followed by deionized water (1 min), 0.5 *M* NaOH (10 min), 0.1 *M* NaOH (5 min), deionized water (1 min), and finally with BGE solution (20 min). Electrocondition the capillary at −15 kV for 15 min.
    b. Conditioning before daily use: flush the capillary with 0.1 *M* NaOH (5 min), with deionized water (2 min), and finally with BGE for 20 min followed by electroconditioning for 15 min at −15 kV.
    c. Conditioning between runs: flush the capillary with 0.1 *M* NaOH, dip ends in water, and rinse with BGE for 2 min (*see* **Note 14**).
    d. Conditioning after daily use: rinse with 0.1 *M* NaOH for 5 min followed by deionized water for 5 min and methanol for 2 min, dip the capillary ends in water and finally reverse the direction of the rinse to dry the capillary (30 s).

4. Extract atmospheric aerosols collected on Teflon filters with 8 mL water for 30 min using a mechanical shaker and analyze them in the same day of extraction. Stabilize the extracts with 0.2% of chloroform to prevent the degradation of the organic acids.
5. Extract the vehicle exhaust samples collected on a-KOH-coated quartz fiber filters with 10 mL of deionized water in an ultrasonic bath for 30 min (*see* **Note 15**).
6. Introduce samples into the capillary by applying a pressure (0.5 psi for 10 s) or a voltage of (−10 kV for 15 s) followed by injection of BGE (0.5 psi, for 2 s).

7. Run samples using reversed polarity and a constant current mode at $6.6 \pm 0.2\,\mu A$ ($-15\,kV$) (*see* **Notes 11**, **16**, and **17**)

3.3. DNB-Based BGE Method (15)

1. This method assumes the use of a 270A-HT CE system (Perkin Elmer, Applied Biosystems Division, Foster City, CA) equipped with a variable-wavelength UV-Vis detector set at 254 nm, and a capillary temperature control device maintained at 25.0 °C or 30.0 °C.
2. Capillary treatment: condition the capillary at the beginning of the day by a flush of 1 *M* NaOH solution for 20 min followed by a flush of deionized water for 10 min and finally, a flush of BGE for 30 min. Replenish the capillary with fresh BGE by flushing for 2 min in between runs.
3. To prepare 100 mL BGE solution, dissolve 0.2121 g DNB and 0.0036 g CTAB in approx 50 mL water, adjust the pH to 5.0 with 0.1 *M* NaOH, and dilute to the mark with water (*see* **Note 8**).
4. Sample extraction: airborne particulate matter samples collected on filters are extracted with 30 mL water at room temperature in a shaker for 90 min. The extract is filtered through a 0.22-μm pore-size membrane filter (HAWP, Millipore, Bedford, MA) and after adding chloroform, stocked in a freezer until analysis; denuders are extracted with pure water and treated in the same way as filters' extracts; vehicle exhaust samples collected in impingers are transferred to 50-mL volumetric flasks and diluted with water to the mark, and filtered through 0.45-μm membrane filters (Millipore). Samples should be kept frozen until analysis.
5. Introduce samples into the capillary hydrodynamically (5 in-Hg for 10 s).
6. Run samples using reversed polarity and constant voltage mode at $-15\,kV$.

3.4. PDA-Based BGE Method (18)

1. This method assumes the use of a P/ACE MDQ CE system (Beckman-Coulter Instruments, Fullerton, CA) equipped with a photodiode array UV detector (190–400 nm) and set up at 266 nm, and a capillary temperature control device maintained at 25 °C.
2. Condition the capillary before the first use by rinsing it with 0.1 *M* NaOH, water and BGE for 15 min each. Between the runs, flush the capillary with BGE solution for 2 min (*see* **Note 18**).
3. Prepare BGE stock solution (25 m*M* PDA–3.125 m*M* TTAB) by dissolving 0.4178 g PDA and 0.1051 g TTAB in 100 mL water, and store it at +4 °C. Immediately before analysis, prepare the working BGE (4 m*M* PDA and 0.5 m*M* MTAB) by the appropriate dilution of the stock BGE. Adjust the pH to 11.0 with 1.0 *M* NaOH just before the filtration of the BGE before use.
4. Extract the analytes from the filters with 5 mL of Milli-Q water and ultrasonicate for 20 min. Extracts can be stored at +4 °C until analysis.
5. Introduce samples into the capillary by applying a pressure of 2 psi for 6 s.
6. Run samples using reversed polarity and a constant voltage at $-24\,kV$.

3.5. CE-LIF Method (19)

1. This method assumes the use of a Spectrophoresis 100 CE instrument (TSP, Egelsbach, Germany) with a KF-2 LIF detector (Sopra, Büttelborn, Germany), equipped with a He-Cd laser, 442-nm excitation (50 mW) and a 470-nm cut-off filter.
2. Derivatization procedure (*see* **Note 19**): to 1.5 mL solution of sample/standard solution adjusted at pH 2.0 using 1 *M* HCl, add 10 μL of a 100 μ*M* caprinic acid solution (IS) and 375 μL of 250 m*M* DDC in diethyl ether (0.1032 g in 2 mL). Mix the reaction phases for 10 min in a vortex mixer (6000 rpm) and then let the organic phase separated. Repeat the procedure with another 375 μL DDC. Combine two organic phases and add 10 μL of 50 m*M* 4-aminofluorscein in dimethylformamide (0.0362 g in 2 mL). Vortex the mixture at 6000 rpm at ambient temperature for 1 h. Extract the organic phase three times with 50 μL of 1 m*M* NaOH solution. Transfer a portion of resulting 150 μL sodium hydroxide solution to a sample vial.
3. Introduce samples into the capillary hydrostatically (15 cm, 30 s; 9 nL).
4. Run samples using a normal polarity and a constant voltage at +30 kV (26 μA).

4. Notes

1. The chromate-based BGEs are usually used for the analysis of high-mobility ions such as inorganic anions.
2. Concentrations of the organic anions in aerosol samples were frequently close or below the detection limit of the analytical procedure. Therefore, on-line preconcentration of these compounds (e.g., electrokinetic injection) is recommended.
3. Inorganic anions could not be separated with this BGE system as they co-migrated before the organic acids. With exception of oxalate, well defined electropherograms are obtained without interferences from matrix constituents such as sulfate, nitrate, and chloride. In addition, under these conditions, carbonate/bicarbonate, usually present in various samples, did not interfere because the pH of the BGE was lower than the pKa_1 of carbonate ($pKa_1 = 6.35$).
4. Compared to the IC, the CE method provides different selectivity with better separation efficiency allowing for example the separation of two classical co-eluted pairs of acetate/lactate and glycolate/butyrate that occurs in IC columns. Thus, both methods are complementary and able to cross-validate each other.
5. The use of electrokinetic injection increases CE sensitivity but it is matrix-dependent. Proper quantitative analysis can, however, be made by employing the internal standard (IS) procedure. Thus, the IS (pentasulfonic acid) was used in order to obtain satisfactory repeatability and accuracy of measurements. In addition, the calibration standards using electrokinetic injection were prepared in the presence of 10 mg/L of sulfate to simulate a real sample matrix.
6. The advantage of this method is its indifference against inorganic matrices such as NaOH, carbonate, chloride, etc., up to the m*M* range.
7. Anion BT (Waters) contains 10 m*M* TTAB, 10 m*M* Tris, and 5 m*M* potassium hydrogenphthalate.

8. All reagents employed are of the highest purity available. Deionized water (18 MΩ/cm) was used for the preparation of all working solutions, BGEs, and standards.
9. Bis-Tris was chosen as the buffering reagent in the BGE because the pH chosen (6.2) is closely matched to the pKa of this counterion (pKa = 6.5).
10. Lithium is used as co-ion because its mobility is 20% smaller than sodium. This lower contribution to the electrolyte conductivity results in a better separation as a result of an increase of the plate numbers.
11. Reliability of the analysis in the extracts of wide concentration range was improved by using constant current separation mode. The analysis is complete once the last anion of interest is detected.
12. In order to prepare 144 m*M* Bis-Tris, dissolve 3.0125 g of Bis-Tris in deionized, degassed water and dilute to 100 mL. Store in plastic bottles in the refrigerator (at 4 °C) for 4 mo or until exhausted.
13. In order to prepare 10 m*M* TTAB dissolve 0.1682 g of TTAB in deionized, degassed water and dilute to 50 mL slowly to avoid producing too many bubbles. Store in plastic bottles in the refrigerator (at 4 °C) until exhausted.
14. In order to keep the electrolyte level in the inlet side constant, use different vials of BGE (4mL) for rinsing. Also, use two vials of water for dipping the capillary ends to avoid cross-contamination after rinsing with 0.1 *M* NaOH.
15. Because of the high content of hydroxide ions in these extracts, these extracts should be passed through a solid phase extraction cartridge (e.g. Dionex OnGuard H) containing strong acid resin in the H^+ form.
16. For the analysis of organic acids in atmospheric aerosols collected on Teflon filters, the internal standard quantitation method with electrokinetic injection was used. The linear dynamic range was established using a minimum four-point calibration curve constructed for every target analyte.
17. For the analysis of organic acids in vehicle emission collected on KOH-coated filters the external standard quantitation method with pressure injection mode is used. An internal standard is used as a reference peak to correct sample migration time shifts. The linear dynamic range is established using a minimum four-point calibration curve constructed for every target analyte.
18. An electroconditioning step (2 min, −15 kV) between runs did not improve the repeatability significantly.
19. Use 2-mL micro test tubes (save lock vial) as reaction vials. These vials can be used for up to 1.5 mL solutions (standards or samples).

References

1. Chebbi, A. and Carlier, P. (1996) Carboxylic acids in the troposphere: occurrence, sources, and sinks: a review. *Atmos. Environ*. **30**, 4233–4249.
2. Dabek-Zlotorzynska, E. and McGrath, M. (2000) Determination of low-molecular-weight carboxylic acids in the ambient air and vehicle emissions: a review. *Fresenius J. Anal. Chem*. **367**, 507–518.

3. Klampfl, C. W., Buchberger, W., and Haddad, P. R. (2000) Determination of organic acids in food samples by capillary zone electrophoresis. *J. Chromatogr. A* **881**, 357–364.
4. Klampfl, C. W. and Buchberger, W. (1997) Determination of low-molecular-weight mass organic acids by capillary zone electrophoresis. *Trends Anal. Chem*. **16**, 221–229.
5. Dabek-Zlotorzynska, E. and Keppel-Jones, K. (2000) The analysis of low-molecular weight carboxylic acids by CE with indirect UV detection. *LCGC Int*. **18**, 950–966.
6. Galli, V., Garcia, A., Saavedra, L., and Barbas, C. (2003) Capillary electrophoresis for short-chain organic acids and inorganic anions in different samples. *Electrophoresis* **24**, 1951–1981.
7. Macka, M., Johns, C., Doble, P., and Haddad, P. R. (2001) Indirect detection in capillary electrophoresis: i. principles. *LCGC* **19**, 38–47.
8. Macka, M., Johns, C., Doble, P., and Haddad, P. R. (2001) Indirect detection in capillary electrophoresis: ii. practical rules. *LCGC* **19**, 178–188.
9. Johns, C., Macka, M., and Haddad, P. R. (2003) Enhancement of detection sensitivity for indirect photometric detection of anions and cations in capillary electrophoresis. *Electrophoresis* **24**, 2150–2167.
10. Krivacsy, Z., Molnar, A., Tarjanyi, E., et al. (1997) Investigation of inorganic ions and organic acids in atmospheric aerosol by capillary electrophoresis. *J. Chromatogr. A* **781**, 223–231.
11. Kiss, G., Gelencser, A., Krivacsy, Z., and Hlavay, J. (1997) Occurrence and determination of organic pollutants in aerosol, precipitation, and sediment samples collected at lake Balaton. *J. Chromatogr. A* **74**, 349–361.
12. Dabek-Zlotorzynska, E. and Dlouhy, J. F. (1994) Capillary zone electrophoresis with indirect UV detection of organic anions using 2,6-naphthalenedicarboxylic acid. *J. Chromatogr. A* **685**, 145–153.
13. Dabek-Zlotorzynska, E., Piechowski, M., McGrath, M., and Lai, E. P. C. (2001) Determination of low-molecular-weight carboxylic acids in atmospheric aerosol and vehicle emission samples by capillary electrophoresis. *J. Chromatogr. A* **910**, 331–345.
14. Dabek-Zlotorzynska, E., Piechowski, M., Keppel-Jones, K., and Aranda-Rodriguez, R. (2002) Determination of hydroxymethanesulfonic acid in environmental samples by capillary electrophoresis. *J. Sep. Sci*. **25**, 1123–1128.
15. Souza, S. R., Tavares, M. F. M., and Carvalho, L. R. F. (1998) Systematic approach to the separation of mono- and hydroxycarboxylic acids in environmental samples by ion chromatography and capillary electrophoresis. *J. Chromatogr. A* **796**, 335–346.
16. Souza, S. R., Vasconcellos, P. C., and Carvalho, L. R. F. (1999) Low molecular weight carboxylic acids in an urban atmosphere: winter measurements in Sao Paulo City, Brazil. *Atmos. Environ*. **33**, 2563–2574.
17. Colombara, R., Massaro, S., and Tavares, M. F. M. (1999) Exploring the versatility of capillary electrophoresis for the analysis of ionic species in vehicular emission. *Anal. Chim. Acta* **388**, 171–180.

18. Adler, H., Siren, H., Kulmala, M., and Riekkola, M. L. (2003) Capillary electrophoretic separation of dicarboxylic acids in atmospheric aerosol particle. *J. Chromatogr. A* **990**, 133–141.
19. Kibler, M. and Bachmann, K. (1999) New derivatization method for carboxylic acids in aqueous solution for analysis by capillary electrophoresis and laser-induced fluorescence detection. *J. Chromatogr. A* **836**, 325–331.
20. Nassar, A. E. F., Lucas, S. V., Myler, C. A., et al. (1998) Quantitative analysis of chemical warfare agent degradation products in reaction masses using capillary electrophoresis. *Anal. Chem*. **70**, 3598–3604.
21. Johns, C., Shaw, M. J., Macka, M. and Haddad, P. R. (2003) Sensitive indirect photometric detection of inorganic and small organic ions by capillary electrophoresis using Orange G as a probe ion. *Electrophoresis* **24**, 557–566.
22. Fung, Y. S. and Lau, K. M. (1998) Development and validation of analytical methodology using capillary electrophoresis for separation and determination of anions in rainwater. *Talanta* **45**, 641–656.
23. Fornaro, A. and Gutz, I. G. R. (2003) Wet deposition and related atmospheric chemistry in the Sao Paulo metropolis; part 2- contribution of formic and acetic acids. *Atmos. Environ*. **37**, 117–128.
24. Tenberken-Potzsch, B., Schwikowski, M., and Gagler, H. W. (2000) Analysis of size-classified ice crystals by capillary electrophoresis. *J. Chromatogr. A* **871**, 391–398.
25. Xu, X., Bryn, P. C. A., Koeijer, J. A., and Logtenberg, H. (1999) Low molecular mass anion screening for forensic environmental analysis by capillary zone electrophoresis with indirect UV detection. *J. Chromatogr. A* **830**, 439–451.
26. Martinez, D., Farre, J., Borrull, F., Calull, M., Ruana, J., and Colom, A. (1998) Capillary zone electrophoresis with indirect UV detection of haloacetic acids in water. *J. Chromatogr. A* **808**, 229–236.
27. Dabek-Zlotorzynska, E., McGrath, M., and Lai, E. P. C. (2000) Determination of haloacetic acids using capillary electrophoresis, in *Proceedings of 3*rd *International Conference on Chemical Measurement and Monitoring of the Environment, EnviroAnalysis* (Clement, R. and Burk, B., eds.) Ottawa, Canada: pp. 115–123.
28. Lopez-Avila, V., van de Goor, T., Gas, B., and Coufal, P. (2003) Separation of haloacetic acids in water by capillary zone electrophoresis with direct UV detection and contactless conductivity detection. *J. Chromatogr. A* **993**, 143–152.
29. Johnson, S. K., Houk, L. L., Johnson, D. C., and Houk, R. S. (1999) Determination of small carboxylic acids by capillary electrophoresis with electrospray- mass spectrometry. *Anal. Chim. Acta* **398**, 1–8.
30. Li, Y. H., Huang, B. X., and Shan, X. Q. (2003) Determination of low molecular weight organic acids in soil, plants and water by capillary zone electrophoresis. *Anal. Bianal. Chem*. **375**, 775–780.
31. Laugere, F., Guijt, R. M., Bastemeijer, J., et al. (2003) On-chip contactless four-electrode conductivity detection for capillary electrophoresis devices. *Anal. Chem*. **75**, 306–312.

32. Mayrhofer, K., Zemann, A. J., Schnell, E., and Bonn, G. K. (1999) Capillary electrophoresis and contactless conductivity detection of ions in narrow inner diameter capillaries. *Anal. Chem.* **71**, 3828–3833.
33. Chovancek, M., Choo, P., and Macka, M. (2004) Development of a fully buffered molybdate electrolyte for capillary electrophoresis with indirect detection and its use for analysis of anions in Bayer liquor. *Electrophoresis* **25**, 437–443.
34. Rivasseau, C. and Blank, P. (2001) Determination of C_4-C_{14} carboxylic acids by capillary zone electrophoresis. Application to the identification of diamide degradation products and partitioning studies. *J. Chromatogr. A* **920**, 345–358.

4

Determination of Aliphatic Low-Molecular-Weight and Biogenic Amines by Capillary Zone Electrophoresis

Agnes Fekete, Majlinda Lahaniatis, Jutta Lintelmann, and Philippe Schmitt-Kopplin

Summary

Low-molecular-weight (LMW) aliphatic amines play a key role in the global nitrogen cycle, are involved in nutrient transfer, and act as buffer in the ecosystem. They are widely used as intermediates in chemical synthesis and were shown to cause occupational asthma. Biogenic amines occur in all living organims and have an effect on the cell growth, although at high concentrations they can be toxic; some are used as cancer markers in health protection or as spoilage markers in foods. Their identification and quantification from different matrices such as human tissues or foods is of high importance. The electrophoretic separation of amines is possible as cations as a result of their high basicity; their detection, however, is more difficult because these amines contain no chromophor group. Indirect ultraviolet (UV) detection is the first presented possibility and widely used for the separation of nonderivatized amines. Otherwise, derivatization of the amines is nesessary to directly detect them with laser-induced fluoresence (LIF) detection. Other detection modes such as pulse amperometric, chemiluminescence, or mass spectrometry have been also used for the determination of LMW and biogenic amines, but not on a routine basis. In this chapter, three capillary electrophoretic methods with indirect UV and LIF detection for detemination of LMW aliphatic and biogenic amines are described.

Key Words: Capillary electrophoresis; biogenic amines; volatile aliphatic amines; indirect UV; derivatisation; laser induced fluoresence.

1. Introduction

Aliphatic mono-, di-, and polyamines are anthropogenic and naturally occurring compounds. Primary and secondary alkylamines such as methylamine,

From: *Methods in Molecular Biology, vol. 384: Capillary Electrophoresis*
Edited by: P. Schmitt-Kopplin © Humana Press Inc., Totowa, NJ

dimethylamine, ethylamine, diethylamine, and butylamine are important raw materials and intermediates in the chemical and pharmaceutical industry. They are also discharged into the atmosphere from cattle feeds, livestock buildings, waste incineration, sewage treatment, and automobile exhaust. In addition to the anthropogenic sources, they occur as biodegradation products of organic materials such as proteins and amino acids. Aliphatic di- and polyamines such as cadaverine, putrescine, spermidine, and spermine are formed during normal metabolic processes in living cells. They have been implicated in a variety of cell functions involving cell growth and differentiation and receptor function. They also impact DNA replication, gene expression, protein synthesis, stabilization of lipids, brain development, and nerve growth and regeneration. Overproduction or overintake of these so-called biogenic amines is toxic to the cells and facilitates cell death by oxidative mechanism or may cause headaches, nausea, hypo- or hypertension, and cardiac palpitations. Moreover, these abovementioned biogenic amines have been proposed as possible cancer markers and are used as quality indicators for raw food materials. Thus the identification and quantification of amines from different food products such as wine ***(1–4)***, cheese ***(5)***, fish ***(6–8)***, soy sauce ***(9,10)***, seafood ***(11,12)***, tobacco leaf ***(13)***, and beer ***(14,15)***; human tissues and fluids such as serum ***(16)***, urine ***(18,17)***, and tumor cells ***(18,19)***; and environmental samples such as lake water ***(20,21)***, pine needles ***(22)***, sewage water ***(23)***, and atmospheric aerosol ***(24)*** is an important and challenging task.

Gas chromatographic and high-performance liquid chromatographic methods have been widely used to analyze these amines; their direct analysis presents, however, chromatographic problems as a result of their extreme basicity and high polarity and reactivity ***(25)***. Therefore, derivatization is frequently needed, and often increases the analysis time given the lower resolution in the separation. Ion chromatography was applied for direct analysis of amines with the drawbacks of long separation time and restricted choice of mobile phases ***(26)***. Capillary electrophoresis (CE) has been used as an alternative to chromatographic methods and has been shown to exhibit a powerful capability for the analysis of amines from complex matrices with high separation speed and efficiency, relatively simple instrumentation, and low running cost.

Capillary electrophoretic separation of aliphatic mono- and polyamines is relatively straight-forward because their electrophoretic mobility in acidic buffer is directly related to their charge and size (*see* Chapter 23 on empiric models). The detection of the separated analytes is more delicate because these molecules do not adsorb light in the ultraviolet (UV)-Vis and thus they can not be directly detected by spectrophotometrically. Because spectrophotometric detection is commercially available in the CE instruments, methods using an indirect UV mode have been developed for the analysis of the

underivatized amines. The advantages of this approach are that primary through quaternary amines can be rapidly separated without any derivatization steps, and the determination of inorganic cations is possible simultaneously. However, indirect UV detection imposes severe limitations on the choice of electrolytes and their concentrations and additives. Moreover, this technique is the least selective and therefore the most subject to interference. To improve selectivity and sensitivity of the determination process, amines can be derivatized before their separation for laser-induced fluoresence (LIF) or direct UV detection. Their signal sensitivity can be improved two or three orders of magnitude and the interference of other present and nonderivatized cations with similar mobilities is eliminated. This technique has some drawbacks: the separation of the derivatized products is more difficult than that of the nonderivatized amines and, in addition, tertiary and quaternary amines cannot be labeled and thus cannot be determined. Recently, other detection techniques such as mass spectrometry ***(4)***, chemiluminescence detection ***(17,27,28)***, and amperometric detection ***(15,21,29)*** have been developed for the determination of amines (*see* **Table 1**), but these have not been used routinely.

1.1. Analysis of Nonderivatized Amines

Indirect UV detection allows simultaneous determination of primary though quaternary mono- and polyamines and aminoalcohols because it offers an universal detection. It uses the addition of an adsorbing co-ion (so-called *probe*) to the separation electrolyte, and negative peaks are detected at the migration zones of the charged and non-UV active solutes. The concentration of the *probe* and its physical properties such as dissociation constant (pK_a), mobility, and absorption coefficient determine the selectivity, the shape of the peak, and also the sensitivity of the method (*see* **Note 1**). The most used *probes* for capillary electrophoretic determination of LMW and biogenic amines are (1) copper(II) sulfate ($CuSO_4$) ***(1,6,7,30,31)***, (2) imidazole ***(25,26,32–34)***, and (3) quinine sulfate ***(16,18,35)***. These *probes* were developed earlier for the determination of inorganic cations, thus they may interfere with the amine peaks. Other substances, such as p-sulphonic calyx[6]arane ***(9)*** in the presence of halide ions and *N*-methyl-imidazole ***(36)*** for the separation of aliphatic monoamines, have also been used in the separation electrolyte. Amino alcohols were determined with the addition of other UV-active compounds, such as histidine ***(23)*** or 2-amino-4,6-dimethylpyrimidin ***(37)***,to the background electrolyte (BGE) because the above-mentioned probes have a higher electrophoretic mobility and are faster than the analytes, causing wider peaks and higher separation duration.

Table 1
Determination of Volatile and Biogenic Amines by Capillary Electrophoresis

Matrix	Analytes	BGE	Capillary	Inj. mode	Detection	LOD	Ref.
Wine	Hist-, putrescine, cadaverine, isoamyl-phenylethyl-, ethyl-, methyl-, tyr-	4 m*M* $CuSO_4$ 4m*M* formic acid, pH 4.5 4 m*M* 18-crown-6	57/50 cm 75 μm ID	Hydrostatic (3.4 kPa 10 s)	Indirect UV (210 nm)	0.05–0.1 mg/L	***1***
Wine, salami	Putrescine, cadaverine, spermidine, spermine, hist-, tyr-	100 m*M* borate, pH 8.9 50 m*M* SDS 10% ACN	55/30 cm 50 μm ID	Hydrostatic (5 s)	UV (200 nm) Pre-cap. der. AccQ	0.05–2 μ*M*	***2***
Wine	Putrescine, cadaverine, hist-, tyr-, ethyl-, phenylethyl-, spermidine, spermine, ethanol-, ammonia	100 m*M* borate, pH 9.3 20 m*M* SDS	75/42 cm 50 μm ID	Hydrostatic (2 s)	LIF Pre-cap. der. FITC		***3***
Wine	Hist-, cadaverine, isopropyl-, ethanol-, isoamyl-, 2-pentyl, heptyl-, tyr-, phenylethyl-	25 m*M* citrate, pH 2.0	75 cm 50 μm ID	Hydrostatic (50 mbar, 7 s)	MS	18–90 μg/L	***4***
Cheese, dairy products	Putrescine, cadaverine, hist-, tyr-, trypt-, phenylethyl-,	100 m*M* borate, pH 9.2 100 m*M* SDS	80/50 cm 75 μm ID	Hydrostatic (2 s)	LIF Pre-cap. der. FITC	5–15 n*M*	***5***

Fish extract	Ammonia, dimethyl-, trimethyl-, trimethylamine-*N*-oxide	4 m*M* formic acid 5m*M* $CuSO_4$ 3 m*M* 18-crown-6	Ext. light, 64.5/56 cm, 50 μm ID	Hydrostatic (50 mbar 2s)	Indirect UV (215 nm)	25 m*M*	***6***
Fish	Methyl-, dimethyl-, trimethyl-, ethyl-, diethyl-, triethyl-, propyl-	4 m*M* $CuSO_4$ 4m*M* formic acid, pH 3.0 5 m*M* 18-crown-6	47/40 cm 75 μm ID	Hydrostatic (3.4 kPa, 10 s)	Indirect UV (210 nm)	0.02–0.1 mg/L	***7***
Fish, urine	Putrescine, cadaverine, spermidine, spermine, hist-, tyr-, trypt-, phenylethyl-	15 m*M* borate, pH 9.0 10% EtOH, 25 m*M* SBCD, 15 m*M* MBCD	47/40 cm 50 μm ID	Hydrostatic (3.44 kPa 5s)	LIF (325/389) Pre-cap. der. OPA/MA	0.3 – 0.6 μ*M*	***8***
Soy sauce	Putrescine, cadaverine, hist-, tyr-, tryp-phenylethyl-, spermidine, spermine	20 m*M* borate, pH 9.5 70 m*M* SDS	65/50 cm 50 μm ID	Hydrostatic (10 cm, 10 s)	LIF (488/514) Pre-cap. der. FITC	0.1 μ*M*	***9***
Soy sauce	Putrescine, cadaverine, hist-, tyr-, tryp-phenylethyl-, spermidine, spermine	100 m*M* borate, pH 9.4 30 m*M* SDS	65/55 cm	Hydrostatic (0.1 bar, 1.2 s)	LIF (488/532) Pre-cap. der. FITC	0.63–35 n*M*	***10***
See food	Histamine, cadaveririne, tyramine,	20 m*M* phosphate/borate,	100/75 cm		LIF (340/450)		***11***

(Continued)

Table 1
(Continued)

Matrix	Analytes	BGE	Capillary	Inj. mode	Detection	LOD	Ref.
	spermidine	pH 10.0, 20 m*M* SDS 2 m*M* OPA/NAC	50 μm ID		in-cap. der. OPA/NAC		***12***
Tobacco leaf	Putrescine, cadaverine, hist-, tyr-, phenylethyl-, spermidine, spermine,	25 m*M* borate, pH 9.35 40 m*M* SDC 10% ACN	65/50 cm 50 μm ID	Hydrostatic (50 mbar, 5 s)	LIF (488/514) Pre-cap. der. FQ	0.5–2.5 n*M*	***13***
Beer	Methy-, dimethyl-, ethyl-, pyrrolidine, isobutyl-, isoamyl-	10 m*M* borate, pH 9.3 50 m*M* SDS		Hydrostatic (50 mbar, 12 s)	LIF (488/540) Pre-cap. der. NBD		***14***
Beer	Histamine	10 m*M* phosphate, pH 5.6		Electrokinetic (15 kV, 5 s)	Amperometric	0.4 μ*M*	***15***
Serum	Putrescine, spermine, spermidine	8 m*M* quinine sulfate 19 % EtOH, pH 3.0 (adj. with HCl)	40.2/35.2 cm 50 μm ID	Elektrokinetic (5 kV, 3 s)	Indirect UV (236 nm)	0.001 n*M*	***16***
Human urine	Putrescine, cadaverine, spermine, spermidine	200 m*M* phosphate, pH 2.0	50 cm 25 μm ID	Elelktrokinetic (10 kV 10 s)	Chem.lum. Post-col der. $Ru(bpy)_3^{3+}$	7.6–190 n*M*	***17***

Tumor cell	Putrescine, spermine, spermidine	8 m*M* quinine sulfate 20% EtOH, pH 5.9 0.5% (w/v) HMC	60/35 cm 75 μm ID	Elektrokinetic (30 kV, 3 s)	Indirect UV (236 nm)		***18***
Tumor cell	Putrescine, spermine, spermidine	100 m*M* borate, pH 9.0	47/40 cm 50 μm ID	Hydrostatic (0.5 psi, 20 s)	LIF (488/520) Pre-cap. der. FITC	0.03–2.5 n*M*	***19***
Water	Diethyl-, propyl-, 1,5-pentane-diamine, 2-(2-aminoethyl)-pyridine,	40 m*M* phosphate, pH 7.0 25% MeOH	57/50 cm 75 μm ID		LIF (488/520) Pre-cap. der. FITC	1 n*M* (matrix: 0.1 mg/L)	***20***
Lake water	Diaminopropane, cadaverine, putrescine, diaminohexane	10 m*M* Tris/phosphate pH 4	65/60 cm 25 μm ID	Electrokinetic (15 kV 15s)	Amperometric Pre der., NDA	0.05–0.4 μ*M*	***21***
Pine needle	Putresine, cadaverine, spermine, spermidine	80 m*M* borate, pH 8.6	47/40 cm 75 μm ID	Hydrostatic (3.44kPa, 5 s)	LIF (488/520) Pre. der., FITC	0.7–3.2 n*M*	***22***
Process water	Diethanol-, *N*-methyl-diethanol-	10 m*M* Histidine, pH 5.0 adj. with AcOH	37.3/28.9 cm 75 μm ID	Hydrostatic (40mbar, 5 s)	Indirect UV (350, 214 nm)	0.2 mg/L	***23***

(Continued)

Table 1
(Continued)

Matrix	Analytes	BGE	Capillary	Inj. mode	Detection	LOD	Ref.
Aerosol	Methyl-, dimethyl-, diethyl-, dipropyl-, piperedine, pyrrolidine, morpholine	20 m*M* borate, pH 9.0 20% acetone 5 m*M* DM-β-CD	47/40 cm 75 μm ID	Hydrostatic (3.44 kPa, 2 s)	LIF (488/520) Pre-cap. der. FITC	0.9–5 n*M*	***24***
Model standards	Propyl-, dipropyl-, tripropyl-, trimethyl-morpholine, pyrrolidine, cadaverine, diaminopropane, putrescine, ethanol-, diethanol-, triethanol-, diethyl-, triethyl-, butyl-, dibutyl-, tributyl-, dimethyl-,	5 m*M* imidazole, pH 5.0		Hydrostatic (5 nL)	Indirect UV (214 nm)	1.5 mg/L without SPE	***25***
Wrapping material	Ethanol-, diethanol-, triethanol-, monocyclohexyl-, dicyclohexyl-, diethylethanol-	10 m*M* imidazole/ α-HIBA, pH 4.3 10 m*M* 18-crown-6	53.5/45 cm 75 μm ID	Hydrostatic (50 mbar, 3 s)	Indirect UV (214 nm)	0.54–1.54 mg/L	***26***
Milk	Putrescine, cadaverine, spermine, spermidine	30 m*M* citrate, pH 3.5	65/60 cm 25 μm ID	Hydrostatic (90 s)	Amperometric	0.1–0.4 μ*M*	***29***

Model standards	Ammonia, methyl-, heptyl-, 1,3-diaminopropane, putrescine, hist-, cadaverine, agmatine, ethyl-, ethanol-, spermidine, propyl-, morpholine, isopropyl-, diethyl-, butyl-, spermine, isobutyl-, amyl-, isoamyl-, tyr-, 1-methylbutyl-, hexyl-, phenylethyl-	4 m*M* $CuSO_4$ 4 m*M* formic acid, pH 3.0 4 m*M* 18-crown-6	63/55 cm 75 μm ID	Elektokinetic (7 kV 10 s) Hydrostatic (3.4 kPa, 15 s)	Indirect UV (210 nm)	0.05–0.1 mg/L	***30***
Water in space	Methyl-, trimethyl-, ethyl-, propyl-	5 m*M* imidazole 10 m*M* α-HIBA	80/72 cm 50 μm ID	Hydrostatic (200 s)	Indirect UV (214 nm)		***33***
Model standards	Dimethyl-, trimethyl-, diethyl-, triethyl-, diethanol-, triethanol-, ammonia	5 m*M* imidazole 10 m*M* acetate, pH 4.5	63/55 cm 75 μm ID	Hydrostatic (10 cm, 3 s)	Indirect UV (214 nm)	0.1 mg/L	***34***
Model standards	Aminobutane, 2-aminobutane, 2-amino-2-methylpropane	10 m*M* *N*-Me-imidazole 30% MeOH 200 m*M* 8-crown-6, pH 4.5 (adj. with H_3PO_4)	80/60 cm 75 μm ID		Indirect UV (210, 214 nm)		***36***

(Continued)

Table 1
(Continued)

Matrix	Analytes	BGE	Capillary	Inj. mode	Detection	LOD	Ref.
Metal-working fluid	1,2-propandiol-3-, 2-(2-aminoethoxy)-ethanol, 2,2-imino-diethanol, isobutyl-, ethanol-, *N*, *N*-dimethylethanol-etc.	10 m*M* 2-amino-4,6-dimethyl-pyrimidine	48.5 cm 50 μm ID	Hydrostatic (185 mbar*s)	Indirect UV (228 nm)	1 mg/L	***37***
Foods	Putrescine, cadaverine, spermidine, spermine, hist-, tyr-, trypt-	15 m*M* borate, pH 9.45 40 m*M* SDS 25% MeOH	43/36 cm 75 μm ID	Hydrostatic (2.5 s)	UV (200 nm) Pre-cap. der. benzoyl-Cl	0.2–0.7 mg/L	***38***
Model standards	Methyl-, ethyl-, methoxy-propyl-, ipropyl-, propyl-, isobutyl-, butyl-, octyl-, cyclohexyl-, pentyl-, hexyl-,	20 m*M* borate, pH 9.0 100 m*M* SDS, (7 *M* urea) 5% ACN, 10 m*M* β-CD	67/55 cm 50 μm ID	Hydrostatic (50 mbar, 12 s)	LIF (325/389) Pre-cap. der. OPA/MA	0.09–0.5 μ*M*	***39***

The mean detection limits are determined to be in the range of 0.05–1 mg/L for each above-mentioned *probe* when standard solutions of amines are separated. The sensitivity of the method can be increased in the sample preparation, but these steps must be suitable to the indirect UV detection. Application of salt-free solvents is recommended because the presence of ions in the solvent may cause interference or matrix effect. Alkaline and alkaline earth metal ions in the extraction solvent in large amounts may interfere and the peak of the inorganic ion may fully overlap the amine peaks. Thus, ammonium solution is usually used when required because the ammonium migrates faster than the amines and metal ions. However, ammonium at high concentration may cause shifting in the migration times ***(23)*** that can be avoided if the BGE used has good buffer capacity. The presence of strong anions in the solvent may cause system peaks (*see* **Note 2**) and unstable baseline ***(1)***.

For sample clean-up and preconcentration of the extract, solid-phase extraction (SPE) is widely used and has commonly been performed with weak cation exchangers and C_{18} phase ***(1,25)***. C_{18} is best suitable to indirect UV detection because in ion exchange resins, inorganic cations are also retained and elute together with the amines, interfering with the indirect UV detection. Two alternative procedures are possible when C_{18} is used for SPE. The first is the application of ion-pairing with octanesulfonate or decanesulfonate ***(10,25)***. This technique has some drawbacks; it poses severe elution problems, and as the ion-pairing reagents are sodium salts, the sodium peak may interfere with the amines. The second alternative is the adsorption of neutral amines onto the solid phase and desorption by charging them. In this case, the pH of the solution medium of the sample must be above 9.0 (set by addition of ammonium solution). The elution solvent is a strong acid such as nitric acid (HNO_3) or hydrogen chloride (HCl) at a concentration lower than 0.1 *M* to avoid the occurrence of system peaks and unstable baseline. SPE with C_{18} phases is suitable to indirect UV detection and can increase the selectivity and the sensitivity of a method, sometimes with results comparable to those of fluorescence detection.

Electrophoretic separations for the determination of LMW and biogenic amines applying the three widely used *probes* (copper, imidazole, and quinine sulfate) in the BGE are discussed as follows.

1.1.1. Copper-Based BGE Methods

The amount of *probe* needed can be determined as follows: the greater the amount of *probe*, the lower the detection limit; however, the baseline noise increases proportionately. The optimum concentration of copper sulfate ($CuSO_4$) is observed at 4 m*M*. The copper-based BGE medium is generally acidic so as to increase protonation of the amines and prevent copper

hydrolization. Generally, formic acid is added to the $CuSO_4$ water solution to obtain acidic medium (pH 3.0).

Crown ethers are usually added into the separation electrolyte to improve the selectivity of the method. In $CuSO_4$-based methods, the addition of 18-crown-6 ether at concentration of 3–4 m*M* in the BGE is generally used. The cavity size of 18-crown-6 is more in conformity with the amine ions than 15-crown-5, resulting in a stronger complexation. The stability of the complex depends strongly on the content of the BGE. On one hand, the BGE does not have to contain small, single-charged cations such as sodium or potassium. On the other hand, the separation pH and the amount of organic modifier, such as methanol in the BGE, strongly affects the complexation. The crown ether cannot complex very well at low pH; this may be attributed to its partial protonation. The presence of methanol in the separation electrolyte increases the complexation constant, although at high methanol content, the lipophilic interaction between the ether and methanol increases, resulting in a weaker amine complex. The complexation of the crown ether agents with LMW amines is weaker than that with metal ions, thus crown ether agents are less effective in amine analysis (*see* **Note 3**). However, addition of this complex agent might be helpful in improving the separation of primary amines and eliminating co-elution with metal ions.

The separation voltage and temperature strongly affects the noise and the stability of the baseline, causing poorer method sensitivity and reproducibility. Increase in the baseline noise as a function of applied voltage is particularly exacerbated when using strongly absorbing electrolytes ***(31)***. The separation temperature is usually set to 20 °C considering the volatility and thermal stability of the analytes.

Generally, hydrostatic injection is used for loading the sample into the capillary; however, the method sensitivity can be increased by a factor of 10–20 by applying the ion-selective electrokinetic injection mode. However, elektrokinetic injection is not recommended in routine work, because the injected amount strongly depends on the ionic strength of the sample (*see* **Note 4**). Moreover, additional peaks may occur that overlap with the analyte peaks ***(7,16)***. On the other hand, the peak area is not necessary proportional to the concentration of the analyte when elektokinetic injection is used even for standard solutions; it has been observed that cubic equation was the best-fitting tool for determining the calibration curve ***(7)***.

Applying copper-based BGE methods, LMW and biogenic amines are separated within 10 min. The mathematical detection limit of these methods is under 0.5 mg/L. Sample clean-up of wine ***(1)*** and drinking water ***(25)*** has been developed by application of SPE with C_{18}. An on-line gas-extraction

sampling device was also coupled with this technique for determination of volatile alkylamines ***(7)***.

1.1.2. Imidazol-Based BGE Methods

Another generally used *probe* for indirect UV detection of amines is imidazole at concentration range of 5–20 m*M* in water solution. The co-ions acetic acid or α-hydroxy-isobutyric acid (α-HIBA) are generally used to set the proper pH of the BGE at 4.3–5.0. α-HIBA creates weak complexes with the amines that may enhance the resolution of the analytes. The complexation of α-HIBA with LMW amines is weaker than with that with inorganic metal ions, and nearly no significant effect is observed in the selectivity when α-HIBA or acetic acid is used for determination of LMW amines.

18-crown-6 ether as a selector has been also used in the imidazole-based electrolytes, and its concentration was optimized to 0.2 *M* ***(36)***. Another complexation agent, namely ethylenediamine tetraacetic acid (EDTA), has been also used to eliminate the co-migration of amines and inorganic cations. The multiple charged cations form stable complexes with EDTA, thus the migration difference of the polyamines and alkaline earth metals increases as a result of the increased volume of the Stoke radii of the molecule. Addition of ionic additives, however, is not recommended in the indirect mode because they may compete for the displacement with the BGE and thereby reduce the response.

Mainly aliphatic LMW amines have been determined with imidazole-based methods from wrapping material and condensed water with a detection limit of 0.5–1.5 mg/L. However, this technique has not been frequently used for real application.

1.1.3. Quinine Sulfate-Based BGE Methods

Quinine sulfate-based BGE has been used for the separation of biogenic polyamines such as cadaverine, putrescine, and spermidine. The used concentration of quinine sulfate is in the range of 5–10 mmol/L and the pH of the buffer is generally set to 3.0 with HCl. The separation buffer always contains ethanol at a volume ratio of 20%, otherwise the quinine sulfate precipitates in the BGE. To block the evaporation of ethanol and to suppress the electroosmotic flow (EOF), hydroxypropylmethyl cellulose (HMC) has been also added to the electrolyte in the amount of 0.5% (w/v)%; however, its addition is not necessary.

The developed quinine sulfate-based BGE methods have been used for biomedical application since the biogenic polyamines have been determined from serum ***(16)*** and tumor cells ***(18)***. When trichloroacetic acid is used for

extraction of tumor cells, its impurities might also be detected ***(35)***. The sample containing the analytes and the internal standard, which is usually 1,7-diaminopentane, are separated within 10 min.

1.2. Analysis of Derivatized Amines

Derivatization is mostly a detection-oriented modification of the analytes associated with the introduction of UV-absorbing or -fluorescing groups into the molecules to increase the detection selectivity and sensitivity. Various derivatization reagents have been applied in the determination of biogenic amines in CE, such as benzoyl chloride ***(38)***, 6-aminoquinoyl-*N*-hydroxysuccinmidyl carbamate (AccQ) ***(2)***, *O*-phthalaldehyde (OPA) ***(39)***, 5-(4,6-dichloro-s-triazin-2-ylamino)fluorescein (DTAF) ***(40)***, fluorescein isothiocyanate isomer I (FITC) ***(3,5,9,10,19,20,22,24)***, fluorescamine (FA) ***(41)***, 3-(2-furoyl)quinoline-2-carboxaldehyde (FQ) ***(13)***, 1-pyrenebutonic acid succinimidyl ester (PSE) ***(42)***, and 7-chloro-4-nitrobenzo-2-oxa-1,3-diazole (NBD) ***(14)***. These labels react with the noncharged primary or secondary amino groups of the analytes and the reaction based on nucleophyl substitution or addition. The proper label reagent is determined by:

1. The type of the analyte (primer or secondary and mono- or polyamine is in the interest).
2. The available detector (UV or flouresence with argon or nitrogen laser).
3. Native fluorescence and mobility of the labeling agent.
4. The speed of the derivatization and the stability of the product.

AccQ and benzoyl chloride show a good reactivity toward biogenic amines, but have poor sensitivity as a result of the UV detection. OPA reacts quantitavely with primary amino compounds within 30 s in the presence of a reducing agent such as 2-mercaptoethanol, but OPA derivatives are not stable (*see* **Note 5**). FITC and DTAF react with primary and secondary amines such as phenyl isothiocyanate under alkaline conditions to form fluoresceine thiocarbamyl derivatives. These derivatives exhibit strong fluorescence, with an excitation wavelength that almost matches the 488-nm light provided by an argon laser, which is used in at least one commercially available CE system with LIF detection ***(24)***. The FTC-amine derivatives are stable at room temperature in the dark over a period of 7 d ***(24)***. FA could react with both primary and secondary amino groups, but only the former derivative is fluorescent. The reaction is rather fast (30 s at 70 °C) in aqueous solution, and the excess reagent is hydrolyzed into a nonfluorescent product. FQ can easily react with primary amino compounds to form highly fluorescent and stable derivatives in the presence of potassium cyanide (KCN). The fluorescent excitation wavelength of the products is close to the wavelength of a commercial argon laser.

Moreover, excess FQ does not interfere with the amine derivatives because of its weak native fluorescence. PSE labels the amines with a fluorescent pyrene group. In analytes with multiple labeling sites, an excited pyrene group can form an intramolecular excimer that emits at longer wavelength (450–520 nm) than mono-labeled analytes (360–420 nm). Thus, high selectivity for polyamines can be achieved with the use of this reagent. NBD has a chlorine atom which is displaceable by nucleophilic groups such as primary and secondary amines and it forms highly fluorescent adducts with good yield and in a reasonable time (1 h). It has strong absorbances at both 488 and 337 nm, allowing for exication by either argon-ion or nitrogen laser. Unreacted NBD exhibits weak fluoresence, but is a strong adsorber ***(14)***. Among these labels, FITC is more frequently used for determination of volatile and biogenic amines from different matrices such as tumor cells ***(19)***, soy sauce ***(9–10)***, aerosol ***(24)***, wine ***(3)***, cheese ***(5)***, water ***(20)***, and pine needle extract ***(22)***, thus its derivatization and derivatization condition are described in more detail.

1.2.1. Precapillary Derivatization and Separation of FTC-Amines

The degree of derivatization of amines with FITC is mainly influenced by the medium of the solvent (pH value), the kind of the buffer used, additional organic solvents, the molecular ratio of the label and the analytes, and the reaction temperature and duration ***(22)***. The reaction rate continuously increases with increasing pH value, although an increase of side reaction products has also been observed ***(22,24)***. In the case of FTC-amines, the best intensity is obtained at pH 10.0 with carbonate buffer compared to the borate and phosphate buffers at similar pH. The reaction rate is not significantly affected by changing the concentration of the buffer components ***(22,24)***. Organic solvent in the reaction media affects mainly the peak intensity of the products, but these effects are negligible as a result of the high apolarity of FITC (*see* **Note 6**). Nearly similar intensity of FITC-derivatized LMW and biogenic amines has been obtained with acetone and acetonitrile, but methanol content decreased the fluorescence intensity to 10–50% ***(22,24)***. When tetrahydrofuran (THF) or dimethylformamide (DMF) were used as stock solutions of FITC, no response for dimethylamine (DMA) derivative was observed ***(24)***. Excess derivatization reagents must be applied for the quantitative analysis of LMW and biogenic amines, especially when polyamines containing two or more amino groups are in the interest. When the excess of FITC is not enough, amines with lower reactivity may be not fully derivatize or polyamines may form more than one product, which may cause problems during the separation (causing interfering peaks). At high concentrations of FITC, the peak of the excess reagent may overlap the analyte peaks and/or additional peaks from side-products or from

matrix compounds with amino groups such as amino acids may appear (*see* **Note 7**). In addition, it was found that FTC-amines are less stable when large amounts of derivatizing reagent are used ***(9)***. The optimum excess of the FITC in standard solution of amines is 50–100 ***(22,24)***. The derivatization reaction is sped up by higher temperature, but side reactions are also enhanced. Thus, heating is not found to be useful and the reaction is usually performed at room temperature. The derivatization is mainly completed within 2 h; however, an overnight (16 h) reaction is recommended if secondary amines are also in the interest of the determination.

Electrophoretic separation of the FTC-amines is more difficult than the separation of underivatized ones because the labeling group with the high-molecular-weight tag mainly determines the mobility of the analyte. FITC has a carboxylic acid group, thus the used separation medium is alkaline because the FTC-amines adducts are negatively charged. The migration times for the amine derivatives are shorter than those for the interfering excess of FITC, thus the amine detection could not be influenced by the nonreacted FITC. However, peak overlapping may be observed if the excess ratio is too high (more than 100).

Borate has been widely used as a separation buffer because of its low current conductivity and its ability to form complexes; thus, it may enhance the selectivity in separation. The separation efficiency is greatly affected by the buffer concentration and medium. Use of higher concentrations of borate led to slightly better resolution, but the migration time and electrophoretic current are also increased, thus the optimal concentration range was determined to be between 20 m*M* and 100 m*M* at a pH range of 8.6 to 9.5. Complete separation of all amine analytes is seldom achieved with a buffer containing no additives such as anionic surfactants, modifier organic solvent, or cyclodextrins (CD) that enrich the mobility differences of the derivatized amines. Sodium dodecyl sulfate (SDS) at higher concentrations than its critical micellar concentration is widely used in micellar electrokinetic chromatography (MEKC) to improve the selectivity of the LMW and biogenic amines. Addtion of 30 m*M* SDS to the separation buffer greatly improved the resolution and peak shape of the FTC-polyamine derivatives, but at concentrations of higher than 100 m*M*, resulted in longer migration times and loss in resolution ***(9)***. Thus the optimal concentration of SDS in the BGE is determined to be between 30 and 100 m*M*; however, decrease in the sensitivity (approx 100 times) has been observed ***(22,24)***. Organic modifiers such as methanol, acetonitrile, or aceton in the BGE have been also introduced because they suppress the EOF and thus increase the migration of the solutes in the capillary. Complete separation of volatile aliphatic amines was achieved with a buffer containing 30% acetone ***(24)***. For further improvement of the resolution, addition of a range of various

cyclodextrins of different cavity size and rim substitution has been also investigated ***(24)***. The electrophoretic mobility of the CD–analyte complexes is lower (shorter migration times) than that of the uncomplexed analytes. Among the unmodified CDs, only addition of β-cyclodextrin to the separation buffer improved the separation efficiency of LMW amines and addition of 2,6-Di-*O*-methyl-β-cyclodextrin yielded better peak shapes than the unmodified buffer ***(24)***.

The optimized methods have been evaluated for the determination of FTC-labeled amines. The linear dynamic concentration range was determined to be between 5 and 1000 n*M* ***(24)*** and is at least two orders of magnitude broad (*see* **Note 8**). For determination of the analyte concentration, calibration is mainly used; however, internal standards have been also evaluated. The most frequently used internal standards are 1,7-diaminohexane and 1,7-diaminoheptane. The relative standard deviation (RSD) of the peak area has been always determined to be under 5%, which shows a good reproducibility of quantification. The detection limits were determined to be in the range of 0.7–10 n*M* for LMW and biogenic amines too (*see* **Note 9**). It should be mentioned that the sensitivity of a method strongly depends on the type of the amines. For example, FTC-spermidine and FTC-spermine show detection limits of one and two orders of magnitude higher than the other biogenic polyamines, which could be caused by their lower reaction yield with FITC ***(10)***.

The application of this method to real samples may present difficulties as a result of the interfering signals from *N*-containing compounds that reacted with FITC and/or from excess reagent that migrates at about the same time as the FTC-amine peaks. Because of this, it is necessary to use the lowest concentration of FITC possible. The other alternative is to remove the excess FITC by derivatizing the analytes on solid phase; however, no method has been developed in combination with CE.

1.2.2. On-Capillary Derivatization Techniques

Generally, precapillary derivatization is used for determination of LMW amines; however, some methods applying in-capillary derivatization have also been developed. In the *on-line mode*, the derivatization takes place by mixing the analytes with the reagent just before the capillary using a T-junction and it is frequently employed in combination with a microdialysis procedure. Until now, no method has been developed in combination with on-line derivatization of LMW amines. The *on-capillary mode* is a form of derivatization that can be used without changing the commercially available CE devices. This technique is divided as a result of the part of the capillary where the reaction takes place. In the *at-inlet on-capillary technique*, a sample and the reagent solution are

introduced into the inlet of a capillary either by tandem or sandwich mode. These reactants are mixed by diffusion and allowed to react for a specified time. Molina and his co-workers ***(40)*** have developed a tandem in-capillary mode for determination of biogenic polyamines separated as DTAF derivatives. However, the detection limit of the method is quite high (0.17–0.43 mg/L) compared with the precapillary LIF methods and it has not been applied for real samples. In the *throughout on-capillary mode*, the BGE containing the reagent and the amines are labeled during their migration through the capillary. In spite the fact that the OPA derivatives are not stable, they have been used for labeling purposes because they are not natively fluorescent and react quickly with the primer amines ***(11,12)***. Biogenic amines such as histidine, putrescine, tyramine, and spermidine have been determined from seafood and human plasma by applying this technique; its detection limit is 1–5 μM, which is two orders of magnitude higher than that of precapillary derivatization. The last on-capillary derivatization technique is the *postcapillary mode*, which requires modification of the commercial CE instrument because the labeling takes place after the separation and before the detection. Postcapillary derivatization has been used in combination with tris(2, 2′-bipyridyl)ruthenium(II) ($Ru(bpy)_3^{3+}$)-based chemiluminescence detection for determination of volatile aliphatic ***(28)*** and biogenic polyamines in human urine ***(17)***.

2. Materials and Equipment

2.1. Analysis of Underivatized Amines

2.1.1. Copper-Based CE–Indirect UV Method ***(1)***

1. Analytes: putrescine, histamine, cadaverine, spermidine, ethanolamine, isopropylamine, isoamylamine, 1-methylbutylamine, phenethylamine, tyramine, methylamine (from Aldrich, Milwaukee, WI).
2. Sample: commercially available wines: spiked wines with analytes and synthetic wine containing ethanol, tartaric acid, citric acid, sucrose, glycerine, calcium chloride, sodium chloride, and potassium hydrogentartrate (from Merck, Darmstadt, Germany).
3. Sample preparation: automated on-line flow-injection (FI) system coupled to CE equipment via programmable arm containing an electronic interface and controlled by a microcomputer (*see* **Fig. 1**). The system contains Gilson Miniplus-3 peristaltic pump, a Rheodyne 5041 injection valve, three switching valves, polytetrafluoroethylene (PTFE) tubing of 0.5 mm inner diamter (ID), and a reactor length of 50 cm. The continous filtration system contains a Millipore microfilter with pore size of 0.45 μm. FI contains C_{18} octadecyl solid phase (from Varian, Palo Alto, CA) in a tube with dimension of 5 cm × 2 mm ID. MeOH and water were used for

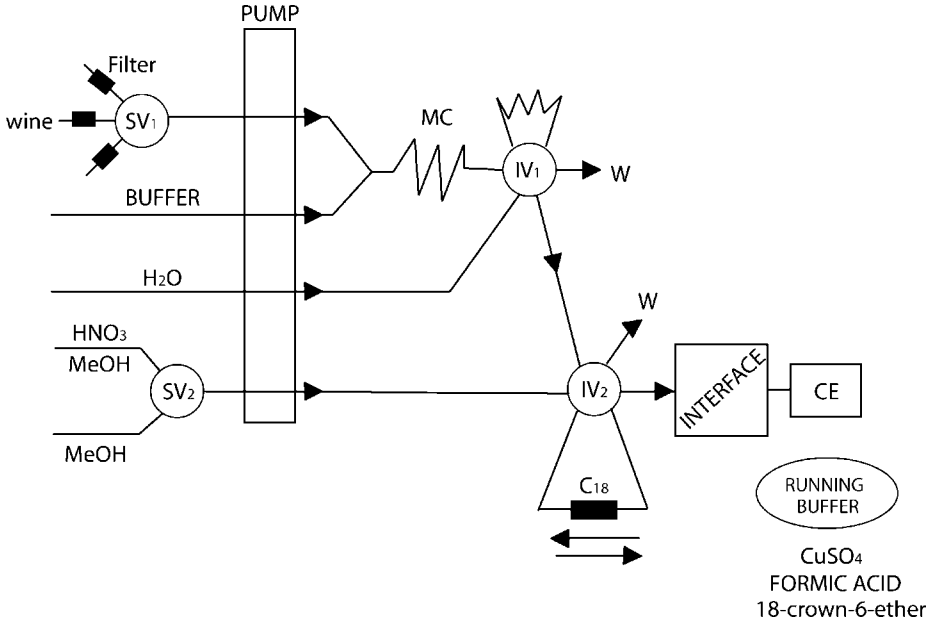


Fig. 1. Scheme of FI system ***(1)***. Abbreviations: IV, injection valve; SV, switching valve; MC, mixing coil; w, waste.

conditioning the microcolumn and 0.1 *M* HNO_3 dissolved in MeOH was used as eluent at 3 mL/min.

4. CE instrument and capillary: Beckman P/ACE 5500 CE unit equipped with a diode array detector (DAD). Normal polarity: anode on the injection side and cathode on the detection side. Detection wavelength at 210 nm. Beckmann capillary tubing of 57 cm long (effective length is 50 cm), 75 μm ID (375 μm outer diamter [OD]). Cartridge temperature is set to 20 °C.
5. CE buffer: 4 m*M* $CuSO_4$, formic acid, 18-crown-6 ether (pH 4.5) (from Sigma, St. Louis, MO).

2.1.2. Imidazole-Based CE-Indirect UV Method

1. Analytes: methylamine, ethylamine, propylamine, butylamine, dimethylamine, diethylamine, cadaverine, putrescin, and spermidine (from Sigma, St. Louis, MO). Standard stock solution of 1000 mg/L dissolved in water.
2. Sample: atmospheric and metalworking fluid (MWF) aerosol collected onto quartz filter by air pump.
3. Sample preparation: the filters are extracted with high-purity water in an ultrasonic bath.

4. CE instrument and capillary: Beckman P/ACE 5500 CE unit equipped with a DAD. Normal polarity: anode on the injection side and cathode on the detection side. Detection wavelength at 214 nm. Capillary tubing of 47 cm length (effective length is 40 cm), 75 μm ID (360 μm OD) (from Polymicro Technologies, Phoenix, AZ). Cartridge temperature is set to 30 °C.
5. CE buffer: 20 m*M* imidazole, acetic acid, 4 m*M* EDTA (*see* **Note 10**), 20% ethanol (pH 3.3) (from Sigma, St. Louis, MO). The running buffer is prepared daily from 100 m*M* imidazole and 100 m*M* EDTA solutions and it is filtered ($d_p = 0.45\,\mu m$) before use.

2.2. Analysis of FTC-Amines (24)

1. Analytes: methylamine, dimethylamine, diethylamine, dimethylamine, diethylamine, dipropylamine, piperidine, pyrrolidine, morpholine (from Aldrich, Milwaukee, WI). Standard stock solution of 1000 mg/L dissolved in water.
2. Sample: atmospheric aerosol collected onto thin PTFE filters.
3. Reagents for derivatization: 1.1 m*M* FITC dissolved in acetone, 0.2 *M* sodium bicarbonate (pH 8.8) (from Aldrich, Milwaukee, WI).
4. CE instrument and capillary: Beckman P/ACE 5500 CE unit equipped with a a Beckman LIF detection system using a 4-mW argon ion laser with exication wavelength of 488 nm and emission wavelength filter of 520 nm. Normal polarity: anode on the injection side and cathode on the detection side. Capillary tubing of 57 cm long (effective length is 50 cm), 75 μm ID (375 μm OD) (from Polymicro Technologies, Phoenix, AZ). Cartridge temperature is set to 20 °C.5. CE buffer: 20 m*M* sodium tetraborate, 20% acetione, 5 m*M* DM-β-CD (pH 9.0). (Sigma, St. Louis, MO). The separation electrolyte are prepared daily from 100 m*M* sodium tetraborate solution and ultrasonicated for 20 min before use.

3. Methods

3.1. Analysis of Underivatized Amines

3.1.1. Copper-Based CE–Indirect UV Method (1)

1. Regenerate the capillary before each measuring day by rinsing it with water for 10 min, with 0.1 *M* sodium hydroxyde (NaOH) for 2 min, again with water for 2 min, and with BGE for 15 min (vacuum pressure of 20 psi).
2. Inject the sample hydrodinamically for 10 s with pressure (*see* **Note 11**).
3. Run sample under 15 kV with running buffer and detect negative peaks at 214 nm. The measured current is approx 14 μA. (*see* **Note 12**).
4. **Figure 2** shows an electropherogram for a red wine sample using the on-line sample clean-up procedure.
5. Calibration is used for the determination of the analyte concentration from integrated peak area.

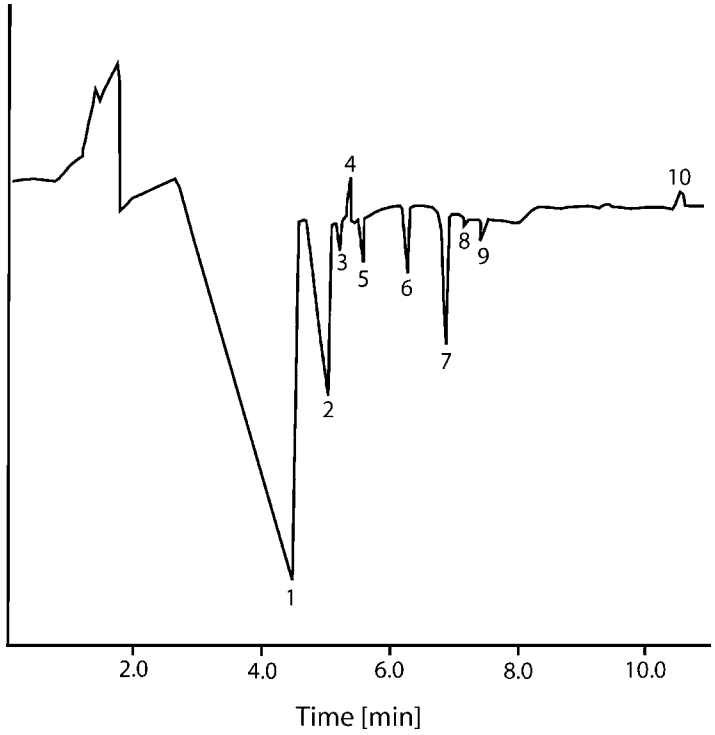


Fig. 2. Electropherogram for a red wine sample using the copper-based background electrolyte (BGE) method for determination of biogenic amines ***(1)***. BGE: 5 m*M* $CuSO_4$, 4 m*M* formic acid, 4 m*M* 18-crown-6, pH 4.5. Injection: 3.44 kPa, 10s. Detection: indirect at 210 nm. Separation voltage: 15 kV. Peaks: 1, 2, 6, 7, 9, unknown peaks; 3, putrescine; 4, histamine; 5, cadaverine; 8, ethanolamine; 10, phenethylamine.

3.1.2. Imidazole-Based CE–Indirect UV Method

1. Condition the new capillary with 0.1 *M* NaOH for 30 min with high pressure (20 psi).
2. Rinse the capillary before each measuring day with 0.1 *M* NaOH for 15 min.
3. Rinse the capillary before each injection for 2 min with 0.1 *M* NaOH and subsequently with buffer for 3 min (vacuum pressure of 20 psi).
4. Inject the sample hydrodinamically (0.5 psi) for 10 s. The calculated injection volume is 59 nL (*see* **Note 13**).
5. Run the sample under 20 kV with running buffer and detect negative peaks at 214 nm. The measured current is approx 28 μA.
6. **Figure 3** shows a typical electropgherogram when standard solution of LMW amines at concentration of 10 mg/L are injected.

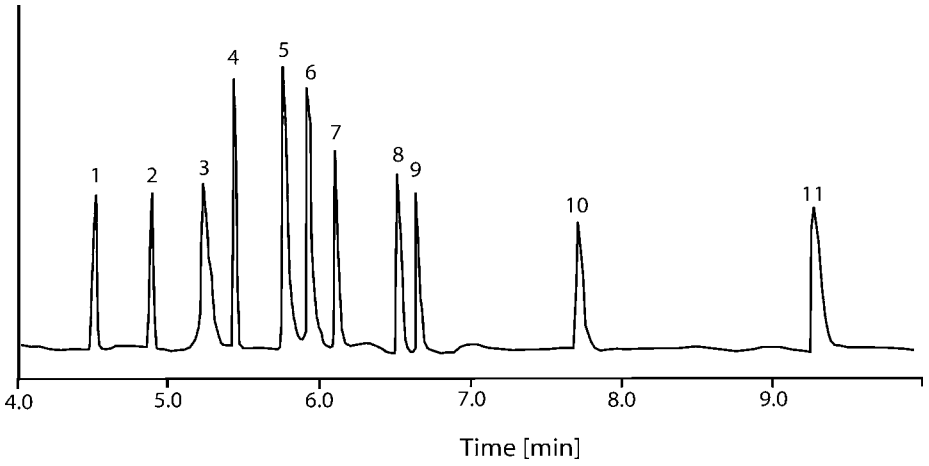


Fig. 3. Corrected electropherogram for standard solution at concentration of 10 mg/L using the imidazole-based background electrolyte (BGE) method for separation of low-molecular-weight amines. BGE: 20 m*M* imidazole, acetic acid, 4 m*M* EDTA, pH 3.3. Injection: 3.44 kPa, 10 s. Detection: indirect at 214 nm. Separation voltage: 20 kV. Peaks: 1, methylamine; 2, dimethylamine; 3, sodium; 4, ethylamine; 5, cadaverine; 6, putrescine; 7, propylamine; 8, diethylamine; 9, butylamine; 10, diethanolamine (int.st); 11, spermidine.

7. Effective mobility calculated from migration time is used for identifying the detected peaks (*see* **Note 14**) and internal standard (diethanolamine) is used for quantification applying effective mobility scale ***(43)*** (*see* **Note 15**).

3.2. Analysis of FTC-Amines (24)

1. Derivatization procedure: derivatization solution containing 100 µL of 0.2 *M* sodium bicarbonate (pH 8.8) and 200 µL of 1.1 m*M* FITC dissolved in acetone is added into the solution containing the standard solution of analytes or water extract of the aerosol sample and filled with water to a volume of 1 mL. This solution then is stored overnight (16 h) in the dark at room temperature (21 °C). Before injection, the mixture is diluted five times with BGE.
2. Each measuring day, the capillary is rinsed with 0.1 *M* NaOH and water for 5 min (vacuum pressure of 20 psi).
3. Before injection, flush the capillary with 0.1 *M* NaOH, water and the BGE continuously for 1 min (*see* **Note 16**).
4. Inject the sample containing the diluted solution by applying 0.5 psi for 2 s (calculated sample volume is 18 nL).
5. Run the injected sample under 25 kV with the proper BGE. The measured current is approx 50 µA.

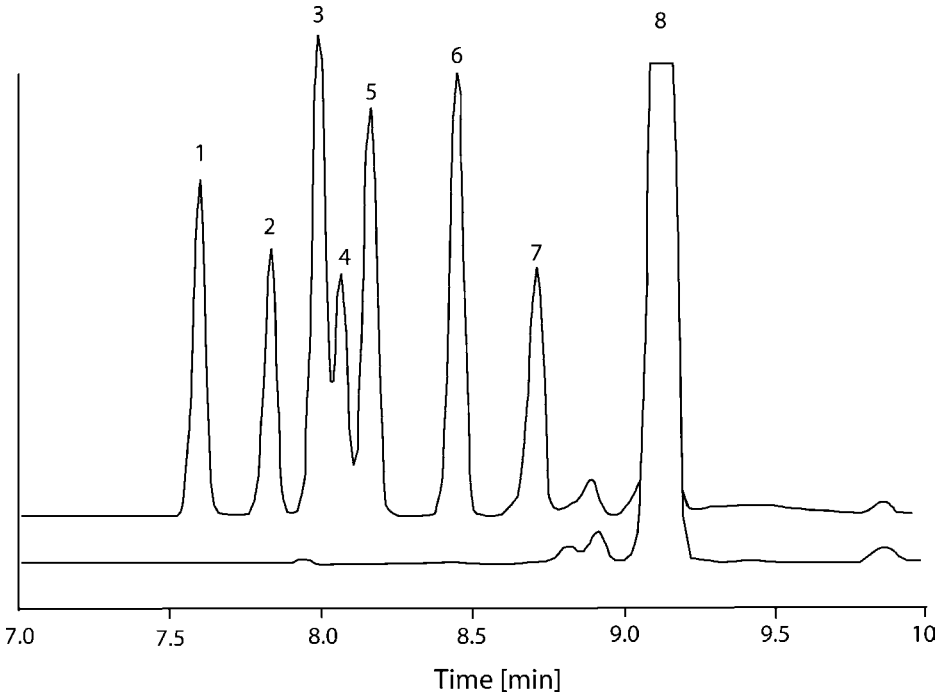


Fig. 4. Laser-induced fluoresence (LIF) electropherogram. LIF electropherograms of fivefold diluted standard (upper chart) and reagent blank (lower chart) ***(24)***. Background electrolyte: 20 m*M* borate, 20% aceton, 5 m*M* DM-β-CD, pH 9.0. Injection: 3.44 kPa, 2s. Detection: LIF, exication wavelength of 488 nm and emission wavelength of 520 nm. Separation voltage: 25 kV. Peaks: 1, dipropylamine; 2, piperidine; 3, diethylamine; 4, pyrrolydine; 5, morpholine; 6, dimethylamine; 7, methylamine; 8, fluorescein isothiocyanate. Diluted concentration of pyrrolidine and dimethylamine (100 mg/L), other peaks (200 mg/L).

6. **Figure 4** shows LIF electropherogram of fivefold diluted standard and blank.
7. Peaks are identified according to their migration times, and calibration using corrected peak areas is used for quantification.

4. Notes

1. The solvent of the probe and the injection duration also affect the peak symmetry. More details about the affecting properties are reviewed elsewhere ***(44)***.
2. The occurrence of system peaks also depends on the concentration and the organic content of the medium.
3. 18-crown-6 ether was originally used for separation of ammonium and potassium.

4. The sample may contain nitrate or sulfate in different amounts that change the ionic strength of the sample and thus the injected amount of the analyte.
5. The sample solution must be injected 2–3 min after mixing together the derivatization solution and the solution containing the analytes ***(14)***.
6. The polarity of the components can be described with its octanol/water coefficient (logP) value. The calculated logP of FITC is 5.03, thus it is 100,000 times more soluble in octanol (apolar solvent) than in water. The calculation was made by Pallas version 3.1 (CompuDrug International, Budapest, Hungary) ***(45)***.
7. Amino acids react slower with FITC than biogenic amines because of the lower nucleophilicity of the amino acids.
8. The range can be varied by changing the injection time.
9. From a practical point of view, the detection limit should be calculated 100 times more when the analytes are derivatized in matrix.
10. EDTA was added to eliminate the interference of alkali earth metals and improve the selectivity of polyamines.
11. The sample solvent of the injected solution is 0.1 *M* HNO_3 dissolved in MeOH.
12. The measured current depends on the total length of the capillary and the type of the instrument, thus this value is typical of CE produced by Beckman-Coulter.
13. The injection volume was calculated with CE Expert Lite (Beckman Coulter, Waldborn, Germany) ***(46)***.
14. Applying effective mobility scale, the identification becomes more precise, and it is independent of the separation voltage and the dimension of the capillary.
15. The performance characteristics were the same when electropherogram and effective mobility scale were used for integration the peaks. Thus, both the identification and quantification can be made at the same time because the same scale is used.
16. Relatively stable migration times could be obtained when the capillary is rinsed with sodium hydroxide after each run.

References

1. Arce, L., Rios, A., and Valcarcel, M. (1998) Direct determination of biogenic amines in wine by integrating continuous flow clean-up and capillary electrophoresis with indirect UV detection. *J. Chromatogr. A* **803**, 249–260.
2. Kovacs, A., Simon-Sarkadi, L., and Ganzler, K. (1999) Determination of biogenic amines by capillary electrophoresis. *J. Chromatogr. A* **836,** 305–313.
3. Nouadje, G., Simeon, N., Dedieu, F., Nertz, M., Puig, P., and Couderc, F. (1997) Determination of twenty eight biogenic amines and amino acids during wine aging by micellar electrokinetic chromatography and laser-induced fluorescence detection. *J. Chromatogr. A* **765,** 337–343.
4. Santos, B., Simonet, B. M., Rios, A., and Valcarcel, M. (2004) Direct automatic determination of biogenic amines in wine by flow injection-capillary electrophoresis-mass spectrometry. *Electrophoresis* **25,** 3427–3433.

5. Nouadje, G., Nertz, M., Ph., V., and Couderc, F. (1995) Ball-lens laser-induced flouresence detector as an easy-to-use highly sensitive detector for capillary electrophoresis Application to the identification of biogenic amines in dairy products. *J. Chromatogr. A* **717,** 335–343.
6. Timm, M. and Jorgensen, B. M. (2002) Simultaneous determination of ammonia, dimethylamine, trimethylamine and trimethylamine-N-oxide in fish extracts by capillary electrophoresis with indirect UV-detection. *Food Chem*. **76,** 509–518.
7. Lista, A. G., Arce, L., Rios, A., and Valcarcel, M. (2001) Analysis of solid samples by capillary electrophoresis using a gas extraction sampling device in a flow system. *Anal. Chim. Acta* **438,** 315–322.
8. Male, K. B. and Luong, J. H. T. (2001) Derivatization, stabilization and detection of biogenic amines by cyclodextrin-modified capillary electrophoresis-laser-induced fluorescence detection. *J. Chromatogr. A* **926,** 309–317.
9. Rodriguez, I., Lee, H. K., and Li, S. F. Y. (1996) Separation of biogenic amines by micellar elektrokinetic chromatography. *J. Chromatogr. A* **745,** 255–262.
10. Rodriguez, I., Lee, H. K. and Li, S. F. Y. (1999) Ion-pair solid-phase extraction of biogenic amines before micellar electrokinetic chromatography with laser-induced fluorescence detection of their fluorescein thiocarbamyl derivatives. *Electrophoresis* **20,** 1862–1868.
11. Oguri, S., Watanabe, S., and Abe, S. (1997) Determination of histamine and some other amines by high-performance capillary electrophoresis with on-line mode in-capillary derivatization. *J. Chromatogr. A* **790,** 177–183.
12. Oguri, S., Tsukamoto, A., Yura, A., and Miho, Y. (1998) Development of a simple high-performance capillary electrophoretic method with on-line mode in capillary derivatization for the determination of spermidine. *Electrophoresis* **19,** 2986–2990.
13. Liu, X., Yang, L. X. and Lu, Y. T. (2003) Determination of biogenic amines by 3-(2-furoyl)quinoline-2-carboxaldehyde and capillary electrophoresis with laser-induced fluorescence detection. *J. Chromatogr. A* **998,** 213–219.
14. Preston, L. M., Weber, M. L., and Murray, G. M. (1997) Micellar electrokinetic capillary chromatography with laser-induced fluorimetric detection of amines in beer. *J. Chromatogr. B* **695,** 175–180.
15. Zhang, L., Huang, W., Wang, Z. L., and Cheng, J. (2002) Determination of histamine by capillary electrophoresis with amperometric detection. *Anal. Sci*. **18,** 1117–1120.
16. Zhou, G., Yu, Q., Ma, Y., Xue, J., Zhang, Y., and Lin, B. (1995) Determination of polyamines in serum by high-performance capillary zone electrophoresis with indirect ultraviolet detection. *J. Chromatogr. A* **717,** 345–349.
17. Liu, J. F., Yang, X. R., and Wang, E. K. (2003) Direct tris(2, 2′-bipyridyl)ruthenium(II) electrochemiluminescence detection of polyamines separated by capillary electrophoresis. *Electrophoresis* **24,** 3131–3138.
18. Ma, Y., Zhang, R., and Cooper, C. L. (1992) Indirect photometric detection of polyamines in biological samples separated by high-performance capillary electrophoreses. *J. Chromatogr*. **608,** 93–96.

19. Du, M., Flanigan, V., and Ma, Y. F. (2004) Simultaneous determination of polyamines and catecholamines in PC-12 tumor cell extracts by capillary electrophoresis with laser-induced fluorescence detection. *Electrophoresis* **25,** 1496–1502.
20. Brumley, W. C. and Kelliher, V. (1997) Determination of aliphatic amines in water using derivatization with fluorescein isothiocyanate and capillary electrophoresis laser-induced fluorescence detection. *J. Liq. Chromatogr.* **20,** 2193–2205.
21. Zhang, L. Y., Liu, Y. M., Wang, Z. L., and Cheng, J. K. (2004) Capillary zone electrophoresis with pre-column NDA derivatization and amperometric detection for the analysis of four aliphatic diamines. *Anal. Chim. Acta* **508,** 141–145.
22. Mattusch, J., Huhn, G., and Wennrich, R. (1995) Sensitive laser induced fluoresence detection of polyamine-fluoresceinisothiocyanate-derivatives after capillary zone electrophoretic separation. *Fresenius J. Anal. Chem.* **351,** 732–738.
23. Bord, N., Cretier, G., Rocca, J. L., Bailly, C., and Souchez, J. P. (2004) Determination of diethanolamine or N-methyldiethanolamine in high ammonium concentration matrices by capillary electrophoresis with indirect UV detection: application to the analysis of refinery process waters. *Anal. Bioanal. Chem.* **380,** 325–332.
24. Dabek-Zlotorzynska, E. and Maruszak, W. (1998) Determination of dimethylamine and other low-molecular-mass amines using capillary electrophoresis with laser-induced fluorescence detection. *J. Chromatogr. B* **714,** 77–85.
25. Matchett, W. H. and Brumley, W. C. (1997) Preconcentration of aliphatic amines from water determined by capillary electrophoresis with indirect UV detection. *J. Liq. Chromatogr.* **20,** 79–100.
26. Pereira, E. A. and Tavares, M. F. M. (2004) Determination of volatile corrosion inhibitors by capillary electrophoresis. *J. Chromatogr. A* **1051,** 303–308.
27. Liu, Y. M. and Cheng, J. K. (2003) Separation of biogenic amines by micellar electrokinetic chromatography with on-line chemiluminescence detection. *J. Chromatogr. A* **1003,** 211–216.
28. Wang, X. and Bobbitt, D. R. (2000) Electrochemically generated Ru(bpy)(3)(3+)-based chemiluminescence detection in micellar electrokinetic chromatography. *Talanta* **53,** 337–345.
29. Sun, X. H., Yang, X. R., and Wang, E. K. (2003) Determination of biogenic amines by capillary electrophoresis with pulsed amperometric detection. *J. Chromatogr. A* **1005,** 189–195.
30. Arce, L., Rios, A., and Valcarcel, M. (1997) Selective and rapid determination of biogenic amines by capillary zone electrophoresis. *Chromatographia* **46,** 170–176.
31. Riviello, J. M. and M. P. H. (1993) Capillary electrophoresis of inorganic cations and low-molecular-mass amines using a copper-based electrolyte with indirect UV detection. *J. Chromatogr. A* **652,** 385–392.
32. Haumann, I., Boden, J., Mainka, A. and Jegle, U. (2000) Simultaneous determination of inorganic anions and cations by capillary electrophoresis with indirect UV detection. *J. Chromatogr. A* **895,** 269–277.

33. Orta, D., Mudgett, P. D., Ding, L., Drybread, M., Schultz, J. R., and Sauer, R. L. (1998) Analysis of water from the Space Shuttle and Mir Space Station by ion chromatography and capillary electrophoresis. *J. Chromatogr. A* **804,** 295–304.
34. Beck, W. and Engelhardt, H. (1992) Capillary electrophoresis of organic and inorganic cations with indirect UV detection. *Chromatographia* **33,** 313–316.
35. Zhang, R., Cooper, C. L., and Ma, Y. (1993) Determination of total polyamines in tumor cells by high-performance capillary zone electrophoresis with indirect photometric detection. *Anal. Chem.* **65,** 704–706.
36. Chiou, C. S. and Shih, J. S. (1998) Application of crown ethers as modifiers for the separation of amines by capillary electrophoresis. *Anal. Chim. Acta* **360,** 69–76.
37. Schubert, B. A., Hohaus, E., Dengel, H. S., Riepe, W., and Maurer, W. (1996) Determination of alkanolamines in water-miscible cooling lubricants by capillary zone electrophoresis. *Gefahrstoffe-Reinhaltung der Luft* **56,** 393–399.
38. Krizek, M. and Pelikanova, T. (1998) Determination of seven biogenic amines in foods by micellar electrokinetic capillary chromatography. *J. Chromatogr. A* **815,** 243–250.
39. Maruszak, W. (1999) Analysis of aliphatic amines by micellar electrokinetic chromatography. *Hrc-J. High Resolut. Chromatogr.* **22,** 126–128.
40. Molina, M. and Silva, M. (2002) In-capillary derivatization and analysis of amino acids, amino phosphonic acid-herbicides and biogenic amines by capillary electrophoresis with laser-induced fluorescence detection. *Electrophoresis* **23,** 2333–2340.
41. Tsuda, T., Kobayashi, Y., Hori, A., Matsumoto, T., and Suzuki, O. (1990) Separation of polyamines in rat tissues by capillary electrophoresis. *J. Microcolumn Sep.* **2,** 21–25.
42. Paproski, R. E., Roy, K. I., and Lucy, C. A. (2002) Selective fluorometric detection of polyamines using micellar electrokinetic chromatography with laser-induced fluorescence detection. *J. Chromatogr. A* **946,** 265–273.
43. Schmitt-Kopplin, P., Garmash, A. V., Kudryavtsev, A. V., et al. (2001) Quantitative and qualitative precision improvements by effective mobility-scale data transformation in capillary electrophoresis analysis. *Electrophoresis* **22,** 77–87.
44. Macka, M., Johns, C., Doble, P., Haddad, P. R., and Altria, K. D. (2001) Indirect photometric detection in CE using buffered electrolytes: part I, principles. *Lc Gc North America* **19,** 38.
45. Fekete, J., Morovjan, G., Csizmadia, F., Darvas, F. (1994) Method development by an expert system: Advantages and limitations. *J Chromatogr. A* **660**, 33–46.
46. Rush, R. S. and B. L., K. (1990) Sample injection with PACE System 200: importance of temperature coontrol withh respect to quantification (technical bulletin TIBC-104). Beckman Instruments, Spinco Division, Paolo Alto, CA, USA. Harry Whatley, CE Expert Lite, Beckmann, Waldborn, Germany. http://www. beckman coulter. com/resourcecenter/labresources/ce/ceexpert.asp

5

Capillary Electrophoretic Analysis of Organic Pollutants

Ashok Kumar Malik, Jatinder Singh Aulakh and Varinder Kaur

Summary

Environmental pollutants comprise a variety of compounds from inorganic anions, cations, ionizable organic compounds and moderately hydrophobic organic compounds to highly hydrophobic organic compounds. Correspondingly different separation strategies are required for their separation. In this chapter, we have presented some methods for the separation and the analysis of the organic pollutants such as polycyclic aromatic hydrocarbons, phenoxy acids, dithiocarbamates, paraquat and diquat, endocrine disruptors, toxins and explosives.

Key Words: Capillary electrophoresis; UV detection; environmental organic pollutants; phenoxy acids; dithiocarbamates; paraquat and diquat; endocrine disruptors; toxins; explosives.

1. Introduction

The monitoring of organic micropollutants is today one of the major challenges of environmental analytical chemistry. More than 10 million compounds have been registered, of which the human and/or animal population can come into contact with at least 76,000 ***(1)***. Many of these compounds can enter the environment via surface and ground water. To prevent pollution, analytical chemists should develop systems that can give fast and reliable information on the identity and amount of suspected pollutants. As regards the surface water, the detection of many organic compounds is typically required at the level of 1–3 $\mu g l^{-1}$. Capillary electrophoresis (CE) has an unrealized potential for analytes of environmental concern, particularly those that are more polar and ionic. Sovocool *et al.* ***(2)*** have reviewed the various organic

From: *Methods in Molecular Biology, vol. 384: Capillary Electrophoresis*
Edited by: P. Schmitt-Kopplin © Humana Press Inc., Totowa, NJ

and inorganic pollutant analyses using CE. Most of the common organic environment pollutants reported are polycyclic aromatic hydrocarbons (PAHs), aromatic and alkyl sulfonates, phenols, small carboxylic acids, explosives, dyes and radioactive materials. Various aspects for the analysis of agrochemicals (pesticides) are reviewed by Malik *et al.* ***(3)*** and Garisson *et al.* ***(4)***.

UV-VIS detection is the most widely used detection method in commercial CE instruments ***(5)*** **(Note 1)**. The majority of the work ***(6)*** with ultra-violet UV-VIS detection is focused on methods that improve analysis precision and detection limits and system miniaturization. Such methods include the use of capillaries with widened inner diameter (ID) at the position of detection and compact light sources such as light-emitting diodes (LEDs). In normal detection systems, the maximum optical path length correspond to the ID of the separation capillary (usually in the range of 30–100 μm), which limits optical detector sensitivity as a result of the small detection volume. Recently, Strasik *et al.* ***(7)*** used a wide-bore capillary tube (320 μm ID) for the detection and identification of the analytes after capillary zone electrophoresis (CZE) separation with fiber optics coupled to a diode array detector (DAD). Concentration detectabilities of 0.2–1.0 μmol l^{-1} of the CZE analyses by this combination were ascribed to a 250-μm mean effective path length of the detection cell that dramatically increased the photon flux through the cell.

A photodiode array detector has also been used for the detection and separation of explosives ***(8)***. The use of LEDs as a light source relies on the formation of a colored derivative between analytes and additives, which shifts the monitoring wavelength into the red (e.g., >500 nm). LED as a light source is particularly attractive for absorption detection because of its excellent output stability, low power requirements and low cost. Most importantly, LED could be easily implemented into an electrophoresis microchip as a result of its small size.

Generally, the main steps ***(9)*** involved in the environmental analysis are (1) sampling and sample preparation, (2) clean-up and/or extraction, (3) preconcentration and (4) final separation with qualitative and quantitative determination. Because the analytes can be contained in a wide variety of matrices (i.e., aqueous samples, which can include water from rain, tap, river, marine ground and industrial wastes; solid samples, which can include soils and sediments and other types of solid waste; and air samples). A great effort has been made to deal with the handling of the environmental samples before CE ***(10,11)***.

This chapter exemplifies some methods taken from literature for separation and analysis of the organic pollutants such as PAHs, phenoxy acids, dithiocarbamates, paraquat and diquat, endocrine- disrupting compounds (EDCs), toxins and explosives.

2. Materials and Equipment

2.1. Analysis of Polycyclic Aromatic Hydrocarbons (11)

The PAHs are very important environmental pollutants. Their analysis is very important because of their toxicity, mutagenicity and carcinogenicity to animals. In this section, a method described by Grimmer *et al.* ***(11)*** is presented as an example.

1. Analytes: the pollutant PAH mixture of anthracene, benzo[a]pyrene, chrysene, fluorene, phenanthrene, pyrene and fluoranthene at a concentration of 1 mg/mL each in acetonitrile.
2. Sample: a mixture of machine oil from a garage and soil sample. For the machine sample, contaminate 30 g of sand (heath) with 1 mL of spent machine oil. Extract after 2 h with acetonitrile. For the soil sample, take 10 g of sand (heath) with 0.5 mL of a solution containing the seven standard PAHs, each at a concentration of 1 mg/mL.
3. Sample preparation: extract the PAHs from the soil samples with the help of 6 mL cyclohexane with vigorous shaking (15 min), wash with an additional 4 mL of cyclohexane and dissolve the residue in 0.5 mL of acetonitrile. Extract the PAHs from the machine oil-contaminated soil with 10 mL cyclohexane, dry the residue and dissolve in 2.5 mL of acetonitrile.
4. CE instrument and capillary: fused-silica capillaries of 50 μm ID are used. Perform the detection with a UV detector.
5. CE buffer: 8.5 m*M* borate buffer (pH 9.9) containing 85 m*M* sodium dodecyl sulfate (SDS) and 50% (v/v) acetonitrile as the electrophoresis buffer. The mobile phase should be thoroughly degassed by ultrasonication. Apply a vacuum of 30 mbar for 5 s.

2.2. Analysis of Phenoxy Acids (12)

Phenoxy acids are an important class of pesticides that have a high toxicity even at low concentrations. Various methods are available for the analysis of phenoxy acids ***(12)*** and their enantiomers. Here, we have presented a simple method for the analysis of the phenoxy acids.

1. Analyte: sample solutions of phenoxy acid herbicides (2,4-dichlorophenoxy) acetic acid (2,4-D); 2-(2,4,5-Tricholorophenoxy) propionic acid (fenoprop); 2-(4-chloro-2-methyl-phenoxy)propionic acid (Mecoprop); and 2-(2,4-dichlorophenoxy)propionic acid (dichloroprop). Dissolve 40 mg of each analyte in 100 mL of pesticide-grade methanol and dilute 1:100 to prepare 4 μg/mL of each analyte. **The acid** structure of phenoxy acids is shown in **Fig. 1**.
2. CE instrument and capillary: Beckman P/ACE 2100 series HPCE with Beckman system Gold chromatography software. The fused-silica CE column (65 cm [50 cm to the detector] × 300 μm, outer diamter [OD] × 75 μm ID) fitted in a 100 × 200 μm aperture cartridge. Maintain temperature is 30 °C, voltage is 20 kV and the detector wavelength is 230 nm.
3. CE buffer: acetate buffer: 0.05 *M* glacial acetic acid and 0.05 *M* sodium acetate (1:1, v:v) at a concentration of 25 m*M*, pH 4.45.

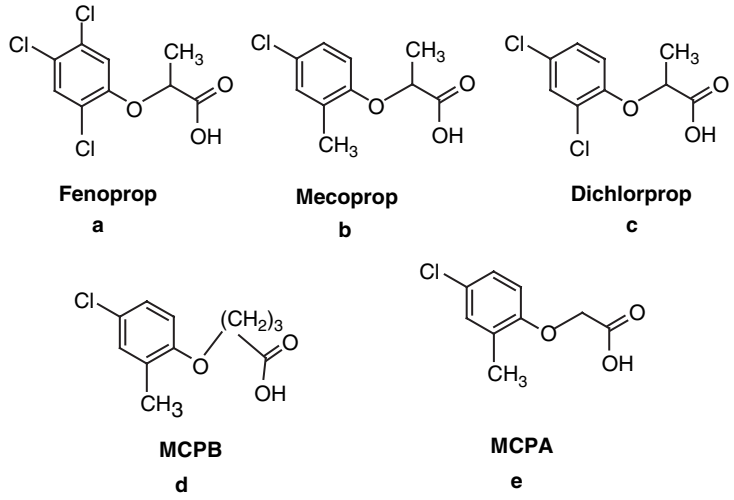


Fig. 1. Structures of phenoxy acids (a) 2-(2,4,5-tricholorophenoxy) propionic acid (Fenoprop), (b) 2-(4-chloro-2-methyl-phenoxy) propionic acid (Mecoprop), (c) 2-(2,4-dichlorophenoxy) propionic acid (Dichloroprop), (d) 4-(4-chloro-2-methylphenoxy) butanoic acid (MCPB) and (e) (4-chloro-2-methylphenoxy) acetic acid (MCPA).

2.3. Analysis of the Dithiocarbamate Pesticides (13,14)

Dithiocarbamates are an important class of compounds that find application in rubber industry as vulcanization accelerators and in agriculture as fungicides. Here, a method for the analysis of these compounds that is applicable for their analysis in grains and in commercial samples is described.

1. Analytes: prepare stock solutions (200 mg/L^{-1}) of maneb and metham (Riedel-de Haën Germany) and sodium diethyl dithiocarbamate trihydrate and potassium o-ethylxanthate (Fluka, Germany) (except maneb) by dissolving 20 mg of each compound in double-distilled water and diluting to 100 mL in a calibrated flask. Prepare stock solution of maneb by dissolving maneb in 0.1 *M* NaOH and diluting further with distilled water. Prepare working solutions of lower concentrations by appropriate dilutions with water.
2. Sample: grains and commercial samples (Dithane M 45).
3. Sample preparation:

   (a) Extraction from grains: weigh about 10 g of grain sample accurately and spray with 5 mL of aqueous dispersions of maneb containing different amounts of 0.1% solution. Dry the samples in the sun for 1 h and thereafter in the shade for 24 h to remove excess moisture. Carry out for each determination a blank assay by spraying the same amount of grain with 5 mL of water. Treat the grounded samples with 50 mL of 0.1 *M* NaOH, fortify for 10 min and

centrifuge at 2000 rpm for 5 min. Filter the aliquots of the resulting solutions through a 45 μm filter and analyze by the general procedure.

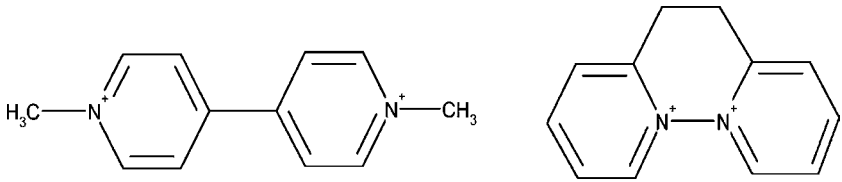
(b) Commercial sample: apply the method to the determination of maneb in a commercial sample of Dithane M 45. Dissolve it in 0.1 *M* NaOH and further dilute with distilled water.

4. CE instrument and capillary: fused-silica capillaries (100 μm ID, 75 cm long and 45 cm to the detector) were used. Inject the solutes for 2 s (injection volume 13.1 nL) in the hydrodynamic mode by vacuum. TSP 1000 software was used for data acquisition. Perform detection by direct UV absorbance at 254 nm.
5. CE buffer: Electrophoretic sodium tetraborate buffer solution (20 m*M*, pH 9.0 Merck, Germany).

2.4. Analysis of Paraquat and Diquat (15,16)

Paraquat and diquat belong to quaternary class of herbicides. These are quick-acting herbicides that are absorbed by the plants and translocated, which results in desiccation of the foliage. These are strongly adsorbed by the soil and are thus deactivated quickly. A representative method for the analysis of paraquat and diquat is given below.

1. Analytes: use chemicals of analytical-reagent grade and double-distilled water for the preparation of solutions of paraquat and diquat. 2-Amino pyridine can be used as the internal standard. Use phenol as the tracer to measure the electroosmotic flow (EOF). Prepare paraquat and diquat solutions in 0.1 *M* sodium phosphate (pH 3.5) running electrolyte. The structures of paraquat and diquat are shown in **Fig. 2**. Filter all the solutions with 0.2 μm filter to avoid capillary plugging.
2. Sample: waste water sample.
3. Sample preparation: filter the water sample through a 0.2 μm filter.
4. CE instrument and capillary: the CE system consists of a 30 kV direct current power supply of positive polarity and a system equipped with a UV absorbance detector. Fused-silica capillaries (50 μm ID, 80 cm long and 50 cm to the detector) were used. Inject paraquat and diquat for 2 s (injection volume 13.1 nL) in the hydrodynamic mode by vacuum and record the electropherogram with a UV-Visible recording spectrophotometer model from Shimadzu.
5. CE buffer: 0.10 *M* sodium phosphate, pH 3.5.



Paraquat Diquat

Fig. 2. Structures of paraquat and diquat.

2.5. Analysis of Endocrine Disruptors (17)

Today, various chemicals are found to have endocrine-disrupting effects. For the assessment of human exposure to these chemicals, analytical methods for their identification are required. In this section, a method developed by Regan *et al.* ***(17)*** as a representative of EDCs is described.

1. Analytes: pentachlorophenol (PCP), trichlorophenol (TCP), 17β-oestradiol, dichlorophenol (DCP), oestrone, oestriol, diethylstilbestrol (DES), ethynyloestradiol, lindane, dieldrin, octylphenol (OP), nonylphenol (NP), bisphenol-α (BPA), 4 nonyl-phenol (85% content of *p*-isomers) and cyclohexylamino-1-propane. The structure of EDCs are shown in **Fig. 3**.
2. Sample: river water
3. Sample preparation: a river water sample was spiked with six test analytes (NP, OP, NPEO, DES, ES and BPA) for analysis using cyclodextrin-modified micellar electrokinetic chromatography (CD-MEKC) in the EOF-suppressed mode. In order to minimize differences between the sample zone and surrounding buffer zone, some of the key buffer components, including cyclodextrin, surfactant and buffer, were added directly to the river water sample prior to analysis. As a result of the limited solubility of analytes in aqueous samples at high concentrations, 10 mL of acetonitrile was added to aid analyte solubility. The analyte concentration was equivalent to 20 mg/L. An unspiked sample was analyzed in order to identify possible matrix effects.
4. CE instrument and capillary: Beckman P/ACE 2100 series HPCE with Beckman system with window P/ACE Station Software version 1.21 For integration, data can be evaluated using P/ACE Station using the United States Pharmacopoeia (USP) method. The fused-silica CE column was 57 cm long with an internal diameter of 50 μm. The temperature was maintained at 30 °C, voltage was 20 kV and the detector wavelength was 230 nm.
5. CE buffer: cyclohexylamino-1-propane sulfonic acid (CAPS), disodium tetraborate, sodium acetate and sodium phosphate (Sigma-Aldrich) HCl, NaOH, methanol (HPLC-grade), acetonitrile (ACN; HPLC grade) and SDS are from Sigma-Aldrich. CAPS buffer pH was adjusted using 0.1 *M* HCl and 0.1 *M* NaOH. α- and β-cyclodextrins are from Sigma-Aldrich.

2.6. Analysis of Toxins (18)

The analysis of toxins is very important because of their food poisoning effect. Here is presented a routine and practicable method for the analysis of toxins that is exemplified with the analysis of Domoic acid from mussel tissue as described by Pineiro *et al.* ***(18)***.

1. Analytes: Domoic acid calibration solution (DACS-1B) and mussel tissue reference material (MUS-1) containing 100 mg DA/mL and 100 mg DA/g, respectively, can

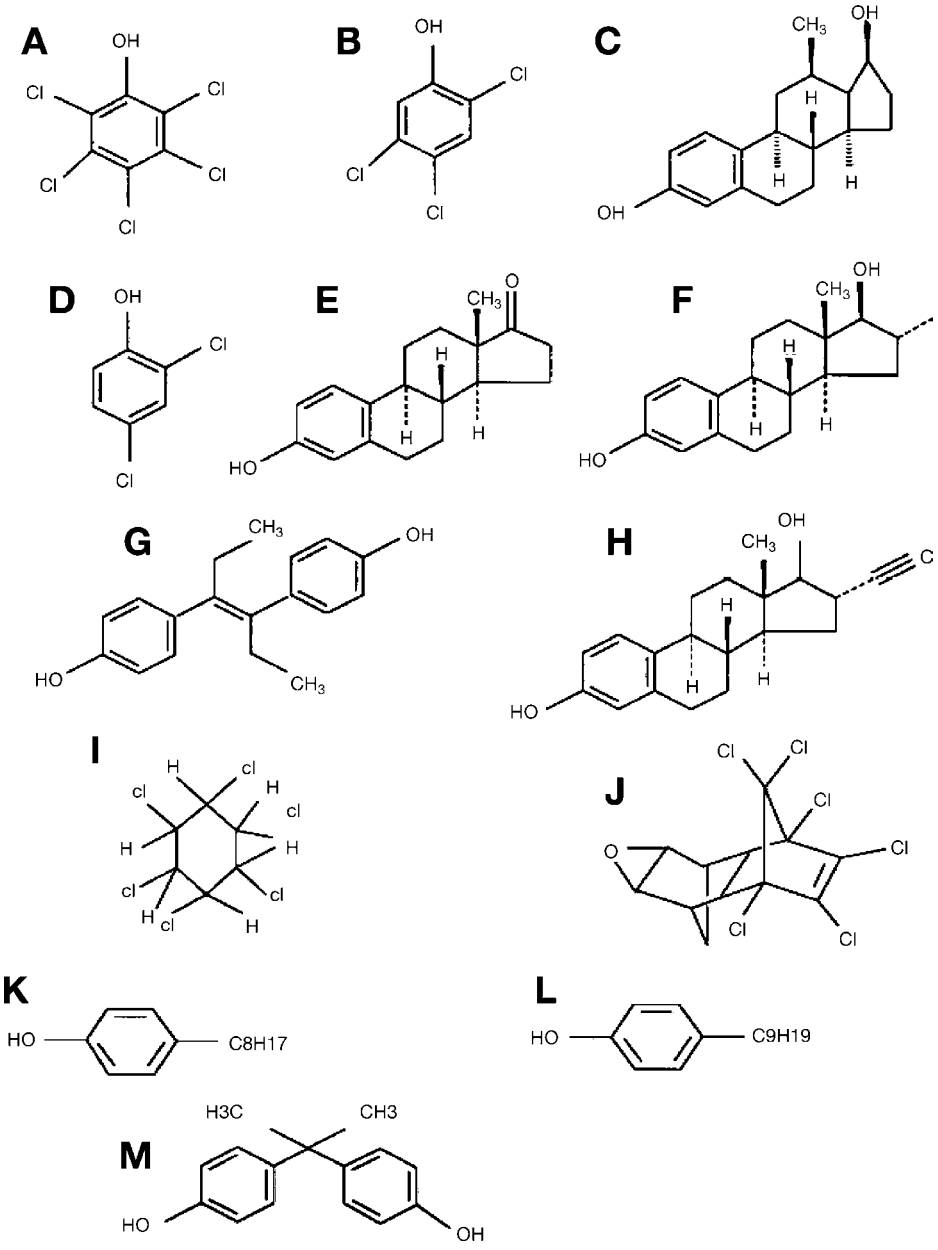
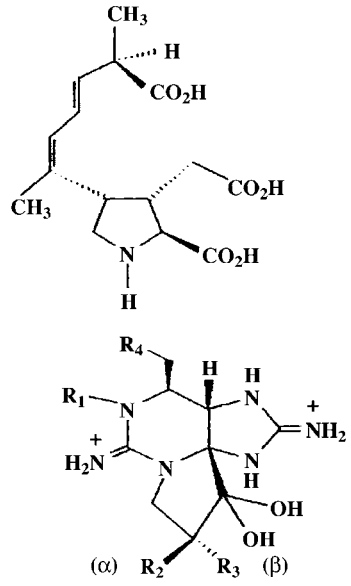


Fig. 3. Structures of some typical endocrine-disrupting compounds used in this study. **(A)** Pentachlorophenol (PCP); **(B)** trichlorophenol (TCP); **(C)** 17β-oestradiol; **(D)** dichlorophenol (DCP); **(E)** oestrone; **(F)** oestriol; **(G)** diethylstilbestrol (DES); **(H)** ethynyloestradiol (EO); **(I)** lindane; **(J)** dieldrin; **(K)** octylphenol (OP); **(L)** nonylphenol (NP); **(M)** bisphenol-A (BPA). (From **ref.** ***17***.)

be obtained from the Marine Analytical Chemistry standards Program, National Research Council of Canada. Acetic acid solutions (0.03 *M*) of saxitoxing (STX) and decarbamoyl saxitoxin (dcSTX) (20 mg/mL) were provided by RIVM hoven, The Netherlands. For breakpoint cluster region (BCR), standard measurements and testing program certification study were used. The chemical structure of domoic acid and paralytic shellfish-poisoning (PSP) toxins are shown in **Fig. 4**.



			R_4		
R_1	R_2	R_3	Caramoyl toxins	N-sulfocarbamoyl toxins	Decarbamoyl toxins
H	H	H	STX	GTX5	dcSTX
H	H	OSO_3^-	GTX2	epiGTX8	dcGTX2
H	OSO_3^-	H	GTX3	GTX8	dcGTX3
OH	H	H	neoSTX	GTX6	dcneoSTX
OH	H	OSO_3^-	GTX1	C3	dcGTX1
OH	OSO_3^-	H	GTX4	C4	dcGTX4

Fig. 4. Chemical structure of **(A)** Domoic acid and **(B)** paralytic shellfish-poisoning toxins. (From **ref.** ***18***.)

2. Sample: amnesic shellfish poisoning (ASP)-contaminated samples of razor clams and mussels from Rıa de Vivero (Lugo) can be obtained from Delegacion 'Provincial de Pesca de Lugo, Conselleria de Pesca, Xunta de Galicia. PSP-contaminated mussel samples from Rıa de Vigo can be obtained from by Conselleria de Sanidade, Xunta de Galicia. Freeze the samples at −18 °C until analysis.
3. Sample preparation:
   (a) Extraction of domoic acid: to 4 g homogenized tissue, add 16.0 mL methanol–water (1:1, v/v). This mixture was homogenized for 3 min and then centrifuged at 4500 rpm for 10 min. Filter the supernatant through a 0.45-mm filter (Millex-HV) and keep in a refrigerator until analysis.
   (b) The conditions required for clean-up of ASP toxins are as follows: (1) Pass 5.0 mL of extract through a strong anion-exchange (SAX) cartridge (3 mL capacity, 500 mg; part No. 1210–2044, lot No. 182639, Varian) previously conditioned with methanol, water and methanol–water (1:1, v/v). Wash the extract with methanol–water (1:1) and elute with 5 ml 0.1 *M* formic acid. (2) Load through a strong cation-exchange (SCX) cartridge (10 mL/500 mg size; part No. 1211–3039, lot No. 171069, Varian) preconditioned with methanol, water and 0.1 *M* formic acid, 5 mL of SAX. Wash the cartridge with 5 mL of 0.01 *M* formic acid. Elute with 0.5 mL of 25 m*M* sodium tetraborate (pH 9.2)–acetonitrile (9:1, v/v). Elute with six portions of 2 mL of 25 m*M* sodium tetraborate (pH 9.2)–acetonitrile (9:1); Domoic acid starts to appear in the third eluate.
   (c) Extraction and clean-up of PSP toxins: extract the PSP toxins from muscle samples for the analysis of PSP toxin in food. Pass the 3.0-mL volume of supernatant obtained in the extraction procedure through a C_{18} cartridge and collect 1.5–2.0 mL of eluate for the analysis. Condition the cartridge with methanol and water. After purification on a C_{18} cartridge, ultrafilter the extracts in a 0.45- to 18-μm membrane (Ultrafree-MC, Millipore) and analyze by CE–UV.
4. CE instrument and capillary: a CE system model HP with diode array detection system. Different capillaries and conditions are required for the ASP and PSP toxin analysis:
   (a) For analysis of ASP toxins, use fused-silica capillaries of 66 cm × 363 μm OD, 50 μm ID with a UV window located 15 cm from the exit end of the capillary at room temperature and perform detection at 242 nm. Inject the sample at 50 mbar for 12 s and apply a voltage of 30 kV.
   (b) For PSP toxins, perform the CE separations in a polyvinyl alcohol (PVA) capillary (104 cm × 75 μm ID) under a constant voltage of 20 kV at the injector end of the capillary. Apply the sample under constant pressure (50 mbar) such that 20% volume of the capillary is introduced. Perform the UV detection at 200 nm.

5. CE buffer: For ASP toxins: 25 m*M* borate buffer. For PSP toxins: The capillary iso-tachophoretic (cITP) electrolyte is 10 m*M* formic acid. cITP preconcentration is performed with 50 m*M* morpholine in water adjusted to pH 5.0 with formic acid.

2.7. Analysis of Explosives

Explosives and their degradation products are important environmental contaminants. Standard methods for their analysis are required forensic activity. Here, the analysis of nitramine, with nitro aromatic explosives as their representative, is described ***(19)***.

1. Analytes: explosives as given in **Table 1**.
2. Sample: extract the small sample of explosive with less than 3–4 mL of acetonitrile.
3. Sample preparation: dilute the extracts with the running electrolyte in a ratio of 1:5.
4. CE instrument and capillary: CE system with detection at 185 nm, 214 nm, 229 nm and 254 nm. AccuSep polyimide fused-silica capillaries (Waters, Milford, MA) of dimension 60 cm × 50 μm ID were used. Computer control and data acquisition was carried out with a Waters Millennium 2010 Chromatography Manager.
5. CE buffer: 25 m*M* mono- and dibasic phosphate (dilute the contents of packet to 200 mL) as electrolyte solution. Add SDS (electrophoresis grade, Millipore) to a final concentration of 50 m*M* of SDS.

Table 1
Names and Abbreviations of Explosives Analyzed by Micellar Electrokinetic Chromatography

Name	Abbreviation
1,3,5,7-tetranitro-*N*-methylaniline	HMX
1,3,5-trinitro- 1,3,5-triazacyclohexane	RDX
1,3,5-trinitrobenzene	TNB
trinitrotoluene	TNT
2,4-dinitrotoluene	2,4-DNT
2,6-dinitrotoluene	2,6-DNT
1,2,3-propanetriol trinitrate (nitroglycerin)	NG
pentaerythritol tetranitrate	PETN
2,4,6-*N*-tetranitro-*N*-methylaniline	Teryl
2-nitrotoluene	2-NT
3-nitrotoluene	3-NT
4-nitrotoluene	4-NT
nitrobenzene	NB
1,3-dinitrobenzene	DNB

3. Methods

3.1. Analysis of PAHs

1. Inject the sample solution into the capillary and record the capillary electropherogram (*see* **Notes 2 and 3**).
2. Prepare the standard calibration curve for the analysis of the PAHs.
3. Inject these samples into the capillary and determine the concentration of the unknown samples.
4. **Figs. 5** and **6** show the separation of the PAHs by the SDS and cetyltrimethylammonium bromide (CTAB) methods.
5. **Fig. 7** shows the capillary electropherogram for the determination of PAHs from soil spiked with machine oil.

3.2. Analysis of Phenoxy Acids

1. Maintain the capillary at a constant temperature of 30 °C.
2. Rinse the capillary with 0.1 *M* NaOH and the separation buffer before each run.
3. Operate the CE system at a voltage of 20 kV.

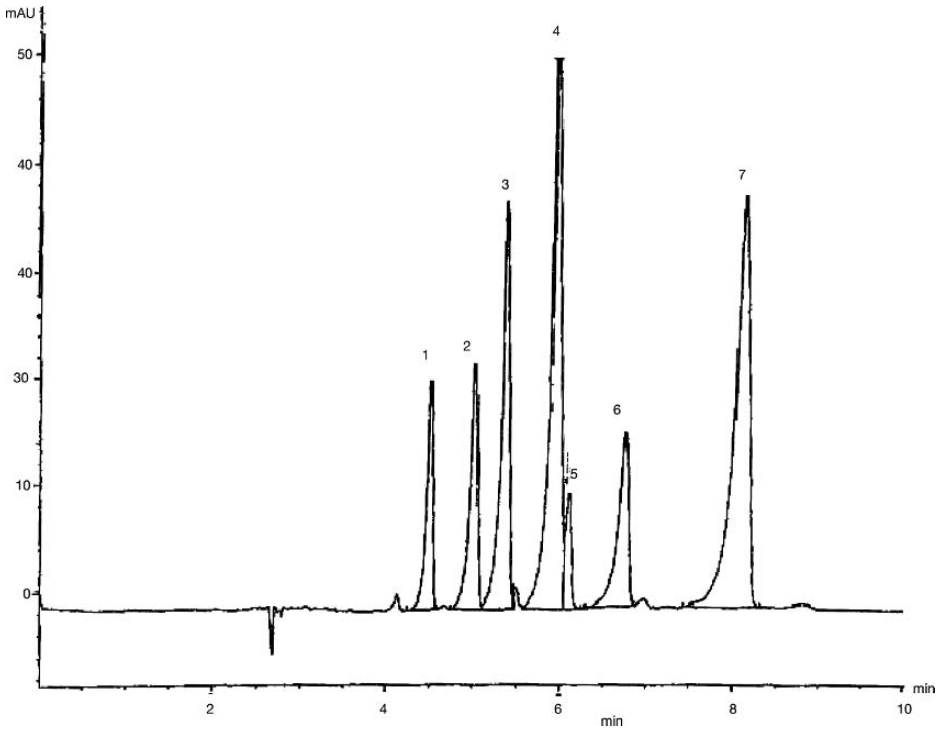


Fig. 5. Separation and calibration graph for the standard polycyclic aromatic hydrocarbons (sodium dodecyl sulfate method). (From **ref.** ***11***.)

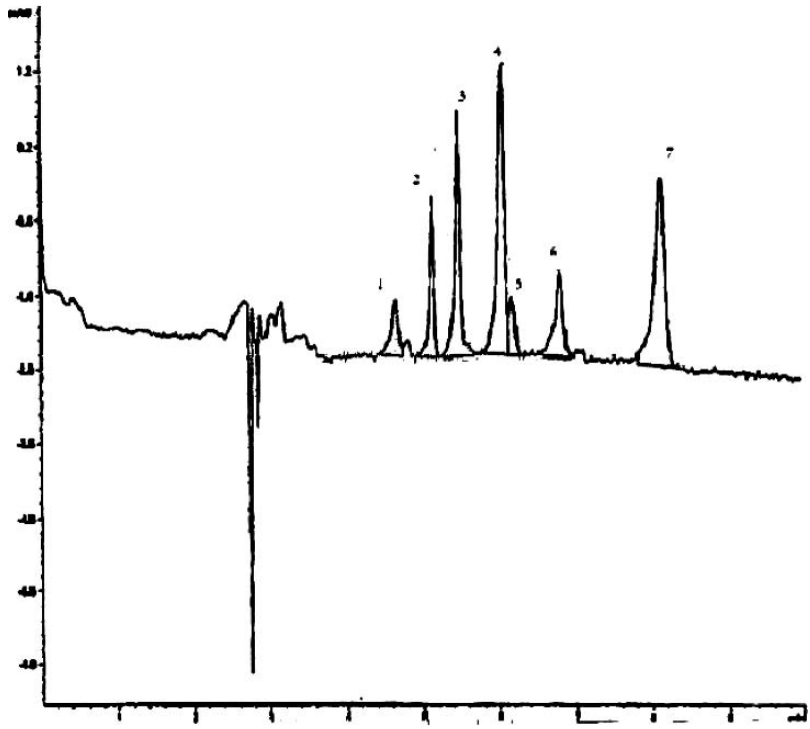


Fig. 6. Separation of a standard mixture of PAH by the CTAB method. (1) anthracene (2) fluorene (3) phenanthrene (4) fluoranthene (5) pyrene (6) chrysene, (7) benzo[a]pyrene (**ref. *11***.)

4. Inject the sample hydrodynamically for 5 s.
5. **Fig. 8** shows the separation of the phenoxy acids.

3.3. Analysis of Dithiocarbamates

1. Rinse the capillary consecutively with 1 *M* NaOH, 0.1 *M* NaOH and water for 2 min and equilibrate with the carrier electrolyte for 2 min.
2. Between the electrophoretic separations, perform equilibrium step with carrier electrolyte. Filter all electrolyte solutions through a 0.45-μm membrane filter.
3. Prepare the calibration graphs by injecting a series of solutions dithiocarbamates into the capillary. **Fig. 9** shows electropherogram for the separation of a mixture of dithiocarbamates using CE.
4. The detection limits reported are 1.33, 174 and 2.16 μ*M* for metham, potassium-o-ethylxanthate and maneb.
5. A typical capillary electropherogram of the commercial sample of maneb is shown in **Fig. 10** (*see* **Note 4**).

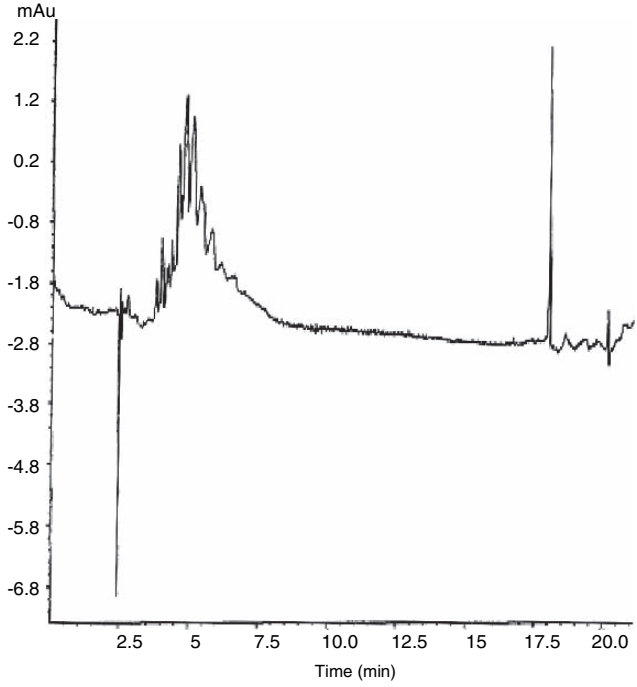


Fig. 7. Analysis of a soil sample contaminated with machine oil. (From **ref. *11***.)

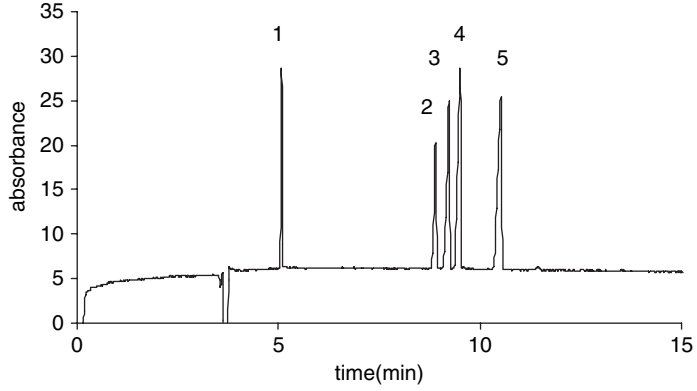


Fig. 8. Electropherogram of the phenoxy acid herbicides (1) MCPB, (2) Fenoprop, (3) Mecoprop, (4) Dichloroprop and (5) MCPA, each at a concentration of 20 ppm. Background electrolyte: 25 mmol acetate buffer, pH 4.5. Capillary dimensions: total length 57 cm, length to detector 50 cm, 75 μm (i.d). Instrumental conditions: P/ACE 5510 CE system, temperature 30 °C, separation voltage 30Kv, wavelength 215 nm, sample injection time 5 second.

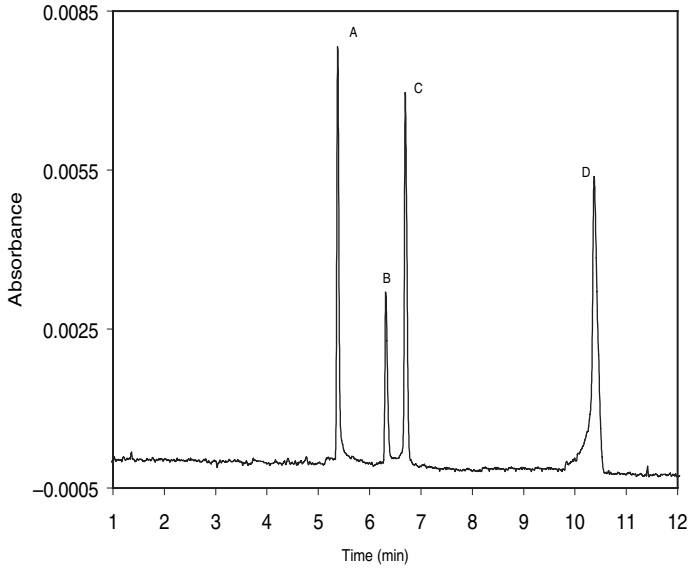


Fig. 9. Capillary electropherogram of sodium diethyldithiocarbamate (0.083 m*M*) **(A)**, potassium o-ethylxanthate (0.017 m*M*) **(B)**, metham (0.018 m*M*) **(C)** and (0.04 m*M*) maneb **(D)** using 20 m*M* boric acid buffer (pH 9.0) as the carrier electrolyte, voltage applied 25 kV, detection at $\lambda = 254$ nm. (From **ref. *14***.)

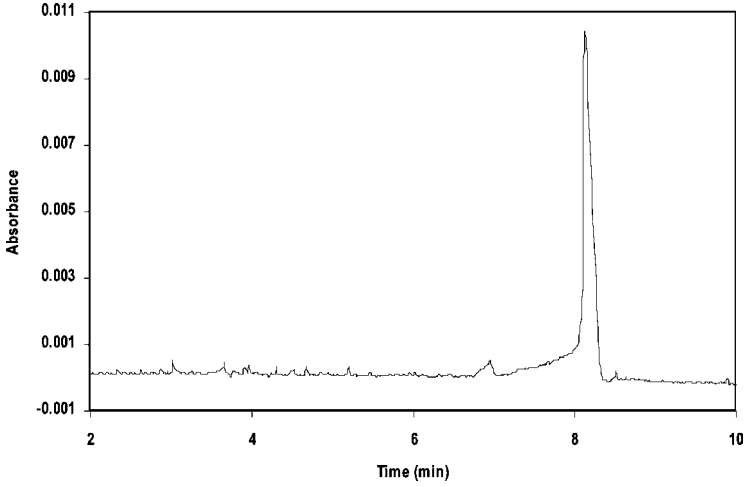


Fig. 10. Capillary electropherogram of a commercial sample of maneb (Dithane M 45) 0.074 m*M*, other conditions same as in **Fig. 9**. (From **ref. *14***.)

6. Analyse the dithiocarbamates extract from wheat grains taking untreated samples of wheat grains as reference.

3.4. Analysis of Paraquat and Diquat

1. Rinse the capillary with 0.1 *M* NaOH and the separation buffer before each run.
2. Operate the CE system at of 15 kV.
3. Inject the samples and prepare the standard calibration curves for the determination of paraquat and diquat.
4. A typical electropherogram is shown in **Fig. 11** for the determination of paraquat and diquat.
5. The λ_{max} and molar absorptivity of paraquat and diquat are 258 and 308 nm, respectively; for 2-aminopyridine, they are 229 and 290 nm, respectively.
6. The limits of detection are found to be 0.40 and 0.50 μg/mL for paraquat and diquat, respectively.

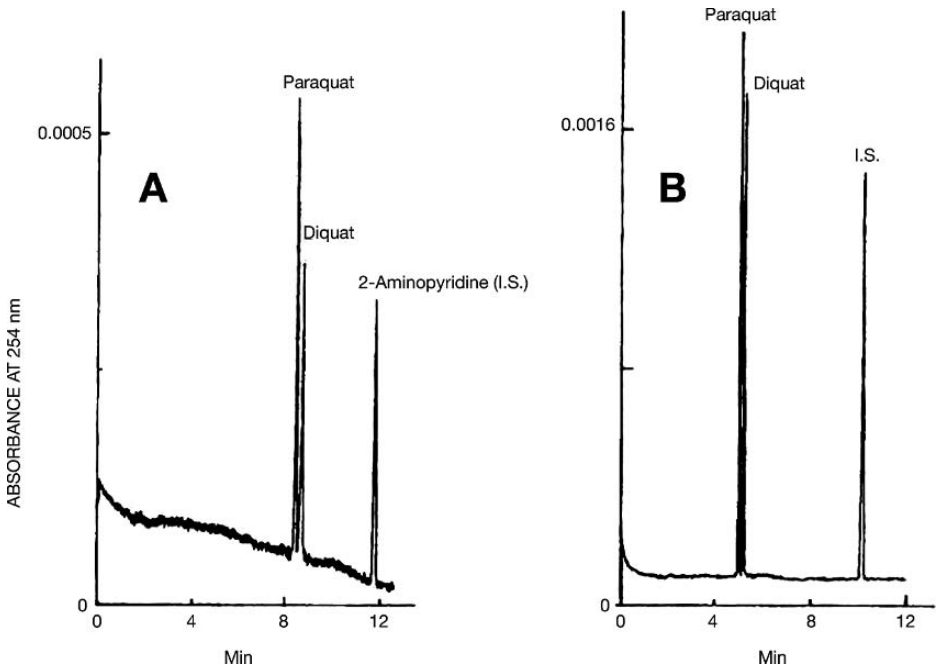


Fig. 11. A typical electropherogram illustrating the rapid separation of herbicides by capillary zone electrophoresis. Separation capillary, untreated fused-silica capillary 50 cm (to the detection point), 80 cm total length, 50 μm (i.d); running electrolyte, 0.10 M sodium phosphate, pH 3.5 in **A** and pH 7.0 in **B**, sample injection time, 5 s, running voltage, 15 kV, internal standard 2-aminopyridine, detection wavelength 254 nm. (From **ref. *16***.)

3.5. Analysis of Endocrine Disruptors

1. Regenerate the capillary before each working day by rinsing it with water for 10 min, with 0.1 *M* sodium hydroxide (NaOH) for 2 min, again with water for 2 min and with BGE for 15 min.
2. Inject the sample hydrodynamically for 5 s with high pressure.
3. Run the sample under 30 kV.
4. Detect the analytes using DAD scanning from 190 to 300 nm.
5. For MEKC and CD-MEKC: add CAPS and SDS to running buffer and perform the separation at 20 kV. The rest of the procedure is same as discussed above.
6. **Fig. 12** shows the separation of 19 EDCs using MEKC.
7. **Fig. 13** indicates the analysis of spiked river water sample.
8. Prepare calibration for the determination of the analytes.

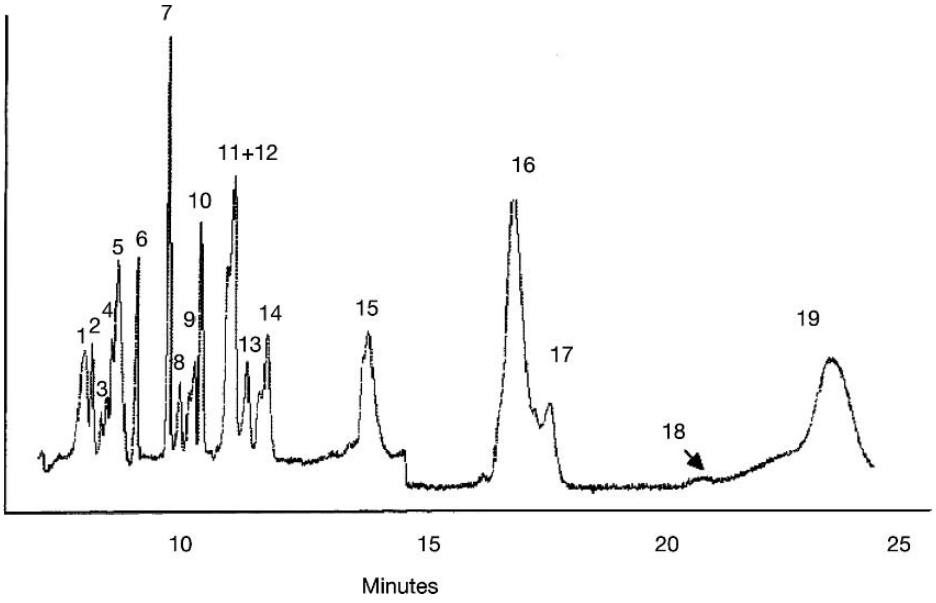


Fig. 12. Separation of 19 target endocrine-disrupting compounds using micellar electrokinetic chromatography. Separation conditions: 20 m*M* cyclohexylamino-1-propane sulfonic acid, pH 11.5 with 15% acetonitrile and 25 m*M* sodium dodecyl sulfate; voltage 20 kV; detection at 200 nm; injection sample MeOH-buffer (50:50, v/v). Peak identification: 1, ethylphenol; 2, oestriol; 3, methylparaben; 4, phenol; propylphenol; 6, lindane; 7, TCP; 8, bisphenol-A; 9, pentachlorophenol; 10 butylphenol; 11, oestrone; 12, 17 β-oestradiol; 13, DES; 14, hexylphenol; 15, dieldrin; 16, ethynyloestradiol; 17, NP12; 18, NP2EO; 19, nonylphenol. (From **ref. *17***.)

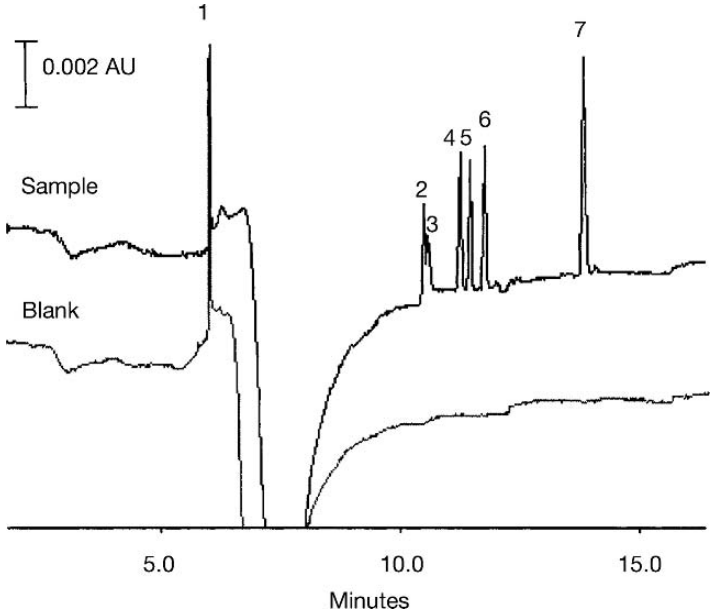


Fig. 13. Analysis of spiked river water sample. Separation conditions: 100 m*M* phosphate, pH 1.8, 25 m*M* sodium dodecyl sulfate, 12.5% acetonitrile (ACN), 1 m*M* HP-b-CD (M.S. 0.8). 1 ve polarity, capillary 57 cm × 50 μm inner diameter; 25 °C. Applied voltage +20 kV; 214 nm. Analytes dissolved in 10% ACN, 90% run buffer. Analyte concentration 20 mg/L. Peak identification: (1) sample matrix, (2) OP, (3) NP, (4) DES, (5) EO, (6) 17 β-oestradiol, (7) BPA. (From **ref. *17***.)

3.6. Analysis of Toxins

3.6.1. CE–UV Analysis of ASP Toxins

1. Perform CE analysis of ASP toxins using fused silica capillaries of 66 cm × 363 μm OD, 50 μm ID with a UV window located 15 cm from the exit end of the capillary at room temperature. Perform the UV detection at a wavelength of 242 nm.
2. For sample injections employ a 50-mbar push for 12 s and the separation voltage of for the separation is 30 kV. Use different buffer–electrolyte concentrations in the range of 10, 25 and 50 m*M* in borate buffer.
3. **Fig. 14** shows CE-UV/DAD analysis of Domoic acid and MUS-1 reference material.

3.6.2. CE–UV Analysis of PSP Toxins

1. CE separation is performed in a polyvinylalcohol (PVA) coated capillary (104 cm × 375 μm ID) under a constant voltage of 20 kV at the injector end of the capillary.

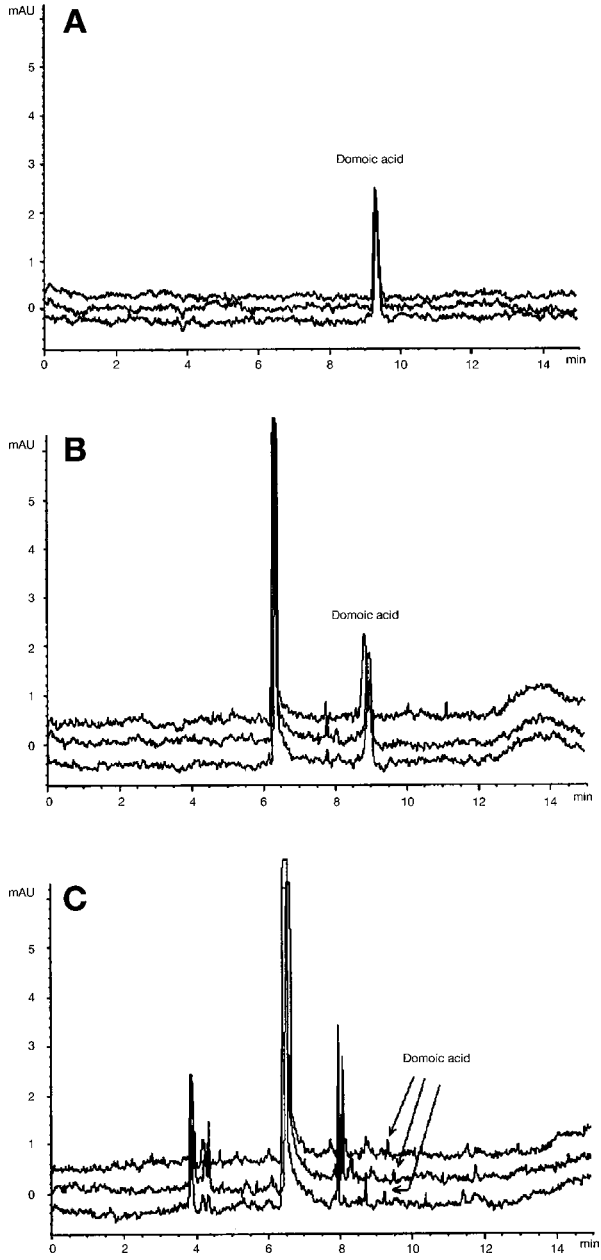


Fig. 14. CE–UV/diode array detector analysis of: **(A)** Domoic acid standard, **(B)** MUS-1 Reference material after strong anion-exchange (SAX)-strong cation-exchange (SCX) clean-up and **(C)** Galician razor clam sample after SAX-SCX clean-up. (From **ref.** ***18***.)

2. Apply the sample under constant pressure (50 mbar) such that 20% volume of the capillary is filled with sample.
3. Operate the UV detector at 200 nm.
4. **Fig. 15** shows CE–UV/DAD analysis of PSP toxins.

3.7. Analysis of Explosives

1. 25 m*M* mono and dibasic phosphate (dilute the contents of packet (Waters) to 200 mL) as electrolyte solution. Add SDS (electrophoresis grade, Millipore) to give a final concentration of 50 m*M* SDS.
2. Prepare solutions of the various explosives as given in **Table 1** in acetonitrile.
3. Take 3–4 mL of extract of the explosives in acetonitrile. Dilute the extracts with the running electrolyte in a ratio of 1:5.
4. Rinse the capillary with 1 *M* NaOH and water for 2 min and equilibrate with the carrier electrolyte for 2 min.
5. Inject the standard samples in to the capillary and prepare the standard calibration curve.
6. **Fig. 16** shows the separation of a mixture of the explosives. The conditions are given as in the caption of the figure.
8. **Figs. 17–19** show the capillary electropherogram for the determination of explosives from different acetonitrile extracts.
9. The detection limit of different explosives is 0.23–0.78 mg/L (S/N = 3).

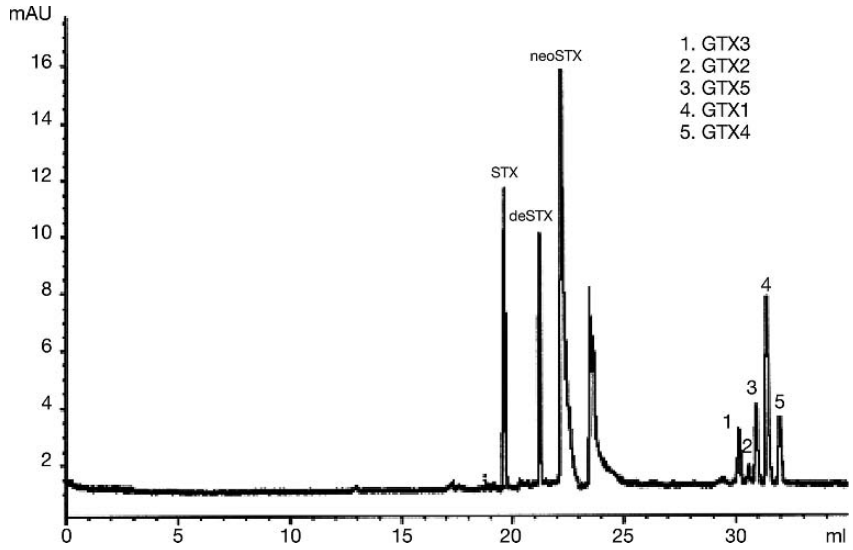


Fig. 15. Standard of paralytic shellfish-poisoning toxins, 20 kV, 50 m*M* morpholine, pH 5.0. (From **ref. *18***.)

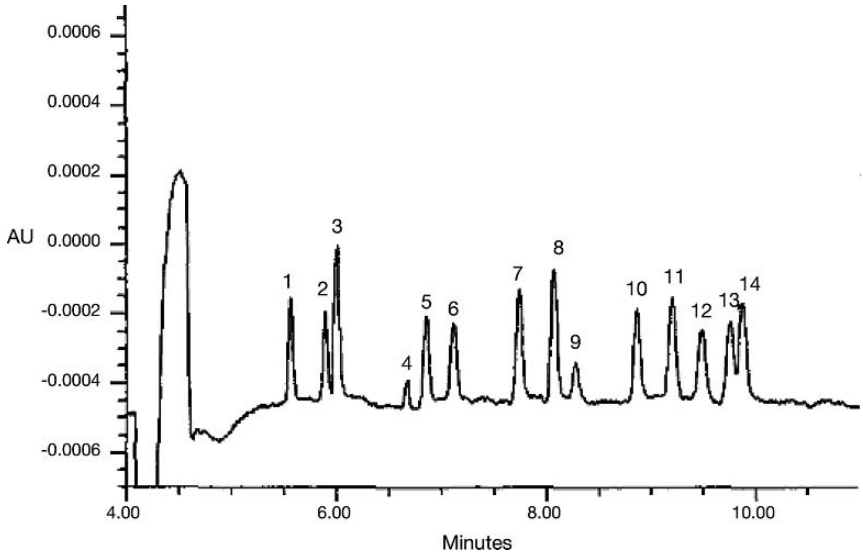


Fig. 16. Electropherogram of a 5 mg/L mixture of explosives standards. Capillary electrophoresis conditions: fused-silica 60 cm × 50 μm inner diamter capillary; voltage, 20 kV; electrolyte, 25 m*M* phosphate-50 m*M* sodium dodecyl sulfate; direct ultraviolet detection at 214 nm; hydrostatic injecton (10 cm for 20 s). Solutes: I, HMX; 2, RDX; 3, TNB; 4, NG; 5, DNB; 6, NB; 7, TNT; 8, Tetryl; 9, PETN; 10-2,4-DNT; I I, 2,6-DNT; 12-2-NT; 13, 3-NT; 14, 4-NT. Refer to **Table 2** for full names of solutes. (From **ref. *19***.)

4. Notes

1. A comparison of various detectors is given in **Table 2**.
2. Wash and rinse the capillary with 0.1 *M* NaOH and with buffer solution, respectively.
3. The buffer in the outlet vial is to be exchanged after each run to improve the reproducibility. After each injection, the capillary was briefly dipped in a second buffer vial to remove all traces of the sample from the outer capillary wall.
4. It was observed that the peak due to maneb appears earlier as compared to a pure sample of maneb in the presence of other dithiocarbamates. The migration time of maneb is different in commercial sample analysis, as there is decrease in EOF due to the presence of other compounds in the test mixture. This observation is similar to the observation that the migration time increases with the buffer concentration. We have carried out the experiment with pure maneb sample and its peak appears at the same time as of the commercial sample. Therefore, we conclude that the presence of other analytes is affecting the migration time.

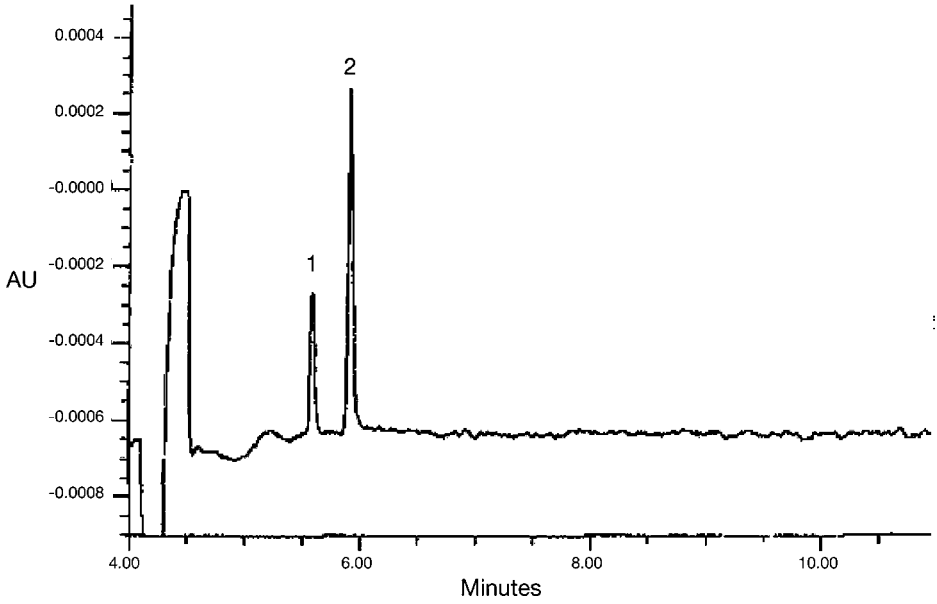


Fig. 17. Electropherogram of composition C-4 extract. Conditions as stated in **Fig. 16**. Solutes: I, HMX; 2, RDX. Refer to **Table 1** for full names of solutes. (From **ref. *19***.)

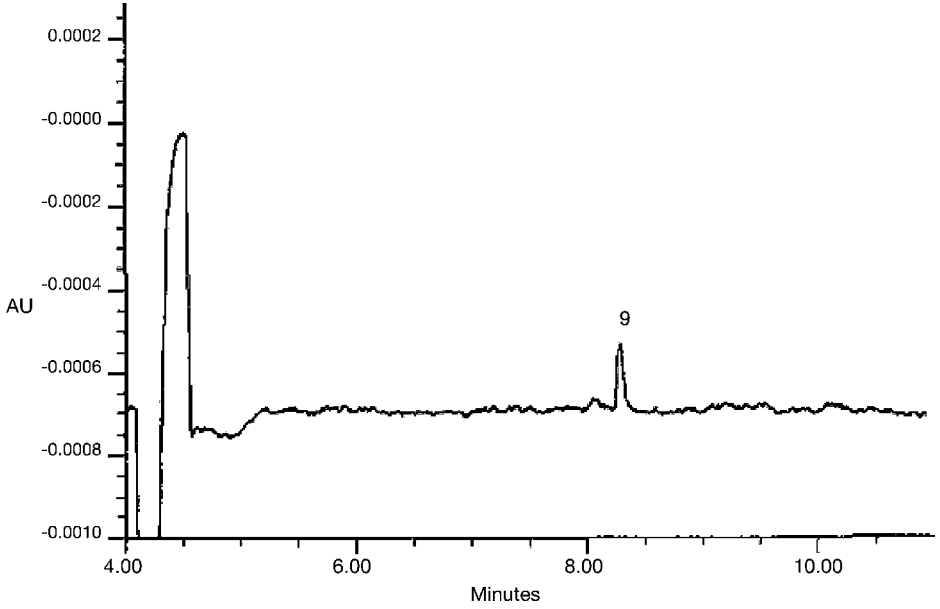


Fig. 18. Electropherogram of detonating cord extract. Conditions as stated in **Fig. 16**. Solutes: 9, PETN. Refer to **Table 2** for full names of solutes. (From **ref. *19***.)

Table 2
Comparison of the Detection Limits for Different Spectroscopic Detectors Used for Capillary Electrophoresis

Detection mode	Approx. Linear range [M] (S/N = 2 or 3)	Approx. mass LOD (Mol)	Applications	Advantages	Disadvantages	References
UV/VIS Absorbance	10^{-6}–10^{-3}	10^{-15}	Pesticides, aromatic amines, etc.	Easy to use	Not so sensitive	***1,2***
Indirect UV/VIS Absorbance	10^{-5}–10^{-3}	10^{-14}	Aliphatic compounds	Selective and sensitive	Imposes limits on choices of buffer	***1,2***
Optical absorbance (LED)	10^{-6}–10^{-3}	10^{-15}	Aliphatic and aromatic amines, etc.	Selective and sensitive	Selective in detection	***1,2***
Laser induced Fluorescence	10^{-18}–10^{-12}	10^{-21}	Formaldehyde acetaldehyde, etc	Highly sensitive	Selective and expensive	***20,21***
Mass Spectrometry	10^{-12}–10^{-9}	10^{-15}	Phenols, PAHs, etc.	Highly sensitive	Selective and expensive	***20,22***

(Continued)

Table 2
(Continued)

Detection mode	Approx. Linear range [M] (S/N = 2 or 3)	Approx. mass LOD (Mol)	Applications	Advantages	Disadvantages	References
ICP-MS	10^{-12}–10^{-9}	10^{-21}	Organophosphorus pesticides, etc.	Highly sensitive	Selective and expensive	***23***
Nuclear magnetic resonance (nmr)	10^{-6}–10^{-3}	10^{-15}	Aromatic sulfonates, etc.	Highly sensitive	Low selectivity and expensive	***24***
Photothermal (Thermal Lensing)	10^{-18}–10^{-12}	10^{-21}	Pesticides, PAHs, etc.	Highly sensitive, short analysis time	Expensive and difficult to handle	***5***

LOD, limit of detection; LED, light-emitting diode; PAH, polycyclic aromatic hydrocarbon; ICP-MS, inductively coupled plasma mass spectrometry.

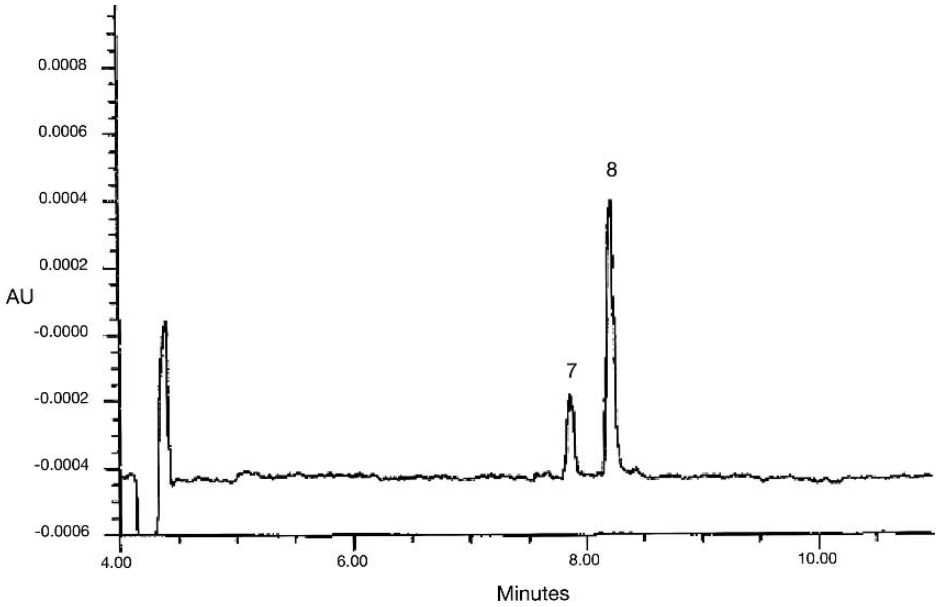


Fig. 19. Electropherogram of Tetrytol extract. Conditions as stated in **Fig. 16**. Solutes: 7, TNT; 8, Tetryl. Refer to **Table 1** for full names of solutes. (From **ref. *19***.)

Acknowledgment

The authors gratefully acknowledge the financial assistance received from DST (New Delhi), DAAD (Germany) research based personnel exchange programme.

References

1. Slobodn, J., Louter, A. J. H., Vreuls, J. J., Lika, I. and Brinkman, U. A. Th. (1997) Monitoring of micropollutant in surface water by automated on line trace enrichment liquid and gas chromatographic systems with ultraviolet diode-array and mass spectrometric detection, *J. of Chromatogr. A* **768,** 239–258.
2. Sovocool,, G. W., Brumley, W. C. and Donelli, J. R. (1999) Capillary electrophoresis and capillary electrochromatography of organic pollutants, *Electrophoresis* **20,** 3297–3310.
3. Malik, A. K. and Faubel, W. (2001) A review of analysis of pesticides using capillary electrophoretsis, *Crit. Rev. Anal. Chem*. **31 (3),** 223–279.
4. Menzinger, F., Schmitt-Kopplin, P., Freitag, D. and Kettrup, A. (2000) Analysis of agrochemicals by capillary electrophoresis, *J. Chromatogr. A*. **891,** 45–66.
5. Malik A. K. and Faubel, W. (2000) Photothermal and light emitting diodes as detector for trace detection in capillary electrophoresis. *Chem. Soc. Rev*. **29,** 275–282.

6. Zlotorzynska, D., Chen, H. and Ding, L. (2003) Recent advances in capillary electrophoresis and capillary electrochromatography of pollutants. *Electrophoresis* **24,** 4128–4149.
7. Strasik, S., Dankova, M., Molnarova, M., Olvecka, E. and Kaniansky, D. (2003) Capillary zone electrophoresis in wide bore capillary tubes with fiber-coupled diode array detection. *J. Chromatogr. A* **990,** 23–33.
8. Lu, Q., Collins, G. E., Smith, M. and Wang, J. (2002) Sensitive capillary electrophoresis microchip determination of trinitroaromatic explosives in nonaqueous electrolyte following solid phase extraction, *Anal. Chim. Acta* **469,** 253–260.
9. Martinez, D., Cugat, M. J., Borrull, F. and Calull, M. (2000) Solid-phase extraction coupling to capillary electrophoresis with emphasis on environmental analysis *J. Chromatogr. A* **902,** 65–89.
10. Yan, C., Dadoo, R. Zhao, H. and Zare, R. N. (1995) Capillary electrochromatography: analysis of polycyclic aromatic hydrocarbons *Anal. Chem.* **67,** 2026–2029.
11. Grimmer, G., Jacob, J., Naujack, K. W. and Dettbarn, G. F. (1981) Inventory and biological impact of polycyclic carcinogens in the environment. Part 13. Profile of the polycyclic aromatic hydrocarbons from used engine oil-inventory GC-GC/MS-PAH in environmental materials, part 2. *Z. Anal. Chem*. **309,** 13–19.
12. Garisson, A. W., Schmitt, P. and Kettrup, A. (1994) Separation of phenoxy acid herbicides and and their enantiomers by high-performance capillary electrophoresis. *J. Chromatogr A* **688,** 317–327.
13. Malik, A. K. and Faubel, W. (1999) Review methods of analysis of dithiocarbamate pesticides. *Pest. Sci*. **55,** 1–6.
14. Malik, A. K. and Faubel, W. (2000) Capillary electrophoretic determination of dithiocarbamates and ethyl xanthate, *Fresenius J. Anal. Chem*. **367,** 211–214.
15. Pico Y, Font, G., Molto, J. C. and Manes, J. (2000) Solid-phase extraction of quaternary ammonium herbicides, *J. Chromatogr A* **885,** 251–271.
16. Cai, J. and Rassi, Z. EL. (1992) Capillary electrophoresis of two cationic herbicides paraquat and diquat., *J. Liq. Chromatogr*. **15 (6,7),** 1193–1200.
17. Regan, F., Moran, A., Fogarty, B. and Dempsey, E. (2003) Novel modes of capillary electrophoresis for the determination of endocrine disrupting chemicals, *J. Chromatogr A* **1014,** 141–152.
18. Pineiro, N., Leao, J. M., Gago Martinez, A. and Rodriguez Vazquez, J. A. (1999) Capillary electrophoresis with diode array detection as an alternative analytical method for paralytic and amnesic shellfish toxins, *J. Chromatogr A* **847,** 223–232.
19. Stuart A. O. (1996) Analysis of nitramine and nitroaromatic explosives by capillary electrophoresis. *J. Chromatogr A* **745,** 233–237.
20. Reemtsma, T. (2003) Liquid chromatography–mass spectrometry and strategies for trace-level analysis of polar organic pollutants. *J. Chromatogr A* **1000,** 477–501.
21. Pereira, E. A., Carrilho, E. and Tavaresa, M. F. M. (2002) Laser-induced fluorescence and UV detection of derivatized aldehydes in air samples using capillary electrophoresis. *J. Chromatogr A* **979,** 409–416.

22. Riu, J, Eichhorn, P., Guerrero, J. A., Knepper, Th. P. and Barcelo, D. (2000) Determination of linear alkylbenzenesulfonates in waste water treatment plants and coastal waters by automated solid-phase extraction followed by capillary electrophoresis–UV detection and confirmation by capillary electrophoresis–mass spectrometry. *J. Chromatogr A* **889,** 221–229.
23. Wuiloud, R. G., Shah, M., Kannamkumarath S. S. and Altamirano, J. C. (2005) The potential of inductively coupled plasma-mass spectrometric detection for capillary electrophoretic analysis of pesticides. *Electrophoresis* **26,** 1598–1605.
24. Malik, A. K. and Faubel, W. (1999) A review on capillary electrophoretic separations and their studies by nuclear magnetic resonance. *J. Capillary Electrophor*. **6(3–4),** 97–108.

6

Capillary Electrophoresis With Laser-Induced Fluorescence

Environmental Applications

Lee Riddick and William C. Brumley

Summary

Capillary electrophoresis (CE), especially free-zone CE, offers a relatively simple separation with moderate selectivity based on the mobility of ions in solution. Laser-induced fluorescence (LIF) detection, an extremely sensitive technique, can be coupled with a variety of separation conditions to achieve sensitive and quantitative results. When these techniques are combined, CE/LIF provides the sensitivity and increased selectivity that makes trace level environmental analysis of fluorescent compounds possible at or below levels typical for gas chromatography (GC)/mass spectrometry (MS). We offer a panoramic review of the role of these tools in solving environmental and related analytical problems before providing a detailed experimental protocol.

Key Words: Capillary electrophoresis; laser-induced fluorescence; pollutants.

1. Introduction

Environmental analytical chemistry is continually refining and exploring new technology to improve the sensitivity, selectivity, separations, interpretation, and adaptability of methodology. Although it is a mature field in many senses, new methods, instruments, and modifications are crucial to analytical chemists and instrumentalists who are challenged with the identification and quantitation of newly recognized compounds of environmental concern ***(1**,**2)***. The workhorse technique of environmental analysis, capillary gas chromatography (GC)/mass spectrometry (MS), is the standard most often used to compare methods in terms of specificity and sensitivity ***(3)***. Liquid chromatography (LC)/MS and capillary electrophoresis (CE)/MS ***(4)*** have become

From: *Methods in Molecular Biology, vol. 384: Capillary Electrophoresis*
Edited by: P. Schmitt-Kopplin © Humana Press Inc., Totowa, NJ

modern standards in their spheres of applicability. However, there is a long history of separation techniques coupled to other types of detectors that have provided a wealth of environmental data valuable in monitoring and remediation studies. Examples of these coupled techniques are: GC/flame ionization detection (FID), GC/electron capture detection (ECD), high-performance liquid chromatography (HPLC)/diode array detection (DAD), and HPLC/fluorescence detection (FLD) ***(3)***.

CE/laser-induced fluorescence (LIF) provides the sensitivity and increased selectivity that makes trace level environmental analysis of fluorescent compounds possible at or below levels typical for GC/MS. Separation in free-zone CE is based on differences in ion mobilities ***(5)***. Thus, CE is particularly well suited to ionic organic compounds in aqueous buffers, but it is not limited to these systems.

As with most analytical methods, sample preparation and cleanup techniques are an integral aspect of the analytical problem and may provide the additional selectivity needed for a successful determination. Innovative methods for sample preparation and cleanup such as accelerated solvent extraction (ASE), solid-phase extraction (SPE), and multidimensional chromatography may be combined with CE/LIF in the total analytical approach ***(6)***.

The purpose of this article is to summarize the current status of CE/LIF detection in its ability to solve important environmental analytical problems. Throughout this chapter, we will highlight areas where additional method development is needed. As environmental analytical requirements change, new analytical procedures provide essential options to environmental chemists engaged in monitoring hazardous compounds in ecological and biological matrices. Specifically, we describe CE/LIF detection and its application in environmental analysis as an example of the continuing expansion of a new class of measurement technologies that meet the challenges of detection limits, complex matrices, green chemistry, and cost effectiveness. A review of some aspects of CE/LIF has been published ***(7)***.

1.1. Separations Science

In environmental analysis, capillary GC is the benchmark separation technique. For liquid separations, a 4.6-mm inner diameter (ID) HPLC column packed with C18-derivatized silica carried out under reversed-phase conditions is commonly used. Capillary GC methods are generally very robust with highly reproducible retention times and responses. They can often resolve more than 100 compounds per analysis, resulting in versatility and high peak capacity. However, typical environmental analysis exhibits the resolution of only 10–30

peaks, although thousands of compounds might be involved in the sample. In view of the rather limited peak capacity of one-dimensional separations, it is not surprising that more powerful separation approaches are sought. LIF is particularly useful in facilitating detection in smaller ID formats such as are used in capillary separations (<1.0 μm ID). The detector cell volume generally decreases by the same scaling factors as do all volume-related parameters, i.e., as a square of the ratio of the two diameters $(de/ds)^2$ ***(8)***, but the concentration detection limit appears to follow an approximate simple linear ratio (de/ds) relation or path length where *de* is the end diameter and *ds* is the starting diameter. For example, assuming that a 4.6-mm ID column system used a 10 μL volume detector cell, then a 0.075-mm ID capillary requires a 2.7-nL cell volume. The obvious advantage of the laser over conventional discharge lamps is the dual ability to focus intense radiation at the wavelength of interest and to do so for a detection cell volume that is the interior diameter of the capillary itself for on-column detection.

A typical schematic of an optical bench setup for CE/LIF is shown in **Fig. 1**. This schematic illustrates the essential parts of the CE/LIF experiment that

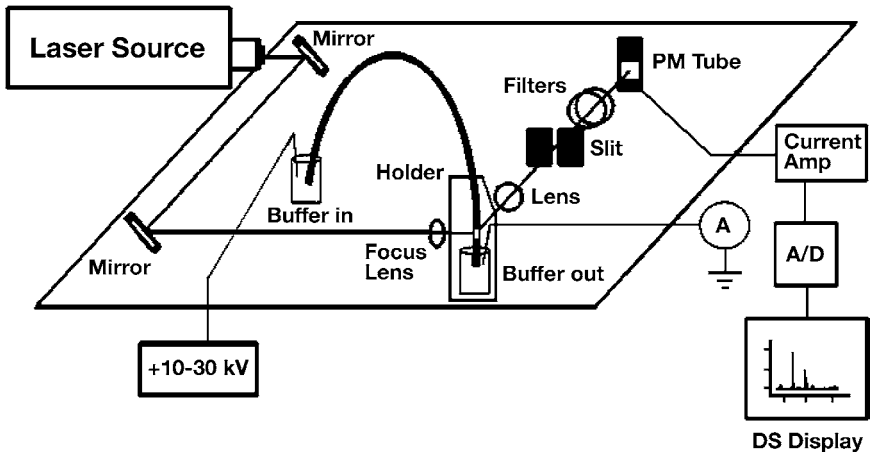


Fig. 1. Schematic diagram of an optical bench with capillary electrophoresis/laser-induced fluorescence experiment and data system acquisition. Laser light is aligned using mirrors, possibly attenuated or subjected to a notch filter at the excitation wavelength (e.g., 325 nm), focused using a microscope objective onto the capillary at the window. Fluorescent light is collected at 90° to the beam, collected and refocused by a second objective to a point, and passes through a slit and band pass filters to the photomultiplier tube for amplification and conversion to a digital signal for the computer.

consists of the buffers, separation capillary column, excitation light (laser), and the detection of the fluorescent emitted light (**Notes 1–5**).

1.2. Capillary Format Separations

It is obvious that there is a strong trend in analytical chemistry toward developments that address research problems in biomedical areas. This has resulted in the development of tools that determine levels of nonvolatile analytes such as polar drugs, proteins, DNA, and biomarkers. These developments have been partially propelled by capillary format separations such as capillary zone electrophoresis (CZE), capillary electrochromatography (CEC), and the ability of MS to ionize large biomolecules via electrospray ionization.

Capillary format separations have an obvious advantage for pollution prevention (low volume of solvent use for separations) and therefore provide a "green" chemistry approach to analysis. They also exhibit high mass sensitivity (amount of sample on-column that can be detected), but a concomitant increase in concentration detection limits due in one sense to the path length limitations described and the practical limits to the volume of sample that may be injected. This relatively high concentration detection limit is a primary concern for environmental analysis where normally large amounts and volumes of samples are available. Typical detection limits ranging from mg/kg to ng/kg are often realized in commonly used techniques such as GC/FID, GC/ECD, GC/MS, and HPLC/DAD or HPLC/FLD, either directly from a solution of the sample or sample extract or by using preconcentration. A useful figure for target analyte amount for sample injection is 1 pg/μL, which is currently practical for GC/MS methods, and 1 fg/nL for CE methods. Capillary format separations are, in a practical sense, limited by the volume of injection possible, but this deficiency is offset by the advantage of a plug-like flow profile which results in sharper peaks and greater selectivity ***(9)*** from the rather limited practical range of ion mobilities. In the case of optical methods of detection, the optical path length is also limited by the geometry of the capillary in any practical detection scheme. Recent work in addressing the short optical path length has been quite creative. An "z-cell" introduces a straight detour into the inside of the capillary, allowing the laser to interact with the contents along a section of the capillary length rather than through a cross-section ***(10)***.

LIF has assumed an important role as a detector for CZE and other capillary techniques because of its inherent sensitivity and resultant low detection limits (typically, $10^{-7}\,M$ to $10^{-13}\,M$) ***(11)***. Ultraviolet (UV) detection methods are unable to achieve these low detection limits, typically being limited to about $10^{-6}\,M$ to $10^{-7}\,M$. For organic ions, the power of LIF increases our ability to sensitively screen for nonvolatile and other analytes.

1.3. Derivatization of Target Analytes With Fluorophores

Because there is a requirement for the target analyte to exhibit fluorescence, some analysts have resorted to derivatization with fluorophores to provide the desired properties. In principle, this approach would produce a derivatized analyte capable of being detected at very low levels.

Two limiting considerations must be addressed within this context, however. One concerns the lowest practical concentration of analyte that will undergo reaction with the derivatizing reagent. Chemical kinetics dictates that some analytes will not react appreciably at concentrations of interest, but must first be preconcentrated in order for the reactions to proceed at useful rates.

The second consideration must address the production of artifacts, coupling products, and derivatives from coextractives, all of which put additional burden on the separation system. To address this very challenging problem, two approaches may be pursued. First, one may apply cleanups to limit the number of coextractives present. Second, one may develop cleanups to remove the bulk of the unwanted side products and other fluorescing background from the reaction mixture.

1.4. Quality Assurance/Quality Control Aspects of CE/LIF

Two primary questions arise in the context of quality assurance/quality control (QA/QC) issues: how reproducible are the run-to-run migration times (MTs) of target analytes, and how transferable and robust are methods developed in one laboratory when ported to another laboratory (or collaborative study)? Unfortunately, the performance to date for both CZE and micellar conditions has not been as good as those methods based on GC/MS, HPLC, and thin-layer chromatography (TLC).

The well known variation in electroosmotic flow (EOF) has been a major source of irreproducibility. One QA/QC tool that has been used is the employment of an internal standard as both a quantitative tool and as a corrective tool for MT variations, especially when those variations are a result of EOF variations. MT corrections can be applied based on the reciprocal relation between intrinsic mobility and MTs ***(12)***. Thus, if a typical standard run is used as a benchmark for the MTs of internal standard and analytes, subsequent runs of samples can be corrected back to this benchmark where the correction factor is based on the relationship between the MT of the internal standard in the two runs. This factor can then be used to correct the analyte MTs to what they would be if the EOF was the same as the benchmark run. Typically, corrected MTs of analytes can be as good as 0.3 % reproducibility.

A more difficult problem to deal with is the change in selectivity that is observed when methods are transferred to a different laboratory. Separations

can no longer be maintained, or the order of analytes that reach the detector is altered. The reproducibility issue is particularly acute under micellar conditions. Adsorption problems also occur in free zone, particularly when nonborate buffers are used or when dealing with ions that are subject to these problems.

Corrected peak areas must be used when on-column detection is implemented. This is usually automatically handled by the data system software, but the analyst may have to factor this in for laboratory built systems. This is a direct result of the difference in time that the analyte spends within the detector window as a function of its apparent mobility as it moves through the capillary.

It is considered good practice to bracket the sample series of runs with standards, validating performance and adherence to the calibration plot. Analysis of reagent blanks (taken through the method) to demonstrate the lack of contamination and solvent blanks between samples and standards is also recommended.

1.5. Environmental Analysis

A number of examples will illustrate the attributes and advantages of CE/LIF for solving the analytical problems posed by various environmental analysis scenarios. The performance or potential of CE/LIF will be compared with the currently used methodology.

1.5.1. Dye Tracers in Groundwater Migration Studies

Groundwater migration using fluorescent dyes presents an analytical problem almost ideally matched to CZE/LIF. The anionic dyes migrate in such a manner that they follow the cations and neutrals in entering the detection window (longer MTs). CZE/LIF has been used for tinopal (near UV, 354 nm excitation) and fluorescein (visible, 488 nm excitation) dyes in actual groundwater migration ***(13–15)***. These applications may result in improved detection limits, specificity, and quality control. Multiwavelength lasers may be applied for multiple dye injection studies ***(16)***. Typical dyes used include fluorescein, tinopal (fluorescent brightener), eosin, and rhodamines. **Figure 2** illustrates results for a groundwater migration study using fluorescein as the indicating dye.

1.5.2. Solid Waste and Contaminants in Solid Matrices

It is possible to screen for a wide range of analytes that fluoresce using frequency-doubled lasers operating in the deep UV (e.g., 257 nm). Alkyl phenols and hydroxylated polynuclear aromatics (hydroxy-PNAs)

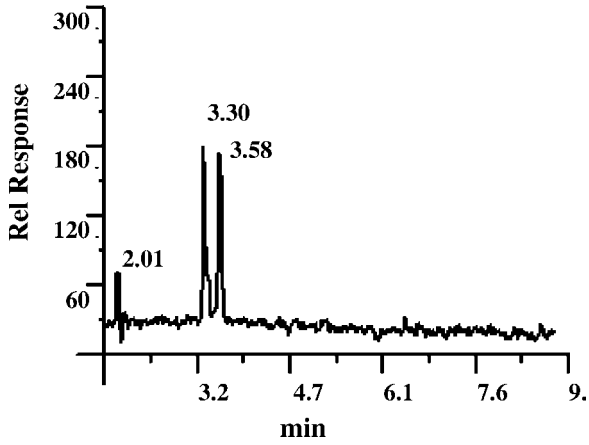


Fig. 2. Capillary electrophoresis/laser-induced fluorescence detection of fluorescein (migration time [MT]=3.58 min) (excitation 488 nm, emission band pass centered at 520 nm) as a groundwater tracer in an actual study. Groundwater was exposed to the charcoal pad, eluted with solvent, and quantitated at 62 ppt in the extract. Internal standard erythrosin B appears at MT=3.30 min and the electroosmotic flow disturbance near 2.0 min. Separation used a 57 cm capillary (0.075 mm inner diameter, 50 cm to the detector) with 40 m*M* borate buffer and 30 kV voltage in a Beckman P/ACE 5000 instrument.

can be detected as migrating anions and therefore separated from neutral hydrophobics ***(17)***.

Conversely, organic bases can be screened by using acidic conditions for their separation and detection as cations. These separations are particularly simple, but may be complicated by surface adsorption and coelutions.

Micellar agents or cyclodextrins offer alternatives and are needed for the resolution of neutral molecules using a technique called micellar electrokinetic chromatography (MEKC). This is accomplished for PNAs based on separations using cyclodextrins with LIF detection resulting from the HeCd laser operated at 325 nm ***(18)***.

Another variant employs CEC, a hybrid of capillary HPLC and electrophoresis wherein the mobile phase flow is generated electrically as the EOF ***(19)***.

1.5.3. Atmospheric Contaminants

CE has been applied to various substances of interest to atmospheric chemistry and particulate matter ***(20)***. Recent work by Dabek-Zlotorzynska et al. shows that CE/LIF can be used to measure dimethylamine and other low-molecular-weight amines in atmospheric aerosol studies ***(21)***.

1.5.4. Chemical Characterization of Matrices

The characterization of a sample can be limited to a list of analytes of interest or it can be expansive enough to encompass the character of the matrix itself. Humic substances include fulvic acid, humic acid, and humin. These constituents, although not frequently considered in environmental analyses, play an important role in the way contamination binds to or flows through soil matrices. CE has been used to study the interaction of free metal cations with fulvic acid ***(22)***. It has also been used to characterize sewage effluent for fluorescent acids ***(23)***.

1.5.5. Drinking Water and Groundwater Contaminants

An area that has stimulated considerable recent interest both publicly and analytically is that of endocrine-disrupting compounds (EDCs). There is a demand for reliable analytical methods capable of detecting trace levels of many pesticides, polychlorinated biphenyls, and dioxin-like compounds, among others. CE/LIF may play a role in applicable cases, provided some type of fluorescent property belongs to the target or can be added to the target analyte. This focus on EDCs has resulted in closer scrutiny of many pesticides and other suspect compounds such as polychlorinated biphenyls. The Safe Drinking Water Act (SDWA) and the Food Quality Protection Act (FQPA) have both adopted new regulations for monitoring thousands of compounds that interfere with the human and ecological hormone systems.

An example of the application of CE to pesticide analysis is the use of MEKC with LIF to analyze for trace levels of phenoxy acid herbicides ***(24)***. This highly sensitive method requires a complex derivatization but is able to achieve femtomole detection levels. CE even has the power and sensitivity to separate enantiomers of phenoxy acid herbicides ***(25)***. CE/LIF in an immunoassay format was also applied to 2, 4-dichlorophenoxy acetic ***(26)***. CE/LIF has been used to determine anilines ***(27)*** and aliphatic amines ***(28)***. Surfactants have also been determined using CE/LIF operating in the UV region ***(29–31)***.

1.5.6. Biomarkers of Exposure

Biomarkers of exposure can be monitored by analyzing certain physical response parameters such as protein adducts, DNA adducts, and other biological indicators. This application seeks to exploit the sensitivity and specificity of LIF and the separation power of CE. However, the area has yet to undergo significant development.

1.5.7. Food Contaminants

The complexity of food analysis is a combination of difficult matrices and low detection level requirements. In addition, the contaminants present in food

may be pesticide residues, natural toxins, such as mycotoxins, or the residues or breakdown products of food additives. CE with fluorescence detection has been used to determine the levels of fumonisin B_1 ***(32)***. Certain food contamination issues have become matters of widespread interest to the media and the public. The low detection limits achieved by CE/LIF make it an excellent choice for food analysis and monitoring where applicable.

MEKC with LIF has been used in a study of aflatoxin contamination in corn. In a laboratory study, aflatoxin spores were introduced onto corn kernels and allowed to grow for 2 wk at room temperature. The complex sample matrix yielded chromatographic peaks that were difficult to resolve. MEKC data showed separation times of less than a minute and, at the time of the study, the detection was the limiting factor ***(33)***.

1.5.8. Emerging Developments

Multidimensional separation separations allow more complete analyses because analytes are separated by more than one method, e.g., GC and LC, supercritical fluid extraction (SFE) and LC, or other combinations. Although in theory, less efficient separation (i.e., peak broadening) is obtained with two-dimensional chromatography, the advantage in separation power greatly outweighs any loss in efficiency ***(34)***. The resolution obtained depends on several factors: the orthogonality of the methods, the effectiveness of transferring from one column to another, and the completeness of the whole sample dispersion.

CZE has been used with reversed-phase HPLC in an automated, comprehensive two-dimensional method. Each separation phase is capable of effecting separations using a different separating principal: they are orthogonal methods. In the first report of an electromigration injection from a flowing stream, Bushey and Jorgenson ***(35)*** presented the advantages (excellent separation, ease of injection into the CZE system) and disadvantages (long analysis time, inefficiency in sampling from the first column).

CEC has been used to separate 16 different polycyclic aromatic compounds (PAHs). In CEC, an electric field is applied across columns that are packed with microparticulates. The EOF becomes a tool for chromatographic separations ***(19)***. CEC has an advantage over CZE in this application because it is capable of separating many uncharged species. However, CEC has yet to be significantly adopted in environmental analysis and seems to suffer from lack of robustness, undue complexity, expensive columns, and poor reproducibility.

2. Materials

2.1. Chemicals

All organic compounds were obtained from Aldrich Chemical Company, Inc. (Milwaukee, WI) and Molecular Probes (Eugene, OR) unless otherwise

specified. Other chemicals were from standard sources of supply, and all were used as received. Deionized (DI) water (18 mohm quality) was used for all aqueous solutions. Buffer solutions were freshly prepared at least weekly. Solutions of dye standards were prepared from solid dye and serially diluted.

2.2. Optics and Fused Silica

Fused-silica glass with polyimide coating was obtained from PolyMicro Technology, Phoenix, AZ. Capillaries of 0.050 mm ID and 0.075 mm ID are acceptable for separations. Optics obtained commercially should be appropriate for the application. If wavelengths below 365 um are used, then fused-silica optics should be employed, with appropriate coatings for the application wavelength region.

3. Methods

3.1. Capillary Electrophoresis of Fluorescein Dyes

A P/ACE Model 5000 Capillary Electrophoresis System (Beckman Instruments, Fullerton, CA) was used for all commercial instrument electrophoretic determinations reported here. The instrument was fitted with a capillary 57 cm in total length (50 cm from the origin to the detector window) and 75 μm ID. Detection was accomplished with an Ar ion laser operated at 488 nm emission and detection using a notch filter (488 nm) and a band pass filter (520DF20). Unless otherwise noted, electrophoresis was carried out at 30 kV. The temperature of the capillary was maintained at 25°C. The capillary was equilibrated with running buffer for 2 min prior to beginning of an experiment, and washed for 2 min with alkali and water between runs. MTs, peak widths, and peak areas were determined directly from peaks displayed by the data system or by processing software. Corrected peak areas, as computed by the instrumental software were further normalized by dividing them by the area of the peak of the internal standard, which was erythrosin B. This computation was necessary to correct for the small variations in injection volumes resulting from the pressure injections typically of 5-s duration (nominally 20 nL).

3.2. Sample Handling

Samples containing dyes or other fluorophores can be preconcentrated from the matrix by several procedures.

3.2.1. Calibration Curve

A regression analysis was carried out on the ratio of corrected areas (fluorescein corrected area divided by internal standard corrected area) vs the ratio of fluorescein concentration to internal standard concentration from

$1\times10^{-7}\,M$ to $1\times10^{-10}\,M$ in half-decade increments resulting in a seven-point calibration curve. Both unforced and forced through the origin regressions were considered and both resulted in correlation coefficients of 0.99. The equation of the line was used to calculate the concentrations of fluorescein in the samples and check standards run during the course of analysis. The concentration of fluorescein was calculable based on the known volume and concentration of internal standard added to the sample and the known volume/weight of the sample being analyzed.

3.2.2. Quality Assurance/Quality Control

Each group of samples to be analyzed was bracketed before and after by a representative standard/internal standard QC sample to establish adherence to the calibration curve equation and MT variations due to changes in EOF and therefore MT. Deviations greater than 15% in agreement with the calibration curve results would be cause for rerunning of standards, construction of a new calibration curve, or replacement of the capillary.

The MT variation on a given day/capillary was approx 5% in agreement with the standards of that day. The variation provides a rough window for anticipating the response of the internal standard and fluorescein. Using MT correction based on the internal standard, the expected and measured MT of the fluorescein peak fell within 0.3%. The position of both the internal standard and fluorescein could also be estimated from the position of the EOF disturbance. The EOF could be seen as a peak on the optical scale or can be monitored as a change in current as the injection plug exits the column. Further confirmation of the internal standard peak can be obtained by overspiking the sample with an additional aliquot of internal standard and observing the appropriate increase in peak area. Fluorescein itself could be confirmed by a similar procedure. In the samples reported in this work, no problems were encountered in identifying internal standard and analyte responses due to the low background level observed with CZE/LIF.

3.2.3. Optical Bench Experiments With Optical Brighteners

An optical bench with components and light-tight enclosure was constructed and used for all LIF experiments. The overall design was based on that of Nie et al. ***(11)***, but modified in certain respects. A special cylindrically symmetric capillary holder was machined to ensure optical alignment with the laser beam, lenses, slit, and the newly installed capillary with window made by removing the polyimide coating. The entrance lens was an L-50X and the exit lens was an M-60X (Newport, Irvine, CA). A mass spectrometer slit (VG 7070EQ source slit, Micromass, Beverly, MA) was mounted in a special holder to exclude wall fluorescence transmitted to the detector as previously

described ***(3)***. The bench was fitted with a fused-silica capillary Polymicro Technologies, Phoenix, AZ) 57 cm × 75 μm ID, 50 cm to the detector, with LIF detection using the 354-nm line of the HeCd ion laser, 3 mW, model 7203N (Liconix, Santa Clara, CA) and two 450DF100 (i.e., 50% transmission at 400 nm and 500 nm) emission filters (Omega Optical, Brattleboro, VT) in series. The power supply for CE was a Series EL (Glassman, White House Station, NJ). The temperature of the capillary was 25 °C, and electrophoretic runs were about 10 min at 20 kV using a 40-m*M* borate buffer at pH 9.1. The buffer was prepared by weighing 0.381 g of sodium tetraborate decahydrate followed by dissolution in 100 mL of DI water. The capillary was equilibrated with running buffer at the start of each experiment, and washed extensively (minimum 2 min each) with 0.1 *M* sodium hydroxide, DI water, and running buffer between analyses. Rinsing was accomplished by using capillary rinse reservoirs (SGE, Austin, TX) at about 20 psi of nitrogen pressure by fitting the injection end of the capillary through septum seals on the reservoirs. MTs, peak widths, and detection limits were either read directly from the monitor or from printouts of the data system (Austin P-90 computer, Austin, TX loaded with Beckman System Gold, Ver. 8.1, Fullerton, CA) with data acquisition using a Beckman 406 analog interface (2 V full scale output). The photomultiplier tube (PMT) was model R928 (185–900 nm) fitted with socket E0719-21 (Hamamatsu Photonics Systems, Bridgewater, NJ) and was operated at 900 V with power supply model 230-03R (Bertan, supplied by Hamamatsu). The current amplifier for the optical signal was a model 428 (Keithley Instruments, Cleveland, OH) and used the auto-current suppression facility of the amplifier to zero the background signal and maintain full amplifier dynamic range (0 to 10 V output). Corrected peak areas, as computed by using a spreadsheet (peak area multiplied by the velocity of the ion [length to the detector divided by time]), were normalized to the corrected peak area of the internal standard (7-hydroxycoumarin-4-acetic acid) as a control for the variations in the nominal volumes of the gravity injections (10 s to 40 s at 30 cm height corresponding to about 40 to 170 nL). A microampere electrometer with 0 to 1 V output (1 V = 200 μA) was constructed for measuring current through the capillary and was also interfaced to the Beckman 406 ADC to provide a record of the electrophoretic current.

Four different dyes (Tinopal CBS-X, fluorescein [acid yellow 73], rhodamine WT, and eosin Y) were injected into four wells at a Resource Conservation and Recovery Act (RCRA) site and were monitored at three wells at a nearby Superfund site. Each dye (10–30 lbs) was injected with 2000 L of water resulting in a 10-m*M* concentration level for each dye. Thereafter, 8000 L of water was used to flush the dyes into the surrounding groundwater. Samples were taken before injection and for about 2 mo afterward, resulting

in about 22 samples. Samples consisted of vial samples of water, "receptors," and 1-L water samples at the monitoring wells. The "receptors" consisted of fiberglass mesh filled with coconut charcoal and weighted to remain near the bottom of the well. The standard protocol called for 1 g of charcoal from the receptor to be extracted with 10 mL of a solution consisting of 5:3:2 (propanol: water: concentrated ammonium hydroxide). Results for fluorescein may be reported as ppt-levels in the 10-mL extractant of the pads or ppt in the water when determined directly from a portion of the water sample.

3.2.4. SPE Sample Handling

Fluorescein was isolated from spiked DI water samples or groundwater samples using SPE with styrene-divinylbenzene (SDVB) extraction disks. The disks were prepared following the manufacturer's directions by soaking in 10 mL acetone and then pulling the solvent through the disk. The process was repeated with 10 mL methanol and then water without letting the disk become dry. Samples were then added, adjusted to pH 5.0, and pulled through at 25 mmHg vacuum. The disks were dried for 2 min and then eluted twice with 6 mL of methanol. The methanol eluant was concentrated as necessary with a gentle stream of nitrogen with gentle warming to achieve a recovered concentration within the detection limits of the CE/LIF technique.

4. Notes

1. New capillaries should be conditioned with generous rinsing with 0.1 *N* NaOH solution and DI water. If the capillary does not perform as expected, it should be discarded and a new one installed in either the commercial holder or the user-designed apparatus. Although commercial capillaries are available in a variety of coatings, their expense compared to the bare silica ones is considerable. The use of inexpensive columns of bare fused silica is one of the strengths of the approach. Unstable current at the operating voltage can be due to a poor capillary as well. As long as the Joule heating (V times i) does not exceed the heat dissipation available to the setup (2.5 W or lower for air-cooled setups), a relatively stable current should be readily achieved. Slow drift of current up or down is not usually a problem for concern. Note also that current will dip and then change after the passage of the EOF disturbance through and out of the capillary.
2. An excellent buffer for CE is borate either as the titrated pH 8.3 (tetraborate vs boric acid) or the tetraborate itself (pH 9.2). Many other buffers are used, but often with poorer performance and ruggedness compared to borate.
3. Remember to replace the anode and cathode buffers on a regular basis because of depletion of ions, sample elution from either intrinsic mobility or EOF, and electrical processes. Continuity must be maintained, therefore a buffer-filled capillary is required and the introduction of a plug of nonconducting liquid or easily boiled liquid could lead to no conductivity. Remember to rinse to a waste container,

not the receiving buffer. For pressure injections, do not exceed about 10% of the capillary length (usually less than 20 s, typically 5 s). Use a diluted buffer for the sample (about 10% of the ionic strength of the working buffer) for focusing effects. Running buffer strengths of 10 to 50 m*M* are often sufficient for good results. Avoid working in the pH 5.0–7.0 region if possible because of the strong dependence of EOF in this region on pH (i.e., the extent of ionization of the silica wall is changing steeply in this region as a function of pH).

4. Doubling the length of the capillary will result in MTs four times longer if all other parameters are kept constant. Efficiency is proportional to field strength if Joule heating is controlled.
5. MT variations are often a consequence of EOF variations from run to run and capillary to capillary. Use internal standard for MT corrections arising from EOF variations and for quantitation. This also serves QA/QC purposes for assessing the performance of each run including MT and relative response. Use corrected areas to account for on-column detection bias (simply area/MT).

Acknowledgment

The US Environmental Protection Agency (EPA), through its Office of Research and Development (ORD), funded the work involved in preparing this article. It has been subject to the Agency's peer review and has been approved for publication. The US Government has the right to retain a nonexclusive, royalty-free license in and to any copyright covering this article.

References

1. Daughton, C. G. and Ternes, T. A. (1999) Pharmaceuticals and personal care products in the environment: agents of subtle change?*Environ. Health Perspect*. **107,** (6), 907.
2. http://www.epa.gov/nerlesd1/chemistry/pharma/index.htm
3. http://www.epa.gov/nerlesd1/chemistry/org-anal/home.htm
4. Brumley, W. C. and Winnik, W. (1996) Applications of capillary electrophoresis/mass spectrometry to environmental analysis, in *Applications of Liquid Chromatography/ Mass Spectrometry in Environmental Chemistry* (D. Barceló, ed.) Elsevier, Amsterdam: pp. 481–527.
5. Heiger, D. N. (1992) High performance capillary electrophoresis. Hewlett-Packard 12-5091–6199E, Walbronn, Germany.
6. Brumley, W. C. (1995) Techniques for handling environmental samples with potential for capillary electrophoresis. *J. Chromatogr. Sci*. **33,** 670–685.
7. Gooier, C., Kok, S. J., and Ariese, F. (2000) Capillary electrophoresis with laser-induced fluorescence detection for natively fluorescent analytes *Analusis* **28,** 679–685.
8. Chervet, J. P., van Ling, R., Evans, K., and Salzmann, (1999) Capillary and nano HPLC using a dedicated instrument. *Am. Lab*. August, 44–50.

9. Dadoo, R., Yan, C., Zare, R. N., Anex, D. S., Rakestraw, D. J., and Hux, G. A. (1997) Advances toward the routine use of capillary electrochromatography. *LC-GC* **15(7),** 630–635.
10. Chervet, J. P., van Soest, R. E. J., and Ursem, M. (1991) Z-Shaped flow cell for UV detection in capillary electrophoresis. *J. Chromatogr*. **543,** 439–449.
11. Nie, S., Dadoo, R., and Zare, R. N. (1993) Ultrasensitive fluorescence detection of polycyclic aromatic hydrocarbons in capillary electrophoresis. *Anal. Chem*. **65,** 3571.
12. Brumley, W. C. and Brownrigg, C. M. (1993) Electrophoretic behavior of aromatic-containing organic acids and the determination of selected compounds in water and soil by capillary electrophoresis. *J. Chromatogr*. **646,** 377–389.
13. Brumley, W. C., Ferguson, P. L., Grange, A. H., Donnelly, J. L., and Farley, J. W. (1996) Applications of capillary electrophoresis/laser-induced fluorescence detection to groundwater migration studies. *J. Capillary Electrophor*. **3,** 295–299.
14. Ferguson, P. L., Grange, A. H., Brumley, W. C., Donnelly, J. L., and Farley, J. W. (1998) Capillary electrophoresis/laser-induced fluorescence detection of fluorescein as a groundwater migration tracer. *Electrophoresis* **19,** 2252–2256.
15. Brumley, W. C., and Gerlach, C. L. (1998) Capillary electrophoresis/laser-induced fluorescence in groundwater migration determination. *Am. Lab*. **31,** 45–49.
16. Brumley, W. C. and Farley, J. W. (2003) Determining eosin as a groundwater migration tracer by capillary electrophoresis/laser-induced fluorescence using a multiwavelength laser@. *Electrophoresis* **24,** 2335–2339.
17. Brumley, W. C., Grange, A. H., Kelliher, V., et al. (2000) Environmental screening of acidic compounds based on CZE/LIF detection with GC/MS and GC/HRMS identifications. *J AOAC Int*. **83,** 1059–1067.
18. Brown, R. S., Luong, J. L. T., Szolar, O., Halasz, H. J., and Hawari, J. A. (1996) Cyclodextrin-modified capillary electrophoresis: determination of polycyclic aromatic hydrocarbons in contaminated soils. *Anal. Chem*. **68,** 287–292.
19. Yan, C., Dadoo, R., Zhao, H., Zare, R. N., and Rakestraw, D. J. (1995) *Gradient* elution in capillary electrochromatography. *Anal. Chem*. **67,** 2026–2029.
20. Dabek-Zlotorzynska, E., Piechowski, M., Liu, F., Kennedy, S., and Dlouhy, J. F. (1997) Routine determination of major ions in atmospheric aerosols by capillary electrophoresis. *J. Chromatogr. A* **770,** 349–359.
21. Dabek-Zlotorzynska, E. and Maruszak, W. (1998) Determination of dimethylamine and other low-molecular-mass amines using capillary electrophoresis with laser-induced fluorescence detection. *J. Chromatogr. B* **714,** 77–85.
22. Nordén, M. and Dabek-Zlotorzynska, E. (1996) Study of metal-fulvic acid interactions by capillary electrophoresis *J. Chromatogr. A* **739,** 421–429.
23. Flaherty, S., Wark, S., Street, G., Farley, J. W., and Brumley, W. C. (2002) Investigation of CE/LIF as a tool in the characterization of sewage effluent for fluorescent acidics: determination of salicylic acid. *Electrophoresis* **23(14),** 2327–2332.
24. Jung, M. and Brumley, W. C. (1995) Trace analysis of fluorescein-derivatized phenoxy acid herbicides by micellar electrokinetic chromatography with laser-induced fluorescence detection. *Chromatogr. A* **717,** 299–308.

25. El Rassi, Z., Mechref, Y., Postlewait, J., and Ostrander, G. K. (1997) Capillary electrophoresis of carboxylated carbohydrates. III. Selective precolumn derivatization of glycosaminoglycan disaccharides with 7-aminonaphthalene-1, 3-disulfonic acid fluorescing tag. *Anal. Biochem.* **244,** 283–290.
26. Rogers, K. R., Apostol, A. B., and Brumley, W. C. (2000) Capillary electrophoresis (CE) immunoassay format for phenoxyacid herbicides. *Anal. Lett.* **33,** 443–453.
27. Wall, W. and El Rassi, Z. (2001) Electrically driven microseparation methods for pesticides and metabolites: V. micellar electrokinetic capillary chromatography of aniline pesticidic metabolites derivatized with fluorescein isothiocyanate and their detection in real water at low levels by laser-induced fluorescence. *Electrophoresis* **22,** 2312–2319.
28. Brumley, W. C., and Kelliher, V. (1997) Determination of aliphatic amines in water using derivatization with fluorescein isothiocyanate and capillary electrophoresis/laser-induced fluorescence detection. *J. Liq. Chromatogr.* **20,** 2193–2205.
29. Kok, S. J., Hoornweg, G., de Ridder, T., Brinkman, U., Velthorst, N. H., and Gooijer, C. (1998) Generation of 275.4-nm UV output from a large-frame argon-ion laser for fluorescence detection in capillary electrophoresis. *J. Chromatogr. A* **806,** 355–360.
30. Kok S. J., Kristenson, E. M., Gooijer, C., Velthorst, N. H., and Brinkman, U. A. Th. (1977) Wavelength-resolved laser-induced fluorescence detection in capillary electrophoresis: naphthalenesulphonates in river water. *J. Chromatogr. A* **771,** 331–341.
31. Kok, S. J., Isberg, I. C. K., Gooijer, C., Brinkman, U. A. Th., and Velthorst, N. H. (1998) Ultraviolet laser-induced fluorescence detection strategies in capillary electrophoresis: determination of naphthalene sulphonates in river water. *Anal. Chim. Acta* **360,** 109–118.
32. Holcomb, M. and Thompson, H. C. (1996) Analysis of fumonisin B_1 in rodent feed by capillary electrophoresis with fluorescence detection of the FMOC derivative. *J. Capillary Electrophor.* **3(4),** 205–208.
33. Cole, R. O., Holland, R. D., and Sepaniak, M. J. (1992) Factors influencing performance in the rapid separation of aflatoxins by micellar electrokinetic capillary chromatography. *Talanta* **39(9),** 1139–1147.
34. de Geus, H. J., de Boer, J., and Brinkman, U. A. Th. (1996). Multidimensionality in gas chromatography. *Trends Anal. Chem.* **15,** 398–408.
35. Bushey, M. M. and Jorgenson, J. W. (1990) Automated instrumentation for comprehensive two-dimensional high performance liquid chromatography of proteins. *Anal. Chem.* **62,** 161–167.

7

Practical Considerations for the Analysis of Ionic and Neutral Organic Molecules With Capillary Electrophoresis/Mass Spectrometry

Moritz Frommberger, Matthias Englmann, and Philippe Schmitt-Kopplin

Summary

This chapter presents the technique of capillary electrophoresis coupled to mass spectrometry (CE/MS). The introductory section is targeted mainly at CE/MS beginners and notes briefly the theoretical background of electrospray ionization (ESI), the most commonly used ionization mode in CE/MS. The specifics of CE/MS are described—also in comparison with more classic methods like LC/MS. Important caveats to be taken into consideration for successful CE/MS operation are noted in the interest of avoiding pitfalls. CE/MS is illustrated with three representative examples, which might serve as starting points for more in-detail experiments: (1) *partial-filling* micellar elektrokinetic chromatography (MEKC) of *neutral* bacterial signaling molecules (*N*-acylhomoserine lactones) extracted from culture supernatants, (2) capillary zone electrophoresis (CZE) of their *anionic* degradation products, and finally (3) CZE separation of *cationic* hydroxy-*s*-triazines.

Key Words: Capillary electrophoresis, mass spectrometry, electrospray ionization, coupling techniques, anions, cations, neutrals, *N*-acylhomoserine lactones, triazines.

1. Introduction

Since its introduction in the late 1980s and the first publication by J. A. Olivares and coworkers ***(1)***, the coupling of capillary electrophoresis to mass spectrometry (CE/MS) has become a well-accepted two-dimensional technique for the analysis of a large number of analytes from small, inorganic ions to biologically important macromolecules ***(2,3)***. It combines CE as an exceptional separation technique with more and more selective and sensitive mass detection

From: *Methods in Molecular Biology, vol. 384: Capillary Electrophoresis*
Edited by: P. Schmitt-Kopplin © Humana Press Inc., Totowa, NJ

possibilities through very mild ionization modes. CE/MS complements, and in some cases substitutes for, classic MS-hyphenated separation techniques. Over the years, CE was coupled to many different types of mass spectrometers, including magnetic sector, quadrupole, ion trap, time-of-flight, and Fourier transform ion cyclotron (reviewed in **refs. *2*,*3***). Many different ionization strategies were followed for the coupling (including continuous flow fast atom bombardment, laser evaporation, and sonic spray), but obviously none of these could make its breakthrough to become some form of "routine": invariably, all application-oriented papers until 2005 ***(2*,*3)*** apply electrospray ionization (ESI) principles for *on-line* ionization of the CE eluent. In a first paragraph, we will therefore shortly describe and characterize fundamental ESI principles and show possibilities and limitations for the practical realization. CE/MS differs fundamentally from the more commonly used LC/MS the reader might be familiar with; a second paragraph will thus focus on basic CE principles particularly with regard to successful and reproducible coupling.

Covering all and any possible application scenarios in one book chapter is illusory; we therefore will demonstrate CE separation with MS detection with three representative examples, that might serve as starting points for own experiments: *partial-filling* micellar elektrokinetic chromatography (MEKC) of *neutral* bacterial signalling molecules (*N*-acylhomoserine lactones) extracted from culture supernatants, capillary zone electrophoresis (CZE) of their *anionic* degradation products, and finally CZE separation of *cationic* hydroxy-*s*-triazines.

1.1. Electrospray Ionization

1.1.1. Principles

The electrospray phenomenon was known a long time before its application as an ionization technique for MS, and it is used for varnishing, nebulization of pharmaceutical formulations, in space thrusters, and in plasma desorption. A first theoretical description of the underlying principles was already given by J. Zeleny in 1917; however, it was not until 1968 that M. Dole and coworkers applied ESI in connection with MS for the first time. For his pioneering work in ESI-MS, J. B. Fenn was rewarded the Nobel prize in 2002 ***(4)***, "for the development of methods for identification and structure analyses of biological macromolecules" (http://nobelprize.org/chemistry/laureates/2002/). The most appealing feature of electrospray, in fact, is the *soft* ionization, which allows for the nondestructive analysis of small metabolites, pharmaceuticals, and environmental and forensic samples up to even large biomolecules.

Figure 1 gives a schematic representation of an ESI ion source. If a high-tension (typically, 0.5 to 5 kV) is applied to the end of a capillary filled with

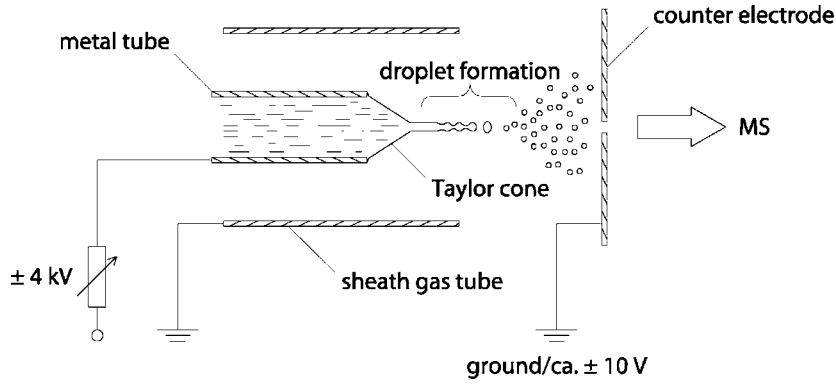


Fig. 1. Schematic setup of an electrospray ionization ion source. An electrified, liquid-filled capillary ("metal tube") is mounted opposite to a grounded counter electrode (or vice versa). The sheath gas tube is optional. For details, refer to text.

a conducting polar liquid opposite to a grounded counter electrode (or, in some configurations, vice versa), a conical meniscus (Zeleny-Taylor Cone, Taylor Cone) is formed as a result of dipole forces and viscosity. The tip of the meniscus, being the most unstable point, elongates to a very narrow liquid column or *jet*. As a consequence of interaction between viscosity and surface tension, so called "varicose waves" are formed in the jet (comparable to the fine liquid thread from an incompletely closed tap), which grow in amplitude until they break the liquid column into droplets of nearly identical diameter. Depending on the polarity of the electric field, the droplets all contain excessive anions or cations on their surface, and, as a consequence of their charge of the same sign (positive or negative), their trajectories diverge to form a conical spray ("electrospray"). While the solvent continues to evaporate from the droplets, their charge-to-surface ratio gets greater and greater until the electrostatic repulsion of the ions supersedes surface tension (the *Rayleigh stability limit* is reached). In consequence, the parent droplets disintegrate into daughter droplets by so-called Coulomb explosions; a process that continues to occur and causes smaller and smaller droplets to be produced.

The exact mechanism by which charged gas-phase ions are produced from ions in charged solvent droplets is still not completely elucidated, but two principal models exist. The *charged residue model* (CRM) by Dole postulates that repetitive Coulomb explosions finally lead to droplets with only one analyte molecule, which retains some of the charge after the last solvent molecule has evaporated. Conversely, the *ion evaporation mechanism* (IEM) by Iribarne and Thomson holds that the high field strength at the droplet surface causes solute molecules to be "lifted" into the gas phase.

In nature, both mechanisms seem to contribute to ionization, but the relative importance of either of the two principles is still the subject of discussion. Detailed information on MS and its coupling to various separation techniques can be found in Elsevier's *Encyclopedia of Mass Spectrometry, Volume 8* ***(5)***.

1.1.2. Theoretical Considerations

An in-detail review on miniaturization issues in ESI devices is given in **ref. *6***, which might serve as a starting point for further reading. In contrast to capillary and nano liquid chromatography, which is a development only of recent years, CE (like capillary gas chromatography) is a *miniaturized* technique. Both *sampling efficiency* and *ionization efficiency* strongly influence sensitivity in ESI applications. Whereas the latter is merely an inherent feature of the molecules under examination, buffer constituents, and the presence of matrix, the fraction of ionized species that *actually reaches* the mass spectrometer (sampling efficiency) is mainly determined by the setup of the ESI source. As already mentioned under **Subheading 1.1.1.,** an electrostatic repulsion of charged droplets in the spray occurs, thus the effect of the flow rate may be simplified to the following conclusion: the higher the flow rate, the higher the number of charged droplets, and, in consequence, the larger the diameter of the droplet cloud. Following the theoretical approach of Smith et al. (1990; *see* **ref. *6***), the ionization yield of a conventional ESI interface with a flow rate of 3 to 6 μL/min is 1 in 100 000; from the produced ions, however, only a fraction (1 in 10,000) actually reaches the mass spectrometer. Low-flow ESI sources may be placed much closer to the front of the MS orifice, and also careful optimization of the flow rates and the diameters of the ionization capillaries may help to increase the sampling efficiency. According to Wilm and Mann (1994; *see* **ref. *6***), droplet formation in ESI can be calculated according to

$$r_e = \left\{ \frac{\rho}{4\pi^2 \gamma \tan\left(\frac{\pi}{2} - \theta\right)\left[\left(\frac{U_T}{U_A}\right)^2 - 1\right]} \right\}^{\frac{1}{3}} \left(\frac{dV}{dT}\right)^{\frac{2}{3}} \quad (1)$$

where r_e is the radius of the emitter region at the tip of the Taylor cone (cf. **Subheading 1.1.1.**), γ the surface tension, θ the angle of the taylor cone, ρ the density of the solution, U_T the threshold voltage, U_A the applied voltage, and dV/dt the flow rate. If the flow rate is lowered, smaller droplets are emitted as a consequence of the hereby reduced r_e. This facilitates the emission of ions into the gas phase as a consequence of the higher surface-to-volume ratio. To maintain Taylor cone stability, the capillary diameter should

be reduced in parallel to the reduction of the flow rate. **Subheading 1.1.3.** shows examples for miniaturized ionization systems; in such "nanospray" devices, the ionization yield can be increased to (theoretically) 1 in 390 (Wilm & Mann, 1996; *see* **ref**. ***6***). Practical limitations, however, are opposed to an universal use of nanospray in CE/MS as also discussed in the next section.

1.1.3. Practical Realization

Under **Subheading 1.1.1.,** the basic setup of the simplest possible ESI interface is presented. The main challenge when coupling CE to MS, however, is the application of high voltage to the contents of the separation capillary, which is necessarily nonconductive. In CE/MS applications, the ESI interface additionally serves as the second electrode for separation; together with this, the flow rates in CE are so low that electrochemistry phenomena may play a substantial role. CE/MS interfaces are today mainly constructed in two ways (the *liquid bridge*, the oldest form of coupling, is intentionally left out as it plays only a minor role in current applications).

In *sheath liquid* (SL) interfaces (*see* **Fig. 2**, left), the CE capillary is surrounded by a second tube, through which a conductive liquid of appropriate organic modifier content (thus viscosity) and conductivity is pumped. The composition of this SL, which establishes the contact to the capillary eluent and closes the electric circuit for separation, may vary from one application to another and it might be necessary to adapt its composition during method

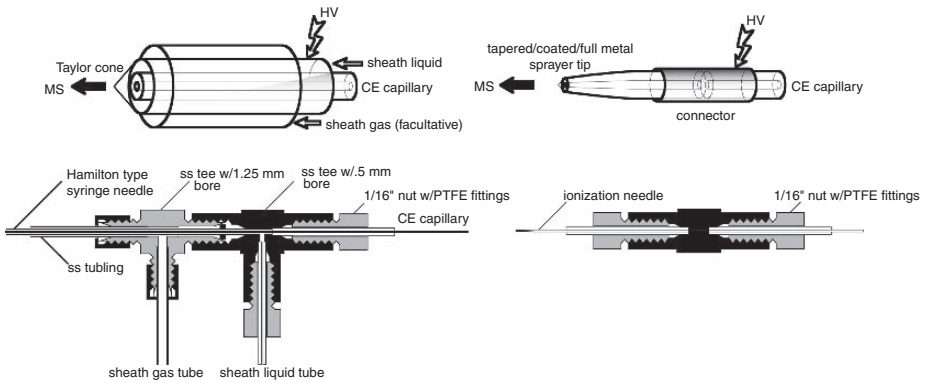


Fig. 2. Theoretical concepts of electrospray ionization (ESI) interfaces (top figures) and suggestions for the practical realization (bottom figures) of ESI interfaces (left, sheath liquid type; right, sheathless type). The interfaces are constructed from commercially available standard components (polyetheretherketone, polytetrafluoroethylene, and stainless steel).

development. The two coaxial capillaries are very often surrounded by a third tube, through which a gas flow is guided. This *sheath gas* is used for stabilization of the Taylor cone and causes a quicker evaporation of solvent from the produced droplets. The next section will discuss caveats to be taken into consideration for both SL and sheath gas.

In *sheathless* systems (**Fig. 2**, right), the voltage is directly applied to the contents of the separation capillary. Miniaturized forms of this setup (e. g., with pulled capillaries with an inner diameter down to 5 μm) are known as "nanospray." Again, there are different possibilities: either the end of the separation capillary is tapered and/or coated with conductive material (e. g., gold or graphite) or the capillary is connected to an ionization tip (either full-metal or coated as above). Numerous, sometimes exceedingly sophisticated, strategies exist for voltage application: the contact can either be established directly with the tip, via a distally mounted metal connector, via a platinum wire inserted into the separation capillary, or via a thinly etched region of the capillary, etc.

From a purely theoretical point of view, all the sheathless systems (especially nanospray) are clearly superior to any SL interface: the electroosmotic flow (EOF)-generated flow in a CE capillary lies in the nL/min range, the SL flow (of typically 1 to 5 μL/min) thus substantially dilutes the sample. From the ESI mechanistics presented under **Subheading 1.1.1.,** it also becomes clear that a higher flow will negatively impact the sampling efficiency, as a lower number of ions will reach the mass spectrometer. From our recent literature surveys, however, it became clear that the large majority (79%) of articles published on CE/MS, and mainly the application-oriented papers, apply SL-type interfaces for their separations (*see*, e. g., the yearly special issues on CE/MS in *Electrophoresis*, Wiley VCH). This finding reflects our personal experience: when carefully optimized, the SL interface is a highly robust and reproducible system. In contrast to that, and despite the substantial improvements over the last years, the stability of the coatings of nanospray tips—and thus the quantitative reproducibility—is still an issue. Another advantage of SL-type interfaces may be the possibility of overcoming buffer incompatibilities somewhat (*see* **Subheading 1.2.3.**).

1.2. Specifics and Caveats in CE/MS

Central features make CE different from more conventional separation techniques such as LC, and almost every one of these has its impact on CE/MS. In the following sections, some of the important "tuning parameters" are noted. They mainly apply to the SL interface; what is possible—and necessary—sometimes depends on the instruments available.

1.2.1. Positioning of the Instruments and Setup of the ESI Source

In an open-tube separation technique such as CE/MS, the inlet end (in the CE instrument) and the outlet end of the separation capillary (in the ESI interface) should be positioned at the same height, as otherwise suction effects are generated through siphoning. This might cause an acceleration or deceleration of the liquid in the capillary, thus a laminar flow superimposed to the EOF and, in consequence, peak-broadening effects. In some commercially available "coupling kits," the minimum capillary length is 80 cm or more—too long for applications with slow EOF. In this case, one might find it necessary to apply low pressure (~0.5 psi) at the inlet of the capillary (accepting the peak broadening effect by the laminar flow) or to modify the instrument positioning (*see* **Note 1**). To control spray stability, one should have the possibility of visually observing the spray with a magnifying video camera. In addition to that, a device for fine-adjustment of the sprayer needle (possible with a *xyz* stage with verniers) is desirable (*see* **Note 2**).

1.2.2. Injection Volumes

In contrast to LC/MS, injection volumes in CE lie in the nanoliter range. With the most commonly used *hydrodynamic injection*, the volume *actually* injected is a function of applied pressure, of capillary dimensions, and of buffer/sample viscosity (*see* **Note 3**). In CE/MS, two other factors must be kept in mind: any sheath gas flow (*see* below) causes suction effects, and the ESI voltage (when switched on before the separation voltage) may cause a reversed EOF (in positive mode) or electrokinetic conditions that result in a larger or lower amount of injected analyte. A solution for these reasons for irreproducibilities is to switch on the ESI voltage and sheath gas only *after* the separation voltage has already reached its target value. Automatization may here increase reproducibility.

1.2.3. Buffer Composition

Nonvolatile and/or high-ionic-strength buffers cause a significant decrease in sensitivity through ion-pairing effects or prevention of ion evaporation from the charged droplets (*see* above and **ref**. *7*), an increase in ESI currents, and, through precipitation, a contamination or blocking of the ESI source. It is therefore advisable to use a volatile buffer salt (ammonium acetate or formate for acidic pH values, ammonium carbonate for basic pH values) at a low concentration (10 to 50 m*M*) in water or a water/organic modifier mixture. A very small concentration of involatile buffers might also be tolerated. Surfactants are especially problematic in CE/MS experiments, as they preferentially accumulate at the surface of the droplets and hinder ion evaporation ***(8)***.

Micellar electrokinetic chromatography (MEKC) can therefore not be coupled to MS via ESI offhand; rather, special precautions must be taken: one possibility is using "ESI-compatible" surfactants such as bile salts or polymeric substances, another is using *partial-filling* MEKC, still another is modifying the pH and capillary surface in a way that the micelles remain stationary in the capillary or elute at a the anodic end (for an overview, *see* **ref**. ***9***).

1.2.4. Separation Voltages

In CE/MS, the complete cooling of the separation capillary is often not possible. In close relation to the ionic strength of the buffer (as discussed above), voltages that are too high cause Joule heating, which might not be completely dissipated in CE/MS. More moderate ionization voltages or a small amount of organic modifier in the buffer can solve this problem but on the other hand, may cause longer separation times. As a general rule, the CE current should not exceed 20 μA.

1.2.5. Sheath Gas Flow

If applied, the sheath gas flow in the ESI source generates a suction effect at the end of the capillary, and thus causes a parabolic flow, which overlays the plug-like flow of the EOF. The EOF is apparently accelerated and the separation time is shortened. This may have a negative impact on resolution and may cause peak-broadening. Some CE instruments offer the possibility of using a slight vacuum at the capillary inlet, which may help to solve these problems; another solution is to keep the sheath gas flow at a minimum (*see* **Note 4**).

1.2.6. Sheath Liquid Flow Rate and Composition

In the ESI interface, the eluent of the CE capillary is mixed with, and substantially diluted by, the SL. In terms of sensitivity, it is desirable to keep the flow rate as low as possible, but to form a stable spray, higher values might be necessary (*see* **Subheading 1.1.3**.). Flow rate and composition of the SL are closely related with the resulting ionization current, which is a measure of the charges that can be converted to gas phase ions. The ionization current, I, can be calculated according to the Hendricks equation (*see* **ref**. ***10***), where H is a constant whose value will vary depending upon the dielectric constant and the surface tension of the solvent, ν is the flow-rate, σ is the specific conductivity, and E is the imposed electric field:

$$I = H\nu\sigma E \tag{2}$$

Throughout the literature, methanol/water or 2-propanol/water (50% to 80%) SLs are most often used. In positive ionization mode, a small amount of acetic

or formic acid (0.1% to 1%) is added; for negative ionization, usually the same amount of ammonium hydroxide is used. Other authors propagate a small amount (about 10 m*M*) of a volatile buffer salt such as ammonium acetate. Additive amounts that are too large will cause a larger value of σ in **eq. 2**; thus the ionization current, *I*, will rise—flow rates that are too high have the same effect. The ESI interface represents a perfect electrochemical half cell, thus electrolysis reactions (bubbles) and numerous other electrochemical effects can occur (for an extensive discussion, *see* **ref**. ***11***). We found it necessary to rinse the interface with SL after each run: **Fig. 3** shows spectra and electropherograms before and after a rinsing step. Usually, the SL is supplied by a syringe pump integrated into the mass spectrometer—often the cause of irreproducibilities and constant annoyance. To yield more reproducible flow rates and to minimize maintenance, the best way is to substitute the syringe pump with an external HPLC pump—eventually equipped with a flow splitter—that can be triggered and is variable over a large range of flow rates (*see* **ref**. ***12*** for an example).

1.2.7. Distance and Position of the Interface

The electric field strength in the ESI interface is calculated from the voltage difference, *V*, the distance between the ionization needle and the counter electrode, *d*, and the needle radius, r, according to

$$E = \frac{V}{r \ln\left(\frac{4d}{r}\right)} \tag{3}$$

Briefly, this means that both the needle diameter and the distance have to be optimized in parallel to gain optimum ionization conditions. In many commercially available interfaces, the position of the ESI needle relative to the MS orifice is fixed or can be adjusted only very roughly, which is certainly a major drawback and a criterion for selecting between interfaces. If the distance is too large, the sampling efficiency drops; if the distance is too small, the ionization current rises, and, even before sparks are observed, the ion intensity may drop dramatically (**Fig. 4**, left). We found no significant differences among an axial, angular, or orthogonal arrangement of the spraying needle; the horizontal and vertical positioning, however, is critical. With the low flow rates in CE/MS (in contrast to classic LC/MS), no negative effects can be expected when the spray goes directly into the MS.

1.2.8. Ionization Voltage

The ionization voltage cannot be sensibly separated from the positioning of the interface, as from **Subheading 1.2.7.** it becomes clear that both *dimension*

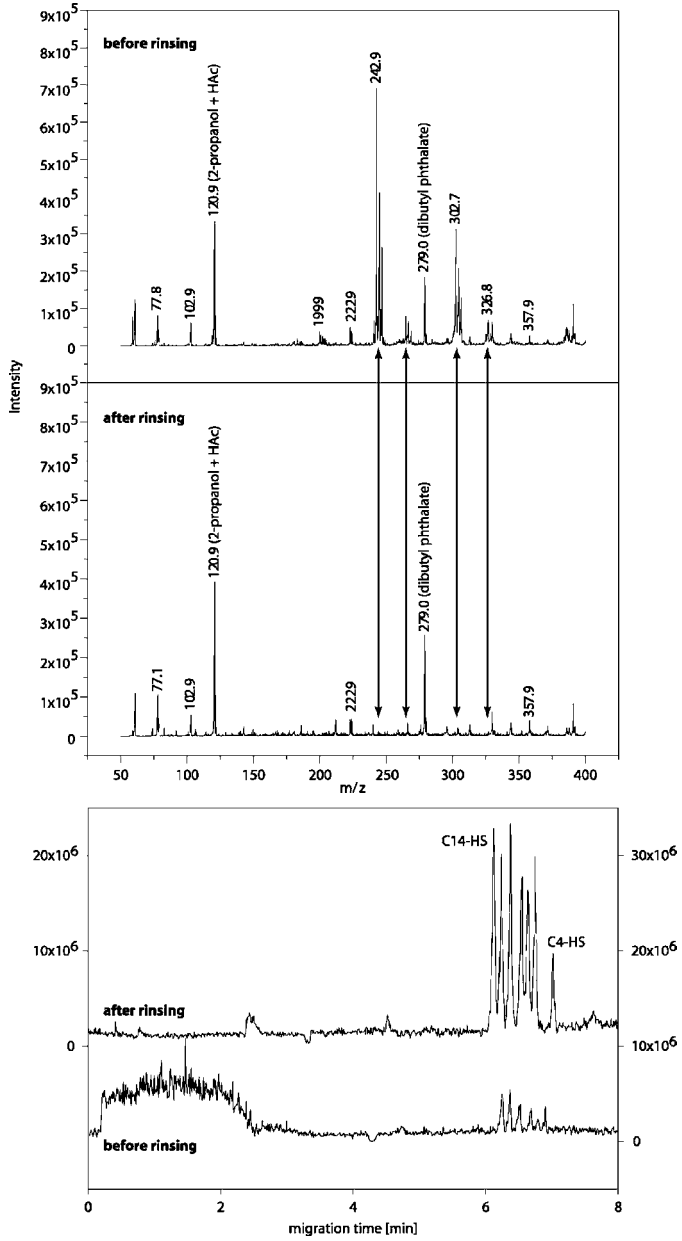


Fig. 3. Effects of intensively rinsing the electrospray ionization interface with sheath liquid (5 mL/min, 1 min). Capillary electrophoresis/mass spectrometry of a homoserine standard mix (*see* **Subheading 3.2.** for details). Top, background after three runs without rinsing; middle, background after rinsing; bottom, total ion currents (TICs) before and after rinsing.

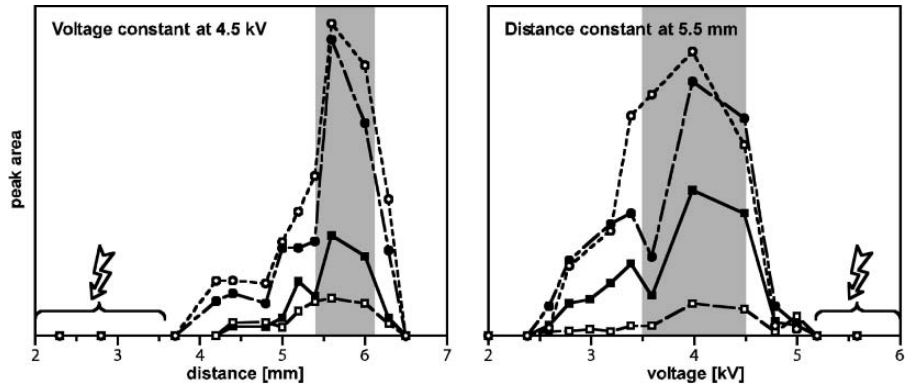


Fig. 4. Example for the optimization of the distance between ionization needle and counter electrode (left) and the ionization voltage (right). Too high a voltage or too short a distance led to arcing problems; best values are shaded. Samples injected in 10 m*M* ammonium acetate buffer, pH 6.8, with 30 kV; coaxial sheath liquid (50% methanol with 1% of acetic acid) at 2.5 µL/min; sheath gas (nitrogen) flow rate 20 arbitrary units; positive electrospray ionization. ■, hydroxydesethylatrazine; □, desisopropylatrazine; ●, hydroxyatrazine; ○, hydroxyterbutylazine.

and *voltage* influence the electric field at the ESI needle. The right part of **Fig. 4** gives an example for a voltage optimization series.

1.2.9. Temperature

In ESI MS, the droplet cloud/gas phase ions are often heated to improve solvent evaporation. This might be achieved by different concepts (a *curtain gas* or a *heated capillary*). The effects, however, are the same: especially in CE/MS, where, in contrast to LC/MS, *buffers* are used for the separation, the optimum temperature for the ionization source sometimes becomes a balancing act among thermal stability, solvent exaporation, and adduct formation. Thus, the optimum temperature for the analyte might not be the optimum temperature for detection (*see* **ref**. ***13*** for a practical example).

2. Materials

2.1. Equipment

1. ThermoQuest (San José, CA) LCQ Duo ion trap mass spectrometer equipped with the commercial CE/MS interface or a laboratory-constructed, coaxial (SL) ESI interface mounted on a *xyz* stage (**Fig. 5**).
2. SL supplied by a Hewlett-Packard (Waldbronn, Germany) 1100 quaternary HPLC pump operated without flow splitter.

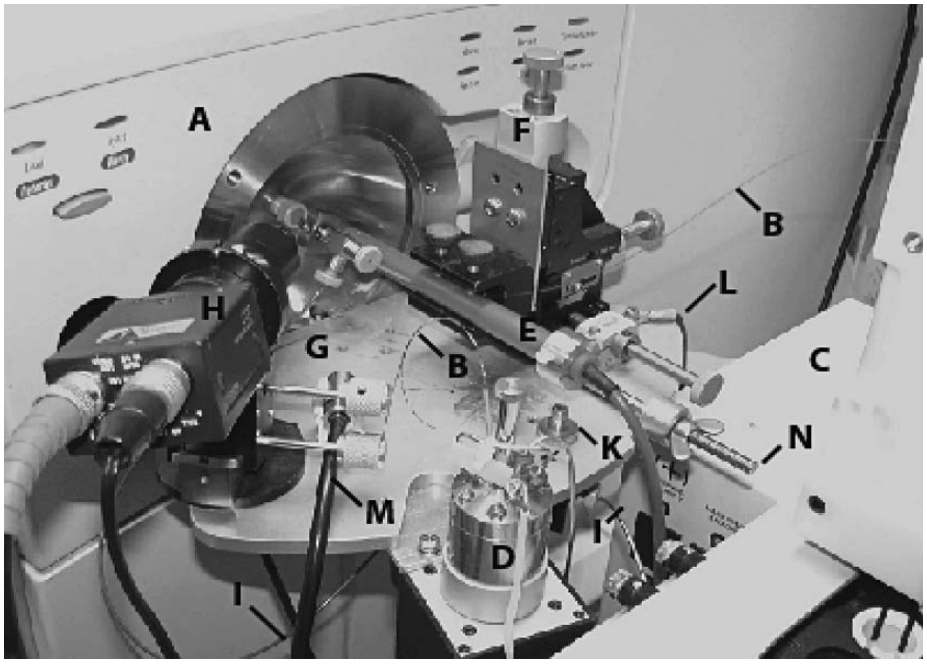


Fig. 5. Setup of the laboratory-constructed electrospray ionization source. **A**, mass spectrometer. The separation capillary **(B)** from the capillary electrophoresis (CE), or, optionally, from the liquid chromatography injection valve **(D)** is inserted into the ionization device (**E**, cf. **Fig. 2**) mounted to a *xyz* stage with verniers **(F)** on a horizontal platform **(G)**. The spray is monitored via a charge-coupled device camera with microscope lenses **(H)**. Sheath liquid is provided via a polyetheretherketone tubing (**I**, grounded at **K**). Other parts: **L**, grounding cable for the CE instrument (Beckman coupling kit); **M**, optical fiber illumination; **N**, fixation screw.

3. Spray observed with a charge-coupled device (CCD) camera with microscope lenses.
4. High-performance capillary electrophoresis system (P/ACE 5010) with CE/MS adapter kit from Beckman (Waldbronn, Germany). Fused-silica capillaries (Polymicro Technologies, Phoenix, AZ); length given below; inner diameter 75 μm, outer diameter 360 μm.
5. Rotavapor R-114 (Büchi, Flawil, Switzerland).

2.2. Chemicals, Standards and Consumables

1. Water was purified using a MilliQ system (Millipore, Eschborn, Germany). All chemicals (analytical grade) provided by Merck (Darmstadt, Germany) or Fluka (Deisenhofen, Germany).

2. *N*-Acylhomoserine lactone standards (C4-HSL, C6-HSL, C7-HSL, C8-HSL, C10-HSL, C12-HSL and C14-HSL) from Fluka were dissolved in methanol (1 mg/mL) and freshly diluted with water or running buffer to reach the desired concentration every day (*see* **Note 5**).
3. A 10-ppm mix of the hydroxy-*s*-triazines (ameline, hydroxydesethylatrazine, hydroxyatrazine, hydroxyterbutylazine; Dr. Ehrenstorfer, Augsburg, Germany) was prepared in 20 m*M* acetic acid.
4. Consumables: 3 MM Whatman paper (Whatman, Maidstone, UK); 6 mL Oasis MAX SPE columns (Waters, Eschborn, Germany); usual laboratory equipment.

2.3. Real Samples

Glycerol stock cultures (e.g., *Burkholderia cepacia* rhizosphere isolates) were plated on NB-Agar (Sigma, Deisenhofen) and were grown over night at 37 °C. Single colonies were transferred to NB liquid medium and were cultivated under shaking to an optical density (OD_{600}) of 1 (typically 8 h). Supernatants were harvested by centrifugation at 5000 rpm for 40 min.

3. Methods

3.1. N-Acylhomoserine Lactones (Neutrals)

N-Acylhomoserine lactones (HSLs, AHLs, etc.) are semiochemicals that play a crucial role in cell density-dependent communication in bacteria (quorum sensing, QS, reviewed, e.g., in ref. ***14***) and in communication processes between bacteria and higher organisms. HSLs are synthesized from *S*-adenosyl-L-methionine and side-products of the fatty acid biosynthesis. They vary in length and saturation of the fatty acid side chain (which normally consists of an even number of carbon atoms), and in substitution of the β-carbon (keto- or hydroxy functions). **Figure 6** gives an overview of naturally produced HSLs from different species.

In their native, and biologically active, form, HSLs are uncharged and cannot be separated by regular CZE. Because their hydrophobicities depend on the chain length and represent a homologous series, HSLs make ideal candidates for systematic studies in MEKC (for MEKC principles, *see* Chapter 30). To overcome the difficulties in MEKC/ESI-MS coupling noted above, different strategies were followed: (1) the use of bile salts, which are no actual "surfactants" but exhibit some features of such ***(15)***, (2) the use of a "polymeric surfactant" such as BBMA (a butylacrylate-/butylmethacrylate-/methacrylate copolymer), which is compatible with ESI/MS according to ***(8)***, and (3) the "reverse migrating micelle" technique in connection with partial-filling MEKC (in the following, RMM-PFMEKC). In the latter, the pH of the separation buffer is kept low, and the capillary is conditioned with hydrochloric acid (instead of sodium hydroxide) to minimize the EOF. In consequence, the mobility vector of the micelle (to the

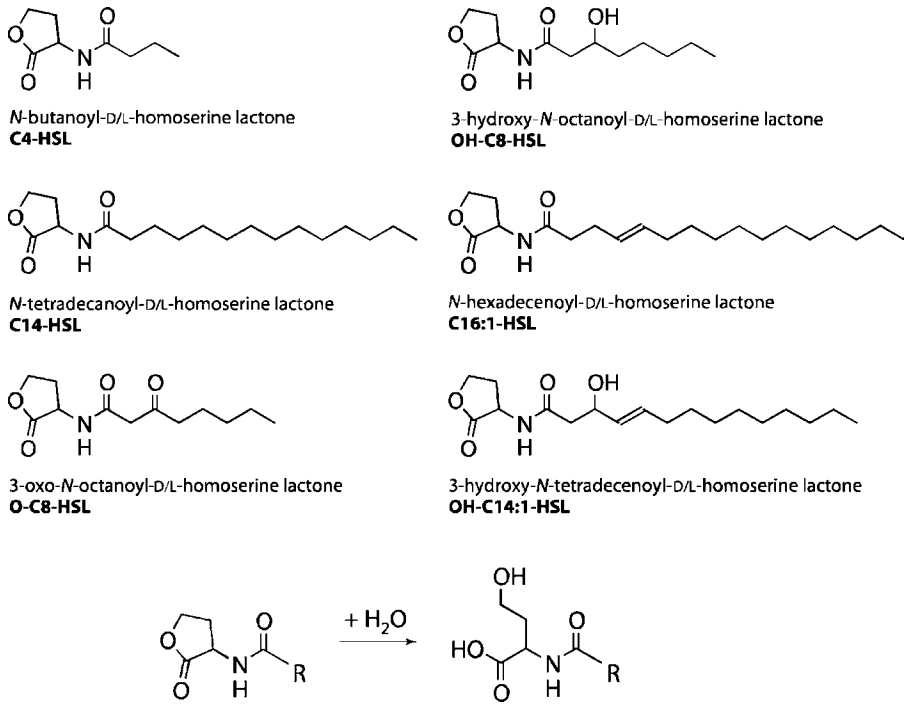


Fig. 6. Examples for naturally occuring *N*-acylhomoserine lactones (top) and hydrolysis to the acid under alkaline conditions (bottom).

anode) will supersede the mobility vector of the EOF (to the cathode) and the micelles will remain stationary in the capillary or even elute to the inlet. This can be assisted by filling the capillary only to a certain percentage with surfactant ***(16)***. In our experiments, all "non-sodium dodecyl sulfate (SDS)" separations (strategies 1 and 2 above) yielded unsatisfactory results in the form of irreproducibilities, precipitation effects, massive contamination of the interface, and/or an insufficient method flexibility. We thus focussed on the optimization of the RMM-PFMEKC. The partial filling degree and SDS and buffer concentrations were optimized, and all of the details are given in **ref**. ***13*** (*see* **Note 6**).

3.1.1. Sample Preparation

1. Shake 250 mL of supernatant (*see* **Subheading 2.3.**) twice with 100 mL of dichloromethane.
2. Dry combined organic phases with magnesium sulfate.
3. Filter with Whatman paper.
4. Evaporate to dryness using a rotation evaporator.
5. Redissolve with 250 μL of methanol and store at −20 °C.
6. Prior to the analyses, dilute extracts 1:10 (v/v) with background electrolyte.

3.1.2. CE/MS Analysis

1. CE conditions: voltage, 30 kV; background electrolyte, 20 m*M* ammonium acetate (pH 6.0, acetic acid); micellar buffer, 10 m*M* SDS in background electrolyte; injection, 5 s with 20 psi; capillary dimensions, 80 cm length/75 μm inner diameter/360 μm outer diameter; initial conditioning and conditioning before/after each day, 30 min with 1 *M* HCl at 20 psi/30 min with buffer; conditioning between runs, 5 min with 1 *M* HCl/5 min with buffer at 20 psi; temperature, ambient. Partial filling with 60% (capillary length) of micellar buffer. Sample injection 10 s with 0.5 psi.
2. Coupling: commercial ThermoFinnigan CE/MS interface. SL 50% methanol with 1% acetic acid delivered by a syringe pump at 1 μL/min. Ionization voltage, 5 kV; distance of needle to MS orifice, 5 mm; no sheath gas.
3. MS conditions: MS tuned on dibutyl phthalate (ubiquitous plasticiser, *see* **Note 10**), acquisition range m/z 100–400; full scan. Heated capillary at 250 °C.
4. **Figure 7** shows the detection of two HSLs from a *Burkholderia cepacia* strain with RMM-PFMEKC/MS. The compounds are identified by their common fragmentation product with m/z 102 (temperature induced degradation).

3.2. N-Acylhomoserines (Anions)

HSL (*see* **Subheading 3.1.** and **Fig. 6**, bottom) readily hydrolyze to the corresponding homoserines (HSs) under alkaline conditions, an effect that opens the possibility to selectively enrich them from cultures, and separate them in CE as anionic organic acids. The hydrolysis process also occurs in nature, presumably also as a way to regulate the HSL turnover. Thus, it was desirable to

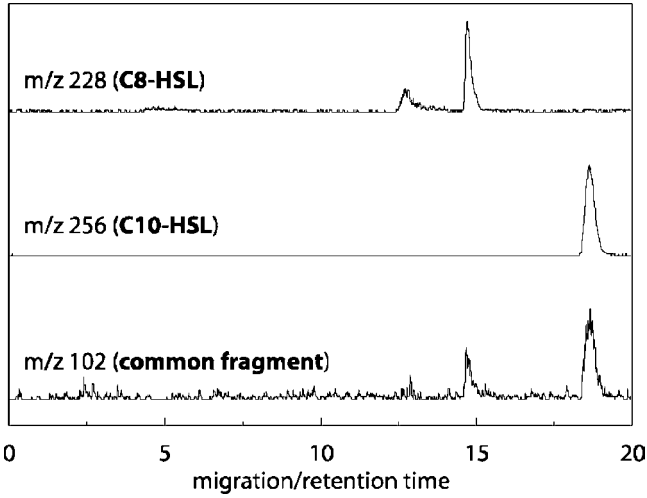


Fig. 7. Detection of C8-HSL and C10-HSL from a *Burkholderia cepacia* culture extract. For details, refer to **Subheading 3.1**.

develop a method for the quantification of autochthonous HSs, and of HSLs and HSs together as a sum parameter. For the determination of HSs plus HSLs, the HSLs in a centrifuged culture supernatant are hydrolyzed by addition of sodium hydroxide solution and the batch is incubated at room temperature (nuclear magnetic resonance [NMR] measurements showed that the hydrolysis reaction is complete in less than 1 min in 0.1 *M* sodium hydroxide). The hydrolyzed sample is then acidified with phosphoric acid and submitted to mixed-mode anion exchange solid-phase extraction (SPE). HSs alone (as natural degradation products of *N*-acylhomoserine lactones) are directly extracted from the supernatant by SPE, but after addition of phosphoric acid and sodium hydroxide (this yields the same matrix concentration, but the pH is kept at a low level). A more detailed description/validation of the method is given in **ref**. ***17***.

The HSs have a pK_a value of about 4.6, thus under (slightly) alkaline conditions, they can be separated in CE as anions. The separations are performed in ammonium carbonate buffer, pH 9.2; quantification is performed via the internal standard C7-HSL/C7-HS (*see* **Note 7**).

3.2.1. Internal Standard

1. To 500 µL of a solution of 1 mg/mL C7-HSL in methanol, add 100 µL of 1 *M* NaOH and 400 µL of water.
2. Mix and incubate for 15 min at room temperature.
3. Fill with water to reach a concentration of 50 µg/mL (*see* **Note 8**).

3.2.2. Sample Preparation: HSLs Plus Autochthonous HSs (Sum Parameter)

1. Add 500 µL of 1 *M* NaOH to 5 mL of culture supernatant.
2. Mix and incubate for 15 min at room temperature.
3. Dilute with 5 mL of water and acidify with 150 µL of 85% phosphoric acid.
4. Add 50 µL of internal standard (*see* **Subheading 3.2.1.**).
5. Extract immediately after hydrolysis.

3.2.3. Sample Preparation: Autochthonous HSs

1. Dilute 5 mL of culture supernatant with 5 mL of water.
2. Acidify with 15 µL of 85% phosphoric acid.
3. Add 500 µL of 1 *M* NaOH.
4. Add 50 µL of internal standard (*see* **Subheading 3.1.1.**).
5. Extract immediately after hydrolysis.

3.2.4. Sample Extraction

1. Condition column with 3 mL of methanol.
2. Condition column with 3 mL of water.
3. Apply sample (*see* **Subheadings 3.2.2.** and **3.2.3.**) sequentially.

4. Rinse with 3 mL of ammonium acetate buffer, pH 7.0.
5. Rinse with 3 mL of methanol.
6. Elute with 2% of formic acid in acetonitrile.
7. Evaporate to dryness under nitrogen.
8. Reconstitute with 500 µL of 50% methanol.
9. Store at −20 °C until analyzed.

3.2.5. CE/MS Analysis

1. CE conditions: voltage, 15 kV; buffer, 20 mi ammonium carbonate (pH 9.2, ammonia) plus 10% 2-propanol; injection, 5 s with 20 psi (*see* **Note 9**); capillary dimensions, 50 cm length/75 µm inner diameter/360 µm outer diameter; initial conditioning and conditioning before/after each day, 30 min with 0.1 *M* NaOH at 20 psi; conditioning between runs, 3 min with 0.1 *M* NaOH/3 min with buffer at 20 psi; temperature, ambient.
2. Coupling: laboratory constructed SL interface similar to **Fig. 2**, left, but without sheath gas: separation capillary guided through polymer tee and 22-G Hamilton syringe needle shortened to 4 cm. SL (50% 2-propanol with 0.5% acetic acid) pumped through side port. Ionization voltage, 4.2 kV; distance of needle to MS orifice, 5 mm; SL flow rate, 4 µL/min.
3. MS conditions: MS tuned on dibutyl phthalate (*see* **Note 10**), acquisition range m/z 100–400. Full scan for analysis of known HSL, 20% source fragmentation for determination of m/z 102 in unknown real samples. Heated capillary at 150 °C.
4. **Figure 8** shows the detection of C8-HS, C10-HS, and C12-HS extracted from a *B. cepacia* culture (different from that described under **Subheading 3.1**.) together with the internal standard C7-HS.

3.3. Hydroxy-s-Triazines

s-Triazines were widely used as herbicides in many parts of the world. After field application, the triazine herbicides are subjected to various degradation processes (photolysis, oxidation, hydrolysis, biodegradation, etc.), leading primarily to dealkylation of the amine groups in positions 4 and 6 (*see* structure in **Fig. 9**) and/or hydrolysis of the substituent in position 2. The latter process gives the corresponding hydroxytriazines, which have been found as contaminants in stream and reservoir water (*see* **ref**. ***18*** and references therein). Depending on structure and pH, these hydroxytriazines may exist as a myriad of species (neutral, charged, zwitterionic, and keto-enol tautomerics). For the optimization of the separation conditions as a function of the pH, please refer to the chapter on semiempiric models within this book.

In this section, we show the separation and detection of four hydroxy-*s*-triazines (ameline, hydroxydesethylatrazine, hydroxyatrazine, hydroxyterbutylazine; *see* **Fig. 9**) as cations at low pH with CE/MS.

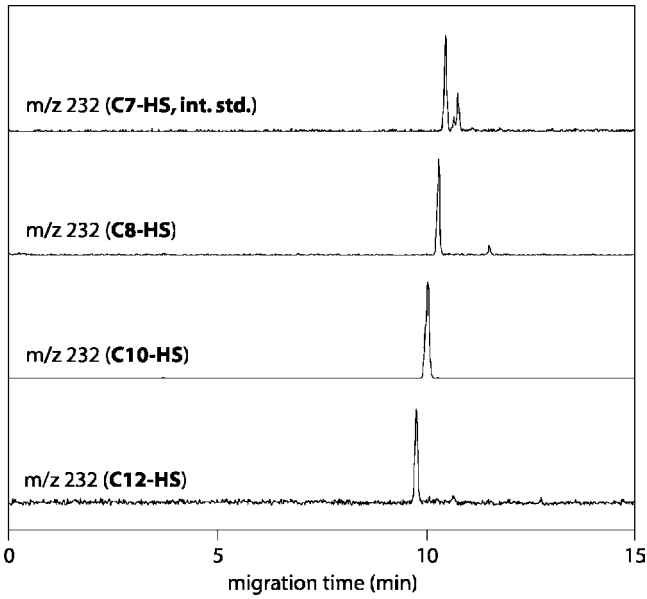
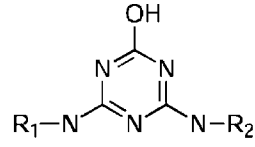


Fig. 8. Detection of C8-HS, C10-HS, and C12-HS extracted from a *Burkholderia cepacia* culture (different from that of **Fig. 7**) together with the internal standard C7-HS. For details, refer to **Subheading 3.2.**

3.3.1. CE/MS Analysis

1. CE conditions: voltage, 25 kV; electrolyte, 20 m*M* acetic acid (pH 3.45); injection, 10 s with 20 psi; capillary dimensions, 50 cm length/75 μm inner diameter/360 μm outer diameter; initial conditioning and conditioning before/after each day, 30 min



commercial name	R1	R2	M_R
hydroxyterbutylazine	CH_2CH_3	$C(CH_3)_3$	127
hydroxyatrazine	CH_2CH_3	$CH(CH_3)_2$	169
hydroxydesethylatrazine	H	$CH(CH_3)_2$	197
hydroxydiaminotriazine, ameline	H	H	211

Fig. 9. Structures of the analyzed hydroxy-*s*-triazines.

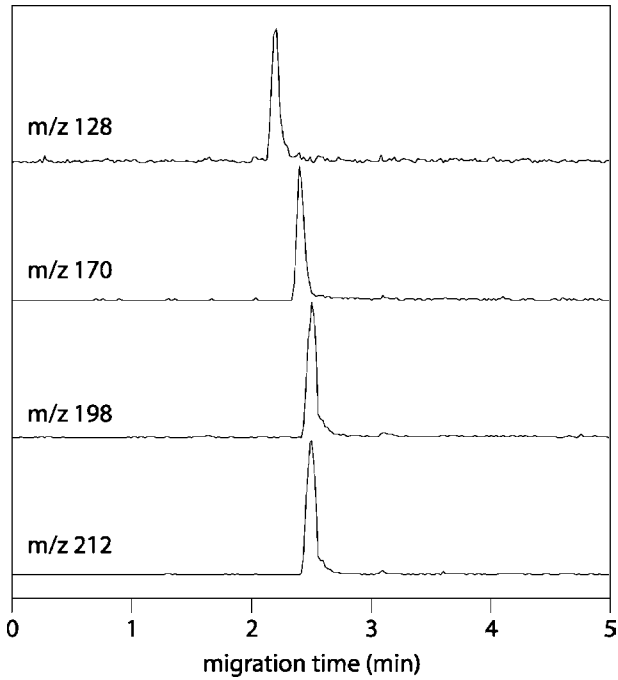


Fig. 10. Preliminary separation of a standard mix of ameline (m/z 128), hydroxydesethylatrazine (m/z 170), hydroxyatrazine (m/z 198), and hydroxyterbutylazine (m/z 212). For details, refer to **Subheading 3.3.** and **Fig. 9**.

with 0.1 *M* NaOH at 20 psi; conditioning between runs, 3 min with 0.1 *M* NaOH/3 min with electrolyte at 20 psi; temperature, ambient.

2. Coupling: laboratory-constructed SL interface similar to that shown in **Fig. 2**, left, but without sheath gas: separation capillary guided through polymer tee and 22-G Hamilton syringe needle shortened to 4 cm. SL (50% methanol with 0.5% acetic acid) pumped through side port. Ionization voltage, 4.0 kV; distance of needle to MS orifice, 5 mm; SL flow rate, 4 μL/min.
3. MS conditions: MS tuned on ameline, acquisition range m/z 100–300. Heated capillary at 125 °C.
4. **Figure 10** shows the detection of the four hydroxy-*s*-triazines in water (1 ppm each; *see* **Note 11**).

4. Notes

1. With the Beckman P/ACE (at least for the 2000 to 5000 series), e. g., a hole can be drilled into the upper left edge of the capillary cartridge, the MS can be turned around, and the CE instrument can be placed right of the MS. In this setup,

only the first few centimeters of the capillary are cooled (this requires special precautions regarding separation voltages and buffer molarity—*see* **Subheading 1.2.4**.). To save cooling liquid, the cooling circle of the P/ACE can be sut down by disconnecting (1) the float lever (remove cover at the left side of the instrument) and (2) the coolant pump (remove respective plugs on the circuit board behind the cover at the right side of the instrument).

2. Again, as a practical example with "our" ThermoQuest LCQ duo, the ESI housing can be removed, and the ionization interface can be mounted on a horizontal platform equipped with a *xyz* stage (*see* **Fig. 5—note** safety regulations).
3. The injected volume is given by the Hagen-Poiseuille equation,

$$I = \frac{\Delta V}{\Delta T} = \frac{\pi R^4}{8\eta l}\Delta P$$

where I is the volume, V, injected over the time, T. R, inner radius of the capillary; η, viscosity; l, capillary length; Δp, pressure difference between inlet and outlet end of the capillary. The Hagen-Poiseuille equation is the core of Beckman's "CE Expert" software by H. Whatley (http://www.beckman.com/resourcecenter/labresources/ce/downpage.asp or the online version: http: //www.beckman.com/resourcecenter/labresources/ce/ceexpert.asp).

4. In our experience, no sheath gas is necessary at least for positive ionization if the SL composition, the flow rate, and the voltage is carefully optimized.
5. HSLs undergo hydrolysis at room temperature even at neutral pH. Even in methanol, degradation (methanolysis) might be observed. Always check the integrity of the standards.
6. Briefly, the minimum concentration of SDS yielding satisfactory peak resolution was chosen. The capillary could be filled with SDS to not more than 80% (otherwise, SDS eluted into the MS despite all precautions).
7. HSLs are synthesized from acylated acyl carrier protein (as a side effect of the fatty acid biosynthesis). C7-HSL (with its odd number of carbons in the side chain) is thus not expected to occur frequently in nature.
8. The internal standard can be stored at room temperature for at least 3 d.
9. Longer injection times (10 s and above) were possible with standard solutions, but caused substantial peak broadening in real samples.
10. Dibutyl phthalate (m/z 279) is an ubiquitous plasticizer and thus an unevitable background signal. However, being in the mass range of the analytes, it may be used for tuning during a CE run and thus under "real" conditions (flow rates and voltages in contrast to direct infusion of the standards).
11. The resolution of the peaks in this run is certainly far from optimum (although resolution in CE/MS is not as important as in CE/UV). Supposable optimization parameters might include the use of a real buffer instead of only 20 m*M* acetic acid, pH changes, and addition of an organic modifier to the buffer.

Acknowledgments

We thank Prof. Dr. A. Hartmann (GSF) and his working group for the microbiological samples. Sarah Jakoby is thanked for real sample measurements with CE/MS.

References

1. Olivares, J. A., Nguyen, N. T., Yonker, C. R., and Smith, R. D. (1987) On-line mass spectrometric detection for CZE. *Anal. Chem*. **59,** 1230–1232.
2. Schmitt-Kopplin, P. and Frommberger, M. (2003) Capillary electrophoresis mass spectrometry: 15 years of developments and applications. *Electrophoresis* **24,** 3837–3867.
3. Schmitt-Kopplin, P. and Englmann, M. (2005) Capillary electrophoresis mass spectrometry: Survey on developments and applications 2003–2004. *Electrophoresis* **26,** 1209–1220.
4. Fenn, J. B. (2003) Electrospray wings for molecular elephants (Nobel lecture). *Angew. Chem. Int. Edit*. **42,** 3871–3894.
5. Caprioli, R. and Gross, M. (2005) *The Encyclopedia of Mass Spectrometry. Volume 8, Hyphenated Methods*. Elsevier, Amsterdam.
6. Abian, J., Oosterkamp, A. J., and Gelpi, E. (1999) Comparison of conventional, narrow-bore and capillary liquid chromatography mass spectrometry for electrospray ionization mass spectrometry: practical considerations. *J. Mass Spectrom*. **34,** 244–254.
7. Kebarle, P. and Tang, L. (1993) From ions in solutions to ions in the gas phase: the mechanism of electrospray mass spectrometry. *Anal. Chem*. **65,** 972–986.
8. Rundlett, K. L. and Armstrong, D. W. (1996) Mechanism of signal suppression by anionic surfactants in capillary electrophoresis electrospray ionization mass spectrometry. *Anal. Chem*. **68,** 3493–3498.
9. Yang, L. and Lee, C. S. (1997) Micellar electrokinetic chromatography-mass spectrometry. *J. Chromatogr. A* **780,** 207–218.
10. Cole, R. B. (2000) Some tenets pertaining to electrospray ionization mass spectrometry. *J. Mass Spectrom*. **35,** 763–772.
11. Fernandez de la Mora, J., van Berkel, G. J., Enke, C. G., Cole, R. B., Martinez-Sanchez, M., and Fenn, J. B. (2000) Electrochemical processes in electrospray ionization mass spectrometry. *J. Mass Spectrom*. **35,** 939–952.
12. Agilent Technologies (1999) CE-ESI-MS: an integrated solution. Publication Number 5968-1328E.
13. Frommberger, M., Schmitt-Kopplin, P., Menzinger, F., *et al*. (2003) Analysis of *N*-acyl-L-homoserine lactones produced by *Burkholderia cepacia* with partial filling micellar electrokinetic chromatography: electrospray ionization-ion trap mass spectrometry. *Electrophoresis* **24,** 3067–3074.
14. Fuqua, C. and Greenberg, E. (2002) Listening in on bacteria: acyl-homoserine lactone signalling. *Nat. Rev. Mol. Cell Biol*. **3,** 685–695.

15. Messina, P., Morini, M. A., Schulz, P. C., and Ferrat, G. (2002) The aggregation of sodium dehydrocholate in water. *Colloid Polym. Sci*. **280,** 328.
16. Molina, M., Wiedmer, S. K., Jussila, M., Silva, M., and Riekkola, M. L. (2001) Use of a partial filling technique and reverse migrating micelles in the study of *N*-methylcarbamate pesticides by micellar electrokinetic chromatography-electrospray ionization mass spectrometry. *J. Chromatogr. A* **927,** 191–202.
17. Frommberger, M., Hertkorn, N., Englmann, M., *et al*. (2005) Analysis of *N*-acylhomoserine lactones after alkaline hydrolysis and anion-exchange solid-phase extraction by capillary zone electrophoresis-mass spectrometry. *Electrophoresis* **26,** 1523–1532.
18. Schmitt, P., Poiger, T., Simon, R., Freitag, D., Kettrup, A., and Garrison, A. W. (1997) Simultaneous determination of ionization constants and isoelectric points of 12 hydroxy-*s*-triazines by capillary zone electrophoresis and capillary isoelectric focusing. *Anal. Chem*. **69,** 2559–2566.

8

Analysis of the Enantiomers of Chiral Pesticides and Other Pollutants in Environmental Samples by Capillary Electrophoresis

Arthur W. Garrison, Philippe Schmitt-Kopplin, and Jimmy K. Avants

Summary

The generic method described here involves typical capillary electrophoresis (CE) techniques, with the addition of cyclodextrin chiral selectors to the electrolyte for enantiomer separation and also, in the case of neutral analytes, the further addition of a micelle-forming compound such as sodium dodecyl sulfate (SDS) for separation by the micellar electrokinetic chromatography (MEKC) mode of CE. This generic method has broad application for the separation and analysis of enantiomers of chiral pesticides and other small molecules in a variety of environmental matrices. Aqueous samples such as surface water are analyzed after simple filtration, but centrifugation is sometimes necessary for soil–water slurry samples. Soils and sediment must be extracted with a polar organic solvent such as methanol, which needs only to be evaporated to near dryness, diluted with water, and filtered before CE analysis. Simple borate or phosphate-based buffers are usually used in the CE electrolyte. The method must be optimized for the electrolyte composition, including the correct chiral selector and its concentration, as well as for column conditions and instrumental variables such as voltage. Specific methodologies for application of this generic CE method to follow the enantioselective microbial transformation of ruelene, a neutral organophosphorus insecticide, dichlorprop, an ionic phenoxyalkanoic acid herbicide, and bromochloroacetic acid, a drinking water disinfection byproduct, are provided.

Key Words: CE; capillary electrophoresis; MEKC; pesticides; ruelene; dichlorprop; bromochloroacetic acid; pollutants; chiral; enantiomer; cyclodextrin; enantiomer separation

From: *Methods in Molecular Biology, vol. 384: Capillary Electrophoresis*
Edited by: P. Schmitt-Kopplin © Humana Press Inc., Totowa, NJ

1. Introduction

As many as 25% of all pesticides, as well as many other environmental pollutants, are chiral and exist as two mirror-image isomers called enantiomers ***(1)***. These isomers differ in their environmental fate and effects, so it is necessary to study them as separate entities ***(2,3)***. This requires enantiomer separation, which may involve gas or high-performance liquid chromatography with chiral columns, or capillary electrophoresis (CE) with chiral selector reagents ***(2–8)***. CE analysis of ionizable chiral pesticides employs capillary zone electrophoresis (CZE) or, for neutral pesticides, the micellar electrokinetic chromatography (MEKC) mode of CE ***(6–9)***. The latter mode involves the addition of a pseudostationary phase, i.e., a negatively charged micelle such as may be formed from sodium dodecyl sulfate (SDS). Relative partitioning of the neutral analyte between the water and the micellar phase results in a differential migration and separation of the analytes as a function of their affinity to the micelles. Either mode of CE requires only addition to the electrolyte of a chiral selector such as a cyclodextrin (CD) to achieve enantiomer separation. These CDs, which are easily dissolved into the existing aqueous electrolyte solutions (run buffers), are chiral and can form complexes with the enantiomers of chiral analytes, including those neutral analytes that have already interacted with SDS, resulting in diastereomers that have different CE migration times. As a result, rapid enantiomer separation and analysis is possible with reliable, reproducible results. This is in contrast to the more frequently used methods for the analysis of enantiomers of chiral pollutants, which include high-performance liquid chromatography (HPLC) and gas chromatography (GC) ***(2,3,7,8)***. Both of these techniques require relatively expensive chiral columns that are specific for separation of a limited number of analyte enantiomers, and GC analysis also requires extraction of the pesticide from an aqueous matrix and sometimes derivatization.

Despite wide use in chiral drug analyses ***(5)***, application of CE to the analysis of pesticides ***(10)***, chiral pesticides ***(2,3,9–15)***, or other environmental pollutants is relatively new. In past investigations using CE, chiral pesticides and other pollutants such as dichlorprop ***(11,13,14)***, ruelene ***(14)***, and bromochloroacetic acid (BCAA; unpublished work of the authors) have exhibited enantioselective transformation rates. In order to study enantiomer transformation under a variety of conditions, a CE separation method was developed for the enantiomers of these pollutants and applied to monitor their transformation in water (BCAA) or in aerobic soil slurries ***(11,14)***. Periodic sampling and analysis of the slurries over several months allowed calculation of kinetic data, enantiomer fractions (EFs), and observation of any enantioselectivity.

The generic method described here involves typical CE techniques with the addition of commonly available cyclodextrins for enantiomer separation and also, in the case of neutral analytes, the further addition of SDS for separation by the MEKC mode of CE. Water samples are analyzed after simple filtration, but centrifugation is sometimes necessary for soil–water slurry samples. Soils and sediment must be extracted with a polar organic solvent, which is evaporated to near dryness, diluted with water, and filtered before CE analysis. Simple phosphate, acetate, or borate-based buffers are usually used in the electrolyte. The method must be optimized for the buffer composition, for the correct chiral selector and its concentration, the concentration of any organic modifier that may be used and, in the case of MEKC analysis, the SDS concentration. Other variables such as the applied voltage and column conditioning must also be optimized. Specific methodology for application of this generic CE method to follow the enantioselective microbial transformation of ruelene, a neutral organophosphorus insecticide, dichlorprop, an ionic phenoxyalkanoic acid herbicide, and bromochloroacetic acid, a drinking water disinfection byproduct, are provided here. **Figures 1** and **2** show partial electropherograms of ruelene and bromochloroacetic acid enantiomers in environmental

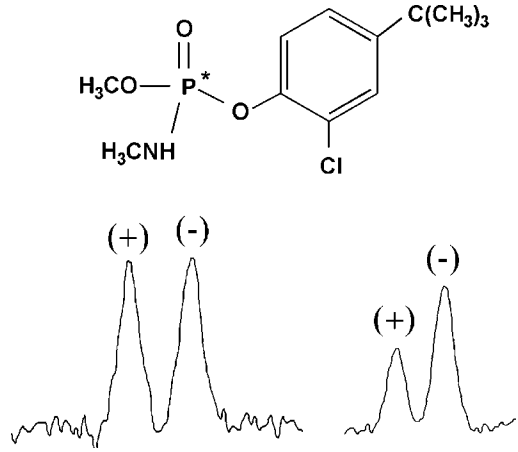


Fig. 1. Partial electropherograms of ruelene enantiomers in a soil–water slurry spiked with 50 mg/L of the ruelene racemate. Micellar electrokinetic chromatography analysis according to the methods specified in this paper allowed calculation of enantiomer fractions (EFs) with time as a measure of microbial transformation. For ruelene at t_o, EF = 0.50 (left electropherogram); at 100 d (right electropherogram), EF = 0.40 [EF = area (+)-enantiomer/area of both enantiomers]. * Designates the chiral center of the molecule.

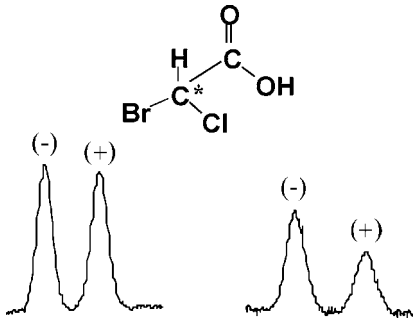


Fig. 2. Partial electropherograms of bromochloroacetic acid (BCAA) enantiomers spiked into a natural river water at 30 mg/L of the BCAA racemate. Capillary electrophoresis analysis according to the methods specified in this paper allowed calculation of enantiomer fractions (EFs) with time as a measure of microbial transformation. For BCAA at t_o (left), EF = 0.50; at 8 d (right), EF = 0.43 [EF = area (+)-enantiomer/area of both enantiomers]. * Designates the chiral center of the molecule.

samples before and after microbial transformation. (For illustrations of similar results with dichlorprop using the methods described here, *see* **refs. *11*** and ***13***.)

2. Materials

2.1. Chemical Reagents

1. SDS: (ACS grade, Sigma-Aldrich, St. Louis, MO) **(Note 1)**
2. CDs: 2-hydroxypropyl β-CD and 2,3,6-tri-O-methyl β-CD (commonly known as trimethyl β-CD) (>99%, Sigma-Aldrich) **(Notes 2** and **3)**
3. Buffer salt: sodium tetraborate (ACS grade, Sigma-Aldrich)
4. Organic modifiers and solvents: acetonitrile, methylene chloride, methanol (HPLC grade, Sigma-Aldrich) **(Note 4)**
5. Analyte standards: dichlorprop, ruelene, bromochloroacetic acid (>98%, Chem Service, West Chester, PA) (**Note 5**)
6. Sodium hydroxide (reagent grade), 0.1 *M* in deionized water, and dilute HCl
7. Deionized water (DIW): Barnstead Nanopure II

2.2. Carrier Electrolytes (Notes 1–4 and 6–8)

1. For dichloprop analysis: 25 m*M* sodium tetraborate in DIW adjusted to pH 8.5 with dilute HCl and containing 25 m*M* trimethyl β-CD.
2. For bromochloroacetic acid analysis: 50 m*M* sodium tetraborate in DIW adjusted to pH 8.5 with dilute HCl and containing 40 m*M* trimethyl β-CD.
3. For ruelene analysis: 20 m*M* sodium tetraborate in DIW adjusted to pH 8.5 with dilute HCl and containing 100 m*M* SDS, 20% acetonitrile, and 40 m*M* 2-hydroxypropyl-β-CD.

2.3. Equipment and Supplies

1. High-performance capillary electrophoresis system: A Beckman P/ACE System 5500 CE, liquid cooled **(Note 9)**, with diode array ultraviolet (UV) detector **(Notes 10** and **11)**, hydrodynamic injection **(Note 12)**, power supply up to 30 kV **(Notes 13** and **14)** and System Gold version 8.1 chromatography software was used for development of these methods.
2. CE column: uncoated fused silica **(Note 15)**, 75 μm inner diameter (OD), 300 μm outer diameter (OD), 57 cm total length, 50 cm effective length (MicroSolv Technology Corporation, Long Branch, NJ) **(Note 16)**
3. Syringe filters: 0.45 μm nylon (SRI, Eatontown, NJ, or equivalent)
4. CE vial inserts for small volumes; mini-vials, 400 μL, or micro-vials, 30 μL (Beckman Instruments, Fullerton, CA).

3. Methods

This method assumes that samples have been collected and stored according to good laboratory practices, keeping in mind the purpose for which the analysis is intended. In the case of the examples given here, the purpose of analysis is to measure the concentration of enantiomers in natural environmental samples, or in laboratory microcosms over time as microbial transformation of a chiral substrate is allowed to proceed. Thus, the method description begins with the natural sample as retrieved from storage, or with each individual microcosm sample as collected with increasing incubation time.

The CE methodology given in detail here is specifically for enantiomers of the analytes dichlorprop ***(11–14)***, ruelene ***(9**,**11**,**14)*** and bromochloroacetic acid; the variables involved in the electrolyte composition and the column and instrumental conditions are specified for these analytes. However, the basic principles and methodology will be similar for any small neutral chiral molecule such as ruelene, which is analyzed by the MEKC mode of CE, and for any small negatively charged chiral molecule such as dichlorprop or BCAA, which are analyzed by the traditional capillary electrophoresis mode (sometimes referred to as capillary zone electrophoresis [CZE]). In adapting the specific CE methods detailed here to other small chiral molecules whose enantiomers are to be separated, there are certain variables for which modification will be necessary. These are listed and briefly discussed in **Notes 11–14**.

3.1. Quality Assurance

1. *Standard curve*. A standard curve should be prepared by analysis of standards of the analyte(s) of interest. There should be at least four standards of different concentrations, covering a range of values expected for the samples of interest, and each point should be the average of three measurements. The standards for the curve should be dissolved in a matrix similar to that of the samples to be analyzed.

These standards should be stored in the cold and analyzed at least once a week (depending upon stability of the standards) to check for variations from the original curve. Changes in sample matrix **(Note 17)**, electrolyte **(Note 6)**, column conditions **(Note 15)**, instrument conditions, or other variables over time may create the need for a new standard curve.

2. *Daily conditioning of the CE column* **(Note 15)**. At the beginning of each day that samples are to be analyzed, the column is prepared by washing in the following order: DIW for 10 min, 0.1 *M* NaOH for 10 min, DIW for 10 min again, and electrolyte solution (prepared for the analyte[s] of interest) for 4 min or until baseline is stable.
3. *Daily QA check of standard analyte(s)*. After conditioning the column, analyze a solution of a standard(s) of the analyte(s) of interest for that day. Compare against the previously prepared standard curve **(step 1)** for accuracy of concentration, enantiomer peak resolution, and analyte migration time. Resolution (R) may be calculated according to the following formula: $R = 2(t^1 - t^2)/(w^1 + w^2)$, where t = migration time, w = width at peak base, and 1 and 2 are enantiomer peaks. Criteria for acceptance of concentration and resolution measurements will depend on the purpose of the day's analysis. If acceptance criteria are not met, check for accuracy of concentration of the daily standard, then for changes in electrolyte, column conditions, or instrument conditions that may have caused differences in peak intensity or resolution.
4. *Internal and external standards*. Where analyte quantitation is most important, an external standard (sometimes called a surrogate analyte) of similar chemical characteristics to the analyte(s), but with a different migration time, may be added to the sample matrix before sample preparation at a concentration level close to the level expected for the analyte. The concentration of the analyte may be corrected for the recovery of the external standard. In addition, such a standard may help in analyte peak identity; if CE migration times change from sample to sample because of differences in the sample matrix or other factors, the time relationship between the standard and analyte peaks will usually remain fairly constant. An internal standard may also be added to the prepared sample just before CE instrumental analysis as a check for consistency in migration times and instrument sensitivity.

3.2. Sample Preparation (Notes 5 and 17)

1. *Surface water*. For surface water samples that contain little suspended solid material, a 5-mL disposable syringe is used to collect about 1 mL of the water. The syringe is then fitted with a nylon syringe filter and the collected sample is transferred to a 2-mL Beckman CE vial. If a limited amount of sample is available, the vial is fitted with a 100-μL insert and about 40 μL of sample is transferred. The split flexible vial cap (Beckman) is fitted to the vial, and the sample is then ready for analysis.
2. *The aqueous phase of soil/sediment slurries*. These samples inherently contain lots of suspended soil particles and centrifugation is necessary to settle solids and avoid plugging the CE column. Centrifuge at about 10,000 rpm for 5 min or until solids have formed a pellets in the bottom of the tube. Then sample the supernatant with a syringe and, if necessary, filter through a syringe filter into a CE vial as for surface

water. For exact quantitation of the analyte associated with the aqueous phase of a slurry, it may be necessary to decant and save the first supernatant, rinse the solid residue with DIW, filter the rinse water through a syringe filter (or centrifuge if necessary), and add it to the first supernatant. In this case, it will be necessary to measure the rinse water volume for accurate calculation of analyte concentration because it will have diluted the original aqueous sample.

3. *The solid phase of sediment slurries*. These are the sediment pellets formed upon centrifugation of slurries. The slurry is centrifuged as in **step 2**, and the solid pellet is separated from the aqueous matrix by decantation. If measurement of only the analyte sorbed onto the solids is desired, the solids are rinsed with DIW to remove any analyte that may be associated with the residual aqueous phase, centrifuged again, and the aqueous phase is again decanted away. The solids are then extracted in a vortex mixer with 1 mL of methanol. This mixture is then mixed with 2 mL of water; this composition makes the final sample more amenable to CE analysis. This aqueous/methanol phase is then centrifuged to remove the solids and the supernatant extract solution is decanted and saved. The solids are rinsed with about 200 μL of methanol by vortexing; this methanol rinse is either centrifuged or filtered through a syringe filter and added to the first extract. The total extract is then made to a known volume; this is critical for concentration calculation because the extract theoretically contains all of the analyte originally sorbed onto the soil. About 1 mL of this solution is transferred into a CE vial.
4. *Soils (13)* **(Note 17)**. Follow the procedure **step 3** above, beginning with the solid extraction step ("The solids are then extracted. . ."). In case of interference with the CE analyte peak, it will be necessary to clean this extract by any of the commonly used cleanup techniques; for example, florisil or silica gel adsorption cartridges.

3.3. CE Instrumental Analysis (Notes 11–14)

1. *Computer control*. The instrumental part of modern CE analysis is completely computer controlled. This includes injection type (usually hydrodynamic with nitrogen pressure) and time (which is equivalent to a certain injection volume), orientation of vials for certain purposes (sample vial for sample injection, electrolyte vials for the sample analysis, NaOH and DIW vials for column rinsing, etc.), run time for each step, etc. The parameters of the "method" to be used for the particular sample to be run are also specified by the operator through the computer; these include voltage, temperature, detector wavelength, and process time. During the analysis, the computer displays these previously set parameters as well as monitors absorbance, voltage, current, temperature, and elapsed time. After analysis, the computer software can be used to expand electropherogram areas, adjust and print the electropherogram display, calculate analyte concentrations, obtain UV spectra of peak components, etc.
2. *Column preparation for each sample* **(Note 15)**. The column is washed in order with DIW for 2 min, 0.10 *M* NaOH for 2 min, water again for 4 min, and the appropriate electrolyte solution for 2 min before each sample run. This procedure should be specified in the computer sample table to be done at the completion of

the preceding sample run. This ensures that the column has been cleaned and is ready for the next run.

3. *Dichlorprop CE analysis*. The two electrolyte vials are filled with the electrolyte containing 25 m*M* sodium tetraborate in DIW adjusted to pH 8.5 with dilute HCl and containing 25 m*M* trimethyl β-CD. The following parameter values are set through the computer: temperature, 23 °C; detector wavelength, 230 nm; voltage, 15 kV; injection type and time (hydrodynamic, usually for 5 s); and run time, 25 min.
4. *Bromochloroacetic acid CE analysis*. The electrolyte vials are filled with the electrolyte containing 50 m*M* sodium tetraborate in DIW adjusted to pH 8.5 with dilute HCl and containing 40 m*M* trimethyl β-CD. The following parameter values are set through the computer: temperature, 23 °C; detector wavelength, 200 nm; voltage, 25 kV; injection type and time (hydrodynamic, usually for 5 s); and run time, 25 min.
5. *Ruelene CE analysis*. The electrolyte vials are filled with the electrolyte containing 20 m*M* sodium tetraborate in DIW adjusted to pH 8.5 with dilute HCl and containing 100 m*M* SDS, 20% acetonitrile, and 40 m*M* 2-hydroxypropyl-β-CD. The following parameter values are set through the computer: temperature, 23 °C; detector wavelength, 200 nm; voltage, 25 kV; injection type and time (hydrodynamic, usually for 5 s); and run time, 25 min.
6. *CE sample run*. After column preparation, filling of the electrolyte vials, and parameter adjustment, the sample table is activated through the computer, voltage is applied, and the sample run commences. A voltage ramp time, previously set through the computer, allows a slow (0.6 min) voltage increase to the desired voltage to avoid overheating the column.

The computer monitors the system for voltage, current, and temperature throughout the run, while sample UV absorbance is displayed on the electropherogram. The current generated by the applied voltage should rise quickly as the voltage ramp increases to the desired voltage level; the final current is determined by the voltage and electrolyte ionic strength, and should remain constant within 2 or 3 μA throughout the run. The maximum current level allowed by the Beckman CE instrument is 250 μA. Higher currents make it difficult to control the column temperature.

3.4. Data Analysis

As mentioned above, the CE computer can calculate concentrations. Manually, analyte concentrations are calculated similarly to the calculation of standard concentrations as described in **Subheading 3.1., step 1**. That is, the analyte peak area is compared to areas from the standard curve. If several samples are run in sequence, a standard should be analyzed with every 10 samples and these standard concentrations should be checked against the standard curve for consistency of their concentrations. A single-point standard procedure for calculation of analyte concentration can be used for less critical

samples, but comparison of analyte areas with the standard curve will provide more accuracy. Correction may be made for recovery of the external standard, if applicable (*see* **Subheading 3.1., step 4**).

3.5. Method Sensitivity and Reproducibility

The detection limit for this method for BCAA in water is about 1 mg/L in the injected sample with a 5-s injection time. For dichlorprop and ruelene, the method detection limit for the aqueous phase of soil slurries was 3 and 5 mg/L, respectively, with a 5-s injection. These limits may be lower for surface water samples in which the matrix is cleaner. Also, longer injection times will lower the detection limit; for cleaner samples, injection times can be as long as 25 s or more. In addition, for increased sensitivity with organic extracts of soil, the analyte may be concentrated by reducing the extract volume to almost dryness, adding only the minimum amount (e.g., 50 μL) of methanol to dissolve the analyte, and diluting with the minimum amount of water (e.g., 150 μL) to facilitate the CE analysis (*see* **Subheading 3.2.**, **step 3**). A CE vial insert must be used for this final sample volume.

Table 1 ***(11)*** shows the means and precision data for repetitive runs of ruelene and dichlorprop standards. CE migration times can vary because of changes with time in the buffer or column surface conditions. However, **Table 1** shows that for eight consecutive runs of both a 25-μg/mL and a 100-μg/mL solution of ruelene, the percent relative standard deviation (RSD) for migration times of each enantiomer is good—about 3.5 for the lower concentration and about 1 for the higher. This degree of migration time reproducibility also means that the resolution between enantiomer peaks is fairly constant, which serves as one indicator of correct analyte identification. The RSDs of the ruelene enantiomer peak areas are also good, less than 2.5 for each enantiomer at the low concentration but higher, about 4.8 and 5.9, for the high concentration. The %RSDs of the EF values calculated from these enantiomer peak areas are about 2 in both cases, indicating good reproducibility. The average EF calculated from these data is 0.50 for the low and 0.48 for the high concentrations of the racemate. [EF is defined as being the area of the (+)-enantiomer/sum of areas of both enantiomers or, if optical rotation is unknown, the area of the first migrating peak/sum of areas of both peaks.]

The quality of the dichlorprop data of **Table 1** is similar to that of ruelene. The migration time %RSDs are better, whereas the peak area %RSDs are close to those of the 100 μg/mL ruelene standard.

It must be realized that these reproducibility data are for standard solutions. With real samples, precision will be less. Co-migrating or closely migrating materials in the sample matrix may interfere with peak area measurements.

Table 1
Capillary Electrophoresis Parameter Means and Precision Data for Ruelene and Dichlorprop

	Migration time (min)		Peak Area		EF
Enantiomer	+	–	+	–	+/(–)+(+)
Ruelene, 25 μg/mL (***n***=8)					
Mean	13.386	13.547	2.724	2.747	0.5
SD	0.462	0.473	0.058	0.068	0.01
%RSD	3.452	3.489	2.131	2.471	2
Ruelene, 100 μg/mL (***n***=8)					
Mean	20.123	20.422	14.667	15.881	0.48
SD	0.2	0.208	0.698	0.934	0.01
%RSD	0.995	1.016	4.756	5.88	2.08
Dichlorprop, 50 μg/mL (***n***=6)					
Mean	7.897	7.791	2.451	2.481	0.5
SD	0.061	0.059	0.106	0.105	0.01
%RSD	0.77	0.76	4.325	4.247	2

EF, enantiomer fraction; SD, standard deviation; RSD, relative standard deviation.

More pronounced deviations may occur in migration times, when components in the sample matrix affect the column surface or otherwise interfere with the mobility of the analyte. The use of internal and/or external standards can help discover and correct for these deviations. In addition, when analyzing for enantiomers, the presence of two peaks with a difference in migration times that corresponds to the difference in times of the standard enantiomers helps identify them.

4. Notes

1. SDS concentration: for MEKC, the concentration of SDS must be optimized and higher than the critical micelle concentration; it is often about 100 m*M*.
2. Chiral selector: there are a large variety of chiral molecules that have been used for this purpose, but only CDs will be considered here. CDs are cyclic oligomers of several D-(+)-glucopyranose units. There are five or six native and substituted CD chiral selectors that are in fairly common use. The native ones are α, β, and γ, possessing six, seven, and eight glucopyranose units, respectively. The substituents, which form ethers with the carbohydrate hydroxyl groups, are methyl groups or, in one common case, a 2-hydroxypropyl group. The appropriate CD for a particular analyte will have the optimum-sized cavity for the analyte plus the optimum type (primary or secondary) and arrangement of hydroxyl or substituted

hydroxyl moieties for best complexation with the analyte. The cavity size for cyclodextrins increase in the order $\alpha < \beta < \gamma$, and a general rule is that β-CDs are best for molecules with a single aromatic ring, whereas γ-CDs are best for larger multiple or fused-ring molecules.

3. Concentration of chiral selector: this usually ranges between 20 and 50 m*M*, although there are lower and higher exceptions.
4. Organic modifier: especially in MEKC, acetonitrile, acetone, methanol, or other organic solvents may be added to the electrolyte at concentrations of 10 to 20% by volume to improve enantiomer separation. They act to help solubilize the analyte or its SDS complex, and also to avoid coating the CE column with electrolyte components. However, the migration time of the analyte often shifts if an organic modifier is added; the presence of an internal standard helps to observe this shift.
5. Sample/analyte solvent: water (DIW) is the normal sample solvent, but sometimes 10 to 30% of methanol or acetonitrile is allowable or even required to maintain solubility of the analyte(s) during the separation process. On the other hand, if sample preparation involves extraction with or dissolution in an organic solvent, this matrix must be either diluted with water to a ratio of 2:1 or 3:1 water:organic or evaporated to dryness and redissolved in water to facilitate CE analysis.
6. Buffer composition: usually borate, phosphate-, or acetate-based buffers are employed to keep the pH relatively constant throughout a separation process. Borate buffers are usually used for MEKC separations. Changes in chemical composition of the buffers can occur as a result of gradual electrolysis of the electrolyte—this is referred to as buffer depletion. There is a corresponding change in electrolyte pH, which usually causes shifts in analyte migration times. Buffer depletion can be avoided by changing the electrolyte in the vials after a number of runs. Electrolyte stability depends on a number of factors, and the number of runs that can be made before electrolyte change is necessary must be determined for each method. The same electrolyte can often last for 4 or more runs; very stable electrolytes may last for 10 or more runs. The automatic sampler on most CE systems can be set up to automatically switch to a new set of electrolyte vials after a certain number of runs, and newer instruments include automatic electrolyte replenishment features.
7. Buffer concentration is usually in the range of 20 to 50 m*M*. Higher buffer concentrations (higher ionic strength) give higher currents and can cause unduly high column temperatures.
8. pH of Electrolyte: for anionic analytes, the pH must be such that the analyte exists at least partially in the negative state; a general rule is that the electrolyte pH should be as close as possible (within one pH unit) to the pKa of the analyte. A good pH for MEKC of neutral analytes is about 8.5.
9. Column temperature: the column must be cooled to dissipate joule heat and maintain a constant temperature, usually close to ambient, e.g., 23 °C. However, temperature control also allows subambient (e.g., 10 °C) and above ambient (e.g., 40 °C) column temperature regulation.

10. Detector window: most CE instruments use an on-line, for in-column detection UV/VIS detector (*see* **Note 16**); this requires removal of the polyimide coating, applied by the manufacturer to give the column more stability, from the window area of the column. The window is usually about 1 cm in length. Some columns come with this area of coating already removed, or tools can be purchased for the polyimide removal.
11. Detector wavelength: commercial CE instruments are equipped with a UV filter detector or UV diode array detector. The response of these detectors depends on the age and condition of the UV lamp; as the lamp ages, analyte response may decrease. The wavelength for optimum detection depends on the UV absorbance profile of the analyte.
12. Injection time/volume and injection method: injection time may range from 1 to 50 s, usually from 2 to 15 s, depending on expected analyte concentration. The injection is usually hydrodynamic (pressure-controlled), but is sometimes electrodynamic. A certain hydrodynamic injection time delivers a known volume of sample, which depends on injection pressure and may be calculated. Most commercial CE instruments are equipped with an automatic sample/reagent tray, which is oriented by the computer to arrange appropriate vials for such operations as column wash and rinse, sample injection, and electrophoresis (actual sample run).
13. Voltage: the voltage is usually set between 5 and 30 kV. Higher voltages increase the electric field strength, which decreases migration/analysis time, but increases the current and temperature.
14. Current: the current is primarily determined by the applied voltage and ionic strength of the electrolyte. Higher currents increase temperatures within the column, making temperature control more difficult. The current is usually kept below 100 μA but, in certain separations, can be allowed to reach 250 μA, which is the limit of the Beckman CE system.
15. Column surface: the entire column is usually fused silica, although there are a variety of surface-coating reagents used to modify separations. Careful column preparation each day and, to a lesser extent, before each run, is important to provide a suitable column interior surface for consistent electrophoresis.
16. Column dimensions are usually 25, 50, or 75 μm ID; total length is 57 cm for the Beckman PACE instruments, with length to detector of 50 cm. An ID of 50 μm usually provides a reasonable path length for adequate sensitivity for in-column detection while being wide enough to avoid plugging. The column ends must be cut square with a cleaving stone or a commercial cutter to avoid detection artifacts.
17. Sample matrix: although CE analysis usually requires a minimum of sample preparation, complicated matrices such as soil, sediment, food, etc. may require cleanup, similar to that required for HPLC or GC analysis. Cleanup steps may involve accumulation from the matrix using solid-phase extraction (SPE) techniques or extraction using typical organic solvent processes. In some cases, additional steps

such as treatment with florisil or silica gel are required. The technology used for sample cleanup depends on characteristics of the sample matrix.

Disclaimer

This paper has been reviewed in accordance with the US Environmental Protection Agency peer and administrative review policies and approved for publication. Use of firm, brand, or trade names in this article is for identification purposes only and does not constitute endorsement by the US Government.

References

1. Eliel, E. L., Wilen, S. H., and Doyle, M. P. (2001) *Basic Organic Stereochemistry*. Wiley-Interscience, New York.
2. Ali, I. and Aboul-Enein, H. Y. (2004) *Chiral Pollutants: Distribution, Toxicity and Analysis by Chromatography and Capillary Electrophoresis*. John Wiley & Sons, Ltd., West Sussex, England.
3. Garrison, A. (2006) Probing the enantioselectivity of chiral pesticides. *Environ. Sci. Technol*. **40**, 16–23.
4. Guzman, N. A. (ed.) (1993) *Capillary Electrophoresis Technology*. Marcel Dekker, Inc., New York.
5. Altria, K. D. (ed.) (1996) *Capillary Electrophoresis Guidebook*. Humana, Totowa, NJ.
6. Vindevogel, J. and Sandra, P. (eds.) (1992) *Introduction to Micellar Electrokinetic Chromatography*. Hüthig Buch Verlag, Heidelberg.
7. Gübitz, G. and Schmid, M. G. (eds.) (2004) *Chiral Separations, Methods and Protocols*. Humana, Totowa, NJ
8. Kallenborn, R. and Hühnerfuss, H. (2001) *Chiral Environmental Pollutants. Trace Analysis and Ecotoxicology*. Springer-Verlag, Berlin.
9. Schmitt, P., Garrison, A., Freitag, D., and Kettrup, A. (1997) Application of cyclodextrin-modified micellar electrokinetic chromatography to the separation of selected neutral pesticides and their enantiomers. *J. Chromatogr. A* **792,** 419–429.
10. Hernandez-Borges, J., Frias-Garcia, S., Cifuentes, A., and Rodriguez-Delgado, M. (2004) Pesticide analysis by capillary electrophoresis. *J. Sep. Sci*. **27,** 947–963.
11. Jarman, J. L., Jones, W. J., Howell, L. A., and Garrison, A. W. (2005) Application of capillary electrophoresis to study the enantioselective transformation of five chiral pesticides in aerobic soil slurries. *J. Agric. Food Chem*., **53,** 6175–6182.
12. Garrison, A. W., Schmitt, P., and Kettrup, A. (1994) Separation of phenoxy acid herbicides and their enantiomers by high-performance capillary electrophoresis. *J. Chromatogr. A* **688,** 317–327.
13. Garrison, A., Schmitt, P., Martens, D., and Kettrup, A. (1996) Enantiomer selectivity in the environmental degradation of dichlorprop as determined by high-performance capillary electrophoresis. *Environ. Sci. Technol*. **30,** 2449–2455.

14. Lewis, D., Garrison, A., Wommack, K., Whittemore, A., Steudler, P., and Melillo, J. (1999) Influence of environmental changes on degradation of chiral pollutants in soils. *Nature* **401,** 898–901.
15. Penmetsa, K., Leidy, R., and Shea, D. (1997) Enantiomeric and isomeric separation of herbicides using cyclodextrin-modified capillary zone electrophoresis. *J. Chromatogr. A* **790,** 225–234.

9

Capillary Electrophoresis of Tropane Alkaloids and Glycoalkaloids Occurring in *Solanaceae* Plants

Tommaso R. I. Cataldi and Giuliana Bianco

Summary

This chapter examines the role of capillary electrophoresis (CE) in the separation of tropane alkaloids, glycoalkaloids, and closely related compounds that have either pharmaceutical value or toxicological effects on humans. The latest significant developments in CE analysis have been selected and critically discussed. When the conventional CE mode was found unable to provide an acceptable selectivity towards the analytes, the addition of either an organic solvent, a chiral selector, or a surfactant to the running buffers was exploited. Likewise, nonaqueous CE (NACE) was also employed to increase solute solubilities and for a better compatibility of this media with mass spectrometry. It turns out that, upon selecting the most appropriate experimental conditions, the CE separation of tropane alkaloids and steroidal glycoalkaloids of *Solanaceae* plants was successfully accomplished. All major steps involved in the separation and detection of these secondary metabolites in complex samples are described and the relevant aspects of each application are examined with emphasis on the main aspects entailed a typical assay. More applications have yet to be developed in order to encourage more labs to exploit the tremendous potential of capillary electrophoresis.

Key Words: Capillary electrophoresis; tropane alkaloids; *Solanum spp*.; alkaloids; glycoalkaloids; plant extracts; electrospray ionization mass spectrometry; enantioseparation; micellar elctrokinetic chromatography; isotachophoresis; nonaqueous capillary electrophoresis.

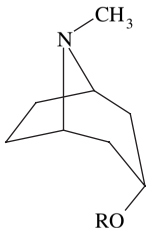
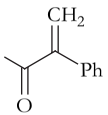
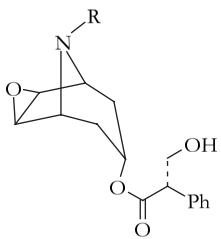
From: *Methods in Molecular Biology, vol. 384: Capillary Electrophoresis*
Edited by: P. Schmitt-Kopplin © Humana Press Inc., Totowa, NJ

1. Introduction

Plants synthesize an enormous variety of compounds that do not appear to play a major role in their primary nutritional or regulatory metabolism. An accepted definition for these naturally produced compounds is secondary metabolites (SMs). Apparently, SMs are involved in communication, attraction, or defense against herbivores, predators, pathogens, and competitors ***(1)***. Plant pigments, alkaloids, isoprenoids, and terpenes are some examples of secondary products. However, the role of many SMs has been rather ambiguous; whereas initially, they were thought to be just waste materials, their bactericidal and toxic effects as well as their role as sedatives and poisons have been re-evaluated. For these reasons, plant secondary metabolites represent a tremendous resource for scientific investigations, clinical trials, and drug development. Two of the largest and most interesting families of plant SMs are represented by tropane alkaloids and glycoalkaloids, which are produced by *Solanaceae* plants. Tropane alkaloids (*see* **Table 1**) are interesting compounds for their pharmaceutical and therapeutic values; they mainly occur in the genera *Atropa, Datura, Duboisia*, and *Hyoscyamus **(2)***. Plants containing these alkaloids have been used throughout recorded history as poisons, but many of the alkaloids do have valuable pharmaceutical properties. Atropine comes from *Atropa belladonna* (deadly nightshade) and is used to dilate the pupils of the eye. Atropine is also a central nervous system stimulant and is used as a treatment for nerve gas poisoning. Scopolamine, another member of this class, is used as a treatment for motion sickness. Glycoalkaloids present in many solanaceous **(Table 2)** possess antimicrobial, insecticidal and fungicidal properties, which provide resistance against several insect pests and herbivores ***(3–5)***. As such, these compounds exhibit pharmacological and toxicological effects on humans ***(6,7)***.

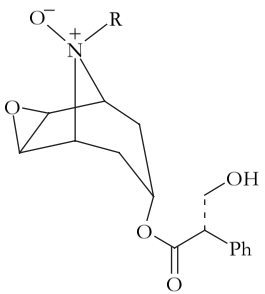
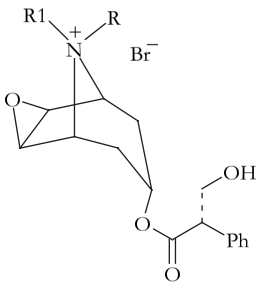
Alkaloids as a whole are among the most frequent applications of capillary electrophoresis (CE) in phytochemical analysis. Determination of SMs has been comprehensively reviewed ***(8–11)***, and it continues to be a very active research area in the Separation Science. Key advantages of CE are its high resolving power, shorter analysis time, and lower operation cost as compared to liquid chromatographic methods. The aim of this chapter is to illustrate the potential of CE and its applications in the analysis of tropane alkaloids and glycoalkaloids occurring in *Solanaceae* plants. Several modes of CE have been developed, namely capillary zone electrophoresis (CZE), micellar elctrokinetic chromatography (MEKC), nonaqueous capillary electrophoresis (NACE), isotachophoresis (ITP), etc. This review contains an extensive listing of CE methodologies in tabular form (*see* **Tables 3** and **4**) and an accompanying list of references that have appeared in the recent literature on the analysis of naturally produced and closely related *Solanaceae* alkaloids.

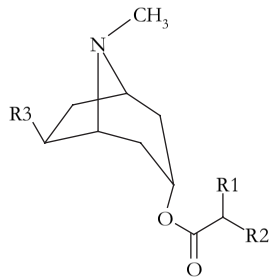
Table 1
Chemical structures of naturally produced and synthetic tropane alkaloids

Structure	Compound*	R	R1	R2	R3
	Tropine: 1αH, 5αH-tropan-3α-ol, $C_8H_{15}NO$ (MW = 141.2)	–H	–	–	–
	Apoatropine: 1αH, 5αH-tropan-3α-ol atropate, $C_{17}H_{21}NO_2$ (MW = 271.3)		–	–	–
	Scopolamine: 6β, 7β-epoxy-1αH, 5αH-tropan-3α-ol (-)-tropate, $C_{17}H_{21}NO_4$ (MW = 303.3)	$-CH_3$	–	–	–
	Nor-(-)-Scopolamine: $C_{16}H_{19}NO_4$ (MW = 289.3)	–H	–	–	–

(*Continued*)

Table 1
(Continued)

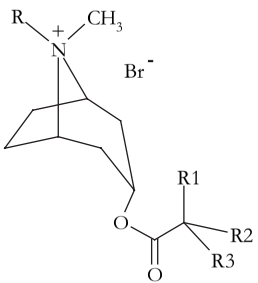
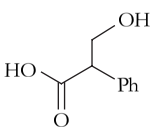
Structure	Compound*	R	R1	R2	R3
	Scopolamine-N-oxide: 6β, 7β-epoxy-1αH, 5αH-tropan-3α-ol (-)-tropate 8-oxide, $C_{17}H_{21}NO_5$ (MW = 319.3)	$-CH_3$	–	–	–
	Oxitropium bromide: (8r)-, 6β, 7β-epoxy-8-ethyl-3α-hydroxy-1αH, 5αH-tropanium bromide (-)-tropate, $C_{19}H_{26}BrNO_4$ (MW = 412.3)	$-CH_2CH_3$	$-CH_3$	–	–
	N-butylscopolamine bromide: 8-butyl-6β, 7β-epoxy-3α-hydroxy-1αH, 5αH-tropanium bromide (-)-tropate, $C_{21}H_{30}BrNO_4$ (MW = 440.4)	$-CH_3$	$-C_4H_9$	–	–
	N-methylscopolamine bromide: 8-methyl-6β, 7β-epoxy-3α-hydroxy-1αH, 5αH-tropanium bromide (-)-tropate, $C_{18}H_{24}BrNO_4$ (MW = 398.4)	$-CH_3$	$-CH_3$	–	–



Hyoscyamine: 1αH, 5αH-tropan-3α-ol (-)-tropate (ester),$C_{17}H_{23}NO_3$ (MW = 289.4)	–	$-CH_2OH$	–Ph	–H
Homatropine: 1αH, 5αH-tropan-3α-ol (-)-mandelate, $C_{16}H_{21}NO_3$ (MW = 275.3)	–	–OH	–Ph	–H
Littorine: 1αH, 5αH-tropan-3α-ol (-)-hydroxy-hydrocinnamate, $C_{17}H_{23}NO_3$ (MW = 289.4)	–	–OH	$-CH_2Ph$	–H
6β-Hydroxyhyoscyamine: 6β-hydroxy-1αH, 5αH-tropan-3α-ol (-)-tropate, $C_{17}H_{23}NO_4$ (MW = 305.4)	–	$-CH_2OH$	–Ph	–OH

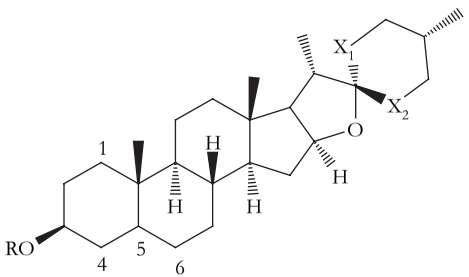
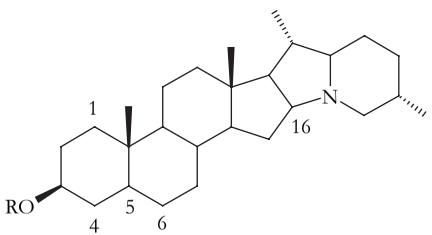
(*Continued*)

Table 1
(Continued)

Structure	Compound*	R	R1	R2	R3
	Ipratropium bromide: 3α-hydroxy-8-isopropyl-1αH, 5αH-tropanium bromide (±)-tropate $C_{20}H_{30}BrNO_3$ (MW = 412.4)	$-CH(CH_3)_2$	–Ph	$-CH_2OH$	H
	Flutropium bromide: (8r)-8-(2-fluoroethyl)-3α-hydroxy-1αH, 5αH-tropanium bromide benzilate $C_{24}H_{29}BrFNO_3$ (MW = 478.4)	$-CH_2CH_2F$	–OH	–Ph	–Ph
	Tropic acid: α-phenyl-β-hydroxypropionic acid, $C_9H_{10}O_3$ (MW = 166.2)	–	–	–	–

* The nomenclature of compounds was taken from The Merck Index 13th edition, Whitehouse Station, NJ, 2001; Ph = $-C_6H_5$

Table 2
Chemical structure of the most common glycoalkaloids

Structure	Compound	Insaturation	R	X_1	X_2
	Solasodine, $C_{27}H_{43}NO_2$ (MW = 413.6)	Δ^5	–H	–NH–	$–CH_2–$
	Solasonine, $C_{45}H_{73}NO_{16}$ (MW = 884.1)	Δ^5	–Solatriosyl	–NH–	$–CH_2–$
	Tomatidine, $C_{27}H_{45}NO_2$ (MW = 415.6)	–	–H	$–CH_2–$	–NH–
	Tomatine, $C_{50}H_{83}NO_{21}$ (MW = 1034.2)	–	–Lycotetraosyl	$–CH_2–$	–NH–
	Solanidine, $C_{27}H_{43}NO$, (MW = 397.6)	Δ^5	–H	–	–
	α-Solanine, $C_{45}H_{73}NO_{15}$ (MW = 868.1)	Δ^5	–Solatriosyl	–	–
	α-Chaconine, $C_{45}H_{73}NO_{14}$ (MW = 852.1)	Δ^5	–Chacotriosyl	–	–
	Demissidine, $C_{27}H_{45}NO$ (MW = 399.7)	–	–H	–	–

Solatriosyl: α-L-rhamnopyranolsyl-β-D-glucopyranosyl-β-galactopyranose; lycotetraosyl: β-D-glucopyranosyl-β-D-xylopyranosyl-β-D-glucopyranosyl-β-D-galactopyranose; chacotriosyl: bis-α-L-rhamnopyranolsyl–β-D-glucopyranose.

Table 3
Capillary Electrophoresis (CE) Applications of Tropane Alkaloids Occurring in Extracts of *Solanaceous* Plants

Compounds	CE mode	Run time	Experimental conditions	Detection	Ref.
Atropine, homatropine, scopolamine	CZE	4–5 min	UFSC (50 μm ID, effective length 56 cm, total length 64.5 cm) HSJ = 20 s (25 mbar) 100 m*M* Tris-phosphate pH 7.0, 30 kV, T = 25 °C	UV = 195 nm	***12,13***
Oxitropium, ipratropium, *N*-butylscopolamine, flutropium (atropine and scopolamine derivatives)	CZE	12 min	UFSC (50 μm ID, effective length 56 cm, total length 64.5 cm) HSJ = 10 s (25 mbar) 80 m*M* citrate, 2.5 m*M* hydroxypropyl-β-cyclodextrin, pH 2.5 30 kV, T = 25 °C	UV = 191 nm	***14***
Atropine, scopolamine, nor-(-)-scopolamine, tropic acid	CZE	13 min	UFSC (75 μm ID, effective length 60 cm, total length 67 cm) 40 m*M* phosphate, pH 7.8, 20 kV, T = 25 °C, HSJ = 4 s (0.5 psi)	UV = 214 nm	***15***
Hyoscyamine, scopolamine	CZE	10 min	UFSC (50 μm ID, total length 85 cm, 22 cm from inlet to UV detector) HSJ = 6 s (50 mbar) 40 m*M* ammonium acetate pH = 8.5, 20 kV, T = 15 °C	UV = 200 nm (+)-ESI-MS/MS	***16***

Enantioseparation of (±)-hyoscyamine, littorine	CZE	5 min	UFSC (50 μm ID, total length 48.5 cm, 40 cm from inlet to UV detector) HSJ = 10 s (50 mbar) 55 m*M* phosphate, 2.9 m*M* sulfated-β-CD, pH = 7.0, 20 kV, T = 20 °C	UV = 195 nm	***17,18***
Scopolamine, hyoscyamine, littorine, 6β-hydroxy hyoscyamine, apoatropine, homatropine, tropic acid	MEKC	20 min	UFSC (50 μm ID, effective length 56 cm, total length 64.5 cm) HSJ = 10 s (25 mbar) 30 m*M* phosphate-borate, 50 m*M* SDS, 10% acetonitrile, pH 8.5 30 kV, T = 25 °C	UV = 195 nm	***19***
Scopolamine *N*-oxide and scopolamine hydrobromide, scopolamine *N*-methylbromide, scopolamine *N*-butylbromide	MEKC	5 min	UFSC (50 μm ID, effective length 30 cm, total length 37 cm) 30 m*M* phosphate, 30 m*M* SDS, pH 7.0, 24 kV, T = 25 °C	UV = 200 nm	***20***

(*Continued*)

Table 3
(Continued)

Compounds	CE mode	Run time	Experimental conditions	Detection	Ref.
Scopolamine, hyoscyamine, littorine, homatropine, tropic acid	MEKC	12 min	UFSC (75μm ID, effective length 56 cm, total length 64.5 cm) HSJ = 5 s (30 mbar) 30 m*M* phosphate-borate, 40 m*M* SDS, 16.5% acetonitrile, pH 8.7	UV = 195 nm	***21***,***22***
Scopolamine, hyoscyamine, littorine	MEKC and CZE	12 min	UFSC (50 μm ID, effective length 56 cm, total length 64.5 cm) HSJ = 5 s, (30 mbar), 30 m*M* phosphate-borate, 40 m*M* SDS, 16.5% acetonitrile, pH 8.7, 30 kV, T = 25 °C, 40 m*M* ammonium acetate at pH 8.5	UV = 195 nm ESI-MS	***23***
Atropine, littorine, apoatropine, ipratropium, scopolamine, *N*-butylscoplamine, methylscoploamine, homatropine	NACE	15 min	UFSC (50 μm ID, effective length 56 cm, total length 64.5 cm) HSJ = 5 s (50 mbar), 25 m*M* ammonium acetate, 1 *M* acetic acid in 25 kV T = 20 °C	UV = 200 nm	***24***

CZE, capillary zone electrophoresis; UFSC, uncoated fused-silica capillary; HSJ, hydrostatic sample injection; UV, ultraviolet; ESI, electrospray ionization; MS/MS, tandem mass spectrometry; MEKC, micellar elctrokinetic chromatography; SDS, sodium dodecyl sulfate; NACE, nonaqueous capillary electrophoresis.

Table 4
Capillary Electrophoresis (CE) Applications of Glycoalkaloids Produced by *Solanaceous* Plants

Compounds	CE mode	Run time	Experimental conditions	Detection	Ref.
α-solanine, α-chaconine, solanidine	ITP	20-25 min	PTFE capillary (150 mm × 0.45 mm ID)	–	***25***
Solasodine, solasonine	NACE	10 min	UFSC (57 cm × 50 μm ID) HSJ = 30 s, (50 mbar), 600 m*M* acetic acid, 10 m*M* sodium hydroxide in methanol, 30 kV, T = 20 °C	UV = 200 nm	***26***
α-solanine, α-chaconine, solanidine, fluorescently labeled (4′-aminomethyl-fluorescein, (AMF)	Immunoassays-CE	5 min	UFSC (50 μm ID, effective length 20 cm, total length 27 cm), 50 m*M* phosphate, 10% (v/v) methanol, 1.5 m*M* SDS, pH 7.5, 10 kV, T = 25 °C	LIF (excitation 488 nm, emission 520 nm)	***27,28***

(*Continued*)

Table 4
(Continued)

Compounds	CE mode	Run time	Experimental conditions	Detection	Ref.
Solasodine, solanidine, tomatidine, demissidine	NACE	13 min	UFSC (50 μm ID, effective length 72 cm, total length 80.5 cm), HSJ = 5 s, (50 mbar), 25 m*M* ammonium acetate, 1 *M* acetic acid, methanol–acetonitrile (20:80, v/v), 30 kV, T = 20 °C	UV = 195 nm ESI-MS	***29***
α-solanine, α-chaconie, α-tomatine, solanidine and tomatidine,	NACE	13 min	UFSC (50 μm ID, 80 cm) HSJ = 5 s, (50 mbar), 50 m*M* ammonium acetate, 1.2 *M* acetic acid, methanol–acetonitrile (10:90, v/v), 25.5 kV, T = 20 °C	(+)-ESI-MS and MS/MS	***30,31***

ITP, isotachophoresis; PTFE, polytetrafluoroethylene; NACE, nonaqueous capillary electrophoresis; UFSC, uncoated fused-silica capillary; HSJ, hydrostatic sample injection; UV, ultraviolet; SDS, sodium dodecyl sulfate; LIF, laser-induced fluorescence; ESI, electrospray ionization; MS, mass spectrometry.

2. Materials

2.1. CZE of Atropine, Homatropine, and Scopolamine

1. Samples: atropine (1%, w/v) and scopolamine (0.25%, w/v) ophthalmic solutions (Ciba Vision, Niederwagen, Switzerland), isotopo-homatropine (1%, w/v) (Alcon, Rueil Malmaison, France).
2. The CE instrument was a HP^{3D} CE system (Hewlett-Packard, Waldbronn, Germany).
3. Separation capillaries: fused silica capillary, 64.5 cm (56 cm effective length) × 50 μm inner diameter (ID).
4. Running buffer: 100 m*M* Tris-phosphate at pH 7.0.

2.2. CZE of Atropine and Scopolamine Derivatives

1. Samples: Buscopan® tablets, suppositories (containing 10 mg of *N*-butylscopolamine bromide) and injections (containing 20 mg of active principle for each ml of injection solution), Atroveny® (ipratropium) inhalation solution (each milliliter containing 0.25 mg ipratropium bromide), Flubron® (flutropium) aerosol (containing 30 μg flutropium bromide per dose) were purchased from a pharmacy.
2. The CE instrument was a HP^{3D} CE system (Hewlett-Packard, Waldbronn, Germany).
3. Separation capillaries: fused-silica capillary, 64.5 cm (56 cm effective length) × 50 μm ID.
4. Running buffer: 80 m*M* sodium citrate pH 2.5, containing 2.5 m*M* hydroxypropyl-β-cyclodextrin.

2.3. CZE of Atropine, Scopolamine, Nor-(-)-Scopolamine, and Tropic Acid

1. Samples: liophilized (50 mg) transgenic plant clones T1 and T2 of the Egyptian henbane *Hyoscyamus muticus* (*L.*) were extracted with 5.0 mL of 80% (v/v) methanol for 16 h at 60 °C.
2. The CE instrument was a Beckman CZE P/ACE System 2200 (Fullerton, CA).
3. Separation capillaries: fused-silica capillary, 67 cm (60 cm effective length) × 75 μm ID.
4. Running buffer: 40 m*M* phosphate buffer at pH 7.8.

2.4. CZE of Hyosciamine and Scopolamine

1. Samples: Belladonna leaf extract (Siegfried, Zofingen-Switzerland).
2. The CE instrument was a HP^{3D} CE system (Hewlett-Packard, Waldbronn, Germany); mass spectrometry (MS): single quadrupole HP Series 1100 MSD (Hewlett-Packard, CA).
3. Separation capillaries: fused-silica capillary, 85 cm (22 cm effective length) × 50 μm ID.
4. Running buffer: 40 m*M* ammonium acetate buffer at pH 8.5.

2.5. CZE Separation of Atropine Enantiomers

1. Samples: atropine (1%, w/v) and scopolamine (0.25%, w/v) ophthalmic solutions (Ciba Vision, Niederwagen, Switzerland).
2. The CE instrument was a HP^{3D} CE system (Hewlett-Packard, Waldbronn, Germany).
3. Separation capillaries: fused silica capillary, 48.5 cm (40 cm effective length) × 50 μm ID.
4. Running buffer: 55 m*M* phosphate buffer at pH 7.0, in the presence of 2.9 m*M* sulfated-β-cyclodextrin (CD).

2.6. MEKC of Scopolamine, Hyoscyamine, Littorine, 6β-Hydroxy Hyoscyamine, Apoatropine, Homatropine, and Tropic Acid

1. Samples: *Datura candida* × *D. aurea* extracts.
2. The CE instruments were a HP^{3D} CE system (Hewlett-Packard, Waldbronn, Germany) and a Beckman CZE P/ACE System 2200 (Fullerton, CA).
3. Separation capillaries: uncoated fused silica capillary, 64.5 cm (56 cm effective length) × 75 μm ID and 37 cm (30 cm effective length) × 50 μm ID.
4. Running buffers: 30 m*M* borate-phosphate buffer at pH 8.5, in the presence of 50 m*M* sodium dodecyl sulfate (SDS) and 30 m*M* phosphate buffer at pH 7.0, in the presence of 30 m*M* SDS.

2.7. MEKC of Scopolamine, Hyoscyamine, Littorine, Homatropine, and Tropic Acid

1. Samples: Belladonna extract (Siegfried Zofingen, Switzerland).
2. The CE instrument was a HP^{3D} CE system (Hewlett-Packard, Waldbronn, Germany).
3. Separation capillaries: uncoated fused-silica capillary, 64 cm (56 cm effective length) × 75 μm ID.
4. Running buffer: 30 m*M* borate-phosphate buffer at pH 8.7, in the presence of 40 *mM* SDS and 16.5% acetonitrile.

2.8. Nonaqueous CE of Atropine, Littorine, Apoatropine, Ipratropium, Scopolamine, N-Butylscopolamine, Methylscopolamine, and Homatropine

1. Samples: Hairy-root extract from *Datura candida* × *D. aurea*.
2. The capillary electrophoresis (CE) instrument was a HP^{3D} CE system (Agilent 3. Separation capillaries: uncoated silica capillary 64.5 cm (56 cm effective length) × 50 μm ID.
3. Running buffers: (a) 25 m*M* ammonium acetate and 1 *M* trifluoroacetic acid (TFA) in acetonitrile, (b) 25 m*M* ammonium acetate and 1 *M* acetic acid in acetonitrile.

2.9. ITP of α-Solanine, α-Chaconine, and Solanidine

1. Samples: potato tubers.
2. The CE instrument was a single capillary isotachophoregraph IONOSEP 900.1 (RECMAN-laboratorni technika, Czech Republic) equipped with a contactless high-frequency conductimer.
3. Separation capillaries: polytetrafluoroethylene (PTFE) capillary (150 mm × 0.45 mm ID).
4. Running buffers: the leading electrolyte was prepared by diluting a solution of 1 *M* hydrochloric acid in methanol, the terminating electrolyte by dissolving zinc nitrate hexahydrate in methanol.

2.10. Nonaqueous CE of Solasodine and Solasonine

1. Samples: plants of *Solanum laciniatum*.
2. The CE instrument was a HP^{3D} CE system (HP, Waldbronn, Germany).
3. Separation capillaries: uncoated fused-silica capillary (57 cm × 50 μm ID).
4. Running buffers: nonaqueous buffer (600 m*M* acetic acid, 10 m*M* sodium hydroxide in methanol).

2.11. CE-Laser-Induced Fluorescence Detection of Glycoalkaloids Based on Solution-Phase Immunoassay

1. Samples: freeze-dried potatoes.
2. The CE instrument was a Beckman P/ACE System 2100 CE with a laser-induced fluorescence (LIF) detector equipped with a 488-nm laser for excitation and a 520-nm emission filter (Beckman Coulter Inc., Fullerton, CA).
3. Separation capillaries: uncoated fused-silica capillary, total length 27 cm, effective length 20 cm × 50 μm ID.
4. Running buffers: 50 m*M* phosphate, 10% (v/v) methanol, 1.5 m*M* SDS, pH 7.5.

2.12. NACE of Solasodine, Solasonidine, Tomatidine, and Demissidine

1. Samples: *Solanum sodomaeum* extracts (leaves and seeds) and *Solanum elaeagnifolium* extracts (berries), and potato tubers extracts (*Solanum tuberosum cv. Desirèe*).
2. The CE instruments was a HP^{3D} CE system (HP, Waldbronn, Germany) and Spectraphoresis Ultra instrument (Thermo Separation Products-Fremont, CA), Beckman P/ACE 5510 capillary electrophoresis system (Beckman Instruments, Fullerton, CA), coupled to an ion trap mass spectrometer Finnigan LCQ DUO (ThermoQuest, San Jose, CA) with an electrospray ionization (ESI) source.
3. Separation capillaries: (a) uncoated fused-silica capillary 80.5 cm of total length, 72 cm to the detector (50 μm id) with a bubble cell (bubble factor 3) and (b) uncoated fused-silica capillary 50 μm ID, 80 cm of total length, 20 cm to the diode array detector.

4. Running buffers: nonaqueous buffer (25 m*M* ammonium acetate, 1 *M* acetic acid in a methanol–acetonitrile mixture [20:80, v/v]) and nonaqueous buffer 90:10 (v/v) of MeCN-MeOH containing 50 m*M* ammonium acetate and 1.2 *M* acetic acid.

3. Methods

3.1. CZE of Atropine, Homatropine, and Scopolamine

Tropane alkaloids are extensively used in ophthalmic diagnosis as mydriatic, anticholinergic, antispasmodic and preanesthesis agents ***(32)***. The most familiar use of atropine, as the sulfate salt, is as a mydriatic to dilate the pupil of the eye during an opthamological examination. Notably, the juice of the berries of *A. Belladonna* was used during the Renaissance by ladies of the Italian courts to exaggerate the size of their eyes by dilating the pupils. These compounds occur mainly in *Solanaceae* and include also the narcotic tropical anesthetic cocaine, which on the contrary is isolated from *Erythroxylaceae* species. Moreover, natural alkaloids have been used as model compounds to synthesize several tropane derivatives that exhibit improved pharmacokinetic properties, higher efficacy, and/or less toxicity. CE has proven to be a powerful tool in investigating the occurrence and the behavior of the major tropane alkaloids in solanaceous.

A CZE method was developed using an uncoated fused-silica capillary for the separation and determination of atropine, homatropine, and scopolamine ***(12,13)***. The influence of buffer concentration on the separation of these compounds was investigated: 100 m*M* Tris-phosphate buffer was chosen. To study the effect of pH on the separation, a value between 6.0 and 8.0—namely, within the pK_a of scopolamine—was selected. A pH value of 7.0 yielded the best compromise in terms of analysis time, selectivity, and separation efficiency ***(12)***. The method was validated and the repeatability, evaluated as relative standard deviation (RSD), was found to be better than 0.6% for migration time and 3.2% for peak area, without adding any internal standard (IS); the reproducibility was also evaluated on the basis of migration time and peak area and was not higher than 0.5% and 2.6%, respectively. A good linear relationship between peak area and analyte concentration was found over a concentration range from 0.01 to 0.125 mg/mL. The limit of detection (LOD) was estimated to be 1 μg/mL. The developed method was applied to assay tropane alkaloids in ophthalmic solutions using an on-column diode array detector set at 195 nm ***(13)*** (*see* **Note 4.1**).

3.2. CZE of Atropine and Scopolamine Derivatives

Cherkaoui et al. ***(14)*** have looked into the potential of chiral selectors for the simultaneous separation of oxitropium, ipratropium, *N*-butylscopolamine, and flutropium, which are atropine and scopolamine derivatives (*see* **Table 1**).

The hydroxypropyl-β-cyclodextrin (HP-β-CD) was chosen to investigate its influence on the resolution and separation selectivity. The following parameters were consecutively optimized: buffer pH, buffer concentration, and cyclodextrin concentration. The pH optimization was carried out with 50 m*M* sodium citrate buffer, with an applied a voltage of 30 kV and a temperature of 25 °C. The best resolution was achieved at pH 2.0, but working at such pH a detrimental effect on the capillary lifetime was observed. Thus, a pH value of 2.5 was chosen for subsequent method development. Buffer concentration was found to significantly affect the separation performance through its influence on the electroosmotic flow (EOF) and the current produced in the capillary. A solution of 80 m*M* citrate buffer was preferred as a compromise among resolution, higher efficiency, and relatively short run time. The influence of HP-β-CD on the selectivity was also investigated. Apparently, the presence of 2.5 m*M* HP-β-CD (*see* **Fig. 1**) was found very suited to separate atropine and scopolamine derivatives.

The method was validated for ipratropium, *N*-butylscopolamine and flutropium; the repeatability was better than 0.2% for the migration time, 4.5% for peak area, and 2.4% for the peak area ratio, using oxitropium as an IS. Detector response linearities were evaluated over a concentration range from 50 to 150 μg/mL ($r > 0.99$). LODs and limits of quantitation (LOQs) were in the range of 0.5–0.8 μg/mL and 1.5–2.4 μg/mL, respectively. The method was successfully applied to identify and quantify compounds closely related to atropine and scopolamine in a series of pharmaceutical formulations, obtaining results in good agreement with the labeled content (*see* **Note 4.2**).

3.3. CZE of Atropine, Scopolamine, Nor-(-)-Scopolamine, and Tropic Acid

Eeva et al. ***(15)*** developed a CE method to separate atropine, scopolamine, nor-(-)-scopolamine, and tropic acid using 40 m*M* phosphate buffer at pH 7.8 and applying a voltage of 20 kV. Under these experimental conditions, the main alkaloids and tropic acid migrated trough the capillary in less than 13 min. The observed linearities were as follows: 5.00–140 μg/mL, 7.50–210 μg/mL and 2.50–70.0 μg/mL for atropine, scopolamine, and tropic acid, respectively. The repeatability of the method was not greater than 7.1% for the smallest and 1.5% for the highest standard concentration reported. The detection limits were 1.0, 1.5, and 1.0 μg/mL for atropine, scopolamine, and tropic acid, respectively. The authors verified the applicability of the method to transgenic Egyptian henbane *Hyoscyamus muticus* (L.) plants. Unfortunately, very low alkaloid concentrations in the crude plant extracts and matrix effects affected the repeatability substantially (*see* **Note 4.3**).

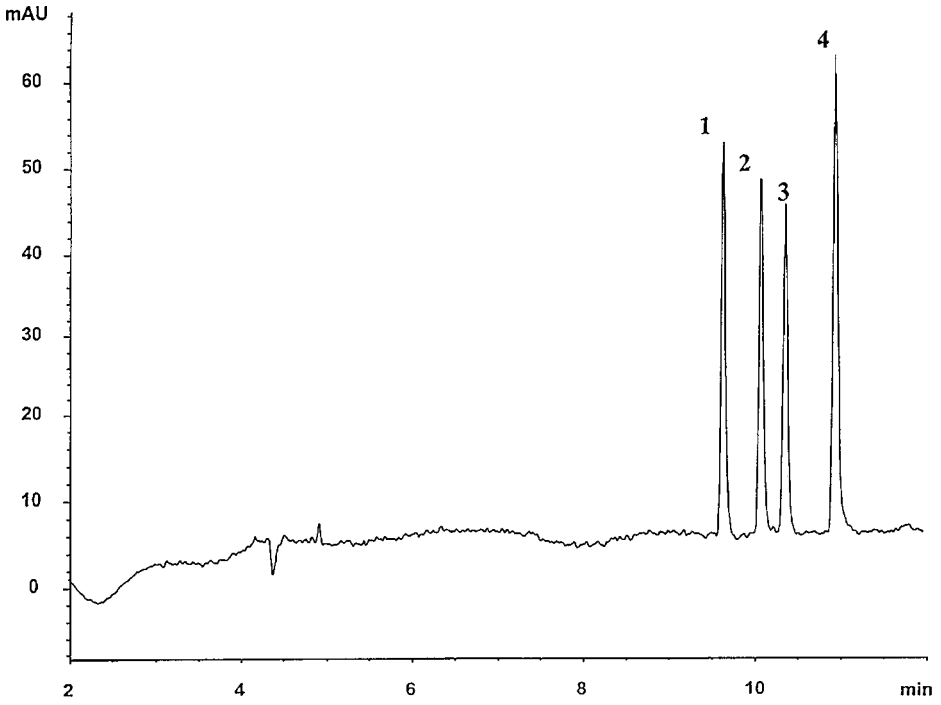


Fig. 1. Typical electropherogram of oxitropium **(1)**, ipratropium **(2)**, *N*-butylscopolamine **(3)**, and flutropium **(4)** obtained by capillary zone electrophoresis, using 80 m*M* citrate buffer pH 2.5 in the presence of 2.5 m*M* HP-β-cyclodextrin. Other operating conditions: uncoated fused-silica capillary $L = 64.5$ cm, $l = 56$ cm, inner diameter = 50 μm; applied voltage 30 kV ($i = 45$ μA), temperature 25 °C, on-column detection at 191 nm. (Reprinted from **ref. *14***, with permission from Elsevier.)

3.4. CZE of Hyoscyamine and Scopolamine

CE interfaced with diode array and mass spectrometry was efficiently used for the separation and detection of hyoscyamine and scopolamine, as well their precursors, littorine, tropine, and 6β-hydroxy-hyoscyamine. A volatile buffer, suitable for coupling CE with ESI-MS, made of 40 m*M* ammonium acetate at pH 8.5 was employed. Upon optimization, such a pH value gave the best resolution of compounds under investigation. The sheath liquid used in the ESI-MS interface was a mixture of isopropanol–water 50/50 v/v in the presence of 0.5% formic acid. To discriminate between hyoscyamine and littorine, which are two positional isomers (MW 289.4 Da), fragmentation was performed by tandem mass spectrometry (MS/MS), as illustrated in **Fig. 2**. Fortunately, a different fragmentation pathway was obtained, and the method was thus applied

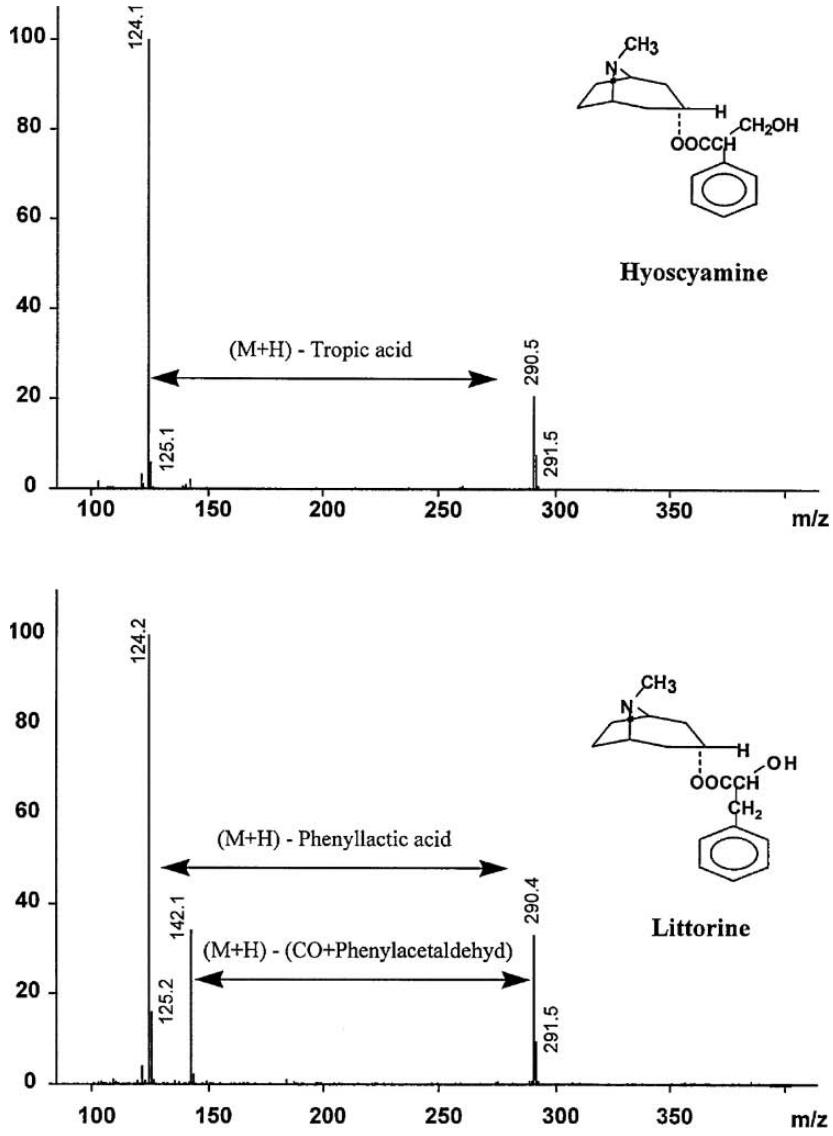


Fig. 2. Mass spectrometry spectra of hyoscyamine and littorine ($[M+H]^+$ at m/z 290) after collision-induced dissociation (CID). The daughter ion at m/z 124 corresponds to the loss of tropic acid and phenillactic acid for hyoscyamine and littorine, respectively. In the case of littorine, the peak at 142 corresponds to the loss of phenylacetaldehyde and carbon monoxide. (Reprinted from **ref. *16***, with permission from Wiley.)

to assay the content of tropane alkaloids in extracts of *Belladonna* leaves and *Datura candida* × *D. aurea* hairy roots ***(16)*** (*see* **Note 4.4**).

3.5. CZE of Atropine Enantiomers

Atropine is a racemic mixture of optical isomers also referred to as (±)-hysoscyamine. However, only the (−)-hyoscyamine stereoisomer exhibits the pharmacological activity, whereas (+)-hyoscyamine is the ineffective component ***(32)***. The use of β-cyclodextrins (β-CDs) in CZE allowed the separation of atropine enantiomers ***(17,18)***. Mateus et al. ***(17)*** showed that the electrophoretic behavior of (±)-hysoscyamine and littorine is critically affected by the substitution degree of the chiral selector. Two sulfated β-CDs of different degree of substitution (DS = 16 and 13) were investigated. Optimization was accomplished by a central composite design in which buffer concentration, buffer pH and sulfated β-CDs were varied simultaneously ***(33)***. Maximizing the resolution between atropine enantiomers, successful results were obtained with 55 m*M* phosphate buffer at pH 7.0 in the presence of 2.9 m*M* sulfated-β-CD at 20 °C and 20 kV (**Fig. 3**). A baseline separation of atropine enantiomers was achieved in less than 5 min. The method was applied to the stereoselective analysis of (±)-hysoscyamine in a commercial ophthalmic solution and to evaluate the effect of three extraction procedures on the (−)-hyoscyamine racemization in hairy root extracts. Comparable results were obtained by Heine et al. ***(18)*** for the enantioseparation of atropine that was performed using a 50 m*M* sodium dihydrogen phosphate solution, pH 9.0, containing a commercially available sulphated β-cyclodextrin (*see* **Note 4.5**).

3.6. MEKC of Tropane Alkaloids

Scopolamine and hyoscyamine (*see* **Table 1**), which have a similar structure, generally occur with other tropane alkaloids in solanaceous plant extracts. The use of a micellar phase in CE was found to be more appropriate for their separation. Thus, MEKC with SDS as a surfactant was exploited by Cherkaoui et al. ***(19)*** for the separation of a mixture of six tropane alkaloids (i.e. scopolamine, hyoscyamine, littorine, 6β-hydroxyhyoscyamine, apoatropine and homatropine) and tropic acid. The authors examined the effects of buffer concentration, pH, micelle concentration and organic modifier. Optimization of the electrophoretic separation with different phosphate–borate buffer concentrations, ranging from 10 to 50 m*M*, at pH 7.0 and 50 m*M* SDS, was investigated. A buffer of 30 m*M* was selected as a compromise between stacking effect, acceptable current, and run time. Besides, the effect of pH on migration time was evaluated in the range between 7.0 and 9.0. A pH value of 8.5 was chosen. The authors noted that both type and amount of the organic modifier

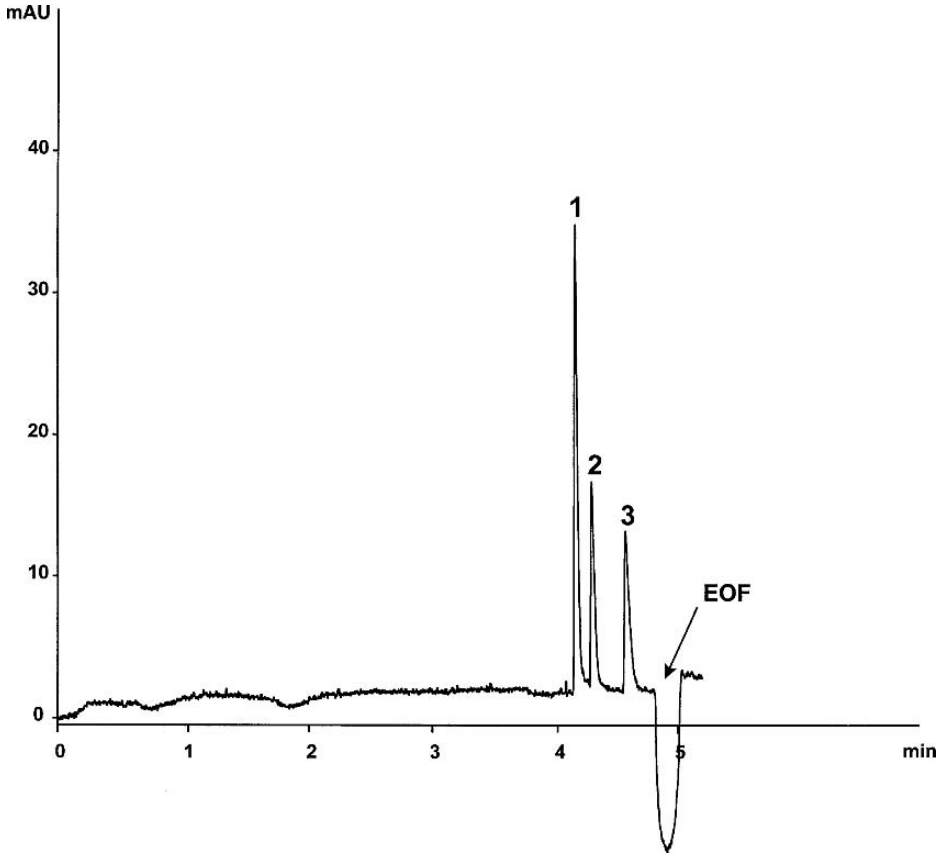


Fig. 3. Typical electropherogram of littorine **(1)**, (−)-hyoscyamine **(2)**, and (+)-hyoscyamine **(3)** obtained by CZE using 55 m*M* phosphate at pH 7.0 and 2.9 m*M* sulfated-β-cyclodextrin. Applied voltage, 20 kV ($i = 69.5\,\mu A$); temperature, 20 °C. Uncoated fused-silica capillary: $L = 48.5$ cm, $l = 40$ cm, inner diameter $= 50\,\mu m$. Detection at 195 nm. (Reprinted from **ref. *17***, with permission from Elsevier.)

strongly affected the selectivity. Methanol lengthens the migration time and widens the migration window available for the separation. However, either CH_3CN or CH_3OH could be employed to improve separation efficiency and resolution in MEKC. A buffer solution consisting of 30 m*M* phosphate–borate, 50 m*M* SDS, and 10% acetonitrile at pH 8.5 was used to separate a plant extract of *Datura candida* × *D. aurea* in less than 18 min.

Another interesting example of scopolamine-related drugs separated by MEKC was reported by Wu et al. ***(20)***. Scopolamine hydrobromide, scopolamine *N*-methylbromide, scopolamine *N*-butylbromide (SB), and *N*-oxide

hydrobromide were separated by an uncoated capillary with 30 m*M* phosphate buffer at pH 7.0, 30 m*M* SDS and an applied voltage of 24 kV. Such an electrolyte gave resolved, sharp, and symmetric peaks in less than 6 min **(Fig. 4)**. Using scopolamine *N*-oxide hydrobromide (300 μ*M*) as an IS the quantitative applicability of the method was evaluated; good linearity between the peak–area ratios of analytes and IS as a function of analyte concentration was observed for the concentration range investigated, that is 50–300 μ*M*. The lower detection limits of scopolamine hydrobromide, scopolamine *N*-methylbromide, and SB were approx 10 μ*M* (S/N = 3). The method applicability was also demonstrated by analyzing SB in tablets (*see* **Note 4.6**).

3.7. Optimized MEKC Methods to Separate Hyoscyamine, Scopolamine, Littorine, Homatropine, and Tropic Acid

The MEKC method ***(19)*** was further optimized and validated using a Doehlert design with a quadratic model by Mateus et al. ***(21)***. Looking at

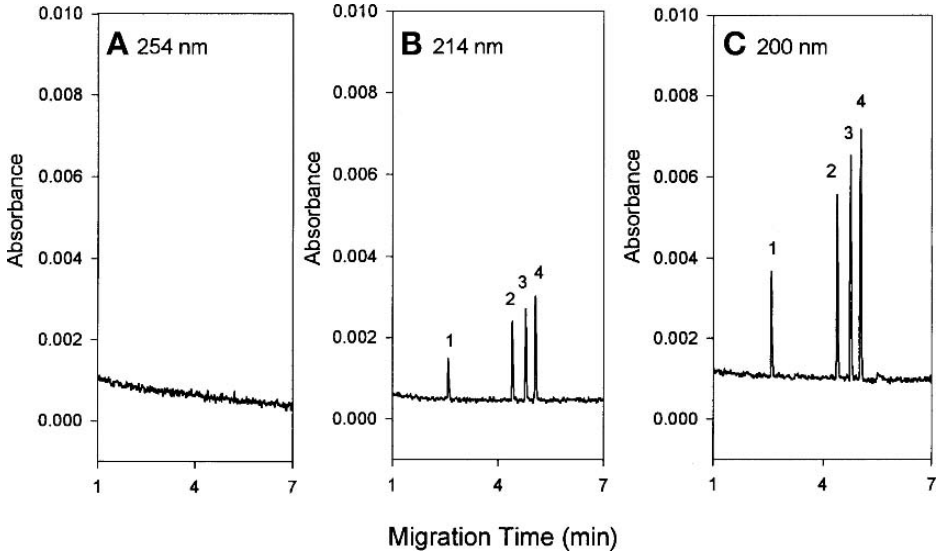


Fig. 4. Electropherograms of scopolamine related drugs each at 300 m*M*, detected at **(A)** 254 nm, **(B)** 214 nm, and **(C)** 200 nm. Peaks: 1, scopolamine *N*-oxide; 2, scopolamine hydrobromide; 3, scopolamine *N*-methylbromide and 4, scopolamine *N*-butylbromide. Micellar electrokinetic chromatography conditions: buffer, 30 m*M* phosphate (pH 7.00) with 30 m*M* sodium dodecyl sulfate; applied voltage, 24 kV (detector at cathode side); uncoated fused-silica capillary, 30 cm (effective length) 50 μm inner diameter. (Reprinted from **ref. *20***, with permission from Elsevier.)

the separation of hyoscyamine, scopolamine, littorine, homatropine, and tropic acid, the buffer pH, SDS concentration, and amount in volume of acetonitrile were investigated. Whereas the resolution between littorine and hyoscyamine was the main feature taken into account in this analytical optimization, run time, power supply, and current generated during electrophoresis were simply fixed as threshold values. Upon optimization, the chosen values were 30 m*M* phosphate–borate buffer at pH 8.7, 40 m*M* SDS, and 16.5% CH_3CN. The applied voltage was 30 kV at 25 °C. This experimental design allowed a better and faster prediction of the optimal conditions than the univariate development described above ***(19)***.

The method was validated showing satisfactory sensitivity, linearity, precision, and accuracy. Method precision for each alkaloid was evaluated by measuring repeatability and intermediate precision (between-day precision) of migration times and normalized peak areas. In all cases, repeatability was better than 1% for migration times and 4% for the peak area ratio. Also, the RSD values relative to intermediate precision were in the same order of magnitude than those obtained for repeatability. Detector response linearities were assessed in the concentration range of 50–125 μg/mL and good correlation coefficients were obtained. The results obtained for hyoscyamine in a *Belladonna* extract attested the precision and accuracy of the method, which was also successfully applied to the dosage of hyoscyamine and scopolamine in various hairy root and plant extracts ***(22)***. Mateus et al. ***(23)*** applied a previously developed MEKC-UV method ***(19,21)*** to investigate the influence of various strains of *Agrobacterium* on the tropane alkaloid content of different *Hyoscyamus muticus* hairy roots clones in order to verify whether transformed root cultures were capable of producing high contents of littorine. ESI-MS/MS was employed to confirm the occurrence of littorine (*see* **Note 4.7**).

3.8. NACE of Selected Tropane Alkaloids in Plant Extracts

Although atropine, scopolamine, and homatropine can be easily separated by CE, the selectivity towards the synthetic version of tropane alkaloids is poor because of their similar mass-to-size ratios ***(12)***. As a result, the potential of NACE was evaluated ***(24)***. Methanol and/or acetonitrile addition up to 30% (v/v) to the aqueous buffer enabled the tailored manipulation of selectivity. Indeed, NACE was used to investigate the separation of atropine, littorine, apoatropine, ipratropium, scopolamine, *N*-butylscopolamine, methylscopolamine, and homatropine. Methanol and acetonitrile were selected because of their low viscosity, which results in a rapid separation with high efficiency; their relatively high ultraviolet (UV) transparency; their larger autoprotolysis constants, which result in improved selectivity for very closely related

compounds; and their high volatility, which makes them appropriate solvents for a successful coupling to a mass spectrometer. With methanol–acetonitrile mixtures, it was demonstrated that, on increasing the percentage of MeOH from 0 to 100%, the electrophoretic mobility of each compound reached a maximum at approx 25% (v/v) MeOH. Most likely, this is due to the viscosity of the mixture, which is minimum at 25% MeOH, thus affecting the EOF in the opposite manner. Replicate injections under nonaqueous conditions gave good precision of migration time and peak area as well, with RSD < 0.2% and < 1.45%, respectively. The method was applied to quantify and confirm the content of hyoscyamine and scopolamine in plant extracts (*see* **Note 4.8**).

3.9. Capillary ITP of α-solanine, α-chaconine, and solanidine

Glycoalklaoids, like many SMs, are thought to play a major role in the chemical defence of plants, acting as nonspecific protectors or repellents against potential pest predators ***(34)***. The inibitory effects of glycoalkaloids on both fungal and insect pests of potato indicate that their evolutionary significance is as natural pesticides ***(35)***. Numerous *Solanaceae* plants synthesize a battery of steroidal glycoalkaloids (SGAs) ***(36)***. The major *Solanum* alkaloids of pharmacological and toxicological interest are steroidal alkamines, all of which possess the C_{27} steroidal skeleton of cholestane. Several analytical methods has been recently described for the detection and determination of steroidal alkaloids by using capillary electrophoresis ***(25–31)***. Potato tubers contain a mixture of the steroidal triglycosides α-solanine and α-chaconine accounting for about 95% of the total glycoalkaloid content ***(37)***. Both possess the same aglycone, solanidine, but differ in their sugar moieties (**Table 2**).

The ITP analysis is based on the fact that both potato glycoalkaloids and solanidine are weak bases and migrate towards the cathode under acidic conditions ***(25)***. Water, methanol, and water–methanol mixtures were tested; 2 m*M* HCl and 5 m*M* $Zn(NO_3)_2$ both in 99% MeOH, were used as leading and terminating electrolytes, respectively. Under these experimental conditions, α-solanine and α-chaconine co-migrated, being exclusively separated from their aglycone. The ITP detection limit was 0.5 mg/mL and 1 mg/mL for solanidine and potato glycoalkaloids, respectively. With such a method, it is not possible to establish the individual content of α-solanine and α-chaconine (*see* **Note 4.9**).

3.10. NACE of Solasodine and Solasonine

Solasodine is a water-insoluble, steroidal alkaloid used as a raw material for steroid drug manufacture. It is mainly isolated from the leaves of some *Solanum* species, where it occurs in the form of a water soluble glycoside, solasonine. Because of the low solubility of solasodine in water and in water–ethanol

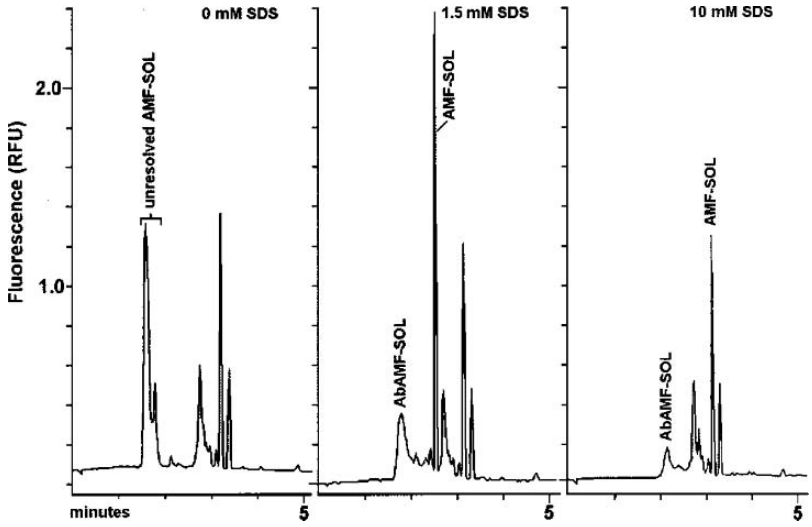


Fig. 5. Effect of sodium dodecyl sulfate (SDS) concentration on the resolution of unbound 4′-aminomethyl-fluorescein solanidine molecule (AMF-SOL) from AMF-SOL–antibody complex. SDS was added to 50 m*M* phosphate, 10% (v/v) methanol, pH 7.5; LIF detection (488 nm for excitation and a 520 nm emission filter). (Reprinted from **ref.** ***27***, with permission from American Chemical Society.)

solutions, a nonaqueous acetic/acetate buffer in methanol was employed ***(26)***. The separation of solasodine and solasonine from other compounds occurring in plant extracts was obtained; the signal was measured at 200 nm with a detection limit of solasodine relatively high, 8 mg/L (*see* **Note 4.10**).

3.11. CE-LIF Detection of Glycoalkaloids Based on Solution-Phase Immunoassay

In this immuno-CE-LIF method, potato glycoalkaloids and a fluorescently labeled alkaloid were allowed to react with a limited amount of anti-glycoalkaloid serum ***(27,28)***. The assay was based on the competition between the fluorescently labelled alkaloid and the native glycoalakloids from the potato extract for antibodies. In particular, solanidine coupled to 4'-aminomethyl-fluorescein, (AMF) and a polyclonal antibody solution were used as immunoreagents. CE was employed to separate and quantify the adduct of the solution-phase glycoalkaloid immunoassay. The peak area of labeled alkaloids was found proportional to the amount of glycoalkaloid in potato extracts. The antibody exhibited strong affinity (K_{aff} approx 4×10^8) for the fluorescent solanidine molecule (AMF-SOL). Nevertheless, the separation of the antibody-bound AMF-SOL from unbound AMF-SOL proved to be difficult. As illustrated in **Fig. 5**,

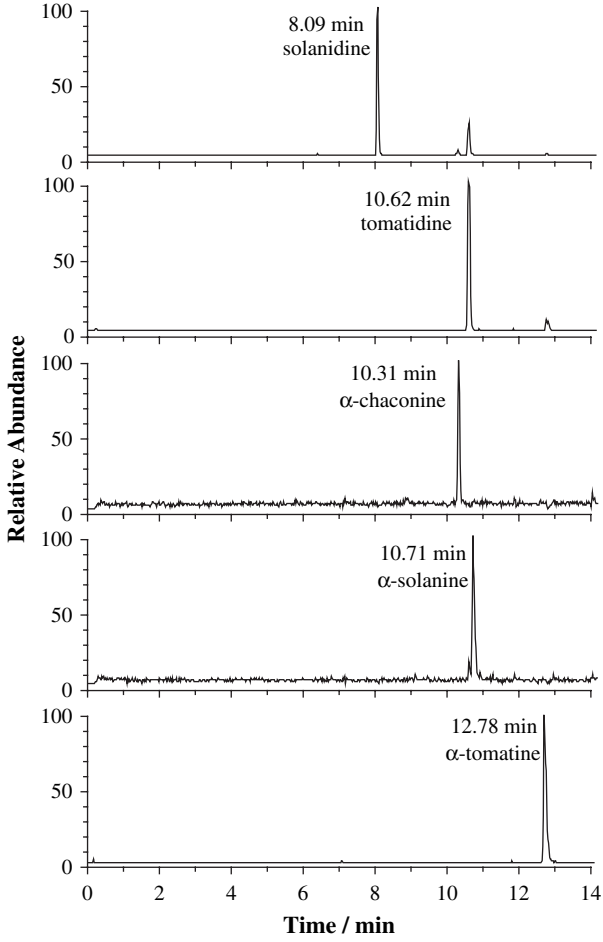


Fig. 6. Selected ion monitoring, (SIM) traces of the electrophoretic separation by nonaqueous capillary electrophoresis (NACE)-electrospray ionization (ESI)-mass spectrometry (MS) of 1 mg/L standard mixture of solanidine, tomatidine, α-chaconine, α-solanine, and α-tomatine. Electrophoretic conditions: buffer, MeCN-MeOH (90:10, v/v) containing 50 m*M* ammonium acetate and 1.2 *M* acetic acid, uncoated fused-silica capillary $L_d = 80$ cm, inner diamter 50 μm, outer diameter 365 μm; injection pressure 0.5 psi for 5 s; effective voltage applied 25.5 kV; T = 20 °C. ESI-needle voltage $V_{es} = +4.5$ kV, spray current $i_{es} = 6–8$ μA (CE on) sheath gas flow rate was set at (N_2) 0 arbitrary units (a.u.), temperature of the aluminium capillary $T_{cap} = 180$ °C and capillary voltage 32 V, coaxial sheath liquid, methanol:water (1:1) with 1% of acetic acid at flow rate of 2.5 μL/min. MS detection in SIM mode: 398, 416, 852, 868, 1034 for solanidine, tomatidine, α-chaconine, α-solanine, and α-tomatine, respectively. (Reprinted from **ref**. ***30***, with permission from Wiley.)

optimum resolution was achieved with an electrolyte consisting of 50 m*M* phosphate, at pH 7.5, 10% methanol (v/v), and 1.5 m*M* SDS (*see* **Note 4.11**).

3.12. Determination of Glycoalkaloids by NACE with DAD and ESI-MS Detection

The use of organic solvents in CE represents an interesting alternative to buffered aqueous media for the separation of closely related and poorly soluble compounds in water ***(38)***. NACE coupled to UV and MS detection was used for the separation and detection of steroidal alkaloids (solasodine, tomatidine, solanidine, and demissidine) and applied to plant specimens of *Solanum spp* ***(29)***. A series of methanol–acetonitrile mixtures, containing a constant amount of ammonium acetate and acetic acid, was investigated; the optimum mixture was MeOH/MeCN 20:80 (v/v). The detection was performed at 195 nm. However, when the NACE method was interfaced with a mass spectrometer by ESI, approx 100-fold sensitivity enhancement was obtained.

Bianco et al. ***(30,31)*** have developed a NACE method to separate the main glycoalkaloids and relative aglycones occurring in solanaceous plants; as shown in **Fig. 6**, an effective separation of α-chaconine, α-solanine and α-tomatine and their aglycones was accomplished in less than 13 min. Good detection sensitivity, selectivity, and reduced analyte-wall interaction along with high separation efficiency and short analysis time were obtained. It should be emphasized that the nonaqueous mixture was well compatible with the MS detection system in terms of low current generation and ease of evaporation, which resulted in better ionization and stable signals.

Interestingly, the whole SGA profile in extracts of commercial potatoes and novel genetically modified varieties was evaluated by NACE-ESI-MS. The samples were potato tubers of a conventional cultivar *Désirée* and its three lines of modified plants: resistant, intermediate, and susceptible to potato virus-Y infection. The main glycoalkaloids were confirmed to be α-solanine and α-chaconine with molecular ions at 852 and 868, respectively (*see* **Note 4.12**).

4. Notes

1. To ensure changes in the ionization degree of scopolamine, buffer electrolytes with pH around the pK_a (7.6) were investigated. Scopolamine, which is partially protonated at pH 7.0, is less influenced by buffer concentration as the electrophoretic mobility is directly proportional to the compound's total charge. In complex plant extracts, as a rule, scopolamine and hyoscyamine occur together with other tropane alkaloids. Having similar structure, MEKC seemed to be more appropriate to separate neutral and ionic analytes in the same run. As tropane alkaloids are stable under mildly acidic pH ***(38)***, it was possible to resolve them with a low EOF. The addition of various amounts of methanol or acetonitrile strongly alters the

selectivity. The effect of organic modifier on the resolution of positional isomers was attributed to solute desolvation. Apparently, the addition of an organic solvent gives rise to a reduced hydration sphere depending on the isomer, which in turns affects the charge-to-size ratios.

2. To reduce the negative charge on the fused silica capillary wall, the investigated pH range was restricted to the acidic region. As the EOF is negligible at low pHs, the selected alkaloids are positively charged with migration mainly controlled by the electrophoretic mobility. An increase of the buffer concentration produced an increase of migration times with better separations. This effect was related to the decrease of the zeta potential at the capillary-wall solution interface. The concentration of HP-β-CD in the buffer influenced the selectivity as well as the migration times; the separation is based upon the complexation differences of alkaloids with the cyclodextrin.
3. The investigated pH range was 5.4–8.2. Although the baseline separation of atropine, scopolamine, and nor-(-)-scopolamine was not possible up to pH 6.6, tropic acid could be separated from the basic compounds because of its smaller molecular weight and acidic character ($pK_a = 4.1$). Changing from acidic to neutral and basic electrolytes enabled the separation of cationic compounds, which migrated in the order of increasing molecular weight. The most suitable pH range proved to be from 7.0 to 7.8. The effect of buffer concentration on migration times and the peak shapes revealed that on increasing buffer concentration, the migration times and peak areas of the solutes also increase substantially.
4. The successful coupling of CE and MS is mainly governed by volatility requirements of the CE running buffer, whereby the use of ammonium acetate appears very suitable. The buffer concentration is also an important parameter to consider during the CE-ESI-MS optimization. Indeed, increasing the ammonium acetate concentration resulted in an important Joule effect with migration times irreproducibility. Working with 40 m*M* ammonium acetate at pH 8.5 ensured changes in the ionization degree of scopolamine, which was partially protonated at this pH and characterized by a lower electrophoretic mobility than that of hyoscyamine. As a result, the resolution was improved. The nature, composition, and flow rate of the sheath liquid have a critical effect on the performance of CE-ESI interface. Isopropanol gave the most stable and highest MS signal; the use of an isopropanol-water mixture (50/50 v/v), in the presence of 0.5% formic acid resulted in the highest ion abundance signal, based on the reconstructed ion current (RIC) pherogram. The make-up flow rate was also studied; whereas higher flow rates resulted in a lower signal-to-noise ratio as a result of the dilution of the separated compounds, lower flow rates negatively affected the signal stability. A compromise was obtained at a flow rate set at 3 μL/min.
5. The substitution degree of a cyclodextrin is of paramount importance in the chiral separations by CE ***(40)***. Under the same electrophoretic conditions, atropine enantiomers and littorine migrated after the EOF with the highly substituted

cyclodextrins, whereas they migrated in front of the EOF with the less substituted ones. In both cases, littorine and atropine enantiomers were baseline-resolved.

6. To begin with, a 30 m*M* phosphate–borate buffer at pH 7.0 and 50 m*M* SDS was chosen as a compromise of stacking effect, acceptable current, and reasonable run time. However, the effect of buffer pH (7.0–9.0) was investigated; scopolamine and 6β-hydroxyhyoscyamine were present in their neutral and cationic forms with migration times which decreased on increasing pH. Other alkaloids, such as hyoscyamine, littorine, apoatropine, homatropine, and tropic acid, were slightly affected by the pH solution. A pH value of 8.5 was preferred while the surfactant level was varied from 0 up to 80 m*M*. Except for tropic acid, which was negatively charged at pH 8.5, the migrations times increased gradually with increasing SDS concentration. On the contrary, neutral and especially positively charged compounds strongly interacted with micelles, resulting in a slow net migration. The best compromise in terms of separation efficiency was found at 50 m*M* SDS. Higher SDS concentrations were not used because of the negative influence on the separation by Joule effect. The separation selectivity was strongly altered when an organic modifier was added. Specifically, the analyte migration time increased on increasing the methanol content, most likely as a result of a modification of the running buffer viscosity ***(41)***. In the case of scopolamine, the migration time remained almost constant as a result of two to opposite effects, i.e., an increase of solution viscosity and a decrease of the partition coefficient with micelles. In the case of acetonitrile, the viscosity of the buffer was found maximum around 10%, which explained the different migration behavior in comparison to methanol. The effects of various methanol and acetonitrile mixtures on the resolution of hyoscyamine and littorine showed that a better resolution was obtained when acetonitrile was used. Such an effect on positional isomers was attributed to solute desolvation. In aqueous phase, littorine and hyoscyamine are totally hydrated and therefore exhibit approximately the same size. Addition of an organic solvent resulted in a change of the hydration sphere depending on the isomer, which in turns means a change in the charge-to-size ratio ***(19)***. In the MEKC method reported by Wu et al. ***(20)***, using a 30 m*M* phosphate buffer at pH 7.0 and SDS (5–10 m*M*) it was possible to obtain resolved peaks but tailing, whereas at higher SDS levels (i.e., 30 m*M*) solute peaks were sharp and symmetric.
7. The separation of hyoscyamine and scopolamine was performed by experimental design in order to optimize all together a series of electrophoretic parameters. Homatropine, structurally related to hyoscyamine and scopolamine, was used as an internal standard ***(21)***.
8. The use of methanol–acetonitrile mixtures with high ε^2/η values under NACE conditions significantly improved the separation of tropane alkaloids. It was noted that upon changing the organic solvent composition, the dissociation constants and solvatation degree of selected compounds underwent a substantial change. Moreover, the influence of buffer pH* on the separation selectivity showed that the use of TFA, instead of acetic acid, was highly advantageous in terms of selectivity because it improved the resolution of the investigated compounds.

9. The ITP analysis was based on the weak basic properties of α-solanine, α-chaconine, and solanidine. An acidic electrolyte was used and several cations were examined as leading and/or terminating ion (hydroxonium, potassium, sodium, β-alanine, etc); water, methanol and water-methanol mixture were tested as electrolyte solvents. α-solanine and α-chaconine were not separated because of their common aglycone (solanidine) bearing a positive charge and also because they have nearly the same molecular weights, 867 and 851, respectively.
10. When a solution composed of 600 m*M* acetic acid and 90 m*M* sodium hydroxide in methanol was used, the analysis time was longer compared to buffers with a lower ionic strength. However, an advantage of using a concentrated buffer was that it enables sample stacking (the effect of focusing the sample molecules from large injection volumes) even when the sample contained up to 15 m*M* sodium hydroxide. The dilute buffer provided sample stacking only with samples containing no sodium hydroxide. The fluorescence intensity of AMF-SOL decreased quickly when the pH was below 7.0, but raising the buffer pH above 8.0 would be expected to affect antigen-antibody binding ***(27)***.
11. The immunoassay method is based on the competition between fluorescently labeled alkaloids and native glycoalkaloids from potato extracts. The antibody used in this experiment recognized an epitope on the alkaloid portion of the glycoalkaloid molecule and hence it was not imperative to preserve the carbohydrate moiety. Buffer composition was found one of the main parameter affecting separation in CE. Indeed, coupling an immunoassay to CE-LIF introduces numerous limitations to buffer selection because harsh conditions may reverse antigen–antibody binding. It was noteworthy that either extremes in pH or high concentrations of organic solvent could induce the antibody to release the antigen. SDS added at levels lower than the critical micellar concentration improved the resolution of free AMF-SOL and AMF-SOL, but the role of SDS was not elucidated ***(27,28)***.
12. NACE was found to be a very suitable approach for the separation of SGAs because of their very low solubility in water. The electrolyte concentration was kept constant (i.e., ammonium acetate and acetic acid) and different methanol–acetonitrile mixtures were investigated between 0% and 100% MeOH with a step of 20%; a MeOH:MeCN (20:80, v/v) mixture resulted in a more efficient and rapid separation ***(29)***. The tailing character of peaks relative to SGAs was observed whatever was the aqueous buffer solution employed, probably as a result of solute interactions with silica wall and/or to the relatively low solubility of these compounds in water ***(30)***. Ammonium acetate is the most frequently used electrolyte in nonaqueous CE system and acetic acid is often added to adjust the apparent pH of the electrophoretic medium. Several MeCN:MeOH mixtures were used; the acetonitrile percentage in methanol was increased from 20% to 100% in 10% steps. Using MeCN:MeOH volume ratios lower than 60%, the migration order was solanidine, tomatidine, α-chaconine, α-solanine, and α-tomatine, whereas on increasing the amount of MeCN up to 70% there was a reversal between migration times of tomatidine and α-chaconine. As the electrophoretic mobility of ions is

mainly governed by charge to size (shape) ratio, the inversion of migration order of tomatidine and α-chaconine was ascribed to changes in their effective charges and solvatation degrees. A good compromise between run time and separation was found with MeCN:MeOH at a ratio of 90:10 (v/v) containing ammonium acetate and acetic acid. This mixture allowed in fact to separate α-chaconine and α-solanine, which normally are both present in potato samples.

Acknowledgments

The financial support by VIGONI-DAAD is gratefully acknowledged.

References

1. Harborne, J. B. (ed.) (1993) *Introduction to Ecological Biochemistry*. Academic, New York.
2. Lounasmaa, M. and Tamminen, T. (1993) The tropane alkaloids, in *The Alkaloids* (Cordell, G. A., ed.) Chap I. Academic Press Inc., San Diego, USA., pp. 1–114.
3. Tingey, W. M. (1984) Glycoalkaloids as pest resistance factors. *Am. Potato J*. **61,** 157–167.
4. Jadhav, S. J., Sharma, R. D., and Salunkhe, D. K. (1981) Naturally occurring toxic alkaloids in food. *Crit. Rev. Toxicol*. **9,** 21–104.
5. Roddick, J. G., Rijnenberg, A. L., and Weissenberg, M., (1990) Membrane-distrupting properties of the steroidal glycoalkaloids solasonine and solamargine. *Phytochemistry* **29,** 1513–1518.
6. van Gelder, W. M. J., (1991) Chemistry, toxicology and occurrence of steroidal glycoalkaloids: Potential contaminants of the potato (Solanum tuberosum L.), in *Poisonous Plant Contamination of Edible Plants*, (A.F.M. Rizk ed.) Boca Raton, Florida: CRC Press, pp. 117–156.
7. Jadhav, S. J., Lutz, S. E., Mazza, G., and Salunkhe, D. K. F. Shahidi (eds.) (1997) *Antinutrients and Phytochemicals in Food*, ACS Symposium Series 662. American Chemical Society, Washington, DC: pp. 94–114.
8. Issaq, H. J. (1997) Capillary electrophoresis of natural products-I. *Electrophoresis* **18,** 2438–2452.
9. Issaq, H. J. (1999) Capillary electrophoresis of natural products-II. *Electrophoresis* **20,** 3190–3202.
10. Tomas-Barberan, F. A. (1995) Capillary electrophoresis: a new technique in the analysis of plant secondary metabolites. *Phytochem. Anal*. **6,** 177–192.
11. Suntornsuk, L. (2002) Capillary electrophoresis of phytochemical substances. *J. Pharm. Biomed. Anal*. **27,** 679–698.
12. Cherkaoui, S., Mateus, L., Christen, P., and Veuthey, J. -L. (1997) Development and validation of a capillary zone electrophoresis method for the determination of atropine, homatropine and scopolamine in ophthalmic solutions. *J. Chromatogr. B* **696,** 283–290.
13. Mateus, L., Cherkaoui, S., Christen, P., and Veuthey, J. -L. (1998) Capillary electrophoresis for the analysis of tropane alkaloids: pharmaceutical and phytochemical applications. *J. Pharm. Biomed. Anal*. **18,** 815–825.

14. Cherkaoui, S., Mateus, L., Christen, P., and Veuthey, J. -L. (1998) Validated capillary electrophoresis method for the determination of atropine and scopolamine derivatives in pharmaceutical formulations. *J. Pharm. Biomed. Anal*. **17,** 1167–1176.
15. Eeva, M., Salo, J. P., and Oksman-Caldentey, K. M. (1998) Determination of the main tropane alkaloids from transformed Hyoscyamus miticus plants by capillary zone electrophoresis. *J. Pharm. Biomed. Anal*. **16,** 717–722.
16. Mateus, L., Cherkaoui, S., Christen, P., and Veuthey, J. -L (1999) Capillary electrophoresis-diode array detection – electrospray mass spectrometry for the analysis of selected tropane alkaloids in plant extracts. *Electrophoresis* **20,** 3402–3409.
17. Mateus, L., Cherkaoui, S., Christen, P., and Veuthey, J. -L. (2000) Enantioseparation of atropine by capillary electrophoresis using sulphated β-cyclodextrin: application to a plant extract. *J. Chromatogr. A*. **868,** 285–294.
18. Heine, S., Ebert, K., and Blaschke, G. (2003) Determination of L-hyoscyamine in atropine and D-hyoscyamine in L-hyoscyamine by chiral capillary electrophoresis as an alternative to polarimetry. *Electrophoresis* **24,** 2687–2692.
19. Cherkaoui, S., Mateus, L., Christen, P., and Veuthey, J. -L. (1997) Micellar electrokinetic capillary chromatography for selected tropane alkaloid analysis in plant extract. *Chromatographia* **46,** 351–357.
20. Wu, H. -L., Huang, C. -H., Chen, S. -H., and Wu, S. -M. (1998) Micellar electrokinetic chromatography of scopolamine-related anticholinergics. *J. Chromatogr. A* **802,** 107–113.
21. Mateus, L., Cherkaoui, S., Christen, P., and Veuthey, J. -L. (1998) Use of a Doehlert design in optimizing the analysis of selected tropane alkaloids by micellar electrokinetic capillary chromatography. *J. Chromatogr. A* **829,** 317–325.
22. Mateus L., Cherkaoui S., Christen P., and Veuthey J. -L. (1999) Application of micellar electrokinetic chromatography to the determination of some tropane alkaloids in various plant extracts. *Current Topics in Phytochemistry* **2,** 175–182.
23. Mateus, L., Cherkaoui, S., Christen, P., and Oksman-Caldentey, K. -M. (2000) Simultaneous determination of scopolamine, hyoscyamine and littorine in plants and different hairy root clones of Hyoscyamus muticus by micellar electrokinetic chromatography. *Phytochemistry* **54,** 517–523.
24. Cherkaoui, S., Mateus, L., Christen, P., and Veuthey, J. -L. (1999) Nonaqueous capillary electrophoresis for the analysis of selected tropane alkaloids in a plant extract. *Chromatographia* **49,** 54–60.
25. Kvasnicka, F., Price, K. R., Ng, K., and Fenwick, G. R. (1994) Determination of potato glycoalakloids using isotachophoresis and comparison with a HPLC method. *J. Liq. Chromatogr*. **17,** 1941–1951.
26. Kreft, S., Zel, J., Pukl, M., Umek, A., and Strukelj, B. (2000) Non-aqueous capillary electrophoresis for the simultaneous analysis of solasodine and solasonine. *Phytochem. Anal*. **11,** 37–40.
27. Driedger, D. R., LeBlanc, R. J., LeBlanc, E. L., and Sporns, P. (2000) A capillary electrophoresis laser-induced fluorescence method for analysis of potato

glycoalkaloids based on a solution-phase immunoassay. 1. Separation and quantification of immunoassay products. *J. Agric. Food Chem*. **48,** 1135–1139.
28. Driedger, D. R., LeBlanc, R. J., LeBlanc, E. L., and Sporns, P. (2000) A capillary electrophoresis laser-induced fluorescence method for analysis of potato glycoalkaloids based on a solution-phase immunoassay. 2. Performance evaluation. *J. Agric. Food Chem*. **48,** 4079–4082.
29. Cherkaoui, S., Bekkouche, K., Christen, P., and Veuthey, J. -L. (2001) Non-aqueous capillary electrophoresis with diode array and electrospray mass spectrometric detection for the analysis of selected steroidal alkaloids in plant extracts. *J. Chromatogr. A* **922,** 321–328.
30. Bianco, G., Schmitt-Kopplin, P., De Benedetto, G., Kettrup, A., and Cataldi, T. R. I. (2002) Determination of glycoalkaloids and relative aglycones by non-aqueous capillary electrophoresis (NACE) coupled with electrospray ionization ion-trap mass spectrometry (ESI-ion-trap MS). *Electrophoresis* **23,** 2904–2912.
31. Bianco, G., Schmitt-Kopplin, P., Crescenzi, A., Comes, S., Kettrup, A., and Cataldi T. R. I. (2003) Evaluation of glycoalkaloids in tubers of genetically modified virus y resistant potato plants (var. Désirée) by non aqueous capillary electrophoresis coupled with electrospray ionisation mass spectrometry (NACE-ESI-MS). *Anal. Bioanal. Chem*. **375,** 799–804.
32. Hardman, J. G. and Limbird, L. E. (eds.) (1995) Goodman and Gilman's *The Pharmacological Basis of Therapeutics*, 9th ed. McGraw-Hill, New York: pp. 141–160.
33. Daali, Y., Cherkaoui, S., Christen, P., and Veuthey, J. -L. (1999) Experimental design for enantioselective separation of celiprolol by capillary electrophoresis using sulfated β-cyclodextrin. *Electrophoresis* **20,** 3424–3431.
34. Roddick, J. G., Rijnenberg, A. L., Osman, S. F. (1988) Synergistic interaction between potato glycoalkaloids α-solanine and α-chaconine in relation to destabilization of cell membranes: ecological implications. *J. Chem. Ecol*. **14,** 889–902.
35. Jadhav, S. J., Kumar, A., Chavan, J. K. (1991) Glycoalkaloids, in *Potato: Production, Processing, and Products* (Salunkhe, D. K., Kadam, S. S., and Jadhav, S. J. eds.) CRC, Boca Raton, FL: pp. 203–245.
36. Maga, J. A. (1994) Glycoalkaloids in solanaceae. *Food Rev. Int*. **10,** 385–418.
37. Friedman, M. and Mc Donald, G. M. (1997) Potato glycoalkaloids: chemistry, analysis, safety, and plant physiology. *Crit. Rev. Plant Sci*. **16,** 55–132.
38. Steiner, F. and Hassel, M. (2000) Nonaqueous capillary electrophoresis: a versatile completion of electrophoretic separation techniques. *Electrophoresis* **21,** 3994–4016.
39. Blaschke, G., Lamparter, E., and Schlüter, J. (1993) Racemization and hydrolysis of tropic acid alkaloids in the presence of cyclodextrins. *Chirality* **5,** 78–83.
40. Salvador, A., Varesio, E., Dreux, M., and Veuthey, J. -L. (1999) Binding constant dependency of amphetamines with various commercial methylated β-cyclodextrins. *Electrophoresis* **20,** 2670–2679.
41. Mc Laughlin, G. M., Nolan, J. A., Lindahl, J. L., et al. (1992) Pharmaceutical drug separations by HPCE: Practical guidelines. *J. Liq. Chromatogr*. **15,** 961–1021.

10

Capillary Electrophoresis for Pharmaceutical Analysis

Alex Marsh, Margo Broderick, Kevin Altria, Joe Power, Sheila Donegan, and Brian Clark

Summary

This chapter describes the application of capillary electrophoresis (CE) to pharmaceutical analysis. The areas of pharmaceutical analysis covered are enantiomer separation, analysis of small molecules such as amino acids or drug counter-ions, pharmaceutical assay, related substances determinations, and physiocochemical measurements such as log P and pKa of compounds. The different electrophoretic modes available and their advantages for pharmaceutical analysis are described. Recent applications of CE for each subject area are tabulated with electrolyte details. Information on electrolyte choice and method optimization to obtain optimal separations is included.

Key Words: Capillary electrophoresis; free solution CE; nonaqueous CE; micellar electrokinetic chromatography; microemulsion electrokinetic chromatography; pharmaceuticals; review; dynamic capillary coating; chiral separation; log P determination; pKa determination; assay.

1. Introduction

The use of capillary electrophoresis (CE) methods for pharmaceutical analysis has become increasingly popular in recent years. The wide range of applications for which its use has proved successful includes ***(1)*** assay of drugs, determination of drug-related impurities, physicochemical measurements of drug molecules, chiral separation, and the analysis of vitamins and pharmaceutical excipients.

Pharmaceutical analysis is dominated by high-performance liquid chromatography (HPLC). Other separative techniques used include thin-layer

From: *Methods in Molecular Biology, vol. 384: Capillary Electrophoresis*
Edited by: P. Schmitt-Kopplin © Humana Press Inc., Totowa, NJ

chromatography (TLC) and gas chromatography (GC), but the range of applications for which they can be used and their quantitative capabilities are not as widespread as for HPLC. Other techniques include ionizing radiation (IR) and ultraviolet (UV) spectroscopy, which are often used for identity testing of pharmaceuticals, and a range of flask-based methods, e.g., titration, which are used for physicochemical parameter determinations.

The advantages of CE for pharmaceutical analysis include its speed and cost of analysis, reductions in solvent consumption and disposal, and the possibility of rapid method development. CE also offers the possibility that a single set of separation conditions can be applicable for a wide range of analyses, giving efficiency savings. CE instruments can be coupled to a variety of detector types, including mass spectrometers, for special applications and more detailed analysis.

1.1. Electrophoretic Modes

There are several electrophoretic modes which can be used to analyse pharmaceuticals.

Free-solution capillary electrophoresis (FSCE) is very popular and involves the use of simple buffered aqueous electrolytes and separation of ionic drugs is achieved through pH control. The addition of reagents to the electrolyte such as organic solvents or ion-pair reagents can also be used to achieve the required separation selectivity. For the separation of drug enantiomers, FSCE with chirally selective agents such as cyclodextrins (CDs) added to the electrolyte to facilitate chiral resolution is the most common method used ***(2)***.

For the separation of water-insoluble or sparingly soluble pharmaceuticals, nonaqueous CE (NACE), which employs electrolytes composed of organic solvents, has been used successfully ***(3–7)***. NACE is also useful for the resolution of water-soluble charged solutes, as the selectivity obtained can be different to aqueous-based separations.

Micellar electrokinetic chromatography (MEKC) and microemulsion electrokinetic chromatography (MEEKC) electrolytes contain surfactant molecules which form micelles (MEKC) and microemulsion droplets (MEEKC) that add a chromatographic element to the separation, enabling analysis and separation of acidic, basic and neutral drugs.

MEEKC is the most flexible of all the separation modes, offering the greatest selectivity to the widest range of compounds and can be considered the separation method of choice when performing CE analysis.

1.1.1. Free-Solution Capillary Electrophoresis

The majority of drugs are basic and thus ionized at low pH. FSCE using low pH buffer systems has been employed to separate a range of basic drugs;

separations are based on analyte size and number of positive charges, but neutral compounds do not migrate through the detector. This offers an advantage over HPLC analysis of formulated pharmaceutical products where the analyte peak can be masked by the co-elution of neutral excipient or flavouring compounds. A low-pH phosphate buffer has been used to analyze 550 different basic drugs ***(8)*** and a similar method has been validated ***(9)*** for analysis of a variety of basic drugs, excipients, and raw materials.

To separate mixtures of acidic and basic drugs (or cationic and anionic species), FSCE at high pH can be utilized ***(10)***. At pH 7.0 or greater, the electroosmotic flow (EOF) generated by the applied current is sufficiently strong to sweep anions to the detector. Analyte migration time is dependent on solute charge type and density; strongly cationic species migrate first whereas small, highly charged anions attempt to migrate against the EOF and are detected last. Neutral species migrate with the EOF, and are unresolved.

1.1.2. Nonaqueous Capillary Electrophoresis

Water-insoluble basic drugs are difficult to separate using FSCE methods, and NACE can be applied for such analyses ***(3–6,11)***. NACE electrolytes do not contain water, and organic solvents such as methanol and acetonitrile are used instead. Selectivities that are difficult to obtain using aqueous buffers, even when using surfactants or complexing agents, may be easily obtained with nonaqueous systems ***(12)*** and separation selectivity can be altered by changing the composition of organic solvent in the electrolyte. The compatibility of mass spectrometric coupling is increased as a result of the solvent volatility and the use of organic buffers ***(3)***. NACE is being considered more frequently and its use for the analysis of basic drugs has been reported, including the separation of a number of opium alkaloids ***(12)***, a mixture of cationic drug substances ***(13)***, a range of tropane alkaloids ***(6)***, a range of β-blockers ***(14)***, tricyclic antidepressants ***(7)***, and different basic drugs ***(5,15)***. NACE has also been successfully used to separate polar acidic and basic drugs ***(16)***, perform chiral separation of pharmaceutical amines ***(17)***, and calculate pK_a^* values of basic analytes in methanol ***(15)***.

1.1.3. Micellar and Microemulsion Electrokinetic Chromatography

To achieve separation of acidic, basic, and neutral pharmaceutical compounds, either MEKC or MEEKC can be employed. Both techniques enhance the electrophoretic separation by providing a chromatographic partitioning mechanism into the micelles (MEKC) or microemulsion droplets (MEEKC), which offers resolution of neutral compounds as well as charged species. Neutral solutes are separated solely based on their solubility. Charged solutes are separated based on their electrophoretic movement, solubility based

partitioning, and potential ion-pair interaction with the charged micelle or droplet. MEEKC has been found to provide superior separation efficiency to MEKC, probably as a result of improved mass transfer between the microemulsion droplet and aqueous phase ***(18)***. Solutes also penetrate the MEEKC droplet more easily than the rigid MEKC micelle, which allows MEEKC to be applied to a wider range of analytes. MEEKC also offers greater separation capability for water-insoluble compounds than MEKC ***(19)*** and a larger separation window ***(18,20)***.

The use of MEEKC to determine compound solubility (log P) has been successfully shown for many types of drugs ***(21–29)*** and is an important pharmaceutical application of the technique.

Many reports have been published detailing the use of MEEKC for pharmaceutical applications, **Table 1** details selected pharmaceutical applications using MEEKC and the composition of the microemulsion used.

Readers are referred to two recent reviews on MEEKC ***(43,44)*** for further examples of MEEKC applications and descriptions of operating parameter effects.

Table 1
Selected Pharmaceutical Applications of Microemulsion Electrokinetic Chromatography

Application	Microemulsion composition	Ref.
Determination of nine preservatives in pharmaceutical and cosmetic products	3.3% *w/w* SDS, 0.81% *w/w* octane, 6.6% *w/w* butan-1-ol, 89.3% *w/w* 50 m*M* borate, pH 9.5	***30***
Analysis of betamethasone and derivatives	1.44% *w/w* SDS, 0.81% *w/w* octane, 6.61% *w/w* butan-1-ol, 91.14% 20 m*M* sodium phosphate, pH 7.5 1.9% *w/w* IPM, 2.0% *w/w* SC/SDC, 3.5% *w/w* PC, 0.81% *w/w* octane, 7.5% *w/w* butan-1-ol, 85.1% 20 m*M* sodium phosphate, pH 7.5	***22***
Analysis of 4-hydroxybenzoate preservatives in pharmaceuticals	3.31% *w/w* SDS, 0.81% *w/w* n-octane, 6.61% *w/w* butan-1-ol, 89.27% *w/w* 50 m*M* phosphate buffer, pH 2.1.	***31***
Analysis of formulated drug products	3.31% *w/w* SDS, 0.81% *w/w* n-octane, 6.61% *w/w* butan-1-ol, 89.27% *w/w* 10 m*M* Borate buffer, pH 9.2.	***32***

Insoluble ingredients of pharmaceutical ointment	3.97% *w/w* SDS, 0.81% *w/w* n-octane, 6.61% *w/w* butan-1-ol, 10% *w/*w propan-2-ol, 78.61% *w/w* 10 m*M* Borate buffer, pH 9.2.	***33***
Levetiracetam from other antiepileptic drugs	1.8% *w/w* SDS, 0.48% *w/w* n-octane, 3.96% *w/w* butan-1-ol, 93.76% *w/w* 10 m*M* Borate buffer, pH 9.2.	***34***
Separation of immunosuppressive drugs	1.44% *w/w* SDS, 0.81% *w/w* octane, 6.61% *w/w* butan-1-ol, 91.14% 20 m*M* sodium phosphate, pH7.5 2.0% *w/w* SDC, 3.5% *w/w* PC, 1.9% *w/w* IPM, 0.81% *w/w* octane, 7.5% *w/w* butan-1-ol, 85.1% 20 m*M* sodium phosphate, pH 7.5 2.0% *w/w* SC, 3.5% *w/w* PC, 1.9% *w/w* IPM, 0.81% *w/w* octane, 7.5% *w/w* butan-1-ol, 85.1% 20 m*M* sodium phosphate, pH 7.5	***35***
Analysis of ephedrine and pseudoephedrine	23.3 m*M* SDS, 16.4 m*M* *n*-heptane, 180.85 m*M* butan-1-ol, 8% acetonitrile, 20 m*M* borate	***36***
Amino acid derivatives using laser-induced fluorescence detection	2.12% *w/w* SDS, 0.52% *w/w* heptane, 4.21% *w/w* butanol, 84 m*M* borate, pH 8.4	***37***
Nicotine-related alkaloids	3.3% *w/w* SDS, 0.8% *w/w* octane, 6.6% *w/w* butan-1-ol, 89.29% *w/w* 10 m*M*, sodium tetraborate, pH 9.15	***38***
Analysis of vitamins	6.0% *w/w* SDS, 0.8% octane, 6.6% butanol, 20.0% propan-2-ol, 66.6% 25 m*M* phosphate, pH 2.75	***39***
Analysis of water and fat-soluble vitamins	80 m*M* SDS, 1% *w/w* octane, 5% *v/v* butanol, 40 m*M* borate, pH 8.5	***40***
Separation of fat-soluble vitamins	6.0% *w/w* SDS, 0.8% octane, 6.6% butanol, 20.0% propan-2-ol, 66.6% 25 m*M* phosphate, pH 2.75	***41***
UV filters in suncreen lotions	2.25% *w/w* SDS/0.75% *w/w* Brij35, 0.8% *w/w* n-alkane, 6.6% *w/w* 1-butanol, 17.5% *w/w* 2-propanol, 72.1% *w/w* 10 m*M* borate buffer, pH 9.2	***42***

IPM, isoprpylmyristate; PC, phosphatidylcholine; SC, sodium cholate; SDC, sodium deoxycholate; SDS, sodium dodecylsulfate.

2. Enantiomer Separation

Chiral analysis has become one of the most studied areas in CE, as it is a powerful analytical technique for separating chiral compounds and of major importance for pharmaceutical applications.

Research in this area has increased over the past few years and fast, efficient, sensitive, and selective methods have been developed. Extensive research has shown chiral analysis by CE can be far superior than conventional techniques such as HPLC and GC, with the added cost benefit that in CE, the chiral selector is added to the background electrolyte in lieu of expensive chiral columns. The possibility of low-UV wavelength detection for CE also allows the separation and detection of analytes with poor chromophores, which are difficult to detect by HPLC.

This section reviews recently developed chiral selectors and chiral separating techniques. Readers are referred to recently published reviews on the fundamental aspects ***(45)*** and applications of chiral CE ***(46)***.

There are many types of chiral selectors that can be applied to the enantioseparation, but the most common are native and derivatized CDs. Other chiral selectors that have been applied to CE separations include natural and synthetic chiral micelles, crown ethers, chiral ligands, proteins, carbohydratesm and macrocyclic antibiotics (***45,47–51)***.

At low pH, basic drugs are positively charged and their migration toward the cathode can be retarded by a chirally selective complexing agent, resulting in separation of enantiomers of differing affinity for the agent. This principle has been demonstrated for the resolution of chiral basic drugs using CDs as the chiral selector ***(52)***. At high pH, chiral acidic drugs are negatively charged and migrate against the EOF toward the anode. Neutral chiral selector agents are swept along the capillary with the EOF toward the detector, thus complexation reduces the migration time of the drug and results in enantioseparation ***(53)***.

2.1. Cyclodextrins

Native and derivatized CDs are employed routinely for enantioseparation, and are naturally occurring carbohydrates with a bucket-like shape. Inside the capillary, analytes can become included in the CD cavity by complexation, and migration time is dependent on analyte mobility and its degree of interaction with the CD. The chiral hydroxyl groups around the rim of the CD can interact enantioselectively with chiral analytes, which can fit inside the CD cavity, leading to the separation of enantiomers with differing binding constants. There are three types—α, β, and γ CDs—each differing in the number of glucose subunits they are composed of. β-CD is the least soluble in water but its solubility can be improved by the addition of urea. Because enantioselection

is based on the formation of inclusion complexes between the CD host and chiral solute, the type of CD chosen is a major factor for achieving efficient resolution of enantiomers. The background to the use of CDs in chiral CE has been the subject of two recent reviews ***(54,55)***.

A systematic approach to the development of CE chiral methods for pharmaceutical basic compounds using sulfated CDs has been reported ***(56)***. Systematic method-development approaches for several compounds have been performed by modifying method parameters, chiral selectors and concentration, buffer pH, type of organic modifiers, buffer type, temperature, and applied voltage.

The robustness of an enantiomeric method for separation of a basic (propanolol), a neutral (praziquantel), and an acidic (warfarin) compound using highly sulfated CDs (HS-CDs) in a low-pH phosphate buffer and short-end injection technique was evaluated; the method showed high selectivity and good resolution, proving that HS-CD is an effective chiral selector ***(50)***. A charged, highly water soluble CD derivative, 2-*O*-(2-aminoethyl-imino-prpyl)- β-*O*-hydroxypropyl-β-CD (2-AIPHP-C-CD) was synthesized and successfully used as a chiral selector for enantiomeric separation of some acidic compounds ***(57)***. New single-isomer sulfated CDs have been synthesized, namely, sodium salt of octakis (2,3-dimethyl-6-o sulfo)- γ-cyclodextrin and β-cyclodextrin; these are stable in basic media and have been used to separate the enantiomers of neutral, weakly acidic, and weakly basic analytes by CE ***(58)***. Ion-pairing reagents, which improve chiral resolution in combination with the CDs, have been added to chiral separations in CE in the presence of CDs,. The use of the cationic ion-pairing reagent quinine is shown as a powerful enantioselector for the chiral resolution of acidic and basic analytes ***(59)***.

2.2. Crown Ethers

Crown ethers are another type of chiral selector that have been developed and synthesized. The only crown that has been studied is 18 crown-6-tetracarboxylic acid, introduced by Kuhn et al. ***(60)***. The capability of crown ethers to host ions was found with alkaline metal, alkali earth metal, ammonium ions, and organic cations derived from primary amines ***(47,48)***. Two new diazo crown ether derivatives have been synthesized ***(61)*** and have shown the potential of enhanced enantioselectivity with different cyclodextrins in dual_ selector systems.

2.3. Macrocyclic Antibiotics

The usefulness of macrocyclic antibiotics as chiral selectors in CE has been reported ***(49)***. Recently, erythromycin and derivatives (types of macrocyclic

antibiotics) were investigated for their potential as chiral selectors. The potential of erythromycin is limited because of its small glycone ring size, which is about half that of β-cyclodextrin ***(62)***.

2.4. Carbohydrates

Chirally selective carbohydrates are often employed in CE. Maltodextrins (mixtures of linear linked D-glucose polymers) have been used for chiral resolution of a range of acidic drugs ***(63)***. Maltodextrins have also been used to separate racemic basic drugs belonging to different pharmacological groups (antifungal, antihistaminic, antidepressant, antipsychotic) ***(64)***.

2.5. Proteins

Proteins have been used for enantiomer separation in CE. Proteins such as bovine serum albumin (BSA), human serum albumin (HAS), and several additional proteins have been used as chiral selectors ***(65)***. A recent review of the use of protein chiral selectors has been written ***(66)***. The high background UV absorbance of proteins limits their utility in chiral CE.

2.6. Chiral MEKC

Enantiomer separation by MEKC involves the addition of a chiral agent such as chiral surfactants, crown ethers, or CDs to the background electrolyte with chiral/achiral micelles. Chiral MEKC with chiral surfactants is an important separation mode for chiral compounds, with chiral surfactants including naturally occurring compounds such as bile salts ***(67)***, amino acids ***(68)***, and glucose ***(69)***. Chiral separation in MEKC is affected by the affinity of the enantiomers toward the micelles, and the concentration of the micellar phase, which depends on the aggregation properties of the chiral surfactants. A mixed MEKC consisting of sodium dodecyl sulfate (SDS) and either sodium cholate (SC) or taurodeoxycholate (TDC) was used for the chiral separation of polychlorinated biphenyls ***(70)***.

An MEKC method with laser-induced florescence detection has been applied to the determination of enantiomeric forms of amino acids derived from antitumor antibiotics ***(51)***.

2.7. Chiral MEEKC

Succesful analyses have also been carried out by MEEKC. To achieve chiral resolution of a range of basic drugs, a chirally selective surfactant in combination with low interfacial tension oils has been used ***(71,72)***, whereas

a chiral oil has been successful for racemic ephedrine ***(73)***. Chiral resolution has been achieved by cyclodextrin-modified microemulsions for racemic levetiracetam ***(74)***.

2.8. Pharmaceutical Applications of Chiral CE

Chiral selectors are used routinely in the pharmaceutical industry for a wide variety of applications and there have been many publications on the subject. **Table 2** contains a selection of such applications and details on the electrolytes used.

N′-nitrosonornicotine is formed by the nitrosation of nicotine. Tumor induction is believed to occur by way of 2′hydroxylation of NNN and others have shown that (S) NNN undergoes more 2′hydroxylation than (R) NNN, thus there is a need to quantify and separate the two enantiomeric forms of this important analyte. Employing HP-β-CD the R and S (NNN) are separated in 4 min ***(75)***.

Enantiomeric purity of levodopa (3,4-dihydroxyphenyl-L-alanine) in the pharmaceutical formulation Madopar also containing benserazide, which is used to treat Parkinson's disease, has been determined. The addition of chiral crown ether to the background electrolyte allowed the enantioseparation of benserazide (added to the formulation to prolong therapeutic effect) and chiral resolution of dextrodopa from the main active for a preparation used to treat Parkinson's disease. The dextrodopa impurity was clearly resolved from the main peak and determined to be 0.5%, as shown in **Fig. 1** ***(76)***.

The validation criteria for chiral CE methods are similar to those employed for the validation of chiral HPLC methods and include limits of detection and quantatition for the undesired enantiomer, linearity of detector response, recovery, precision, and method robustness.

Validation of chiral CE methods has successfully been carried out and reported ***(77–80)***. Using a low-pH background electrolyte and heptakis (2,6-di-O-methyl)-β-CD as the chiral selector, validated chiral methods have been developed for the novel direct thrombin inhibitor Melagatran, its oral prodrug Ximelagatran, and their enantiomers ***(78)***, and for the local anaesthetic ropivacaine hydrochloride in pharmaceutical formulations ***(77)***, which showed the required limit of quantatition of 0.1% of the enantiomeric impurity. A limit of detection (LOD) of 0.04% was reported for a validated chiral separation of the enantiomers of the Alzheimer's treatment galantamine hydrobromide using α-cyclodextrin in pH-3.0 phosphate buffer, and the method was successfully included in a New Drug Application (NDA) ***(80)***, whereas an LOD of 0.05% was achieved for the undesired enantiomer of an M3 agonist using highly sulfated γ-cyclodextin in low pH buffer ***(81)***. A CE method for the determination of ephedrine enantiomers has been validated for the European

Table 2
Chiral Separation of Pharmaceuticals Application Table

Application	Buffer	Ref.
Enantiomeric separation of *N′*-nitrosonornicotine found in tobacco smoke	Citric acid buffer, pH 2.8, 30 m*M* HP-β-CD	***75***
Chiral antimalaria drug erythro-MQ and its analoques	100 m*M* triethanolamine phosphate buffer, pH 3.0, 0.2–150 mg mL^{-1} HP-α-CD, acetyl-β-CD, HE-β-CD	***84***
nine racemic arylglyine amides used in the systhesis of amino acids	20 m*M* 3-(*N*-morpholino propanesulfonic acid, pH 6.5, 10% methanol, 1.5% w/v HS-β-CD	***85***
Novel antidepressant drug E-6006	25 m*M* sodiumphosphate, pH 3.0, 10 m*M* S-β-CD	***86***
4 diastereomers of an antiviral agent with 2 chiral centres	25 m*M* phosphate buffer, pH 2.5, 1–7% w/v S-β-CD	***87***
(+/−) methamphetamine (+/−) ephedrine and (+/−) pseudoephedrine (+/−) amphetamine in clandestine tablets	150 m*M* phosphate, 12.5 m*M* β-CD	***88***
Analgesic drug	25 m*M* borate buffer, pH 9.0, 40 m*M* SBE-β-CD	***89***
Enantioseparation of methotrexate antifolate drug	70 m*M* phosphate, pH 7.0, 12.5–200 μ*M* HP-β-CD	***79***
nonsteroidal anti-inflammatory drug (NSAID),S-naproxen	Phosphoric acid-triethanolamine, pH 3.0, 5 m*M* SB-β-CD, 20 m*M* TM-β-CD	***90***
Dopa enantiomers used to treat parkinsons disease	10 m*M* Tris buffer, pH 2.5 12 m*M* 18 C_6H_4	***76***
Local anaesthetic bupivacaine	125 m*M* L-ZGP, 50 m*M* ammonium acetate in MeOH	***17***
β-adrenoceptor blocker pindolol	125 m*M* L-ZGP, 50 m*M* NH_4 ammonium acetate in MeOH, 55% 1,2dichloroethane	***17***

S-β-CD, Sulfate-β-CD-cyclodextrin; HE-β-CD, hydroxyethyl-β-CD; HP-β-CD, Hydroxypropyl-β-cyclodextrin; SB-β-CD, Sulfobutyl-β-cyclodextrin; SU-β-CD, sulfated-β-CD; TMCD, Trimethyl-β-CD; $18C_6H_4$, (18-crown-6)-2,3,11,12-tetracarboxylicacid; L-ZGP, *N*-benzocarbonylglycyl-L-proline.

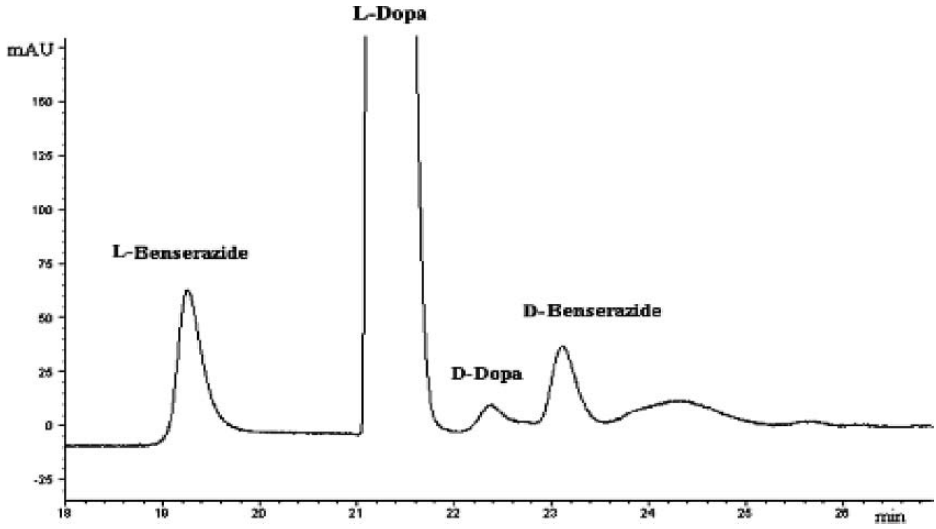


Fig. 1. Chiral separation of benserazide and dopa enantiomers for L-dopa pharmaceutical preparation. Separation conditions: fused-silica capillary was 56 cm × 50 μm inner diameter extended light path; buffer Tris-citric acid (10 m*M*) citrate adjusted to pH 2.5 12 m*M* $18C_6H_4$ 15% MeOH; operating temperature 15 °C. (From **ref. *76***.)

pharmcopia with a detection limit of 0.1% for (+) ephedrine, with a relative standard deviation (RSD) of less than 20% for trace-level enantiomer determination and good linearity from 0.1 to 1% ***(82)***, and the chiral separation of methotrexate, an antifolate, has been validated ***(79)***. A separation method compatible with mass spectrometry was developed for quarternary ammonium compounds by CE using 50 m*M* ammonium formate, pH 3.0, and 50 m*M* γ-cyclodextrin. Chiral separation of the pentamers was not possible using HPLC ***(83)***.

3. Analysis of Small Molecules and Ions

The separation and detection of small organic and inorganic ions is an important activity in the pharmaceutical industry. Most drug molecules are charged and as such, are manufactured with a counter-ion; commonly, a metal cation (e.g., K^+) for acidic drugs or an ionic salt (e.g., Cl^-) or small organic acid (e.g., acetate) for basic drugs. It is important to characterize analytically the drug stoichiometry (ratio of drug:counter ion) to ensure that the potency of the batch of drug substance is known. Because such counter-ions usually have little or no chromphore, popular techniques for the analysis of small ions include ion-exchange chromatography (IEC) and flame atomic absorption spectrometry,

Table 3
Small Molecules and Ions Pharmaceutical Analysis Application Table

Application	Electrolyte	Ref.
Anions—indirect detection		
Determination of Br, Cl, & SO_4 as impurities in calcium acamprosate	Chromate + 1 m*M* borate, pH 9.15	***94***
TFA counter-ion of an opioid peptide analgesic	Phthalate, CTAB	***95***
Acetate content in acetate drug salt	Phthalate, OFM	***96***
Acetate residues in drug substance	Phthalate, OFM	***97***
Drug inorganic counter ion determination	Chromate, TTAB	***98***
Drug organic acid counter ion determination	Phthalate, MES, TTAB	***99***
Inorganic anion contaminant in drug substance	Chromate, OFM	***100***
Anions—direct detection		
Determination of residual Br in excess of Chloride for local anaesthetic analysis	60:40 MeCN: methanesulfonic acid buffer, pH 1.3	***101***
Drug organic acid counter-ion determination e.g. benzoate, hydroxynapthoate	Borate, pH 9.5	***102***
Cations—indirect detection		
Ca, Li, K & Na counterions of glycosaminoglycans	4-aminopyridine buffer, pH 9.0	***103***
Ca in calcium acamprosate drug substance	Imidazole, sulfuric acid	***104***
Cationic counter ion content in drug substance	Imidazole, formic acid	***105***
	Imidazole, low pH	***98***
K in drug substance	Imidazole, formic acid	***106***
Quarternary amine residues in drug substance	Quinine, THF	***107***
Cations—direct detection		
K counter-ion and inorganic cationic impurities of acidic drugs by conductivity detection	Creatine, acetic acid, 18-crown-6	***108***

CTAB, cetyltrimethylammonium bromide; MES, 4-morpholineethanesulfonic acid; OFM, proprietary Waters chemical; TTAB, tetradecyltrimethylammoniumbromide.

but CE is becoming increasingly popular for such applications because of its simplicity. Commercial kits are available for ion analysis and are frequently used; consequently, methods are simple to operate, with analysis times of 2–10 min, which compares favorably with IEC. Additionally, IEC columns are expensive and require regeneration, so CE offers both reduced analysis times and costs.

Ions with a poor UV response can be analyzed by indirect UV detection, using a UV-absorbing background electrolyte, and metal ions can be detected directly through on-capillary complexation to form UV-active metal chelates. Some simple organic acids are sufficiently UV-active to be detected directly ***(91)***. **Table 3** contains a selection of CE methods that have been used to analyze ions for pharmaceutical applications.

The separation of amino acids can be quite complicated by HPLC, as they must first be derivatized to provide a chromophore for detection. However, CE can be used at lower operating wavelengths. Amino acids, usually zwitterionic, become cations at low pH, and a pH-2.8 electrolyte of 50 m*M* ethanesulfonic acid was used to resolve a number of amino acids, which were detected directly at 185 nm without requiring sample pretreatment as shown in **Fig. 2** ***(92)***.

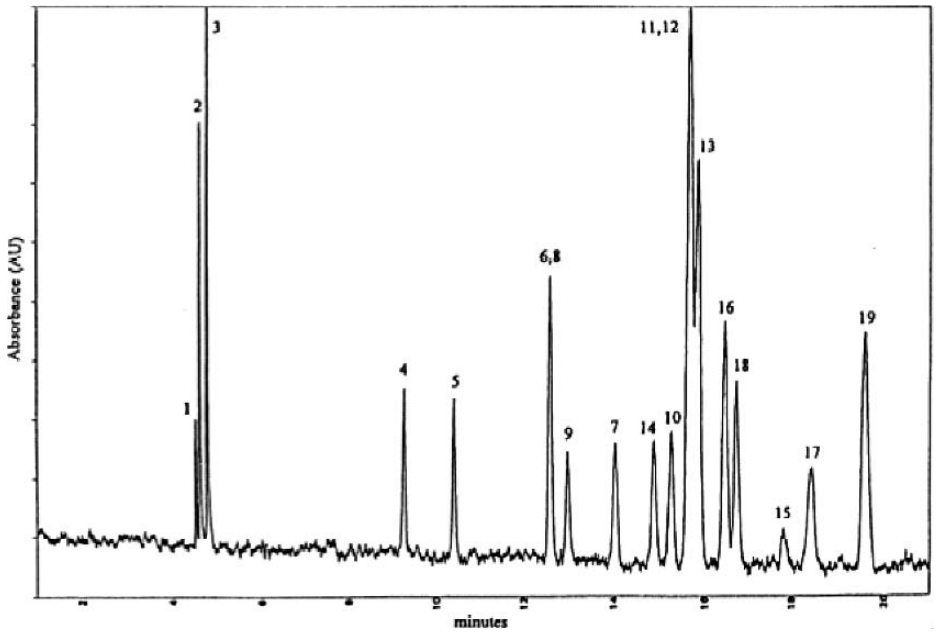


Fig. 2. Electropherogram of 20 common amino acids. 50 m*M* Ethanesulfonic acid, pH 2.8; applied voltage, 30 kV; injection time, 10 s. Peaks: 1, Lys; 2, Arg; 3, His; 4, Gly; 5, Ala; 6, Val; 7, Ser; 8, Ile; 9, Leu; 10, Thr; 11, Asn; 12, Met; 13, Gln; 14, Trp; 15, Glu; 16, Phe; 17, Pro; 18, Tyr; 19, Cys. (From **ref. *93***.)

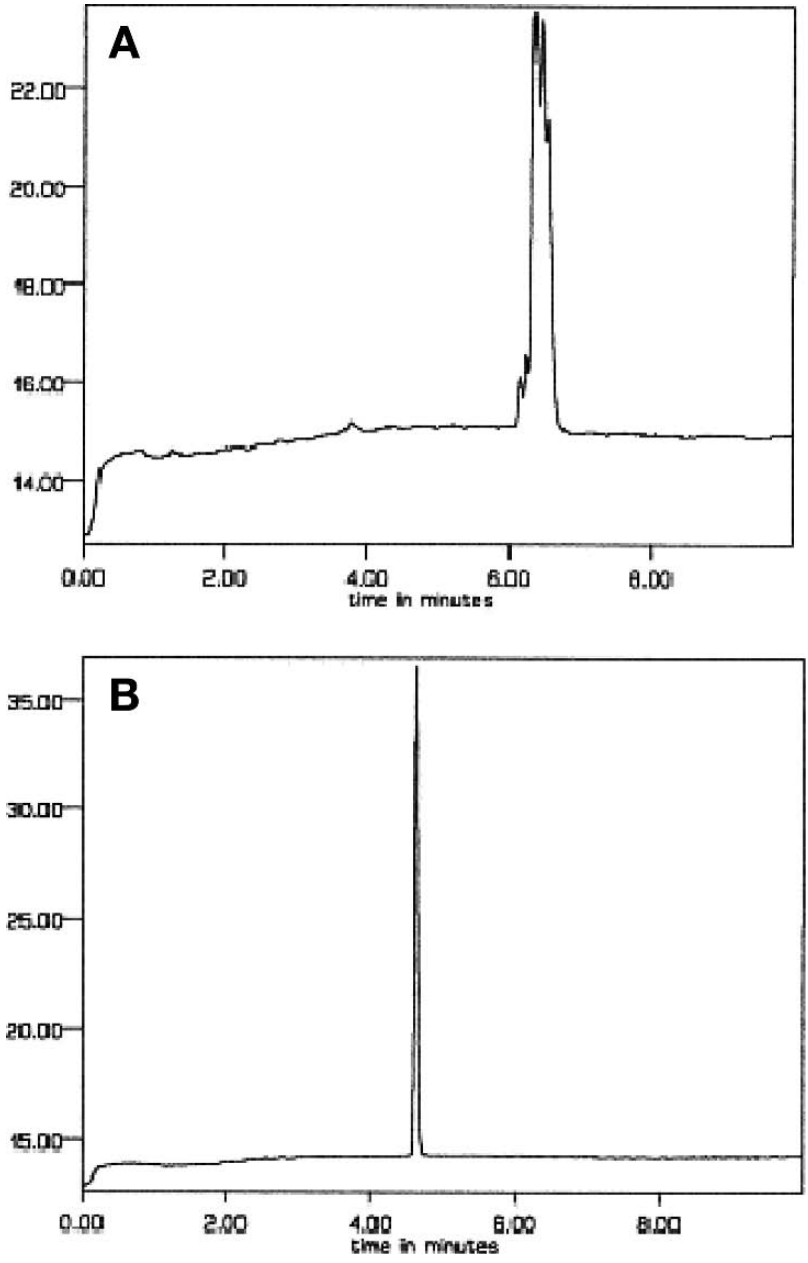


Fig. 3. Separations on a multibore capillary using phosphate buffer or CElixir buffer. **(A)** Separation using phosphate buffer: 50 m*M* phosphate 2.5, multibore capillary 19 × 25 μm channels, 27 cm long, 130 μA, +5 kV, 30 °C, detection at 200 nm, sample salbutamol 1 mg/mL, 1 s injection. **(B)** Separation using CElixir™

A background electrolyte of 100 m*M* sodium tetraborate, pH 10.0, 20 m*M* sodium deoxycholate, and 15 m*M* β-CD was used to separate all major and minor components of gentamicin amino sugar antibiotic and its impurities by derivatization with σ-phthaldialdehyde ***(93)***.

4. Assay of Pharmaceuticals

For pharmaceutical analysis, assay of drug substance and formulated products is a very important and regulated activity. Analytical methods must be validated to strict standards to show that they are robust, accurate, repeatable, and suitable for their purpose. Most routine analytical assay determinations in the pharmaceutical industry are performed by HPLC, a well established separative technique. One of the major advantages of implementing CE methods in place of HPLC is its relatively small level of solvent consumption (milliliters compared to the liters of mobile phase used in an HPLC run). An additional advantage is that sample pretreatment requirements are often reduced compared to HPLC, as the CE capillary can be washed with NaOH between injections and many interfering components do not migrate, as they are neutral. The ability to quantify a range of sample types using a single set of CE conditions is another strong feature, as this can considerably reduce analysis and system set-up times ***(9***,***10***,***109–112)***.

The electrophoretic conditions inside the capillary vary slightly between injections, which leads to greater variability in peak migration times and area than that seen in HPLC. A number of approaches can overcome this problem. Migration times and peak areas can be calculated relative to those of an internal standard peak, which results in great improvement in method repeatability ***(113)***. Greater migration time reproducibility can also be achieved by applying the separation voltage across the capillary for a very short time prior to injection and separation ***(114)***. A commercial capillary treatment system of buffers and rinse solutions has been shown to improve CE repeatability, as the capillary is coated with a bilayer of surfactants, ensuring that the surface coverage and EOF is consistent between injections and between capillaries. **Figure 3** highlights the consistency of EOF when using the buffer-coating system compared to a standard phosphate buffer using a capillary composed of 19 separate channels. In **Fig. 3A**, the peaks in the channels have different speeds and the separation

Fig. 3. buffer: 50 m*M* phosphate 2.5, multibore capillary 19 × 25 μm channels, 27 cm long, 90 μA, +5 kV, 30 °C, detection at 200 nm, sample salbutamol 1 mgmL^{-1} 1 s injection. Multibore capillary 19 × 25 μm channels, 27 cm long,+5 kV, 30 °C, Elixir buffer pH 2.5, 90 μA, 200 nm. (From **ref. *115***.)

is poor, whereas in **Fig. 3B**, the EOF is consistent in each channel and the peaks move at the same speed, resulting in a single peak ***(115)***. For a more comprehensive guide to improving the precision of CE methods, readers are referred to a review on the subject ***(116)***.

An FSCE method with CDs in the electrolyte has been developed ***(117)*** for analysis of the diabetic therapy ragalitazar and its counter-ion arginine in Active Pharmaceutical Ingredients (API) and low-dose tablets. The method is suitable for 12 different analyses of the API and tablets—assay and identification of ragaglitazar and arginine, chiral purity of ragaglitazar, and purity of ragaglitazar. The accuracy of the method (% recovery) was found to be 101–106% for ragaglitazar and 101–125% for arginine, whereas precision for the detection of peaks (% RSD) was found to be 0.63% for ragaglitazar and 3.50% for arginine. A MEEKC method was used for the quantitative determination of folic acid in tablets ***(118)***, giving a precision of $<1.2\%$ RSD and recovery of $99.8 \pm 1.8\%$ at three concentration levels.

CE methods have been reported that monitor both drugs and polymers released from drug delivery systems in a single run (HPLC methods allow the monitoring of either the drug or the polymer alone). FSCE was used for monitoring of the controlled delivery of recombinant growth hormone from a system based in VP-HEMA copolymer. The CE method used a running buffer of 100 m*M* sodium tetraborate, pH 9.0 and allowed the simultaneous monitoring of both the liberation of rHGH and the polymer's degradation by solubilization ***(119)***. A CE method has been reported to monitor R- and S-ibuprofen released from hydrophilic copolymer systems using dextrin 10 as a chiral selector. The method allowed detection at concentrations of $1\,\mu g mL^{-1}$ and 0.5% of the R-ibuprofen enantiomer ***(120)***. An assay method has been reported ***(121)*** for quantitative determination of the weakly acidic antibiotic benzylpenicillin and procaine, benzathine, and clemizole, the basic forms of benzylpenicillin found in pharmaceutical preparations. The separation is shown in **Fig. 4**. **Table 4** contains a selection of CE methods that have been validated for the quantitative assay of various pharmaceutical substances and dosage forms.

5. Impurities Determination of Pharmaceuticals

CE can be used for the determination of structural related impurities from main active drug. Impurity profiling is generally been carried out by HPLC and cross-correlated with TLC or another HPLC method. CE offers a completely different selectivity process than chromatography, and thus is a complementary technique to HPLC.

CE has been proven an alternative to TLC or HPLC for quantitation of compounds and the determination of drug-related impurities ***(135–137)***.

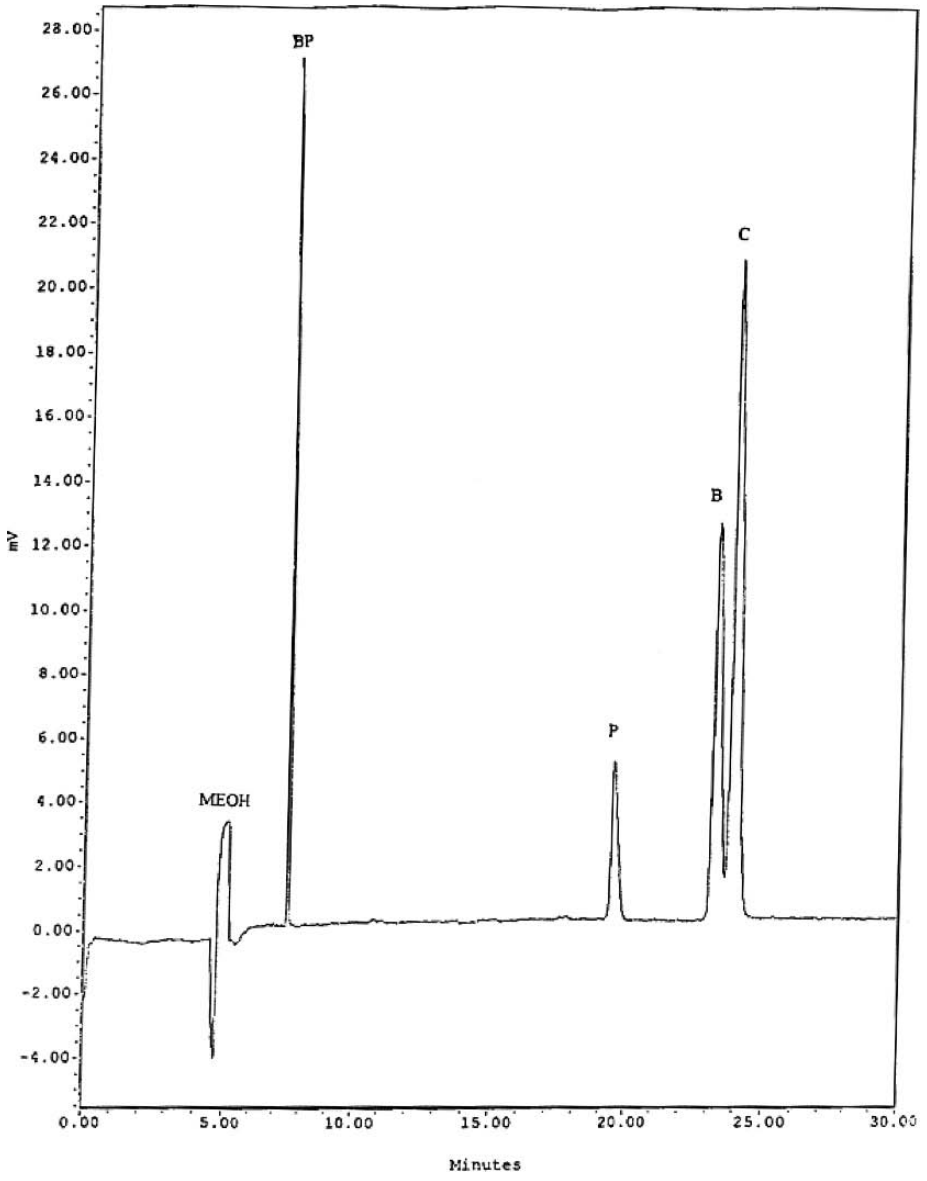


Fig. 4. Electropherogram of benzylpenicillin and procaine, benzathine and clemizole. Buffer phosphate–borate pH 8.7, supplemented with 14.4 g/L sodium dodecyl sulfate. Ultraviolet 214 nm 60 cm (52 cm effective length) × 75 μm inner diameter fused-silica capillary at 25 °C, 18 kV. Hydrodynamic injection by gravity-driven siphoning 10 s. was used. P, procaine; B, benzathine; C, clemizole; BP, benzylpenicillin; MEOH, methanol (EOF marker). (From **ref. *121***.)

Table 4
Validated Capillary Electrophoresis (CE) Methods for Pharmaceutical Assay

Application	Method details	Ref.
FSCE methods		
Simultaneous determination of procaine, dihydrostreptomycin and penicillin G in multiantibiotic veterinary preparations	0.08 *M* borate, pH 8.0	***122***
Determination of indinavir sulfate, a protease inhibitor used in HIV therapy in capsule formulations	20 m*M* phosphate, pH 2.52	***123***
Method for assay of raloxifene, an estrogen agonist in bone	20 m*M* acetate, pH 4.5	***124***
Assay and identification of ragaglitazar, a diabetic therapy, and its counter-ion arginine, chiral purity of ragaglitazar and purity of ragaglitazar in Active Pharmaceutical Ingredients and low dose tablets	90% v/v 25 m*M* phosphate buffer, pH 8.0 + 10% v/v acetonitrile + 2% w/v sulfobutylether β-CD + 0.7% w/v dimethyl β-CD	***117***
Determination of pravastatin, a cholesterol reducing agent, in tablet formulation	10 m*M* borate, pH 8.5 + 10% MeCN	***125***
Determination of the anti-fungal ketoconazole in tablets and creams	10 m*M* phosphate buffer, pH 2.3	***126***
Stability indicating, validated method for cyclizine hydrochloride tablets and suppositories (motion sickness)	50 m*M* phosphate, pH 2.3	***127***
Determination and separation of antipsychotics—clothiapine, clozapine, olanzapine, quetiapine	80 m*M* phosphate, pH 3.5	***128***

Simultaneous determination of 6 angiotensin-II-receptor antagonists – candesartan, eprosartan, irbesartan, losartan potassium, telmisartan and valsartan	FSCE: 60 m*M* phosphate, pH 2.5 MEKC: 55 m*M* phosphate, pH 6.5, 15 m*M* SDS	***129 130***
Dynamic capillary coating system methods		
Analysis of benzodiazepines	CEofix™[a] buffer system	***131***
Characterization and quantification of heroin and its basic impurities and adulterants	CElixir[b] buffer system	***132***
NACE methods		
Analysis of quinolizidine alkaloids in Chinese herbs, which are difficult to separate in aqueous media	1% acetic acid, 50 m*M* ammonium acetate, 20% acetonitrile in methanol	***133***
MEKC methods		
Determination of acyclovir in Zovirax cream	20 m*M* borate buffer, pH 10.0 + 10 m*M* SDS	***134***
Benzylpenicillin salts	phosphate-borate buffer, pH 8.7 + 14.4 gL^{-1} SDS	***121***
MEEKC methods		
Quantitative determination of folic acid (a water soluble vitamin) in tablets	0.5% w/w ethyl acetate, 1.2% w/w butan-1-ol, 0.6% w/w SDS, 15% v/v propan-2-ol, 82.7% w/w 10 m*M* tetraborate, pH 9.2	***118***
Quantitative determination of the fat-soluble vitamin E acetate. (suppressed EOF environment enabled timely migration of the analyte peak)	0.8% w/w n-octane, 6.6% w/w butan-1-ol, 6% w/w SDS, 20% v/v propan-2-ol, 66.6% w/w 25 m*M* phosphate, pH 2.5	***41***

[a] Analis proprietary chemical.
[b] MicroSolv proprietary chemical.

The structural impurities of a drug will possess similar structural properties to the main component, which makes achieving their resolution challenging. The high separation efficiencies possible for CE often allows a small degree of selectivity to provide an acceptable resolution. Standard requirements of an impurity method are that all likely synthetic and degradative impurities are

Table 5
Drug-Related Impurity Pharmaceutical Analysis Application Table

Application	Electrolyte	Ref.
Ximelagatran thrombin inhibitor and related substances in drug substance and tablet formulation	phosphate buffer, pH 1.9, 22% v/v MeCN, 11 m*M* hydroxypropyl β-CD	***145***
Penicillin and related impurities	20 m*M* ammonium acetate, pH 6.5.	***146***
N-acetylcysteine and its impurities	100 m*M* borate, pH 8.40	***147***
Ciprofloxacin and its impurities	phosphate buffer, pH 6.0 0.075 *M* pentane-1-sulfonic acid sodium salt	***148***
Metacycline and its related substances	160 m*M* sodium carbonate + 1 m*M* EDTA, pH 10.35, 13% v/v MeOH	***149***
Loratadine and related impurities	100 m*M* H_3PO_4, pH 2.5 10% acetonitrile.	***150***
Heroin and its basic impurities	100 m*M* DM-β-CD in Celixir[a] reagent B, pH 2.5, 100 m*M* HP-β-CD in Celixir[a] reagent B ph2.5, 103.2 m*M* SDS, 50 m*M* phosphate-borate ph 6.5	***132***
Ranitidine hydrochloride and related substances	190 m*M* trisodium citrate, pH 2.6.	***138***
vancomycin and related impurities	120 m*M* Tris-phosphate buffer, pH 5.2 containing 50 m*M* CTAC	***144***
Ketorolac tromethamine and its known related impurities	13 m*M* boric acid-phosphoric acid, pH 9.1	***143***
Homotaurine as an impurity in calcium acamprosate	40 m*M* borate, pH 9.2	***140***
New substance LAS 35917)	60 m*M* tetraborate, pH 9.2	***141***
3,4-diaminopyridine and 4,aminopyridine potassium channel blockers	50 m*M* phosphate buffer, pH 2.5	***139***
5-aminosalicylic acid and its major impurities	120 m*M* CAPS buffer, pH 10.2, 65 m*M* SDS, 55 m*M* TBAB, 5% MeOH	***142***

CAPS, 3-(Cyclohexylamino)-1-propanesulfonic acid; CTAC, cetyltrimethylammonium chloride; EDTA, ethylenediaminetetraacetic acid; SDS, sodium dodecyl sulfate; TBAB, tetrabutylammonium bromide.

[a] MicroSolv proprietary chemical.

resolved from one another, and from the main drug peak, and that impurities can be monitored at 0.1% area/area level or below. **Table 5** contains a selection of successful CE methods for impurity determination for pharmaceuticals.

5.1. Low pH

Basic drug impurities can be separated at pH 2.0–4.0, and a low-pH electrolyte is often employed in analysis of basic drugs and their related impurities. A CE assay was developed and validated for ranitidine (Zantac) and potential related substances in bulk drug and pharmaceutical preparations ***(138)***, with the ionic strength and pH of the electrolyte shown to be the most critical parameters affecting selectivity. **Figure 5** illustrates the separation of ranitidine and related impurities from the analysis of a batch of Zantac injection. The CE assay gave detection limits of: diamine (0.03% a/a), oxime (0.04%, a/a), Bis (0.1%a/a), nitroacetamide (0.24%a/a), and a number of unknown peaks, which were not resolved by either TLC or HPLC.

All known impurities of 3,4-diaminopyridine, a potassium channel blocker, were separated and quantified at a level of 0.05% ***(139)***.

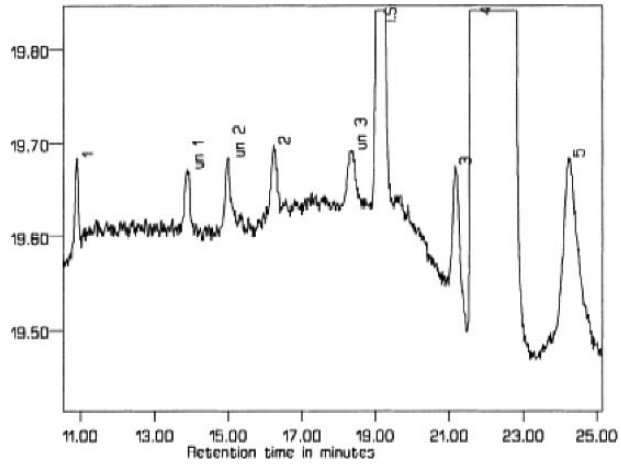


Fig. 5. Resolution of ranitidine and the seven related substances in 10 mg/mL Zantac injection. Separation conditions: fused-silica capillary was 27cm × 50 μm inner diameter; buffer 190 m*M* trisodium citrate adjusted to pH 2.6 with citric acid. Voltage 6 kV; detection wavelength 230 nm;operating temperature 25 °C. diamine(1), oxime(2), Nitroacetamide(5), unknown1(un1), unknown(un2), unknown(un3). (From **ref. *138***.)

5.2. High pH

High-pH buffers, such as phosphate and borate, are employed in the analysis of acidic components. At high pH, the acidic components migrate against the EOF, maximizing mobility differences.

High-pH borate buffer at pH 9.2 has been used in CE for the determination of homotaurine (HT), a doubly charged anion at this pH, as an impurity in calcium acamprosate by capillary zone electrophoresis ***(140)***. The method was validated and detection limits of between 0.01 and 0.15% homotaurine with respect to drug substance were reported.

A high-pH CE method was successfully developed to quantitatively profile the chloromethylated, monomethylated, and hydroxylated impurities of a new substance (LAS 35917) ***(141)***. These impurities co-eluted when analyzed by HPLC; the CE method allowed detection and quantitation of impurities present at levels of 0.04–0.08% of the parent drug.

5.3. MEKC

As a result of its chromatographic-style separation mechanism, MEKC is often employed to separate mixtures of charged and neutral components. A MEKC method was developed for the quantification of mesalazine 5-aminosalicylic and its major impurities ***(142)***. A fast, selective MEKC method was used for the simultaneous assay of ketorolac tromethamine and its known related impurities ***(143)***, and quantitative analysis of vancomycin antibiotic and related impurities has also been carried out by MEKC ***(144)***.

The separation and determination of drug-related impurities using CE has been extensively studied, and the method performance and validation data obtained clearly shows that CE methods are successful applications in this area and give equal or superior performance to HPLC methods.

6. Physicochemical Measurements

In the early stages of drug discovery, it is important to determine the pharmacokinetic properties of compounds in order to predict their bioavailability and blood–brain barrier distribution and to develop appropriate formulations. There are a large number of compounds requiring such screening, mainly because of the high volume of syntheses that can be carried out by combinatorial chemistry. Consequently, there is a need for rapid and reliable methods of physicochemical determination in order to maintain high throughput and efficiency. CE has been applied successfully for physicochemical analysis of many pharmaceutical compounds and has many advantages over the traditional methods of log P and pKa determination. An integrated automated process of measuring the log P, pKa, and chemical stability of compounds has been reported ***(152)***.

6.1. Log P

Extremes of pH, i.e., pH 1.19 and pH 12.0, can be used in CE to measure the log P of acids and bases, respectively in their uncharged forms ***(153)***. This is an advantage compared to HPLC, where stationary phase stability must be considered.

Early work in this area was performed ***(154–156)*** using MEKC with solute partitioning with the micelle being related to its log P (solubility).

The wider range of solutes that are separated in MEEKC has enabled its use ***(21–23,26,27,30,156–158)*** for compound solubility measurement techniques. The MEEKC method of octanol-water partition coefficient determination has been demonstrated for pharmaceuticals ***(21–29,153)***. The compound solubility is assessed by bracketing it with neutral "marker" compounds of known Log P, which are used to create a calibration graph of log P against migration time, as shown in **Fig. 6**. The log P of the analyte of interest can then be calculated by its migration time using the graph. The higher the compound's log P value,

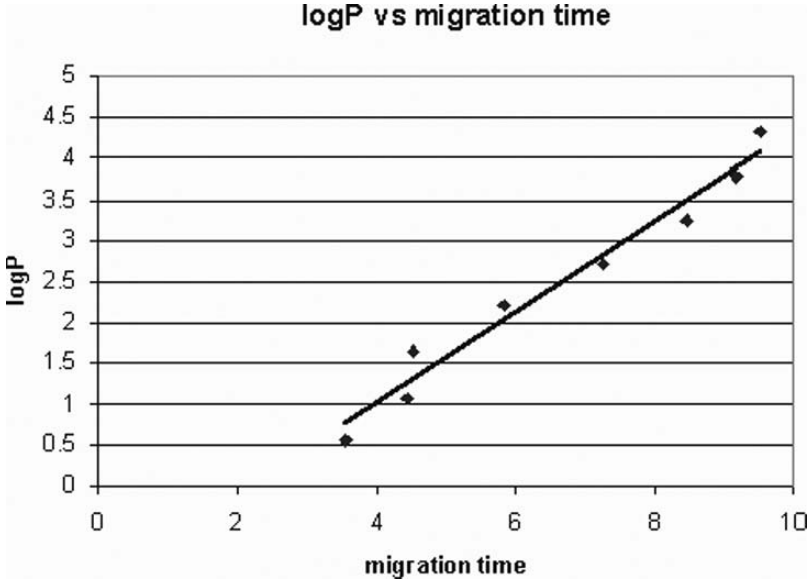


Fig. 6. Use of microemulsion electrokinetic chromatography (MEEKC) to determine partition coefficients: plot of MEEKC migration times vs log P data for a range of phenones. Separation conditions: 0.81% (w/w) octane, 6.61% (w/w) butan-1-ol, 3.31% (w/w) sodium dodecyl sulfate, and 89.27% (w/w) 10 m*M* sodium tetraborate buffer, 15 kV, 30 cm × 50 μm inner diameter capillary (detection window at 22 cm), 40 °C, 200 nm. (From **ref.** ***160***.)

the more it partitions into the microemulsion droplet and the longer it takes to migrate *(23,159,160)*.

A rapid screening assay for the determination of log P that uses pressure-assisted MEEKC has been developed *(28)*. This technique applies pressure to the capillary, driving its contents through the capillary at a faster rate than that offered by the EOF.

The use of MEEKC for log P determinations has also been demonstrated with a 96-capillary array instrument for the high-throughput screening of compound solubility *(21,161)*. **Table 6** contains a selection of published applications of CE for log P determination.

6.2. pKa

The dissociation constants (pKa) of pharmaceuticals can be determined from migration time data obtained by running the compound with FSCE electrolytes of a range of pH values *(162–174)*, and **Table 7** details a selection of reported applications. The mobility of the solute at each pH can be calculated from its migration time and the EOF (measured using a neutral marker such as dimethylsulfoxide), and a plot of mobility against pH constructed. **Figure 7** shows the mobility of the antibiotic cephalexin plotted over a range of electrolyte pH values. The pKa value of a compound is calculated using the electrophoretic mobilities, and cephalexin is calculated to have an acidic and a basic pKa of 2.49 and 7.08, respectively, compared to its literature values of 2.53 and 7.14 *(175)*.

The dissociation constants of water-insoluble and sparingly soluble compounds have been measured by CE through adding solvents such as methanol to the electrolyte *(164)*.

A medium-throughput method of pKa screening by pressure-assisted CE has been developed and demonstrated successfully for 48 acidic, basic, and multivalent pharmaceutical compounds of known pKa *(165)*. The pressure assistance can greatly reduce the measurement time, especially for the low-pH analyses, which can be very slow as a result of the low EOF level.

By combining pressure assistance with the "short-end injection" technique and a short capillary, pKa determinations can be performed even more rapidly, and this method was also found to give greater repeatability of mobility measurements *(166)*.

CE compares very favorably to other methods of pKa analysis *(176)*. CE instruments are highly automated and can be used for high-throughput applications. Unlike titration methods, precise information on sample concentration is not required, as only analyte mobilities are used to calculate pKa by CE. Sparingly soluble compounds are easily analyzed and only very small amounts of material are required, which is especially useful for the screening of newly

Table 6
log P Application Table

Application	Method details	Ref.
Neutral pharmaceuticals	25 m*M* borate buffer, pH 8.5–30 to 150 m*M* SDS (MEKC)	***154***
Neutral pharmaceuticals and steriods	0.05 M phosphate buffer, pH 7.0 (pH 9.0 for steroids)–80 m*M* SC, 100 m*M* SDS or 100 m*M* CTAB surfactant (MEKC)	***155***
24 acidic and basic pharmaceuticals	Heptane-butanol-SDS borate, pH 12.0	***23***
Anionic pharmaceuticals	Heptane-butanol-SDS borate, pH 7.0	***159***
45 weakly acidic, weakly basic and neutral pharmaceuticals	50 m*M* SDS, 82 m*M* nheptane, 50 m*M* borate-phosphate buffer, pH 10.0, 0.87 *M* butan-1-ol	***28***
Carbonate esters and small organic molecules	1.80% *w/w* SDS, 0.82 *w/w*% nheptane, 6.49 *w/w*% butan-1-ol, 0.1 *M* borate-0.5 *M* phosphate buffer, pH 7.4 1.44-2.88% *w/w* SDS, 0.82% *w/w* nheptane, 6.49% *w/w* butan-1-ol, 0.05 *M* acetate buffer, pH 4.75 2.16% *w/w* SDS, 0.82% *w/w* nheptane, 6.49% *w/w* butan-1-ol, 0.1 *M* borate-0.05 *M* HCl, pH 1.4	***22***
Multiplexed 96-capillary method for neutral and basic compounds	3.3% *w/w* SDS, 0.8% *w/w* nheptane, 6.6% *w/w* butan-1-ol, 92% *w/w* 68 m*M* (cyclohexylamino)-1-propanesulfonic acid, pH 10.3	***22***
Neutral and weakly acidic compounds using dynamically coated capillary columns	1.4% *w*/*v* SDS, 1.2% *v/v* nheptane, 8% v/*v* butan-1-ol, 85% *v/v* 50 m*M* sodium phosphate buffer, pH 3.0	***29***

SDS, sodium dodecyl sulfate; SC, sodium cholate; CTAB, cetyltrimethylammonium bromide.

synthesized pharmaceutical entities of which only small quantities exist ***(172)*** or for applications where the molecule of interest is present only in very small quantities, such as radiopharmaceuticals. A CE system equipped with a radioactivity detector has been used to determine the dissociation constants of ^{99m}Technetium radiopharmaceuticals ***(177)***. By using the "stacking" technique (explained in an earlier section) of sample introduction, concentrations of pharmaceutical compounds as low as 2 μM have resulted in successful pKa determinations ***(166)***. Techniques commonly used for pKa determination such

Table 7
pKa Application Table

Application	Method details	Ref.
Medium throughput pKa of 48 pharmaceutical compounds —acidic, basic and multivalent	pH range 2.5–11.0. Electrolytes of 0.1 *M* ionic strength composed of phosphate, acetate and borate buffers adjusted to required pH with phosphoric, acetic or boric acid or NaOH. PACE at 2 psi	***165***
Rapid pKa screening of 26 acidic, basic and multivalent pharmaceuticals	pH range 2.5–11.0 electrolytes of 0.05 *M* ionic strength composed of 0.5 *M* phosphate and 1 *M* acetate buffers mixed to obtain required pH PACE at 25 mbar "short-end" injection	***166***
PKa determination of labile drug compounds	PH range 2.0-12.0 electrolytes of 0.05 *M* ionic strength composed of 1 *M* phosphate, 0.1 *M* borate and 1 *M* acetate buffers mixed and adjusted with phosphoric acid, acetic acid and NaOH to obtain required pH "short-end" injection	***167***
PKa determination of ^{99m}Technetium radiopharmaceuticals	pH range 1.3–6.6 50 mbar PACE Citric acid adjusted with NaOH	***177***
pKa of N imidazole derivative aromatase inhibitors	pH range 3.88–9.16 25 m*M* phosphate buffer adjusted with triethylamine	***185***
2-amino-2-oxazolines (anti-hypertensive agents)	pH 4.77–9.69	***172***
Anthrocyclines (antibiotics)	pH 4.20–8.20	***179***
Cephalosporins (antibiotics)	pH 2.0–9.0	***173***
Cytokinins (phytohormones)	pH 1.5–6.0	***180***
Dihydrofolate reductase inhibitors	pH 2.1–4.5 50 m*M* phosphate buffer adjusted with phosphoric acid/NaOH	***181***
Quinolines (antibiotics)	pH 2.0–11.0	***182***
Ropinirole and impurities (Parkinsons treatment)	pH 2.20–11.42	***183***
pKa of organic bases in aqueous methanol (0–70% v/v)	pH range 4.76–9.5 Tris, ethanolamine & acetate buffers	***184***
pKa* values of bases	pH* range 4.9–9.7 Methanol and sodium acetate buffer + acetic acid	***15***

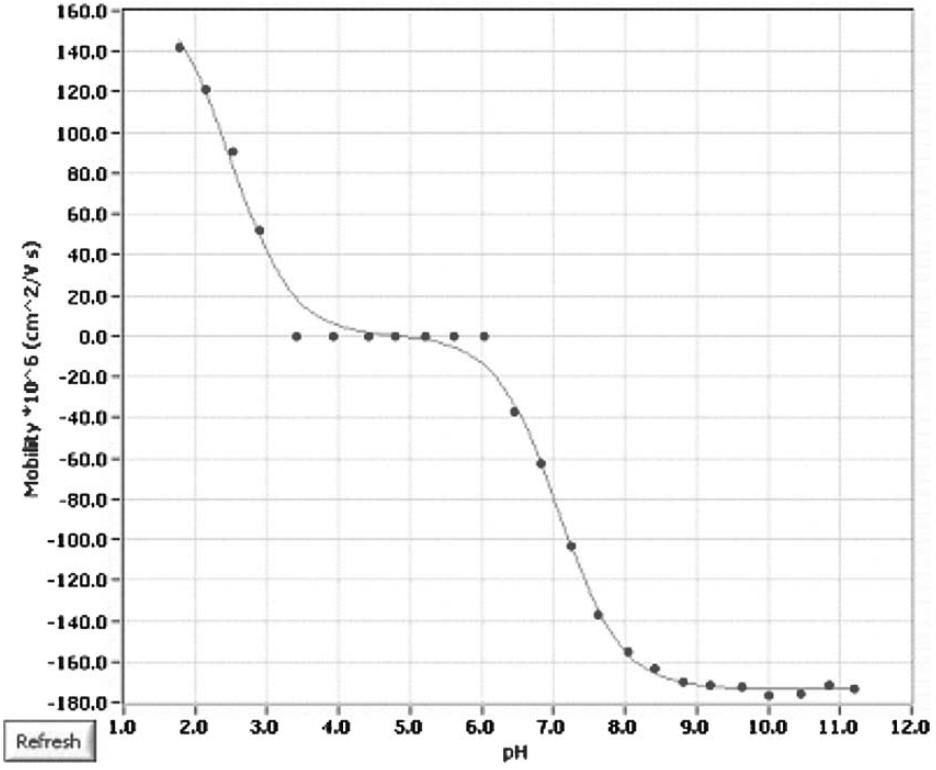


Fig. 7. Plot of cephalexin electrophoretic mobility against electrolyte pH, used to calculate compound pKa. Analysis performed using CombiSep 96-capillary array instrument, CombiSep pKa determination buffers and CombiSep pKa determination software.

as potentiometric titration or UV-VIS spectroscopy do not differentiate in analytical response between the analyte of interest and any analog impurities, which causes problems when attempting to measure compounds that are not highly pure or are unstable in solution. Because CE is a separative technique, it is appropriate for pKa determination of impure or unstable samples, and also, electrolyte purity is not essential. The CE method of pKa determination has been demonstrated successfully for sets of labile drug compounds, which are unstable in neutral and acidic or in basic solution ***(167)***.

The standard pH scale for aqueous acids and bases has limited applicability to organic solvents where pH^* is used instead. Correspondingly, the pKa^* values of compounds in nonaqueous solvents have been calculated by CE ***(178)***. The pKa^* values in methanol of a series of bases have been determined ***(15)***.

7. Conclusion

For pharmaceutical analysis, the range of applications for which CE can be used is extensive, possibly eclipsing that of HPLC. CE also offers a number of advantages over HPLC and other analytical techniques: analysis and method development speed, reduced consumable and solvent expenses, simplicity of operations, and a greater possibility of implementation of a single set of method conditions for the analysis of several different samples, giving the large efficiency savings which are desirable in today's busy laboratory.

For some pharmaceutical applications, such as chiral analysis or the measurement of physicochemical properties, CE is a superior technique to the conventional methods in terms of cost, ease of use, and automation possibilities. CE does have its disadvantages, but with considered method development, such as the incorporation of internal standards to overcome poor injection precision, its performance can match that of HPLC. This has been shown by the number of reported validated CE methods and also by several CE methods that have been accepted by regulatory authorities in new drug product submissions. CE also suffers from a comparative lack of experience on the part of pharmaceutical analysts, but with its routine applications increasing, this is improving. In many analytical laboratories, CE is regularly used to provide complementary information to HPLC or other methods and is even the technique of choice for certain applications. As the instrumentation further improves, automation possibilities expand, and the list of applications increases, the use of CE for pharmaceutical analysis is certain to continue to be popular and become more widespread.

References

1. Altria, K. D. (ed.) (1998) *Quantitative Analysis of Pharmaceuticals by Capillary Electrophoresis*. Vieweg, Weisbaden: pp. 1–285.
2. Altria, K. D. (ed.) (1998) *Quantitative Analysis of Pharmaceuticals by Capillary Electrophoresis*. Vieweg, Weisbaden: pp. 70–78.
3. Esaka, Y., Okumura, N., Uno, B., and Goto, M. (2001) Non-aqueous capillary electrophoresis of p-quinone anion radicals. *Anal. Sci*. **17,** 99–102.
4. Yuqin, L., Shuya, C., Yuqiao, C., Xingguo, C., and Zhide, H. (2004) Application of nonaqueous capillary electrophoresis for quantitative analysis of quinolizidine alkaloids in Chinese herbs. *Anal. Chim. Acta*. **508,** 17–22.
5. Leung, G. N. W., Tang, H. P. O., Tso, T. S. C., and Wan, T. S. M. (1996) Separation of basic drugs with non-aqueous capillary electrophoresis. *J. Chromatogr. A* **738,** 141–154.
6. Cherkaoui, S., Varesio, E., Christen, P., and Veuthey, J. -L. (1998) Selectivity manipulation using nonaqueous capillary electrophoresis. Application to tropane alkaloids and amphetamine derivatives. *Electrophoresis* **19,** 2900–2906.

7. Cantú, M. D., Hillebrand, S., Costa Queiroz, M. E., Lanças, F. M., and Carrilho, E. (2004) Validation of non-aqueous capillary electrophoresis for simultaneous determination of four tricyclic antidepressants in pharmaceutical formulations and plasma samples. *J. Chromatogr. B* **799,** 127–132.
8. Hudson, J., Golin, M., Malcolm, M., and Whiting, C. (1998) Capillary zone electrophoresis in a comprehensive screen for drugs of forensic interest in whole blood: an update. *Can. Soc. Forens. Sci. J*. **31,** 1.
9. Altria, K. D., Frake, P., Gill, I., Hadgett, T. A., Kelly, M. A., and Rudd, D. R. (1995) Validated capillary electrophoresis method for the assay of a range of basic drugs. *J. Pharm. Biomed. Anal*. **13,** 951–957.
10. Altria, K. D., Bryant, S. M., and Hadgett, T. (1997) Validated capillary electrophoresis method for the assay of a range of acidic drugs and excipients. *J. Pharm. Biomed. Anal*. **15,** 1091–1101.
11. Hansen, S., Tjornelund, J., and Bjornsdottir, I. (1996) Selectivity enhancement in capillary electrophoresis using non-aqueous media. *Trends Anal. Chem*. **15,** VII.
12. Bjørnsdottir, I. and Hansen, S. H. (1995) Determination of opium alkaloids in crude opium using non-aqueous capillary electrophoresis. *J. Pharm. Biomed. Anal*. **13,** 1473–1481.
13. Bjørnsdottir, I. and Hansen, S. H. (1995) Comparison of separation selectivity in aqueous and non-aqueous capillary electrophoresis *J. Chromatogr. A* **711,** 313–319.
14. Servais, A. C., Fillet, M., Chiap, P., Abushoffa, A. M., Hubert, P., and Crommen, J. (2002) Optimization of the separation of beta-blockers by ion-pair capillary electrophoresis in non-aqueous media using univariate and multivariate approaches. *J. Sep. Sci*. **25,** 1087–1095.
15. Porras, S. P. and Riekkola, M. -L. (2001) Capillary zone electrophoresis of basic analytes in methanol as non-aqueous solvent: Mobility and ionisation constant. *J. Chromatogr. A*. **905,** 259–268.
16. Siren, H., Hiissa, T., and Min, Y. (2000) Aqueous and non-aqueous capillary electrophoresis of polar drugs. *Analyst* **9,** 1561–1568.
17. Hedeland, Y., Hedeland, M., Bondesson, U., and Pettersson, C. (2003) Chiral separation of amines with N-benzoxycarbonylglycyl-L-proline as selector in non-aqueous capillary electrophoresis using methanol and 1,2-dichloroethane in the background electrolyte. *J. Chromatogr. A* **984,** 261–271.
18. Hansen, S. H., Gabel-Jensen, C., Mohamed El-Sherbiny, D. T., and Pedersen-Bjergaard, S. (2001) Microemulsion electrokinetic chromatography – or solvent-modified micellar electrokinetic chromatography. *Trends Anal. Chem*. **20,** 614–619.
19. Altria, K. D. (1999) Application of microemulsion electrokinetic chromatography to the analysis of a wide range of pharmaceuticals and excipients. *J. Chromatogr. A* **844,** 371–386.
20. Cherkaoui, S. and Veuthey, J. -L. (2002) Micellar and microemulsion electrokinetic chromatography of selected anesthetic drugs. *J. Sep. Sci*. **25,** 1073–1078.

21. Wong, K. S., Kenseth, J., and Strasburg, R. (2004) Validation and long-term assessment of an approach for the high throughput determination of lipophilicity (log P_{OW}) values using multiplexed, absorbance-based capillary electrophoresis. *J. Pharm. Sci*. **4,** 916–931.
22. Lucangioli, S. E., Carducci, C. N., Scioscia, S. L., Carlucci, A., Bregni, C., and Kenndler, E. (2003) Comparison of the retention characteristics of different pseudostationary phases for microemulsion and micellar electrokinetic chromatography of betamethasone and derivatives. *Electrophoresis* **24,** 984–991.
23. Gluck, S. J., Benko, M. H., Hallberg, R. K., and Steele, K. P. (1996) Indirect determination of octanol-water partition coefficients by microemulsion electrokinetic chromatography. *J. Chromatogr. A* **744,** 141–146.
24. Ostergaard, J., Hansen, S. H., Larsen, C., Schou, C., and Heegaard, N. H. H. (2003) Determination of octanol-water partition coefficients for carbonate esters and other small organic molecules by microemulsion electrokinetic chromatography. *Electrophoresis* **24,** 1038–1046.
25. Gong, S., Bo, T., Huang, L., Li, K. A., Liu, H. (2004) Separation and determination of biphenyl nitrile compounds by microemulsion electrokinetic chromatography with mixed surfactants. *Electrophoresis* **25,** 1058–1064.
26. Klotz, W. L., Schure, M. R., and Foley, J. P. (2001) Determination of octanol–water partition coefficients of pesticides by microemulsion electrokinetic chromatography. *J. Chromatogr. A* **930,** 145–154.
27. Reinhard, N. and Mrestani, Y. (2001) Use of affinity capillary electrophoresis for characterising pharnaceutical colloidal vahicle systems thermodynamically. *Biopharm. Drug Dispos*. **22,** 265–271.
28. Jia, Z., Mei, L., Lin, F., Huang, S., and Killion, R. B. (2003) Screening of octanol–water partition coefficients for pharmaceuticals by pressure-assisted microemulsion electrokinetic chromatography. *J. Chromatogr. A* **1007,** 203–208.
29. Poole, S. K., Patel, S., Dehring, K., Workman, H., and Dong, J. (2003) Estimation of octanol–water partition coefficients for neutral and weakly acidic compounds by microemulsion electrokinetic chromatography using dynamically coated capillary columns. *J. Chromatogr. B* **793,** 265–274.
30. Huang. H., Lai, Y. C., Chiu, C. W., and Yeh, J. M. (2003) Comparing micellar electrokinetic chromatography and microemulsion electrokinetic chromatography for the analysis of preservatives in pharmaceutical and cosmetic products. *J. Chromatogr. A* **993,** 153–164.
31. Mahuzier, P. E., Altria, K. D., and Clark, B. J. (2001) Selective and quantitative analysis of 4-hydroxybenzoate preservatives by microemulsion electrokinetic chromatography. *J. Chromatogr. A* **924,** 465–470.
32. Mahuzier, P. E., Clark, B. J., Crumpton, A. J., and Altria, K. D. (2001) Quantitative microemulsion electrokinetic capillary chromatography analysis of formulated drug products. *J. Sep. Sci*. **24,** 784–788.
33. Okamoto, H., Uetake, A., Tamaya, R., Nakjima, T., Sagara, K., and Ito, Y. (2000) Simultaneous determination of ingredients in an ointment by hydrophobic interaction electrokinetic chromatography. *J Chromatogr. A* **929,** 133–141.

34. Ivanova, M., Piunti, A., Marziali, E., Komarova, N., Raggi, M. A., and Kenndler, E. (2003) Microemulsion electrokinetic chromatography applied for separation of levetiracetam from other antiepileptic drugs in polypharmacy. *Electrophoresis* **24,** 992–998.
35. Lucangioli, S. E., Carducci, C. N., Scioscia, S. L., Carlucci, A., Kenndler, E., and Tripodi, V. P. (2003) Relation between retention factors of immunosuppressive drugs in microemulsion electrokinetic chromatography with biosurfactants and octanol-water partition coefficients. *J. Pharm. Biomed. Anal*. **33,** 871–878.
36. Zhang, J., Xie, J., Liu, J., Tian, J., Chen, X., and Hu, Z. (2004) Microemulsion electrokinetic chromatography with laser-induced fluorescence detection for sensitive determination of ephedrine and pseudoephedrine. *Electrophoresis* **25,** 74–79.
37. Jianping, X., Jiyou, Z., Huanxiang, L. et al. (2004) MEEKC with laser induced fluorescence detection: as tested with amino acid derivatives. *Biomed. Chromatogr*. **18,** 600–607.
38. Marsh, A., Altria, K. D., and Clark B. J. (2004) Orthogonal separations of nicotine and nicotine-related alkaloids by various capillary electrophoretic modes. *Electrophoresis* **259,** 1270–1277.
39. Hansen, S. H., Gabel-Jensen, C., and Pedersen-Bjergaard, S. (2001) Comparison of microemulsion electrokinetic chromatography and solvent-modified micellar electrokinetic chromatography. *J. Sep. Sci*. **24,** 643–650.
40. Sanchez, J. M. and Salvado, V. (2002) Comparison of micellar and microemulsion electrokinetic chromatography for the analysis of water- and fat-soluble vitamins. *J. Chromatogr. A* **950,** 241–247.
41. Pedersen-Bjergaard, S., Naess, O., and Moestue, S. (2000) Microemulsion electrokinetic chromatography in suppressed electroosmotic flow environment. Separation of fat-soluble vitamins. *J. Chromatogr. A* **876,** 201–211.
42. Klampfl, C. W. and Leitner, T. (2003) Quantitative determination of UV filters in sunscreen lotions using microemulsion electrokinetic chromatography. *J. Sep. Sci*. **26,** 1259–1262.
43. Hansen, S. H. (2003) Recent applications of microemulsion electrokinetic chromatography. *Electrophoresis* **24,** 3900–3907.
44. Marsh, A., Broderick, M., Altria, K., Clark, B., Power, J., and Donegan, S. (2004) Recent Advances in Microemulsion Electrokinetic Chromatography. *Electrophoresis* **25,** 3970–3980.
45. Rizzi, A. (2001) Fundamental aspects of chiral separations by capillary electrophoresis. *Electrophoresis* **22,** 3079–3106.
46. Amini, A. (2001) Recent developments in chiral capillary electrophoresis and applications of this technique to pharmaceutical and biomedical analysis. *Electrophoresis* **22,** 3107–3130
47. Haginaka, J. (2000) Enantiomer separation of drugs by capillary electrophoresis using proteins as chiral selectors. **875,** 235–254.
48. Stover, S. F. (1984) Isotachophoresis of metal—neutral ligand complexes: 18-crown-6 ether complexes with alkali metals. *J. Chromatogr. A* **298,** 203–210.

49. Desiderio, C. and Fanali, S. (1998) Chiral analysis by capillary electrophoresis using antibiotics as chiral selector. *J. Chromatogr. A* **807,** 37–56.
50. Perrin, C., Fabre, H., Maftouh, M., Massart, D. L., and Vander Heyden, Y. (2003) Robustness testing of chiral separations by capillary electrophoresis using highly-sulfated cyclodextrins. *J. Chromatogr. A* **1007,** 165–177.
51. Liu, J., Dabrah, T. T., Matson, J. A., et al. (1997) Analysis of amino acid enantiomers derived from antitumor antibiotics using chiral capillary electrophoresis. *J. Pharm. Biomed. Anal*. **16,** 207–214.
52. Sanger-van de Griend, C., Groningsson, K., and Westerlund, D. (1996) Chiral separation of local anaesthetics with capillary electrophoresis. Evaluation of the inclusion complex of the enantiomers with heptakis(2,6-di-O-methyl)-beta-cyclodextrin. *Chromatographia* **42,** 263–268.
53. Liu, L. and Nussbaum, M. A. (1995) Control of enantiomer migration order in capillary electrophoresis separations using sulfobutyl ether beta-cyclodextrin. *J. Pharm. Biomed. Anal*. **14,** 65–72.
54. Fillet, M., Hubert, P., and Crommen, J. (1998) Method development strategies for the enantioseparation of drugs by capillary electrophoresis using cyclodextrins as chiral additives. *Electrophoresis* **19,** 2834–2840.
55. De Boer. T., De Zeeuw, R. A., De Jong, G. J, and Ensing, K. (2000) Recent innovations in the use of charged cyclodextrins in capillary electrophoresis for chiral separations in pharmaceutical analysis. *Electrophoresis* **21,** 3220–3239.
56. Zhou, L., Thompson, R., Song, S., Ellison, D., and Wyvratt, J. M. (2002) A strategic approach to the development of capillary electrophoresis chiral methods for pharmaceutical basic compounds using sulfated cyclodextrins. *J. Pharm. Biomed. Anal*. **27,** 541–553.
57. Lin, X., Zhu, C., and Hao, A. (2004) Enantiomeric separations of some acidic compounds with cationic cyclodextrin by capillary electrophoresis. *Anal. Chim. Acta* **517,** 95–101.
58. Busby, B. M., Maldonado, O., and Vigh, G. (2003) Electrophoretic enantiomer separations at high pH using the new, single-isomer octakis (2,3-dimethyl-6-O-sulfo)- -cyclodextrin as chiral resolving agent. *J. Chromatogr. A* **990,** 63–73.
59. Jira, T., Bunke, A., and Karbaum, A. (1998) Use of chiral and achiral ion-pairing reagents in combination with cyclodextrins in capillary electrophoresis. *J. Chromatogr. A* **798,** 281–288.
60. Kuhn, R. (1999) Enantiomeric separation by capillary electrophoresis using a crown ether as chiral selector. *Electrophoresis* **20,** 2605–2613.
61. Ivanyi, T., Pál, K., Lázár, I., Massart, D. L., and Vander Heyden, Y. (2004) Application of tetraoxadiaza-crown ether derivatives as chiral selector modifiers in capillary electrophoresis. *J. Chromatogr. A* **1028,** 325–332.
62. Thanh Ha, P. T., Van Schepdael, A., Roets, E., and Hoogmartens, J. (2004) Investigating the potential of erythromycin and derivatives as chiral selector in capillary electrophoresis. *J. Pharm. Biomed. Anal*. **34,** 861–870.

63. D'Hulst, A. and Verbeke, N. (1996) Chiral analysis of basic drugs by oligosaccharide-mediated capillary electrophoresis *J. Chromatogr. A* **735,** 283–293.
64. D'Hulst, A. and Verbeke, N. (1994) Quantitation in Chiral Capillary Electrophoresis-Theoretical and Practical considerations. *Electrophoresis* **15,** 854–863.
65. Fanali, S. (1997) Controlling enantioselectivity in chiral capillary electrophoresis with inclusion–complexation. *J. Chromatogr. A* **792,** 227–267.
66. Haginaka, J. (2000) Enantiomer separation of drugs by capillary electrophoresis using proteins as chiral selectors. *J. Chromatogr. A* **875,** 235–254.
67. Terabe, S., Shibata, M., and Miyashita, Y. J. (1989) Chiral separation by electronkinetic chromatography while bile salt micelles. *J. Chromatogr. A* **480,** 403–411.
68. Dobashi, A., Ono, T., Hara, S., and Yamaguchi, J. (1989) Optical resolution of enantiomers with chiral mixed micelles by electrokinetic chromatography. *Anal. Chem*. **61,** 1984–1986.
69. Tickle, D. C., Okafo, G. N., Camilleri, P., Jones, R. F. D., and Kirby, J. (1994) Glucopyranoside-based surfactants as pseudostationary phases for chiral separations in capillary electrophoresis. *Anal. Chem*. **66,** 4121–4126.
70. Grego, A. L. and Garcia, M. L. (2000) Enantiomeric separation of chiral polychlorinated biphenyls by micellar electrokinetic chromatography using mixtures of bile salts and sodium dodecyl sulphate with and without -cyclodextrin in the separation buffer *J. Microcol. Sep*. **12,** 33–40.
71. Mertzman, M. D. and Foley, J. R. (2004) Effect of oil substitution in chiral microemulsion electrokinetic chromatography. *Electrophoresis* **25,** 723–732.
72. Pascoe, R. and Foley, J. (2002) Rapid separation of pharmaceutical enantiomers using electrokinetic chromatography with a novel chiral microemulsion. *Analyst* **127,** 710–714.
73. Aiken, J. H. and Huie, C.W. (1993) Use of a Microemulsion system to incorporate a lipophilic chiral selector in Electrokinetic Capillary Chromatography. *Chromatographia* **35,** 448–450.
74. Mertzman, M. D. and Foley, J. P. (2004) Chiral cyclodextrin-modified microemulsion electrokinetic chromatography. *Electrophoresis* **25,** 1188–1200.
75. McCorquodale, M. E., Boutrid, H., and Colyer, C. L. (2003) Enantiomeric separation of N'-nitrosonornictine by capillary electrophoresis. *Anal. Chim. Acta* **496,** 177–184.
76. Blanco, M. and Valverde, I. (2003) Chiral and non chiral determination of Dopa by capillary electrophoresis *J. Pharm. Biomed. Anal*. **31,** 431–438.
77. Singer-van de Griend, C., Wahlstrom, H., Groningsson, K., and Widahl-Nasman, M. (1997) A chiral capillary electrophoresis method for ropivacaine hydrochloride in pharmaceutical formulations: validation and comparison with chiral liquid chromatography. *J. Pharm. Biomed. Anal*. **15,** 1051–1061.
78. Wikstrorm, H. and Owens, K. P. (2002) Development and validation of a chiral capillary electrophoresis method for melagatran and ximelagatran drug substances. *J. Sep. Sci*. **25,** 1167–1174.

79. Kuo, C. Y., Wu, H. L., and Wu, S. M. (2002) Enantiomeric analysis of methotrexate in pharmaceuticals by cyclodextrin-modified capillary electrophoresis. *Anal. Chim. Acta* **471,** 211–217.
80. Jimidar, M., Van Ael, W., De Smet, M., and Cockaerts, P. (2002) Method validation and robustness testing of an enantioselective CE method for chemical quality control. *LCGC Eur*. **15,** 230–243.
81. Song. S., Zhou, L., Thompson, R., Yang, M., Ellison, D., and Wyvratt, J. M. (2002) Comparison of capillary electrophoresis and reversed-phase liquid chromatography for determination of the enantiomeric purity of an M3 antagonist. *J. Chromatogr. A* **959,** 299–308.
82. Miller, J. H. McB., and Rose, U. (2001) Comparison of chiral liquid chromatographic methods and capillary electrophesis separation of the enantiomers of ephedrine hydrochloride. *Pharmeuropa* **13,** 3.
83. Zhang, B., Krull, I. S., Cohen, A., et al. (2004) Separation of quaternary ammonium diastereomeric oligomers by capillary electrophoresis. *J. Chromatogr. A* **1034,** 213–220.
84. Chankvetadze, B., Burjanadze, N., and Blaschke, G. (2003) Enantioseparation of erythro-mefloquine and its analogues in capillary electrophoresis. *J. Pharm. Biomed. Anal*. **32,** 41–49.
85. Guo, l., Lin, S. J., Yang, Y. F., Qi, L., Wang, M. X, and Chen, Y. (2003) Fast enantioseparation of arylglycine amides by capillary electrophoresis with highly sulfated- -cyclodextrin as a chiral selector. *J. Chromatogr. A* **998,** 221–228.
86. Gomez-Gomar, A., Ortega, E., Calvet, C., Andaluz, B., Merce, R., and Frigola, J. (2003) Enantioseparation of basic pharmaceutical compounds by capillary electrophoresis using sulphated cyclodextrins. *J. Chromatogr. A* **990,** 91–98.
87. Lipka, E., Selouane, A., Postel, D., et al. (2004) Enantioseparation of four cis and trans diastereomers of 2′, 3′-didehydro-2′, 3′-dideoxythymidine analogs, by high-performance liquid chromatography and capillary electrophoresis *J. Chromatogr. A* **1034,** 161–167.
88. Liau, A. S., Liu, J. T., Lin, L. C., et al. (2003) Optimisation of a simple method for chiral separation of methamphetamine and related compounds in clandestine tablets and urine samples by β-cyclodextrine modified capillary electrophoresis: acomplementary method to GC-MS. *Forensic Sci. Int*. **134,** 17–24.
89. Ferrara, G., Santagati, N. A., Aturki, Z., and Fanali, S. (1999) Optical isomer separation of potential analgesic drug candidates by using capillary electrophoresis. *Electrophoresis* **20,** 2432–2437.
90. Fillet, M., Fotsing, L., Bonnard, J., and Crommen, J. (1998) Stereoselective determination of S-naproxen in tablets by capillary electrophoresis. *J. Pharm. Biomed. Anal*. **18,** 799–805.
91. Timerbaev, A. R. (2002) Recent advances and trends in capillary electrophoresis of inorganic ions. *Electrophoresis* **23,** 3884–3906.
92. Fritz, S. (2000) Recent developments in the separation of inorganic and small organic ions by capillary electrophoresis. *J. Chromatogr. A* **884,** 261–275.

93. Wienen, F. and Holzgrabe, U. (2003) A new micellar electrokinetic capillary chromatography method for separation of the components of the aminoglycoside antibiotics. *Electrophoresis* **24,** 2948–2957.
94. Fabre, H., Blanchin, M. D., and Bosc, N. (1999) Capillary electrophoresis for the determination of bromide, chloride and sulfate as impurities in calcium acamprosate. *Anal. Chim. Acta* **381,** 29–37.
95. Hettiarachchi, K., Ridge, S., Thomas, D. W., Olson, L., Obi, C. R., and Singh, D. (2001) Characterization and analysis of biphalin: an opioid peptide with a palindromic sequence. *J. Peptide Res*. **57,** 151.
96. Zhou, L. and Dovletoglou, A. (1997) Practical capillary electrophoresis method for the quantitation of the acetate counter-ion in a novel antifungal lipopeptide. *J. Chromatogr. A* **763,** 279–284.
97. Chen, D., Klopchin, P., Parsons, J., and Srivatsa, G. S. (1997) Determination of sodium acetate in antisense oligonucleotides by capillary zone electrophoresis. *J. Liq. Chrom. Rel. Tech*. **20,** 1185–1195.
98. Altria, K. D., Goodall, D. M., and Rogan, M. M. (1994) Quantitative-determination of drug counterion stoichiometry by capillary electrophoresis. *Chromatographia* **38,** 637–642.
99. Altria, K. D., Assi, K. H., Bryant, S. M., and Clark, B. J. (1997) Determination of organic acid drug counter-ions by capillary electrophoresis. *Chromatographia* **44,** 367–371.
100. Nair, J. B. and Izzo, C. G. (1997) Anion screening for drugs and intermediates by capillary ion electrophoresis. *J. Chromatogr. A* **640,** 445–461.
101. Stålberg, O., Sander, K., Singer-van de Griend, C. (2002) The determination of bromide in a local anaesthetic hydrochloride by capillary electrophoresis using direct UV detection. *J. Chromatogr. A* **977,** 265–275.
102. Assi, K., Clark, B., and Altria, K. D. (1997) Simultaneous determination of basic drugs and their acidic counter-ions by capillary electrophoresis. *Pharm. Sci*. **3,** 593–596.
103. Malsch, R. and Harenberg, J. (1996) Purity of glycosaminoglycan-related compounds using capillary electrophoresis. *Electrophoresis* **17,** 401–405.
104. Fabre, H., Blanchin, M. D., Julien, E., Segonds, C., Mandrou, B., and Bosc, N. (1997) Validation of a capillary electrophoresis procedure for the determination of calcium in calcium acamprosate. *J. Chromatogr. A* **772,** 265–269.
105. Filbey, S. D. and Altria, K. D. (1994) Robustness testing of a capillary electrophoresis method for the determination of potassium content in the potassium salt of an acidic drug. *J. Capillary Electrophor*. **1,** 190–195.
106. Altria, K. D., Clayton, N. G., Harden, R. C., Makwana, J. V., and Portsmouth, M. J. (1995) Inter-company cross-validation exercise on capillary electrophoresis—quantitative-determination of drug counterion level. *Chromatographia* **40,** 47–50.
107. Johnson, B. D., Grinberg, N., Bicker, G., and Ellison, D. (1997) The quantitation of a residual quaternary amine in bulk drug and process streams using capillary electrophoresis. *J. Liq. Chrom. Rel. Tech*. **20,** 257–272.

108. Williams, R. C. and Boucher, R. J. (2000) Analysis of potassium counter ion and inorganic cation impurities in pharmaceutical drug substance by capillary electrophoresis with conductivity detection. *J.Pharm. Biomed. Anal*. **22,** 115–122.
109. Bechet, I., Fillet, M., Hubert, Ph., and Crommen, J. (1995) Quantitative analysis of non-steroidal anti-inflammatory drugs by capillary zone electrophoresis. *J.Pharm. Biomed. Anal*. **13,** 497–503.
110. Fujiwara, S. and Honda, S. (1987) Determination of ingredients of antipyretic analgesic preparations by micellar electrokinetic capillary chromatography. *Anal. Chem*. **59,** 2773–2776.
111. Ong, C. P., Ng, C. L., Lee, H. K., and Li, S. F. Y. (1991) Determination of antihistamines in pharmaceuticals by capillary electrophoresis. *J. Chromatogr. A* **588,** 335–339.
112. Bechet, I., Fillet, M., Hubert, P., and Crommen, J. (1994) determination of benzodiazepines by micellar electrokinetic chromatography. *Electrophoresis* **15,** 1316–1321
113. Dose, E. and Guiochon, G. (1991) Internal standardisation technique for capillary zone electrophoresis. *Anal. Chem*. **63,** 1154–1158.
114. Ross, A. G. (1995) Voltage pre-conditioning technique for optimisation of migration-time reproducibility in capillary electrophoresis. *J. Chromatogr. A* **718,** 444–447.
115. Altria, K. D. (2003) Enhanced pharmaceutical analysis by CE using dynamic surface coating system. *J. Pharm. Biomed. Anal*. **31,** 447–453.
116. Mayer, B. X. (2001) How to increase precision in capillary electrophoresis. *J. Chromatogr. A* **907,** 21–37.
117. Jamali, B. and Lehmann, S. (2004) Development and validation of a high-resolution capillary electrophoresis method for multi-analysis of ragaglitazar and arginine in Active Pharmaceutical Ingredients and low-dose tablets. *J. Pharm. Biomed. Anal*. **34,** 463–472.
118. Aurora Prado, M. S., Silva, C. A., Tavares, M. F., and Altria, K. D. (2004) Determination of folic acid in tablets by microemulsion electrokinetic chromatography. *J. Chromatogr. A* **1051,** 291–296.
119. Cifuentes, A., Diez-Masa, J. C., Montenegro, C., *et al*. (2000) Recombinant growth hormone delivery systems based on vinylpyrrolidone-hydroxyethyl methacrylate copolymer matrices: Monitoring optimization by capillary zone electrophoresis. *J. Biomater. Sci. Polym. Ed*. **11,** 993–1005.
120. Simó, C., Cifuentes, A., and Gallardo, A. (2003) Drug delivery systems: polymers and drugs monitored by capillary electromigration methods. *J. Chromatogr. B* **797,** 37–49.
121. Pajchel, G., Michalska, K., and Tyski, S. (2004) Application of capillary electrophoresis to the determination of various benzylpenicillin salts. *J. Chromatogr. A* **1032,** 265–272.
122. Michalska, K., Pajchel, G., and Tyski, S. (2004) Capillary electrophoresis method for simultaneous determination of penicillin G, procaine and dihydrostreptomycin in veterinary drugs. *J. Chromatogr. B* **800,** 203–209.

123. Aurora Prado, M. S., Kedor-Hackmann, E. R., Santoro, M. I., Pinto, T. J., and Tavares, M. F. (2004) Capillary electrophoretic method for determination of protease inhibitor indinavir sulfate used in human immunodeficiency virus therapy. *J. Pharm. Biomed. Anal*. **34,** 441–450.
124. Pérez-Ruiz, T., Martínez-Lozano, C., Sanz, A., and Bravo, E. (2004) Development and validation of a quantitative assay for raloxifene by capillary electrophoresis. *J. Pharm. Biomed. Anal*. **34,** 891–897.
125. Krcal, K., Tuncel, M., and Aboul-Enein, H. Y. (2004) Determination of pravastatin in tablets by capillary electrophoresis. *Farmaco* **59,** 241–244.
126. Velikinac, I., Cudina, O., Jankovic, I., Agbaba, D., and Vladimirov, S. (2004) Comparison of capillary zone electrophoresis and high performance liquid chromatography methods for quantitative determination of ketoconazole in drug formulations. *Farmaco* **59,** 419–424.
127. Mohammadi, A., Kanfer, I., and Walker, R. (2004) A capillary zone electrophoresis (CZE) method for the determination of cyclizine hydrochloride in tablets and suppositories. *J. Pharm. Biomed. Anal*. **35,** 233–239.
128. Hillaert, S., Snoeck, L., and Van den Bossche, W. (2004) Optimization and validation of a capillary zone electrophoretic method for the simultaneous analysis of four atypical antipsychotics. *J. Chromatogr. A* **1033,** 357–362.
129. Hillaert, S. and Van den Bossche. W. (2002) Optimization and validation of a capillary zone electrophoretic method for the analysis of several angiotensin-II-receptor antagonists. *J. Chromatogr. A*. **979,** 323–339.
130. Hillaert, S., De Beer, T. R., De Beer, J. O., and Van den Bossche, W. (2003) Optimization and validation of a micellar electrokinetic chromatographic method for the analysis of several angiotensin-II-receptor antagonists *J. Chromatogr. A* **984,** 135–146.
131. Vanhoenacker, G., de l'Escaille, F., De Keukeleire, D., and Sandra, P. (2002) Analysis of benzodiazepines in dynamically coated capillaries by CE-DAD, CE-MS and CE-MS2. *J. Pharm. Biomed. Anal*. **34,** 595–606.
132. Lurie, I. S., Hays, P. A., Garcia, A. E., and Panicker, S. (2004) Use of dynamically coated capillaries for the determination of heroin, basic impurities and adulterants with capillary electrophoresis. *J. Chromatogr. A* **1034,** 227–235.
133. Li, Y., Cui, S., Cheng, Y., Chen, X., and Hu, Z. (2004) Application of nonaqueous capillary electrophoresis for quantitative analysis of quinolizidine alkaloids in Chinese herbs. *Anal. Chim. Acta* **508,** 17–22.
134. Neubert, R. H., Mrestani, Y., Schwarz, M., and Colin, B. (1998) Application of micellar electrokinetic chromatography for analyzing antiviral drugs in pharmaceutical semisolid formulations. *J. Pharm. Biomed. Anal*. **16,** 893–897.
135. Altria, K. D. (1993) Determination of salbutamol-related impurities by capillary electrophoresis. *J. Chromatogr. A* **634,** 323.
136. Altria, K. D. and Fabre, H. (1995) Approaches to optimisation of precision in capillary electrophoresis. *Chromatographia* **40,** 313–320.

137. Emaldi, P., Fapanni, S., and Baldini, A. (1995) Validation of a capillary electrophoresis method for the determination of cephradine and its related impurities. *J. Chromatogr. A* **711,** 339.
138. Kelly, M. A., Altria, K. D., Grace, C., and Clark, B. J. (1998) Optimisation, validation and application of a capillary electrophoresis method for the determination of ranitidine hydrochloride and related substances. *J. Chromatogr. A* **798,** 297–306.
139. Sabbah, S. and Scriba, G. K. (2001) Development and validation of a capillary electrophoresis assay for the determination of 3,4-diaminopyridine and 4-aminopyridine including related substances. *J. Chromatogr. A* **907,** 321–328.
140. Fabre, H., Perrin, C., and Bosc, N. (1999) Determination of homotaurine as impurity in calcium acamprosate by capillary zone electrophoresis. *J. Chromatogr. A* **853,** 421–430.
141. Toro, I., Dulsat, J. F., Fabregas, J. L., and Claramunt, J. (2004) Development and validation of a capillary electrophoresis method with ultraviolet detection for the determination of the related substances in a pharmaceutical compound. *J. Chromatogr. A* **1043,** 303–315.
142. Gotti, R., Pomponio, R., Bertucci, C., and Cavrini, V. (2001) Determination of 5-aminosalicylic acid related impurities by micellar electrokinetic chromatography with an ion-pair reagent. *J. Chromatogr. A* **916,** 175–183.
143. Orlandini, S., Fanali, S., Furlanetto, S., Marras, A. M., and Pinzauti, S. (2004) Micellar electrokinetic chromatography for the simultaneous determination of ketorolac tromethamine and its impurities: Multivariate optimization and validation. *J. Chromatogr. A* **1032,** 253–263.
144. Kang, J. W., Van Schepdael, A., Roets, E., and Hoogmartens, J. (2001) Analysis of vancomycin and related impurities by micellar electrokinetic capillary chromatography. Method development and validation. *Electrophoresis* **22,** 2588–2592.
145. Owens, P. K., Wikström, H., Någård, S., and Karlsson, L. (2002) Development and validation of a capillary electrophoresis method for ximelagatran assay and related substance determination in drug substance and tablets. *J. Pharm. Biomed. Anal*. **27,** 587–598.
146. Hilder, E. F., Klampfl, C. W., Buchberger, W., and Haddad, P. R. (2002) Comparison of aqueous and nonaqueous carrier electrolytes for the separation of penicillin V and related substances by capillary electrophoresis with UV and mass spectrometric detection. *Electrophoresis* **23,** 414–420.
147. Jaworska, M., Szulinska, G., Wilk, M., and Tautt, J. (1999) Capillary electrophoretic separation of N-acetylcysteine and its impurities as a method for quality control of pharmaceuticals. *J. Chromatogr. A* **853,** 479–485.
148. Michalska, K., Pajchel, G., and Tyski, S. (2004) Determination of ciprofloxacin and its impurities by capillary zone electrophoresis. *J. Chromatogr. A* **1051,** 267–272.
149. Gil, E. C., Dehouck, P., Van Schepdael, A., Roets, E., and Hoogmartens, J. (2001) Analysis of metacycline by capillary electrophoresis. *Electrophoresis* **22,** 497–502.

150. Ferandez, H., Ruperez, F. J., and Barbas, C. (2003) Capillary electrophoresis determination of loratadine and related impurities. *J. Pharm. Biomed. Anal*. **31,** 499–506.
151. Kang, J. W., Van Schepdael, A., Roets, E., and Hoogmartens, J. (2001) Analysis of vancomycin and related impurities by micellar electrokinetic capillary chromatography. Method development and validation. *Electrophoresis* **20,** 2588–2592.
152. Kibbey, C. E., Poole, S. K., Robinson, B., Jackson, J. D., and Durham, D. (2001) An integrated process for measuring the physicochemical properties of drug candidates in preclinical discovery environment. *J. Pharm. Sci*. **90,** 1164–1175.
153. Mahuzier, P. E., Aurora Prado, M. S., Clark, B. J., Kedor-Hackmann E. R., and Altria, K.D. (2003) An introduction to the theory and application of microemulsion electrokinetic chromatography. *LCGC Europe* **16,** 22–29.
154. Chen, N., Zhang, Y., Terabe, S., and Nakagawa, T. (1994) Effect of physicochemical properties and molecular structure on the micelle—water partition coefficient in micellar electrokinetic chromatography. *J. Chromatogr. A* **678,** 327–332.
155. Yang, S., Bumgarner, J. G., Kruk, L. F., and Khaledi, M. G. (1996) Quantitative structure-activity relationships studies with micellar electrokinetic chromatography influence of surfactant type and mixed micelles on estimation of hydrophobicity and bioavailability. *J. Chromatogr. A* **721,** 323–335
156. Herbert, B. J. and Dorsey, J. G. (1995) Octanol-water partition coefficient estimation by micellar electrokinetic chromatography. *Anal. Chem*. **67,** 744–749.
157. Ishihama, Y., Oda, Y., Uchikawa, K., and Asakawa, N. (1995) Evaluation of solute hydrophobicity by microemulsion electrokinetic chromatography. *Anal. Chem*. **67,** 1588–1595.
158. Oestergard, J., Hansen, S., Larsen, C., Schou, C., and Heegard, N. (2003) Determination of octanol-water partition coefficients for carbonate esters and other small organic molecules by microemulsion electrokinetic chromatography. *Electrophoresis* **24,** 1038–1046.
159. Ishihama, Y., Oda, Y., and Asakawa, N. (1996) A hydrophobicity scale based on the migration index from microemulsion electrokinetic chromatography of anionic solutes *Anal. Chem*. **68,** 1028–1032.
160. Altria, K. D. (2000) Background theory and applications of microemulsion electrokinetic chromatography. *J. Chromatogr. A* **892,** 171–186.
161. Wehmeyer, K., Tu, J., Jin, Y., et al.(2003) The application of multiplexed MEEKC for the rapid determination of log Pow values for neutral and basic compounds. *LCGC N. America* **21,** 1078–1088.
162. Gluck, S. J., Cleveland, Jr., J. A. (1994) Capillary zone electrophoresis for the determination of dissociation constants. *J. Chromatogr. A* **680,** 43–48.
163. Gluck, S. J., Cleveland, Jr., J. A. (1994) Investigation of experimental approaches to the determination of pKa values by capillary. *J. Chromatogr. A* **680,** 49–56.
164. Bellini, S., Uhrová, M., and Deyl, Z. (1997) Determination of the thermodynamic equilibrium constants of water-insoluble (sparingly soluble) compounds by capillary electrophoresis. *J. Chromatogr. A*. **772,** 91–101.

165. Jia, Z. J., Ramstad, T., and Zhong, M. (2001) Medium-throughput pKa screening of pharmaceuticals by pressure-assisted capillary electrophoresis. *Electrophoresis* **22,** 1112–1118.
166. Wan, H., Holmén, A., Någård, M., and Lindberg, W. (2002) Rapid screening of pKa values of pharmaceuticals by pressure-assisted capillary electrophoresis combined with short-end injection. *J. Chromatogr. A* **979,** 369–377.
167. Örnskov, E., Linusson, A., and Folestad, S. (2003) Determination of dissociation constants of labile drug compounds by capillary electrophoresis. *J. Pharm. Biomed. Anal*. **33,** 379–391.
168. Beckers, J. L., Everaerts, F. M., and Ackermans, M. T. (1991) Determination of absolute mobilities, pK values and separation numbers by capillary zone electrophoresis: effective mobility as a parameter for screening. *J. Chromatogr. A* **537,** 407–428.
169. Cleveland, Jr., J. A., Martin, C. L., and Gluck, S. J. (1994) Spectrophotometric determination of ionization constants by capillary zone electrophoresis. *J. Chromatogr. A* **679,** 167–171.
170. Gluck, S. J., Steele, K. P., Benkö, M. H. (1996) Determination of acidity constants of monoprotic and diprotic acids by capillary electrophoresis. *J. Chromatogr. A* **745,** 117–125.
171. Caliaro, G. A. and Herbots, C. A. (2001) Determination of pKa values of basic new drug substances by CE. *J. Pharm. Biomed. Anal*. **26,** 427–434.
172. Matoga, M., Laborde-Kummer, E., Langlois, M. H., *et al*. (2003) Determination of pKa values of 2-amino-2-oxazolines by capillary electrophoresis. *J. Chromatogr. A* **984,** 253–260.
173. Mrestani, Y., Neubert, R., Munk, A., and Wiese, M. (1998) Determination of dissociation constants of cephalosporins by capillary zone electrophoresis. *J. Chromatogr. A* **803,** 273–278.
174. Cleveland, Jr., J. A., Benko, M. H., Gluck, S. J., and Walbroehl, Y. M. (1993) Automated pKa determination at low solute concentrations by capillary electrophoresis. *J. Chromatogr. A* **652,** 301–308.
175. Takacs-Novak, K., Box, K. J., and Avdeef, A. (1997) Potentiometric pKa determination of water-insoluble compounds: validation study in methanol/water mixtures. *Int. J. Pharm.* **151,** 235–248.
176. Poole, S. K., Patel, S., Dehring, K., Workman, H., and Poole, C. F. (2004) Determination of acid dissociation constants by capillary electrophoresis. *J. Chromatogr. A* **1037,** 445–454.
177. Jankowsky, R., Friebe, M., Noll, B., and Johannsen, B. (1999) Determination of dissociation constants of 99mTechnetium radiopharmaceuticals by capillary electrophoresis. *J. Chromatogr. A* **833,** 83–96.
178. Porras, S. P. and Kenndler, E. (2004) Capillary zone electrophoresis in non-aqueous solutions: pH of the background electrolyte. *J. Chromatogr. A* **1037,** 455–465.
179. Hu, Q., Hu, G., Zhou, T., and Fang, Y. (2003) Determination of dissociation constants of anthrocycline by capillary zone electrophoresis with amperometric detection. *J. Pharm. Biomed. Anal*. **31,** 679.

180. Barták, P., Bednár, P., Stránsky, Z., Bocek, P., Vespalec, R. (2000) Determination of dissociation constants of cytokinins by capillary zone electrophoresis. *J. Chromatogr. A* **878,** 249–259.
181. Cao, J. and Cross, R. F. (1995) The separation of dihydrofolate reductase inhibitors and the determination of pKa,1 values by capillary zone electrophoresis. *J. Chromatogr. A* **695,** 297–308.
182. Jimenez-Lozano, E., Marques, I., Barron, D., Beltran, J. L., and Barbosa, J. (2002) Determination of pK(a) values of quinolones from mobility and spectroscopic data obtained by capillary electrophoresis and a diode array detector. *Anal. Chim. Acta* **464,** 37–45.
183. Coufal, P., Stulik, K., Claessens, H. A., Hardy, M. J., and Webb, M. (1998) Determination of the dissociation constants of ropinirole and some impurities and their quantification using capillary zone electrophoresis. *J. Chromatogr. B* **720,** 197–204.
184. Buckenmaier, S. M., McCalley, D. V., and Euerby, M. R. (2004) Determination of ionisation constants of organic bases in aqueous methanol solutions using capillary electrophoresis. *J. Chromatogr. A* **1026,** 251–259.
185. Foulon, C., Danel, C., Vaccher, C., Yous, S., Bonte, J. -P., and Goossens, J. -F. (2004) Determination of ionization constants of N-imidazole derivatives, aromatase inhibitors, using capillary electrophoresis and influence of substituents on pKa shifts. *J. Chromatogr. A* **1035,** 131–136.

11

Capillary Electrophoresis of Neutral Carbohydrates

Mono-, Oligosaccharides, and Glycosides

Cristiana Campa and Marco Rossi

Summary

This chapter reports an overview of the recent advances in the analysis of neutral sugars by capillary electrophoresis (CE); furthermore, some relevant reviews and research articles in the field are tabulated. Comparison of CE with chromatography is also presented, with special attention to separation efficiency and sensitivity. The main routes aimed at pretreatment and CE analysis of uncharged mono-, oligosaccharides, and glycosides are described. Representative examples of such procedures are reported in detail, upon describing robust methodologies for the study of (1) neutral mono- and oligosaccharides derivatized by reductive amination and by formation of glycosylamines; (2) underivatized mono- and di-saccharides analyzed using highly alkaline buffers; and (3) anomeric couples of glycosides separated using borate-based buffers.

Key Words: Capillary electrophoresis; neutral sugars; glycosides; monosaccharides; oligosaccharides; alditols; reductive amination; glycosylamines; tabulated review.

1. Introduction

Carbohydrates are the most abundant organic compounds in nature. According to the published IUPAC Recommendations ***(1)***, the term "carbohydrate" includes monosaccharides, oligosaccharides, and polysaccharides, as well as substances derived from monosaccharides by reduction of the carbonyl group (alditols) by oxidation of one or more terminal groups to carboxylic acids, or by the replacement of one or more hydroxyl group(s) by a hydrogen atom, an amino group, a thiol group, or similar heteroatomic groups. It also includes derivatives of these compounds. The term "sugar" is frequently applied to monosaccharides and lower oligosaccharides. Carbohydrates can

From: *Methods in Molecular Biology, vol. 384: Capillary Electrophoresis*
Edited by: P. Schmitt-Kopplin © Humana Press Inc., Totowa, NJ

also be linked to noncarbohydrate natural products (such as proteins or lipids), giving rise to the so-called glycoconjugates. Characterization of carbohydrates is a fundamental tool for a full understanding of their numerous functions: besides their structural relevance in plants and invertebrates, they play a key role in molecular recognition events, acting as highly specific receptors or as antigens ***(2,3)***; structural elucidation of carbohydrates therefore has potential in the biomedical and pharmaceutical fields for the design of new and specific diagnostic and therapeutic tools. Analysis of carbohydrates requires the use of highly sensitive and selective techniques, because these compounds often constitute highly complex mixtures, which can have a wide distribution of branching patterns, positions and substitutions of hydroxyl groups, and α- or β-anomericity of the glycosidic linkages. For instance, two identical monosaccharides can potentially give rise to eleven disaccharides, whereas two identical amino acids can originate only one dipeptide.

This chapter will focus on the analysis of neutral sugars by capillary electrophoresis (CE), with special attention to mono-, oligo-saccharides and glycosides. In order to better clarify the advantages introduced by CE, emergent chromatographic approaches that can be successfully used for complex mixtures of carbohydrates will be briefly introduced ***(4–24)***. Among the liquid chromatographic techniques, anion-exchange chromatography with pulsed amperometric detection (HPAEC-PAD) deserves a special mention, as it provides selective separation and sensitive detection without the need of derivatization ***(8–16)***. This technique exploits the weak acidity of sugars and alditols for their anion-exchange chromatographic separation with highly alkaline eluents. Detection, which is based on the oxidation at gold electrodes, allows an unprecedented sensitivity for underivatized carbohydrates (100–250 times better than refractive index detector ***[4]***). One drawback of HPAEC-PAD for neutral monosaccharide analysis is the loss in resolution and irreproducibility of retention times due to the uptake of atmospheric carbon dioxide in the alkaline eluents, which can only be prevented by suitable modification of the mobile phase with alkaline-earth cations forming poorly soluble carbonate salts ***(11,12)*** or by extensive washes of the column with concentrated sodium hydroxide. Moreover, detector response must be optimized upon changing the eluent additives and also depends on the size and nature of the sugars ***(13)***.

CE provides several benefits, which are partially counterbalanced by some drawbacks with respect to chromatographic techniques. Such aspects make these methodologies complementary, as demonstrated in various comparative studies ***(13,25–30)***. Like HPLC, CE is particularly suited for the characterization of isomeric complex mixtures, but the volume of sample required for the analysis is much lower (typically, it is decreased by three orders of magnitude). Moreover, the resolving power of CE is generally higher and

analyses take place in a shorter time. It may be claimed that this is also a feature typical of micro-HPLC; in CE, however, a less extensive clean-up of samples is required with respect to HPLC, because no column fouling can take place; moreover, post-run washes are much shorter, because nonrelevant compounds from the matrix can be simply flushed out. A few milliliters of buffer are necessary to run a separation, and no changes of columns are required for different categories of carbohydrates. Moreover, CE makes it possible to analyze, together to carbohydrates, a wider range of nonsaccharidic compounds eventually present in the matrix ***(31–32)***. Such features make CE very suitable for the analysis of biological samples. On the other hand, ultraviolet (UV) detection sensitivity in on-capillary detection is limited by the small path length ***(33)***. The use of electrochemical detection is advised in such cases, because it is independent of path lengths, allowing typical limits of detection equal to 10^{-8} *M* without derivatization ***(34–36)***. Alternatively, the sensitivity drawback can be overcome upon using pre-concentration techniques ***(37,38)*** and/or upon suitable derivatization of the saccharidic compounds with fluorescent labels. Commercially available detectors based on laser-induced fluorescence (LIF) allow narrow focusing of excitation light onto capillaries, leading to extremely low detection limits, typically equal to 10^{-11} *M* ***(33)***. The use of CE for the analysis of neutral sugars and glycosides has been summarized in several books and excellent reviews (*see* **Table 1**) ***(4,25,33,39–52)***. To date, the main applications of CE for neutral mono- and oligosaccharides, glycosides, and alditols found in the literature include:

1. CE method developments aimed to improve resolution/sensitivity ***(53–79)***;
2. Mono- and oligosaccharide composition in glycoproteins ***(80–94)***;
3. Food and beverage analysis ***(27,28,31,32,35,95–104)***;
4. Pharmaceutical and clinical applications ***(18,105–110)***;
5. Plant extracts ***(71,111–126)***;
6. Polysaccharide hydrolysis mixtures ***(55,62,79,127–132)***;
7. Monitoring of reactions involving carbohydrates ***(133–138)***.

A selection of some relevant papers regarding these topics is reported in **Table 2**, where experimental details as well as specific applications are reported. Despite the well established use of CE for their characterization, neutral sugars are not structurally suitable to routine CE, because they are not easily ionizable. Moreover, they do not carry strong chromophoric groups, and this is a challenge for spectrophotometric detectors, which are the most widely used in CE. In the present chapter, we show the main routes that can be used to overcome these difficulties.

Table 1
Selected Reviews Reporting Capillary Electrophoresis (CE) Analysis of Neutral Sugars

Reference	Carbohydrate species	CE modes	Detection modes
33	Mono- and oligosaccharides from glycoconjugates and glycosaminoglycans Maltoheptaose Maltooligosaccharides Cyclodextrins Chitooligosaccharides Sialic acids	CZE MEKC	UV LIF ED RI TOA
41	Monosaccharides Amino sugar derivatives Glycoprotein oligosaccharides Polysaccharides Proteoglycans Sialic acids	CZE MEKC CITP CIEF	UV LIF RI ED MS
42	Flavonoid aglycone and glycosides, phenolic acids, Quinones, Coumarins, Alkaloids, Capsacinoids, Glucosinolates Polyamines, Monoterpenes, Diterpenes, Triterpenes, Phytoecdysteroids, Cardiac glycosides, Saponins	CZE MEKC	UV
43	Neutral carbohydrates Acidic carbohydrates	CZE MEKC	UV LIF

	N-acetylhexosamines Maltooligosaccharides with various DP *N*-acetylated-chitooligosaccharides Poly(galacturonic acid) hydrolyzed	Size-exclusion electrophoresis	ED
44	Mono- and oligosaccharides Intact and hydrolized glycoproteins, glycopeptides, glycosaminoglycans, pectins and hyaluronic acid Cyclodextrins	CZE CITP MEKC CIEF	UV ED LIF MS
45	Mono- and oligosaccharides Plant glycosides Uronic acids, glyconic acids Glycoconjugates Glycopeptides and glycoproteins Glycosaminoglycans Sialic acids	CZE MEKC CGE CIEF	UV LIF ED RI MS
46	Oligosaccharides from glycosaminoglycans *N*-acetylneuraminic acid polymers Acidic, neutral and amino sugars and sugar alcohols Oligosaccharides from lipopolysaccharides and glycoproteins Carrageenan polysaccharides unhydrolyzed	CZE MEKC CITP	UV ED Biosensors RI MS LIF

(Continued)

Table 1
(Continued)

Reference	Carbohydrate species	CE modes	Detection modes
47	Neutral and acidic carbohydrates from glycoconjugates such as glycoproteins, proteoglycans and gangliosides	CZE MEKC CGE	ED UV LIF RI Biosensors
48	Simple sugars (mono- to tetrasaccharides) Sugar derivatives (Alditols, Glucosamines, Sugar acids) Polysaccharides Sugar conjugates (Glycopeptides, aminoglycosides)	CZE	ED
49	*N*-linked oligosaccharides released from glycoproteins	Paper electrophoresis CGE FACE CZE	LIF UV ED
52	Component monosaccharides in glycoconjugates Naturally occurring oligosaccharides Glycans in glycoproteins	CZE MEKC Ion-interaction	UV ED MS

Unsatured oligosaccharides derived from proteoglycans Oligosaccharides in glycolipids Plant oligosaccharides	electrokinetic chromatography Size exclusion electrophoresis Affinity electrophoresis Hydrogen bonding formation electrophoresis

2-ABA, 2-aminobenzoic acid; 3-ABA, 3-aminobenzoic acid; 4-ABA, 4-aminobenzoic acid; 4-ABN, 4-aminobenzonitrile; All, allose; Alt, altrose; 2,6-ANS, 2-anilinonaphtalene-6-sulfonic acid; ANTS, 8-aminonaphtalene-1,3,6-trisulfonic acid; APTS, 1-aminopyrene-3,6,8-trisulfonate; Ara, arabinose; BCDC, N-benzylcinchonidium chloride; BGE, background electrolyte; BHZ, p-hydrazine-benzenesulfonic acid; CBQCA, 3-(4-carboxybenzoyl)2-quinoline-carboxyaldehyde; CCD, contactless conductivity detection; Cell, cellobiose; CGE, capillary gel electrophoresis; CIEF, capillary isoelectric focusing; CITP, capillary isotachophoresis; CTAB, cetyltrimethylammonium bromide; CTAH, cetyltrimethylammonium hydroxide; CZE, capillary zone electrophoresis; DEA, diethylamine; DNBA, 3,5-dinitrobenzoic acid; d-Rib, 2-Deoxyribose; ED, electrochemical detection; ESI-MS, electrospray ionization-mass spectrometry detector; FACE, fluorophoreassisted carbohydrates electrophoresis; Fru, fructose; Fuc, fucose; Gal, galactose; GalA, galacturonic acid; GalN, galactosamine; GalNAc, *N*-Acetylgalactosamine; Glc, glucose; GlcA, glucuronic acid; GlcN, glucosamine; GlcNAc, *N*-Acetylglucosamine; Gul, gulose; HDB, hexadimethrine bromide; HPAEC, high performance anion-exchange chromatography; Ido, idose; Lac, lactose; LIF, laser-induced fluorescence; LOD, limit of detection; Lyx, lyxose; MALDI-TOF, matrix-assisted laser desorption/ionization-time of flight-mass spectrometry detector; Man, mannose; MEKC, micellar electrokinetic capillary chromatography; MS, mass spectrometry detector; n.a., not available; NAA, 1-naphthylacetic acid; NACE, non aqueous capillary electrophoresis; Neu5Ac, *N*-Acetylneuraminic acid; PAD, pulsed amperometric detection; PAGE, polyacrilamide gel electrophoresis; PDC, 2,6-pyridinedicarboxylic acid; PEG, polyethylene glycol; PF-MEKC, partial filling MEKC; PMP, 1-phenyl-3-methyl-2-pyrazolin-5-one; PNP, p-nitrophenol; Rha, rhamnose; RI, refractive index detector; Rib, ribose; RT, room temperature; S/N, signal/noise ratio; SDS, sodium dodecyl sulfate; std, standard; Tag, tagatose; Tal, talose; TBAB, tetra-butylammonium bromide; TEA, triethylamine; TFA, trifluoroacetic acid; TOA, thermooptical absorbance; UV, ultraviolet detector; Xyl, xylose.

Table 2
Selected Articles Reporting Capillary Electrophoresis (CE) Analysis of Neutral Sugars

Ref.	Carbohydrate species	Matrix	Derivatizing agent	CE mode	Capillary; T	Buffer, Voltage	Detection mode	LOD	Results
27	Sucrose, Glc and Fru	Orange, apple and grape juice. Sugar std	None	CZE	Fused silica (**1.** $L = 42$ cm; $l = 35$ cm; ID = 50 μm; **2.** $L = 90$ cm; $l = 83$ cm; ID = 50 μm) T = 15 °C	6 m*M* potassium sorbate pH 12.2–12.3; 230 V/cm^{-1} Outlet: cathode	Indirect UV (256 nm)	CZE: sucrose: 0. 29 m*M*; Glc: 0.23 m*M*; Fru: 0.24 m*M* HPAEC: sucrose: 0.58 μM; Glc: 1.11 μM; Fru: 1.11 μM	• The CZE method showed a 10–20-fold increase in separation efficiency compared with the HPAEC-PAD method. • In order to increase the dissociation and improve the resolution of the sugars, it is best to choose low temperature and high pH.
31	Inorganic anions, organic acids, amino acids, carbohydrates, nucleotides, aromatic acids, alcohols,	Std and sea urchin and sake	None	CZE	Fused silica (L = 112.5 cm; l = 104 cm; ID = 50 μm) T = 15 °C	BGE: 20 m*M* 2,6-pyridinedicarboxylic acid (PDC) and 0.5 m*M* cetyltrimethylam-monium hydroxide (CTAH) pH 12.1; 30 kV Outlet: anode	Indirect UV (350 nm)	Anions and amino acids: range 6–12 mg/L; carbohydrates: range 23–37 mg/L	• More than 50 carbohydrates including acidic, neutral, and amino sugars, sugar alcohols and phosphorylated saccharides could be separated.

	phosphorylated saccharides, oxyhalides, metal oxoacids, metal-EDTA complexes, forensic anions, Good's buffers and herbicides								• Maltooligosaccharides higher than maltotriose comigrated at the same time and the separation is not sufficient by this method.
54	Underivatized compounds: **1.** D-Xyl, D-Ara, D-Rib, D-Glc, D-Gal, L-Fuc, D-Man, D-Fru, D-GlcNAc, D-GalNAc, Gentiobiose, Lac, Maltose, Cell, Sucrose, Maltotriose, Raffinose, Stachyose, Maltotetraose, Trehalose, L-Sorbose,	Std mixtures	None	CZE	**1., 2., 3.** Fused silica (L = 94 cm; l = 87 cm; ID = 75 μm); temperature comprised between 20 °C and 60 °C **4.** Fused silica (L = 58 cm; l = 54 cm; ID := 75 μm) T = 20 °C	**1., 2., 3.** 50–60 mM tetraborate, pH 9.3; 20 kV; **4.** 50, 100, 150, 200 mM boric acid, pH 10.0; 20 kV Outlet: cathode	UV (195 nm)	n.a.	• Complexation with borate results in an increase of the sugars absorbance at 195 nm. • Resolution and efficiency is improved by performing the CE separation at high temperatures up to 60 °C. • CE analysis of a hexapeptide

(Continued)

Table 2
(Continued)

Ref.	Carbohydrate species	Matrix	Derivatizing agent	CE mode	Capillary; T	Buffer, Voltage	Detection mode	LOD	Results
	2. Polyols: Myo-inositol, Sorbitol **3.** Syalic acid, GlcA, GalA **4.** Glycosylated hexapeptide								containing glucose O-glycosydically bound to serine demonstrates that not only the open-chain glucose, but also its pyranose form can complex with borate.
56	**1.**, **2.** Ara, Rib, Gal, Glc, Lyx, Xyl and Man. **3.**: component monosaccharides commonly found in glycoproteins: Gal, Man, Fuc, GalNAc, GlcNAc	Std mixtures	PMP	CZE	**1.**, **3.**: Fused silica (L = 49 cm; l = 34 cm; ID = 50 μm) **2.** Fused silica (L = 53 cm; l = 38 cm : ID = 50 μm)	**1.** 100 m*M* sodium acetate or potassium acetate or ammonium acetate; 10 kV **1a.** 20 m*M* calcium acetate, 2 h, 7 h, 12 h after changing the carrier from **1.** **2.** 20–100 m*M* calcium acetate 13 h after changing the carrier from **1.** 100 m*M* barium acetate or 100 m*M* strontium acetate **3.** 100 m*M* barium acetate **1.**, **3.**: Outlet: cathode; **2.**: Outlet: anode	UV (245 nm)	n.a.	• The direction of electro-osmotic flow was the reverse of that observed for ordinary carriers not containing alkaline earth metal ions. • The order of mobility for the derivatives of aldopentose isomers was different from that observed in borate buffer, suggesting formation of different types of complexes.

									• The barium salt-containing carrier gave sharper peaks and better separation; the strontium salt-containing carrier also gave good separation but longer migration times.
62	Glc, Maltose and linear malto-oligosaccharides (with up to 40 Glc residues)	Starch hydrolysis mixture; Dextrin 15; Maltrin M040	ANTS	CZE	Fused silica (**1.** $L =$ 27 cm; $l =$ 20 cm; ID = 50 μm; **2.** $L =$ 37 cm; $l =$ 30 cm; ID = 50 μm; **3a.** $L =$ 47 cm; $l =$ 40 cm; ID = 20 μm; **3b.** $L =$ 67 cm;	**1a.** 50 m*M* phosphate at pH 2.5; 15 kV (25 °C) **1b.** 30 m*M* phosphate at pH 2.5; 17 kV (50 °C) **1c.** 50 m*M* sodium/ triethylammonium phosphate pH 2.5 containing 10.8 m*M* triethylamine (TEA) **2.** 50 m*M* phosphate at pH 9.0; 17 kV **3.** 200 m*M* phosphate at pH 2.0; **a.** 30 kV;	UV (214 nm) and LIF (λ_{EXC}: 325 nm; λ_{EM}: 525 nm)	n.a.	• Optimal resolution of higher oligomers obtained by using low-pH buffers. • The addition of triethylamine in the background electrolyte improved reproducibility and resolution.

(Continued)

Table 2
(Continued)

Ref.	Carbohydrate species	Matrix	Derivatizing agent	CE mode	Capillary; T	Buffer, Voltage	Detection mode	LOD	Results
					l=60 cm; ID = 20 μm;) T = 25 °C	**b**. 15 kV Buffers at pH 9.0 and 9.4: outlet: cathode Buffers at pH 2.0 and 2.5:outlet: anode			• The mobility of malto-oligosaccharides conjugates was a linear function of the molecular mass to the negative two-thirds power (buffer at pH 2.5). • Mobility of ANTS-derivatized malto-oligosaccharides is higher than the mobility observed in PAGE (factor: 22) and in CGE of 3-(4-carboxybenzoyl)2-quinoline-carboxyaldehyde (CBQCA)-derivatized malto-oligosaccharides (factor: 6).

63	**1**. Neutral mono-, di- and trisaccharides (Maltotriose, Maltose, Lac, L-Rha, D-Lyx, D-Xyl, Cell, Melibiose, L-Sorbose, D-Rib, D-Glc, D-Fru,D-Man, L-Ara, D-Fuc, D-Gal) **2**. Sugar acids (D-GlcA, D-GalA)	Std mixtures	4-ABN	CZE MEKC	CZE Fused silica (L=72 cm; l=50 cm; ID = 75 μm) MEKC Fused silica (**1**. $L = 80$ cm; $l = 60$ cm; ID = 50 μm; **2**. $L = 55$ cm; $l = 35$ cm; ID = 50 μm) T = 30 °C	CZE 175 m*M* borate, pH 10.5; 24 kV MEKC 25 m*M* tris-phosphate, 100 m*M* SDS, pH 7.5; 30 kV Outlet: cathode	UV (285 nm)	0.3 μM; 1 fmol, S/N 3	• Optimization of the reductive amination conditions. • 4-amino-benzonitrile allows the CZE separation of a larger number of sugars with respect to 2-aminobezonitrile. • MEKC vs RP-HPLC: MEKC provides the resolution of structurally similar carbohydrates; RP-HPLC only resolves carbohydrates belonging to different families. • MEKC is more efficient than CZE.

(Continued)

Table 2
(Continued)

Ref.	Carbohydrate species	Matrix	Derivatizing agent	CE mode	Capillary; T	Buffer, Voltage	Detection mode	LOD	Results
64	α-, β- and γ-cyclodextrins (CD)	**1**. Std **2**. components in 2,6–di-*O*-methyl-β-cyclodextrins	2,6-ANS (*Dynamic labelling*)	CZE	Fused silica ($L = 100$ cm; ID = 50 μm)	**1**. 40 m*M* sodium phosphate pH 11.76 with 1.0 m*M* 2,6-ANS **2a**. 30 m*M* benzoate pH 8.0 with 1.0 m*M* 2,6-ANS and 20 % methanol; 30 kV **2b**. 30 m*M* benzoate pH 4.0 with 40 μM (TBAB) tetra-butylammonium bromide and 1.0 m*M* 2,6-ANS; 30 kV	LIF (λ_{EXC}: 363 nm, λ_{EM}: 424 nm)	62 μM for α-CD; 2.4 μM for β-CD; 24 μM for γ-CD	• Dynamic fluorescence labelling provides a simple, sensitive and selective means for analysis of the CD. • Addition of organic modifiers and an ammonium salt allowed to separate components of DM-β-CD with differing degrees of substitution.
65	**1**. GalNAc, GlcNAc, Rha, Man, Glc, Fru, Xyl, Fuc, Gal **2**. Maltooligosaccharides (with up to 18 Glc residues)	**1**. Std mixtures **2a**. Dextrin 15 **2b**. Maltotetraose and α-Glc-(1–6)-α-Glc-(1–4)-α-Glc	APTS	CZE	Fused silica ($L = 27$ cm; $l = 20$ cm; ID = 20 μm)	**1**. 100 m*M* borate, pH 10.2 ; 20 kV **2a**. 200 m*M* borate, pH 10.2; 17 kV; 50 m*M* phosphate pH 2.2 ; 20 kV **2b**. 150 m*M* borate pH 10.2; 20 kV Outlet: cathode	LIF (λ_{EXC}: 488 nm; λ_{EM}: 520 nm); conversion of 2 pmol of sugar in the APTS-derivative	0.4 nM, 0.8 amol, S/N 10	• Drastic reduction of the signal of the excess APTS by choice of the appropriate excitation and emission wavelength for the selective detection of APTS-derivatized sugars.

		(1–4)-α-Glc hydrolyzed with α-amylase							• Similar separation order of malto-oligosaccharides analyzed by CZE with respect to PAGE. • Monitoring of the specificity action of glycosidases.
69	Fuc, Gal, Glc, Ara, Tag, Xyl, Sor, Man, Fru, Rib, Lyx, Sucrose, Melibiose, Cell, Lac, Gentiobiose, Maltose, Meleziose, Raffinose, Stachyose, Galactonic acid,	Std	None	CZE	Fused silica ($L = 56 - 57$ cm; $l = 32 - 35$ cm; ID = 25 or 50 μm) RT	Phosphate buffer pH 12.1 or NaOH at various concentrations, with tryptophan or BCDC as markers; various voltages Outlet: cathode	Indirect UV (280 nm) with tryptophan as the marker. Indirect UV (290 nm) with a cationic marker:	Range of fmol	• Use of cationic marker: the system gives a similar separation profile but much lower response magnitudes. • It is demonstrated that the choice of electrolyte conditions

(Continued)

Table 2
(Continued)

Ref.	Carbohydrate species	Matrix	Derivatizing agent	CE mode	Capillary; T	Buffer, Voltage	Detection mode	LOD	Results
	Gluconic acid, GalN, GlcN, mannitol, sorbitol						*N*-benzyl-cin choni-dium chloride (BCDC)		regarding pH and marker concentration is crucial; different conditions are required in order to optimize selectivity or sensitivity.
70	Glc, Rha, Man, Fru, Lyx, Xyl, Gal, Ara, Rib, Fuc, Lac, lactulose, turanose, sucrose, raffinose, trehalose, maltotriose, gluconic acid	Std	None	CZE	Fused silica ($L =$ 90 cm; $l =$ 85 cm; ID = 50 μm) RT	6 m*M* sorbic acid with **1**. 5% diethylamine pH 12.6 or with **2**. NaOH pH 12.2; 17 kV; **3**. 6 m*M* riboflavin with 50 m*M* borate pH 9.5; 17 kV Outlet: cathode	Indirect UV (256 nm for **1**. and **2**.; 267 nm for **3**.)	**1**.: 1 m*M* for sucrose, Gal, Glc and Fru; 2 m*M* for Rib; 0.1 m*M* for gluconic acid; **2**.: 0.1 m*M* for sucrose, Gal, Glc and Fru; 0.5 m*M* for Rib; 0.05 m*M* for gluconic acid	• DEA was used as an electrolyte additive to decrease the conductivity of the electrolyte, so that a higher buffer pH could be used and separation of carbohydrates was improved. • Slight decrease in the LOD was observed using benzoic acid as a BGE due to its low molar absorptivity.

									• Sucrose and raffinose were completely separated due to borate complexation.
71	**1**. Gal, Fuc, Ara, Man, Fru, Glc, Lac, GlcNAc, Rib, Sorbose, Xyl, Melibiose, Cell, Lyx, Maltose, Rha, Maltotetraose, GalNAc, Gentiobiose, Maltotriose, 2-deoxy-Rib **2**. GlcA, GalA, ManA **3**. Sialic acid (Neu5Ac)	Std mixtures; plant hydrolyzates	Ethyl 4-aminobenzoate and 4-ABN	CZE	Fused silica ($L = 57.5$ cm or 66 cm; $l = 50$ cm or 58.5 cm)	100–500 m*M* tetraborate, 0.001% hexadimethrine bromide (HDB) *Ethyl 4-aminobenzoate*: , pH 9.5–11.5, containing 0–20% of methanol, ethanol, n-propanol, i-propanol, acetonitrile, or ethyl-glycol *4-aminobenzonitrile*: pH 9.75–10.5, containing 0–5% of methanol, ethanol, n-propanol, or acetonitrile Outlet: anode	UV (280 nm)	1 ppm, 50 fmol (ethyl 4-aminobenzoate); 0.6 ppm, 30 fmol (4-aminobenzonitrile)	• With this method it is possible to resolve specific carbohydrates, such as Ara, Man and Glc, which are difficult to separate by other CE methods. • The high run-to-run repeatability for derivatization reagents also enables reliable determination of carbohydrates in real samples like plant hydrolizates.

(Continued)

Table 2
(Continued)

Ref.	Carbohydrate species	Matrix	Derivatizing agent	CE mode	Capillary; T	Buffer, Voltage	Detection mode	LOD	Results
72	Sucrose, isomaltose, Cell, maltose, Lac, 4-*O*-galactosyl-mannopyrano-side, melibiose, Fru, Glc	Std	None	CZE	Fused silica (L = 70 cm; l = 50 cm; ID = 75 μm) RT	175 m*M* sodium borate, pH 10.0 + 6 m*M* *p*-nitrophenol (PNP); 6 kV Outlet: cathode	Indirect VIS (400 nm)	Sucrose: 0.6 m*M*	• Is it possible to use borate complexation as a separation principle under the indirect detection conditions. • PNP as a background chromophore which allows the separation process to be monitored in a visible range.
75	**1**. GalNAc, GlcNAc, Rib, Fuc, Glc, Man, Gal **2**. GlcA, GalA	Std mix-tures	2-ABA	CZE	Fused silica (L = 60 cm; l = 50 cm; ID = 75 μm) T = 25 °C	150 m*M* sodium borate- 50 m*M* sodium phosphate, pH 7; 20 kV Outlet: cathode	UV (214 nm)	n.a.	• Study of the effect of pH, reaction solvent, temperature and reaction time for the derivatization reaction with 2-ABA. • Best derivatization conditions: solvent: water; pH 5.7; 40 °C for 16h.

									• Increment of average peak areas (two-fold increase for Man and GlcA, ten-fold increase for GlcNAc).
77	12 disaccharides containing Glc, Man and Gal	Std	4-ABA	CZE	Fused silica ($L = 92$ cm; $l = 84$ cm; ID = 50 μm)	**1**. 10 m*M* borate pH 10.0; 20 kV **2**. 50 m*M* ammonium acetate with 10 m*M* α-cyclodextrin pH 5.5; 20 kV Outlet: cathode	UV (254 nm) ESI-MS/MS (negative mode); electro-spray voltage: −4.5 kV; sheath liquid: water-2-propanol (20:80) containing 0.5 % NH_3	n.a.	• In negative mode ESI, the glycosylamine approach (closed ring) provides more information on linkage and anomeric configuration than reductive amination. • Although ammonium acetate/α-CD provided the best resolution of linkage isomers, the borate buffer was superior to α-CD in the separation of disaccharides with the same

(Continued)

Table 2
(Continued)

Ref.	Carbohydrate species	Matrix	Derivatizing agent	CE mode	Capillary; T	Buffer, Voltage	Detection mode	LOD	Results
									linkage but different anomeric configuration and/or monosaccharide composition.
78	Malto-oligosaccharides	Solution std	PMP (*on-capillary derivatization*)	MEKC	Fused silica (L = 71 cm; l = 49 cm; ID = 50 μm) T = 57 °C	200 m*M* borate, 200 m*M* SDS pH 8.2; 10 kV Outlet: cathode	UV (195 and 245 nm)	10^{-6} M	• Application of in-capillary derivatization to condensation of reducing carbohydrates with PMP. • Analysis by this technique was shown to be useful for kinetic study of derivatization reaction.
87	*N*-linked oligosaccharides	**1**. Std **2**. enzymatically released products from	APTS	CZE	Fused silica (l = 27 cm; ID = 19 μm)	**1**. 100 m*M* sodium borate pH 10.2; 25 kV **2**. 150 m*M* sodium phosphate pH 2.5; 18 kV	LIF	n.a.	• The role of various organic acid catalyst on the reductive amination of

		bovine fetuin and ribonuclease B				**1**. Outlet: cathode **2**. Outlet: anode				monosaccahrides with APTS is investigated. • The labelling efficiency is greatly improved for *N*-linked oligosaccharides with GlcNAc on the reductive end using catalysts more acidic than acetic acid: derivatization at 37°C with malic, citric and malonic acids produced high labelling yields with retention of more than 90% of sialic acid residues on the oligosaccharides.
96	Glc, Fru, Rha, Rib, maltose, Lac, sucrose, GlcA.	Std, beverages and drinks, serum	None	CZE	Fused silica (L = 120 cm; l = 113 cm; ID = 50 μm) T = 25 °C (best)	Investigated the suitability of six BGEs: 1-naphthylacetic acid (NAA), 2-naphthalensulfonic	Indirect UV (222 nm)	Rib: 0.2 m*M* GlcA: 0.01 m*M* Others: 0.1 m*M*	• NAA shows a 3–6 fold increase in the separation efficiency and 2–5 fold improvement in the detection limit with respect

(Continued)

Table 2
(Continued)

Ref.	Carbohydrate species	Matrix	Derivatizing agent	CE mode	Capillary; T	Buffer, Voltage	Detection mode	LOD	Results
						acid, 1,3-dihydroxy-naphthalene, phenylacetic acid, *p*-cresol and sorbic acid. Best composition: 2 m*M* NAA pH 12.2; 25 kV Outlet: cathode			to a commonly used BGE, i.e. sorbate. • CE separations between the Gal-Lac pair and between the Glc-Maltose pair were very difficult; Gal and Man, on the contrary, were resolved. • HPLC showed a complementary separation efficiency.
100	Gal, Glc, Man, Fru, inositol, d-Rib, Xyl, raffinose, Ara, Fuc, mannitol, Rib, GlcN, sucrose, GalN, maltose, xylitol and deoxyribose as internal std	Std and wine samples	None	CZE	Fused silica (L = 70 cm; ID = 50 μm)	50–400 m*M* Diethylamine (DEA), pH 12.15–12.40 with methanol or acetonitrile (0–40 %); 15–20 kV (voltage ramp 10 kV/s)	ESI-MS (negative mode) with sheath liquid: 80% 2-propanol and 20% water	Range of 0.5 (raffinose)-3.0 (deoxyribose) mg/L	• Best results without organic modifiers (optimized buffer: 300 m*M* DEA). • The use of ESI-MS allows the correct analysis of

							containing 0.25% DEA at 4 μL/min.		comigrating analytes because it provides a much higher accuracy in the assignment of peaks.
101	Sucralose, sucrose, Glc and Fru	Low-calorie soft drinks and std mixture	None	CZE	Fused silica (L = 112.5 cm; ID=50 μm) RT	3 m*M* 3,5-dinitrobenzoic acid (DNBA) pH 12.1; 20 kV Outlet: cathode	Indirect UV (238 nm)	Sucralose: 28 mg/L	• This method is a suitable tool for the determination of sucralose in low-calorie beverages; in contrast, HPLC methods involve sample clean-up steps and analyte concentration to overcome poorer sensitivity.
102	Glc, Gal, Lac, Fru and sucrose	Soft drinks, isotonic beverages, fruit juice and sugarcane spirits.	None	CZE	Fused silica (**1**. L = 68.5 cm; l = 60 cm; ID = 50 μm; **2**. L = 44 cm; l = 35.5 cm; ID = 20 μm) T = 30 °C	**1**. 30 m*M* NaOH; 30 m*M* NaOH and 12% v/v CH_3OH; 30 m*M* NaOH with 15 m*M* Na_2HPO_4 (all contained 200 μM CTAB); 11 kV **2**. 10 m*M* NaOH, 4.5 m*M* Na_2HPO_4,	CCD	Fru: 16 μM; Glc: 31 μM; Gal: 18 μM; sucrose: 13 μM	• The addition of phosphate resulted in good baseline and resolution but the sensitivity was reduced and analysis time was increased.

(Continued)

Table 2
(Continued)

Ref.	Carbohydrate species	Matrix	Derivatizing agent	CE mode	Capillary; T	Buffer, Voltage	Detection mode	LOD	Results
		Gal use as internal std				200 μm CTAB; 25 kV Outlet: anode			• With addition of MeOH the resolution of the critical pair, lactose-galactose, was improved. • Use of 20 μm capillary ID gives impressive results.
107	Fuc, Glc, Gal and Ara	Human serum	BHZ	CZE	Fused silica ($L = 67$ cm; $l = 60$ cm; ID = 50 μm) RT	100 m*M* boric acid pH 10.4; 23.1 kV Outlet: cathode	UV (200 nm)	15.6 μM for Gal; 31.2 μM for Glc	• The Glc peak was completely separated from other serum components.
110	*N*-linked oligosaccharides	Digestion products from antibody pharmaceutical sample and std	**1**. APTS **2**. 3-ABA	CZE	**1., 2a.** DB-1 capillary coated with dimethylpolysiloxane ($L = 30$ cm; $l = 20$ cm) **1.** ID = 50 μm); **2a.** ID = 100 μm; **2b.**	**1**. 50 m*M* Tris-acetate buffer pH 7.0 with 0.5% PEG70000; 18 kV **2**. 100 m*M* Tris-borate buffer pH 8.3 with 10% PEG70000; **a**. 25 kV; **b**. 30 kV	LIF **1**. (λ_{EXC}: 488 nm; λ_{EM}: 520 nm); **2**. (λ_{EXC}: 325 nm; λ_{EM}: 405 nm)	n.a.	• 3-ABA advantages: highest grade reagent is commercially available; it reacts with reducing sugars in the mildest conditions without release of

					Fused silica ($L = 80$ cm; $l = 70$ cm; ID = 100 μm) T = 25 °C				sialic acid residues; the derivatization products can be analyzed by normal- or reverse-phase HPLC and they are stable at −20 °C for several months.• Rapidness in analysis time is a merit for APTS.
119	Glycoalkaloids and relative aglycones: solanidine, tomatidine, chaconine, solanine and tomatine	Std and potato extracts	None	NACE	Fused silica ($L = 80$ cm; $l = 20$ cm; ID = 50 μm) T = 20 °C	90/10 CH_3CN/CH_3OH + 50 m*M* ammonium acetate +1.2 M acetic acid; 25.5 kV (30 kV to the anode and 4.5 kV to the cathode-electrospray tip) Outlet: cathode	ESI-MS (positive mode) with sheath liquid: methanol-water 1/1 with 1% acetic acid at 2.5 μL/min	Solanidine and α-chaconine: 10 μg/L; α-solanine: 50 μg/L	• An effective separation of glycoalkaloids and their aglycones, natural toxins and their metabolites can be achieved by NACE in conjunction with ESI-MS: a very powerful approach to study the presence of GAs in wild and transgenic plants.

(Continued)

Table 2
(Continued)

Ref.	Carbohydrate species	Matrix	Derivatizing agent	CE mode	Capillary; T	Buffer, Voltage	Detection mode	LOD	Results
120	11 neutral iridoid glycosides	Std and 7 plant samples	None	PF-MEKC	Fused silica ($L = 80\,cm$; l = 71.5 cm; ID = 50 μm) T = 25 °C	20 m*M* ammonium acetate +100 m*M* sodium/ammonium/ lithium dodecyl sulfate pH 9.5; 20 kV Outlet: cathode	ESI-MS with sheath liquid : 1.0 m*M* lithium acetate in water-methanol 50–50; UV (197, 235, 239 and 283 nm)	Range 3–25 mg/L	• Ammonium dodecyl sulfate, lithium dodecyl sulfate and sodium dodecyl sulfate were compared in the MEKC separation and MS analysis: SDS gave the best results in MEKC and the noise at the MS was diminished when the SDS was dissolved in the BGE instead of pure water.
121	Cyanogenic allosides, D/L-Glc and D/L-All	Std and extracts of leaf and stem	(*S*)-(-)-phenylethy-lamine	CZE	Fused silica ($L =$ 57 cm; ID = 50 μm) T = 27 °C	50 m*M* $Na_2B_4O_7$, 2.7 M CH_3CN pH 10.3; 30 kV Outlet: cathode	UV (200 nm)	n.a.	• Determination of the absolute D/L-configuration of the β-allose moiety, performed by CZE using the

										(*S*)-phenylethylamine derivatives of the free sugars obtained after hydrolysis with TFA. Authentic (*S*)-phenylethylamine derivatives of D- and L-allose used as references.
123	Raffinose family oligosaccharides (α-galactosides): sucrose, raffinose, stachyose, verbascose and ajugose Galactinol Maltitol and methyl-α-D-glucopyranoside as internal std	Std and samples of legu-minous seed (Lupine)	None	CZE	Fused silica ($L = 80$ cm; $l = 70$ cm; ID = 50 μm) T = 30 °C	Pyridine-2,6-dicarboxylic acid (BGE), 5–150 m*M* $Na_2B_4O_7 \times 10\,H_2O$, 0.5 m*M* hexadecyltrimethy-lammonium bromide pH 8.0–10.0; 10 kV Outlet: anode	Indirect UV (350 nm)	110 μg/mL corresponding to 150–320 μM for sucrose, raffinose and stachyose and 130 μg/ml for verbascose	• No borate complexes with α-galactosides were seen at pH values below 9; in these conditions, the 3 oligosaccharides and sucrose migrated as a single peak. Best borate conc.: 50 m*M* at pH 9.2. with a free carbonyl group (hemiacetals or hamiketals) without including

(Continued)

Table 2
(Continued)

Ref.	Carbohydrate species	Matrix	Derivatizing agent	CE mode	Capillary; T	Buffer, Voltage	Detection mode	LOD	Results
									nonreducing carbohydrates of the aldose type.
125	Amygdalin epimers	Apricot kernel extract and std	None	MEKC	Fused silica ($L =$ 127 cm; $l =$ 120 cm; ID = 50 μm) T = 25 °C	20 m*M* ammonium acetate +30 m*M* SDS pH 7; 20- − 30 kV + 0.5 psi Outlet: cathode	ESI-MS with sheath liquid: methanol/ water/ formic acid 49.5/50/0.5 at 10 μL/min.	n.a.	• The author suggests that co-application of applied voltage with the low pressure (< 3.4 kPa) could be a good technique to decrease the migration time when a long capillary is employed in CE-ESI-MS.
126	Rha, Cell, Xyl, Rib, Melibiose, Ara, Glc, Man, Fuc, Gal, GlcA, and D-thyminose (2-deoxy-D-ribose) as internal std	Std and plant extracts from *Lupinus angus-tifolius*	Tryptamine	MEKC	Coated fused silica ($L =$ 76 cm; $l =$ 53 cm : ID = 50 μm) T = 30 °C	35 m*M* cholic acid, 100 m*M* borate with 2% 1-propanol pH 9.7; 30 kV Outlet: cathode	UV (220 nm)	Picomole range	• The presence of a carboxylated group as in uronates increases the migration time.

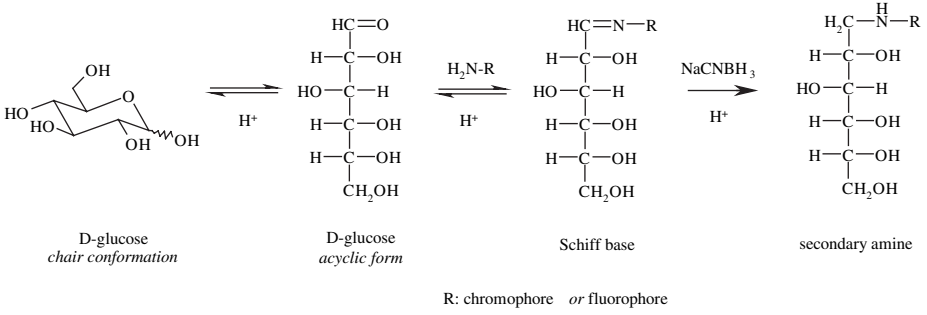
(Continued)

									• This method is selective with respect to determination of carbohydrates with a free carbonyl group (hemiacetals or hamiketals) without including nonreducing carbohydrates of the aldose type.
131	Mannooli gosaccharide caps from *Mycobacterium tuberculosis* H37rv mannosylated lipoarabino-mannans (ManLAMs)	Acidic hydro-lysis extracts and std	APTS	CZE	Analytical CE: fused silica (L = 47 cm; l = 40 cm; ID = 50 μm) Micro reparative CE: fused silica (L = 47 cm; l = 40 cm; ID = 75 μm) T = 25 °C	15 m*M* triethylamine in a 1% (w/v) solution of acetic acid in water, pH3.5 20 kV for analytical CE; 10 kV for micropreparative CE Outlet: anode	UV (254 nm) LIF (λ_{EXC}: 488 nm; λ_{EM}: 520 nm) MALDI-TOF (off-line) linear and reflectron modes in negative ion mode	50 fmol of std APTS-maltotriose; 100 fmol using a 200-ns extraction delay time	• A single CE collection yielded enough material for MALDI-TOF experiments. • The combination of CE and MALDI-TOF-MS is more sensitive than the on-line coupling between CE and ESI-MS for the structural analysis of APTS-derivatized oligosaccharides.

For abbreviations, see **Table 1**.

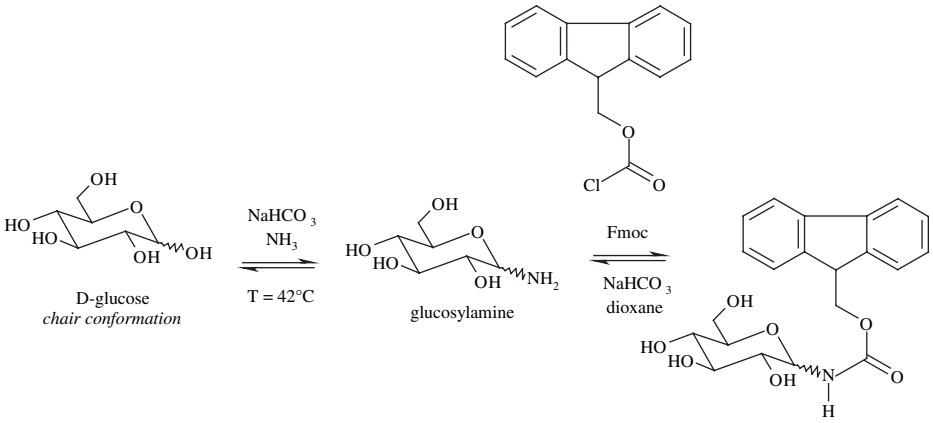
1.1. Derivatization of Neutral Reducing Sugars

Linkage of sugars with chromophoric or fluorophoric tags, eventually carrying ionizable groups, guarantees the lowest detection limits without sacrificing highly selective electrophoretic separations. Sugar derivatization is generally carried out before injection in the capillary. It is always preferable to exploit the reactivity of one only functional group, in order to minimize the presence of by-products. Furthermore, the yield of the reaction should be as high as possible. The most widely used pre-column derivatization procedure is reductive amination **(Scheme 1)**, a reproducible, one-pot reaction. It uses suitable chromophores or fluorophores carrying a primary amino group capable of reacting with the carbonyl group of reducing sugars in the presence of sodium cyanoborohydride ***(33,45,47,51)***. In order to shift the initial equilibrium (Schiff base formation) into the direction of the condensation, at least a fivefold excess of the derivatizing agent is necessary ***(33)***. Derivatization efficiency depends on the nature of the sugars as well as on the reaction conditions. As an example, 2-aminopyridine is not suitable for derivatization of ketoses, whereas 4-aminobenzonitrile, 4-aminobenzoic acid and its ethyl ester have been successfully used for the CE analysis of fructose and sorbose ***(71)***. Glycoprotein monosaccharides, like 2-deoxy-2-acetamido-sugars, are successfully derivatized with 2-aminobenzoic acid ***(74,75)*** Concerning the reaction conditions, the yield is related to the nature of the organic acid used as the catalyst; whereas acetic acid (pK_a 4.75) is the most widely employed, it has been demonstrated that the highest yield for the reductive amination of *N*-linked oligosaccharides with 1-aminopyrene-3,6,8-trisulfonate (APTS) is obtained using citric acid (pK_a 3.13) or malic acid (pK_a 3.40) as catalysts ***(87)***. This effect is much more relevant for sugars having *N*-acetylglucosamine
at the reducing end. APTS and 8-aminonaphtalene-1,3,6-trisulfonic acid (ANTS) are extremely advantageous, because they introduce negative charges



Scheme 1.

to the sugars for a wide pH range (i.e., pH $\geq$ 2.0), with consequent wide possibilities in the buffer composition optimization ***(62,65,66,87,88)***. They have been used not only as derivatizing agents for fluorescence detection, but also for on-line electrospray mass spectrometry detection and off-line matrix-assisted laser desorption/ionization mass spectrometry ***(79,131,139)***. Among the chromophores, 4-aminobenzonitrile (4-ABN) allows a relatively high sensitivity with respect to other commonly used chromophores, such as 2-aminopyridine, 4-aminobenzoic ethyl ester, 8-aminonaphtalene-1,3,6-trisulfonic acid ***(33,47)***. Another efficient derivatization strategy that includes reductive amination is the conversion of reducing sugars in 1-amino-1-deoxyalditols and subsequent reaction with 3-(4-carboxybenzoyl)-2-quinolinecarboxyaldehyde (CBQCA) ***(81)*** or with 5-carboxytetramethylrhodamine succinimidyl ester (TRSE) ***(134)***. Finally, condensation between carbonyl group of reducing carbohydrates and the active hydrogens of 1-phenyl-3- methyl- 5-pyrazolone (PMP) has been successfully employed for the characterization of various biological matrices ***(39,52,55)***. In **Table 3**, the structures of the most widely used derivatizing agents together with their main applications are reported. A disadvantage of all the previously mentioned derivatization strategies is that they are destructive. This is not generally a big drawback, because the sample volumes required for derivatization in CE are in the microliter range. Nevertheless, some approaches to minimizing the sample consumption have been proposed. The first is on-capillary derivatization, which reduces the sample volume by two to three orders of magnitude ***(78,107)***. A second approach, the so-called "dynamic labeling" of carbohydrates, has been mainly used for cyclodextrins, which have the capacity to form inclusion complexes with charged fluorophores or chromophores added to the separation buffer. Electrophoretic migration as well as sensitive detection is thus achieved ***(64,140)***. A third interesting approach makes it possible to re-convert the labeled products in the starting sugars, and is based on the formation of chromophoric or fluorophoric glycosylamines; this strategy has been reported for both HPLC and CE analysis of reducing sugars: as an example, formation of *N*-(2-pyridinyl)-glycosylamines has been successfully used to label malto-oligosaccharides or pullulan oligomers prior to their HPLC analysis ***(136,141)***. Glycosylamines originated from reaction with 4-aminobenzoic acid and various disaccharides have been analyzed with CE and negative-mode electrospray mass spectrometry: the glycosylamines approach turned out to provide more information on linkage and anomeric configuration than reductive amination ***(77,142)***. Another procedure based on the formation of glycosylamines consists in the preparation of 1-amino-1-deoxy-derivatives from the reducing sugars, which can then react with acylic groups of suitable tags like 9-fluorenyl-methyloxycarbonyl



Scheme 2.

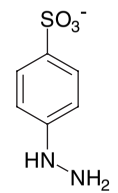
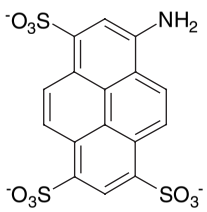
chloride (Fmoc) **(Scheme 2)** ***(135,143)***. In all of the cases related to the glycosylamines-based strategies, the starting oligosaccharides can be recovered from glycosylamines upon weak acid hydrolysis ***(135,136,141,143)***.

In this chapter, we report the protocols for derivatization and CE analysis of reducing sugars by this last method as well as by reductive amination using 4-aminobenzonitrile (4-ABN).

1.2. Use of Highly Alkaline Buffers for Underivatized Neutral Sugars

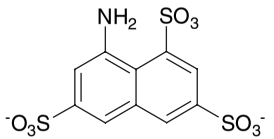
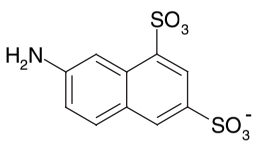
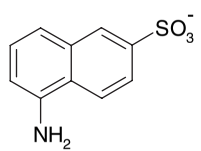
Highly alkaline buffers (pH >12.0) are capable of inducing acidic dissociation of underivatized sugars ($11.9 < pK_a < 12.8$) and of alditols ($pK_a = \sim 13.5$) ***(51)***, which can migrate in the capillary through zone electrophoresis. This analysis mode is normally associated with electrochemical, mass spectrometry, or indirect ultraviolet/fluorescence detection ***(43,50,51,99,100)***. Electrochemical detection allows the highest sensitivity achievable for underivatized carbohydrates ***(33)***. Upon using volatile bases in the separation buffer, negative-mode electrospray mass spectrometry turns out to be a suitable detector for alditols and reducing and nonreducing neutral sugars ***(100)***. When coupled with highly alkaline buffers, the most common UV or LIF detectors are successfully used in "indirect" mode, which is based on the displacement of the chromophores or fluorophores in the background electrolyte by any charged molecule in the sample, resulting in negative peaks ***(33,144)***. Limits of detection (LOD) in indirect UV (or fluorescence) depend on the nature of the chromophore (or fluorophore) in the background electrolyte as well as on the type of sugar: for instance, neutral carbohydrates analyzed with

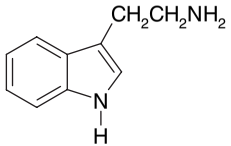
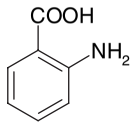
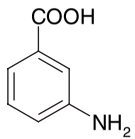
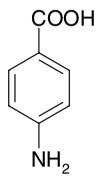
Table 3
-main derivatizing tags suitable for CE analysis of neutral sugars.

Derivatizing agent	Detection	Carbohydrates species	References
 **BHZ** *p*-hydrazine-benzenesulfonic acid	UV (200 nm)	Fuc, Glc, Gal, Ara	**[107]**
 **APTS** 1-aminopyrene-3,6,8-trisulfonic acid	LIF (λ_{EXC}: 455 nm; λ_{EM}: 512 nm) UV (254 nm)	GalNAc, GlcNAc, Rha, Man, Glc, Fru, Xyl, Fuc, Gal, Maltooligosaccharides (with up to 18 Glc residues) Mannooligosaccharide caps from *Mycobacterium tuberculosis* H37rv mannosylated lipoarabinomannans (ManLAMs) *N*-linked oligosaccharides Gluco-oligosaccharide regioisomers with a degree of polymerization (DP) ranging from 2 to 9; several glucose disaccharide regioisomers GalNAc, GlcNAc, Rha, Man, Glc, Xyl, Fuc, Gal, Ara, Rib, Gentibiose, maltose, Lac, Cell, Melibiose, Maltotetraose and its α-1–6 isomer, Sialyllactose Amylodextrin oligomers (up to 40 glucose units) GalNAc, GlcNAc, Man, Glc, Gal, Fuc, GlcNAc-Gal	**[65]** **[131]** **[110], [87]** **[138]** **[66]** **[106]** **[89]**

(Continued)

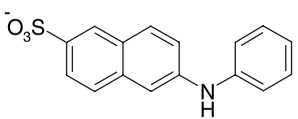
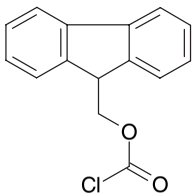
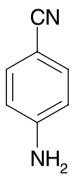
Table 3
(Continued)

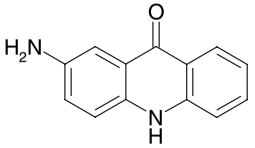
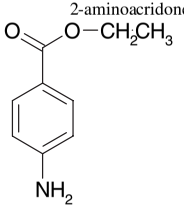
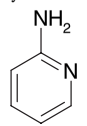
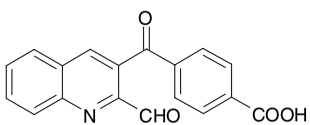
Derivatizing agent	Detection	Carbohydrates species	References
 **ANTS** 8-aminonaphtalene-1,3,6-trisulfonic acid	LIF (λ_{EXC}: 370 nm; λ_{EM}: 520 nm) UV (214 e 223 nm)	Glc, Maltose and linear malto-oligosaccharides (with up to 40 Glc residues) Malto-oligosaccharides	**[62]** **[79]**
 **ANDSA** 7-aminonaphtalene-1,3-disulfonic acid	LIF (λ_{EXC}: 315 nm; λ_{EM}: 420 nm) UV(247 nm)	Amylodextrin oligomers (up to 40 glucose units)	**[106]**
 **ANMS** 5-aminonaphtalene-2-sulfonic acid	LIF (λ_{EXC}: 325 nm; λ_{EM}: 514 nm)	Amylodextrin oligomers (up to 40 glucose units)	**[106]**

 Tryptamine	UV (220 nm)	Rha, Cell, Xyl, Rib, Melibiose, Ara, Glc, Man, Fuc, Gal, GlcA, and D-thyminose	**[126]**
 **2-ABA** 2-aminobenzoic acid	UV (214 nm)	GalNAc, GlcNAc, Rib, Fuc, Glc, Man, Gal, GlcA, GalA GalNAc, GlcNAc, Rib, Fuc, Glc, Man, Gal	**[75]** **[74]**
 **3-ABA** 3-aminobenzoic acid	LIF (λ_{EXC}: 325 nm; λ_{EM}: 405 nm)	*N*-linked oligosaccharides	**[110]**
 **4-ABA** 4-aminobenzoic acid	UV (285 nm)	12 disaccharides containing Glc, Man and Gal	**[77]**

(Continued)

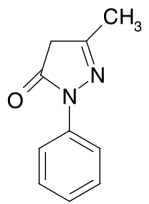
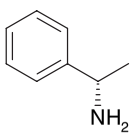
Table 3
(Continued)

Derivatizing agent	Detection	Carbohydrates species	References
 **2,6-ANS** 2-anilinonaphtalene-6-sulfonic acid	LIF (λ_{EXC}: 363 nm; λ_{EM}: 424 nm)	α−, β−and γ-cyclodextrins	**[64]**
 **Fmoc** *N*-fluorenyl-methyloxycarbonyl chloride	UV (260 nm)	Glc, Gal and Lac previously converted in the corresponding glycosylamines	**[135]**
 **4-ABN** 4-aminobenzonitrile	UV (285 nm)	Neutral mono-, di- and trisaccharides (Maltotriose, Maltose, Lac, L-Rha, D-Lyx, D-Xyl, Cell, Melibiose, L-Sorbose, D-Rib, D-Glc, D-Fru,D-Man, L-Ara, D-Fuc, D-Gal); sugar acids (D-GlcA, D-GalA) Gal, Fuc, Ara, Man, Fru, Glc, Lac, GlcNAc, Rib, Sorbose, Xyl, Melibiose, Cell, Lyx, Maltose, Rha, Maltotetraose, GalNAc, Gentiobiose, Maltotriose, 2-deoxy-Rib, GlcA, GalA, ManA, Sialic acid (Neu5Ac)	**[63]** **[71]** **[136]**

 **AMAC** 2-aminoacridone	LIF (λ_{EXC}: 425 nm; λ_{EM}: 520 nm)	Isomaltose, maltose, Glc, Glcα1→6Glcα1→6Glc, Glcα1→6Glcα1→4Glc Sialic acid (Neu5Ac) Neutral sugars (see also reference 77 in Chapter 12)	**[89]**
 Ethyl 4-aminobenzoate	UV (305 nm)	Gal, Fuc, Ara, Man, Fru, Glc, Lac, GlcNAc, Rib, Sorbose, Xyl, Melibiose, Cell, Lyx, Maltose, Rha, Maltotetraose, GalNAc, Gentiobiose, Maltotriose, 2-deoxy-Rib, GlcA, GalA, ManA, Sialic acid (Neu5Ac)	**[71]**
 **2-AP** 2-aminopyridine	UV (240 nm)	GalA, GlcA, Gal, GalNAc, Ara, Fuc, Rha, Xyl, Lyx, GlcNAc, Glc, Rib	**[53]**
 **CBQCA** 3- (4- carboxybenzoyl)- 2-quinolinecarboxyaldehyde	LIF (λ_{EXC}: 457 nm; λ_{EM}: 552 nm)	GlcN, GalN, 1-amino-1-deoxyglucosamine, 1-amino-1-galactosamine, 6-amino-6-deoxy-glucose, glucosaminic acid, galactosaminic acid, 1-amino-1-deoxyglucose, 1-amino-1-deoxygalactose, 2-amino-2-deoxyglucose, 2-amino-2-deoxygalactose	**[81]**

(Continued)

Table 3
(Continued)

Derivatizing agent	Detection	Carbohydrates species	References
 **PMP** 1-phenyl-3-methyl-2-pyrazolin-5-one	UV (245 nm)	Maltooligosaccharides Ara, Rib, Gal, Glc, Lyx, Xyl and Man, Fuc, GalNAc, GlcNAc Xyl, Ara, Rib, Lyx, Glc, All, Alt, Man, Ido, Gul, Tal, Gal, Oligoglucans (up tp 13 glucose residues)	**[78]** **[56]** **[55]**
 (S)-(-)-1-phenylethylamine	UV (200 nm)	D/L-Glc, D/L-All	**[121]**

For abbreviations, see Table 1

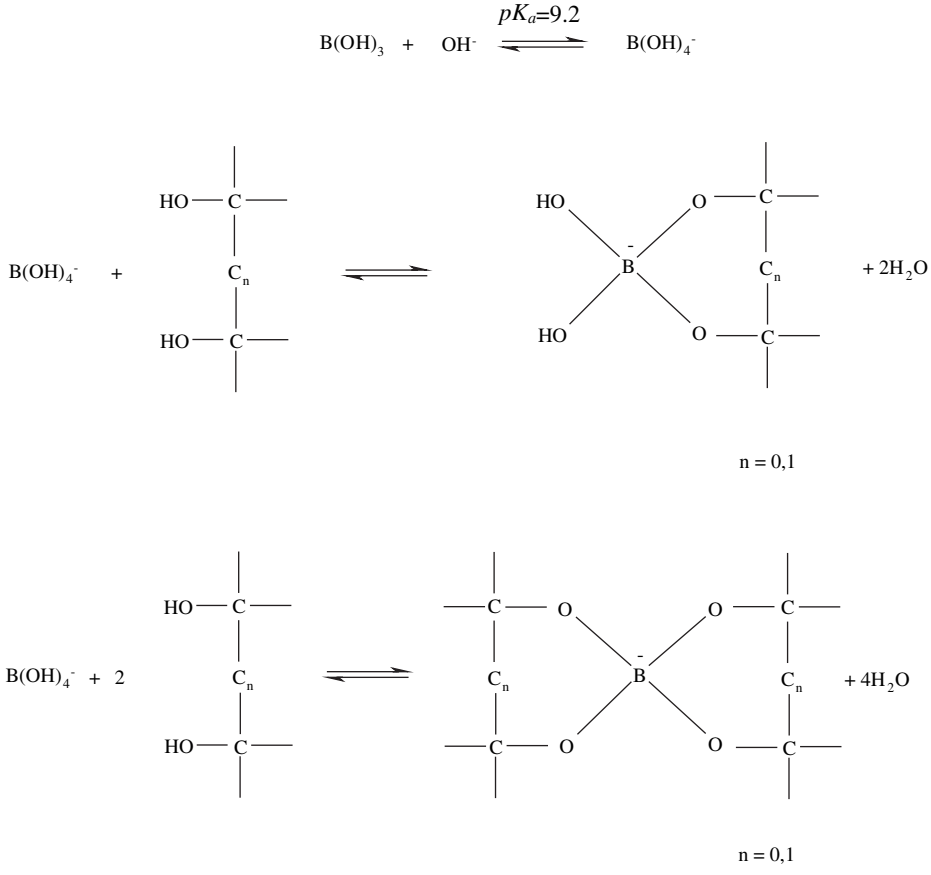
indirect UV detection show typical limits of detection (LODs) equal to 10^{-4} *M* whereas, in the same analysis conditions, sugar acids have LOD values of 10^{-6} *M* ***(27,33,145)***. The separation efficiency of CE using highly alkaline buffers shows a 10- to 20-fold increase with respect to HPAEC-PAD ***(27,50)***. It should be mentioned that the use of highly alkaline buffers is advised not only for alditols, but also for reducing sugars, when some relevant matrix components can be degraded under the typical derivatization conditions ***(135)***.

In this chapter, a protocol for the CE analysis of reducing sugars using highly alkaline buffers and indirect UV detection is shown ***(135)***.

1.3. Use of Borate-Based Separation Buffers for Derivatized and Underivatized Sugars

The use of borate-based buffers is widespread for the CE analysis of carbohydrates (***47,51,53–55,70,72,137,146***). Using such separation electrolytes, sugars can be converted *in situ* to anionic borate complexes **(Scheme 3)**. The stability of the mentioned complexes depends on the pH (typically, between 7.0 and 10.0); moreover, it is related to the configuration of the hydroxyl groups involved in the interaction with boron: for cyclic carbohydrates, only vicinal hydroxyl groups with cis configuration can form stable complexes; for polyols, *cis*-1,2-diols are preferred in complexation over *trans*-1,2-diols; moreover, in general the stability of complexes increases with the number of hydroxyl groups ***(54,146)***. These features imply that borate-based buffers can exert a strong influence on the selectivity of the electrophoretic separation of carbohydrates, because the differential stability of *in situ*-formed complexes contributes to the mobility of the analytes. As a consequence, borate is a useful additive for the analysis of derivatized carbohydrates ***(53,55,63,70,72,136)***. Besides the introduction of the charge, borate-carbohydrate complexes show an increase in UV response at 195 nm with respect to uncomplexed carbohydrates. As a consequence, borate-based buffers can make sugars suitable for CE analysis without the need of derivatization ***(54)***. The use of borate-based buffers is one of the methods of choice for capillary electrophoresis of glycosides, because they are not amenable to derivatization at the reducing end.

In this chapter, we will show a specific example relative to the CE analysis of allyl-glycosides, where the usefulness of the borate complexation is shown, in terms of sensitivity and separation selectivity.



Scheme 3.

2. Materials

2.1. Derivatization of Neutral Reducing Sugars

2.1.1. Reductive Amination of Gluco-oligosaccharides with 4-aminobenzonitrile

1. Samples: isomaltose (6-*O*-α-D-Glucopyranosyl-D-glucose), glucose and maltose; gluco-oligosaccharides synthesized upon treatment of 1 g of maltose (in 5 mL of 50 m*M* CH_3COONa, pH 5.5) with 100 μL (2.5 U) of *Aspergillus niger* α-D-glucosidase (gift) at 37 °C (all reagents from Sigma, St. Louis, MO). Kinetic study was carried out upon collecting aliquots of the synthesis mixture at 5, 10, 15, 60, and 90 min and inactivating the enzyme at 100 °C for 10 min ***(136)***.

2. Reagents for derivatization: sodium cyanoborohydride ($NaCNBH_3$), 4-ABN, glacial acetic acid, and methanol (all reagents from Sigma, St. Louis, MO); the structure of 4-ABN is reported in **Table 3**.
3. CE buffer: 100 m*M* sodium tetraborate (borax) +100 m*M* sodium dodecyl sulfate (SDS) pH 9.2 (all reagents from Sigma, St. Louis, MO).

2.1.2. Derivatization of Glycosylamines With N-fluorenyl-methiloxycarbonyl (Fmoc) Chloride and Subsequent Regeneration of Starting Reducing Sugars

1. Samples: D-galactose, D-glucose and lactose (Sigma, St. Louis, MO).
2. Reagents for derivatization: ammonium hydrogen carbonate, concentrated ammonia, *N*-fluorenyl-methyloxycarbonyl (Fmoc) chloride, sodium hydrogen carbonate ($NaHCO_3$), dioxane and methanol (all reagents from Sigma, St. Louis, MO); the structure of Fmoc is reported in **Table 3**.
3. Reagent for Fmoc-removal: 15% aqueous ammonia solution (diluted from 28% ammonium hydroxide, Sigma, St. Louis, MO).
4. Reagent for sugar regeneration: 2% aqueous acetic acid solution (diluted from glacial acetic acid, Sigma, St. Louis, MO).
5. CE buffer: 20 m*M* sodium tetraborate (borax) +25 m*M* SDS pH 9.2 (all reagents from Sigma, St. Louis, MO).

2.2. Use of Highly Alkaline Buffers for Underivatized Neutral Sugars (Analysis of Synthesis Mixtures of Glycosylamines)

1. Samples: D-glucose, D-galactose, and lactose; glycosylamines synthesis mixtures (all reagents from Sigma, St. Louis, MO) (*see* **Subheading 3.1.2.** for details).
2. CE buffer: 6 m*M* sorbate (Sigma, St. Louis, MO) +0.5 m*M* tetradecyltrimethylammonium bromide (TTAB), pH 12.5 (Aldrich, St. Louis, MO).

2.3. Use of Borate-Based Separation Buffers for Derivatized and Underivatized Sugars (Identification of Anomeric Forms of O-and C-Allyl Glycosides)

1. Samples: *O*-allyl-α-glucopyranoside, *O*-allyl-β-glucopyranoside, and *O*-allyl-α-galactopyranoside (from Glycon Biochemicals, Luckenwalde, GER); *O*-allyl-β-galactopyranoside previously synthesized according to the procedure reported in literature *(137)*. α- and β-*C*-allyl galactopyranosides and glucopyranosides were synthesized following the protocol reported in **Note 1**.
2. CE buffer: *C*-allyl-glycosides: 100 m*M* borax +100 m*M* SDS (pH 9.2); *O*-allyl-glycosides: 25 m*M* borax +250 m*M* SDS (pH 9.2) (all reagents from Sigma, St. Louis, MO).

2.4. Equipment

1. High-performance CE system (Applied Biosystems Model 270A-HT; Foster City, CA), with Turbochrom Navigator (4.0) software.
2. Uncoated fused-silica column (Supelco, St. Louis, MO); inner diameter (ID): 50 μm; capillary length: 72 cm (50 cm to detector).
3. Detection: UV on-column (285 nm **[Subheading 3.1.1.]**; 260 nm **[Subheading 3.1.2.]**; 256 nm **[Subheading 3.2.]**; 195 nm **[Subheading 3.3.]**).
4. C18 cartridge (Sep-Pak®, 10 g).
5. Nylaflo membrane filters: 0.45 μm (Sigma, St. Louis, MO).
6. Bio-Gel P2 (Bio-Rad, Hercules, CA).
7. Dry-bath heating block.

3. Methods

3.1. Derivatization of Neutral Reducing Sugars

3.1.1. Reductive Amination of Gluco-Oligosaccharides With 4-Aminobenzonitrile

1. Derivatization of reducing sugars with 4-ABN: prepare a solution containing 60 mg of 4-ABN and 10 mg of $NaCNBH_3$ in 950 μL of CH_3OH and 50 μL of glacial acetic acid. Add 250 μL of this solution to 50 μL of sugar(s) dissolved in water (0.5–5 mg/mL) in a screw-cap vial. Heat the mixture at 90 °C (in dry-bath heating block) for 15 min. Before injection in the CE system, a 1:5 dilution with water is necessary.
2. Operate a flush of the capillary for 2 min with a 0.1 *N* NaOH solution at a vacuum pressure of 67.6 kPa.
3. Condition the silica capillary by flushing with the separation buffer at a vacuum pressure of 67.6 kPa for 4 min.
4. Load sample under vacuum at a pressure of 16.9 kPa for 1.5 s.
5. CE conditions: voltage: 15 kV; UV detection at 285 nm, carried out at the cathode; temperature: 30 °C; buffer: 100 m*M* tetraborate +100 m*M* SDS (pH 9.2).
6. **Figure 1** demonstrates the usefulness of MEKC-UV for monitoring the enzymatic synthesis of pullulan oligosaccharides: the high separation selectivity of the method allowed the identification of two trisaccharidic products, a dextran (Glcα1→6Glcα1→6Glc) and a pullulan (Glcα1→6Glcα1→4Glc) fragment. Glucose, maltose, and isomaltose were also very satisfactorily separated. The micellar electrokinetic chromatography (MEKC)-UV kinetic analysis demonstrated that the synthetic strategy was not effective for the synthesis of pullulan trisaccharide, which was only formed during the first minutes of the reaction, and subsequently hydrolyzed in favor of the dextran trisaccharide ***(136)***.

3.1.2. Derivatization of Glycosylamines with N-fluorenyl-methiloxycarbonyl (Fmoc) Chloride and Subsequent Regeneration of Starting Reducing Sugars

1. Conversion of glucose, galactose, and lactose in the corresponding glycosylamines: dissolve the reducing sugar (0.2 *M*) in an aqueous solution containing ammonia

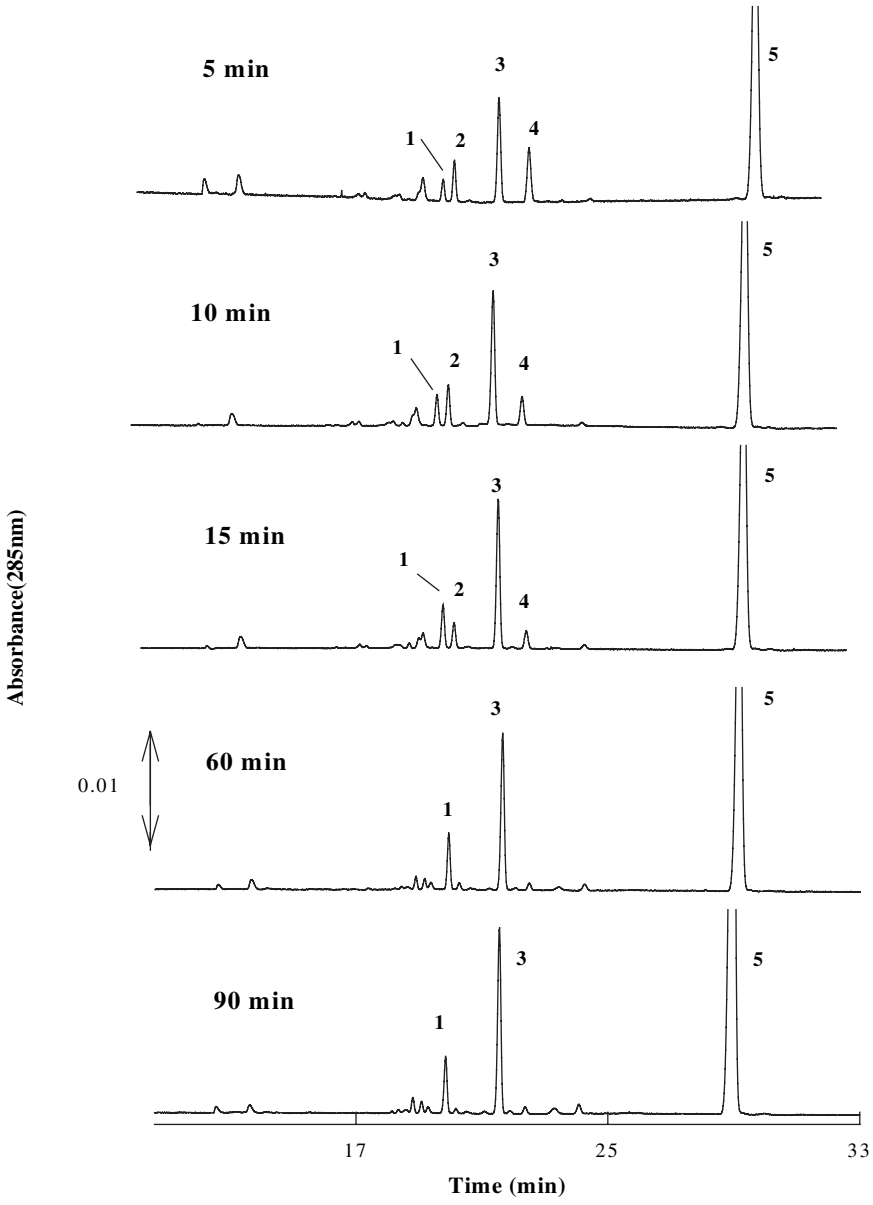


Fig. 1. Micellar electrokinetic chromatography-ultraviolet analysis of the synthesis mixtures of pullulan and dextran trisaccharide using α-D-glucosidase; peak attributions: 1, dextran trisaccharide; 2, pullulan trisaccharide; 3, isomaltose; 4, maltose; 5, glucose; operative conditions: voltage: 15 kV; detection: 285 nm at the cathode; temperature: 30 °C; buffer: 100 m*M* tetraborate+100 m*M* sodium dodecyl sulfate, pH 9.2. (Reprinted from **ref. *134***, with permission from Elsevier.)

(16 *M*) and ammonium hydrogen carbonate (0.2 *M*). Leave the mixture for 36 h at 42 °C ***(135,147)*** (*see* **Note 2**).

2. Derivatization of glycosylamines with Fmoc: prepare 5 mL of a solution containing 0.1 mmol of glycosylamine in saturated aqueous sodium hydrogen carbonate; add this solution to 5 mL of Fmoc-Cl (0.4 mmol) in dioxane; stir the resulting mixture overnight at ambient temperature. Load the sample on a C18 cartridge conditioned in water, wash it with water to remove salt and reducing carbohydrates, and then with methanol to recover the condensation product (*see* **Note 3**).
3. Rinse the capillary for 2 min with a 0.1 *N* NaOH solution at a vacuum pressure of 67.6 kPa.
4. Condition the capillary by flushing with separation buffer for 4 min at a vacuum pressure of 67.6 kPa.
5. Inject the sample under vacuum at a pressure of 16.9 kPa for 1.5 s.
6. CE conditions: voltage: 20 kV; detection: 260 nm at the cathode; temperature: 30 °C; buffer: 20 m*M* borax at +25 m*M* SDS, pH 9.2
7. **Figure 2** shows the electropherograms relative to the analysis of glucose, galactose, and lactose converted in the corresponding glycosylamines and derivatized with Fmoc (*see* **Note 4**).
8. Fmoc removal: keep the solution of glycosylamine-Fmoc (0.2 mmol, 20 mL) in 15% ammonia overnight at ambient temperature. Filter (Nylon, 0.45 μm), concentrate and freeze-dry the resulting mixture.
9. Recovery of the starting reducing sugar: glycosylamines are hydrolyzed with 2% aqueous acetic acid solution (2 mL) at 65 °C for 2 d.
10. An alternative nondestructive derivatization of carbohydrates based on the formation of glycosylamines is reported in **Note 5**.

3.2. Use of Highly Alkaline Buffers for Underivatized Neutral Sugars (Analysis of Synthesis Mixtures of Glycosylamines)

1. Rinse the capillary for 2 min with a 0.1 *N* NaOH solution at a vacuum pressure of 67.6 kPa.
2. Condition the capillary by flushing with separation buffer for 4 min at a vacuum pressure of 67.6 kPa.
3. Load the samples under vacuum at a pressure of 16.9 kPa for 1.5 s.
4. CE conditions: voltage: 10 kV; detection: 256 nm at the anode; temperature: 30 °C; buffer: 6 m*M* sorbate +0.5 m*M* TTAB, pH 12.5 (*see* **Note 6**).
5. **Figure 3** shows the results obtained for analysis of glucose, fructose, galactose, lactose and lactulose, resulting in synthesis mixture of glucosylamine **(Fig. 3A)**, galactosylamine **(Fig. 3B)**, and lactosylamine **(Fig. 3B)** (*see* **Note 7**). Molar percentages of the mentioned reducing sugars were between 5.4 and 7.1%. As a result of the selectivity of CE, the occurrence of partial isomerization of glucose and lactose during the synthesis of the corresponding glycosylamines was evidenced. The extent of such isomerization was also elucidated upon assessment of carbohydrate composition in the reaction mixtures ***(135)***.

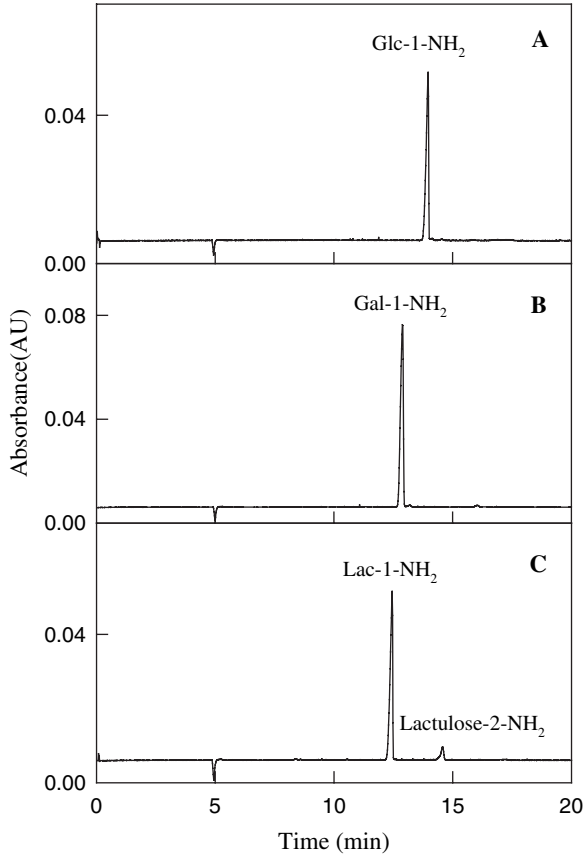


Fig. 2. Micellar electrokinetic chromatography-ultraviolet analysis of: **(A)** glucose (0.8 mg/mL); **(B)** galactose (1.26 mg/mL); and **(C)** lactose (1.0 mg/mL), all converted in glycosylamines and derivatized with Fmoc; voltage: 20 kV; detection at 260 nm (cathode); temperature: 30 °C; buffer: 20 m*M* borax+25 m*M* SDS, pH 9.2. (Reprinted from **ref**. ***135***, with permission of CRC Press.)

3.3. Use of Borate-Based Separation Buffers for Derivatized and Underivatized Sugars (Identification of Anomeric Forms of O- and C-Allyl Glycosides)

1. Wash the capillary for 2 min at a vacuum pressure of 67.6 kPa with NaOH 0.1 *N*.
2. Condition the capillary for 2 min by flushing the working buffer under a vacuum pressure of 67.6 kPa.
3. Load the samples under vacuum at a pressure of 16.9 kPa for 1.5 s.

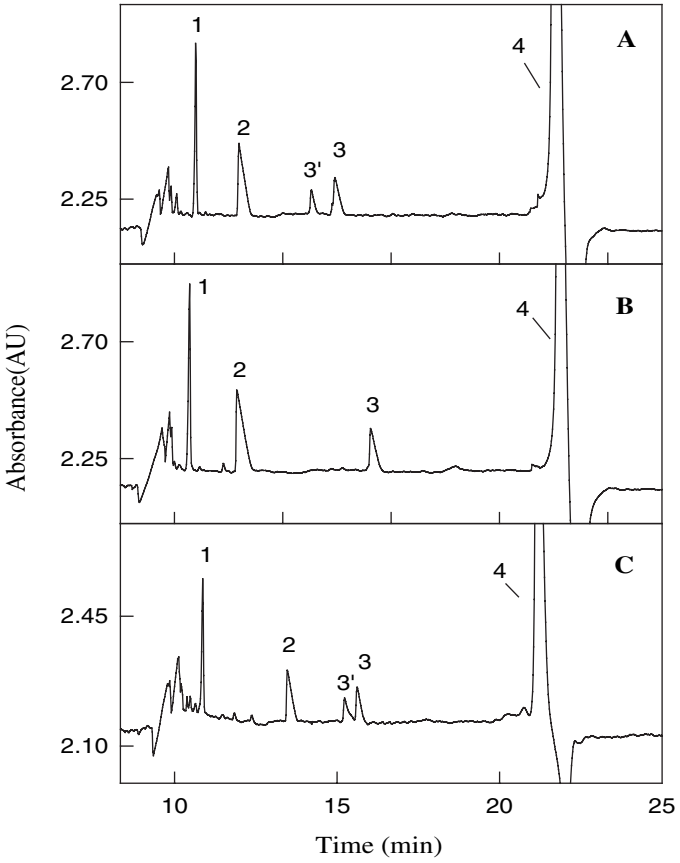


Fig. 3. Capillary zone electrophoresis-indirect ultraviolet analysis of: **(A)** glucosylamine: (1) 0.7 m*M* galacturonic acid (i.s.), (2) glucosylcarbamate, (3′) fructose, (3) glucose, (4) contribution from glucosylamine; **(B)** galctosylamine: (1) 0.7 m*M* galacturonic acid (i.s.), (2) galactosylcarbamate, (3) galactose, (4) contribution from galactosylamine; **(C)** lactosylamine: (1) 0.7 m*M* galacturonic acid (i.s.), (2) lactosylcarbamate, (3′) lactulose, (3) lactose, (4) contribution from lactosylamine. Voltage: 10 kV; indirect detection: 256 nm at the anode (*see* **Note 6**); temperature: 30 °C; buffer: 6 m*M* sorbate+0.5 m*M* tetradecyltrimethylammonium bromide, pH 12.5. (Reprinted from **ref**. ***135***, with permission of CRC Press.)

4. CE conditions: voltage: 15 kV; detection: 195 nm at the cathode; temperature: 30 °C; buffer for *C*-allyl-glycosides: 100 m*M* borax +100 m*M* SDS (pH 9.2); buffer for *O*-allyl-glycosides: 25 m*M* borax +250 m*M* SDS (pH 9.2).

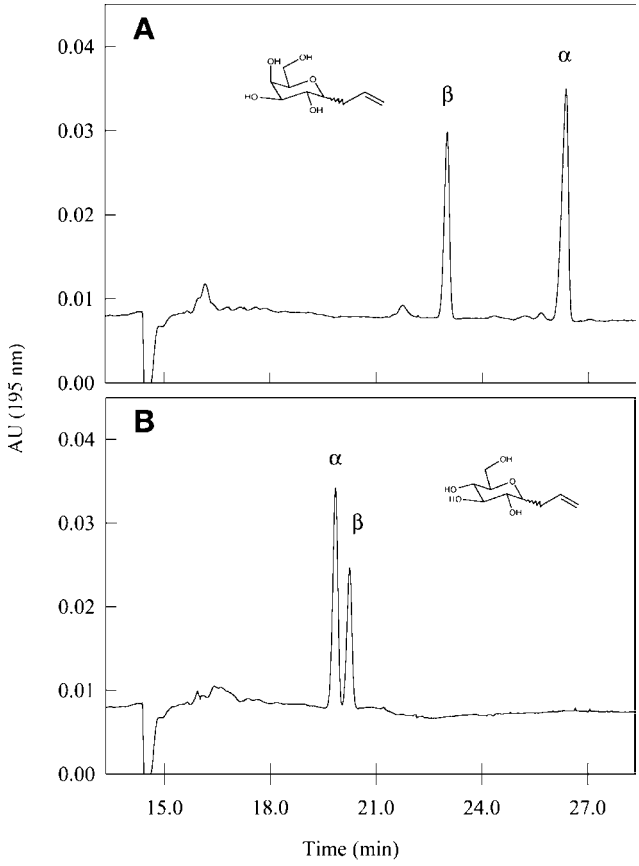


Fig. 4. Micellar electrokinetic chromatography-ultraviolet analysis of *C*-allyl-galactopyranosides **(A)** and *C*-allyl-glucopyranosides **(B)** anomeric mixtures from crude synthesis mixtures diluted 1:5 with water. Operative conditions: voltage, 15 kV; detection: 195 nm at the cathode; temperature, 30 °C; buffer, 100 m*M* borax+100 m*M* sodium dodecyl sulfate, pH 9.2 (*see* **Note 8**).

5. **Figure 4** shows the electropherograms relative to a mixture of α-and β-*C*-allyl glucopyranosides **(Fig. 4A)** and galactopyranosides **(Fig. 4B)** (*see* **Note 8**) diluted 1:10 with water before injection in the CE system.
6. **Figure 5** reports the results of the electrophoretic analysis of α- and β-*O*-allyl-galactopyranosides and α- and β-*O*-allyl-glucopyranosides (4.5–5 m*M*).
7. The presence of borate and SDS in the separation buffer improved both separation selectivity and detection sensitivity (*see* **Notes 9** and **10**).

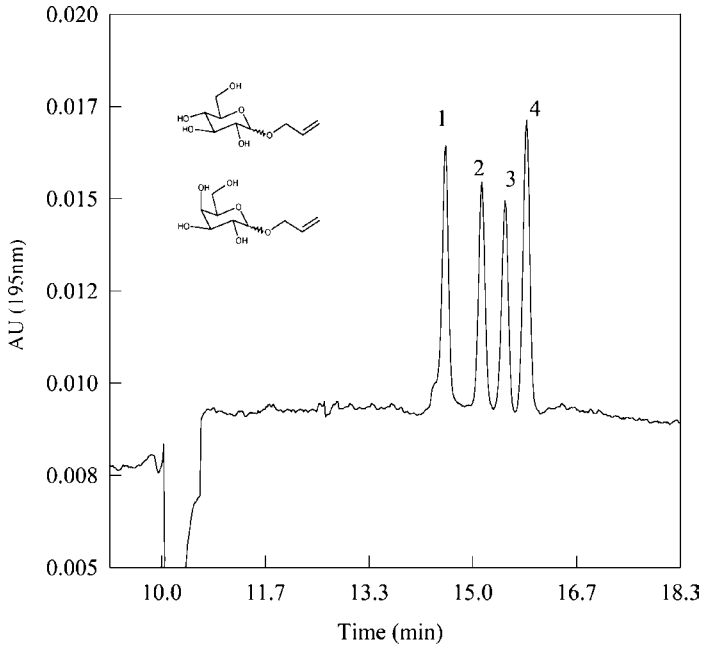


Fig. 5. Micellar electrokinetic chromatography-ultraviolet analysis of a mixture of 5 m*M* *O*-allyl-α-glucopyranoside **(1)**, 4.5 m*M* *O*-allyl-β-glucopyranoside **(2)**, 4.5 m*M* *O*-allyl-β-galactopyranoside **(3)**, and 5 m*M* *O*-allyl-α-galactopyranoside **(4)**. Operative conditions: voltage, 15 kV; detection: 195 nm at the cathode; temperature, 30 °C; buffer, 25 m*M* borax+250 m*M* sodium dodecyl sulfate, pH 9.2.

4. Notes

1. Procedure for the synthesis of *C*-allyl-galactospyranoside and *C*-allyl-glucopyranoside anomeric couples: glucose or galactose pentaacetate (1 mmol) in dichloroethane (2 mL) with allyl trimethylsilane (5 eq) and boron trifluoride diethyl etherate (5 eq) were heated at 60 °C overnight. After extraction and purification with flash chromatography, the products were deacetylated in methanol solution (5 mL) with 2 mL of 0.5 *M* sodium methoxide overnight under reflux (all reagents from Sigma, St. Louis, MO).
2. Glycosylamines are readily hydrolyzed in neutral or weakly acidic solutions ***(135***, ***143***,***147)***. The pH of the reactions in which glycosylamines are involved should not be in this range, in order to avoid the formation of the starting reducing sugars.
3. Typically, the yield of the synthesis of glycosylamines is 75% ***(135)***. Considering that subsequent reaction with Fmoc is quantitative, the value of the yield of the overall derivatization procedure is 75%. Careful calibration with standard amounts of sugars must be carried out for a reliable quantitative analysis.

4. The presence of lactulosylamine-Fmoc **(Fig. 2C)** is originated by the isomerization of lactose in the highly alkaline conditions in which glycosylamines are synthetized (*see also* **Subheading 3.2.**) ***(135)***.
5. Another convenient nondestructive derivatization of carbohydrates is formation of *N*-(2-pyridinyl)-glycosylamines with the use of 2-aminopyridine ($\lambda_{max} = 240$ nm). This reaction gives rise to UV-detectable glycosylamines: sugar (10 mg) is dissolved in 500 μL of aqueous 2-aminopyridine solution at pH 7.0 (prepared by dissolving 1 g of 2-AP in 0.8 mL 6 *N* HCl and 1.6 mL of water) at 65 °C for 10 h ***(136,141)***. The regeneration of the original sugars is an acidic hydrolysis with 2% aqueous acetic acid solution (2 mL) at 65 °C for 2 d.
6. TTAB is a quaternary ammonium salt, usually added to the working buffer in order to reverse the electroosmotic flow and to induce rapid migration of anionic analytes. Separation is carried out in reversed polarity.
7. When detection is performed with indirect UV monitoring, positive signals can be obtained instead of the typical negative peaks by simply reversing the output polarity of the detector.
8. The attribution of the peaks was possible by comparing the migration times obtained with the analysis of a solution containing 95% of α-anomer and 5% of β-anomer; this was achieved by simply performing the synthesis in acetonitrile instead of dichloroethane (*see* **Note 1**).
9. Comparison between the results obtained using borate-based buffers and acetate-based buffers (195 nm) demonstrated that complexation of glycosides with borate imply an increase in UV response of two times for glucosides and four times for galactosides. This different behavior reflects the different stabilities of the borate complexes for galactosides and glucosides ***(54)***.
10. The peculiar behavior of the galactoside and glucoside anomeric couples can be attributed to the various stabilities of borate-glycoside complexes as well as to the interaction with SDS micelles.

Acknowledgments

We wish to express our thanks to Professor Paoletti and his research group (Department of Biochemistry, Biophysics and Macromolecular Chemistry, University of Trieste) for introducing us to the wonders of glycobiology.

References

1. McNaught, A. D. (1997) Nomenclature of carbohydrates (Recommendations 1996). *Carbohydr. Res*. **297**, 1–90.
2. Varki, A., Cummings, R., Esko, J., Freeze, H., Hart, G., and Marth, J., (eds.) (1999) *Essentials of glycobiology*, Cold Spring Laboratory Press, Cold Spring Harbor, NY (available on-line in the Bookshelf of the PubMed site http://www.ncbi.nlm.nih.gov/entrez/query.fcgi).
3. Lindhorst, T. K. (2000) *Essentials of Carbohydrate Chemistry and Biochemistry*. Wiley-VCH Verlag, Wheinheim.

4. El Rassi, Z. (ed.) (2002) *Carbohydrate Analysis by Modern Chromatography and Electrophoresis*. Journal of Chromatography Library, Vol. 66, Elsevier, Amsterdam.
5. Churms, S. (1990) Recent developments in the chromatographic analysis of carbohydrates. *J. Chromatogr*. **500**, 555–583.
6. Bleton, J., Mejanelle, P., Sansoulet, J., Goursaud, S., and Tchapla, A. (1996) Characterization of neutral sugars and uronic acids after methanolysis and trimethylsilylation for recognition of plant gums. *J. Chromatogr. A* **720**, 27–49.
7. Whiton, R. S., Lau, P., Morgan, L, Gilbart, J., and Fox, A. (1985) Modifications in the alditol acetate method for analysis of muramic acid and other neutral and amino sugars by capillary gas chromatography- mass spectrometry with selected ion monitoring. *J. Chromatogr*. **347**, 109–120.
8. Paskach, T. J., Lieker, H. P., Reilly, P. J., and Thielecke, K. (1991) High-performance anion-exchange chromatography of sugars and sugar alcohols on quaternary ammonium resins under alkaline conditions. *Carbohydr. Res*. **215**, 1–14.
9. Lee, Y. C. (1996) Carbohydrate analysis with high-performance anion- exchange chromatography. *J. Chromatogr. A*. **720**, 137–149.
10. Cataldi, T. R. I., Campa, C., and De Benedetto, G. E. (2000) Carbohydrate analysis by high-performance anion-exchange chromatogrphy with pulsed amperometric detection: the potential is still growing. *Fresenius J. Anal. Chem*. **368**, 739–758.
11. Cataldi, T. R. I., Campa, C., Margiotta, G., and Bufo, S. A. (1998) Role of barium ions in the anion-exchange chromatographic separation of carbohydrates with pulsed amperometric detection. *Anal. Chem*. **70**, 3940–3945.
12. Cataldi, T. R. I., Campa, C., Angelotti, M., and Bufo, S. A. (1999) Isocratic separations of closely- related mono- and disaccharides by high- performance anion-exchange chromatography with pulsed amperometric detection using dilute alkaline spiked with barium acetate. *J. Chromatogr. A* **855**, 539–550.
13. Campa, C., Oust, A., Skjåk Bræk, G., et al. (2004) Determination of average degree of polymerisation and distribution of oligosaccharides in a partially acid-hydrolysed homopolysaccharide: a comparison of four experimental methods applied to mannuronan. *J. Chromatogr. A* **1026**, 271–281.
14. Conboy, J. J. and Henion, J. (1992) High-performance anion-exchange chromatography coupled with mass spectrometry for the determination of carbohydrates. *Biol. Mass Spectrom*. **21**, 397–407.
15. Wunschel, D. S., Fox, K. F., Fox, A., et al. (1997) Quantitative analysis of neutral and acidic sugars in whole bacterial cell hydrolysates using high- performance anion- exchange liquid chromatography- electrospray ionization tandem mass spectrometry. *J. Chromatogr. A* **776**, 205–219.
16. Okatch, H., Torto, N., and Armateifio, J. (2003) Characterisation of legumes by enzymatic hydrolysis, microdialysis sampling, and micro-high-performance anion-exchange chromatography with electrospray ionisation mass spectrometry. *J. Chromatogr. A* **992**, 67–74.

17. Karlsson, N. G., Schulz, B. L., and Packer, N. H. (2004) Structural determination of neutral O-linked oligosaccharide alditols by negative ion LC-Electrospray-MS^n. *J. Am. Soc. Mass Spectrom.* **15**, 659–672.
18. Schmid, D., Behnke, B., Metzger, J., and Kuhn, R. (2002) Nano-HPLC- mass spectrometry and MEKC for the analysis of oligosaccharides from human milk. *Biomed. Chromatogr.* **16**, 151–156.
19. Todoroki, K., Hayama, T., Ijiri, S., et al. (2004) Rhodamine B amine as a highly sensitive fluorescence derivatization reagent for saccharides in reversed-phase liquid chromatography. *J. Chromatogr. A* **1038**, 113–120.
20. Blanken, W. M., Bergh, M. L. E., Koppen, P. L., and van den Eunden, D. H. (1985) High-pressure liquid chromatography of neutral oligosaccharides: effects of structural parameters. *Anal. Biochem.* **145**, 322–330.
21. Churms, S. C. (1996) Recent progress in carbohydrate separation by high-performance liquid chromatography based on hydrophilic interaction. *J. Chromatogr. A* **720**, 75–91.
22. Stefansson, M. and Westerlund, D. (1996) Ligand-exchange chromatography of carbohydrates and glycoconjugates. *J. Chromatogr. A* **720**, 127–136.
23. Churms, S. C. (1996) Recent progress in carbohydrate separation by high-performance liquid chromatography based on size exclusion. *J. Chromatogr. A* **720**, 151–166.
24. Takahashi, N. (1996) Three-dimensional mapping of N-linked oligosaccharides using anion-exchange, hydrophobic and hydrophilic interaction modes of high-performance liquid chromatography. *J. Chromatogr. A* **720**, 217–225.
25. Lamari, F. N., Kuhn, R., and Karamanos, N. K. (2003) Derivatization of carbohydrates for chromatographic, electrophoretic and mass spectrometric structure analysis. *J. Chromatogr. B* **793**, 15–36.
26. Okafo, G., Burrow, L., Carr, S. A., Roberts, G. D., Johnson, W., and Camilleri, P. (1996) A coordinated high-performance liquid chromatographic, capillary electrophoretic, and mass spectrometric approach for the analysis of oligosaccharide mixtures derivatized with 2-aminoacridone. *Anal. Chem.* **68**, 4424–4430.
27. Klockow, A., Paulus, A., Figuereiso, V., Amadò, R., and Widmer, H. M. (1994) Determination of carbohydrates in fruit juices by capillary electrophoresis and high-performance liquid chromatography. *J. Chromatogr. A* **680**, 187–200.
28. Cabálková, J., Zidková, J., Pribyla, L., and Chmelík, J. (2004) Determination of carbohydrates in juices by capillary electrophoresis, high-performance liquid chromatography, and matrix-assisted laser desorption/ionization-time of flight-mass spectrometry. *Electrophoresis* **25**, 487–493.
29. Kang, S. H., Jung, H., Kim, N., Shin, D. H., and Chung, D. S. (2000) Micellar electrokinetic chromatography for the analysis of D-amigdalin and its epimer in apricot kernel. *J. Chromatogr. A* **866**, 253–259.
30. Chmelík, J., Chemlíková, J., and Novotny, M. (1997) Characterization of dextrans by size-exclusion chromatography on silica gel columns, with light-scattering detection, and capillary electrophoresis with laser-induced fluorescence. *J. Chromatogr. A* **790**, 93–100.

31. Soga, T. and Imaizumi, M. (2001) Capillary electrophoresis method for the analysis of inorganic anions, organic acids, amino acids, nucleotides, carbohydrates and other anionic compounds. *Electrophoresis* **22**, 3418–3425.
32. Soga, T. and Ross, G. A. (1999) Simultaneous determination of inorganic anions, organic acids, amino acids and carbohydrates by capillary electrophoresis. *J. Chromatogr. A* **837**, 231–239.
33. Paulus, A. and Klockow, A. (1996) Detection of carbohydrates in capillary electrophoresis. *J. Chromatogr. A* **720**, 353–376.
34. Ye, J. and Baldwin, R. P. (1993) Amperometric detection in capillary electrophoresis with normal size electrodes. *Anal. Chem*. **65**, 3525–3527.
35. Ye, J. and Baldwin, R. P. (1994) Determination of carbohydrates, sugar acids and alditols by capillary electrophoresis and electrochemical detection at a copper electrode. *J. Chromatogr. A* **687**, 141–148.
36. Baldwin, R. P. (2002) Electrochemical detection of carbohydrates at constant potential after HPLC and CE separations, in *Carbohydrate Analysis by Modern Chromatography and Electrophoresis* (El Rassi, Z., ed.), Journal of Chromatography Library, Vol. 66, Elsevier, Amsterdam: pp. 947–959.
37. Auriola, S., Thibault, P., Sadovskaya, I., and Altman, E. (1998) Enhancement of sample loadings for the analysis of oligosaccharides isolated from *Pseudomonas aeruginosa* using transient isotachophoresis and capillary zone electrophoresis-electrospray mass spectrometry. *Electrophoresis* **19**, 2665–2676.
38. Li, J., Thibault, P., Martin, A., Richards, J. C., Wakarchuk, W. W., and van der Wilp, W. (1998) Development of an on-line preconcentration method for the analysis of pathogenic lipopolysaccharides using capillary electrophoresis-electrospray mass spectrometry. Application to small colony isolates. *J. Chromatogr. A* **817**, 325–326.
39. Thibault, P., and Honda, S. (eds.) (2003) *Capillary Electrophoresis of Carbohydrates*, Humana, Totowa, NJ.
40. El Rassi, Z. (1996) *High Performance Capillary Electrophoresis of Carbohydrates*. Beckman Instruments, Fullerton, CA.
41. Novotny, M., and Sudor, J. (1993) High-performance capillary electrophoresis of glycoconjugates. *Electrophoresis* **14**, 373–389.
42. Tomás-Barberán, F. A. (1995) Capillary electrophoresis: a new technique in the analysis of plant secondary metabolites. *Phytochem. Anal*. **6**, 177–192.
43. Honda, S. (1996) Separation of neutral carbohydrates by capillary electrophoresis. *J. Chromatogr. A* **720**, 337–351.
44. El Rassi, Z. (1997) Recent developments in capillary electrophoresis of carbohydrate species. *Electrophoresis* **18**, 2400–2407.
45. Suzuki, S. and Honda, S. (1998) A tabulated review of capillary electrophoresis of carbohydrates. *Electrophoresis* **19**, 2539–2560.
46. El Rassi, Z. (1999) Recent developments in capillary electrophoresis and capillary electrochromatography of carbohydrate species. *Electrophoresis* **20**, 3134–3144.
47. Lamari, F. and Karamanos, N. K. (1999) High performance capillary electrophoresis as a powerful analytical tool of glycoconjugates. *J. Liq. Chrom. Rel. Technol*. **22**, 1295–1317.

48. Baldwin, R. P. (1999) Electrochemical determination of carbohydrates: Enzyme electrodes and amperometric detection in liquid chromatography and capillary electrophoresis. *J. Pharm. Biomed. Anal*. **19**, 69–81.
49. Raju, T.S. (2000) Electrophoretic methods for the analysis of *N*-linked oligosaccharides. *Anal. Biochem*. **283**, 125–132.
50. Soga, T. (2002) Analysis of carbohydrates in food and beverages by HPLC and CE, in *Carbohydrate Analysis by Modern Chromatography and Electrophoresis* (El Rassi, Z., ed.). Journal of Chromatography Library, Vol. 66, Elsevier, Amsterdam: pp.483–502.
51. El Rassi, Z. (2002) Capillary electrophoresis and electrochromatography of carbohydrates, in *Carbohydrate Analysis by Modern Chromatography and Electrophoresis* (El Rassi, Z.,ed.), Journal of Chromatography Library, Vol. 66, Elsevier, Amsterdam: pp. 597–676.
52. Honda, S., Suzuki, S., and Taga, A. (2003) Analysis of carbohydrates as 1-phenyl-3-methyl-5-pyrazolone derivatives by capillary/microchip electrophoresis and capillary electrochromatography. *J. Pharm. Biomed. Anal*. **30**, 1689–1714.
53. Honda, S., Iwase, S., Makino, A., and Fujiwara, S. (1989) Simultaneous determination of reducing monosaccharides by capillary zone electrophoresis as the borate complexes of N-2-pyridylglycamines. *Anal. Biochem*. **176**, 72–77.
54. Hoffstetter-Kuhn, S., Paulus, A., Gassmann, E., and Widmer, H. M. (1991) Influence of borate complexation on the electrophoretic behaviour of carbohydrates in capillary electrophoresis. *Anal. Chem*. **63**, 1541–1547.
55. Honda, S., Suzuki, S., Nose, A., Yamamoto, K., and Kakehi, K. (1991) Capillary zone electrophoresis of reducing mono- and oligo-saccharides as the borate complexes of their 3-methyl-1-phenyl-2-pyrazolin-5-one derivatives. *Carbohydr. Res*. **215**, 193–198.
56. Honda, S., Yamamoto, F., Suzuki, S., Ueda, M., and Kakehi, K. (1991) High-performance capillary zone electrophoresis of carbohydrates in the presence of alkaline earth metal ions. *J. Chromatogr*. **588**, 327–333.
57. Oefner, P. J., Vorndran, A. E., Grill, E., Huber, C., and Bonn, G. K. (1992) Capillary zone electrophoretic analysis of carbohydrates by direct and indirect UV detection. *Chromatographia* **34**, 308–316.
58. Arentoft, A. M., Michaelsen, S., and Sørensen, H. (1993) Determination of oligosaccharides by capillary zone electrophoresis. *J. Chromatogr. A* **652**, 517–524.
59. Stefansson, M. and Westerlund, D., (1993) Capillary electrophoresis of glycoconjugates in alkaline media. *J. Chromatog*. **632**, 195–200.
60. Morin, Ph., Villard, F., and Dreux, M. (1993) Separation of flavonoid-7-O-glycosides differing in their flavonoid aglycone. *J. Chromatogr*. **628**, 153–160.
61. Morin, Ph., Villard, F., Dreux, M., and André, P. (1993) Separation of flavonoid-3-O-glycosides differing in their sugar moiety. *J. Chromatogr*. **628**, 161–169.
62. Chiesa, C. and Horváth, C. (1993) Capillary zone electrophoresis of maltooligosaccharides derivatized with 8-aminonaphtalene-1,3,6-trisulfonic acid. *J. Chromatogr*. **645**, 337–352.

63. Schwaiger, H., Oefner, P. J., Huber, C., Grill, E., and Bonn, G. K. (1994) Capillary electrophoresis and micellar electrokinetic chromatography of 4-aminobenzonitrile carbohydrate derivatives. *Electrophoresis* **15**, 941–952.
64. Penn, S. G., Chiu, R. W., and Monnig, C. A. (1994) Separation and analysis of cyclodextrins by capillary electrophoresis with dynamic fluorescence labelling and detection. *J. Chromatogr. A* **680**, 233–241.
65. Evangelista, R. A., Liu, M.-S., and Chen, F.-T. A. (1995) Characterization of 9-Aminopyrene-1,4,6-trisulfonate- derivatized sugars by capillary electrophoresis with laser-induced fluorescence detection. *Anal. Chem*. **67**, 2239–2245.
66. Chen, F. A. and Evangelista, R. A. (1995) Analysis of mono- and oligosaccharide isomers derivatized with 9-aminopyrene-1,4,6-trisulfonate by capillary electrophoresis with laser-induced fluorescence. *Anal. Biochem*. **230**, 273–280.
67. Noe, C. R. and Freissmuth, J. (1995) Capillary zone electrophoresis of aldose enantiomers: separation after derivatization with S-(-)-1-phenylethylamine. *J. Chromatogr. A* **704**, 503–512.
68. Xu, X., Kok, W. Th., and Poppe, H. (1995) Sensitive determination of sugars by capillary zone electrophoresis with indirect UV detection under highly alkaline conditions. *J. Chromatogr. A* **716**, 231–240.
69. Lu, B. and Westerlund, D. (1996) Indirect UV detection of carbohydrates in capillary zone electrophoresis by using tryptophan as a marker. *Electrophoresis* **17**, 325–332.
70. Liu, Y., Shu, C., and Lamb, J. D. (1997) High-performance capillary electrophoretic separation of carbohydrates with indirect UV detection using diethylamine and borate as electrolyte additives. *J. Capillary Electrophor*. **4**, 97–103.
71. Nguyen, D. T., Lerch, H., Zemann, A., and Bonn, G. (1997) Separation of derivatized carbohydrates by co-electroosmotic capillary electrophoresis. *Chromatographia* **46**, 113–121.
72. Plocek, J. and Chmelik, J. (1997) Separation of disaccharides as their borate complexes by capillary electrophoresis with indirect detection in visible range. *Electrophoresis* **18**, 1148–1152.
73. Honda, S., Taga, A., Kotani, M., and Grover, E. R. (1997) Separation of aldose enantiomers by capillary electrophoresis in the presence of optically active N-dodecoxycarbonylvalines. *J. Chromatogr. A* **792**, 385–391.
74. Sato, K., Sato, K., Okubo, A., and Yamazaki, S. (1997) Determination of monosaccharides derivatized with 2-aminobenzoic acid by capillary electrophoresis. *Anal. Biochem*. **251**, 119–121.
75. Sato, K., Sato, K., Okubo, A., and Yamazaki, S. (1998) Optimization of derivatization with 2-aminobenzoic acid for determination of monosaccharide composition by capillary electrophoresis. *Anal. Biochem*. **262**, 195–197.
76. Akiyama, T., Yamada, T., and Maitani, T. (2000) Analysis of enzymatically glucosylated flavonoids by capillary electrophoresis. *J. Chromatogr. A* **895**, 279–83.
77. Li, D. T., Sheen, J. F., and Her, G. R. (2000) Structural analysis of chromophore-labeled disaccharides by capillary electrophoresis tandem mass spectrometry using ion trap mass spectrometry. *J. Am. Soc. Mass Spectrom*. **11**, 292–300.

78. Taga, A., Suzuki, S., and Honda, S. (2001) Capillary electrophoretic analysis of carbohydrates derivatized by in-capillary condensation with 1-phenyl-3-methyl-5-pyrazolone. *J. Chromatogr. A* **911**, 259–267.
79. Larsson, M., Sundberg, R., and Folestad, S. (2001) On-line capillary electrophoresis with mass spectrometry detection for the analysis of carbohydrates after derivatization with 8-aminonaphtalene-1,3,6- trisulfonic acid. *J. Chromatogr. A* **934**, 75–85.
80. Honda, S., Makino, A., Suzuki, S., and Kakehi, K. (1990) Analysis of the oligosaccharides in ovalbumin by high-performance capillary electrophoresis. *Anal. Biochem*. **191**, 228–234.
81. Liu, J., Shirota, O., Wiesler, D., and Novotny, M. (1991) Ultrasensitive fluorometric detection of carbohydrates as derivatives in mixtures separated by capillary electrophoresis. *Proc. Nat. Acad*. Sci. **88**, 2302–2306.
82. Liu, J., Shirota, O., and Novotny, M. (1991) Capillary electrophoresis of amino sugars with laser-induced fluorescence detection. *Anal. Chem*. **63**, 413–417.
83. Hermentin, P., Doenges, R., Witzel, R., et al. (1994) A strategy for the mapping of N-glycans by high-performance capillary electrophoresis. *Anal. Biochem*. **221**, 29–41.
84. Kakehi, K., Susami, A., Taga, A., Suzuki, S., and Honda, S. (1994) High performance capillary electrophoresis of O-glycosidically linked sialic acid-containing oligosaccharides in glycoproteins as their alditol derivatives with low-wavelenght UV monitoring *J. Chromatogr. A*. **680**, 209–215.
85. Camilleri, P., Harland, G. B., and Okafo, G. (1995) High resolution and rapid analysis of branched oligosaccharides by capillary electrophoresis. *Anal. Biochem*. **230**, 115–122.
86. Weber, P. L. and Lunte, S. M. (1996) Capillary electrophoresis with pulsed amperometric detection of carbohydrates and glycopeptides. *Electrophoresis* **17**, 302–309.
87. Evangelista, R. A., Chen, F. A., and Guttman, A. (1996) Reductive amination of N-linked oligosaccharides using organic acid catalysis. *J. Chromatogr. A* **745**, 273–280.
88. Guttman, A., Chen, F. T., Evangelista, R. A., and Cooke, N. (1996) High-resolution capillary gel electrophoresis of reducing oligosaccharides labelled with 1-aminopyrene-3,6,8-trisulfonate. *Anal. Biochem*. **233**, 234–242.
89. Guttman, A. (1997) Analysis of monosaccharide composition by capillary electrophoresis. *J. Chromatogr. A* **763**, 271–277.
90. Soga, T. and Heiger, D. N. (1998) Simultaneous determination of monosaccharides in glycoproteins by capillary electrophoresis. *Anal. Biochem*. **261**, 73–78.
91. Iwase, H., Tanaka, A., Hiky, Y., et al. (1999) Mutual separation of hinge-glycopeptide isomers bearing five N-acetylgalactosamine residues from normal human serum immunoglobulin A1 by capillary electrophoresis. *J. Chromatogr. B* **728**, 175–183.
92. Kakehi, K., Funakubo, T., Suzuki, S., Oda, Y., and Kitada, Y. (1999) 3-aminobenzamide and 3-aminobenzoic acid, tags for capillary electrophoresis of complex carbohydrates with laser-induced fluorescent detection. *J. Chromatogr. A* **863**, 205–218.

93. Huang, Y., Mechref, Y., and Novotny, M. (2001) Microscale nonreductive release of O-linked glycans for subsequent analysis through MALDI mass spectrometry and capillary electrophoresis. *Anal. Chem*. **73**, 6063–6069.
94. Gennaro, L. A., Delaney, J., Vouros, P., Harvey, D. J., and Domon, B. (2002) Capillary electrophoresis/electrospray ion trap mass spectrometry for the analysis of negatively charged derivatized and underivatized glycans. *Rapid. Commun. Mass. Spectrom*. **16**, 192–200.
95. Colón, L. A., Dadoo, R., and Zare, R. N. (1993) Determination of carbohydrates by capillary zone electrophoresis with amperometric detection at a copper microelectrode. *Anal. Chem*. **65**, 476–481.
96. Lee, Y.-H. and Lin, T.-I. (1996) Determination of carbohydrates by high-performance capillary electrophoresis with indirect absorbance detection. *J. Chromatogr. B* **681**, 87–97.
97. Chen, M-C. and Huang, H-J. (1997) Application of a nickel-microelectrode-incorporated end-column detector for capillary electrophoretic determination of alditols and alcohols. *Anal. Chim. Acta*. **341**, 83–90.
98. Zemann. A., Nguyen, D. T., and Bonn, G. (1997) Fast separation of underivatized carbohydrates by coelectroosmotic capillary electrophoresis. *Electrophoresis* **18**, 1142–1147.
99. Soga, T. and Serwe, M. (2000) Determination of carbohydrates in food samples by capillary electrophoresis with indirect UV detection. *Food Chemistry* **69**, 339–344.
100. Klampfl, C. W. and Buchberger, W. (2001) Determination of carbohydrates by capillary electrophoresis with electrospray-mass spectrometric detection. *Electrophoresis* **22**, 2737–2742.
101. Stroka, J., Dossi, N., and Anklam, E. (2003) Determination of the artificial sweetener Sucralose by capillary electrophoresis. *Food. Addit. Contam*. **20**, 524–527.
102. Carvalho, A. Z., da Silva, J. A., and do Lago, C. L. (2003) Determination of mono- and disaccharides by capillary electrophoresis with contactless conductivity detection. *Electrophoresis* **24**, 2138–2143.
103. Gel-Moreto, N., Streich, R., and Galensa, R. (2003) Chiral separation of diastereomeric flavanone-7-O-glycosides in citrus by capillary electrophoresis. *Electrophoresis* **24**, 2716–2722.
104. Simonet, B. M., Rios, A., Grases, F., and Valcarcel, M. (2003) Determination of myo-inositol phosphates in food samples by flow injection-capillary zone electrophoresis. *Electrophoresisis* **24**, 2092–2098.
105. Lambertsen Larsen, K. Mathiesen, F., and Zimmermann, W. (1997) Separation and analysis of cyclodextrins by capillary zone electrophoresis. *Carbohydr. Res*. **298**, 59–63.
106. Hong, M., Soini, H., Baker, A., and Novotny, M. V. (1998) Complexation between amylodextrin oligomers and selected pharmaceutical measured through capillary electrophoresis. *Anal. Chem*. **70**, 3590–3597.
107. Wang, X. Y., Chen, Y., Li, Z., and Wang, Z. (2002) Analysis of carbohydrates by capillary zone electrophoresis with on-capillary derivatization. *J. Liq. Chrom. & Rel. Technol*. **25**, 589–600.

108. Song, J. F., Weng, M. Q., Wu, S. M., and Xia, Q. C. (2002) Analysis of neutral saccharides in human milk derivatized with 2-aminoacridone by capillary electrophoresis with laser-induced fluorescence detection. *Anal. Biochem.* **304**, 126–129.
109. Jamali, B. and Nielsen, H. M. (2003) Development and validation of a capillary electrophoresis-indirect photometric detection method for the determination of the non-UV-absorbing 1,4-dideoxy-1,4-imino-D-arabinitol in active pharmaceutical ingredients, solutions and tablets using an internal standard. *J. Chromatogr. A* **996**, 213–223.
110. Kamoda, S., Nomura, C., Kinoshita, M., et al. (2004) Profiling analysis of oligosaccharides in antibody pharmaceuticals by capillary electrophoresis. *J. Chromatogr. A* **1050**, 211–216.
111. Kenndler, E., Schwer, C., Fritsche, B., and Pöhm, M. (1990) Determination of arbutin in uvae-ursi folium (bearberry leaves) by capillary zone electrophoresis. *J. Chromatogr.* **514**, 383–388.
112. Honda, S., Suzuki, K., Kataoka, M., Makino, A., and Kakehi, K. (1990) Analysis of the components of *Paeonia radix* by capillary zone electrophoresis. *J. Chromatogr.* **515**, 653–658.
113. Morin, Ph. and Dreux, M. (1993) Factors influencing the separation of ionic and non-ionic chemical natural compounds in plant extract by capillary electrophoresis. *J. Liq. Chrom.* **16**, 3735–3755.
114. Frias, J., Price, K. R., Fenwick, G. R., Hedley, C. L., Sørensen, H., and Vidal-Valverde, C. (1996) Improved method for the analysis of alpha-galactosides in pea seeds by capillary zone electrophoresis. Comparison with high-performance liquid chromatography-triple-pulsed amperometric detection. *J. Chromatogr. A.* **719**, 213–219.
115. Campa, C., Schmitt-Kopplin, P., Cataldi, T. R. I., Bufo, S. A., Freitag, D., and Kettrup, A. (2000) Analysis of cyanogenic glycosides by micellar capillary electrophoresis. *J. Chromatogr. B* **739**, 95–100.
116. Suomi, J., Sirén, H., Hartonen, K., and Riekkola, M-L. (2000) Extraction of iridoid glycosides and their determination by micellar electrokinetic capillary chromatography. *J. Chromatogr. A* **868**, 73–83.
117. Kang, S.H., Jung, H., Kim, N., Shin, D-H., and Chung, D. S. (2000) Micellar electrokinetic chromatography for the analysis of D-amygdalin and its epimer in apricot kernel. *J. Chromatogr. A* **866**, 253–259.
118. Warren, C. R. and Adams, M. A. (2000) Capillary electrophoresis for the determination of major amino acids and sugar in foliage: application to the nitrogen nutrition of sclerophyllus species. *Journal Experimental Botany* **51**, 1147–1157.
119. Bianco, G., Schmitt-Kopplin, P., De Benedetto, G., Kettrup, A., and Cataldi, T. R. I. (2002) Determination of glycoalkaloids and relative aglycones by nonaqueous capillary electrophoresis coupled with electrospray ionization-ion trap mass spectrometry. *Electrophoresis* **23**, 2904–2912.
120. Suomi, J., Wiedmer, S. K., Jussila, M., and Riekkola, M-L. (2002) Analysis of eleven iridoid glycosides by micellar electrokinetic capillary chromatography (MECC) and screening of plant samples by partial filling (MECC)-electrospray ionisation mass spectrometry. *J. Chromatogr. A* **970**, 287–296.

121. Seigler, D.S., Pauli, G.F., Nahrstedt, A., and Leen, R. (2002) Cyanogenic allosides and glucosides from Passiflora edulis and Carica papaya. *Phytochemistry* **60**, 873–882.
122. Marchart, E., Kopp, B. (2003) Capillary electrophoretic separation and quantification of flavone-*O*- and *C*-glycosides in *Achillea setacea*. *J. Chromatogr. B* **792**, 363–368.
123. Andersen, K. E., Bjergegaard, C., Møller, P., Sørensen, J. C., and Sørensen, H. (2003) High-performance capillary electrophoresis with indirect UV detection for determination of alpha-galactosides in Leguminosae and Brassicaceae. *J. Agric. Food. Chem*. **51**, 6391–6397.
124. Marchart, E., Krenn, L., and Kopp, B. (2003) Quantification of the flavonoid glycosides in Passiflora incarnata by capillary electrophoresis. *Planta Med*. **69**, 452–456.
125. Kang, S. H. (2003) On-line micellar electrokinetic chromatography-electrospray ionization mass spectrometry for the direct analysis of amygdalin epimers. *Bull. Korean. Chem. Soc*. **24**, 144–146.
126. Andersen, K. E., Bjergegaard, C., and Sørensen, H. (2003) Analysis of reducing carbohydrates by reductive tryptamine derivatization prior to micellar electrokinetic capillary chromatography. *J. Agric. Food. Chem*. **51**, 7234–7239.
127. Stefannson, M. and Novotny, M. (1994) Resolution of the branched forms of oligosaccharides by high-performance capillary electrophoresis. *Carbohydr. Res*. **258**, 1–9.
128. Stefannson, M. and Novotny, M. (1994) Separation of complex oligosaccharide mixtures by capillary electrophoresis in the open-tubular format. *Anal. Chem*. **66**, 1134–1140.
129. Rydlund, A. and Dahlman, O. (1996) Efficient capillary zone electrophoretic separation of wood-derived neutral acidic mono- and oligosaccharides. *J. Chromatogr. A* **738**, 129–140.
130. Monsarrat, B., Brando, T., Condouret, P., Nigou, J., and Puzo, G. (1999) Characterization of mannooligosaccharide caps in mycobacterial lipoarabinomannan by capillary electrophoresis/electrospray mass spectrometry. *Glycobiology* **9**, 335–342.
131. Ludwiczak, P., Brando, T., Monsarrat, B., and Puzo, G. (2001) Structural characterization of *Mycobacterium tuberculosis* lipoarabinomannans by the combination of capillary electrophoresis and matrix-assisted laser desorption/ionization time of flight mass spectrometry. *Anal. Chem*. **73**, 2323–2330.
132. Cescutti, P., Campa, C., Delben, F., and Rizzo, R. (2002) Structure of the oligomers obtained by enzymatic hydrolysis of the glucomannan produced by the plant Amorphophallus konjac. *Carbohydr. Res*. **337**, 2505–2511.
133. Zhang, Y., Le, X., Dovichi, N. J., et al. (1995) Monitoring biosynthetic transformations of N-acetyllactosamine using fluorescently labelled oligosaccharides and capillary electrophoretic separation. *Anal. Biochem*. **227**, 368–376.
134. Le, X., Scaman, C., Zhang, Y., et al. (1995) Analysis by capillary electrophoresis-laser-induced fluorescence detection of oligosaccharides produced from enzyme reactions. *J Chromatogr. A*. **716**, 215–20.

135. Campa, C., Donati, I., Vetere, A., Gamini, A., and Paoletti, S. (2001) Synthesis of glycosylamines: identification and quantification of side-products. *J. Carbohydr. Chem*. **20**, 263–273.
136. Campa, C., Vetere, A., Gamini, A., Donati, I., amd Paoletti, S. (2002) Enzymatic synthesis and characterization of oligosaccharides structurally related to the repeating unit of pullulan. *Biochem. Biophys. Res. Commun*. **297**, 382–389.
137. Vetere, A., Medeot, M., Campa, C., Donati, I., Gamini, A., and Paoletti, S. (2003) High-yield enzymatic synthesis of O-allyl-β-D-galactopyranoside. *J. Molec. Catalysis B: Enzymatic* **21**, 153–156.
138. Joucla, G., Brando, T., Remaud-Simeon, M., Monsan, P., and Puzo, G. (2004) Capillary electrophoresis analysis of glucooligosaccharide regioisomers. *Electrophoresis* **25**, 861–869.
139. Che, F. Y., Song, J. F., Zeng, R., Wang, K. Y., and Xia, Q. C. (1999) Analysis of 8-aminonaphtalene-1,3,6-trisulfonate-derivatized oligosaccharides by capillary electrophoresis- electrospray ionization quadrupole ion trap mass spectrometry. *J. Chromatogr. A* **858**, 229–238.
140. Lee, Y.-H. and Lin, T.-I. (1996) Capillary electrophoretic analysis of cyclodextrins and determination of formation constants for inclusion complexes. *Electrophoresis* **17**, 333–340.
141. Her, G. R., Santikarn, S., Reinhold, V. N., and Williams, J. C. (1987) Simplified approach to HPLC precolumn fluorescent labeling of carbohydrates: N-(2-pyridinyl)-glycosylamines. *J. Carbohydr. Chem*. **6**, 129–139.
142. Li, D. T. and Her, G. R. (1993) Linkage analysis of chromophore-labeled disaccharides and linear oligosaccharides by negative ion fast atom bombardment ionization and collisional-induced dissociation with B/E scanning. *Anal. Biochem*. **211**, 250–257.
143. Kallin, E., Lönn, H., Norberg, T., Sund, T., and Lunqvist, M. l. (1991) Derivatization procedures for reducing oligosaccharides.4. Use of glycosylamines in a reversible derivatization of oligosaccharides with the 9-fluorenylmethoxycarbonyl group, and HPLC separations of the derivatives. *J. Carbohydr. Chem*. **10**, 377–386.
144. Yeung, E. S. and Kuhr, W. G. (1991) Indirect detection methods for capillary separations. *Anal. Chem*. **63**, 275A–282A.
145. Damm, J. B. and Overklift, G. T. (1994) Indirect UV detection as a non-selective detection method in the qualitative and quantitative analysis of heparin fragments by high-performance capillary electrophoresis. *J Chromatogr. A* **678**, 151–65.
146. Shmitt-Kopplin, P., Fischer, K., Freitag, D., and Kettrup, A. (1998) Capillary electrophoresis for the simultaneous separation of selected carboxylated carbohydrates and their related 1,4-lactones. *J. Chromatogr*. **807**, 89–100.
147. Lubineau, A., Augé, J., and Droillat, B. (1995) Improved synthesis of glycosylamines and a straighforward preparation of *N*-acylglycosylamines as carbohydrate-based detergents. *Carbohydr. Res*. **266**, 211–219.

12

Capillary Electrophoresis of Sugar Acids

Cristiana Campa, Edi Baiutti, and Anna Flamigni

Summary

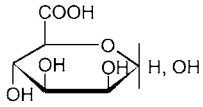
This chapter illustrates the usefulness of capillary electrophoresis (CE) for the analysis of sugar acids, that is, monosaccharides and lower oligosaccharides carrying carboxylate, sulphate or phosphate groups. In order to provide a general description of the main results and challenges in the field, some relevant applications and reviews on CE of such saccharidic compounds are tabulated. Furthermore, some detailed experimental procedures are shown, regarding the CE analysis of sugar acids released upon hydrolysis of acidic polysaccharides and of glycans linked to glycoproteins. In particular, the protocols will deal with the following compounds: (i) unsaturated, underivatized oligosaccharides from lyase-treated alginate; (ii) oligosaccharides derivatized with 4-aminobenzonitrile, arising from chemical hydrolysis of alginate; (iii) sialic acid derivatized with 2-aminoacridone, released from human serum immunoglobulin G.

Key Words: Capillary electrophoresis; sugar acids; sugar phosphates; carboxylated sugars; sulphated sugars; glycosaminoglycans oligosaccharides; uronic acids; sialic acids; tabulated review.

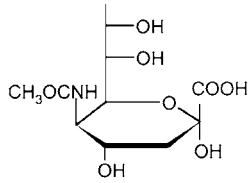
1. Introduction

Sugar acids are monosaccharides and lower oligosaccharides carrying carboxylate, sulphate or phosphate groups. **Scheme 1** reports the structures of some representative components of this category, that is, (i) uronic acids, (ii) glycosaminoglycans disaccharides and (iii) sialic acids. Uronic acids [monocarboxylic acids formally derived from aldoses by replacement of the C-6 alcohol group with a carboxy group ***(1)***] are the building blocks of polysaccharides extensively used in food and pharmaceutical industry, like alginates and pectins ***(2–4)***. The repeating disaccharide units of the glycosaminoglycans (i.e. hyaluronic acid, heparin, keratan sulphate, chondroitin sulphate

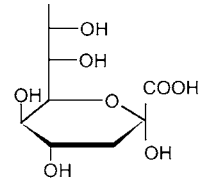
From: *Methods in Molecular Biology, vol. 384: Capillary Electrophoresis*
Edited by: P. Schmitt-Kopplin © Humana Press Inc., Totowa, NJ



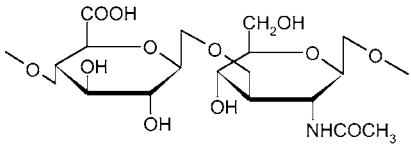
D-Mannuronic acid



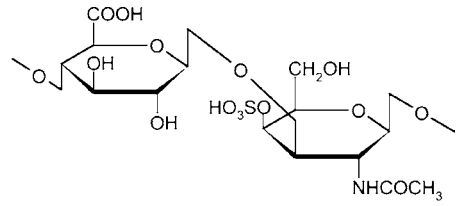
α-D-Neu5Ac



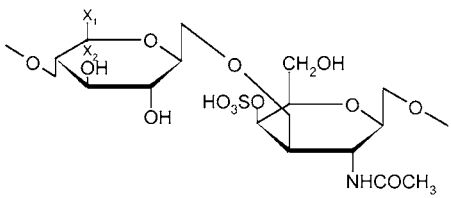
α-D-KDN



Hyaluronic acid

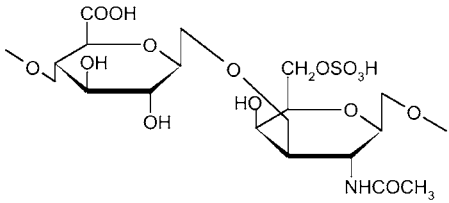


Chondroitin 4-sulfate



X_1= COOH/H;
X_2= H/COOH

Dermatan sulfate



Chondroitin 6-sulfate

Scheme 1.

and dermatan sulphate) consist of one hexosamine and one uronic acid or neutral hexose, where any of the free hydroxyl groups may carry a sulphate, with the exception of hyaluronic acid; moreover, the hexosamine units can be *N*-acetylated or *N*-sulphated ***(2,5,6)***. Sialic acids are typically found at the

'outermost' ends of *N*-glycans, *O*-glycans and glycosphingolipids as well as in polysialic acid, a homopolymer found only on few animal glycoproteins and in the capsular polysaccharides of certain pathogenic bacteria. The basic structures of sialic acids, 2-keto-5-acetamido-3,5-dideoxy-D-glycero-D-galactononulosonic acid (*N*-Acetylneuraminic acid, Neu5Ac) and 2-keto-3-deoxy-D-glycero-D-galactonononic acid, can be subjected to a wide variety of modifications, including de-acetylation, *N*-hydroxylation, methylation, sulphation and phosphorylation. Additional complexity derives from the various possibilities of glycosidic linkages ***(2**,**5**,**7**,**8)***.

The biological relevance of sugar acids is increasingly being recognized, due to their key role in a wide variety of processes ***(2**,**5)***. For instance, sialic acids are involved in cell–cell interactions ***(2**,**5**,**7**,**9)***; the activation of antithrombin III depends on a specific pentasaccharidic sequence of heparin, having a characteristic sulphation pattern ***(10**,**11)***; differential disaccharide composition of glycosaminoglycans has been suggested as an indicator for malignancies in gastrointestinal carcinomas ***(12)***; an increase in sialylation is often manifested in tumours ***(13**,**14)***, like in the case of α2-6-linked sialic acids attached to inner GalNAc-*O*-Ser/Thr units on *O*-glycans. Siaα2-6GalNAcα 1-*O*-Ser/Thr (called sialyl-Tn) is currently a target for attempts in cancer immunotherapy ***(5)***; sugar phosphates, which will be shortly mentioned below (*see* **Table 2**), are involved in cell-signalling pathways ***(15)***. Moreover, short oligomeric fragments of acidic polysaccharides have great relevance in biotechnology: in alginate, for example, distribution of mannuronic acid and guluronic acid strongly influence the stability, strength and porosity of the gels formed from this polysaccharide in the presence of calcium ions ***(3**,**16**,**17)***, which are used for cell encapsulation, drug delivery and tissue engineering.

Evaluation of the structure and distribution of short oligosaccharidic building blocks of acidic polysaccharides, as well as the characterization of sialic acid pattern in glycoconjugates, is then of fundamental significance in the understanding of their biological functions, structure and biosynthesis ***(5**,**18)***. Due to the structural complexity and heterogeneity, however, characterization of sugar acids is really challenging. Unlike polypeptides and polynucleotides, polysaccharides cannot be sequenced using automated, 'universal' approaches ***(11)***. Nevertheless, highly selective separative techniques provide a powerful tool for the characterization of complex mixtures of acidic monosaccharides and oligosaccharides. In particular, capillary electrophoresis (CE) ***(19–24)*** and chromatographic techniques ***(24–27)*** are widely used for this purpose, providing complementary advantages, as demonstrated in various comparative approaches ***(28–32)***. Among the chromatographic methodologies, high performance anion-exchange chromatography with pulsed amperometric detection (HPAEC-PAD) ***(33–36)*** ensures good selectivity of separation as well as very high sensitivity

for underivatized carbohydrates, which is typical of electrochemical detection *(9,21,37,38)* [100–250 times better than refractive index detector *(24)*]. The response, however, depends on the size and nature of the sugars *(32)* and must be optimized upon changing the eluent additives. The mobile phase is typically based on concentrated sodium hydroxide containing acetate or nitrate salts, which are added for a fast elution of acidic analytes, with poor possibilities in the optimization of the eluent composition. CE, on the other hand, gives the possibility to explore a wide variety of buffer compositions, owing to the low consumption of sample and separation buffer. Moreover, in CE, a less extensive clean-up of samples is required with respect to chromatographic techniques, and post-run washes are much shorter, because no column fouling can take place. Up to date, CE gives the possibility to analyze, together with carbohydrates, a wider range of saccharidic and non-saccharidic compounds possibly present in the matrix with respect to chromatography *(39–41)*: Soga and Ross *(40)*, for instance, reported the CE analysis of underivatized neutral sugars, alditols, sialic acids, aminoacids and inorganic anions in one run. Such versatility can be achieved upon using nonselective detection modes, like indirect UV (or fluorescence) detection, which is successfully carried out without derivatization. This detection methodology is based on the displacement of the chromophore (or fluorophore) in the background electrolyte by the analyte molecules, which give rise to negative peaks *(42–45)*. Indirect UV detection allows limits of detection (LOD) in the 10^{-6} M range for negatively charged saccharides, using 6 mM sorbate at pH 4–5 as the background electrolyte *(39,43,45,84)*. Such LOD value is higher by two orders of magnitude with respect to that achieved for neutral sugars. Another advantage over neutral analogues is that acidic sugars are charged in a much wider pH range; as a consequence, they are more intrinsically suited to CE. It is not surprising that CE is increasingly being considered one of the techniques of choice for sugar acids, as fully described in excellent books *(24,46)* and in several reviews, which are summarized in **Table 1** *(9,19–23,38,45,47–49)*. Furthermore, some relevant articles published in this field are reported in **Table 2**. The contents of these publications are really heterogeneous, considering the differences in structure and functions of sugar acids. For simplicity, we can group the main applications of CE in this field in the following way:

1. Analysis of sugar acids released from polysaccharides, like polyuronic acids, xylans or glycosaminoglycans. This characterization is carried out following two main methodologies:

   a. Hydrolysis of polysaccharides with enzymes called lyases, which give rise to unsaturated products, and subsequent CE analysis of the underivatized sugar acids with direct UV detection *(12,50–62)*; other reported detection methodologies include electrospray mass spectrometry *(63–66)* and indirect UV detection *(44)*.

Table 1
Relevant Reviews Reporting CE Analysis of Sugar Acids

Reference	Carbohydrate species	CE modes	Detection mode
(9)	Oligosaccharides from glycoproteins	CZE, MEKC, FACE	UV, fluorescence, LIF, ED
(19)	CS, DS and HA oligosaccharides; sialic acids	CZE, MEKC	UV, LIF, fluorescence
(20)	CS, DS, heparin and hyaluronan oligosaccharides	CZE, MEKC	UV,
(21)	Unsatured acidic disaccharides; neutral saccharides, gluconic and galactonic acids, heparin oligosaccharides, phosphorilated monosaccharides; neutral monosaccharides and glycopeptides	CZE, MEKC, CGE	UV, LIF, ED, RI, Biosensors UV,
(22)	Intact GAGs; hyaluronic oligosaccharides polysialic acid, oligomers of sialic acid	CZE, MEKC	UV, LIF, ESI-MS
(23)	Intact hyaluronan, heparin and heparan sulphate, chondroitin sulphate and dermatan sulphate and corresponding oligosaccharides	CZE, MEKC	UV, LIF, ESI-MS, fluorescence
(38)	Underivatized monosaccharides and oligosaccharides; derivatized monosaccharides and oligosaccharides; intact and hydrolyzed glycoconjugates, polyuronic acids and GAGs	CZE, CITP, MEKC, CIEF	UV, ED, LIF, ESI-MS
(45)	Neutral sugars from glycoconjugates; heparin/heparin sulphate; chondroitin/dermatan sulphate oligosaccharides; cyclodextrins; sialic acids; uronic acids	CZE, MEKC	UV, LIF, fluorescence, ED, TOA, RI

(Continued)

Table 1
(Continued)

Reference	Carbohydrate species	CE modes	Detection mode
(47)	Neutral sugars, uronic acids and acidic oligosaccharides; glycoproteins hydrolyzates; sialic acids; polysaccharides and proteoglycans	CZE, MEKC, CIEF, CITP	UV, ED, fluorescence, LIF
(48)	Sialic acids and sialylated glycans; glyconic acids; uronic acids; HA, heparan sulphate, CSs digests; neutral sugars and glycosides; glycoconjugates	CZE, MEKC, CGE, CIEF	UV, LIF, ED, RI, ESI-MS
(49)	Neutral and acidic carbohydrates; carbohydrate from lypo-polysaccharides cleavage and from glycoconjugates; carrageenan poly-sialic acids	CZE, tCITP-CZE, MEKC	UV, ED, Enzymatic OCE, ESI-MS, MIBD, RI

CE, capillary electrophoresis; CGE, capillary gel electrophoresis; CIEF, capillary isoelectric focusing; CITP, capillary isotachophoresis; CS, chondroitin sulphate; CZE, capillary zone electrophoresis; DS, dermatan sulphate; ED, electrochemical detection; ESI-MS, electrospray ionization mass spectrometer; FACE, fluorophore-assisted capillary electrophoresis; GAG, glycosaminoglycan; HA, hyaluronic acid; LIF, laser-induced fluorescence; MEKC, micellar elctrokinetic capillary chromatography; MIBD, micro-interferometric backscatter detector; RI, refractive index; OCE, on-capillary electrode; tCITP, transient capillary isotachophoresis; TOA, thermooptical absorbance.

   b. Hydrolysis of polysaccharides by chemical or enzymic routes and subsequent CE analysis of sugar acids derivatized with a suitable chromophore or fluorophore ***(29,32,62,67–75)***.

2. Analysis of sialic acids released from glycoconjugates using sialidases or mild acidic hydrolysis; study of neutral oligosaccharidic fragments carrying a sialic acid at the nonreducing terminus. Again, derivatization can be carried out in order to improve the performances of CE ***(76–78,83,85)***, even if analysis of underivatized sialic acids and sialylated oligosaccharides has been successfully carried out at low UV wavelength (195–205 nm) ***(13,79–81)***.
3. Development of CE methods for acidic sugars, including glyconic, glycaric, uronic, sialic acids, as well as sulphated and phosphated sugars ***(40–44,82–91)***.

In this chapter, some detailed experimental procedures will be shown, reporting the CE analysis of sugar acids released upon hydrolysis of acidic polysaccharides and of glycans linked to glycoproteins.

Table 2
Selected Articles Reporting Capillary Electrophoresis (CE) Analysis of Sugar Acids

Reference	Carbohydrate species	Matrix	Derivatizing agent	CE mode	Capillary; T	Buffer; voltage	Detection mode	LOD	Results
(12)	GAGs disaccharides	Std and chondro-itinase-treated HA, CS and DS from normal and neoplastic tissues	None	CZE	Fused silica (L = 55 cm, l = 50 cm; ID = 75 μm) T = 25 °C	15 mM ortho-phosphate, pH 3, 20 kV, Outlet: anode	UV ($\lambda = 232$ nm)	n.a.	• Significant increase in GAGs disaccharides in gastrointestinal carcinomas • Specimen from gastric, colon and rectum carcinomas contained increased amounts (about twofold to threefold) of uronic acid and hexosamines, compared to the normal tissues • Increase was more pronounced in pancreatic carcinoma (about fivefold)
(13)	Neu5Ac Neu5Gc	Std Samples from human serum	None	CZE	Fused silica (L = 50 cm, l = 45.5 cm; ID = 50 μm)	50 mM $Na_2B_4O_7$ + 50 mM Na_2HPO_4, pH 8.95, 10 kV, Outlet: cathode	UV ($\lambda = 195\,nm$)	Neu5Ac: 9.6 μM; 39 fmol (S/N = 3)	• Neu5Ac in sera of cancer-affected patients increased significantly as compared with normal human • Linear range for Neu5Ac: 0.02–2 mg/mL • Neu5Gc was not found in the sera of healthy and cancer-affected patients

(Continued)

Table 2
(Continued)

Reference	Carbohydrate species	Matrix	Derivatizing agent	CE mode	Capillary; T	Buffer; voltage	Detection mode	LOD	Results
(32)	Mannuronan oligomers	From acid hydrolysis mixtures	4-ABN	MEKC	Fused silica (L = 72 cm, l = 50 cm, ID = 50 μm); T = 30 °C	660 mM H_3BO_3 + 75–100 mM SDS, pH8, 18 kV, Outlet: cathode	UV (λ = 285 nm)	μM range	• NMR allowed determination of the DP_n with n up to approximately 20 • ESI-MS directly evaluates weight distribution, but reliability decreases upon size increase • In contrast to HPAEC-PAD, MEKC-UV molar response factors were independent of oligosaccharide chain length • MEKC-UV was less effective than HPAEC-PAD in detecting high molecular weight components present in low amounts

(39)	Neu5Ac, Neu5Gc, GlcA, GalA, ManA, Fru, Man, Xyl, Glc, Gal, Rib, GlcN, GalN, Fuc; mannitol, sorbitol, xylitol, inositol	Std and mixture from calf serum fetuin	None	CZE	Fused silica (L = 80.5 cm, l = 72 cm; ID = 50 μm) T = 20°C	20 mM PDC + 0.5 mM CTAB, pH 12.1 (NaOH 1 M), 25 kV, Outlet: anode	Indirect UV ($\lambda = 350\,nm$)	20–70 μM (S/N = 3)	• Resolution between GlcA and GalA and between Neu5Gc and Neu5Ac were improved at higher pH values, but separation of GalN and Gal deteriorated at pH > 12.2 • This method yields a threefold to sevenfold increase in sensitivity for Glc detection compared with the previously reported indirect UV detection using sorbate buffer • No reacetilation of amino sugars deacetilated during hydrolysis is needed • With a single electrophoretic condition, it is possible to have a well-resolved and reproducible separation of sialo, neutral and amino saccharides

(Continued)

Table 2
(Continued)

Reference	Carbohydrate species	Matrix	Derivatizing agent	CE mode	Capillary; T	Buffer; voltage	Detection mode	LOD	Results
(43)	D-galactonic and D-gluconic acids	Std	None	CZE	Fused silica (L = 100 cm, l = 92.4 cm; ID = 50 μm) RT	6 mM sorbic acid, pH 3.8–11 and 6 mM sorbic acid + 15 mM β-CD, pH 4.1–7.9, 20 kV, Outlet: cathode	Indirect UV (λ = 254 *nm*)	18 fmol, (S/N = 3, pH 4.1; S/N = 5, pH 5)	• Separation of chiral compounds by CZE is very sensitive to pH • Best resolution at pH 4.1 and 5. • Addition of β-CD to the buffer did not improve separation at the optimal pH
(53)	Mono-, di-, tri-, and non-sulphated disaccharides (GAGs)	Std and released from squid skin, shark fine cartilage, porcine skin and human umbilical cord (HA and CS)	None	CZE	Fused silica (L = 55 cm, l = 50 cm; ID = 75 μm) T = 25°C	15 mM sodium orthophosfate, pH 3, 20 kV, Outlet: anode	UV (λ = 232 nm)	32–250 pM (S/N = 2)	• This method can be used as a diagnostic test for human malignant mesothelioma • It has been possible to distinguish anomeric forms of various GAGs disaccharides • Sulphation patterns obtained from analysis of pure HA were in close agreement with those obtained from the tissue extracts RSD: 2.6–3.2%

(57)	Heparin sulphate disaccharides	Released from porcine, bovine and ovine intestinal mucosa and bovine lung	None	CZE	Fused silica (L = 57 cm, l = 50 cm; ID = 75 μm) T = 25°C	60 mM formic acid, pH 3.4, 15 kV, Outlet: anode	UV (λ = 232 nm)	1.33–5.05 μg/mL (S/N = 3)	• A significant reduction in analysis time (from 60 to 25 min) and increase of reproducibility was obtained by application of a pressure gradient
(59)	Heparin oligosaccha-rides	Std and released from hydrolysis of porcine intestine and bovine lung treated with heparin lyase	None	CZE	Fused silica (L = 57 cm, l = 50 cm; ID = 75 μm) T = 25°C	30 mM ammonium hydrogen carbonate, pH 8.5 + 10 mM triethylamine, 22 kV, Outlet: cathode	UV (λ = 232 and 200 nm)	0.9–6.9 μM (S/N = 3)	• A CE method for the separation of high molecular mass heparin oligosaccharides compatible with MS detection was developed • Various buffer compositions were tested, differing in pH and additives • Ammonium hydrogencarbonate (30 mM, pH8.5) + 10 mM triethylamine was the optimal buffer Daily calibration was required in quantitative applications

(Continued)

Table 2
(Continued)

Reference	Carbohydrate species	Matrix	Derivatizing agent	CE mode	Capillary; T	Buffer; voltage	Detection mode	LOD	Results
(63)	Heparin unsatured oligosaccharides	Std and released from porcine mucosa heparin treated with heparinase II and III	None	CZE	Fused silica CE/UV: L = 57 cm, l = 50 cm, ID = 50 μm; CE/MS: L = 110 cm; ID = 50 μm; T = 25°C	Std: 530 mM acetic acid/ammonium acetate, pH 3.5, 23 kV, Outlet: anode; Std and hydrolyzed: 40 mM ammmonia/ ammonium acetate, pH 9.2, 30 kV, Outlet: cathode	UV (λ = 230 nm); ESI-MS: negative and positive ionization mode; spray voltage = 4 kV; sheat gas = 1.56 l/min; sheat liquid = acetonitrile/ water, 1:1 (v/v) [+0.1% formic acid (v/v)]; flow rate = 5 μL/min	n.a. (S/N = 5–70)	• Analysis of standard mixture of oligosaccharides completed within 35 min • Work assesses the feasibility of direct CE/MS coupling to characterize heparine oligosaccharides • Method was applied to separation and characterization of heparin enzymatic digests produced by heparinases II and III especially to detect disaccharides and terasaccharides

(66)	HA oligosaccharides	Enzymatic digestion of HA with hyaluronidase	None	CZE	Fused silica (L = 80 cm, l = 71.5 cm; ID = 50 μm); Polyacrylamide coated (L = 90 cm ID = 50 μm) T = 25°C	40 mM ammonium acetate, pH 9, 30 kV, Outlet: cathode	UV (λ = 195 nm); ESI-MS: negative ion mode; capillary voltage = 4 kV; T = 260°C; sheat gas = 0.9 L/min; auxiliary gas = 6 L/min; sheat liquid: 1% triethylamine, methanol/water (v/v), 80:20 (v/v), flow rate: 10 μL/min	n.a.	• Analysis of fragmentation patterns of even and odd oligosaccharides • Polyacrylamide coated with respect to uncoated capillaries offers highly reproducible migration times
(67)	GalA oligomer mixture	Poly-(GalA) subjected to autoclave hydrolysis (120 °C, 50 min)	CBQCA	CZE	Fused silica deactivated capillary filled with poly(acrilamide) gels at high concentrations (L = 32 cm, l = 23 cm; ID = 50 μm)	0.1 M Tris + 0.25 M boric acid + 2 mM EDTA, pH 8.48, 234 V/cm, Outlet: cathode	LIF (λ_{exc} = 457 nm)	amol range	• Electromigration depended only on size and charge • Sensitivity was several orders of magnitude greater than the best results reported prior to this paper

(Continued)

Table 2
(Continued)

Reference	Carbohydrate species	Matrix	Derivatizing agent	CE mode	Capillary; T	Buffer; voltage	Detection mode	LOD	Results
(68)	GAGs oligosaccharides	Std and chondroitinase digested CS-A, CS-C, CS-D, CS-E and HA from pig skin	PMP	CZE	Fused silica (l = 51 cm; ID = 50–75 μm) T = 30 °C	100 mM borate, pH 9 (25 kV) and 100 mM borate, pH 9+polybrene (0.1% w/w) (15–25 kV) Outlet: cathode	UV (λ = 214 and 254 nm)	10 fmol	• Separation and sensitivity were much improved by conversion of these unsatured disaccharides into the PMP derivates • Range of linearity: 0.5–10 μg

(70)	GalA oligomers	Pectic acid hydrolyzed by autoclave and digested by EPGs	ANTS	CZE	Fused silica (L = 60 cm, l = 34 cm; ID = 50 μm)	0.1 mM phosphate buffer, pH 2.5, 17 kV, Outlet: anode	Fluorescence ($\lambda_{exc} = 364$ nm, $\lambda_{em} \geq 440$ nm)	n.a.	• About 20 GalA residues in length were well separated • No difference observed between either polyacrilamide-coated or un-coated capillary • High resolution for long oligomers of glucans, not of GalA (relatively poorly soluble at low pH) • Electrophoresis separation exhibited a lower apparent concentration of the larger oligomers compared to HPLC data
(71)	Xyl, Glc, Man, Ara, Gal, ManA, GlcA, GalA;	Std	6-AQ	CZE	Fused silica (L = 61 cm, l = 56 cm; ID = 50 μm)	220 mM alkaline borate, pH 9, 20 kV	UV ($\lambda = 245$ nm)	1–5.6 μM	• High sensitivity and good separation • Accurate quantitative analysis • Powerful analytical tool for the characterization of hemicelluloses obtained from wood pulps

(Continued)

Table 2
(Continued)

Reference	Carbohydrate species	Matrix	Derivatizing agent	CE mode	Capillary; T	Buffer; voltage	Detection mode	LOD	Results
	Glc, Man, Ara;	Std			Fused silica (L = 61 cm, l = 56 cm; ID = 50 μm)	420 mM alkaline borate, pH 9, 20 kV			
	Rha, Xyl, Glc, Ara, Man, Gal, 4-O-MeGlcA, GlcA, GalA;	Std			Fused silica (L = 43 cm, l = 38 cm; ID = 30 μm)	420 mM alkaline borate, pH 9, 1200 mW, Outlet: cathode			
	Xyl_n (n = 1–6), 4-O-MeGlcA, aldobiuronic acid, aldotriuronic acid, aldotetrauronic acid	Std			Fused silica (L = 43 cm, l = 38 cm; ID = 30 μm)	420 mM alkaline borate, pH 9, 20 kV			

	Xyl, Glc, Man, Ara, aldobiuronic acid, Gal, 4-O-MeGlcA	Hydrolized sample of spruce wood xylan (enzymatic or chemical hydrolysis)			Fused silica (L = 43 cm, l = 38 cm; ID = 30 μm)	420 mM alkaline borate, pH 9, 20 kV			
(72)	Mono-, di-, tri- and non-sulphated chondroitin disaccharides	Std	ANDSA	CZE	Polyether coated (L = 50/80 *cm*, *ID* = 50 μm) T = 30 °C	100 mM sodium phosfate, pH 3; 100 mM sodium acetate, pH 4–5; 50 mM MES, pH 6–7 spermine, 20 kV, Outlet: anode	LIF (λ_{exc} = 325 nm; λ_{em} = 420 nm)	5 nM	• Yield of derivatization with ANDSA was ≥ 85% • The use of the additive spermine was studied in function of the pH (3–7): at pH 7, a fast migration of the disaccharides was observed and this additive improved the separation of analytes from the excess of ANDSA

(Continued)

Table 2
(Continued)

Reference	Carbohydrate species	Matrix	Derivatizing agent	CE mode	Capillary; T	Buffer; voltage	Detection mode	LOD	Results
							UV ($\lambda_{underiv} = 231$ nm, $\lambda_{deriv} = 250$ nm) Spectro-fluorescence ($\lambda_{exc} = 315$ nm)	5 μM (underivatized) 2.5 μM (derivatized) 0.1 μM	
(73)	CS and DS disaccharides	Std and from normal and aneurysmal human abdominal aortas after treatment with chond-roitinase ABC and AB	AMAC	CZE	Fused silica (L = 55 cm, l = 50 cm; ID = 75 μm) T = 20 °C	15 mM orthophosfate buffer, pH 3, 20 kV, Outlet: anode	LIF ($\lambda_{exc} = 488$ nm) UV ($\lambda = 254$ nm)	LIF: 0.51 pM; UV: 5–8 pM (S/N = 3)	• In aneurismal abdominal aortas, a 65% decrease in CS content was noted, whereas that of DS remained constant • The modified sulphation profiles in aneurismal aortas may well be related with development of the disease All mixture of known tri-, di- and mono-sulphated disaccharides were well resolved within 25 min

(75)	Maltooligosaccharide ladder, cellooligosaccharide ladder, cellohexaose, digestion products of cellohexaose, GlcA, Xyl, Ara, Glc, Gal	Std and lignocellulosic biomass, corn fiber	APTS	CZE	eCAP™ neutral coated (l = 10 cm or 48 cm); bare fused silica (L = 58 cm, l = 48 cm) ID = 50 μm T = 25 °C	25 mM lithium acetate, pH 5, 500 V/cm, Outlet: anode	LIF (λ_{exc} = 488 nm; λ_{em} = 520 nm)	n.a.	• Good methodology for large-scale carbohydrate analysis for oligosaccharide and monosaccharide profiling • Excellent resolution under suppressed electrosmotic flow conditions • Efficient tool for elucidation and optimization of biomass degradation processes
(76)	Neu5Ac, GalNAc, GlcNAc, Man, Glc, Fuc, Gal	Std and monosaccharides released from different acidic hydrolysis of bovine fetuine	APTS; AMAC (for Neu5Ac)	CZE	Fused silica (L = 37 cm, l = 30 cm; ID = 25 μm) T = 20 °C	25 mM lithium tetraborate buffer pH 10, 750 V/cm, Outlet: cathode	LIF (λ_{exc} = 488 nm; λ_{em} = 520 nm)	n.a.	• Different hydrolysis conditions are recommended for the analysis of sialylated, neutral and N-acetylated sugars • After the N-acetylated sugar hydrolysis a re-N-acetylation step is necessary before the labelling step

(Continued)

Table 2
(Continued)

Reference	Carbohydrate species	Matrix	Derivatizing agent	CE mode	Capillary; T	Buffer; voltage	Detection mode	LOD	Results
(77)	Neu5Ac, GalNAc, Xil, Rib,GlcNAc, Glc, Man, Ara, Fuc, Gal, cinnamic acid, GlcA, GalA	Std	AMAC	CZE	Fused silica (L = 72 cm, l = 50 cm; ID = 50 μm) T = 30 °C	0.3 M H_3BO_3/NaOH, pH 10.5, 20 kV, Outlet: cathode	UV ($\lambda = 260\,nm$)	Neu5Ac: 1 μM	• Linear range for Neu5Ac: 10–120 μM • AMAC-Neu5Ac is unstable at room temperature and under light exposure, as it spontaneously undergoes decarboxylation reaction • AMAC-Neu5Ac can be isolated and valuated in biological samples
	Neu5Ac	Samples released from acidic hydrolysis of hu-UTI, bovine α_1-AGP and rhu-EPO							

(78)	Neu5Ac	Std and released from human serum	Benzoic anhydride	CZE	Fused silica (l = 56 cm; ID = 50 μm) T = 25 °C	25 mM buffer phosphate, pH 3.5: containing 50% (v/v) CH_3CN, 30 kV, Outlet: anode	UV (λ = 231 nm)	Neu5Ac: 2 μM; 5 pg (S/N = 3)	• In contrast to reductive amination, this method requires mild conditions that prevent any decomposition of sialic acid residues • Range of linearity: 5 μg/mL to 5 mg/mL • The method is highly reproducible, RSD < 1%
(80)	3′-SL, 6′-SL, 3′-SLN, 6′-SLN, DST, 3′-S-3-FL, SLNT-a, SLNT-b, SLNT-c, DSLNT, DSFLNH	Std	None	MEKC	Fused silica (l = 56 cm; ID = 50 μm) T = 25 °C	376 mM Trizma buffer +150 mM SDS, pH 7.9; 6 % MeOH (v/v), 30 kV, Outlet: cathode	UV (λ = 205 nm)	30–68 fmol	• Detector response is influenced by structure, not merely by the number of N-acetyl and carboxyl groups • The method can be used to determine if the type and the amount of sialylated oligosaccharides vary depending on the milk donor or on her stage of lactation

(Continued)

Table 2
(Continued)

Reference	Carbohydrate species	Matrix	Derivatizing agent	CE mode	Capillary; T	Buffer; voltage	Detection mode	LOD	Results
	Sialylated oligosaccharides	Human milk after acidic hydrolysis							
(81)	Neu5Ac	Std	None	CZE	Coated with linear polyacrylamide (L = 50 cm; ID = 50 μm) T = 37 °C	50 mM acetate buffer, pH 5 (+ sialidases, 250 mU/mL) 5 kV (20 min)/20 kV (10 min) Outlet: anode	UV ($\lambda = 200$ nm)	Neu5Ac: 25 μg/mL	• In-capillary digestion of sialoglycans • Total time of analysis reduced to approximately 25 min • Linear range for Neu5Ac: 0.025–10 mg/ml
	Neu5Ac	From fetuins				5, 10, 15 kV 5 kV (20 min)/20 kV (10 min) Outlet: anode			

	Mix of 3′ and 6′ Neu5Ac-Lac	After treatment with sialidases				5 kV (20 min)/20 kV (10 min) Outlet: anode			
(83)	Neu5Ac, gluconic acid, GalA, glyceric acid	Std	SA; ANDSA	CZE	Fused silica (L = 80 cm, l = 50 cm; ID = 50 μm)	100 mM phosphate, pH 2, 2.5, 3, 20 kV, Outlet: anode	UV ($\lambda = 247$ nm);	Approximately 30 fmol (SA derivatives); approximately 15 fmol (ANDSA derivatives)	• Low pH increases separation efficiency • At high pH, SA and ANDSA derivatives of GalA were completely separated from those of gluconic acid • Borate complexation enhances selectivity • Glyceric acid gives stronger complexation with borate than other derivatized sugars, thus it is the most retarded solute
			ANDSA			50 mM phosphate, pH 10, 20 kV, Outlet: cathode	UV ($\lambda = 247$ nm);	Approximately 30 fmol (SA derivatives); approximately 15 fmol (ANDSA derivatives)	
			ANDSA			100 mM borate, pH 10, 20 kV, Outlet: cathode	Fluorescence (λ_{exc} = 315)	0.6 fmol (ANDSA derivatives); extanded path capillary: 5.3 fmol (ANDSA derivatives), 10.5 fmol (SA derivatives)	

(Continued)

Table 2
(Continued)

Reference	Carbohydrate species	Matrix	Derivatizing agent	CE mode	Capillary; T	Buffer; voltage	Detection mode	LOD	Results
(84)	Inositol phosphates	Water and plasma	None	CZE	Fused silica (L = 57 cm, l = 50 cm; ID = 75 μm)	0.5 mM NDSA +30 mM acetic acid, pH 3 + 0.01% HPMC and 10 mM ammonium acetate, pH 5.0 + 0.01% HPMC, 25 kV, Outlet: anode	Indirect UV ($\lambda = 214$ nm)	10 μM	• Good reproducibility and linearity without the use of an internal standard
(85)	Glyceric acid, gluconic acid, GalA, Neu5Ac	Std	ANDSA	CZE	PVA coated (L = 47 cm, l = 40 cm; ID = 50 μm) T = 15 °C	Sodium acetate buffer at various concentrations, pH 5, 20 kV, Outlet: anode	LIF ($\lambda_{exc} = 325$ nm; $\lambda_{em} = 420$ nm)	n.a.	• Linear dependence of effective mobility of solutes on $1/\sqrt{C}$ (C = buffer concentration) • Study of the effect of ionic strength on separation resolution and selectivity • Influence of buffer concentration is more evident for trisialooligosaccharides than for disialo- and monosialo-oligosaccharides
	Sialo-oligosaccha-rides	Sialo-oligosaccha-rides ganglio-sides treated with ceramide glycanase							

(89)	Poly(GalA), GalA and tri(GalA)	Std	APTS	CGE	Linear polyacrylamide coated (L = 62 cm, l = 47 cm; ID = 50 μm)	24 mM citric acid +2 M urea +4% LPAA, pH 3, pH 3.5, pH 4.2 (trizma base)	LIF (λ_{exc} = 488 nm; λ_{em} = 514 nm)	n.a.	• CE proves the capacity of acidic polysaccharides to interact with heavy metals • CGE allows a size-dependent separation • ELFSE changes solutes' frictional attributes. • For larger oligomers, polymer solutions are mandatory. • ELFSE allows investigation of metal binding (due to the necessity of high pH values) and because of its speed and convenience it is a good alternative for other interaction studies • ELFSE avoids interactions between gel matrix (absent) and metals
			N-(1-maltoheptaosamine)-3,6-diaminoacridine	ELFSE		24 mM citric acid, pH = 5 (trizma base) + metal chlorides (0–15 mM), 25 kV, Outlet: cathode			

(Continued)

Table 2
(Continued)

Reference	Carbohydrate species	Matrix	Derivatizing agent	CE mode	Capillary; T	Buffer; voltage	Detection mode	LOD	Results
(90)	Fru and Glc phosphates	Std mixture and metabolites obtained from *Bacillus subtilis*	None	CZE	SMILE (+) capillary (cationic capillary coated with multiple ionic polymer layers); (L = 100 cm; ID = 50 μm) T = 20°C	50 mM ammonium acetate, pH 9, 30 kV, Outlet: anode	ESI-MS; negative ion mode; capillary voltage = 3500 V; T = 300°C; N_2 flow = 10 L/min; Sheat liquid = 10 μL/min ammonium acetate in 50 % (v/v) methanol/water	0.3–6.7 μM (S/N = 3)	• SMILE (+) capillary is used to avoid the current drop that occurs when using surfactants on capillary walls (necessary to reverse EOF). Such drop may in fact be due to migration of the surfactants toward the inlet vial (cathode) • Migration times of all 20 metabolites gradually decrease over time (RSD for migration times = 1.8 − −3.3%, $n = 6$); but they were increased and stabilized when capillary is flushed with low-pH buffer • Mass LOD is 130–83,000-fold better than with HPLC

(91)	Sulphated Fuc	Std and fucose 2-O-sulfohydro-lase hydrolyzate	None	NACE	Fused silica (L = 40 cm, l = 31.5 cm; ID = 50 μm) T = 12 °C	12 mM ethanol amine +2 mM trimesic acid mixture in methanol-ethanol (50:50, v/v) solvent mixture, 20 kV, Outlet: anode	Indirect UV ($\lambda = 200$ nm)	n.a.	• Increased solubility of analytes sparingly soluble in purely aqueous electrolytes • Reduced Joule heating, consequent increase of the electric field improved efficiency and reduced analysis time • Modification of the EOF without surfactant addition • The method could be used for the screening of sulphoesterases of unknown activity • Best isomeric separations were obtained with EtOH/MeOH (1:1, v/v) as solvent mixture and at a temperature of 12 °C
(92)	Glucaric acid, GlcA, gluconic acid, Glc, glucitol	Std	None	CZE	Fused silica (l = 20 cm; ID = 25 μm)	50 mM NaOH +0.25 mM CTAB, 2 kV, Outlet: anode	n.a.	Cu OCE	• Nearly complete resolution of the mixtures is achieved in less than 5 min; excellent quantitative reproducibility • OCE eliminates problems raised by aligning the detecting electrode with the capillary outlet

(Continued)

Table 2
(Continued)

Reference	Carbohydrate species	Matrix	Derivatizing agent	CE mode	Capillary; T	Buffer; voltage	Detection mode	LOD	Results
(95)	Xylonic acid; GalA; MeGlcA; aldobiuronic acid; aldotriuronic acid; aldotetrauronic acid	Enzymatic hydrolyzates of pulps and unbleached birch and pine kraft pulps	SA	CZE	Fused silica (L = 44 cm; ID = 50 μm)	100 mM phosphate +10 mM β-CD and 15 mM triethanolamine, pH 2.3, 20 kV, Outlet: anode	UV (λ = 247 nm)	< 3μM	• Possible quantification within a concentration range of at least 2 orders of magnitude down to about 10 μM • Both saturated and unsaturated acidic xylo-oligosaccharides could be separated and detected • Highly selective and sensitive determination of the amount of MeGlcA and Δ UA units in samples of a few μmol/g pulp

4-ABN, 4-aminobenzonitrile; AGP, acid glycoprotein; AMAC, 2-aminocridone; ANDSA, 7-aminonaphtalene-1.3-disulfonic acid; ANTS, 8-aminonaphtalene-1.3.6-trisulfonic acid; APTS, 1-aminopyrene-3,6,8-trisulfonate; Ara, arabinose; 6-AQ, 6-aminoquinoline; CBQCA, 3-(carboxybenzoyl)-2-quinoline carboxy-aldehyde; CGE, capillary gel electrophoresis; CS, chondroitin sulphate; CTAB, cetylmethylammonium bromide; CZE, capillary zone electrophoresis; DS, dermatan sulphate; DSFLNH, disialomonofucosyllacto-*N*-neohexaose; DSLNT, disialyllacto−*N*-tetraose; DST, disialyltetraose; EDTA, ethylenediaminotetracetic acid; ELFSE, end-label free solution; EPG, endopolygalacturonase; ESI-MS, electrospray isonization mass spectrometer; Fru, fructose; Fuc, fucose; GAG, glycosaminoglycan; Gal, galactose; GalA, galacturonic acid; Glc, glucose; GlcA, glucuronic acid; GalNAc, *N*-acetyl galactosamine; GlcNAc, *N*-acetyl glucosamine; HA, hyaluronic acid; HPAEC-PAD, high performance anion-exchange chromatography with pulsed amperometric detection; HPMC, hydroxypropylmethylcellulose; hu-UTI, human urinary trypsin inhibitor; ID, internal diameter; LIF, laser-induced fluorescence; LOD, limit of detection; LPAA, linear polyacrilamide; Man, mannose; NDSA, 1-naphtol-3,6-disulfonic acid; Neu5Ac, *N*-acetylneuraminic acid; ManA, mannuronic acid; MeGlcA, methyl-glucuronic acid; MEKC, micellar elctrokinetic capillary chromatography; MES, 2-(N-morpholino) ethansulfonic acid; n.a., non available; NACE, non-aqueous capillary electrophoresis; NMR, nuclear magnetic resonance; OCE, on-capillary electrode; PDC, 2.6-pyridinedicarboxylic acid; PMP, 1-phenyl-3-methyl-5-pyrazolone; Rha, rhamnose; rhu-EPO, recombinant human erythropoietin; Rib, ribose; RSD, relative standard deviation; RT, room temperature; 3′-S-3-FL, 3′-syalil-3-fucosyllactose; SA, sulfanilic acid; SDS, sodium dodecyl sulphate; SL, syalillactose; SLN, syalillactosamine; SLNT, sialyllacto−*N*-tetraose; std, standard; Xyl, xylose for other abbreviations, see table 1.

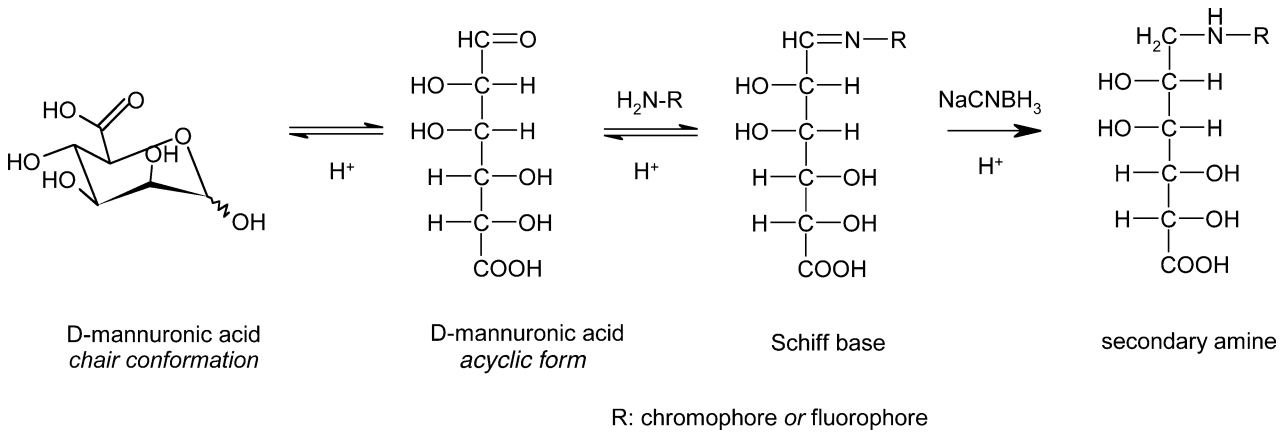
1.1. Acidic Sugars Released from Alginates

1.1.1. CZE-UV of Unsaturated, Underivatized Acidic Sugars

UV detection of underivatized, unsaturated sugar acids is typically carried out at 232 nm (i.e. the absorption wavelength of the double bond). Many buffer compositions can be chosen to separate such compounds ***(12,50–62)***. In order to optimize the selectivity of the electrophoretic separation, borate-based buffers are often used, as carbohydrates can be converted in situ to anionic borate complexes ***(87,92)***; the stability of these adducts depends on the pH (typically, comprised between 7 and 10) and on the configuration of the hydroxyl groups involved in the interaction with boron. The following sessions will report the protocol for the capillary zone electrophoresis (CZE) analysis of the unsaturated oligosaccharides arising from treatment of an alginate sample with G-lyase, an enzyme which is specific for guluronic acid in GG and GM glycosidic linkages ***(62)***, where G represents α-L-guluronic acid and M β-D-mannuronic acid units. The reported CE methodology can be extended to other relevant lyase-treated acidic polysaccharides, like glycosaminoglycans.

1.1.2. Analysis of Derivatized Acidic Sugars

Derivatization with chromophoric or fluorophoric agents is a powerful strategy used to increase the sensitivity and selectivity of CE analysis of sugar acids ***(19–23,48)***. It is generally carried out before injection in the CE system. The most popular route used to achieve this goal is reductive amination, a one-pot reaction, which takes place between the carbonyl group of reducing sugars and the amino group of a suitable chromophore or fluorophore; sodium cyanoborohydride is used as the reductant agent ***(38,45,69–71,73–75)*** (*see* **Scheme 2**). In order to achieve a high and reproducible yield, it is necessary to shift the initial equilibrium (Schiff base formation) into the direction of the condensation; at least a fivefold excess of the derivatizing agent is therefore used ***(45)***. Derivatization efficiency depends on the nature of the analyte as well as on the reaction conditions ***(93)***. Among the chromophores, 4-aminobenzonitrile (4-ABN) provides extremely low values of detection limits (LODs) ***(21,45,94)***. Fluorophoric tags used in reductive amination include 1-aminopyrene-3,6,8-trisulphonic acid (APTS) and 2-aminoacridone (AMAC), which give rise to unprecedented sensitivity [LODs down to the pM range ***(73)***], due to the commercially available detectors based on laser-induced fluorescence that allow narrow focusing of excitation light onto capillaries. Another efficient derivatization strategy which can be considered as a variant of reductive amination is the conversion of reducing sugar acids in 1-amino-1-deoxyalditols and subsequent reaction with the fluorophore 3-(4-carboxybenzoyl)-2-quinolinecarboxyaldehyde (CBQCA) ***(9,45,67)***. Moreover,


D-mannuronic acid
chair conformation
H+
D-mannuronic acid
acyclic form
H2N-R
H+
Schiff base
NaCNBH3
H+
secondary amine
R: chromophore or fluorophore

Scheme 2.

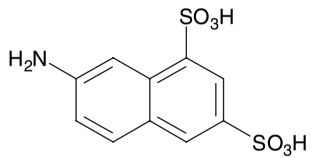
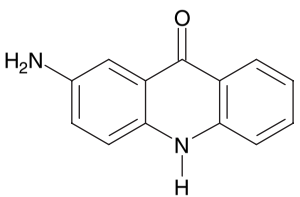
condensation between the carbonyl group of reducing carbohydrates and the active hydrogens of 1-phenyl-3-methyl-5-pyrazolone has been successfully employed for sugar acids ***(68)***. The previously mentioned strategies can be applied to both neutral and acidic sugars. A selective method for the labelling of carboxylated carbohydrates deserves a special mention. It is based on the formation of an amide bond between the carboxylate group of the sugar and the amino group of the tag in the presence of water-soluble carbodiimide; the amount of this catalyst has to be lower than that of the sugar acid, in order to avoid the formation of side products ***(45)***. 7-Aminonaphtalene-1,3-disulfonic acid (ANDSA) ***(72,83,95)*** and sulphanilic acid (SA) ***(72,95)*** have been successfully used for this approach. The most used tags for derivatization of sugar acids are reported in **Table 3**, together with their main applications.

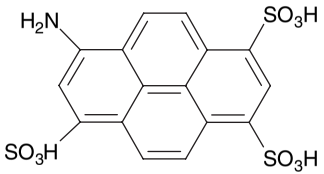
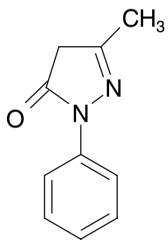
In this chapter, a protocol for the CE analysis of alginate oligomers derivatized with 4-ABN by reductive amination will be reported.

1.2. Sialic Acids

Direct UV detection of sialic acids after their CE separation has been successfully applied in various instances, like the analysis of oligosaccharides from human milk, containing Neu5Ac ***(80)***. As for other sugar acids, derivatization can be carried out in order to improve the sensitivity and selectivity of the separation. The most used strategy, again, is reductive amination; AMAC is the most popular agent used for sialic acid ***(76,77)***, while oligosaccharides containing sialic acid at the nonreducing terminus can be derivatized using other tags, like those previously mentioned for neutral or acidic sugars. Other procedures for sialic acid derivatization include condensation with ANDSA and SA (*see* **Subheading 1.1.2.**) ***(83,85)*** and perbenzoylation with benzoic anhydride ***(78)***. A method specific for sialic acids exploits the ability of α-ketoacids to form a quinoxaline ring structure upon reaction with ortho-diamines ***(47)***. It must be mentioned, however, that sometimes the characterization procedures for sialoglycoconjugates do not take into account sialic acid complexity, as substitutions can slow down or even completely prevent release of sialic acids, and many methods used in the structural analysis of intact glycans cause disruption of sialic acid modifications ***(5)***. As an example, during reductive amination of sialo-oligosaccharides, the use of catalysts having stronger acidity than acetic acid may lead to a loss of sialic acid. An interesting study on de-sialylation of sialyl-*N*-acetyllactosamine in different conditions of reductive amination with APTS has been reported by Evangelista et al. ***(93)***. **Table 3** summarizes the most used derivatizing agents reported in literature up to date for sialic acids, as well as for other sugar acids.

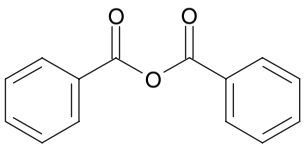
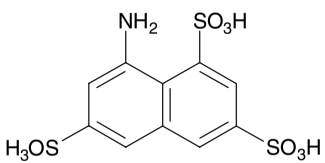
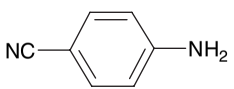
Table 3
Main Derivatizing Tags Suitable for CE Analysis of Sugar Acids

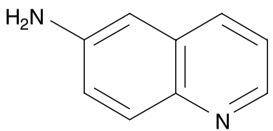
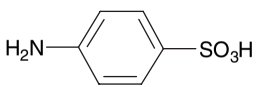
Derivatizing agent	Detection	Carbohydrate species	Reference
 **ANDSA** 7-aminonaphtalene-1,3-disulfonic acid	LIF (λ_{exc} = 315 nm; λ_{em} = 420 nm); UV (247 nm)	Chondroitin sulphate saccharide	*(72)*
		Neu5Ac, gluconic acid, GalA, glyceric acid	*(83)*
		Sialooligosaccharides	*(85)*
 **AMAC** 2-amino-acridone	UV (260 nm); LIF (λ_{exc} = 425 nm; λ_{em} = 520 nm)	Variously sulphated chondroitin/dermatan Δ-disaccharides	*(73)*
		Neu5Ac, cinnamic acid, GlcA, GalA and neutral sugars	*(76,77)*

 **APTS** 1-Aminopyrene-3-6-8-trisulfonate	LIF (λ_{exc} = 455 nm; λ_{em} = 512 nm)	Neu5Ac and neutral sugars	***(76)***
		GlcA and neutral sugars	***(75)***
		PolyGalA, GalA and triGalA	***(89)***
 **PMP** 1-phenyl-3methyl-5-pyrazolone	UV (245 nm)	Chondroitin sulphate disaccharides	***(68)***

(Continued)

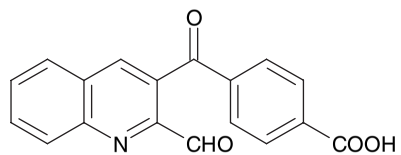
Table 3
(Continued)

Derivatizing agent	Detection	Carbohydrate species	Reference
 **BA** Benzonic anhydride	UV (231 nm)	Sialic acids	***(78)***
Benzoic anhydride  **ANTS** 8-aminonaphtalene-1,3,6-trisulfonic acid	LIF (λ_{exc} = 370 nm; λ_{em} = 520 nm)	GalA oligomers	***(70)***
 **4-ABN** 4-aminobenzonitrile	UV (285 nm)	ManA oligomers GalA, GlcA	***(32,62)*** ***(94)***

 **6-AQ** 6-aminoquinoline	UV (245 nm); LIF (λ_{exc}=270 nm; λ_{em} > 495 nm)	Monosaccharides, uronic acids, xylo-oligosaccharides, xylan-derived acidic oligosaccharides	***(71)***
 **SA** Sulfanilic acid	UV (247 nm)	Neu5Ac, gluconic acid, GalA, glyceric acid	***(83)***
		Xylonic acid, MeGlcA, aldobiuronic acid, aldotriuronic acid, aldotetrauronic acid	***(95)***

(Continued)

Table 3
(Continued)

Derivatizing agent	Detection	Carbohydrate species	Reference
 **CBQCA** 3-(4-carboxybenzoyl)-2-quinoline carboxy-aldehyde	LIF (λ_{exc} = 457 nm; λ_{em} = 552 nm)	Glucosaminic acid, GlcA, Glc6P and neutral sugars	***(67,82)***

GalA, galacturonic acid; GlcA, glucuronic acid; Glc6P, glucose-6-phosphate; LIF, laser-induced fluorescence; MeGlcA, methyl-glucuronic acid; Neu5Ac, *N*-acetylneuraminic acid for other abbreviations, see tables 1 and 2.

In this chapter, the procedure for analysis of Neu5Ac released from immunoglobulin G (IgG) and derivatized with AMAC will be reported.

2. Materials

2.1. Acidic Sugars Released from Alginates

2.1.1. CZE-UV of Unsaturated, Underivatized Acidic Sugars

1. Samples: Unsaturated oligomers (2 mg/mL of freeze-dried mixture in water) released from alginate upon treatment with G-lyase (from *Klebsiella Pneumoniae*; from the University of Science and Technology NTNU, Throndheim, Norway) as previously described ***(62)***. Alginate containing 47% of a-L-guluronic acid was prepared treating poly-mannuronic acid with recombinant mannuronan C-5 epimerase (62), AlgE4.
2. CE buffer: 50 mM sodium tetraborate (pH 9.2) (from Sigma Chemical Co., St. Louis, MO, USA).

2.1.2. Analysis of Derivatized Acidic Sugars

1. Samples: Oligo-mannuronic acids (hexamer, heptamer and octamer) purified from a chemical hydrolysis mixture of polymannuronic acid ***(32,62)*** before and after epimerization with recombinant mannuronan C-5 epimerase, AlgE4 ***(62)***.
2. Reagents for derivatization: Sodium cyanoborohydride ($NaCNBH_3$), 4-ABN, glacial acetic acid and methanol (all reagents from Sigma Chemical Co.); the structure of 4-ABN is reported in **Table 3**.
3. CE buffer: 660 mM boric acid +100 mM sodium dodecyl sulphate (SDS) (pH 8) (all reagents from Sigma Chemical Co.).

2.2. Sialic Acids (N-Acetylneuraminic Acid from Human IgG)

1. Samples: *N*-Acetylneuraminic acid (*Escherichia coli*) (Neu5Ac) was from Fluka (Buchs, Switzerland); the procedure for release of Neu5Ac with neuraminidase (*Arthrobacter ureafaciens*) (Calbiochem, Merck, Darmstadt, Germany) from human serum IgG (Sigma Chemical Co.) is reported in **Note 1**.
2. Reagents for derivatization: Sodium cyanoborohydride ($NaCNBH_3$), dimethyl sulphoxide and acetic acid were from Merck; AMAC was from Fluka; the structure of AMAC is reported in **Table 3**.
3. CE buffer: 50 mM sodium tetraborate (pH 9.2) (from Sigma Chemical Co.).

2.3. Equipment

2.3.1. Alginate Oligosaccharides

1. High-performance CE system from Applied Biosystems (Foster City, CA, USA), Model 270-HT, with Turbochrom Navigator (4.0) software.
2. Fused silica column (Supelco, St. Louis, MO, USA); total length, 72 cm; effective length, 50 cm; internal diameter, 50 μm.

3. UV detection, wavelength equal to 232 nm (for procedure described in **Subheading 2.1.1**.) and 285 nm (for procedure described in **Subheading 2.1.2**.).
4. Dry-bath heating block.

2.3.2. Sialic Acid

1. High-perfomance CE system from Hewlett-Packard (Agilent Technologies, Waldbronn, Germany), Model HP^{3D}CE, with HP Chemstation software.
2. Fused silica column with extended light path (Agilent Technologies); total length, 80 cm; effective length, 72.5 cm; internal diameter, 50 μm.
3. UV detection, wavelength equal to 254 nm.
4. Filters: 0.45-μm pore size membrane (Millipore, Billerica, MA, USA).
5. Dry-bath heating block.

3. Methods

3.1. Acidic Sugars Released from Alginates

3.1.1. CZE-UV of Unsaturated, Underivatized Acidic Sugars

1. Wash the capillary for 2 min with 0.1 M NaOH and subsequently with buffer for 4 min (vacuum pressure 67.6 kPa).
2. Load sample under vacuum at a pressure of 16.9 kPa (1.5 s).
3. CE conditions: voltage, 15 kV; detection, 232 nm (at cathode); temperature, 27 °C; buffer, 50 mM tetraborate (pH 9.2).
4. **Figure 1** shows the CE analysis of underivatized alginate oligomers released from alginate after G-lyase digestion. Tetramer and dimer were the major constituents of the hydrolysis mixture; this result confirmed that AlgE4 works by a processive made of action ***(62)***.

3.1.2. Analysis of Derivatized Acidic Sugars

1. Wash the capillary for 2 min with 0.1 M NaOH and subsequently with buffer for 4 min (vacuum pressure 67.6 kPa).
2. Load sample under vacuum at a pressure of 16.9 kPa (1.5 s).
3. CE conditions: voltage, 18 kV; detection, 285 nm (at cathode); temperature, 27 °C; buffer, 660 mM boric acid +100 mM SDS (pH 8 with 3 N NaOH).
4. Derivatization procedure: 50 μL of carbohydrate solution in water (0.5–5 mg/mL) is added to 450 μL of a solution containing 4-ABN (0.5 M) and $NaCNBH_3$ (0.16 M) in methanol/acetic acid (95/5 v/v). Reaction is carried out in a screw-capped vial for 15 min at 90 °C (dry-bath heating block). Prior to injection in the CE system, derivatization mixtures should be diluted five times with water (*see* **Notes 2** and **3**).
5. **Figure 2** shows the micellar electrokinetic capillary chromatography (MEKC)-UV analysis of 4-ABN-derivatized hexamer (0.1 mg/mL) (*see* **Fig. 2A**), heptamer (0.3 mg/mL) (*see* **Fig. 2B**) and octamer (0.25 mg/mL) (*see* **Fig. 2C**) of mannuronan. The high selectivity of MEKC allows the purity assessment of the oligomers arising from separation by size exclusion chromatography ***(62)***: in each fraction, contamination of the (n + 1) oligomer can be clearly seen.

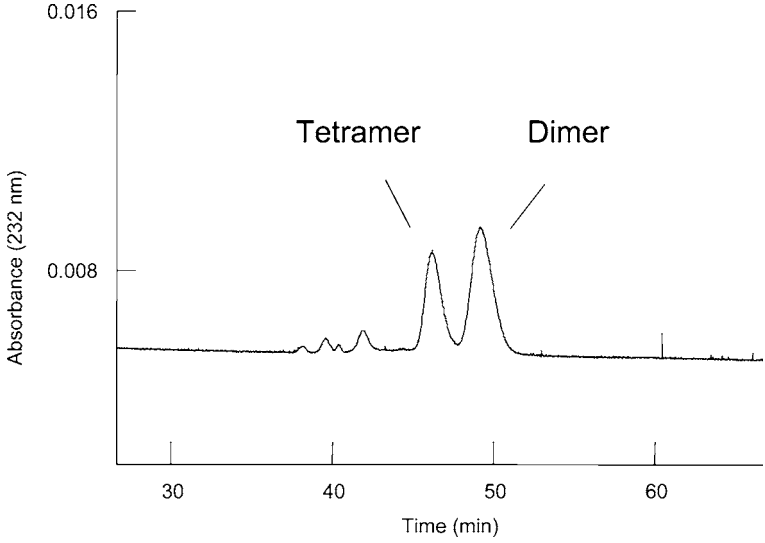


Fig. 1. Capillary electrophoresis (CE) analysis of underivatized alginate oligomers released from 47% GulA alginate after G-lyase digestion; buffer: 50 mM sodium tetraborate (pH 9.2); voltage: 15 kV; UV detection: 232 nm; temperature: 27 °C; fused silica capillary, L = 72 cm, l = 50 cm, internal diameter = 50 μm (reproduced with permission from **ref. *62***; © The Biochemical Society).

6. In **Fig. 3** is demonstrated the selectivity of MEKC-UV for isomeric alginate oligomers: it shows the analysis of the same mannuronic acids after treatment with AlgE4, an enzyme which catalyzes the in-chain epimerization of β-D-mannuronic acid in α-L-guluronic residues in the last step of alginate biosynthesis. The new peaks appearing in **Fig. 3** belong to oligomers containing G-units, which are well distinguished between each other these results show that the efficiency of the epimerase action is higher for the octa-mannuronic acid than for lower oligomers.

3.2. Sialic Acids (N-Acetylneuraminic Acid from Human IgG)

1. Wash the capillary for 2 min with 0.1 M NaOH and for 4 min with the separation buffer at a pressure equal to 960 mbar.
2. Load the sample at a pressure of 25 mbar for 3 s.
3. CE conditions: voltage, 15 kV; detection at 254 nm (cathode); temperature, 25 °C; buffer, 50 mM sodium tetraborate (pH 9.2).
4. Derivatization procedure: 200 μL of Neu5Ac standard solution (16 mM) or Neu5Ac released from human IgG (*see* **Note 1**) is added to 200 μL of derivatizing solution [0.05 M AMAC, in dimethyl sulphoxide/acetic acid (17/3), containing 1 M sodium cyanoborohydride, $NaCNBH_3$] in a screw-capped vial. The reaction mixture is

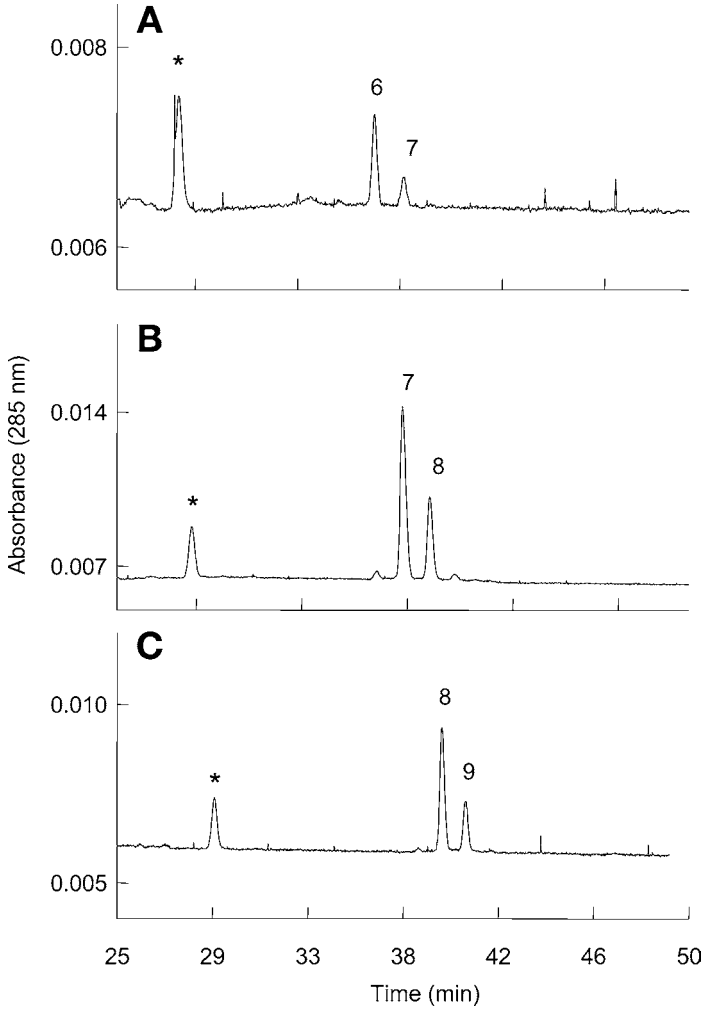


Fig. 2. Micellar electrokinetic capillary chromatography-UV analysis of 4-aminobenzonitrile-derivatized hexamer (0.1 mg/mL) ***(6)*** (**A**), heptamer (0.3 mg/mL) ***(7)*** (**B**) and octamer (0.25 mg/mL) ***(8)*** (**C**) of mannuronan; buffer: 660 mM boric acid +100 mM sodium dodecyl sulphate (pH 8); voltage: 18 kV; detection: 285 nm; temperature: 27 °C; fused silica capillary, L = 72 cm, l = 50 cm, internal diameter = 50 μm (reproduced with permission from **ref. *62***; © The Biochemical Society)(*) from ABN.

heated in the dark at 70 °C for 2 h in a dry-bath heating block ***(96)*** (*see* **Note 4**). Before injection, the sample can be diluted (e.g., 1:10) with water.

5. **Figure 4** shows the capillary zone electrophoretic analysis of Neu5Ac released from human IgG (panel B). Peak attribution has been confirmed upon injection of standard Neu5Ac (panel A).

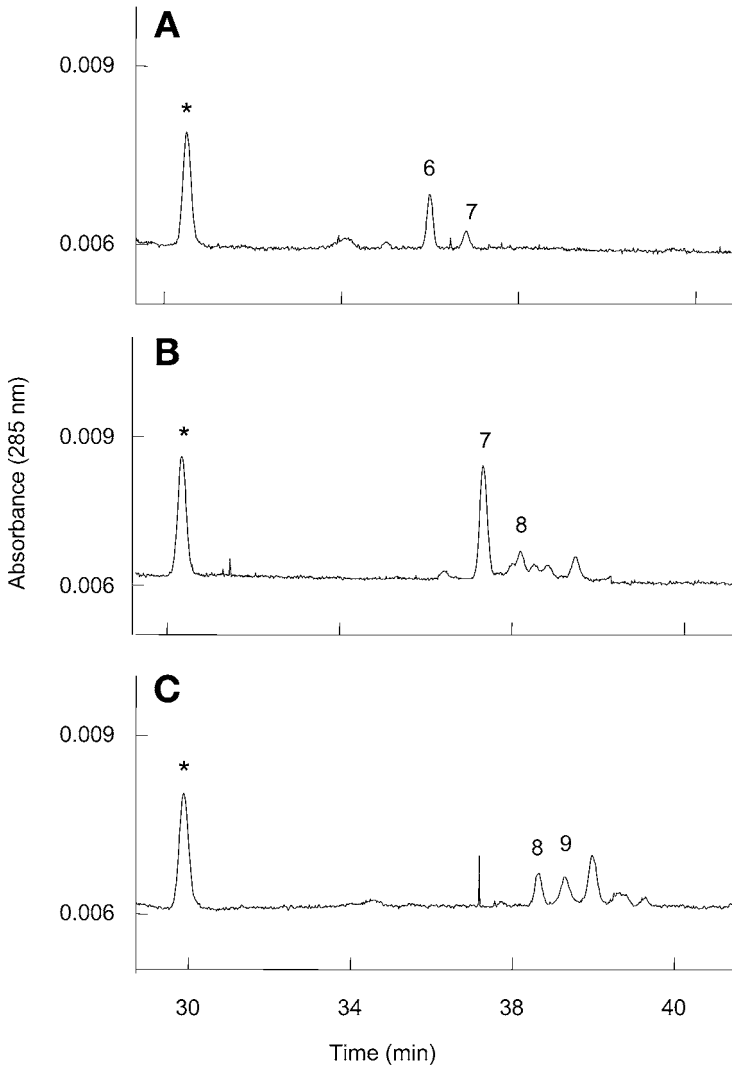


Fig. 3. Micellar electrokinetic capillary chromatography-UV analysis of aminobenzonitrile-derivatized hexamer (0.1 mg/mL) (**A**), heptamer (0.3 mg/mL) (**B**) and octamer (0.25 mg/mL) (**C**) after treatment with AlgE4; buffer: 660 mM boric acid +100 mM SDS (pH 8); voltage: 18 kV; detection: 285 nm; temperature: 27 °C; fused silica capillary, L = 72 cm l = 50 cm, internal diameter = 50 μm (reproduced with permission from **ref. *62***; © The Biochemical Society).

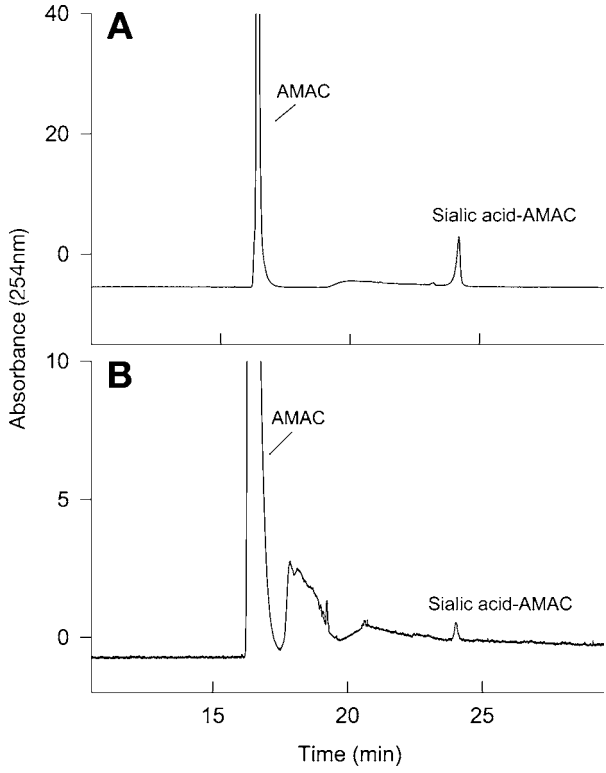


Fig. 4. Capillary zone electrophoresis-UV analysis of sialic acid derivatized with 2-aminoacridone (AMAC) (diluted 1:20 with water). (**A**) Standard Neu5Ac-AMAC; (**B**) Neu5Ac-AMAC from IgG; buffer: 50 mM sodium tetraborate (pH 9.2); voltage: 15 kV; UV detection: 254 nm; temperature: 25 °C; fused silica capillary, L = 80 cm; l = 72.5 cm; internal diameter = 50 μm.

4. Notes

1. IgG from human serum (10 mg in 2 mL of 50 mM KH_2PO_4 buffer, pH 6) is treated with 50 mU of neuraminidase from *A. ureafaciens* and incubated for 22 h at 37 °C.
2. 4-ABN has been successfully used for alginate oligomers containing up to 20 monomeric units ***(32)***. Response factors are independent of chain length because there is only one ABN chromophore attached to each oligomer. This is a clear advantage of CE (in the derivatization approaches which exploit the reactivity of reducing end) with respect to HPAEC-PAD, where the response factors must be determined for each oligomer, as mentioned previously. It must be stressed, however, that this discussion has been experimentally proven only for relatively short oligosaccharides. For higher molecular weights, the yield of reductive amination may decrease with consequent loss in reliability of the CE method for quantitative purposes ***(97)***.

3. Store ABN-derivatized samples at +4 °C.
4. Store derivatized samples at −20 °C in the dark, since at room temperature, a spontaneous conversion of the product into a de-carboxylated species is observed *(77)*.

Acknowledgments

We gratefully thank Prof. Gudmund Skjåk Bræk and his research group (University of Science and Technology NTNU, Throndheim, Norway) for giving us the opportunity to discover the world of alginates.

References

1. McNaught, A.D. (1997) Nomenclature of carbohydrates (Recommendations 1996). *Carbohydr. Res*. **297,** 1–90.
2. Lindhorst, T.K. (2000) *Essentials of Carbohydrate Chemistry and Biochemistry*, Wiley-VCH Verlag, Wheinheim.
3. Smidsrod, O., Skjåk Bræk, G. (1990) Alginate as immobilization matrix for cells. *Trends Biotechnol*. **8,** 71–78.
4. Draget, K.I., Skjåk Bræk, G., Smidsrod, O. (1997) Alginate based new materials. *Int. J. Biol. Macromol*. **21,** 47–55.
5. Varki, A., Cummings, R., Esko, J., Freeze, H., Hart, G., Marth, J., (eds.). (1999) *Essentials of Glycobiology*, Cold Spring Laboratory Press, NY (available on-line in the Bookshelf of the PubMed site http://www.ncbi.nlm.nih.gov/entrez/query.fcgi).
6. Karamanos, N.K., Hjerpe, A. (2002) Capillary electrophoresis of intact and depolymerised glycosaminoglycans and proteoglycans, in *Carbohydrate Analysis by Modern Chromatography and Electrophoresis* (El Rassi, Z., ed.), *Journal of Chromatography Library*, Vol. 66, Elsevier, Amsterdam, pp. 799–826.
7. Angata, T., Varki, A. (2002) Chemical diversity in sialic acids and related a-keto acids: an evolutionary perspective. *Chem. Rev*. **102,** 439–469.
8. Reuter, G., Schauer, R. (1994) Determination of sialic acids. *Methods Enzymol*. **230,** 168–199.
9. Mechref, Y., Novotny, M.V. (2002) Structural investigations of glycoconjugates at high sensitivity. *Chem. Rev*. **102,** 321–369.
10. Lindahl, U., Lidholt, K., Spillmann, D., Kjellen, L. (1994) More to "heparin" than anticoagulation. *Thromb. Res*. **75,** 1–32.
11. Venkataraman, G., Shriver, Z., Raman, R., Sasisekharan, R. (1999) Sequencing complex polysaccharides. *Science* **286,** 537–542.
12. Theocharis, A.D., Theocaris, D.A. (2002) High-performance capillary electrophoretic analysis of hyaluronan and galactosaminoglycan-disaccharides in gastrointestinal carcinomas. Differential disaccharide composition as a possible tool-indicator for malignances. *Biomed. Chromatogr*. **16,** 157–161.
13. Dong, X., Xi, X., Han, F., Ping, X., Yuang, X., Lin, B. (2001) Determination of sialic acids in the serum of cancer patients by capillary electrophoresis. *Electrophoresis* **22,** 2231–2235.

14. Ciolczyk-Wierzbicka, D., Gil, D., Hoja-Lukowicz, D., Litynska, A., Laidler, P. (2002) Carbohydrate moieties of N-cadherin from human melanoma cell lines. *Acta Biochim. Pol*. **49,** 991–998.
15. Alberts, B., Johnson, A., Lewis, J., Raff, M., Roberts, K., Walter, P. (2002) *Molecular Biology of the Cell*, 4th edn., Garland Publishing, New York (available on-line in the Bookshelf of the PubMed site http://www.ncbi.nlm.nih.gov/entrez/query.fcgi).
16. Draget, K.I., Strand, B., Hartmann, M., Valla, S., Smidsrod, O., Skjåk Bræk, G. (2000) Ionic and acid gel formation of epimerised alginates; the effect of AlgE4. *Int J Biol Macromol*. **27,** 117–122.
17. Donati, I., Gamini, A., Skjåk Bræk, G., Vetere, A., Campa, C., Coslovi, A., Paoletti, S. (2003) Determination of the diadic composition of alginate by means of circular dichroism: a fast and accurate improved method. *Carbohydr. Res*. **338,** 1139–1142.
18. Hizukuri, Y., Yamanishi, Y., Hashimoto, K., Kanehisa, M. (2004) Extraction of species-specific glycan substructures. *Genome Inform*. **15,** 69–81.
19. Linhardt, R.J., Pervin, A. (1996) Separation of negatively charged carbohydrates by capillary electrophoresis. *J. Chromatogr. A* **720,** 323–335.
20. Grimshaw, J. (1997) Analysis of glycosaminoglycans and their oligosaccharide fragments by capillary electrophoresis. *Electrophoresis* **18,** 2408–2414.
21. Lamari, F., Karamanos, N. K. (1999) High performance capillary electrophoresis as a powerful analytical tool of glycoconjugates. *J. Liq. Chrom. Rel. Technol*. **22,** 1295–1317.
22. Koketsu, M., Linhardt, R.J. (2000) Electrophoresis for the analysis of acidic oligosaccharides. *Anal. Biochem*. **283,** 136–145.
23. Mao, W., Thanawiroon, C., Linhardt, R.J. (2002) Capillary electrophoresis for the analysis of glycosaminoglycans and glycosaminoglycan- derived oligosaccharides. *Biomed. Chromatogr*. **16,** 77–94.
24. El Rassi, Z. (ed.) (2002) *Carbohydrate Analysis by Modern Chromatography and Electrophoresis, Journal of Chromatography Library*, Vol. 66, Elsevier, Amsterdam.
25. Bleton, J., Mejanelle, P., Sansoulet, J., Goursaud, S., Tchapla, A. (1996) Characterization of neutral sugars and uronic acids after methanolysis and trimethylsilylation for recognition of plant gums. *J. Chromatogr. A* **720,** 27–49.
26. Heyraud, A., Leonard, C. (1991) Analysis of oligouronates by reversed-phase ion-pair HPLC: role of the mobile phase. *Carbohydr. Res*. **215,** 105–115.
27. Knutsen, S.H., Sletmoen, M., Kristensen, T., Barbeyron, T., Kloareg, B., Potin, P. (2001) A rapid method for the separation and analysis of carrageenan oligosaccharides released by iota- and kappa- carrageenase. *Carbohydr. Res*. **331,** 101–106.
28. Klockow, A., Paulus, A., Figuereiso, V., Amadò, R., Widmer, H.M. (1994) Determination of carbohydrates in fruit juices by capillary electrophoresis and high-performance liquid chromatography. *J. Chromatogr. A* **680,** 187–200.
29. Kitagawa, H., Kinoshita, A., Sugahara, K. (1995) Microanalysis of glycosaminoglycan-derived disaccharides labelled with the fluorophore 2-

aminoacridone by capillary electrophoresis and high- performance liquid chromatography. *Anal. Biochem.* **232,** 114–121.
30. Ferro, V., Li, C., Fewings, K., Palermo, M. C., Lindhardt, R.J., Toida, T. (2002) Determination of the composition of the oligosaccharide phosphate fraction of *Pichia (Hansenula) holstii* NRRL Y-2448 phosphomannan by capillary electrophoresis and HPLC *Carbohydr. Res*. **337,** 139–146.
31. Soga, T. (2002) Analysis of carbohydrates in food and beverages by HPLC and CE, in *Carbohydrate Analysis by Modern Chromatography and Electrophoresis* (El Rassi, Z., ed.), *Journal of Chromatography Library*, Vol. 66, Elsevier, Amsterdam, pp. 483–502.
32. Campa, C., Oust, A., Skjåk Bræk, G., Smestad Paulsen, B., Paoletti, S., Christensen, B.E., Ballance, S. (2004) Determination of average degree of polymerisation and distribution of oligosaccharides in a partially acid- hydrolysed homopolysaccharide: a comparison of four experimental methods applied to mannuronan. *J. Chromatogr. A* **1026,** 271–281.
33. Smits, H.P., Cohen, A., Buttler, T., Nielsen, J., Olsson, L. (1998) Cleanup and analysis of sugar phosphates in biological extracts by using solid-phase extraction and anion-exchange chromatography with pulsed amperometric detection. *Anal. Biochem*. **261,** 36–42.
34. Cataldi, T.R.I., Campa, C., Casella, I.G. (1999) Study of sugar acids separation by high-performance anion-exchange chromatography-pulsed amperometric detection using alkaline eluents spiked with Ba^{2+}, Sr^{2+}, or Ca^{2+} as acetate or nitrate salts. *J. Chromatogr. A* **848**, 71–81.
35. Cataldi, T.R.I., Campa, C., De Benedetto, G.E. (2000) Carbohydrate analysis by high-performance anion-exchange chromatography with pulsed amperometric detection: the potential is still growing. *Fresenius J. Anal. Chem*. **368**, 739–758.
36. Roher, J.S. (2000) Analyzing sialic acids using high-performance anion-exchange chromatography with pulsed amperometric detection. *Anal. Biochem*. **283,** 3–9.
37. Ye, J., Baldwin, R.P. (1994) Determination of carbohydrates, sugar acids and alditols by capillary electrophoresis and electrochemical detection at a copper electrode. *J. Chromatogr. A* **687,** 141–148.
38. El Rassi, Z. (1997) Recent developments in capillary electrophoresis of carbohydrate species. *Electrophoresis* **18,** 2400–2407.
39. Soga, T., Heiger, D.N. (1998) Simultaneous determination of monosaccharides in glycoproteins by capillary electrophoresis. *Anal. Biochem*. **261,** 73–78.
40. Soga, T., Ross, G.A. (1999) Simultaneous determination of inorganic anions, organic acids, amino acids and carbohydrates by capillary electrophoresis. *J. Chromatogr. A* **837,** 231–239.
41. Soga, T., Imaizumi, M. (2001) Capillary electrophoresis method for the analysis of inorganic anions, organic acids, amino acids, nucleotides, carbohydrates and other anionic compounds. *Electrophoresis* **22,** 3418–3425.
42. Yeung, E.S., Kuhr, W.G. (1991) Indirect detection methods for capillary separations. *Anal. Chem*. **63,** 275A–282A.

43. Bergholdt, A., Overgaard, J., Colding, A. (1993) Separation of D-galactonic and D-gluconic acids by capillary zone electrophoresis. *J. Chromatogr.* **644,** 412–415.
44. Damm, J.B., Overklift, G.T. (1994) Indirect UV detection as a non-selective detection method in the qualitative and quantitative analysis of heparin fragments by high-performance capillary electrophoresis. *J. Chromatogr. A* **678,** 151–165.
45. Paulus, A., Klockow, A. (1996) Detection of carbohydrates in capillary electrophoresis. *J. Chromatogr. A* **720,** 353–376.
46. Thibault, P., Honda, S. (eds.) (2003) *Capillary Electrophoresis of Carbohydrates, Methods in Molecular Biology Series*, Vol. 213, Humana Press, Totowa, New Jersey.
47. Novotny, M.V., Sudor, J. (1993) High performance electrophoresis of glycoconjugates. *Electrophoresis* **14,** 373–389.
48. Suzuki, S., Honda, S. (1998) A tabulated review of capillary electrophoresis of carbohydrates. *Electrophoresis* **19,** 2539–2560.
49. El Rassi, Z. (1999) Recent developments in capillary electrophoresis and capillary electrochromatography of carbohydrate species. *Electrophoresis* **20,** 3134–3144.
50. Carney, S.L., Osborne, D.J. (1991) Separation of chondroitin sulphate disaccharides and hyaluronan oligosaccharides by capillary zone electrophoresis. *Anal. Biochem.* **195,** 132–140.
51. Michaelsen, S., Schrøder, M., Sørensen, H. (1993) Separation and determination of glycosaminoglycans disaccharides by micellar electrokinetic capillary chromatography for studies of pelt glycosaminoglycans. *J. Chromatogr. A* **652,** 503–515.
52. Pervin, A., Al-Hakim, A., Lindhart, R.J. (1994) Separation of glycosaminoglycans-derived oligosaccharides by capillary electrophoresis using reverse polarity. *Anal. Biochem.* **221,** 182–188.
53. Karamanos, N.K., Axelsson, S., Vanky, P., Tzanakakis, G.N., Hjierpe, A. (1995) Determination of hyaluronan and galactosaminoglycan disaccharides by high-performance capillary electrophoresis at the attomole level. Applications to analyses of tissue and cell culture proteoglycans. *J. Chromatogr. A* **696,** 295–305.
54. Scapol, L., Marchi, E., Viscomi, G.C. (1996) Capillary electrophoresis of heparin and dermatan sulphate unsaturated disaccharides with triethylamine and acetonitrile as electrolyte additives. *J. Chromatogr. A* **735,** 367–374.
55. Karamanos, N.K., Hjerpe, A. (1997) High-performance capillary electrophoretic analysis of hyaluronan in effusions from human malignant mesothelioma. *J. Chromatogr. B* **697,** 277–281.
56. Rydlund, A., Dahlman, O. (1997) Rapid analysis of unsatured acidic xylooligosaccharides from kraft pulps using capillary electrophoresis. *J. High. Resolut. Chromatogr.* **20,** 72–76.
57. Ruiz-Calero, V., Puignou, L., Galceran, M.T. (1998) Use of reversed and pressure gradient in the analysis of disaccharide composition of heparin by capillary electrophoresis. *J. Chromatogr. A* **828,** 497–508.
58. Payan, E., Presle, N., Lapicque, F., Jouzeau, J.Y., Bordji, K., Oerther, S., Miralles, G., Mainard, D., Netter, P. (1998) Separation and quantification by ion-association capillary zone electrophoresis of unsaturated disaccharide units of

chondroitin sulfates and oligosaccharides derived from hyaluronan. *Anal. Chem*. **70,** 4780–4786.
59. Gunay, N.S., Linhardt, R.J. (2003) Capillary electrophoretic separation of heparin oligosaccharides under conditions amenable to mass spectrometric detection. *J. Chromatogr. A* **1014,** 225–233.
60. Militsopoulou, M., Lamari, F., Karamanos, N.K. (2003) Capillary electrophoresis: a tool for studying interactions of glycans/proteoglycans with growth factors. *J. Pharm. Biomed. Anal*. **32,** 823–828.
61. Stöm, A., Williams, M.A.K. (2004) On the separation, detection and quantification of pectin derived oligosaccharides by capillary electrophoresis. *Carbohydr. Res*. **399,** 1711–1716.
62. Campa, C., Holtan, S., Nilsen, N., Bjerkan, T.M., Stokke, B.T., Skjåk-Bræk, G. (2004) Biochemical analysis of the processive mechanism for epimerisation of alginate by mannuronan C-5 epimerase AlgE4. *Biochem. J*. **381,** 155–164.
63. Duteil, S., Gareil, P., Girault, S., Mallet, A., Feve, C., Siret, L. (1999) Identification of heparin oligosaccharides by direct coupling of capillary electrophoresis/ionspray-mass spectrometry. *Rapid Commun. Mass Spectrom*. **13,** 1889–1898.
64. Ruiz-Calero, V., Moyano, E., Puignou, L., Galceran, M.T. (2001) Pressure-assisted capillary electrophoresis-ion trap mass spectrometry for the analysis of heparin depolymerised disaccharides. *J. Chromatogr. A* **914,** 277–291.
65. Zamfir, A., Seidler, D.G., Kresse, H., Peter-Katalini, J. (2002) Structural characterization of chondroitin/dermatan sulfate oligosaccharides from bovine aorta by capillary electrophoresis and electrospray ionization quadrupole time-of-flight tandem mass spectrometry. *Rapid Commun. Mass Spectrom*. **16,** 2015–2024.
66. Kühn, A.V., Rüttinger, H.H., Neubert, R.H.H., Raith, K. (2003) Identification of hyaluronic acid oligosaccharides by direct coupling of capillary electrophoresis with electrospray ion trap mass spectrometry. *Rapid Commun. Mass Spectrom*. **17,** 576–582.
67. Liu, J., Shirota, O., Novotny, M.V. (1992) Sensitive, laser-assisted determination of complex mixtures separated by capillary gel electrophoresis at high resolution. *Anal. Chem*. **64,** 973–975.
68. Honda, S., Ueno, T., Kakehi, K. (1992) High-performance capillary electrophoresis of unsaturated oligosaccharides derived from glycosaminoglycans by digestion with chondroitinase ABC as 1-phenyl-3-methy-5-pyrazolone derivatives. *J. Chromatogr*. **608,** 289–295.
69. Sudor, J., Novotny, M.V. (1995) End-label, free-solution capillary electrophoresis of highly charged oligosaccharides. *Anal. Chem*. **67,** 4205–4209.
70. Mort, A.J., Chen, E.M.W. (1996) Separation of 8-aminonaphtalene-1,3,6-trisulfaste (ANTS)-labeled oligomers containing galacturonic acid by capillary electrophoresis: application to determining the substrate specificity of endopolygalacturonases. *Electrophoresis* **17,** 379–383.
71. Rydlund, A., Dahlman, O. (1996) Efficient capillary zone electrophoretic separation of wood-derived neutral and acidic mono- and oligosaccharides. *J. Chromatogr. A* **738,** 129–140.

72. El Rassi, Z., Postlewait, J., Mechref, Y., Ostrander, G.K. (1997) Capillary electrophoresis of carboxylated carbohydrates III. Selective precolumn derivatization of glycosaminoglycan disaccharides with 7-aminonaphthalene-1,3-disulfonic acid fluorescing tag for ultrasensitive laser-induced fluorescence detection. *Anal. Biochem*. **244,** 283–290.
73. Lamari, F., Theocaris, A., Hjerpe, A., Karamanos, N.K. (1999) Ultrasensitive capillary electrophoresis of sulfated disaccharides in chondroitin/dermatan sulfates by laser-induced fluorescence after derivatization with 2-aminoacridone. *J. Chromatogr. B* **730,** 129–133.
74. Ruiz-Calero, V., Puignou, L., Galceran, M.T. (2003) Determination of glycosaminoglycan monosaccharides by capillary electrophoresis using laser-induced fluorescence detection. *J. Chromatogr. B* **791,** 193–202.
75. Khandurina, J., Blum, D., Stege, J., Guttman, A. (2004) Automated carbohydrate profiling by capillary electrophoresis: a bioindustrial approach. *Electrophoresis* **25,** 2326–2331.
76. Guttman, A. (1997) Analysis of monosaccharide composition by capillary electrophoresis. *J. Chromatogr. A* **763,** 271–277.
77. Che, F.-Y., Shao, X.-X., Wang, K.-Y., Xia, Q.-C. (1999) Characterization of derivatization of sialic acid with 2-aminoacridone and determination of sialic acid content in glycoproteins by capillary electrophoresis and high performance liquid chromatography-ion trap mass spectrometry. *Electrophoresis* **20,** 2930–2937.
78. Strousopoulou, K., Militsopoulou, M., Stagiannis, K., Lamari, F. N., Karamanos, N.K. (2002) A capillary zone electrophoresis method for determining N-acetylneuraminic acid in glycoproteins and blood sera. *Biomed. Chromatogr*. **16,** 146–150.
79. Kakehi, K., Kinoshita, M., Hayase, S., Oda, O. (1999) Capillary electrophoresis of *N*-acetylneuraminic acid polymers and hyaluronic acid: correlation between migration order reversal and biological functions. *Anal. Chem*. **71,** 1592–1596.
80. Shen, Z., Warren, C.D., Newburg, D.S. (2000) High-performance capillary electrophoresis of sialylated oligosaccharides of human milk. *Anal. Biochem*. **279,** 37–45.
81. Taga, A., Sugimura, M., Suzuki, S., Honda, S. (2002) Estimation of sialic acid in a sialoglycan and a sialoglycoprotein by capillary electrophoresis with in-capillary sialidase digestion. *J. Chromatogr. A* **954,** 259–266.
82. Liu, J., Shirota, O., Wiesler, D., Novotny, M. (1991) Ultrasensitive fluorometric detection of carbohydrates as derivatives in mixtures separated by capillary electrophoresis. *Proc. Natl. Acad. Sci. U. S. A*. **88,** 2302–2306.
83. Mechref, Y., El Rassi, Z. (1994) Capillary zone electrophoresis of derivatized acidic monosaccharides. *Electrophoresis* **15,** 627–634.
84. Buscher, B.A.P., Tjaden, U.R., Irth, H., Andersson, E.M., van der Greef, J. (1995) Determination of 1,2,6-inositol triphosphate (derivatives) in plasma using iron(III)-loaded adsorbents and capillary zone electrophoresis-(indirect) UV detection. *J. Cromatogr. A* **718,** 413–419.

85. Mechref, Y., Ostrander, G.K., El Rassi, Z. (1997) Capillary electrophoresis of carboxylated carbohydrates IV. Adjusting the separation selectivity of derivatized carboxylated by controlling the electrolyte ionic strength at subambient temperature and in absence of electroosmotic flow. *J. Chromatogr. A* **792,** 75–82.
86. Hauri, D.C., Shen, P., Arkin, A.P., Ross, J. (1997) Steady state measurements on the fructose 6-phosphate/fructose 1,6-bisphosphate interconversion cycle. *J. Phys. Chem. B* **101,** 3872–3876.
87. Schmitt-Kopplin, Ph., Fisher, K., Freitag, D., Ketrup, A. (1998) Capillary electrophoresis for the simultaneous separation of selected carboxylated carbohydrates and their related 1,4-lactones. *J. Chromatogr. A* **807,** 89–100.
88. Soga, T., Serwe, M. (2000) Determination of carbohydrates in food samples by capillary electrophoresis with indirect UV detection. *Food Chem.* **69,** 339–344.
89. Wiedmer, S.K., Cassely, A., Hong, M., Novotny, M.V., Riekkola, M.L. (2000) Electrophoretic studies of polygalacturonate oligomers and their interactions with metal ions. *Electrophoresis* **21,** 3212–3219.
90. Soga, T., Ueno, Y., Naraoka, H., Ohashi, Y., Tomita, M., Nishioka, T. (2002) Simultaneous determination of anionic intermediates for *Bacillus subtilis* metabolic pathways by capillary electrophoresis electrospray ionization mass spectrometry. *Anal. Chem.* **74,** 2233–2239.
91. Descroix, S., Varenne, A., Goasdou, N., Abian, J., Carrascal, M., Daniel, R., Gareil, P. (2003) Non-aqueous capillary electrophoresis of positional isomers of a sulphated monosaccharide. *J. Chromatogr. A* **987,** 467–476.
92. Hoffstetter-Kuhn, S., Paulus, A., Gassmann, E., Widmer, H.M. (1991) Influence of borate complexation on the electrophoretic behaviour of carbohydrates in capillary electrophoresis. *Anal. Chem.* **63,** 1541–1547.
93. Evangelista, R.A., Chen, F.A., Guttman, A. (1996) Reductive amination of N-linked oligosaccharides using organic acid catalysis. *J. Chromatogr. A* **745,** 273–280.
94. Schwaiger, H., Oefner, P.J., Huber, C., Grill, E., Bonn, G.K. (1994) Capillary electrophoresis and micellar electrokinetic chromatography of 4-aminobenzonitrile carbohydrate derivatives. *Electrophoresis* **15,** 941–952.
95. Lindquist, A., Rydlund, A., Dahlman, O. (1997) Selective determination of acidic carbohydrates using capillary electrophoresis. *ISWPC,* 22/1–22/4.
96. Camilleri, P., Harland, G.B., Okafo, G. (1995) High resolution and rapid analysis of branched oligosaccharides by capillary electrophoresis. *Anal. Biochem.* **230,** 115–122.
97. Chmelík, J., Chmelíková, J., Novotny, M.V. (1997) Characterization of dextrans by size-exclusion chromatography on unmodified silica gel columns, with light-scattering detection, and capillary electrophoresis with laser-induced fluorescence detection. *J. Chromatogr. A* **790,** 93–100.

13

Use of Capillary Electrophoresis for Polysaccharide Studies and Applications

Amelia Gamini, Anna Coslovi, Isabella Rustighi, Cristiana Campa, Amedeo Vetere, and Sergio Paoletti

Summary

Capillary electrophoresis (CE) applications to charged polysaccharides are briefly reported. A simple procedure is presented to determine the esterification degree of a hyaluronan derivative. In this case, the degree of substitution was as low as 14%. The molecular weight distribution of mannuronic oligosaccharides mixture produced by hydrolysis of native polymannuronic is readily calculated from peak area of the species resolved by CE on the basis of a specific degree of polymerization. The influence of the applied electric field strength on the free solution mobility of hyaluronan samples is briefly addressed for molar masses of the order of 10^5 and 10^6 g/mol. The data are compared with the results obtained for a 50% galactose-substituted hyaluronic acid (HA). Mobility data obtained as a function of buffer pH for a native HA sample as well as for two galactose-amide HA derivatives, having slightly different degrees of substitution, are presented and discussed in terms of the polymer charge density parameters ξ. In most cases, more questions than answers arise from the application of CE to charged polysaccharides. However, perspectives are disclosed for a further understanding of the reliability of CE applied for the structural elucidation of such macromolecules.

Key Words: Charged polysaccharides; hyaluronan; capillary electrophoresis; electrophoretic mobility; charge density; molar mass distribution; random degradation; glycoconjugates.

1. Introduction

In the polysaccharide field, capillary electrophoresis (CE) studies have followed two main streams. One is dealing mainly with identification and

From: *Methods in Molecular Biology, vol. 384: Capillary Electrophoresis*
Edited by: P. Schmitt-Kopplin © Humana Press Inc., Totowa, NJ

quantification of native biopolymers in pharmaceuticals, biological samples and foods ***(1–15)***. The other is dealing with the elucidation of chemical structure in terms of molar mass, polydispersity and degree of substitution ***(16–29)***. In this respect, **Table 1** reports, more explicatively than exhaustively, the experimental details of the applied procedure as well as the main results achieved by CE technique applied to polysaccharides. By inspection of **Table 1**, it turns out that the glycosaminoglycans are in general the most studied polysaccharides, and important reviews have been also devoted to this subject (*see*, for instance, ***30***). Besides, to overcome the experimental limit of mass separation when large biopolymers are studied, polysaccharides have also found wide application on CE techniques as sieving matrix ***(8,16,24,31–41)***. In this respect, however, much care should be taken on considering polysaccharide chains as inert sieving material, especially when the objective of their use is to separate structurally similar molecules. Certain cellulose derivatives, for instance, have peculiar features strictly related to their rather rigid backbone. As an example, hydroxypropyl cellulose ***(24,33,40)*** not only goes to phase separation in water at temperature slightly higher than 40 °C but is also known to aggregate in ordered structures leading, at sufficiently high concentration, to liotropic mesophases of cholesteric type ***(41)***. Indeed, most polysaccharides easily form aggregated structures, in line with their more common, although less specialized, biological role. To mention only a few, viscoelastic, mechanical, protective and gelling properties are indeed strictly related to polysaccharide secondary (if not tertiary) structures assumed in aqueous environment. These may range from coiled to worm-like type, the stiffness of which strongly depends on the chain molecularity (single-, double-, triple- and multi-chain) which itself may depend on the solution environment (temperature, salt concentration and salt type).

1.1. Determination of the Degree of Substitution of Hyaluronic Acid Butyric Ester: CZE-UV of Released Butyric Acid

In recent years, great attention has been directed towards synthetic glyco-polymers as well as naturally occurring glyco-polymers (i.e. polysaccharides) for their potential use as biomaterials. Polymer engineering is a term usually referred to a pre-existing polymer chain *ad hoc* modified by introducing biologically active ligands developing third-generation biomaterials that are able to directly intervene in cell growth, differentiation, adhesion and extracellular matrix production ***(42–47)***. At the level of isolated molecules, the ligand-receptor affinity is very low and can be dramatically increased by increasing the ligand density within the glyco-conjugate (‘cluster’ effect). A similar approach can be used by anchoring a biological and pharmacological active molecule,

Table 1
Capillary electrophoresis (CE) Technique(s) Applied to Polysaccharide Investigations

Reference	Carbohydrate species	Matrix	Derivatizing agent	CE mode	Capillary, T	Buffer, Voltage	Detection mode	LOD	Results
Identification and quantification of polysaccharides									
(1)	Heparin	Deproteinized plasma samples Std	None	MEKC	Fused silica ($l = 30$cm, ID $= 50\,\mu$m); T $= 20\,^{\circ}$C;	25 mM boric acid +25 mM SDS (pH 8.5); 20 kV Outlet: cathode	UV (270 nm)	25 units/L	• HPCE quantified free heparin in plasma, suitable for measuring high doses of heparin in clinical therapy
(2)	HA	Water-extracted fractions from pharmaceuticals	None	CZE	Fused silica ($L = 64.5$ cm. $l = 56$ cm, ID $= 50\,\mu$m); T $= 25\,^{\circ}$C	20 mM phosphate (pH 7.4); 30 kV; Outlet: cathode	UV (195 nm, 200 nm)	10 μg/mL	• Compared to photometric determination with carbazole reaction, quantification of HA with CE: – not influenced by the presence of other carbohydrates – lower LOD but a twofold lower SD – suitable method for semisolid formulations: absence of interactions with the matrix

(Continued)

Table 1
(Continued)

Reference	Carbohydrate species	Matrix	Derivatizing agent	CE mode	Capillary, T	Buffer, Voltage	Detection mode	LOD	Results
(3)	HA	Std From vitreous humour	None	MEKC	Fused silica ($l = 50$ cm, ID = 75 μm); T = 30 °C	50 mM disodium hydrogenphosphate, 40 mM SDS, 10 mM sodium tetraborate (pH 9); 15 kV; Outlet: cathode	UV (200 nm)	25 μg/mL	• Quantification of hyaluronan in the complex matrix of vitreous humor (bovine and human) CE powerful tool to investigate vitreous humour diseases
(4)	Chondroitin 4-sulphate, HA, heparan sulphate, heparin (LMW and HMW)	Intact and degraded GAGs	None	CZE	Fused silica ($L = 68$ cm, ID = 75 μm); RT	Intact GAGs: $CuSO_4$ 5 mM (pH 4.5); −20 kV Enzymatically treated GAGs: sodium phosphate (pH 3.5); 20 kV Outlet: anode	UV (240 nm) UV (232 nm)	10–9 g n.a.	• GAGs separation based on Cu (II)-carboxylate complex formation. • Optimized conditions (pH 4.5, 240 nm, 20 kV, 20 mM $CuSO_4$) led to distinct GAG migration times. Broad peaks (due to polydispersity) are observed, only LMW heparin and dermatan sulphate show narrower peaks

(5)	K4 and defructosylated K4 native polysaccharides	K4 anionic polysaccharide from *Escherichia coli*	None	MEKC	Fused silica ($L = 85$ cm; $l = 65$ cm, ID = 50 μm); T = 25 °C	40 mM disodium hydrogen phosphate, 10 mM sodium tetraborate, 40 mM SDS (pH 9); 20 kV; Outlet: cathode	UV (200 nm)	Less than 30 ng (0.5 μg/μL)	• HPCE separation for qualitative and quantitative determination of native K4 and its defructosylated product before, during and after defructosylation process
(6)	LMW heparin fragments	Colominic acid (hydrolyzate), heparin fragments, synthetic heparin pentasaccharides	None	CZE	Fused silica ($L = 57$ cm, $l = 50$ cm, ID = 75 μm); T = 40 °C	200 mM NaH_2PO_4 (pH 2, 3, 4); 7.5 kV; Outlet: anode	UV (214 nm)	n.a.	• Optimized conditions with std colominic oligosaccharides led to good separation of heparin disaccharides and short heparin fragments according to their MW, charge and structural heterogeneity • CE can be applied to assess the quality of synthetic heparin pentasaccharide preparation

(Continued)

Table 1
(Continued)

Reference	Carbohydrate species	Matrix	Derivatizing agent	CE mode	Capillary, T	Buffer, Voltage	Detection mode	LOD	Results
(7)	Starch	Glc (from starch depoly-mer-ization) **2**. Linear oligosac-charides (DP 3/85) isoamylase treatment	APTS	CZE	Neutrally coated with eCAP™ buffer (Beckman), ($L = 47\,\text{cm}$ ID = .50 μm) T = 25 °C	eCAP™ buffer (Beckman); V = 23.5 kV; Outlet: cathode	LIF ($\lambda_{ecc} = 488\,nm$)	n.a.	• Capillary electrophoresis provides a highly resolving and sensitive alternative method to gel electrophoresis • Separation of APTS-labelled oligosaccharides turned out to be both higher resolving and a more reproducible method than DNA sequencer analysis

(8)	Derivatized HA mixtures	HA samples (from bovine trachea and S*treptococcus zooepi-demicus*) also degraded by ultrasoni-cation or enzyme treatment	APTS	CGE	Various lengths of coated (LPAA) (ID = 50 μm) $l = 50$ cm $l = 45$ cm $l = 45$ cm, RT	Intact HA: 25 mM citric acid, 12.5 mM Tris buffer; 5% LPAA (pH 3); 430 V/cm **2**. Enzymatic HA digests: 25 mM citric acid, 12.5 mM Tris buffer (pH 3), 4 M urea, 0.03% aminodextran, 3% LPAA; 416 V/cm Ultrasonic degraded HA: as in intact HA, 416 V/cm; Outlet: anode	LIF (λ_{exc} = 488 nm; λ_{em} = 514 nm)	n.a.	• Using LPAA, polydispersity of intact HA is highlighted. Polysaccharides differing in one disaccharide unit are resolved • Decrease of polydispersity with HA degradation • Satellite peaks appeared after ultrasonication are ascribed to pH-dependent conformers

(Continued)

Table 1
(Continued)

Reference	Carbohydrate species	Matrix	Derivatizing agent	CE mode	Capillary, T	Buffer, Voltage	Detection mode	LOD	Results
(9)	κ-, ι- and λ-carrageenan	Stds and commercial food additives in water at RT and thermally treated (70–90 °C)	APTS	CZE	Fused silica ($l = 47$ cm; ID = 50 μm); T = 25, 37 and 50 °C	25 mM citrate (pH 3); 30 kV Outlet: anode	LIF (λ_{exc} = 488 nm; λ_{em} = 520 nm)	0.3 μg/mL	• Capillary electrophoresis provides a simple, rapid method for the quantitative detection and separation of κ-, ι-carrageenans. λ-carrageenan identified by migration times and peak shape
					For lower DP components: CHO-coated capillary ($l = 47$ cm; ID = 50 μm); T = 20 °C	Beckman gel buffer; 30 kV; Outlet: anode			
(10)	Chitosan	Stds Chitosan in plasma and foods (acidified with 10% TFA)	None	CZE	Fused silica ($L = 27$ cm, $l = 20$ cm, ID = 50 μm); RT	100 mM TEA-phosphate buffer (pH 2); 15 kV; Outlet: cathode	UV (195 nm)	0.25 mg/mL	• Excellent linear responses were obtained in the range of 1.25–20 mM • Applicable to chitosan determination in real biological samples

(11)	Pectins	Stds Enzimatically de-esterified pectins from lemon peel	None	CZE	Fused silica ($L = 57$ cm, $l = 50$ cm, ID = 100 μm); T = 30 °C	Phosphate (pH 7); 20 kV; Outlet: cathode	UV (192 nm)	0.5 mg/mL	• Capillary electrophoresis provides a simple, rapid method for the quantitative detection and separation of pectins with different DE • This technique has the potential of quantifying the charge polydispersity directly
(12)	Two starch-hydrolyzed sample and four dextran samples	stds	None	CZE	Coated (LPAA) ($l = 80$ cm, ID = 25 μm); RT	Aqueous NaOH (50–200 mM), eventually containing CTAB at a concentration between 0.25 and 10 mM; 20 kV; Outlet: cathode	ED. Working electrode: 127-μm Cu magnet wire whose side areas were covered with a non-conductive coating	1.0×10^{-6} –1.0×10^{-7} M	• Coupling of the high separation efficiency of CE with high sensitivity detection methods for the analysis of complex carbohydrate samples, without the need for derivatization procedures

(Continued)

Table 1
(Continued)

Reference	Carbohydrate species	Matrix	Derivatizing agent	CE mode	Capillary, T	Buffer, Voltage	Detection mode	LOD	Results
(13)	Poly-galacturonic acid	Oligo-saccharides mixture (wide DP range) from partially hydrolyzed polygalac-turonic acid	CBQCA	CGE	Deactivated fused silica filled with LPAA gels at high concentration ($L = 30$ cm, $l = 23$ cm; ID = 50 μm); RT	0.1 M Tris, 0.25 M boric acid, 2 mM EDTA (pH 8.48); 5 kV; Outlet: cathode	LIF ($\lambda_{exc} =$ 487 nm; $\lambda_{em} =$ 550 nm)	85 fM	• Resolution of highly complex mixtures of oligosaccharides
(14)	Poly-galacturonic acids	Stds	APTS	CGE	Coated with a layer of linear polyacry-lamide (ID = 50 μm, $L =$ 62 cm, $l = 47$ cm) ELFSE, RT	24 mM citric acid, 2 M urea, pH3, 4% LPAA; 25 kV; Outlet: cathode	LIF ($\lambda_{exc} =$ 488 nm; $\lambda_{em} =$ 514 nm)	n.a.	• Metals–polysaccharide interactions as detected by CE • CGE size-dependent separation • Use of CE-LIF to separate polygalacturonic molecules in both entangled matrices (mandatory for larger oligomers) and free solutions media
			N-(1-malto-heptaosamine)-3,6-diaminoacridine	ELFSE					

(15)	Chitin and glucan hydrolyzates	Stds of Glc and GlcNAc	6-AQ	CZE, CEC	Fused silica (L = 57 cm; l = 50 cm; ID = 50 μm); RT	100 mM sodium phosphate monobasic, pH 5.0; V = 15 kV	UV (254 nm)	1.2×10^{-5} M	• Qualitative and quantitative analyses of chitin and glucan content of two peanut fungal pathogens and baker's yeast
		Total enzimatically digested chitin and glucan				Same, V = 20 kV Same containing 50 mM tetrabutylammonium bromide, pH 5; 15 kV; Outlet: cathode			• The study revealed the differences in chitin and glucan content of the *Sclerotium rolfsii fungus* isolates from various locations

(Continued)

Table 1
(Continued)

Reference	Carbohydrate species	Matrix	Derivatizing agent	CE mode	Capillary, T	Buffer, Voltage	Detection mode	LOD	Results
Structural characterization of polysaccharides									
(16)	HA	Hyaluronic acid samples, from pig skin, human ombelical cord and pharmaceuticals (MW 40–60 kDa, 0.8–2.1 and 1.5–2.1 MDa, respectively)	None	CGE	Fused silica (L = 58 cm, l = 50 cm; ID = 75 μm) T = 25 °C	50 mM phosphate (pH 4) PU of various MW (48, 212, 380, 1600 kDa) and dextran (MW 60–90 kDa); 20 kV; Outlet: anode	UV (185 nm)	1 μg/mL	• Quantitative determination of HA samples of different Mw from different sources • With PU as sieving matrix, HA samples migrate according to their MW • Peak broadening due to both size-exclusion effect of PU network to sample polydispersity

(17)	Hydrolyzed fucoidan and heparin	Commercial samples	None	CZE	Fused silica (L = 34.5 cm, l = 26 cm, ID = 50 μm) T = 25 °C	Anisic acid, sulfosalicilic acid with Bis-Tris or Tris (various concentrations and pHs); 30 kV; Outlet: anode or cathode;	Indirect UV (450 nm)	n.a.	• CE characterization of LMW fucoidan and heparin samples as a function of pH, ionic strengths and counterions
(18)	Derivatized polysaccharide samples	Alginate (200 kDa); HA (185, 750, 900, 1350, 3600, 9300 kDa)	APTS	CZE	Coated with LPAA and EHEC, (various lengths, ID = 50 μm), RT	50 mM phosphate, 55 mM Tris (pH 6.2); 5–300 V/cm; Outlet: cathode	LIF (λ_{exc} = 488 nm; λ_{em} = 515 nm)	n.a.	• Aggregation into sample-rich domain occur at a specific electric field value (i.e. E_t) for an initially homogeneous solution • At E_t, electropherograms distortion and formation of sharp distinct peaks occurs

(Continued)

Table 1
(Continued)

Reference	Carbohydrate species	Matrix	Derivatizing agent	CE mode	Capillary, T	Buffer, Voltage	Detection mode	LOD	Results
									• Segregation phenomenon increases with increasing sample molecular weight and charge as well as with sieving polymer molecular weight and concentration
(19)	GAG mimotope (chondroitine sulphate oligomer recognized by hydrolytic enzymes like chondroitinase and hyaluronidase)	Desulphated (by methanolysis or enzyme digestion) chondroitine sulphate	None	MEKC	Fused silica (L = 72 cm, l = 50 cm, ID = 50 μm) T = 40 °C	40 mM phosphate, 40 mM SDS, 10 mM borate (pH 9); 15 kV; Outlet: anode	UV (200 nm)	n.a.	• Sulphation degree of intact and partly desulphated GAGs (by methanolysis) was determined • Real-time sulphate ester removal was analyzed: 6-sulphate ester was more resistant to removal than the corresponding 4-sulphate

									• From coupled results of PAGE and CE, a GAG mimotope structure is suggested
(20)	Colominic acid or Neu5Ac polymers of different molecular weights (14,17,29, 59,69 kDa)	Neu5Ac polymersr	None	CZE	Coated (dimethyl polysiloxane) (L = 27 cm, l = 20 cm, ID = 100 μm) (L = 57 cm, l = 50 cm,	50 mM Tris-borate (pH 8.5) containing 10% PEG 70000; 6 kV	UV (200 nm)	n.a.	• Mobilities of Neu5Ac polymer Stds are related to their molecular mass • Method applied to the determination of molecular weight of polysulphated esters of HA (extensively degraded during sulfonation reaction)
	HA	Polysulphated hyaluronans (HAPS) from *Streptococcus zooepidemicus*		ID = 100 μm)	50 mM Tris-borate (pH 8.5) containing 10% PEG 70000; 15 kV; Outlet: anode				

(Continued)

Table 1
(Continued)

Reference	Carbohydrate species	Matrix	Derivatizing agent	CE mode	Capillary, T	Buffer, Voltage	Detection mode	LOD	Results
(21)	Colominic acid	Hydrolyzates of different oligo/polySia chains	None	CZE	Fused silica (L = 108 cm, ID = 75 μm); T = 25 °C	100 mM SDS, 100 mM sodium bicarbonate (pH 8); 20 kV; Outlet: cathode	UV (200 nm)	n.a.	• Colominic acid shows unresolved peaks due to formation of lactonization products under mild acid conditions. After alkaline treatment and saponification of lactone rings, overlapping peaks are resolved
	Polysialo-glycoprotein (and other oligo/polySia acid chains with different interketosidic linkages) Glycoprotein (KDN-gp)								• Three homologous series of α2 → 8 linked oligoSia acid with identical DP (with different substituents at C-5 position) (oligoNeu5Ac, oligoNeu5Gc and oligoKDN) are separated; separation improves as DP increases

									• Two oligoNeu5Gc with different interketosidic linkages are also resolved
(22)	Dextrans (of various molecular weights) and carboxy methyl-cel-lulose stds	Debranched polydextran (enzyme treatment) and cleaved carboxy-methyl cellulose (enzyme treatment)	CBQCA	MEKC	Fused silica (L = 15–60 cm, ID = 50 μm) uncoated or filled with different concentration of LPAA, Istacryl, Synergel; RT	25 mM boric acid, 25 mM sodium phosphate, 50 mM Tris (pH 9.1); 15 kV	LIF (λ_{exc} = 457 nm; λ_{em} = 555 nm)	n.a.	• Under pulse-field conditions, migration behaviour is dramatically altered. Overcoming the reptation behaviour a highly efficient polysaccharide separation according to increasing MW is obtained
					L = 55 cm;	50 mM boric acid, 50 mM sodium phosphate, 100 mM Tris (pH 8.81); 5–11 kV			
					L = 20 cm;	50 mM boric acid, 50 mM sodium phosphate, 100 mM Tris (pH 8.81); 10 kV, 3 Hz			

(Continued)

Table 1
(Continued)

Reference	Carbohydrate species	Matrix	Derivatizing agent	CE mode	Capillary, T	Buffer, Voltage	Detection mode	LOD	Results
					L=15 cm	100 mM boric acid/100 mM Tris (pH 8.5); 10 kV; 5 Hz			
					L = 15 cm	50 mM Tris borate, 1 mM EDTA (pH 8.2); 10 kV; 3 Hz; Outlet: cathode or alternatively cathode/anode in pulse field conditions			
(23)	Carboxy-methyl-, hydroxy-propylmethyl- (300 and 60), hydroxyethyl- and methyl-hydroxyethyl-cellulose	CBQCA-Stds	CBQCA	MEKC	Various lengths of fused silica capillaries (ID = 25 μm) coated with a layer of LPAA; RT	50 mM MES, 25 mM Tris and 20 mM sodium acetate (pH from 2.85 to 8.65); further addictions of SDS; 350–400 V/cm; Outlet: anode	LIF (λ_{exc} = 442 nm; λ_{em} = 550 nm)	n.a.	• Migration of neutral or highly charged polysaccharides (like chemically modified celluloses and heparins) can be regulated by suitable buffer additives (SDS, spermine, Tris and ethylendiamine).

Heparin	CZE	• Mono- or multi-layer adsorption on different sites of detergents on analyte molecules governs migration rates • For highly charged polysaccharides (like heparins) high electrophoretic mobility can be modulated by use of ion-pairing reagents

(Continued)

Table 1
(Continued)

Reference	Carbohydrate species	Matrix	Derivatizing agent	CE mode	Capillary, T	Buffer, Voltage	Detection mode	LOD	Results
(24)	Oligomers of Neu5Ac Oligomers of HA	Colominic acid (from partial hydrolysis) HA oligomer mixture (hyaluronidase digestion)	None	CZE	Fused silica (L = 57 cm, l = 50 cm, ID = 100 μm) coated with dimethyl-polysiloxane or (50% phenyl) methyl-polysiloxane	0.1 M Tris–0.25 M borate (pH 8.5) containing PEG 70000 or HPC and HPHC having different viscosities as sieving material; 10 kV; Outlet: anode	UV (200 nm)	n.a.	• Neu5Ac oligomers with DP smaller than 5 as well as HA oligomers with DP smaller than 8 migrate in reverse order of their MW • The unusual migration patterns are related to the stereochemistry of the structures. The oligomers migrating the fastest are the minimum unit forming 3D structures required for biological function

(25)	Dextran PU HPG (modified guar gum where some hydroxyl groups are replaced by hydrox-ypropyl units)	Stds	APTS	MEKC	Various lengths of fused silica capillaries (ID = 50 μm) LPAA Uncoated, RT	40 mM clorimipramine in citric acid-Tris (pH 3.95); Outlet: cathode	LIF (λ_{exc} = 488 nm; λ_{em} = 515 nm)	n.a.	• Neutral and uncharged polysaccharides were electrophoreti-cally mobilized and characterized through choice of detergent and type of derivatization reagent • Correlation between mobility and polymer conformation is attempted

(Continued)

Table 1
(Continued)

Reference	Carbohydrate species	Matrix	Derivatizing agent	CE mode	Capillary, T	Buffer, Voltage	Detection mode	LOD	Results
(26)	Pectins of varying DE (side chains consisting in 200–1000 GalA units linked together by α-(1 → 4) glycosidic bonds	Stds pectins from lemon peels, (different DE by using pectin esterase of *Aspergillus*)	None	CZE	Fused silica (L = 57 cm; l = 50 cm; ID = 100 μm); T = 30 °C	50 mM phosphate (pH7); 20 kV; Outlet: cathode	UV (192 nm)	n.a.	• The electrophoretic mobility is seen to scale linearly with the average charge per residue over the investigated range. This technique allows the quantitative detection and separation of pectins having different DE

(27)	Cellulose and cellulose derivatized at a hydroxyl group with a hydrophilic substituent	Stds and enzymatically and chemically hydrolyzed	APTS	MECK	Various lengths of fused silica capillaries (ID = 50 μm) coated with a layer of linear polyacry-lamide; RT	Various compositions of a citric acid/Tris buffer; Further addictions of SDS Further addictions of decylsulphate; Electric field strength = 350–500 V/cm; Outlet: anode	LIF (λ_{exc} = 488 nm; λ_{em} = 515 nm)	n.a.	• Electrophoretic migration of uncharged chemically modified celluloses was induced by the adsorption of charged surfactants added to the electrolyte buffer • Carboxymethy-lated celluloses of different DS were resolved

(Continued)

Table 1
(Continued)

Reference	Carbohydrate species	Matrix	Derivatizing agent	CE mode	Capillary, T	Buffer, Voltage	Detection mode	LOD	Results
(28)	Pectins	Deesterified std pectins at different DE (enzyme treated)	None	CZE	Fused silica (L = 46.5 cm, l = 40 cm, ID = 50 μm) T = 25 °C	Phosphate buffer (pH 7); V = 20 kV; Outlet: cathode	UV (191 nm)	n.a.	• The electrophoretic mobility of polysaccharide pectin is determined largely by its chain-averaged charge density, irrespective of how that charge is distributed
(29)	Pectins	Deesterified pectins at different DE (pectin-esterase treatment) Alkaline-deesterified pectins	None	CZE	Fused silica (ID = 75 μm, l = 30 cm and l = 60 cm) T = 25 °C	50 mM phosphate (pH 6.5); V = 15 kV; Outlet: cathode	UV (192 nm)	n.a.	• Results shows that pectins with higher DE exhibit shorter migration times

											• There is a different correlation between time and DE of chemically and enzymatically de-esterified pectins, dependent on the random or block-wise charge distribution

APTS, 1-aminopyrene-3,6,8-trisulphonate; 6-AQ, 6-aminoquinoline; CBQCA, 3-(4-carboxybenzoyl)2-quinoline-carboxyaldehyde; CEC, capillary electrochromatography; CGE, capillary gel electrophoresis; CTAB, cetyltrimethylammonium bromide; CZE, capillary zone electrophoresis; DE, degree of esterification; DP, degree of polymerization; ED, electrochemical detection; EHEC, ethyl(hydroxyethyl)cellulose; ELFSE, end labelled free solution electrophoresis; GAG, glycosaminoglycans; GalA, galacturonic acid; Glc, glucose; GlcNAc, *N*-Acetylglucosamine; HA, hyaluronic acid; HMW, high molecular weight; HPCE, high performance capillary electrophoresis; LIF, laser-induced fluorescence; LMW, low molecular weight; LOD, limit of detection; LPAA, linear polyacrylamide; MEKC, micellar electrokinetic capillary chromatography; MES, 2-[*N*-morpholino]ethanesulphonic acid; n.a., not available; Neu5Ac, *N*-Acetylneuraminic acid; Neu5Gc, *N*-glycolylneuroaminic acid; PAGE, polyacrilamide gel electrophoresis; PEG, polyethylene glycol; PU, pullulan; RT, room temperature; SD, standard deviation; SDS, sodium dodecyl sulphate; std, standard; TEA, triethylamine; TFA, trifluoroacetic acid; UV, ultraviolet detector.

like butyric acid ***(48,49)*** to a selective vehicle such as hyaluronan (HA) recognized by CD44 receptor overexpressed in stem and neoplastic cells ***(50,51)***. The CE as rapid and reliable technique to identify and quantify biologically active molecules anchored to polymer chains ***(47)*** is here applied to a HA butyric ester derivative (HA-but). The degree of substitution for the glycoconjugate is here determined by quantification of butyric acid released upon hydrolysis of the HA-but derivative.

1.2. MEKC-UV Determination of the Degree of Polymerization and Distribution of Oligosaccharides in a Partially Acid-Hydrolyzed Homopolysaccharide

Degradation studies are particularly useful for naturally occurring macromolecules, the polymerization of which cannot be performed in laboratory. Although high molar mass polymers represent a challenge for CE characterization, macromolecular study in terms of de-polymerization mechanisms can be easily performed. As an example, the molecular weight distribution of an oligo-mannuronic mixture resulted from acid hydrolysis of high molecular weight mannuronan turned out to be satisfactorily interpreted in terms of the most probable distribution for an early stage of polycondensation reaction ***(52)***. Besides the definition of polysaccharides (and proteins) as condensation polymers, it is since long known that hydrolysis of cellulose occurs randomly for degree of polymerization x lower than 500 ***(53)***. In this respect, if the polymer degradation consists of non-specific (random) bond scission, a mixture from an extensively hydrolyzed polysaccharide solution might be considered as a snapshot of a polycondensation reaction taken at sufficiently low extent of condensation p (i.e. fraction of bond formed). Then, in the polymer mixture containing in total N_0 sugar residues, there are $N_0 p$ intact linkages and $N_0(1-p)$ unbound residues, the latter corresponding also to the total number of chains N. The expected molecular weight distribution function (i.e. the frequency of occurrence of a given degree of polymerization x) expressed in terms of mole fraction, $N_x = n_x/N$, and weight fraction $\mathrm{W}_x = xn_x/N_0$ of the $n_x x$-mers is then ***(53)***:

$$N_x = (1-p)\,p^{(x-1)} \tag{1}$$

$$W_x = x\,(1-p)^2\,p^{(x-1)} \tag{2}$$

The number average molecular weight $< M >_{\mathrm{n}}$ and the weight-average molecular weight $< M >_{\mathrm{w}}$ can as well be obtained by:

$$< M >_{\mathrm{n}} = \mathrm{Mo}/\,(1-p)$$

and

$$< M >_{w} = \mathrm{Mo}\,(1+p)\,/\,(1-p)$$

1.3. Influence of Electric Field on the Electrophoretic Mobility of Polysaccharides: Application to Hyaluronic Acid

It is generally reported that application of CE to large charged (bio)polymers in free solution cannot provide for their size separation when sharing the same mass to charge ratio (i.e. for regular structures). Then, the general approach to achieve CE separation on molar mass basis is to let highly charged polymers of relatively big size migrate through an entangled polymer solution that is believed to act as an inert sieving matrix ***(20,24,31–40,54)***. Depending on the type, dimensions and concentration of the host polymer, different separation models have been developed and reported ***(37,38)***. The electrophoretic studies in free solutions dealing with charged (bio)polymers of relatively large sizes are in comparison sensibly fewer ***(55–60)***. Before electrophoretic technique can be applied to macromolecular characterization beyond the qualitative size separation, more systematic studies should be performed to asses and develop polyelectrolyte models that can better mimic electrophoretic behaviour (**ref.** ***59*** and herein citations). Discrepancies on experimental data as well as on theoretical predictions are such to render the assumption of a molar mass-independent electrophoretic mobility in free solution somewhat doubtful (refs ***55,56,59*** and herein citations). Additional and systematic experimental data are needed especially to better understand when and how a dependence of electrophoretic mobility on macromolecular features such as chain conformation and chain stiffness may disclose and/or be predicted. In this respect, the wide spectrum of charge, chain conformation and stiffness covered by native and modified charged polysaccharides might represent a resource for deeper studies on a wider range of polymer types. Besides the unsuccessful size separation in free solution, electrophoretic mobilities of charged polymers measured on increasing electric field strength generally showed a relatively steeper increase than the expected ***(38,59)***. A similar trend can be also observed when naturally occurring or synthetic polyelectrolytes migrate through entangled polymer solutions ***(38,39,54)***. A phenomenon the origin of which, generally ascribed either to chain distorsion or to a viscosity drop by Joule heating, would likely deserve for deeper investigations. As an example, the electrophoretic mobility of five hyaluronan samples of different molar mass is here reported as a function of the applied voltage. The data obtained for molar masses of the order 10^5–10^6 g/mol are also compared with the electric field

dependence of electrophoretic mobility observed when 50% of the charged groups of one of those HA sample are substituted by an amide-linked galactose residue.

The dependence of the intrinsic mobility on electric fields strength, here only shortly addressed, shows interesting features. In line with elsewhere reported findings ***(38,39,59)***, an increase of the mobility is observed on increasing the applied voltage value in the entire investigate field strength range (i.e. 124–420 V/cm). Heating effects are reported to occur at field strength higher than 250 V/cm (i.e. $\geq$ 16 kV in our case) ***(39,59)***. Although their presence cannot be excluded, the much smoother increase of the mobility presently observed with respect to steeper variations elsewhere reported ***(38,39,59)*** should more likely come from field-induced perturbation of the ion cloud.

1.4. Influence of pH on the Electrophoretic Mobility of Polysaccharide: Application to Hyaluronic Acid and Related Glycoconjugates

Electrokinetic models have been generally applied more successfully to electrophoretic migration of colloidal particles ***(61–63)***. Indeed, accurate models as those elaborated by Booth and Overbeek that take into account polarization and relaxation of the ion cloud induced by the flow/electric field well represent the electrophoretic behaviour of spherical charged particles ***(64–66)***. However, a solid non-conducting spherical model hardly applies to real macroions. Even if their shape can approximately be spherical, their charge distribution is not expected to be spherically simmetrical.

However, to have simple estimation of approximate values of the electrophoretic mobility of spherical macroions with low potential surface, the Henry's equation is often used ***(67)***:

$$\mu = \frac{Ze}{6\pi\eta R} \cdot \frac{\mathrm{f}(kR)}{1+kR}, \tag{3}$$

where Z is the number of charge units, e is the elementary charge, R is the radius and k is the Debye–Hückel parameter. f(kR) is a complicated function which, however, lies between 1 and 1.5 in the $0.1–10^3\,kR$ range and departs very little from unit for $kR \leq 1$. **Equation 1** coincides with the first term of the more elaborate Booth equation ***(62)***.

Hyaluronan is a low charged polymer, its chain, when fully ionized, has approximately one fixed charge per nm length. The charge state being generally represented by the charge density parameter ξ defined as the ratio between the Bjerrum length l_b and the average distance b separating two consecutive

charged sites on the polymer backbone: $\xi = l_b/b = (e^2/4\pi Dk_B Tb)$, where e is the elementary charge, D is the dielectric permittivity of the medium, k_B the Boltzmann's constant and T the absolute temperature (i.e. $l_b = 0.714$ nm in water at 25 °C). The mobility of the unsubstituted HA4 hyaluronan and of the HA7 and HA8 galactose-substituted hyaluronans, all having an identical molar mass, measured as a function of pH and at constant ionic strength is here reported. The fully ionized state is characterized by a linear charge density parameter ξ of 0.72, 0.55 and 0.48 for HA4, HA7 and HA8, respectively. In this case, for which potentiometric data are also available, the mobility dependence on the ionization degree α_{ion} can then be resorted by using:

$$\alpha_{ion} = \alpha_N + 10^{-pH} \Big/ C_p, \tag{4}$$

where α_N is given by the added base to total carboxyl equivalent ratio and C_p is expressed in equivalent of repeating units/L. Furthemore, the very same data can be plotted as well as a function of the linear charge density varying with α_{ion} (i.e. $\xi' = \xi\alpha_{ion}$).

It has been reported that the electrophoretic mobility of hyaluronan can be reproduced rather well by the so-called frozen-worm-like model ***(60,67)***. In the present case, a very simple approach is used: **Eq. 3** is taken as a reference point to compare the electrophoretic mobilities of hyaluronan samples on a qualitative basis. Indeed, besides the above-mentioned restrictions for **Eq. 3**, to apply an additional one is given by the 'conducting' surface of a weak polyacid, as hyaluronan, with carboxyl groups rapidly exchanging protons. What we will use are the two statements implied in **Eq. 3**: one that the electrophoretic mobility is directly proportional to the charge Z of the polyion and the other that is inversely proportional to the frictional coefficient under the assumption of a spherical macroion shape.

2. Materials

2.1. Determination of the Degree of Substitution of Hyaluronic Acid Butyric Ester: CZE-UV of Released Butyric Acid

1. Samples: Hyaluronic acid (85 kDa) (Bioibérica, Barcelona, Spain).
2. Reagents for linkage of butyric acid to HA: butyric anhydride, tertrabutylammonium (Sigma, St Louis, MO, USA). The derivatization procedure was previously described **ref. *50***.
3. Reagents for basic hydrolysis: Sodium hydroxide (Sigma).
4. CE buffer: 50 mM sodium tetraborate (borax), pH 9.2 (Sigma).

2.2. MEKC-UV Determination of the Degree of Polymerization and Distribution of Oligosaccharides in a Partially Acid-Hydrolyzed Homopolysaccharide

1. Samples: Mannuronan oligomers released upon hydrolysis from high molecular weight mannuronan (from fermentation broth of a mannuronan C-5 epimerase negative strain of *Pseudomonas fluorescens*) ***(52)***.
2. Reagents for oligosaccharides derivatization: 4-Aminobenzonitrile (ABN) (Aldrich, St. Louis, MO, USA), sodium cianoborohydride, glacial acetic acid and methanol (Merck, Darmstadt, Germany).
3. CE buffer: Boric acid 660 mM (pH 8) containing 100 mM sodium dodecyl sulphate (SDS).

2.3. Influence of Electric Field on the Electrophoretic Mobility of Polysaccharides: Application to Hyaluronic Acid

1. Samples: Sodium hyaluronate (rooster comb) samples were kindly provided from FIDIA S.p.A (Abano Terme, Padova, Italy). The details of the different hyaluronic acid samples are summarized in **Table 2**. Samples were prepared dissolving 1 mg of intact or galactose-modified sodium hyaluronate in 1 mL of bi-distilled water and analyzed without further dilution.
2. Reagents for linkage of galactose to HA: 1-Amino-1-deoxy-β-D-galactose (galactosylamine) was prepared as reported in literature ***(68)***, 2-[*N*-morpholino] ethanesulphonic acid (MES), *N*-hydroxysuccinimide (NHS) and 1-ethyl-3-[3-(dimethtlamino)-propyl]carbodiimide hydrochloride (EDC). All reagents were from Sigma.
3. CE buffer: 50 mM sodium tetraborate (borax), pH 9.2 (Sigma).

Table 2
HA Samples Analyzed by Capillary Electrophoresis-UV

HA Samples	MW (kDa)	DS
HA1	120	(−)
HA2	160	(−)
HA3	160	0.5
HA4	210	(−)
HA5	850	(−)
HA6	1050	(−)
HA7	210	0.2
HA8	210	0.3

DS, degree of substitution.

2.4. Influence of pH on the Electrophoretic Mobility of Polysaccharide: Application to Hyaluronic Acid

1. Samples: *See* **Subheading 2.3**.
2. Reagents for linkage of galactose on HA: *See* **Subheading 2.3**.
3. CE-buffer: A series of potassium phosphate buffers (KH_2PO_4/K_2HPO_4, Merck) at constant ionic strength (0.05 M) and at different pH values (pH range between 3 and 9).

2.5. Equipment

1. High-performance CE system (Applied Biosystems HPCE Model 270A-HT; Foster City, CA, USA) with Turbochrom Navigator (4.0) software (*see* **Subheadings 2.1., 2.2**. and **2.4**.). High-performance CE (HP3D CE system; Waldbronn, Germany), with HP Chemstation software (*see* **Subheading 2.3**.).
2. Uncoated fused silica column (Supelco, St. Louis, MO, USA) with an inner and outer diameter of 50 μm and 375 μm, respectively, capillary length 92 cm (70 cm to detector) (*see* **Subheadings 2.1**. and **2.2**.).
3. Uncoated fused silica column (Agilent Technologies, Waldbronn, Germany) with internal diameter of 50 μm, capillary length 64.2 cm (56 cm to detector) extended light path (*see* **Subheading 2.3**.).
4. Linear polyacrilamide (LPA)-coated capillary (Bio-Rad Laboratories, Hercules, CA, USA) with an inner diameter and outer diameter of 50 μm and 375 μm, respectively, capillary length 80 cm (62 cm to detector) (*see* **Note 1**) (*see* **Subheading 2.4**.).
5. Detection: UV on column 195 nm for all samples but oligo-mannuronic acids (285 nm).

3. Methods

3.1. Determination of the Degree of Substitution of Hyaluronic Acid Butyric Ester: CZE-UV of Released Butyric Acid

Besides the low sample consuming, CE is shown to be an easy and rapid technique to accurately quantify pendent species, chemically introduced onto polymer chain ***(44)***, in amounts that are in the detection limit range of the important and widespread nuclear magnetic resonance technique.

1. Rinse the capillary for 2 min with a 0.1 N NaOH solution at a pressure equal to 67.6 kPa.
2. Condition the silica capillary with electrophoresis buffer (pressure 67.6 kPa) for 4 min.
3. Program the instrument to load the sample under vacuum at a pressure of 16.9 kPa for 1.5 s.
4. Operative conditions: Voltage, 20 kV; detection, 195 nm at the cathode; temperature, 27 °C; buffer, borax 50 mM (pH 9.2).

5. Hydrolysis procedure: Dissolve 4 mg of the substituted polymer in 1 mL of 0.1 N NaOH solution. Incubate the mixture at room temperature (RT) and after 2 h neutralize it with 1 mL 0.1 N HCl.
6. **Figure 1** shows the electropherogram of intact HA derivative (*see* **Fig. 1A**); hydrolyzed mixture (*see* **Fig. 1B**) before and (*see* **Fig. 1C**) after co-injection of a standard butyric acid solution. A degree of substitution as low as 0.14 was determined. The calibration curve from peak area to migration time ratio (A/t) versus solute concentration ($A/t = 15.151\text{x} + 2.558,\ r^2 = 0.999$) was linear in the investigated 1 mM to 4.5 mM butyric acid concentration range ***(50)***.

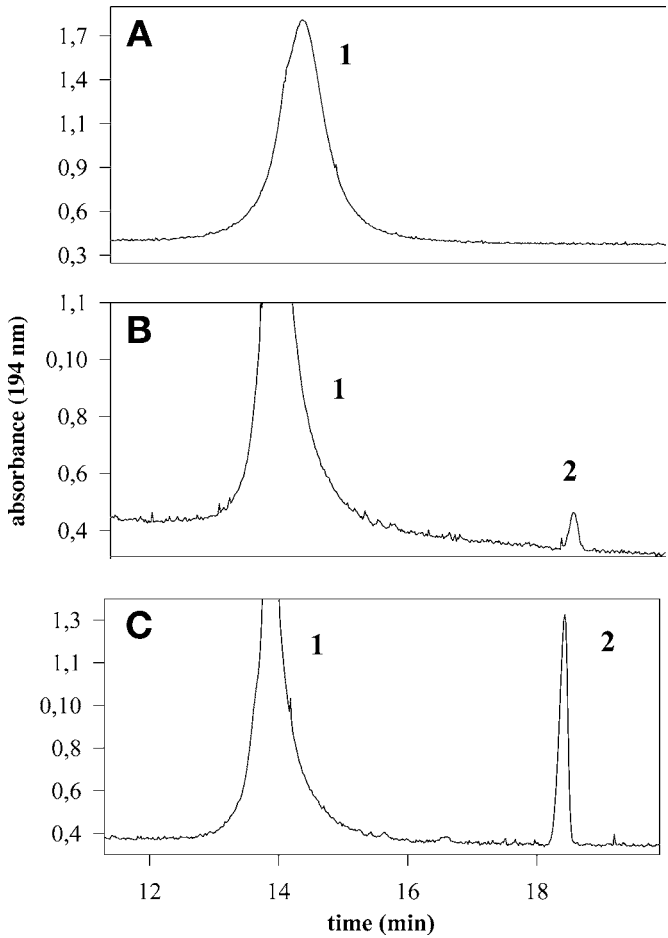


Fig. 1. Electropherogram of intact HA butyric ester (**A**); hydrolyzed mixture before (**B**) and after (**C**) co-injection of butyric acid solution.

3.2. MEKC-UV Determination of the Degree of Polymerization and Distribution of Oligosaccharides in a Partially Acid-Hydrolyzed Homopolysaccharide

As far as the CE is concerned, the relatively short mannuronic chains are singularly tagged so that the peak area to retention time ratios for the CE resolved x values (i.e. 1–18 monomeric units) are proportional to the number (moles) of chains containing x-monomers (i.e. n_x). Both mole and weight fractions as a function of x can then be obtained and compared with the theoretically expected distribution functions.

Operatively:

$$n_x = (A/t)_x\,,$$
$$N_0 = \Sigma_x\; x\,(A/t)_x\,,$$
$$N = \Sigma_x\,(A/t)_x\,.$$

1. Rinse the capillary for 2 min with 0.1 N NaOH solution at a pressure of 67.6 kPa.
2. Condition the silica capillary with electrophoresis buffer.
3. Program the instrument to load the sample under vacuum at a pressure of 16.9 kPa for 1.5 s.
4. Operative conditions: Voltage, 18 kV; detection, 285 nm at the cathode; Temperature, 30 °C; Buffer: H_3BO_3 660 mM (pH 8) containing 100 mM SDS.
5. Derivatizing procedure: Derivatize standards (1 mg/mL) or hydrolysis mixture (4 mg/mL) with 0.5 M ABN in the presence of 0.16 M $NaCNBH_3$ in 1 mL MeOH/AcOH (95/5) for 15 min at 90 °C. For CE analysis, dilute the samples five times with H_2O or buffer.
6. Weight, W_x, (*see* **Fig. 2A**) and mole N_x, fractions of mannuronic oligomers (*see* **Fig. 2B**) obtained from A/t of resolved x species in the electropherogram of the hydrolyzed mannuronic mixture. Solid curves are best fitting curves obtained from **Eqs 1** and **2** at values of 0.72 and 0.75 for the fraction of unbroken linkages, p, respectively.

3.3. Influence of Electric Field on the Electrophoretic Mobility of Polysaccharides: Application to Hyaluronic Acid

Field dependence of the free solution mobility of HA samples having different molar masses is here reported together with mobility data observed for HA having lower charge density.

1. Rinse the capillary for 2 min with a 0.1 N NaOH solution at a pressure of 960 mbar.
2. Condition the silica capillary with electrophoresis buffer (pressure 960 bar) for 4 min.
3. Program the instrument to load the sample under vacuum at a pressure of 25 mbar for 3 s.

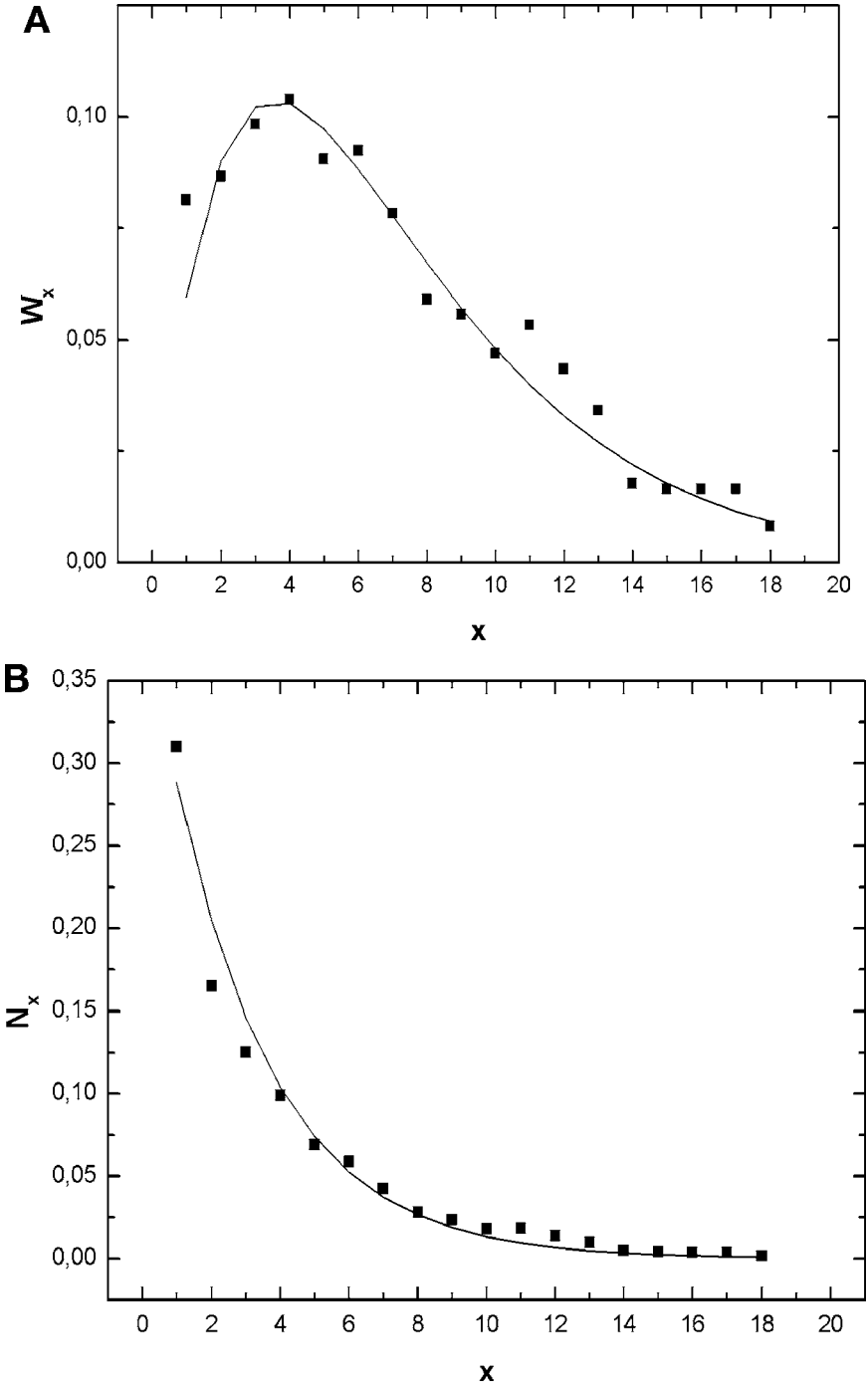


Fig. 2. Continued

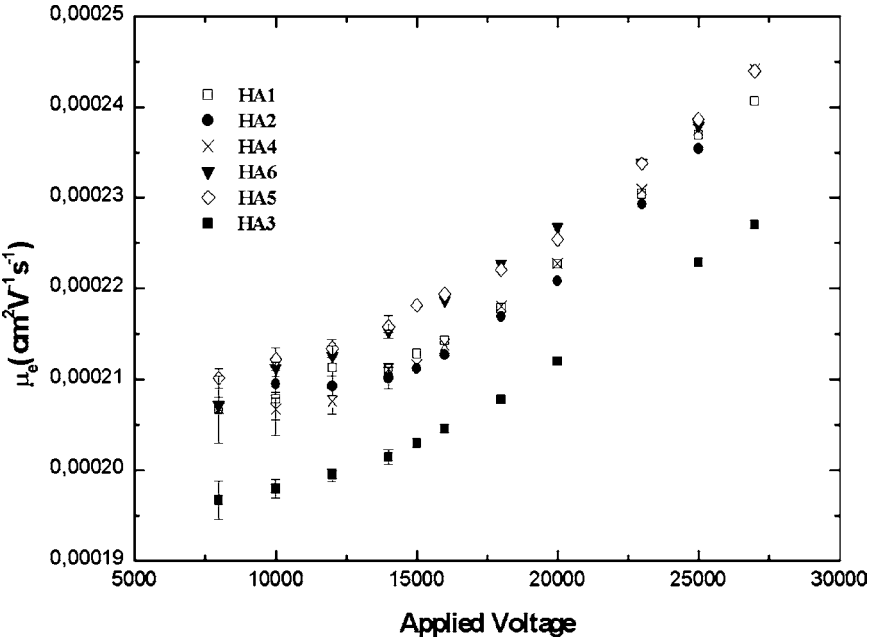


Fig. 3. Electrophoretic mobility as a function of the applied voltage (V) for HA1, HA2, HA4, HA5 and HA6 samples.

4. Operative conditions: Different values of voltage, ranging from 8 to 27 kV (*see* **Fig. 3**); detection, 195 nm at the cathode; temperature, 25 °C; buffer, 50 mM borax (pH 9.2).
5. Galactose-substituted hyaluronan synthesis procedure: *see* **Note 2**.
6. **Figure 3** shows that the mobilities measured for the HA samples increase smoothly from approximately a common low field asymptotic value to merge to an overlapping value at high fields. Just above the asymptotic low field behaviour, a window in the range of applied field values exists where the mobility of the larger molecules is slightly but distinctively higher than that measured for shorter HA chains. Albeit small the measured differences are above the standard errors. Any mobility difference can instead be deduced neither between HA5 and HA6 nor between HA1, HA2 and HA4. From the linear increase of the current in the 8–20 kV voltage range and from the relatively low conductivity of the used buffer ***(56)***, the presence of heat artefacts below 16 kV (i.e. $E = 250\,V/cm$) should be

Fig. 2. (**A**) Weight fraction of mannuronic oligomers as a function of the degree of polymerization x. (**B**) Mole fraction. Solid curves are calculated from **Eqs 1** and 2 with p equal to 0.75 and 0.72 for weight and number fractions, respectively (*see* **Subheadings 1.2**. and **3.2**.).

safely excluded. Additional measurements are needed to clarify the role that borax may as well play in the electrolyte-polymer system ***(56)***. As an example, at low field strength (i.e. 50–150 V/cm), free solution mobility of DNA molecules has been reported to increase with molar mass in a very limited range of chain length (i.e. 20–400 bp) and to attain molecular mass-independent values beyond that upper limit ***(56)***, the rise being ascribed to electrolyte drag forces, the effects of which are vanishing with chain dimensions. Such an increase, although over estimated by 10–15%, has as well been predicted by molecular modelling of short DNA fragments (20–60 bp), in the rod limit diffusion behaviour, that included ion relaxation. In our case, if retardation effects of deformed ion clouds are responsible for the distinct migration behaviour reported in **Fig. 3**, they appear to be either weaker for, or better recovered by, expanded coiled shapes of large sizes. The HA samples investigated here not only have larger sizes than the above-reported DNA molecules but also are less charged and, perhaps more important, are much more flexible. A worm-like chain model with a persistence length of roughly 10 nm applies reasonably well in the entire range of chain lengths here investigated ***(69)***. As indicated by the expected low electrophoretic mobility disclosed by the low charge bearing galactose-substituted hyaluronan, HA3 ($M_w = 1.6 \times 10^5$), the charge-to-size value that contribute to the electrophoretic mobility of HA5 and HA6 measured in the 13–18 kV range must apparently be higher than that of the low molecular weight hyaluronans. Only for comparison purposes we may try to treat the polymer samples simply as charged bodies and to compute the charge Q by which they contribute to the electrophoretic mobility measured at 15 kV ($\mu = Q/f$), assuming the frictional coefficient being described by Stokes law, $f = 6\pi\eta R$, and taking R equal to the measured average root mean square radius of gyration ***(69)***. It can then be shown that low molar mass hyaluronans (HA1, HA2 and HA4) contribute to the electrophoretic mobility with approximately 18–19% of the total charge actually carried by the chains, whereas the charge contribution to the mobility of the higher HA5 and HA6 is roughly 10% of the charge they actually have; this suggests, as expected, that much higher electrostatic and hydrodynamic screening effects are characterizing the expanded larger sized coils. The electrophoretic mobility of the low charged HA3 sample is compatible with that observed for the parent HA2 polymer if a degree of substitution of 0.6 is considered (to be compared with DS = 0.5 independently measured by traditional methods, *see* **Note 3**) assuming a charge contribution of 18% and, moreover, disregarding R_g variations that likely occur with substitution, assuming that both HA2 and HA3 share an identical average size. In this specific case, the CE technique although sensitive cannot substitute the more assessed methodologies for the determination of chemical structural parameters like the degree of substitution. Unfortunately, disclosure of differences in migration behaviour eventually present at low fields is precluded by the large standard errors affecting the experimental data. Unclear as well are the reasons for the high field behaviour where the overlapping mobility value is apparently more rapidly reached by HA1 and HA2 (low molar mass samples) than by HA5 and HA6 samples. Long flexible chains can be oriented by an electric/flow field and even deformed at high flow field strengths as resulted, for instance, from viscoelastic and flow/electric birefrangence measurements. Besides the need to ascertain the

influence of heat artefacts, deeper investigations of the field dependence migration on well-characterized and differently charged macromolecules, in general, and on charged polysaccharides, in particular, should be addressed to gain better insights on the several and not too well understood mutual influences of dynamic, conformation and electrostatic features that actually contribute to the electrophoretic behaviour of worm-like chains.

3.4. Influence of pH on the Electrophoretic Mobility of Polysaccharides: Application to Hyaluronic Acid

1. Rinse the capillary for 2 min with bi-distilled water at a pressure of 67.6 kPa.
2. Condition the silica capillary with electrophoresis buffer (pressure 67.6 kPa) for 4 min.
3. Program the instrument to load the sample under vacuum at a pressure of 16.9 kPa for 3 s.
4. Operative conditions: Voltage, 20 kV; detection, 190 nm at the anode; temperature, 30 °C; buffer, potassium phosphate solutions in a pH range between 3 and 9 and constant ionic strength (0.05 M).

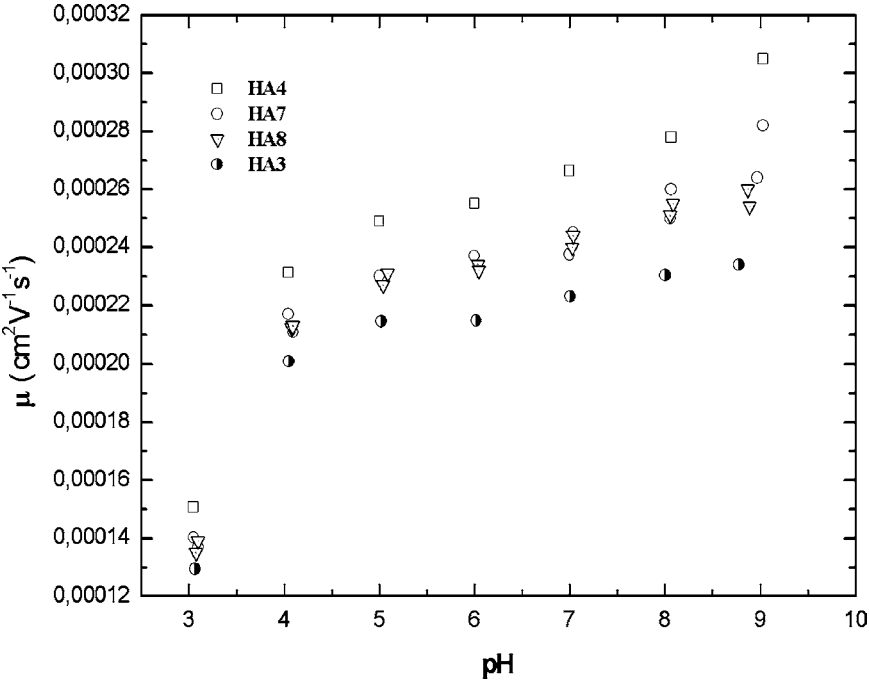


Fig. 4. Electrophoretic mobility as a function of pH for native (HA4) and galactose-substituted HA7 and HA8 samples. For comparison purposes, mobility measured for the higher substituted HA3 sample are also reported (*see* **Table 2**).

5. **Figure 4** shows the electrophoretic migration measured as a function of pH for native hyaluronan (HA4, $M_w = 2.1 \times 10^5$ g/mol) and for the galactose-substituted HA7 (DS 0.24) and HA8 (DS 0.34) samples. The higher charge density of HA4 accounts for the higher mobility measured with respect to the less charged HA7 and HA8 (and, even more, for HA3 sample, *see* **Table 2**).
6. **Figure 5** reports the mobility values as a function of the degree of ionisation measured for HA4, HA7 and HA8, for which potentiometric data were available. There, the pH values were transformed into α_{ion} by applying **Eq. 4**.
7. More interesting features (*see* **Fig. 6**) are disclosed by analyzing the mobility data in terms of the linear charge density that depends on the degree of ionization, $\xi' = \xi\alpha_{ion}$. In all cases, as expected, an approximately linear dependence of the mobility is observed as a function of the charge density parameter. Different instead is the rate by which the mobility changes on charging the polymer chains. On the basis of the simple statements made in the introduction, data of **Fig. 6** show that the potential surface of HA7 and HA8 increases with chain charging more rapidly than that of HA4. In turn, on increasing the degree of substitution, a decrease of the chain frictional coefficient is suggested for the galactose-substituted hyaluronans in comparison with a more 'unperturbed' behaviour of HA4.

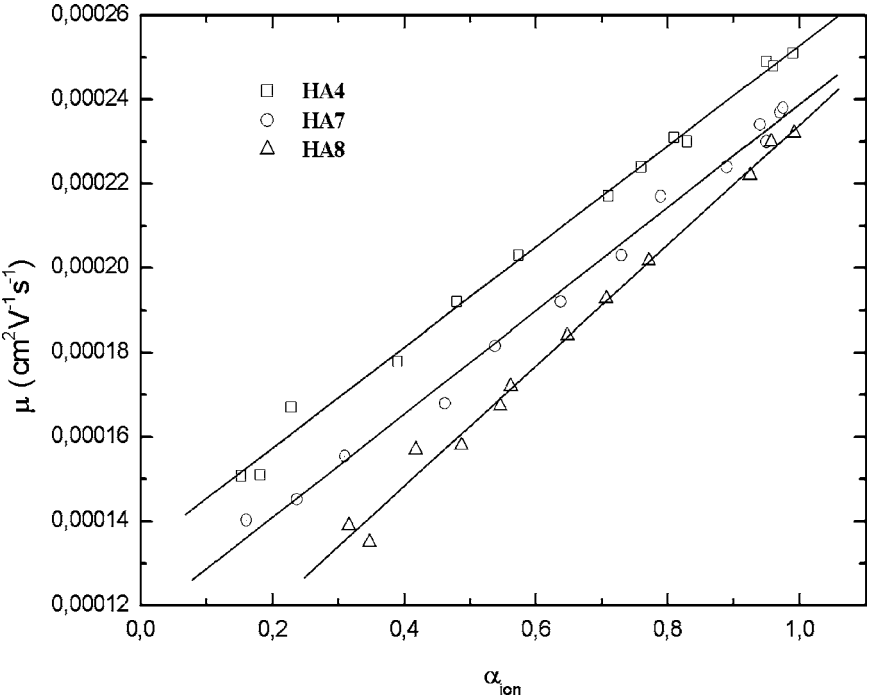


Fig. 5. Data of **Fig. 4** are plotted as a function of the degree of ionization α_{ion} (*see* **Eq. 4**). Solid lines are least-square fits of the experimental points.

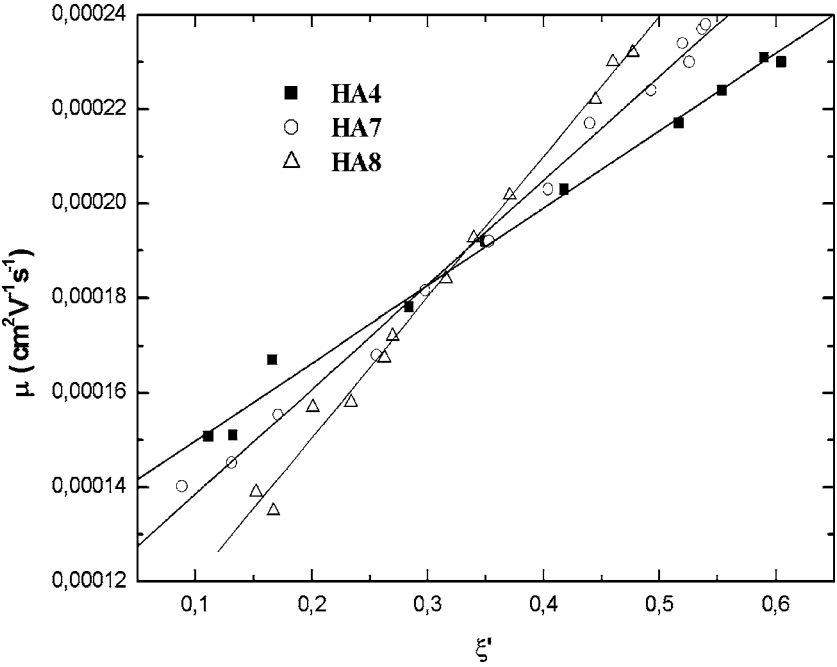


Fig. 6. Mobility data are here reported as a function of the charge density parameter $\xi' = \xi\alpha_{ion}$. Solid lines are least-square fits of the experimental points.

4. Notes

1. Differently from what recommended for polyvinyl alchol (PVA)-coated capillary, LPA-coated one is a general-purpose capillary which is suitable to be used in a wide pH range (typically, from 2 to 9).
2. Add galactosylamine (2.70 mg, 1.35 mg or 0.95 mg to yield respectively DS of 0.5, 0.3 and 0.2) to a stirred solution of hyaluronan sodium salt (1.5 g) in 0.2 M MES buffer (pH 4.5, 400 mL) containing NHS and EDC ([EDC]/[HA repeating unit] = 1.5; [NHS]/[EDC] = 1). Stir the solution for 24 h at RT, dialyze the polymer at 4 °C against 0.05 M $NaHCO_3$ for 1 day and then exhaustively against mQ water. Adjust, if necessary, the pH to 6.5, filter the polymer solution and freeze-dry it to obtain the modified hyaluronans.
3. The determination of the degree of substitution was made by potentiometric titration and elemental analysis.

References

1. Zhou, X.-M., Liu, J.-W., Zhang, M.-E., Chen, S.-J. (1998) Determination of plasma heparin by micellar electrokinetic capillary chromatography. *Talanta* **46,** 757–760.

2. Plätzer, M., Ozegowski, J.H., Neubert, R.H.H (1999) Quantification of hyaluronan in pharmaceutical formulations using high performance capillary electrophoresis and the modified uronic acid carbazole reaction. *J. Pharm. Biomed. Anal*. **21,** 491–496.
3. Grimshaw, J. et al. (1996) Quantitative analysis of hyaluronan in vitreous humor using capillary electrophoresis. *Electrophoresis* **15,** 936–940.
4. Toida, T., Linhardt, R.J. (1996) Detection of glycosaminoglycans as a copper (II) complex in capillary electrophoresis. *Electrophoresis* **17,** 341–346.
5. Volpi, N. (2004) Separation of capsular polysaccharide K4 and defructosylated K4 by high-performance capillary electrophoresis. *Electrophoresis* **25 (4–5),** 692–696.
6. Damm, J.B.L., Overclift, G.T., Vermeulen, B.W.M. (1992) Separation of natural and synthetic heparin fragments by high-performance capillary electrophoresis. *J. Chromatogr*. **608,** 297–309.
7. Morell, M.K., Samuel, M.S., O'Shea, M.G. (1998) Analysis of starch structure using fluorophore-assisted carbohydrate electrophoresis. *Electrophoresis* **19,** 2603–2611
8. Hong, M., Sudor, J., Stefansson, M., Novotny, M. (1998) High-resolution studies of hyaluronic acid mixtures through capillary electrophoresis. *Anal. Chem*. **70 (3),** 568–573.
9. Roberts, M.A., Zhong, H.-J., Prodolliet, J., Goodall, D.M. (1998) Separation of high-molecular-mass carrageenan polysaccharides by capillary electrophoresis with laser-induced fluorescence detection. *J. Chromatogr. A* **817,** 353–366.
10. Eunmi, B., et al. (2001) Capillary electrophoresis of high-molecular chitosan: The natural carbohydrate polymer. *Electrophoresis* **22,** 2217–2221.
11. Zhong, H.-J., Williams, M.A.K., Keenan, R.D., Goodall, D.M., Rolin, C. (1997) Separation and quantification of pectins using capillary electrophoresis: A preliminary study. *Carbohydr. Polym*. **32,** 27–32.
12. Zhou, W., Baldwin, R. P. (1996) Capillary electrophoresis and electrochemical detection of underivatized oligo- and poly-saccharides with surfactant-controlled electroosmotic flow. *Electrophoresis* **17,** 319–324.
13. Liu, J., Shirota, O., Novotny, M.V. (1992) Sensitive, laser-assisted determination of complex oligosaccharide mixtures separated by capillary gel electrophoresis at high resolution. *Anal. Chem*. **64,** 973–975.
14. Wiedmer, S.K., Cassely, A., Hong M., Novotny, M.N., Riekkola, M.-L. (2000) Electrophoretic studies of polygalacturonate oligomers and their interactions with metal ions. *Electrophoresis* **21,** 3212–3219.
15. Zhang, M., Melouk, H.A., Chenault, K., El Rassi, Z. (2001) Determination of cellular carbohydrates in peanut fungal pathogenesis and Baker's yeast by capillary electrophoresis and electrochromatography. *J. Agric. Food Chem*. **49 (11),** 5265–5269.
16. Hayase, S., Oda, Y., Honda, S., Kakehi, K. (1997) High-performance capillary electrophoresis of hyaluronic acid: Determination of its amount and molecular mass. *J. Chromatogr. A* **768,** 295–307.

17. Kim, M.Y., Varenne, A., Daniel, R., Gareil, P. (2003) Capillary electrophoresis profiles of fucoidan and heparin fractions: Significance of mobility dispersity for their characterisation. *J. Sep. Sci*. **26,** 1154–1162.
18. Stefansson, M. (1999) Electrohydrodynamic instabilities and segregation of polysaccharides in capillary polymer solution electrophoresis. *Biopolymers* **49 (6),** 515–524.
19. Carney, S.L, Caterson, B., Penticost, H.R. (1996) The investigation of glycosaminoglycan mimotope structure using capillary electrophoresis and other complementary electrophoretic techniques. *Electrophoresis* **17,** 384–390.
20. Kinoshita, M., Shiraishi, H. (2002) Determination of molecular mass of acidic polysaccharides by capillary electrophoresis. *Biomed. Chromatogr*. **16,** 141–145.
21. Cheng, M.-C., Lin, S.-L., Wu, S.-H., Inoue, S., Inoue, Y. (1998) High-performance capillary electrophoresis characterization of different types of oligo- and polysialic acid chains. *Anal. Biochem*. **260,** 154–159.
22. Sudor, J., Novotny, M. (1993) Electromigration behaviour of polysaccharides in capillary electrophoresis under pulsed-field conditions. *Proc. Natl. Acad. Sci. U. S. A*. **90,** 9451–9455.
23. Stefansson, M., Novotny, M. (1994) Modification of the electrophoretic mobility of neutral and charged polysaccharides. *Anal. Chem*. **66,** 3466–3471.
24. Kakehi, K., Kinoshita, M., Hayase, S., Oda, Y. (1999) Capillary electrophoresis of N-acetylneuraminic acid polymers and hyaluronic acid: Correlation between migration order reversal and biological functions. *Anal. Chem*. **71,** 1592–1596.
25. Tokarz, M., Gustavsson, P., Stefansson, M. (2002) Employment of detergent-tag/solute interactions in capillary electrophoresis of neutral polysaccharide. *Biomed. Chromatogr*. **16,** 134–140.
26. Zhong, H.-J., Williams, M.A.K., Goodall, D.M., Hansen, M. (1998) Capillary electrophoresis studies of pectins. *Carbohydr. Res*. **308,** 1–8.
27. Stefansson, M. (1998) Characterization of cellulose derivatives and their migration behaviour in capillary electrophoresis. *Carbohydr. Res*. **312,** 45–52.
28. Williams, M.A.K., Foster, T.J., Schols, H.A. (2003) Elucidation of pectin methylester distributions by capillary electrophoresis. *J. Agric. Food Chem*. **51 (7),** 1777–1781.
29. Jiang, C.-M., Wu, M.-C., Chang, W.H., Chang, H.-M. (2001) Determination of random- and blockwise-type de-esterified pectins by capillary zone electrophoresis. *J. Agric. Food Chem*. **49 (11),** 5584–5588.
30. Karamanos, N.K., Hjerpe, A. (2002) Capillary electrophoresis of intact and depolymerized glycosaminoglycans and proteoglycans. In: *Carbohydrate Analysis by Modern Chromatography and Electrophoresis*. Journal of Cromatography Library, vol. 22., Z. El Rassi, Ed., Elsevier Sci. Amsterdam, NL
31. Kakehi, K., Kinoshita, M., Yasueda, S-I. (2003) Hyaluronic acid: Separation and biological implications. *J. Chromatogr*. **797,** 347–353.
32. Kakehi, K., Kinoshita, M., Nakano, M. (2002) Analysis of glycoproteins and the oligosaccharides thereof by high performance capillary electrophoresis - significance in regulatory studies on biopharmaceutical products. *Biomed. Chromatogr*. **16,** 103–115.

33. Magnusdottir, S., Isambert, H., Heller, C., Viovy, J.-L., (1999) Electrodynamically induced aggregation during constant and pulsed field capillary electrophoresis of DNA. *Biopolymers* **49,** 385–401.
34. Quesada, M.A. (1997) Replaceable polymers in DNA sequencing by capillary electrophoresis. *Curr. Opin. Biotechnol*. **8,** 82–93.
35. Welch, C.F., Hoagland, D.A. (2001) Molecular weight analysis of polycations by capillary electrophoresis in a solution of neutral polymer. *Polymer* **42,** 5915–5920.
36. Bohrisch, J., Grosche, O., Wendler, U., Jaeger, W., Engelhard, H. (2000) Electroosmotic mobility and aggregation phenomena of model polymers with permanent cationic groups. *Macromol. Chem. Phys*., **201,** 447–452.
37. Clos, H.N., Engelhard, H. (1998) Separation of ionic and cationic synthetic polyelectrolytes by capillare gel electrophoresis. *J. Chromatogr. A,* **802,** 149–157.
38. Cottet, H., Gareil, P. (1997) Electrophoretic behaviour of fully sulfonated polystyrenes in capillary filled with entangled polymer solutions. *J. Chromatogr. A,* **772,** 369–384.
39. Starkweather, M.E., Hoagland, D.A., Muthukumar, M. (2000) Polyelectrolyte electrophoresis in a dilute solution of neutral polymer: Model studies. *Macromolecules* **33,** 1245–1253.
40. Heller, C. (1995) Capillary electrophoresis of proteins and nucleic acids in gels and entangled polymer solutions. *J. Chromatogr. A* **698,** 19–31.
41. a) Guido, S. (1995) Phase behaviour of aqueous solutions of hydroxypropylcellulose. *Macromolecules,* **28,** 4530–4539. b) Guido, S. (1995) Cholesteric textures of aqueous hydroxypropylcellulose solutions. *Mol. Cryst. Liq. Crist*. **266,** 111–119.
42. Kobayashi, A., Akaike, H. (1986) Enhanced adhesion and survival efficiency of liver cell in culture disches coated with a lactose carrying styrene homopolymer. *Makromol. Chem. Rapid Commun*. **7,** 645–650.
43. Maeda, H., Ueda, M., Morinaga, T., Matsumoto, T. (1985) Conjugation of poly(styrene-*co*-maleic acid) derivatives to the antitumor protein neocarzinostatin: pronounced improvements in pharmacological properties. *J. Med. Chem,* **28,** 455.
44. Donati, I., Gamini, A. Vetere, A., Campa, C., Paoletti, S. (2002) Synthesis, characterization and preliminary biological study of glyco-conjugates of poly(styrene-*co*-maleic acid). *Biomacromolecules* **3,** 805–812.
45. Hubbel, J.A. (1999) Bioactive biomaterials. *Curr. Opin. Biotechnol* **10,** 123–129.
46. Henc, L., Polak, G.M. (2002) Third generation biomedical materials. *Science* **5557,** 1014–1017.
47. Donati, I., Stredanska, S., Silvestrini, G., Vetere, A., Marcon, P. Marsich, E., Mozetic, P., Gamini, A., Paoletti, S., Vittur, F. (2005) The aggregation of pig articular chondrocyte and synthesis of extracellular matrix by lactose modified chitosan. *Biomaterials* **26,** 987–998.
48. Pellizzaro, C., Coradini, D., Abolafio, G., Daidone, M.G. (2001) Modulation of cell cycle-related proteins but not of p53 expression by sodium butyrate in a human non-small cell lung cancer cell line. *Int. J. Cancer* **91,** 658–664.
49. Yamamoto, H., Fujimoto, J., Okamoto, E., Furujama, J., Tamaoki, T., Hashimoto-Tamaoki, T. (1998) Suppression of growth of hepatocellular carcinoma by sodium butyrate in vitro and in vivo. *Int. J. Cancer* **76,** 897–902.

50. Coradini, D., Pellizzaro, C., Abolafio, G., Bosco, M., Scarlata, I., Cantoni, S., Stucchi, L., Zorzet, S., Turrin, C., Sava, G., Perbellini, A., Daidone, M.G. (2004) Hyaluronic-acid butyric esters as promising antineoplastic agents in human lung cancer carcinoma: A preclinical study. *Invest. New Drugs* **22,** 207–217.
51. Ventura, C., Maioli, M., Asara, Y., Santoni, D., Scarlata, I., Cantoni, S., Perbellini, A. (2004) Butyric and retinoic mixed ester of hyaluronan. A novel differenting glycoconjugate affording a high throughput of cardiogenesis in embryonic stem cells. *J. Biol. Chem*. **279,** 23574–23579.
52. Campa, C., Oust, A., Skjåk-Bræk, G., Paulsen, B.S., Paoletti, S., Christensen, B.E., Ballance, S. (2004) Determination of average degree of polymerization and distribution of oligosaccahrides in partially acid hydrolysed homopolysaccharide: A comparison of four experimental method applied to mannuronan, *J. Chromogr*. **1026,** 271–281.
53. Flory, P.J. (1953) *Principles of Polymer Chemistry,* Cornell University Press, Ithaca, N.Y.
54. Cottet, A., Gareil, P. (2001) On the use of the activation energy concept to investigate analyte and network deformations in entangled polymer solution capillary electrophoresis of synthetic polyelectrolytes. *Electrophoresis* **22,** 684–691.
55. Allison, A., Mazur, S. (1998) Modeling free solution electrophoretic mobility of short DNA fragments. *Biopolymers* **46,** 359–373.
56. Stellwagen, N.C., Gelfi, C., Righetti, P.G. (1997) The free solution mobility of DNA. *Biopolymers* **42,** 687–703.
57. Gao, J.Y., Dubin, P., Sato, T., Morishima, Y. (1997) Separation of polyelectrolytes of variable composition by free-zone capillary electrophoresis. *J. Chromogr*. **766,** 233–236.
58. Popov, A., Hoagland, D.A. (2004) Electrophoresis evidence for a new type of counterion condensation. *J. Polym. Sci. Part B, Polym. Phys*. **42,** 3616–3627.
59. Hoagland, D.A., Arvanitidou, E., Welch, C. (1999) Capillary electrophoresis measurements of free solution mobility for several model polyelectrolyte systems. *Macromolecules* **32 (19),** 6180–6190.
60. Cleland, R.L. (1991) Electrophoretic mobility of wormlike chains. 1. Experiment: hyaluronate and chondroitin-4-sulfate. *Macromolecules,* **24 (15),** 4386–4390.
61. Overbeek, J.T.G. (1943) Theorie der elektrophorese. *Kolloid-Beih*. **54,** 287–364.
62. Booth, F. (1950) The cataphoresis of spherical, solid non conducting particles in a symmetrical electrolyte. *Proc. R. Soc. Lond*. **203,** 533–551.
63. Saville, D.A. (1994) Dielectric behavior of colloidal dispersions. *Colloids Surf. A* **92,** 29–40.
64. Ohshima, H. (2002). Modified Henry function for the electrophoretic mobility of a charged spherical colloid particle covered with an ion-penetrable uncharged polymer layer. *J. Colloid Interface Sci*. **252,** 119–125.
65. Cohen, J.A., Korosheva, V.A. (2001) Electrokinetic measurement of hydrodynamic properties of grafted polymer layers on liposome surfaces. *Colloids Surfaces A: Physicochem. Eng. Aspects* **195,** 113–127.

66. Tanford, C. (1965) *Physical Chemistry of Macromolecules*. J. Wiley & Sons Eds, Inc., N.Y.
67. Cleland, R.L. (1991) Electrophoretic mobility of wormlike chains. 2. Theory. *Macromolecules* **24 (15),** 4391–4402.
68. Campa, C., Donati, I., Vetere, A., Gamini, A., Paoletti, S. (2001) Synthesis of glycosylamines: Identification and quantification of side products. *J. Carbohydr. Chem*., **20 (3& 4),** 263–273.
69. Gamini, A., Paoletti, S., Zanetti, F. (1992) Chain rigidity of polyuronates: Static light scattering of aqueous solutions of hyaluronate and alginate. In: *Laser Light Scattering in Biochemistry,* S. E. Harding, D.B. Sattelle, and V.A. Bloomfield, Ed., Royal Society of Chemistry, U.K.

14

Analysis of Oligonucleotides Using Capillary Zone Electrophoresis and Electrospray Mass Spectrometry

An Willems, Dieter L. Deforce, and Jan Van Bocxlaer

Summary

This chapter illustrates the usefulness of capillary zone electrophoresis (CZE) coupled to high-resolution electrospray ionization quadrupole time-of-flight mass spectrometry for the single-step desalting, and separation, as well as characterization of oligonucleotides in the framework of quality control after synthesis. Separation is performed using a 25 mM ammonium carbonate buffer supplemented with 0.2 mM *trans*-1,2-diaminocyclohexane-*N*, *N*, *N*′, *N*′-tetraacetic acid (CDTA) (pH 9.7). During the electrophoretic process, sodium and potassium ions are removed from the polyanionic backbone of the oligonucleotides by exchange of these ions with ammonium ions or by chelation on CDTA, thus eliminating a sample preparation step. A sample stacking procedure used to concentrate the samples on the CZE capillary is described. After analysis, the obtained spectrum is deconvoluted to the zero charge spectrum to yield the molecular mass of the oligonucleotide. A misincorporation of one nucleotide can be detected by a difference in mass.

Key Words: Capillary zone electrophoresis; electrospray mass spectrometry; quadrupole time-of-flight mass spectrometer; oligonucleotides; quality control.

1. Introduction

Today, synthetic oligonucleotides have become indispensable tools in the fields of biochemistry, molecular biology, medicine, microbiology and forensics. They are extensively used as primers for DNA amplification by the polymerase chain reaction (PCR), as probes for in situ hybridization techniques for the detection of PCR products, and as antisense oligonucleotide therapeutic agents for the treatment of several viral infections and cancer. Oligonucleotide quality is of prime importance to give the results the needed degree of certainty.

From: *Methods in Molecular Biology, vol. 384: Capillary Electrophoresis*
Edited by: P. Schmitt-Kopplin © Humana Press Inc., Totowa, NJ

Therefore, quality control and characterization of these oligonucleotides after synthesis are needed to confirm the expected oligonucleotide sequence, to verify the product purity and to identify the presence of eventually failure sequences, as a defect in length or sequence is not tolerated ***(1–7)***.

Until recently, the analytical methods used for this purpose were polyacrylamide slab gel electrophoresis, capillary gel electrophoresis (CGE), and high-performance liquid chromatography (HPLC). These methods are based on the separation of the oligonucleotides according to their length, regardless of their base sequence or composition and are thus not sufficient for absolute identification ***(1–6)***. During the past decade, mass spectrometry (MS) has become another important tool in the analysis of oligonucleotides. MS provides a basis for detecting both length and sequence variations of oligonucleotides, based on a difference in mass ***(4,8,9)***. Under electrospray ionization (ESI) conditions, multiply charged ions are produced, resulting in a mass spectrum containing an envelope of peaks which correspond to ions with various charge states, having a relatively low mass-to-charge ratio ($m/z < 2500$). Computer algorithms can transform this spectrum to a zero charge spectrum to yield the molecular mass of the oligonucleotide, called a deconvoluted spectrum ***(10,11)***. Because ESI forms ions directly from a liquid solution, it is ideally suited for the direct interfacing to HPLC (mainly ion-pair reversed-phase HPLC) ***(2,3,7,8,12,13)*** and capillary electrophoresis (CE) ***(4,14–20)***.

However, oligonucleotide mass measurements are complicated due to the affinity of the polyanionic backbone for cations such as sodium and potassium. These cations lower the sensitivity for the analyte by dispersing the ion abundance among multiple adducted ions. In the case of ESI-MS, these multiple cation adduct ions result in highly complex spectra, which decrease the ability to characterize mixtures of oligonucleotides. Moreover, accurate mass measurements are hampered. A high-resolution mass spectrometer is necessary to prevent overlap of spectral peaks. Less resolving MS systems (i.e. ion trap) are unsuitable as peak broadening due to adduct formation entailing overlap of spectral peaks can occur with the consequence that charge states of the multiply charged envelope cannot be distinguished in the worst case. Effective removal of these cations is required to obtain better interpretable mass spectra, high mass accuracy, and satisfactory sensitivity. Several strategies were developed for the reduction of cation adduction ***(21–23)***. A first approach involves the competition of an excess of ammonium ions with sodium and potassium ions for the negative charges at the sugar-phosphate backbone. Ammonium ions appear to be less tightly bound to the phosphodiester groups than sodium or potassium ions, and they can dissociate during the electrospray process, leaving one proton with the oligonucleotide ***(21,22,24,25)***. A second approach is based on the use

of a chelator, such as *trans*-1,2-diaminocyclohexane-*N*, *N*, *N′*, *N′*-tetraacetic acid (CDTA), to remove cations from the oligonucleotide sample ***(26)***.

CE is one of the most important techniques for the separation of charged analytes, being the method of choice for the analysis of the negatively charged oligonucleotides. CE itself has one major disadvantage: the volumes of sample loading are limited resulting in low concentration sensitivity. However, preconcentration techniques, such as sample stacking, have been devised to increase the loadability of the capillary and improve detection limits for CE-MS ***(27)***. The coupling of CE and MS for the analysis of oligonucleotides after synthesis combines all the advantages of CE with the ability of the mass spectrometer to provide sensitivity and selectivity and the ability to detect both the intact oligonucleotide (and eventually failure sequences) and fragments thereof formed by collision-induced dissociation. Until now, only a few reports were found dealing with the CE-ESI-MS analysis of oligonucleotides. The research group of Schrader et al. ***(14–16)*** used capillary zone electrophoresis (CZE)-negative ion ESI-MS and ESI-MS/MS in an ammonium carbonate buffer for the detection and identification of styrene oxide-modified oligonucleotides. Deforce et al. ***(4)*** investigated an on-line CZE-negative ion ESI-quadrupole time-of-flight (Q-TOF)-MS separation for its ability to enhance the detection and characterization of oligonucleotides of up to 120 bases. During separation in an ammonium carbonate buffer, the sodium and potassium ions were exchanged for ammonium ions, thus eliminating the need for any sample preparation. Prior to CZE-ESI-MS analysis, the oligonucleotide samples were preconcentrated using the sample stacking technique with compensating pressure. The use of the CZE-ESI-Q-TOF system not only enhances the sensitivity by a factor of 20 compared to that of the conventional quadrupole, but it also has a superior mass resolution. The deconvoluted spectra exhibit high mass accuracy [about 50 ppm and 100 ppm for the long (120 bases) and short (18–27 mers) oligonucleotides, respectively] and high resolution (peak widths at half height of 4 Da). The absolute mass accuracy obtained is about 0.8 (short oligos) to 1.8 Da (long oligos). A misincorporation of one base, in the worst case a thymine to adenine switch having a mass difference of 9 Da, would easily be detected. Barry et al. ***(17)*** and Harsch et al. ***(18)*** coupled CE in a fused silica capillary coated with poly-(vinyl alcohol) and filled with a poly-(*N*-vinylpyrrolidone) matrix to negative ion ESI-MS for the analysis of short modified oligonucleotides. It was observed that, in addition to size differentiation, the physical network formed by the linear polymer acts as a pseudo-phase and allows separation on the basis of hydrophobic interactions. Oligonucleotides with minor hydrophobic modifications were retained longer than their normal unmodified analogues. Freudemann et al. ***(19)*** and von Brocke et al. ***(20)*** reported the on-line coupling of CGE with negative ion

ESI-MS for oligonucleotide analysis (5–20 mers) using an entangled polymer solution consisting of poly-(ethylene glycol), Bis-Tris, boric acid, and acetonitrile in poly-(vinyl acetate)- or poly-(vinyl alcohol)-coated capillaries. More detailed information about the analysis of oligonucleotides with CE-MS can be found in a recent review article summarized by our research group ***(28)***.

Methods utilized for the quality control of oligonucleotides after synthesis should be rapid, low cost, and reliable and use minimal labor. This chapter focuses on the application of CZE- nano-ESI-Q-TOF-MS for the single-step desalting, and separation, as well as characterization of oligonucleotides. Separation is performed using a 25 mM ammonium carbonate buffer supplemented with 0.2 mM CDTA (pH 9.7). During the electrophoretic process, sodium and potassium ions are removed from the polyanionic backbone of the oligonucleotides by exchange of these ions with ammonium ions or by chelation on CDTA, thus eliminating a sample preparation step. A sample stacking procedure used to concentrate the samples on the CZE capillary is described. After analysis, the obtained spectrum is deconvoluted to the zero charge spectrum to yield the molecular mass of the oligonucleotide. A misincorporation of one nucleotide can be detected by a difference in mass.

2. Materials

2.1. Chemicals

1. All reagents and solvents used were of analytical grade and were used without further purification. Ammonium carbonate, ammonium hydroxide, isopropanol and sodium hydroxide were obtained from Aldrich (St. Louis, MO, USA). CDTA (>99%) was from Sigma (St. Louis, MO, USA).
2. For the preparation of all aqueous solutions, high purity water, provided from a Synergy 185 system (Millipore, Bedford, MA, USA), was used.
3. Samples: Synthetic oligonucleotides (Applied Biosystems, Warrington, Cheshire, UK) were used without further purification (125 and 180 pmol/μL).

2.2. CZE-ESI-MS, On-line Sample Stacking

1. The CZE instrument used is a Lauerlabs PRINCE system (Lauerlabs, Emmen, The Netherlands) with autosampler and control software version 4.201. In theory, any other CZE instrument should also allow the coupling to ESI-MS. Important features are that the CZE instrument can measure the current leaving its high voltage power supply, instead of the current going through the capillary. This is a prerequisite to be able to perform the sample stacking when coupled to ESI-MS because there is no outlet vial in that configuration.
2. A quadrupole time-of-flight (Q-TOF®) mass spectrometer (Waters, Manchester, UK) was applied for mass spectrometric detection.
3. CZE-ESI ionization was performed using a nano-electrospray source, which was equipped with a coaxial CZE-nano-ESI probe (Waters). This interface consisted of

three capillaries with the separation capillary as innermost capillary. The second capillary, which was made from stainless steel, carries the sheath flow and the electrospray potential, while the outermost capillary (also a stainless steel tube) allows addition of a nebulization gas to assist droplet formation and to provide a certain amount of cooling for the CZE capillary.

4. Data were collected and analyzed using the MassLynx® 3.5 software (Waters). The expected average molecular masses of all oligonucleotides were calculated using the Biolynx® software, which is part of the MassLynx® software package. Using the MaxEnt® algorithm (Waters), deconvoluted spectra were calculated, displaying the observed masses of the uncharged molecules.
5. Buffer: 25 mM ammonium carbonate, 0.2 mM CDTA, pH 9.7. A 20 mM solution of CDTA is prepared in ammonium hydroxide (30%). Two hundred and fifty microliters of this solution is added to 25 mL of a 25 mM ammonium carbonate solution and adjusted to pH 9.7 with ammonium hydroxide (*see* **Notes 1** and **2**).
6. Sheath liquid: 80% isopropanol, 15% high purity water and 5% 5 mM ammonium carbonate (pH 9.7). This sheath liquid was introduced in the probe using a sheath liquid capillary, at a flow rate of 0.7 μL/min, delivered by a Harvard syringe pump (Harvard Apparatus, South Natick, MA, USA) (*see* **Notes 2** and **3**).
7. Nucleotide solution [0.1 mg/mL deoxynucleotide triphosphates (dNTPs)]: 10 mg of each nucleotide, 2′-deoxyadenosine-5′-monophosphate (dAMP), 2′-deoxycytidine-5′-monophosphate (dCMP), 2′-deoxyguanosine-5′-monophosphate (dGMP) and thymidine-5′-monophosphate (TMP) (all from Sigma), were combined and dissolved in 100 mL in 25 mM ammonium carbonate + 0.2 mM CDTA (pH 9.7) buffer.

3. Methods

3.1. Sample Preparation

1. The synthetic oligonucleotides arrive as lyophilized samples.
2. Dissolve each sample in high purity water to become the appropriate concentration (*see* **Note 4**).
3. Divide each sample into aliquots.
4. Analyze the samples without further purification or manipulation.

3.2. CZE-ESI-MS

1. The procedure described here was optimized for the quality control of negatively charged oligonucleotides after synthesis.
2. Cut a fused silica capillary [dimensions: 50 μm inner diameter (i.d.) and 365 μm outer diameter (o.d.)] to the desired length (±15 cm) using a ceramic cutter (*see* **Note 5**). The polyimide coating needs to be removed over a length of ±3 cm from the sprayer end of the capillary which will be inside the inner sheath capillary of the ESI probe, this is because the polyimide coating loosens during operation and may cause malfunctions and clog the sample orifice. Thread this extension capillary from the rear of the sprayer through the sleeve and T piece in the inner sheath capillary of the coaxial ESI probe. Attach the fused silica to the microtight

union in the adjuster assembly using the correct sleeve and nut and ensure that dead volumes are eliminated by use of a blanking nut. Using the adjuster screw alter the position of the microtight union so that the union sleeve touches the back end of the sprayer sleeve (this will reduce the length of the extension capillary to a minimum) and then cut the capillary so that approximately 2 mm of fused silica protrudes from the stainless steel make up capillary. The sheath capillary is positioned to protrude approximately 1 mm from the nebulizing capillary. Connect a syringe pump to the sheath capillary and attach this capillary to the port at the top of the sprayer. The nut supporting the sleeving for the CE extension capillary should now be tightened. The correct tightness is achieved when it is still possible to adjust the fused silica at the tip using the adjuster screw, but no liquid leakage is observed through the sleeve. It is best to tighten the sleeve in stages while checking the movement at the tip regularly.

3. Cut a fused silica capillary (same dimensions as above) to the desired length (0.85 m) using a ceramic cutter (*see* **Note 5**). The polyimide coating needs to be removed from the injection end (±5 cm). Insert the injection end of the capillary in the CZE instrument and attach the other end to the microtight union in the adjuster assembly of the ESI probe using the correct sleeve and nut.
4. Before its first use, the capillary should be preconditioned (*see* **Note 6**).
5. The positioning of the capillaries needs slight optimization (*see* **Note 7**).
6. Pump the sheath liquid at a flow rate of 0.7 μL/min (*see* **Note 8**). A nitrogen gas flow of 1.2 bar is delivered to the ESI tip through the nebulizing capillary to aid the ESI process. A drying gas flow of 125 L/h nitrogen is delivered to the source. Set the temperature in the source to 80 °C.
7. The liquid level in the anode buffer reservoir should be at the same height as the ESI probe tip when inserted in the source of the mass spectrometer. This is necessary to prevent hydrodynamic effects during electrophoresis. Set the current control of the CZE instrument to the inlet electrode which measures the amount of current going out of the CZE high voltage source. This is necessary to be able to monitor the current during electrophoresis (*see* **Note 9**).
8. Next, the mass spectrometer should be tuned to obtain the optimized ESI and MS conditions. Fill the capillary with the nucleotide solution (0.1 mg/mL dNTPs) by applying a pressure of 500 mbar on the vial at the inlet of the capillary (*see* **Note 10**), position the ESI probe in the source of the mass spectrometer, apply an electrospray voltage of −3 kV to the ESI probe and a cone voltage of 35 V and wait for about 20 min to proceed. This time is necessary to let the temperature of the ESI probe reach 80 °C. Apply a pressure of 60 mbar and 14 kV over the electrophoresis capillary and monitor the signal at m/z 306 (dCMP), 321 (TMP), 330 (dAMP) and 346 (dGMP) on the mass spectrometer for tuning purposes. Optimize the x-, y- and z-axis position of the ESI probe in the MS source to obtain an optimal signal for dCMP, TMP, dAMP and dGMP. This step needs to be done with great care as slight deviations from the optimal position result in a dramatic decrease in sensitivity.
9. Tune the mass spectrometer to attain optimal sensitivity.

10. Position a vial containing the electrophoresis buffer (25 mM ammonium carbonate + 0.2 mM CDTA, pH 9.7) at the capillary inlet and rinse the CZE capillary with electrophoresis buffer by applying a pressure of 500 mbar (*see* **Note 11**). When the capillary is properly rinsed, set the pressure on the CZE instrument to zero.
11. Fill the CZE autosampler tray with the properly prepared samples (*see* **Subheading 3.1.**).
12. Select the appropriate data collection settings on the mass spectrometer. In most cases, full scan spectra were acquired over the m/z 500–2500 range at a scan accumulation rate of 2 s/scan and an interscan delay of 0.1 s. All spectra were collected in continuum mode (*see* **Note 12**).
13. Before injecting a sample on the CZE capillary, turn off the electrospray voltage in the ESI probe, the sheath flow and the nanoflow gas pressure. Inject the sample on the CZE capillary by applying a pressure of 100 mbar for 1 min, followed by the on-line sample stacking procedure (*see* **Subheading 3.3.**). Move the autosampler back to the electrophoresis buffer and start the electrophoresis process by applying a voltage of 14 kV and a pressure of 60 mbar over the CZE capillary. Turn the electrospray voltage, the sheath flow and the nanoflow gas pressure back on and start the data collection on the mass spectrometer (*see* **Notes 13** and **14**).
14. Monitor an extracted ion electropherogram of the sum of the m/z values of all the multiply charged ions that can be observed between 500 and 2500 Da on the mass spectrometer to follow the electrophoresis process. A typical reconstructed mass electropherogram is shown in **Fig. 1**.

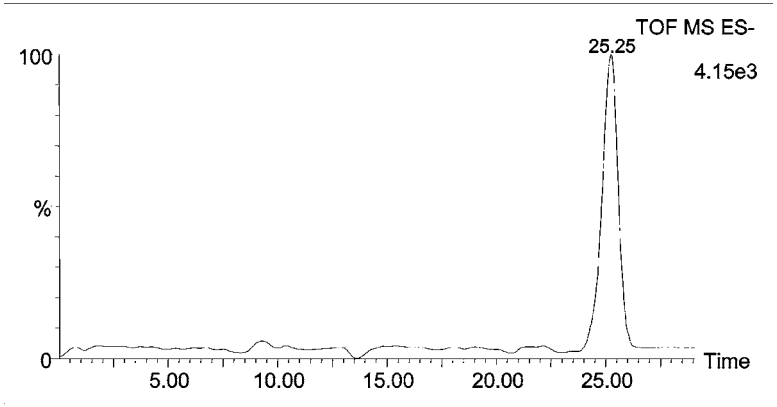


Fig. 1. Reconstructed mass electropherogram obtained after capillary zone electrophoresis-electrospray ionization-quadrupole time-of-flight-mass spectrometry (CZE-ESI-Q-TOF-MS) analysis of oligonucleotide 5′-CCC TGG GCT CTG TAA AGA ATA GTG-3′ (theoretical mass: 7392.8587 Da). Buffer: 25 mM ammonium carbonate + 0.2 mM *trans*-1,2-diaminocyclohexane-*N*, *N*, *N*′, *N*′-tetraacetic acid, pH 9.7. Electrophoretic conditions: 14 kV, 60 mbar. Sheath liquid: isopropanol-water-5 mM ammonium carbonate, pH 9.7 (80/15/5). Reproduced with permission from **ref. *29***; © Wiley-VCH Verlag.

15. When the analysis is completed, switch off the electrophoresis voltage and apply a pressure of 500 mbar during 5 min to rinse the CZE capillary with electrophoresis buffer. The system is now ready for the analysis of a new sample (repeat from step 12) (*see* **Note 15**).
16. Inspect the CZE-ESI-MS results for the confirmation of the oligonucleotide and for the detection of eventually failure sequences. This can best be performed by taking a summation of all m/z values present in the electrophoretic zone of interest to obtain a spectrum consisting of a series of peaks, each of which represents a multiply charged ion of the intact oligonucleotide that has a specific number of protons removed from the phosphodiester groups (*see* **Fig. 2**). Process the Maxent algorithm of the signals of the multiply charged series to yield the molecular mass of the oligonucleotide (*see* **Note 16**). No cation adducts are observed (*see* **Fig. 3**).

3.3. On-Line Sample Stacking

1. The sample stacking procedure described here is only suited for the concentration of negatively charged analytes, such as oligonucleotides. In order to be able to perform this sample stacking procedure, it is a prerequisite that the samples are present in a solution with a lower electrolyte concentration than the electrophoresis buffer, or ideally in a solution containing no electrolytes. In our case, the samples are present in high purity water.

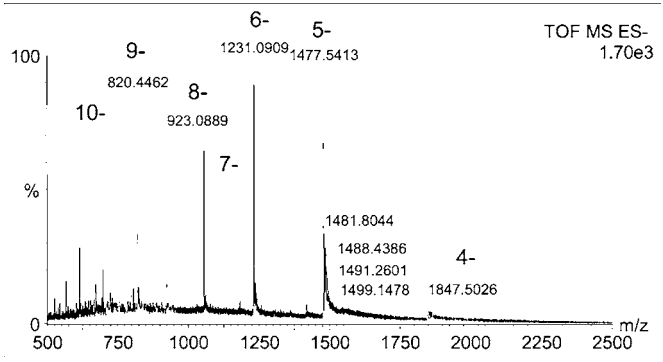


Fig. 2. Raw electrospray negative ion spectrum obtained after capillary zone electrophoresis-electrospray ionization-quadrupole time-of-flight-mass spectrometry (CZE-ESI-Q-TOF-MS) analysis of oligonucleotide 5′-CCC TGG GCT CTG TAA AGA ATA GTG-3′ (theoretical mass: 7392.8587 Da). Buffer: 25 mM ammonium carbonate + 0.2 mM *trans*-1,2-diaminocyclohexane-*N*, *N*, *N*′, *N*′-tetraacetic acid, pH 9.7. Electrophoretic conditions: 14 kV, 60 mbar. Sheath liquid: isopropanol-water-5 mM ammonium carbonate, pH 9.7 (80/15/5). Reproduced with permission from **ref. *29***; © Wiley-VCH Verlag.

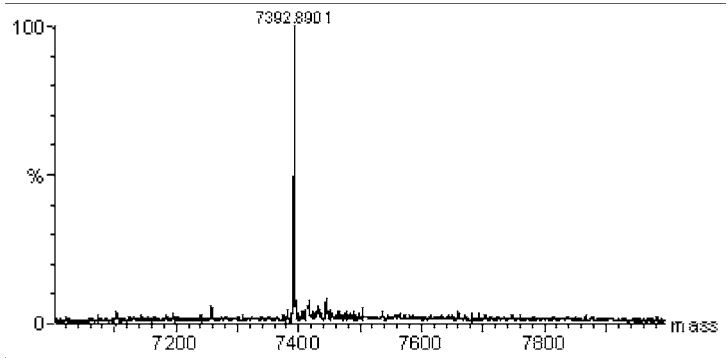


Fig. 3. Deconvoluted (zero charge) spectrum obtained after capillary zone electrophoresis-electrospray ionization-quadrupole time-of-flight-mass spectrometry analysis of oligonucleotide 5′-CCC TGG GCT CTG TAA AGA ATA GTG-3′ (theoretical mass: 7392.8587 Da). Buffer: 25 mM ammonium carbonate + 0.2 mM *trans*-1,2-diaminocyclohexane-*N*, *N*, *N*′, *N*′-tetraacetic acid, pH 9.7. Electrophoretic conditions: 14 kV, 60 mbar. Sheath liquid: isopropanol-water-5 mM ammonium carbonate, pH 9.7 (80/15/5). Reproduced with permission from **ref. *29***; © Wiley-VCH Verlag.

2. Perform the **steps 1–12** described in **Subheading 3.2.** CZE-ESI-MS, if you have not yet done so.
3. Set the pressure on the CZE instrument to zero and turn off the electrospray voltage, the sheath liquid and the nanoflow gas pressure.
4. Hold an Eppendorf vessel filled with running buffer manually in place over the sprayer needle (*see* **Note 17**).
5. Apply a voltage of −20 kV to the CZE capillary. Monitor the current and write it down as the stack limit current (−12.8 μA). Program the CZE instrument to start the normal electrophoresis when the stack limit current +0.5 μA is reached.
6. Set the voltage over the CZE capillary to zero, remove the Eppendorf vessel from the sprayer needle and rinse the capillary with CZE buffer by applying a pressure of 200 mbar for 2 min.
7. Again, hold an Eppendorf vessel filled with running buffer manually in place over the sprayer needle. Inject the sample on the CZE capillary by applying a pressure of 100 mbar for 1 min (*see* **Note 18**). Move the autosampler back to the electrophoresis buffer and start the sample stacking process by applying a voltage of −20 kV to the CZE capillary. Let the CZE instrument monitor the current (*see* **Note 9**) and start the normal electrophoresis when the stack limit current +0.5 μA (using the program made in **step 5**, the CZE instrument performs this switch automatically) is reached by applying a voltage of 14 kV and a pressure of 60 mbar over the CZE capillary. Remove the Eppendorf vessel from the sprayer needle and switch the electrospray voltage, the sheath liquid and the nanoflow gas pressure back on.
8. Start the data collection on the mass spectrometer.
9. Continue with **steps 14–16** described in **Subheading 3.2.**

4. Notes

1. As any capillary is prone to blocking, all separation and wash solutions were filtered through a 0.22-μm membrane filter (Millipore) to remove any particular matter, followed by degassing for 10 min in an ultrasonic bath prior to use.
2. All buffers and sheath liquids are made fresh each day.
3. Sheath liquids are thoroughly degassed by sonication for 5 min.
4. Take great care during the sample preparation to avoid contamination, especially if the oligonucleotide sample will be used as primer. Perform all procedures in laminar air flow cabinets and use only autoclaved recipients. Avoid any contact with glass ware to minimize the amount of sodium and potassium ions in the oligonucleotide sample.
5. The o.d. of the capillary needs to be chosen in function of the i.d. of the inner sheath capillary of the ESI probe. The cut at both capillary ends should be straight, this is extremely important for the capillary end in the ESI probe. Otherwise, this can have a negative impact on the ESI process at the capillary tip. The cut can best be examined under a stereomicroscope. The polyimide coating is removed by holding it in the flame of a cigarette lighter and cleaning off the burned coating with a cloth dampened with methanol.
6. This preconditioning procedure needs to be performed with the ESI probe outside the source. Wash the capillary with 0.1 M NaOH for 30 min applying a pressure of 1000 mbar, followed subsequently by a 30-min flush with high purity water (1000 mbar) and a rinse with the electrophoresis buffer (1000 mbar for 30 min).
7. In order to optimize the positioning of the capillaries at the ESI probe tip, the spray can be observed under a stereomicroscope. For this purpose, a pressure of 60 mbar is applied to the CZE capillary in order to deliver electrophoresis buffer at the capillary end, a sheath flow of 0.7 μL/min, a nebulizing back pressure of 1.2 bar and an electrospray voltage of −3 kV is applied. The positioning of the capillaries may need slight adjustments in order to obtain a fine and stable electrospray mist. Great care needs to be taken to prevent the different capillaries to touch each other at the ESI tip, which has a detrimental effect on the electrospray.
8. This sheath liquid is optimal for the analysis of negatively charged species such as oligonucleotides. For the analysis of positively charged species, a sheath liquid of 50% methanol in water is to be preferred.
9. In order to be able to monitor the electrophoresis process, it is important to be able to follow the current going through the CZE capillary. An indication that the electrophoresis process is disturbed is that the current is not stable at a certain level (using our conditions ~12μA) or drops to zero (e.g. bubbles in the capillary). In addition, the sample stacking procedure cannot be performed when the current cannot be monitored.
10. Optimization of ESI conditions was investigated using dAMP, dCMP, dGMP and TMP in the electrophoresis buffer as test sample. The ESI-MS instrumental parameters, such as capillary positioning, capillary voltage, cone voltage, N_2 nanoflow gas pressure and N_2 desolvation gas flow rate, were optimized to produce the highest signal intensity of the four deprotonated molecules at m/z 306, 321,

330 and 346. This approach for the optimization of the ESI conditions was necessary, because it was not possible to perform an adequate optimization of the ESI-MS parameters using oligonucleotide samples. When oligonucleotide samples were infused in order to optimize the ESI conditions, no significant signal was obtained to tune the mass spectrometer, mainly because the signal was dispersed among the various multiple adducted ions.

11. The CZE capillary is properly rinsed when there is no detectable signal at m/z 306, 321, 330 and 346.
12. As under ESI conditions, multiply charged ions are produced, resulting in a mass spectrum containing an envelope of peaks which correspond to ions with various charge states, and having a relatively low mass-to-charge ratio ($m/z < 2500$), most peaks are observed between 500 and 2500 Da.
13. No oligonucleotide could be detected without the use of the on-line sample stacking technique.
14. When the electrospray voltage is not turned off during sample injection, the negative analytes, such as oligonucleotides, are prevented from entering the CZE capillary due to the electrostatic repulsion from the negative potential at the ESI tip and sensitivity drops dramatically. Also, the sheath liquid flow was turned off. Otherwise, the sheath liquid could be drawn into the capillary, because of the reversed electroosmotic flow (EOF) during the sample stacking procedure. Due to the low conductivity of the sheath liquid, this would render the sample stacking procedure unusable when connected to ESI-MS. During electrophoresis, an additional constant pressure of 60 mbar is applied at the injection (inlet) end to cut down analysis time. This results in a slight decrease in resolution of the CZE separation. The analysis can be performed without the 60 mbar pressure to maintain the high resolution; however, analysis time exceeding 1 hour is to be expected in that case. Data collection on the mass spectrometer can be started with a fixed delay (e.g. 10 min) in order to save disk space, as the oligonucleotides migrate only after the EOF.
15. Using the described injection procedure (100 mbar, 1 min), a calculated volume of around 110 nL was applied on the capillary. The calculated amount of oligonucleotide, which was injected on the capillary in our case, was about 15–20 pmol. Spectra which could still be deconvoluted were obtained from the injection of 2 pmol of oligonucleotide (24 bases) on the CZE-ESI-Q-TOF-MS using the sample stacking technique. This resulted in a signal-to-noise ratio of 5 in the mass electropherogram extracted from the total ion current.
16. The molecular masses could be obtained with an accuracy of better than 40 ppm or 0.5 Da for oligonucleotides less than 10,000 Da. It is obvious from these data that the use of the combination of CZE and ESI-Q-TOF-MS allows the identification of oligonucleotides differing in length by one nucleotide, so a misincorporation of the smallest mass difference (adenine to thymine switch differing 9 Da in mass) can be detected without any problem.
17. In order to be able to perform the sample stacking procedure, it is a prerequisite that electrophoresis buffer is present at the capillary end. This is necessary because

during the sample stacking procedure, a potential of −20 kV is applied over the CZE capillary which causes an EOF in the direction of the injection side of the capillary thus aspirating buffer into the capillary at the ESI probe end. When no electrophoresis buffer would be present at the capillary end during sample stacking, this would lead to a failure of the sample stacking process. In our case, an Eppendorf vessel filled with running buffer was held manually in place over the sprayer needle until the preconcentration was finished. Alternatively, two HPLC pumps can be connected to the sheath capillary using a Valco six-way switching valve to select the flow from the first or the second HPLC pump to enter the sheath capillary: one to deliver the normal sheath flow and a second to deliver the buffer necessary to perform sample stacking. Flow splitters can be used to be able to deliver the low volume flows at a constant flow rate. In that case, monitor the m/z value of 59, this is the $[M\text{-}H]^-$ ion of isopropanol, on the mass spectrometers tuning page and apply a constant pressure of 20 mbar on the buffer vial at the CZE inlet to deliver a constant flow of electrophoresis buffer through the CZE capillary. Then, switch the Valco six-way valve to deliver the flow from the second HPLC pump to the ESI probe. After some time, the signal at m/z 59 will decrease and eventually drop down to zero (about 10 min after switching the valve).

18. Injection of more sample of course increases the sensitivity of the method. In theory, the complete CZE capillary can be filled with sample solution for sample stacking concentration. In practice, the CZE capillary can be filled up to three quarters with sample.

Acknowledgements

We thank Ing. S. Vande Casteele for all her help with the analysis of the samples. This work was supported by grant GOA99-120501-99 (Bijzonder OnderzoeksFonds Universiteit Gent).

References

1. De Bellis, G., Salani, G. (1997) Oligonucleotide analysis by capillary zone electrophoresis at low pH. *Anal. Chim. Acta* **345**, 1–4.
2. Gaus, H. J., Owens, S. R., Winniman, M., Cooper, S., Cummins, L. L. (1997) On-line HPLC electrospray mass spectrometry of phosphorothioate oligonucleotide metabolites. *Anal. Chem.* **69**, 313–319.
3. Apffel, A., Chakel, J. A., Fisher, S., Lichtenwalter, K., Hancock, W. S. (1997) Analysis of oligonucleotides by HPLC-electrospray ionization mass spectrometry. *Anal. Chem.* **69**, 1320–1325.
4. Deforce, D. L. D., Raymackers, J., Meheus, L., Van Wijnendaele, F., De Leenheer, A., Van den Eeckhout, E. G. (1998) Characterization of DNA oligonucleotides by coupling of capillary zone electrophoresis to electrospray ionization Q-TOF mass spectrometry. *Anal. Chem.* **70**, 3060–3068.

5. Mangano, M. F., Battaglia, C., Salani, G., Rossi Bernardi, L., De Bellis, G. (1999) Composition dependent separation of oligonucleotides by capillary electrophoresis in acidic buffers with application to the quality control of synthetic oligonucleotides. *J. Chromatogr. A* **848**, 435–442.
6. Pietta, P. G., Mangano, M. F., Battaglia, C., Salani, G., Rossi Bernardi, L., De Bellis, G. (1999) Application of capillary electrophoresis at low pH to oligonucleotides quality control. *J. Chromatogr. A* **853**, 355–358.
7. Fountain, K. J., Gilar, M., Gebler, J. C. (2003) Analysis of native and chemically modified oligonucleotides by tandem ion-pair reversed-phase high-performance liquid chromatography/electrospray ionization mass spectrometry. *Rapid Commun. Mass Spectrom.* **17**, 646–653.
8. Huber, C. G., Krajete, A. (1999) Analysis of nucleic acids by capillary ion-pair reversed-phase HPLC coupled to negative-ion electrospray ionization mass spectrometry. *Anal. Chem.* **71**, 3730–3739.
9. Nordhoff, E., Kirpekar, F., Roepstorff, P. (1996) Mass spectrometry of nucleic acids. *Mass Spectrom. Rev.* **15**, 67–138.
10. Doktycz, M. J., Hurst, G. B., Habibi-Goudarzi, S., McLuckey, S. A., Tang, K., Chen, C. H., Uziel, M., Jacobson, K. B., Woychik, R. P., Buchanan, M. V. (1995) Analysis of polymerase chain reaction-amplified DNA products by mass spectrometry using matrix-assisted laser desorption and electrospray: current status. *Anal. Biochem.* **230**, 205–214.
11. Walters, J. J., Fox, K. F., Fox, A. (2002) Mass spectrometry and tandem mass spectrometry, alone or after liquid chromatography, for analysis of polymerase chain reaction products in the detection of genomic variation. *J. Chromatogr. B* **782**, 57–66.
12. Huber, C. G., Oberacher, H. (2001) Analysis of nucleic acids by on-line liquid chromatography-mass spectrometry. *Mass Spectrom. Rev.* **20**, 310–343.
13. Bleicher, K., Bayer, E. (1994) Analysis of oligonucleotides using coupled high-performance liquid chromatography-electrospray mass spectrometry. *Chromatographia* **39**, 405–408.
14. Janning, P., Schrader, W., Linscheid, M. (1994) A new mass spectrometric approach to detect modifications in DNA. *Rapid Commun. Mass Spectrom.* **8**, 1035–1040.
15. Schrader, W., Linscheid, M. (1995) Determination of styrene oxide adducts in DNA and DNA components. *J. Chromatogr. A* **717**, 117–125.
16. Schrader, W., Linscheid, M. (1997) Styrene oxide DNA adducts: in vitro reaction and sensitive detection of modified oligonucleotides using capillary zone electrophoresis interfaced to electrospray mass spectrometry. *Arch. Toxicol.* **71**, 588–595.
17. Barry, J. P., Muth, J., Law, S.-J., Karger, B. L., Vouros, P. (1996) Analysis of modified oligonucleotides by capillary electrophoresis in a polyvinylpyrrolidone matrix coupled with electrospray mass spectrometry. *J. Chromatogr. A* **732**, 159–166.

18. Harsch, A., Vouros, P. (1998) Interfacing of CE in a PVP matrix to ion trap mass spectrometry: analysis of isomeric and structurally related (*N*-acetylamino)fluorene-modified oligonucleotides. *Anal. Chem.* **70**, 3021–3027.
19. Freudemann, T., von Brocke, A., Bayer, E. (2001) On-line coupling of capillary gel electrophoresis with electrospray mass spectrometry for oligonucleotide analysis. *Anal. Chem.* **73**, 2587–2593.
20. von Brocke, A., Freudemann, T., Bayer, E. (2003) Performance of capillary gel electrophoretic analysis of oligonucleotides coupled on-line with electrospray mass spectrometry. *J. Chromatogr. A* **991**, 129–141.
21. Liu, C., Wu, Q., Harms, A. C., Smith, R. D. (1996) On-line microdialysis sample cleanup for electrospray ionization mass spectrometry of nucleic acid samples. *Anal. Chem.* **68**, 3295–3299.
22. Huber, C. G., Buchmeiser, M. R. (1998) On-line cation exchange for suppression of adduct formation in negative-ion electrospray mass spectrometry of nucleic acids. *Anal. Chem.* **70**, 5288–5295.
23. Griffey, R. H., Greig, M. J., Gaus, H. J., Liu, K., Monteith, D., Winniman, M., Cummins, L. L. (1997) Characterization of oligonucleotide metabolism in vivo via liquid chromatography/electrospray tandem mass spectrometry with a quadrupole ion trap mass spectrometer. *J. Mass Spectrom.* **32**, 305–313.
24. Ragas, J. A., Simmons, T. A., Limbach, P. A. (2000) A comparative study on methods of optimal sample preparation for the analysis of oligonucleotides by matrix-assisted laser desorption/ionization mass spectrometry. *Analyst* **125**, 575–581.
25. Huber, C. G., Krajete, A. (2000) Comparison of direct infusion and on-line liquid chromatography/electrospray ionization mass spectrometry for the analysis of nucleic acids. *J. Mass Spectrom.* **35**, 870–877.
26. Limbach, P. A., Crain, P. F., McCloskey, J. A. (1995) Molecular mass measurement of intact ribonucleic acids via electrospray ionization quadrupole mass spectrometry. *J. Am. Soc. Mass Spectrom.* **6**, 27–39.
27. Wolf, S. M., Vouros, P. (1995) Incorporation of sample stacking techniques into the capillary electrophoresis CF-FAB mass spectrometric analysis of DNA adducts. *Anal. Chem.* **67**, 891–900.
28. Willems, A. V., Deforce, D. L., Van Peteghem, C. H., Van Bocxlaer, J. F. (2005) Analysis of nucleic acid constituents by on-line capillary electrophoresis-mass spectrometry. *Electrophoresis* **26**, 1221–1253.
29. Willems, A. V., Deforce, D. L., Van Peteghem, C. H., Van Bocxlaer, J. F. (2005) Development of a quality control method for the characterization of oligonucleotides by capillary zone electrophoresis-electrospray ionization quadrupole time-of-flight mass spectrometry. *Electrophoresis* **26**, 1412–1423.

15

Separation of DNA by Capillary Electrophoresis

Bruce McCord, Brittany Hartzell-Baguley, and Stephanie King

Summary

This chapter reports an overview of the analytical techniques used to perform genetic analysis of polymerase chain reaction products using capillary electrophoresis. Three separate but related techniques are described: the separation of native DNA with detection using fluorescent intercalating dyes, the separation of denatured DNA using fluorescently labeled primers, and the detection of single-strand conformation polymorphisms using denatured DNA separated under native conditions. The various techniques involve electrokinetic injection of the DNA onto a narrow band at the head of the column, sieving the DNA through various entangled polymer matrices, and detection via single or multichannel laser-induced fluorescence. Analytical protocols are provided, and a series of representative electropherograms are included.

Key Words: DNA; capillary electrophoresis; genotyping; SSCP; fluorescence; PCR.

1. Introduction

Capillary electrophoresis (CE) is an attractive separation technique for DNA analysis due to its high resolving capability, speed, low sample consumption, and its capability to automate sample loading ***(1,2)***. Applications include DNA sequencing, restriction mapping of chromosomal DNA, and genotyping ***(3)***. In electrophoresis, molecules are usually separated as a result of their different mobilities. However, because DNA molecules have a constant charge/size ratio, their electrophoretic mobility in free solution is equally regardless of their chain length ***(4)***. For this reason, a sieving matrix must be used within the capillary to provide size-dependent DNA fragment separation.

From: *Methods in Molecular Biology, vol. 384: Capillary Electrophoresis*
Edited by: P. Schmitt-Kopplin © Humana Press Inc., Totowa, NJ

In early work with this technique, capillaries were filled with cross-linked solutions of polyacrylamide when performing DNA separations ***(5)***. These gels were analogous to the standard slab gel methods used. However, this approach was hindered by the difficulty in preparing homogeneous gels in capillaries when highly sensitive polymerization reactions were being utilized for gel formation ***(4)***. Furthermore, these capillaries had very short lifetimes due to gel shrinkage and breakdown with time and the repeated use of high electric fields. With the introduction of non-cross-linked (linear) polyacrylamide systems in the early 90s, the separation matrix could be replaced after every run, eliminating the need to replace the capillary in order to maintain high separation efficiency ***(5)***. A wide variety of hydrophilic polymers have been adopted for this purpose, including solutions formulated with derivatized celluloses, N-substituted acrylamides, poly(vinyl pyrrolidone) (PVP), poly(ethylene oxide), poly(ethylene glycol), and more recently copolymers such as acrylamide-dimethylacrylamide ***(1,2,6)***. The key issue in applying these polymers to DNA separations is to optimize the concentration and molecular weight in order to achieve high resolution and to utilize polymers with dynamic wall coating characteristics in order to permit refilling and reuse of the capillary.

With the advent of commercial DNA sequencers from companies such as Beckman and Applied Biosystems (AB), Foster city, CA, DNA separations have become more standardized. Specialized mixtures of soluble polymers and buffers can be easily purchased to perform different types of DNA separations. There have also been a number of published reviews of techniques for DNA separation by CE as well as several books ***(3,7–10)***. In this chapter, three major applications of CE for DNA analysis will be discussed. These include separation of native DNA for the analysis of polymerase chain reaction (PCR) and other enzymatic products, the separation of denatured DNA for high resolution genotyping, and the application of single-strand conformation polymorphisms (SSCPs) for bacterial identification.

2. Native DNA Analysis

A number of sieving matrices exist for the separation of native DNA ***(11)***. Of these, PVP is attractive because of its low viscosity compared to other polymers at the same concentration and molecular weight, and its excellent dynamic coating ability ***(12,13)***. More viscous polymer solutions can require high pressures resulting in longer fill times when loaded into capillaries. Furthermore, these viscous solutions can make rinsing and refilling the capillary difficult, resulting in a gradual loss of efficiency. For the separation of DNA by CE, a polymer with a high dynamic coating ability is also preferred. This property allows for the reduction of the electroosmotic flow without having to

use expensive, coated capillaries. It is thought that hydrogen bonding between the PVP carbonyl groups and the capillary wall is responsible for the formation of this polymer's coating. Other polymer matrices can require more specialized capillaries or extended wall treatments ***(14)***. In addition to these properties, we have chosen to utilize a solution of PVP in our lab for double-stranded DNA (dsDNA) separation because of its short preparation time, long shelf life, and good reproducibility. Following the procedure described below, which has been adapted from Gao and Yeung ***(12)***, we can achieve greater than 8 bp resolution for DNA fragments ranging in size from 60 to 600 bp. Fluorescence detection occurs through the application of YO-PRO-1, an intercalating dye ***(14)***.

2.1. Materials

2.1.1. Capillary Electrophoresis Using Poly(Vinyl Pyrrolidone)

1. Run buffer (1 × Tris-borate EDTA (TBE)): 89 mM Tris, 89 mM boric acid, 2 mM ethylenediamine tetra acetic acid (EDTA). Store at room temperature.
2. Sieving matrix (PVP in TBE): PVP powder, MW 1,000,000 (Polysciences Inc., Warrington, PA) added to buffer solution to yield 5.5% (w/w) polymer solution. Store at room temperature.
3. Plasmid digest for sizing: 148 μg/mL pBR322 Hae III digest (Sigma, St. Louis, MO).
4. Fluorescent intercalating dye: 1 mM YO-PRO-1 iodide in dimethyl sulfoxide (DMSO), excitation and emission wavelengths, 491 and 509 nm, respectively (Molecular Probes, Eugene, OR). Store at −20 °C.
5. Uncoated, fused silica capillaries with an internal diameter of 50 μm (Polymicro Technologies, Phoenix, AZ).

2.2. Methods

The following instructions assume the use of the P/ACE 2050 system (Beckman Coulter, Fullerton, CA) with an Ar-ion laser, 488 nm emission (National Laser Company, Salt Lake City, UT); however, they are easily adaptable to other CE systems and lasers. Also, if a fluorescent dye is incorporated on the 5′ end of a PCR primer, an intercalating dye is not necessary; however, the use of intercalating dyes improves sensitivity as multiple sites along the DNA are labeled. In our studies, unlabeled DNA or strands labeled with functional groups other than dyes were analyzed, and therefore, an intercalating dye was used for detection. We found that the dye, YO-PRO-1, could be added either to the separation system (run buffers and sieving matrix) or directly to the DNA sample as follows.

2.2.1. Preparation of Poly(Vinyl Pyrrolidone) Sieving Matrix

1. Add 5.5 g of PVP powder to 100 mL of TBE to make approximately 5.5% (w/w) polymer solution.
2. Cover solution and mix evenly using a magnetic stirrer for 1 h.

2.2.2. Addition of Intercalating Dye to Buffer System or DNA Sample

1. If dye is added to the run buffers and the sieving matrix, 1 μL of 1 mM YO-PRO-1 iodide is added per 5 mL of solution. Solutions are then vortexed to mix evenly and sonicated for 1 min to remove any bubbles that have formed.
2. If dye is added to the sample, 0.5 μL of 148 μg/mL pBR322 Hae III digest (or the DNA sample to be tested) and 0.2 μL of 1 mM YO-PRO-1 iodide are added to 100 μL deionized water. This solution is then vortexed to mix evenly.

2.2.3. Double-stranded DNA Separation and LIF Detection

1. Cut capillary to a total length of 37 cm, effective length 29 cm.
2. Fill capillary with polymer solution for 6 min using high pressure.
3. Place both ends of the capillary in deionized water for 0.1 min, prior to injection.
4. Zero the detector output and then electrokinetically inject sample for 2 s at 2 kV.
5. Use a run voltage of 5 kV for DNA separation (i.e., an electric field of 135 V/cm). An electropherogram displaying the separation of the pBR322 Hae III digest fragments using this system is shown in **Fig. 1**. **Figure 2** shows the separation

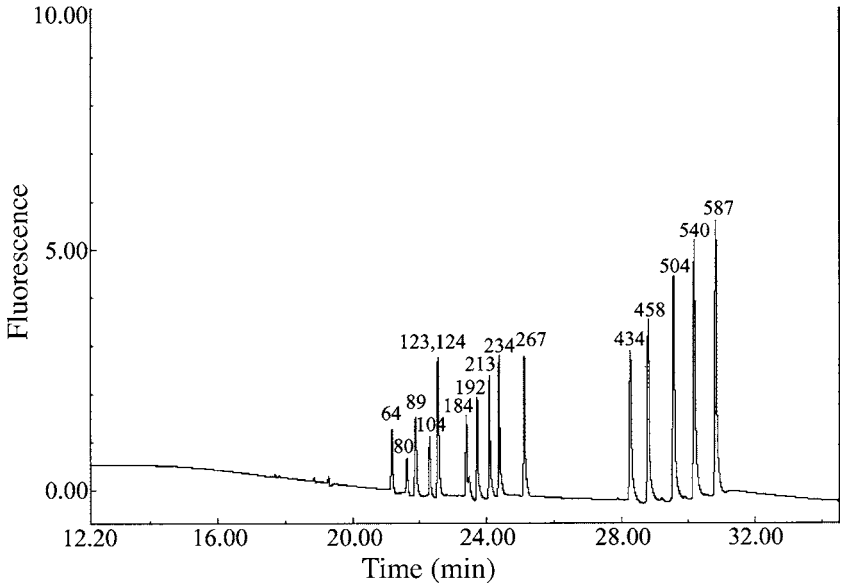


Fig. 1. Electropherogram of pBR322 Hae III digest, separated using 5.5% poly(vinyl pyrrolidone) in TBE buffer and YO-PRO-1 dye mixed with the DNA sample. Fragment size (in bp) shown above each peak.

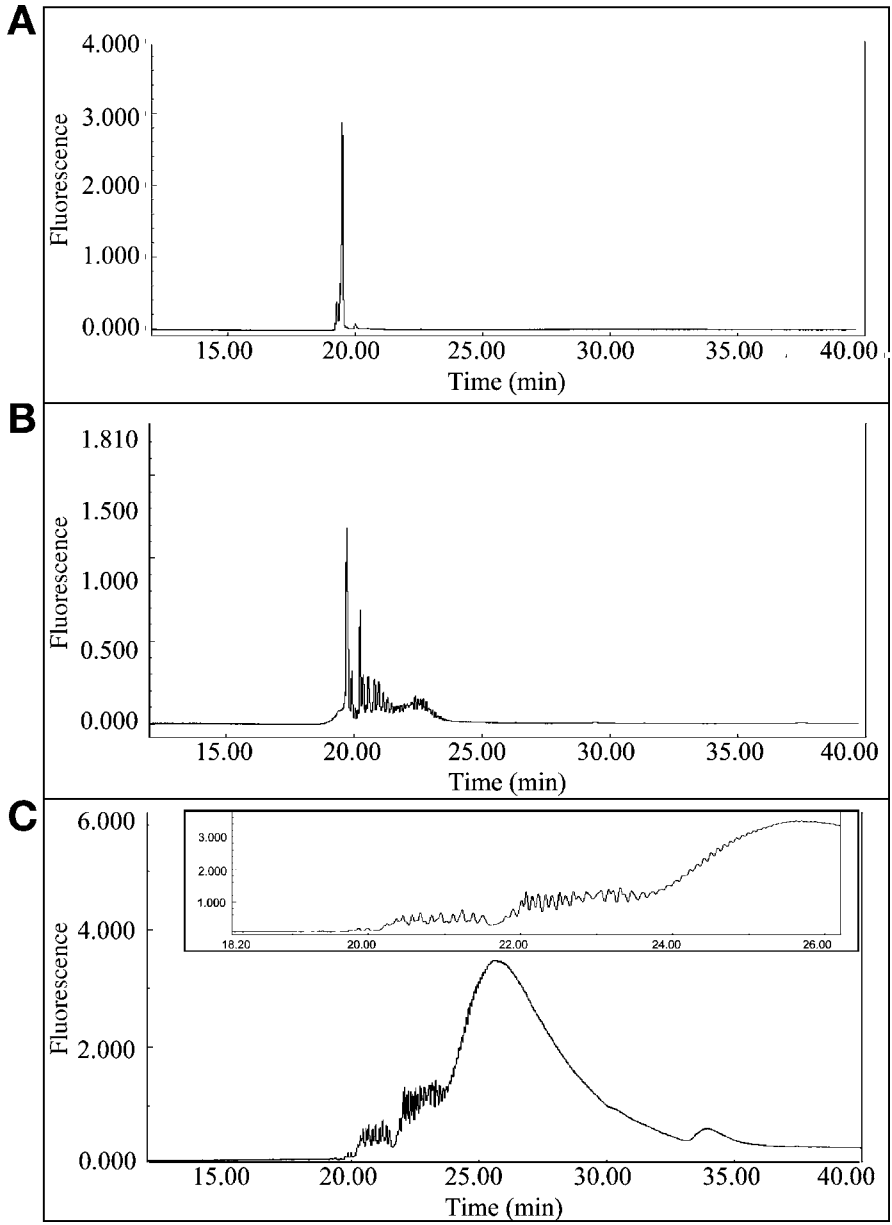


Fig. 2. (**A**) Electropherogram of hybridized starting material: 30-base single-stranded poly(A), annealed to 30-base single-stranded poly(T). The multiple peaks are due to the imperfect nature of hybridization for repetitive sequences (if the DNA is run under denaturing conditions, a single peak is present). (**B**) Electropherogram of the blunt-ended, double-stranded product that results from treating the hybridized material shown in panel A with T4 DNA polymerase. This enzyme catalyzes

of dsDNA fragments with a repetitive sequence after both an enzymatic blunt-ending step and a ligation reaction.

6. Between runs rinse the capillary with deionized water for 2 min using high pressure and then methanol for 2 min using high pressure. PVP is readily soluble in both water and methanol. After the capillary has been rinsed accordingly and then re-filled with the polymer solution, it is ready for the next run.

3. Analysis of Denatured DNA

In situations where it is important to precisely characterize the fragment length of the DNA or where higher resolution is desired, DNA must be denatured prior to analysis. This is because denatured DNA is more flexible and interacts more effectively with the separation matrix, yielding separations with up to single-base resolution ***(15)***. In addition, under proper conditions of buffer and temperature, the mobility of fragments from 100 bases up to 350 bases is linearly dependent on size ***(16)***. These characteristics are particularly important for DNA sequencing where high resolution is necessary in order to distinctly characterize each fragment. Multicolor fluorescent analyzers can then be used for dye-labeled DNA fragments, permitting simultaneous detection of all four bases based on the fluorescence output ***(10)***. Another example where denatured DNA must be used is in forensic genotyping. In this process, highly polymorphic short tandem repeat DNA is used to establish the identity of biological stains at crime scenes. The DNA loci analyzed are generally composed of repetitive four base motifs that vary from one individual to the next, however, one and two base variants can also occur ***(17)***. Here, both high precision and high resolution are required as each individual fragment must be fully separated and its mobility precisely defined in order to clearly distinguish it from other nearby alleles. To do this, two different control samples are used. A ROX dye-labeled sizing standard is added to each sample as an internal standard to correct for internal migration shifts, and an allelic ladder is run as an external standard to correct for run to run migration shifts. Multicolor detection is also used in these analyses to permit the simultaneous detection of the internal standard and multiplexed PCR amplified products. The result

Fig. 2. *(Continued)* the 5′ to 3′ synthesis of DNA and also possesses 3′ to 5′ exonuclease activity. (**C**) Electropherogram of the product yielded from the addition of T4 DNA ligase to the blunt-ended material shown in panel B. The inset in this figure shows an enlarged region of the electropherogram for a clearer view of the multiple fragment lengths present. This particular ligation yielded a mixture of products up to approximately 745 bp in length. All separations were completed using 5.5% PVP in TBE buffer, with YO-PRO-1 dye in the run buffers and sieving matrix.

is a precise analysis with high information content and standard deviation of size estimates of better than 0.17 bp ***(18)***.

3.1. Materials

3.1.1. Capillary Electrophoresis of Short Tandem Repeats for Forensic Genotyping

1. Run buffer: 100 mM N-Tris(hydroxymethyl)methyl-3-aminopropanesulfonic acid (TAPS), 1 mM EDTA, pH adjusted to 8 with NaOH.
2. Sieving matrix: POP4, Applied Biosystems [4% poly(dimethylacrylamide), 100 mM TAPS (pH 8), 8 M urea, and 5% 2-pyrrolidinone].
3. Internal size standard: Genescan ROX-500 (Applied Biosystems).
4. Uncoated, fused silica capillary with a 50 μm internal diameter (Polymicro Technologies).
5. Allelic ladder: Obtained from Applied Biosystems or Promega, Madison, WI.

3.2. Methods

Denatured DNA analysis was performed on the AB Prism 310 genetic analyzer (PE Applied Biosystems). Designed in 1995, the AB 310 is a single-capillary instrument with a multiple wavelength fluorescent detection system. Fluorescent-based CE systems from other vendors may also be used. DNA samples run on this system are labeled with a fluorescent dye at the 5′ end during PCR amplification through the use of fluorescent primers. Samples are prepared from blood, buccal swabs, or other biological samples by digestion and organic extraction. Other techniques may also be used ***(20)***. The samples are then quantified using slot blot techniques or real-time PCR ***(21)*** and 250 pg–1 ng of DNA template is amplified via PCR ***(18)***. Amplifications can be multiplexed to permit 16 or more simultaneous PCRs. To avoid overlap, PCR products are labeled with different dyes, and the fragment sizes are adjusted by careful choice of primer binding sites ***(19)***. **Figure 3** provides an example of the simultaneous analysis of four different short tandem repeats along with a ROX-labeled internal standard. **Figure 4** provides an example of the analysis of six different short tandem repeats using multiple dye labels.

3.2.1. Sample Preparation for ssDNA Analysis

1. DNA is removed from blood stains or buccal swabs through digestion with proteinase K and detergent followed by an organic extraction with phenol chloroform isoamyl alcohol ***(20)***.
2. Total DNA is quantified using real-time PCR ***(21)***.
3. Template DNA, 0.25–1 ng, is then targeted for multiplex PCR amplification using dye labeled primers ***(19)***.

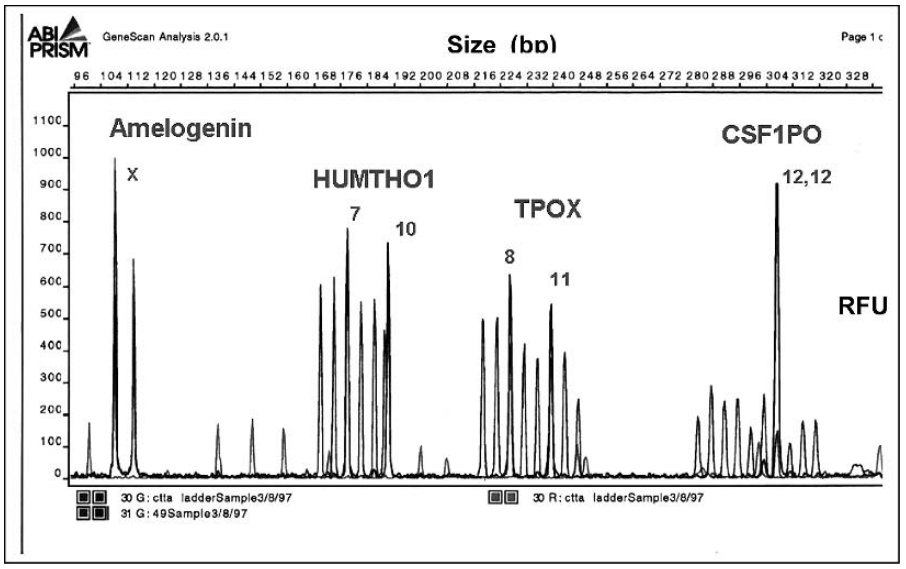


Fig. 3. The analysis of a set of three polymerase chain reaction amplified STR loci and the amelogenin sex typing marker (AB AmpFlSTR green multiplex typing kit). The sample is overlayed with an allelic ladder consisting of all common polymorphisms of the four loci. In addition, an internal standard is added to permit calculation of the relative size of each allele. The results of these analyses can be used to assist in determining the identity of an unknown blood stain at a crime scene or for paternity testing.

4. An internal standard is prepared by diluting a ROX sizing ladder 1:25 in high purity formamide (conductance under 80 micro Siemens).
5. One microliter of amplified DNA is added to 12 μl of the ROX-formamide mixture. This step denatures the DNA, and the sample is loaded onto the CE system for injection.

3.2.2. DNA Separation and Detection

1. Cut a 50-μm id capillary to a total length of 43 cm.
2. Flush capillary with polymer matrix for 120 s using the ABI 310's syringe pump.
3. Electrokinetically inject sample for 5 s at 15 kV.
4. Collect data for 25 min at 60 °C and 15 kV.
5. Determine the size of individual DNA fragments by reference to the ROX internal standard, using the Global Southern alignment tool in the GeneScan Analysis software.
6. Convert fragment sizes to allele calls using Genotyper, a second software package that compares the fragment sizes with a previously run allelic ladder.

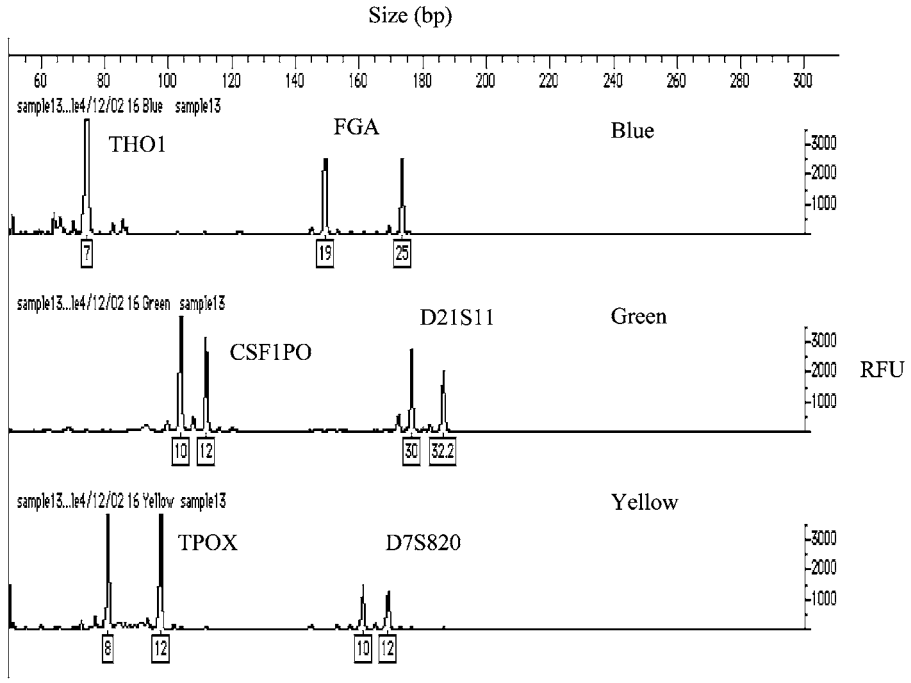


Fig. 4. The simultaneous analysis of six different polymerase chain reaction-amplified short tandem repeats using capillary electrophoresis with multichannel fluorescence detection. The figure is split into three different panels, each representing the fluorescence response from a different dye. The red-labeled internal standard is not shown in this figure. Full experimental details are given in **ref. *19***. Figure courtesy of Kerry Opel, Florida International University.

4. DNA Analysis Using Single-Strand Conformation Polymorphisms

When performing analysis of a bacterial community, universal primers must be used in order to amplify all the species present. These primers typically target the single subunit ribosomal ribonucleic acid gene, because the ribosomes are essential to cell function, and these genes contain some of the most highly conserved sequences in the genome. This gene is widely studied in bacteria and has facilitated a more complete understanding of microbial phylogeny and identification of bacteria ***(22,23)***. However, because universal primers are utilized, the bacterial DNA fragments will all be of the same length. Therefore, a different type of sieving matrix is necessary that does not separate based on size alone.

SSCP is a powerful structural analysis technique in which DNA fragments of the same length can be separated based on their sequence ***(24)***. In this technique,

electrophoretic separation is performed under non-denaturing conditions and reduced temperatures, allowing the fragments to partially renature and form folded conformations due to the intramolecular interactions between the bases. These secondary structures result in different electrophoretic mobilities, and separation of DNA strands differing by as little as a single base pair is possible. SSCP analysis is optimal for DNA fragments ranging from 150 to 400 base pairs in length, as the sensitivity of mutation detection decreases with increasing fragment length *(25)*. There are many reports of SSCP analysis of bacterial soil communities using slab gels *(26,27)*, and only recently has this been done by CE *(28)*.

In order to obtain precise results, GeneScan Analysis software is used to align the peaks in reference to the internal standard. Under denaturing conditions, such as those performed for forensic DNA analysis, the ROX 500 internal standard fragments migrate based on the number of base pairs in the fragment. In non-denaturing SSCP conditions, the migration rates of the ROX 500 fragments do not necessarily correspond to their size, because they too will adopt unpredictable conformations based on their sequence. This is not an issue for this study because the purpose of the internal size standard is to align samples in order to compare mobility values, not assign fragment sizes. **Figure 5** shows two electropherogram panels displaying the separation of ROX-labeled fragments. The top panel shows ROX-labeled fragments separated under denaturing conditions, where the fragments migrate according to their size. The bottom panel displays ROX-labeled fragments separated under non-denaturing or SSCP conditions. Clearly, no correlation can be observed regarding the size of the fragment and the relative mobility. In both denaturing and non-denaturing conditions, the same values are assigned to the peaks that correlate to the size of the fragments, although for SSCP analysis, the number no longer represents the fragment length.

4.1. Materials

4.1.1. Capillary Electrophoresis Single-Strand Conformation Polymorphism

1. Run buffer: 1× genetic analyzer buffer with EDTA (PE Applied Biosystems)
2. Sieving matrix (GeneScan 5% non-denaturing polymer): 7.14 g 7% Genescan polymer (PE Applied Biosystems), 1 g glycerol, 1.03 g 10× genetic analyzer buffer with EDTA (PE Applied Biosystems), and deionized water to reach a total of 10 g. Vortex solution for 30 s to mix evenly.
3. Internal size standard: Genescan ROX-500 (PE Applied Biosystems).
4. Uncoated, fused silica capillary with a 50 μm internal diameter (Polymicro Technologies).

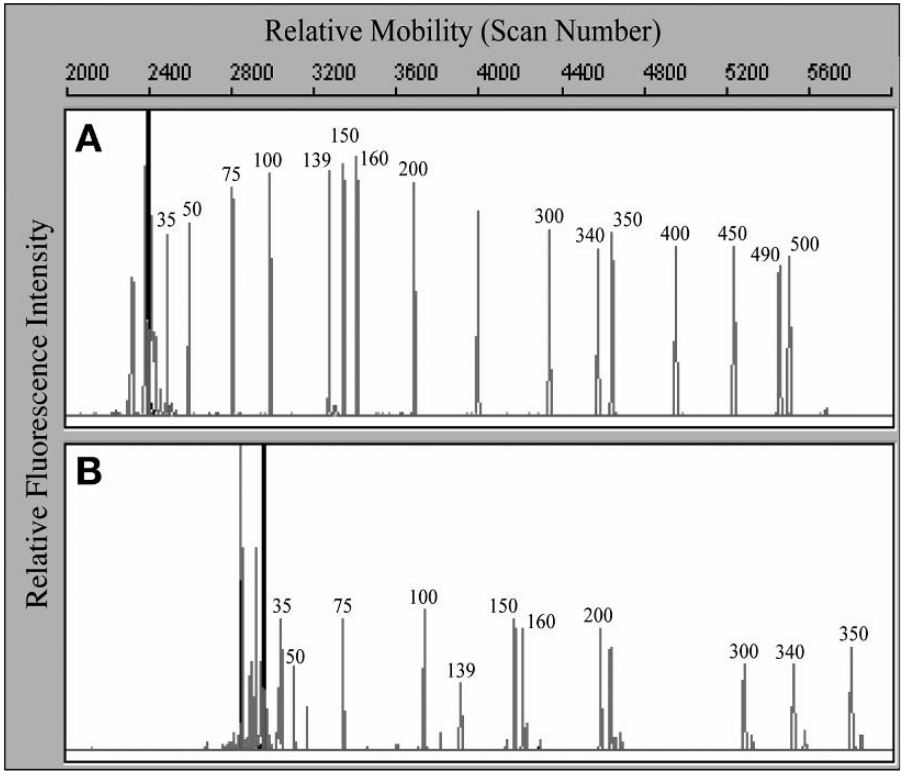


Fig. 5. Electropherograms of ROX internal standard under (**A**) denaturing and (**B**) non-denaturing conditions. The numbers assigned to each peak correspond to the fragment sizes of Genescan ROX 500.

4.2. Methods

CE-SSCP analysis was performed using PCR-amplified DNA labeled at the 5′ end with various fluorescent dyes. Analyses were carried out using the ABI Prism 310 genetic analyzer (PE Applied Biosystems). The ABI 310 is only equipped with a capillary heater, not a cooling device. This can be problematic because CE-SSCP analysis is best performed at 30 °C to promote the likelihood of the strands forming secondary structures. Therefore, in certain instances of higher laboratory temperatures, the capillary door was kept open and an electric fan was used to cool the capillary.

4.2.1. Sample Preparation for CE-SSCP Analysis

1. DNA was extracted from broth and soil using MoBio Ultraclean DNA isolation kits. DNA was diluted to 10 μg/ml with 10 mM Tris (pH 8) before use in PCR.

2. Prepare internal standard by diluting ROX 1:25 in deionized formamide.
3. Add 1 μl of properly diluted, fluorescently labeled amplified DNA to 12.5 μl of the ROX-formamide mixture.
4. Heat to 95 °C for 3 min and immediately cool in an ice water bath to freeze fragments in their single-stranded form.

4.2.2. DNA Separation and Detection

1. Cut and install a 50-μm id capillary with a total length of 43 cm length onto the CE system.

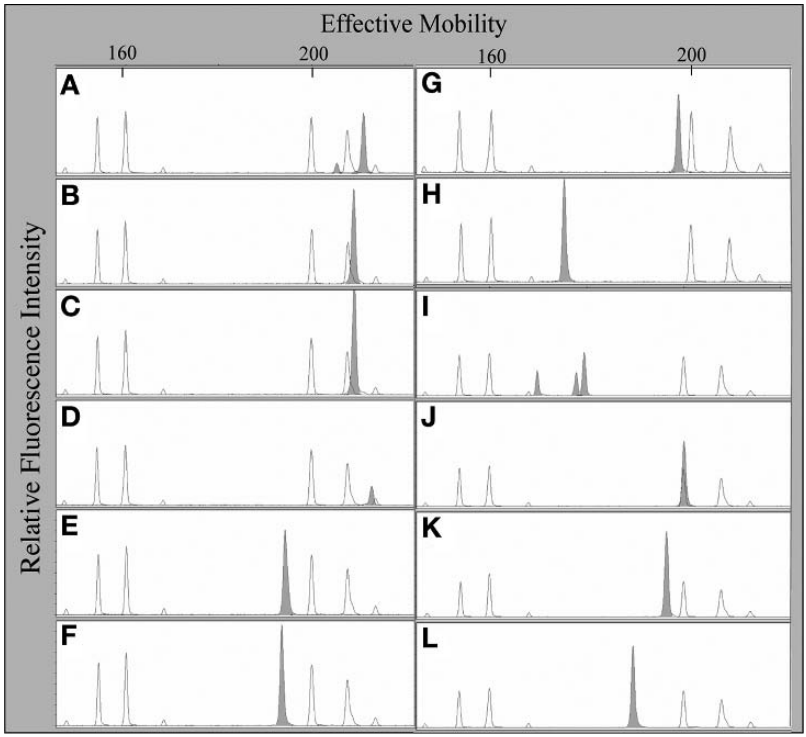


Fig. 6. Capillary electrophoresis-single-strand conformation polymorphism peak patterns of polymerase chain reaction-amplified 16S rRNA gene sequences of pure-culture bacteria, using primer set 341–534. Bacteria peak patterns, shown as filled peaks, were assigned an effective mobility value relative to the red internal standard peaks. (**A**) *Pseudomonas putida* ATCC 47054D, (**B**) *Pseudomonas putida* ATCC 700478, (**C**) *Pseudomonas aeruginosa*, (**D**) *Pseudomonas fluorescens*, (**E**) *Bacillus subtilis*, (**F**) *Bacillus megaterium*, (**G**) *Clostridium perfringens*, (**H**) *Clostridium sporogenes*, (**I**) *Rhizobium trifolii* ATCC 14479, (**J**) *Staphylococcus aureus*, (**K**) *Escherichia coli*, (**L**) *Enterococcus faecalis*.

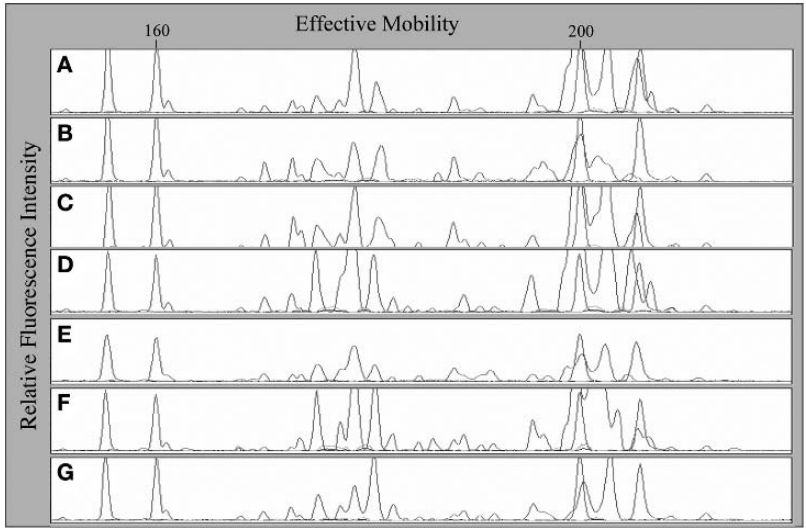


Fig. 7. Capillary electrophoresis-single-strand conformation polymorphism peak patterns of polymerase chain reaction-amplified soil bacteria DNA using primer set 341–534. Samples were extracted after 5 weeks from non-sterile soil spiked with 150 mg/kg trinitro toluene (TNT). Each panel shows a different combination of grass seed with bacteria. (**A**) Rye/*Pseudomonas putida* (**B**) Rye/*Rhizobium trifolii*, (**C**) Rye/Killed, (**D**) Sweet vernal/*Pseudomonas* putida, (**E**) Sweet vernal/*Rhizobium* trifolii, (**F**) Sweet vernal/Killed, (**G**) Killed/Killed.

2. Flush capillary with polymer matrix for 120 s with a syringe pump.
3. Electrokinetically inject sample for 5 s at 13 kV.
4. Collect data for 25 min at 30 °C. Electropherograms showing the separation of 12 common soil bacteria are shown in **Fig. 6**. The results for extraction from plants inoculated with different bacteria and planted in contaminated soil are shown in **Fig. 7**.
5. Align the peaks in reference to the internal standard using the Global Southern alignment method in the GeneScan Analysis software.
6. Set analysis parameters to target the specific region of amplification and only label two internal standard size peaks on either side of the peaks of interest.
7. Increase the threshold of the internal standard dye to limit interferences that result from smaller peaks and disrupt the size calling of the software.

Acknowledgments

Major support for this work was provided by the National Institute of Justice, the National Science Foundation, and Ohio University. Points of view in this document are those of the authors and do not necessarily represent the official position of the U.S. Department of Justice. The authors thank Nancy

Tatarek, Jiri Drabek, Denise Chung, Kerry Opel, and Guy Riefler for technical assistance in support of this work.

References

1. Ulfelder, K. J. and McCord, B. R. (1996) Capillary Electrophoresis of DNA, In *Handbook of Capillary Electrophoresis*, Landers, J., ed., CRC Press: NY, 347–378.
2. Righetti, P. G. and Gelfi, C. J. (1999) Capillary electrophoresis of DNA in the 20–500 bp range: recent developments, *Biochem. Biophys. Methods* 41, 75–90.
3. Mitchelson, K. R. and Cheng, J. eds. (2001) *Capillary Electrophoresis of Nucleic Acids, Vol II: Practical Applications of Capillary Electrophoresis*, Humana Press: Totowa, NJ.
4. Chiari, M. and Melis, A. (1998) Low viscosity DNA sieving matrices for capillary electrophoresis, *Trends Anal. Chem*. 17, 623–632.
5. Quesada, M. A. (1997) Replaceable polymers in DNA sequencing by capillary electrophoresis, *Curr. Opin. Biotechnol*., 8, 82–93.
6. Chiari, M., Cretich, M., and Consonni, R. (2002) Separation of DNA fragments in hydroxylated poly(dimethylacrylamide) copolymers, *Electrophoresis* 23, 536–541.
7. Mitchelson, K. R. and Cheng, J. eds. (2001) *Capillary Electrophoresis of Nucleic Acids, Vol I: Introduction to the Capillary Electrophoresis*, Humana Press: Totowa, NJ.
8. Christoph Heller, ed. (1997) *Analysis of Nucleic Acids by Capillary Electrophoresis*, Vieweg: Wiesbaden.
9. Righetti, P. G., Gelfi, C., and D'Acunto, M. R. (2002) Recent progress in DNA analysis by capillary electrophoresis, *Electrophoresis*, 23(10), 1361–1374.
10. Dolník, V. (1999) DNA sequencing by capillary electrophoresis, *J. Biochem. Biophys. Methods*, 41(2–3), 103–119.
11. Xu, F. and Baba, Y. (2004) Polymer solutions and entropic-based systems for double-stranded DNA capillary electrophoresis and microchip electrophoresis, *Electrophoresis*, 25(4), 2332–2345.
12. Gao, Q. and Yeung, E. S. (1998) A matrix for DNA separation: genotyping and sequencing using poly(vinylpyrrolidone) solution in uncoated capillaries, *Anal. Chem*., 70, 1382–1388.
13. Song, J. M. and Yeung, E. S. (2001) Optimization of DNA electrophoretic behavior in poly(vinyl pyrrolidone) sieving matrix for DNA sequencing, *Electrophoresis*, 22, 748–754.
14. McCord, B. R., McClure, D. M., and Jung, J. M. (1993), Capillary electrophoresis of PCR-amplified DNA using fluorescence detection with an intercalating dye, *J. Chromatogr*., 651, 75–82.
15. Heller, C. (1999) Separation of double-stranded and single-stranded DNA in polymer solutions: I. Mobility and separation mechanism, *Electrophoresis*, 20, 1962–1977.

16. Rosenblum, B. B., Oaks, F., Menschen, S., and Johnson, B. (1997) Improved single-strand DNA sizing accuracy in capillary electrophoresis, *Nucleic Acids Res*., 25, 3925–3929.
17. Butler, J., Buel, E., Crivelente, F., and McCord B. (2004) Forensic DNA typing by capillary electrophoresis, *Electrophoresis*, 25(10–11), 1397–1412.
18. Lazaruk, K., Walsh, P. S., Oaks, F., Gilbert, D., Rosenblum, B. B., Menchen, S., Scheibler, D., Wenz, H. M., Holt, C., and Wallin, J. (1998) Genotyping of forensic short tandem repeat (STR) systems based on sizing precision in a capillary electrophoresis instrument, *Electrophoresis*, 19, 86–93.
19. Butler, J., Shen, Y., and McCord, B. (2003) The development of reduced size STR amplicons as tools for analysis of degraded DNA, *J. Forensic Sci*., 48(5), 1054–1064.
20. Comey, C. T., Koons, B. W., Presley, K. W., Smerick, J. B., Sobieralski, C. A., Stanley, D. M., and Baechtel, F. S. (1994) DNA extraction strategies for amplified fragment length polymorphism analysis, *J. Forensic Sci*., 39(5), 1254–1269.
21. Nicklas, J. A. and Buel, E. J. (2003) Development of an Alu-based, real-time PCR method for quantitation of human DNA in forensic samples, *J. Forensic Sci*., 48(5), 936–944.
22. Chèneby, D., Philippot, L., Hartmann, A., Hénault, C., and Germon, J. C. (2000) 16S rDNA analysis for characterization of denitrifying bacteria isolated from three agricultural soils, *FEMS Microbiol. Ecol*., 34, 121–128.
23. Schmalenberger, A., Schwieger, F., and Tebbe, C. C. (2001) Effect of primers hybridizing to different evolutionarily conserved regions of the small-subunit rRNA gene in PCR-based microbial community analyses and genetic profiling, *Appl. Environ. Microbiol*., 67, 3557–3563.
24. Tebbe, C. C., Schmalenberger, A., Peters, S., and Schweiger, F. (2001) Single-strand conformation polymorphism (SSCP) for microbial community analysis, In Rochelle, P. A., ed., *Environmental Molecular Microbiology: Protocols and Applications*, Horizon Scientific Press: Wymondham, UK, 161–175.
25. Kourkine, I. V., Hestekin, C. N., and Barron, A. E. (2002) Technical challenges in applying capillary electrophoresis-single strand conformation polymorphism for routine genetic analysis, *Electrophoresis*, 23, 1375–1385.
26. Junca, H. and Pieper, D. H. (2004) Functional gene diversity analysis in BTEX contaminated soils by means of PCR-SSCP DNA fingerprinting: comparative diversity assessment against bacterial isolates and PCR-DNA clone libraries, *Environ. Microbiol*. 6, 95–110.
27. Schmalenberger, A. and Tebbe, C. C. (2003) Bacterial diversity in maize rhizospheres: conclusions on the use of genetic profiles based on PCR-amplified partial small subunit rRNA genes in ecological studies, *Mol. Ecol*., 12, 251–262.
28. King, S., McCord, B. R., and Riefler, R. G. J. (2005) Capillary electrophoresis single-strand conformation polymorphism analysis for monitoring soil bacteria, *J. Microbiol. Methods*, 60, 83–92.

16

Capillary Electrophoresis of Oxidative DNA Damage

Guowang Xu, Xianzhe Shi, Surong Mei, Qinghong Yao, Qianfeng Weng, and Caiying Wu

Summary

Urinary 8-hydroxy-2′-deoxyguanosine (8OHdG) is an excellent marker of oxidative DNA damage. Until now, urinary 8OHdG has been measured by high-performance liquid chromatography with electrochemical detection. A simple and sensitive method for the analysis of urinary 8OHdG by capillary electrophoresis with end-column amperometric detection has been developed and is described in this chapter. A single-step solid-phase extraction procedure was optimized and used for extracting 8OHdG from human urine. To improve the sensitivity of this method, a new focusing technique based on a dynamic pH junction was used. In the end, the urinary concentration of 8OHdG in healthy persons, patients with cancer, patients with diabetic nephropathy, and smokers was determined. Emphasis is focused on the establishment and application of the methods.

Key Words: Capillary electrophoresis; electrochemical detection; oxidative DNA damage.

1. Introduction

Oxidative damage of DNA is considered to be one of the most important contributors to aging, cancer, and other age-related degenerative processes ***(1,2)***. Of about 20 known products of oxidative DNA damage, 8-hyrdoxy-2′-deoxyguanosine (8OHdG) has received considerable attention because of its demonstrated mutagenic potential ***(3)***, and it must be a good biomarker of carcinogenesis. Because 8OHdG produced is excreted in urine without any

From: *Methods in Molecular Biology, vol. 384: Capillary Electrophoresis*
Edited by: P. Schmitt-Kopplin © Humana Press Inc., Totowa, NJ

further metabolism ***(4)***, determination of urinary 8OhdG has been proposed as a noninvasive assay of in vivo oxidative DNA lesions.

During the last decade, several methodologies for the measurement of 8OHdG in urine have been developed including high-performance liquid chromatography (HPLC) ***(5,6)***, gas chromatography ***(7,8)***, and enzyme-linked immunosorbent assay (ELISA) ***(9)***. In former study from our group, capillary electrophoresis (CE) with ultraviolet (UV) method was used to analyze urinary 8OHdG with a good resolution ***(10)***; because of the low sensitivity of UV detection, that method could not be used to determine the low concentration of 8OHdG in urine, which is reported to be at the range of 10^{-8}–10^{-9} *M*. Compared with the CE-UV method, CE with electrochemical detection (ECD) can provide greater selectivity and lower limit of detection.

The aim of this study is to develop a simple, sensitive, and selective method for analyzing urinary 8OHdG. When a capillary with very small inside diameters ($\leq$25 μm) is used in CE ***(11)***, no significant effects from the high electric field on amperometric detection are observed; therefore, a simple CE with end-column amperometric detection without complex porous decoupler is developed in this study. In the meantime, a new focusing technique—dynamic pH junction—is used to improve efficiently the sensitivity for detection of 8-OHdG, and the operational conditions are systemically investigated.

2. Materials

2.1. Agents

1. **Urine samples** were collected from healthy persons, patients with cancer, patients with diabetic nephropathy, and smokers.
2. **Sample pretreatment**: solid-phase extraction (SPE) columns (C_{18}/OH 500 mg, 6 mL, Chrom Expert Co.)
3. **Standard sample**: stock solutions of 8OHdG (from Sigma, St. Louis, MO) were stored at 4 °C in a refrigerator when not in use.
4. **Sample buffer**: 30 m*M* phosphate solution, pH 6.5 (from Shanghai Reagent Co., Shanghai, China)
5. **CE buffer**: 30 m*M* sodium tetraborate, pH 9.12 (from Shanghai Reagent Co., Shanghai, China)

2.2. Equipment

1. CE instrument from Shandong Institute of Chemical engineering (Shandong, China), model HPCE-01; electrochemical detector from Shandong Institute of Chemical engineering (Shandong, China), model JF-01. Electrochemical current was recorded on a 3066 recorder (Yokogawa Hokuskin, Tokyo, Japan).

2. Fused-silica column (Yongnian Optical Fiber Factory, Hebei, China), total length, 75 cm; effective length, 75 cm; internal diameter, 25 μm.
3. Electrochemical detection: 0.8V vs SCE. Carbon fiber microcolumn electrode was fabricated according to the method of Huang and Cheng ***(11,12)***. Before use, the working electrode must be cleaned in the supersonic cleaner for 2 min.

3. Methods

3.1. Electrophoresis Sample Reparation

1. The pH of urine was adjusted to 4.0–5.0 with 1 *M* HCl, then 5-mL aliquots of urine were kept frozen at −20 °C.
2. The sample underwent at least one freeze–thaw step and was centrifuged at 4000 rpm for 5 min in order to remove precipitates. Before SPE, urine sample was filtered through a 0.2-μm micropore filter membrane.
3. The SPE columns were preconditioned with 10 mL methanol and 10 mL water in turn, and then 1 mL of urine was applied. The column was washed with 5 mL of water and 8-OHdG was eluted with 2 mL of 15% methanol.
4. The eluate was evaporated to dryness under vacuum at 39–40 °C and the residue was dissolved in 0.1 mL 30 m*M* phosphate solution (pH 6.5).

3.2. Sample Focusing Method—A Dynamic pH Junction

1. Sample stacking is one of the most common approaches to improving concentration sensitivity in CE (*see* **Note 1**).
2. A focusing technique of dynamic pH junction (*see* **Note 2**) was used in detection of 8-OHdG becausee a phenolic hydroxyl group exists in its structure. 8OHdG is neutral at pH 6.5, but becomes partially ionized at pH >7.0.
3. **Figure 1** showed the effect of the focusing of 8OHdG in a different pH of background electrolyte (BGE) using a dynamic pH junction. As can be seen, a pH difference of only 1.65 units is sufficient to focus 8OHdG into a sharp zone, with a column efficiency greater than 5×10^5 theoretical plate number. Optimal focusing of 8OHdG was observed at pH 8.15.

3.3. CE Conditions

1. Although at pH 8.15, both the peak current and theoretical plate were highest among the whole pH range of 7.0–10.0, the 8OHdG could not be baseline-separated from other urinary components (*see* **Fig. 2A**).
2. It was found that a low pH of BGE was not beneficial to focusing. While increasing pH of BGE to 8.5, the separation efficiency became worse (*see* **Fig. 2B**).
3. The separation efficiency became better T when the pH of BGE sequentially increased to 9.12 (*see* **Fig. 2C**,**D**).
4. The 8OHdG could not be separated completely from other urinary components again when the pH increased to 9.18 (see **Fig. 2E**), so the optimal pH of BGE was 9.12.

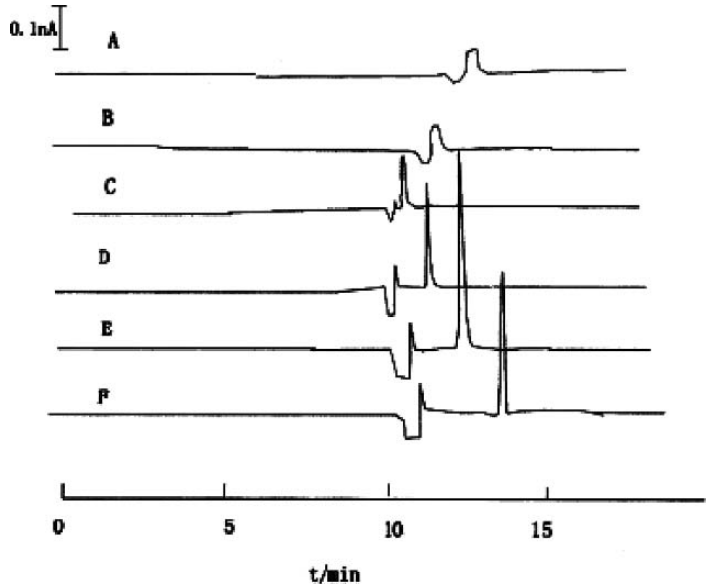


Fig. 1. Series of electropherograms showing the focusing of 8-OHdG in a different running buffer system using a dynamic pH junction. The pH of 30 m*M* borate buffer is varied from **A**, 6.5; **B**, 7.0; **C**, 7.5; **D**, 8.0; **E**, 8.15, to **F**, 8.50. All sample solution contained 5×10^{-6} *M* 8OHdG in 30 m*M* phosphate (pH 6.5). Capillary electrophoresis conditions: fused-silica capillary, $L = 75$ cm, inner diameter $= 25$ μm; injection, 20 kV, 20 s; voltage, 20 kV; electrochemical detection, 0.8V vs SCE. (Reproduced from **ref. *14***, with permission of John Wiley & Sons Limited.)

5. The optimal CE conditions: buffer, 30 m*M* borate (pH 9.12); electrokinetic injection, 20 kV for 10 s; separation voltage, 20 kV; electrochemical detection, a two-electrode system (*see* **Note 3**); detection potential, 0.8V vs SCE.
6. **Figure 3** shows a typical electropherogram of a urine extraction from a healthy person. A good separation was obtained for 8OHdG from other urinary matrix components. 8OHdG in urine was identified by comparison of the retention time, spiking, and peak current ratios.

3.4. Reproducibility, Limit of Detection, and Linear Range

1. The reproducibility of the migration time and the peak current was tested by repeatedly ($n = 8$) injecting 1 μ*M* 8-OHdG standard. The relative standard deviation (RSD) was found to be 0.57% for migration time, and 4.79% for peak current.
2. The linear range was 50 n*M*–10 μ*M*, and the correlation coefficient was better than 0.999. The limit of detection was 20 n*M* (signal to noise ratio [S/N] = 3), which

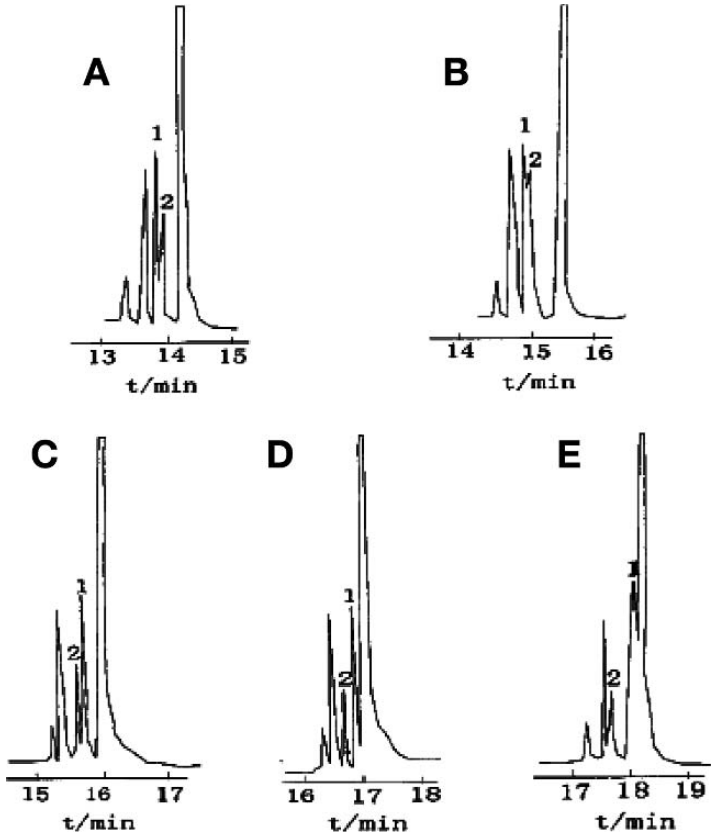


Fig. 2. Effect of pH of background electrolyte on urinary 8OHdG separated from other components. pH is **A**, 8.15; **B**, 8.50; **C**, 9.00; **D**, 9.12; and **E**, 9.18, respectively. Peak 1, unknown component, peak 2, 8-OHdG. (Reproduced from **ref. *14***, with permission of John Wiley & Sons Limited.)

was higher than that of the CE-ECD method for determining 8OHdG reported by Weiss and Lunte (50 n*M*) ***(13)***.

3. The recovery of 8-OHdG spiked into urine in this method was 99.36 ± 4.03% in the concentration range of 10–100 n*M*, and the average inter-day and intra-day coefficients of variation for quantitation were 1.14% and 4.88%, respectively.

3.5. Analysis of Urinary 8-OHdG in Cancer Patients

1. The concentration of urinary 8OHdG from 9 healthy persons and 10 patients with cancer was determined.
2. It was found that the urinary concentration of 8OHdG in healthy persons varied from 6.34 n*M* to 21.33 n*M*, with an average concentration of 13.51 ± 5.08 n*M*, and

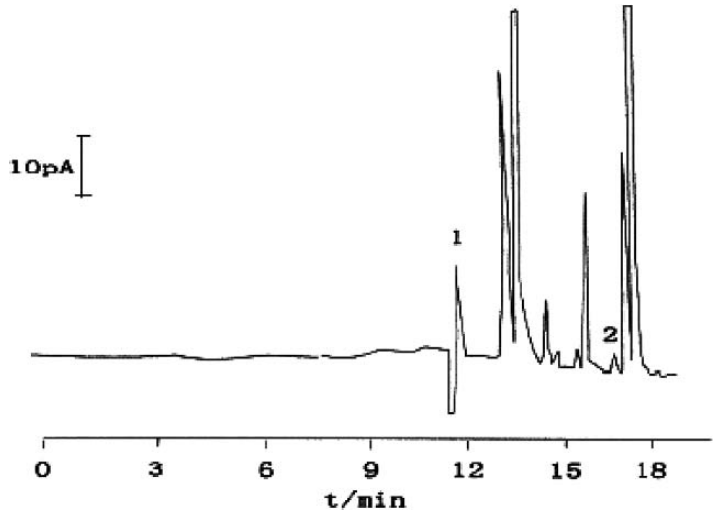


Fig. 3. Electrophoretogram of 8-OHdG in an extract urine from a healthy person. Electrophoretic conditions: fused-silica capillary, $L = 75$ cm, inner diameter $= 25\,\mu$m; injection, 20 kV, 10 s; voltage, 20 kV; buffer: 30 m*M* borate buffer pH 9.12; sample matrix, 30 m*M* phosphate buffer pH 6.5. Electrochemical detection, 0.8V vs SCE. Peak 1, unknown component; peak 2, 8-OHdG. (Reproduced from **ref. *14***, with permission of John Wiley & Sons Limited.)

that in patients with cancer varied from 13.83 n*M* to 130.12 n*M*, with an average concentration of 35.26 ± 27.96 n*M*.

3. The excretion level of 8OHdG in cancer patients was significantly higher than that in healthy persons; this result might support the assumption that oxidative DNA damage leading to cytotoxicity occurs actively in the body of a patient with cancer, and cancer maybe have a relationship with 8OHdG, which is a marker of oxidative DNA damage ***(14)***.

3.6. Analysis of Urinary 8-OHdG in Patients With Diabetic Nephropathy

1. The mean level of urinary 8-OHdG excretions was 4.15 ± 4.85 mol/mol creatinine in diabetic nephropathy patients and 2.33 ± 2.83 mol/mol creatinine in control subjects ($P = 0.058$).
2. The levels of 8-OHdG in urine of the three groups divided according to the urinary albumin excretion rate (UAER) are shown in **Table 1**. No difference was observed between the healthy group and L group. Although the M group had higher averaged 8-OHdG contents in urine than the healthy group, there was no significant difference between the two groups ($P = 0.069$). A significant difference was found between H group and the healthy group ($P = 0.018$).

Table 1
The Levels of 8-OHdG in Urine of the Patients Compared to the Healthy Group

Subject Group	Subject number	8-OhdG/creatinine (μmol/mol)	8 – OhdG (μg/24 h)
Healthy group	30	2.33 ± 2.83	–
Diabetic neuphropathy patients			
L	18	2.63 ± 2.94	8.1 ± 1.7
M	28	3.84 ± 3.37	12.5 ± 10.3
H	23	5.72 ± 6.89	19.2 ± 16.8

Data in the table are mean ± S.D. Reproduced from **ref. *15***, with permission of Elsevier Limited.

3. The differences of 24-h urinary excretions of 8-OHdG were compared among the three patient groups. It was found that a noticeable difference existed between the H and L groups ($P = 0.015$), and no significant difference was found between the M and L groups ($P = 0.15$).
4. 8-OHdG is known as a sensitive biomarker of oxidative DNA damage and also of oxidative stress. The high urinary 8-OHdG levels in the patients with high albuminuria investigated in this study suggested that the increased oxidative stress has a primary role in the pathogenesis of diabetic nephropathy.
5. Our study showed that the patients with normoalbuminuria had a lower urinary 8-OHdG level than the patients with high albuminuria. We speculated that the increased urinary 8-OHdG in the patients with diabetic nephropathy might have resulted not only from the increased systemic oxidative stress, but also from the kidney in which oxidative stress increased caused by hyperglycemia ***(15)***.

3.7. Analysis of Urinary 8-OHdG in Smokers

1. To provide a direct evidence for the association between cigarette smoking and oxidative stress, we evaluated urinary 8OHdG levels in smokers and nonsmokers.
2. **Table 2** summarized levels of 8OHdG, age, sex, and body weight, smoking status, and cigarette consumption of every volunteer. there was significant difference both in the urinary 8OHdG excretion ($P = 0.0004$) and in the ratio of 8OHdG-to-creatinine ($P = 0.028$) between smokers and non-smokers.
3. To further know the association of urinary 8OHdG with the smoking amount, smokers were divided into two groups according to the number of cigarettes smoked per day. As reported in **Table 3**, urinary 8OHdG contents in subjects smoking less than 10 cigarettes per day have no significant difference from those in nonsmokers ($P = 0.22$), but significantly higher levels ($P = 0.003$) were observed in the ratio of urinary 8OHdG-to-creatinine of the two groups. There was a significant difference both in the urinary 8OHdG excretion ($P = 0.0007$) and in the ratio

Table 2
Descriptive Date and 8-OHdG Levels of the Smokers and Nonsmokers

	Smokers	Nonsmokers
Number	21	21
Age (years)	48.2 ± 12.5	30.7 ± 9.3
Body weight (kg)	69.9–13.3	67.7 ± 10.5
Cigarettes per day	15.5–5.5	–
8OhdG (n*M*)	31.4 ± 18.9	14.4 ± 7.6
8OhdG ($\mu g g^{-1}$ Cr)	23.5 ± 21.3	12.6 ± 13.2

Data in the table are mean ± S.D. Cr, creatinine. Reproduced from **ref. *16***, with permission of Elsevier Limited.

of urinary 8OHdG-to-creatinine ($P = 0.002$) between subjects smoking more than 10 cigarettes per day and nonsmokers. From the above results, we observed that cigarette smoking has a strong effect on 8OHdG content in urine, especially for those heavy smokers.

4. The high urinary 8OHdG levels in the subjects with heavy smoking habits suggested that smoking has an important role in increasing oxidative stress in the human body. Although the biochemical physiological basis is unknown, it may be related to smoke constituents, which include or generate reactive oxygen species or consume antioxidants or enhance the effect of smoking on the metabolic rate ***(16)***.

Table 3
Effect of Smoking Habits on 8-OHdG Content in Urine

	Group	*N*	8OhdG (n*M*)	8OhdG ($\mu g g^{-1}$ Cr)
Smokers	Less than 10 cigarettes per day	7	28.6 ± 15.8	18.2 ± 12.7
	More than 10 cigarettes per day	14	32.8 ± 20.7	26.9 ± 24.5
Nonsmokers		21	14.4 ± 7.6	12.6 ± 13.2

Data in the table are mean ± S.D. Reproduced from **ref. *16***, with permission of Elsevier Limited.

4. Notes

1. One major prerequisite for most sample stacking methods is that the analyte should be in a low-salt environment (low conductivity) relative to the BGE. Thus, samples of biological or environmental origin often require desalting prior to analysis.
2. A dynamic pH junction can achieve selective focusing when analytes possess different velocities in the sample and the BGE zones caused by pH difference in the two segments of electrolyte in the capillary. Thus, an analyte must possess an appropriate chemical functional group so that it may exist in two distinct states with different velocities in the capillary. This technique is different from conventional stacking methods since the conductivity of the sample matrix may be less, similar, or greater than that of BGE.
3. A 400 μm long, 7 μm diameter carbon fiber is used as the working electrode and an SCE as the reference electrode.

Acknowledgments

We gratefully acknowledge financial support for this research by grants from National Natural Science Foundation of China (No.90209048), (No. 20425516) for Distinguished Young Scholars, the Knowledge Innovation Program of the Chinese Academy of Sciences (KSCX2-SW-329, KGCX2-SW-213),and Liaoning province foundation of science and technology. Moreover, We gratefully thank prof. Ben-li Su and his research group (The Secondary Affiliated Hospital of Dalian Medical University, Dalian, China) for providing the partial clinical samples.

References

1. Richter, C., Park, J. W., and Ames, B. N. (1988) Normal oxidative damage to mitochondrial and nuclear DNA is extensive. *Proc. Natl. Acad. Sci. USA* **85,** 6465–6467.
2. Fraga, C. G., Shigenaga, M. K., Park, J. W., Degan, P., and Ames, B. N. (1990) Oxidative damage to DNA during aging: 8-hydroxy-2′-deoxyguanosine in rat organ DNA and urine. *Proc. Natl. Acad. Sci. USA* **87,** 4533–4537.
3. Moriya, M. and Grouman, A. P. (1993) Mutations in the mut Y gene of Escherichia coli enhance the frequency of targeted G:C–>T:A transversions induced by a single 8-oxoguanine residue in single-stranded DNA. *Mol. Gen. Genet*. **239,** 72–76.
4. Shigenaga, M. K. and Ames, B. N. (1991) Assays for 8-hydroxy-2′-deoxyguanosine: a biomarker of in vivo oxidative DNA damage. *Free Radic. Biol. Med*. **10,** 211–216.
5. Shigenaga, M. K., Gimeno, C. J., and Ames, B. N. (1989) Urinary 8-hydroxy-2′-deoxyguanosine as a biological marker of in vivo oxidative DNA damage. *Proc. Natl. Acad. Sci. USA* **86,** 9697–9701.

6. Helbock, H. J., Beckman, K. B., Shigenaga, M. K., et al. (1998) DNA oxidation matters: the HPLC-electrochemical detection assay of 8-oxo-deoxyguanosine and 8-oxo-guanine. *Proc. Natl. Acad. Sci. USA* **95,** 288–293.
7. Mei, S., Xu, G., Xing, J., and Wu, C. (2001) Method for the analysis of 8-hydroxy-2′-deoxyguanosine in urine by gas chromatography. *Anal. Sci*. **17,** 779–781.
8. Teixeira, A., Gommers-Ampt, H., Werken, G., Westra, J., and Stavenuiter, J. (1993) Method for the analysis of oxidized nucleosides by gas chromatography/mass spectrometry *Anal. Biochem*. **214,** 474–483.
9. Yin, B., Whyatt, R., Perera, F., Randall, M., Cooper, T., and Santella, R. (1995) Determination of 8-hydroxydeoxyguanosine by an immunoaffinity chromatography-monoclonal antibody-based ELISA. *Free Radic. Biol. Med*. **18,** 1023–1032.
10. Mei, S., Xu, G., and Wu, C. (2001) Analysis of urinary 8-hydroxydeoxyguanosine by capillary electrophoresis and solid-phase extraction *Anal. Lett*. **34,** 2063–2076.
11. Huang, X., Zare, R. N., Stoss, S., and Ewing, A. G. (1991) End-column detection for capillary zone electrophoresis *Anal. Chem*. **63,** 189–192.
12. Huang, W., Pang, D., Tong, H., Wang, Z., and Cheng, J. (2001) A method for the fabrication of low-noise carbon fiber nanoelectrodes. *Anal. Chem*. **73,** 1048–1052.
13. Weiss, D. and Lunte, C. (2000) Detection of a urinary biomaker for oxidative DNA damage 8-hydroxydeoxyguanosine by capillary electrophoresis with electrochemical detection *Electrophoresis* **21,** 2080–2085.
14. Mei, S., Yao, Q., Cai, L., Xing, J., Xu, G., and Wu, C. (2003) Capillary electrophoresis with end-column amperometric detection of urinary 8-hydroxy-2′-deoxyguanosine. *Electrophoresis* **24,** 1411–1415.
15. Xu, G. W., Yao, Q. H., Weng, Q. F., Su, B. L., Zhang, X., and Xiong, J. H. (2004) Study of urinary 8-hydroxydeoxyguanosine as a biomarker of oxidative DNA damage in diabetic nephropathy patients. *J. Pharm. Biomed. Anal*. **36,** 101–104.
16. Yao, Q., Mei S., Weng Q., Zhang, P., Yang, Q., Wu, C., and Xu, G. (2004) Determination of urinary oxidative DNA damage marker 8-hydroxy-2_-deoxyguanosine and the association with cigarette smoking. *Talanta* **63,** 617–623.

17

Capillary Electrophoresis of Gene Mutation

Guowang Xu, Xianzhe Shi, Chunxia Zhao, Kailong Yuan, Qianfeng Weng, Peng Gao, and Jing Tian

Summary

This chapter illustrates the usefulness of capillary electrophoresis (CE) for the detection of gene mutation, i.e., point mutation, methylation, and microsatellite analysis. In order to provide a general description of the main results and challenges in the field, some relevant applications and reviews on CE of gene mutation are tabulated. Furthermore, some detailed experimental procedures are shown. Several CE methods of gene mutation detection were developed including the following: (1) single-strand conformation polymorphism with capillary electrophoresis; (2) SNaPshot analysis; (3) constant denaturant capillary electrophoresis; (4) microsatellite analysis; and (5) Methylation analysis.

Key Words: Capillary electrophoresis; gene mutation; DNA methylation; microsatellite instability.

1. Introduction

Mutations in human genome may result in the occurrence of heritable genetic diseases and malignant tumors. Therefore, efficient and reliable detection of these mutations in human genome is becoming more and more important. Various methods for mutation detection have been developed and used in basic research and clinical diagnosis of genetic disorders.

1.1. SSCP-CE

Single-strand conformation polymorphism (SSCP) analysis is thought to be the most common technique for rapid identification of known or unknown

From: *Methods in Molecular Biology, vol. 384: Capillary Electrophoresis*
Edited by: P. Schmitt-Kopplin © Humana Press Inc., Totowa, NJ

mutations. The basis of SSCP analysis is that the conformational change of single-strand DNA caused by mutation results in a mobility shift on nondenaturing electrophoresis. The combination of SSCP technique with CE was first developed by Kuypers ***(1)***. When the technique is coupled with laser-induced fluorescence detection, it is more suited for clinical analysis because of its higher sensitivity and resolution ***(2–5)***.

1.2. SNaPshot Analysis

SNaPshot analysis is a new automated fluorescent method that can rapidly and accurately genotype multiplex known single-nucleotide polymorphisms (SNPs). As an efficient and reliable identification method of known mutations in human genome, it has been used to type multiplex SNPs of Y chromosome ***(6)***, cytokine gene ***(7)***, and k-ras gene ***(8,9)***.

1.3. Constant Denaturant Capillary Electrophoresis

Constant denaturant capillary electrophoresis (CDCE) ***(10)***, based on cooperative melting equilibrium, has the resolving power to separate single nucleotide mutants from wild-type sequences. This technique has previously been used to analyze low-frequency mutations in the human mitochondrial genome with contiguous high- and low-melting domains ***(11)***, and is also used for mutation detection in the p53, N-ras, K-ras, and HPRT genes with an attached GC-clamp to provide the necessary high melting domain ***(12–14)***.

1.4. Microsatellite Analysis

Alterations in the length or strength of microsatellite alleles in tumor tissue compared with normal tissue from the same individual are referred to as microsatellite instability (MSI) or loss of heterozygosity (LOH), which reflects a defect in DNA replication or repair. Microsatellite instability was analyzed using capillary electrophoresis (CE) instruments with ultraviolet (UV) detection ***(15)*** or laser-induced fluorescence detection of a single color ***(16)***. In these cases, the microsatellite alleles were easily interfered with the internal size standards. Recently, the dedicated instrument equipped with multicolor fluorescence detection (e.g., ABI 310 Genetic Analyzer) resolved this question and was widely applied ***(17,18)***.

1.5. Methylation Analysis

Promoter methylation plays a crucial role in the regulation of gene transcription, X chromosome inactivation, genomic imprinting, and carcinogenesis ***(19,20)***. Aberrant Promoter methylation has been detected by a variety

of methods. Bisulfate-single strand conformation polymorphism (bisulfite-SSCP) combined the chemical modification of cytosine to uracil by sodium bisulfite treatment with SSCP is an sensitive and reliable method for methylation analysis ***(21,22)***.

In this chapter, several different methods based on CE for gene mutation have been developed. Tumor gene K-ras, tumor suppression gene p53, and mismatch repair gene hMLH1 are as the model genes. Emphasis is placed on the procedure and establishment of each method.

2. Materials

2.1. SSCP-CE

1. **Clinical sample treatment**: genomic DNA was extracted from cancer tissue by proteinase K digestion and phenol-chloroform extraction. The primers of p53 exon 7 and 8 were labeled FAM or HEX ***(5)***. PCR was performed in 50 μL solution containing 100 ng genomic DNA, 20 pmol of each primer, 200 μ*M* each of dNTPs, 1.5 U Taq DNA polymerase, and carried out for 30 cycles under the following program: 40 s at 94 °C, 1 min at 50 °C, and 1 min at 72 °C.
2. **Electrophoresis sample**: 2-μL PCR products were diluted 25- to 50-fold with Milli-Q water, then denatured at 95 °C for 5 min, chilled on ice, and placed in the tray of the analyzer.
3. **CE buffer**: 89 m*M* Tris, 89 m*M* boric acid, 2 m*M* EDTA, pH 8.3 (TBE I).
4. **CE sieving medium**: short-chained linear polyacrylamide (LPA) was synthesized according to the procedure described ***(23)*** with minor modifications, 6% (w/v) LPA in TBE I buffer.

2.2. SNaPshot Analysis

1. **Clinical sample treatment**: Genomic DNA was extracted from cancer tissue by proteinase K digestion and phenol-chloroform extraction. PCR of K-ras exon 1 was performed in 50 μL solution containing 100 ng genomic DNA, 20 pmol of each primer, 200 μ*M* each of dNTPs, 1.5 U Taq DNA polymerase, and carried out for 30 cycles under the following program: 40 s at 94 °C, 1 min at 50 °C, and 1 min at 72 °C ***(8)***. After PCR amplification, add 2 U Exonuclease I (Exo I) and 5 U shrimp alkaline phosphatase (SAP) (ABI, Foster City, CA) to 15 μL PCR product, mix thoroughly and incubate at 37 °C for 1 h, followed by a 15-min incubation at 75 °C to inactivate the enzymes (*see* **Note 1**). Multiplex single base extension reactions were performed in 12 μL solution containing 6 μL purified PCR product, 2 μL SNaPshot Ready Reaction Mix, 0.5∼2 pmol of each primer and were carried out for 25 cycles under the following program: 10 s at 96 °C, 5 s at 50 °C, and 1 min at 60 °C. Then, each reaction product was treated with 1 U SAP for 1 h at 37 °X, and followed by a 15-min incubation at 75 °C for SAP inactivation (*see* **Note 2**).
2. **Electrophoresis sample**: 5 μL purified extension product was diluted with 10 μL formamide, denatured at 95 °C for 5 min, chilled on ice, and placed in the tray of the analyzer.

3. **CE buffer**: 89 m*M* Tris, 89 m*M* boric acid, 2 m*M* EDTA, 5 *M* urea, pH 8.3 (TBE II).
4. **CE sieving medium**: short-chained linear polyacrylamide (LPA) was synthesized according to the procedure described ***(23)*** with minor modifications, 8% (w/v) LPA in TBE II buffer.

2.3. CDCE Analysis

1. Clinical sample treatment: genomic DNA was extracted from cancer tissue by proteinase K digestion and phenol-chloroform extraction. PCR of K-ras exon 1 was performed in 50 μL solution containing 100 ng genomic DNA, 20 pmol of each primer, 200 μ*M* each of dNTPs, 1.5 U Taq DNA polymerase, and carried out for 30 cycles under the following program: 40 s at 94 °C, 1 min at 53 °C, and 1 min at 72 °C. Then PCR products were denatured 5 min at 94 °C and incubated 1 h at 65 °C for heteroduplex formation (***14***).
2. Electrophoresis sample: 1 μL PCR products were diluted in 100 μL water, denatured at 95 °C for 5 min, chilled on ice, and placed in the tray of the analyzer.
3. CE buffer: 89 m*M* Tris, 89 m*M* boric acid, 2 m*M* EDTA, 20% formamide. pH 8.3 (TBE III).
4. CE sieving medium: short-chained LPA was synthesized according to the procedure described ***(23)*** with minor modifications, 6% (w/v) LPA in TBE III buffer.

2.4. Microsatellite Analysis

1. Clinical sample treatment: genomic DNA was extracted from cancer tissue and corresponding normal tissue by proteinase K digestion and phenol-chloroform extraction. PCR of five microsatellite loci was performed in 25 μL solution containing 50 ng genomic DNA, 10 pmol of each primer, 100 μ*M* each of dNTPs, 1 U Taq DNA polymerase, and carried out for 30 cycles under the following program: 40 s at 94 °C, 1 min at 58 °C, and 1 min at 72 °C ***(18)***.
2. Electrophoresis sample: 0.5 μL of each PCR products was mixed with 1 μL of GeneScan 500 size standard labeled TAMRA (ABI, Foster City, CA) and 12 μL of formamide. Each sample was denatured at 95 °C for 5 min, chilled on ice, and placed in the tray of the analyzer.
3. CE buffer: 89 m*M* Tris, 89 m*M* boric acid, 2 m*M* EDTA, 8 *M* urea, pH 8.3 (TBE IV).
4. CE sieving medium: short-chained LPA was synthesized according to the procedure described ***(23)*** with minor modifications, 6% (w/v) LPA in TBE IV buffer.

2.5. Methylation Analysis

1. Clinical sample treatment: genomic DNA was extracted from cancer tissue by proteinase K digestion and phenol-chloroform extraction. Bisulfite modification of genomic DNA was performed as the following steps: first, 1 μg of genomic DNA was denatured in 0.2 *M* NaOH at 55 °C for 10 min. 30 μL of 10 m*M* hydroquinone and

520 μL of 4.8 *M* sodium bisulfite at pH 5.0, both freshly prepared, were added and mixed, and then sample were incubated at 55 °C for 4 h. Modified DNA was purified using the Wizard DNA purification resin (Promega, Madison, WI), and eluted into 50 μL of water. Modification was completed by NaOH (0.3 *M* final concentration) treatment for 5 min at room temperature, followed by ethanol precipitation. Then PCR amplification of hMLH1 promoter was performed in 50 μL solution containing 100 ng genomic DNA, 20 pmol of each primer, 200 μ*M* each of dNTPs, 1.5 U Taq DNA polymerase, and carried out for 30 cycles under the following program: 30 s at 94 °C, 30 s at 58 °C, and 30 s at 72 °C ***(25)***.

2. Electrophoresis sample: 2 μL PCR products were diluted 25- to 50-fold with Milli-Q water, then. denatured at 95 °C for 5 min, chilled on ice, and placed in the tray of the analyzer.
3. CE buffer: 89 m*M* Tris, 89 m*M* boric acid, 2 m*M* EDTA, 10% glycerol, pH 8.3 (TBE V).
4. CE sieving medium: short-chained LPA was synthesized according to the procedure described ***(23)*** with minor modifications, 6% (w/v) LPA in TBE V buffer.

2.6. Equipment

2.6.1. SSCP-CE, SNaPshot, CDCE and Microsatellite Analysis

1. High-performance capillary electrophoresis system from Applied Biosystems (Foster City, CA), Model 310, with Gene-Scan 3.1 software.
2. Fused-silica column (Yongnian Optical Fiber Factory, Hebei, China); total length, 47 cm; effective length, 36 cm; internal diameter, 50 μm. The inner surface of the capillary was modified by covalent bonding of hydrophilic polymer ***(24)***.
3. Laser-induced fluorescence (LIF) and charge-coupled device (CCD) camera detection, excitation wavelength from 494 nm to 587 nm, emission wavelength from 517 nm to 607 nm.
4. PCR system from Applied Biosystems (Foster City, CA), Model 2700.

2.6.2. Methylation Analysis

1. High-performance capillary electrophoresis system from Beckman (Palo Alto, CA), Model P/ACE MDQ, with MDQ software.
2. Fused-silica column (Yongnian Optical Fiber Factory, Hebei, China); total length, 40 cm; effective length, 30 cm; internal diameter, 50 μm. The inner surface of the capillary was modified by covalent bonding of hydrophilic polymer ***(24)***.
3. LIF detection, excitation wavelength equal to 488 nm, emission wavelength equal to 520 nm
4. PCR system from Applied Biosystems (Foster City, CA), Model 2700

3. Methods

3.1. SSCP-CE Analysis

1. Rinse the capillary with sieving medium (6% LPA) at high pressure for 2 min.
2. Load sample at high voltage 15 kV for 5 s.

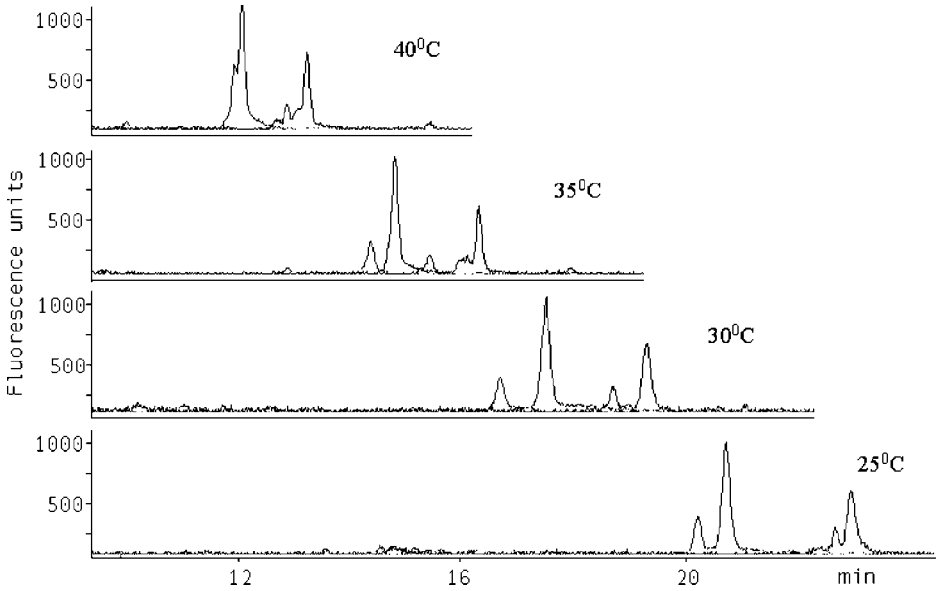


Fig. 1. Effect of temperature on the SSCP analysis of mutant sample of p53 exon 7. Electrophoretic conditions: neutral coated capillary, $L = 47\,cm$, $l = 36\,cm$, I.D. = 50 μm; sieving medium, 6% LPA; DNA fragment, p53 exon 7; voltage, -15 kV; temperature, 25–40 °C; LIF detection. (Reproduced from **ref. *5***, with permission of the Japan Society for Analytical Chemistry.)

3. CE conditions: voltage, 15 kV; detection, LIF and CCD camera detection; temperature, 30 °C; buffer, TBE I.
4. **Figure 1** shows the effect of temperature on SSCP analysis. 30 °C was selected as the most appropriate temperature
5. **Figure 2** shows the SSCP electropherograms of different DNA fragments of p53 gene. The patterns of ssDNA from different gene regions showed a high degree of variation. For example, a single peak was observed for each strand (p53 exon 7), but a complex peak pattern was observed for each single strand (p53 exon 8). The additional peaks can be explained as the additional stabilized conformers of the single strands ***(5)***.

3.2. SNaPshot Analysis

1. Rinse the capillary with sieving medium (8% LPA with 5 *M* urea) at high pressure for 2 min.
2. Load sample at high voltage 15 kV for 5 s.
3. CE conditions: voltage, 15 kV; detection, LIF and CCD camera detection; temperature, 50 °C; buffer, TBE II.

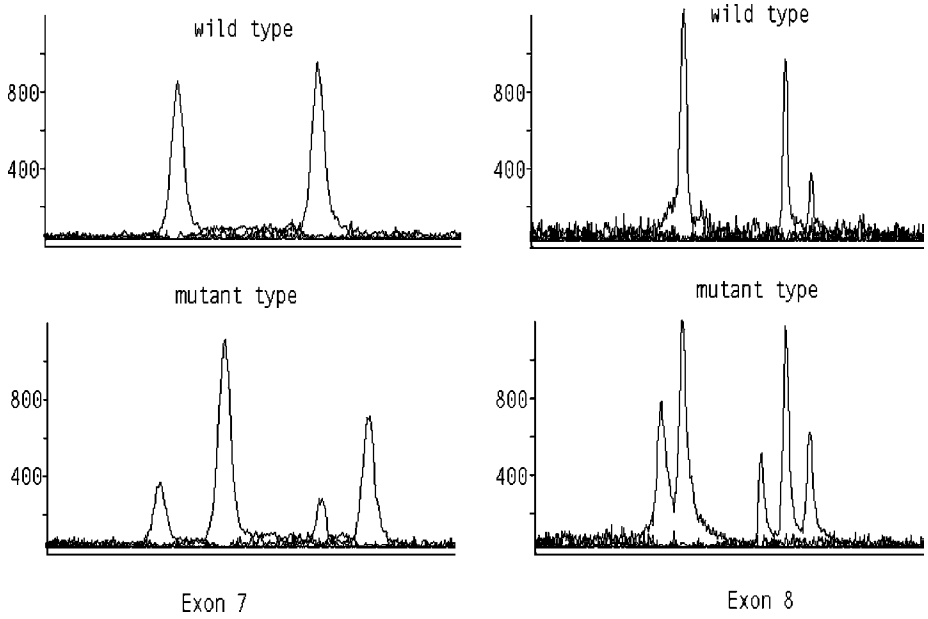


Fig. 2. SSCP electropherogram of different DNA fragments of p53 gene. Electrophoretic conditions: neutral coated capillary, $L = 47$ cm, $l = 36$ cm, I.D. = 50 μm; sieving medium, 6% LPA; DNA fragment, p53 exon 7; voltage, -15 kV; temperature, 30 °C; LIF detection. (Reproduced from **ref. *5***, with permission of the Japan Society for Analytical Chemistry.)

4. **Figure 3** shows the electropherograms of the wild type and mutant (codon 12) sample of K-ras gene exon 1 by SnaPshot analysis. The lengths of all SNaPshot reaction products are less than 40 bp (*see* **Note 3**). There are four peaks indicate four known SNPs of codon 12-2, codon 22-2, codon 12-1, and codon 13-1 in the electropherograms. The first peak is indicative of a "C" genotype in codon 12-2 of wild-type sample; but in the mutant sample, there are two peaks showing "C" and "T" genotype, which indicate a C→T heterozygosity mutation ***(8)***.

3.3. CDCE Analysis

1. Rinse the capillary with sieving medium (6% LPA with 4 *M* urea) at high pressure for 2 min.
2. Load sample at high voltage 15 kV for 5 s.
3. CE conditions: voltage, 15 kV; detection, LIF and CCD camera detection; temperature, 50 °C; buffer, TBE III.
4. **Figure 4** shows the effect of temperature on CDCE analysis of K-ras gene exon 1 (*see* **Note 4**). Separation of the two homoduplex peaks and the two heteroduplex

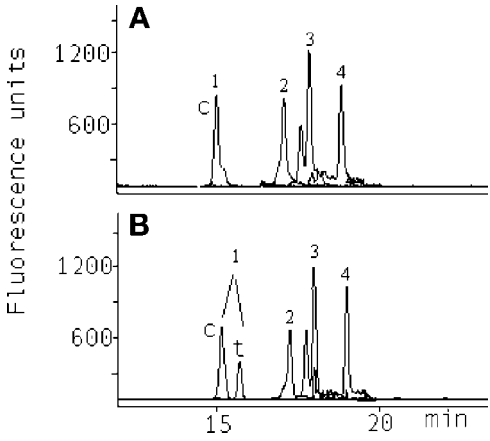


Fig. 3. SNaPshot electropherograms of wild-type **(A)** and mutant-type **(B)** of K-ras exon 1. Electrophoretic conditions: neutral coated capillary, L=47 cm, l=36 cm, *I.D.* = 50 μm; sieving medium, 8% LPA with 5 *M* urea; voltage, -15 kV; temperature, 50 °C; LIF detection. Peak 1, codon 12-2; peak 2, codon 22-2; peak 3, codon 12-1; peak 4, codon 13-1. (Reproduced from **ref. *8***, with permission of Elsevier Limited.)

peaks ws achieved at temperature between 56 °C and 58 °C, so 57 °C was chosen as an optimal temperature.

5. **Figure 5** shows the electropherograms of different mutations in K-ras gene exon 1. Except for a codon 13 GGC to AGC mutation, other mutated samples displayed the complete separation of two homoduplex peaks (wt and mut) and two heteroduplex peaks (hetro), all the different mutations displayed distinct peak patterns ***(14)***.

3.4. Microsatellite Analysis

1. Rinse the capillary with sieving medium (6% LPA with 8 *M* urea) at high pressure for 2 min.
2. Load sample at high voltage 15 kV for 5 s.
3. CE conditions: voltage, 15 kV; detection, LIF and CCD camera detection; temperature, 60 °C; buffer, TBE IV.
4. **Figure 6** shows the electropherograms of five microsatellite loci in the normal tissue and tumor tissue of a patient with cancer. GeneScan-500 standard fragments in the size range of 35 to 350 bp were used for the calculation of relative sizes of microsatellite alleles by Local Southern Method. The fragment size of five microsatellite loci is shown in **Table 1**. The result showed that the three loci, BAT-26, D17S261, and D3S1283 display shift, but the two loci, D2S123 and D3S1611, have no shift (*see* **Note 5**).

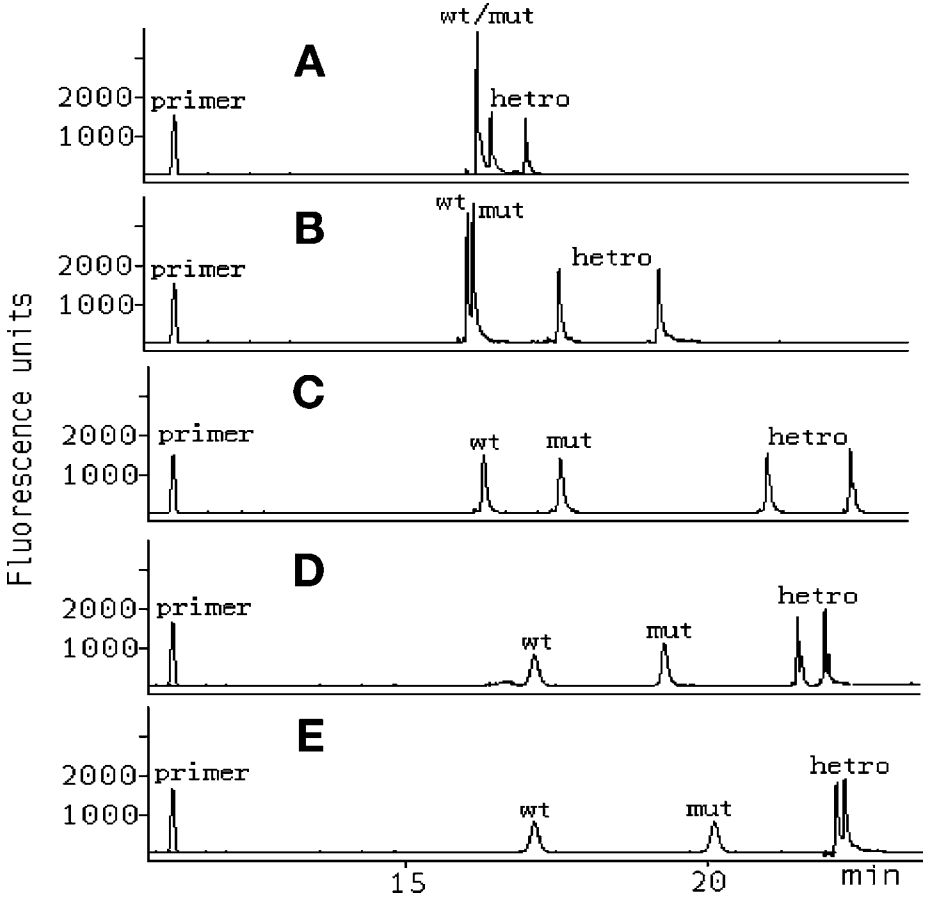


Fig. 4. Effect of temperature on CDCE analysis of K-ras exon 1. Electrophoretic conditions: neutral coated capillary, $L = 47\,\text{cm}$, $l = 36\,\text{cm}$, I.D. $= 50\,\mu\text{m}$; sieving medium, 6% LPA with 4 *M* urea; voltage, -15 kV. temperature, a. 55 °C; b. 56 °C; c. 57 °C; d. 58 °C; e. 59 °C. LIF detection. (Reproduced from **ref. *14***, with permission of John Wiley & Sons Limited.)

5. **Figure 7** shows the electropherogams of five microsatellite loci analysis of normal and tumor tissue of another patient with cancer. The smaller allele of D17S261 locus reduced 67% (>50%) in the tumor tissue compared to that in the normal tissue, which implicated LOH. On the contrary, there was no LOH in D3S1283 locus because the allelic ratios of D3S1283 locus reduced only 34% (< 50%). In addition, LOH is obvious that the larger alleles of D2S123 and D3S1611 loci were completely loss in the tumor tissue (*see* **Note 6**).

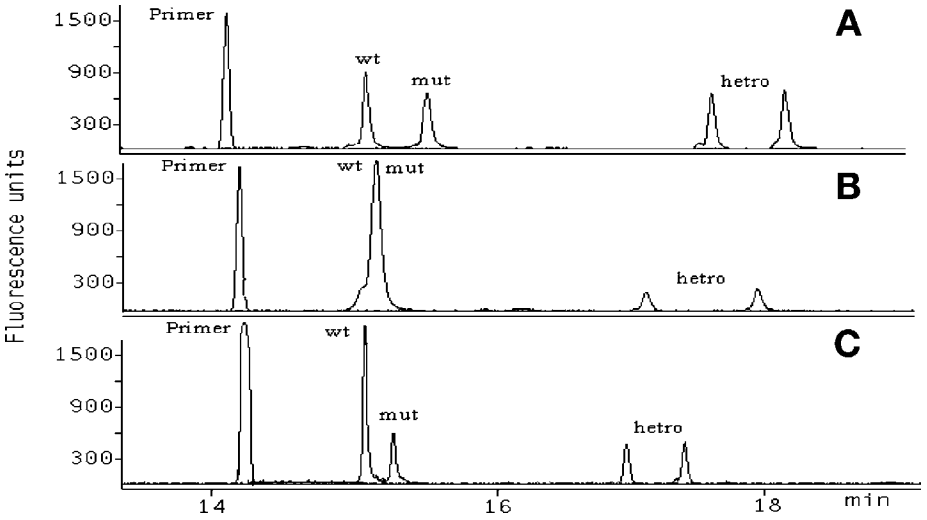


Fig. 5. Different mutation patterns of K-ras exon 1. Electrophoretic conditions: neutral coated capillary, $L = 47\,cm$, $l = 36\,cm$, I.D. $= 50\,\mu m$; sieving medium, 6% LPA with 4 *M* urea; voltage, -15 kV; temperature, 57 °C. LIF detection. a. GGT→GAT; b. GGC→AGC; c. GGT→AGT. (Reproduced from **ref. *14***, with permission of John Wiley & Sons Limited.)

3.5. Methylation Analysis

1. Rinse the capillary with sieving medium (6% LPA with 10% glycerol) at high pressure for 2 min.
2. Load sample at high voltage 10 kV for 5 s.
3. CE conditions: voltage, 12 kV; detection, LIF; temperature, 25 °C; buffer, TBE V.
4. **Figure 8** shows the electropherograms of unmethylated and methylated of hMLH1 promoter by bisulfite SSCP-CE analysis ***(25)***. The unmethylated sample gives two peaks of ssDNA but the methylated sample gives four peaks of ssDNA, which represented the heterogeneous methylation status (*see* **Note 7**).

Table 1
The Length of Representative Fragments of Five Microsatellite Loci in the Normal Tissue and Tumor Tissue of a Cancer Patient

	BAT-26 (bp)	D17S261 (bp)		D3S1283 (bp)		D2S123 (bp)	D3S1611 (bp)
Normal	119.15	127.52	133.78	149.12	157.25	209.42	262.76
Tumor	112.30	121.63	131.65	153.23	157.36	209.30	262.85

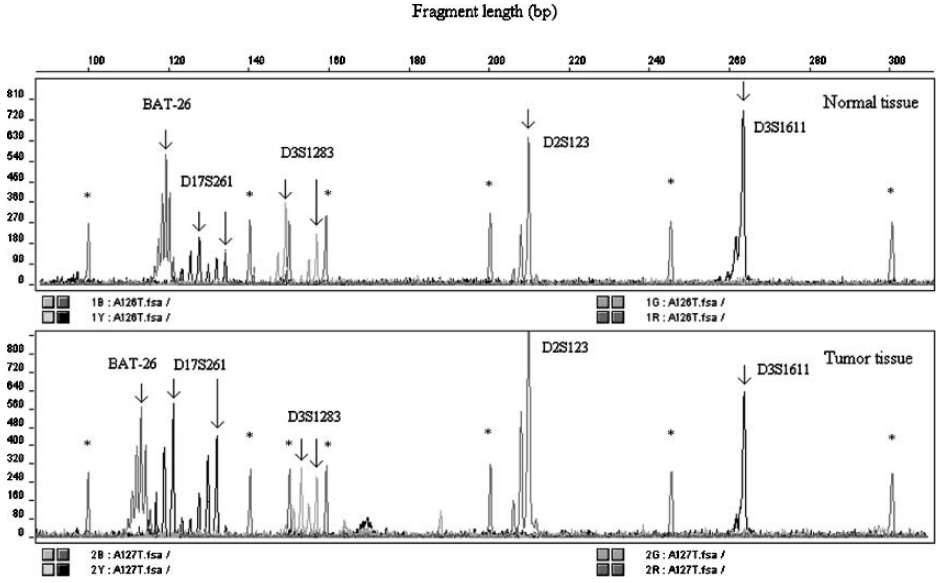


Fig. 6. Electropherograms of five microsatellite loci in the normal tissue and tumor tissue of a patient with cancer. Electrophoretic conditions: neutral coated capillary, $L = 47\,\text{cm}$, $l = 36\,\text{cm}$, I.D. $= 50\,\mu\text{m}$;.sieving medium, 6% LPA with $8\,M$ urea; voltage, -15 kV; temperature, 60 °C. LIF detection. Arrowheads indicate the predominant peaks for each alleles at five loci. The peaks with * are GeneScan 500 size standard (Reproduced from **ref.** ***18***, with permission of Elsevier Limited.).

4. Notes

1. To avoid participation in the subsequent primer-extension reaction, primers and unincorporated dNTPs must be removed.
2. Multiplex SNaPshot reaction to genotype multiplex SNPs in a single reaction can not only decrease reagent consumption but also increase the throughput of detection. Through choosing a suitable ratio of template and corresponding primer and mixing all the primers and PCR products, several SNPs can simultaneously be genotyped by any four-color or five-color fluorescent detection device. After multiplex single base extension, removal of the 5′ phosphoryl groups by phosphatase treatment can alter the migration of the unincorporated ddNTPs and prohibit interference.
3. The sequence diversity can result in different mobility and even cause the overlap of the peaks. In order to avoid this overlap, the difference of adjacent primer in length must be longer than 5–6 bp.
4. At a suitable separating temperature, low-melting domain of the PCR product will unwind, whereas the high-melting domain will keep the strands together. This

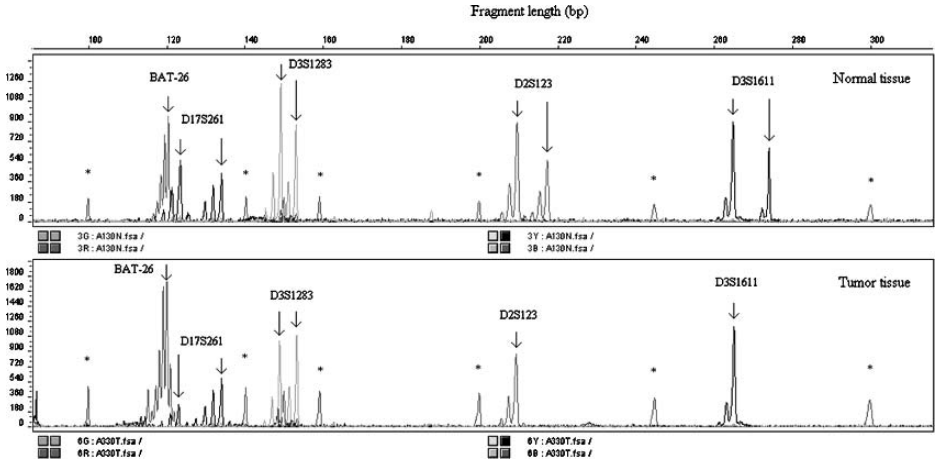


Fig. 7. Electropherograms of five microsatellite loci in the normal tissue and tumor tissue of another patient with cancer. Electrophoretic conditions: neutral coated capillary, $L = 47\,\text{cm}$, $l = 36\,\text{cm}$, I.D. $= 50\,\mu\text{m}$; sieving medium, 6% LPA with $8\,M$ urea; voltage, -15 kV; temperature, 60 °C. LIF detection. Arrowheads indicate the predominant peaks for each alleles at five loci. The peaks with * are GeneScan 500 size standard (Reproduced from **ref. *18***, with permission of Elsevier Limited.).

will allow separation of less stable mutants and heteroduplexes compared to the wild type.

5. Arrowheads in **Fig. 6** indicate the predominant peaks for each alleles at five microsatellite loci (the greatest peak heights). The fragment size of microsatellite loci could be calculated in comparison with TAMRA-labelled GeneScan-500 size standard using the local southern method.
6. LOH was assigned if the relative intensity of two alleles of microsatellite locus in tumor tissue showed at least a 50% reduction compared with that in matched normal tissue ***(26)***. To estimate the degree of LOH, reduced ratios are calculated as the following formula: {1-(T1/T2)/(N1/N2)} × 100%, where T1 and N1 are the peak heights of the smaller alleles and T2 and N2 are the peak heights of the larger alleles in tumor tissue or in normal tissue, respectively.
7. The differences of methylation-dependent sequence are introduced into the genomic DNA by sodium bisulfite modification, and then modified DNA is amplified by PCR using FAM-labeled primers without CpG repeats and complementary to the deaminated DNA strand. This combination of bisulfite modification and PCR results in the conversion of unmethylation cytosine residues to thymine, whereas methylation cytosine residues, present at CpG sites, are retained as cytosine. This sequence conversion can lead to the methylation-dependent alteration of single-strand conformation, which can be detected by single-strand conformation polymorphism with CE.

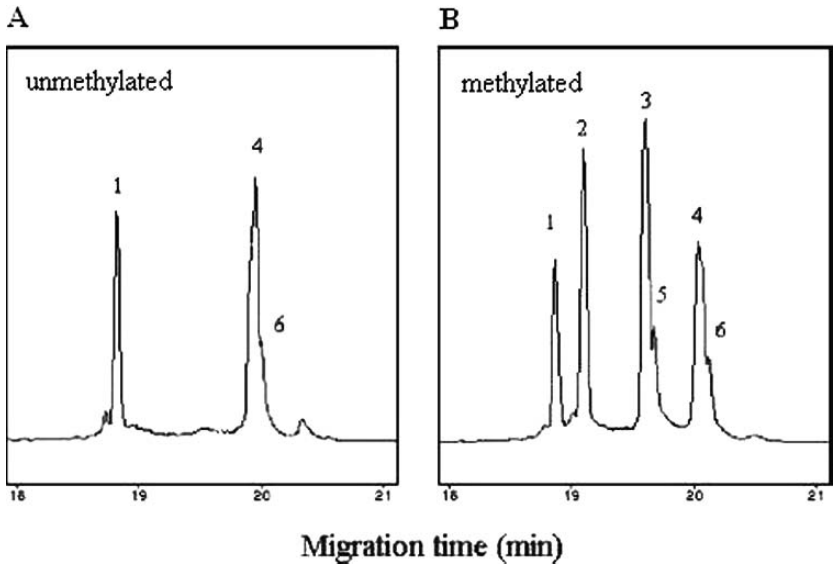


Fig. 8. Electropherograms of unmethylated and methylated of hMLH1 promoter by bisulfite SSCP-CE analysis Electrophoretic conditions: neutral coated capillary, $L = 40\,\text{cm}$, $l = 30\,\text{cm}$, I.D. $= 50\,\mu\text{m}$; sieving medium, 6% LPA with 10% glycerol; voltage, -12 kV; temperature, 25 °C. LIF detection. Peaks 1 and 4, unmethylated ssDNA of hMLH1 promoter; peaks 2 and 3, methylated ssDNA of hMLH1 promoter; peaks 5 and 6, primer-ssDNA complexes. (Reproduced from **ref. *25***, with permission of John Wiley & Sons Limited.)

Acknowledgements

We gratefully acknowledge financial support for this research by grants from National Natural Science Foundation of China (No.90209048), (No. 20425516) for Distinguished Young Scholars, the Knowledge Innovation Program of the Chinese Academy of Sciences (KSCX2-SW-329, KGCX2-SW-213), and Liaoning province foundation of science and technology. Moreover, We gratefully thank Prof. Shen Lv and his research group (The Secondary Affiliated Hospital of Dalian Medical University, Dalian, China) for providing the clinical samples.

References

1. Kuypers, A. W., Willems, P. M., Van der Schans, M. J., et al. (1993) Detection of point mutations in DNA using capillary electrophoresis in a polymer network. *J. Chromatogr.* **621,** 149–156.

2. Kutach, L. S., Bolshakov, S., and Ananthaswamy, H. N. (1999) Detection of mutations and polymorphisms in the p53 tumor suppressor gene by single-strand conformation polymorphism analysis. *Electrophoresis* **20,** 1204–1210.
3. Shi, X., Xu, G., Zhao, C., et al. (2003) A single-strand conformation polymorphism method by capillary electrophoresis with laser-induced fluorescence for detection of the T1151A mutation in hMLH1 gene. *Electrophoresis* **24,** 2316–2321.
4. Shi, X., Li, J., Zhao, C., et al. (2005) K-ras gene mutation detection by Single-Strand Conformation Polymorphism with Capillary Electrophoresis. *Chin. J. Anal. Chem*. **33,** 177–180.
5. Zhao, C., Xu, G., Shi, X., et al. (2004) Fluorescent-based single-strand conformation polymorphism/heteroduplex capillary electrophoretic mutation analysis of p53 gene. *Anal. Sci*. **20,** 1001–1005.
6. Inagaki, S., Yamamoto, Y., Doi, Y., et al. (2002) Typing of Y chromosome single nucleotide polymorphism in a Tapanese population by a multiplexed single nucleotide primer extension reaction. *Legal Medicine* **4,** 202–206.
7. Turner, D., Choudhury, F., Reynard, M., Railton, D., and Navarrete, C. (2002) Typing of multiple single nucleotide polymorphisms in cytokine and receptor genes using SNaPshot. *Hum. Immunol*. **63,** 508–513.
8. Zhao, C., Xu, G., Shi, X., et al. (2003) Simultaneous genotyping of multiplex single nucleotide polymorphisms of K-ras gene with homemade kit. *J. Chromatogr. B*. **795,** 55–60.
9. Zhao, C., Shi, X., Zhang, Y., et al. (2003) Simultaneous detection of several single nucleotide polymorphisms. *Chin. J. Anal. Chem*. **31,** 906–910.
10. Khrapko, K., Hanekamp, J. S., Thilly, W. G., Belenkii, A., Foret, F., and Karger, B. L. (1994) Constant denaturant capillary electrophoresis (CDCE): a high resolution approach to mutational analysis. *Nucleic Acids Res*. **22,** 364–369.
11. Khrapko, K., Coller, H., Andre, P., et al. (1997) Mutational spectrometry without phenotypic selection: human mitochondrial DNA. *Nucleic Acids Res*. **25,** 685–693.
12. Ekstrom, P. O., Borresen-Dale, A. L., Qvist, H., Giercksky, K. E., and Thilly, W. G. (1999) Detection of low-frequency mutations in exon 8 of the TP53 gene by constant denaturant capillary electrophoresis (CDCE). *BioTechniques* **27,** 128–134.
13. Kumar, R., Hanekamp, J. S., Louhelainen, J., et al. (1995) Separation of transforming amino acid-substituting mutations in codons 12, 13 and 61 the N-ras gene by constant denaturant capillary electrophoresis (CDCE). *Carcinogenesis* **16,** 2667–2673.
14. Zhao, C., Xu, G., Shi, X., Ma, J., Lu, S., and Yang, Q. (2004) Detection of K-ras exon 1 mutations by constant denaturant capillary electrophoresis. *Biomed. Chromatogr*. **18,** 538–541.
15. McCord, B. R., Jung, J. M., and Holleran, E. A. (1993) High resolution capillary electrophoresis of forensic DNA using a non gel sieving buffer. *J. Liq. Chromatogr*. **16,** 1963–1981.
16. Marino M. A., Devaney J. M., Davis P. A., and Girard J. E. (1999) Optimization of intercalation dye concentration for short tandem repeat allele

genotyping using capillary electrophoresis with laser-induced fluorescence detection. *J. Chromatogr. B*. **732,** 365–374.
17. Klintschar, M., Ebner, A., and Reichenpfader, B. (1999) Population genetic studies on nine tetrameric short tandem repeat loci using fluorescence dye-labeled primers and capillary electrophoresis in the Austrian population. *Electrophoresis* **20,** 1740–1742.
18. Shi, X., Li, J., Li, A., Lu, S., and Xu, G. (2006) Simultaneous analysis of microsatellite instability and loss of heterozygosity by capillary electrophoresis with a homemade kit. *J. Chromatogr. B.* **834,** 122–127.
19. Jones P. A. (1996) DNA methylation errors and cancer. *Cancer Res*. **56,** 2463–2467.
20. Monk M. (1995) Epigenetic programming of differential gene expression in development and evolution. *Dev. Genet*. **17,** 188–197.
21. Bianco T., Hussey D., and Dobrovic, A. (1999) Methylation-sensitive, single-strand conformation analysis (MS-SSCA): A rapid method to screen for and analyze methylation. *Hum. Mutat*. **14,** 289–293.
22. Bian, Y. S., Yan P., Osterheld, M. C., Fontolliet C., and Benhattar J. (2001) Promoter methylation analysis on microdissected paraffin-embedded tissues using bisulfite treatment and PCR-SSCP. *BioTechniques* **30,** 66–72.
23. Ren, J. C., Ulvik, A., Ueland, P. M., and Refsum, H. (1997) Analysis of single-strand conformation polymorphism by capillary electrophoresis with laser-induced fluorescence detection using short-chain polyacrylamide as sieving medium. *Anal. Biochem*. **245,** 79–84.
24. Hjerten, S. (1985) High-performance electrophoresis elimination of electroendosmosis and solute adsorption. *J. Chromatogr*. **347,** 191–198.
25. Shi, X., Li, J., Zhao, C., Lu, S., and Xu, G. (2006) Methylation analysis of hMLH1 gene promoter by a bisulfite-sensitive single strand conformation polymorphism—capillary electrophoresis method. *Biomed. Chromatogr*. **20,** 815–820.
26. Ohtani, H., Yashitro, M., Onoda, N., Nishioka, N., Kato, Y., Yamamoto, S., Fukushima, S., Hirakawa-Ys, Chung, K. (2000) Synchronous multpile primary gastrointestinal cancer exhibits frequent microsatellite instability. *Int. J. Cancer* **86**, 678–683.

18

Biomedical Applications of Amino Acid Detection by Capillary Electrophoresis

Giuseppe E. De Benedetto

Summary

Capillary electrophoresis (CE) is an efficient tool for amino acid (AA) analysis. However, its role can be fully accounted for only by examining the applications on real matrices. Methods must be successfully transferred into working environments for use by non-CE experts before their power can be realized. This transfer of technology is rapidly increasing. In this chapter, some applications to real samples are presented with the precise intent to illustrate the great capabilities of CE to AA analysis in clinical applications.

Key Words: Capillary zone electrophoresis; micellar electrokinetic chromatography; amino acids; chiral separations; biomedical applications.

1. Introduction

Amino acids (AAs) have an important role in different areas, such as biochemistry and medicine. Determination of AAs can help in the diagnosis or treatment of diseases or the assessment of quality and taste of foodstuffs ***(1–4)***. Their analysis has been widely pursued by many authors with the goal of determining more amino acids in a single run with lower detection limits. Moreover, many AAs lack a strong chromophore and their different behavior, whether acidic, neutral, or basic, makes their determination both interesting and intriguing. As a result, AAs represent perhaps the only class of compounds that have been analyzed by all of the standard electrophoretic methods. Another related, burgeoning analytical field is the chiral separation of amino acids: the determination of enantiomeric purity is fundamental to pharmaceutical

From: *Methods in Molecular Biology, vol. 384: Capillary Electrophoresis*
Edited by: P. Schmitt-Kopplin © Humana Press Inc., Totowa, NJ

and food industries, and racemization studies receive extensive attention ***(4,5)***. Again, the number of proposed methods matches the importance of the topic. Unfortunately, few applications to real problems of the chiral capabilities of electrophoresis in resolving AAs racemates can be found in literature. Surely more applications of chiral CE to real problems of biomedical importance will appear in the next future if the numerous separations of the standard racemic mixtures are considered.

The wealth of papers continuously published on AA analysis is continuously reviewed, and a review of the reviews could be useful to evidence the peculiar aspects. Presently, it is important to mention the general reviews published every 2 yr in *Electrophoresis* ***(1–3)***.

Tables 1 and **2** provide a general overview of a few significant methods, mainly related to biomedical applications and set up to separate and detect AAs, along with the most relevant experimental information on normal ***(6–30)*** and enantiomeric ***(31–53)*** separations, respectively. Within each table, both capillary zone electrophoresis (CZE) and micellar electrokinetic chromatography (MEKC) have been described. All of the referred-to methods can also be carried out on simple, commercial instruments and, as a rule, could be transferred to every CE system.

Different matrices, as far as the biomedical applications are concerned, have been analyzed: physiological fluids such as urine, saliva, or plasma; cells such as lymphocytes or erythrocytes; neurotransmitters; and different hydrolysates (*see* column "Matrix" in **Tables 1** and **2**). Moreover, the hyphenation of microdialysis with the CE apparatus deserves attention as it allows both continuous and in vivo analysis: a fraction of the analytes can diffuse through the membrane dialysis and depending on the temperature and probe characteristics, a definite recovery is attainable and quantitative measurements can be accomplished. Also fast monitoring of AAs is carried out by hyphenating microdialysis with CE: in particular if LIF is used as detector, thank to the high separation efficiency and low volume sample requirement of CE and the very low detection limits of LIF detector, the sampling rate has been increased to levels not attainable by other analytical common techniques, like HPLC, and short-lasting changes in AAs concentration could be recorded. For example, it was successfully employed in physiological studies in which variations lasting less than 3–4 minutes (up to 5 s) occurred ***(54,55)***.

As already pointed out, detection is a general concern, common to all of the different separation schemes. Indeed, nonaromatic, nonderivatized AAs can only be efficiently detected by means of indirect methods; upon derivatization, the selected dye/tag determines the appropriate or most useful detector. Derivatization can be effectively employed to overcome both the lack of

Table 1
Selected Applications of Capillary Zone Electrophoresis (CZE) and Micellar Electrokinetic Chromatography (MEKC) to Biomedical Applications

Sample	Matrix	Detection	Capillary total/ effective length (cm), ID/OD (μm)	Separation method	Derivati zation	Injection	BGE	Run time (min)	L.O.D.	Ref.
19 protein amino acids	Fish flour	UV, 254 nm	75.0/65.0, 50/–	CZE, 25 kV, 20 °C	Pre-capillary, PITC	Hydrodynamic, 3000 Pa, 5 s	30 m*M* phosphate buffer (pH 7.4), 4 m*M* β-CD	50	0.08–0.50 mg/L	***6***
Arg, Lys, Trp, Asn, Ser, Ala, Cys, Gly, Glu	Single erythrocyte	LIF, 488/520 nm	60.2/50.0, 25/375	CZE, 25 kV, 25 °C	Intracellular derivati-zation by electropo-ration, FITC	Electrokinetic, Cell injection, 3.0 kV	12.5 mM borate, 12.5 mM NaOH, 0.12 m*M* spermine (pH 9.45)	25	2–94 n*M*	***7***
20 Aas (16 separated)	Urine, beer	Contactless conductivity detection	60.0/60.0, 25/360	CZE, 25 kV, 20 °C	No	Electrokinetic, 5 kV, 7 s	50 m*M* 2-amino-2-methyl-1-propanol, 10 m*M* CAPS (pH 10.8)	8	0.2–10 μ*M*	***8***
20 Aas	Urine, saliva, yeast	Contactless conductivity detection	80.0/66.5, 50/375	CZE, 30 kV, 25 °C	No	Hydrodynamic, 300 mbar s	2.3 *M* acetic acid, 0.1 % w/w hydroxyethyl-cellulose	30	9.1–29 μ*M*	***9***

(Continued)

Table 1
(Continued)

Sample	Matrix	Detection	Capillary total/ effective length (cm), ID/OD (μm)	Separation method	Derivati zation	Injection	BGE	Run time (min)	L.O.D.	Ref.
Ser, Ala, Tau, Gly	Human lymphocyte	ED, C electrode, 1.00 V	77.0/77.0, 20/375	CZE, 25 kV, 30 °C	In-capillary, NDA	Electrokinetic, Cell injection, 2.0 kV, 3–4 min	20 m*M* $Na_2B_4O_7$, 5 m*M* NaOH (pH 9.84), 5% acetonitrile	30	3–8 μ*M*	***10***
18 Aas	Feed samples and pharma-ceutical preparations	UV, 230 nm	67/58.7, 75/375	CZE, 20 kV + 0.5 psi to the CE inlet	Continuous flow, naphto-quinone-sulfonate	Electrokinetic, 7 kV, 10 s	40 m*M* $Na_2B_4O_7$, isopropanol 70:30 (v/v)	65	0.4–8.5 mg/L	***11***
27 aromatic Aas (24 separated)	Plant seeds	UV, 200 nm	57/50, 50/–	CZE, 25 kV, 15 °C	No	Hydrodynamic, 3.4 kPa, 5 s	75 m*M* phosphoric acid (pH 1.85)	33	4–30 μ*M*	***12***
Arg, Lys, Asp, Gln, Ala, Gly, Glu, GABA	Micro-dialysate from rat hypo-thalamus	LIF, 488/520 nm	57.0/42.0, 75/–	CZE, 12.5 kV, 25 °C	Pre-capillary, FITC	Hydrodynamic, 0.5 psi, 3 s	10 mM $Na_2B_4O_7$ (pH 10.0)	22	< 0.7 n*M*	***13***
Met, Cys, Homocys-teine	Plasma	Fluorometric, 488/520 nm	67/60, 75/–	CZE, 30 kV, 25 °C	Pre-capillary, 5-bromo-methylflu-oresceine	Hydrodynamic, 0.5 psi, 1.5 s	0.25 M phosphate (pH 7.4)	13	1 fmol injected	***14***
Tau, Asp, Ala, Gly, Glu, GABA	Neuro-transmitters in the rat dorsal root ganglion	LIF, 488 nm/CCD 510–670 nm	51/46, 75/375	CZE, 12.5 kV, 25 °C	Pre-capillary, FITC	Gravity, 10 cm, 10 s	15 mM borate buffer (pH 9.2)	20	1.7–17.2 n*M*	***15***

17 Aas (15 separated)	Soybean hydrolysate	Fluorometric, 340/450 nm	75.0/75.0, 50/–	CZE, 22 kV, 20 °C	In-capillary, OPA	Gravity, 10 cm, 10 s	15 m*M* β-CD, 2 m*M* OPA/NAC, 0.1 *M* phosphate/borate buffer (pH 10.0)	55	2.5–10 μ*M*	***16***
Asp, Glu	Continuous in vivo monitoring of AA neuro-transmitters	LIF, 442/520 nm	27/14, 75/150	CZE, 25 kV, 20 °C	On line in-capillary, NDA	Dialysate 1 μL/ min, NDA + fluorescein 1 μL/ min, NaCN 1 mL/min, run buffer 3.5 μL/ min	0.1 *M* Tris (pH 8.65)	2	0.03 μ*M*	***17***
Lys, His, Met, Thr, Asn, Ser, Gly, Tyr	Urine	ED, 127-μm-diameter Cu electrode, 0.60 V vs Ag/AgCl	80.0/80.0, 25/360	CZE, 20 kV, 20 °C	No	Electrokinetic, 20 kV, 3 s	50 m*M* NaOH	36	0.8–6.4 fmol	***18***
20 Aas (18 separated)	Infusion fluids	UV (indirect), 266 nm for PAS or 288 nm for DMAB	90.0/83.0, 75/365	CZE, 20 kV, 25 °C	No	Hydrodynamic, 1s	10 m*M* PAS or DMAB, 20 m*M* of α-CD (pH 11.0)	36/50	–	***19***
cys, cystine, homocystine and met	Urine, nutritive complement	DRC-ICP-MS	70/–, 75/–	CZE, −22 kV	No	Gravity, 10 cm, 40 s	10 m*M* $Na_2B_4O_7$ (pH 9.8), 0.1 m*M* EDTA, 0.5 m*M* Triton X-100	9	1.3–1.6 pg S (27 nL)	***20***
Arg, Glu, Asp	microdialysis in freely moving rats	LIF, 488/510 nm	60/–, 25/360	CZE, 21 kV	Pre-capillary, FITC	Hydrodynamic, 19 psi, 0.2 s	10 m*M* $NaHCO_3$ (pH 7.4)	–	–	***21***

(Continued)

Table 1
(Continued)

Sample	Matrix	Detection	Capillary total/ effective length (cm), ID/OD (μm)	Separation method	Derivati zation	Injection	BGE	Run time (min)	L.O.D.	Ref.
Arg, Tyr, Glu	human serum	LIF, 488/520 nm	47/40, 75/–	CZE, 20 kV, 25 °C	Pre-capillary, FITC	Hydrodinamic, 0.5 psi, 3 s	20 m*M* borate (pH 10.05)	13	0,96–11.1 nM	***22***
32 Aas	human urine	ESI-MS/MS	100/–, 50/–	CZE, 30 kV, 20 °C	No	Hydrodynamic, 50 mbar, 3 s	1 *M* formic acid (pH 1.8)	16	0.1–14 μ*M*	***23***
21 Aas	Blood	ESI-MS (quadrupole), scan m/z 74–250	115–130.0, 20/150	CZE, 30 kV + 5 psi to the CE inlet	No	Hydrodynamic, 300 mbar s	1 *M* formic acid, sheathless	35	1.0–14-0 fmol injected	***24***
homocysteine and cysteine sulfinic acids, homocysteic and cysteic acids	cerebrospinal fluid	LIF, 488/520 nm	57.0/50.0, 75/375	MEKC, 25 kV, 19 °C	Pre-capillary, CFSE	Hydrodynamic, 0.5 psi, 5 s	0.1 *M* borate (pH 9.0), 10 m*M* SDS, 10 % (v/v) methanol	23	9–60 n*M*	***25***
16 Aas and biogenic amines	Brain micro-dyalisate	LIF, 448/630 nm	47/40, 50/140	MEKC, 8.2 kV	Pre-capillary, 5-furoylquinoline-3-carboxaldehyde	Electrokinetic, 4 kV, 5 s	20 m*M* borate (pH 9.0) and 60 m*M* SDS or 15 m*M* borate (pH 8.5), 45 m*M* SDS and 5 m*M* β-CD	18	0.1–80 n*M*	***26***

GABA, Glu, and Asp	in vivo brain monitoring using micro-dialysis sampling	LIF, 442/520 nm	63/52, 50/–	MEKC, 25 kV, 36–38 °C	Pre-capillary, NDA	Hydrodynamic, 10 s, 0.6 psi	75 mmol/L borate buffer (pH 9.2), 70 mmol/L SDS and 10 mmol/L HP-β-CD	10	3–15 n*M*	***27***
18 Aas	Protein hydrolysate	UV, 200 nm	87.0/80.0, 75/365	MEKC, 27 kV, 24 °C	Pre-capillary, PITC	Hydrodynamic, 10 s, 0.6 psi	29 m*M* phosphate buffer (pH 7.4), 168.3 mM SDS	30	Pmol-fmol range	***28***
32 Aas	Human plasma	LIF, 488/520 nm	67.0/60.0, 50/–	MEKC, 30 kV, 25 °C	pre-capillary, CBQC	Hydrodynamic, 5 s, 0.5 psi	160 m*M* borate, 130 m*M* SDS, 7.5 m*M* γ-CD, 20 m*M* NaCl (pH 9.5)	60	40–1000 n*M*	***29***
homocysteine, glutathione, cysteinyl-glycine, and cysteine	Blood samples	LIF, 488/515 nm	85.0/50.0, 50/–	CZE, 30 kV, 25 °C	pre-capillary, IAF	Hydrodynamic, 3 s, 50 mbar	50 m*M* boric acid, 20 m*M* CAPS (pH 10.0)	–	–	***30***

Table 2
Chiral Separation of Amino Acids Enantiomers by Capillary Zone Electrophoresis (CZE) and Micellar Electrokinetic Chromatography (MEKC)

Sample	Matrix	Detection	Capillary total/effective length (cm), ID/OD (μm)	Separation method	Derivatization	Injection	BGE	Chiral selector	Run time (min)	Ref.
11 D/L Aas	standard	ESI-q-MS, m/z 74–250 and 515–700	130.0/130.0, 20/150	CZE, 30 kV + 5 psi to the CE inlet	No	Hydrodynamic, 300 mbar s	5 m*M* (+)-18C6-TCA	5 m*M* (+)-18C6-TCA	28	***31***
20 D/L Aas, 6 in a single run	standard	LIF, 488/520 nm	57.0/50.0, 50/–	CZE, 20 kV, 20 °C	FITC	Hydrodynamic, 1 s, 0.5 psi	80 m*M* borate buffer (pH 9.3)	20 m*M* β-CD, 30 m*M* STC	55	***32***
15 D/L aromatic Aas	Seed extract	UV, 200 nm	50.2/40.0, 50/–	CZE, 25.1 kV, 20 °C	No	Hydrodynamic, 3 s, 3.4 kPa	60 m*M* phosphoric acid (pH 2.5)	175 m*M* HP-α-CD or 2.3 m*M* HS-γ-CD	60	***33***
9 D/L Aas	albumen racem-ization	UV, 254 nm	47.0/40.0, 75/–	MEKC, 15 kV, 25 °C	Dansyl	Hydrodynamic, 5 s, 0.5 psi	250 m*M* borate buffer (pH .5), 100–200 m*M* SDS, 0–30 % (v/v) methanol	75 m*M* β–CD	26	***34***
6 D/L Aas	standard	UV, 254 nm	52.0/38.0, 50/–	CZE, 25 kV, 23 °C	Dansyl	Electrokinetic, 10 s, 10 kV	40 m*M* ammonium acetate (pH 7.0)	1 m*M* $CuSO_4 \cdot 5H_2O$, 1 m*M* L-arginine	–	***35***
33 D/L DNP-Aas	standard	UV, 254 nm	80/54, 75/–	CZE, 24 kV	DNP	Gravity, 10 cm, 2–10 s	100 m*M* MES, 10 m*M* His (pH 5.2)	20 m*M* methylamino-β-CD, 2 m*M* γ-CD	80	***36***

21 D/L Aas, 7 in a single run	standard	LIF, 488/520 nm	85/99, 50/–	MEKC, 30 kV, RT	FITC	Hydrodynamic, 5 s, 75 mbar	100 mm borate (pH 9.5), 30 m*M* SDS	10 m*M* γ-CD	35	***37***
13 D/L Aas, 10 in a single run	standard	UV, 256 nm	67/46, 25/360	MEKC, 30 kV, 25 °C	APC	Hydrodynamic, 15 s, 50 mbar	50 m*M* phosphate buffer (pH 7.5), 40 m*M* SDS, 15 % (v/v) 2-propanol, 1 *M* urea	45 m*M* β-CD	–	***38***
17 D/L Aas	standard	LIF, 351/412	70.0/62.0, 21/–	MEKC, 30 kV, 25 °C	APC	Gravity, 11 cm, 20–80 s	20 m*M* borate buffer (pH 9.95), 15 m*M* SDS	indirect, (+)–APC	15	***39***
D/L-Phe, Tyr, Trp	standard	UV, 220 nm	50/37.5, 50/–	CZE, 12 kV, 20 °C	No	Electrokinetic, 10 kV, 10 s	20 m*M* ammonium acetate (pH 6.8)	0.6–1.8 m*M* AD-β-CD, 0.5–1.5 m*M* $CuSO_4$	10	***40***
6 D/L Aas	standard	UV, 254 nm	35.0/28.0, 75/375	CZE, 20 kV, 25 °C	Dansyl	Gravity, 10 cm, 5 s	0.2 *M* β-alanine/acetate, pH 4.20 – methanol (1/1, v/v)	20 m*M* 1-allyl-5R,8S,10R-terguride	17	***41***
34 D/L Aas	standard	UV, 340 nm	27.0/19.0, 50/–	CZE, 11 kV, 25 °C	OPA/TATG	Hydrodynamic, 2 s, 0.5 psi	sodium borate buffer (pH 9.55, I = 0.04 *M*), 0.045 *M* SDS, 4 % (v/v) acetonitrile	indirect, 2,3,4,6–tetra-O-acetyl-1-thio-β-D-glucopyranose	5	***42***

(Continued)

Table 2
(Continued)

Sample	Matrix	Detection	Capillary total/effective length (cm), ID/OD (μm)	Separation method	Derivatization	Injection	BGE	Chiral selector	Run time (min)	Ref.
Gly	reagent purity	UV, 256 nm	65.0/45.0, 50/–	CZE, 20 kV, 25 °C	FEC		100 m*M* acetate (pH 6.0) 18 % 2-propanol	indirect, 14 m*M* β-CD	15	***43***
15 D/L Aas	Sequence analysis	UV, 269 nm	50.0/30.0, 50/–	MEKC, −15 kV, 26 °C	PTH	Gravity, 5 cm, 4–20 s	10 m*M* formic acid, 50 m*M* SDS	17.5 m*M* TM-β-CD, 12.5 m*M* digitonin, 12.5 m*M* β-escin	65	***44***
D/L aspartic and glutamic acids	teeth dentine, beer	indirect, UV, 238 nm	75.0/45, 75/–, polyacrylamide coated	CZE, −30 kV, 25 °C	No	Hydrodynamic, 26.1 psi s	10 m*M* sorbic acid/histidine (pH 5.0)	10 m*M* vancomycin	11	***45***
D/L-Trp	urine	UV, 220 nm	−/−, 300/–, fluorinated ethylene propylene copolymer	CZE, 70 μA	No	20 μl	50 m*M* borate buffer (pH 9.0), 0.2 % w/v Methyl-hydroxyethyl-cellulose	80 m*M* α-CD	70	***46***

3 D/L β-methyl-Aas	standard	UV, 208 nm	40.0/31.5, 50/–	CZE, 30 kV, 25 °C	No	Hydrodynamic, 30 mbar, 3 s	5 m*M* phosporic acid/ammonia (pH 4.3)	40 m*M* Cu(II), 80 m*M* L-4-hydroxyproline or 10 m*M* Cu(II), 20 m*M* PHP or 10 m*M* Cu(II), 20 m*M* OHP	15	***47***
seleno-methionine, seleno-ethionine	commercial sample	UV, 230 nm	67.0/50.0, 50/–	MEKC, 12 kV, 25 °C	NDA	Hydrodynamic, 70 mbar, 0.6 s	30 m*M* phosphate/10 m*M* boric acid (pH 7.0), 50 m*M* SDS	20 m*M* β-CD, 50 m*M* taurodeoxy-cholic acid	32	***48***
10 D/L-Aas	racemization in peptide synthesis	UV, 200 nm	73.0/60.0, 75/–	MEKC,15 kV, 25 °C	FMAC		20 m*M* borate buffer (pH 9.2), 0–80 m*M* SDS	indirect, FMOC-L-Ala-NCA	12	***49***
galanthamine and narwedine derivatives		UV	64.5/56.0, 50/–	CZE, 26 kV, 20 °C	No	Hydrodynamic, 20–60 mbar, 2–5 s	50 m*M* tetrabutylam-monium dihydrogen phosphate (pH 2.5)	30 m*M* HM-β-CD	40	***50***
8 D/L-Aas	standard	UV, 246 nm	66.0/48.0, 50/–	MEKC, 15 kV, 25 °C	Dansyl	Vacuum, 3s	25 m*M* Na_2HPO_4, 100 m*M* H_3BO_3 (pH 6.5), 25–100 m*M* SDS	36–90 m*M* OTP, 10 m*M* β-CD	21	***51***

(Continued)

Table 2
(Continued)

Sample	Matrix	Detection	Capillary total/effective length (cm), ID/OD (μm)	Separation method	Derivatization	Injection	BGE	Chiral selector	Run time (min)	Ref.
D/L- Asp	rat pineal gland, wine	fluorescence, 470/530 nm	95.0/65.0, 50/–	CZE, 25 °C	FNB	Hydrodynamic, 50 mbar, 12 s	50 m*M* phosphate buffer (pH 4.0)	30 m*M* HM-β-CD	20	***52***
8 D/L-Aas	standard	UV, 254 nm	75.0/55.0, 50/–	CZE, 25 kV, 22 °C	Dansyl	Electrokinetic, 10 kV, 10 s	60 m*M* H_3BO_3-KCl/40 mM NaOH (pH 9.0), 4 *M* urea, 10% (v/v) methanol	100 m*M* β-cyclodextrin	19	***53***

a chromophore on many AAs and the interferences caused by extraneous compounds in real samples: it results in both improved detection sensitivity and selectivity. Hence, the choice of a derivatization reagent is of crucial importance, and great demands are therefore put on its properties. Different approaches have been devised: pre-capillary and in-capillary ***(10,15,16)***. Pre-capillary derivatization is time-consuming, as it requires batch procedures, but it is affordable and widely diffused. In-capillary (or on-column) derivatization is classified into either "on-site in-capillary derivatization" or "throughout in-capillary derivatization." In the former, the inlet of a separation capillary is used as a reaction chamber, and the reaction is performed by introducing an analyte into the capillary between two plugs of labeling reagent. In the latter, the separations and derivatizations of analytes are performed simultaneously during the electromigration of native analytes in a separation capillary tube filled with a run buffer containing a derivatization reagent.

In the last few years, however, two detection systems have been acknowledged as valuable: contactless conductivity and, above all, mass spectrometry detection. Both allow detection of free AAs without derivatization—the former is universal and does not interact with the analytes or separation system; the latter is expensive but offer great selectivity. MS detection for CE is viewed, indeed, as more universal than ultraviolet (UV) or electrochemical detection. The selectivity and specificity of MS compensate for variations in migration times of the analytes and provide molecular weight and structural information. Most importantly, MS adds a second dimension in separation selectivity for co-eluting molecules having different fragmentation patterns. This is of great importance in chiral separation of AAs, where this possibility greatly enhances the capability of the technique ***(31)***.

As to the background electrolyte, an impressing variety with respect to the pH (from 2.2 to 11.0) or the nature (from acetic or formic acid to borate or phosphate buffers) is found. Moreover, the electrolyte modification with organic modifiers or chemicals like cyclodextrin (CD) derivatives is an emerging trend: the former may cause an improvement of the separation, possibly because of a decrease in electroosmotic flow (EOF), lower solute adsorption to the capillary, and Joule heating. Different roles have also been attributed to CD, mainly related to the host–guest interaction with the solute ***(56)***. Similarly, in chiral separation, blends of chiral selectors separated AA enantiomers better than did a single chemical ***(36,44)***. As a result, to fulfill the great complexity of the method setup, experimental designs are often employed ***(57,58)***.

The protocols described in the following paragraphs represent different approaches to the AA analysis, and all could possibly be applied to biomedical problems.

2. Materials

2.1. Analysis of the Amino Acid Standards and the Blood Samples

1. 48% Hydrogen fluoride (Merck, Darmstadt, Germany).
2. Background electrolyte (BGE): 1 *M* formic acid solution: dilute 1.90 mL of 98–100% Suprapur formic acid (Merck) to 50 mL with water in a volumetric flask. Store at room temperature (*see* **Note 1**).
3. Sheath liquid: 5 m*M* ammonium acetate (Merck) in methanol/water (50:50, v/v).
4. Preparation of the blood sample: soak a 5-mm diameter blood spot on filter paper in 100 μL of water for 10 min. Then, take a 20-μL aliquot of this solution and dilute to 200 μL with a solution of acetonitrile/water/formic acid (49.9/49.9/0.2; v/v).
5. High-performance capillary electrophoresis/mass spectrometry system.
6. Uncoated 115 cm long, 20 μm inner diameter (I.D.), 150 μm outer diameter (O.D.) fused-silica capillary (Polymicro Technologies, Inc., Phoenix, AZ).

2.2. Capillary Electrophoresis Combined with Microdialysis: Analysis of Trace Amino Acids Neurotransmitters

1. Ringer solution: 140.0 m*M* NaCl, 4.0 m*M* KCl, 1.2 m*M* $CaCl_2$, 1.0 m*M* $MgCl_2$, 10 m*M* $NaHCO_3$ at pH 7.4 (*see* **Note 1**).
2. Prepare the 1 m*M* γ-Aminobutyric acid (GABA), glutamate (Glu), and L-Aspartate (L-Asp) (all from Sigma-Aldrich) standard solutions in 0.1 *M* hydrogen chloride (prepared from 30% Suprapur hydrogen chloride, Merck) and store at 4 °C.
3. NDA solution: 3.0 m*M* Naphthalene-2,3-dicarboxaldehyde (NDA) (Buchs, Switzerland) in acetonitrile (hypergrade LiChrosolv, Merck)/water 50:50 v/v.
4. Borate/NaCN solution: 0.5 *M* borate buffer pH 9.2/87 m*M* NaCN in water (100:20 v/v).
5. Internal standard: 0.1 m*M* cysteic acid in 0.1 *M* hydrogen chloride.
6. BGE: 75 m*M* sodium borate, 10 m*M* hydroxypropyl-β-cyclodextrin (HP-β-CD), 70 m*M* sodium dodecyl sulfate (SDS) buffer (pH 9.20). (Sigma-Aldrich). (*see* **Note 2**)
7. A microdialysis apparatus composed by a microinfusion pump and a microdialysis probe equipped with a polycarbonate ether dialysis membrane having a molecular mass cut-off of 20,000 D.
8. High-performance CE equipped with a laser induced fluorescence detector and Helium Cadmium laser (8 mW, 442 nm).
9. Uncoated 63 cm long, 50 μm I.D. fused-silica capillary (Polymicro Technologies, Inc.). Effective length 52 cm.

2.3. Analysis of Protein Hydrolysates

1. Hydrochloric acid solution: 6 *M* HCl (Suprapur, Merck) containing 0.5% (w/v) phenol (Merck) (*see* **Note 1**).
2. Triethylamine solution: mix 2 ml of 99.5% ethanol, 2 mL of water and 1 mL triethylamine.

3. PITC solution: mix 70 μL of 99.5% ethanol, 20 μL of triethylamine, and 10 μL of phenylisothiocyanate (Sigma-Aldrich).
4. Bovine serum albumin (BSA, 607 residues) was obtained from Sigma-Aldrich.
5. BGE: 29 m*M* phosphate buffer, pH 7.4, 168.3 m*M* SDS (Sigma-Aldrich) (*see* **Note 3**).
6. Glass tubes for hydrolysis and derivatization.
7. High performance capillary electrophoresis with UV-vis detection.
8. Uncoated 57 cm long, 50 μm I.D. fused silica (Polymicro Technologies). The length to the detector is 50 cm.

3. Methods

The methods described herein outline the use of different electrophoretic techniques to separate and detect AAs in biomedical applications. In the first example, a CE-MS system is effectively used to detect phenylketonuria and tyrosinemia, two metabolic diseases, in blood samples. A sheath-flow interface is used because of its easy and reproducible setup. It also imposes fewer constraints on the buffer used in the separation. Pressure-assisted CE also minimizes loss of resolution due to the diffusion of counter ion from the sheath liquid back into the capillary. This hyphenation, as already observed, deserves great attention: the results are interesting, and the methods can be further improved, for example, by separating AAs after derivatization. MS, indeed, has a greater sensitivity when higher-molecular-weight compounds are detected, and a simpler tuning of the spectrometer is feasible if the tag represents the main part of the molecule.

CE-LIF is the method of choice for monitoring simultaneously neurotransmitters. Its sensitivity and the low injected volume, typical of CE, make it an ideal technique for the analysis of biological samples, such as microdialysate from discrete brain areas, whose absolute amounts are very small. No clean-up procedures are required, as the dialysis membrane is not crossed by high-molecular weight-substances like the proteins. By selecting the proper membrane cutoff, different real samples can be analyzed without time-consuming purification procedures. Also, if the perfusate is compatible with the derivatization mixture, the derivatized AAs can be collected and promptly analyzed, avoiding batch operation.

The microdialysis-CE-LIF experiment, herein described, permitted to monitor the extracellular concentration of neurotransmitters, which have a key role in the understanding of human chemical, physiological, and behavioral events.

The last protocol is a rapid and sensitive tool for analysis of AAs in polypeptide or protein hydrolysates, which can find application in different fields, from protein analysis to glue identification. Its compatibility with

conventional methods and the better sensitivity (the needed amounts are 100–1000 times lower than those used for the ninhydrin-based determinations) made the method valuable for real samples.

3.1. CE-ESI-MS

1. Sample vial is sample holder SI:A1. In some instruments, for electrical reasons, the outlet terminal in normal mode becomes the inlet terminal with the external adapter.
2. BGE (2.0 mL) in sample holder position BI:A1.
3. 1 *M* NaOH solution (2.0 mL) in sample holder position B1:D1 and water (2.0 mL) in sample holder position BI:E1; place an empty vial in sample holders BI:C1.
4. Fill the syringe with the sheath liquid solution and place it in its holder on mass spectrometer.
5. Before the run, rinse at high forward pressure (20 psi) the capillary sequentially with NaOH (1 min), water (1 min), and electrophoresis buffer (4 min) (*see* **Note 4**).
6. CE programmed to inject electrophoresis sample for 5 s at low pressure (0.5 psi, 3.45 kPa).
7. The conditions used in the CE were as follows: voltage 30 kV, temperature 25 ± 0.5 °C, pneumatic assistance to classical electrophoretic driving force, 10 psi. (*see* **Note 5**).
8. 1.5 kV were applied to the CE outlet/ESI electrode and the heated capillary used in these measurements is kept at 200 °C. The source temperature is maintained at 80 °C and nitrogen is used for both nebulising (35 L/h) and drying (100 L/h). The sheath liquid flow at a flow rate of 5 μL/min is provided by the mass spectrometer controlled syringe pump (*see* **Note 6**).
9. Set up the mass spectrometer detector to scan the m/z range between 74 and 250 amu under positive ionization mode at unit mass resolution to monitor free AAs.
10. The UV detector, located 20 cm from the capillary injection end, can be operated continuously at 200 nm for coarse control of analyte migration.
11. **Figure 1** shows the electropherograms of blood sample of both healthy and afflicted individuals.

3.2. CE-LIF

1. Perfuse the microdialysis probe with the Ringer's solution at high flow rate (10 μL/min) for 1 h, then lower the flow rate to 2 μL/min and implant the probe. Monitor the basal level of the analytes for at least 30 min before stimulus.
2. Collect the perfusate fraction in microvials every 1 min (2 μL sample volume) and immediately store each of them at –40 °C before derivatization. Stop the fraction collection 30 min after the stimulus.
3. After recovery to room temperature, derivatize the microdialysate as follows: add 0.2 μL of the internal standard, 0.4 μL of the borate/NaCN and 0.2 μL of the NDA solutions to the sample (2 μL). Let the mixture react for about 1 h (*see* **Note 7**).

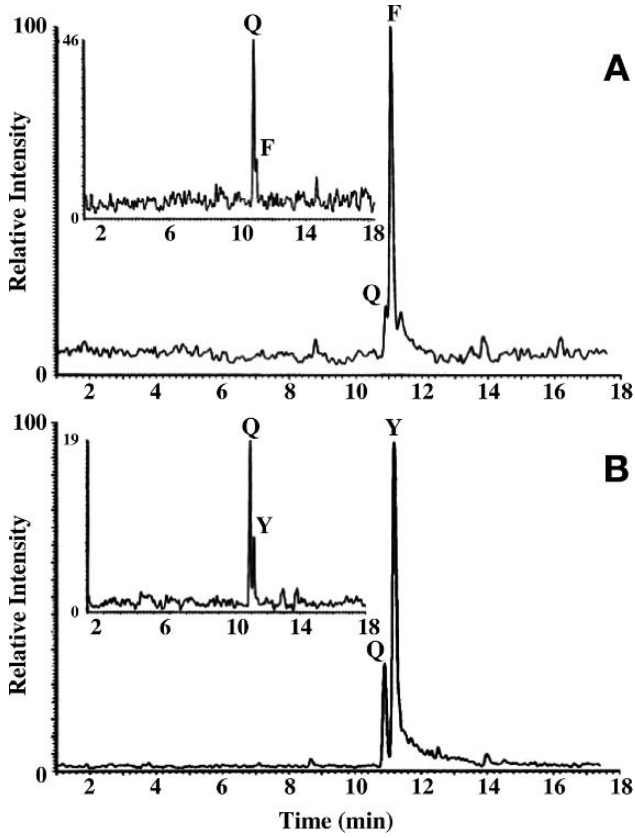


Fig. 1. Analysis by CE-MS. **(A)** Amino acid analysis of the blood of an individual afflicted with PKU and its comparison to that of a healthy one (inset). **(B)** Amino acid analysis of the blood of an infant afflicted with tyrosinemia. The inset contains the electropherogram of the blood of a healthy individual. (Reprinted from **ref.** ***24***, with permission of the American Chemical Society.)

4. Electrophoresis buffer (2 × 2.0 mL) in sample holder position BI:A1 and BO:A1. Electrophoresis sample in sample holder SI:A1. Standard solution in sample holder SI:B1.
5. 0.25 *M* NaOH solution (2.0 mL) in sample holder position B1:D1 and water (2.0 mL) in sample holder position BI:E1; place empty vials in sample holders BI:C1 and BO:B1.
6. CE programmed to inject electrophoresis sample for 10 s at 0.5 psi.
7. The conditions used in the CE were as follows: voltage, 25 kV, temperature 25 ± 0.5 °C. The excitation was performed with a Helium Cadmium laser (8 mW, 442 nm) whereas the fluorescence emission intensity was recorded at 490 nm.

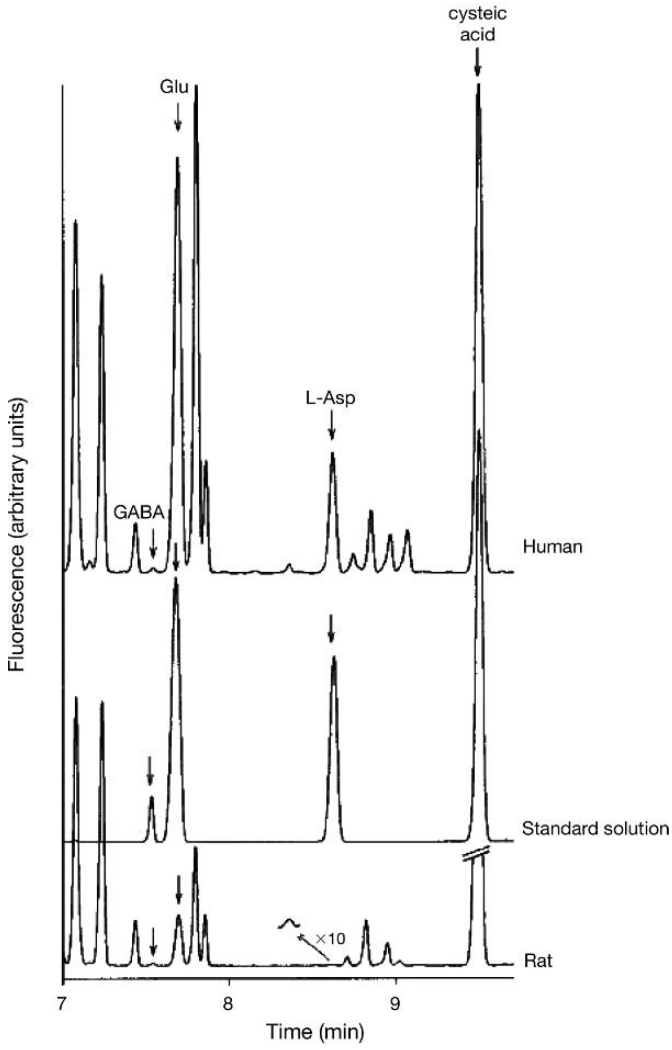


Fig. 2. Analysis by CE-LIF. Typical electropherograms of a microdialysate obtained from the spinal dorsal horn in a patient with chronic pain (top), a standard solution (middle) containing 5×10^{-7} mol/L GABA, 5×10^{-6} mol/L Glu/L-Asp compared to a brain dialysate obtained from rat striatum (bottom). Cysteic acid is the internal standard. (Reprinted from **ref. *59***, with permission of Wiley-VCH.)

8. Between runs, rinse at high pressure (20 psi) the capillary sequentially with 0.25 NaOH (30 s), water (1 min) and electrophoresis buffer (1 min).
9. **Figure 2** shows the electropherograms relevant to the analysis of a microdialysate obtained from the spinal dorsal horn, a standard solution and a brain dialysate from a rat striatum.

3.3. CE-UV

1. Hydrolysis of Proteins and Peptides: vacuum dry the solution of proteins or peptides in 5 × 35-mm glass tubes. Then add to each tube 40 μL of hydrochloric solution. Evacuate and flame seal the tubes. Put the tubes in a oven at 110 °C for 24 h. After opening of the tubes, dry with a gentle nitrogen flow. (*see* **Note 8**)
2. Derivatization with phenylisothiocyanate (PITC): add to each tube 40 μL of triethylamine solution, vortex shortly and evaporate (*see* **Note 9**). Then, add 3 μL 50% ethanol to each tube followed by subsequent addition of 7 μL of PITC solution. Vortex and incubate the samples for 30 min at room temperature. Dry the derivatized samples under vacuum overnight in a desiccator. Dissolve the PITC-AAs in water before CE analysis (*see* **Note 10**)
3. BGE (2 × 2.0 mL) in sample holder position BI:A1 and BO:A1. Electrophoresis sample-to-sample holder SI:A1.
4. CE programmed to inject electrophoresis sample for 5 s at 0.5 psi.
5. The conditions used in the CE were as follows: voltage, 27 kV, temperature 24 ± 0.5 °C. The on-line UV detector, located 7 cm from the capillary end, is operated continuously at 200 nm for control of analyte migration.
6. Change the BGE after each run and wash the capillary with the fresh electrolyte at least 5 min.
7. **Figure 3** shows the electropherograms of a hydrolysate of BSA.

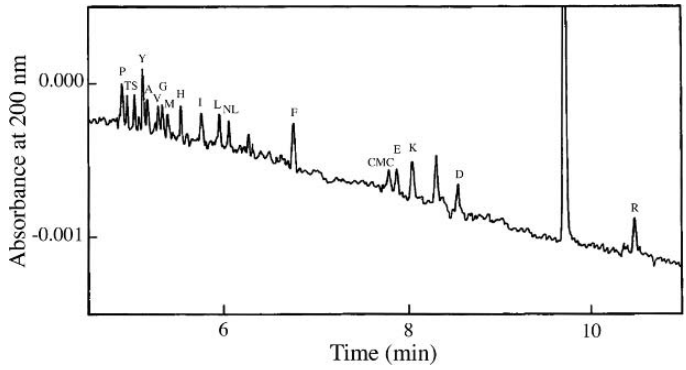


Fig. 3. Analysis by CE-UV. Capillary electrophoresis of PTC–amino acid standard in the femtomole range (100 fmol). CMC denotes PTC–carboxymethylcysteine and NL, PTC–norleucine (internal standard). (Reprinted from **ref. *28***, with permission from Elsevier.)

4. Notes

1. All solutions were prepared in water that has a resistivity of 18.2 MΩ-cm and total organic content of less than 5 ppb. An UltraClear system (SG Water, Hamburg, Germany) equipped with a UV lamp was used.
2. Filter the BGE through a 0.2-μm filter to prevent blockage of the CE capillary and for degassing.
3. The running buffer may conveniently be prepared by titration of phosphoric acid (Merck) with NaOH (Sigma-Aldrich). Then, dissolve the SDS and filter through 0.2-μm membranes before use. It could be stored at room temperature for at least 6 mo.
4. Either a chemical or a mechanical method can be used to sharpen the outlet tip of a new capillary, before mounting it in the cartridge. If nitrile gloves and a fume hood are available, the chemical etching in 49% hydrofluoric acid could be accomplished by soaking 2–4 mm of the capillary end for 5 min while passing nitrogen through the capillary to minimize the etching of the inner wall of the capillary. Otherwise, the tip could also be sharpened mechanically with fine emery paper: in this case, pay attention to the debris so as to avoid clogging the capillary. Moreover, before use, new capillaries should be eluted with 1 *M* NaOH for 2–4 h under constant pressure. At the beginning of each day, the capillary should be conditioned by flushing with 1 *M* NaOH solution (5 min), followed by a 5-min flush with water and a 30-min flush with electrolyte solution.
5. If available, use an HPLC pump, as generally, the baseline noise is halved.
6. With different CE equipment, the pneumatic assistance, which is used to shorten analysis time, is not available.
7. NDA is a fluorescent tag not fluorescent itself (in contrast with fluorescin isothiocyanate, for instance) and rapidly reacts to give stable fluorescent derivatives. However, because the internal standard cysteic acid reacts less quickly than Glu, L-Asp and GABA, a reaction time of 1 h at room temperature is necessary to complete the derivatization reaction.
8. To eliminate the metal ions eventually present in the sample, it is possible to extract the proteic fraction in 6 *N* NH_3 first, then to dry the extract and hydrolyze it. For biomedical applications, the glass tube should be pyrolyzed (400 °C, 3–4 h) before use.
9. This step is essential to remove residual hydrolysis acid.
10. Reagent mixtures were made fresh daily, and stock PITC was stored at about 20 °C under nitrogen. Triethylamine and 50% ethanol were stored at 4 °C. PTC–amino acids were stored at −20 °C.

References

1. Marchelli, R., Dossena, A., and Palla, G. (1996) The potential of enantioselective analysis as a quality control tool. *Trends Food Sci. Technol.* **7,** 113–119.
2. Smith, J. T. (1999) Recent advances in amino acid analysis by capillary electrophoresis. *Electrophoresis* **20,** 3078–3083.

3. Prata, C., Bonnafous, P., Fraysse, N., Treilhou, M., Poinsot, V., and Couderc, F. (2001) Recent advances in amino acid analysis by capillary electrophoresis. *Electrophoresis* **22,** 4129–4138.
4. Poinsot, V., Bayle, C., and Couderc, F. (2003) Recent advances in amino acid analysis by capillary electrophoresis. *Electrophoresis* **24,** 4047–4062.
5. Chankvetadze, B. (1997) *Capillary Electrophoresis in Chiral Analysis*, John Wiley & Sons, New York.
6. Komarova, N. V., Kamentsev, J. S., Solomonova, A. P., and Anufrieva, R. M. (2004) Determination of amino acids in fodders and raw materials using capillary zone electrophoresis. *J. Chromatogr. B*. **800,** 135–143.
7. Zhang, H. and Jin, W. (2004) Analysis of amino acids in individual human erythrocytes by capillary electrophoresis with electroporation for intracellular derivatization and laser-induced fluorescence detection. *Electrophoresis* **25,** 480–486.
8. Tanyanyiwa, J., Schweizer, K., and Hauser, P. C. (2003) High-voltage contactless conductivity detection of underivatized amino acids in capillary electrophoresis. *Electrophoresis* **24,** 2119–2124.
9. Coufal, P., Zuska, J., van de Goor, T., Smith, V., and Gas, B. (2003) Separation of twenty underivatized essential amino acids by capillary zone electrophoresis with contactless conductivity detection. *Electrophoresis* **24,** 671–677
10. Weng, Q. and Jin, W. (2003) Assay of amino acids in individual human lymphocytes by capillary zone electrophoresis with electrochemical detection. *Anal. Chim. Acta* **478,** 199–207.
11. Latorre, R. M., Saurina, J., and Hernandez-Cassou, S. (2002) Continuous flow derivatization system coupled to capillary electrophoresis for the determination of amino acids. *J. Chromatogr. A*. **976,** 55–64.
12. La, S., Kim, A., Kim, J. -H., Choi, O. -K., and Kim, K. -R. (2002) Profiling and screening analysis of 27 aromatic amino acids by capillary electrophoresis in dual modes. *Electrophoresis* **23,** 1080–1089.
13. Zhang, D., Zhang, J., Ma, W., et al. (2001) Analysis of trace amino acid neurotransmitters in hypothalamus of rats after exhausting exercise using microdialysis. *J. Chromatogr. B*. **758,** 277–282.
14. Vecchione, G., Margaglione, M., Grandone, E., et al. (1999) Determining sulfur-containing amino acids by capillary electrophoresis: A fast novel method for total homocyst(e)ine human plasma *Electrophoresis* **20,** 569–574.
15. Zhang, L., Chen, H., Cheng, J., Li, Z., and Shao, M. (1998) Determination of the amino acid neurotransmitters in the dorsal root ganglion of the rat by capillary electrophoresis with a laser-induced fluorescence-charge coupled device. *J. Chromatogr. B*. **707,** 59–67.
16. Oguri, S., Yokoi, K., and Motohase, Y., (1997) Determination of amino acids by high-performance capillary electrophoresis with on-line mode in-capillary derivatization. *J. Chromatogr. A*. **787,** 253–260.
17. Zhou, S. Y., Zuo, H., Stobaugh, J. F., Lunte, C. E., and Lunte, S. M. (1995) Continuous in Vivo Monitoring of Amino Acid Neurotransmitters by Micro-

dialysis Sampling with Online Derivatization and Capillary Electrophoresis Separation. *Anal. Chem*. **67,** 594–599.
18. Ye, J. and Baldwin, R. P. (1994) Determination of amino acids and peptides by capillary electrophoresis and electrochemical detection at a copper electrode. *Anal. Chem*. **66,** 2669–2674.
19. Lee, Y. -H. and Lin, T. -I. (1995) Capillary electrophoretic determination of amino acids Improvement by cyclodextrin additives. *J. Chromatogr. A*. **716,** 335–346
20. Yeh, C. -F. Jiang, S. -H., and Hsi, T. -S. (2004) Determination of sulfur-containing amino acids by capillary Electrophoresis dynamic reaction cell inductively coupled plasma mass spectrometry. *Anal. Chim Acta* **502,** 57–63.
21. Silva E., Hernandez L., Quinonez B., Gonzalez, L. E., and Colasante, C. (2004) Selective amino acids changes in the medial and lateral preoptic area in the formalin test in rats. *Neuroscience* **124,** 395–404.
22. Zhang, J., Tian, J., Liu, J., Gao, H., Chen, X., and Hu, Z. (2003) Quantification of neurotransmitter amino acids in human serum by capillary electrophoresis with laser-induced fluorescence detection. *Mikrochim. Acta* **143,** 241–244.
23. Soga, T., Kakazu, Y., Robert, M., Tomita, M., and Nishioka, T. (2004) Qualitative and quantitative analysis of amino acids by capillary electrophoresis-electrospray ionization-tandem mass spectrometry. *Electrophoresis* **25,** 1964–1972.
24. Schultz C. L. and Moini M. (2003) Analysis of underivatized amino acids and their D/L-enantiomers by sheathless capillary Electrophoresis/electrospray ionization mass spectrometry. *Anal. Chem*. **75,** 1508–1513.
25. Becker, E., Scheuch, U., Bode, and Jaehde, U. (2002) Simultaneous analysis of sulfur-containing excitatory amino acids using micellar electrokinetic chromatography with diode array and laser-induced fluorescence detection. *Electrophoresis* **23,** 2457–2464.
26. Chen, Z., Wu, J., Baker, G. B., Parent, M., and Dovichi, N. J. (2001) Application of capillary electrophoresis with laser-induced fluorescence detection to the determination of biogenic amines and amino acids in brain microdialysate and homogenate samples. *J. Chromatogr. A*. **914,** 293–298.
27. Sauvinet, V., Parrot, S., Benturquia, N., Bravo-Moraton, E., Renaud, B., and Denoroy, L. (2003) In vivo simultaneous monitoring of γ-aminobutyric acid, glutamate, and L-aspartate using brain microdialysis and capillary electrophoresis with laser-induced fluorescence detection: Analytical developments and in vitro/in vivo validations. *Electrophoresis* **24,** 3187–3196.
28. Zahou, E., Jornvall, H., and Bergman, T. (2000) Amino acid analysis by capillary electrophoresis after phenylthiocarbamylation. *Anal. Biochem*. **281,** 115–122.
29. Boulat, O., McLaren, D. G., Arringa, E. A., and Chen, D. D. Y. (2001) Separation of free amino acids in human plasma by capillary electrophoresis with laser induced fluorescence: potential for emergency diagnosis of inborn errors of metabolism. *J. Chromatogr. B*. **754,** 217–228.
30. Causse, E., Issac, C., Bayle, C., Salvayre, R., and Couderc, F. (2002) Assays for total homocysteine and other thiols by capillary electrophoresis–laser-induced

fluorescence detection. II. Pre-analytical and analytical conditions. *J. Chromatogr. A*. **979,** 255–260.
31. Moini, M., Schultz, C. L., and Mahmood, H. (2003) CE/electrospray ionization-MS analysis of underivatized d/l-amino acids and several small neurotransmitters at attomole levels through the use of 18-crown-6-tetracarboxylic acid as a complexation reagent/background electrolyte. *Anal. Chem*., **75,** 6282–6287
32. Lu, X. and Chen, Y. (2002) Chiral separation of amino acids derivatized with FITC by CE and LIF detection using mixed selectors of β-CD and sodium taurocholate. *J. Chromatogr. A*. **955,** 133–140.
33. La, S., Ahn, S., Kim, J. -H., Goto, J., Choi, O. -K. and Kim, K. -R. (2002) Enantioseparation of chiral amino acids by capillary electrophoresis in neutral and charged cyclodextrin selector modes. *Electrophoresis* **23,** 4123–4131.
34. Chang, H. -M., Tsai, C. -F., and Li, C. -F. (1999) Quantification of racemization of amino acids in alkaline-treated duck eggs by micellar capillary electrophoresis. *J. Agric. Food Chem*. **47,** 479–484.
35. Yuan, Z., Yang, L. and Zhang, S. (1999) Enantiomeric separation of amino acids by copper(II)-L-arginine ligand exchange capillary zone electrophoresis. *Electrophoresis* **20,** 1842–1845.
36. Mikus, P., Kaniansky, D. and Fanali, S. (2001) Separation of multicomponent mixtures of 2,4-dinitrophenyl labelled amino acids and their enantiomers by capillary zone electrophoresis. *Electrophoresis* **22,** 470–477.
37. Jin, L. J., Rodriguez, I., and Li, S. F. Y. (1999) Enantiomeric separation of amino acids derivatized with fluorescein isothyocyanate isomer I by micellar electrokinetic chromatography using β- and γ-cyclodextrin as chiral selectors. *Electrophoresis* **20,** 1538–1545.
38. Wan, H., Engström, A and Blomberg, L. G. (1996) Direct chiral separation of amino acids derivatized with 2-(9-anthryl)ethyl chloroformate by capillary electrophoresis using cyclodextrins as chiral selector. Effect of organic modifiers on resolution and enantiomeric elution order. *J. Chromatogr. A*. **731,** 283–292.
39. Thorsen, G., Engstrom, A., and Josefsson, B. (1997) Enantiomeric determination of amino Compounds with high sensitivity using the chiral reagents (+)- and (−)-1-(9-antryl)-2-propyl chloroformate. *J. Chromatogr. A*. **786,** 347–354.
40. Cucinotta, V., Giuffrida, A., La Mendola, D., et al. (2004) 3-Amino derivative of β-cyclodextrin: thermodynamics of copper(II) complexes and exploitation of its enantioselectivity in the separation of amino acid racemates by ligand exchange capillary electrophoresis. *J. Chromatogr. B*. **800,** 127–133.
41. Honzátko, A., Votruba, J., Olšovská, J., et al. (2003) Enantioseparation of dansyl amino acids on terguride-based chiral selectors. Part I: Capillary electrophoretic separation. *J. Sep. Sci*. **26,** 851–856.
42. Tivesten, A. and Folestad, S. (1995) Separation of precolumn labelled D- and L-amino acids by micellar electrokinetic chromatography with UV and fluorescence detection. *J. Chromatogr. A*. **708,** 323–337.

43. Engstrom, A., Wan, H., Andersson, P. E., and Josefsson, B. (1995) Determination of chiral reagent purity by capillary electrophoresis. *J. Chromatogr. A*. **715,** 151–158.
44. Kurosu, Y., Murayama, K., Shindo, N., et al. (1998) Optical resolution of phenylthiohydantoin-amino acids and identification of phenylthiohydantoin-D-amino acid residue of [D-Ala]-methionine enkeohalin by capillary electrophoresis. *J. Chromatogr. A*. **802,** 129–134.
45. Bednar, P., Aturki, Z., Stransky, Z., and Fanali, S. (2001) Chiral analysis of UV nonabsorbing compounds by capillary electrophoresis using macrocyclic antibiotics: 1. Separation of aspartic and glutamic acid enantiomers, *Electrophoresis* **22,** 2129–2135.
46. Danková, M., Kaniansky, D., Fanali, S., and Iványi, F. (1999) Capillary zone electrophoresis separations of enantiomers present in complex ionic matrices with on-line isotachophoretic sample pretreatment, *J. Chromatogr. A*. **838,** 31–43.
47. Grobuschek, N., Schmid, M. G., Tuscher, C., Ivanova, M., and Gübitz, G. (2002) Chiral separation of ß-methyl-amino acids by ligand exchange using capillary electrophoresis and HPLC. *J. Pharm. Biomed. Anal*. **27,** 599–605.
48. Méndez, S. P., González, E. B., Sanz-Medel, A. (2000) Enantiomeric separation of selenoaminoacid derivatives by cyclodextrin-modified micellar electrokinetic chromatography using a mixed micellar system of sodium dodecyl sulphate and taurodeoxycholic acid. *Anal. Chim. Acta* **416,** 1–7
49. Pumera, M., Flegel, M., Lepa, L., and Jelínek I. (2002) Chiral analysis of biogenic DL-amino acids derivatized by urethane - protected -amino acid N-carboxyanhydride using capillary zone electrophoresis and micellar electrokinetic chromatography. *Electrophoresis* **23,** 2449–2456.
50. Rizzi, A., Schuh, R., Brückner, A., et. al. (1999) Enantiomeric resolution of galanthamine and related drugs used in anti-Alzheimer therapy by means of capillary zone electrophoresis employing derivatized cyclodextrin selectors. *J. Chromatogr. B*. **730,** 167–175.
51. Tran, C. D. and Kang, J. (2002) Chiral separation of amino acids by capillary electrophoresis with octyl-ß-thioglucopyranoside as chiral selector. *J. Chromatogr. A*. **978,** 221–230.
52. Tsunoda, M., Kato, M., Fukushima, T., et al. (1999) Determination of aspartic acid enantiomers in bio-samples by capillary electrophoresis. *Biomed. Chromatogr*. **13,** 335–339.
53. Yang, L. and Yuan, Z. (1999) Comparison of enantioseparation of amino acid derivatives in aqueous and mixed aqueous-organic media by capillary zone electrophoresis. *Fresenius J Anal. Chem*. **365,** 541–544.
54. Lada, M. W., Vickroy, T. W., and Kennedy, R. T. (1997). High temporal resolution monitoring of glutamate and aspartate in vivo using microdialysis on-line with capillary electrophoresis with laser-induced fluorescence detection. *Anal. Chem*. **69,** 4560–4565.
55. Lada, M. W., Vickroy, T. W., and Kennedy, R. T. (1998). Evidence for neuronal origin and metabotropic receptor-mediated regulation of extracellular glutamate

and aspartate in rat striatum in vivo following electrical stimulation of the prefrontal cortex. *J. Neurochem*. **70,** 617–625.
56. Wagner, B. D. and McManus, G. J. (2003) Enhancement of the fluorescence and stability of o-phthalaldehyde-derived isoindoles of amino acids using hydroxypropyl-beta-cyclodextrin. *Anal. Biochem*. **317,** 233–239.
57. Perrin, C., Fabre, H., Vander Heyden, Y.; Maftouh, M.; and Massart, D. L. (2003) Robustness testing of chiral separations by capillary electrophoresis using highly-sulfated cyclodextrins. *J. Chromatogr. A*. **1007,** 165–177.
58. Perrin, C., Vargas, M. G., Vander Heyden, Y., Maftouh, M., and Massart, D. L. (2000) Fast development of separation methods for the chiral analysis of amino acid derivatives using capillary electrophoresis and experimental designs. *J. Chromatogr. A*. **883,** 249–265.
59. Parrot, S., Sauvinet, V., Xavier, J. -M., et al. (2004) Capillary electrophoresis combined with microdialysis in the human spinal cord: A new tool for monitoring rapid peroperative changes in amino acid neurotransmitters within the dorsal horn. *Electrophoresis* **25,** 1511–1517.

19

Separation of Peptides by Capillary Electrophoresis

Gerhard K. E. Scriba and Arndt Psurek

Summary

Peptides are an important class of analytes in chemistry, biochemistry, and food chemistry as well as medical and pharmaceutical sciences. As a high-resolution technique, capillary electrophoresis (CE) is well suited for the analysis of polar compounds such as peptides. In addition, CE is orthogonal to high-performance liquid chromatography, as both techniques are based on different physico-chemical separation principles. For the successful development of peptide separations by CE, operational parameters including buffer pH, buffer concentration and buffer type, applied voltage, and capillary dimensions, as well as background electrolyte additives such as detergents, ion-pairing reagents, cyclodextrins, (poly)amines, soluble polymers, etc. must be considered and optimized.

Key Words: Capillary electrophoresis; peptides; peptide analysis; method development; review.

1. Introduction

Peptides represent an important class of biologically active compounds acting as hormones, neurotransmitters, immunomodulators, coenzymes, enzyme inhibitors, toxins, or antibiotics. In addition, peptides and peptidomimetics comprise an important class of approved drugs and drug candidates under development. Although high-performance liquid chromatography (HPLC) has been traditionally the method of choice for the separation and analysis of peptides, capillary electrophoresis (CE) has emerged as a very useful technique for peptide analysis in recent years. CE is complementary to HPLC, as the selectivities of both techniques are based on different physico-chemical principles. Whereas HPLC separations are primarily based on the lipophilicity/hydrophobicity of the analytes separations in CE are accomplished

From: *Methods in Molecular Biology, vol. 384: Capillary Electrophoresis*
Edited by: P. Schmitt-Kopplin © Humana Press Inc., Totowa, NJ

as a result of differences in the charge density (charge-to-mass ratio) of compounds. Thus, separations that are difficult to achieve with one technique may be easily performed by the other method. In addition, CE offers rapid method development and is an extremely flexible technique that offers high peak resolution. CE is very economical, as only low amounts of chemicals and sample are required and no or little organic solvent is used.

Natural peptides are composed of about 20 amino acids. Depending on the number, composition, and number of amino acid residues, peptides may differ in charge, size, shape, hydrophobicity, and binding capabilities. These physico-chemical properties allow their separation by the various capillary electromigration techniques, i.e., capillary zone electrophoresis (CZE), micellar electrokinetic chromatography (MEKC), capillary isoelectric focusing (CIEF), or capillary electrochromatography (CEC). The present chapter will focus on the analysis of peptides by CZE. Following a short general overview of peptide CE separations, important considerations for method development will be discussed and a practical example will be presented. For further details, including specifics of the other electromigration techniques in peptide analysis, the reader is referred to recent reviews ***(1–7)*** and book chapters ***(8,9)***.

1.1. Overview

1.1.1. Analyte Separation

In CE, analytes are separated on the basis of the applied field as a function of the physico-chemical properties, such as its charge density (charge-to-mass ratio), depending on the background electrolyte. The overall charge of the peptide is the sum of the charge of the deprotonated (negative) groups and protonated (positive) groups. Negatively charged groups can arise from the carboxyl acid terminus as well as the side chain groups of Asp, Glu, Cys, and Tyr. Groups that can be positively charged are the terminal amino function and the lateral groups of Lys, Arg, and His. The charge of a peptide at a certain pH value can be calculated provided that the exact pK_a values of the ionizable groups of a given peptide are known. However, the pK_a values of peptides are a complex function not only of the amino acid sequence but of the whole structure (i.e., the secondary and tertiary structure) of the peptides. For theoretical considerations approximations of the pK_a values can be used ***(1,8)***.

For the prediction of peptide mobility using the basic electrophoretic equation

$$\mu = \frac{q}{6\pi\eta r}$$

the Stokes radius, r, of the peptides must be known. As this information cannot be obtained from the amino acid sequence, two different approaches have been taken. The first approach correlates the radius to the number of amino acids elevated to the power of a parameter, whereas the second group of models use molecular weight, M_r, elevated to the power of different parameters ***(2**,**3**,**6**,**8)***. In several studies, good correlation between the electrophoretic mobility, μ, and the ratio q/M_r^A was observed with the parameter A between one-third and two-thirds. However, these models are mostly applicable only to a relatively narrow set of peptides differing not too much with respect to size, charge, and charge distribution.

Background electrolyte pH is the most important factor in CE, as it regulates the charge of the peptides. Theoretical considerations ***(8)*** suggest that the best resolution between peptides occurs at a pH value at which the peptide mobility is not very high. However, because short analysis time is often required, separations are often performed at a lower pH value where resolution is still good and peptide charge is high. Other requirements such as stability or suppression of wall interactions may also apply. Overall, good separations are often achieved at buffer pH close to the pK_a values of the terminal carboxyl group or side chain carboxyl groups when Asp or Glu are present. Further variables influencing the electrophoretic analyte mobility may have to be optimized if buffer pH modulation cannot achieve sufficient resolution. These factors include the ionic strength (concentration) of the buffer, capillary temperature, applied voltage, or the use of buffer additives such as organic solvents, surfactants, ion pair reagents, metal ions, or chiral selectors (*see* **1.2 Method Development**).

Different separation modes are available in CE. CZE (often simply also referred to as CE) is the most universal, most powerful, and most frequently used separation mode for peptide analysis. The peptides are resolved based on charge and size, i.e., differences in the electrophoretic mobility due to different charge densities. In MEKC, a detergent is added at concentrations above the critical micelle concentration, resulting in the formation of micelles as a pseudostationary phase. In this mode, analytes are separated based on the partition coefficients between the aqueous and the micellar phase. MEKC can be applied to the analysis of electroneutral (uncharged) peptides but it can also be utilized for charged compounds when sufficient resolution by CZE cannot be obtained. Analyte separation in capillary isotachophoresis (CITP) is based on the mobilities of the compounds between a leading electrolyte and a terminating electrolyte leading to distinct zone of the individual analytes immediately following each other. CITP as such has not been widely applied to peptide separations, but isotachophoretic principles are used in preconcentration stacking procedures. In CIEF, peptides are separated in a pH gradient based on their isoelectric point. However, because the effective charge of

small peptides similar to amino acids approaches zero over a rather broad pH range, the application of CIEF to oligopeptide analysis is rather limited. It is used for the characterization of large polypeptides as well as for the determination of microheterogeneity of polypeptides. Capillary gel electrophoresis (CGE) utilizing separations based on molecular size in sieving media (gels) is primarily used for the analysis of oligonucleotides and macromolecules such as DNA or proteins. CEC is considered a hybrid of HPLC and CE, combining the high peak efficiency of CE with the separation selectivity of a stationary phase. The driving force in CEC is the electroosmotic flow (EOF) generated upon application of the electric field along the capillary as a consequence of the charged surface of the capillary or the packing material. Although currently not considered a mature technique, CEC has been also applied to peptide analysis.

1.1.2. Detection

As for other analytes, the detection of peptides in CE can be a challenging task because of the microscale capillary dimensions and the small amount of injected sample. Ultraviolet (UV) detection in the short wavelength region at 200–220 nm is the most commonly used method of detection of peptides in CE. The absorbance in this UV region is due to the absorbance of the peptide amide bonds. Some structural information such as the presence of aromatic amino acids such as Phe, Tyr, or Trp can be obtained by scanning the UV spectrum when using a diode array detector (DAD). UV detection limits are typically not better than the low micromolar range (10^{-5}–10^{-6} M). Lower detection limits may be achieved by increasing the optical pathlength by applying different capillary detection cell geometries such as bubble cells or Z-cells. Another approach to increase the sensitivity is the derivatization of the peptides yielding derivatives with higher molar absorptivities ***(10,11)***.

Fluorescence as a more sensitive method of detectiing native peptides is only possible when the aromatic amino acids Tyr or Trp are present, but both amino acids are poor fluorophores and require excitation in the 210–290 nm wavelength range. Detection limits may be improved by a factor of 10–100. More commonly, laser-induced fluorescence (LIF) detection of peptides in CE is based on labeling the peptides with a fluorescent tag that can be excited at the wavelength of the commercially available He-Cd laser (325 nm) or argon-ion laser (488 nm). Several chemistries have been developed mostly derivatzing the amine residues in peptides ***(10,11)***. Examples include o-phthalaldehyde, naphthalene-2,3-dicarboxyladehyde, and fluoresceamine or 3-(4-carboxybenoyl)-2-quinoline carboxylaldehyde as reagents for primary amino groups. 9-fluorenylmethyl chloroformate and fluorescein isothiocyanate label primary and secondary amino groups. When multiple reactive sites are

available, the chemistry must be optimized to yield a single product. Derivatization is performed either after the CE separation (post-column) or more frequently before injecting the samples into the system (pre-column). Typically, the detection limit of LIF is in the 10^{-9} *M* range, corresponding to an increase in sensitivity of 1000 compared to UV detection.

Mass spectrometry (MS) is an ideal detection technique in peptide CE analysis, especially for complex mixtures of biomolecules ***(12)***. CE-MS not only allows high-accuracy determination of the relative moleuclar masses of the separated peptides but also provides important structural data on the amino acid sequence of sites of posttranslational modifications via tandem MS (MS/MS). Electrospray ionization (ESI) MS is the preferred mode for on-line coupling of CE with MS ***(13)***. Unfortunately, CE-ESI-MS is not extremely sensitive because a sheath liquid flow is necessary in most applications in order to obtain a stable electrospray. This results in a dilution of the sample with concomitant loss of sensitivity. Nevertheless, very sensitive applications have also been developed. Matrix-assisted laser desorption/ionization (MALDI) is applied primarily in the off-line mode. Experimental systems further evaluated Fourier transformation ion cyclotron resonance (FT-ICR) MS ***(14)***.

Further detection modes applied in CE peptide analysis include electrochemical, conductometric, and chemoluminescence detection, but no commercial detectors for CE employing these modes are available to date.

1.1.3. Suppression of Adsorption

It may be necessary to suppress the adsorption of larger peptides to the inner surface of unmodified fused-silica capillaries, whereas small peptides normally do not trend to adsorb to the capillary wall. Wall adsorption is primarily due to ionic interactions between the ionized silanol groups of the fused-silica wall and the peptides, especially basic peptides. Subsequently, several strategies for a suppression of wall adsorption may be employed. The analysis can be performed at extreme pH values of the background electrolyte where either the silanol groups are not dissociated (low pH) or the peptide is negatively charged (high pH), leading to electrostatic repulsion. High ionic strength buffers also reduce analyte–wall interactions as a result of competition of the buffer ions with the binding sites on the capillary wall. However, their use is limited as a result of the high electrical current generated, leading to excessive Joule heating and subsequent loss in separation efficiency. More appropriate and effective suppression of wall adsorption can be achieved by dynamic or permanent coating of the capillary surface blocking the silanol interaction sites for the analytes. Dynamic (reversible) coating can be performed by the addition of (oligo)amines, neutral polymers, or neutral and zwitterionic surfactants to the background electrolyte ***(15,16)***. Permanent coatings require the formation of

a chemical bond between the silanol groups of the fused silica capillary and the coating material usually a polymer. The reactions typically involve the formation of a covalent bond with a reagent containing a double bond and subsequent binding of a polymer to this intermediate layer. Several chemistries have been developed for the reproducible formation of hydrolytically stable, covalently bound polymers including poly(acrylamide) derivatives, polyvinyl alcohol, polyethylene glycol, and cellulose derivatives ***(16–18)***.

1.1.4. Sample Concentration

The concentration of peptides in synthetic samples usually does not represent a problem. However, for the analysis of compounds in biological samples preconcentration may be required in order to achieve the appropriate sensitivity. Generally, the same principles are applied in peptide CE analysis as for nonpeptide analytes. Sample concentration can be either performed off-line by solid-phase or liquid–liquid extraction or on-line by chromatographic or, more frequently, by electrophoretic stacking techniques. CE with on-line enrichment for the analysis of biological samples by chromatographic and electrophoretic preconcentration ***(19)*** as well as general sample stacking strategies ***(20)*** have been summarized. Further specific examples in peptide analysis can be found in **refs. *2***, ***3***, and ***6***.

1.1.5. Applications

The separation of peptides by CE has been described in numerous publications. Especially, the increasing number of recombinant DNA technology products has expedited the use of CE in peptide analysis as the major technique for peptide characterization as well as a complementary method to HPLC in quality control of synthetic and fermentation products. Any reaction resulting in a change of the charge and/or size of a peptide can be monitored by CE. These changes include degradation reactions such as hydrolysis, oxidation, or deamidation as well as posttranslational modifications such as glycosylation or phosphorylation. In addition, sample microheterogeneity resulting from multiple modification sites may be analyzed.

CE is primarily used as an analytical technique, although micropreparative applications have also been reported. Analytical CE of peptides can be divided into the following categories: (1) the use of peptides as model compounds to study fundamental aspects of CE or to demonstrate the feasibility of a certain concept or technique; (2) the analysis of synthetic peptides for purity control; (3) the analysis of bioactive peptides in biological samples; and (4) the analysis of peptide maps following tryptic digestion of proteins. Applications of CE to peptide analysis have been summarized in **Table 1**. Further examples include monitoring reactions such as homo- and heterodimer

Table 1
Examples of the Application of Capilary Electrophoresis to the Analysis of Peptides

Type of analysis	Examples
Peptide mapping	Growth hormones, erythropoietin, granulocyte stimulating factor, ovalbumin, human tissue plaminogen activator, somatotropin, interleukins
Peptide identification/ separation of closely related peptides	Natural and synthetic peptides including enkephalins, insulins, dynorphin analogs
Purity of peptides	Adrenocorticotropic hormone, endorphins, cholecystokinin, insulin, neuropeptide Y, hirudin, insulin-like growth factor, bradykinin, ginseng polypeptide, protergin IB-367, somatostatin, vasopressin
Peptide degradation/stability	Insulin, goserelin, Asp tripeptides, Asp hexapeptide, neuropeptide Y, LHRH analogs
Stereoisomer analysis	Di- tri- and tetrapeptides, *N*-derivatized peptides, peptide-derived drugs, neuropeptide Y
Bioanalysis of physiological peptides	Enkephalins, vasoactive intestinal peptide, cytokines, gonadorelin, angiotensin II, glutathione, neurotensin, vasopressin, somatostatin, thyreotropin-releasing hormone
Determination of reaction kinetics	Peptide oxidation, kinase and phosphatase activity, angiotensin-converting enzyme activity
Determination of pK_a	Di-, tri-and tetrapeptides, enkephalins, phosphinic pseudopeptides

formation, cis/trans interconversion of Pro-peptides, and peptide folding and unfolding as well as the complexation between peptides and natural or synthetic polymers (*see also* **refs. *1*–*9***).

A specific application of CE is the separation of peptides stereoisomers. Such analyses are important to monitor stereoisomer purity of synthetic peptides in quality control. Peptide diastereomers can often be separated in CE without chiral background electrolyte additives, as diastereomers differ in

their physico-chemical properties. Thus, careful manipulation of the buffer pH can exploit the small differences in the pK_a values. Most peptide diastereomer separations reported so far have been achieved in the acidic pH region. The resolution of peptide enantiomers can be performed by the indirect or direct method. The indirect method involves the derivatization with a stereochemically pure agent to form diastereomers, which can be subsequently separated in an achiral system ***(21,22)***. The direct enantioseparation is based on the formation of transient diastereomeric complexes between the analyte enantiomers and a stereochemically pure chiral selector. Native and derivatized cyclodextrins (CDs), the chiral crown ether (+)-(18-crown-6)-2,3,11,12-tetracarboxylic acid, the macrocyclic antibiotics vancomycin and teicoplanin, chiral ligand exchange complexation, and chiral ion pair formation have been applied for peptide enantioseparations ***(21,22)***.

1.2. Method Development

Generally, method development in CE analysis of peptides follows the principal considerations for method development of nonpeptide analytes. The effect of important variables on peptide analysis will be briefly discussed here; a more general and detailed discussion of the various parameters can be found in the literature ***(23,24)***.

1.2.1. Separation Capillary

In CE, the resolution and efficiency are proportional to the length of the capillary under a constant electric field. Efficiency and migration times increase linearly while resolution depends on the square root of length. Therefore, improving efficiency and resolution by increasing the length of the capillary occurs at the expense of increased analysis time. Generally, longer capillaries may be required for the analysis of complex mixtures whereas short capillaries are preferred for less complex mixtures or in the case of very long analysis times.

With respect to the inner diameter (ID) of the capillary, some loss of efficiency and resolution is observed when increasing the capillary diameter. Small-ID capillaries allow the use of higher ionic strength buffers and higher applied voltages because less Joule heat is generated. The capillary diameter has only little effect on the EOF. On the other hand, the sensitivity increases with diameter because the optical path is increased. Moreover, large-bore capillaries allow higher mass loading.

The temperature of the capillary has significant effects on the viscosity of the background electrolyte, the electric current, and the migration time. Therefore, efficient capillary temperature control is required for reproducible analyses.

Increasing the temperature results in a lower viscosity of the separation buffer and faster electrophoretic mobility of the analytes (**Fig. 1**). Both are inversely proportional to temperature. High temperatures also result in high currents. In addition, temperature can affect analyte solubility and buffer pH, resolution, and efficiency. High temperatures should be avoided when organic solvents are used as buffer additives.

In CE peptide separations, unmodified fused-silica capillaries are used most often. If surface interaction of the analytes is observed, intermediate rinses with sodium hydroxide solutions may be required. Alternatively, coated capillaries can be used to suppress wall interactions. Hydrophilicity and hydrophobicity of the inner wall can be manipulated. In addition, coated or surface-modified capillaries modify, stabilize, eliminate, or reverse the EOF by producing a stable, reproducible surface. Surface coating may also alter the separation

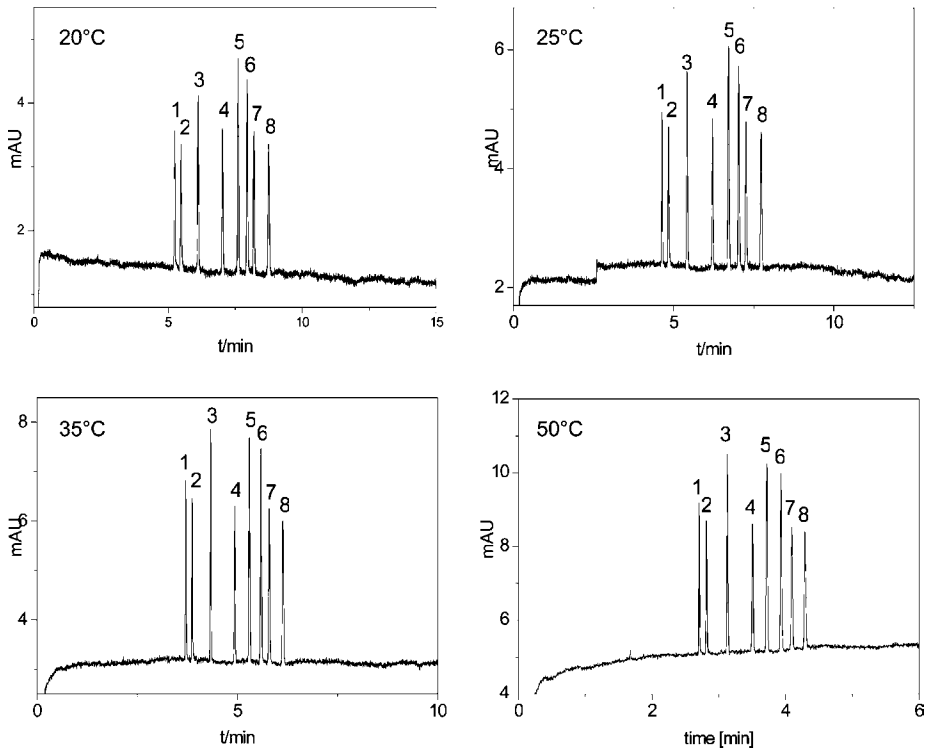


Fig. 1. Separation of model peptides at different temperatures. Experimental conditions: fused-silica capillary, 50 cm effective length, 57 cm total length, 50 μm inner diamter; 50 m*M* sodium phosphate buffer, pH 2.7; 25 kV; detection wavelength 215 nm. For peptide identification, *see* **Table 2**.

selectivity. For the various chemistries for dynamic and permanent surface modifications, *see* **refs. *16–18***.

1.2.2. Applied Voltage

The applied voltage affects efficiency, resolution, and migration time **(Fig. 2)**. Efficiency and resolution increase with increasing voltage while migration time decreases. However, high voltage produces high Joule heat. The optimum applied voltage can be derived from an Ohm's plot depicting the current as a function of the applied voltage. Deviation of current from the linear relationship signals the generation of Joule heat. Certain buffers, such as the so-called "Good's buffers," produce only relatively low currents even at high concentrations. It has also been shown that it may be feasible to use a voltage gradient during the electrophoretic run instead of a constant applied voltage in order to increase the separation efficiency ***(25)***.

1.2.3. Separation Buffer

In CE, solute migration velocity, separation efficiency, and peak shape are sensitive to characteristics of the buffer (background electrolyte). The buffer controls not only the ionization and migration of the analytes but also the magnitude of the EOF, which is driven by the residual charges of the inner wall of the separation capillary. Moreover, the buffer capacity must be high enough to ensure that the local pH and conductivity will not change as the result of the introduction and migration of the sample across the capillary. Additional factors that should be considered when selecting an appropriate buffer in CE are the compatibility of the background electrolyte with the stability of the analytes and other additives, running current (see applied voltage above), or UV absorbance. A detailed discussion can be found in **ref. *26***.

The pH of the separation buffer is the most important parameter for optimizing the separation selectivity. Although CE peptide analysis has been reported over a wide range of pH, two pH regions appear to be especially useful. At low pH, i.e., pH 2.0–4.0, the basic groups of the peptides are protonated and the peptides migrate as cations. Selectivity (differences in the electrophoretic mobilities) can be achieved by exploiting small differences in the dissociation equilibria of the acidic groups. The pK_a of the C-terminal carboxyl groups is around 3, the pK_a of side chain carboxyl groups of Asp and Glu range between 3.5 and 4.5. The exact pK_a depends not only on the individual amino acid but also on the amino acid sequence and the microenvironment within the peptide, resulting in small pK_a differences even of closely related peptides that can be exploited for their CE separation. In addition, at pH less than 3.0, the dissociation of the silanol groups of the capillary wall is negligible so that wall adsorption of analytes onto the surface is suppressed.

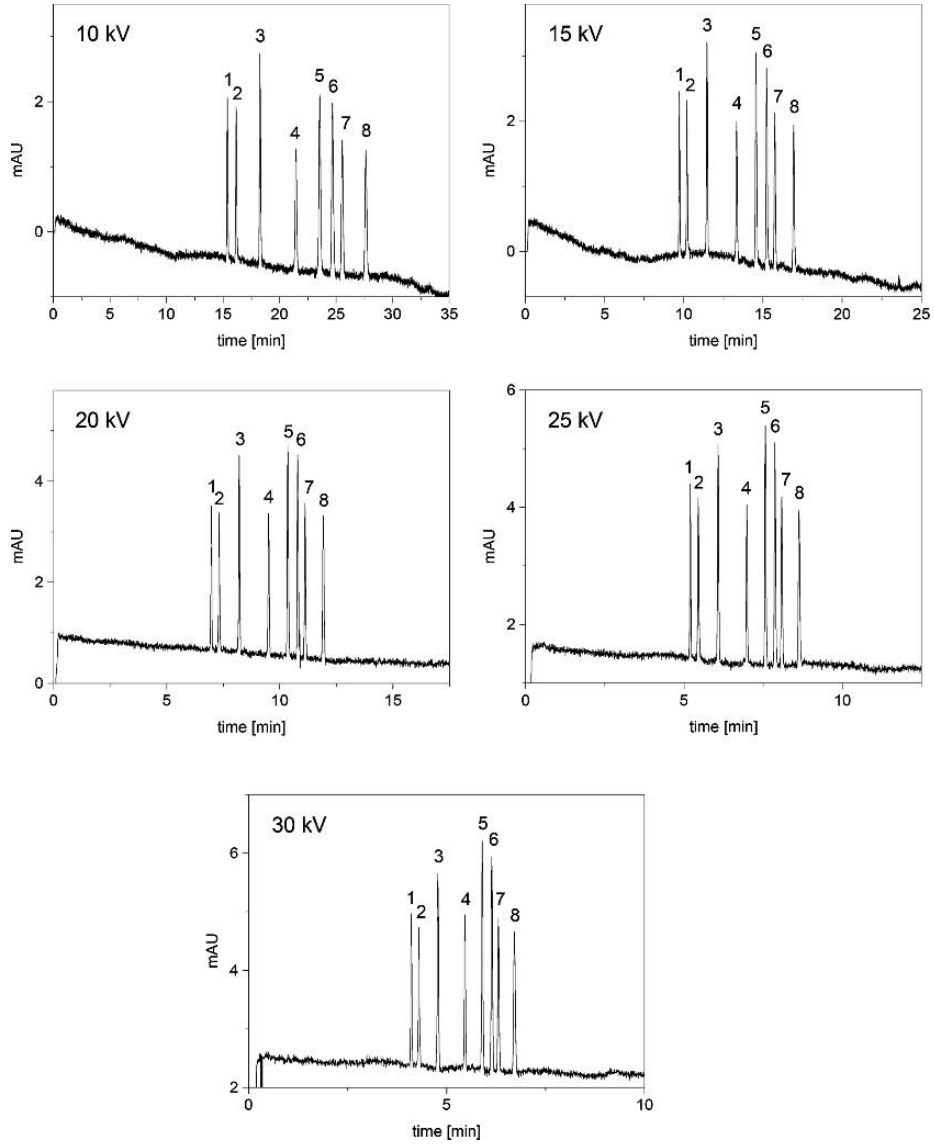


Fig. 2. Separation of model peptides at different applied voltages. Experimental conditions: fused-silica capillary, 50 cm effective length, 57 cm total length, 50 μm inner diameter; 50 m*M* sodium phosphate buffer, pH 2.7; 20 °C; detection wavelength 215 nm. For peptide identification, *see* **Table 2**.

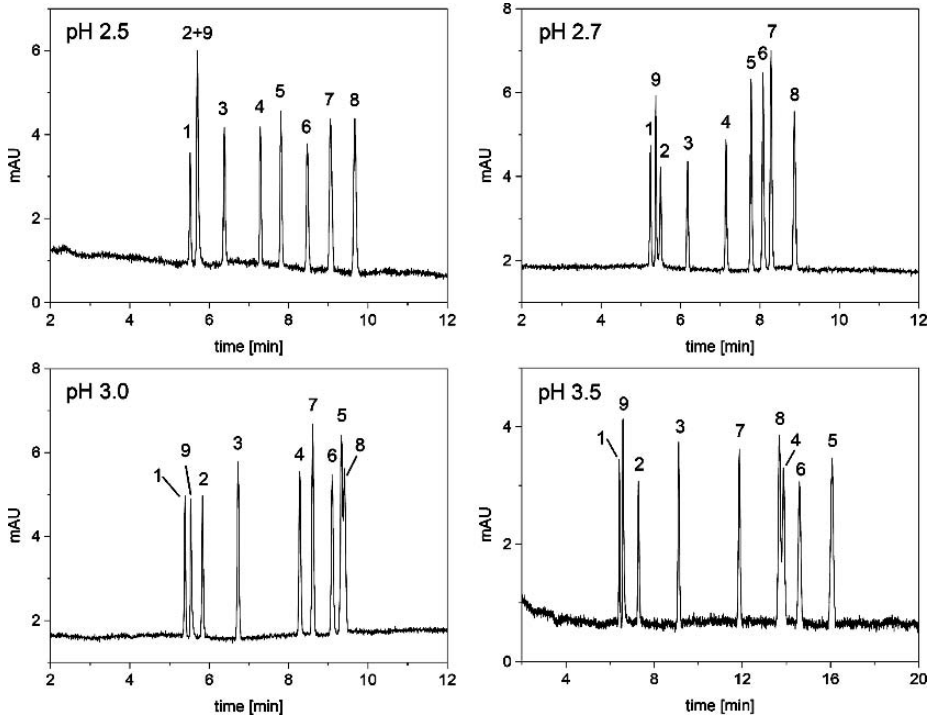


Fig. 3. Separation of model peptides at different buffer pH values. Experimental conditions: fused-silica capillary, 50 cm effective length, 57 cm total length, 50 μm inner diameter; 50 m*M* sodium phosphate buffer; 25 kV, 20 °C; detection wavelength 215 nm. For peptide identification, *see* **Table 2**.

Figure 3 illustrates the effect of pH between 2.5 and 3.5 for a set of nine peptides. At pH 2.5, two peptides comigrate (bradykinin and angiotensin I). Increasing the pH results in a separation of these two peptides, but interference between other peptides is observed. In addition, the migration order of peptides 5–8 changes. For example, the dipeptide L-Ala-D-Phe (peptide 5) migrates faster than the tripeptide Gly-Leu-Tyr (peptide 6) below pH 3.0, whereas the migration order is reversed at pH values of 3.0 and above. Apparently the carboxylic acid group of L-Ala-D-Phe is more acidic, resulting in a lower overall positive charge of the smaller peptide that translates into slower electrophoretic migration at pH 3.0 and above. An example of the separation of closely related peptides based on differences in the pK_a values is shown in **Fig. 4**. The peptides differ only in the position of the amide bond with respect to Asp. In one peptide, Asp is connected to the following amino acid via the α-carboxyl group, whereas the amide bond is formed with the β-carboxyl

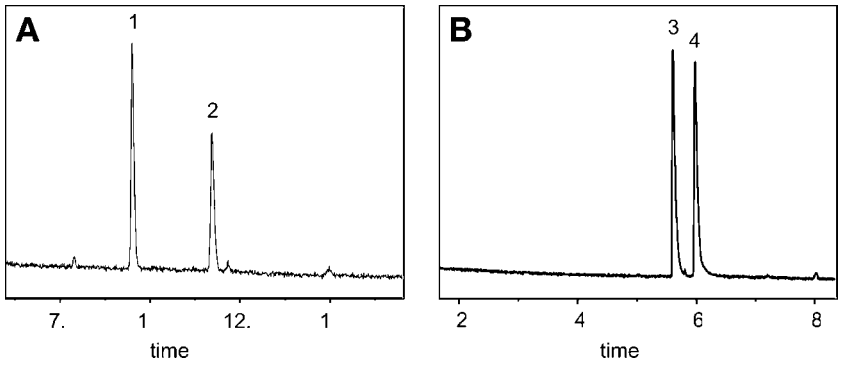


Fig. 4. Separation of α-Asp and β-Asp peptides. **(A)** Isomeric angiotensin 2 peptides Asp-Arg-Val-Tyr-Ile-His-Pro-Phe (1) and β-Asp-Arg-Val-Tyr-Ile-His-Pro-Phe (2); **(B)** isomeric β-amyloid peptide fragment (4) Phe-Arg-His-Asp-Ser-Gly (3) and Phe-Arg-His-β-Asp-Ser-Gly. Experimental conditions: fused-silica capillary, 40 cm effective length, 47 cm total length, 50 μm inner diameter; 50 m*M* sodium phosphate buffer, pH 2.5 **(A)** or pH 3.0 **(B)**; 20 kV, 20 °C; detection wavelength 215 nm.

group of the side chain of Asp in the case of the other peptide (so-called β-Asp linkage). Moreover, peptide diastereomers can also be separated at acidic pH because of small differences in the dissociation equilibria of the diastereomers. This is illustrated by the separation of L-Ala-L-Phe and L-Ala-D-Phe in **Fig. 3** as well as by the examples of the pair of isomeric tripeptides Phe-Asp-GlyNH_2 and Phe-β-Asp-GlyNH_2 in **Fig. 5**. The latter example shows the simultaneous separation of isomeric α-Asp and β-Asp peptides and their diastereomers.

Phosphate buffers are often used at acidic pH values. Substituting the buffer cation by organic amines such as triethylamine or triethanolamine may be beneficial for peptide separations. The amines are positively charged at low pH, covering residual charges on the capillary wall and, thus, suppressing analyte wall interactions. In addition, an anodic EOF is generated, often resulting in increased efficiency. **Figure 6** compares the effect for a mixture of peptides at pH 2.7 using sodium phosphate buffer and triethanolamine-phosphate buffer obtained by titration of phosphoric acid with triethanolamine to pH 2.7.

A further useful pH range, especially for basic peptides, is pH 8.0–10.0. At this pH, the peptides bear negative charges and migrate as anions. The dissociation equilibria of basic groups can be targeted to achieve selectivity. The pK_a values of peptide N-termini rage between 7.5 and 9 depending on the amino acid whereas pK_a values of His and Lys are about 6 and 10, respectively. The pK_a of Arg is too high to be useful. At high pH, the fused-silica silanol groups are also deprotonated so that the adsorption of peptides onto the capillary wall is minimized as a result of electrostatic repulsion.

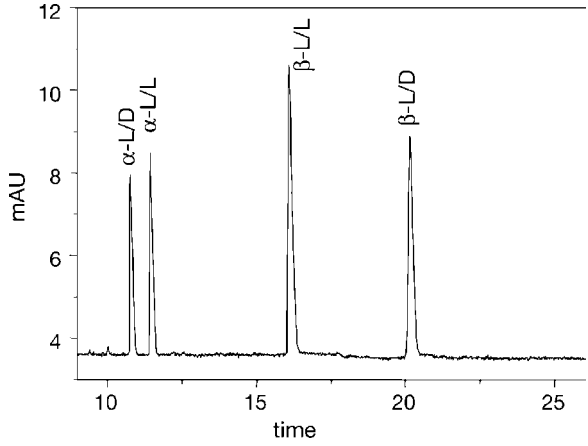


Fig. 5. Simultaneous separation of the diastereomers of the isomeric tripeptides Phe-α-Asp-GlyNH_2 and Phe-β-Asp-GlyNH_2. Experimental conditions: fused-silica capillary, 40 cm effective length, 47 cm total length, 50 μm inner diameter; 50 m*M* sodium phosphate buffer, pH 3.0; 23 kV, 20 °C; detection wavelength 215 nm.

Buffer capacity must be high enough to provide a stable pH throughout the separation. The capacity is directly proportional to the overall concentration of the buffer as well as the concentration ratio of the acidic and basic buffer

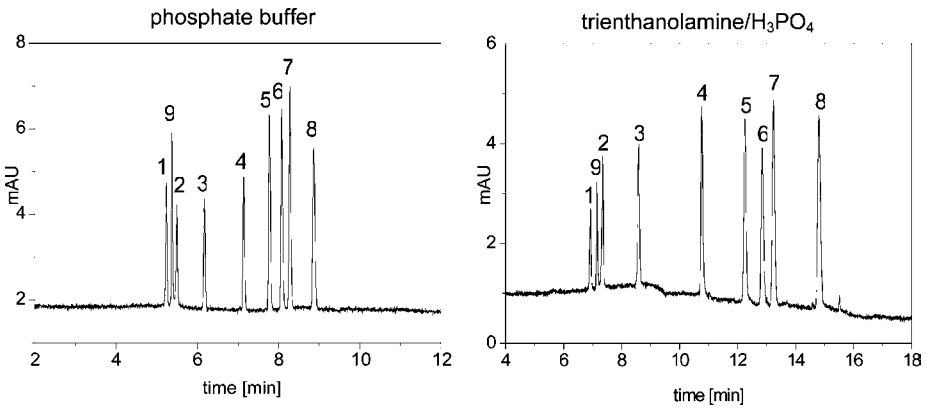


Fig. 6. Influence of the buffer type on the separation of model peptides. **(A)** 50 m*M* sodium phosphate buffer, pH 2.7; **(B)** 50 m*M* phosphoric acid titrated to pH 2.7 with triethanolamine. Experimental conditions: fused-silica capillary, 50 cm effective length, 57 cm total length, 50 μm inner diameter; 25 kV, 20 °C; detection wavelength 215 nm. For peptide identification, *see* **Table 2**.

species. A buffer is most effective at pH values close to the pK_a of the buffer acid. Generally, a buffer should only be applied in the pH range within ±1 U of the pK_a. High buffer concentrations (ionic strength) reduce analyte wall interactions, EOF, and electrophoretic analyte mobility, resulting in an increase in resolution and efficiency **(Fig. 7)**. In addition, analyte stacking effects can be achieved using high concentrations of separation buffers. On the other hand, the concentration of the electrolytes influences the electrical current and Joule heating, thus limiting the buffer concentration. Buffer anions as well as buffer cations can influence the EOF, analyte mobility, selectivity, and resolution so that careful adjustment of the buffer can improve a separation. A special class of buffers are the so-called isoelectric buffers. These buffers, consisting of amphoteric compounds such as cysteic acid, iminodiacetic acid, aspartic acid,

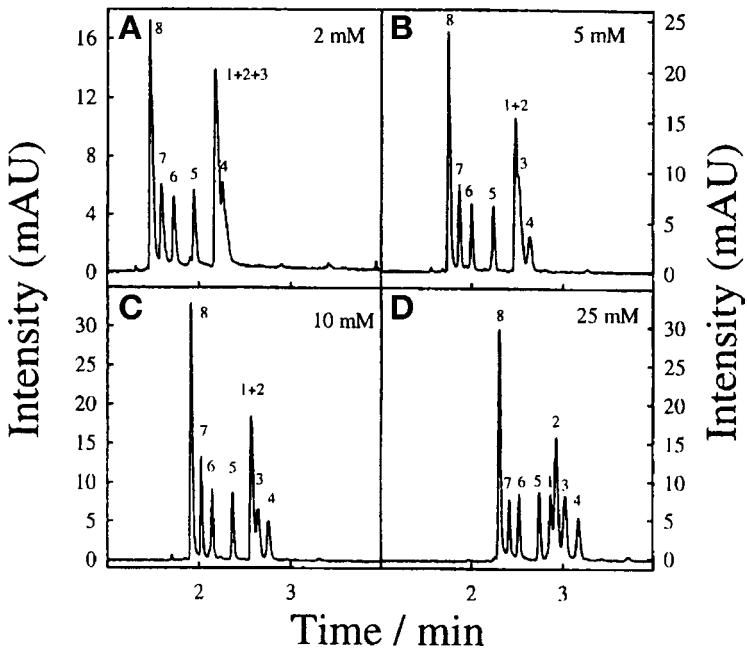


Fig. 7. Influence of buffer concentration on the separation of a mixture of synthetic peptides. Experimental conditions: fused-silica capillary, 8.5 cm effective length, 37 cm total length, 100 μm inner diameter; sodium phosphate buffer, pH 2.0; −6.8 kV, 22 °C; detection wavelength 214 nm. Peptides: 1, Asp-His-Asp-Ile-Asn-Arg; 2, Trp-Asp-His-Asp-Ile-Asn-Arg; 3, Ser-Trp-Asp-His-Asp-Ile-Asn-Arg; 4, Asn-Ser-Trp-Asp-His-Asp-Ile-Asn-Arg; 5, His-Asn-Ser-Trp-Asp-His-Asp-Ile-Asn-Arg; 6, His-His-Asn-Ser-Trp-Asp-His-Asp-Ile-Asn-Arg; 7, His-His-His-Asn-Ser-Trp-Asp-His-Asp-Ile-Asn-Arg; 8, his-His-His-Asn-Ser-Trp. Reprinted from **ref. *30***, with permission.

or glutamic acid, possess a much lower conductivity compared to ionic salt buffers so that high operating voltages can be applied. For a detailed discussion of the theory and application of these buffers, *see* **ref. *27***.

1.2.4. Buffer Additives

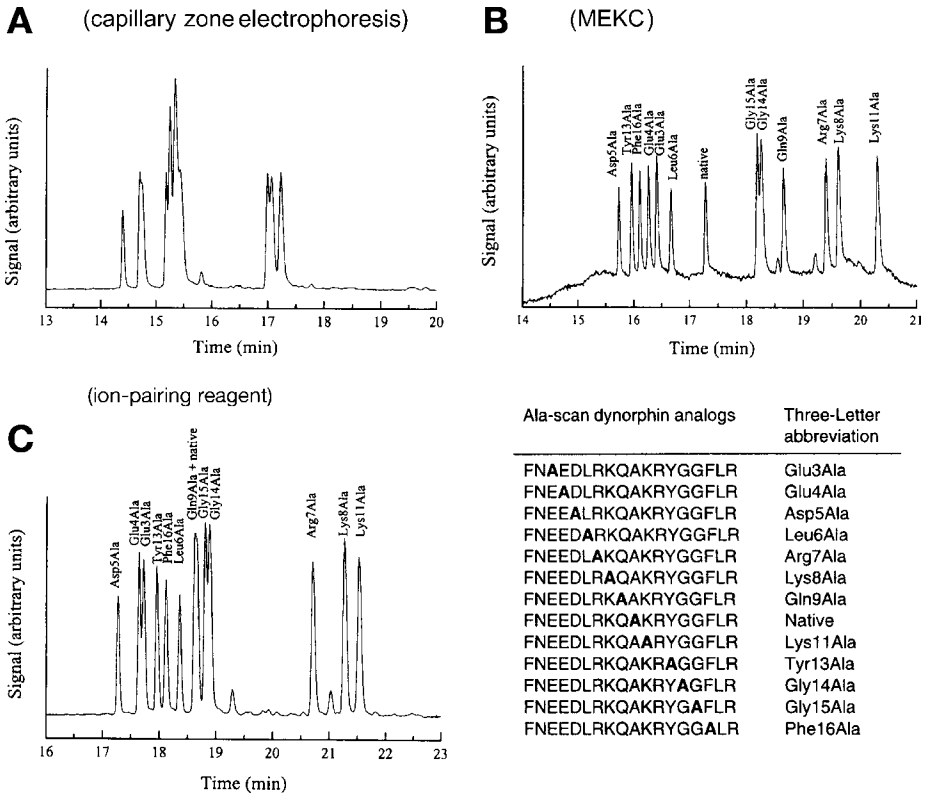
If pH optimization does not result in a sufficient resolution, buffer additives can be applied in order to maximize differences between the analytes and/or suppress undesired interactions. The most important classes of additives will be briefly addressed. Additives may be combined.

Organic solvents such as methanol, ethanol, 1-propanol, 2-propanol, or acetonitrile modify buffer viscosity, separation selectivity, and EOF. The electrical current decreases as the concentration of the organic solvent is increased. The effect of the organic solvents on a separation is difficult to predict. Acetonitrile typically leads to an increase of the EOF and a reduction of the analysis time whereas methanol increases the migration time of the analytes. Trifluoroethanol has also been successfully applied to peptide separations ***(28)***. Organic solvents also affect the dissociation equilibria of solutes resulting in a change of the electrophoretic mobility compared to pure aqueous buffers. Thus, resolution and separation efficiency can change.

The addition of detergents above the critical micelle concentration (cmc) yields micelles as pseudostationary phase. This separation mode, MEKC, was developed for the separation of neutral (uncharged) analytes. A separation is based on the partitioning of the analytes between the micelles and the buffer according to the lipophilicity of the compounds. With respect to peptide analysis, MEKC is suitable for the separation of hydrophobic peptides and peptides derivatized at the N- or C-terminus. But the method can also be employed to modulate the selectivity in the separation of closely related charged peptides by introducing lipophilicity as an additional differentiating parameter. Sodium dodecyl sulfate (SDS) is probably the most frequently used surfactant in MEKC, working well in alkaline to neutral pH buffers, but separations in low pH buffers have also been reported. Cationic surfactants, for example cetyltrimethylammonium bromide (CTAB) or dodecyltrimethylammonium bromide (DTAB), reverse the EOF as a result of the formation of a bilayer producing a positively charged capillary surface. Zwitterionic surfactants such as 3-[(3-cholamidopropyl)dimethylammonio]-1-propanesulfonate (CHAPS) and neutral detergents (for example, derivatives of the Tween or Brij series), as well as combinations of detergents, have also been used. Altering the nature of the surfactant greatly affects the analyte interactions with the micelles and, therefore, separation selectivity and analyte migration order. Detergents are often combined with organic solvents or CDs. For a detailed discussion on theoretical considerations and surfactant selection in MEKC of peptides,

see **ref. *29***. **Figure 8** illustrates the effect of MEKC in the separation of a set of dynorphin analogs obtained by an Ala scan using the zwitterionic detergent CHAPS as additive.

Addition of ion-pair reagents, for example, trifluoroacetic acid or the sodium salts of alkylsulfonic acids such as hexanesulfonic acid or heptanesulfonic acid, have been especially useful for the separation of smaller hydrophilic peptides. The ion-pair reagent neutralizes ionic groups of opposite charge and increases



Ala-scan dynorphin analogs	Three-Letter abbreviation
FN**A**EDLRKQAKRYGGFLR	Glu3Ala
FNE**A**DLRKQAKRYGGFLR	Glu4Ala
FNEE**A**LRKQAKRYGGFLR	Asp5Ala
FNEED**A**RKQAKRYGGFLR	Leu6Ala
FNEEDL**A**KQAKRYGGFLR	Arg7Ala
FNEEDLR**A**QAKRYGGFLR	Lys8Ala
FNEEDLRK**A**AKRYGGFLR	Gln9Ala
FNEEDLRKQ**A**KRYGGFLR	Native
FNEEDLRKQA**A**RYGGFLR	Lys11Ala
FNEEDLRKQAK**A**GGFLR	Tyr13Ala
FNEEDLRKQAKRY**A**GFLR	Gly14Ala
FNEEDLRKQAKRYG**A**FLR	Gly15Ala
FNEEDLRKQAKRYGG**A**LR	Phe16Ala

Fig. 8. Comparison of the separation of peptides in **(A)** capillary zone electrophoresis mode, **(B)** micellar electrokinetic chromatography mode, and **(C)** addition of an ion-pair reagent. Experimental conditions: fused-silica capillary 61.2 cm effective length, 69.7 cm total length, 50 mm inner diameter; **(A)** 100 m*M* sodium phosphate buffer, pH 3.5, **(B)** 100 m*M* sodium phosphate buffer, pH 3.5, containing 35 m*M* 3-[(3-cholamidopropyl)dimethylammonio]-1-propanesulfonate (CHAPS), and **(C)** 100 m*M* sodium phosphate buffer, pH 3.5, containing 100 m*M* 1-hexanesulfonic acid sodium salt; 25 kV, 17 °C; detection wavelength 200 nm. Modified from **ref. *31***, with permission.

the hydrodynamic radius of the analytes. In addition, the ionic strength of the background electrolyte is increased and the EOF is reduced. The combined effects may or may not improve the resolution depending on the nature of the analytes. In addition, selectivity changes may be observed. An example comparing the separation of dynorphin analogs using "plain" buffer and upon addition of the ion-pair reagent hexanesulfonic acid sodium salt is illustrated in **Fig. 8**.

CDs are typically employed as chiral selectors for enantioseparations. CDs are cyclic oligosaccharides. The most commonly used compounds are α-CD, β-CD and γ-CD consisting of 6, 7, and 8 α-1,4-linked glucopyranose units, respectively. Many neutral and charged derivatives especially of β-CD are commercially available. CDs have the shape of a truncated cone with a hydrophobic cavity and a hydrophilic outer side. They form complexes with a variety of solutes by inclusion of lipophilic moieties of these molecules into the cavity. CDs have been effectively used for the separation of the enantiomers of small peptides (for a review also on the use of other chiral selectors for peptide enantioseparations, *see* **refs. *21***, ***22***). However, the compounds can also be used to alter resolution and selectivity of peptide separations when the chiral resolution of analytes is not an issue. Complexation results in an altered hydrodynamic radius and, subsequently, in a different electrophoretic mobility of the solutes.

Further additives include amines, zwitterions, urea, soluble polymers, water-miscible solvents with high viscosity, and metal ions. (Poly)amines are modifiers of the EOF and suppress analyte–wall interactions, as do soluble polymers. Metal ions such as Zn^{2+} can be useful for the analysis of His-containing peptides.

1.2.5. Sample Matrix and Injection

The type of sample matrix can range from a (simple) aqueous solution to a complex biological sample such as plasma. Interactions of matrix components with analytes or the capillary wall may be the reason for reduced efficiency and reproducibility. Ideally, the sample has a lower conductivity than the run buffer, allowing on-line focusing (stacking) of the components. High salt content of the sample results in peak broadening. In addition, the injected amount of the sample should be considered. The injected amount can be increased either by increasing the sample concentration or by applying longer injection times. Although sufficiently high concentrations are needed to achieve the desired sensitivity, concentrations that are too high lead to mass overload. A long injection plug, i.e., the use of long injection times, results in reduced resolution.

1.2.6. Method Development Strategy

According to the points outlined above, a successful method development strategy includes evaluation of the following parameters:

1. Peptide solubility: ensure that the analytes are soluble and stable in all separation solutions. If large amounts of organic solvents are necessary, evaluate the application of MEKC for peptide analysis.
2. Capillary dimensions: a fused-silica capillary with an effective length of 40–50 cm and an inner diameter of 50 μm is a good first choice with respect to resolution, effective heat dissipation, and detection sensitivity. For increased detection sensitivity or increased mass loading capacity, capillaries with larger inner diameters (100–200 μm) may be required. Coated capillaries can be used for specific applications and modification of the EOF.
3. Capillary temperature: 20–25 °C is a good starting point. For fast separations, use 30–60 °C; for high-concentration buffers or difficult separations, 15–20 °C may apply. For optimization, vary the temperature in 5-Kelvin increments.
4. Optimization of buffer pH: pH 2.5–4.0 (pK_a of acidic groups) and pH 8.0–10.0 (pK_a of basic groups) can be used for most peptides. The buffer should be selected to provide good pH control of the specific pH (pK_a of buffer acid close to pH). Optimization of the pH should be performed in 0.1- to 0.5-pH increments.
5. Optimization of buffer concentration: start with 50–100 m*M* buffers for 50 μm ID capillaries. Use higher ionic strength buffers for the separations of closely related peptides or if a large number of peptides must be analyzed simultaneously.
6. Optimization of separation voltage: construction of an Ohm's plot (observed current vs applied voltage) for a given separation buffer indicates the voltage that will give the best resolution and efficiency within the shortest analysis time. Use 2.5- to 5-kV increments for the construction of Ohm's plots.
7. Selection of buffer additives: the use of buffer additives may be required in order to maximize selectivity and/or to mask interactions. Organic solvents (1–50%) increase the solubility of lipophilic peptides and modify the EOF. Ionic surfactants (5–200 m*M*, depending on the surfactant) can be applied in the case of hydrophobic and neutral peptides; the additional use of nonionic surfactants (5–50 m*M*) or organic solvents (1–20%) can modify analyte partitioning. Ion-pair reagents (10–100 m*M*) are effective for the separation of small hydrophilic peptides. CDs (10–50 m*M*) may also be used for selectivity enhancement for separations of smaller peptides. (Poly)amines and soluble polymers suppress hydrophobic interactions between peptides and the capillary wall.

2. Materials

1. A commercially available CE apparatus (for example, Beckman P/ACE 5500, Beckman, Fullerton, CA) with a high voltage source (up to 30 kV) and UV or photodiode array detector should be used (*see* **Note 1**). The capillary was kept at a constant temperature of 20 °C. Uncoated fused-silica capillaries (for example, from Polymicro Technologies, Phoenix, AZ) with an internal diameter of 50 μm

Table 2
Peptides and Amino Acid Sequence

No.	Amino acid sequence	Peptide
1	Arg-Val-Tyr-Ile-His-Pro-Phe	angiotensin III
2	Asp-Arg-Val-Tyr-Ile-His-Pro-Phe-His-Leu	angiotensin I
3	Asp-Arg-Val-Tyr-Ile-His-Pro-Phe	angiotensin II
4	L-Ala-L-Phe	
5	L-Ala-D-Phe	
6	Gly-Leu-Tyr	
7	Trp-Met-Asp-PheNH_2	gastrin tetrapeptide
8	Tyr-Gla-Gly-Phe-Leu	leucine enkephalin
9	Arg-Pro-Pro-Gly-Phe-Ser-Pro-Phe-Arg	bradykinin

were used for the separations presented below. The effective length of the capillary was 50 cm while the total length was 57 cm.

2. Conditioning of the capillary: the following solutions are required:
   a. 0.1 *M* sodium hydroxide solution.
   b. 0.1 *M* phosphoric acid.
   c. Double-distilled water.
3. Separation buffer: the separation buffer is prepared by dissolution of 50 m*M* sodium dihydrogen phosphate monohydrate ($NaH_2PO_4 \times H_2O$) in double-distilled water. The pH is adjusted using 0.1 *M* phosphoric acid under control of a pH meter (*see* **Notes 2** and **3**). The buffer solution is filtered through a 0.47-μm membrane filter and degassed by sonication.
4. Peptide analytes: the peptides, e.g., L-Ala-L-Phe, L-Ala-D-Phe, Gly-Leu-Tyr, gastrin tetrapeptide, leucine enkephalin, angiotensin I, angiotensin II, angiotensin III, and bradykinin were obtained from commercial sources (for example, Sigma-Aldrich, Bachem, or Calibochem) and used without further purification. Stock standard solutions of 500 μg/mL are prepared by dissolution of the solid peptide preparations in double-distilled water. In some cases, the addition of 0.2% phosphoric acid is required for complete dissolution of the peptide. Before injection the stock solution is diluted 1:10 with double-distilled water (*see* **Table 2**).

3. Methods

3.1. Preconditioning of the Fused-Silica Capillary

1. Rinse the capillary hydrodynamically (at an inlet pressure of about 140 kPa) with 0.1 *M* phosphoric acid for 10 min and then with 0.1 *M* aqueous sodium hydroxide solution for 20 min.
2. Wash the capillary hydrodynamically with water for 5 min.
3. Flush the capillary hydrodynamically with separation buffer for 10 min.

4. Between the runs, rinse the capillary with 0.1 *M* sodium hydroxide solution for 2 min followed by separation buffer for 2 min (see Note **4**).

3.2. Injection of the Sample Solution

Sample solutions were introduced hydrodynamically at a pressure of 3.5 kPa (0.5 p.s.i.) for 3 s (*see* **Note 5**).

3.3. CE Analysis

After conditioning of the capillary (*see* **Note 4**) and introduction of the analyte solution, the CE measurement is carried out at a high voltage of +25 kV. The UV detection wavelength is set at 215 nm. The separation is monitored by personal computer controlling the CE instrument. Typical electropherograms of the separation of the peptides at pH 2.5–3.5 are shown in **Fig. 3** (*see* **Note 6**).

4. Notes

1. Different CE instruments from the same supplier as well as instruments from different companies may yield slightly different results using otherwise identical experimental procedures. Thus, the variables may require slight changes when transferring a certain analytical method from one instrument to another. Therefore, fine tuning of the parameters of a published method can be necessary.
2. Preparation of buffers according to different procedures yields buffers that differ in concentration, which may affect the separation selectivity as discussed above. For example, a 50 m*M* phosphate buffer, pH 2.5, may be prepared (1) by mixing 50 m*M* sodium dihydrogen phosphate (monobasic sodium phosphate, NaH_2PO_4) and 50 m*M* disodium hydrogen phosphate (dibasic sodium phosphate, Na_2HPO_4) in appropriate proportions to obtain the desired pH, (2) by adjusting 50 m*M* phosphoric acid to pH 2.5 by addition of a sodium hydroxide solution, and (3) by adjusting 50 m*M* sodium dihydrogen phosphate to pH 2.5 by addition of diluted phosphoric acid. In the first case, the buffer concentration is 50 *M* with respect to phosphate; in the second case, the molarity of phosphate is below 50 m*M*; and in the third case, phosphate molarity is higher than 50 m*M*. The deviation from the desired molarity will depend on the dilution of the sodium hydroxide solution and phosphoric acid used for pH adjustment. In addition, when using different salts, e.g., the potassium or lithium phosphate salts, or different bases, e.g., potassium hydroxide or lithium hydroxide, for the preparation, the resulting buffers differ in the counterions, which may also affect a separation. Thus, careful characterization of the buffer is required for reproducible results. In addition, buffers can only be stored for a limited period of time even at low temperatures.
3. Because of the temperature dependence of dissociation equilibria, buffer pH should be adjusted at the temperature that is used during the electrophoretic run. Specifically, the change of the pK_a per Kelvin (or degree Celsius) of organic zwitterionic buffers is significant.

4. Conditioning of the capillary is important in order to obtain reproducible conditions of the inner wall of the capillary. Therefore, careful preconditioning of the capillary is required. Moreover, it is necessary to include all rinsing steps in validation procedures when developing CE procedures for quality control. Capillaries from different manufacturers may also produce different results.
5. When applying hydrodynamic injection, the amount of the sample that is actually injected may vary depending on the temperature or the viscosity of the solution. Thus, adjustment of the injection time and/or pressure may be required. In the present example, the samples were injected at ambient temperature.
6. The separation between bradykinin (peptide 9) and angiotensin I (peptide 2) at pH 2.7 may not always be achieved, depending on the commercial source and separation "history" of the capillary. If baseline resolution cannot be achieved with the present capillary, a longer separation capillary or increased buffer concentration may fix the problem. If the buffer pH is raised to 2.8, comigration of Gly-Leu-Try (peptide 6) and gastrin tetrapeptide (peptide 7) is observed.

References

1. Messana, I., Rossetti, D. V., Cassiano, L., Misiti, F., Giardina, B., and Castagnola M. (1997) Peptide analysis by capillary (zone) electrophoresis. *J. Chromatogr. B*. **699**, 149–171.
2. Kasicka, V. (1999) Capillary electrophoresis of peptides. *Electrophoresis* **20**, 3084–3105.
3. Kasicka, V. (2001) Recent advances in capillary electrophoresis of peptides. *Electrophoresis* **22**, 4139–4162.
4. Hearn, M. T. W. (2001) Peptide analysis by rapid, orthogonal technologies with high separation selectivities and sensitivities. *Biologicals* **29**, 159–178.
5. Hu, S. and Dovichi, N. J. (2002) Capillary electrophoresis for the analysis of biopolymers. *Anal. Chem*. **74**, 2833–2850.
6. Kasicka, V. (2003) Recent advances in capillary electrophoresis and capillary electrochromatography of peptides. *Electrophoresis* **24**, 4013–4046.
7. Bandilla, D., Skinner, C. D. (2004) Capillary electrochromatography of peptides and proteins. *J. Chromatogr. A* **1044**, 113–129.
8. Castagnola, M., Messana, I., and Rossetti, D. V. (1996) Capillary zone electrophoresis for the analysis of peptides, in *Capillary Electrophoresis in Analytical Biotechnology* (Hancock, W. S., ed.) CRC, Boca Raton, FL: pp. 239–275.
9. Van de Goor, T., Apffel, A., Chakel, J., and Hancock, W. (1997) Capillary electrophoresis of peptides, in *Handbook of Capillary Electrophoresis*, 2nd ed. (Landers, J. P., ed.) CRC, Boca Raton, FL: pp. 213–258.
10. Underberg, W. J. M. and Waterval, J. C. M. (2002) Derivatization trends in capillary electrophoresis: an update. *Electrophoresis* **23**, 3922–3933.
11. Bardelmeijer, H. A., Waterval, J. C. M., Lingeman, H., et al. (1997) Pre-, on-, and post-column derivatization in capillary electrophoresis. *Electrophoresis* **18**, 2214–2227.

12. Hernandez-Borges, J., Neususess, C., Cifuentes, A., and Pelzing, M. (2004) On-line capillary electrophoresis-mass spectrometry for the analysis of biomolecules. *Electrophoresis* **25**, 2257–2281.
13. Moini, M. (2004) Capillary electrophoresis-electrospray ionization mass spectrometry of amino acids, peptides and proteins, in *Capillary Electrophoresis of Proteins and Peptides* (Strege, M. A., Lagu, A. L., ed.) *Methods in Molecular Biology*, Totowa, NJ: pp. 253–290.
14. Tsybin, Y. O., Ramstroem, M., Witt, M., Baykut, G., and Hakansson, P. (2004) Peptide and protein characterization by high-rate electron capture dissociation Fourier transform ion cyclotron resonance mass spectrometry. *J. Mass Spectrom*. **39**, 719–729.
15. Righetti, P. G., Gelfi, C., Verzola, B., and Castelletti, L. (2001) The state of the art of dynamic coatings. *Electrophoresis* **22**, 603–611.
16. Rodriguez, I. and Si, S. F. Y. (1999) Surface deactivation in protein and peptide analysis by capillary electrophoresis. *Anal. Chim. Acta* **383**, 1–26.
17. Horvath, J. and Dolnik, V. (2001) Polymer wall coatings for capillary electrophoresis. *Electrophoresis* **22**, 644–655.
18. Doherty, E. A. S., Meagher, R. J., Albarghouthi, M. N., and Barron A. E. (2003) Microchannel wall coatings for protein separation by capillary and chip electrophoresis. *Electrophoresis* **24**, 34–54.
19. Sentellas, S., Puignou, L., and Galceran, M. T. (2002) Capillary electrophoresis with on-line enrichment for the analysis of biological samples. *J. Sep. Sci*. **25**, 975–987.
20. Urbanek, M., Krivankova, L., and Bocek, P. (2003) Stacking phenomena in electromigration: From basic principles to practical procedures. *Electrophoresis* **24**, 466–485.
21. Wan, H. and Blomberg, L. G. (2000) Chiral separation of amino acids and peptides by capillary electrophoresis. *J. Chromatogr. A*. **875**, 43–88.
22. Scriba, G. K. E. (2003) Recent advances in enantioseparations of peptides by capillary electrophoresis. *Electrophoresis* **24**, 4063–4077.
23. Wätzig, H., Degenhardt, M., and Kunkel, A. (1998) Strategies for capillary electrophoresis: method development and validation for pharmaceutical and biomedical applications. *Electrophoresis* **19**, 2695–2752.
24. McLaughlin, G. M., Anderson, K. W., and Hauffe, D. K. (1998) Peptide analysis by capillary electrophoresis: Method development and optimization, sensitivity enhancement strategies, and applications, in *High Performance Capillary Electrophoresis* (Khaledi, M. G., ed.) John Wiley & Sons, New York, NY: pp. 637–681.
25. Yang, Y., Boysen, R. I., and Hearn, M. T. W. (2004) Analysis of synthetic peptides by capillary electrophoresis. Effect of organic solvent modifiers and variable electrical potentials on separation efficiencies. *J. Chromatogr. A* **1043**, 91–97.
26. Janini, G. M. and Issaq, H. J. (2001) Selection of buffers in capillary zone electrophoresis: application to peptide and protein analysis. *Chromatographia* **53**, S18–S26.

27. Righetti, P. G., Gelfi, C., Perego, M., Stoyanov, A. V., and Bossi, A. (1997) Capillary zone electrophoresis of oligonucleotides and peptides in isoelectric buffers. theory and methodology. *Electrophoresis* **18**, 2145–2153.
28. Castagnola, M., Cassiano, L., Messana, I., Paci, M., Rossetti, D. V., and Giardina, B. (1996) Effect of 2,2,2-trifluoroethanol on capillary zone electrophoretic peptide separations. *J. Chromatogr. A* **735**, 271–281.
29. Matsubara, N. and Terabe, S. (1996) Micellar electrokinetic chromatography in the analysis of amino acids and peptides, in *Capillary Electrophoresis in Analytical Biotechnology* (Hancock, W. S., ed.), CRC, Boca Raton, FL: pp. 155–182.
30. Yang, Y., Boysen, R. I., Chen, J. C., Keah, H. H., and Hearn M. T. W. (2003) Separation of structurally related synthetic peptides by capillary zone electrophoresis. *J. Chromatogr. A* **1009**, 3–14.
31. Fürtös-Matei, A., Day, R., St-Pierre, S. A., St-Pierre, L. G., and Waldron K. C. (2000) Micellar electrokinetic chromatography separations of dynorphin peptide analogs. *Electrophoresis* **21**, 715–723.

20

Analysis of Proteins by Capillary Electrophoresis

Christian W. Huck and Günther K. Bonn

Summary

This chapter describes the basic *principles* of protein analysis by capillary electrophoresis, and provides an overview of the literature and thus a comprehensive summary of special topics in this field. The "Materials and Methods" section includes the main experimental points to be taken into consideration, namely, sample pretreatment, reduction of protein adsorption to capillary wall, increase of selectivity, detection modes, and special electrophoretic modes. Because there are many capillary electrophoretic methods for protein analysis, not all experimental steps are listed; however, the main references are cited. Additional experimental information can be found in the Notes. Finally, an overview of the most relevant *applications*, divided according to the origin of the samples into human proteins, food and agricultural products, pharmaceutical proteins, proteome, and special proteins, is given with the relevant literature.

Key Words: Capillary electrophoresis; proteins; sample pretreatment; wall interaction; detection modes; special electrophoretic modes; application fields; review.

1. Introduction

Since its commercial introduction in 1987, capillary electrophoresis (CE) has been developed into a high-sensitivity, high-resolution, quantitative separation technique for the analysis of both small molecules (e.g., inorganic cations and anions) and large molecules (e.g., proteins).

1.1. Principal Considerations for Capillary Electrophoresis of Proteins

Today, CE is a modern analytical method that offers the advantages of short analysis time and minimum consumption of both reagents and samples. It is well suited for the separation of proteins and has been used for this purpose

From: *Methods in Molecular Biology, vol. 384: Capillary Electrophoresis*
Edited by: P. Schmitt-Kopplin © Humana Press Inc., Totowa, NJ

Table 1
Reviews Dealing With Capillary Electrophoretic Separation of Proteins Published Between 1999 and Early 2004

Publication year	Short description	Reference
2004	Techniques and applications of gel electrophoresis and peptide analyses, and probing folding/unfolding/refolding/misfolding of proteins by capillary zone electrophoresis	***1***
2004	Food proteins	***2***
2004	Serum proteins	***3***
2004	Miniaturized proteomics by capillary electrophoresis (CE)-mass spectrometry (MS)	***4***
2004	CE-MS	***5***
2004	Past, present, and future of electrophoresis	***6***
2004	Protein–protein interaction	***7***
2003	Developments in CE from 2001–2003	***8***
2003	Recent progress in high-performance capillary bioseparation	***9***
2003	Gel and polymer-solution mediated separation	***10***
2003	Analysis of single mammalian cells	***11***
2003	Methodological challenges of protein analysis in blood serum and cerebrospinal fluid	***12***
2003	CE and its application in the clinical laboratory	***13***
2003	CE for exploring protein stability	***14***
2001	Microfabricated fluidic devices for preparation, injection, separation, derivatization, and detection	***15***
2001	CE of proteins 1999–2001	***16***
2000	CE of proteins in acidic, isoelectric buffers	***17***
2000	CE for the analysis of biopolymers	***18***
1999	Capillary zone electrophoresis, capillary isoelectric focusing, sieving sodium dodecyl sulfate CE	***19***
1999	Developments in capillary zone electrophoresis of proteins until 1999	***20***

for over three decades. The importance of CE in protein analysis increases with the growing effort to learn more about the composition and function of proteins in living bodies, and has great potential to become one of the key tools in proteome research.

1.2. Electrophoretic Behavior of Proteins

In CE, proteins behave differently in terms of separation efficiency than small molecules. They differ in electric charge, relative molecular mass, conformation, hydrophobicity, and even specific binding capability. Owing to these properties, electrophoretic separation can be achieved as a result of differences in (1) electrophoretic mobility (i.e., separation by capillary zone electrophoresis [CZE] and isotachophoresis [ITP]), (2) size (i.e., separation in sieving media such as gels and entangled polymeric networks), (3) charge (i.e., separation by isoelectric focusing [IEF], elektrokinetic chromatography [EKC] with ion-exchanger pseudophases), (4) hydrophobicity (i.e., separation by micellar elektrokinetic chromatography [MEKC]), and (5) specific integration(s) with other biomolecules (i.e., separation by bioaffinity electrophoresis [BAE] with molecular pseudophases, e.g., cyclodextrins) (*see* **Note 1**).

1.3. Literature Overview

Since the beginnings of capillary electrophoresis, more than 6000 papers have been published dealing with proteins. Generally, this huge number of publications can be divided into (1) methodological papers, (2) theoretical papers, (3) applications, and (4) reviews summarizing these. Because of the huge amount of reviews, an overview of the main representative and most important contributions since 1999 is provided in **Table 1**.

2. Methods

2.1. Sample Pretreatment

In real samples, analytes of interest are very often only available in very small amounts. Therefore, concentration of the sample (preconcentration) or chemical modification of the sample (derivatization) is very important.

2.1.1. Preconcentration

Preconcentration can be carried out both on- and off-line. An overview of on-line preconcentration techniques as well as affinity interactions for preconcentrations can be found in **refs. *21*** and ***22***. The simplest and most popular on-line preconcentration technique is sample stacking. In this method, a sample plug is introduced in either a lower concentration or a buffer with a higher

pH than the separation buffer. Because the mobility of the analytes in the sample differs from that of the analytes in the separation buffer, the sample will focus at the interface between the two buffers. Recently, pH-mediated stacking, using a plug of 1–2 *M* NH_3 before the sample and 4 *M* formic acid after the sample, was used with CE-ESI-MS ***(23)***. Using this technique, a 10-fold improvement in sensitivity can be achieved. The so-called large-volume sample stacking using electroosmotic flow pump (LVSEP) technique can be employed as an alternative; it operates on the same principle, but requires a capillary coating, which compresses electroosmotic flow (EOF) ***(22)***. This technique allows a concentration factor of about 100-fold. For samples in high-conductivity media, a sample stacking method that does not require desalting has been developed ***(24)***. For this method, a poly(ethylene oxide) solution is prepared in a 400 m*M* Tris-borate buffer and follows the injection with a short plug of low-pH buffer. Concentration factors of more than 100 are reported. Another technique uses a porous joint to connect the concentration region of the capillary to the separation region. This technique is suitable for the concentration of samples in low-ionic strength solutions, acidic solutions, and dissolved in running buffer.

Several other techniques suitable for preconcetration prior to analysis are solvent extraction, chromatography, IEF, and ITP. For the concentration and analysis of neuropeptide Y, the coupling of capillary liquid chromatography (LC) to CE via a flow-gating interface was reported ***(25)***, and improved the lower detection limit 20-fold. The use of carrier ampholyte-free isoelectric focusing (CAF-IEF) shows a concentration factor of about 10^7 ***(26)***. The formation of a microfluidic channel from two gold or palladium electrodes can be used for continuous concentration and fractionation of proteins ***(27)***. Alternatively, an extraction device to transfer separated proteins from a polyacrylamide slab gel to a capillary can be used ***(28)***. Thereby, the extracted proteins are stacked as they enter the capillary. ITP separates the sample into a series of zones between a leading and tailing ion ***(29)***. Solid-phase extraction (SPE) uses the partitioning of molecules into a solid-phase—typically, C18-coated particles—to extract hydrophobic analytes from dilute aqueous solutions ***(30)***. An easy-to-construct, mechanically stable on-line SPE system was developed from poly(styrene-divinylbenzne) PS-DVB particles in a teflon matrix **(Fig. 1)** ***(31)***. Consequently, no frit is needed to keep the stationary phase in place. This SPE device allows to improve the detection limit three to four orders of magnitude for model compounds.

2.1.2. Derivatization Techniques

Limits of detection can also be improved through the use of derivatization to impart better detection properties, such as absorption, fluorescence,

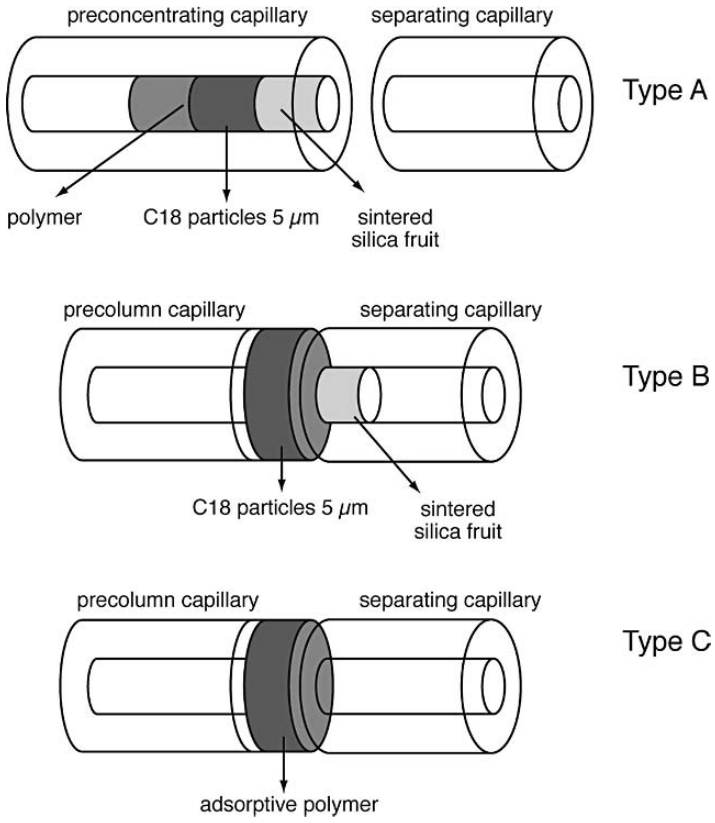


Fig. 1. Schemes of on-line preconcentration capillary electrophoresis systems. Reprinted from **ref. *31***, with permission.

or electroactivity, to the sample. Although labeling is normally homogenous throughout the sample, a technique to prefentially label cationic proteins, anionic proteins, or proteins with a specific isoelectric point has been described ***(32)***. Fluorescent agents, associating with a protein but not covalently bound, have gained significant popularity ***(33,34)***. These dyes have a strong fluoresence when associated with a protein, but only a very slight fluorescence when free in solution ***(35)***. The use of pyrenebutanoate for this purpose results in attomole-range detection limits ***(36)***. The use of green fluorescent protein (GFP) fusion proteins has also increased in poularity ***(37–39)***. On-column derivatization with phthalic anhydride by differential mobility is described by Zhang et al. ***(40)***. Using this technique, a sample plug of derivatizing agent is injected separately, and the derivatization reaction occurs as the faster migrating

band "penetrates" the slower migrating band. For IEF, 6-aminoquinolyl-*N*-hydroxysuccinimidyl carbamate was described ***(41)***. Single-label fluorescent derivatization via protein's α-amino groups is based on the application of an amine reactive probe, fluorescein isothiocyanate (FITC), at a lower-than-normal derivatization buffer pH, which discriminated between the derivatization of the ε-amino groups and α-amino groups ***(42)***. A method for the homogeneous derivatization of large proteins requires the sample to be reduced and alkylated, and then reacted with an excess of the derivatization agent ***(43)***. Under evaluation with three model proteins, this method showed 100% of the amino sites derivatized for α-chymotrypsinogen A and ovalbumin and 96% of the amino sites derivatized for bovine serum albumin.

2.1.3. Alternative Methods

Microfabricated devices can include an enzymatic microreactor for on-chip protein digestion ***(28,44)***, whereby hydrodynamic flow is used to introduce the sample to the chip and a gating voltage is used to introduce the sample to the separation channel.

2.2. Reduction of Protein Adsorption to the Capillary Wall

Adsorption of proteins to capillary walls is a serious problem in CE, resulting in changes in EOF, peak broadening, and loss of separation efficiency. Models for analyte adsorption allow a mathematical correction of migration times and changes in EOF ***(45)***. Usually, dynamic or static wall coatings are applied to minimize protein adsorption.

2.2.1. Dynamic Wall Coating

For dynamic wall coating, a polymer, detergent, or other molecule that interrupts the interaction of the analytes with the inner capillary wall is added ***(46)***. Poly(diallyldimethyl ammonium chloride) (PDMAC) at a concentration of 0.5% w/v can be used, e.g., for the suppression of insuline-like growths factors ***(47)***. It forms a positively charged layer at the fused-silica surface, which reverses electroosmosis and leads to electrostatic repulsion of the positively charged analytes. Cetyltrimethylammonium bromide (CTAB), Brij, or sodium dodecyl sulfate (SDS) can be added to the sample as a zwitterionic surfactant ***(48,49)***. Phospholipids, e.g., 1,2-dilauroyl-*sn*-phosphatdidylcholine (DLPC), can be used as a semipermanent wall coating ***(50)***. Bilayer capillary coating with fluorosurfactants has the advantage of excluding oily and fatty phases ***(51)***. To reduce the adsorption of glycoproteins to the wall, amines, e.g., α–ω-diamine alkanes and bis(aminoalkyl amines) ***(52)***, are found to be effective but less efficient than polymeric wall coating. Hexadimethrine bromide reverses

EOF and prevents adsorption of cationic proteins. For poly(dimethylsiloxane) (PDMS) microfabricated devices, less adsorption and improved separation efficiency is achieved by applying a coating with 2-morpholinoethanesulfonic acid (MES) ***(53)***.

2.2.2. Static Wall Coating

Permanent static inner wall coatings generally eliminate analyte interaction more effectlively and are even more stable than dynamic wall coating. Nevertheless, they are more difficult to produce. One type of static wall coating is made by reacting the capillary wall with a small molecule with double functionality, which is then used to bind the polymer to the wall. Epoxy-based hydrophilic wall coatings allow separation efficiences as high as 200,000 theoretical plates per meter ***(54)***. As an alternative, grafting can be carried out with poly(glycidyl methacrylate) (GMA) ***(55)***, epoxy-poly(dimethylacrylamide) ***(56,57)***, 2-hydroxyethyl methacrylate ***(58)*** or derivatized polystytrene nanoparticles ***(59)*** **(Fig. 2)**. Modification of the inner wall under mild conditions can be achieved by dextrane coating ***(60)*** **(Fig. 3)**. Polyvinyl alcohol and Polybrene can also be used to reduce wall adsorption effects ***(61)***.

For microfabricated devices, static coatings necessitate the use of a broader range of materials. Thereby, the difficulty lies in the introduction of derivatization reagents. Glass chips can be coated with acrylamide and hexadimethyldisiloxane (HDMS) ***(62)***. Finally, the application of polycarbonate microfluidic devices is also reported ***(63)***.

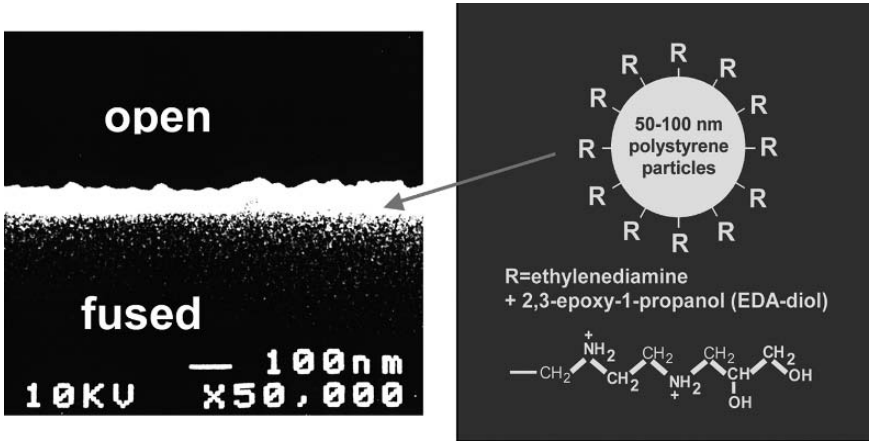
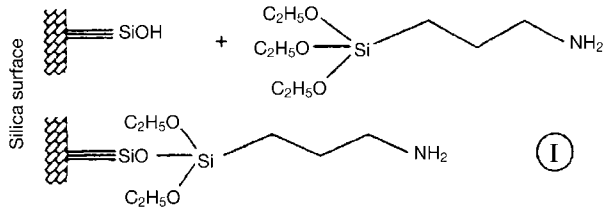
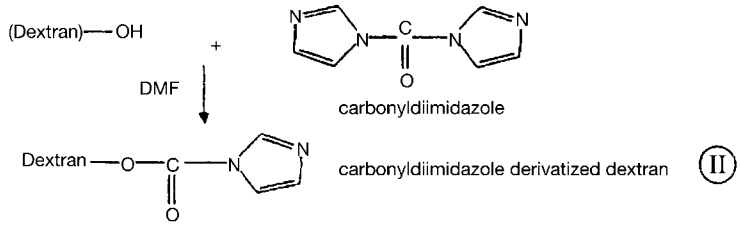


Fig. 2. Permanent coating of fused-silica capillaries with functionalized polystyrene particles.

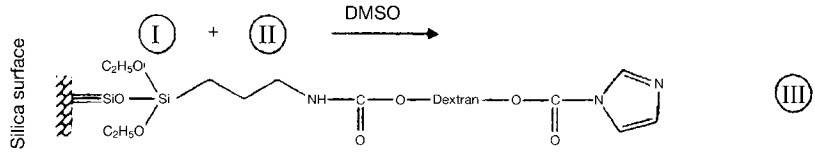
Step 1. Aminosilanization of the inner wall of fused silica capillaries



Step 2. Activation of dextran particles suspended in DMF solution of carbonyldiimidazole



Step 3. The activated dextran particles are dissolved in DMSO and reacted with the primary amino groups at the silanized surface



Step 4. Residual reactive sites on dextran bound to the silica surface are reacted with ethanolamine

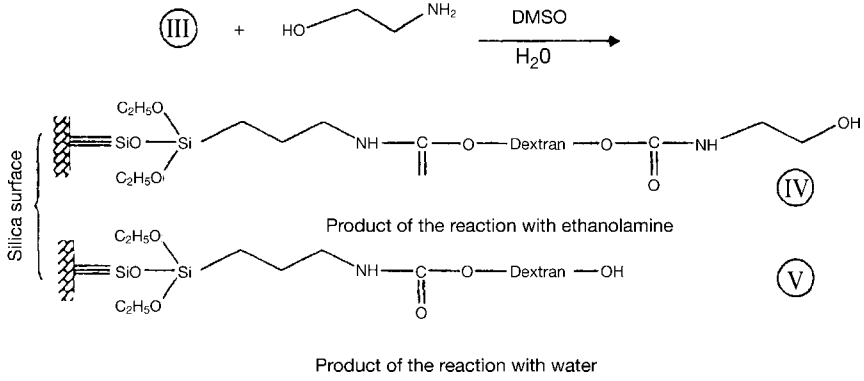


Fig. 3. Four steps of the coating procedure for preparation of dextran-coated fused-silica capillaries for capillary electrophoresis. Reprinted from **ref. *60***, with permission.

2.3. Increasement of Selectivity

In most cases, selectivity and resolution are improved by the manipulation of the separation pH and buffer additives in order to change the analyte mobilities. Effects of voltage and temperature are summarized in **Note 2**. For the analysis of monoclonal antibodies, fluorescent latex particles were developed as additives ***(64)*** to allow separation of protein–latex immunocomplex from the unbound latex particles. Polyamines are helpful buffer modifiers for the separation of glycoforms in polyacrylamide-coated capillaries ***(65)***. The addition of curdlan ***(66)*** and *N*-carboxymethylated polyethyleneimine (CMPEI) ***(67)*** was shown to reduce analysis time without reducing resolution and to alter EOF. Finally, SDS and poly(ethylene oxide) (PEO) can improve resolution without any further sample pretreatment ***(68)***.

2.4. Detection Modes

After separation, proteins are detected in CE using ultraviolet (UV) absorbance, laser-induced fluorescence (LIF), and mass spectrometric (MS). Other detection methods mainly include amperometric or chemoluminiscence detection and nuclear magnetic resonance (NMR).

2.4.1. UV Absorption

UV absorption is the most common but also the least sensitive detection mode. Typically, wavelengths between 200 and 220 nm, at which absorption is proportional to the number of peptide bonds, are chosen. Alternatively, detection can be accomplished at wavelengths of 254 or 280 nm, at which the aromatic residues have absorption bands. The advantage of UV absorption is that no sample pretreatment is necessary. To detect cells with small volumes, z-shape and bubble cells can be used ***(69)***. For short separation capillaries, whole-column imaging can be applied; this makes it possible to observe the separation dynamics more fully ***(70,71)***.

2.4.2. LIF

As a result of its high sensitivity, laser-induced fluorescence detection is often the method of choice for the analysis of low concentrations. It requires pre-, on-, or post-column derivatization. For detection, the native fluorescence of aromatic residues, or a fluorogenic complexing agent, can be used ***(36,72–76)***. Green fluorescent protein (GFP) ***(37–39)*** has become very popular. As an alternative, fluorescence detection using UV laser or two-photon excitation can be used ***(77)***, the latter allowing attomole detection limits ***(78)***. A twofold improvement of the detection limit can be achieved by phase-sensitive lifetime detection ***(79)***. Fluorescence correlation spectroscopy

monitors the fluorescence fluctuations arising from individual molecules passing the detection point and autocorrelates the electrophoretic mobilities ***(80)***. Fluorescence polarization can be applied for the monitoring of complex formation in affinity capillary electrophoresis (ACE) ***(81)***. For microfabricated devices, fluorescence emission ***(82)*** or acousto-optical deflection for whole-channel imaging have been shown to be useful ***(83)***.

2.4.3. Mass Spectrometry

Although LIF is the most sensitive detection technique, MS provides the most information. Therefore, CE is often coupled with Fourier-transform ion cyclotron resonance (FTICR)-mass spectrometry ***(84,85)***. The high efficiency of this system was demonstrated for the analysis of 1500 peaks, which allowed the identification of 30 proteins on a 95% confidence interval with mass measurement errors less than 5 ppm ***(84)***. CE-MALDI with vacuum deposition produces a more reproducible and uniform signal intensity compared to the "dried droplet" method, resulting in lower limits of detection (LODs) (10 n*M*). To improve the ionization process, many optimizations, e.g., modifications of the buffer systems ***(86)***, sheath conditions ***(87)***, and sheath flow configuration ***(88)*** as well as the use of a sheathless metal-liquid ESI interface, have been reported ***(89)***. In order to minimize dead volume, disposable nanospray emittors have been developed ***(90)***. The rapid open-access channel electrophoresis (ROACHE) technique employs a microfabricated device with open channels ***(91)***. The separation buffer contains the MALDI matrix and the solvents are simply evaporated at the end of the separation. For CE-inductively-coupled plasma (ICP), a self-aspirating total consumption micronebulizer is used ***(92)***, which decreases LOD by a factor of 100.

2.4.4. Other Detection Methods

In addition to the traditionally used detection methods, a number of novel detection modes have been developed. Such methods are amperometric detection of, e.g., myoglobin in human urine ***(90)***, chemiluminescence detection for capillary isoelectric focusing (CIEF) ***(93)***, and NMR for capillary isotachophoresis (CITP) ***(94)***. Four electrode contactless conductivity detection can be applied to glass microfabricated devices ***(95,96)***. Post-capillary affinity detection, e.g., for immunoglobulin G, is described in **ref. *97***.

2.5. Special Chromatographic Modes

Beside CZE, several older modes of CE are commonly in use. In the following sections, affinity electrophoresis, capillary SDS electrophoresis, CIEF, and the combination of CE and high-performance liquid chromatography (HPLC) are discussed.

2.5.1. Affinity Capillary Electrophoresis

ACE comprises a group of techniques in which a ligand interacts with a protein ***(98,99)***. ACE is used to calculate a binding constant for a protein–ligand complex, or to determine the amount of protein or ligand present ***(100)***. It must be considered that during the determination of the binding ligand, a positive error will occur if the sample concentration is too high ***(101)***. Nevertheless, mathematical models enable the calculation of the correct concentration ***(102)***. A modified ACE technique is the partial filling technique ***(103)***. In this technique, the capillary is first filled with the ligand and then with the receptor and a noninteracting standard. Mobility of the receptor, relative to the standard, changes with the concentration of the ligand, and this enables the binding constant to be calculated. A GFP fused to the C-terminus of rDmCyo20 and ACE was used to determine the dissociation constant for a cyclophin (rDmCyp20) and capsid protein p24 of HIV-1 to be $20 \pm 1.5 \times 10^{-}6\ M$. Further applications include the measurement of binding constants of the immunosuppressive drug cyclosporin A to enzyme cyclophilin ***(104)***, a noncompetititve immunoassay of digoxin ***(105)***, DNA binding of homo- and heterodimers ***(106)***, and drugs measured in the presence of HAS ***(107)***.

2.5.2. Capillary SDS Electrophoresis (see **Note 3**)

Capillary SDS electrophoresis enables separation of proteins on the basis of differences in molecular mass. As sieving matrices polymer materials, e.g., dextran, polyethylene oxide (PEO), linear polyacrylamide (LPA) ***(108)***, and hydroxypropylcellulose ***(109)*** are the most commmonly used polymers. The suitability for microchip separation has been demonstrated ***(110)***. For detection, the proteins are labeled with a fluorescent dye, e.g., 5-carboxytetramethylrhodamine succinimidyl ester, allowing resolution and sensitivity comparable to that obtained with silver-stained SDS page. At the end of the capillary, the SDS concentration is decreased by the addition of a sheath liquid below its critical micelle concentration (CMC). Detection is then based on a decrease in the fluorescent background caused by the fluorescent dye bound to SDS micelles. SDS-CE can successfully be applied to the analysis of single HT29 human colon adeno-carcinoma cells ***(109,111,112)***, **(Fig. 4)**. This method, which used 8% pullulan as the sieving matrix, provided reproducible separations with peak capacities around 30 with a total analysis time of about 45 min.

2.5.3. Capillary Isoelectric Focusing

CIEF allows the separation of proteins based on their isoelectric points (p*I*). In this technique, a pH gradient is established within the capillary, and each

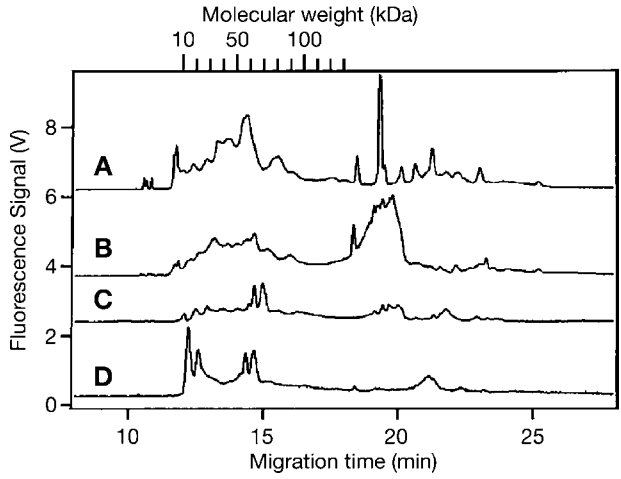


Fig. 4. Electropherograms of **(A)** cytosolic fraction, **(B)** membrane/organelle fraction, **(C)** nuclear fraction, and **(D)** cytoskeletal/nuclear matrix fraction of HT29 human colon cancer cells. Capillary, 40 cm × 50 μm; PEO concentration, 2.5%. Experimental conditions: separation, 300 V/cm; injection, 100 V/cm for 5 s; sieving buffer, 0.1 *M* Tris-0.1 *M* CHES with 2% poly(ethylene oxide) and 0.1% sodium dodecyl sulfate; protein concentration, 200 n*M* each. Reprinted from **ref. *112***, with permission.

protein focuses at the region where the pH is equal to its p*I*. By the analysis of cell lysates from *Saccharomyces cerevisiae, Escherichia coli*, and *Deinococcus radiodurans*, it was shown that proteins differing in p*I* only by 0.004 can be separated by this technique ***(113)***. In this work, CIEF of proteins in the pH interval 3-8.8 allowed the separation of 210 peaks. Compared to flat-bed IEF, CIEF allows better separation in a shorter time. In order to prevent protein precipitation at a pH near the p*I*, urea, sucrose, and 3-(cyclohexylamino)-1-propanesulfonic acid may be added to the system ***(114)***. For the determination of the isoelectric points, the CIEF system with UV detection must be calibrated with synthetic oligopeptides as p*I* markers ***(115)***. Imaging detection of a whole column has been developed using refractive index, UV absorption, and LIF detection **(Fig. 5)** ***(116)***. Real-time monitoring can shorten the anaylsis time to 3–5 min for one sample. Microfabricated devices for direct ESI-MS have been constructed (6 cm × 50 μm × 30 μm) ***(117)***. CIEF has also been used for the investigation of noncovalent protein complexes and HIV envelope glycoproteins ***(118)***, as well as for the analysis of the recombinant human erythropoietin ***(119)***. Studies have validated the use of CIEF as a quantitative method for impurity detection in drug studies. Both a degradation product

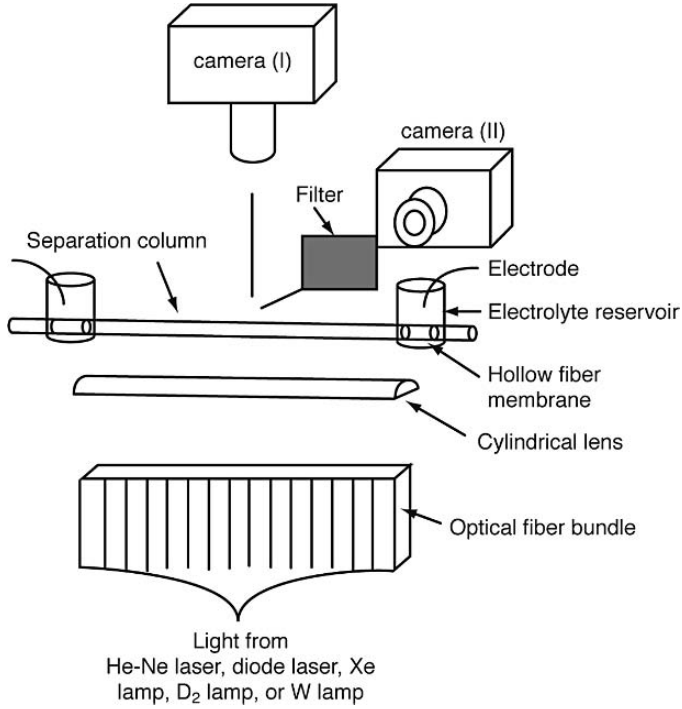


Fig. 5. Instrumental setup for whole-column detection for capillary isoelectric focusing. Reprinted from **ref. *116***, with permission.

(monodeamidation of a protein) and an aggregated form of the molecule were evaluated, and RSD values were found to be under 20% for both species ***(120)***.

2.5.4. Combination of CE and HPLC

A two-dimensional (2-D) LC-CE system offers a superior performance of certain separations, particularly of samples with a large number of components, such as proteomes; this is very helpful, as the peak capacity of a one-dimensional separation is insufficient. The primary concern is the design of a suitable interface. A microdialysis junction, constructed by joining the capillaries with a short length of dialysis tubing, was used to couple CIEF with transient CITP-CZE to analyze protein digests ***(121)***. The peptides were first hydrodynamically injected into the CIEF capillary and focused, and then hydrodynamically injected into the ITP/CZE capillary and further separated. Sheng and Pawliszyn used a 10-port valve to couple MEKC with IEF ***(122)***. The MEKC capillary was connected to a dialysis loop, which consisted of a microporous hollow fiber inside a tygon tube. Fractions were collected

from the MEKC separation, dialyzed, transferred via a transfer capillary, and injected into a CIEF cartridge via an eight-port valve. LC fractions are collected in a microtiter plate with a microfraction collector, and the fractions are dried under vaccuum and analyzed by CE ***(123)***. In another approach, proteins can first be separated by CIEF, which is followed by reversed-phase LC ***(124)***. Each LC peak obtained is collected and characterized by further proteolytic digestion, MALDI-time-of-flight (TOF)-MS, and database search. Low molecular mass and basic proteins of human cell lysates line were resolved with better resolution by the 2-D capillary method than with 2-D slab-gel electrophoresis. Another method combines size-exclusion chromatography (SEC) with CIEF ***(125)***. Fractions eluted from an SEC column are transferred to a hollow fiber membrane microdialysis device where they are desalted and mixed with carrier ampholytes and then injected into a column for separation by CIEF. There is also a great deal of interest in methods for performing 2-D separations on microfabricated devices. To this end, a rearrangable PDMS chip was developed ***(126)***. This chip could be used for a first dimension of IEF and then peeled apart and reassembled for SDS-capillary gel electrophoresis (CGE) as the second dimension. Another 2-D separation microfabricated device was developed that coupled IEF and CE with a simple cross geometry ***(127)***. To facilitate this, a CZE separation compatible with the IEF ampholyte system was developed, and it was shown that the separation behavior in the first dimension was consistent with a CZE mechanism.

3. Application Fields

Real applications play an important role in the develeopment and success of any analytical method. The number of CE applications continues to increase with time, and this is a sign of great interest of this analytical method. As a result of the large number of published applications, in this chapter they have been divided into several sections according to the origin of the samples. Finally, special applications are grouped together.

3.1. Human Proteins

Analysis of proteins in body fluids by CE is focused primarily on blood, urine, and CSF. Today, analysis of serum proteins by CE has become a routine method in many clinical laboratories. For the analysis of serum proteins, CZE was found to be comparable to slab gel ***(128)***. It was described as suitable for the analysis of serum proteins obtained from children between 1 and 14 yr of age ***(128,129)***. In this case, monoclonal proteins in sera were analyzed by CE employing UV detection ***(130)***. Other methods include CIEF of plasma proteins in the absence of denaturing agents followed by cathodic

mobilization ***(131)***. In this method, isoelectric points of proteins are estimated by using synthetic peptide p*I* markers. In a different approach, an affinity-probe CIEF method was developed to quantitate α_1-antitrypsin in human serum ***(132)***. For the preparation of the affinity probe, a recombinant fragment of mouse IgG1 against human α_1-antitrypsin was labeled with tetramethylrhodamine on a single cysteine residue and purified by IEF in agarose gel. For the analysis of blood samples obtained from patients with Alzheimer disease, CZE-MS together with nano-LC has been successfully applied for the analysis of amyloid that circulates in blood and might be deposited in the brain ***(133)***. CIEF-MS was used to compare the protein content in cerebrospinal fluid (CSF) and whole blood ***(134)***. Another approach is the application of CE combined online with CE-FTICR-MS for the proteomic analysis of human CSF after digestion. CE-FTICR allowed the identification of 30 proteins on 95% confidence level with a mass measurement error of less than 5% ***(84)***. A split-flow CE-MS interface was used to analyze carbonic anhydrase in human erythrocytes ***(135)***. By this technique, four major erythrocyte proteins, i.e., the α- and β-chains of hemoglobin and carbonic anhydrase I and II, were separated and detected at the low attomole level. A CE method was setup for the analysis of urinary proteins, e.g., glomerular proteins from the tubular proteinuria ***(136)***. Other applications include the analysis of saliva, pleural transudates ***(137)***, and HT29 human colon adenocarcinoma cells by LIF detection after labeling with 3-(2-furoyl] quinoline-2-carboxyaldehyde ***(109,111,138)***. Some unusual proteins from patients with IgD myeloma, IgG heavy chain disease, a triple IgG (kappa] monoclonal band, rapid changing abnormal/monoclonal band, and a mixed type-11 cryoglobulinemia could be identified using CE ***(139)***. Other atypical proteins analyzed by CE are monoclonal M-protein, albumin, and α_2-macroglobulin in serum of patients with neurological disorders **(Fig. 6)** ***(140)***. Chronic or repeated alcohol abuse can be detected by the analysis of carbohydrate-deficient transferrin in human serum, and the analysis of lipoproteins (very-low-density lipoprotein [VLDL], low-density lipoprotein [LDL], high-density lipoprotein [HDL]) ***(16)***.

3.2. Food and Agricultural Product Proteins

The analysis of proteins in food and agricultural samples is an important application of CE. It serves as a method for quality control and for the identification of cultivars and food adulteration. Milk, egg, meat, and fish are the foods and agricultural products most frequently analyzed for proteins by CE ***(141,142)***. High-molecular mass glutenins can be separated and quantitated by SDS-CE after extraction from flour by 50% *n*-propanol and precipitation with 40% acetone ***(143)***. CE could be used to identify different wheat cultivars by

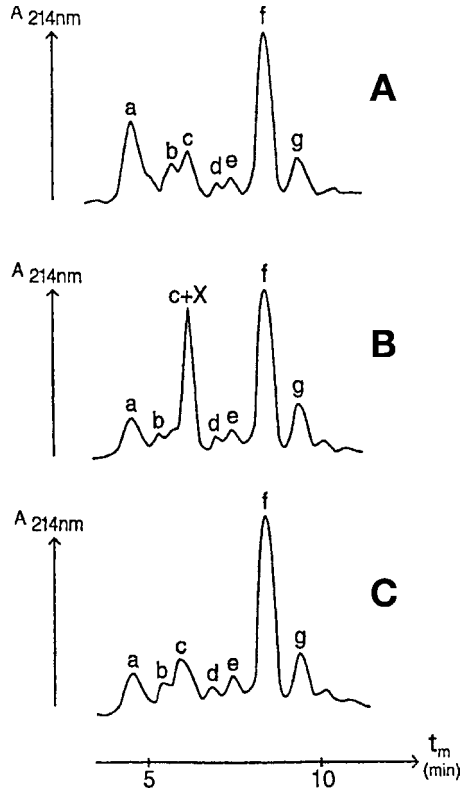


Fig. 6. Capillary zone electrophoresis of human cerebrospinal fluid from **(A)** a patient with multiple sclerosis approaching the malignant phase, **(B)** a patient with cerebral infarction in the recovery phase, and **(C)** a patient with neurosis with no organic damage in the central nervous system. Peak a, γ-globulin; b, β2-globulin; c, β1-globulin; d, α2-globulin; e, α1-globulin; f, albumin; g, prealbumin. Reprinted from **ref.** ***140***, with permission.

analysis of gliadins extracted from flour with 30% ethanol and comparison of the protein profile ***(144)***. Wheat maturation can be monitored by CE of proteins, namely gliadin ***(145)***. Changes in protein fractions of different wheat cultivars were studied to determine the effect of damage by the wheat bugs *Aelia* spp. and *Eurygaster* spp. In some damaged wheat cultivars, glutenin fractions were detected as a result of hydrolysis of the proteins by the bug proteinases. Proteins and their degradation products in milk, cheese, and whey products have been analyzed by CE ***(146,147)***. CZE and IEF have also been used to monitor the deterioration of milk powder upon storage due to the Maillard reaction. CZE proved to be a fast, easy, and sensitive method for

monitoring the quality of milk powders during storage ***(148,149)***. Lactosylation of milk proteins during production and storage was also investigated by CE. It was found that both temperature and moisture content affect the lactosylation level ***(150)***. Whey proteins were analyzed after partial hydrolysis with enzyme systems pancreatin, protease, or alcalase ***(151)***. Capillary SDS electrophoresis was also used for the analysis of milk from horses and donkeys ***(152)***, and to analyze the composition of casein fraction in Iberico cheese made from more than one cow ***(153)***. For the quality control of meat, CE can be applied to distinguish between raw, mechanically recovered chicken meat and hand-deboned chicken breast meat ***(154)***. Microbial proteolysis in meat products was studied by CGE, and changes in sarcoplasmic and myofibrillar proteins were detected ***(155)***. Other applications include the analysis of fish proteins ***(156)*** and, more and more, also wine proteins, which influence aroma ***(157,158)***.

3.3. Pharmaceutical Proteins

CE is a powerful analytical tool for the separation of protein therapeutics ***(159,160)*** and recombinant proteins, e.g., recombinant human erythropoietin (hEPO). hEPO, which controls formation of red blood cells and is used therapeutically, can be analyzed by CIEF. Glycosylation of recombinant hEPO differs from manufacturer to manufacturer, mainly as a result of the cell lines used. CZE can separate individual glycosylation forms to distinguish them from endogenous hEPO and to identify its source ***(119)***. Recombinant proteins such as human deoxyribonuclease I and human epiderimal growth factor ***(161)*** were also analyzed by CE. Stability of placental alkaline phosphatase, a potential therapeutic agent in the treatment of sepsis, was investigated by CZE after exposure to high temperatures, extreme pH, and freeze-drying ***(162,163)***. Investigations showed that temperatures higher than 65 °C result in degradation.

3.4. Analysis of the Proteome

In the post-genomic era, the analysis of the proteome is gaining importance, as posttranslational changes in protein structure cannot be deduced from the DNA sequence. Model proteomes of *E. coli* and *Deinococcus radodurans* were analyzed by IEF with (FT-ICR)-MS ***(164)***. 2-D CE has been applied to the analysis of tryptic digests of model proteins including horse heart cytochrome c, bovine pancreatic ribonuclease A, and bovine erythrocyte carbonic anhydrase II. This method was combined with transient isotachophoresis-zone electrophoresis (**Fig. 7**). The maximum peak capacity was estimated to be around 1600 ***(121)***. Sheng and Pawliszyn used a 2-D electrophoretic system with whole-column imaging (*see* **ref. *122***, chapter II5d). Dovichi's group ***(165)*** developed a system for automated protein

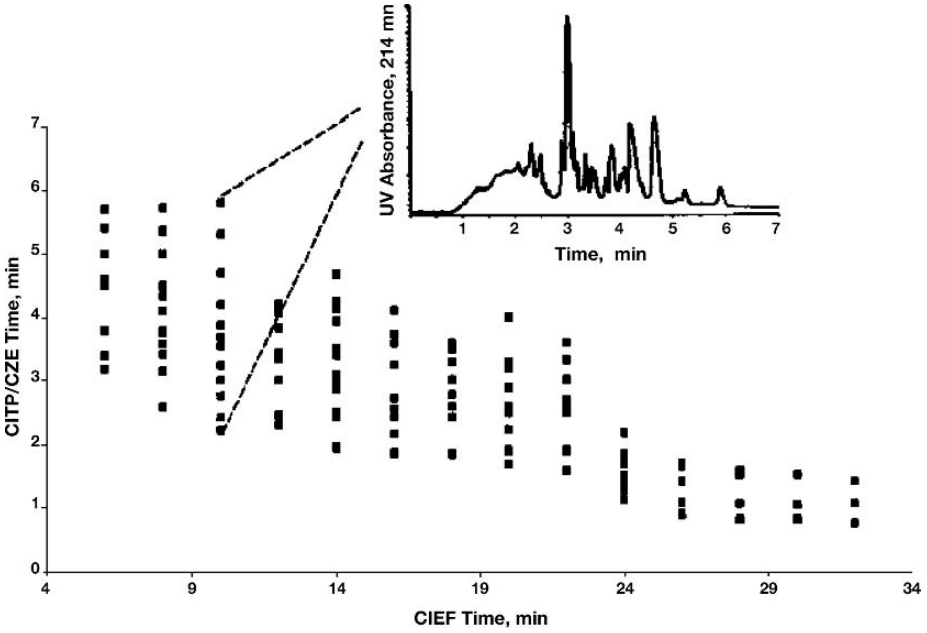


Fig. 7. Two-dimensional plot of tryptic protein digest (cytochrome c, ribonuclease A, carbonic anhydrase II) resolved by capillary isoelectric focusing and transient capillary isotachophoresis -capillary zone electrophoresis in a two-dimensional separation system. The inset shows separation of peptides from the fifth fraction. Reprinted from **ref. *211***, with permission.

analysis. Proteins labeled with 3-(2-furoyl)quinoline-2-carboxaldehyde were first separated by submicellar CE at pH 7.5. Once the first component migrated from the capillary, successive fractions were transferred under computer control without any operator intervention to a second-dimension capillary, and proteins were further separated by CZE at pH 11.1. Proteins from *Neisseria meningitidis* have been analyzed in an integrated microfabricated system by CE-nanoelectrospray ***(166)***.

3.5. Special Proteins

CE is applied to a number of various groups of proteins that can not be classified into the above-mentioned groups. These applications include analysis of peanut allergenic proteins ***(167)***, GFP-extracellular signal-related kinase 2 fusion protein ***(38)***, alanine glyoxalate aminotransferase in rat liver ***(38)***, phycobiliproteins ***(168,169)***, protein YjeQ from *E. coli*, human high-density lipoproteins ***(170)***, mitochondrial proteins ***(171)***, heterologous

bovine pancreatic trypsin inhibitor ***(172)***, rubisco in spinach leaves ***(173)***, albumins ***(174)***, alkaline phosphatase ***(162,175)***, IgG ***(97)***, IgG4 monoclonal antibody ***(176)***, β-glucuronidase and mitogen-activated protein kinase ***(177)***, amyloid β-A4-related peptides ***(178)***, parasporal crystal protein from *Bacillus thuringiensis* ***(179)***, polyethylene modified proteins, luteinizing hormone-releasing hormones ***(180)***, UDP-*N*-acetylglucosamine enolpyruvyl transferase [MurA] ***(181)***, insulin antibodies ***(182)***, partially structured β_2-microglobulin ***(183)***, neuropeptide Y ***(25)***, amyloidogenic β_2-microglobulin ***(184)***, μ- and m-calpain ***(185)***, IgMκ M-protein ***(186)***, embryo proteins from *Caenorhabditis elegans* ***(187)***, and protein kinase substrates ***(188)***.

Structural changes and interactions in proteins include measurement of electrostatic interactions in protein folding with the use of protein charge ladders ***(189)***, structural differentiation of parallel β-helical pectate lysates ***(190)***, salt-promoted protein folding ***(191)***, characterization of secondary structure of antifreeze protein from *Ammopiptanthus mongolis* ***(192)***, unfolded conformation of β_2-microglobulin ***(193)***. The use of CE to exploring protein conformational stability ***(194)*** as well as folding/unfolding/refolding of proteins ***(195)***, has been described.

CE in different formats, including zone electrophoresis and frontal analysis, was used in a number of binding studies, including the binding of ribonuclease and ovalbumin to agglutinin from *Lens culinaris* ***(196)***, drugs to human seru albumin and α_1-acid glycoprotein ***(131)***, heparin to BSA ***(197)***, anionic drugs and oxybutinin to plasma proteins ***(198)***, drugs to plasma lipoproteins ***(199)*** and subdomain III of HAS ***(200)***, porfyrin to HAS ***(201,202)***, phosphates to lysozyme, lactoferrin, and α-lactoglobulin ***(203)*** DNA to proteins ***(80)***, and basic drugs to human α_1- acid glycoprotein ***(204)***. CE has also been used to study the interaction of pUC19DNA with ovalbumin ***(205)*** and of herbizides with HAS ***(206)*** as well as to identify drug-binding sites in HAS ***(107)***.

Finally, CZE was also applied to the study of the thermal and conformational stability of several protein modifying processes, e.g., glycosylation and oxidation ***(207)***. SDS-CGE was applied to characterize H- and L- subunit ratios of ferritins ***(208)*** and to quantitate murine monoclonal antibodies ***(209)***. CE combined with MALDI-MS and radionuclide detection was used to analyze the content of single neuron cell from *Aplysia californica* ***(210)***.

4. Notes

1. Capillaries with an internal diameter of 25–75 μm are usually employed. Fused silica is the material of choice because of its UV transparency, durability (when polyamide coated), and zeto potential.
2. Precise temperature control is important. As the temperature increases, the viscosity decreases, thus the electrophoretic mobility increases as well. Some

buffers such as Tris are known to be pH-sensitive with temperature. Most separations are performed at 25 °C. Whenever temperature control starts to become a problem, the usual strategy is to use a smaller-bore capillary (less current reduces the heat produced) or a longer capillary (more surface area dissipates the heat generated).

3. Good starting conditions are usually 100 m*M* SDS in pH 7.0 and 50 m*M* phosphate-borate buffer, after which adjustments in SDS concentration, pH, and organic modifier may be necessary. Some guidelines are:

   a. In the case of long separation times and good resolution, increase pH and decrease SDS.
   b. In the case of long separation times and poor resolution, use an organic modifier.
   c. In the case of short separation times and poor resolution, increase SDS.
   d. In the case of short separation times and moderate resolution, decrease pH and increase SDS.

   The use of an organic modifier is especially powerful in MECC. Acetonitrile is the solvent of choice.

References

1. Righetti, P. G., Hamdan, M., Antonucci, F., Verzola, B., and Bossi, A. (2004) Electrophoresis of proteins and peptides. *J. Chromatogr. Libr*. **69B,** 633–668.
2. Ferranti, P. (2004) Mass spectrometric approach for the analysis of food proteins. *Eurp. J. Mass Spectrom*. **10,** 349–358.
3. Bossuyt, X. (2004) Interferences in clinical capillary zone electrophoresis of serum proteins. *Electrophoresis* **25,** 1485–1487.
4. Ramstrom, M. and Bergquist, J. (2004) Miniaturized proteomics and peptidomics using capillary liquid separation and high resolution mass spectrometry. *FEBS Lett*. **567,** 92–96.
5. Hernandez-Borges, J., Neususs, C., Cifuentes, A., and Pelzing, M. (2004) On-line capillary electrophoresis-mass spectrometry for the analysis of biomolecules. *Electrophoresis* **25,** 2257–2281.
6. Righetti, P. G. (2004) Bioanalysis: its past, present, and some future. *Electrophoresis* **25,** 2111–2127.
7. Pierceall, W. E., Zhang, L., and Hughes, D. E. (2004) Affinity capillary electrophoresis analyses of protein-protein interactions in target-directed drug discovery. *Meth. Mol. Biol*. **261,** 187–197.
8. Hutterer, K. and Dolnik, V. (2003) Capillary electrophoresis of proteins 2001–2003. *Electrophoresis* **24,** 3998–4012.
9. Huck, C. W., Stecher, G., Bakry, R., and Bonn, G. K. (2003) Recent progress in high-performance capillary bioseparations. *Electrophoresis* **24,** 3977–3997.
10. Guttman, A. (2003) Gel and polymer-solution mediated separation of biopolymers by capillary electrophoresis. *J. Chromatogr. Sci*. **41,** 449–459.

11. Woods, L. A. and Ewing, A. G. (2003) Analysis of single mammalian cells. *Anal. Bioanal. Chem.* **376,** 281–283.
12. Lamari, F. N. and Karamanos, N. K. (2003) Methodological challenges of protein analysis in blood serum and cerebrospinal fluid. *Chromatographia* **58,** 349–356.
13. Petersen, J. R., Okorodudu, A. O., Mohammad, A., and Payne, D. A. (2003) Capillary electrophoresis and its application in the clinical laboratory. *Clin. Chim. Acta* **330,** 1–30.
14. Rochu, D. (2003) Capillary electrophoresis for exploring protein stability. *BIOforum Eur.* **7,** 37–39.
15. Lacher, N. A., Garrison, K. E., Martin, R. S., and Lunte, S. M. (2001) Microchip capillary electrophoresis/electrochemistry. *Electrophoresis* **22,** 2526–2536.
16. Dolnik, V. and Hutterer, K. M. (2001) Capillary electrophoresis of proteins 1999–2001. *Electrophoresis* **22,** 4163–4178.
17. Righetti, P. G., Gelfi, C., Bossi, A., et al. (2000) Capillary electrophoresis of peptides and proteins in isoelectric buffers: an update. *Electrophoresis* **21,** 4046–4053.
18. Krylov, S. N. and Dovichi, N. J. (2000) Capillary electrophoresis for the analysis of biopolymers. *Anal. Chem.* **72,** 11R–128R.
19. Manabe, T. (1999) Capillary electrophoresis of proteins for proteomic studies. *Electrophoresis* **20,** 3116–3121.
20. Dolnik, V. (1999) Recent developments in capillary zone electrophoresis of proteins. *Electrophoresis* **20,** 3106–3115.
21. Stroink, T., Paarlberg, E., Waterval, J. C. M., Bult, A., and Underberg, W. J. M. (2001) On-line sample preconcentration in capillary electrophoresis, focused on the determination of proteins and peptides. *Electrophoresis* **22,** 2375–2383.
22. Guzman, N. A. and Stubbs, R. J. (2001) The use of selective adsorbents in capillary electrophoresis-mass spectrometry for analyte preconcentration and microreactions: a powerful three-dimensional tool for multiple chemical and biological applications. *Electrophoresis* **22,** 3602–3628.
23. Neususs, C., Pelzing, M., and Macht, M. (2002) A robust approach for the analysis of peptides in the low femtomole range by capillary electrophoresis-tandem mass spectrometry. *Electrophoresis* **23,** 3149–3159.
24. Tseng, W. L. and Chang, H. T. (2001) Regulation of electroosmotic flow and electrophoretic mobility of proteins for concentration without desalting. *J. Chromatogr. A*. **924,** 93–101.
25. German, I., Roper, M. G., Kalra, S. P., Rhineart, E., and Kennedy, R. T. (2001) Capillary liquid chromatography of multiple peptides with on-line capillary electrophoresis immunoassay detection. *Electrophoresis* **22,** 3659–3667.
26. Pospichal, J. and Glovinova, E. (2001) Analytical aspects of carrier ampholyte-free isoelectric focusing. *J. Chromatogr. A* **918,** 195–203.
27. Macounova, K., Carbera, C. R., and Yager, P. (2001) Concentration and separation of proteins in microfluidic channels on the basis of transverse IEF. *Anal. Chem.* **73,** 1627–1633.

28. Copper, J.W.; Gao, J.and Lee, C.S. (2002) Gel Protein Capillary Extraction Apparatus. Electronic Protein Transfer. *Anal. Chem*. **74,** 1182–1186.
29. Larsson, M. and Lutz, E. S. M. (2000) Transient isotachophoresis for sensitivity enhancement in capillary electrophoresis-mass spectrometry for peptide analysis. *Electrophoresis* **21,** 2859–2865.
30. Huck, C. W. and Bonn, G. K. (2000) Review: polymer based sorbents for solid-phase extraction. *J. Chromatogr. A* **885,** 51–72.
31. Waterval, J. C., Hommels, G., Teeuwsen, J., Bult, A., Lingeman, H., and Underberg, W. J. (2000) Transient isotachophoresis for sensitivity enhancement in capillary electrophoresis-mass spectrometry for peptide analysis. *Electrophoresis* **21,** 2851–2858.
32. Zhang, Z., Carpenter, E., Puyan, X. L., and Dovichi, N. J. (2001) Manipulation of protein fingerprints during on-column fluorescent labeling: protein fingerprinting of six *Staphylococcus* species by capillary electrophoresis. *Electrophoresis* **22,** 1127–1132.
33. Hansen, L. C. and Sievers, R. E. (1974) Highly permeable open-pore polyurethane columns for liquid chromatography. *J. Chromatogr*. **99,** 123–133.
34. Hjerten, S., Liao, J. -L., and Zhang, R. (1974) High-performance liquid chromatography on continuous polymer beds. *J. Chromatogr*. **473,** 273–275.
35. Benito, I., Marina, M. L., Saz, J. M., and Diez-Masa, J. C. (1999) Detection of bovine whey proteins by on-column derivatization capillary electrophoresis with laser-induced fluorescence monitoring. *J. Chromatogr. A* **841,** 105–114.
36. Horka, M. and Slais, K. (2002) Pyrenebutanoate as a dynamic protein modifier for fluorometric detection in capillary zone electrophoresis. *Electrophoresis* **23,** 1090–1095.
37. Tan, W., Fan, Z. H., Qiu, C. X., Ricco, A. J., and Gibbons, I. (2002) New technique for capillary electrophoresis directly coupled with end-column electrochemiluminescence detection. *Electrophoresis* **23,** 3683–3691.
38. Yoon, S., Ban, E., and Yoo, Y. S. (2002) Direct monitoring of the expression of the green fluorescent protein–extracellular signal-regulated kinase 2 fusion protein in transfected cells using capillary electrophoresis with laser-induced fluorescence detection. *J. Chromatogr. A* **976,** 87–93.
39. Kiessig, S., Reissmann, J., Rascher, C., Kullertz, G., Fischer, A., and Thunecke, F. (2001) Application of a green fluorescent fusion protein to study protein-protein interactions by electrophoretic methods. *Electrophoresis* **22,** 1428–1435.
40. Zhang, Y. and Gomez, F. A. (2000) On-column derivatization and analysis of amino acids, peptides, and alkylamines by anhydrides using capillary electrophoresis. *Electrophoresis* **21,** 3305–3310.
41. Strong, R. A., Liu, H., Krull, I. S., Cho, B. -Y., and Cohen, S. A. (2000) Advantages and limitations of derivatization of peptides for improved performance and detectability in capillary isoelectric focusing (CIEF). *J. Liq. Chromatogr. Relat. Technol*. **23,** 175–187.
42. Little, M. J., Paquette, D. M., Harvey, M. D., and Banks, P. R. (1997) Single-label fluorescent derivatization of peptides. *Anal. Chim. Acta* **339,** 279–288.

43. Liu, H. J., Cho, B. Y., Krull, I. S., and Cohen, S. A. (2001) Homogeneous fluorescent derivatization of large proteins. *J. Chromatogr. A* **927,** 77–89.
44. Peterson, D. S., Rohr, T., Svec, F., and Frechet, J. M. J. [2002) Enzymatic microreactor-on-a-chip: protein mapping using trypsin immobilized on porous polymer monoliths molded in channels of microfluidic devices. *Anal. Chem*. **74,** 4081–4088.
45. Ghosal, S. (2002) Effect of analyte adsorption on the electroosmotic flow in microfluidic channels. *Anal. Chem*. **74,** 771–775.
46. Righetti, P. G., Gelfi, C., Verzola, B., and Castelleti, L. (2001) The state of the art of dynamic coatings. *Electrophoresis* **22,** 603–611.
47. Morand, M., Blaas, D., and Kenndler, E. (1997) Reduction of wall adsorption in capillary zone electrophoresis of a basic single-chain antibody fragment by a cationic polymeric buffer additive. *J. Chromatogr. B* **691,** 192–196.
48. Ding, W. and Fritz, J. S. [1997) Separation of basic proteins and peptides by capillary electrophoresis using a cationic surfactant. *J. High Resolut. Chromatogr*. **20,** 575–580.
49. Kasicka, V., Prusik, Z., Sazelova, P., Barth, T., Brynda, E., and Machova, L. (1997) Capillary zone electrophoresis with external radial electric field control of electroosmotic flow and its application to the separation of synthetic oligopeptides. *J. Chromatogr. A* **772,** 221–230.
50. Cunliffe, J.M.; Baryla, N.E. and Lucy, C.A. (2002) Phospholipid bilayer coatings for the separation of proteins in capillary electrophoresis. *Anal. Chem*. **74,** 776–783.
51. Emmer, A. and Roeraade, J. (2001) Wall deactivation with fluorosurfactants for capillary electrophoretic analysis of biomolecules. *Electrophoresis* **22,** 660–665.
52. Pacakova, V., Hubena, S., Ticha, M., and Madera, M. S. K. (2001) Effects of electrolyte modification and capillary coating on separation of glycoprotein isoforms by capillary electrophoresis. *Electrophoresis* **22,** 459–463.
53. Dou, Y. H., Bao, N., Xu, J. J., and Chen, H. Y. (2002) A dynamically modified microfluidic poly(dimethylsiloxane) chip with electrochemical detection for biological analysis. *Electrophoresis* **23,** 3558–3566.
54. Bao, J. J. (2000) Separation of proteins by capillary electrophoresis using an epoxy based hydrophilic coating. *J. Liq. Chromaatogr. Rel. Technol*. **23,** 61–78.
55. Belenkii, B. G., Kassalainen, G. E., and Nasledov, D. G. (2000) Modified capillary electrophoresis system for peptide, protein and double-stranded DNA analysis. *J. Chromatogr. A* **879,** 189–196.
56. Cretich, M., Stastna, M., Chrambach, A., and Chiari, M. (2002) Decreased protein peak asymmetry and width due to static capillary coating with hydrophilic derivatives of polydimethylacrylamide. *Electrophoresis* **23,** 2274–2278.
57. Chiari, M., Cretich, M., Stastna, M., Radko, S. P., and Chrambach, A. (2001) Rapid capillary coating by epoxy-poly-(dimethylacrylamide): performance in capillary zone electrophoresis of protein and polystyrene carboxylate. *Electrophoresis* **22,** 656–659.

58. Leinweber, F. C., Stein, J., and Otto, M. (2001) Capillary zone electrophoresis of proteins with poly(2-hydroxyethyl methacrylate)-coated capillaries: fundamentals and applications. *Fresenius J. Anal. Chem.* **370,** 781–788.
59. Kleindienst, G., Huber, C. G., Gjerde, D. T., Yengoyan, L., and Bonn, G. K. (1998) Capillary electrophoresis of peptides and proteins in fused-silica capillaries coated with derivatized polystyrene nanoparticles. *Electrophoresis* **12,** 262–269.
60. Zhang, J. and Horvath, C. (2003) Capillary electrophoresis of proteins in dextran-coated columns. *Electrophoresis* **24,** 115–120.
61. Le Potier, I., Taverna, M., Fattal, E., Benzaki, J., Chevalier, M., and Ferrier, D. (2001) Performance evaluation of capillary surface treatments for peptide mapping by capillary zone electrophoresis. *Chromatographia* **53,** 563–570.
62. Tsai, S. W., Loughran, M., Hiratsuka, A., Yano, K., and Karube, I. (2003) Application of plasma-polymerized films for isoelectric focusing of proteins in a capillary electrophoresis chip. *Analyst* **128,** 237–244.
63. Gaudioso, J. and Craighead, H. G. (2002) Characterizing electroosmotic flow in microfluidic devices. *J. Chromatogr. A* **971,** 249–253.
64. Nilsson, H., Wiklund, M., Johansson, T., Hertz, H. M., and Nilsson, S. (2001) Microparticles for selective protein determination in capillary electrophoresis. *Electrophoresis* **22,** 2384–2390.
65. Kubo, K. and Hattori, A. (2001) Assessment of the capillary zone electrophoretic behavior of proteins in the presence of electroosmotic modifiers: protein-polyamine interaction studied using a polyacrylamide-coated capillary. *Electrophoresis* **22,** 3389–3394.
66. Tabuchi, M. and Baba, Y. (2001) A separation carrier in high-speed proteome analysis by capillary electrophoresis. *Electrophoresis* **22,** 3449–3457.
67. Macka, H., Johns, C., Grosse, A., and Haddad, P. R. (2001) New isoelectric buffers for capillary electrophoresis: *N*-carboxymethylated polyethyleneimine as a macromolecular isoelectric buffer. *Analyst* **126,** 421–425.
68. Tseng, W. L., Lin, Y. W., and Chang, H. T. (2002) Improved separation of microheterogeneities and isoforms of proteins by capillary electrophoresis using segmental filling with SDS and PEO in the background electrolyte. *Anal. Chem.* **74,** 4828–4834.
69. Mosulishvili, L. M., Barnov, V. A., Tsibakhashvili, N. Y., Engelhardt, H., and Beck, W. J. (2001) Enhancing detection sensitivity in capillary electrophoresis. *J. Anal. Chem.* **56,** 512–514.
70. Wu, X. Z. and Pawliszyn, J. (2002) Whole-column imaging capillary electrophoresis of proteins with a short capillary. *Electrophoresis* **23,** 542–549.
71. Wu, X. Z., Sze, N. S. K., and Pawliszyn, J. (2001) Miniaturization of capillary isoelectric focusing. *Electrophoresis* **22,** 3968–3971.
72. Jin, L. J., Giordano, B. C., and Landers, J. P. (2001) Dynamic labeling during capillary or microchip electrophoresis for laser-induced fluorescence detection of protein-SDS complexes without pre- or postcolumn labeling. *Anal. Chem.* **23,** 1090–1095.

73. McCorquodale, E. M. and Coyler, C. L. (2001) Indocyanine green as a noncovalent, pseudofluorogenic label for protein determination by capillary electrophoresis. *Electrophoresis* **22,** 2403–2408.
74. Sze, N. S. K., Huang, T. M., and Pawliszyn, J. (2002) Laser-induced fluorescence detection of non-covalently labeled protein in capillary isoelectric focusing. *J. Sep. Sci*. **25,** 1119–1122.
75. Sowell, J., Agnew-Heard, K. A., Mason, J. C., Mama, C., Strekowski, L., and Patonay, G. (2001) Use of non-covalent labeling in illustrating ligand binding to human serum albumin via affinity capillary electrophoresis with near-infrared laser induced fluorescence detection. *J. Chromatogr. B* **755,** 91–99.
76. Harvey, M. D., Bablekis, V., Banks, P. R., and Skinner, C. D. (2001) Utilization of the non-covalent fluorescent dye, NanoOrange, as a potential clinical diagnostic tool. nanomolar human serum albumin quantitation. *J. Chromatogr. B* **754,** 345–356.
77. Zhang, X. and Sweedler, J. V. (2001) Ultraviolet native fluorescence detection in capillary electrophoresis using a metal vapor NeCu laser. *Anal. Chem*. **73,** 5620–5624
78. Okerberg, E. and Shear, J. B. (2001) Attomole-level protein fingerprinting based on intrinsic peptide fluorescence. *Anal. Chem*. **73,** 1610–1613.
79. He, Y. and Geng, L. (2001) Phase-sensitive fluorescence lifetime detection in capillary electrophoresis. *Anal. Chem*. **73,** 943–950.
80. LeCaptain, D. J., Michel, M. A., and Van Orden, A. (2001) Characterization of DNA-protein complexes by capillary electrophoresis-single molecule fluorescence correlation spectroscopy. *Analyst* **126,** 1279–1284.
81. Le, X. C., Wang, Q. H., and Lam, M. T. (2002) Fluorescence polarization detection for affinity capillary electrophoresis. *Electrophoresis* **23,** 903–908.
82. Chabinyc, M. L., Chiu, D. T., McDonald, J. C., et al. (2001) An integrated fluorescence detection system in poly(dimethylsiloxane) for microfluidic applications. *Anal. Chem*. **73,** 4491–4498.
83. Sanders, J. C., Huang, Z. L., and Landers, J. P. (2001) Acousto-optical deflection-based whole channel scanning for microchip isoelectric focusing with laser-induced fluorescence detection. *Lab on a Chip* **1,** 167–172.
84. Wetterhall, M., Palmblad, M., Hakansson, P., Markides, K. E., and Bergquist, J. (2002) Rapid analysis of tryptically digested cerebrospinal fluid using capillary electrophoresis-electrospray ionization-fourier transform ion cyclotron resonance-mass spectrometry. *J. Proteome Res*. **1,** 361–366.
85. Tsybin, Y. O., Hakansson, P. W. M., Markides, K. E., and Bergquist, J. (2002) Capillary electrophoresis and electron capture dissociation Fourier transform ion cyclotron resonance mass spectrometry for peptide mixture and protein digest analysis. *Eur. J. Mass Spectrom*. **8,** 389–395.
86. Huber, C. G., Premstaller, A., and Kleindienst, G. (1999) Evaluation of volatile eluents and electrolytes for high-performance liquid chromatography–electrospray

ionization mass spectrometry and capillary electrophoresis–electrospray ionization mass spectrometry of proteins: II. capillary electrophoresis. *J. Chromatogr. A* **849,** 175–189.

87. Lynen, F., Zhao, Y., Becu, C., Borremans, F., and Sandra, P. (1999) Considerations concerning interaction characterization of oligopeptide mixtures with vancomycin using affinity capillary electrophoresis-electrospray mass spectrometry. *Electrophoresis* **20,** 2462–2474.
88. Zhang, C. X., Xiang, F., Pasa-Tolic, L., Anderson, G. A., Veenstra, T. D., and Smith, R. D. (2000) Stepwise mobilization of focused proteins in capillary isoelectric focusing mass spectrometry. *Anal. Chem*. **72,** 1462–1468.
89. Tong, W., Link, A., Eng, J. K., and Yates III, J. R. (1999) Identification of proteins in complexes by solid-phase microextraction/multistep elution/capillary electrophoresis/tandem mass spectrometry. *Anal. Chem*. **71,** 2270–2278.
90. Li, J., Kelly, J. F., Chernushevich, I., Harrison, D. J., and Thibault, P. (2000) Separation and identification of peptides from gel-isolated membrane proteins using a microfabricated device for combined capillary electrophoresis/nanoelectrospray mass spectrometry. *Anal. Chem*. **72,** 599–609.
91. Liu, J., Tseng, K., Garcia, B., et al. (2001) Electrophoresis separation in open microchannels. a method for coupling electrophoresis with MALDI-MS. *Anal. Chem*. **73,** 2147–2151.
92. Hiraoka, A., Tominaga, I., and Hori, K. (2002) One-step capillary isoelectric focusing of the proteins in cerebrospinal fluid and serum of patients with neurological disorders. *J. Chromatogr. A* **961,** 147–153.
93. Hashimoto, M., Tsugoagoshi, K. N. R., and Kondo, K. (1999) Chemiluminescence detection of heme proteins separated by capillary isoelectric focusing. *J. Chromatogr. A* **852,** 597–601.
94. Kautz, R. A., Lacey, M. E., Wolters, A. M., et al. (2001) Sample concentration and separation for nanoliter-volume NMR spectroscopy using capillary isotachophoresis. *J. Am. Chem. Soc*. **123,** 3159–3160.
95. Guijt, R. M., Baltussen, E., van der Steen, G., et al. (2001) Capillary electrophoresis with on-chip four-electrode capacitively coupled conductivity detection for application in bioanalysis. *Electrophoresis* **22,** 2537–2541.
96. Kuijt, J., van Teylingen, R., Nijbacker, T., Ariese, F., Brinkman, U. A. T., and Gooijer, C. (2001) Detection of nonderivatized peptides in capillary electrophoresis using quenched phosphorescence. *Anal. Chem*. **73,** 5026–5029.
97. Chen, J. Z. and Lee, C. S. (2002) On-line post-capillary affinity detection of immunoglobulin G for capillary zone electrophoresis. *J. Chromatogr. B* **768,** 105–111.
98. Guijt-van Duijn, R. M., Frank, J., van Dedem, G. W., and Baltussen, E. (2000) Recent advances in affinity capillary electrophoresis. *Electrophoresis* **21,** 3905–3918.
99. Heegaard, N. H. H. and Kennedy, R. T. (1999) Identification, quantitation, and characterization of biomolecules by capillary electrophoretic analysis of binding interactions. *Electrophoresis* **20,** 3122–3133.

100. Tanaka, Y. and Terabe, S. (2002) Estimation of binding constants by capillary electrophoresis. *J. Chromatogr. B* **768,** 81–92.
101. Lynen, F., Borremans, F., and Sandra, P. (2001) Practical evaluation of the influence of excessive sample concentration on the estimation of dissociation constants with affinity capillary electrophoresis. *Electrophoresis* **22,** 1974–1978.
102. Galbusera, C., Thachuk, M., De Lorenzi, E., and Chen, D. D. Y. (2002) Affinity capillary electrophoresis using a low-concentration additive with the consideration of relative mobilities. *Anal. Chem.* **74,** 1903–1914.
103. Heintz, J., Hernandez, M. and Gomez, F. A. (1999) Use of a partial-filling technique in affinity capillary electrophoresis for determining binding constants of ligands to receptors. *J. Chromatogr. A* **840,** 261–280.
104. Kiessig, S., Bang, H., and Thunecke, F. (1999) Interaction of cyclophilin and cyclosporins monitored by affinity capillary electrophoresis. *J. Chromatogr. A* **853,** 469–477.
105. Hafner, F. T., Kautz, R. A., Iverson, B. L., Tim, R. C., and Karger, B. L. (2000) Noncompetitive immunoassay of small analytes at the femtomolar level by affinity probe capillary electrophoresis: direct analysis of digoxin using a uniform-labeled scFv immunoreagent. *Anal. Chem.* **72,** 5779–5786.
106. Foulds, G. J. and Etzkorn, F. A. (1999) DNA-binding affinities of MyoD and E47 homo- and hetero-dimers by capillary electrophoresis mobility shift assay. *J. Chromatogr. A* **862,** 231–236.
107. Kim, H. S., Austin, J., and Hage, D. S. (2002) Identification of drug-binding sites on human serum albumin using affinity capillary electrophoresis and chemically modified proteins as buffer additives. *Electrophoresis* **23,** 956–963.
108. Bean, S. R. and Lookhart, G. L. (1999) Sodium dodecyl sulfate capillary electrophoresis of wheat proteins. 1. uncoated capillaries. *J. Agric. Food Chem.* **47,** 4246–4255.
109. Hu, S., Zhang, Z., Cook, L. M., Carpenter, E. J., and Dovichi, N. J. (2000) Separation of proteins by sodium dodecylsulfate capillary electrophoresis in hydroxypropylcellulose sieving matrix with laser-induced fluorescence detection. *J. Chromatogr. A* **894,** 291–296.
110. Bousse, L., Mouradian, S., Minalla, A., Yee, H., Williams, K., and Dubrow, R. (2001) Protein sizing on a microchip. *Anal. Chem.* **73,** 1207–1212.
111. Hu, S., Ye, Y. L., Surh, G., Clark, J. I., and Dovichi, N. J. (2002) Analysis of proteins by capillary SDS-DALT electrophoresis with laser-induced fluorescence detection. *LC-GC* **15,** 166.
112. Hu, S., Zhang, L., Cook, L. M., and Dovichi, N. J. (2001) Capillary sodium dodecyl sulfate-DALT electrophoresis of proteins in a single human cancer cell. *Electrophoresis* **22,** 3677–3682.
113. Shen, Y., Xiang, F., Veenstra, T. D., Fung, E. N. and Smith, R. D. (1999) High-resolution capillary isoelectric focusing of complex protein mixtures from lysates of microorganisms. *Anal. Chem.* **71,** 5348–5353.

114. König, S. and Welsch, T. (2000) Moderation of the electroosmotic flow in capillary electrophoresis by chemical modification of the capillary surface with tentacle-like oligourethanes. *J. Chromatogr. A* **894,** 79–88.
115. Shimura, K., Wang, Z., Matsumoto, H., and Kasai, K. -I. (2000) Synthetic oligopeptides as isoelectric point markers for capillary isoelectric focusing with ultraviolet absorption detection. *Electrophoresis* **21,** 603–610.
116. Mao, Q. and Pawliszyn, J. (1999) Capillary isoelectric focusing with whole column imaging detection for analysis of proteins and peptides. *J. Biochem. Biophys. Methods* **39,** 93–110.
117. Wen, J., Lin, Y., Xiang, F., Matson, D. W., Udseth, H. R., and Smith, R. D. (2000) Microfabricated isoelectric focusing device for direct electrospray ionization-mass spectrometry. *Electrophoresis* **21,** 191–197.
118. Tran, N. T., Taverna, M., Chevalier, M., and Ferrier, D. (2000) One-step capillary isoelectric focusing for the separation of the recombinant human immunodeficiency virus envelope glycoprotein glycoforms. *J. Chromatogr. A* **866,** 121–135.
119. Lopez-Soto-Yarritu, P., Diez-Masa, J. C., Cifuentes, A., and De Frutos, M. (2002) Improved capillary isoelectric focusing method for recombinant erythropoietin analysis. *J. Chromatogr. A* **968,** 221–228.
120. Ladsun, A. M., Kurumbail, R. R., Leimgruber, N. K., and Rathore, A. S. (2001) Validatibility of a capillary isoelectric focusing method for impurity quantitation. *J. Chromatogr. A* **917,** 147–158.
121. Mohan, D. and Lee, C. S. (2002) On-line coupling of capillary isoelectric focusing with transient isotachophoresis-zone electrophoresis: a two-dimensional separation system for proteomics. *Electrophoresis* **23,** 3160–3167.
122. Sheng, L. and Pawliszyn, J. (2002) Comprehensive two dimensional separation based on coupling micellar electrokinetic chromatography with capillary isoelectric focusing. *Analyst* **127,** 1159–1163.
123. Issaq, H. J., Chan, K. C., Janini, G. M., and Muschik, G. M. (1999) A simple two-dimensional high performance liquid chromatography/high performance capillary electrophoresis set-up for the separation of complex mixtures. *Electrophoresis* **20,** 1533–1537.
124. Wall, D. B., Kachman, M. T., Gong, S., et al. (2000) Isoelectric focusing nonporous RP HPLC: a two-dimensional liquid-phase separation method for mapping of cellular proteins with identification using MALDI-TOF mass spectrometry. *Anal. Chem.* **72,** 1099–1111.
125. Tragas, C. and Pawliszyn, J. (2000) On-line coupling of high performance gel filtration chromatography with imaged capillary isoelectric focusing using a membrane interface. *Electrophoresis* **21,** 227–237.
126. Chen, X. X., Wu, H. K., Mao, C. D., and Whitesides, G. M. (2002) A prototype two-dimensional capillary electrophoresis system fabricated in poly(dimethylsiloxane). *Anal. Chem.* **74,** 1772–1778.
127. Herr, A. E., Molho, J. I., Drouvalakis, K. A., et al. (2003) On-chip coupling of isoelectric focusing and free solution electrophoresis for multidimensional separations. *Anal. Chem.* **75,** 1180–1187.

128. Claeys, R., Groven, C., and Gorus, F. K. (2001) Capillary zone electrophoresis of proteins in body Fluids: comparison of capillary and agarose gel electrophoresis. *Clin. Chem*. **47,** 967–970.
129. Bossuyt, X., Claeys, R., Bogaert, G., et al. (2001) Reference values for the five electrophoretic serum protein fractions in Caucasian children by capillary zone electrophoresis. *Clin. Chem. Lab*. **39,** 970–972.
130. Le Bricon, T., Launay, E., Houze, P., Bengoufa, D., Bousquet, B., and Gourmel, B. (2002) Determination of poorly separated monoclonal serum proteins by capillary zone electrophoresis. *J. Chromatogr. B* **775,** 63–70.
131. Jia, Z. J., Ramstad, T., and Zhong, M. (2002) Determination of protein–drug binding constants by pressure-assisted capillary electrophoresis (PACE)/frontal analysis (FA). *J. Pharm. Biomed. Anal*. **30,** 405–413.
132. Shimura, K., Hoshino, M., Kamiya, K., et al. (2002) Immunoassay of serum α_1-antitrypsin by affinity-probe capillary isoelectric focusing using a fluorescence-labeled recombinant antibody fragment. *Electrophoresis* **23,** 909–917.
133. Varesio, E., Rudaz, S., Krause, K. H., and Veuthey, J. L. (2002) Nanoscale liquid chromatography and capillary electrophoresis coupled to electrospray mass spectrometry for the detection of amyloid- peptide related to Alzheimer. *J. Chromatogr. A* **974,** 135–142.
134. Clarke, N. J. and Naylor, S. (2002) Capillary isoelectric focusing-mass spectrometry: analysis of protein mixtures from human body fluids. *Biomed. Chromatogr*. **16,** 287–297.
135. Moini, M., Demars, S. M., and Huang, H. L. (2002) Analysis of carbonic anhydrase in human red blood cells using capillary electrophoresis/electrospray ionization-mass spectrometry. *Anal. Chem*. **74,** 3772–3776.
136. Kolios, G., Bairaktari, E., Tsolas, O. and Seferiadis, K. (2001) Routine differential diagnosis of proteinurias by capillary electrophoresis. *Clin. Chem. Lab. Med*. **39,** 784–788.
137. Porcel, J. M., Vives, M., Esquerda, A., and Rivas, M. C. (2001) Pleural protein capillary electrophoresis for the separation of transudates and exudates. *Clin. Chem*. **47,** 975–976.
138. Hu, S., Jiang, J., Cook, L. M., et al. (2002) Capillary sodium dodecyl sulfate-DALT electrophoresis with laser-induced fluorescence detection for size-based analysis of proteins in human colon cancer cells. *Electrophoresis* **23,** 3136–3142.
139. Jenkins, M. A. and Ratnaike, S. (1999) Five unusual serum protein presentations found by capillary electrophoresis in the clinical laboratory. *J. Biochem. Biophys. Methods* **41,** 31–47.
140. Hiraoka, A., Tominaga, I., and Hori, K. (2000) Sodium dodecylsulfate capillary gel electrophoretic measurement of the concentration ratios of albumin and alpha2-macroglobulin in cerebrospinal fluid and serum of patients with neurological disorders. *J. Chromatogr. A* **895,** 339–344.
141. Frazier, R.A. (2001) Recent advances in capillary electrophoresis methods for food analysis. *Electrophoresis* **22,** 4197–4206.

142. Recio, I., Ramos, M., and Lopez-Fandino, R. (2001) Capillary electrophoresis for the analysis of food proteins of animal origin. *Electrophoresis* **22,** 1489–1502.
143. Zhu, J. and Khan, K. (2001) Separation and quantification of HMW glutenin subunits by capillary electrophoresis. *Cereal Chem*. **78,** 737–742.
144. Siriamornpun, S., Wootton, M., Cox, J. M., Bekes, F., and Wrigley, C. W. A. (2001) Capillary electrophoresis of wheat gliadin proteins and its potential for wheat varietal identification using pattern matching software. *Aust. J. Agr. Res*. **52,** 839–843.
145. Scholz, E., Ganzler, K., Gergely, S., and Salgo, A. (2002) Use of capillary electrophoresis to monitor wheat maturation. *Chromatographia* **56,** S127–S130.
146. Strickland, M., Johnson, M. E., and Broadbent, J. R. (2001) Qualitative and quantitative analysis of proteins and peptides in milk products by capillary electrophoresis. *Electrophoresis* **22,** 1510–1517.
147. Miralles, B., Rothbauer, V., Manso, M. A., Amigo, L., Krause, I., and Ramos, M. (2001) Improved method for the simultaneous determination of whey proteins, caseins and *para*-casein in milk and dairy products by capillary electrophoresis. *J. Chromatogr. A* **915,** 225–230.
148. De Block, J., Merchiers, M., Mortiers, L., et al. (2003) Monitoring nutritional quality of milk powders: capillary electrophoresis of the whey protein fraction compared with other methods. *Int. Diary J*. **13,** 87–94.
149. Fayle, S. E., Healy, J. P., Brown, P. A., Reid, E. A., Gerrard, J. A., and Ames, J. M. (2001) Novel approaches to the analysis of the Maillard reaction of proteins. *Electrophoresis* **22,** 1518–1525.
150. Guyomarch, F., Warin, F., Muir, D. D., and Leaver, J. (2000) Lactosylation of milk proteins during the manufacture and storage of skim milk powders. *Int. Diary J*. **10,** 863–872.
151. Bertoldo Pacheco, M. T., Amaya-Farfan, J., and Sgarbieri, V. (2002) Partial characterization of a whey protein concentrate and its enzyme hydrolysates. *J. Food Biochem*. **26,** 327–338.
152. Civardi, G., Curadi, M. C., Orlandi, M., Cattaneo, T. M. P., and Giangiacomo, R. (2002) Capillary electrophoresis (CE) applied to analysis of mare's milk. *Milchwissenschaft* **82,** 1240–1245.
153. Molina, E., Ramos, M., and Amigo, L. (2002) Characterisation of the casein fraction of Iberico cheese by electrophoretic techniques. *J. Sci. Food Agric*. **82,** 1240–1245.
154. Day, L. and Brown, H. (2001) Detection of mechanically recovered chicken meat using capillary gel electrophoresis. *Meat Sci*. **58,** 31–37.
155. Martin A., Cordoba J. J., Rodriguez M. M., Nunez F., and Asensio, M. A. (2001) Evaluation of microbial proteolysis in meat products by capillary electrophoresis. *J. Appl. Microbiol*. **90,** 163–171.
156. Larrain, M. A., Abugoch, L., Quitral, V., Vinagre, J., and Segovia, C. (2002) Capillary zone electrophoresis as a method for identification of golden kinglip (Genypterus blacodes) species during frozen storage. *Food Chem*. **76,** 377–384.

157. Rodriguez-Delgado, M. A., Malovana, S., Montelongo, F. J., and Cifuentes (2002) Fast analysis of proteins in wines by capillary gel electrophoresis. *Eur. Food Res. Technol*. **214,** 536–540.
158. Mazhar, H., Basha, S. M., and Lu, J. (2002) Variation in berry protein composition of muscadine cultivars. *Am. J. Enol. Viticul*. **53,** 87–91.
159. Righetti, P. G. (2001) Capillary-electrophoretic analysis of proteins and peptides of biomedical and pharmacological interest. *Biopharm. Drug Disp*. **22,** 337–351.
160. Gawron, A. J., Martin, R. S., and Lunte, S. (2001) Microchip electrophoretic separation systems for biomedical and pharmaceutical analysis. *Eur. J. Pharm. Sci*. **14,** 1–12.
161. Hwang, K. -H., Lee, K. W., Kim, C. S., Han, K., Chung, Y. -B. and Moon, D. -C. (2001) Determination of recombinant human epidermal growth factor (rhEGF) in a pharmaceutical preparation by capillary electrophoresis. *Arch. Pharm. Res*. **24,** 601–606.
162. Eriksson, H. J. C., Somsen, G. W., Hinrichs, W. L. J., Frijlink, H. W., and de Jong, G. J. (2001) Characterization of human placental alkaline phosphatase by activity and protein assays, capillary electrophoresis and matrix-assisted laser desorption/ionization time-of-flight mass spectrometry. *J. Chromatogr. B* **755,** 311–319.
163. Eriksson, H. J. C., Wijngaard, M., Hinrichs, W. L. J., Frijlink, H. W., Somsen, G. W., and De Jong, G. J. (2003) Potential of capillary electrophoresis for the monitoring of the stability of placental alkaline phosphatase. *J. Pharm. Biomed*. **31,** 351–357.
164. Jensen, P. K., Pasa-Tolic, L., Anderson, G. A., et al. (1999) Probing proteomes using capillary isoelectric focusing-electrospray ionization Fourier transform ion cyclotron resonance mass spectrometry. *Anal. Chem*. **71,** 2076–2084.
165. Michels, D. A., Hu, S., Schoenherr, R. M., Eggerston, M. J., and Dovichi, N. J. (2002) Fully automated two-dimensional capillary electrophoresis for high sensitivity protein analysis. *Mol. Cell. Proteomics* **1,** 69–74.
166. Li, J. J., Tremblay, T. L., Wang, C., Attiya, S., Harrison, D. J., and Thibault, P. (2001) Integrated system for high-throughput protein identification using a microfabricated device coupled to capillary electrophoresis/nanoelectrospray mass spectrometry. *Proetomics* **1,** 975–986.
167. Wu, X. Z., Huang, T. M., Mullett, W. M., and Yeung, J. M. (2001) Determination of isoelectric point and investigation of immunoreaction in peanut allergenic proteins-rabbit IgG antibody system by whole-column imaged capillary isoelectric focusing. *J. Microcol. Sep*. **13,** 322–326.
168. Viskari, P. J., Kinkade, C. S., and Colyer, C. L. (2001) Determination of phycobiliproteins by capillary electrophoresis with laser-induced fluorescence detection. *Electrophoresis* **22,** 2327–2335.
169. Viskari, P. J. and Colyer, C. L. (2002) Separation and quantitation of phycobiliproteins using phytic acid in capillary electrophoresis with laser-induced fluorescence detection. *J. Chromatogr. A*. **972,** 269–276.

170. Deterding, L. J., Cutalo, J. M., Khaledi, M., and Tomer, K. B. (2002) Separation and characterization of human high-density apolipoproteins using a nonaqueous modifier in capillary electrophoresis-mass spectrometry. *Electrophoresis* **23,** 2296–2305.
171. Presley, A. D., Poe, B. G., and Arriaga, E. A. (2002) Separation and detection of fluorescently-labeled mitochondrial proteins by capillary electrophoresis with laser-induced fluorescence detection. *Abstr. Papers ACS* **223,** 259.
172. Galli, A., Ghezzi, L., Raspi, G., Secco, F., and Spinetti, M. (2002) Detection of heterologous bovine pancreatic trypsin inhibitor by capillary zone electrophoresis. *Polyhedron* **21,** 1405–1410.
173. Nicholas, K., Forney, C. F., and Paulson, A. T. (2002) A rapid capillary gel electrophoresis method for the quantitative determination of RuBisCo in spinach. *Phytochem. Anal*. **13,** 39–44.
174. Tseng, W. L., Chiu, T. C., Weng, J. M., and Chang, H. T.(2001) Analysis of albumins, using albumin blue 580, by capillary electrophoresis and laser-induced fluorescence. *J. Liq. Chromatogr*. **24,** 2971–2982.
175. Murakami, Y., Morita, T., Kanekiyo, T., and Tamiya, E. (2001) On-chip capillary electrophoresis for alkaline phosphatase testing. *Biosens. Bioelectron*. **16,** 1009–1014.
176. Soundararajan, S., Guariglia, L., Sydor, W., and Mercorelli, S. (2001) Analysis of an IgG4 monoclonal antibody by protein lab-on-chip technology, SDS-capillary gel electrophoresis and SDS-polyacrylamide gel electrophoresis. *Abstr. Papers ACS* **222,** 16.
177. Starkey, D. E., Han, A., Abdelaziez, Y., et al. (2001) Fluorogenic assays for β-glucuronidase and mitogen activated protein kinase using microchip capillary electrophoresis (μ CE). *Abstr. Papers ACS* **222,** 70.
178. Schrum, D. P. and Worthington, M. (2001) Analysis of amyloid β-A4-related peptides, amyloid protein fibrils, and their interactions by capillary electrophoresis. *Abstr. Papers ACS* **221,** 720.
179. Liu, C. M. and Tzeng, Y. M. (2001) Quantitative analysis of parasporal crystal protein from *Bacillus thuringiensis* by capillary electrophoresis. *J. Food Drug Anal*. **9,** 79–83.
180. Ledger, R., Tucker, I. G., and Walker, G. F. (2002) Quantitative capillary electrophoresis assay for the proteolytic stability of luteinizing hormone-releasing hormones. *J. Chromatogr. B* **769,** 235–242.
181. Dai, H. J., Parker, C. N., and Bao, J. J. (2002) Characterization and inhibition study of MurA enzyme by capillary electrophoresis. *J. Chromatogr. B* **766,** 123–132.
182. Sowell, J., Parihar, R., and Patonay, G. (2001) Capillary electrophoresis-based immunoassay for insulin antibodies with near-infrared laser induced fluorescence detection. *J. Chromatogr. B* **752,** 1–8.
183. Chiti, F., De Lorenzi, E., Grossi, S., et al. (2001) A partially structured species of β2-microglobulin is significantly populated under physiological conditions and involved in fibrillogenesis. *J. Biol. Chem*. **276,** 46714–46721.

184. Heegaard, N. H. H., Sen, J. W., Kaarsholm, N. C., and Nissen, M. H. (2001) Conformational intermediate of the amyloidogenic protein β2-microglobulin at neutral pH. *J. Biol. Chem.* **276,** 32657–32662.
185. Gu, X. L., Whipple-Vanpatter, G., O'Dwyer, M., and Zeece, M. (2001) Capillary electrophoretic analysis of μ- and m-calpain using fluorescently labeled casein substrates. *Electrophoresis* **22,** 2336–2342.
186. Keren, D. F., Gulbranson, R., Carey, J. L., and Krauss, J. C. (2001) 2-Mercaptoethanol treatment improves measurement of an IgMκ M-protein by capillary electrophoresis. *Clin. Chem.* **47,** 1326–1327.
187. Hu, S., Lee, R., Zhang, Z., Krylov, S. N. and Dovichi, N. J. (2001) Protein analysis of an individual Caenorhabditis elegans single-cell embryo by capillary electrophoresis. *J. Chromatogr. B* **752,** 307–310.
188. Li, H., Wu, H. Y., Wang, Y., Sims, C. E., and Allbritton, N. L. (2001) Improved capillary electrophoresis conditions for the separation of kinase substrates by the laser micropipet system. *J. Chromatogr. B* **757,** 79–88.
189. Negin, R. S. and Carbeck, J. D. (2002) Measurement of electrostatic interactions in protein folding with the use of protein charge ladders. *J. Am. Chem. Soc.* **124,** 2911–2916.
190. Hurlbert, J. and Preston, J. F. (2002) Differences in the solution structures of the parallel beta-helical pectate lyases as determined by limited proteolysis. *Biochim. Biophys. Acta* **1599,** 9–20.
191. Stellwagen Earle, O. E. and Righetti, P. G. (2002) Salt-promoted protein folding, preferential binding, or electrostatic screening? *Proteins* **49,** 147–153.
192. Fei, Y., Wei, L., Gao, S., et al. (2001) Isolation, purification and characterization of secondary structure of antifreeze protein from Ammopiptanthus mongolicus. *Chin. Sci. Bulletin* **46,** 495–498.
193. De Lorenzi, E., Grossi, S., Massolini, G., et al. (2002) Capillary electrophoresis investigation of a partially unfolded conformation of $beta_2$-microglobulin. *Electrophoresis* **23,** 918–925.
194. Rochu, D. and Maasson, P. (2002) Multiple advantages of capillary zone electrophoresis for exploring protein conformational stability. *Electrophoresis* **23,** 189–202.
195. Righetti, P. G. and Verzola, B. (2001) Folding/unfolding/refolding of proteins: present methodologies in comparison with capillary zone electrophoresis. *Electrophoresis* **22,** 2359–2374.
196. Uegaki, K., Taga, A., Akada, Y., Suzuki, S., and Honda, S. (2002) Simultaneous estimation of the association constants of glycoprotein glycoforms to a common protein by capillary electrophoresis. *Anal. Biochem.* **309,** 269–278.
197. Hattori, T., Kimura, K., Seyrek, E., and Dubin, P. L. (2001) Binding of bovine serum albumin to heparin determined by turbidimetric titration and frontal analysis continuous capillary electrophoresis. *Anal. Biochem.* **295,** 158–167.
198. Shibukawa, A., Ishizawa, N., Kimura, T., et al. (2002) Plasma protein binding study of oxybutynin by high-performance frontal analysis. *J. Chromatogr. B* **768,** 177–188.

199. Onishi, T., Mohamed, N. A. L., Shibukawa, A., et al. (2002) Frontal analysis of drug–plasma lipoprotein binding using capillary electrophoresis. *J. Pharm. Biomed. Anal*. **27,** 607–614.
200. Sowell, J., Mason, J. C., Strekowski, L. and Patonay, G. (2001) Binding constant determination of drugs toward subdomain IIIA of human serum albumin by near-infrared dye-displacement capillary electrophoresis. *Electrophoresis* **22,** 2512–2517.
201. Zhang, W. B., Zhang, L. H., Ping, G. C., Zhang, Y. K., and Kettrup, A. (2002) Study on the multiple sites binding of human serum albumin and porphyrin by affinity capillary electrophoresis. *J. Chromatogr. B* **768,** 211–214.
202. Ding, Y. S., Lin, B. C., and Huie, C. W. (2001) Binding studies of porphyrins to human serum albumin using affinity capillary electrophoresis. *Electrophoresis* **22,** 2210–2216.
203. Rabiller-Baudry, M. and Chaufer, B. (2001) Specific adsorption of phosphate ions on proteins evidenced by capillary electrophoresis and reversed-phase high-performance liquid chromatography. *J. Chromatogr. B* **753,** 67–77.
204. Kuroda, Y., Kita, Y., Shibukawa, A., and Nakagawa, T. (2001) Role of biantennary glycans and genetic variants of human alpha1-acid glycoprotein in enantioselective binding of basic drugs as studied by high performance frontal analysis/capillary electrophoresis. *Pharm. Res*. **18,** 389–393.
205. He, X. Y., Xiao, H. B., Liang, X. M., and Lin, B. C. (2002) Quantitative evaluation of the interaction between pUC19DNA and ovalbumin by capillary zone electrophoresis. *J. Sep. Sci*. **25,** 711–714.
206. Purcell, M., Neault, J. F., Malonga, H., Arakawa, H., and Tajmir-Riahi, H. A. C. (2001) Interaction of human serum albumin with oxovanadium ions studied by FT-IR spectroscopy and gel and capillary electrophoresis. *Can. J. Chem*. **79,** 1415–1421.
207. Liu, T., Li, J. D., Zeng, R., Shao, X. X., Wang, K. Y., and Xia, Q. C. (2001) Capillary electrophoresis-electrospray mass spectrometry for the characterization of high-mannose-type N-glycosylation and differential oxidation in glycoproteins by charge reversal and protease/glycosidase digestion. *Anal. Chem*. **73,** 5875–5885.
208. Grady, J. K., Zang, J., Laue, T. M., Arosio, P., and Chasteen, N. D. (2002) Characterization of the H- and L-subunit ratios of ferritins by sodium dodecyl sulfate–capillary gel electrophoresis. *Anal. Biochem*. **302,** 263–268.
209. Lee, H. G., Chang, S., and Fritsche, E. (2002) Rational approach to quantitative sodium dodecyl sulfate capillary gel electrophoresis of monoclonal antibodies. *J. Chromatogr. A* **947,** 143–149.
210. Page, J. S., Rubakhin, S. S., and Sweedler, J. V. (2002) Single-neuron analysis using CE combined with MALDI MS and radionuclide detection. *Anal. Chem*. **74,** 497–503.
211. Mohan, D. and Lee, C. S. (2002) On-line coupling of capillary isoelectric focusing with transient isotachophoresis-zone electrophoresis: a two-dimensional separation system for proteomics. *Electrophoresis* **23,** 3160–3167.

21

Separation of Synthetic (Co)Polymers by Capillary Electrophoresis Techniques

Hervé Cottet and Pierre Gareil

Summary

Capillary electrophoresis (CE) is a very efficient tool for separating and characterizing synthetic polymers, copolymers, and polyelectrolytes. Different modes of CE (free solution capillary electrophoresis [FSCE], entangled polymer solution CE [EPSCE], capillary gel electrophoresis [CGE], or micellar electrokinetic chromatography [MEKC]) can be used depending on the characteristics of the polymer solutes (end charged, evenly charged, or uncharged polymers) and on the polymer solute heterogeneities (molecular mass, functionality, chemical composition). To illustrate the potential of CE, four different methods are proposed using either nonaqueous or aqueous electrolytes. The first method describes the separation of synthetic organic polypeptides according to their functionalities and molar masses in a nonaqueous electrolyte. In a second method, polyelectrolyte oligomers are separated by FSCE in aqueous buffer. The third method demonstrates the great potential of EPSCE for the size-based separation of evenly charged polyelectrolytes on a wide range of molar masses. The last method describes a simple two-dimensional approach realized in a single capillary that combines a separation according to the chemical composition (FSCE) with a size-based separation (EPSCE).

Key Words: Free solution capillary electrophoresis; entangled polymer solution; size-based separations; chemical composition; nonaqueous capillary electrophoresis; background electrolyte composition; synthetic polymers; oligomers; copolymers; polyelectrolytes; polypeptides; poly(Nε-trifluoroacetyl-L-lysine); polystyrenesulfonates; poly(acrylamide-co-2-acrylamido-2-methylpropanesulfonate).

From: *Methods in Molecular Biology, vol. 384: Capillary Electrophoresis*
Edited by: P. Schmitt-Kopplin © Humana Press Inc., Totowa, NJ

1. Introduction

The complete characterization of synthetic polymers requires the use of various experimental techniques. Indeed, synthetic polymer samples have multiple sources of heterogeneity that make their characterization very complex. First, they are usually made of macromolecules differing in their degrees of polymerization (N). Second, the macromolecules can differ in their functionality (chemical nature of the end group[s]). The information concerning this second source of heterogeneity is very important for the polymer chemist because the physico-chemical properties and reactivity of the polymer highly depend on it. In the case of copolymers, macromolecules differ in chemical composition (proportion of each type of monomers in the chain). Polymers can also have different architectures (block or random copolymers, star, branched or hyperbranched polymers, dendrimers, etc.).

Among the techniques used for polymer characterization, separation techniques can give interesting information on the distribution of the polymer sample according to one of the aforementioned parameters (molecular mass, functionality, chemical composition, etc.). The most popular separation technique for polymer characterization is undoubtedly size-exclusion chromatography (SEC), which separates macromolecules according to their hydrodynamic volumes, a molecular parameter strongly correlated to the molecular mass ***(1,2)***. Other chromatographic techniques such as interaction chromatography or chromatography at the critical point were investigated more recently and can bring interesting information on the distributions in chemical composition or in functionality ***(3)***.

Capillary electrophoresis (CE) has been widely used for the separation of natural polymers such as proteins, peptides, DNA, or polysaccharides ***(4–6a)***. More recently, various electrokinetic separation techniques were used for the characterization of synthetic polymers. Indeed, in response to the need for analytical tools suitable for characterizing the wide variety of synthetic (co)polymers, different CE modes have been used and were recently the topic of a few review articles ***(7–10)***. To provide an overview of the potential of the CE techniques for synthetic polymer analysis, some examples taken from the literature are presented in **Table 1** and have been classified according to: (1) the polymer characteristics (end-charged, evenly charged, or uncharged polymers), (2) the polymer heterogeneity on which the separation should be based (molecular mass, functionality, chemical composition), (3) the implemented CE technique (free solution capillary electrophoresis [FSCE], entangled polymer solution CE [EPSCE], capillary gel electrophoresis [CGE], micellar electrokinetic chromatography [MEKC]), and (4) the nature of the solvent used in the electrolyte (aqueous, hydro-organic, or nonaqueous). For each case, at least one example is described (when available in the literature), with some

Table 1
Examples of separations of synthetic polymers by CE techniques

				Examples				
Polymer characteristics	Polymer heterogeneity	CE technique	Potentiality	Solvent type	Buffer	Polymer sample	capillary	ref.
End-charged (co)polymers	Molecular mass	FSCE	Size-based separation in the oligomeric range of mass (typically, DP < 50)	Aqueous	30 mM creatinine buffer + acetic acid pH 4.8 + PEO 1g/L	Polyethylene oxide diamine (Jeffamine)	Fused silica	[11]
					Phosphate buffer pH 6.8	Hydroxy acid oligomers	Fused silica or DEAE-dextran coated	[12]
				Hydro-organic	Phosphoric acid in hexafluoroiso-propanol/water	Polyamide-6 oligomers	Fused silica	[13]
					Borate buffer in THF/water or MeOH/water or ACN/water	Polyethylene glycols, polypropylene glycols and their copolymers derivatized by phtalic anhydride	Fused silica	[14–15]

(Continued)

Table 1
(Continued)

Polymer characteristics	Polymer heterogeneity	CE technique	Potentiality	Examples				
				Solvent type	Buffer	Polymer sample	capillary	ref.
				Non-aqueous	Ammonium acetate + acetic acid in MeOH/ACN	Poly(N_{ε}-trifluoroacetyl-L-Lysines)	Fused silica	[16]
					THF/MeOH or dichloromethane/MeOH or chloroform/MeOH +10 mM perchloric acid	N-phenylaniline oligomers	Fused silica	[17]
		EPSCE or CGE	Size-based separation in the oligomeric range of mass (typically, DP< 100)	Aqueous	TRIS/Borate pH 8.3 containing 3%T/3%C crosslinked polyacrylamide	Ionic ethoxylated polymers	μ-PAGE-3	[18]

Functionality	FSCE	Separation according to the charge of the end groups and/or the number of the end groups	Aqueous	30 mM creatinine buffer + acetic acid pH 4.8+1g/L PEO	Polyethylene oxide diamine (Jeffamine) and monoamine	Fused silica	[11]
			Hydro-organic	Borate buffer + THF	Polyethylene glycols derivatized by benzene tricarboxylic anhydride	Fused silica	[14]
			Non-aqueous	Ammonium acetate + acetic acid in MeOH/ACN	Dead and living poly (N_{ε}- trifluo-roacetyl-L-Lysines)	Fused silica	[16]
Chemical composition	FSCE	Separation of block copolymers according to the polymer structure (micelle/ unimer) and according to the chemical composition of the micelles	Aqueous	Borate buffer	Associative diblock copolymers of poly(styrene-co-methacrylic acid) or poly(styrene-co-ethyleneoxide)	Fused silica	[19, 20]

(Continued)

Table 1
(Continued)

Polymer characteristics	Polymer heterogeneity	CE technique	Potentiality	Examples				
				Solvent type	Buffer	Polymer sample	capillary	ref.
				Hydro-organic	Borate buffer	Associative diblock copolymers of poly(ethylene propylene-co-styrenesulfonate) or poly(tert-butylstyrene-co-styrenesulfonate)	Fused silica	[20]
Evenly charged (co)polymers	Molecular mass	EPSCE or CGE	Size-based separation on large range of molecular masses	Aqueous	Phosphate buffer pH 5.0 + hydroxyethylcellulose	Polystyrene-sulfonates	Fused silca	[21]
					Borate buffer + hydroxyethylcellulose or polyoxyethylene	Polystyrene-sulfonates	Fused silca	[22, 23]
					Phosphate buffer pH 2.5 + 5% Dextran	Poly(2-vinylpyridines)	PVA-coated	[24, 25]

				Pyridine + PEO (200 10^3) 5%	Poly (diallyldimethy-lammonium)	PVA-coated	[26]
				Tris buffer pH 7.2 + 12% crosslinked polyacrylamide	Polyphosphoric acids	Polyacrylamide coated	[27]
			Non-aqueous	Poly(dimethy-lacrylamide) gels in NMF	DNA fragments	Coated	[28]
Evenly charged (co)polymers	FSCE	Size-based separation in the oligomeric range of mass (typically DP < 10) for polyelec-trolytes and on a wider range for dendrimers or non free-draining polymers	Aqueous	pyromellitic acid + triethylamine+ hexamethonium hydroxide pH 7.7	polyphosphates	Fused silica	[29]

(Continued)

Table 1
(Continued)

Polymer characteristics	Polymer heterogeneity	CE technique	Potentiality	Examples				
				Solvent type	Buffer	Polymer sample	capillary	ref.
					Borate buffer	Oligomers of polystyrenesul-fonates	Fused silica	[30, 31]
					Phosphate/acetic acid buffer pH 2.0	Polycarboxy-betaines (non free draining polyelectrolytes)	PVA coated	[26]
					Phosphate buffer pH 2.7	Poly(amidoamine) dendrimers	Fused silica	[33]
				Non-aqueous	CAPS buffer in MeOH+ Brij 35	Porphyrins oligomers	Fused silica	[32]
	Chemical composition	FSCE	Separation according to the charge rate or the chemical nature	Aqueous	Phosphate buffer pH 10	Poly (acrylamide-co-acrylic acids)	Fused silica	[34]
					Borate or phosphate buffer	Poly (acrylamide-co-2-acrylamido-2-propanesulfonates)	Fused silca	[35]

Evenly charged (co)polymers					Borate buffer + neutral or zwitterionic surfactant	Hydrophobically modified poly(acrylic acids)	Fused silica or PEG-coated	[36]
					Buffer pH 9.0	Poly (2-acrylamido-2-methylpropanesulfonate-co- *N*-dodecylmethyl-acrylamide)	Fused silica	[37]
					Phosphate + acetic acid pH 2.0	Polycarboxy- betaines	PVA-coated	[26]
				Hydro-organic	Borate in MeOH/water	Variously sulfonated polystyrenesulfonates	Fused silica	[31]
				Non-aqueous	CAPS buffer in MeOH+ Brij 35	Porphyrins oligomers	Fused silica	[32]
		MEKC		Hydro-organic	Borate buffer +SDS + 5% ACN, pH 9	Poly(2-hydroxyethyl methacrylate-co-2-acrylamido-2-methylpropanesulfonic acid)	Fused silica	[38]
Uncharged (co)polymers	Molecular mass	FSCE	Size-based separation in the oligomeric range of mass	Non-aqueous	Ammonium chloride + triethylamine in MeOH	Nonionic polyether	Fused silica	[39]

(Continued)

Table 1
(Continued)

Polymer characteristics	Polymer heterogeneity	CE technique	Potentiality	Examples				
				Solvent type	Buffer	Polymer sample	capillary	ref.
		EPSCE or CGE	Size-based separation	Non-aqueous (mainly)	Ammonium acetate + stearyl-tributylphosphonium bromide + PEO in DMF with (1–6%) water.	Polystyrenes and polymethyl-methacrylates	PVA coated	[41]
		Inverse CGE	Size-based separation on large range of molecular masses	Aqueous	Phosphate buffer pH 6.0 + 2% poly(vinyl sulfate)	Dextran derivatives	Fused silica	[9]
		(after derivatization of the end group(s) of the neutral polymer by a charged molecule, the problematic is similar to section: end-charged polymer/molecular mass)						
	Functionality	(after derivatization of the end group(s) of the neutral polymer by a charged molecule, the problematic is similar to section: end-charged polymer/functionality)						

	Chemical composition	MEKC	Separation according to the polymer hydrophobicity	Hydro-organic	Borate buffer + SDS in MeOH/water	Poly(vinyl-pyrrolidone-co-2-hydroxyethyl methacrylate)	Fused silica	[40]

Abbreviation: ACN, acetonitrile; Brij 35, polyoxyethylene 23 dodecyl ether; CAPS, 3-cyclohexylamino-1-propanesulfonic acid; DEAE, diethylaminoethyl; MeOH, methanol; PAGE, polyacrylamide gel electrophoresis; PEO, polyethylene oxide; PVA, polyvinyl alcohol; THF, tetrahydrofurane; TRIS, tri(hydroxymethyl)aminomethane.

details on the nature of the buffer, of the analyzed polymer, and on the type of capillary (bare vs coated silica capillaries). The merit of this presentation is that it emphasizes the potential of CE techniques (*see* **Table 1**) as a function of the polymer characteristics and heterogeneities. It also points out the areas that have not been yet researched. All of the application examples belong to the field of synthetic polymers, except for one category for which no synthetic polymer application was available in the literature. Of course, synthetic polymer samples often present different sources of heterogeneity and, for that reason, the same polymer can be classified in more than one category of the table.

1.1. End-Charged (co)Polymers

End-charged polymers are generally separated by FSCE according to their charge-to-mass ratio. Size-based separation in the oligomeric range of mass (typically $N < 20$ to 50) can be obtained either in aqueous, hydro-organic or in nonaqueous FSCE ***(11–17)***. The choice of the solvent highly depends on the polymer solubility. CGE can even improve the resolution for higher molecular masses (typically up to $N < 100$) ***(18)***.

End-charged polymers can also be separated according to their functionalities (difference in charge of the end groups) by aqueous, hydro-organic or nonaqueous FSCE ***(11,14–16)***. End-charged associative diblock copolymers were also separated according to the polymer structure in solution (micelle/unimer) and according to the chemical composition of the micelles ***(19,20)***.

1.2. Evenly Charged (co)Polymers

Evenly charged polymers are usually separated according to their molecular mass by EPSCE or by CGE ***(21–28)***. The size-based separation in such sieving medium is usually performed in aqueous electrolyte ***(21–27)*** because polyelectrolytes are generally water-soluble. The size-based separation can be obtained on a large range of molecular masses (typically from 10^3 to 10^6 g/mol). EPSCE is usually preferred to CGE for practical reasons (bubble formation, capillary conditioning, capillary lifetime, etc.). The main experimental parameters that influence the separation by EPSCE are: (1) chemical nature, concentration, and molecular mass of the separating polymer, ionic strength of the electrolyte, and (2) electric field. Some details on optimal conditions are given in **Note 1**. One example of CGE in nonaqueous mode has been reported ***(28)***, but it concerns natural polymers (DNA).

Size-based separation of evenly charged polyelectrolytes can be obtained by FSCE in some specific cases: (1) for low-molecular-mass oligomers (Typically $N < 10$) ***(30–32)***, (2) for intermediate molecular masses in the crossover region between the rod-like and the coil conformation (*see* **Note 2**) ***(31)***, (3) for

non-free draining polyelectrolytes (such as polycarboxybetaines ***[26]*** or highly charged dendrimers ***[33]***).

Evenly charged copolymers can also be separated according to their chemical composition. For copolymers varying in charge density (for example, when one of the monomers is charged and the other is uncharged), the separation is possible up to a certain chemical charge rate (*see* **Note 3**) ***(31,34,35)***. However, the chemical nature of the backbone (hydrophilic or hydrophobic) was found to change the electrophoretic behavior of variously charged copolymers ***(31)***. The separation of hydrophobic/hydrophilic random copolymers according to their hydrophobic content is also possible in FSCE containing neutral micelles ***(36)*** or in MEKC ***(38)***. Changes in copolymer conformations were also monitored by FSCE ***(37)***.

1.3. Uncharged (co)Polymers

Uncharged polymers cannot be separated by electrokinetic techniques unless an electric charge is conferred to them. This can be obtained by either (1) derivatizing one or both of its ends (and thus the problem is similar to that described under **Subheading 1.2.**), or (2) creating interactions with charged additives (cation in nonaqueous solvent ***[39]***, ionic surfactants ***[40]***, charged polyelectrolytes ***[9]***). When the neutral polymer becomes evenly charged by interaction with a small molecule (e.g., with ammonium in methanolic electrolyte ***[39]***), the electrophoretic behavior and the potential of the CE techniques are similar to those obtained for the separation of evenly charged polyelectrolytes (*see* **Note 4**). MEKC also appeared to be a very effective mode for the separation of neutral copolymers according to their chemical composition ***(40)***. Recently, Li et al. described the use of poly(ethylene oxide) (PEO) as a sieving polymer for the separation of neutral polymers (polystyrenes and polymethylmethacrylates) in almost completely nonaqueous electrolytes (dimethylformamide [DMF] containing 1–6% water) ***(41)***. The neutral polymer solutes were mobilized owing to the presence of a cationic surfactant in the electrolyte (stearyltributylphosphonium bromide). Engelhardt and Martin ***(9)*** demonstrated that inverse capillary gel electrophoresis (CGE) is feasible. In this mode, the neutral polymers are interacting with a charged sieving matrix.

2. Materials

2.1. Nonaqueous Free-Solution Capillary Electrophoresis of End-Charged Polypeptides

1. Samples: Poly(N_ε-trifluoroacetyl-L-lysine) (PTLL) were synthesized by ring-opening polymerization of N_ε-trifluoroacetyl-L–lysine *N*-carboxyanhydride in DMF. The polymerization was initiated by *n*-hexylamine ***(16)***.

2. The CE instrument was an Agilent Technologies CE system (Waldbronn, Germany).
3. Separation capillaries: they were prepared from bare silica tubing purchased from Composite Metal Services (Worcester, UK). Capillary dimensions were: 48 cm (39.8 cm to the detector) × 50 μm inner diameter (ID).
4. Running buffer: 1 *M* acetic acid, 20 m*M* ammonium acetate in a MeOH-ACN (87.5 : 12.5 v/v) mixture (*see* **Note 5**).
5. Denaturing electrolyte for electrophoretic desorption: 60 m*M* sodium dodecyl sulfate (SDS), 5 M urea in 25 m*M* phosphate buffer, pH 7.0.

2.2. Free Solution Capillary Electrophoresis of Evenly Charged Polyelectrolytes

1. Samples: the polystyrenesulfonate standards (PSSs; 1.4, 5, and 990 10^3 g/mol, 80 to 100% sulfonated), were purchased from American Polymer Standards Corporation (Mentor, OH), under their sodium salt form.
2. CE was performed with an Agilent Technologies CE system (Waldbronn, Germany) (*see* **Fig. 1**) or a Perkin-Elmer-Applied Biosystems ABI 270A (Foster City, CA) (*see* **Fig. 2**).

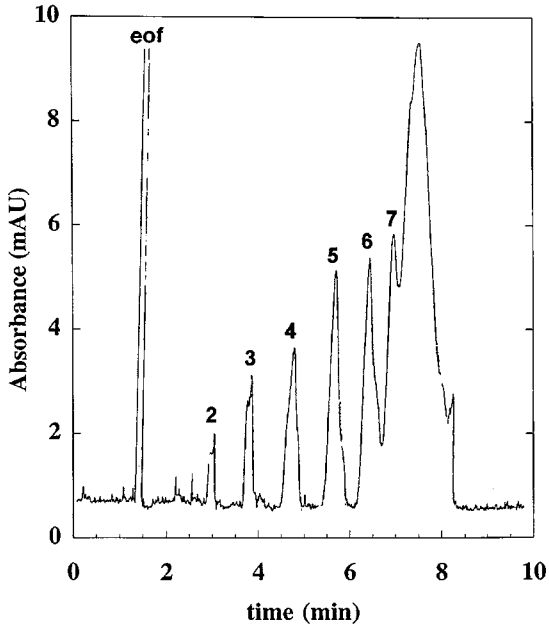


Fig. 1. Oligomeric separation of a low-molecular-mass, fully sulfonated polystyrenesulfonate standard (M_w 1430 g/mol) by free solution capillary electrophoresis. Electrophoretic conditions as described under **Subheading 3.2**. Peak numbering refers to degree of polymerization. Eof, electroosmotic flow marker.

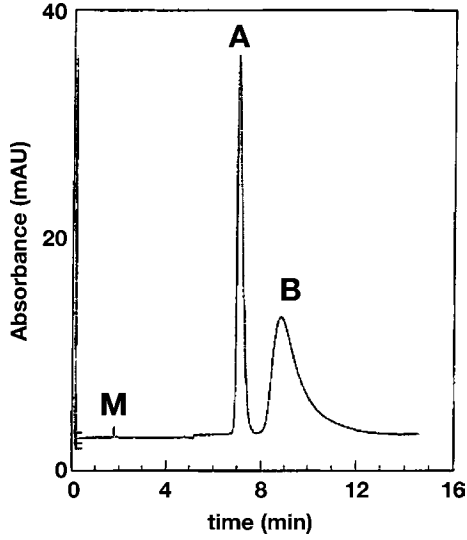


Fig. 2. Separation of two polystyrenesulfonate molecular weight standards (M_w 990 10^3 **[A]** and 5 10^3 **[B]**, >88% sulfonated) by free solution capillary electrophoresis. Electrophoretic conditions as described under **Subheading 3.2**. M: neutral marker. Reprinted from **ref**. ***31***, with permission.

3. Separation capillaries: bare silica capillaries were purchased from Supelco, Bellefonte, PA. Capillary dimensions were: 33.5 cm (25 cm to the detector) × 50 μm ID **(Fig. 1)** and 47 cm (25 cm to the detector) × 50 μm ID **(Fig. 2)**.
4. Running buffers: 150 m*M* or 40 m*M* sodium borate buffers, pH 9.2, were prepared with borax (disodium tetraborate, decahydrate).

2.3. Size-Based Separation of Polyelectrolytes by Entangled Polymer Solution Capillary Electrophoresis

1. Samples: the PSSs (16, 41, 88, 177, 350, and 990 kDa weight average molecular masses, 80 to 100% sulfonated), were purchased from American Polymer Standards Corporation (Mentor, OH), under their sodium salt form.
2. CE was performed with an Applied Biosystems (ABI) Model 270 A capillary electrophoresis instrument (Santa Clara, CA). Data were recorded on a Spectra-Physics (San Jose, CA) 4400 integrator.
3. Separation capillaries: bare silica capillaries were purchased from Supelco, Bellefonte, PA. The capillary dimensions were: 45 cm (25 cm to the detector) × 50 μm ID
4. Running electrolyte: 145 m*M* sodium borate buffer, pH 9.2, containing 0.5 g/100 mL HEC (250 kDa). A 50- to 100-mL volume was prepared at a time. For better dissolution, the separating polymer was added to the buffer the day before the electrophoresis experiment and stirred gently overnight.

2.4. Bidimensional Separations of Polyelectrolytes by Capillary Electrophoresis

1. Samples: PSSs (weight average molar masses M_w 3.33×10^5 and 1.45×10^5 g/mol) were purchased from Polymer Standards Service (Mainz, Germany). The polydispersity indexes of both PSSs were below 1.2. Random copolymer (PAMAMPS) of acrylamide (90% in mole) and 2-acrylamido-2-methylpropanesulfonate (10% in mole) was synthesized by radical polymerization intiated by potassium persulfate and *N*, *N*, *N′*, *N′*-tetramethylethylenediamine. The copolymer was purified by precipitation in absolute ethanol. The number average molecular weight of the PAMAMPS ($M_n \sim 3 \times 10^5$ g/mol) was evaluated by size-exclusion chromatography using polyethylene oxide standards for the calibration.
2. CE was carried out with a PACE MDQ Beckman Coulter (Fullerton, CA) apparatus.
3. Separation capillaries: bare silica tubings used for preparing separation capillaries were purchased from Composite Metal Services (Worcester, UK). Capillary dimensions were: 30 cm (20 cm to the detector) × 50 μm ID.
4. Running electrolyte: 80 m*M* borate buffer pH 9.2 (first dimension) +0.5 g/100 mL HEC, M_w 250 10^3 g/mol (second dimension). For better dissolution, the separating polymer was added to the buffer the day before the electrophoresis experiment and gently stirred overnight.

3. Methods

Subheading 3.1. exemplifies a unique combination of nonaqueous electrolyte and specific rinsing for the separation of water-insoluble, end-charged synthetic polypeptides. **Subheading 3.2**. illustrates the potentiality of FSCE for the separation of evenly charged polyelectrolytes. **Subheading 3.3.** emphasizes the extend of the range of molecular masses that can be separated by EPSCE. **Subheading 3.4**. introduces a two-dimensional (2-D) strategy that combines a separation according to the chemical nature with a size-based separation.

3.1. Nonaqueous Free-Solution Capillary Electrophoresis of End-Charged Polymers

Nonaqueous free-solution capillary electrophoresis (NAFSCE) allows (1) the separation poly(N_ε-trifluoroacetyl-L-Lysine) oligomers according to their molar mass and (2) the separation of the polymers according to the nature of the end groups **(Fig. 3)**. Because of the tendency of the solutes (polypeptides) to adsorb onto the fused-silica capillary wall, a careful attention should be paid to the rinsing procedure of the capillary in between runs in order to keep the capillary surface clean. For that purpose, the use of the electrophoretic desorption under denaturating conditions is very effective.

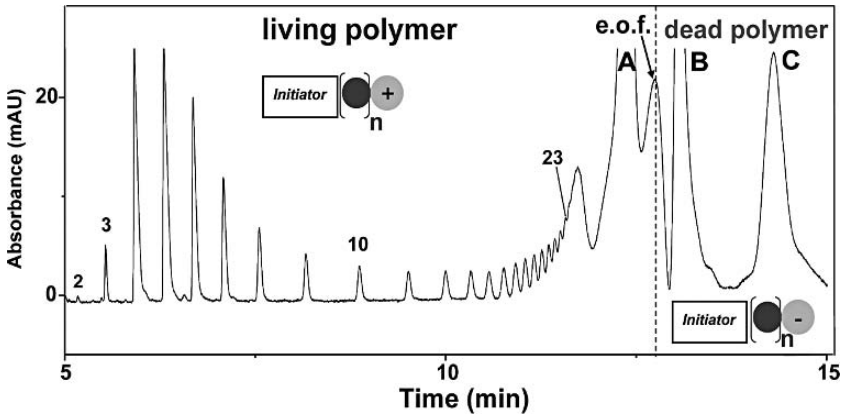


Fig. 3. Separation of end-charged poly(Nε-TFA-L-lysine) according to functionality and molecular mass by free solution nonaqueous capillary electrophoresis (NACE) using a bare silica capillary. Electrophoretic conditions are given under **Subheading 3.1.** Identification: number of monomeric units of the living (cationic) poly(Nε-TFA-L-lysine) as indicated; **A**, living polymer of high molecular mass; **B** and **C**, dead polymers; e.o.f., electroosmotic flow. Reprinted from **ref**. ***16***, with permission.

1. Sample preparation: the reactional mixture containing the synthetic polypeptides was dissolved at 5 g/L in a MeOH/electrolyte (50:50 v/v) mixture and filtered through a 0.45-μm polytetrafluoroethylene membrane. If necessary, 0.05% (v/v) mesityl oxide was added to the sample as a neutral marker for electroosmotic flow (EOF) monitoring.
2. Capillary conditioning: new capillaries were conditioned by performing the following washes: 1 *M* NaOH for 20 min, 0.1 *M* NaOH for 15 min, and water for 2 min.
3. Rinsing procedure using electrophoretic desorption (*see* **Note 6**). Before each injection, perform the following rinsing procedure:

   a. Flush with water for 1 min.
   b. Flush with the denaturing electrolyte for 2 min, both under 930 mbar.
   c. Perform electrokinetic desorption by applying 15 kV between vials containing the denaturing electrolyte for 15 min.
   d. Flush with denaturing electrolyte for 2 min.
   e. Flush with water for 1 min.
   f. Flush with the running electrolyte for 3 min.
   g. Electrokinetically condition the capillary filled with the running buffer under 15 kV for 5 min.
   h. Flush with the running buffer for 1 min.

   Step 3g was found to improve the baseline stability.

4. Electrophoretic conditions (*see* **Note 7**): positive voltage (30 kV) was applied for uncoated capillaries. The resulting current intensity was ca 18 μA. Sample volumes of approx 4 nL were introduced hydrodynamically applying 17 mbar for 3 s. The temperature of the capillary cassettes was maintained constant at 25 °C. Ultraviolet absorbance was monitored at 200 nm.

3.2. Free Solution Capillary Electrophoresis of Evenly Charged Polyelectrolytes

As already discussed in introduction and in **Note 2**, the plot of the electrophoretic mobility of an evenly charged polyelectrolyte as a function of its degree of polymerization (N) is a bell-shaped curve ending with a plateau **(Fig. 4)**. Thus, small oligomers (with $N < 10$, typically $M < 2000$ g/mol for PSSs) can be separated according to their molecular mass by FSCE, as shown in **Fig. 1**. A high-molecular-mass polyelectrolyte ($N > 200$, typically $M > 20\,000$ g/mol for PSSs) in a coil conformation can also be separated from low to

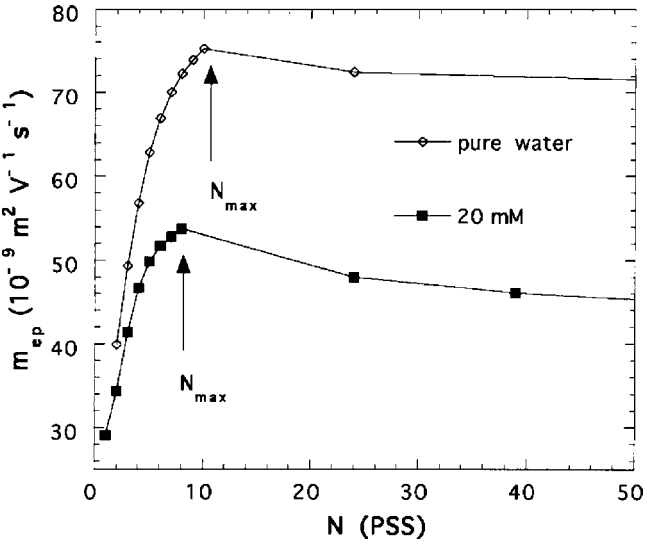


Fig. 4. Influence of the degree of polymerization N on the free solution electrophoretic mobility (m_{ep}) of fully sulfonated polystyrenesulfonate standards (PSSs) for different ionic strengths. Fused-silica capillary, 50 μm inner diameter × 33.5 cm (detector, 25 cm). Electrolytes: 40 mM borate buffer (20 mM ionic strength), pH 9.2 and pure water. Applied voltage: 7.5 kV. PSS concentration: 0.5 g/L each. Hydrodynamic injection (5 kPa, 2 s). UV detection at 225 nm. Temperature: 27 °C. N_{max}: degree of polymerization at the maximum of the mobility vs N curve. The solid lines are guides for the eye. Reprinted from **ref. *31***, with permission.

moderate molecular mass polyelectrolytes (typically 20 000 > M > 2 000 g/mol for PSSs) having a conformation in the crossover from rod-like to coil **(Fig. 2)**.

1. Sample preparation: PSSs were dissolved at 0.5 g/L each in pure water. If necessary, 0.05% (v/v) mesityl oxide was added to the sample as a neutral marker for EOF monitoring.
2. Capillary conditioning: new capillaries were conditioned by performing the following washes: 1 M NaOH for 20 min, 0.1 M NaOH for 15 min, and water for 2 min, each under 670 mbar.
3. Electrophoretic conditions. Electrolyte: 150 mM **(Fig. 1)** or 40 mM **(Fig. 2)** sodium borate buffer, pH 9.2. The influence of the ionic strength is discussed in **Note 8**. Positive voltages were applied: 7.5 kV (224 V/cm, **Fig. 1**) and 20 kV (425 V/cm, **Fig. 2**). Solutes were injected in hydrodynamic mode: 50 mbar for 2 s **(Fig. 1)** or 165 mbar for 1 s **(Fig. 2)**. Solutes were monitored spectrophotometrically at their local absorbance maximum of 225 nm. The temperature was set at 27 °C.
4. Rinsing procedure between runs: capillaries were flushed with 0.1 M NaOH for 3 min and running buffer for 3 min, both under 930 mbar.

3.3. Size-Based Separation of Polyelectrolytes by Entangled Polymer Solution Capillary Electrophoresis

EPSCE is a very effective method for the size-based separation of evenly charged polyelectrolytes (free-draining behavior; *see* **Note 2**). In the presence of chemical (cross-linked) gels or entangled polymer solutions, the electrophoretic mobility of an evenly charged polyelectrolyte is a decreasing function of the molar mass due to the retarding (sieving) effect of the separating matrix on the solute (*see* **Note 9**). Separation on a large range of molar masses, as well as oligomeric separations, can be obtained depending on the separating polymer concentration and molar mass **(Note 10)**. **Figure 5** shows the separation obtained for six PSSs with molecular masses varying between 18×10^3 and 990×10^3 g/mol. The separation is performed in counter-electroosmotic mode **(Note 11)** in an unmodified fused silica capillary. It is worth noting that, in this mode, broader peaks were detected for low molecular mass standards **(Note 11)**.

1. Samples: PSSs were dissolved in pure water at 0.5 g/L each. If necessary, 0.05 (v/v) mesityl oxide was added to the sample as a neutral marker.
2. Capillary conditioning. new, uncoated capillaries were conditioned by performing the following washes: 1 M NaOH for 10 min, 5 mM NaOH solution containing 0.5 M NaCl for 10 min, water for 5 min, and the separating electrolyte for 10 min (all under 670 mbar).
3. Electrophoretic conditions: positive voltage (10 kV) was applied. Samples were introduced hydrodynamically by application of a negative pressure of 167 mbar on the outlet side of the capillary. The temperature setting was at 27 °C. Solutes were

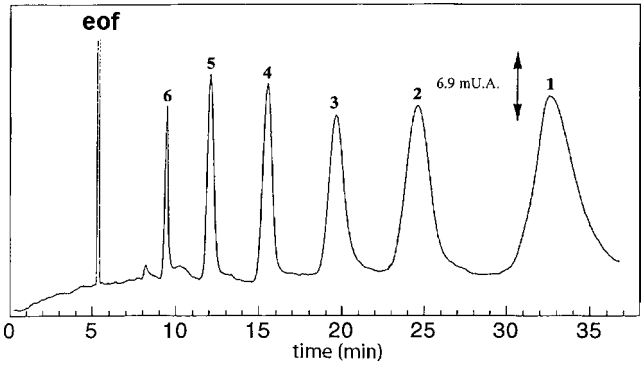


Fig. 5. Separation of a mixture of six polystyrenesulfonate standards by entangled polymer solution capillary electrophoresis on a bare silica capillary. PSS molecular masses in 10^3 g/mol: 16 (1), 41 (2), 88 (3), 177 (4), 350 (5), and 990 (6). Electrophoretic conditions given under **Subheading 3.3.** Reprinted from **ref.** ***22***, with permission.

monitored spectrophotometrically at their local absorbance maximum of 225 nm. For more details on the choice of the HEC concentration, ionic strength, and electric field, *see* **Note 10**.

4. Rinsing procedure between runs: capillaries were flushed with 0.1 *M* NaOH for 3 min and plain buffer for 1 min (both under 670 mbar), and finally flushed with about two capillary volumes of running electrolyte. The time required for rinsing the capillaries with twice their volume of separating electrolyte is dependent on electrolyte viscosity (10 min for this electrolyte under 670 mbar).

3.4. Bidimensional Separations of Polyelectrolytes by Capillary Electrophoresis

The possibility of performing 2-D CE in a single capillary was recently investigated ***(42,43)*** **(Note 12)**. Three synthetic polyelectrolytes were separated by heart-cutting 2-D CE separations in a single capillary according to: (1) the charge density (or chemical composition) by FSCE in the first dimension, and (2) the molar masses by CE in the presence of an entangled polymer solution in the second dimension. **Figure 6** shows the 2-D CE separation of a 10% charged PAMAMPS and two standards of PSS in a 50-μm-ID fused-silica capillary. In the first dimension (**step 1**; *see* also **Fig. 6**), the PSSs were separated from the 10% charged copolymer by free solution capillary electrophoresis in counter-electroosmotic mode. Peak A in **Fig. 6** corresponds to the 10% charged PAMAMPS and was thus detected before the peak assigned to the two comigrating PSSs of different molar masses (**Fig. 6**, Peak B). Before proceeding to the second separation of the PSSs according to their

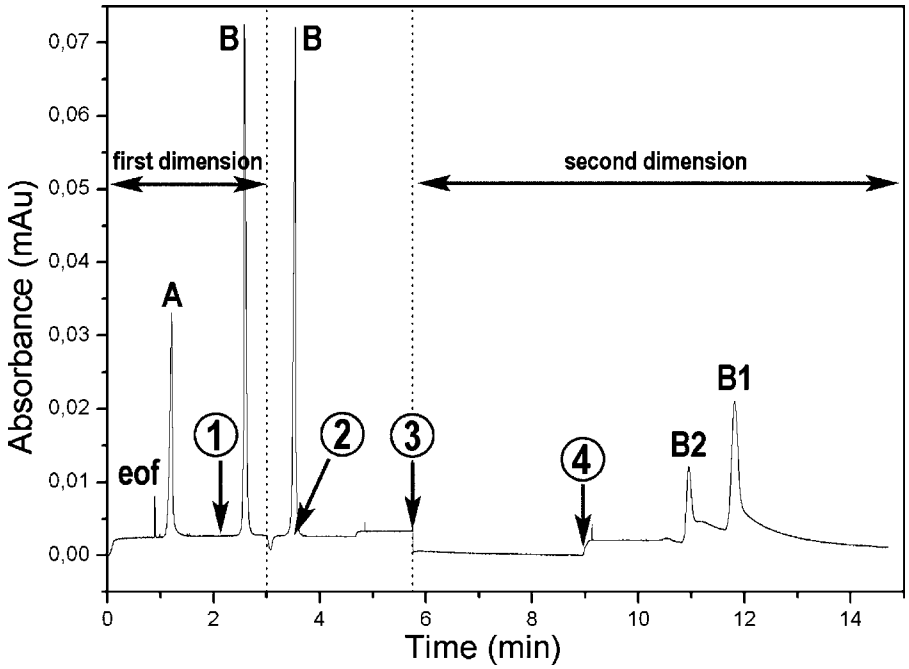


Fig. 6. Separation of three synthetic polymers by two-dimensional capillary electrophoresis. Electrophoretic conditions as given under **Subheading 3.4**. Identification: **A**, PAMAMPS; **B1**, PSS (M_w 3.33×10^5 g/mol); **B2**, PSS (M_w 1.45×10^5 g/mol); **B**, B1 + B2; eof, electroosmotic flow. The circled numerals correspond to four different key steps that are described in the text. Reprinted from **ref.** ***42***, with permission.

molar masses, the polarity of the applied voltage was switched (-20 kV; **step 2**) for 2.75 min, so that fraction B could reach the inlet end of the capillary without being evacuated. The second separation medium was then electroosmotically introduced into the capillary by the application of a relatively low positive voltage (+6 kV; **step 3**). In the second dimension of the separation, the separation of the two PSSs according to their molar masses was obtained as a result of the presence of the entangled polymer solution (**step 4**).

1. Samples: PSSs were dissolved in pure water at 0.5 g/L each. PAMAMPS was dissolved at 5 g/L in water. 0.05% (v/v) of mesityl oxide was added to the sample mixtures as a neutral marker.
2. Capillary conditioning: new capillaries were conditioned by washing with 1 *M* NaOH for 20 min and then with the electrolyte for 10 min.
3. Electrophoretic conditions: sample was introduced hydrodynamically (20 mbar, 3 s). The temperature of the capillary cassettes was maintained constant

at 25 °C. Data were collected at 214 nm. The applied voltage followed this sequence: t = 0–3 min, +20 kV (first dimension); t = 3–5.75 min, -20 kV; t > 5.75 min,+6 kV (second dimension).

4. Rinsing procedure between runs: capillary was successively washed by water for 5 min, 1 *M* NaOH for 5 min, and the electrolyte for 5 min.

4. Notes

1. The mesh size of the separating matrix is a decreasing function of the separating polymer concentration. For the separation of oligomers, concentrated polymer solutions are required so that mesh size matches solute size. On the contrary, less concentrated solutions are required for the separation of longer polymer chains. Quantitative estimations of the mesh size as a function of the separating polymer concentration are given in **ref. *23***. Unlike crosslinked chemical gels, entangled polymer solutions lead to dynamic networks. In this later case, the lifetime of the mesh is highly dependent on the molecular mass of the separating polymer. In practice, separating polymers with molecular masses of the same order of magnitude as the largest polymer solute will lead to a good compromise between size selectivity and electrolyte viscosity. Interestingly, it was shown experimentally that when the size selectivity becomes independent of the molecular mass of the separating polymer (i.e., for high enough molecular masses), the PSS electrophoretic mobility is close to being a universal function of the ratio of mesh size to solute radius of giration ***(23)***.
2. Generally, the electrophoretic mobility of evenly charged polyelectrolytes is independent of molecular mass (the so-called free draining behavior). This behavior is explained by the proportionality of both charge and frictional coefficient to molecular mass. The linear dependence of frictional coefficient to molecular mass is due to the friction of the counterions all along the polyelectrolyte backbone. Consequently, free-draining polyelectrolytes are permeable to the solvent during their electrophoretic migration. Furthermore, during an FSCE separation under currently used ionic strengths (1–100 m*M*), the polyelectrolyte conformation is not altered. However, it was experimentally demonstrated that polyelectrolytes should adopt a true coil conformation to exhibit the free-draining behavior. In other words, the molecular mass must be superior to a threshold value that depends on ionic strength. Small, evenly charged oligomers, i.e., with length smaller than or similar to Debye length, must be considered small molecules, and their electrophoretic mobility is an increasing function of *N* as a result of the hydrodynamic coupling of monomers. In conclusion, the peak assignment for evenly charged polymers according to *N* is not always straightforward, because the variation of the electrophoretic mobility with DP is not monotonous (bell-shaped curve ending with a plateau; *see* **Fig. 4**).
3. The electrophoretic mobility of evenly charged polyelectrolytes is a linear function of their chemical charge rate up to a threshold value that corresponds to the onset of the Manning's condensation. For chemical charge rates superior to this threshold value (about 35% for vinylic polymers), the electrophoretic mobility becomes

almost constant, according to Manning's theory of charge condensation, as was experimentally verified for variously charged copolymers having hydrophilic backbone ***(34,35)***. This ruins any possibility of electrophoretic separations.

4. Okada ***(39)*** reported that the electrophoretic mobility of neutral polyoxyethylene oligomers interacting with ammonium ions follows a bell-shaped variation in accordance with that observed for evenly charged polymers (*see* **Note 1**).
5. Methanol and acetonitrile, as well as ammonium acetate and acetic acid, are volatile. The use of ermetically closed vials is recommended for a better repeatability. An advantage of such volatile electrolytes is their compatibilty for coupling with a mass spectrometer ***(44)***.
6. To avoid early capillary breaking, prepunchers and electrodes should be cleaned twice a week to remove crystalline deposits (SDS, urea, etc.). This precaution is only required for uncoated capillaries (electrokinetic desorption).
7. With the acidic running buffer retained, the so-called living PTLL bears one protonated amine group at one end of the chain, and a neutral group (hexylamide), originating from the initiation step, at the other end. Living PTLLs are thus detected before the EOF marker. Dead polymers bearing a carboxylic group instead of the amine group were detected after the EOF marker and were thus separated from the living polymers (see **Figure 1**). Size-based separation of the living oligomers (up to about the 20 mers) was obtained since the electrophoretic mobility of such end-charged oligomers is a decreasing function of the degree of polymerization.
8. Low ionic strength is preferred for the separation of low-molecular-mass oligomers. At very low ionic strength (1 m*M* or less), separation of up to nine monomers was observed (instead of the seven in **Fig. 1**).
9. Different migration mechanisms (reptation, biaised reptation, Ogston model, etc.), depending on the electric field strength and the solute molar mass, were proposed to model the electrophoretic behavior of polyelectrolytes in sieving matrices ***(4)***. To avoid the loss of size-based selectivity due to orientation and stretching of the solute in the direction of the electric field, low electric field strength is generally required, especially for the separation of the largest solutes.
10. The mesh size ξ_b (in nm) of entangled HEC solution is related to the polymer concentration C (in g/mL) by $\xi_b = 0.729\,C^{-0.76}$. At 0.5 g/100mL, $\xi_b = 41$ nm ***(23)***. The mesh size should be of the same order as the radius of gyration of the largest PSS. The lower the electric field, the greater the size selectivity, especially for the largest polymer solutes (detrimental effect of field induced orientation of the solute). In this method, a moderate electric field (220 V/cm) was selected to compromise between selectivity and analysis time. Increasing the ionic strength of the electrolyte was found to give better resolution for the largest polymer solutes because of the more compact and less deformable coil conformations ***(22,45)***. However, the user can decrease the ionic strength to speed up the analysis by increasing EOF. Lower ionic strengths are especially recommended for solutes of moderate molecular masses, which would be less affected by coil deformation.
11. Counter-electroosmotic mode refers to a solute migration in the opposite direction of the EOF. In the counter-electroosmotic mode, higher resolutions are obtained

for solutes detected at longer migration times than if separations were performed without EOF. This explains why the low-molecular-mass polymers produce broader peaks than those with high-molecular-mass which are detected first. Changing the time scale into an electrophoretic mobility scale would suppress this effect.

12. For performing 2-D CE in a single capillary, a fraction stemming from the first dimension of the separation was selected and isolated into the capillary by evacuating the other undesirable compounds from the capillary. Next, the isolated fraction was submitted to a second separation medium that was introduced in the capillary by EOF. The second separation medium was able to reach the isolated fraction because the solutes were migrating in counter-electroosmotic mode. Because only one fraction is submitted to the second dimension of the separation, this new methodology is closer to a heart-cutting approach than to a true comprehensive 2-D separation. However, it has the advantage of not requiring any special coupling device between capillaries, because the two dimensions of the separation are performed in the same capillary.

Acknowledgment

H. C. gratefully acknowledges the Ministère de la Recherche (ACI jeunes chercheurs n° 4093) for their support on the 2-D CE methodology.

References

1. Barth, H. G., Boyes, B. E., and Jackson, C. (1998) Size exclusion chromatography and related separation techniques. *Anal. Chem*. **70**, 251R–278R.
2. Dubin, P. L. (Ed) (1988) *Aqueous Size Exclusion Chormatography*. J. Chromatogr. Lib. Vol. 40, Elsevier, Amsterdam.
3. Pasch, H. and Trathnigg, B. (1998) *HPLC of Polymers*. Springer, New York.
4. Righetti P.G. (Ed.) (1996) *Capillary Electrophoresis in Analytical Biotechnology*. CRC, Boca Raton, FL.
5. Khaledi, M. G. (Ed) (1998) *High-Performance Capillary Electrophoresis, Theory, Techniques and Applications*. Chemical Analysis Series, vol. 146. John Wiley & Sons, Inc., New York.

6a. Mitchelson, K. R. and Cheng, J. (2001) *Capillary Electrophoresis of Nucleic Acids: Volume 1, Introduction to the Capillary Electrophoresis of Nucleic Acids*. Methods in Molecular Biology, vol 162. Humana, Totowa, NJ.

6b. Mitchelson, K. R. and Cheng, J. (2001) *Capillary Electrophoresis of Nucleic Acids: Volume 2, Practical Applications of Capillary electrophoresis*. Methods in Molecular Biology, vol 163. Humana, Totowa, NJ.

7. Engelhardt, H., and Grosche, O. (2000) Capillary electrophoresis in polymer analysis. *Adv. Polym. Sci*. **150,** 189–217.
8. Kok, W. Th., Stol, R., and Tijssen, R. (2000) Electrokinetic separations for synthetic polymers *Anal. Chem*. **72,** 468A–476A.

9. Engelhardt, H. and Martin, M. (2004) Characterization of synthetic polyelectrolytes by capillary electrophoretic. *Adv. Polym. Sci.* **165,** 211–247.
10. Cottet, H., Simó, C., Vayaboury, W., and Cifuentes, A. (2005) Non-aqueous and aqueous capillary electrophoresis of synthetic polymers. *J. Chromatogr. A*. **1068**, 59–73.
11. Bullock, J. (1993) Application of capillary electrophoresis to the analysis of the oligomeric distribution of polydisperse polymers. *J. Chromatogr. A*. **645,** 169–177.
12. Braud, C., Devarieux, R., Atlan, A., Ducos, C., and Vert, M. (1998) Capillary zone electrophoresis in normal or reversed polarity separation modes for the analysis of hydroxy acid oligomers in neutral phosphate buffer. *J. Chromatogr. A*. **706,** 73–82.
13. Mengerink, Y., Van der Wal, S., Claessens, H. A., and Cramers, C. A. (2000) Analysis of higher polyamide-6 oligomers on a silica-based reversed-phase column with a gradient of formic acid as compared with hexafluoroisopropanol. *J. Chromatogr. A*. **871**, 259–268.
14. Oudhoff, K. A., Schoenmakers, P. J., and Kok, W. Th. (2003) Characterization of polyethylene glycols and propylene glycols by capillary zone electrophoresis and micellar electrokinetic chromatography. *J. Chromatogr. A*. **985,** 479–491.
15. Oudhoff, K. A., VanDamme, F. A., Mes, E. P. C., Schoenmakers, P. J., and Kok, W. Th. (2004) Characterization of gycerin-based polyols by capillary electrophoresis. *J. Chromatogr. A*. **1046,** 263–269.
16. Cottet, H., Vayaboury, W., Kirby, D., Giani, O., Taillades, J., and Schué, F. (2003) Nonaqueous capillary zone electrophoresis of synthetic organic polypeptides. *Anal. Chem*. **75,** 5554–5560.
17. Cottet, H., Struijk, M. P., Van Dongen, J. L. J., Claessens, H. A., and Cramers, C. A. (2001) Non-aqueous capillary electrophoresis using non-dissociating solvents. application to the separation of highly hydrophobic oligomers. *J. Chromatogr. A* **915,** 241–251.
18. Wallingford, R. A. (1996) Oligomeric separation of ionic and nonionic ethoxylated polymers by capillary gel electrophoresis. *Anal. Chem*. **68,** 2541–2548.
19. Stepanek, M., Podhajecka, K., Tesarova, E., and Prochazka, K. (2001) Hybrid polymeric micelles with hydrophobic cores and mixed polyelectrolyte/nonelectrolyte shells in aqueous media. 1. preparation and basic characterization. *Langmuir* **17,** 4240–4244.
20. Cottet, H., Gareil, P., Guenoun, P., et al. (2001) Capillary electrophoresis of associative diblock copolymers. *J. Chromatogr. A* **939,** 109–121.
21. Poli, J. B., and Schure, M. R. (1992) Separation of poly(styrenesulfonates) by capillary electrophoresis with polymeric additives. *Anal. Chem*. **64**, 896–904.
22. Cottet, H. and Gareil, P. (1997) Electrophoretic behaviour of fully sulfonated polystyrenes in capillaries filled with entangled polymer solutuions. *J. Chromatogr. A* **772,** 369–384.
23. Cottet, H., Gareil, P., and Viovy, J. L. (1998) The effect of blob size and network dynamics on the size-based separation of polystyrenesulfonates by capillary electrophoresis in the presence of entangled polymer solution. *Electrophoresis* **19,** 2151–2162.

24. Clos, H. N. and Engelhardt, H. (1998) Separations of anionic and cationic polyelectrolytes by capillary gel electrophoresis. *J. Chromatogr. A* **802,** 149–157.
25. Welch, C. F. and Hoagland, D. A. (2001) Molecular weight analysis of polycations by capillary electrophoresis in a solution of neutral polymers. *Polymer*. **42,** 5915–5920.
26. Grosche, O., Bohrisch, J., Wendler, U., Jaeger, W., and Engelhardt, H. (2000) Characterization of synthetic polyelectrolytes by capillary electrophoresis. *J. Chromatogr. A* **894,** 105–116.
27. Wang, T. and Li, S. F. (1998) Separation of synthetic inorganic polymers of condensed phosphates by capillary gel electrophoresis with indirect photometric detection. *J. Chromatogr. A* **802,** 159–165.
28. Lindberg, P. and Roeraade, J. (1999) Gel matrices in N-methylformamide for separation of DNA fragments. *J. Liq. Chrom. Relat. Technol*. **22,** 307–321.
29. Stover, F. S. (1997) Capillary electrophoresis of longer-chain polyphosphates (1997) *J. Chromatogr. A* **769,** 349–351.
30. Cottet, H. and Gareil, P. From small charged molecules to oligomers: a semi-empirical approach to the modeling of actual mobility in free solution. *Electrophoresis* **21,** 1493–1504.
31. Cottet, H., Gareil, P., Theodoly, O., and Williams, C. A. (2000) Semi-empirical approach to the modeling of the electrophoretic mobility in free solution: application to polystyrenesulfonates of various sulfonation rates. *Electrophoresis* **21,** 3529–3540.
32. Bowser, M. T., Sternberg, E. D., and Chen, D. D. Y. (1996) Development and application of a nonaqueous capillary electrophoresis system for the analysis of porphyrins and their oligomers (photofrin). *Anal. Biochem*. **541,** 143–150.
33. Ebber, A., Vaher, M., Peterson, J., and Lopp, M. (2002) Application of capillary zone electrophoresis to the separation and characterization of poly(amidoamine) dendrimers with an ethylenediamine core. *J. Chromatogr. A* **949,** 351–358.
34. Hoagland, D. A., Smisek, D. L., and Chen, D. Y. (1996) Gel and free solution electrophoresis of variably charged polymers. *Electrophoresis* **17,** 1151–1160.
35. Gao, J. Y., Dubin, P. L., Sato, T., and Morishima, Y. (1997) Separation of polyelectrolytes of variable compositions by free-zone capillary electrophoresis. *J. Chromatogr. A* **766,** 233–236.
36. Collet, J., Tribet, C., and Gareil, P. (1996) Use of neutral surfactants for the capillary electrophoretic separation of hydrophobically modified poly(acrylic acids). *Electrophoresis* **17,** 1202–1209.
37. Morishima, Y. (2000) Self-assembling amphiphilic polyelectrolytes and their nanostructures. *Chin. J. Polym. Sci*. **18,** 323–336.
38. Aguilar, M. R., Gallardo, A., San Román, J., and Cifuentes, A. (2002) Micellar electrokinetic chromatography: a powerful analytical tool to study copolymerization reactions involving ionic species. *Macromolecules* **35,** 8315–8322.
39. Okada, T. (1995) Non-aqueous capillary electrophoretic separation of polyethers and evaluation of weak complex formation. *J. Chromatogr. A* **695,** 309–317.

40. Gallardo, A., Lemus, A. R., San Román, J., Cifuentes, A., and Díez-Masa, J. C. (1999) Micellar electrokinetic chromatography applied to copolymer systems with heterogeneous distribution. *Macromolecules* **32,** 610–617.
41. Li, G., Zhou, W., Wang, Y., et al. (2004) The analysis of synthetic organic, neutral polymers using nonaqueous capillary gel electrophoresis. *J. Liq. Chromatogr. Relat. Technol*. **27 (6),** 939–964.
42. Cottet, H., Biron, J. -P., and Taillades, J. (2004) Heart-cutting two-dimensional electrophoresis in a single capillary. *J. Chromatogr. A* **1051,** 1–2, 25–32.
43. Cottet, H. and Biron, J. -P. Charge- and size-based separations of polyelectrolytes by heart-cutting two-dimensional capillary electrophoresis (2005) *Macromol. Chem. Phys*. **206,** 628–634.
44. Simo, C., Cottet, H., Vayaboury, W., Giani, O., Pelzing, M., and Cifuentes, A. (2004) Nonaqueous capillary electrophoresis-Mass spectrometry of synthetic polymers. *Anal. Chem*. **76,** 335–344.
45. Cottet, H. and Gareil, P. (2001) On the use of the activation energy concept to investigate analyte and network deformation in entangled polymer solution capillary electrophoresis of synthetic polyelectrolytes. *Electrophoresis* **22,** 684–691.

22

Capillary Electrophoresis Separation of Microorganisms

Bartolomé M. Simonet, Angel Ríos, and Miguel Valcárcel

Summary

Microorganisms can be considered a bio-colloid. That is, they have a characteristic outer surface that carries, or can carry, a charge. Precisely, differences in the surface can be exploited for separation by capillary electrophoresis (CE). In fact, methods based on CE seem to be very promising because they should produce rapid and high-efficiency separations. Although CE can be used to separate microbial (i.e., bacteria, virus, fungi, and whole cells) and subcellular particles (i.e., mitochondria and nuclei), this chapter is focused mainly on the determination of bacteria and virus for their interest. At difference to the separation off molecules, microorganisms are characterized as living. This makes their analysis more difficult because several aspects such as possible lysis, aggregation, evolution, growing etc. must be taken into count.

Key Words: Microorganisms analysis, bacteria, virus, aggregates, capillary electrophoresis, capillary isoelectric focusing, affinity capillary electrophoresis.

1. Introduction

During the past decade, a variety of techniques has been developed for the analysis of microorganisms. These techniques include, among others, flow cytometry, serological methods, and protein analysis or genetic analysis including the comparison of DNA nucleotides sequences, for example. Moreover, these techniques based on capillary electrophoresis (CE) or microfluidic devices have been also developed during the past decade. Although these newer methods will not replace the traditional plate-counting methods involving cultures and microscopy, their development and use will continue to expand.

From: *Methods in Molecular Biology, vol. 384: Capillary Electrophoresis*
Edited by: P. Schmitt-Kopplin © Humana Press Inc., Totowa, NJ

Like other colloidal particles, microorganisms carry charged or chargeable groups on their outer surface, and their respective electrical double layer is created when the charged microorganism is in contact with an aqueous solution. Therefore, under an electrical field, microorganisms such as bacteria and viruses present a characteristic electrophoretic mobility, which is a function of the size of the microorganism, the charge of its surface, and the electrical double layer. As it is well known, CE produces rapid and high-efficiency separations of biologically important molecules such as proteins or nucleotides. But these advantages can also be realized for the analysis of microorganisms because CE methods permit the rapid and simultaneous analysis of several microorganisms in one sample, including their identification, quantification, and also viability evaluation.

Hjerten et al. ***(1)*** describe for the first time the possibility of analyzing viruses and bacteria by using CE. They determined *Lactobacillus casei* and tobacco mosaic virus by using a fused-silica capillary coated with methylcellulose in order to avoid the adsorption of microorganisms onto the capillary wall. Although the microorganisms could not be separated under the experimental conditions used, these experiments revealed the possibility of moving microorganisms through a capillary by applying an electrical field. The first separation of bacteria was reported in 1993 by Ebersole and McCormick ***(2)***. They were able to separate or partially separate *Enterococcus faecalis, Streptococcus pyrogenes, Streptococcus aureus, Streptococcus agalactiae*, and *Streptococcus pneumoniae*; the process, however, took 70 min, and *S. pyrogenes* and *S. pneumoniae* were separated as broad peaks. Four years after, in 1997, Pfetsch and Welsch ***(3)*** accomplished the CE separation of three different types of bacteria (*Pseudomonas putida, Pseudomonas sd*., and *Alcaligenes euthrophus*); although the analysis time was slightly shorter than in the earlier study, the electrophoretic bands were relatively broad. Another important aspect of achieving this separation is the necessity of using long capillaries, typically fused-silica capillaries of 1–3 mm length (0.25 mm innder diameter [ID]). Glynn et al. ***(4)*** investigated the electrophoretic mobilities of three bacteria strains by CE and compared their results with results obtained by microelectrophoresis (ME). The results obtained show for the first time that surface charge variations within a monoclonal population can be resolved by CE. In this work, bacteria electrophoretic mobilities were measured using a fused-silica capillary that was not coated on the inside and only 57 cm long (75 μm ID). The first high-efficiency separation of a mixture of bacteria was reported in late 1999 ***(5)***. In this work, two different capillary electrophoretic approaches were utilized. The first approach used a dissolved polymer-containing CE running buffer that may have been affected by size and shape considerations and the second approach uses capillary isoelectric focusing to separate

bacteria by their surface charge or isoelectric point (pI). The dissolved polymer used in the first approach was the poly-(ethylene oxide) (PEO), and it was used as an unbounded coating for the purpose of altering the electroosmotic flow (EOF). This CE assay was used to identify the causative pathogens of urinary tract infections in only 15 min with no sample work-up or pre-treatment ***(6)***.

Because bacteria are living organisms, their analysis presents some difficulties that are not encountered with molecule separations. For example, many bacteria release biomolecules (e.g., enzymes, proteins, etc.) which can affect other microbes in the mixture and can even produce the lysis cell. Bacteria also can cause experimental variations in cellular composition due to age or changes in growth conditions, etc., and some bacteria also can adhere to several substrates including other bacteria of the same or a different species. In fact, self-aggregation, i.e., forming several clusters or associations, can be a natural part of the behavior of many microorganisms. In this way, Armstrong and co-workers described a method of managing microbial aggregates by using CE ***(7)***. Obviously, aggregates can produce changes in surface charge as well as diffusional properties. It is therefore possible to have multiple peaks in electropherograms of a single species of bacteria if different aggregates are present and are not dispersed before analysis.

Recently, the addition of ions that can interact with the bacteria surface and change its charge has been used to improve electrophoretic resolution. In this way, Valcárcel and co-workers described a method based on the addition of calcium and myo-inositolhexakisphosphate as specific ions that interact with the bacterial surface in the background electrolyte ***(8)***. This method allows the effective separation of eight different types of bacteria in only 25 min using a fused-silica capillary of only 47 cm length (75 μm ID).

In **Table 1** are summarized the experimental conditions used in several works for the characterization and separation of bacteria using CE. For a general review of the analysis of colloid/nano particles, including microorganism and subcellular particles, by CE, interested readers can find more information in **refs. *9–12***.

The applicability of capillary zone electrophoresis (CZE) for the analysis of viruses was demonstrated for first time by Hjerten ***(1)*** by running a tobacco mosaic virus. The electrophoretic properties of the same virus were investigated by Grossman and Soane ***(13)*** as a function of the electric field strength. The authors found that the mobility increased with increasing field strength. This was attributed to the preferential orientation of the road-shaped virus in the direction of the field leading to a reduction of the frictional resistance.

Kenndler and co-workers exhaustively studied the human rhinovirus (HRV) in a number of publications ***(14–18)***. In the first study, the pI of the HRV was

Table 1
Experimental Electrophoretic Conditions for the Analysis OF Bacteria by Capillary Electrophoresis

Bacteria	BGE	Instrumental conditions	Ref.
Pseudomona species *Pseudomona putida* *Alcaligenes eutrophus*	Tris:Borate:EDTA (4.45:4.45:0.1) pH = 9.60; I = 0.5 mmol/l	Voltage 30 kV Fused-silica capillary 250 cm × 0.25 mm UV detection 208 nm	***3***
Pseudomonas fluorescens *Enterobacter aerogenes* *Micrococcus luteus*	Tris:Borate:EDTA:PEO (4.5; 4.5; 0.1 m*M*; 0.0125%) pH 8.4	Voltage 10 kV, 23 °C Fused-silica capillary 27 cm × ×100 μm UV detection 214 nm	***5***
Escherichia coli *Pseudomonas putida* *Serratia rubidae*	Bio-Lyte Ampholyte pH 3.0–10.0 (Isoelectric focusing)	Voltage 20 kV, 23 °C Methylcellulose-coated capillary UV detection 280 nm	***5***
Escherichia coli *Staphylococcus* *saprophyticus*	Tris:Borate:EDTA:PEO (4.5; 4.5; 0.1 m*M*; 0.0125%) pH 8.4	Voltage 10 kV, 23 °C Fused-silica capillary 27cm × 100μm UV detection 214 nm	***6***

Aggregates of: *Micrococcus luteus* *Saccharomyces cerevisiae* *Alcaligenes faecalis*	Tris:Borate:EDTA:PEO (4.5; 4.5; 0.1 m*M*; 0.0125%) pH 8.4	Voltage 10 kV, 23 °C Fused-silica capillary 27 cm × 100 μm UV detection 214 nm	***7***
Yersinia enterolitica *Leuconostoc mesenteroides* *Salmonella enteriditis* *Escherichia coli* *Listeria monocitogenes* *Lactobacillus plantarum* *Staphylococcus aureus* *Enterococcus faecium*	Phosphate 25m*M* (pH 7.0) +25 μ*M* calcium chloride +35 μ*M* myo-inositol-hexakisphosphate	Voltage 15kV, 20 °C Fused-silica capillary 47cm × 75μm UV detection 210 nm	***8***

determined ***(14)***. In a second study, the authors demonstrated that the HRV peaks present a reproducible migration time that permits its identification ***(15)***. In this work, small amounts of sodium dodecyl sulfate (SDS), deoxycholate, Triton X-100R, or some combination of these surfactants were added to the run buffer to prevent adsorption of the virus to the capillary wall. A number of different serotypes of HRV were also studied by Okun and co-workers ***(17)***. Affinity CE was also used by Okun et al. to determine the extent of interaction between HRV and certain monoclonal antibodies ***(18)***. Another example is the work of Mann and co-workers ***(19)***, who develop a method for free-zone CE separation of adenovirus 5.

If we compare bacteria microorganisms with viruses, the most important difference is the size. Bacteria can be as much as 10^2–10^3 times larger than viruses. This increased size leads to increased complexity. For example, viruses only exist in two forms, helical or icosahedral, whereas bacteria can adopt an enormous variety of shapes and sizes. Another important difference is the composition of the outer surface. Whereas viral capsides are composed entirely of proteins (only a few types), the bacteria outer membrane has a large number of lipids, proteins, and glycoproteins. These wide varieties of physiological differences make the characterization of bacteria by CE more difficult than characterization of viruses by CE.

2. Materials and Equipment

2.1. Separation of Bacteria Using Polymer-Containing CE Running Buffer

1. Microorganisms: *Pseudomonas fluorescens* type IV, *Enterobacter aerogenes* type III, and *Micrococcus luteus* were purchased as freeze-dried samples from Sigma (St. Louis, MO) (*see* **Note 1**).
2. Stock buffer solution: 4.5 m*M* Tris, 4.5 m*M* boric acid, and 0.1 m*M* EDTA prepared in deionized water yielding a buffer of pH 8.4.
3. Stock dilution buffer solution: the stock buffer solution was diluted 8:1 with deionized water.
4. Stock polymer solution: 0.2 g of PEO were added to 40 mL of the diluted buffer solution (*see* **Note 2**).
5. Electrophoresis sample: bacteria samples were prepared by dispersing appropriate amounts of the bacteria cells in the diluted stock buffer to a concentration of 1 mg/mL (*see* **Note 3**).
6. Background electrolyte: the running buffer was prepared by diluting the polymer stock solution with the diluted stock buffer to give a final polymer concentration of 0.0125%.
7. Apparatus: experiments were performed on a Beckman P/ACE 2100 coupled to a computer equipped with Gold data acquisition software.

8. Electrophoretic capillary: fused-silica capillary 100 μm ID × 27 cm (20 cm to the detector).
9. Detector: ultraviolet (UV)-Vis detector.

2.2. Separation of Bacteria Using Specific Ions-Containing CE Running Buffer

1. Microorganisms: *Escherichia coli, Salmonella enteriditis, Leuconostoc mesenteroides, Listeria monocitogenes, Yersinia enterolitica, Enterococcus faecium, Lactobacillus plantaru*, and *Staphylococcus aureus* were obtained from Spanish Collection od Strains (CECT) of the University of Valencia.
2. Rehydratation: microorganisms were rehydrated from freeze-dried pellets using tryptosa soya broth and cultured in this medium for 24 h (*see* **Note 4**) prior to frozen storage of 500-μL aliquots in Microbank tubes with pellets (Pro-lab Diagnostic, Canada).
3. Bacterial growth: a pellet from a frozen stock culture containing the studied strains was cultured in 10 mL of TSB at 30 °C for 24 h. Several dilutions of the mother growth medium were subsequently made (*see* **Note 5**).
4. Background electrolyte: the CE running buffer was a mixture of 25 m*M* phosphate buffer (pH 7.0), 25 μ*M* calcium chloride, and 35 μ*M* myo-inositol hexakisphosphate (*see* **Note 6**).
5. Electrophoresis sample: the bacterial solution was passed through a sterile filter of 0.2-μm pore size to retain bacteria. Therefore, bacteria were resuspended in electrophoretic buffer for CE analysis.
6. Preparation of food sample: to monitor the bacterial contamination in food samples, 1 g of solid sample or 1 mL of liquid sample was mixed with 10 mL of 25 m*M* phosphate buffer (pH 6.9) containing 150 mg of dehydrated TSB/L. This bacterial suspension was allowed to stand at 37 °C for 7 h for enable amplification (*see* **Note 7**). Then, the suspension was centrifuged and the supernadant was passed through 5-μm sterile Teflon filters. This bacterial solution obtained was passed through a sterile filter of 0.2-μm pore size to retain the bacteria, which were finally resuspended in electrophoretic buffer for analysis (*see* **Note 8**).
7. Apparatus: CE runs were conducted on a P/ACE 5500 instrument from Beckman. Control and data processing were done with a Beckman P/ACE Station Software.
8. Electrophoretic capillary: uncoated fused silica capillaries of 75 μm ID × 47 cm (39.5 cm effective length).
9. Detector: detection was performed at 210 nm with a diode array detector.

2.3. Separation of Bacteria Using Capillary Isoelectric Focusing

1. Microorganisms: *Escherichia coli, Pseudomonas putida*, and*Serratia ribidae* were grown in-house. The starting cultures were transferred from solid agar to Nutrient Broth (Difco Laboratories, Franklin Lakes, NJ) and were growth for 24–26 h at 25–30 °C.

2. Electrophoretic sample: the bacteria were pelleted for 3–5 min using a centrifuge at 5000 g. The supernatant was removed, and the cells were washed with water to remove culture media constituents. This procedure was repeated twice. Finally, bacteria were resuspended in diluted Bio-Lyte Ampholyte (Bio-Rad, Hercules, CA), pH 3.0–10.0 (*see* **Note 9**).
3. Background electrolyte: the pH gradient was generated with diluted Bio-Lyte Ampholyte pH 3.0–10.0 (*see* **Note 9**). The anolyte and the catholyte were 20 m*M* phosphoric acid and sodium hydroxide, respectively.
4. Apparatus: a Beckman P/ACE 2100 coupled to a computer equipped with Gold data acquisition software was used for experiments.
5. Electrophoretic capillary: separations were performed using 50 μm × 47 cm (40 cm to the detector) coated silica capillaries. The methylcellulose coating of the capillaries was prepared using the procedure described by Hjertén ***(20)***.
6. Detector: UV-Vis detector.

2.4. Separation of Bacteria Aggregates Using CE

1. Microorganisms: the bacteria *Micrococcus luteus* and*Alcaligenes faecalis* were grown in-house. The starting cultures were transferred from solid agar to Nutrient Broth (Difco Laboratories, Franklin Lakes, NJ) and were growth for 24–26 h at 25–30 °C (*see* **Note 10**).
2. Electrophoretic sample: the bacterial sample was pelleted for 3–5 min in a small sample vial using a centrifuge. The supernatant was decanted and 1 mL of the CE run buffer was added to the pelleted cells. The vial sample was shaken and the bacterial suspension was centrifugated again. Finally, the washed cells were suspended in 1–2 mL of the CE run buffer and either used for CE analysis (*see* **Note 11**).
3. Background electrolyte: the CE running buffer solution was prepared by diluting the stock polymer solution (**Subheading 2.1., item 4**) with the diluted stock buffer solution (**Subheading 2.1., item 3**) to a final polymer concentration of 0.0125% (*see* **Note 12**).
4. Apparatus: CE separations were performed on a Beckman P/ACE 2100 coupled to a computer equipped with Gold data acquisition software.
5. Electrophoretic capillary: fused-silica capillary 100 μm ID × 27 cm (20 cm effective length).
6. Detector: on-line UV-detector.

2.5. Separation of Recombinant Adenovirus Using CE

1. Microorganisms: recombinant Ad5 preparations with different transgenes were prepared at Berlex Biosciences usinh HEK 293 or PER. C6 packaging cells adapted to serum free medium and suspension culture were purified by anion-exchange chromatography and ultrafiltration. Finally, Ad5 with a fibroblast growth factor (FGF)-4 transgene was used in CE experiments (*see* **Note 13**).
2. Electrophoresis sample: samples were filtered with Nanosep MF 0.45-μm microconcentrators (Pall Filtron, Northborough, MA). Unless otherwise noted, the samples were then dialyzed into 10 m*M* phosphate, pH 7.0 before CZE analysis

using 8000 M_r cutoff membrane with a 10,000-fold or greater volume excess and with a minimum dialysis time of 1 h.
3. Background electrolyte: 25 m*M* phosphate buffer at pH 7.0.
4. Equipment: experiments were made on a Beckman P/ACE 5500 CE equipment.
5. Electrophoretic capillary: the capillaries were apolyvinyl alcohol (PVA) capillaries with a buble cell with a pathlength of 3 times the inner diameter of the capillary. The capillary was 57 cm (effective length 50 cm) × 50 μm ID.
6. Detector: UV detector.

2.6. Study of Affinity Complexes Between Virus and Ligands Using CE

1. Microorganisms: human rhinovirus (HRV) serotypes 2 and 14, as originally obtained from the American Type Culture Collection (ATCC), were produced and purified from infected cell pellets.
2. Ligand: monoclonal antibody 8F5, directed against a linear antigenic determinant of VP2, was purified from hybridoma tissue culture supernatants.
3. Background electrolyte: the electrolyte was 100 m*M* boric acid containing 10 m*M* SDS. The pH was adjusted with 1 *M* NaOH to 8.3.
4. Electrophoresis sample: samples were dissolved in a buffer solution corresponding to half-diluted background solution without the surfactant (SDS).
5. Affinity CE: for evaluation of the immunoaffinity interaction between HRV2 and mAb 8F5, virus and antibody were mixed in a microvial. After incubation, CE separation was performed.
6. Stability: the stability of the affinity complex was studied by programming the CE instrument to switch off the voltage after 4 min of separation time. Separation was then continued after that time period.
7. Apparatus: experiments were performed with an automated HP3D capillary electrophoresis system (Hewlett-Packard).
8. Electrophoretic capillary: uncoated fused-silica capillary 50 μm ID × 60 cm total length (51.5 cm effective length).
9. Detector: UV-Vis detector.

3. Methods

The methods described in this chapter for the determination and analysis of microorganisms by CE can be classified in two groups: (1) determination of bacteria microorganism and (2) determination of virus microorganisms. With regard to the determination of bacteria, four methods are presented. Two of them are based on CZE using a background electrolyte containing a polymer or containing specific ions that alter the outer bacteria surface. Another is based on capillary isoelectric focusing, whereby separation is achieved based on the characteristic bacterial pI. Finally, a method of studying the formation of bacterial aggregate clusters is also presented. With regard to the determination of virus, two procedures are shown. The first is based on free CZE and the second on affinity CE.

3.1. Separation of Bacteria Using Polymer-Containing CE Running Buffer

1. Capillary conditioning: the capillary was washed for 1.5 min with 0.5 *N* phosphoric acid, 0.5 min water, 1.5 min with 1 *N* KOH, and 0.5 min with water, followed by 1 min with the running buffer.
2. The conditions used in CE were as follows: voltage, 10 kV; temperature, 23 °C; detection, 214 nm.
3. Sample injection: bacteria samples were injected by pressure for 8–10 s.
4. The RSDs ($n = 4$) for the electrophoretic mobilities of individual bacteria using this CE approach ranged from 1.5% to 2.0%.
5. The electrophoretic mobilities of bacteria were function of the polymer concentration. **Figure 1** shows the effect of the concentration of 600,000 molecular weight PEO on the electrophoretic mobility of four microorganisms.
6. As can be deduced from **Fig. 1**, as the curves are not parallel to one another; different elution orders can be obtained at different PEO concentrations.

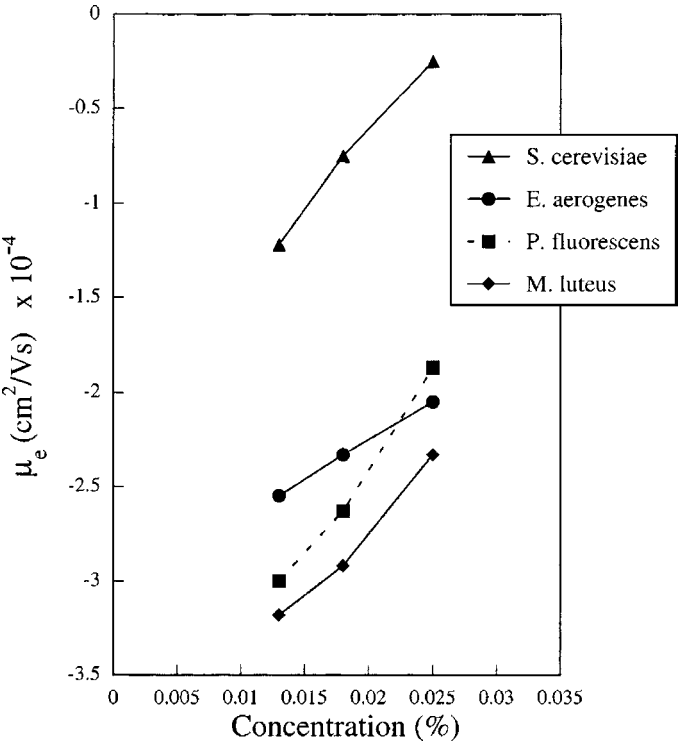


Fig. 1. Effect of the concentration of 600,000 molecular weight poly-(ethylene oxide) (dissolved in the running buffer) on the electrophoretic mobility of four microorganisms. (Reproduced from **ref. *5***, by permission of ACS Publications.)

7. **Figure 2** shows a representative electropherogram of the separation of three bacteria and baker's yeast (*S. cerevisiae*) (*see* **Note 14**). Note the relatively short migration times, the high efficiency, and the good peak shapes.
8. Under the conditions of this method, bacteria are negatively charged and migrate in a direction opposite to that of the EOF.
9. The analysis of a bacterium sample treated with 0.15 % SDS prior injection shows that surfactants cannot be used in the electrophoretic buffer because they produce the lysis of the cells.

3.2. Separation of Bacteria Using Specific Ions-Containing CE Running Buffer

1. Capillary conditioning: a new capillary was conditioned by rinsing with 1 *M* HCl for 5 min, followed by 0.1 *M* NaOH for 10 min and ultrapure Milli-Q water for 5 min. The capillary was filled with 0.1 NaOH for 2 min and with running buffer for 5 min prior to each CZE run.
2. Instrumental CE conditions: voltage, 15 kV; capillary temperature, 20 °C; detection, 210 nm.
3. Sample injection: sample solutions containing the bacteria were injected into the capillary for 10 s with the aid of pressure (20 psi).
4. The method provided migration times reproducible to an RSD of 1.8%.

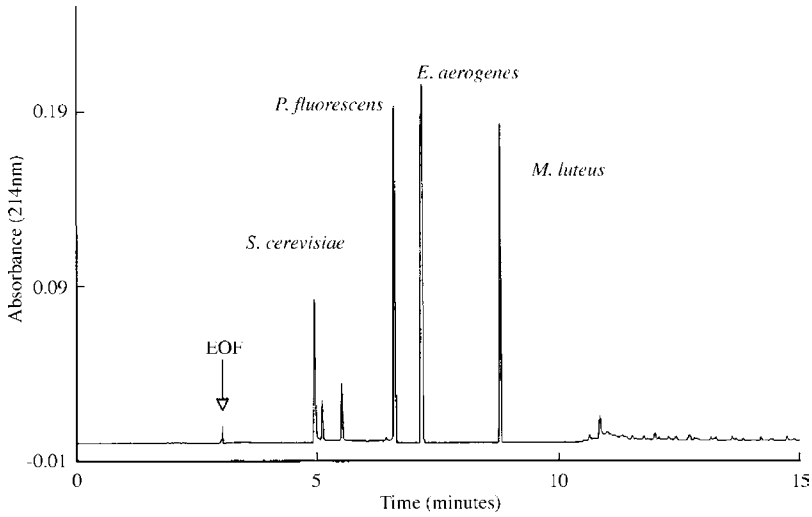


Fig. 2. Capillary electropherogram of the separation of three bacteria (*Pseudomonas fluorescens, Enterobacter aerogene*, and *Micrococcus luteus*) and a baker's yeast (*Saccharomyces cerevisiae*) obtained using the method described under **Subheading 2.1.** (Reproduced from **ref. *5***, by permission of ACS Publications.)

5. The electrophoretic mobility of Gram-positive bacteria was found to increase on raising the pH from 4.0 to 7.0. This was consistent with the fact that Gram-positive bacteria exhibit negative electric charge above pH 5.0.
6. The electrophoretic mobility of Gram-negative bacteria changed very little over the pH range of 4.0–7.0.
7. Extreme pH values (4.0 and 10.0) resulted in broad peaks, probably through partial lysis of the bacteria.

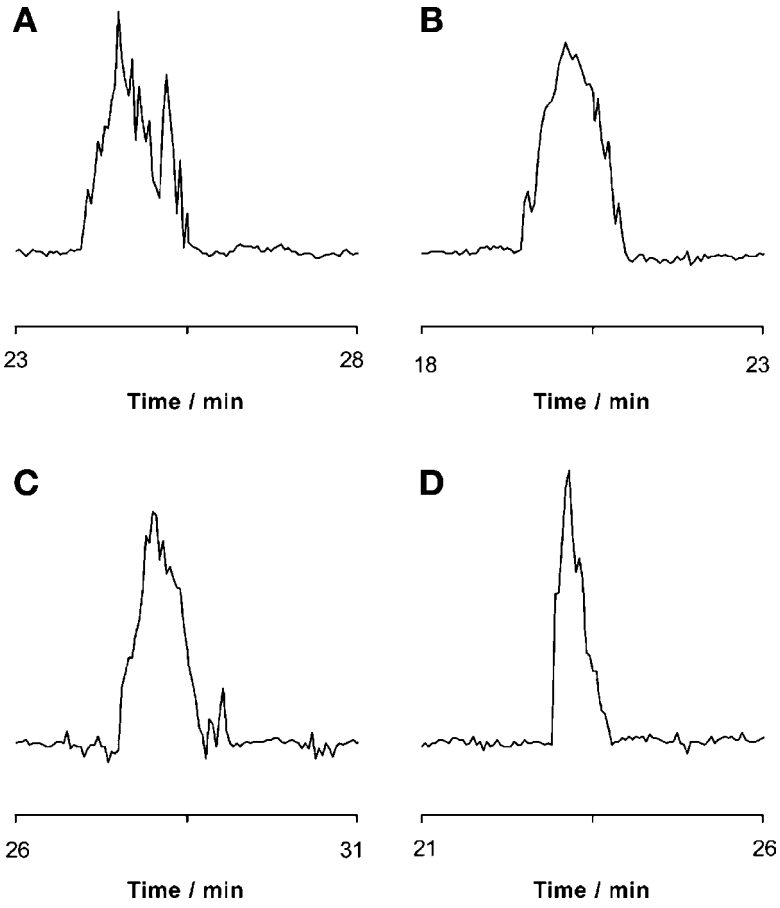


Fig. 3. Dependence of the peak bandwidth and shape for *Escherichia coli* on the concentration of calcium and myo-inositol hexakisphosphate ($InsP_6$) in the electrophoretic buffer. **(A)** 0 μ*M* Ca2++0 μ*M* InsP6. **(B)** 25 μ*M* Ca2++0 μ*M* InsP6. **(C)** 0 μ*M* Ca2++35 μ*M* InsP6. **(D)** 25 μ*M* Ca2++35 μ*M* InsP6. (Reproduced from **ref. *8***, by permission of ACS Publications.)

8. The addition of cations such as calcium and anions such as myo-inositol hexakisphosphate to the running buffer has a positive and synergistic effect on peak width and shape (*see* **Fig. 3**).
9. **Figure 4** shows a representative electropherogram for a mixture of eight types of contaminating bacteria. As can be seen, the method allows the effective separation of eight different bacteria in only 25 min.
10. **Figure 5** shows the electropherograms obtained for the analysis of samples without contamination and contaminated with bacteria. It is important to remark that the precision of the analysis of real spiked samples ranges from 3.3 to 7.0%.

3.3. Separation of Bacteria Using Capillary Isoelectric Focusing

1. Capillary conditioning: before each separation, the capillary was washed for 2 min with water and ampholyte.
2. Instrumental conditions: the focusing of the sample was performed for 5 min at 20 kV. Afterward, samples were mobilized with a low-pressure (0.5 psi) rinse while the 20 kV voltage was maintained. Experiments were carried out at 23 °C and detection was made at 280 nm using an on-line UV detector.

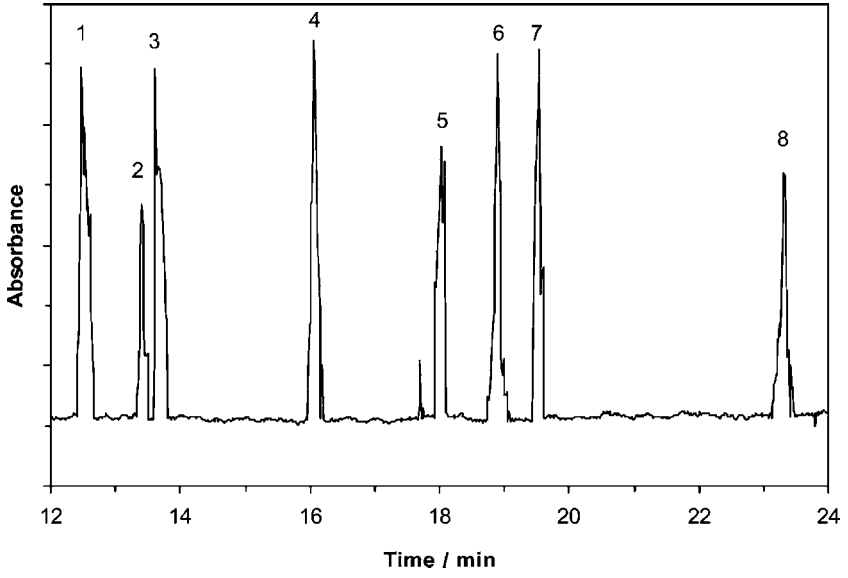


Fig. 4. Electropherogram for a mixture of eight types of contaminating bacteria. Peaks: 1, *Yersinia enterocolitica*; 2, *Leuconostoc mesenteroides*; 3, *Salmonella enteriditis*; 4, *Listeria monocitogenes*; 5, *Escherichia coli*; 6, *Lactobacillus plantarum*; 7, *Staphylococcus aureus*; 8, *Enterococcus faecium*. (Reproduced from **ref. *8***, by permission of ACS Publications.)

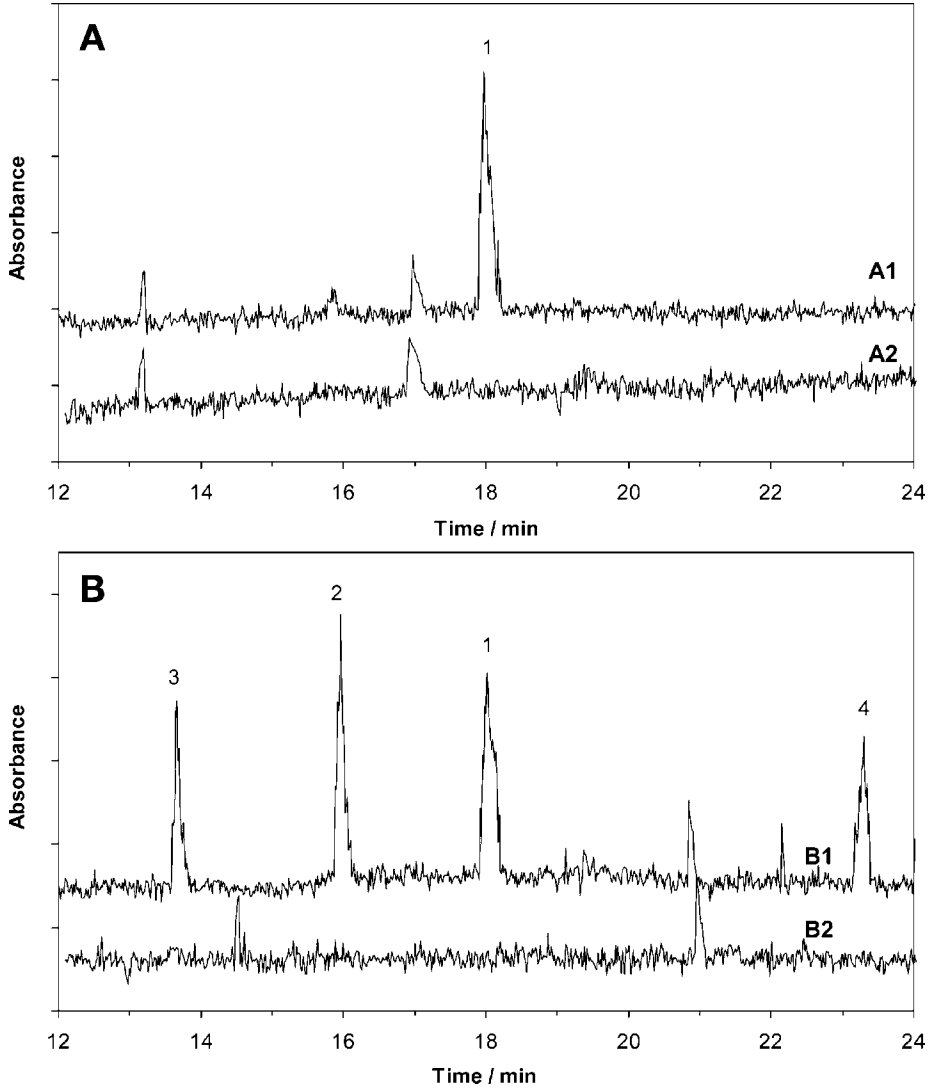


Fig. 5. Electropherograms for a **(A)** corn flakes and **(B)** juice samples using the proposed method. Electropherograms A1 and B1 correspond to spiked samples, and A2 and B2 are the respective blank samples. Peaks: 1, *Escherichia coli*; 2, *Salmonella enteriditis*; 3, *Listeria monocitogenes*; 4, *Enterococcus faecium*. (Reproduced from **ref. *8***, by permission of ACS Publications.)

3. Sample injection: bacteria samples were introduced into the capillary by a 0.5 psi pressure injection for 90 s followed by a second injection of ampholyte for 129 s.
4. **Figure 6** shows as bacteria can be resolved from one another by using their difference in the pI.
5. In order to achieve reproducible results for the isoelectric focusing of bacteria, the capillary and microbial pretreatment must be carried out exactly.

3.4. Separation of Bacteria Aggregates Using CE

1. Capillary conditioning: prior to each injection, the capillary was washed for 1.5 min with 1 *N* phosphoric acid, for 0.5 min with water, for 1.5 min with NaOH, for 0.5 min with water, and for 0.5 min with the running buffer.
2. CE conditions: voltage, 10 kV; temperature, 23 °C, and detection, 214 nm.
3. Sample injection: samples were injected by pressure for 10–12 s at 0.5 psi.

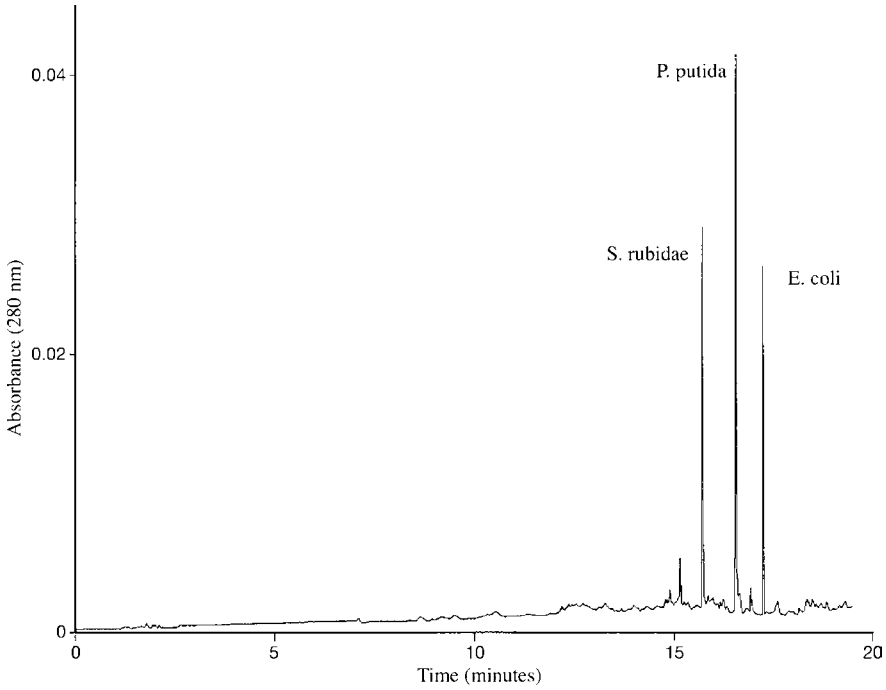


Fig. 6. Electropherogram showing the capillary isoelectric foscusing separation of three bacteria of similar size. (Reproduced from **ref. *5***, by permission of ACS Publications.)

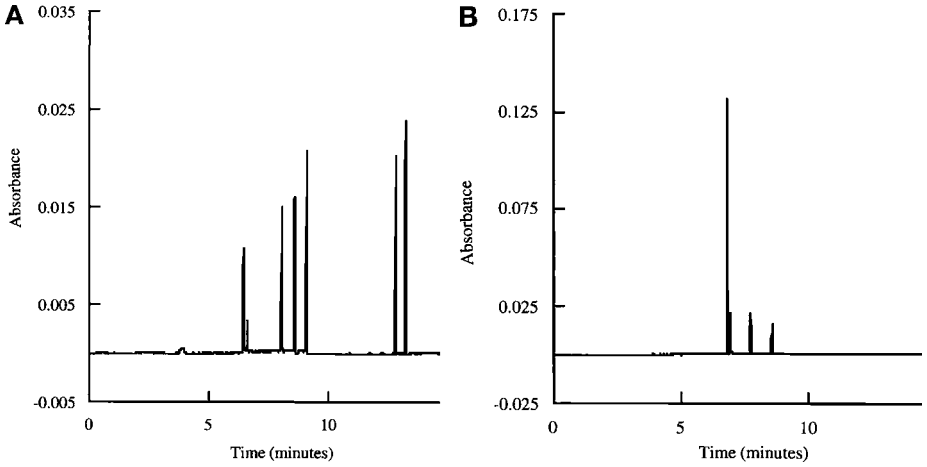


Fig. 7. **(A)** Electropherogram showing the capillary electrophoresis separation of clusters of *Micrococcus luteus* and **(B)** the electropherogram of the same sample of *M. luteus* after the cells were dispersed in an ultrasonic bath for 3 min. (Reproduced from **ref. *7***, by permission of Elsevier Science B.V.)

4. One phenomenon that must be studied and controlled in microbiological analysis is the self-aggregation in an aqueous matrix. In general, bacterial aggregates can be partially dispersed using a small amount of ultrasound energy.
5. **Figure 7A** clearly shows the resolution of bacterial clusters of *M. luteus* into several highly efficient peaks. When the aggregated bacterial sample is immersed in an

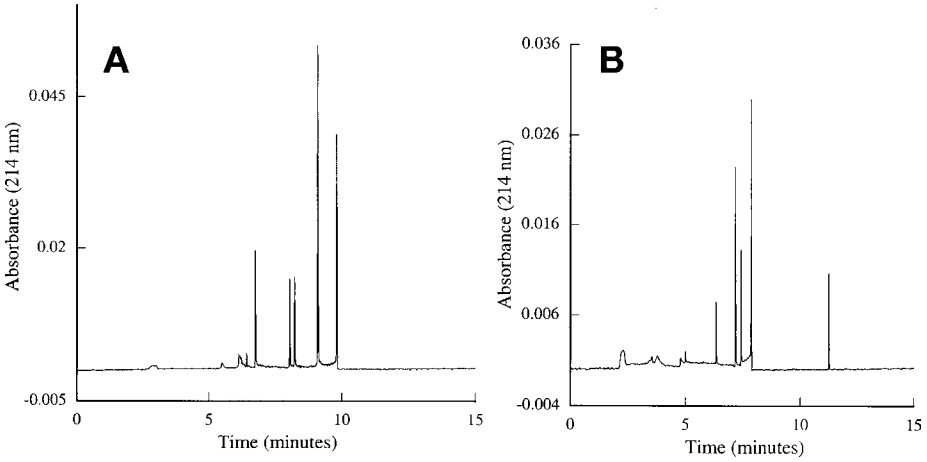


Fig. 8. Electropherogram corresponding to the capillary electrophoresis separations of *Aerogenes. faecalis* **(A)** before immersion in an ultrasound bath and **(B)** after immersion in an ultrasound bath. (Reproduced from **ref. *7***, by permission of Elsevier Science B.V.)

ultrasound bath, the later eluting peaks, which correspond to the larger clusters, disappear (*see* **Fig. 7B**) and the first peak, which corresponds to the single cell, increases in intensity (*see* **Note 15**).

6. Some microorganisms display the phenomenon of cell aggregation more strongly than others. One example is *A. faecalis*. In **Fig. 8A**, five highly efficient peaks corresponding to cell aggregates are observed in the electropherogram. After the sample is immersed in an ultrasonic bath, the same five peaks remain with only slight variations in intensity (**Fig. 8B**).
7. The tendency of the bacteria to form aggregates depends of the bacteria surface composition and also of the medium composition.
8. An alternative method of dispersing the aggregates cell can be the use of mild detergents or the treatment of the cells with hydrolytic enzymes which cleaves these extracellular proteins, saccharides, and lipopolysaccharides. However, the conditions must be controlled carefully in order to avoid the lysis cell.

3.5. Separation of Recombinant Adenovirus Using CE

1. Capillary conditioning: a new capillary was conditioned by flushing with water for 5 min. Between runs, the capillary was conditioned with 60 m*M* HCl for 4 min by applying 13.8 kPa pressure.

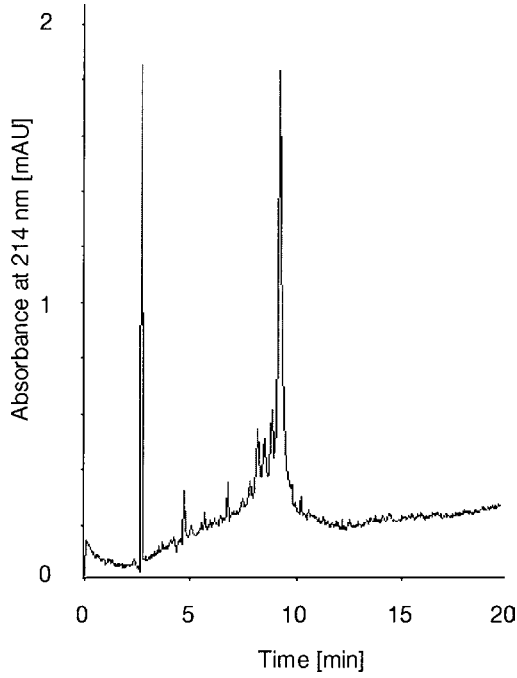


Fig. 9. Electropherogram of a recombinant adenovirus type 5 carrying fibroblast growth factor-4 transgene (Ad5FGF-4). (Taken from **ref. *19***, with permission.)

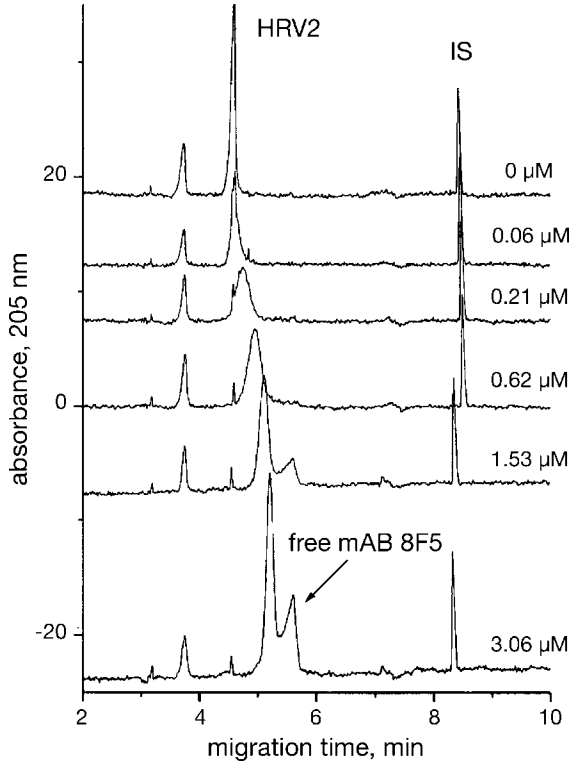


Fig. 10. Formation of HRV2-mAb 8F5 complexes as a function of the amount of antibody added as analyzed by capillary electrophoresis. (Reproduced from **ref.** ***18***, by permission of ACS Publications.)

2. The conditions used in CE were as follows: voltage, reverse polarity at 29.5 kV; capillary temperature, 20 °C; detection, 214 nm.
3. Sample injection: samples were injected by applying 3.4 kPa pressure for 30 s.
4. The use of a PVA-coated capillary is recommended because the PVA kept the virus from adsorbing onto the walls of the capillary.
5. **Figure 9** shows a typical electropherogram obtained with a PVA-coated capillary. The major peak at approx 9–10 min and the minor peaks in the 7- to 9-min interval were consistently present in all batches of Ad5 tested independent of the transgenes present.
6. The minor peaks observed in electropherograms were not the result of clonal difference in the parent virus. These peaks were the result of modifications caused by events after virus purification. One would have expected that arbitrary damage to the capsid surface would have resulted in multiple species producing broadening of the virus peak in the electropherogram.

3.6. Study of Affinity Complexes Between Virus and Ligands Using CE

1. Capillary conditioning: between all runs, the capillary was conditioned with 100 m*M* NaOH, water, and background electrolyte for 2 min each by applying 950 mbar pressure.
2. Instrumental CE conditions: voltage, 25 kV; temperature, 20 °C; detection, 205 nm.
3. Sample injection: injection of samples was performed at 50 mbar pressure for 9 s.
4. At low antibody-to-virus ratio, broad peaks were observed, which points to the presence of a heterogeneous population of virions with several numbers of attached antibodies. In contrast, the peak became narrow at a high molar ratio, indicating saturation of the equivalent epitopes with the antibody (*see* **Fig. 10**).
5. This method proved to be useful for a rapid assessment of complex formation and allows for an estimation of the binding stoichiometry.
6. **Figure 11** shows a series of electropherograms showing the complex formation as a function of the incubation time. Stopping the voltage for periods of time permits one to study easily the kinetics of the complex formation.

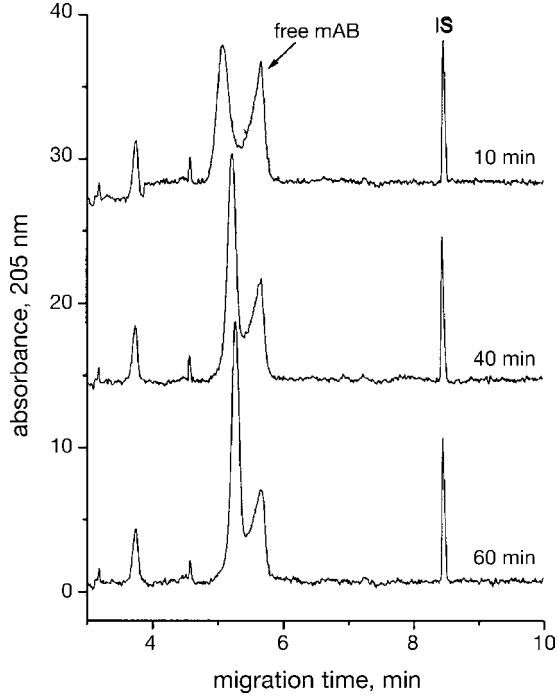


Fig. 11. Virus–antibody complex formation as a function of the incubation time. Virus (HVR2) and antibody (mAb 8F5) were mixed and analysed immediately after incubation at room temperature for the times indicated. (Reproduced from **ref. *18***, by permission of ACS Publications.)

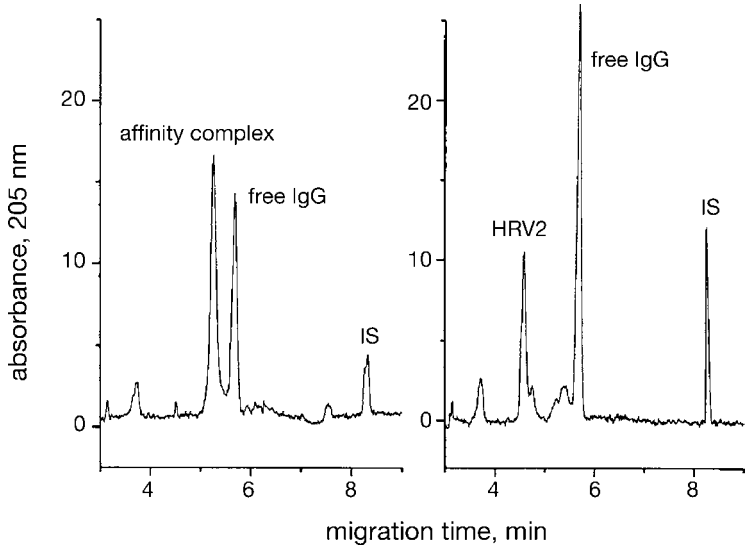


Fig. 12. Stability of the complex between virus and antibody (HRV2 and mAb 8F5) **(A)** without and **(B)** in presence of sodium dodecyl sulfate (SDS). SDS was present in the mixture sample from the beginning. (Reproduced from **ref. *18***, by permission of ACS Publications.)

7. The virus–antibody complex can be prevented by the addition of SDS to the sample (*see* **Fig. 12**). Note the different migration times of the virus–antobody complex with the free virus.

4. Notes

1. The viability of bacteria was checked by microscopy and growth in culture.
2. The heterogenous polymer solution was dispersed by placing it in an ultrasound bath for 4 h. The mixture was removed from the bath and left overnight to dissolve completely. It should be noted that extensive sonication may cause some degradation of the dissolved polymer.
3. Bacteria cells were immersed in the buffer solution for 45 min, yielding a turbid solution. The cells were then centrifugated, the supernadant was decanted, and freshly diluted buffer was added. The tubes containing the sample were placed in an ultrasound bath for 3 min in order to disperse the cells.
4. Bacteria viability was checked by microscopy.
5. The bacterial concentration was determined by plate counting on tryptosa soya agar after incubation at 37 °C for 24h.
6. The background electrolyte solution was filtered prior use with a Nylon filter of 0.45 μm pore size.

7. To obtain a higher sensitivity, let the sample stand for more time until there is enough amplification.
8. The bacteria resuspension was performed with magnetic stirrer. If the bacteria have an affinity for forming aggregates, then the resuspension can be performed with ultrasonic radiation.
9. The ampholyte was diluted with water to a final concentration of 0.5% (v/v).
10. Fresh cultures were prepared weekly.
11. This sample vial was sonicated for 2–3 min in the ultrasound bath prior to CE analysis in order to disperse the aggregates.
12. All buffers and polymer solution were prepared fresh daily.
13. Virus samples were stored frozen in phosphate-buffered saline (PBS) +2% sucrose +2 m*M* $MgCl_2$ and thawed before the analysis.
14. The migration time of the EOF was established using mesityl oxide as marker.
15. The presence of aggregates in the sample was confirmed by examining the sample by visible microscopy.

Acknowledgment

Financial support from Spain's Ministry of Education and Science within the framework of project CTQ2004-01220 is gratefully acknowledged.

References

1. Hjerten, S., Elebring, K., Kilar, F., et al. (1987) Carrier-free zone electrophoresis, displacement electrophoresis and isoelectric focusing in a high-performance electrophoresis apparatus. *J. Chromatogr*. **403,** 47–61.
2. Ebersole, R. C. and McCormick, R. M. (1993) Separation and aisolation of viable bacteria by capillary zone electrophoresis. *Biotechnology* **11,** 1278–1282.
3. Pfetsch, A. and Welsch, T. (1997) Determination of the electrophoretic mobility of bacteria and their separation by capillary zone electrophoresis. *Fresenius J. Anal. Chem*. **359,** 198–201.
4. Glynn, J. R., Belongia, B. M., Arnold, R. G., Ogden, K. L., and Baygents, J. C. (1998) Capillary electrophoresis measurements of electrophoretic mobility for colloidal particles of biological interest. *App. Environ. Microbiol*. **64,** 2572–2577.
5. Armstrong, D. W., Schulte, G., Scheiderheinze, J. M., and Westenberg, D. J. (1999) Separating microbes in the manner of molecules. 1. capillary electrokinetic approaches. *Anal. Chem. t* **71,** 5465–5469.
6. Armstrong, D. W. and Schneiderheinze, J. M. (2000) Rapid identification of the bacterial pathogens responsible for urinary tract infections using direct injection CE. *Anal. Chem*. **72,** 4474–4476.
7. Schneiderheinze, J. M., Armstrong, D. W., Schulte, G., and Westenberg, D. J. (2000) High efficiency separation of microbial aggregates using capillary electrophoresis. *FEMS Microbiol. Lett*. **189,** 39–44.

8. Palenzuela, B., Simonet, B. M., García, R. M., Ríos, A., and Valcárcel, M. (2004) Monitoring of bacterial contamination in food simples using capillary zone electrophoresis. *Anal. Chem*. **76,** 3012–3017.
9. Kenndler, E. and Blaas, D. (2001) Capillary electrophoresis of macromolecular biological assemblies: bacteria and viruses. *Trends Anal. Chem*. **20,** 543–551.
10. Desai, M. and Armstrong, D. W. (2003) Separation, identification and characterization of microorganisms by capillary electrophoresis. *Microbiol. Mol. Biol. Rev*. **67,** 38–51.
11. Rodriguez, M. A. and Armstrong, D. W. (2004) Separation and analysis of colloidal/nano-particles including microorganisms by capillary electrophoresis: a fundamental review. *J. Chromatogr.B*. **800,** 7–25.
12. Kremser, L., Blaas, D., and Kenndler, E. (2004) Capillary electrophoresis of biological particles: viruses, bacteria and eukaryotic cells. *Electrophoresis* **25,** 2282–2291.
13. Grossman, P. D. and Soane, D. S. (1990) Orientation effects on the electrophoretic mobility of rod-shaped molecules in free solution. *Anal. Chem*. **62,** 1592–1596.
14. Scnabel, U., Groiss, F., Blaas, D., and Kenndler, E. (1996) Determination of the pI of Human Rhimovirus Serotype 2 by capillary isoelectric focusing. *Anal. Chem*. **68,** 4300–4303.
15. Okun, V. M., Ronacher, B., Blaas, D., and Kenndler, E. (1999) Analysis of common cold virus (Human Rhinovirus serotype 2) by capillary zone electrophoresis: the problem of peak identification. *Anal. Chem*. **71,** 2028–2032.
16. Okun, V. M., Blaas, D., and Kenndler, E. (1999) Separation and biospecific indentification of subviral particles of human Rhinovirus serotype 2 by capillary zone electrophoresis. *Anal. Chem*. **71,** 4480–4485.
17. Okun, V. M., Ronacher, B., Blaas, D., and Kenndler, E. (2000) Capillary electrophoresis with postcolumn infectivity assay for the analysis of different serotypes of human Rhinovirus (common cold virus). *Anal. Chem*. **72,** 2553–2558.
18. Okun, V. M., Ronacher, B., Blaas, D., and Kenndler, E. (2000) Affinity capillary electrophoresis for the assessment of complex formation between viruses and monoclonal antibodies. *Anal. Chem*. **72,** 4634–4639.
19. Mann, B., Traina, J. A., Soderblom, C., et al. (2000) Capillary zone electrophoresis of a recombinant adenovirus. *J. Chromatogr. A* **895,** 329–337.
20. Hjertén, S. and Kubo, K. (1993) Celular automation simulation of pulsed field gel electrophoresis. *Electrophoresis* **14,** 390–395.

II

Methods-Oriented

23

A Semi-Empirical Approach for a Rapid Comprehensive Evaluation of the Electrophoretic Behaviors of Small Molecules in Free-Zone Electrophoresis

Philippe Schmitt-Kopplin and Agnes Fekete

Summary

A phenomenological model is proposed for the evaluation of relative electrophoretic migration of charged substances present in mixtures and for the rapid pH optimization prior to capillary zone electrophoresis method development. The simple and robust model is based on the Offord model, which takes account of the chemical structure. The effective charge and the molecular mass of the molecule are needed; the charge can easily be calculated from pK_a obtained from known sources or simulated with existing pK-calculation programs. A first example was chosen with the separation of hydroxy-s-triazines to illustrate the applicability of this simple approach for determination of the first buffer-pH conditions prior experimental method optimization when separation of different ions is needed. In a second example, the confirmation of aminialcohols in the CZE method development of unsaturated hexahydro-triazines and oxasolidines.

Key Words: Semi-empiric model; mobility simulation; separation optimization; s-triazines; aminoalcohols; formaldehyde releasers.

1. Introduction

Especially within the fields of genomics, proteomics, and peptidomics, models for a better understanding of the free-zone electrophoresis of DNA fragments (few basepairs up to several thousands of basepairs), proteins, or peptides were developed. These models intended an optimization of the separation conditions, a prognosis of electrophoretic separations of these mixtures, and identification of structures based on standardized experimental separation conditions (i.e., small peptide structures obtained after tryptic digestion) ***(1–5)***.

From: *Methods in Molecular Biology, vol. 384: Capillary Electrophoresis*
Edited by: P. Schmitt-Kopplin © Humana Press Inc., Totowa, NJ

Since the introduction of capillary electrophoresis (CE) in the 1980s, different simulations of the capillary zone electrophoretic processes were proposed. Some of the simulations aimed at the evaluation of equilibrium (binding toward ions and mobility pH dependency) in capillary zone electrophoresis (CZE) ***(6)*** and can also be used for optimization of separation parameters ***(7,8)***. Others were principally aimed at understanding peak anomaly/shape ***(9)***, peak sharpening effects ***(10)***, anomalous spikes, and boundary structures using the Kohlrausch regulating function ***(11)***, allowing correct interpretation of experimental CZE results ***(12)***. A last approach allowed the determination of physical–chemical parameters that can be deduced from the electrophoretic behavior under variable experimental conditions (dissociation constants pK ***(13,14)***, isoelectric points [pIs] ***(14)***, hydrophobicities Log[P] ***(15)***, charge ***(16,17)***, binding constants ***(18)***).

We propose to simulate electrophoretic mobilities with a *simple and robust guideline for a rapid method development in CE* based on a model involving easily accessible structural data of the analyte (pK, molecular mass). On the other hand, screening of unknown components through a series of CE experiments at different pH allows the evaluation determination of charge variations of these analytes. The proposed model was verified for low-molecular-weight components.

2. Semi-Empirical Models

Semi-empirical models were already described from the mid-1960s to predict the mobilities of peptides in electrophoretic separation systems and to obtain information on their amide groups ***(19)***. These descriptions were rapidly adapted to capillary electrophoretic separations of polypeptides and proteins ***(20)***. The effective mobility of an analyte can be generally described with a charge-to-size model where the size of the molecules is approximated by their molecular mass M. It was found to be a continuous function of $M^{-1/3}$ to $M^{-2/3}$, depending on the magnitude of M and the ionic strength of the buffer.

The mobility of an analyte in free solution is defined as the ratio of its electric charge Z (Z = q.e, with e the charge on an electron and q the valency) to its electrophoretic friction coefficient (f) **(eq. 1)**.

$$\mu = \frac{q \cdot e}{f} \tag{1}$$

All models are based on **eq. 1**, with two parameters needing to be estimated: the net charge and the frictional coefficient.

2.1. Charge Estimation

The ζ potential of charged spherical particle is expressed with **eq. 2**:

$$\zeta = \frac{Z}{4\pi \cdot \varepsilon \cdot R \cdot (1 + \kappa \cdot R)} \tag{2}$$

where R is the sphere radius, κ^{-1} the Debye length, ε the permitivity, and Z the particle charge.

The charge Z can be estimated from the pK of the analytes as a function of the pH with the Henderson–Hasselbach equation. However, for a series of analyzed components, the pK values found in literature databases are often not comparable or useable for the chosen experimental conditions (measured at different ionic strength, temperatures or in different solvents). In this case, several simulation programs are available and can be used; some were tested within this study. Best results (relative values) are obtained when taking a homogeneous set of values (i.e., calculated with identical programs or from the same database).

2.2. Frictional Coefficient Estimation

The frictional coefficient (f) corresponds to the drag (viscous) force that the particle experiences when moving with a given velocity under an electrical field, and its estimation is more ambiguous than for charge. An approach would be usable to derive it from the Nernst-Einstein equation:

$$D = \frac{K \cdot T}{f} \tag{3}$$

where D is the diffusion coefficient, k the Bolztmann constant, and T the temperature.

Because this relationship is rarely used, diffusion coefficients (D) can be determined ***(21)*** with **eq. 4** when the mobility and the charge are known:

$$\mu = \frac{q \cdot e}{k \cdot T} \cdot D \tag{4}$$

where k is the Boltzmann constant, T the temperature, z the charge, and μ the mobility.

A first approximation of f can be used for spherical shaped and rigid ions through the Stokes equation **(eq. 5)**:

$$f = 6\pi \cdot \eta \cdot R \tag{5}$$

where η is the viscosity, and R the radius of the ion.

$$\mu = \frac{q \cdot e}{6\pi \cdot \eta \cdot R} \tag{6}$$

This leads to mobility equation **(eq. 6)**:

The resulting approximation, however, is very imprecise because R is often unknown and can only be determined on basis of diffusion, sedimentation, or electrophoretic mobility. Moreover, the solvent/water and ions moving with the analyte are not taken account. This effect can be estimated taking account of the Debye theory presented above and the nature of the solution contiguous to the ion (ionic strength, conterions). The ion cloud can influence the mobility and lead to *relaxation* effects. Cifuentes and Poppe ***(2)*** combined the relaxation effects and electrophoretic retardation effects into a reducing effect on the mobility. They presented a model in which the effects of the deformation of the ion cloud around the moving ion was included and leads to formation of a electric force that counteracts the applied field ***(2)***. In the case of large, moving ions (compared to the buffer ions), the relation could be reduced **eq. 7**:

$$\mu = A \cdot \frac{q \cdot e}{6\pi \cdot \eta \cdot R^2} \tag{7}$$

with A is a constant.

Theoretical approaches give much insight into the mobility of smaller ions, but fail for highly charged and larger ions. Following a more empirical approach is therefore often the best strategy ***(2)***.

3. Mobility Prediction from Structural Data

Many empirical models can be found in studies that were developed to fit the experimental and predicted data for very specific compounds classes (mainly peptides). These mobility expressions usually include in the formula the charge (Z) of the analyte, its molecular mass (M), or the number of amino acids (n). These formulations include:

1. Grossman's equation **(eq. 8)** ***(4)***:

$$\mu = A \cdot \frac{\log(\mathrm{Z}+1)}{n^B} \tag{8}$$

   where Z the charge, A and B are constants, and n the number of amino acids.
2. Offords approach **(eq. 9)** ***(5,19,22)***:

$$\mu = A \cdot \frac{Z}{M^{2/3}} \tag{9}$$

   where Z the charge, A a constants, and M the molecular mass.

3. Compton's equations (**eqs. 10** and **11**) ***(3,20)***:

$$\mu = A \cdot \frac{Z}{M^m} \tag{10}$$

$$\mu = A \cdot \frac{Z}{B \cdot M^{1/3} + C \cdot M^{2/3}} \tag{11}$$

where Z is the charge, A, B, C and m constants, and M the molecular mass.

Cifuentes and Poppe developed this further and came up with a relation giving the best mobility prediction for peptides **(eq. 12)** with a combination of **eqs. 8** and **9** ***(1,2,23)***.

$$\mu = A \cdot \frac{\log(1 + \mathrm{BZ})}{M^C} \tag{12}$$

where Z is the charge, A and B are constants, and M is the molecular weight.

An interesting approach is the one of Fu and Lucy ***(24)***, which integrated the effects of hydration using the McGovan hydration increments ***(25)*** to further improve the prediction. It is, however, limited to monoamines, and the equations are far from being phenomenological.

4. Experimental Approach

4.1. A Semi-Empirical Model for Small Molecules

For the development of a general mobility model, we wanted to stay as close as possible to the phenomenological approach **(eq. 7)**. Any purely mathematical data linearization and curve fitting would improve the prediction but would limit the possibility of data interpretation with the particular samples used for the fitting (*see* equations above).

Originally, we wanted to use the equation for anionic natural organic matter (NOM); we chose substances similar in structure and mobility, like phenolic, aliphatic, and sugar acids. The relation $\mu = f$ (charge, size) had to be tested over different pH ranges so that mobility changes vs pH, as derived from charge and size effects, could be interpreted.

The first problem was to find a homogeneous data set of pK values. The values found in the literature often varied by about 50%, as a result of the use of different solvents and temperatures. We chose to simulate pK with three available pK-simulation software programs and to compare the obtained values within the phenomenological models. We estimated all pKs with the Pallas 3.1 ***(26)***, ACD-Labs pK calculator 3.5, and the SPARC chemical reactivity model (the latter was available thanks to Dr. S.W Karickhoff, Dr. A.W Garisson, and Dr. J.M. Long, USEPA, Athens, GA) ***(27,28)***. For a given pH, different

charged states are calculated in each of the three pK calculation possibilities; when calculating the hydration effect with the McGovan increment method, this had to be taken into account.

The Stoke's radius can be obtained by treating the molecule as a sphere and using the van der Waals volumes calculated by molecular modeling (Alchemy III and ACD Sotware). From the volumes, the corresponding radii were calculated assuming spherical shapes. Because the size data obtained in this way are not always available, it was important to compare these models with systems using the molecular mass only.

The tested models are listed in **Fig. 1**. From all tested combinations (three different pK sources, size modeled with M, r, s, v, and the hydration effect H),

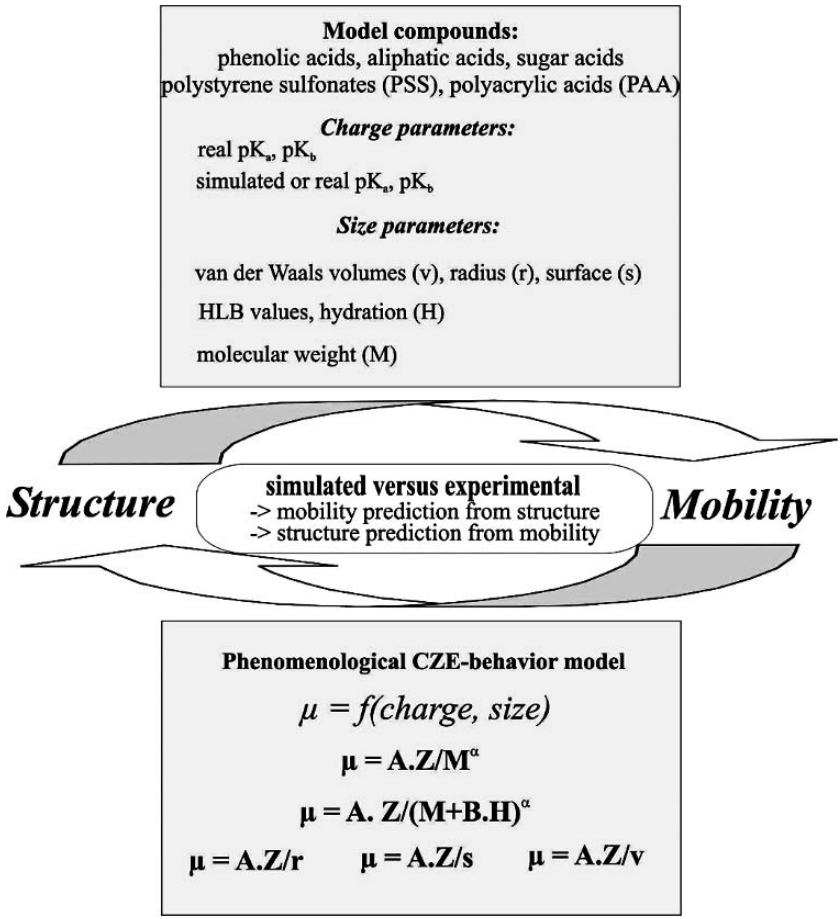


Fig. 1. The applied approach for determinating of the phenomenological model.

we selected the one that gave the best regression coefficient. Hydration factors were calculated for each substance and added to the molecular weight (weight factor taken from the table in **ref. *25*** as a function of the present structures [calculations needed to be done at each pH to take account of the partial ionisation of the acidic groups]) ***(24,25)***. These values are given in **Table 1** for selected data combinations and include phenolic acids only. Other attempts to include additional molecular characteristics such as the hydrophobicity (LogP) or the ovality of the molecules were not successful.

It was required that the separation buffer be noncomplexing toward the analytes so that the measured mobility could be attributed to structural effects only. Borate, for example, is a buffer that interacts with diol groups and therefore induces some mobility shifts as a function of the binding strength. For all of the tested combinations, we compared the experimental data (all data sets were calculated with the phenolic compounds at three pHs) with simulated mobility values involving the van der Waals volumes/surface/radius and additional hydration volumes. The simplest model (already proposed by Offord in 1966) was found to be the best with a linearity of $R^2 = 0.9384$ (*see* **Table 2**).

Including the experimental data of the aliphatic acids in the Offord model, the data also fit into the linearity **(Fig. 2)**. Aliphatic acids were measured at pH 11.0 using CTAB to invert the electroosmotic flow (EOF) and 2,6-naphthalenedicarboxylic acid as an ultraviolet (UV)-absorbing background electrolyte ***(29)***. Acetic acid was used as an internal standard for mobility correction.

The shape and the size of the molecules are thus directly responsible for their mobility. Assuming a homogeneous density of the molecules and a spherical shape, the radius is proportional to the power of one-third. This hypothesis was verified for all of the model phenolic acids studied above and found the relation $r = 0.59385.\ M^{1/3}$ with $R^2 = 0.901$, where r was obtained from the calculated volumes of the phenolic acids with Alchemy 2000 software.

When substituting this relation in the Stoke's equation **(eq. 6)**, the proportionality of the mobility to $M^{-2/3}$ is verified. It was also found previously by many authors that Offord's model is verified for peptides ***(2,5,22)***.

This result signifies that surface charge density governs the mobility of these analytes. However, an universal model could never been verified among all available data sets because the dependency on $M^{-\alpha}$ (α between one-third and two-thirds) was a function of the used amino acid residues and the composition of the separation buffer (complexing or noncomplexing, ionic strength effects on the Debye length). In the studies presented here, we systematically used noncomplexing (acetate and carbonate buffers) at the same ionic strength (25 m*M*) and in all calculations, structural data were from the same source (identically simulated).

Table 1
pKa (Calculated From the Pallas Software Package) and Molecular Weight of Selected Aliphatic, P,henolic, and Sugar Acids.

	pKa (Pallas)	Molecular weight
Aliphatic acids		
formic acid	3.55	46.0
acetic acid	4.56	60.1
oxalic acid	0.99, 6.68	74.0
propionic acid	4.76	74.1
glycolic acid	3.75	76.1
butyric acid	4.63	88.1
pyruvic acid	2.26, 2.26	88.1
glyoxylic acid	1.18	90.0
lactic acid	3.75	90.1
valerianic acid	4.84	102.2
malonic acid	2.77, 5.38	104.1
glyceric acid	3.41	106.1
fumaric acid	4.09, 4.69	116.1
levulinic acid	4.69	116.1
succinic acid	4, 5.24	118.1
erythronic acid - 1,4-lacton	12.38	118.1
tartronic acid	2.31, 4.64	120.1
malic acid	3.16, 4.59	134.1
threonic acid	3.86	136.1
adipic acid	4.37, 5.06	146.2
tartaric acid	2.7, 3.99	150.1
galactonic acid -1,4-lacton	12.13	178.2
isosacharin	3.19	180.2
citric acid	2.39, 4.01, 4.9	192.1
mannonic acid -1,4-lacton	3.16, 12.73	192.1
2-keto-gluconic acid	3.08	194.1
5-keto-gluconic acid	3.26	194.1
gluconic acid	3.27	196.2
galactaric acid	2.92, 3.63	210.2
glucaric acid	2.92, 3.64	210.2
Phenolic acids		
phenol	9.92	94.1
catechol	9.53, 12.67	110.1
resorsinol	9.33, 11.27	110.1
benzoic acid	4.2	122.1
o-hydroxybenzoic acid	4.07, 9.72	122.1
methylcatechol	9.96, 12.69	124.1

transcinamaldehyd	13.15	132.2
2,4-hydroxybenzaldehyd	7.33, 9.3	138.1
m-hydroxybenzoic acid	2.66, 10.03	138.1
p-hydroxybenzoic acid	4.58, 10.03	138.1
p-hydroxyphenyl acetic acid	4.497.85	152.2
protocatechoic acid	4.45, 9.94, 12.17	154.1
alpha-methylcinamic acid	5.17	162.2
m-coumaric acid	4.39, 9.59	164.2
o-coumaric acid	4.63, 9.87	164.2
p-coumaric acid	4.63, 9.58	164.2
phthalic acid	2.95, 5.41	166.1
4-tertiobuthylcatechol	10.03, 12.71	166.2
vanillic acid	4.47	168.2
gallic acid	4.32, 8.86, 10.68	170.1
ascorbic acid	3.94, 12.78	176.1
t-3,4,-dimethoxycinamic acid	4.54	176.2
4-hydroxy, 3-methoxycinamaldehyde	9.63, 13.31	178.2
coffeic acid	4.57, 9.5, 12.04	180.2
Conyferyl alcohol	10.09	180.2
homovanillic acid	4.43, 7.85	182.2
ferulic acid	4.58, 9.58	194.2
syringic acid	4.36, 10.03	198.2
trimellitic acid	2.81, 4.16, 4.76	210.1
2,6-naphthalene dicarboxylic acid	3.67, 4.51	216.2
sinapic acid	4.53, 9.58	224.2
pyromellitic acid	1.86, 3.03, 4.5, 5.67	254.2
quercetin	8.9, 9.95, 11.23, 12.83	302.2
conidendrin	9.8, 10.36	356.4
matairesinol	9.98, 10.06	358.4
pinoresinol	9.92, 10.53	358.4
hydroxymatairesinol	9.95, 10.05	374.4
rutin	8.92, 10.1, 11.38, 12.63	610.5

This best empiric relation for mobility found with all tested combinations, which can systematically be used in CZE method development, is:

$$\mu = A \cdot \frac{Z}{M^{2/3}} \tag{13}$$

with $A = 2.219$ in our experimental conditions for these analytes.

More information on mobility variation with pH is gained with this approach than using the simple relation between the mobility and the pK of the substances, which can only be taken as a preliminary assessment of separation

Table 2
Selected Best R^2 Results From the Data Linearization Using Different Models for Charge (pKa from ACD, Pallas, SPARCS) and Size∗.

H from ACD Size pKa	$Mw^{2/3}$ Hydr.	$MW^{2/3}$ Corrected	H from SPARC r^2 Alchemy	r^2 ACD	H from PALLAS hydr. R^2 Alchemy	hydr. R^2 ACD	hydr. R^2 Alchemy	hydr. R^2 ACD	hydr. R^2 Alchemy	hydr. R^2 ACD
ACD	0.9151	0.8689	0.9146	0.8847	0.8776	0.8747	0.8587	0.853	0.8581	0.8522
SPARC	0.94	0.8786	0.9395	0.9163	0.8754	0.8761	0.8866	0.8877	0.861	0.8599
PALLAS	**0.9384**	**0.9134**	**0.9355**	**0.9097**	**0.9191**	**0.9187**	**0.9086**	**0.907**	**0.9213**	**0.9208**

∗Molecular weight (Mw), van der Walls radius r^2, hydration factor H-corrected van der Waals radius R^2.

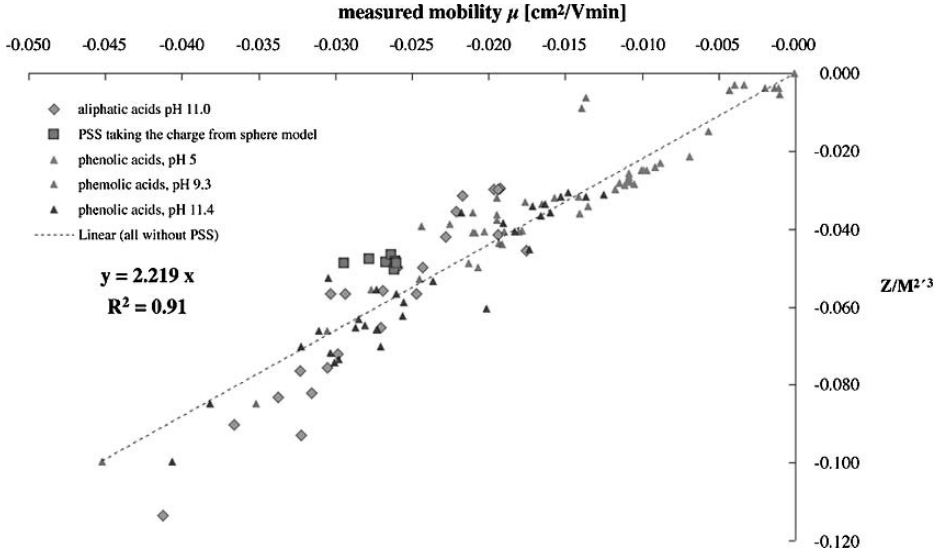


Fig. 2. All experimental datasets involving phenolic acids at three different pH and aliphatic acids at pH 11.0.

(30). The Offord model can be used in a general manner to simulate systematically the electrophoretic mobility of the components of interest over the pH range. An example of theoretical evolution of the mobilities by pH is illustrated for aliphatic and phenolic acids in **Fig. 3**. Different pH zones can be differentiated (arrows) in which the mobilities of the components are governed alone by COOH groups (carboxylic acidity, pH 5.0) or OH and COOH groups (total acidity, pH 11.4). At a pH of around 9.0, the phenols (low mobility) can be additionally distinguished from the phenolic acids (high mobility).

4.2. Simulation and Separation of Hydroxy-S-Triazines as Cations and Anions in CZE

An example of the application of this approach is given for the optimization of the separation of 12 hydroxy-s-triazines, all hydroxylated metabolites of s-triazine pesticides presenting different side chain substituents (**Table 3**). Based on **eq. 13**, the pKa, and the molecular mass values in **Table 3**, an evolution of the theoretical mobility can be calculated as a function of pH. The resulting curves are shown in **Fig. 4**.

From **Fig. 4**, it can easily been seen that the optimum separation pH is at low or high pH values; at neutral pH, the mobility of the analytes is zero (all analytes migrate with the EOF) as a result of the zwitterionic character of

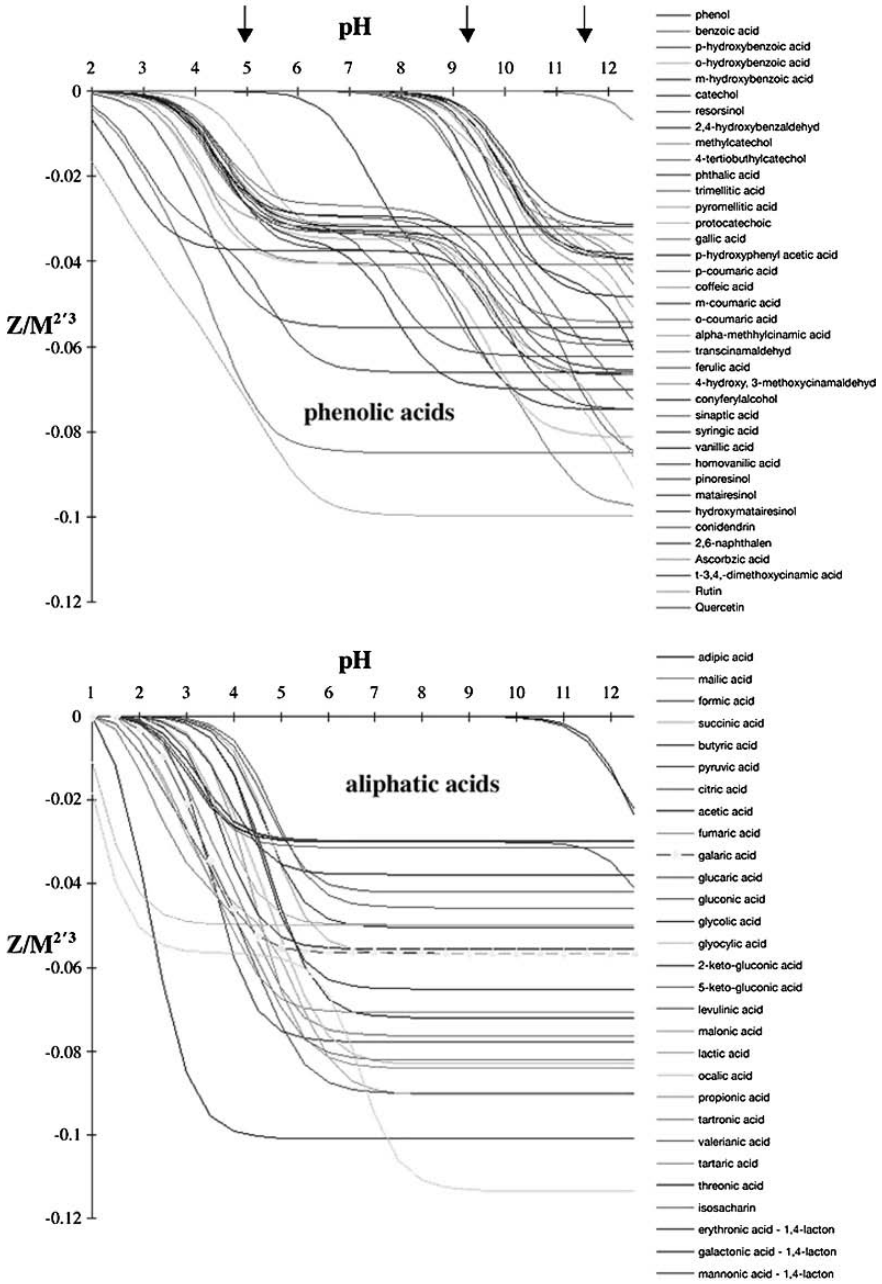
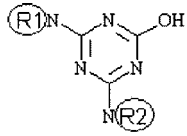


Fig. 3. Theoretical mobility evolution by pH using the Offord model for phenolic and aliphatic acids. Important in this figure is not to recognize the different traces but actually to see the potential of the simmulation in rapidly recognize best pH for the optimal separation of components in mixtures.

Table 3
Substituted Hydroxy-s-Triazines (1–12 in Fig. 4), Their Mass (M) and Acidic pKa and Basic pKb.



R1, R2		M	pKa	pKb
H, H	1	127	4.44	9.54
H, Et	2	155	4.64	9.93
H, iPr	3	169	4.71	9.96
H, tBu	4	183	4.91	10.34
Et, Et	5	183	4.94	10.31
H, mAr	6	233	3.96	9.48
Et, iPr	7	197	4.95	10.39
Et, tBut	8	211	5.2	10.88
iPr, iPr	9	211	5.01	10.88
iPr, Ar	10	245	4.24	9.78
H, Ar	11	203	4.02	9.49
iPr, mAr	12	275	4.29	9.73

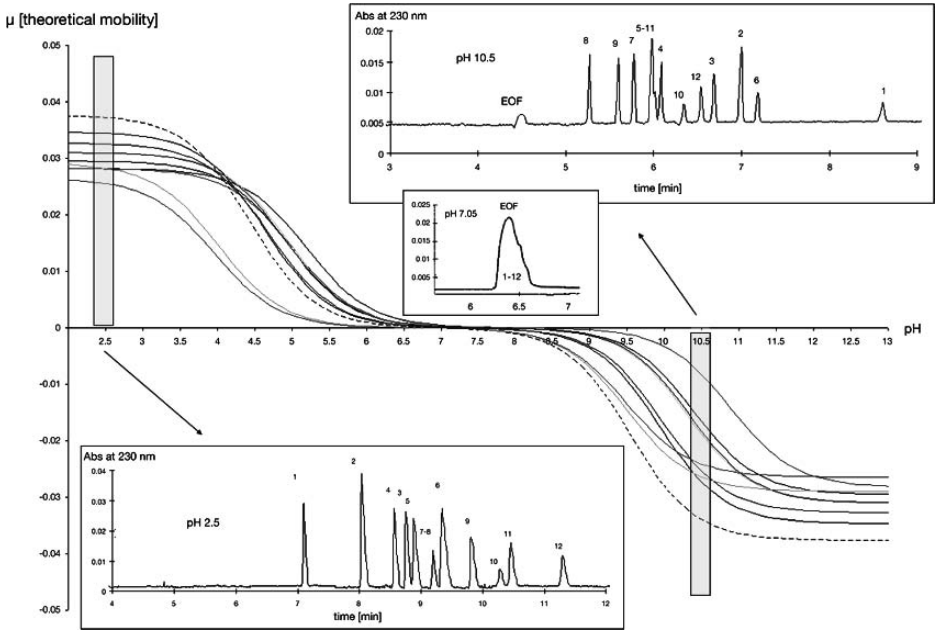


Fig. 4. Theoretical evolution of the mobility by pH for the substituted hydroxy-s-triazines in **Table 3**.

the substances. Indeed, the electropherograms shown in **Fig. 4** verify nicely this separation selectivity.

Actually, the knowledge of the variations in electrophoretic mobility by pH can be used to determine precisely pK values as illustrated with the same analytes in **ref.** ***14***, and in Chapter 10.

4.3. Confirmation of Aminoalcohol in the CZE-Indirect Detection of Formaldehyde Releasers

Unsaturated triazines and oxasolidines used as biocides in metalworking fluid were separated at neutral pH condition because they are not stable under acidic medium; they hydrolyze releasing formaldehyde and different derivatives of corresponding aminoalcohols. According to Offord's model, the $Z/M^{2/3}$ values of the analytes calculated at pH 7.0 differ from each other, meaning that they can be separated with CE. However, after separation with a noncomplexing buffer, the measured mobilities did not match the corresponding $Z/M^{2/3}$ values (all measured mobilities were much lower than those estimated). Moreover, two substances migrated together in spite of the fact that their calculated $Z/M^{2/3}$ was totally different (linear correlation between the theoretical and measured values were as low as $r^2 = 0.320$). Because the hydrolysis products of these two analytes are identical, we calculated the

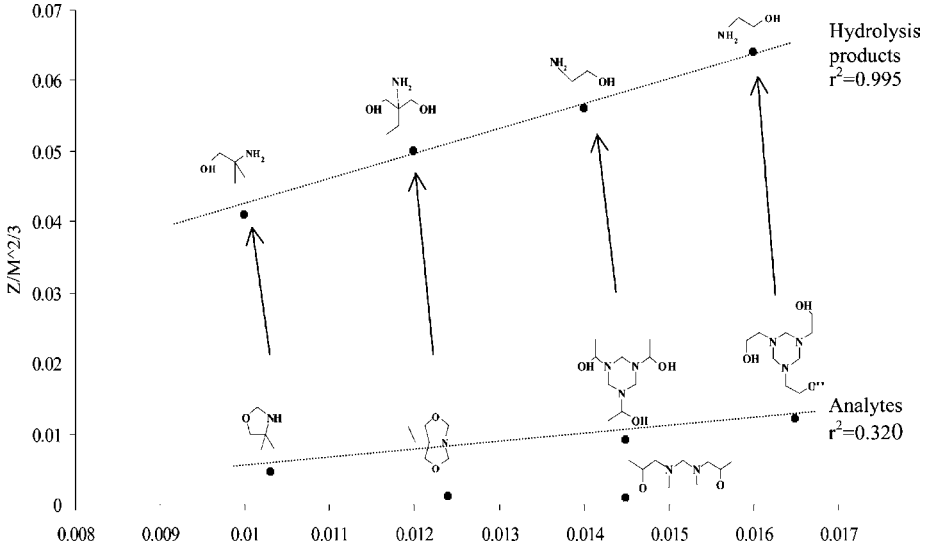


Fig. 5. Comparison of the measured mobility and Offord model ($Z/M^{2/3}$) of the selected unsaturated triazines and oxasolidines and their hydrolysis products.

$Z/M^{2/3}$ of all possible aminoalcohols and compared them to their measured mobility. Strong linear correlation ($r^2 = 995$) was found between the calculated and measured mobility of the aminoalcohols as shown in **Fig. 5**.

Thus, applying this semi-empirical approach, it was possible to verify that the selected hexahydro-triazines and oxasolidines were rapidly hydrolyzed under the separation condition, and thus the hydrolysis products were detected. This hypothesis was verified with CE/mass spectrometry and nuclear magnetic resonance studies not shown here. Consequently, these biocides can be indirectly identified with CE if the sample does not contain the hydolysis product (derivatives of aminoalcohols).

Conclusion

The Offord model (effective mobility linearly correlated to $Z/M^{2/3}$) was verified as the simplest and most accurate approach by which to rapidly simulate the relative mobility of ions in free-zone electrophoresis based on their chemical structure. The charge can easily be calculated from the pK values (as from the literature or databases, or calculated by simulation programs), and the mass can be used to evaluate the frictional force. The accuracy of the model is robust enough to give at least a good estimation of a starting pH when developing methods by which to separate known substances in mixtures or to confirm charge to mass ratios of known/unknown structures in method development.

Acknowledgment

H. Neumeir and B. Look are thanked for their technical assistance and their kind support during the past years.

References

1. Cifuentes, A. and Poppe, H. (1995) Effect of ph and ionic strength of running buffer on peptide behavior in capillary electrophoresis: theoretical calculation and experimental evaluation. *Electrophoresis* **16,** 516–524.
2. Cifuentes, A. and Poppe, H. (1997) Behavior of peptides in capillary electrophoresis: effect of peptide charge, mass and structure. *Electrophoresis* **18,** 2362–2376.
3. Chen, N., Wang, L., and Zhang, Y. K. (1993) Correlation free-solution capillary electrophoresis migration times of small peptides with physicochemical properties. *Chromatographia* **37,** 429–432.
4. Grossman, P. D., Colburn, J. C., and Lauer, H. H. (1989) A semiempirical model for the electrophoretic mobilities of peptides in free-solution capillary electrophoresis. *Anal. Biochem*. **179,** 28–33.

5. Rickard, E. C., Strohl, M. M., and Nielsen, R. G. (1991) Correlation of electrophoretic mobilities from capillary electrophoresis with physicochemical properties of proteins and peptides. *Anal. Biochem*. **197,** 197–207.
6. Havel, J. and Janos, P. (1997) Evaluation of capillary zone electrophoresis equilibrium data using the CELET program. *J. Chromatogr. A* **786,** 321–331.
7. Britz-McKibin, P. and Chen, D. D. Y. (1997) Prediction of the migration behavior of analytes in capillary electrophoresis based on three fundamental parameters. *J. Chromatogr. A* **781,** 23–34.
8. Sahota, R. S. and Khaledl, M. G. (1994) Target factor modeling of migration behavior in capillary electrophoresis. *Anal. Chem*. **66,** 2374–2381.
9. Ermakov, S. V., Bello, M. S., and Righetti, P. G. (1994) Numerical algorithms for capillary electrophoresis. *J. Chromatogr. A* **661,** 265–278.
10. Gas, B., Vacik, J., and Zelensky, I. (1991) Computer-aided simulation of electromigration. *J. Chromatogr*. **545,** 225–237.
11. Kohlrausch, F. (1897) Ueber Concentrations-Verschiebungen durch Electrolyse im Inneren von Lösungen und Lösungsgemischen. *Annalen der Physik und Chemie*, Band **62,** 210–239.
12. Ermakov, S. V., Mazhorova, O. S., and Zhukov, M. Y. (1992) Computer simulation of transient states in capillary zone electrophoresis and isotachophoresis. *Electrophoresis* **13,** 838–848.
13. Gluck, S. J., Steele, K. P., and Benkö, M. H. (1996) Determination of acidity constants of monoprotic and diprotic acids by capillary electrophoresis. *J. Chromatogr. A* **745,** 117–125.
14. Schmitt, P., Poiger, T., Simon, R., Garrison, A. W., Freitag, D., and Kettrup, A. (1997) Simultaneous ionization constants and isoelectric points determination of 12 hydroxy-s-triazines by capillary zone electrophoresis (CZE) and capillary electrophoresis isoelectric focusing (CIEF). *Anal. Chem*. **69,** 2559–2566.
15. Freitag, D., Schmitt-Kopplin, P., Simon, R., Kaune, A., and Kettrup, A. (1999) Interactions of hydroxy-s-triazines with SDS-micelles by micellar electrokinetic capillary chromatography (MEKC). *Electrophoresis* **20,** 1568–1577.
16. Gao, J., Gomez, F. A., Härter, R., and Whitesides, G. M. (1994) Determination of the effective charge of a protein in solution by capillary electrophoresis. *Proc. Natl. Acad. Sci. U. S. A*. **91,** 12027–12030.
17. Menon, M. K. and Zydney, A. L. (1998) Measurement of protein charge and ion binding using capillary electrophoresis. *Anal. Chem*. **70,** 1581–1584.
18. Schmitt, P., Trapp, I., Garrison, A. W., Freitag, D., and Kettrup, A. (1997) Binding of s-triazines to dissolved humic substances: electrophoretic approaches using affinity capillary electrophoresis (ACE) and micellar electrokinetic chromatography (MEKC). *Chemosphere* **35,** 55–75.
19. Offord, R. E. (1966) Electrophoretic mobilities of peptides on paper and their use in the determination of amide groups. *Nature* **211,** 591.
20. Compton, B. J. (1991) Electrophoretic modeling of proteins in free solution zone capillary electrophoresis and its application to monoclonal antibody microheterogeneity analysis. *J. Chromatogr*. **559,** 357.

21. Nikodo, A. E., Garnier, J. M., Tinland, B., et al. (2001) Diffusion coefficient of DNA molecules during free solution electrophoresis. *Electrophoresis* **22,** 2424–2432.
22. Cross, R. F. and Cao, J. (1997) Salt effects in capillary zone electrophoresis 1. Dependence of electrophoretic mobilities upon the hydrodynamic radius. *J. Chromatogr. A* **786,** 171–180.
23. Cifuentes, A. and Poppe, H. (1994) Simulation and optimization of peptide separation by capillary electrophoresis. *J. Chromatogr. A* **680,** 321–340.
24. Fu, S. and Lucy, C. A. (1998) Prediction of electrophoretic mobilities. 1. Monoamines. *Anal. Chem*. **70,** 173–181.
25. McGowan, J. C. (1990) A new approach for the calculation of HLB values of surfactants. *Analysis* **27,** 229–230.
26. Fekete, J., Morovjan, G., Csizmadia, F., and Darvas, F. (1994) Method development by an expert system: Advantages and limitations. *J. Chromatogr. A* **660,** 33–46.
27. Hilal, S. H. and Karickhoff, S. W. (1995) A rigorous test for SPARC's chemical reactivity models: estimation of more than 4300 ionization pk_as. *Quantitative Structures - Activity Relationships* **14,** 348–355.
28. Karickhoff, S. W., McDaniel, V. K., Melton, C., Vellino, A. N., Nute, D. E., and Carreira, L. A. (1991) Predicting chemical reactivity by computer. *Environ. Toxicol. Chem*. **10,** 1405–1416.
29. Dabek-Zlotorzynska, E. and Dlouhy, J. F. (1994) Capillary zone electrophoresis with indirect UV detection of organic ions using 2,6-naphthalenedicarboxylic acid. *J. Chromatogr. A* **685,** 145–153.
30. Souza, S. R., Tavares, M. F. M., and Carvalho de, L. R. F. (1998) Systematic approach to the separation of mono- and hydroxycarboxylic acids in environmental samples by ion chromatography and capillary electrophoresis. *J. Chromatogr. A* **796,** 335–346.

24

The CE Way of Thinking

"All is Relative!"

Philippe Schmitt-Kopplin and Agnes Fekete

Summary

Over the last two decades, the development of capillary electrophoresis (CE) instruments has lead to systems with programmable samplers, separation columns, separation buffers, and detection devices comparable visually in many aspects to the setup of classical chromatography.

Two characteristics make CE essentially different from chromatography and are the basis of the *CE way of thinking*: first is the injection type and the liquid flow within the capillary. When the injection is made hydrodynamically (such as in most of the applications found in the literature), the injected volumes are directly dependent on the type and size of the separation capillary. The second characteristic is that in CE, buffer velocity is not pressure-driven, as in liquid chromatography, but is electrokinetically governed by the quality of the capillary surface (separation buffer dependant surface charge) inducing an electroosmotic flow (EOF). The EOF undergoes small variations and is not necessarily identical from one separation or day to the other. The direct consequence is that the migration time of the analytes apparently nonreproducible, although the velocity of the ions is the same.

The effective mobility (field strength normalized velocity) of the ions is a possible parameterization from acquired time-scale to effective mobility-scale electropherograms leading to a reproducible visualization and better quantification with a direct relation to structural characters of the analytes (i.e., charge and size; *see* Chapter 23).

Key Words: Hydrodynamic injection; electroosmotic flow; effective mobility; mobility scale.

From: *Methods in Molecular Biology, vol. 384: Capillary Electrophoresis*
Edited by: P. Schmitt-Kopplin © Humana Press Inc., Totowa, NJ

1. Introduction

It has already been more than two decades since Jorgenson and Lukacs ***(1,2)*** presented zone electrophoresis in open-tubular glass capillaries and capillary electrophoresis (CE). This chapter does not aim to reiterate the fundamentals of CE, which can be found very easily in many good books and reviews articles ***(3–11)***, but rather will concentrate on some essential specifics of CE relative to liquid chromatographic techniques. In liquid chromatography, the injection volume is determined by the syringe volume or the injection loop size, and the solvent velocity in the column is determined by the pressure governed with the pumps. The well known instrumental setup of CE is remembered in **Fig. 1**; the main differences from chromatography are the *column setup-dependent injection volumes* and *separation buffer-dependent liquid flux* in the column. These two specifics are detailed in this chapter, along with some practical aspects and implications.

2. The Injection Mode

The hydrodynamic injection mode is by far the most used injection type in CE; the electrokinetic injection sometimes can offer higher selectivity and even sensitivity, but is seldom used because it is very sensitive to the constitution and quality of the sample. In the hydrodynamic injection mode, pressure forces a small portion of the sample into the open-tube capillary plunged into the sample vial. A difference in pressure is applied across the capillary by pressurizing

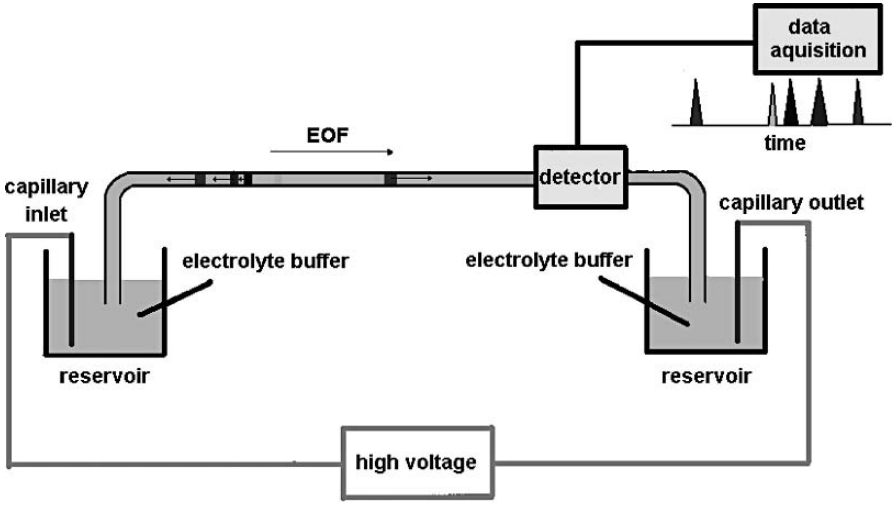


Fig. 1. Schematic representation of capillary electrophoresis.

the sample vial, and the injected sample volume is proportional to following solution parameters:

$$Vinj \approx \frac{\Delta P \cdot d^4 \cdot t}{\eta \cdot L} \quad (1)$$

where ΔP is the difference in pressure across the capillary, d is the capillary inner diameter (ID), t is the time of pressure application, η is the viscosity, and L is the capillary length.

Sample zones that are too large may result in distortions of the signals in the detector because the sample zone does not reach equilibrium before being detected. The general rule in CE is that the sample plug should never exceed 3–4% of the total column length. **Table 1** gives a representative overview of the column volume and the respective injected volumes when applying 0.5 psi for 1 s to different column dimensions. The injection volume is directly proportional to the injection time: 10% of the column is thus filled when applying 10 s of pressure to a 37-cm column of 100 μm ID.

It is important to remember these rules when adapting some methods from the literature to various instruments when the injection pressure conditions and/or column lengths are not necessarily identical.

Additionally, it should be noted that identical injection times with different column IDs or lengths lead not only to different column volumes, but also to different local sample concentrations when passing the detector. This is particularly important when analyzing analytes with concentration-dependent aggregation properties such polymeric materials or natural organic matter.

Table 1
Calculated Total Volumes, Volumes Injected per Second Hydrodynamic Injection at 0.5 psi for Different Column Lengths and Inner Diameter

Column Ld/Lt*	Total volume/ID, 50 μm	Volume injected ID, 75 μm	1n 1 s ID, 100 μm
30/37	0.7 μL/1.8 nL	1.6 μL/9 nL	2.9 μL/28.6 nL
40/47	0.9 μL/1.4 nL	2.1 μL/7.1 nL	3.6 μL/22.5 nL
50/57	1.1 μL/1.1 nL	2.5 μL/5.8 nL	4.5 μL/18.5 nL
60/67	1.3 μL/0.9 nL	2.9 μL/5 nL	5.2 μL/15.8 nL
70/77	1.5 μL/0.8 nL	3.4 μL/4.3 nL	6 μL/13.7 nL

* Ld, length to detector; Lt, total length; ID, inner diameter.

3. The Driving Force: The Electroosmotic Flow

3.1. Origin and Implications

Electroosmosis is a fundamental process in CE. The electroosmotic flow (EOF) is a direct consequence of the surface charge on the wall of the uncoated fused-silica capillary.

The wall of the fused-silica capillary contains silanol groups (pK_a between 3 and 5, depending on the quality of the charge production), which ionize as a function of the pH of the electrolyte solution. This dissociation to silanate ions (SiO^-) produces a negatively charged wall. An electrical double layer is established at solid/liquid interface to preserve electroneutrality.

An externally imposed tangential flow of the medium over the surface leads to a distortion of the ions, creating a "streaming potential." This process is reversible, and when a voltage is applied, the counter ions and their associated solvating water molecules migrate toward the cathode. The produced movement of ions and the associated water molecules result in a flow of solution toward the detector. This flow effectively pumps solute ions along the capillary, generally toward the detector, and is called the "electrically driven pump."

The electroosmotic flow (μ_{eo}) is directly dependent on the chemistry of the buffer, such as the viscosity η and its dielectric constant ε:

$$\mu_{eo} = \frac{\varepsilon\zeta}{4\pi\eta r} \tag{2}$$

ζ is the zeta potential measured at the plane of shear close to the liquid-solid interface and is thus directly related to the pH of the buffer. Because ζ is related to the inverse of the charge per unit surface area, the number of valence electrons, and the square root of the concentration of the electrolyte, an increase in the concentration of the electrolyte decreases EOF; strongly adsorbed cations will have the same effects. The direct implication of these effects is that the liquid flow through the capillary depends both on pH and capillary size. Some flows are illustrated in theoretical **(Table 2)** and real values **(Fig. 2)**.

The EOF is generated by the entire surface and therefore produces a constant flow rate all along the capillary. As a consequence, the electrophoretic flow profile is plug-like in nature. Because analytes are swept at the same rate in the capillary sample, dispersion is minimized. This is an advantage compared to the flow encountered in pressure-driven systems such as liquid chromatography (LC), where frictional forces at the liquid–solid interface, such as the packing and the walls of the tubing, result in substantial pressure drops. Even in an open tube, frictional forces are severe enough at low flow rates to result in

Table 2
Theoretical Buffer Flow (nL/min) in 50-cm Long Capillaries of Different Internal Diameters (i.d. in μm) as a Function of the Observed Time of the Electroosmotic Flow

t_{eof} min.	i.d. 100 μm nL/min	i.d. 75 μm nL/min	i.d. 50 μm nL/min	i.d. 20 μm nL/min
2.0	1964	1105	491	79
2.5	1571	884	393	63
3.0	1309	736	327	52
3.5	1122	631	280	45
4.0	982	552	245	39
4.5	873	491	218	35
5.0	785	442	196	31
5.5	714	402	178	29
6.0	655	368	164	26
6.5	604	340	151	24

A t_{eof} of 2.0 min corresponds to a buffer velocity of 25 cm/min.

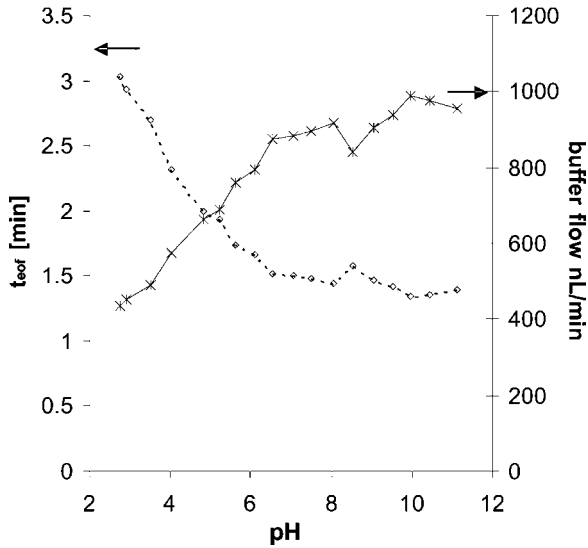


Fig. 2. Real t_{eof} and corresponding buffer flow in a 37-cm capillary, 20 kV.

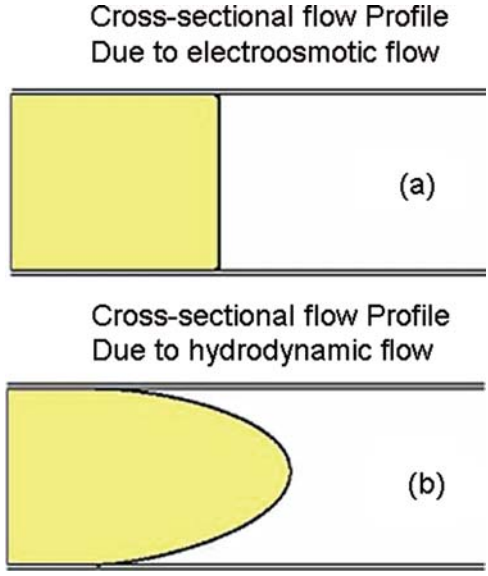


Fig. 3. Flow profiles in electrophoretic and pressure-driven separation columns.

laminar or parabolic flow profiles **(Fig. 3)**. In laminar flow, the solution is pushed from one end of the column and the solution at the edges of the column is moving slower than the solution in the middle of the column, which results in different solute speeds across the column. Therefore, laminar flow broadens peaks as they travel along the column.

4. "All is Relative!", or the CE Mode of Thinking

4.1. Qualitative/Quantitative Implications of μ-Scale Transformations

The "*CE mode of thinking*," as it was already called by Whatley ***(12)***, is a prerequisite for handling CE problems and reaching the goal of robust results. Reaching good reproducibility in migration times (qualitative aspects) and in peak integration (quantitative aspects) is part of this goal: the low reproducibility in these parameters is very often related to small changes in EOF due to uncontrollable alterations of the capillary surface, leading to migration time shifts that are not always understandable, especially when analyzing real samples (matrix effects). A first step toward increase qualitative and quantitative precision is the choice and standardization of the proper operating, calibrating, and equilibrating conditions, leading to stable EOF and reproducible migration times. This goal can be reached with different experimental setups, such as, for example, adequate rinse steps or voltage preconditioning techniques ***(13)***.

The standardization/normalization of raw electrophoretic datasets cannot only be accomplished by experimental optimization, but also by how they are visualized and analyzed. Available software with which to control and process CE signals has been mainly derived from existing classical chromatography techniques and has allowed the description of the signal variation only as a function of time. Electrophoretic separations, however, as seen before are not based on the same separation processes as in chromatography, and the time-based plots are not necessarily representative of the fundamental parameter controlling mobility, which is the velocity of the sample per unit of field strength (not linear with time). An extensive study demonstrated recently the high reproducibility that is afforded by using effective mobility (thus independent of small EOF changes), making this parameter a more robust reproducibility tool than migration times ***(14)***. Only recently has available software been adapted to these needs so as to allow high-precision calculations of the now-automated mobility and effective mobility calculations of selected peaks with a CE-adapted integration algorithm ***(15)***. This qualitative improvement allows the effective mobility value of a component at given separation pHs (combined with its ultraviolet (UV)-visible spectrum, and the use of a spectral library as obtained by diode array detectors) to be used as a decision-making tool for accurate peak assignments ***(16,17)***. Hudson et al. clearly showed the advantages of this alternative for the use of CE-diode array detection (instead of the classical gas chromatography/nitrogen-phosphorous detection technique) in forensic toxicology when screening for the "general unknown" among basic drugs in body fluids ***(18,19)***.

Various attempts to normalize total raw electrophoretic data for improved qualitative comparison have already proposed, including plotting the signals vs the *quantity of electric charge* ***(20)***, the *1/time domain* ***(21)***, using *migration indices* ***(22)***, and *migration time ratios* ***(23)***, or using dimensionless parameters such as the *reduced mobility* ***(24,25)***. These transformations increase significantly the reproducibility of the calculated parameters but cannot be used directly for the quantification of the analytes. The transformation of the entire time-scaled electropherograms to the corresponding effective mobility scale (using EOF markers or internal standards of known/calculated mobility) is another recent approach toward normalizing CE datasets, and opens news possibilities in qualitative as well as in quantitative data treatment. This last approach has been followed in our group for several years in different applications ***(26–28)***.

4.2. The Mobility Scale Transformation

It is essential to identify some basic rules of capillary zone electrophoresis (CZE) ***(29)*** that support the proposed x-scale transformation. Each molecule has

a specific effective mobility as a function of its own physico-chemical characteristics (charge, size) within a given separation buffer (pH and ionic strength governing its charge and hydrodynamic radius). The measured electrophoretic mobility, μ_{mes}, (cm^2/Vs or $cm^2/Vmin$) is calculated from the measured electrophoretic velocity, v_e, (cm/s or cm/min) and the applied electric field strength E (V/cm), taking account of the migration time (t_{mes}), length of the capillary to the detector (L_d), the total length of the capillary (L_t), and the applied voltage (V):

$$\mu_{mes} = \frac{v_e}{E} = \frac{L_d \cdot L_t}{t_m \cdot V} \tag{3}$$

The measured migration time (t_m) and the corresponding measured mobility do not reflect the velocity (directly correlated to the effective electrophoretic mobility, μ_{eff}) of the analytes in the separation system because they are also dependent on the EOF acting as pump for the buffer towards the cathode (*see* CZE setup in **Fig. 4**). The effective mobility can thus be regarded as a $V.cm^{-1}$-normalized velocity of the molecules in the capillary obtained by changing the reference system from the observer (time measurement of signals through the detection device) to the buffer system itself; this absolute value

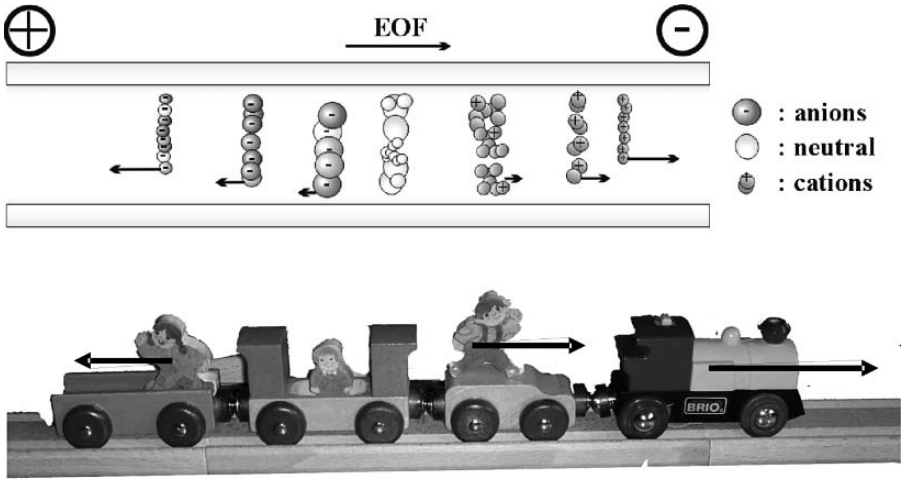


Fig. 4. Capillary zone electrophoresis standard setup. The sample is injected at the anode; the electroosmotic flow is governing a liquid flow toward the cathode; and the sample is separated based on the differences in velocities of the ions in the capillary. Comparison of the setup to a train with a given velocity in which persons are running with always the same velocity in the same direction as the train (anions), are running in the contrary direction (cations), or are sitting in the train (neutrals).

becomes independent of the used column lengths, voltages, and even buffer velocity fluctuations (EOF changes). The effective electrophoretic mobility (μ_{eff}) of the analytes is calculated by subtracting the electroosmotic flow (μ_{eof}) from the measured electrophoretic mobility (μ_{mes})—*EOF-correction*—and is used as an absolute electrophoretic value. Its value is negative in sign for anions and positive for cations:

$$\mu_{eff} = \mu_{mes} - \mu_{eof} \tag{4}$$

$$\mu_{eff} = \frac{L_d \cdot L_t \cdot (t_{eof} - t_m)}{V \cdot t_m \cdot t_{eof}} \tag{5}$$

During measurements, the detection signals (from UV/Vis, laser-induced fluorescence, mass spectrometry, etc.) are plotted against time: $signal = f(t_m)$. Transforming the data into the μ-scale does not give any loss in information because of the bit-to-bit correspondence is similar to the transformation into the 1/t domain or in infrared spectroscopy from wavelength to frequency terms ***(21)***. The input parameters for the transformation in μ_{eff}-scale are only L_d, L_t, V, and t_{eof} (the EOF-peak is determined manually after addition of mesithyl oxide) according to **eq. 5**: $signal = f(\mu_{eff})$.

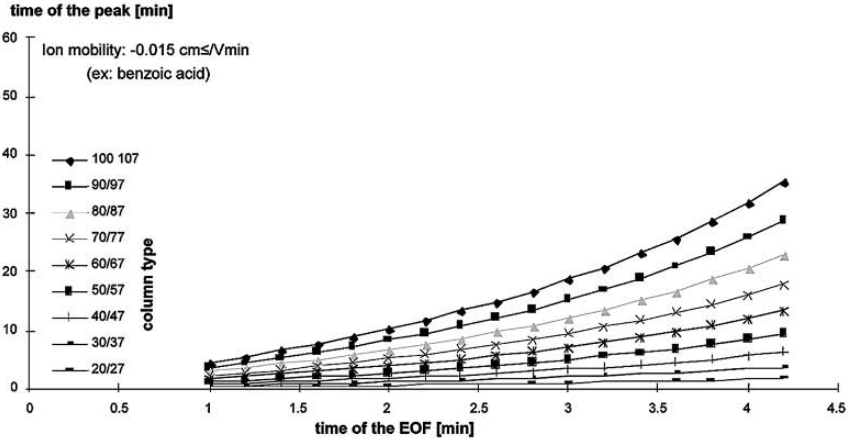
If an internal standard with known (or measurable) mobility μ_{int} (time t_{int}) is used, the transformation is similar by calculating first t_{eof} from **eq. 5** and substituting the value of t_{eof} to **eq. 5** to obtain the signal as a function of μ_{eff}. A software program was written for these two alternatives; normal spreadsheet calculation software can be used as well. Thus, one obtains **eq. 6** as:

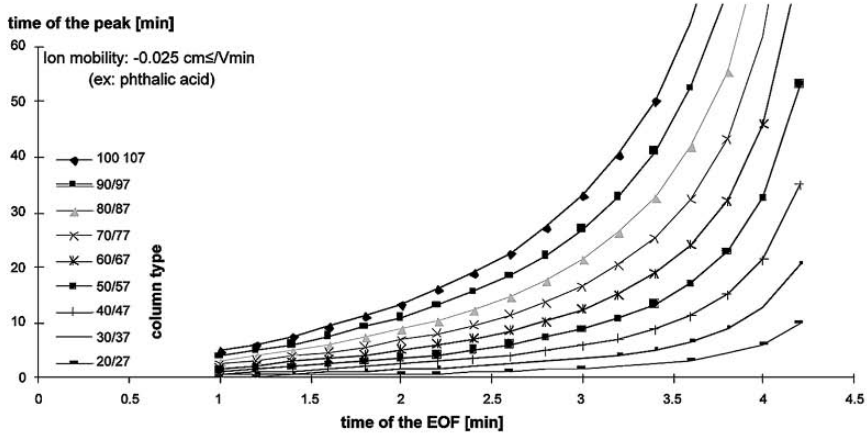
$$\mu_{eff} = \mu_{int} + \frac{L_d \cdot L_t \cdot (t_m - t_{int})}{V \cdot t_m \cdot t_{int}} \tag{6}$$

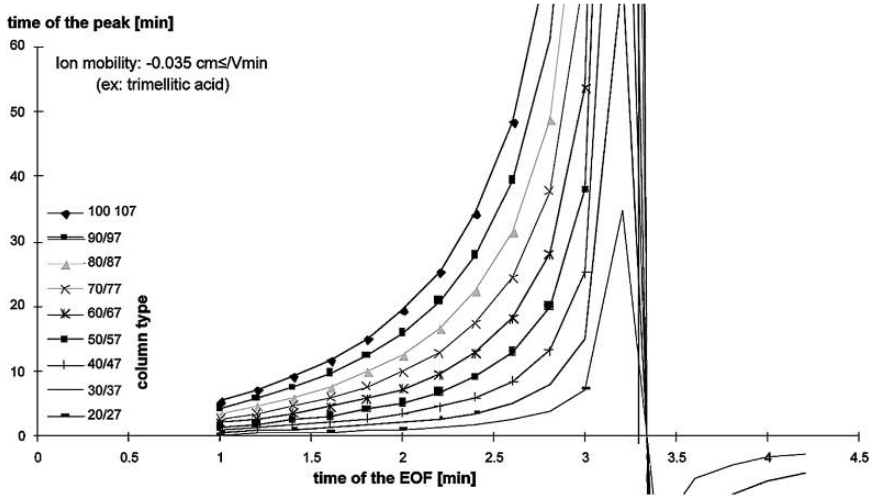
4.3. EOF-Dependent Migration Time Fluctuations

In Albert Einstein's Year 2005, no better sentence fits better with the CE mode of thinking than "*all is relative*." How explain better the need for effective mobility transformation than by: all is relative to the endoosmotic flow!

When assuming only small changes in the viscosity of the buffer (a parameter that is nearly impossible to measure systematically in the laboratory), i.e., when operating at constant temperature, **eq. 5** governs the changes of the migration time (t_m) of a component with the EOF (t_{eof}) as a function of the column lengths (L_d and L_t), the applied voltage (V) and the effective mobility (μ_{eff}) of the analyzed molecule (μ_{eff} has a constant value in the same separation buffer). Illustrated in **Fig. 5** is the relationship between these key parameters in plots of migration time (t_m) vs the time of the endoosmotic flow (t_{eof}).


time of the peak [min]
Ion mobility: -0.015 cm≤/Vmin
(ex: benzoic acid)
100 107
90/97
80/87
70/77
60/67
50/57
40/47
30/37
20/27
column type
time of the EOF [min]


time of the peak [min]
Ion mobility: -0.025 cm≤/Vmin
(ex: phthalic acid)
100 107
90/97
80/87
70/77
60/67
50/57
40/47
30/37
20/27
column type
time of the EOF [min]


time of the peak [min]
Ion mobility: -0.035 cm≤/Vmin
(ex: trimellitic acid)
100 107
90/97
80/87
70/77
60/67
50/57
40/47
30/37
20/27
column type
time of the EOF [min]

The four chosen μ_{eff} correspond to three components bearing charges of 1, 2, and 3 respectively (for example, fully ionized benzoic, phthalic, trimellitic, and pyromellitic acid in alkaline pH). Clearly, small fluctuations in the EOF from one measurement to another can have big effects on the migration time of components. For example, at 25 kV and with a 60- to 67-cm column, the change in EOF from 2.2 min to 2.6 min would induce a shift in the migration time of a highly charged molecule from 13.4 min to more than 60 min.

Molecules with lower mobility, however, would not be affected as much **(Fig. 5)**. This effect is increased for higher applied voltages and lower column lengths.

Small variations in the EOF affecting the migration time of a component (and thus the reproducibility of the observed electropherogram) may occur when analysing samples from real matrices ***(30)*** or trying to follow variations in mobility of samples by addition of some ligands in the separation buffer within affinity capillary electrophoresis (ACE) studies ***(31,32)***.

However, under identical separation buffer conditions, the effective mobility of a component is, by definition, constant and independent of any changes in EOF. As a response to this fact, we proposed a representation of the primary data in the mobility scale (μ-scale) ***(16,26,33)***. The plots of the measured signal in the 1/time domain (also possible in an online mode) have already been proposed by other authors as useful way to represent electropherograms ***(21)***. Although the difference between two peaks becomes a linear function of their difference in mobility in the 1/t domain, variations may occur when the EOF is not stable within a measurement series, so that different separation conditions (column length, voltage) cannot be compared directly.

5. Qualification and Quantification Implications

Improvements on the performance characteristics of capillary electrophoretic separations when applying μ-scale transformation according to **eq. 5** are illustrated with an example. Derivatives of benzotriazoles and benzothiazole used as corrosion inhibitors in metalworking fluid (MWF) were determined with CE under highly basic condition (25 m*M* CAPS, pH 11.75, 15% acetonitrile) ***(34)***. Because of the alkaline separation medium needed for deprotonization of the analytes, the system is sensitive to any changes in the local activity of the buffer and the silanol groups on the capillary surface. To increase the method

◀

Fig. 5. Theoretical implication on migration times by changes in electroosmotic flow times for different experimental column lengths (constant voltage separation of 25 kV) for three substances of different effective mobility (corresponding from their mobility to mono-, di-, and tricarboxylated benzenes)

robustness to the level necessary for routine application, mobility scale transformation was tested, because (1) it is easy to use, (2) it is fast, (3) no additional measurement are needed, and (4) the measurements can be compared directly even they were made on different days and different instruments, because the effective mobility is independent of the capillary length and applied voltage. An electropherogram and effective mobility scale of the five analytes is shown in **Fig. 6**. The *x*-axis of the mobility scale is minus-scaled, which shows that the analytes were separated as anions. Because the data acquisition rate is linear with time, and the mobility is a function of 1/t, an increased number of data points will be found from cations to anions in the μ-scale electropherograms. For fast-moving cations, a high data acquisition rate should thus be chosen to get good visual peak separation, quantification, and reproducibility. The transformed μ-scale can be handled in the same way as the electropherogram in terms of peak integrations. Thus, the needed qualification and quantification parameters can be easily determined, and thus the μ-scale is fitting tool for validation and routine application.

A reliable peak assignment requires a highly precise identification parameter and sharp and resolved peaks. Thus, the within-run, day-to-day and capillary-to-capillary reproducibility of migration time and effective mobility,

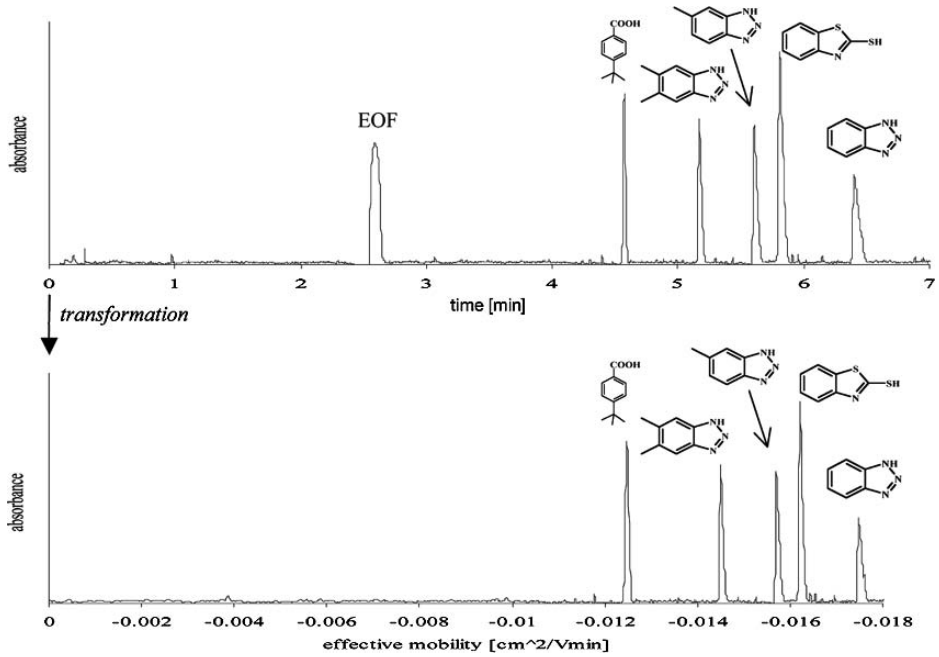
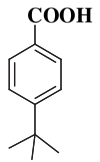
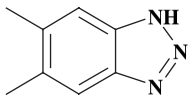
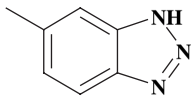
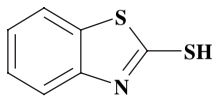
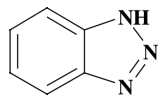


Fig. 6. Electropherogram in time and transformed μ-scale of the anionic analytes

experimental theoretical number plate, symmetry factor, and resolution were determined before and after μ-scale transformation, as shown in **Table 3**. The experimental number plates (N) decreased by more than one-third in the migration window of 2 min and was linearly dependent ($r^2 = 0.925$) on the time. The experimental number of plates increased from 77,000–289,000 in time scale to 230,000—408,000 after μ-scale transformation. Additionally, when N were determined from effective mobilities, they were independent on the migration of the analytes (no correlation was found between N and mobilities). Because the endoosmotic flow and the effective mobility of the components are the driving force in most CE separation techniques, the peak width of the analytes is migration time-dependent. Cations moving with the EOF will show sharp peaks, and anions (moving against the buffer flux in the capillary) become wider with longer migration times in the time domain. In the mobility scale, peak widths becomes very similar for all analytes, including cations to anions, showing that this distortion effect is not only due to diffusion but mainly results from the endoosmotic flow effect (the final velocity through the detection window becomes slower through the increase of the absolute effective mobility for anions). As a direct consequence of this dependency, a higher reproducibility is found after mobility scale transformation. The within-day precision of the identification was 10–15 times higher when effective mobilities were used as an identification parameter determined from μ-scale. The same phenomenon was concluded in the case of day-to-day and capillary-to-capillary precision. The day-to-day and capillary-to-capillary RSDs decreased from 5–7% to 1–2% (the RSD between capillaries have to be lower than 4–6% for fused-silica tubes with 50 μm to 250 μm ID, as described in the literature). Thus, the absolute values of the determined mobilities from one day and capillary to the other can be applied, and therefore the CE instrument and separation capillary can be effectively controlled.

The applicability of the mobility scale was also tested when a highly complex mixture was analyzed. The standard solution was spiked with MWF< which is a stable emulsion of oil and water. As shown in **Fig. 7**, systematic shifting in the migration time of the solutes was observed in the function of MWF content. It can be caused by different unpredictable factors such as small a difference in the viscosity of the injected sample or by matrices differentiating the surface of the capillary wall and thus the activity of the silanol groups, resulting in changes in the endoosmotic flow. Therefore, additional measurements or clean-up steps in the sample preparation would have to be added for reliable identification of the target compounds from real samples. When the electropherograms were transformed into μ-scale, the effective mobility became independent of the MWF content. Therefore, we can conclude that the matrices affected the EOF and not the electrophoretic mobility of the solutes directly.

Table 3
Performance Characteristics of Identification Using Time- and μ-Scale

					
Migration time [min]	4.57	5.17	5.60	5.81	6.40
μ_{eff} [$cm^2/Vmin$]	*−0.0124*	*−0.0144*	*−0.0157*	*−0.0162*	*−0.0174*
N* from time-scale	289644	176096	134367	144427	77816
N from μ-scale*	*408080*	*313269*	*333943*	*404880*	*228975*
A_S from time-scale	*1.50*	*2.22*	*2,60*	*2,60*	*5*
A_S from μ-scale	*1.44*	*2.10*	*2.46*	*2.31*	*4.78*
Resolution R_s from time-scale	9.55	5.27	2.22	5.20	
Resolution R_s from μ-scale	*13.16*	*6.85*	*2.97*	*6.57*	
run-to-run RSD from time-scale	2.77 %	3.04 %	3.37 %	3.67 %	3.77 %
run-to-run RSD from μ-scale	*0.47 %*	*0.34 %*	*0.29 %*	*0.80 %*	*0.26 %*
day-to-day RSD from time-scale	4.86 %	5.51 %	6.01 %	6.26 %	6.97 %
day-to-day RSD from from μ-scale	*0.81 %*	*0.87 %*	*0.97 %*	*0.90 %*	*1.10 %*
cap-to-cap from time-scale	5.27 %	5.34 %	6.01 %	6.32 %	6.63 %
capillary-to-capillary from μ-scale	*1.91 %*	*1.36 %*	*1.61 %*	*1.57 %*	*1.45 %*

Abbreviations: N*: apparent theoretical number plate obtained experimentally, A_S: symmetry factor, R_s: resolution RSD: relative standard deviation.

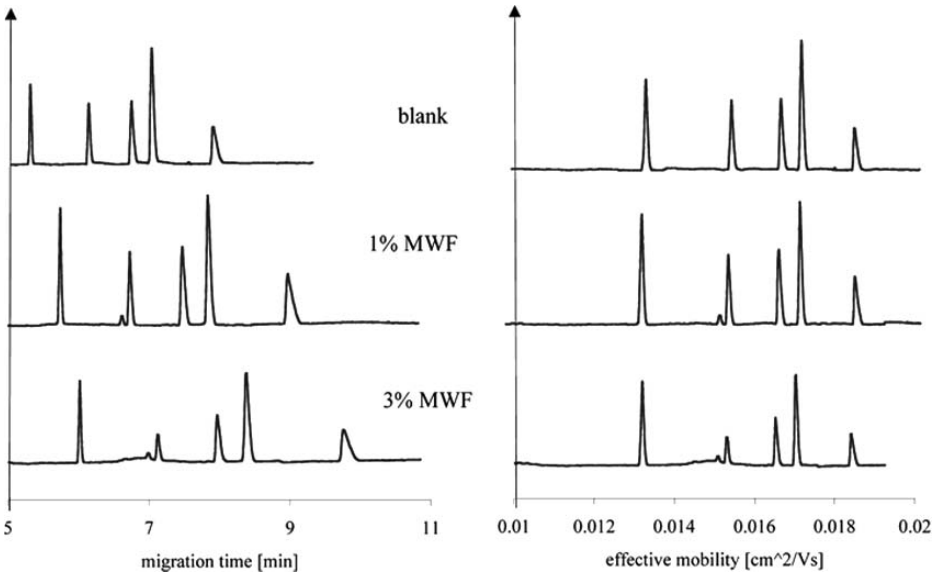


Fig. 7. Electopherogram in time and and μ-scale of spiked standard solution of MWF emulsion.

The applicability of the μ-scale was also tested and quantification was also checked through the validation. Thus, the quantification performance characteristics were also determined from the transformed scale. The precision, linearity, detection limit, and accuracy were identical as determined from the electropherogram and μ-scale, because no systematic differences between the RSDs of the peak area, the regression coefficient, the limit of detection, and the recoveries were observed. A significant difference in the slope of the calibration curve was determined as shown in **Fig. 8** when taking the areas calculated from time scale. To explain this phenomenon, the absorption coefficient of the benzotriazole derivatives was determined in the separation electrolyte with a UV spectrophotometer, because the absorbance depends on the length of the light and absorption coefficient concentration, and only this parameter has influence on the slope of the calibration curve. Because the coefficient values were similar, the differences in the slope values determined from electropherogram can be caused by the differences in the time the plug took to migrate through the detection window. This difference is eliminated by the mobility scale transformation; therefore, the slopes of the benzotriazole derivatives became similar when determined from μ-scale. The μ-scale therefore can be used not only for identification but for quantification without any restrictions.

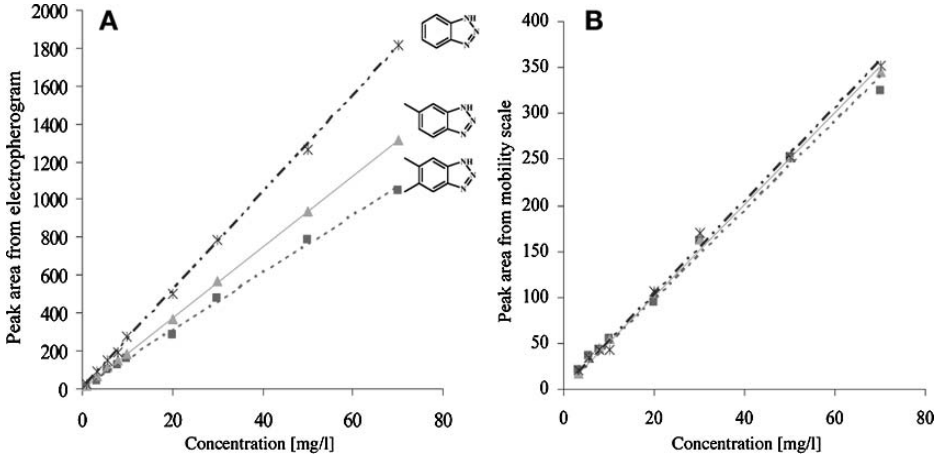


Fig. 8. Calibration curves determined from electropherograms in **(A)** time and **(B)** μ-scale.

Concluding Remarks on Mobility Transformations

For possible routine analysis, CE techniques must give comparable qualitative and quantitative results from run-to-run and day-to-day measurements. Modern technology allows these goals to be reached by new instrumentation. However, for electrophoretic separations where the migration time of an analyte are directly related to the EOF (as affected by the matrice), "*chromatographic mode of thinking*" and data processing must be re-adapted. Representing electropherograms in the μ-scale brings both qualitative and quantitative advantages. Conversion of the primary time-scaled data to the mobility scale (μ-scale) leads to a better interpretation of electropherograms in terms of separation processes. The benefits include better direct comparison of electropherograms and an easier "peak tracking" when trying to identify single components with complex matrices, especially when the UV-visible signatures of the components are also available. Peak integration also is often more precise when done in μ-scale as compared to the time, especially when wide ranges of concentration and voltage are involved. The data can be treated in the same way when comparing measurements made with columns of different lengths or upscaling methods from one instrument to the other. Furthermore, this data presentation was proven to be necessary when describing the distribution of effective mobility for polydisperse samples such as charged synthetic polymers and NOM. This transformation is also applicable to other CE techniques where changes in the EOF can alter the stability of migration times, such as capillary gel electrophoresis, micellar electrokinetic chromatography, and ACE.

It is certainly unusual for *chromatography-mode thinkers* to make the transformation from the time-scale to the μ-scale, but this shift is probably "trivial" for *CE-mode thinkers* who are used to inducing differences in the velocities of the molecules that they want to separate. The fact is that software designed to process electrophoretically based CE data is needed.

References

1. Jorgenson, J. W. and Lukacs, K. D. (1981) Zone electrophoresis in open-tubular glass capillaries. *Anal. Chem*. **53,** 1298–1302.
2. Jorgenson, J. W. and Lukacs, K. D. (1983) Capillary zone electrophoresis. *Science* **222,** 266–272.
3. Shintani, H. and Polonski, J. (1996) *Handbook of Capillary Electrophoresis Applications*. Blackie Academic & Professional, London.
4. Rhighetti, P. G. (1996) *Capillary Electrophoresis in Analytical Biotechnology*. CRC Press, Boca Raton.
5. Li, S. F. Y., (1993) Capillary electrophoresis. principles, practice and applications. *J. Chromatogr. Library* **52,** 582.
6. Kuhn, R., and Hoffstetter-Kuhn, S. (1993) *Capillary Electrophoresis: Principles and Practise*. Springer-Verlag, Berlin Heidelberg.
7. Khaledi, M. G. (1998) *High-performance Capillary Electrophoresis: Theory Techniques, and Applications*. John Wiley & Sons, Chichester: p. 1050,
8. Guzman, N. A. (1993) *Capillary Electrophoresis Technolog*y. Marcel Decker Inc., New York: p. 857.
9. Baker, D. R. (1995) *Capillary Electrophoresis*. John Wiley & Sons, New York: p. 244
10. Chankvetadze, B. (1997) *Capillary Electrophoresis in Chiral Analysis*. John Wiley & Sons, Chichester: p. 555.
11. Deyl, Z., Miksik, I., Tagliaro, F., and Tesarova, E. (1998) Advanced chromatographic and electromigration methods in bioSciences. *J. Chromatogr. Library* 60.
12. Whatley, H. (1999) Making CE work - points to consider. *LC - GC Europe***12,** 762–766.
13. Shihabi, Z. K. and Hinsdale, M. (1995) Some variable affecting reproducibility in capillary electrophoresis. *Electrophoresis* **16,** 2159–2163.
14. Chapman, J. and Hobbs, J. (1999) Putting capillary electrophoresis to work. *LC - GC Europe* **12,** 266–279.
15. Faler, T. and Engelhardt, H. (1999) How to achieve higher repeatability and reproducibility in capillary electrophoresis. *J. Chromatogr. A* **853,** 83–94.
16. Schmitt-Kopplin, P., Fischer, K., Freitag, D., and Kettrup, A. (1998) Capillary electrophoresis for the simultaneous separation of selected carboxylated carbohydrates and their related 1,4-lactons. *J. Chromatogr. A*. **807,** 89–100.
17. Hudson, J. C., Malcom, M. J., and Golin, M. (1998) Advancements in forensic toxicology. *Pace Setter Beckman Coulter,* **2**, 1–5.

18. Hudson, J. C., Golin, M., and Malcom, M. (1995) Capillary zone electrophoresis in a comprehensive screen for basic drugs in whole blood. *Canadian Society of Forensic Science* **28,** 153–164.
19. Hudson, J. C., Golin, M., Malcom, M., and Whiting, C. F. (1998) Capillary zone electrophoresis in a comprehensive screen for drugs of forensic interest in whole blood: an update. *Canadian Society of Forensic Science* **31,** 1–29.
20. Iwata, T., Koshoubu, J., and Kurosu, Y. (1998) Electropherograms in capillary zone electrophoresis plotted as a function of the quantity of electric charge. *J. Chromatogr. A*. **810,** 183–191.
21. Mammen, M., Colton, I. J., Carbeck, J. D., Bradley, R., and Whitesides, G. M. (1997) Representing primary electrophoretic data in the 1/time domain: comparison to representations in the time domain. *Anal. Chem*. **69,** 2165–2170.
22. Lee, T. T. and Yeung, E. S. (1991) Facilitating data transfer and improving precision in capillary zone electrophoresis with migration indices. *Anal. Chem*. **63,** 2842–2848.
23. Yang, J., Bose, S., and Hage, D. S. (1996) Improved reproducibility in capillary electrophoresis through the use of mobility and migration time ratios. *J. Chromatogr. A*. **735,** 209–220.
24. Kenndler, E. (1996) Effect of electroosmotic flow on selectivity, effiency and resolution in capillary zone electrophoresis expressed by the dimensionless reduced mobility. *J. Capillary Electrophor*. **3,** 191–198.
25. Kenndler, E. (1998) Dependence of analyte separation on electroosmotic flow in capillary zone electrophoresis: quantitative description by the reduced mobility. *J. Microcolumn Sep*. **10(3),** 273–279.
26. Schmitt-Kopplin, P., Garmash, A. V., Kudryavtsev, A. V., Perminova, I. V., Hertkorn, N., Freitag, D., and Kettrup, A. (1999) Mobility distribution description of synthetic and natural polyelectrolytes with capillary zone electrophoresis. *J. AOAC Int*. **82,** 1594–1603.
27. Schmitt-Kopplin, P., Menzinger, F., Freitag, D., and Kettrup, A. (2001) Improving the use of CE in a chromatographer's world. *LC-GC Europe* **14,** 284–388.
28. Schmitt-Kopplin, P., Garmash, A. V., Kudryavtsev, A. V., et al. (2001) Quantitative and qualitative precision improvements by effective mobility-scale data transformation in capillary electrophoresis analysis. *Electrophoresis* **22,** 77–87.
29. Whatley, H. (1997) Mobility determinations in capillary electrophoresis. *Technical Information Beckman*.
30. Garrison, A. W., Schmitt, P., Martens, D., and Kettrup, A. (1996) Enantiomeric selectivity in the environmental degradation of Dichlorprop as determined by high performance capillary electrophoresis. *Environ. Sci. Technol*. **30,** 2449–2455.
31. Schmitt-Kopplin, P., Burhenne, J., Freitag, D., Spiteller, M., and Kettrup, A. (1999) Developement of capillary electrophoresis methods for the analysis of fluoroquinolones and applications to the study of the influence of humic substances on their photodegradation in aqueous phase. *J. Chromatogr. A*. **837,** 253–265.
32. Schmitt, P., Trapp, I., Garrison, A. W., Freitag, D., and Kettrup, A. (1997) Binding of s-triazines to dissolved humic substances: electrophoretic approaches using

affinity capillary electrophoresis (ACE) and micellar electrokinetic chromatography (MEKC). *Chemosphere* **35,** 55–75.
33. Schmitt-Kopplin, P., Garrison, A. W., Perdue, E. M., Freitag, D., and Kettrup, A. (1998) Capillary electrophoresis in humic substances analysis, facts and artifacts. *J. Chromatogr. A*. **807,** 101–109.
34. Breuer, D., Fischer, K., Hansen, K., Fekete, A., Lahaniatis, M., and Ph., S.-K. (2003) "Benzotriazole (1,2,3-Benzotriazole, 5-Methyl-1H-benzotriazole, 5,6-Dimethylbenzotriazole)." Analytische Methoden Band 1″, Deutschen Forschungsgemeinschaft, Senatskommosion zur Prüfung gesundheitsschädlicher Arbeitsstoffe-Arbeitsgruppe "Analytische Chemie" 13 (A. Kettrup, ed.).

25

Adsorbed Cationic Polymer Coatings for Enhanced Capillary Electrophoresis/Mass Spectrometry of Proteins

Sara Ullsten, Aida Zuberovic, and Jonas Bergquist

Summary

The combination of capillary electrophoresis (CE) with mass spectrometry (MS) constitutes a powerful microanalytical system for the analysis of biological samples. The anionic and hydrophobic surface of the fused-silica capillary is, however, known to cause severe analyte–wall interactions in protein analysis. In order to control surface properties and eliminate protein adsorption, a capillary coating can be applied. A fast and simple strategy is to coat the anionic capillary with a cationic polymer via multisite electrostatic interaction. This generates a stable deactivation layer, without the need for addition of coating agent to the background electrolyte solution.

This chapter reviews the present knowledge of capillary coatings and especially cationic polymers in CE-MS, and describes the synthesis of a cationic polymer, PolyE-323, for deactivation of fused-silica capillaries. The capillary coating procedure is a simple three-step rinsing protocol comprising deprotonation of surface silanol groups using a base, adsorption of polymer, and a final rinse to remove excess polymer not adsorbed to the surface. As a result of the simplicity of the coating procedure, highly reproducible coatings can be prepared with little or no expert skills. Some practical aspects on using cationic-coated capillaries in CE-MS protein analysis are also discussed.

Key Words: Capillary electrophoresis; mass spectrometry; cationic coating; proteins; surface properties

1. Introduction

The interest in characterizing the human proteome has in recent years created a growing demand in biology and medicine for sensitive and informative methods for protein identification and characterisation. An attractive approach

From: *Methods in Molecular Biology, vol. 384: Capillary Electrophoresis*
Edited by: P. Schmitt-Kopplin © Humana Press Inc., Totowa, NJ

to meet these needs is development of analysis systems combining high-efficiency separations with mass spectrometry (MS). This has increased the interest in capillary electrophoresis (CE) as a protein separation tool. Compared to two-dimensional (2D)-polyacrylamide gel electrophoresis (PAGE), CE allows the use of small sample volumes and offers fast separations, quantitation ability, and instrumentation that is easy to automate. The capability for online mass spectrometric detection provides high sensitivity and, equally importantly, a tool for protein identification and structure elucidation.

The implementation of CE as a routine protein analysis technique has, however, been obstructed as a result of the anionic and hydrophobic nature of the fused-silica capillary surface, which has long been known to present a problem. Adsorption of protein, either irreversibly or with slow desorption, causes bad reproducibility and impaired efficiencies. Although cationic proteins present the greatest problem because of electrostatic analyte–wall interactions, any protein having a region of net positive charge or an external hydrophobic domain (i.e., almost all known proteins) can be adsorbed to the silica surface.

Over the years, a number of approaches have been explored to eliminate the detrimental analyte–wall interactions caused by the fused-silica capillary surface. When using mass spectrometric detection with electrospray ionization (ESI), surface deactivation strategies based on modification of the background electrolyte by using high salt concentration ***(1)*** or unvolatile additives (such as amines ***(2)*** or zwitterions ***(3)***), are not recommended because of the risk of signal suppression and contamination of the mass spectrometer, respectively, which may deteriorate the MS response. Further, strategies based on the use of extreme pH buffers are not advisable because of the risk of protein denaturation. The need for capillary surface coatings for elimination of protein adsorption has thus been recognized for many years. Although a wide range of capillary coatings have been described in the literature, there are few coatings in routine use. Partly, this is because the general CE practitioner experiences many coating procedures that are elaborate, with a large batch-to-batch variability and a limited stability of the generated surface. Further, coated capillaries that are commercially available are expensive, and details of the surface chemistry are often not given. There is thus a need for stable coatings that can be prepared with little or no expertise in a highly reproducible way.

When chemically modifying the capillary surface, the two main routes are to utilize the surface silanol groups for covalent bonding or electrostatic interaction. By using the covalent route, a variety of both neutral and charged capillary coatings have been developed ***(4–6)***. One of the most commonly used cationic coatings is 3-aminopropyltriethoxysilane (APS) ***(7)***, depicted in **Fig. 1A**. It is a monomeric coating prepared by covalent binding of the silane to the surface silanols through one or more siloxane (Si-O-Si) bonds. Although

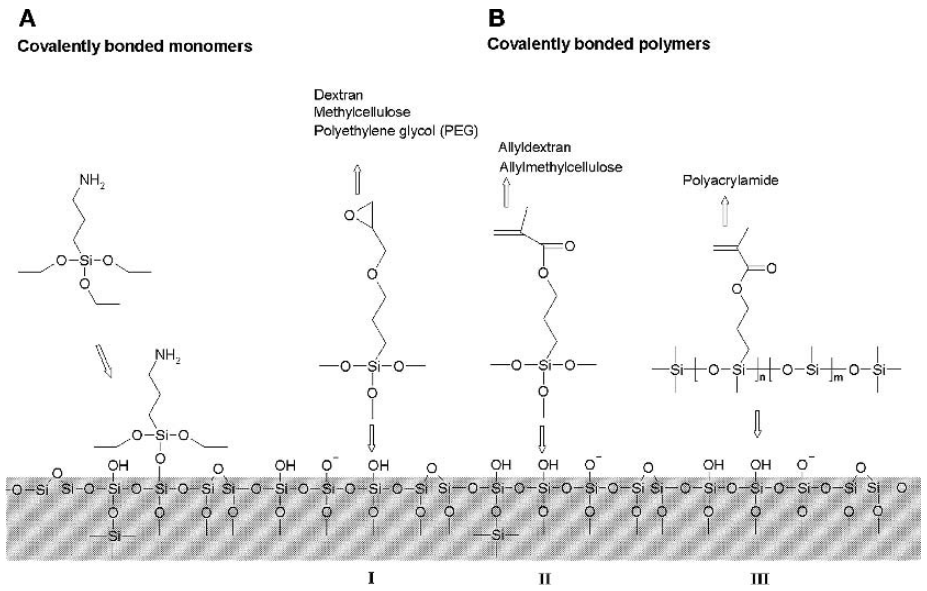


Fig. 1. **(A)** Silanization of the fused-silica capillary wall using APS. **(BI)** Silanization using γ-glycidoxypropyltrimethoxysilane. The reactive expoxy group provides a reaction site for covalent binding of a polymeric top layer. **(BII)** Silanization using γ-methacryloxypropyltrimethoxysilane. The reactive allyl group provides a reaction site for covalent binding of a polymeric top layer. **(BIII)** Covalent binding of polymeric siloxane through a silicon hydride dehydrocondensation reaction. The methacrylic substituents provide reaction sites for covalent binding of a polymeric top layer.

highly stable surfaces can be produced by silanization, monomers often fail to provide complete coverage of a silica surface as a result of steric effects during reaction. This is especially problematic when bulky silanes are used.

Polymeric coatings, on the other hand, have a better surface coverage, but the coating procedures used are often elaborate and time-consuming multi-step processes. One of the most common strategies is to use a bifunctional silane, such as γ-glycidoxypropyltrimethoxysilane **(Fig. 1B[I])** or γ-methacryloxypropyltrimethoxysilane **(Fig. 1B[II])**, as a subcoating. The bifunctional reagent works as an anchor, where the silane is bonded to the surface silanols in one end whereas reactive epoxy or allyl groups are exposed in the other end, and can be used for subsequent attachment of a hydrophilic polymer layer, such as polyacrylamide ***(8)***. Using highly crosslinked siloxane resins as subcoatings increases the shielding of the surface silanol groups more than silanization, ***(9)***. These resins can be prepared by covalently binding a

polymeric siloxane containing methacrylic substituents to the capillary surface through a silicon hydride dehydrocondensation reaction (**Fig. 1B[III]**). As a result of the methacrylic groups of the resin, the subcoating provides reaction sites for covalent binding of a polymeric top layer.

When utilizing the electrostatic route, the coating mechanism is based on multisite electrostatic interaction between a polycationic polymer and the anionic capillary surface. This generates a stable deactivation layer without the need to add coating agent to the background electrolyte solution. Electrostatically adsorbed coatings are prepared by a general and simple rinsing protocol comprising (1) a base to deprotonate surface silanol groups, (2) polymer solution, and (3) buffer to remove excess polymer not adsorbed to the surface. Because of the simplicity of the coating procedure, highly reproducible coatings can be prepared with little or no expertise.

To date, a broad range of cationic polymers have been used for deactivation of fused-silica surfaces by electrostatic binding. Demonstrated examples include polyethyleneimine (PEI) ***(10,11)***, polybrene ***(12,13)***, poly (diallyldimethylammonium chloride) (PDADMAC) ***(14,15)***, polyarginine ***(16)***, chitosan ***(17,18)***, pyrrolidone-containing copolymers ***(19)***, and ammonium substituted agarose ***(20)***. Demonstrated application areas of the coated capillaries are separation of basic proteins, determination of protein p*I* ***(21)***, glycoprotein analysis ***(22–25)***, peptide sequencing ***(26)***, and biofluid protein analysis ***(27–30)***. As shown in **Fig. 2**, the polymers differ widely in structure regarding, e.g., carbon chain length, functional groups, degree of branching, and class of amine. Consequently, the polymers have different properties (e.g., pK_a, flexibility, hydrophobicity/hydrophilicity), which will be reflected in the generated surfaces. By selecting the proper coating polymer, the properties of the capillary surface, such as magnitude and pH dependency of the generated electroosmotic flow (EOF), can be tailored. The ability to control EOF is of prime importance, and cationic coatings have been used for directing both the EOF and the analyte mobility toward the mass spectrometer ***(31)***. Another way of tailoring the coating properties is to use a polymer mix as coating agent. This approach is commonly used for polybrene to increase the coating hydrophilicity by mixing with ethylene glycol ***(22,23)***.

Physically adsorbed coatings can be prepared favorably in a sandwich fashion ***(28,32–34)*** to form a polyelectrolyte multilayer (PEM). By utilizing electrostatic binding, an anionic polymer (often containing sulphate groups) is used as intermediate layer in between a top and a bottom layer of a cationic polymer. Consequently, by utilizing electrostatic binding, the charge of the capillary coating (positive/negative) can easily be controlled and is dependent on the number of polymer rinses applied.

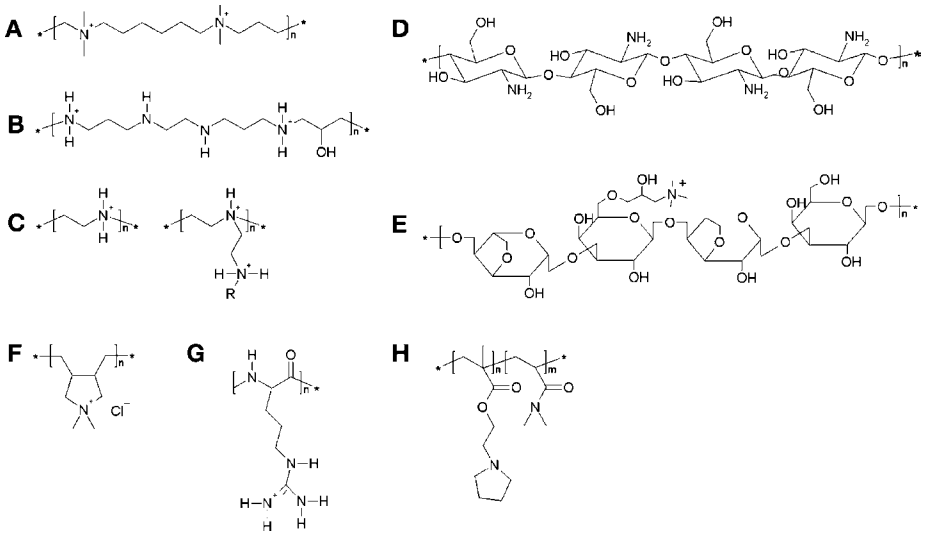


Fig. 2. Schematic structures of the cationic polymers **(A)** polybrene, **(B)** PolyE-323, **(C)** PEI, **(D)** chitosan, **(E)** Q-agarose, **(F)** PDADMAC, **(G)** Polyarginine, and **(H)** DMA-EpyM.

The need to deactivate coatings in order to eliminate the detrimental influence of surface groups on the separation performance is not restricted to separations in the capillary format. Developments in chip technology have further increased the interest in tailor-made surface coatings. When a separation system is minaturized, the surface-to-volume ratio increases, which emphasizes the importance of controlling surface properties. Because of the short lifetime of a disposable chip, coatings prepared by fast and simple procedures are desirable, which makes development of electrostatically bonded coatings particularly interesting. The chemical functionalities of plastic surfaces differ, however, from those of glass. It is therefore attractive to use electrostatically bonded coatings, because these can be applied to all materials containing anionic surface sites. Electrostatic bonding of polyelectrolyte multilayers has been demonstrated for polystyrene and acrylic microfluidic devices ***(35***,***36)*** as well as for chips of PDMS ***(37)***.

In this chapter, a protocol for deactivation of fused-silica capillaries using the cationic polymer, PolyE-323, developed in our research group ***(30***,***38***,***39)***, is described. The protocol is divided into three parts describing (1) synthesis of the polymer, (2) the capillary coating protocol, and (3) some considerations regarding using the coated capillaries in CE-MS protein analysis.

2. Materials

2.1. Polymer Synthesis

1. 1,2-bis(3-aminopropylamino)-ethane (CAS Number [10563-26-5]) of practical grade (LabKemi, Stockholm, Sweden). This is a toxic, corrosive substance, which may cause heritable genetic damage; care should be taken to avoid exposure. It should be stored well capped in a cool and dry place.
2. Epichlorohydrine of puriss grade (Fluka Chemie GmbH, Buchs, Switzerland). This is a toxic substance, which may cause cancer. Care should be taken to avoid exposure as well as special risks to health and the environment. It should be stored, well capped, far from heat, spark, and fire.

2.2. Capillary Coating Protocol

1. 1 *M* sodium hydroxide solution for activation of the fused-silica capillary wall.
2. 1 *M* acetic acid for pH adjustment of the polymer solution.
3. PolyE-323, synthesized according to the procedure described under **Subheading 3.1.** Store PolyE-323 at 8 °C in darkness.

2.3. CE-ESI-MS

The selection of background electrolyte (e.g., pH and amount of organic modifier) is dependent on both analyte properties and instrumentation used (*see* **Subheading 3.3.** for further details). In our laboratory, the CE-ESI-MS experiments were conducted using a home-built capillary electrophoresis instrument interfaced to a time-of-flight mass spectrometer, using a sheath-flow electrospray interface. Both acidic and basic proteins were separated using:

1. Separation solution: 10 m*M* acetic acid.
2. Sheath-flow solution: 10 m*M* acetic acid in 80 % methanol (p.a. grade, Sigma-Aldrich Chemie GmbH, Steinheim, Germany).

3. Methods

3.1. Polymer Synthesis

1. Mix 17.65 g (0.10 mol) 1,2-bis(3-aminopropylamino)-ethane with 20 g water in a 250-mL Erlenmeyer flask. Place the flask in an ice bath and add 9.3 g (0.10 mol) epichlorohydrine dropwise during intensive magnetic stirring (*see* **Notes 1** and **2**).
2. Seal the flask and continuously stir the mixture at room temperature for 48 h while the reaction mixture is thickened (*see* **Note 3**).
3. Add 100 g water during stirring (*see* **Note 4**).
4. Let the equilibration reaction continue for 1 wk. Stir occasionally (*see* **Note 5** and **Fig. 3**).
5. After synthesis, store the polymer solution in darkness at 8 °C (*see* **Note 6**).



Fig. 3. PolyE-323 polymer synthesis scheme. The polymer is schematically depicted and the charge of the polymer is dependent on pH. PolyE-323 has a low degree of branching, which is not indicated in the schematic structure.

3.2. Capillary Coating Protocol

1. Rinse the fused-silica capillary (e.g., 50 μm inner diameter [i.d.], 35–50 cm length) with 1 *M* NaOH at 950 mbar for 30 min to deprotonate the silanol groups on the capillary surface (*see* **Note 7** and **Fig. 4**).
2. Rinse the capillary with water at 950 mbar for 5 min in order to remove the sodium hydroxide solution.
3. Rinse the capillary at 950 mbar for 10 min with a 7.5 % (w/w) solution of PolyE-323 adjusted to pH 7.0. The polymer solution is prepared by mixing 200 μL PolyE-323 (19% w/w, synthesized as described under **Subheading 3.1.**) with 160 μL 1 *M* acetic acid and 140 μL water (*see* **Notes 8** and**9** and **Fig. 5**).
4. Rinse the capillary with background electrolyte (*see* **Notes 10** and **11**).

3.3. CE-ESI-MS

The methods used during CE-ESI-MS are dependent on the instrumental setup, e.g., type of CE instrument, mass spectrometer, and electrospray interface. Some general aspects to consider will thus be discussed first.

Capillaries coated with PolyE-323 can be used in combination with both the sheath-flow and the sheathless electrospray ionization interface, which

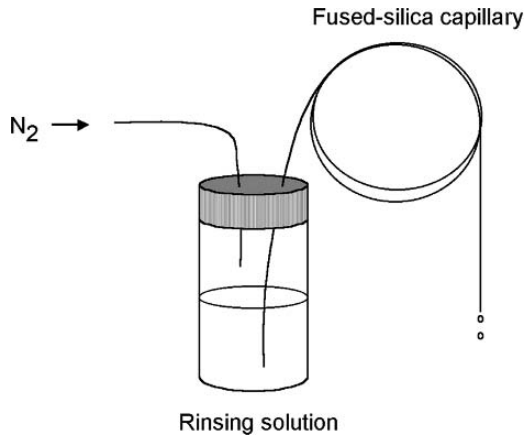


Fig. 4. Schematic experimental setup for manual coating of fused-silica capillaries.

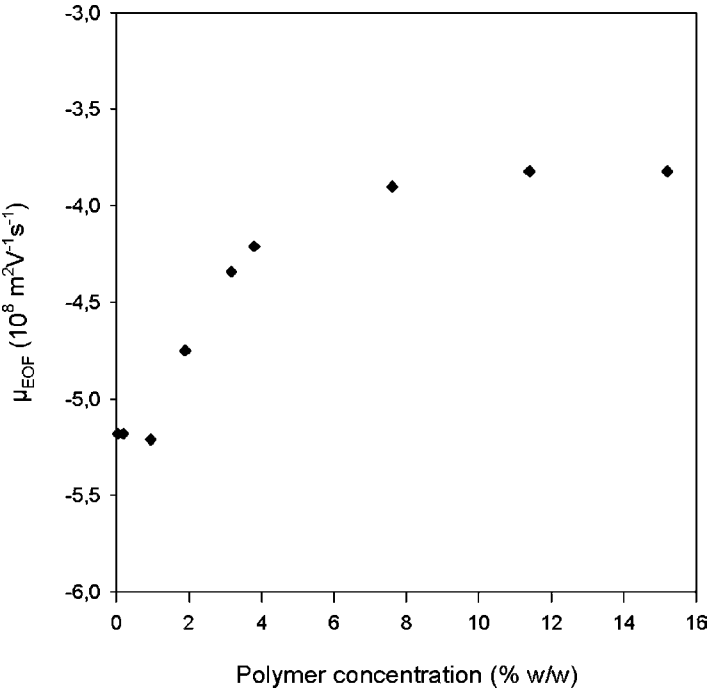


Fig. 5. Electroosmotic flow as a function of PolyE-323 concentration in the coating solution. Conditions: capillary of 50 μm i.d., 365 μm o.d., total length 33.5 cm and 25 cm to the detection window. Injection of water at 50 mbar for 5 sec. Applied negative voltage of 450 V/cm. Detection at 190 nm. Background electrolyte of 50 m*M* ammonium acetate, pH 5.

are the two most commonly used configurations. The type of interface used will, however, affect the selection of background electrolyte for the separation system. The spray formation in the sheathless interface is solely dependent on the capillary effluent, in contrast to the sheath-flow interface, where a coaxial flow is added postcolumn to aid in the spray formation. Consequently, a background electrolyte containing an organic modifier must be used in combination with the sheathless ESI interface in order to increase the volatility of the eluent and thereby enhance spray formation. PolyE-323-coated capillaries have been demonstrated as being compatible with both acetonitrile and methanol, which are commonly used modifiers ***(31)***. This strategy can, preferentially, be used in peptide analysis. Proteins are, however, sensitive to large amounts of organic solvents, which can cause denaturation or even precipitation. By using an electrospray interface of sheath-flow configuration, the organic solvent

needed for stable electrospray formation is added post-column, which reduces the risk of protein precipitation during analysis.

The next parameter to consider is selection of pH of the background electrolyte. Capillaries coated with PolyE-323 have been demonstrated to be stable over the entire range of pH 2.0–11.0, which gives a high degree of freedom. Albeit, acidic background electrolytes can be recommended for two reasons. First, when using MS instruments, such as quadrupole mass analyzers, with a limited mass range of typically m/z 2500, acidic buffers are commonly required during separation in order to create multiply charged species of the proteins that fit in the m/z window. Second, an acidic background electrolyte reduces adsorption of acidic proteins at pH <pI as a result of electrostatic repulsion between the proteins and the cationic coating. This effect is illustrated in **Fig. 6**, where a set of model proteins, differing in p*I* and M_r as listed in **Table 1**, was analyzed on a PolyE-323 coated capillary at different pH. Electrostatic forces play a key role in protein adsorption and a correlation between protein pI and adsorption can be seen in **Fig. 6**. At neutral pH, basic proteins show high performance as a result of electrostatic repulsion from the cationic coating, whereas acidic proteins are adsorbed as a result

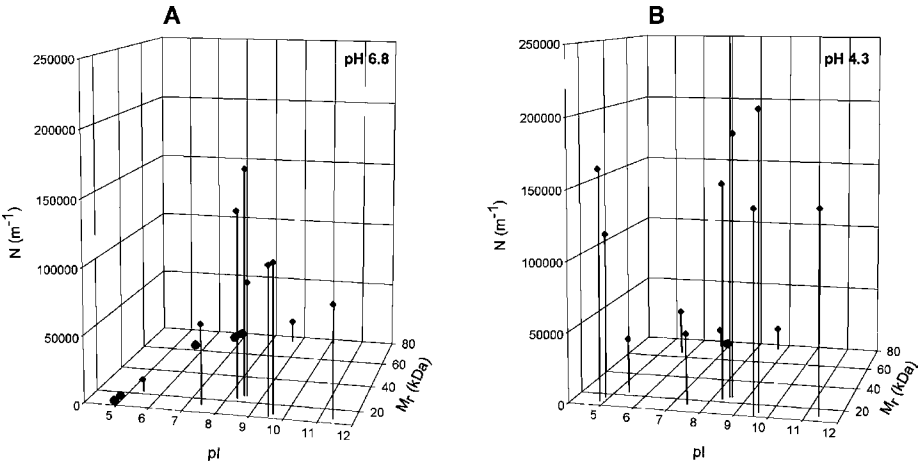


Fig. 6. Model proteins (identities given in **Table 1**) analyzed on a PolyE-323-coated capillary at **(A)** pH 6.8 and **(B)** pH 4.3. Solid circles, proteins eluting; open circles, proteins irreversibly adsorbed. Conditions: protein concentration of 0.17 mg/mL, applied voltage of 15 kV, capillary (50 μm i.d. and 365 μm o.d.) of 33.5 cm total length and 25 cm to detection window, UV detection at 190 nm and 214 nm, pressure injection at 50 mbar for 5 s (corresponding to approx 13 nL), background electrolyte of **(A)** 50 m*M* Tris/HCl pH 6.8 and **(B)** 50 m*M* ammonium acetate, pH 4.3.

Table 1
Isoelectric Point (p*I*) and Molecular Weight (M_r) of the Proteins Analyzed in Fig. 6

Protein	p*I*	M_r (kDa)
α-Lactalbumin	4.8	14
β-Lactoglobulin A	4.8	18
Lentil lectin	5.4	23
Bovine serum albumin	5.6	66
Ovotransferrin	6.7	76
Alcohol dehydrogenase	6.8	80
Myoglobin	7.4	17
Trypsin	8.3	23
Elastase	8.4	26
α-Chymotrypsinogen A	8.5	26
Lactofrrin	8.7	76
Cytochrome c	9.5	12
Ribonuclease A	9.6	14
Lysozyme	11.4	14

of electrostatic attraction **(Fig. 6A)**. By lowering the pH of the background electrolyte solution, the separation performance of acidic proteins is improved as a result of protein charge reversal at pH <pI **(Fig. 6B)**. It is also evident from **Fig. 6** that protein adsorption is strongly influenced by molecular weight, where small proteins show higher performance compared to large ones. This is in accordance with findings reported by Córdova et al ***(13)***. The explanation for the greater tendency toward adsorption for larger proteins is, however, still unclear, but may be due to a larger number of surface sites and a larger contact surface area.

Another aspect to consider is selection of buffer ions in the background electrolyte. Separation buffers traditionally not used in combination with MS detection, such as phosphate, are today increasingly explored in CE-MS because of the development of new electrospray interfaces with a higher tolerance toward unvolatile eluents, and by the development of new ionisation techniques, such as atmospheric pressure photo ionization (APPI). Background electrolytes composed of anionic buffering ions (especially of high valence) are, however, not compatible with cationic-coated capillaries as a result of electrostatic interactions between the coating and the buffer ions. This causes an irreproducible EOF, and the effect is increased with an increased valence of the anion (e.g., $PO_4^{3-} > HPO_4^{2-}$). It is thus recommended that cationic buffering ions or anions of low valence, such as ammonium salts of formate and acetate,

be used. When ultraviolet detection is used, the cationic (but unvolatile) buffer Tris is an excellent choice.

In our laboratory, the CE-ESI-MS experiments were conducted using a home-built CE instrument (high-voltage power supply from Spellman, model SL80PN10/LR/230, Hauppauge, NY, with a platinum electrode placed in a vial for the background electrolyte solution) and a Jaguar orthogonal time-of-flight instrument (Leco, St. Joseph, MI). An x, y, z-micromanipulator (Protana, Odense, Denmark) was used to house a sheath-flow interface in which the CE capillary (50 μm i.d. 185 μm outer diameter [o.d.]) was threaded through a metal tee and centered in a stainless steel capillary. Make-up liquid was delivered by a Harvard 22 syringe pump (Harvard Apparatus, Saint-Laurent, Canada).

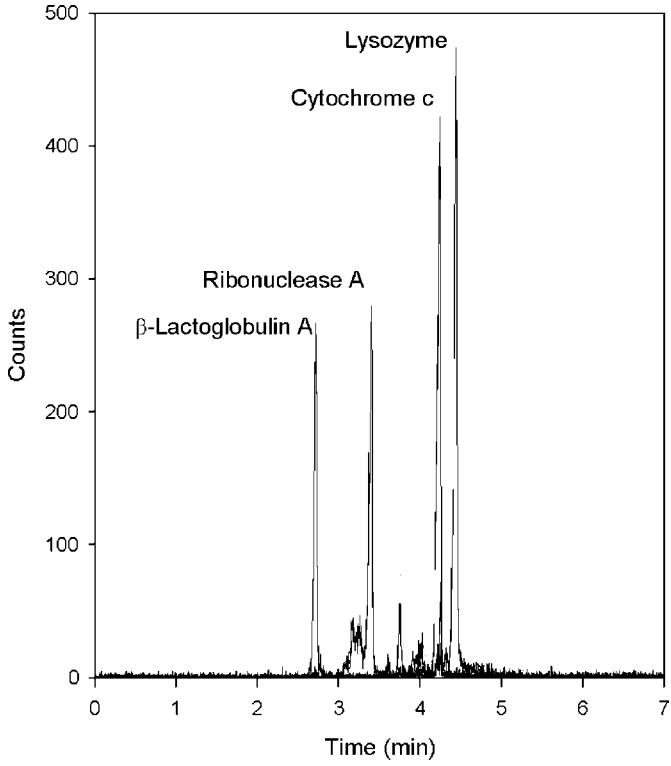


Fig. 7. CE separation of proteins on a PolyE-323 coated capillary using sheath-flow ESI-MS. Conditions: PolyE-323 coated capillary of 50 μm i.d., 185 μm o.d. of total length 40 cm. Hydrodynamic injection of an approx 10 μ*M* protein mixture at 10 cm for 5 s (corresponding to approx 2 nL). Applied negative CE voltage of 500 Vcm^{-1} and positive ESI voltage of 3.9 kV. BGE of 10 m*M* acetic acid and sheath liquid composed of 10 m*M* acetic acid in 80% methanol.

Typical values used during analysis were: negative CE voltage of $-500\,\mathrm{Vcm^{-1}}$, positive ESI voltage of +3.5–4.0 kV, sheath-flow of 1 μL/min, and 7 nL injection of a 10 μ*M* protein sample prepared in water. No conditioning of the capillary was perfored between runs. (*see* **Note 12**). An example of a separation using PolyE-323 coated capillaries is shown in **Fig. 7**.

4. Notes

1. The water used should have a resistivity of 18.2 MΩ-cm and total organic content of less than five parts per billion. This standard is referred to as "water" throughout the text.
2. Heat is produced during the reaction and the size of the synthesis batch is limited by the ability to effectively cool the reaction mixture. If the mixture is not sufficiently cooled, side reactions can take place.
3. The flask is sealed to prevent absorption of carbon dioxide, which might disturb the reaction.
4. After 48 h, the reaction mixture is thickened. Water is added to decrease the viscosity of the solution during the final, slow reaction of epichlorohydrine. If the reagents are very fresh, the initial rate of reaction might be higher and the water can, in that case, be added in less than 48 h as a result of the fast thickening of the reaction mixture.
5. The polymer synthesis is an addition reaction where the ring tension of epichlorohydrine drives the reaction. The synthesis generates a viscous, light yellow, alkaline solution with a polymer concentration of 19 % (w/w), given by the polymer synthesis stoicheometry, schematically depicted in **Fig. 3**.
6. The polymer is sensitive to light and oxygen and the solution turns from light yellow to dark yellow/brown upon storage in light and at room temperature, which should be avoided.
7. The coating protocol consists of four simple rinsing steps, which preferably can be carried out using the inbuilt rinsing ability of a commercial CE instrument. Alternatively, the coating protocol can be carried out manually by flushing nitrogen gas into a gastight vial containing the rinsing solution and into which the fused-silica capillary (or several capillaries) is inserted, according to **Fig 4**.
8. The coating mechanism is based on ionic interaction between the cationic polymer and the anionic capillary surface. The pH of the alkaline PolyE-323 solution is thus adjusted with acetic acid in order to protonate the polymer to get a high cationic charge density. Because the anionic charge density of the capillary wall is decreased at acidic conditions, a coating solution of pH 7.0 is used as a compromise between high cation and anion charge density. Preliminary results from our laboratory, however, show that a stable coating can be generated using acidic as well as basic coating conditions (no addition of acid). The characteristics of the resulting coating layers have not yet been evaluated thoroughly and it cannot be excluded that coating pH has an effect on the properties of the resulting coating, such as EOF generation. It must also be noted that when varying pH of

the coating solution by adding acid, the ionic strength is changed which has been reported to influence surface coverage ***(15)***.

The best way to measure the pH of the PolyE-323 coating solution is to put a droplet of the solution onto a pH-indicator strip. It is not advisable to use a pH meter because the cationic polymer will stick to the glass electrode.

9. The concentration of PolyE-323 in the coating solution has been shown to affect the resulting coating ***(31)***. As shown in **Fig. 5**, the EOF is decreased with an increase in coating solution polymer concentration. Notably, stable coatings can be formed even at very low concentrations of polymer (<0.0002 %). In contrast to polymer concentration, no effect of rinsing time on the resulting coating has been found ***(31)***.
10. Analogously to the discussion above about the pH of the PolyE-323 coating solution, it cannot be excluded that pH of the background electrolyte used for removing excess coating polymer has an effect on the properties of the resulting coating. Consistency during coating preparation is thus recommended for high reproducibility.
11. For high reproducibility, it is preferable to coat the capillary just before the CE-MS experiments are conducted. If the capillary is coated in advance, it can be stored filled with background electrolyte. No effect on the capillary coating upon drying has been observed for the EOF, but the effect of drying on protein separation performance has not been evaluated.
12. When using bare fused-silica capillaries in CE, extensive rinsing procedures are often employed between each injection in order to control the capillary surface for a high analysis reproducibility. This is, however, not required when using capillaries coated with PolyE-323. Analyses can be performed consecutively without any treatment prior to injection. Rinsing with background electrolyte is only needed to, e.g., remove gas bubbles or change background electrolyte. If the capillary is extensively rinsed, the coating might deteriorate by bleeding as a result of mechanical stress. In order to regenerate the coating in the case of deterioration (or irreversible adsorption of material from a crude sample), a simple regeneration protocol can be used consisting of rinsing the capillary at 950 mbar with 1 *M* NaOH for 15 min, water for 5 min, 0.1 *M* HCl for 5 min, water for 5 min, 7.5% w/w PolyE-323 for 10 min, and finally background electrolyte for 5 min.

Acknowledgments

Financial support from the Swedish Strategic Foundation and the Swedish Research Council, Projects K-5104-706/2001, 621-2002-5261, is acknowledged. J.B. holds a senior research position at the Swedish Research Council, 629-2002-6821.

References

1. Green, J. S. and Jorgenson, J. W. (1989) Minimizing adsorption of proteins on fused-silica in capillary zone electrophoresis by the addition of alkali metal salts to the buffer. *J. Chromatogr*. **478,** 63–70.

2. Corradini, D., Rhomberg, A., and Corradini, C. (1994) Electrophoresis of proteins in uncoated capillaries with amines and amino sugars as electrolyte additives. *J. Chromatogr. A*. **661,** 305–313.
3. Bushey, M. M. and Jorgenson, J. W. (1989) Capillary electrophoresis of proteins in buffers containing high concentrations of zwitterionic salts. *J. Chromatogr*. **480,** 301–310.
4. Rodriguez, I. and Li, S. F. Y. (1999) Surface deactivation in protein and peptide analysis by capillary electrophoresis. *An. Chim. Acta*. **383,** 1–26.
5. Horvath, J. and Dolnik, V. (2001) Polymer wall coatings for capillary electrophoresis. *Electrophoresis* **22,** 644–655.
6. Millot, M.-C. and Vidal-Madjar, C. (2000) Overview of the surface modification techniques for the capillary electrophoresis of proteins. *Adv. Chromatogr*. **40,** 427–466.
7. Moseley, M. A., Deterding, L. J., Tomer, K. B., and Jorgenson, J. W. (1991) Determination of bioactive peptides using capillary zone electrophoresis/mass spectrometry. *Anal. Chem*. **63,** 109–114.
8. Hjertén, S. (1985) High-performance electrophoresis. elimination of electroendosmosis and solute adsorption. *J. Chromatogr*. **347,** 191–198.
9. Fridström, A., Lundell, N., Nyholm, L., and Markides, K. E. (1997) Polymethacryloxypropylhydrosiloxane deactivation as pretreatment of polymer-coated fused silica columns for capillary electrophoresis. *J. Microcol. Sep*. **9,** 73–80.
10. Towns, J. K. and Regnier, F. E. (1990) Polyethyleneimine-bonded phases in the separation of proteins by capillary electrophoresis. *J. Chromatogr*. **516,** 69–78.
11. Erim, F. B., Cifuentes, A., Poppe, H., and Kraak, J. C. (1995) Performance of a physically adsorbed high-molecular-mass polyethyleneimine layer as coating for the separation of basic proteins and peptides by capillary electrophoresis. *J. Chromatogr. A*. **708,** 356–361.
12. Córdova, E., Gao, J., and Whitesides, G. M. (1997) Noncovalent polycationic coatings for capillaries in capillary electrophoresis of proteins. *Anal. Chem*. **69,** 1370–1379.
13. Li, M. X., Liu, L., Wu, J. -T., and Lubman, D. M. (1997) Use of a polybrene capillary coating in capillary electrophoresis for rapid analysis of hemoglobin variants with on-line detection via an ion trap storage/reflectron time-of-flight mass spectrometer. *Anal. Chem*. **69,** 2451–2456.
14. Wang, Y. and Dubin, P. L. (1999) Capillary modification by noncovalent polycation adsorption: effects of polymer molecular weight and adsorption ionic strength. *Anal. Chem*. **71,** 3463–3468.
15. Liu, Q., Lin, F., and Hartwick, R. A. (1997) Poly(diallylmethylammonium chloride) as a cationic coating for capillary electrophoresis. *J. Chromatogr. Sci*. **36,** 126–130.
16. Chiu, R. W., Jimenez, J. C., and Monnig, C. A. (1995) High molecular weight polyarginine as a capillary coating for separation of cationic proteins by capillary electrophoresis. *Anal. Chim. Acta*. **307,** 193–201.

17. Sun, P., Landman, A., and Hartwick, R. A. (1994) Chitosan coated capillary with reversed electroosmotic flow in capillary electrophoresis for the separation of basic drugs and proteins. *J. Microcol. Sep*. **6,** 403–407.
18. Yao, Y. J., Li, S. F. Y. (1994) Capillary Zone Electrophoresis of Basic Proteins with Chitosan as a Capillary Modifier*J. Chromatogr. A*. **663,** 97–104.
19. González, N., Elvira, C., Román, J. S., and Cifuentes, A. (2003) New physically adsorbed polymer coating for reproducible separations of basic and acidic proteins by capillary electrophoresis. *J. Chromatogr. A*. **1012,** 95–101.
20. Ullsten, S., Söderberg, L., Folestad, S., and Markides, K. E. (2004) Quaternary ammonium substituted agarose as surface coating for capillary electrophoresis. *Analyst* **129,** 410–415.
21. Yao, Y. J., Khoo, K. S., Chung, M. C. M., and Li, S. F. Y. (1994) Determination of isoelectric points of acidic and basic proteins by capillary electrophoresis. *J. Chromatogr. A*. **680,** 431–435.
22. Kelly, J. F., Locke, S. J., Ramaley, L., and Thibault, P. (1996) Development of electrophoretic conditions for the characterization of protein glycoforms by capillary electrophoresis-electrospray mass spectrometry. *J. Chromatogr. A*. **720,** 409–427.
23. Liu, T., Li, J. -D., Zeng, R., Shao, X. -X., Wang, K. -Y., and Xia, Q. -C. (2001) Capillary electrophoresis-electrospray mass spectrometry for the characterization of high-mannose-type N-glycosylation and differential oxidation in glycoproteins by charge reversal and protease/glycosidase digestion. *Anal. Chem*. **73,** 5875–5885.
24. Boss, H. J., Watson, D. B., and Rush, R. S. (1998) Peptide capillary electrophoresis mass spectrometry of recombinant human erythropoietin: an evaluation of the analytical method*Electrophoresis* **19,** 2654–2664.
25. Lai, C. -C. and Her, G. -R. (2000) Analysis of phospholipase A2 glycosylation patterns from venom of individual bees by capillary electrophoresis/electrospray ionization mass spectrometry using an ion trap mass spectrometer. *Rapid Commun. Mass Spectrom*. **14,** 2012–2018.
26. Naylor, S., Ji, Q., Johnson, K. L., Tomlinson, A. J., Kieper, W. C., and Jameson, S. C. (1998) Enhanced sensitivity for sequence determination of major histocompatibility complex class I peptides by membrane preconcentration - capillary electrophoresis - microspray - tandem mass spectrometry. *Electrophoresis* **19,** 2207–2212.
27. Rohde, E., Tomlinson, A. J., Johnson, D. H., and Naylor, S. (1998) Protien analysis by membrane preconcentration-capillary electrophoresis: systematic evaluation of parameters affecting preconcentration and separation. *J. Chromatogr. B*. **713,** 301–311.
28. Katayama, H., Ishihama, Y., and Asakawa, N. (1998) Stable cationic capillary coating with successive multiple ionic polymer layers for capillary electrophoresis*Anal. Chem*. **70,** 5272–5277.
29. Nedelkov, D. and Bieber, A. L. (1997) Detection of isoforms and isomers of rattlesnake myotoxins by capillary electrophoresis and matrix-assisted laser desorption time-of-flight mass spectrometry. *J. Chromatogr. A*. **781,** 429–434.

30. Ullsten, S., Zuberovic, A., Wetterhall, M., Hardenborg, E., Markides, K. E., and Bergquist, J. (2004) A polyamine coating for enhanced capillary electrophoresis-electrospray ionization-mass spectrometry of proteins and peptides. *Electrophoresis* **25,** 2090–2099.
31. Soga, T., Ueno, Y., Naraoka, H., Ohashi, Y., Tomita, M., and Nishioka, T. (2002) Simultaneous determination of anionic intermediates for bacillus subtilis metabolic pathways by capillary electrophoresis electrospray ionization mass spectrometry. *Anal. Chem*. **74,** 2233–2239.
32. Rodríguez-Delgado, M. A., Garcia-Montelongo, F. J., and Cifuentes, A. (2002) Ultrafast sodium dodecyl sulfate micellar electrokinetic chromatography with very acidic running buffers. *Anal. Chem*. **74,** 257–260.
33. Catai, J. R., Somsen, G. W., and de Jong, G. J. (2004) Efficient and reproducible analysis of peptides by capillary electrophoresis using noncovalently bilayer-coated capillaries. *Electrophoresis* **25,** 817–824.
34. Graul, T. W. and Schlenhoff, J. B. (1999) Capillaries modified by polyelectrolyte multilayers for electrophoretic separations. *Anal. Chem*. **71,** 4007–4013.
35. Barker, S. L. R., Ross, D., Tarlov, M., Gaitan, M., and Locascio, L. E. (2000) Control of flow direction in microfluidic devices with polyelectrolyte multilayers. *Anal Chem*. **72,** 5925–5929.
36. Barker, S. L. R., Tarlov, M. J., Canavan, H., Hickman, J. J., and Locascio, L. E. (2000) Plastic microfluidic devices modified with polyelectrolyte multilayers. *Anal. Chem*. **72,** 4899–4903.
37. Makamba, H., Kim, J. H., Lim, K., Park, N., and Hahn, J. H. (2003) Surface modification of poly(dimethylsiloxane) microchannels. *Electrophoresis* **24,** 3607–3619.
38. Hardenborg, E., Zuberovic, A., Ullsten, S., Söderberg, L., Heldin, E., and Markides, K. E. (2003) Novel polyamine coating providing non-covalent deactivation and reversed electroosmotic flow of fused-silica capillaries for capillary electrophoresis. *J. Chromatogr. A*. **1003,** 217–221.
39. Zuberovic, A., Ullsten, S., Hellman, U., Markides, K. E., and Bergquist, J. (2004) Capillary electrophoresis-off-line-matrix-assisted laser desorption/ionisation mass spectrometry of intact and digested proteins using cationic-coated capillaries. *Rapid Commun. Mass Spectrom*. **18,** 2946–2952.

26

On-Column Ligand/Receptor Derivatization Coupled to Affinity Capillary Electrophoresis

Jose Zavaleta, Dinora Chinchilla, Alvaro Gomez, Catherine Silverio, Maryam Azad, and Frank A. Gomez

Summary

The coupling of on-column derivatization of small molecules to affinity capillary electrophoresis (ACE) has only been realized during the past 5 yr. In this technique, multiple zones of reagent(s) and ligand or receptor are injected into the capillary column. Upon electrophoresis, zones of sample overlap, yielding product. Continued electrophoresis results in the product overlapping with receptor (or ligand, if the receptor was derivatized), thereby causing a shift in migration time of the compound in question. Subsequent Scatchard analysis using noninteracting standards realizes a binding constant. Herein, we describe the use of on-column-ligand and receptor derivatization coupled to partial-filling ACE (PFACE) to probe the binding of vancomycin (Van) from *Streptomyces orientalis* and teicoplanin (Teic) from *Actinoplanes teicomyceticus* to D-Ala-D-Ala terminus peptides.

Key Words: Affinity capillary electrophoresis; binding constants; receptor–ligand interactions; vancomcyin; teicoplanin; ristocetin; Scatchard plot.

1. Introduction

The use of on-column methodologies in the derivatization of molecules is a growing area of capillary electrophoresis (CE) ***(1–3)***. In this technique, samples are injected separately onto the capillary column and electrophoresed. Differential transport velocities permit the separate zones of sample to penetrate each other under an applied field, thereby facilitating reaction. These techniques provide for both simultaneous reaction and analysis of the reaction. The majority of these studies have focused on examining enzyme-catalyzed

From: *Methods in Molecular Biology, vol. 384: Capillary Electrophoresis*
Edited by: P. Schmitt-Kopplin © Humana Press Inc., Totowa, NJ

microreactions. Few studies have documented the use of on-column reaction techniques in the analysis of nonenzymatic reactions.

During the past decade, affinity capillary electrophoresis (ACE) has emerged as a useful and sensitive technique for studying bimolecular noncovalent interactions and for determining binding and dissociation constants of formed complexes ***(4–33)***. Since the initial reports in 1992 documenting the use of CE to study receptor–ligand interactions, ACE has been successfully used to examine a wide array of interactions including protein–drug, protein–DNA, peptide–carbohydrate, peptide–peptide, DNA–dye, carbohydrate–drug, and antigen–antibody ***(4–8)***. The underlying principle of ACE is that the electrophoretic mobility of a receptor (or ligand), μ_R, changes upon binding to a ligand (or receptor) that is present in the electrophoresis buffer. The change in μ (or other parameter based on the form of analysis used) as a function of ligand (or receptor) concentrations allows binding constants to be determined via Scatchard analysis.

A modification of standard ACE techniques is partial filling ACE (PFACE), whereby the capillary is only partially filled with receptor or ligand ***(2,3,10,11)***. As long as an equilibrium is established between the two biomolecules prior to the point of detection, a binding constant can be estimated. PFACE offers a number of advantages over traditional ACE and other assay techniques. First, it requires smaller quantities of both receptor and ligand than do traditional ACE techniques. Second, purified ligand and/or receptor are not always required as long as the peak(s) of interest can be differentiated from other peaks in the electropherogram. Third, most of the commercially available instruments are automated, making it experimentally convenient to use.

Few studies have demonstrated on-column derivatization of compounds using capillary electrophoresis (CE). Even fewer studies have coupled on-column techniques to ACE. Herein, on-column-ligand and receptor derivatization coupled to ACE (**Figs. 1** and **2**) is described to probe the binding of vancomycin (Van) and teicoplanin (Teic) to small peptides.

2. Materials

2.1. On-Column Ligand Derivatization of D-Ala-D-Ala Terminus Peptides and Binding to Van

1. 0.02 *M* phosphate, pH 7.5 (*see* **Note 1**).
2. 1.0 mg D-Ala-D-Ala-D-Ala-D-Ala (BACHEM California Inc., Torrance, CA, U.S.A.) in 1.0 mL 0.02 *M* phosphate buffer (*see* **Note 2**).
3. 1.0 mg fluorenylmethoxy carbonyl (Fmoc)-Ala-*N*-hydroxysuccinimide (NHS) ester in 1.0 mL acetonitrile.
4. 0.3 mg Vancomycin (Van) (Sigma Chemical Company, St. Louis, MO) in 1.0 mL 0.02 *M* phosphate buffer.

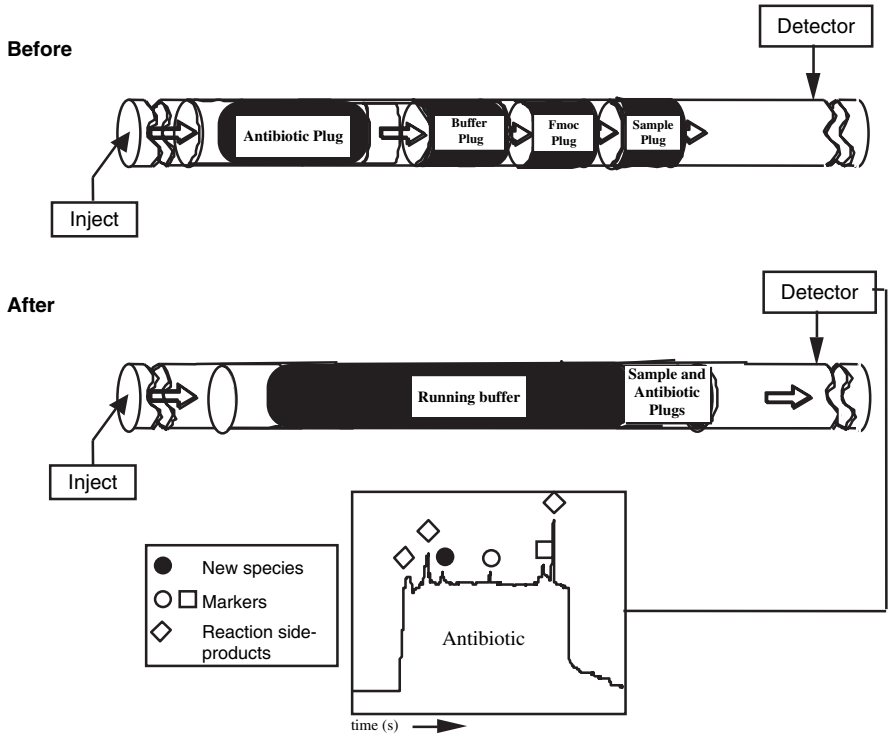


Fig. 1. Schematic of an on-column synthesis partial-filling affinity capillary electrophoresis experiment.

5. 1.0 mg Nicotinamide adenine dinucleotide (NAD) (Sigma Chemical Company, St. Louis, MO) in 1.0 mL 0.02 *M* phosphate buffer (*see* **Note 3**).
6. 1.0 mg 4-carboxybenzene sulfonamide (CBSA) (Sigma Chemical Company (St. Louis, MO) 1.0 mL 0.02 *M* phosphate buffer (*see* **Note 3**).
7. Electrophoresis sample one: 20 µL D-Ala-D-Ala-D-Ala-D-Ala solution, 20 µL NAD solution, 20 µL CBSA solution, in 200 µL sample vial.
8. Electrophoresis sample two: 20 µL Fmoc-Ala-NHS ester in acetonitrile solution.
9. Make up six solutions (10.0 mL total with addition of electrophoresis buffer) of the following concentrations of Van: 3.0, 6.0, 16, 24, 40, 60 µ*M* and divide into two sample vials (4.2 mL) each (*see* **Note 4**).

2.2. On-Column Receptor Derivatization Derivation of Teic and Rist Binding to D-Ala-D-Ala Peptides

1. 0.02 *M* phosphate, pH 6.9 (*see* **Note 5**).
2. 0.4 mg Teicoplanin (Teic) (Advanced Separation Products, Whippany, NJ) in 1.0 mL 0.02 *M* phosphate buffer (*see* **Note 6**).

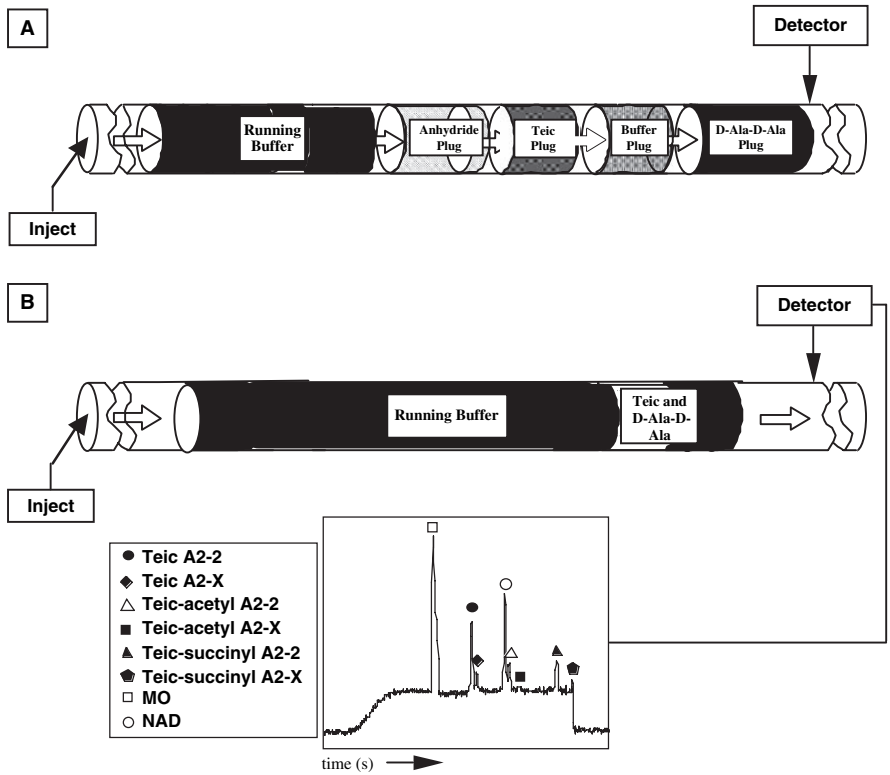


Fig. 2. Schematic of on-column receptor synthesis coupled with partial-filling affinity capillary electrophoresis experiment **(A)** before reaction and **(B)** after reaction.

3. 1.0 mg Nicotinamide adenine dinucleotide (NAD) (Sigma Chemical Company) in 1.0 mL 0.02 *M* phosphate buffer (*see* **Note 7**).
4. 50 μg MO (Calbiochem) in 1.0 mL 0.02 *M* phosphate buffer (*see* **Note 7**).
5. 1.0 mg acetic anhydride (Sigma Chemical Company, St. Louis, MO) in 1.0 mL acetonitrile.
6. 1.0 mg succinic anhydride (Sigma Chemical Company, St. Louis, MO) in 1.0 mL acetonitrile (*see* **Note 3**).
7. 1.0 mg *N*-acetyl-D-Ala-D-Ala (**1**) (Sigma Chemical Company; St. Louis, MO, U.S.A.) in 1.0 mL 0.02 *M* phosphate buffer (*see* **Note 3**).
8. Electrophoresis sample one: 20 μL Teic, 20 μL NAD solution, 20 μL MO solution, in 200 μL sample vial.
9. Electrophoresis sample two: 20 μL acetic anhydride and succinic anhydride in acetonitrile.

10. Make up eight solutions (10.0 mL total with addition of electrophoresis buffer) of the following concentrations of **1**: 25.0, 50.0, 75.0, 100, 200, 300, 400, 500 μ*M* and divide into two sample vials (4.2 mL) each (*see* **Note 4**).

2.3. Equipment

1. High performance CE system (Beckman Model P/ACE 5510; Fullerton, CA).
2. Uncoated fused silica capillaries (Polymicro Technologies, Inc., Phoenix, AZ) with an internal and external diameter of 50 μm and 360 μm, respectively, a length from inlet to detector of 40.5 cm, and a length from detector to outlet of 6.5 cm (*see* **Note 8**).
3. Detection: 205 nm for on-column ligand derivatization coupled to ACE; 200 for on-column receptor derivatization coupled to ACE (*see* **Note 9**).
4. Polyethylene solution vials.
5. pH meter.

3. Methods

The methods described herein outline the use of on-column derivatization techniques coupled to ACE and PFACE to probe the binding of glycopeptide antibiotics to small peptides. Specifically, we examine the binding of vancomycin and teicoplanin to D-Ala-D-Ala terminus peptides.

Standard ACE has several advantages as a method for measuring affinity constants over assay techniques. First, it requires small quantities of both protein and ligand. Second, purification of the sample prior to injection is not necessary as long as the component to be analyzed can be separated from other species. Third, it does not require radiolabelled or chromophoric ligands. Fourth, the commercial availability of automated instrumentation, and the high reproducibility of data, make it experimentally convenient. PFACE is more advantageous than standard ACE in that less quantities of material are needed for a given assay.

3.1. On-Column Ligand Derivatization Coupled to Affinity Capillary Electrophoresis

1. Electrophoresis sample #1 containing D-Ala-D-Ala-D-Ala-D-Ala, NAD, and CBSA to sample holder 21.
2. Electrophoresis sample #2 containing Fmoc-Gly-NHS to sample holder 20.
3. Van solution in vials 12 and 2, 13 and 3, respectively in order of increasing concenration of Van (*see* **Note 10**).
4. Electrophoresis buffer (2 × 4.2 mL) in sample holder positions 11 and 1.
5. 3.0 min rinse at high pressure (20 psi) with electrophoresis buffer.
6. Instrument programmed to inject electrophoresis sample for 3.0 s at low pressure (0.5 psi), followed by sample #2 for 3 s at low pressure (0.5 psi), buffer for 3.0 s at

low pressure (0.5 psi) and to run increasing concentrations of Van in electrophoresis buffer for 5.0 min (*see* **Note 11**).

7. The conditions used in CE were as follows: voltage, 24 kV; current, 35.4 μA depending on the capillary length; detection, 205 nm; temperature, 23 ± 0.5 °C.
8. Run three to five repetitions of each concentration of Van (*see* **Note 12**).
9. For each new concentration of peptide, fill the capillary column for 1.0 min (20 psi) with Van.
10. Upon completion of the electrophoresis runs, record the migration times of the new peptide Fmoc-Ala-D-Ala-D-Ala-D-Ala-D-Ala (**2**), MO, and CBSA and compute the binding constant by Scatchard analysis.
11. In this form of Scatchard analysis, K_b is estimated using a dual-marker form of analysis, which we term the relative migration time ratio (RMTR) **(Eq. 1)**,

$$\mathrm{RMTR} = (t_r - t_{s'})/(t_{s'} - t_s) \quad (1)$$

of a receptor referenced to two non-interacting standards. Here, t_r, t_s, and t_s' are the measured migration times of **2**, and the two noninteracting standard peaks, respectively. A Scatchard plot can be obtained via **Eq. 2**.

$$\Delta\mathrm{RMTR}_{R,L}/[L] = K_b\Delta\mathrm{RMTR}_{R,L}{}^{\max} - -k_b\Delta\mathrm{RMTR}_{R,L} \quad (2)$$

Here, $\Delta\mathrm{RMTR}_{R,L}$ is the magnitude of the change in the relative migration time ratio as a function of the concentration of Van. **Equation 2** allows for the estimation of K_b on a relative time scale using two noninteracting standards and compensates for fluctuations in voltage in the capillary column (*see* **Note 13**).

12. Upon electrophoresis, a dynamic equilibrium is achieved between the plug of **2** and Van resulting in a shift in migration time of the **2**-Van complex. The complexation between **2** and Van resulted in the formation of a complex with greater mass than the beginning peptide and the complex is detected later than the uncomplexed peptide.
13. **Figure 3** shows a representative series of electropherograms of **2** in capillaries partially-filled with increasing concentrations (0 to 60 μ*M*) of Van.
14. **Figure 4** is a Scatchard plot of the data for **2**. A binding constant of 22.6 × 10^3 M^{-1} was obtained for the binding of **2** to Van.

3.2. On-Column Receptor Derivatization Coupled to Partial-Filling Affinity Capillary Electrophoresis

1. Electrophoresis sample #1 containing Teic, NAD, and MO to sample holder 21.
2. Electrophoresis sample #2 containing acetic and succinic anhydride in acetonitrile to sample holder 21.
3. Peptide solution in vials 12 and 2, 13 and 3, respectively in order of increasing concentration of **1** (*see* **Note 10**).
4. Electrophoresis buffer (2 × 4.2 mL) in sample holder positions 11 and 1.

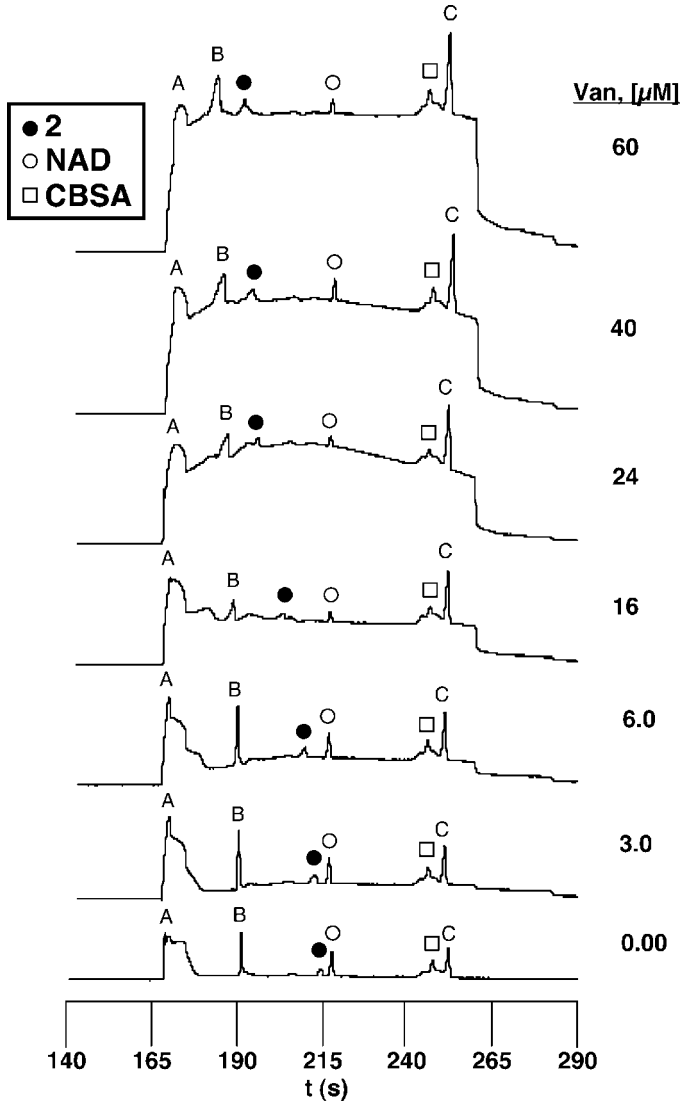


Fig. 3. A representative series of electropherograms of Fmoc-Ala-D-Ala-Ala-D-Ala-D-Ala (2) in 20 m*M* phosphate buffer (pH 7.5) at 205 nm containing various concentrations of Van using the on-column synthesis partial-filling affinity capillary electrophoresis technique. The total analysis time in each experiment was 5.0 min at 24 kV (current: 35.4 μA) using a 40.5-cm (inlet to detector), 50-μm I.D. open, uncoated quartz capillary. Nicotinamide adenine dinucleotide (NAD) and 4-carboxybenzenesulfonamide (CBSA) were used as internal standards. A-C are **(A)** unreacted Fmoc-Ala-NHS, **(B)** D-Ala-D-Ala-D-Ala-D-Ala, and **(C)** Fmoc-Ala-acid.

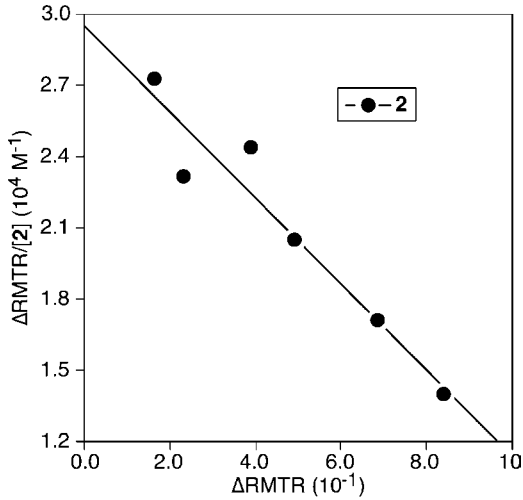


Fig. 4. Scatchard plot of the data for Fmoc-Ala-D-Ala-Ala-D-Ala-D-Ala (2) according to **Eq. 2**.

5. 3.0-min rinse at high pressure (20 psi) with electrophoresis buffer.
6. Instrument programmed to inject solutions of **1** at low pressure (0.5 psi) for 8–12 s, buffer for 3.0 s at low pressure (0.5 psi), electrophoresis sample #1 for 1–2.0 s at low pressure (0.5 psi), and electrophoresis sample #2 for 1.2 s at low pressure (0.5 psi) and electrophoresed for 4.0 min.
7. The conditions used in CE were as follows: voltage, 20 kV; current, 22 μA; detection, 200 nm; temperature, 23 ± 0.5 °C.
8. Run three to five repetitions of each concentration of **1** (*see* **Note 12**).
9. Upon completion of the electrophoresis runs, record the migration times of Teic and its derivatives, MO, and NAD, and compute the binding constant by Scatchard analysis (*see* **Note 13**).
10. Upon increasing the concentration of **1** in the capillary column, a shift in the migration time of Teic and its derivatives is observed. The Teic-**1** complexes are more negative than Teic and upon binding shifts to the right (longer migration time). The markers, MO and NAD, are unaffected by the change in the concentration of **1** and its migration time does not vary significantly during the course of the experiment, hence, they can be used as a marker in the analysis of K_b. As shown in **Fig. 2A**, the change in concentration of **1** in the column is visualized as an increased height in the ligand plateaus. The box-like structure of the ligand peak at all concentrations of ligand denotes both a uniform injection of ligand into the column and a stable concentration of peptide in the capillary column. For the sample plug to elute on top of the ligand boxes, care was taken to ensure that a long enough time of ligand was injected into the capillary; otherwise, incomplete overlap will occur, making analysis of the interaction problematic.

Table 1
Experimental Values of Binding Constants $K_b(10^4\,M^{-1})$ of Teic-A2-2 and A2-X with Ligand 2 Measured by the On-Column Receptor Synthesis Partial-Filling Affinity Capillary Electrophoresis Technique

Antibiotic	$K_b(10^4\,M^{-1})$ 1	$K_b(10^4\,M^{-1})$ (corr. coeff.)
Teic	37	(0.94)
Teic-A2-X	20	(0.98)
Teic-acetyl-A2-2	13	(0.98)
Teic-acetyl-A2-X	6.2	(0.99)
Teic-succinyl-A2-2	6.2	(0.99)
Teic-succinyl-A2-X	3.4	(0.99)

11. **Figure 5** shows a representative series of electropherograms of Van in a capillary partially filled with **2**.
12. **Figure 6** is a Scatchard plot of Teic and its derivatives using varying concentrations of **1** in the running buffer using the RMTR form of analysis. Table 1 summarizes the binding data for Teic and its derivatives to **2**.

4. Notes

1. The use of phosphate buffer is niether critical for ACE analysis nor is a pH of 7.5. Our labs use this buffer concentration and pH because of the importance of conducting the experiments at physiological pH as previous binding studies, both ACE and non-ACE in nature, have been conducted at this pH. We have also conducted experiments at pH 8.3 to reduce protein absorption onto the walls of the capillary columns when using other receptor–ligand combinations.
2. Other D-Ala-D-Ala terminus peptides can be used because they all have similar binding affinities to Van as the peptide being derivatized here.
3. NAD and CBSA are noninteracting standards used in the data analysis. They do not have any affinity to either the glycopeptide antibiotic or the peptide ligands. Other markers can be used as long as they do not migrate at or near the migration times of the derivatized peptide.
4. Other concentrations of Van can be used as long as they are in the same range of values stated here. Values of concentrations are dependent on the strength of the receptor–ligand interaction and, hence, other concentrations must be used if other interactions are to be examined.
5. The use of phosphate buffer and pH of 6.9 is not required for ACE and/or on-column derivatizations. It is critical that the buffer used not be reactive to the reagents used for derivatization.

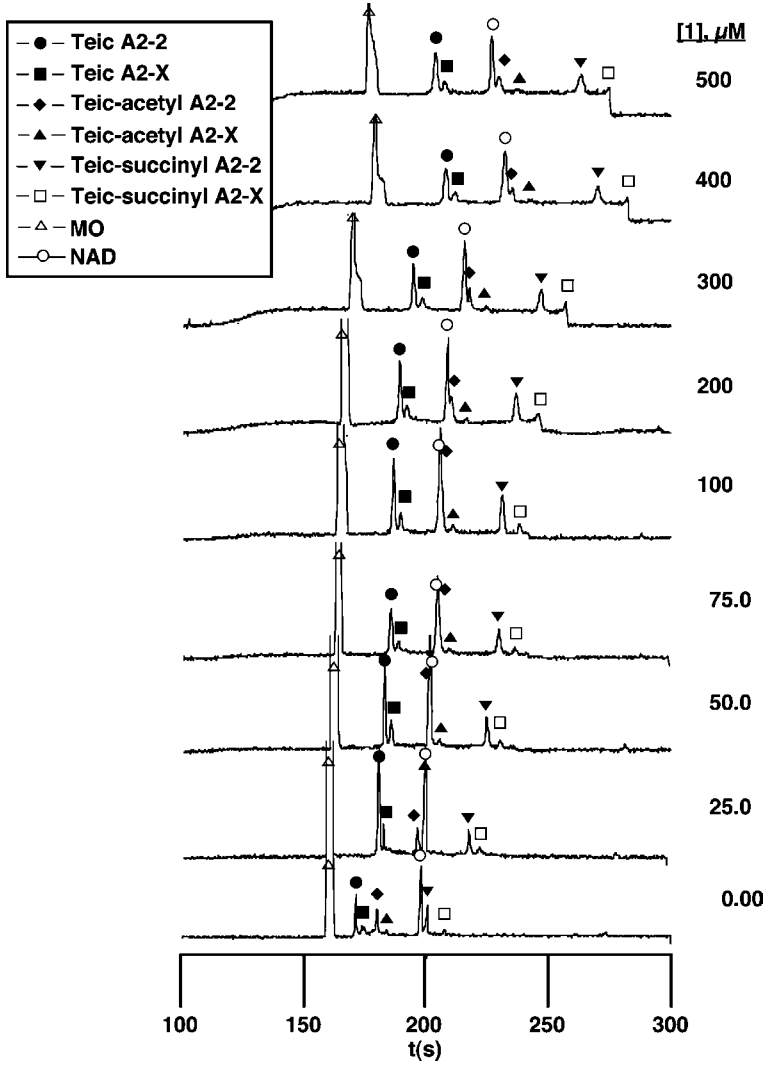


Fig. 5. A representative series of electropherograms of Teic and its derivatives in 20 m*M* phosphate buffer (pH 6.9) containing various concentrations of 1, using on-column receptor synthesis coupled to partial-filling affinity capillary electrophoresis. The total analysis time in each experiment was 5.0 min. at 20 kV using a 46.5 cm (inlet to detector) 50 μm I.D. open, uncoated quartz capillary.

6. Other glycopeptide antibiotics can be used as long as they have an amine moiety available for derivatization and where reactions occurs at the given pH.
7. MO and NAD are noninteracting standards used in the data analysis. They do not have any affinity to either the glycopeptide antibiotic or the peptide ligands.

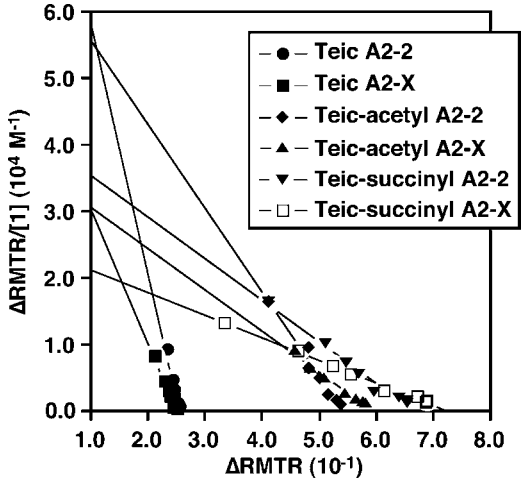


Fig. 6. Scatchard plot of Teic and its derivatives with 1.

Other markers can be used as long as they do not migrate at or near the migration times of the derivatized peptide.

8. Length of column is not critical in ACE as long as a dynamic equilibrium is achieved prior to detection. For PFACE, length of column is critical as the zone of ligand (or receptor) must encompass the peaks of interest and an equilibrium achieved before the point of detection.
9. The detection wavelength used in ACE can be varied depending on the system being studied. We chose 205 and 200 nm in order to achieve the maximal peak response and because little peak overlap with other species was observed at this wavelength.
10. The instrument can be programmed to run the electrophoresis buffers at increasing concentrations.
11. High- and low-pressure settings can be programmed using the instrument software.
12. A greater number of repetitions can be run depending on the amount of sample and time available for the ACE study.
13. There are other forms of Scatchard analysis available which can be used to analyze the data obtained using ACE. We have found a dual-marker form of analysis to work best especially when there are fluctuations in the electroosmotic flow.

Acknowledgments

The authors gratefully acknowledge financial support for this research by grants from the National Science Foundation (CHE-0136724 and DMR-0351848), and the National Institutes of Health (R15 AI055515-01).

References

1. Zhang, Y. and Gomez, F. A. (2000) On-column derivatization and analysis of amino acids, peptides, and alkylamines by anhydrides using capillary electrophoresis. *Electrophoresis* **21,** 3305–3310.
2. Zhang, Y., Kodama, C., Zurita, C., and Gomez, F. A. (2001) On-column ligand synthesis coupled to partial-filling affinity capillary electrophoresis to estimate binding constants of ligands to a receptor. *J. Chromatogr. A*. **928,** 233–241.
3. Silverio, C. S., Azad, M., and Gomez, F. A. (2003) On-column derivatization of the antibiotics teicoplanin and ristocetin coupled to affinity capillary electrophoresis. *Electrophoresis* **24,** 808–815.
4. Kraak, J. C., Busch, S., and Poppe, H. (1992) Study of protein-drug binding using capillary zone electrophoresis. *J. Chromatogr. A*. **608,** 257–264.
5. Chu, Y. H. and Whitesides, G. M. (1992) Affinity capillary electrophoresis can simultaneously measure binding constants of multiple peptides to vancomycin. *J. Org. Chem*. **57,** 3524–3525.
6. Chu, Y. H., Avila, L. Z., Biebuyck, H. A., and Whitesides, G. M. (1992) Use of affinity capillary electrophoresis to measure binding constants of ligands to proteins. *J. Med. Chem*. **35,** 2915–2917.
7. Heegaard, N. H. H. and Robey. F. A. (1992) Use of capillary zone electrophoresis to evaluate the binding of anionic carbohydrates to synthetic peptides derived from human serum amyloid P component. *Anal. Chem*. **64,** 2479–2482.
8. Baba, Y., Tsuhako, M., Sawa, T., Akashi, M, and Yashima, E. (1992) Specific base recognition of oligodeoxynucleotides by capillary affinity gel electrophoresis using polyacrylamide-poly(9-vinyladenine) conjugated gel. *Anal. Chem*. **64,** 1920–1925.
9. Azad, M., Hernandez, L., Plazas, A., Rudolph, M., and Gomez, F. A. (2003) Determination of binding constants between the antibiotic ristocetin A and D-Ala-D-Ala terminus peptides by affinity capillary electrophoresis. *Chromatographia* **57,** 339–344.
10. Heintz, J., Hernandez, M., and Gomez, F. A. (1999) Use of a partial-filling technique in affinity capillary electrophoresis for determining binding constants of ligands to receptors. *J. Chromatogr. A*. **840,** 261–268.
11. Mito, E. and Gomez, F. A. (1999) Flow-through partial-filling affinity capillary electrophoresis can estimate binding constants of ligands to receptors. *Chromatographia* **50,** 689–694.
12. Zhang, Y. and Gomez, F. A. (2000) Multiple-step ligand injection affinity capillary electrophoresis for determining binding constants of ligands to receptors. *J. Chromatogr. A*. **897,** 339–347.
13. Mito, E., Zhang, Y., Esquivel, S., and Gomez, F. A. (2000) Estimation of receptor-ligand interactions by the use of a two-marker system in affinity capillary electrophoresis. *Anal. Biochem*. **280,** 209–215.
14. Chu, Y. -H., Avila, L. Z., Gao, J., and Whitesides, G. M. (1995) Affinity capillary electrophoresis. *Acc. Chem. Res*. **28,** 461–468.

15. Qian, X. –H. and Tomer, K. B. (1998) Affinity capillary electrophoresis investigation of an epitope on human immunodeficiency virus recognized by a monoclonal antibody. *Electrophoresis* **19,** 415–419.
16. Kiessig, S., Bang, H., and Thunecke, F. (1999) Interaction of cyclophilin and cyclosporins monitored by affinity capillary electrophoresis. *J. Chromatogr. A*. **853,** 469–477.
17. Jameson, E. E., Cunliffe, J. M., Neubig, R. K., Sunahara, R. K., and Kennedy, R. T. (2003) Detection of G proteins by affinity probe capillary Electrophoresis using a fluorescently labeled GTP analogue. *Anal. Chem*. **75,** 4297–4304.
18. Erim, F. B. and Kraak, J. C. (1998) Vacancy affinity capillary electrophoresis to study competitive protein-drug binding. *J. Chromatogr. B*. **710,** 205–210.
19. Shimura, K. and Kasai, K. (1997) Affinity capillary electrophoresis: a sensitive tool for the study of molecular interactions and its use in microscale analyses. *Anal. Biochem*. **251,** 1–16.
20. Gomez, F. A., Avila, L. Z., Chu, Y. -H., and Whitesides, G. M. (1994) Determination of binding constants of ligands to proteins by affinity capillary electrophoresis: compensation for electroosmotic flow. *Anal. Chem*. **66,** 1785–1791.
21. Zhang, X., Davidson, E. W., Nguyen, T. H., Evans, R. W., Im, S. J., and Barker, G. E. (1996) Investigation of chiral resolution using displacement interactions with polymer networks in capillary affinity zone electrophoresis. *J. Chromatogr. A*. **745,** 1–8.
22. Colton, J. J., Carbeck, J. D., Rao, J., and Whitesides, G. M. (1998) Affinity capillary electrophoresis: a physical-organic tool for studying interactions in biomolecular recognition. *Electrophoresis* **19,** 367–382.
23. Heegaard, N. H. H., Hansen, B. E., Svejgaard, A., and Fugger, L. H. (1997) Interactions of the human class 11 major histocompatibility complex protein HLD-DR4 with a peptide ligand demonstrated by affinity capillary electrophoresis. *J. Chromatogr. A*. **781,** 91–97.
24. Nakajima, K., Oda, Y., Kinoshita, M., and Kakehi, K. (2003) Capillary affinity electrophoresis for the screening of post-translational modification of proteins with carbohydrates. *J. Proteome Res*. **2,** 81–88.
25. VanderNoot, V. A., Hileman, R. E., Dordick, J. S., and Linhardt, R. J. (1998) Affinity capillary electrophoresis employing immobilized glycosaminoglycan to resolve heparin-binding peptides. *Electrophoresis* **19,** 437–441.
26. Chu, Y. –H., Dunayevskiy, Y. M., Kirby, D. P., Vouros, P., and Karger, B. L. (1996) Affinity capillary electrophoresis-mass spectrometry for screening combinatorial libraries. *J. Am. Chem. Soc*. **118,** 7827–7835.
27. Busch, M. H. A., Carels, L. B., Boelens, H. F. M., Kraak, J. C., and Poppe, H. (1997) Comparison of five methods for the study of drug-protein binding in affinity capillary electrophoresis. *J. Chromatogr. A*. **777,** 311–328.
28. Lin, S., Hsiao, I. –Y., and Hsu, S. –M. (1997) Determination of the dissociation constant of phosvitin-anti-phosphoserine interaction by affinity capillary electrophoresis. *Anal. Biochem*. **254,** 9–17.

29. Larsen, K. L. and Zimmermann, W. (1999) Analysis and characterisation of cyclodextrins and their inclusion complexes by affinity capillary electrophoresis. *J. Chromatogr. A*. **836,** 3–14.
30. Taga, A., Uegaki, K., Yabusako, Y., Kitano, A., and Honda, S. (1999) Simultaneous determination of the association constants of oligosaccharides to a lectin by capillary electrophoresis. *J. Chromatogr. A*. **837,** 221–229.
31. Amini, A. and Westerlund, D. (1998) Evaluation of association constants between drug enantiomers and human alpha-1-acid glycoprotein by applying a partial-filling technique in affinity capillary electrophoresis. *Anal. Chem*. **70,** 1425–1430.
32. Dunayevskiy, Y. M., Lyubarskaya, Y. V., Chu, Y. –H., Vouros, P., and Karger, B. L. (1998) Simultaneous measurement of nineteen binding constants of peptides to vancomycin using affinity capillary electrophoresis-mass spectrometry. *J. Med. Chem*. **41,** 1201–1204.
33. Villareal, V. J., Kaddis, M., Azad, C., et al. (2003) Partial-filling affinity capillary electrophoresis. *Anal. Bioanal. Chem*. **376,** 822–831.

27

On-Line Concentration of Environmental Pollutant Samples by Using Capillary Electrophoresis

Janpen Intaraprasert and Philip J. Marriott

Summary

This chapter reviews the theory and methodological developments of on-line concentration techniques for the determination of environmental pollutant samples, such as organic and inorganic compounds in capillary zone electrophoresis (CZE) and also in micellar electrokinetic chromatography (MEKC). Topics covered include a variety of on-line preconcentration strategies, which are now generally referred to as sample stacking and sweeping techniques. For each technique, surveyed methods are tabulated in order to assist in method selection. Innovative applications of sample stacking and sweeping to advanced environmental research are also emphasized. In addition, other comparative on-line concentration methods for environmental samples, namely, isotachophoretic stacking and anion and cation selective exhaustive injection-sweeping are briefly discussed.

Key Words: Sample concentration; large volume sample stacking; sweeping-micellar electrokinetic capillary electrophoresis; cation selective exhaustive injection-sweeping; anion selective exhaustive injection-sweeping; environmental samples; chlorophenoxy acetic acids.

1. Introduction

One of the general problems in capillary electrophoresis (CE) is its relatively poor detectability in terms of concentration sensitivity with spectrophotometric detection. This is attributable to both the short on-column optical path length, which is effectively controlled by the capillary diameter (50–75 μm), and the minute amount (volume, and mass) of sample injected (in the range of pg or nL magnitude). To overcome this limitation, or to enhance component detectability, several on-line sample preconcentration techniques have been

From: *Methods in Molecular Biology, vol. 384: Capillary Electrophoresis*
Edited by: P. Schmitt-Kopplin © Humana Press Inc., Totowa, NJ

developed and applied to the CE system and specifically aimed at decreasing limits of detection (LODs) by permitting the insertion of a large volume of sample into the capillary, but concurrently without compromising peak efficiency and resolution. This can only be achieved by some means of zone compression of each of the target analytes, which leads to the on-column concentration step. In a general sense, sample concentration can be accomplished by physical means, such as liquid- and solid-phase extraction (SPE), which tend to be pre-column sample handling methods. It also can be accomplished much more easily, and more conveniently, by several electrokinetic maneuvers within the capillary, such as stacking, field amplified injection, isotachophoresis or focusing, and sweeping that are performed individually or in combination ***(1–5)***. On-line techniques are easily transferable technologies because of their simplicity and economy, and effectively only rely on buffer composition/chemistry and electrophoresis principles. These techniques can be applied to charged and neutral analytes, except that isotachophoresis cannot be applied to neutral components. In this chapter, two principles of on-line sample concentration will be reviewed. The first one is based on electromigration effects only, and a term of sample stacking will be used for this. The second principle involves chromatographic or partitioning effects, and it will be denoted as sweeping. The focus will be on processes that largely occur in the CE buffer itself. Although different concentration methods for the analysis of environmental samples are briefly discussed, emphasis is placed on those that have demonstrated the greatest analytical potential, and a range of applications are summarized in **Table 1.** Note that traditionally, environmental analysis is focused on low-level (trace) constituents, for either target or multiresidue analysis, and so the importance of concentration effects to extend the applicability of CE methods to this area is readily apparent.

1.1. Sample Stacking

Sample stacking is one of the desirable features of CE that had not been fully explored or utilized for environmental samples or related compounds in the early development of CE. Stacking in CE is similar to on-column sample enrichment in high-performance liquid chromatography (HPLC), but the former should be considered easier to perform. In CE, there is no need for convoluted eluent change steps or special equipment, such as valves and switching systems; it should have better flexibility. Sample stacking in capillary zone electrophoresis (CZE) has been discussed or noted for widely differing compounds, such as inorganic ions and compounds of pharmaceutical and environmental samples ***(38–42)***. Electrophoretic on-column preconcentration methods for CE are usually easier to implement than other pre-column

Table 1
Examples for Selected Environmentally Relevant Compounds Analyzed in Capillary Zone Electrophoresis and Micellar Electrokinetic Chromatography (MEKC) Based on Different Stacking and Sweeping Concentration Processes.

Analytes	Concentration principle (×enrichment factor)	Background electrolyte	Limit of detection	*Ref.*
Phenols, Chlorophenols, Nitrophenols	Sample stacking with polarity switching (NS)	40 m*M* borate buffer (pH 9.8)	0.5 μg/L	***1***
Ametryn, Carbendazim, Atrazine, Propoxur, Propazine, Linuron, Diuron, Simazine and Carbaryl	SRMM (×3–18)	25 m*M* SDS in 20 m*M* phosphate buffer and 10% MeOH (pH 2.5, 2.12 mS/cm)	2.5 μg/L	***6***
Dibenzodioxin, Dibenzofuran and Polychlorinated dibenzo-p-dioxins	SRW (×200)	100 m*M* SDS–40 m*M* γ-CD in 50 m*M* phosphate buffer (pH 2.5)	0.1 mg/L	***7***
Phenoxy acid herbicides	Stacking with FASI (×200)	(1) 50 m*M* SDS in 20 m*M* phosphate buffer–40% MeOH (pH 7.0 and 9.0)	50 μg/L	***8***
Glyphosate and Aminomethylphosphoric acid (AMPA)	Stacking with FASI (×1000)	10 m*M* phthalate buffer and 0.5 m*M* TTAB (pH 7.5)	2 μg/L	***9***
Quaternary ammonium compounds	Sample stacking with matrix removal (NS)	0.8 m*M* CTAB in 50 m*M* acetic acid–ammonium acetate (pH 4.5)	0.3–2.2 μg/L	***10***
Phenolic compounds	Sample stacking using FASI (NS)	20 m*M* borate buffer (pH 9.9)	0.035–0.05 mg/L	***11***
Phenylurea herbicides	Stacking with SRMM (× 500)[a]	50 m*M* SDS–15 m*M* γ-CD in 50 m*M* phosphate buffer (pH 2.5)	0.01–0.02 mg/L	***12***

(Continued)

Table 1
(Continued)

Analytes	Concentration principle (×enrichment factor)	Background electrolyte	Limit of detection	*Ref.*
Fenoprop, mecoprop and dichloroprop	Stacking-CDEKC (×10)	20 m*M* hepta-6-sulfato-β-CD in 15 m*M* phosphate buffer (pH 1.9)	NS	***13***
Fungicide (triadimenol)	Stacking with SRMP and sweeping-CD-MEKC (×10)	50 m*M* SDS–25 m*M* HP-γ-CD in 50 m*M* in 50 m*M* phosphate buffer and 15% MeOH (pH 7.0)	0.8–3.8 mg/L	***14***
s-Triazines	Stacking by sweeping (NS)	40 m*M* TTAB in 40 m*M* phosphate buffer (pH 6.0)	9–15 μg/L	***15***
Haloacetic acids	LVSS (×97–120)	4 m*M* DDAPS in 100 m*M* phosphate buffer (pH 3.0)	27–53 μg/L	***16***
Phenoxy acids	LVSS with FASI and water removal with EOF pump (×3000)[b]	0.1 % HEC in borate-phosphate buffer (pH 3.2)	10 μg/L	***17***
Chlorophenoxy acids	FASS with polarity switching (×10)	0.3 m*M* HP-β-CD in 3.0 m*M* ammonium-HCl (pH 9)	1–4 μg/L	***18***
Quaternary ammonium herbicides	Sample stacking with sample matrix removal using reversed EOF	0.8 m*M* CTAB in 50 m*M* acetic acid-ammonium acetate (pH 4.0)	11–154 μg/L	***19***
Chlorophenoxy acids and chlorophenols	Stacking (×10), LVSS with polarity switching (×40) and sweeping (×7)	2 m*M* TM-β-CD in 35 m*M* borate-60 m*M* phosphate buffer (stacking mode) and 26 m*M* β-CD, 2 m*M* TM-β-CD, 50 m*M* SDS in 35 m*M* borate-60 m*M* phosphate buffer (sweeping mode) (pH 8.5)	0.1–0.25 mg/L	***20***

Phenol derivatives	FASI with RMM (×20)	50 m*M* SDS in 50 m*M* phosphate buffer (pH 2.0)	NS	***21***
Pesticides	FASS (×30)	15 m*M* β-CD, 50 m*M* SDS in 10 m*M* borate buffer-22 acetonitrile (pH 2.0)	0.04–0.46 μg/L	***22***
Triazine	Stacking with REPSM (×4–10)	125 m*M* SDS in 10 m*M* borate buffer-20 MeOH (NS)	3.3–8.5 μg/L	***23***
Phenols, Chlorophenols and Alkylphenols	Sweeping-MEKC (×100)	(1) 50 m*M* Brij-58 in 50 m*M* phosphate buffer (pH 8.5) (2) 100 m*M* Brij-35 in 20 m*M* borate buffer (pH 11.25)	19–28 μg/L	***24***
Phenol derivatives	Sweeping-MEKC (NS)	50 m*M* SDS in 50 m*M* phosphate buffer (pH 1.9)	NS	***25***
Quaternary ammonium compounds	Sweeping-MEKC (×500) and cation selective exhaustive injection (CSEI-sweeping-MEKC) (×50,000)	80 m*M* SDS in 50 m*M* phosphate buffer-20% acetonitrile (pH 2.5)	< 1 μg/L	***26***
Organic amines	Sweeping-MEKC (×500-700)	50 m*M* SDS in 10 m*M* phosphate-20 m*M* borate buffer (pH 7.0, 4.0 mS/cm)	0.4−0.6 mg/L	***27***
Aromatic amines	CSEI-sweeping-MEKC ($\times 10^4$ to 10^5)	5 m*M* SDS in 50 m*M* phosphoric acid, 5 m*M* triethanolamine, 50 m*M* urea and 20% acetonitrile (pH 2.0)	0.1 μg/L	***28***

(Continued)

Table 1
(Continued)

Analytes	Concentration principle (×enrichment factor)	Background electrolyte	Limit of detection	*Ref.*
Phenoxy acidic herbicides	Anion-selective exhaustive injection sweeping-MEKC (×100,000)	75 m*M* SDS in 25 m*M* phosphate buffer-20% acetonitrile and 1 *M* urea (pH 2.5)	100 ng/L	***29***
N-Methylcarbamate pesticides	Stacking-ESI-MS (NS)	40 m*M* SDS 20 m*M* ammonium acetate (pH 9.0)	0.04–2 mg/L	***30***
Dimethylarsinic acid, Monomethylarsonic acid and Arsenic acid	LVSS with buffer removal using polarity switching at 95% of normal current (×10–20)	20 m*M* phosphate buffer (pH 6.0)	NS	***31***
Monophenylarsinic acid, Monomethylarsonic acid Arsenic acid	LVSS with buffer removal using TTAB as a pump (×30–40)	0.41 m*M* TTAB in 20 m*M* phosphate buffer (pH 6.0)	NS	***32***
Herbicides	LVSS with high-conductivity sample matrix (NS)	20 m*M* SDS, 10 m*M* DOSS in 0.5 m*M* borate and 8% MeOH (pH 9.2)	0.13–2.73 μg/L	***33***
Arsenic compounds	NSM (NS), LVSS with polarity switching (×62), co-EOF with NSM (×11–15)	20 m*M* carbonate buffer (pH 10.0)	18–573 μg/L	***34***

Arsenic compounds	FASS and LVSS with polarity switching (NS)	15 m*M* phosphate buffer (pH 6.5)	11–479 μg/L (LVSS)	***35***
Industrial dyes (hydrolyzed Remazol dyes)	Stacking with reverse polarity (NS)	6 m*M* DETA in 20 m*M* borate buffer and 10% acetonitrile (pH 9.26)	1.0×10^{-6} –2.5×10^{-6} mol dm^{-3}	***36***
Metal ions (Fe^{2+} and Fe^{3+} in water)	LVSS with buffer removal using TTAB as a pump (×50)	0.25 m*M* TTAB in 5 m*M* 2,6-PDCA and 5% acetonitrile (pH 4.0)	<0.1 μ*M*	***37***

[a]Using a Z-shape detector cell.

[b]Combined with solid-phase extraction.

NS, not stated; SRMM, stacking with reverse migrating micelles; SDS, sodium dodecyl sulfate; SRW, SRMM with water; CD, cyclodextrin; FASI, field-amplified sample injection; CDEKC, cyclodextrin-modified electrokinetic chromatography; SRMP, reverse migrating pseudostationary phase; LVSS, large volume sample stacking; FASS, field-amplified sample stacking; EOF, electroosmotic flow; RMM, reverse migrating micelles; REPSM, reverse electrode polarity stacking mode; CSEI, cation selective exhaustive injection; ESI, electrospray ionization; MS, mass spectrometry; NSM, normal stacking mode; DOSS, dioctyl sulfosuccinate.

concentration methods, as most of the former do not require instrumental modification—the separation channel (capillary column) is also the preconcentration channel. The majority of these techniques have a common objective of changing the velocity (ν) of the sample analyte ions, within the sample introduction zone, by some maneuver that involves changing the field strength, the charge, or the ionic shell to achieve sample concentration, based on the following formulae:

$$\nu = \mu H \tag{1}$$

$$\nu = q/6\pi\eta r \tag{2}$$

where μ = electrophoretic mobility, H = field strength, q = charge on the molecule, η = viscosity, and r = ionic radius ***(43)***.

In all of the stacking techniques, having a discontinuous buffer, of different kinds, is the basic means for altering the charge and field strength to modify the ion velocity, which leads to sample concentration. Buffer discontinuity can be brought about in a very simple manner by altering the sample conductivity or pH, so that it is different from that of the separation buffer.

1.1.1. Field-Amplified Sample Stacking or Normal Stacking Mode

Field-amplified sample stacking (FASS) or normal stacking mode (NSM) is one of the earliest on-column sample concentration techniques in high-performance capillary electrophoresis (HPCE), first introduced for ionic analytes in CZE by Mikkers et al. ***(44)***. In this method, a long plug of low concentration buffer (or water, which functions as an extremely diluted buffer) containing analytes to be separated is introduced hydrodynamically (giving the mode known as sample stacking) or electromigration (the field amplified sample injection mode) into the capillary pre-filled with buffer of the same composition but of a higher concentration. This establishes a discontinuous electrolyte system, with sample ions in the low ionic strength buffer zone, and results in discontinuity of some basic parameters, especially of electric field strength and electroosmotic flow (EOF) velocity, that are increased compared with their values in the original background electrolyte (BGE) zone. Sample stacking is defined as the movement of sample ions towards and across a boundary zone that separates the region of the injected sample buffer from the rest of the column containing the running buffer, such that sample ions are collected or concentrated at the boundary. Because of the matrix difference between those two regions, the ions experience a lower electric field in the running buffer region than in the sample region. Thus, the velocity of the ions decreases as they cross the boundary. The slower-moving ions will "stack up" in a narrow zone, thereby increasing the concentration in the sample zone. This

focused zone of ions then electrophoretically migrates through the separation buffer and separates into individual zones by conventional CZE. The stacking mechanism occurs for both positively and negatively charged species. For conventional polarity operation (anode = injection end), the positive species stack up in front of the sample plug and the negative species stack up at the back of the sample plug. The neutral compounds are left uncharged in the sample plug and coelute without any stacking (i.e., they are not concentrated). If the analytes pass the boundaries to the separation buffer compartment, their electrophoretic separation begins. Because the EOF velocity in the separation compartment is higher than the electrophoretic velocities of the analytes, the anions and the cations as well as the sampling compartment are pushed to the cathode. The basic principle of sample stacking of anions is summarized in **Fig. 1.**

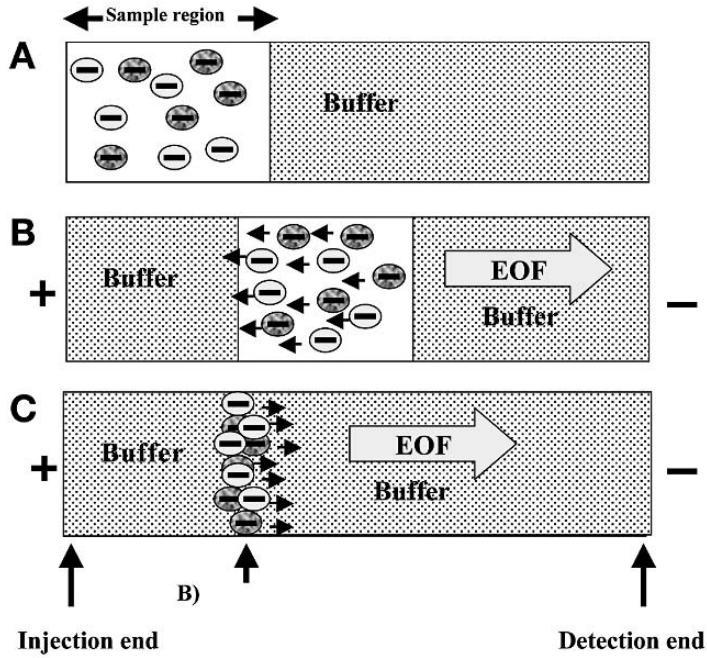


Fig. 1. Schematic representation of the normal sample stacking: **(A)** hydrodynamic injection of sample (prepared in water or low conductivity buffer), after conditioning the capillary with running buffer; **(B)** application of voltage at positive polarity with the running buffer in the inlet and outlet vials (the arrows indicate direction of stacking of analyte anions); **(C)** starting separation of stacked zone, orginally focused at point B.

Theoretically, the amount of stacking for a given sample is proportional to the field enhancement ratio; the larger the difference in buffer concentrations (ionic strength), the narrower the peak (less dispersion in the stacked zone) and the greater the amount of stacking. An extrapolation can be made that a rather long sample plug prepared in water or very low concentration buffer should give stacked ions in a narrowest possible zone in the higher concentration separation buffer. However, a laminar flow (backpressure effect) is generated inside the column caused by the mixing of low-conductivity and high-conductivity areas at the concentration boundary. The laminar flow will broaden the sharp zone generated by the stacking process. The larger the difference in concentration will result in a larger laminar flow. Stacking and broadening work against each other, creating an optimal length of water plug that can be introduced into the column and still achieve high resolution ***(45)***.

Chien and Burgi ***(46)*** investigated the case of field-amplified sample injection, where samples were prepared in a low-conductivity buffer and injected electrically into the column; the number of positive ions injected was proportional to the field enhancement factor at the injection point. The negative ions were not enhanced, but were pushed away from the column by this high field strength. However, because the electroosmotic velocity of the bulk solution is much slower than the electrophoretic velocity of sample ions under the enhanced field, one can inject and concentrate both positive and negative ions into the column by switching polarity of the electrodes at the proper time.

Kruaysawat et al. ***(20)*** found that the sensitivity of detection could be improved around 10 times (as can be seen in **Fig. 2**) for the separation of chlorophenols and chlorophenoxy acids using normal stacking mode.

da Silva et al. ***(6)*** presented on-line preconcentration strategies, sweeping and stacking with reverse migration of micelle (SRMM) for the multi-residue analysis of pesticides in drinking water and vegetable extracts using micellar electrokinetic chromatography (MEKC). Enrichment factors of 3- to 18-fold were obtained using a BGE composed of 20 m*M* phosphate buffer at pH 2.5, containing 25 m*M* sodium dodecyl sulfate (SDS) and 10% methanol.

1.1.2. Large Volume Sample Stacking

To overcome a limitation in NSM (i.e., the short optimum sample plug length that can be injected into the capillary without the loss of efficiency or resolution), the possibility of using large injection volume in CE has been evaluated. When the long plug of sample injected is greater than that of optimum found in NSM, the sample matrix must be pumped out from the capillary before the electrophoretic separation begins, in order to preserve

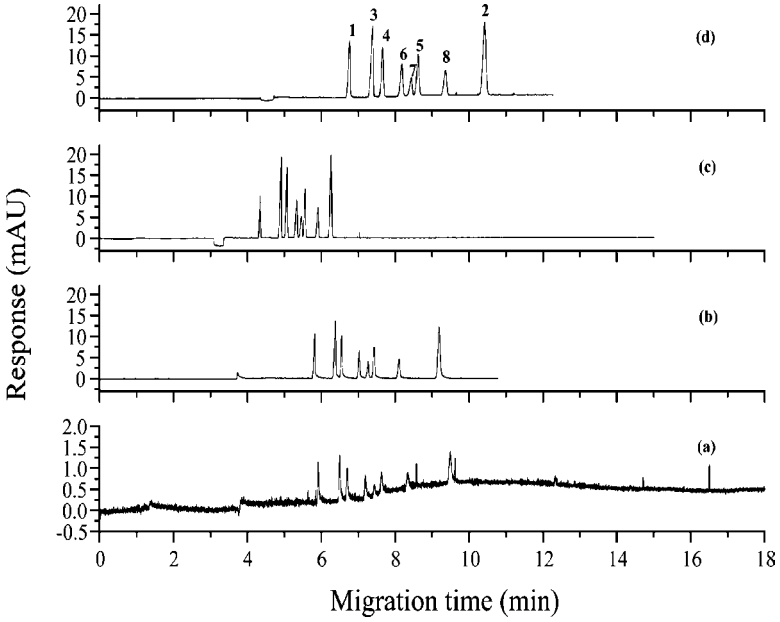


Fig. 2. Electropherograms showing the separation of chlorophenols and chlorophenoxyacetic acids by normal stacking mode in comparison to standard injection (5 s). Buffer composition; 35 m*M* borate-60 m*M* phosphate buffer pH 8.65 containing 2 m*M* β-CD, 214 nm, L = 64.5/56 cm effective length. Peaks identification: 1 = 2,4-DCP, 2 = 2,6-DCP, 3 = 2,4,6-TCP, 4 = 2,4,6-T, 5 = 2,6-D, 6 = 2,4-D, 7 = 4-ClPAA, 8 = 2-ClPAA (*see* **Table 2** for details). Panel **A** is expanded vertically 10 times for comparison purposes.

separation efficiency. Many researchers described the normal stacking mode, in which a large plug of sample dissolved in a lower concentration buffer or water is injected to stack anions in such separation conditions. An alternative to the above sample stacking method is termed the "large volume sample stacking" (LVSS) procedure ***(47,48)***. The direction of pumping, which can be

Table 2
Experimental Parameters Used for Fig. 2

Parameters	Fig. 2A	Fig. 2B	Fig. 2C	Fig. 2D
Applied voltage (kV)	25	25	30	25
Concentration (mg/L)	5	50	5	5
Injection time (second)	5	5	50	50

controlled with the external pressure or with the EOF, is always opposite to the electrophoretic movement of charged analytes. Therefore, the velocity of pumping must be lower than that of the velocity of the charged analytes. LVSS will effectively concentrate either positively or negatively charged analytes in a given experiment.

Using the EOF as a pump, the maximum percentage filled length of the column that is possible without loss of any analytes (χ_{max}) is given by the following equation:

$$\chi_{max} = -\mu_{ep}/\mu_{eof} \quad (3)$$

where μ_{ep} and μ_{eof} are the electrophoretic mobilities of the charged analytes and the coefficient of EOF, respectively ***(45)***. For example, if the electrophoretic mobility of the analytes is half of the electroosmotic mobility of the buffer, the fraction of the capillary filled with sample solution should be up to 50%.

There have been several excellent review articles published recently on the theory and applications of LVSS. These methods have been used to concentrate and investigate charged analytes, such as drugs, dyes, chemicals of environmental concern, and other applications. Smyth et al. ***(49)*** reported LVSS with hydrodynamic injections of up to 240 s can be used to significantly decrease the LODs of selected cationic basic drugs, such as clenbuterol, nacrotine, flurazepam, codeine, and pethidine, by CZE. In addition, they investigated whether cationic and anionic chelates can also be subjected to LVSS. Tu et al. ***(16)*** performed LVSS as an on-capillary sample concentration method in CZE for the investigation of effect of NaOH on LVSS of haloacetic acids. Moreover, Liu et al. ***(50)*** developed MEKC coupled with on-line LVSS to analyze plant hormones including gibberellic acid, abscisic acid, indole-3-acetic acid, α-naphthaleneacetic acid, 2,4-dichlorophenoxyacetic acid, kinetin-6-furfurylaminopurine, and N^6-benzyladenine.

1.1.2.1. LVSS with Polarity Switching

LVSS was first developed by Burgi and Chien ***(48)*** in the polarity switching form and is illustrated in **Fig. 3.** At the beginning, a substantial part of the separation capillary is occupied by a sample dissolved in a low-conductivity matrix that is introduced hydrodynamically into the capillary (up to 90% of the capillary may be filled with sample) and a negative voltage is applied at the injection extremity so that the EOF is directed to the injection end of the capillary. The large solvent plug is then electroosmotically pushed out of the column while the negative species stack-up at the boundary between the sample zone and the background electrolyte. Thus, the stacking and removal of solvent occurs concurrently. When the sample buffer is almost completely

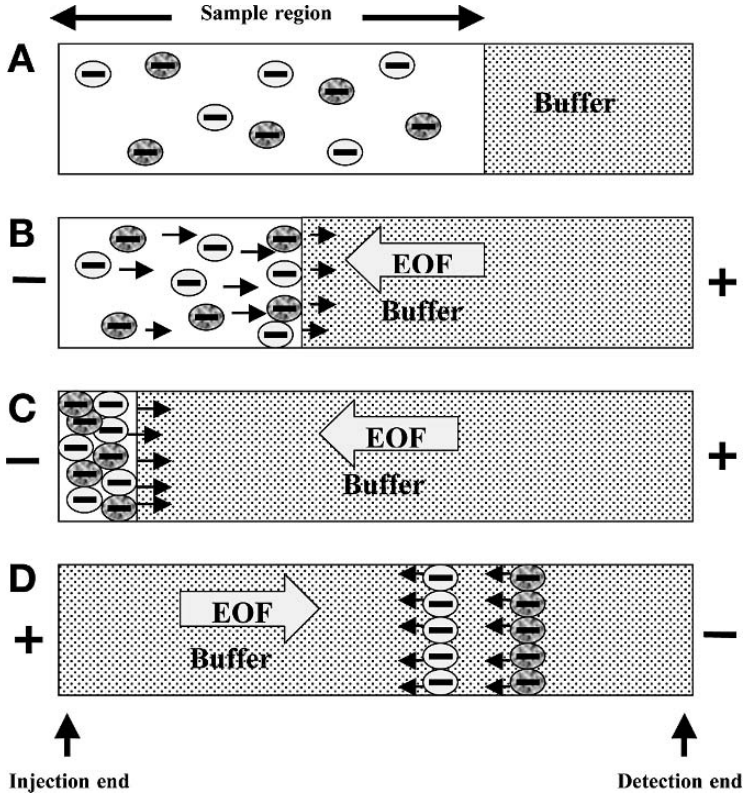


Fig. 3. Schematic representation of the large volume sample stacking with polarity switching: **(A)** large volume of sample (prepared in low conductivity buffer or water hydrodynamic injection, no voltage is used; **(B)** reverse voltage is applied to the capillary so that the analytes stack on the rear boundary between the sample and the running buffer, which moves back towards the inlet as a result of the electroosmotic flow [EOF]; **(C)** sample matrix is pushed out of the column while the capillary column retains the anions; **(D)** polarity is switched to normal when current reaches 90–95% of the original value, and the stacked analytes separate normally in a counter EOF mode.

out of the column (which can be determined by monitoring the electric current, usually defined as 80–95% of the normal level), the polarity is reversed back to the normal configuration and separation of the negative species can proceed.

While LVSS with polarity switching is a significant development in the improvement of detection sensitivity, there are some procedural problems regarding the method. First, it is essential that the current be monitored correctly to ensure that no anions are lost from the capillary inlet during the removal of

sample matrix. Second, analytes must possess mobility greater than that of the EOF in the sample zone, otherwise they will be pushed out from the capillary. Third, automatic polarity switching may not be possible in all commercial instrumentation.

The quantitative analysis of anions with polarity switching has been reported by Albert et al. ***(31)***. They investigated large-volume stacking by injection under high vacuum for 12 s, followed by the removal of the large plug of low-conductivity sample matrix out of the capillary using polarity switching. A 10- to 20-fold sensitivity enhancement can be reached for the quantitative analysis of highly diluted samples in low-conductivity matrices. Chen and Ding ***(40)*** employed LVSS with electrode polarity switching to investigate the optimal conditions for analyzing the positional isomers of multi-charged naphthalenesulfonate compounds by cyclodextrin-mediated CE. Significant sensitivity improvement was observed and a more than 100-fold enrichment was achieved based on peak area.

1.1.2.2. LVSS without Polarity Switching

Burgi ***(51)*** showed that the limitations of LVSS with polarity switching can be overcome by using the EOF modifier, diethylenetriamine (DETA), added to the BGE to reverse the EOF. The mechanism, which involves pumping the sample matrix out of the capillary, is illustrated in **Fig. 4.** After the sample is introduced into the column, DETA in the BGE (but not in the sample solution) dissolves or desorbs from the capillary wall into the water of the sample zone, and causes the direction of EOF to be toward the capillary inlet (cathode end). The surface of capillary wall will be recoated with modifier, supplied by the BGE, as the electrolyte is drawn through the capillary from the detection end. This gradually slows down the EOF in the sample zone, finally reversing its direction toward the anode, at which stage sample matrix removal stops and the analytes are then separated in the normal manner.

It can be concluded that for the separation of anions, the EOF should be reduced or should always be lower than the electrophoretic velocity of the analyte achieved by adding a buffer additive to the BGE. For cations, aside from reducing the EOF, the direction of the EOF should also be reversed. A reduced and reversed EOF can be achieved by using a low pH buffer containing a low concentration of cationic surfactant or using specially coated capillaries. Using an EOF modifier and/or adjusting the pH, the analysis of anions ***(51,52)*** and cations ***(53)*** separately can surpass the performance of the polarity-switching process, which is not accessible in every commercial instrument, and can cause irreproducibility.

Albert et al. ***(32)*** also evaluated a method of large volume stacking without polarity switching, but with removal of the large plug of low conductivity

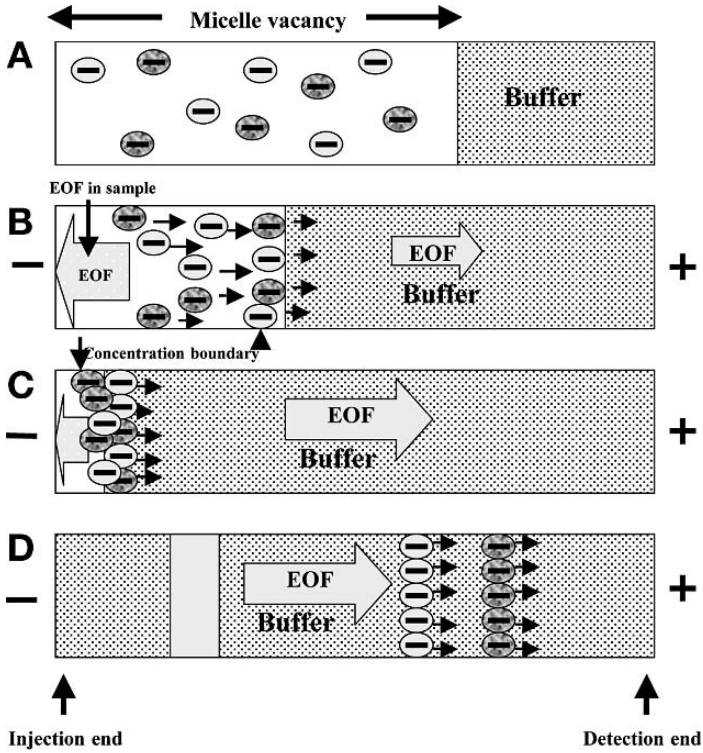


Fig. 4. Schematic representation of large volume sample stacking without polarity switching (surfactant dissolution used to remove sample matrix): **(A)** large volume of sample (prepared in low conductivity buffer or water hydrodynamic injection, no voltage is used); **(B)** voltage is applied to the capillary so that the analytes stack on the rear boundary between the sample and the running buffer (this boundary moves towards the inlet as the electroosmotic flow [EOF] in the sample is of higher magnitude and opposite direction to that in the running buffer); **(C)** as the sample matrix is removed, the speed as which the concentration boundary moves is reduced as more of the capillary has a reversed EOF; **(D)** when almost all of the sample matrix is removed, the concentration boundary stops and reverses its direction, after which the analytes separate as in the normal configuration.

matrix achieved using the redissolution of an EOF modifier (tetradecyltrimethyl ammonium bromide) that will act as an EOF pump. In this case, there is no need for polarity switching.

A novel approach for sample matrix removal of high-ionic-strength samples was presented by Zhao et al. ***(54)***. It was found that when using a microbore LC system with a C_{18} reversed-phase material packing to separate analytes from

the high-ionic-strength matrix, sample anions could subsequently be introduced into a capillary in a low-conductivity sample zone, and this zone concentrated according to the FASS principle. This realized a 500-fold enhancement in sensitivity of detection over conventional injection.

He and Lee ***(55)*** reported a convenient methodology for LVSS in acidic buffer for analysis of small organic and inorganic anions by CE without intermediate polarity switching. In their work, EOF was suppressed simply by adjusting pH at the acidic range so that the EOF was slower than the electrophoretic mobilities of the analytes, allowing stacking and separation to proceed simultaneously. An effect similar to that achieved using an EOF modifier was also brought about by Quirino and Terabe ***(52)*** using a BGE pH of 2.5. In this case, as the pH of the sample is higher than that of the BGE, and there is a greater EOF in the sample zone, which can remove the sample matrix out of the capillary column. The potential of this method for preconcentration of fast-moving inorganic anions, such as bromide, nitrate, and bromate, was demonstrated by a 100-fold increase in sensitivity of detection.

1.1.3. Field-Amplified Sample Injection

An alternative approach toward increasing the amount of charged analytes introduced is to use electrokinetic (or electromigration) injection, in which analytes migrate into the capillary under an applied electric field. Electrokinetic injection itself can be considered to be a form of preconcentration, and its greatest potential is when combined with FASS. It has been termed different names, such as field-amplified sample injection (FASI) ***(56)***, field-enhanced sample injection (FESI) ***(52)***, head-space FASS ***(57,58)*** and electro-stacking ***(59)***. The sample is prepared in diluted buffer, and is similar in all forms to FASS with the exception of the sample injection step. Analytes are injected under an electric field and the low conductivity of the sample zone causes it to adopt a high field strength. Therefore, ions migrate rapidly across the sample zone and stack at the sample/buffer boundary zone in a similar fashion to FASS. Sensitivity improvements especially are achieved for small, highly charged solutes, such as metal ions and inorganic anions.

Sample stacking with electrokinetic injection provided larger sensitivity enhancements than those of hydrodynamic injection as a result of the fact that, in hydrodynamic injection mode, the injected amount of sample will be limited by the volume of sample solution that can be injected, whereas in electrokinetic mode, the injection period can be extended to provide greater sampling of analyte ions into the capillary. However, only either positive or negative ions can be concentrated effectively using a single electrokinetic injection. This is a similar problem to that encountered with LVSS. For example, only positive ions can be injected and concentrated when the negative electrode is at the

outlet end during electrokinetic injection. Chien and Burgi ***(46)*** investigated how both cations and anions can be injected and concentrated in the capillary column in a single run by employing the proper polarity of the electrodes during injection. Unlike the other forms of sample stacking, the application of this technique was not extended to any sample ions. In many cases, a water plug is introduced prior to beginning electromigration injection. The water plug provides an enhanced electric field zone for effective stacking. A useful discussion on current views on the necessity of a water plug can be found in a review by Quirino and Terabe ***(60)***, who stated that a short plug of water before electrokinetic injection of the sample provides proper electric field enhancement at the injection point and renders an empty region to concentrate ions deeper into the column and away from the inlet end.

Sample stacking using FASI in CZE in the analysis of phenolic compounds was investigated by Martínez et al. ***(11)***, who found the limit of detection to be in the μg/L range.

1.2. Sweeping

Sweeping, a more recent on-line sample concentration technique in EKC, is defined as the sorption and accumulating of analyte molecules by a pseudostationary phase (PS) that enters and fills the sample zone upon application of voltage ***(61)***. This phenomenon, initially observed by Gilges ***(62)***, was, however, not further studied until more recently. It occurs whenever the sample matrix is void of a charged carrier phase, and it operates irrespective of whether the sample matrix has a conductivity that is higher than, similar to, or lower than that of the background electrolyte. In sweeping, the analyte zones are narrowed or focused as a result of the chromatographic or partitioning mechanism that the sample molecules experience, causing their sorption into the pseudostationary (PS) phase zone. **Figure 5** shows the schematic representation of neutral micelles (PS) and analyte molecules during sweeping under the suppression of EOF.

In sweeping, the length of the resulting zone after sweeping (l_{sweep}) is given by ***(61)***

$$l_{sweep} = l_{inj}\frac{1}{1+k} \tag{4}$$

Where l_{inj} is the length of the injected sample zone and k is the retention factor of analyte. The k values in the sample zone when filled with PS are assumed equal to those in the separation zone. Sweeping enhancement is then basically dependent on the retention factor and the length of the initial zone.

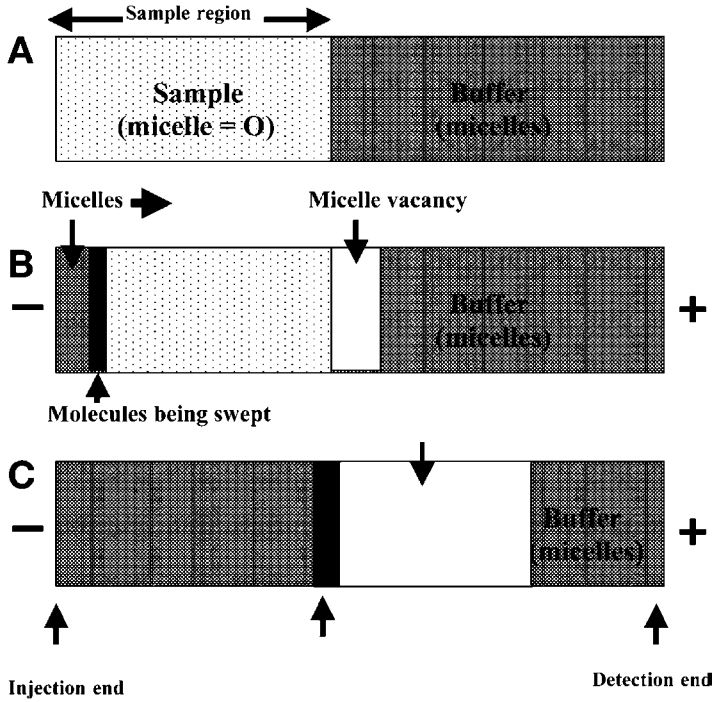


Fig. 5. Schematic representations of sweeping of neutral molecules under the suppressed electroosmotic flow. **(A)** Starting situation: a longer-than-typical injection of sample solution prepared in sample matrix having conductivity similar to the anionic micelles background solution (running buffer). **(B)** Application of voltage at negative polarity: micelles enter the sample region and sweep (concentrate) the analyte molecules. **(C)** The injected analyte zone is assumed completely swept and separated in the micellar zone following the concentrated sample zone by micellar electrokinetic chromatography, because the micelle migrates faster than neutral analytes. The micellar vacancy zone migrates ahead of the analytes zone.

Several papers have been published on the use of this concentration technique in MEKC. Quirino et al. ***(61)*** reported exceeding 5000-fold concentration of dilute analytes in MEKC using sweeping as an on-line concentration technique without off-line treatment. Quirino et al. ***(13)*** developed the sample concentration technique by sample stacking and sweeping using microemulsion and a single isomer sulfated β-CD as pseudostationary phase in MEKC. Monton et al. ***(24)*** used the sweeping technique for on-line preconcentration of charged analytes in MEKC with nonionic micelles to yield peak height enhancements up to 100-fold. Núñez et al. ***(26)*** reported analysis of the herbicides paraquat, diquat and difenzoquat in drinking water by MEKC using

sweeping and cation selective exhaustive injection (CSEI-sweeping-MEKC). More recently, the sweeping principle has been extended to CZE separations of neutral solutes involving complexation reaction of *cis*-diols with borate to generate a dynamic charge on the solutes, demonstrating the versatility and wide applicability of the sweeping technique ***(5)***. Again, Quirino et al. ***(25)*** have explained the concentrating mechanism in MEKC when the sample matrix is a high-resistivity nonmicellar aqueous solution. Theoretical and experimental studies were undertaken. It was found that the total focusing effect is brought about by the cumulative effect of sweeping and sample stacking. For better analytical results, compounds showing low to moderate retention factor (k) and compounds showing high values of k must be dissolved in low and high conductivity matrices, respectively.

The concept of sweeping neutral analytes applying a high-salt-containing matrix or under a reduced electric field in MEKC using anionic micelles, and in the presence of EOF, was presented by Quirino et al. Three important processes were identified. First, stacking of the micelles at the cathodic interface between the sample solution and background solution zone was identified, then followed by the sweeping of the analyte molecules by the stacked micelles that enter the sample zone. Finally, the destacking of the stacked micelle at the anodic interface between the sample and background electrolyte zones occurred ***(63)***. The reason that high-salt-concentration sample matrices can produce a high concentration efficiency may be that retention factors are significantly increased in high-salt concentration matrices ***(5)***.

Lately, microfabricated fluidic devices (microchips) have received much attention and have been successfully demonstrated for CE. In particular, on-line concentration by sweeping was successfully applied to microchip MEKC for the analysis of rhodamine B by Sera et al. ***(64)***.

1.3. Selective Exhaustive Injection Sweeping

Recently, a combination of two on-line preconcentration procedures, sample stacking and sweeping, referred to as cation- or anion-selective exhaustive injection sweeping (CSEI or ASEI), has achieved almost a million-fold enhancement in detector response for cationic hydrophobic analytes ***(65)***. SEI is FESI or sample stacking with electrokinetic injection performed for a longer period of time than is typical. This method was presented by Quirino and Terabe. They devised a mixed mode for the further stacking of analytes in which the sample is concentrated first by field-amplified injection under nonmicellar conditions. The buffers are changed, and the polarity is reversed to induce sweeping of the analytes into a micellar (SDS) solution, giving about a million-fold increase in sensitivity for some cations. **Figure 6** illustrates the

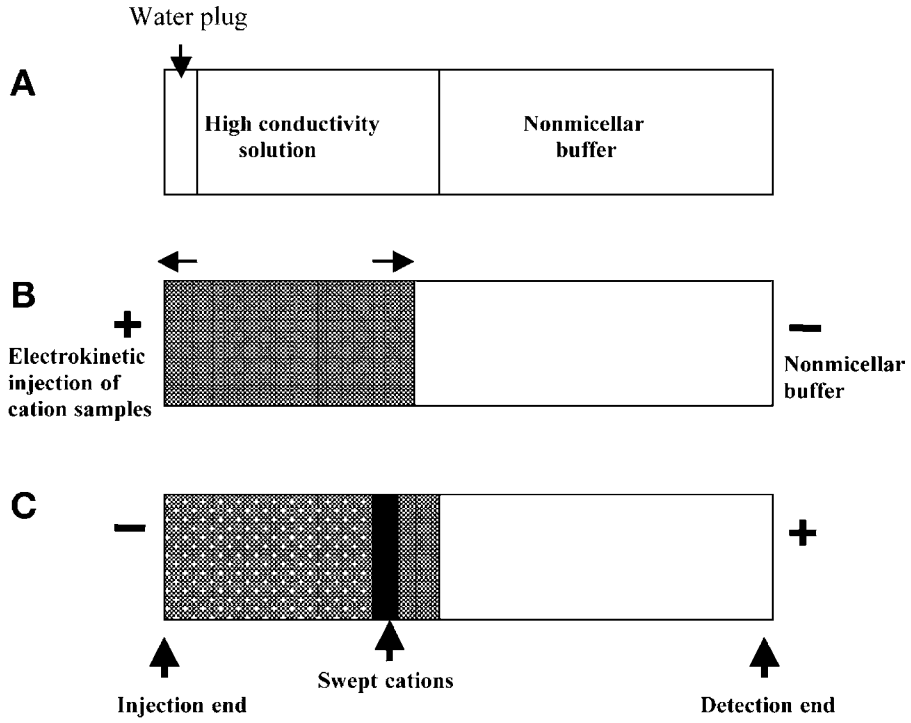


Fig. 6. Schematic representations of cation selective exhaustive injection-sweep-micellar electrokinetic chromatography. **(A)** Starting situation: the capillary is first conditioned with a nonmicellar buffer, after which a zone of high-conductivity buffer containing no micelles (HCB) and then a short plug of water are introduced hydrodynamically. **(B)** The cation sample prepared in a low-conductivity solution is introduced by electrokinetic injection at positive polarity for a longer period than usual. **(C)** Injection is stopped and micellar buffers are placed at both end of the capillary; this is followed by application of a voltage at negative polarity for the normal separation.

model of CSEI-sweep-MEKC. In **Fig. 6A**, a zone of high-conductivity buffer (HCB) free of micelles, and a short plug of water, are introduced with hydrodynamic injection. The water plug helps maintain field enhancement at the tip of the capillary, especially when the sample matrix contains salt, and may also improve reproducibility ***(5)***.

Here, the cation analytes are stacked prior to being swept and separated in the micellar BGE. In **Fig. 6B**, the cation sample prepared in a low-conductivity solution is injected electrokinetically at positive polarity. The sample cations enter the capillary through the water plug with high velocities. When the cations reach the interface between the water and HCB zone, they will slow down

and focus at this interface. In **Fig. 6C**, once the separation voltage is applied at negative polarity with the micellar BGE in the inlet vial, anionic micelles enter the capillary and sweep the analytes. The stacked cations are completely swept by the micelle and are separated by MEKC in the reverse migration mode. It should be noted that in CSEI. EOF is significantly suppressed under acidic conditions with anionic micelles, such as SDS. The principle of ASEI-sweep-MEKC technique is basically the same as CSEI, but the procedure is slightly modified. To suppress EOF, a polyacrylamide (PAA)-coated capillary is employed for the presence of cationic micelles. The polarity for injection and separation is reversed compared to a CSEI. CSEI and ASEI techniques are not applicable to neutral analytes.

Núñez et al. ***(26)*** presented the efficiency of CSEI as an on-line concentration method for the analysis of quaternary ammonium compounds **(Fig. 7)**. CSEI-sweep-MEKC was successfully applied to the determination of three herbicides in spiked tap water below the level established by the US Environmental Protection Agency. SEI in the mode of ASEI could also apply to some aromatic carboxylic acids, dansyl amino acids, and naphthalenedisulfonic acids, and about 1000- to 6000-fold increases in detection sensitivity were obtained in terms of peak heights ***(66)***. Zhu et al. ***(29)*** reported a method that could obviate the need for a coated capillary by using a low pH (2.5) BGE to suppress the EOF in ASEI technique. This method afforded about 100,000-fold improvement in peak height for some phenoxy acidic herbicides.

1.4. Isotachophoresis

Isotachophoresis (ITP) is an electrophoretic technique that is carried out in a discontinuous buffer system. In this procedure, a small quantity of sample is introduced at the interface of a discontinuous buffer system, consisting of a leading (L) and a terminating (T) electrolyte as illustrated in **Fig. 8**. The leading electrolyte contains a high concentration of a high-mobility ion of like charge to the analytes of interest and the terminal electrolyte contains an ion of lower mobility than that of the analytes. Upon the application of voltage, a steady-state migration will be established in which the analytes migrate as consecutive zones. ITP can be used as a preconcentration technique for diluted samples in CZE ***(3,67)***. This is done after injection of the sample, so that the components from a relatively broad sample segment can be stacked into very narrow zones before the separation begins. The requirement for successful ITP stacking is to find suitable leading and terminating ions. Isotachophoretic preconcentration can be performed in a coupled-capillary or single-capillary approach (on-column).

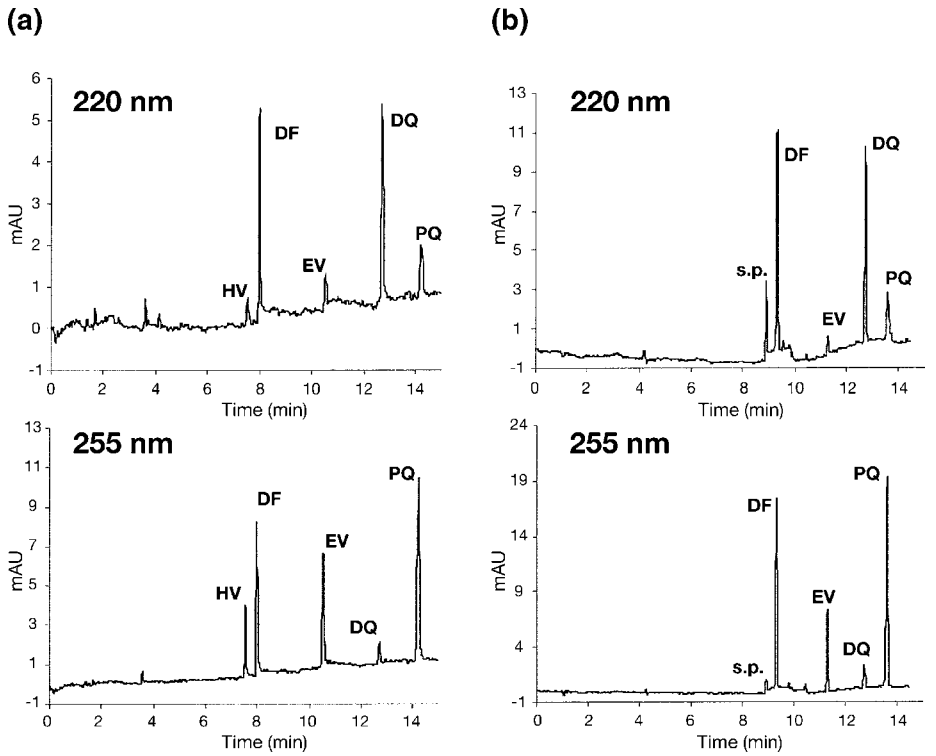


Fig. 7. Conventional micellar electrokinetic chromatography (MEKC) and cation selective exhaustive injection (CSEI)-sweeping-MEKC of quaternary ammonium herbicides. Nonmicellar background electrolyte (BGE): 100 m*M* phosphate buffer (pH 2.5) containing 20% acetonitrile; micellar BGE: 80 m*M* sodium dodecyl sulfate in 50 m*M* phosphate buffer (pH 2.5) containing 20% acetonitrile; HCB: 200 m*M* phosphate buffer (pH 2.5); conditioning solution before injection, (a) micellar BGE, (b) nonmicellar BGE: (a) MEKC: sample prepared in BGE; sample concentration, 100 mg l^{-1}; injection time, 1 s at 5 kPa. (b) CSEI-sweeping-MEKC: sample prepared in water; sample concentration, 10 μg l^{-1} PQ, DQ and EV, 50 μg l^{-1} DF. Injection scheme: hydrodynamic injection of HCB for 200 s (5 kPa), hydrodynamic injection of water for 6 s (5 kPa), electrokinetic injection of sample for 400 s (+22 kV); separation conditions (a) and (b): separation voltage, -22 kV with the micellar BGE at both ends of the capillary. s.p. = system peak. (Used with Permission from Elsevier ***(26)***.)

The application of ITP as a stacking procedure prior to the CZE analysis is the most effective method. Even large volumes of sample can be preconcentrated during the ITP step; trace amounts of analytes can be stacked in a very sharp and short ITP zone between L and T electrolyte. The potential of this technique for environmental trace analysis of herbicides, such as diquat

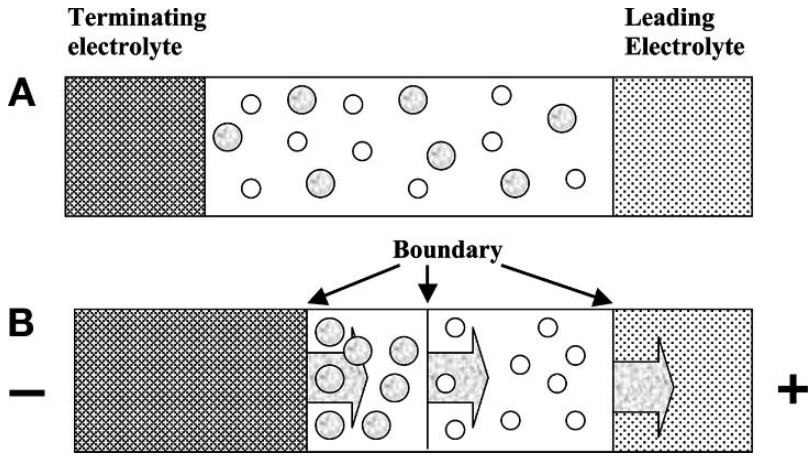


Fig. 8. Schematic representations of isotachophoresis stacking. **(A)** Sample solution is placed between a leading and terminating electrolyte. **(B)** After the application of voltage, analytes migrate as discrete zones.

and paraquat, and for other polar pollutants, has been shown by Kaniansky et al. ***(68)***. In the former case, a number of tap waters spiked with these compounds at 10^{-8} mol/L concentration levels were analyzed. The minimum detectable concentration of these analytes can be reduced by a factor of 10^3–10^4 when using the ITP coupled-column approach.

1.5. Stacking Efficiency

Stacking efficiencies in terms of peak height (SE_{height}) for each test analyte were computed to evaluate quantitatively the degree of stacking. A stacking efficiency of 10 and 100 is comparable to one and two orders of magnitude improvement in concentration detection limit, respectively ***(69)***. It is expressed as the ratio of the height obtained with stacking, H_{stack}, versus the height obtained with a normal CE injection, H, where the same sample solution is used.

$$SE_{height} = \frac{H_{stack}}{H} \tag{5}$$

The percentage of sample effectively stacked into a peak from the total volume of sample injected (%SE) is then described by **Eq. 6** ***(70)***.

$$\%SE_{height} = \frac{SE_{height}}{SE_{height}(\text{expected})} \times 100\% \tag{6}$$

Table 3
Comparison of Stacking Efficiencies and Reproducibility for Preconcentration Methods (Adapted from ref. *71*)

Technique	Limit of detection	Stacking efficiency (x-fold increase in peak height)	Reproducibility (RSD peak height, n≥3)
FASS	80 n*M*	1000	3–6% 2.5–25%
LVSS (pH-mediated)	2 ng/L	100	5–12%
	35–50 μ*M*	8–20	1.4–8.8%
	300 n*M*	66	1.4–1.7%
LVSS (polarity switching)	0.6–10 n*M*	500–7000	10%
ITP—single capillary	50 n*M*	100–200	0.7–1.5%
ITP—double capillary	10 n*M*	300–10000	0.3–2.6%
FASS with MEKC	15.5–21.6 ng/L	28–102	1.2–4.6%
Sweeping	1.7–9.6 ng/L	88–5044	3.9–13.8%

See **Table 1** for definitions.

where SE_{height} (expected) is the expected stacking enhancement factor base on peak height.

In conclusion, several methods of on-line sample preconcentration in CZE and MEKC are now available. These should cover most of the applications of interest to routine users. Moreover, the understanding of the on-line sample preconcentration mechanism will provide effective application of the techniques to a variety of classes of compounds of interest (i.e., pharmaceutical, biomedical, and environmental), especially for diluted solutions. Therefore, such a capability will result in an extension of utility of CE as a powerful and broadly applicable analytical technique. **Table 3,** which was taken and adapted from Osbourn et al. review paper ***(71)***, shows the comparison of stacking efficiencies and reproducibility for preconcentration methods.

2. Case Study: Manufacture of 2,4-D

This section considers a specific example of sample stacking used for various process steps for the analysis of chlorophenoxy acid herbicides and

related chlorophenols during the manufacture and subsequent purification of 2,4-dichlorophenoxy acetic acid (2,4-D). Various solutions in the analysis protocol, such as in process clarifier overflow water, require sample stacking for improved detection limits. **Figure 9** shows the sampling points in an abbreviated schematic diagram of the process. It should be noted that the experimental procedure and materials (capillaries, chemicals, buffer) is included here for completeness. The value of CE is that all key components of the analysis can be analyzed in the one analytical run, within about 5 min. Because the sample contains free acids and phenols, conventional methods such as GC (with derviatization) or reversed-phase HPLC with appropriate buffer choice to suppress ionization of the acid (and even then, the satisfactory analysis of the two classes of compounds within reasonable time can be problematic), can be tedious; hence, this is a suitable analytical task for investigation using CE. The only consideration is whether the analyzed sample has components of interest whose concentrations can be adequately measured by normal injection procedures, or which may require stacking injection to concentrate up minor constituents. The bulk synthesis pot may be tested during the manufacturing process to provide feedback as to reaction completeness, or to indicate whether additional reagent must be added to optimize the reaction or maximize product formation. Various steps in the subsequent (downstream) purification process will usually be targeted to ensure that undesirable or unwanted by-products or impurities are removed; discharge waters can be tested for levels of impurities to ensure compliance with discharge regulations. Each sample taken at selected

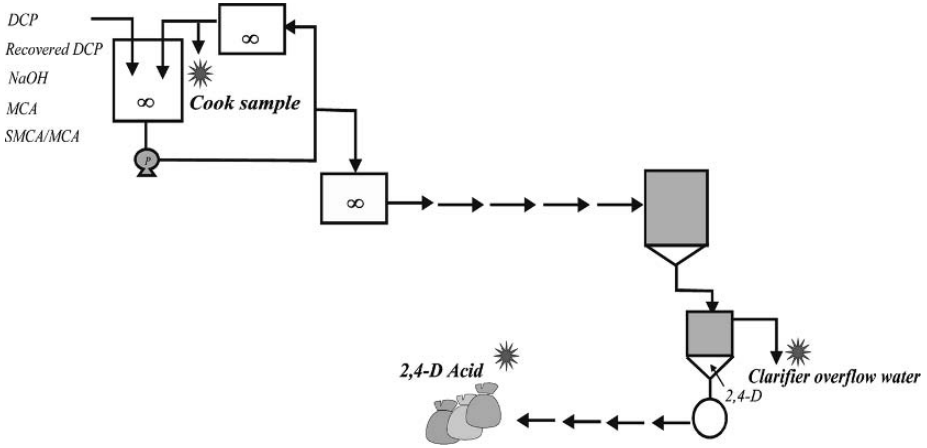


Fig. 9. Three capillary electrophoresis sampling points (asterisked) illustrated on a summary schematic diagram of 2,4-dichlorophenoxy acetic acid (2,4-D) manufacturing process: DCP, 2,6-dichlorophenol; MCA, monocarboxylic acid.

test points of the manufacturing sample process can thus be analyzed using the same CE run buffer system, but with varied injection protocols depending on whether regular or stacking injection is necessary at that step.

2.1. Equipment Details

2.1.1. CE Instrument

An Agilent ^{3D}CE instrument (Agilent Technologies, Burwood, Australia) was used for all capillary electrophoresis results reported here. An ABI 2000 CE instrument was used for some exploratory studied and initial optimization of buffer composition.

2.2. Capillary Columns

Uncoated fused silica capillary columns of 50 μm inner diamter (i.d.), 363 μm outer diameter (o.d.) capillary tubing was purchased from Supelco (Bellefonte, PA) and Polymicro (Polymicro Technologics, Phoenix, AZ). A wide variety of experimental parameters, such as the capillary column i.d., effective column length, running electrolyte composition, concentration, and sample plug-length, should be studied in order to achieve optimum separation conditions—here, speed of analysis, with acceptable resolution of neighboring components, were the primary considerations in selection of optimum conditions.

As an alternative column format, an extended light path column of length 64.5 cm (56 cm effective length) (Agilent Technologies) may be employed. The extended light path column, or bubble cell, incorporates a special capillary column design at the detection region that can be used to extend the optical pathlength without increasing the overall capillary area. The bubble i.d. is three times larger than the regular inner diameter. This yields nearly a threefold increase in response signal, as can be seen in **Fig. 10**.

2.2.1. Preparation of Capillary Columns

Capillaries used for analysis were prepared by cutting the appropriate length of uncoated fused silica capillary. Detection windows were created by either removing the polyimide coating using hot 97% sulfuric acid or burning it off using a gas flame at an appropriate distance from the outlet end of the capillary. A capillary window of about 0.5 cm was created to accommodate the light path slit on the detector of the CE instruments used. The new capillary columns were pressure-rinsed with 1 *M* NaOH for 15 min, followed by water for 30 min in order to activate the silica on the wall. The columns were treated with 1 *M* NaOH, then Milli-Q water, followed by the carrier electrolyte at the

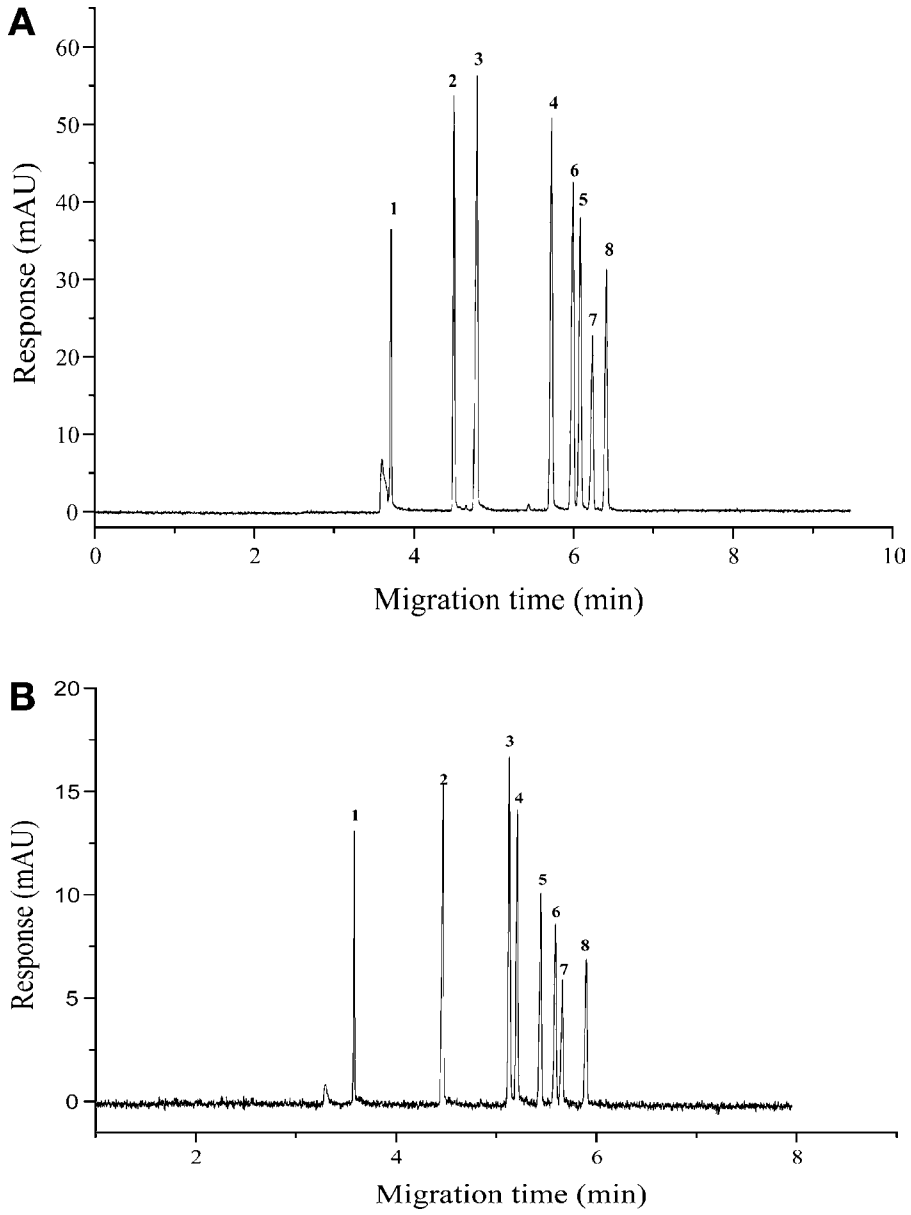


Fig. 10. Electropherogram of the separation of standard compounds. Conditions used: (a) extended light path column, 64.5/56 cm effective length; (b) normal straight capillary column, 64.5/56 cm effective length, 28.3 kV at 214 nm. Buffer compositions: 37 m*M* borate-60 m*M* phosphate pH 6.5 containing 1.62 m*M* TM-β-CD. Concentration of each compound: 50 mg/L. Peaks identification: 1 = 2,4-DCP, 2 = 2,6-DCP, 3 = 2,4,6-TCP, 4 = 2,4,6-T, 5 = 2,6-D, 6 = 2,4-D, 7 = 4-ClPAA, 8 = 2-ClPAA.

start of each working day. The following washing steps were used prior to each electrophoretic run: (1) water for 3 min; (2) background electrolyte for 3 min. The capillary column was cleaned daily by washing it with 1 *M* NaOH for 3 min and then water for 5 min.

2.3. Buffers and Chemical Standards

2.3.1. Chemical Standards

These were obtained from various sources as follows: β-cyclodextrin (β-CD), trimethyl-β-cyclodextrin (TM-β-CD), and dimethyl-β-cyclodextrin (DM-β-CD) were purchased from Aldrich Chemical Company (Milwaukee, WI). Carboxymethyl-β-cyclodextrin (CM-β-CD) (degree of substitution ≈ 3) was purchased from Cyclolab (Budapest, Hungary). 2-chlorophenoxy acetic acid (2-ClPAA), 4-chlorophenoxy acetic acid (4-ClPAA), 2,6-dichlorophenoxy acetic acid (2,6-D), 2,4-dichlorophenoxy acetic acid (2,4-D), 2,4,6-trichlorophenoxy acetic acid (2,4,6-T), 2,4,6-trichlorophenol (2,4,6-TCP), 2,6-dichlorophenol (2,6-DCP), 2,4-dichlorophenol (2,4-DCP), and commercial production samples were obtained from commercial sources (Nufarm Limited, Victoria, Australia).

2.3.2. Buffer Preparation

Following initial buffer optimization studies, a final mixed borate/phosphate buffer was chosen as the most appropriate for this study. It was prepared from separate stock buffers, with pH adjustment using phosphoric acid or NaOH as required. Stock 200 m*M* borate buffer was prepared in Milli-Q water using boric acid; stock 200 m*M* phosphate buffer was prepared from sodium dihydrogen phosphate and disodium hydrogen phosphate. Cyclodextrins (CDs) as the shape selectivity host additives were dissolved in mixed borate-phosphate buffer at concentrations as required. Stock solutions of 1.6 mg/mL of the standard phenoxy acetic acid and compounds recognized as possible impurities or interferences were prepared in 100% methanol. The stock sample was diluted with buffer giving a final concentration of 0.05 mg/mL for most studies. All solutions were filtered with 0.45 μm syringe filters (Advantec MFS Inc., Dublin, CA). Phosphate and borate buffer with SDS additive as the anionic surfactant can be used for analysis using the MEKC mode.

The final running buffer consisted of 35 m*M* borate and 60 m*M* phosphate buffer, and was prepared from separate stock buffers, with pH adjustment to 7.4 and 8.65 using NaOH and phosphoric acid as required. Although different CDs were tested for their capability to provide improved separation, β-CD was found to be the most suitable; it was dissolved in mixed borate-phosphate buffer at the concentration of 2 m*M*.

For samples requiring stacking analysis, to achieve complete sample stacking, the running buffer was changed to an alkaline buffer electrolyte to ensure complete dissociation of the phenols.

2.4. Stacking Details

Stock solutions for sample concentration by stacking were prepared with 100% methanol. Appropriate amounts of the sample stock solutions were combined and diluted with either the sample matrix or water to obtain sample solutions in which the analytes had comparable peak heights.

2.4.1. Normal Stacking Mode

Hydrodynamic injections for 30, 40 50, 60, and 70 s were used to study the effect of sample plug length that may be introduced into the capillary. The subsequent separation efficiency or resolution that is achieved, and the peak height increment under each injection plug condition, is recorded for each experiment. After injection, positive voltage of 25 kV was applied to the system. Note that the optimum sample plug length that can be injected into the capillary without loss of separation efficiency or resolution should be investigated.

Clarifier overflow water samples were diluted 10 times for normal stacking mode. Introduction of clarifier overflow water samples into the CE directly either without dilution or without passing through SPE cartridges gave the interference problems observed as shown in **Fig. 11**.

It was found that peak no. 4 (2,4,6-T) could not be seen. A 10-fold dilution of process water could achieve better separation, but the sensitivity for some components was poor, even though normal stacking technique was used **(Fig. 12)**. This is due to the low concentration of these analytes in water sample. It should be noted that LVSS cannot be applied to this clarifier overflow water because the concentration of the major compound (2,4-D) is very high and will cause severe overlapping of its peak with that of its neighbor (4-ClPAA). However, in the case of LVSS for standard investigation, hydrodynamic injections for 130 s were used, which corresponds to an injected volume representing 13.8% of the capillary volume. The length of sample plug is computed based on the equation as follows *(72)*;

$$\sigma_{inj}^2 = \frac{W_i^2}{12} \tag{7}$$

where w_i is injection plug length.

After injection, a negative voltage (–20 kV) was applied and the large plug of sample carrier solution was electroosmotically pumped out of the capillary

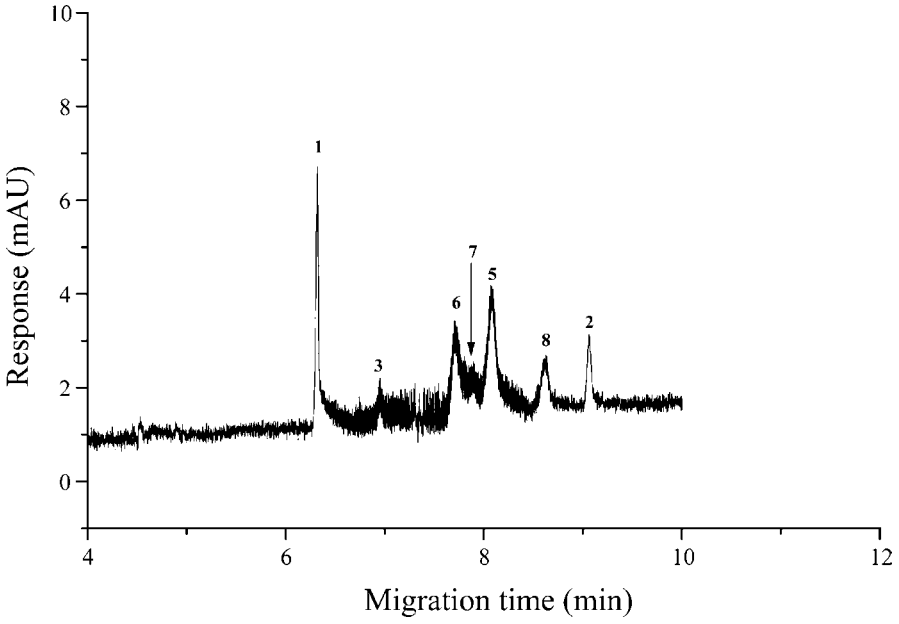


Fig. 11. Electropherogram of the separation of chlorophenoxyacetic acids and chlorophenols in clarifier overflow water without using solid-phase extraction and dilution. Conditions used: buffer composition, 35 m*M* borate-60 m*M* phosphate buffer containing 2 m*M* β-CD pH 8.5; separation voltage +25 kV, 214 nm. L = 64.5/56 cm effective length. Peaks identification: 1 = 2,4-DCP, 2 = 2,6-DCP, 3 = 2,4,6-TCP, 5 = 2,6-D, 6 = 2,4-D, 7 = 4-ClPAA, 8 = 2-ClPAA.

at the injection extremity while stacking occurred. The electric current was monitored to indicate when the sample buffer was almost removed from the column. As the low-conductivity injected zone was pumped out of the capillary, the current continuously increased up toward its normal value. This meant that the bulk of the low-conductivity injected plug had been pushed out of the capillary and the stacking process could be considered complete. Subsequently, the high voltage was then switched from a negative to a positive value. It should be noted that polarity switching is not available for some commercial CE instruments. The experimental current was monitored very carefully and polarity switching conditions were maintained until the current reached 36.8 μA, i.e., 95% of its standard value at 20 kV (the best voltage to monitor the current). This corresponds to a backout time ($t_{backout}$) equal to 0.6 min. The time needed for polarity switching from –20 kV to 20 kV (t_{+-}) was equal to 0.6 min. Electropherograms showing LVSS with polarity switching of chlorophenol and chlorophenoxyacetic acid standard solutions are shown in **Fig. 13**.

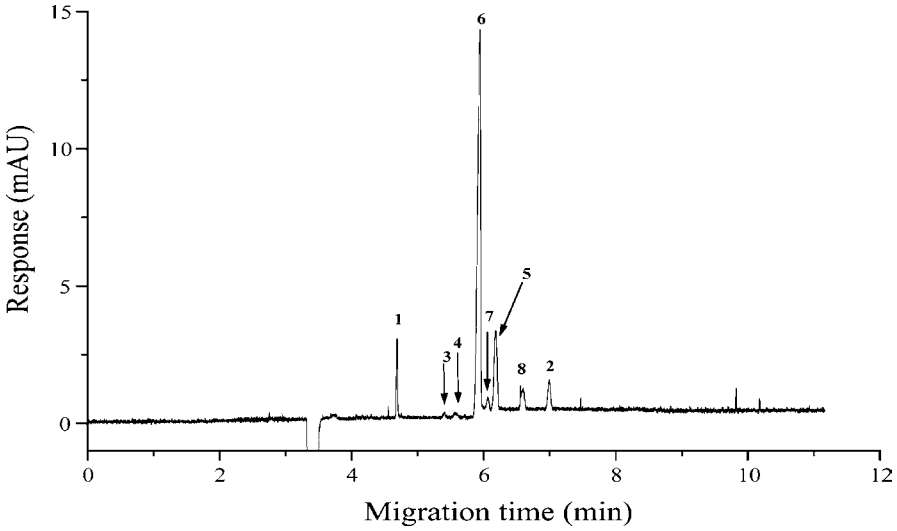


Fig. 12. Electropherogram of the separation of chlorophenoxyacetic acids and chlorophenols in clarifier overflow water (diluted 10 times) obtained with the normal stacking mode technique. Conditions used and peaks identification are the same as in **Fig. 10**, but with an injection time of 50 s and separation voltage of +30 kV.

2.5. Results

As shown in **Fig. 9**, measurement of three different types of sample was required. The first was the process or cook sample, where reasonably high concentrations of a variety of components may be expected. This bulk process involves charging the vessel with starting material and reagents in order to produce the 2,4-D product, while, it is hoped, reducing or minimizing the by-products. Reaction temperature and time are controlled to produce the required final mix. The mixture may be monitored during the process in order to evaluate the extent of the reaction, changes in reagent and product concentrations, and whether further reagent addition may be required. The use of CE here is generally not to give trace analytical measurement, but to study bulk compositions. Hence, direct analysis using CZE can be employed, following dilution of the sample in methanol prior to injection. If analysis of minor components is required, LVSS may also be needed. After the bulk preparation, the process of purification of the product by precipitation and other steps yields an enriched 2,4-D sample. The clarifier water can be monitored for trace composition prior to discharge, and this can be achieved by using CE with LVSS. Additionally, SPE can be also used to increase analyte concentration. The final isolated 2,4-D solid should be essentially a high-purity product, with

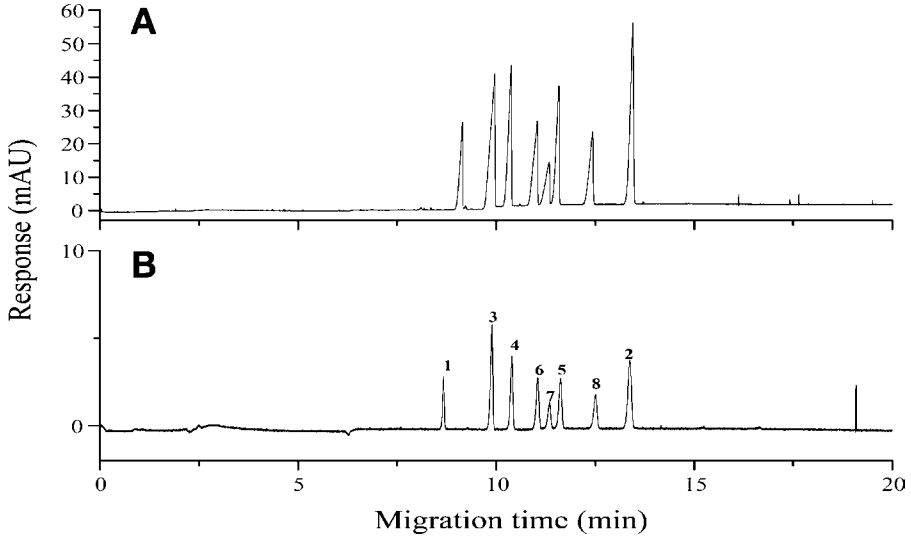
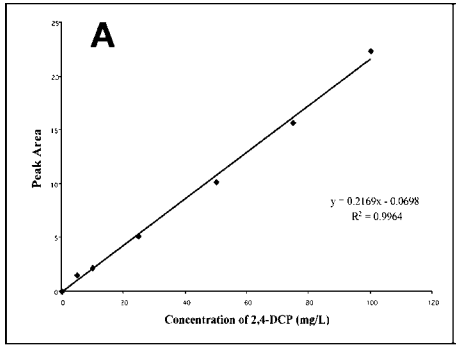


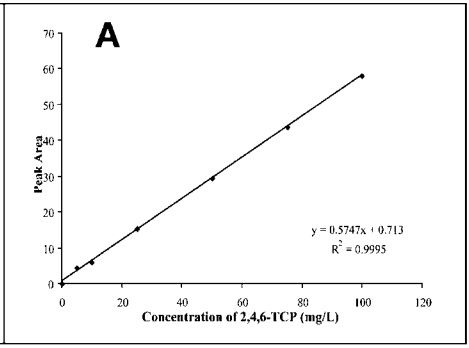
Fig. 13. Electropherogram showing large volume sample stacking with polarity switching of chlorophenols and chlorophenoxyacetic acids. Conditions used: buffer composition, 35 m*M* borate-60 m*M* phosphate buffer containing 2 m*M* β-CD at pH 8.65; injection, 50 mbar for 130 s; applied voltage during stacking and sample matrix removal, -20 kV; separation voltage, +20 kV at 214 nm. L = 64.5/56 cm effective length. Concentration of analytes; (a) 5.0 mg/L each and (b) 0.5 mg/L each. Peaks identification: same as in **Fig. 11**.

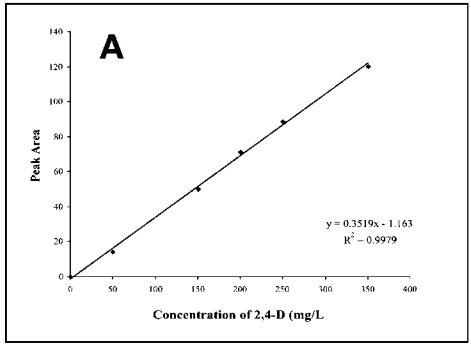
only very minor co-products or impurities. Here, CZE will be required to permit analysis of trace components in the presence of a single major compound, according to the demands of the product purity.

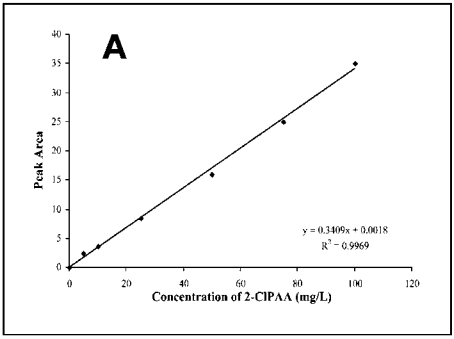
Calibration solutions were prepared in the ranges suited for each component in each sample type. Thus, in the bulk sample preparation, the calibration curve for 2,4-D was constructed over the range of 0–350 mg/L, and for the by-products/impurities, from 0 to 100 mg/L. Where low concentrations required the use of LVSS, calibration curves over the range 0.05–1 mg/L were prepared. **Figure 14** presents example calibration curves for this study. To aid improved CE separation, SPE was also employed in the clarifier water analysis. SPE recoveries using C-18 media were generally in the range of 90–110%. **Figure 15** illustrates a CE trace for this sample analysis.

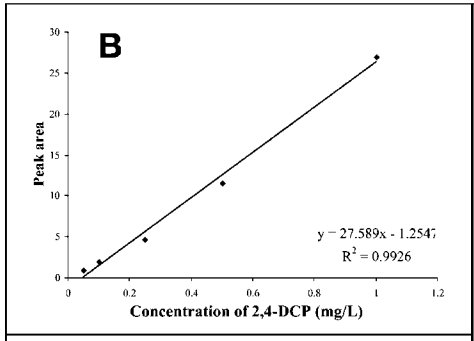
Figure 16 is an example of the process sample, where the component 2,4-D (analyte 6) has been produced as the major product. Using the slightly higher voltage of 30 kV than used for **Fig. 15** results in a total analysis time of about 7 min. Some components are undetectable (analyte 3, 2,4,6-TCP) and minor analyte 7 (4-ClPAA) is only just resolved from 2,4-D under these

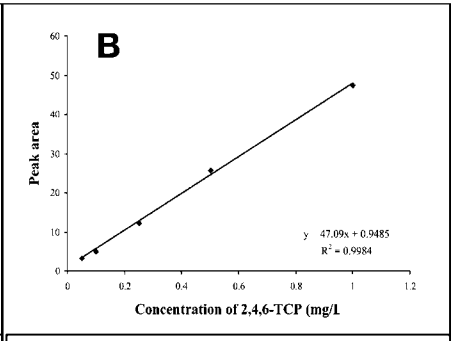

A
Peak Area
y = 0.2169x - 0.0698
R² = 0.9964
Concentration of 2,4-DCP (mg/L)

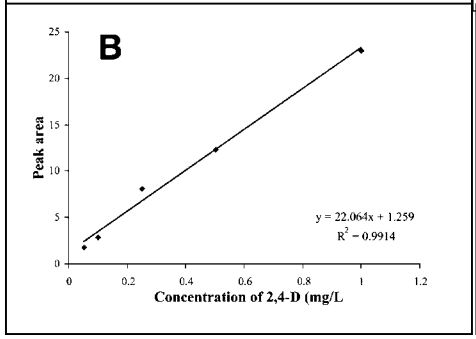

A
Peak Area
y = 0.5747x + 0.713
R² = 0.9995
Concentration of 2,4,6-TCP (mg/L)

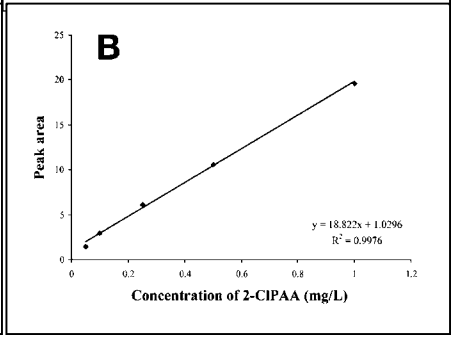

A
Peak Area
y = 0.3519x - 1.163
R² = 0.9979
Concentration of 2,4-D (mg/L


A
Peak Area
y = 0.3409x + 0.0018
R² = 0.9969
Concentration of 2-ClPAA (mg/L)


B
Peak area
y = 27.589x - 1.2547
R² = 0.9926
Concentration of 2,4-DCP (mg/L)


B
Peak area
y = 47.09x + 0.9485
R² = 0.9984
Concentration of 2,4,6-TCP (mg/L


B
Peak area
y = 22.064x + 1.259
R² = 0.9914
Concentration of 2,4-D (mg/L


B
Peak area
y = 18.822x + 1.0296
R² = 0.9976
Concentration of 2-ClPAA (mg/L)

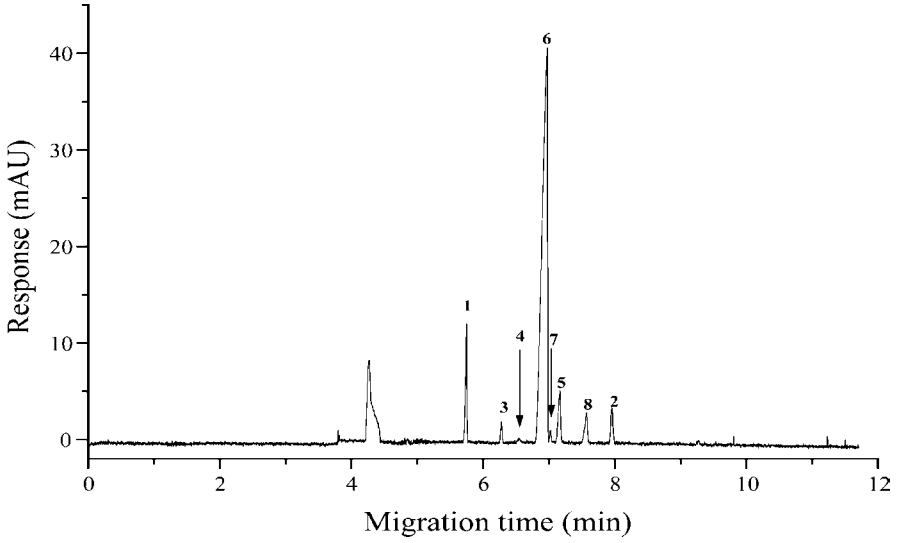


Fig. 15. CE trace for clarifier overflow water sample, following solid-phase extraction. Normal sample injection (5 s). Buffer conditions: 35 m*M* borate, 60 m*M* phosphate, 2 m*M* β-CD at pH 8.5. Separation voltage +25 kV.

conditions; however, it can be still readily seen. The major impurities are seen to be 2,4-DCP (peak 1, starting material), and 2,6-D (peak 5, by-product). The inset CE trace shows the relative peak responses of all components. The final purified 2,4-D product gave the electropherogram shown in **Fig. 17**. Here, the largest impurity peak is still 2,6-D; however, as the inset shows, this is almost negligible compared with the required 2,4-D product.

In regard to the change in products/reactants during the reaction process, samples taken every 30 min during a production run gave the data presented in **Fig. 18**. Major reactant (2,4-DCP) and desired product (2,4-D) gave the trend of reducing/increasing amounts (based on total peak area response in the CE result) as reactant is consumed to produce the 2,4-D product.

For this study of chemical process monitoring, samples were analyzed in triplicate at each of the sample points for three different production runs. To the extent that it was possible, samples taken downstream of the bulk synthesis process were sampled approximately according to when the bulk sample batch was predicted to be at that sampling location (the process of

Fig. 14. Representative calibration curves for selected analytes in the manufacture of 2,4-D, using direct capillary zone electrophoresis (a) and large volume sample stacking (b).

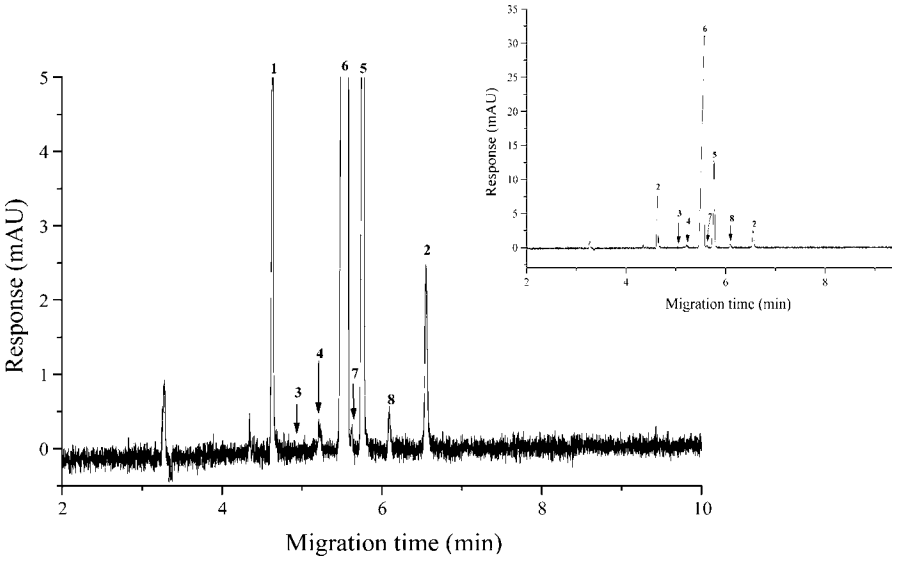


Fig. 16. Electropherogram of 2,4-D and production by-products and impurities. 0.063 g sample/25 mL of methanol.

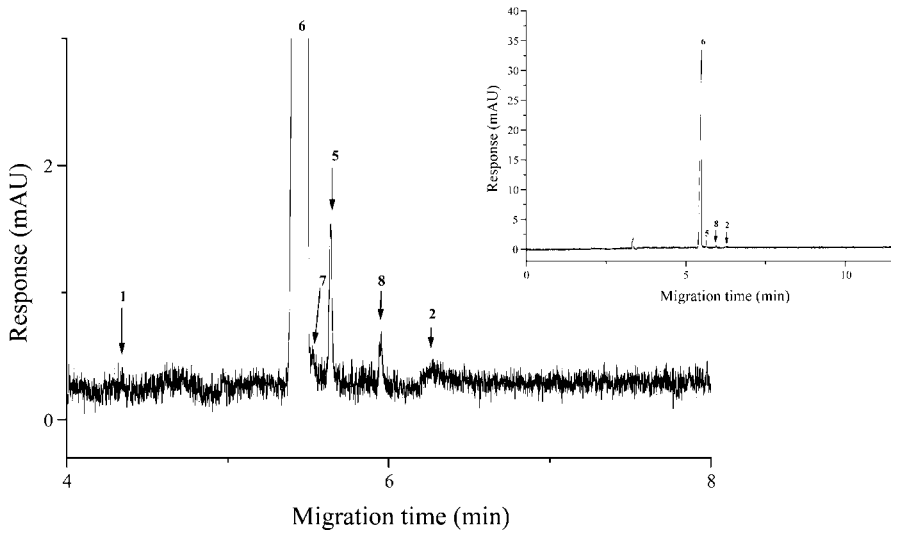


Fig. 17. Electropherogram of final 2,4-D product (2,4-D = peak 6).

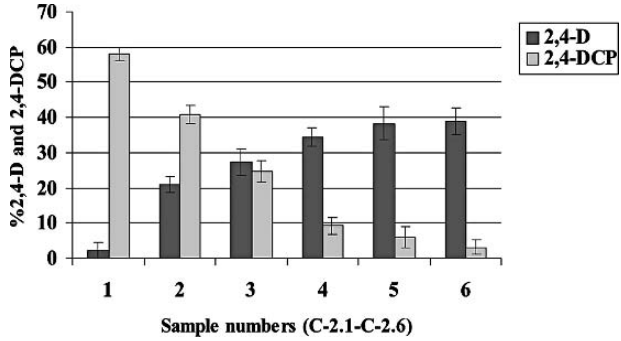


Fig. 18. Relative amounts of 2,4-D and 2,4-DCP in production sample C-2 vs the sampling interval times for C-2.1 (0 min) to C-2.6 (150 min), samples taken every 30 min.

purification is continuous, rather than batchwise); however, this cannot be guaranteed precisely. Tables of data need not be presented here, because this case study is intended to demonstrate the application of CE to process chemical analysis, where the CE analysis is fast, reliable, and reproducible, and has considerable merit over the slower conventionally used HPLC method (details of the comparative HPLC data are not presented here).

Acknowledgments

The authors wish to acknowledge the provision of a Thai Government research studentship to J. I. Support for capillary electrophoresis equipment from Agilent Technologies is gratefully recognized.

References

1. Rodriguez, I., Turnes, M. I., Bollain, M. H., Mejuto, M. C., and Cela, R. (1997) Determination of phenolic pollutants in drinking water by capillary electrophoresis in the sample stacking mode. *J. Chromatogr. A*. **778(1–2),** 279–288.
2. Szucs, R., Vindevogel, J., Sandra, P., and Verhagen, L.C., (1993) Sample stacking effects and large injection volumes in micellar electrokinetic chromatography of ionic compounds: Direct determination of iso-α-acids in beer. *Chromatographia* **36,** 323–329.
3. Stegehuis, D. S., Irth, H., Tjaden, U. R., and Van der Greef, J. (1991) Isotachophoresis as an on-line concentration pretreatment technique in capillary electrophoresis. *J. Chromatogr*. **538,** 393–402.
4. Palmarsdottir, S. and Edholm, L. -E. (1995) Enhancement of selectivity and concentration sensitivity in capillary zone electrophoresis by on-line coupling with column liquid chromatography and utilizing a double stacking procedure allowing for microliter injections. *J. Chromatogr. A*. **693,** 131–143.

5. Quirino, J. P., Kim, J. -B., and Terabe, S. (2002) Sweeping: concentration mechanism and applications to high-sensitivity analysis in capillary electrophoresis. *J. Chromatogr. A*. **965,** 357–373.
6. da Silva, C. L., de Lima, E. C., and Tavares, M. F. M. (2003) Investigation of preconcentration strategies for the trace analysis of multi-residue pesticides in real samples by capillary electrophoresis. *J. Chromatogr. A*. **1014,** 109–116.
7. Otsuka, K., Hayashibara, H., Yamauchi, S., Quirino, J. P., and Terabe, S. (1999) Highly-sensitive micellar electrokinetic chromatographic analysis of dioxin-related compounds using on-line concentration. *J. Chromatogr. A*. **853,** 413–420.
8. Farran, A., Ruiz, S., Serra, C., and Aguilar, M. (1996) Comparative study of high-performance liquid chromatography and micellar electrokinetic capillary chromatography applied to the analysis of different mixtures of pesticides. *J. Chromatogr. A*. **737,** 109–116.
9. Cikalo, M. G., Goodall, D. M., and Matthews, W. (1996) Analysis of glyphosate using capillary electrophoresis with indirect detection. *J. Chromatogr. A*. **745,** 189–200.
10. Núñez, O., Moyano, E., and Galceran, M. T. (2002) Solid-phase extraction and sample stacking-capillary electrophoresis for the determination of quaternary ammonium herbicides in drinking water. *J. Chromatogr. A*. **946,** 275–282.
11. Martínez, D., Borrull, F., and Calull, M. (1997) Sample stacking using field-amplified sample injection in capillary zone electrophoresis in the analysis of phenolic compounds. *J. Chromatogr. A*. **788,** 185–193.
12. Quirino, J. P., Inoue, N., and Terabe, S. (2000) Reversed migration micellar electrokinetic chromatography with off-line and on-line concentration analysis of phenylurea herbicides. *J. Chromatogr. A*. **892,** 187–194.
13. Quirino, J. P., Terabe, S., Otsuka, K., Vincent, J. B., and Vigh, G. (1999) Sample concentration by sample stacking and sweeping using a microemulsion and a single-isomer sulfated [beta]-cyclodextrin as pseudostationary phases in electrokinetic chromatography. *J. Chromatogr. A*. **838(1–2),** 3–10.
14. Otsuka, K., Matsumaru, M., Kim, J. B., and Terabe, S. (2003) On-line preconcentration and enantioselective separation of triadimenol by electrokinetic chromatography using cyclodextrins as chiral selectors. *J. Pharm. Biomed. Anal*. **30,** 1861–1867.
15. Lin, C. -E., Liu, Y. -H., Yang, T. -Y., Wang, T. -Z. and Yang, C. -C. (2001) On-line concentration of *s*-triazine herbicides in micellar electrokinetic chromatography using a cationic surfactant. *J. Chromatogr. A*. **916,** 239–245.
16. Tu, C., Zhu, L., Ang, C. H., and Lee, H. K. (2003) Effect of NaOH on large-volume sample stacking of haloacetic acids in capillary electrophoresis with a low-pH buffer. *Electrophoresis* **24,** 2188–2192.
17. Zhu, L. and Lee, H. K., (2001) Field-amplified sample injection combined with water removal by electroosmotic flow pump in acidic buffer for analysis of phenoxy acid herbicides by capillary electrophoresis. *Anal. Chem*. **73,** 3065–3072.

18. Qin, W. and Li, S. F. Y. (2003) Determination of chlorophenoxy acid herbicides by capillary electrophoresis with integrated potential gradient detection. *Electrophoresis* **24,** 2174–2179.
19. Núñez, O., Moyano, E., Puignou, L., and Galceran, M. T. (2001) Sample stacking with matrix removal for the determination of paraquat, diquat and difenzoquat in water by capillary electrophoresis. *J. Chromatogr. A*. **912,** 353–361.
20. Kruaysawat, J., Marriott, P. J., Hughes, J., and Trenerry, C. (2003) Large-volume stacking with polarity switching and sweeping for chlorophenols and chlorophenoxy acids in capillary electrophoresis. *Electrophoresis* **24,** 2180–2187.
21. Quirino, J.P. and Terabe, S., (1998) On-line concentration of neutral analytes for micellar electrokinetic chromatography. 5. Field-enhanced sample injection with reverse migrating micelles. *Anal. Chem*. **70,** 1893–1901.
22. Fung, Y. S. and Mak, J. L. L. (2001) Determination of pesticides in drinking water by micellar electrokinetic capillary chromatography. *Electrophoresis* **22,** 2260–2269.
23. Turiel, E., Fernández, P., Pérez-Conde, C., and Cámara, C. (2000) On-line concentration in micellar electrokinetic chromatography for triazine determination in water sample: evaluation of three different stacking modes. *Analyst* **125,** 1725–1731.
24. Monton, M. R. N., Quirino, J. P., Otsuka, K., and Terabe, S. (2001) Separation and on-line preconcentration by sweeping of charged analytes in electrokinetic chromatography with nonionic micelles. *J. Chromatogr. A*. **939(1–2),** 99–108.
25. Quirino, J. P. and Terabe, S. (1999) Sweeping with an enhanced electric field of neutral analyte zones in electrokinetic chromatography. *J. High Resol. Chromatogr*. **22(7),** 367–372.
26. Nùñez, O., Kim, J. -B., Moyano, E., Galceran, M. T., and Terabe, S. (2002) Analysis of the herbicides paraquat, diquat and difenzoquat in drinking water by micellar electrokinetic chromatography using sweeping and cation selective exhaustive injection. *J. Chromatogr. A*. **961(1),** 65–75.
27. Isoo, K., Otsuka, K., and Terabe, S. (2001) Application of sweeping to micellar electrokinetic chromatography-atmospheric pressure chemical ionization-mass spectrometric analysis of environmental pollutants. *Electrophoresis* **22,** 3426–3432.
28. Quirino, J. P., Iwai, Y., Otsuka, K., and Terabe, S. (2000) Determination of environmentally relevant aromatic amines in the ppt level by cation selective exhaustive injection-sweeping-micellar electrokinetic chromatography. *Electrophoresis* **21,** 2899–2903.
29. Zhu, L., Tu, C., and Lee, H. K. (2002) On-line concentration of acidic compounds by anion-selective exhaustive injection-sweeping-micellar electrokinetic chromatography. *Anal. Chem*. **74,** 5820–5825.
30. Molina, M., Wiedmer. S. K., Jussila, M., Silva, M., and Riekkola, M. -L. (2001) Use of a partial filling technique and reverse migrating micelles in the study of *N*-methylcarbamate pesticides by micellar electrokinetic chromatography-electrospray ionization mass spectrometry. *J. Chromatogr. A*. **927,** 191–202.

31. Albert, M., Debusschere, L., Demesmay, C., and Rocca, J. L. (1997) Large-volume stacking for quantitative analysis of anions in capillary electrophoresis. I. large-volume stacking with polarity switching. *J. Chromatogr. A*. **757,** 281–289.
32. Albert, M., Debusschere, L., Demesmay, C., and Rocca, J. L. (1997) Large-volume stacking for quantitative analysis of anions in capillary electrophoresis. II. large-volume stacking without polarity switching. *J. Chromatogr. A*. **757,** 291–296.
33. Carabias-Martínez, R., Rodríguez-Gonzalo, E., Revilla-Ruiz, P., and Domínuez-Álvarez, J. (2003) Solid-phase extraction and sample stacking-micellar electrokinetic capillary chromatography for the determination of multiresidues of herbicides and metabolites. *J. Chromatogr. A*. **990,** 291–302
34. Sun, B., Macka, M., and Haddad, P. R., (2003) Trace determination of arsenic species by capillary electrophoresis with direct detection using sensitivity enhancement by counter-or co-electroosmotic flow stacking and a high-sensitivity cell. *Electrophoresis* **24,** 2045–2053.
35. Gil, E. P., Ostapczuk, P., and Emons, H. (1999) Determination of arsenic species by field amplified injection capillary electrophoresis after modification of the sample solution with methanol. *Anal. Chim. Acta* **389,** 9–19.
36. Farray, L., Oxspring, D. A., Smyth, W. F., and Merchant, R. (1997) A study of the effects of injection mode, on-capillary stacking and off-line concentration on the capillary electrophoresis limits of detection for four structural types of industrial dyes. *Anal. Chim. Acta* **349,** 221–229.
37. Chen, Z. and Naidu, R. (2004) On-column complexation capillary electrophoretic separation of Fe^{2+} and Fe^{3+} using 2,6-pyridinedicarboxylic acid coupled with large-volume sample stacking. *J. Chromatogr. A*. **1023,** 151–157.
38. Nuria, M., Alejandro, C., Coral, B., and Analitica, S. Q., (2004) Large-volume sample stacking-capillary electrophoresis used for the determination of 3-nitrotyrosine in rat urine. *J. Chromatogr. B*. **809(1),** 147–152.
39. Kim, J. -B., Quirino, J. P., Otsuka, K., and Terabe, S. (2001) On-line sample concentration in micellar electrokinetic chromatography using cationic surfactants. *J. Chromatogr. A*. **916,** 123–130.
40. Chen, H. -C. and Ding, W. -H. (2003) Analysis of naphthalenesulfonate compounds by cyclodextrin-mediated capillary electrophoresis with sample stacking. *J. Chromatogr. A*. **996,** 205–212.
41. Huang, H. -Y., Chiu, C. -W., Sue, S. -L., and Cheng, C. -F., (2003) Analysis of food colorant by capillary electrophoresis with large-volume sample stacking. *J. Chromatogr. A*. **995,** 29–36.
42. Hou, L., Wen, X., Tu, C., and Lee, H. K. (2002) Combination of liquid-phase microextraction and on-column stacking for trace analysis of amino alcohols by capillary electrophoresis. *J. Chromatogr. A*. **979,** 163–169.
43. Shihabi, Z. K. (2000) Stacking in capillary zone electrophoresis. *J. Chromatogr. A*. **902,** 107–117.
44. Mikkers, F. E. P., Everaerts, F. M., and Verheggen, T. P. E. M. (1979) High-performance zone electrophoresis. *J. Chromatogr*. **169,** 11–20.

45. Chien, R. L. and Burgi, D. S., (1992) On-column sample concentration using field amplification in CZE. *Anal. Chem*. **64(8),** 489A–496A.
46. Chien, R. L. and Burgi, D. S. (1991) Field-amplified polarity-switching injection in high-performance capillary electrophoresis. *J. Chromatogr*. **559,** 153–161.
47. Chien, R. L. and Burgi, D. S. (1992) Sample stacking of a extremely large injection volume in high-performance capillary electrophoresis. *Anal. Chem*. **64,** 1046–1050.
48. Burgi, D. S. and Chien, R. L. (1992) Improvement in the method of sample stacking for gravity injection in capillary electrophoresis. *Anal. Biochem*. **202,** 306–309.
49. Smyth, W. F., Harland, G. B., McClean, S., McGrath, G., and Oxspring, D. (1997) Effect of on-capillary large volume sample stacking on limits of detection in the capillary zone electrophoretic determination of selected drugs, dyes and metal chelates. *J. Chromatogr. A*. **772,** 161–169.
50. Liu, B. -F., Zhong, X. -H., and Lu, Y. -T. (2002) Analysis of plant hormones in tobacco flowers by micellar electrokinetic capillary chromatography coupled with on-line large volume sample stacking. *J. Chromatogr. A*. **945,** 257–265.
51. Burgi, D. (1993) Large volume stacking of anions in capillary electrophoresis using an electroosmotic flow modifier as a pump. *Anal. Chem*. **65,** 3726–3729.
52. Quirino, J. P. and Terabe, S. (1999) Sample stacking of fast-moving anions in capillary zone electrophoresis with pH-suppressed electroosmotic flow. *J. Chromatogr. A*. **850(1–2),** 339–344.
53. Quirino, J. P. and Terabe, S. (2000) Large volume sample stacking of positively chargeable analytes in capillary zone electrophoresis without polarity switching: use of low reversed electroosmotic flow induced by a cation surfactant at acidic pH. *Electrophoresis* **21(2),** 355–359.
54. Zhao, Y. P., Mclaughlin, P., and Lunte, C. E. (1998) On column sample preconcentration using sample matrix switching and field amplification for increased sensitivity of capillary electrophoretic analysis of physiological samples. *Anal. Chem*. **70,** 4578–4585.
55. He, Y. and Lee, H. K. (1999) Large-volume sample stacking in acidic buffer for analysis of small organic and inorganic anions by capillary electrophoresis. *Anal. Chem*. **71,** 995–1001.
56. Chien, R. L. and Burgi, D. S. (1991) Field amplified sample injection in high-performance capillary electrophoresis. *J. Chromatogr*. **559**, 141–152.
57. Zhang, C. -X. and Thormann, W. (1996) Head-column field-amplified sample stacking in binary system capillary electrophoresis: A robust approach providing over 1000-fold sensitivity enhancement. *Anal. Chem*. **68,** 2523–2532.
58. Leung, S. -H. and de Mello, A. J. (2002) Electrophoretic analysis of amines using reversed-phase, reversed-polarity, head-column field-amplified sample stacking and laser-induced fluorescence detection. *J. Chromatogr*. A. **979,** 171–178.
59. Lee, T. T. and Yeung, E. S. (1992) Compensating for instrumental and sampling biases accompanying electrokinetic injection in capillary zone electrophoresis. *Anal. Chem*. **64,** 1226–1231.

60. Quirino, J. P. and Terabe, S. (2000) Sample stacking of cationic and anionic analytes in capillary electrophoresis. *J. Chromatogr*. A. **902,** 119–135.
61. Quirino, J. P. and Terabe, S. (1998) Exceeding 5000-fold concentration of dilute analytes in micellar electrokinetic chromatography. *Science* **282,** 465–468.
62. Gilges, M. (1997) Determination of impurities in an acidic drug substance by micellar electrokinetic chromatography. *Chromatographia* **44,** 191–196.
63. Quirino, J. P., Terabe, S., and Bocek, P. (2000) Sweeping of neutral analytes in electrokinetic chromatography with high-salt-containing matrixes. *Anal. Chem*. **72,** 1934–1940.
64. Sera, Y., Matsubara, N., Otsuka, K., and Terabe, S. (2001) Sweeping on microchip: Concentration profiles of the focused zone in micellar electrokinetic chromatography. *Electrophoresis* **22,** 3509–3513.
65. Quirino, J. P. and Terabe, S. (2000) Approaching a million-fold sensitivity increase in capillary electrophoresis with direct ultraviolet detection: cation-selective exhaustive injection and sweeping. *Anal. Chem*. **72(5),** 1023–1030.
66. Kim, J. -B., Otsuka, K., and Terabe, S. (2001) Anion selective exhaustive injection-sweep-micellar electrokinetic chromatography. *J. Chromatogr. A*. **932,** 129–137.
67. Kaniansky, D. and Marák, J. (1990) On-line coupling of capillary isotachophoresis with capillary zone electrophoresis. *J. Chromatogr*. **498,** 191–204.
68. Kaniansky, D., Iványl, F., and Onuska, F. I. (1994) On-line isotachophoretic sample pretreatment in ultratrace determination of paraquat and diquat in water by capillary zone electrophoresis. *Anal. Chem*. **66,** 1817–1824.
69. Quirino, J. P. and Terabe, S. (1997) On-line concentration of neutral analytes for micellar electrokinetic chromatography. I. normal stacking mode. *J. Chromatogr. A*. **781,** 119–128.
70. Quirino, J. P. and Terabe, S. (1997) On-line concentration of neutral analytes for micellar electrokinetic chromatography. I. reversed electrode polarity stacking mode. *J. Chromatogr. A*. **791,** 255–267.
71. Osbourn, D. M., Weiss, D. J., and Lunte, C. E. (2000) On-line preconcentration methods for capillary electrophoresis. *Electrophoresis* **21,** 2768–2779.
72. Heiger, D. N. (1992) High-performance capillary electrophoresis: *An Introduction*. Hewlett-Packard, France, 32.

28

Free-Flow Electrophoresis System for Proteomics Applications

Gerhard Weber and Robert Wildgruber

Summary

This chapter describes the technology and selected applications in the field of protein analysis for free flow electrophorsis (FFE). FFE is a highly versatile technology for applications in this field as a result of its continuous processing of sample and the possibility of separating almost any kind of charged or chargeable particles in an aqueous medium without any solid matrix such as acrylamide. Possible applications are separation of ions, proteins, peptides, organelles, or whole cells for subsequent analysis.

Key Words: Free flow electrophoresis; isotachophoresis; zone electrophoresis; organelle separation; isoelectric focusing.

1. Introduction

Free flow electrophoresis (FFE) is a well established and highly versatile technology for the separation of a wide variety of charged or chargeable analytes from low-molecular-weight organic compounds, peptides, proteins, protein complexes, membranes, and organelles to whole cells. The separation is performed in aqueous media under native as well as denaturing conditions.

The analyte is injected into a thin, laminar separation buffer film (which defines the electrophoretic mode such as zone electrophoreses, isoelectric focusing [IEF], or isotachophoresis) and is deflected by an electric field perpendicular to the flow direction. The absence of any kind of solid separation matrix prevents unspecific adsorption of analytes or precipitation through concentration effects of analytes. The separation conditions are identical from the sample application through the complete separation process. These unique

From: *Methods in Molecular Biology, vol. 384: Capillary Electrophoresis*
Edited by: P. Schmitt-Kopplin © Humana Press Inc., Totowa, NJ

features of a continuous electrophoretic separation process are directly linked to highly reproducible separations of a duration of less than 20 min and matrix-free fractionations with almost quantitative recovery.

The resolution of the separation is comparable to the high resolution of standard polyacrylamide gel electrophoresis (PAGE). Because FFE is compatible with almost any downstream method, the combination of FFE with two-dimensional (2D)-PAGE and/or liquid chromatography (LC)-mass spectrometry (MS) as well as activity tests and enzyme-linked immunosorbent assay (ELISA) allows access to low abundant proteins species as well as to proteins with extreme physical–chemical properties such as high mass range, hydrophobicity, and extreme isoelectric points (IEPs).

1.1. Free Flow Isoelectric Focusing

IEF in FFE allows for high-resolution fractionation of proteins with recovery rates of up to 98%. The separation of sample can be conducted in preparative quantities from up to 50 mg protein/h continously. The pH gradient for the separation process is formed by the separation media under constant voltage either with ampholytes or with proprietary separation reagents, which consist of well defined compounds with low molecular mass and specific isoelectric points (pIs).

In the pH range of 3.0–12.0, almost any pH gradient can be calculated and used for specific high-resolution separations either in wide or narrow ranges, depending on the application.

1.1.1. Separation of Isoforms

The analysis of isoforms is a essential step, for example, in the development of protein-based pharmaceuticals. Food and Drug Administration (FDA) regulations today demand the characterization of every protein species and the exact documentation of the specific activity of any active substances. In recombinant proteins and artificial peptides, isoforms appear during synthesis by nature.

It is also known now that protein isoforms affect the regulation and are responsible for the conduction of many cellular functions, such as gene expression and stress responses as well as signal transduction. Some pathological states occur even just as a result of the improper expression or function of protein isoforms, for example prion diseases and some cancers. Thus it is crucial today to be able to separate and identify protein isoforms from clinical or pharmaceutical samples quickly and with high resolution.

We analyzed protein isoforms of different origins such as Ovalbumin, IgGs, and Protease DPPIV as proof-of-principle with FFE and subsequent IEF-PAGE. The separations shown here were conducted under native as well as

in denaturing conditions. Native FFE separations, for example, can be used directly for activity tests or ELISA analysis.

1.1.2. FFE Depletion of Human Serum Albumin from Human Plasma

Plasma is a prolific source of potential disease and biological markers and is readily available in large amounts for clinical analysis. The large dynamic range of proteins present in plasma, as well as lipids, salts, and the proteolytic activity limit the consistency, efficiency, sensitivity, and resolution of many analytical techniques to identify biomarkers.

As a consequence, the reduction of sample complexity is becoming widely accredited as a mandatory first step in protein analysis. It is commonly accepted that proteins such as albumin and IgGs should be depleted prior to in-depth analysis of human plasma, but losses caused by unspecific protein interactions with other proteins or separation matrices limit the effectiveness and reproducibility of some depletion techniques. As an alternative to human serum albumin (HSA) depletion, we have used FFE as a preliminary step to separate the HSA from the proteins of interest.

A demonstration of this method is shown for human plasma fractionated by FFE. For high-throughput and pre-fractionation needs, a so called depletion-fractionation-enrichment (DFE) protocol, which fractionates the protein content into three pools: an acidic, an albumin, and a basic pool, respectively, was introduced. The separation is conducted in newly designed separation buffers that are delivering a sophisticated pH gradient within the separation area for exactly this application.

First results of digested FFE-fractions analyzed by LC-MS/MS showed several 100-protein identifications per fraction. We further demonstrate that FFE can be used for large-scale sample preparation for high-throughput proteomic analyses of plasma to create new dimensions in the search for biological markers.

1.2. Zone Electrophoresis

In zone electrophoresis (ZE), the separation of charged particles is performed in a constant pH field as a result of the net charge of the compounds to be separated, and therefore enables rapid separation and purification of organelles, membranes, and whole cells for the study of subproteomes.

1.2.1. Zone Electrophoretic Enrichment of Yeast Mitochondria

Subcellular and organelle fractionation can be a fundamental first step to increase resolution in analysis, but it frequently leads to preparations contaminated with other cellular structures. We chose mitochondria of *Saccharomyces*

cerevisiae to demonstrate that a zone electrophoretic purification step, with an FFE device, can assist in overcoming this problem while significantly improving cells' degree of purity.

Whereas mitochondrial preparations isolated by means of differential centrifugation include a considerable degree of nonmitochondrial proteins (16%), this contamination could be effectually removed by the inclusion of a ZE-FFE purification step (2%). This higher degree of purity led to the identification of many more proteins in subsequent 2D-electrophoretic analysis from ZE-FFE-purified mitochondrial protein extracts ($n = 129$), compared to mitochondrial protein extracts isolated by differential centrifugation ($n = 80$). Moreover, a marked decrease of degraded proteins was found in the ZE-FFE purified mitochondrial protein extracts. It is noteworthy that even at a low 2D-electrophoresis (2-DE) resolution level, a four-fold higher number (17 vs 4) of presumably low-abundance proteins could be identified in the ZE-FFE-purified mitochondrial protein extracts. Therefore, these results represent a feasible approach for an in-depth proteome analysis of mitochondria and possibly other organelles.

1.3. Technology

The FFE system performs electrophoretic separations in patented and well defined separation solutions without the use of a solid polyacrylamide matrix. It provides fluid–phase separation in three different operating modes: ZE, which separates particles (cells, organelles, and protein complexes) by their electrophoretic mobility; IEF, which separates proteins or peptides in a pH gradient by their isoelectric point; and isotachophoresis, which separates proteins or peptides in a pH step gradient. This enables the separation of cell organelles, proteins, and other charged or chargeable entities on a fast, preparative, and continuous basis (*see* **Fig. 1**).

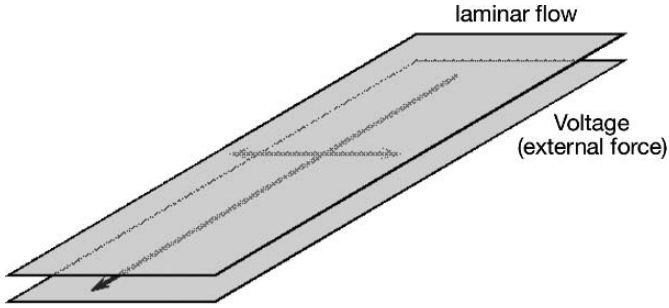


Fig. 1. Schematic overview of the free flow electrophoresis principle.

The system allows researchers to reduce sample complexity using such subproteomics applications as cell or organelle purification in ZE mode, or enrich low-abundance proteins with high reproducibility in IEF or isotachophoresis. The FFE technology ensures that separated samples are compatible with all downstream concentration procedures (e.g., ultrafiltration), separation techniques (1- and 2-DE), and analytical methods (matrix-assisted laser desorption/ionization [MALDI]-time-of-flight [TOF]-MS or LC-MS). As a result of the continuous process, the sample throughput can be adjusted individually from microgram to multigram levels, i.e., from analytical to highly preparative ranges, delivering recovery rates of more than 97%.

The sample is applied using a peristaltic pump and is injected into a separation chamber consisting of two parallel plates. Under laminar flow, the sample is transported within a thin (0.4-mm) film of aqueous medium (ProLyte reagent, FFE Weber GmbH, Planegg, Germany) formed between the two plates. The plates are bordered by two electrodes that generate a high-voltage electric field perpendicular to the laminar flow. Charged particles (ions, peptides, proteins, organelles, membrane fragments, or whole cells) are deflected in this electric field, permitting subsequent separation and/or fractionation.

Three different operational modes can be used for FFE (*see* **Fig. 2**):

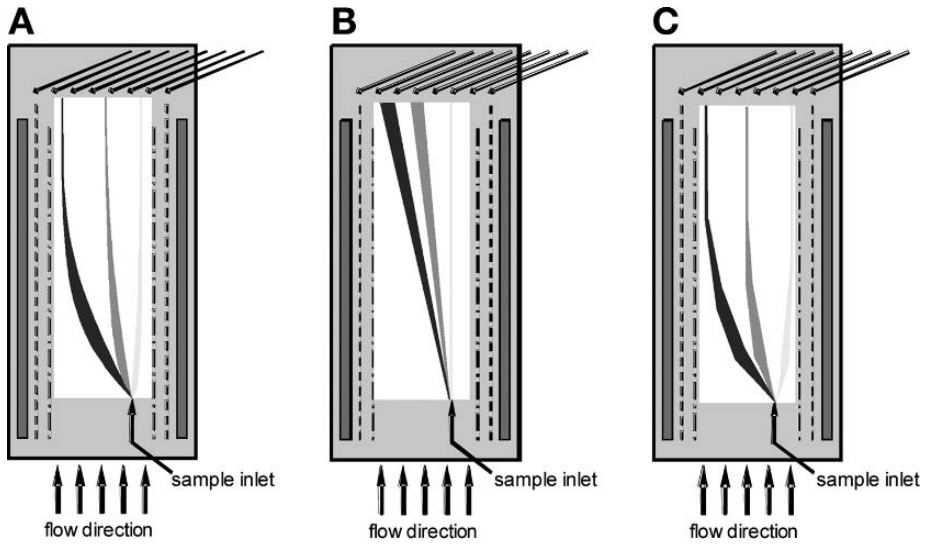


Fig. 2. Free flow electrophoresis (FFE) operating modes. **(A)** Isoelectric focusing mode for separation of proteins/peptides in a pH gradient. **(B)** Zone electrophoresis for separation of particles such as cells and organelles based on their net charge. **(C)** Isotachophoresis for separations of particles based on their electrophoretic mobility.

1. Preparative IEF, which is used for the high-resolution fractionation of proteins with recovery rates of up to 98%; separation of quantities up to 50 mg protein/hr can be achieved.
2. ZE, which permits the rapid separation of organelles, membranes, and whole cells for the study of subproteomes.
3. Isotachophoresis, which offers an enhanced range of separation methods based on electrophoretic mobility.

2. Materials

2.1. Sample Preparation

Tolerable additives for sample preparations are: urea up to 8 *M*; 0.1–1% of detergents such as CHAPS, CHAPSO, Digitonin, Dodecyl-β-D-maltoside, Octyl-β-D-glucoside, Triton-X-114 (IEF); up to 50 m*M* dithiothreitol.

1. Commercially available Ovalbumin (Serva) was diluted with FFE carrier ampholyte running buffer (described below) to a final concentration of 3 mg protein/mL.
2. Protease DPPIV was diluted with ProLyte running buffer to a final concentration of 4 mg/mL.
3. Human IgG was diluted with Ampholyte FFE running buffer to a final concentration of 4 mg/mL.

2.2. Free Flow Isoelectric Focusing

2.2.1. Media for Native ProLyte™ Runs

1. Anodic stabilization medium (I1) 14.5% (w/w) glycerol; 0.2% (w/w) HPMC; 100 m*M* H_2SO_4.
2. Separation medium 1 (I2) 14.5% (w/w) glycerol; 0.2% (w/w) HPMC; 17% (w/w) Prolyte™ 1.
3. Separation medium 2 (I3–5) 14.5% (w/w) glycerol; 0.2% (w/w) HPMC; 17% (w/w) Prolyte 2.
4. Separation medium 3 (I6) 14.5% (w/w) glycerol; 0.2% (w/w) HPMC; 17% (w/w) Prolyte 3.
5. Cathodic stabilization medium (I7) 14.5% (w/w) glycerol; 0.2% (w/w) HPMC; 100 m*M* NaOH.
6. Counterflow medium 14.5% (w/w) glycerol.
7. Anodic circuit electrolyte 100 m*M* H_2SO_4.
8. Cathodic circuit electrolyte 100 m*M* NaOH.

2.2.2. Media for Native Ampholyte Runs

1. Anodic stabilization medium (I1) 14.5% (w/w) glycerol; 0.2% (w/w) HPMC; 100 m*M* H_2SO_4.
2. Separation medium 3 (I2–I6) 14.5% (w/w) glycerol; 0.2% (w/w) HPMC; 0,5% (w/w) Servalyte 4–6.

3. Cathodic stabilization medium (I7) 14.5% (w/w) glycerol; 0.2% (w/w) HPMC; 100 m*M* NaOH.
4. Counterflow medium 14.5% (w/w) glycerol.
5. Anodic circuit electrolyte 100 m*M* H_2SO_4.
6. Cathodic circuit electrolyte 100 m*M* NaOH.

2.2.3. Media for Denaturing Runs

1. Anodic stabilization medium (I1) 14.5% (w/w) glycerol; 42% (w/w) 8 *M* urea; 0.12% (w/w) HPMC; 100 m*M* H_2SO_4.
2. Separation medium (I2) 14.5% (w/w) glycerol; 42% (w/w) 8 *M* urea; 0.12% (w/w) HPMC; 14.5% (w/w) Prolyte 1.
3. Separation medium (I3–5) 14.5% (w/w) glycerol; 42% (w/w) 8 *M* urea; 0.12% (w/w) HPMC; 14.5% (w/w) Prolyte 2.
4. Separation medium (I6) 14.5% (w/w) glycerol; 42% (w/w) 8 *M* urea; 0.12% (w/w) HPMC; 14.5% (w/w) Prolyte 3.
5. Cathodic stabilization medium (I7) 14.5% (w/w) glycerol; 42% (w/w) 8 *M* urea; 0.12% (w/w) HPMC; 100 m*M* NaOH.
6. Counterflow medium 14.5% (w/w) glycerol; 42% (w/w) 8 *M* urea.
7. Anodic circuit electrolyte 100 m*M* H_2SO_4.
8. Cathodic circuit electrolyte 100 m*M* NaOH

2.3. FFE Depletion of HSA from Human Plasma

2.3.1. Media for FF-HSA Depletion

1. Anodic stabilization medium 1 (I1): 10% (w/w) glycerol; 100 m*M* H_2SO_4.
2. Anodic stabilization medium 2 (I2–I3): 10% (w/w) glycerol; 200 m*M* Tris, 100 m*M* HAc
3. Separation medium (I4): 10% (w/w) glycerol; 10 m*M* Tris; 10 m*M* HAc.
4. Cathodic stabilization medium 2 (I5–I6): 10% (w/w) glycerol; 100 m*M* Tris,200 mM HAc.
5. Cathodic stabilization medium 1 (I7): 10% (w/w) glycerol; 100 m*M* NaOH.
6. Counterflow medium 10% (w/w) glycerol.
7. Anodic circuit electrolyte 100 m*M* H_2SO_4.
8. Cathodic circuit electrolyte 100 m*M* NaOH.

2.4. Zone Electrophoretic Enrichment of Yeast Mitochondria

1. Anodic and cathodic circuit electrolytes: 100 m*M* acetic acid; 100 m*M* triethanolamine; 10 m*M* EDTA; the pH was adjusted to 7.4 by 1 *M* NaOH.
2. Anodic/cathodic electrolyte stabilizer (media inlet 1 and 7): 200 m*M* sucrose; 100 m*M* acetic acid; 100 m*M* Triethanolamine; 10 m*M* EDTA pH 7.4.
3. Separation media (media inlet 2–6): 280 m*M* sucrose; 10 m*M* acetic acid; 10 m*M* triethanolamine; 1 m*M* EDTA pH 7.4.
4. Counterflow media: 280 m*M* sucrose.

3. Methods

3.1. Isolation of Isoforms

3.1.1. Sample Preparation

General comments for FFE sample preparation: the chemical and physical properties of sample and separation media should be as similar as possible: density, viscosity, and conductivity should be equal, meaning that the sample should be dissolved or diluted in separation media. Turbid protein samples are cleared by centrifugation; turbid cell or organelle samples do not have to be cleared (*see also* **Note 1**).

3.1.2. Free-Flow Electrophoresis

FFE separations were conducted at 10 °C using the following conditions and media (*see also* **Note 2**): the experiments were run in a horizontal separation using a 0.4 mm spacer. A flow rate of approx 60 g/h (Inlet I1–7) was used in combination with a voltage of 400–1000 V, which resulted in a current of approx 20–30 mA. Samples were perfused into the separation chamber using the cathodic inlet at approx 5 g/h. Residence time in the separation chamber was approx 20 min. Fractions were collected in polypropylene microtiter plates, numbered 1 (anode) through 96 (cathode).

3.1.3. Data Analysis

The pH values of the individual microtiter plate fractions were measured manually. Subsequently, the protein fractions were analysed either by sodium dodecyl sulfate (SDS)-PAGE using an XCell SureLock™ Mini-Cell (Novex) in combination with precast NuPAGE® Novex 4–12% Bis-Tris gels or IEF-PAGE on a flatbed chamber. Silver staining of the proteins was carried out using the SilverQuest' kit (Novex). 2-DE analysis was performed according to Görg et al. using an IPGphor (Amersham Biosciences) and multiple SDS-PAGE on a vertical system.

3.2. FFE Depletion of HSA from Human Plasma

3.2.1. Sample Preparation

Human plasma was diluted 1:10–1:20 directly with separation medium and applied directly to FFE.

3.2.2. Free-Flow Electrophoresis

FFE separations were conducted at 10 °C using the following conditions. The experiments were run in a horizontal separation using a 0.4-mm spacer. A flow rate of approx 60 g/h (Inlet I1–7) was used in combination with a voltage

of 250 V which resulted in a current of approx 20 mA. Samples were perfused into the separation chamber using the cathodic inlet at approx 5 g/h. Residence time in the separation chamber was approx 20 min. Fractions were collected in polypropylene microtiter plates, numbered 1 (anode) through 96 (cathode).

3.2.3. Data Analysis

The pH values of the individual microtiter plate fractions were measured. Subsequently, the protein fractions were analysed either by SDS-PAGE using an XCell SureLock Mini-Cell in combination with precast NuPAGE 4–12% Bis-Tris gels. Silver-staining of the proteins was carried out using the SilverQuest kit (Novex). 2-DE analysis was performed according to Görg et al. using an IPGphor (Amersham Biosciences) and multiple SDS-PAGE on a vertical system.

3.3. Conclusions

3.3.1. Separation of Isoforms

FFE in the isoelectric focusing mode is an indispensable tool for the separation of proteins under nondenaturing conditions. The absence of any matrix (such as a polyacrylamide gel) guarantees highly reproducible results combined with quantitative sample recoveries in a fast and straight forward manner. The native separations are crucial for keeping proteins functional for further activity tests and ELISA analysis. The also samples stay in liquid media from sample preparation **Figures 3–5** show the 1D IEF electropherograms of the native FFE separated isoforms in comparison to the original samples. The separations were performed in narrow pH gradients (pH 4.0–6.0) revealing a

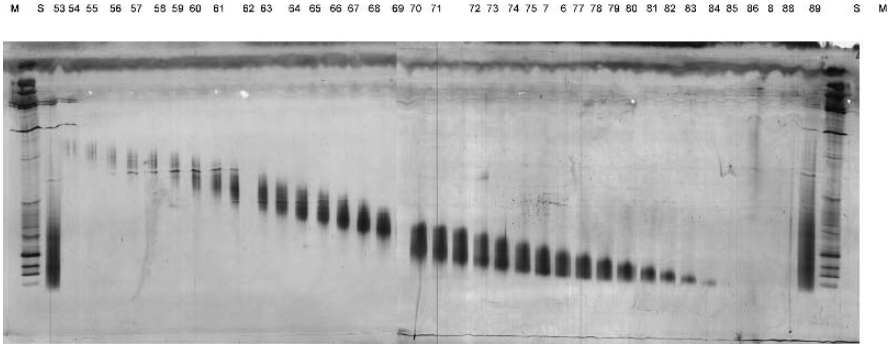


Fig. 3. Subfraction of human IgG, first native separation with free flow electrophoresis, second analytical isoelectric focusing-polyacrylamide gel electrophoresis without urea and without detergent.

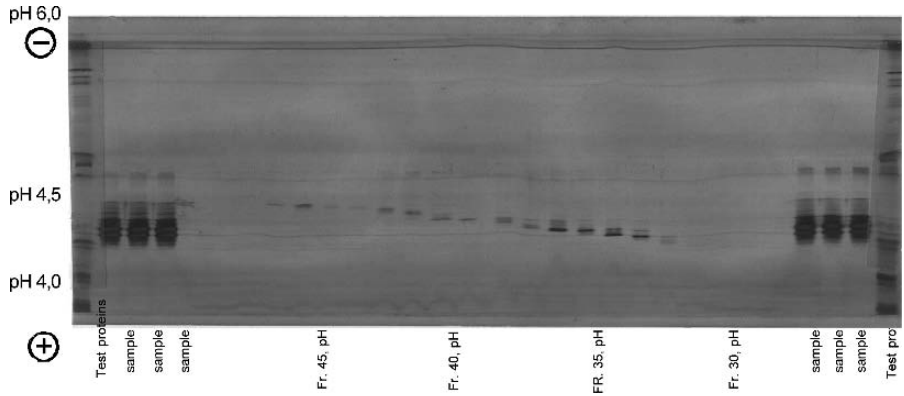


Fig. 4. Subfraction of Ovalbumine, first native separation with free flow electrophoresis, second analytical isoelectric focusing-polyacrylamide gel electrophoresis without urea and without detergent.

high-resolution separation to effectively isolate the different isoforms of the proteins for further analysis.

3.3.2. Native Depletion of HSA from Human Plasma

Figure 6 shows the comparison of 2D electropherograms of a crude plasma sample to the sum of the depleted and fractionated samples of an acidic pool, which were subsequently analyzed. Laboratory results demonstrate an improvement in the resolution on 2D-PAGE by more than a factor

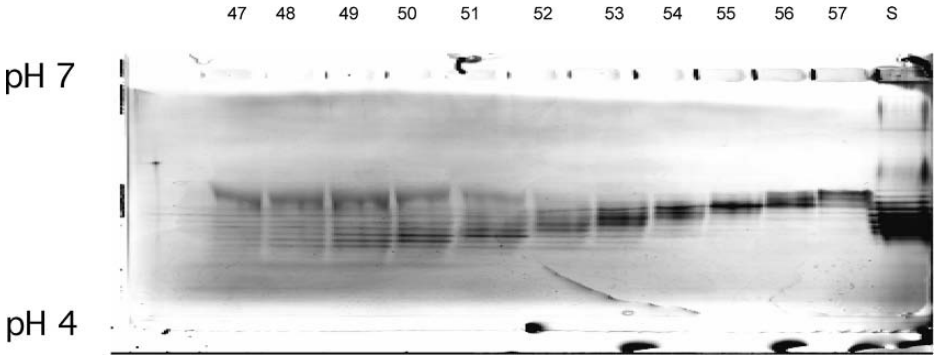


Fig. 5. Subfraction of Protease DPPIV, first native separation with free flow electrophoresis, second analytical isoelectric focusing-polyacrylamide gel electrophoresis with 8 *M* urea.

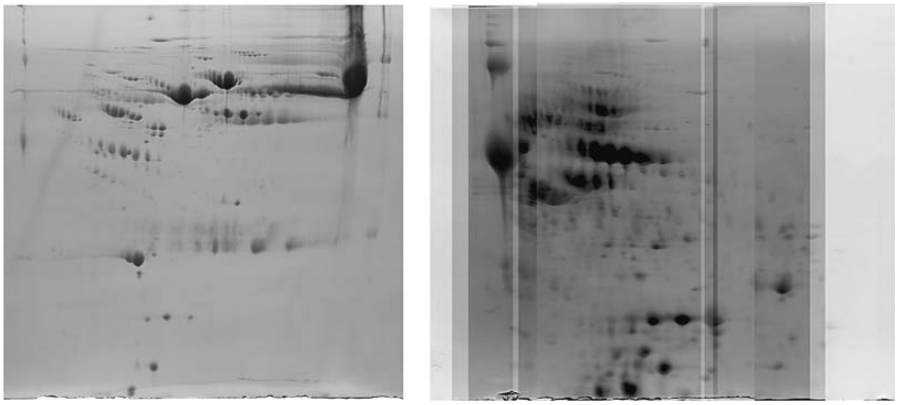


Fig. 6. Native depletion of human serum albumin from human Plasma, Comparison of two-dimensional electrophoretic protein patterns of unprocessed sample (left) and the summarized images as overlay of free flow electrophoresis-processed samples (right).

of three, when compared to unfractionated samples. Additionally, digested fractions analyzed by LC-MS/MS yielded hundreds of protein identifications per fraction.

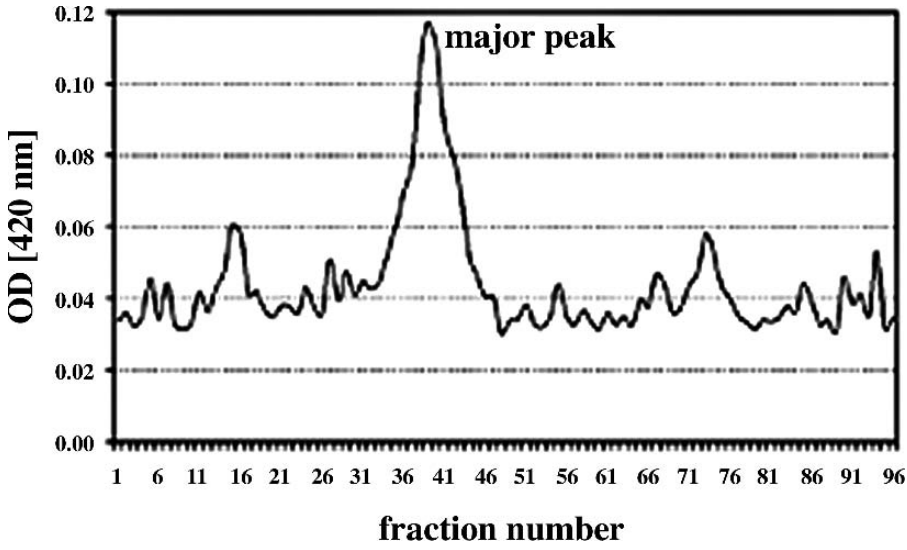


Fig. 7. Zone electrophoretic enrichment of yeast mitochondria. The major peak shows the main mitochondria fraction.

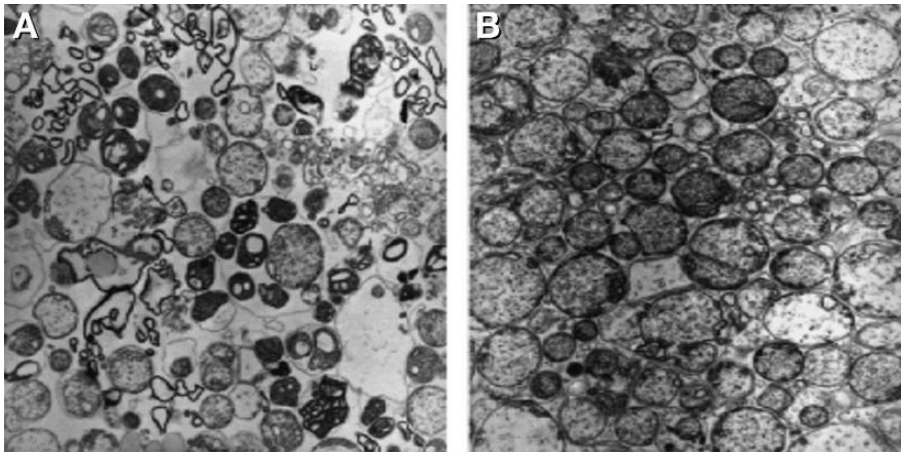


Fig. 8. Electron microscopy of zone electrophoretic-enriched yeast mitochondria **(B)** compared to starting sample **(A)**.

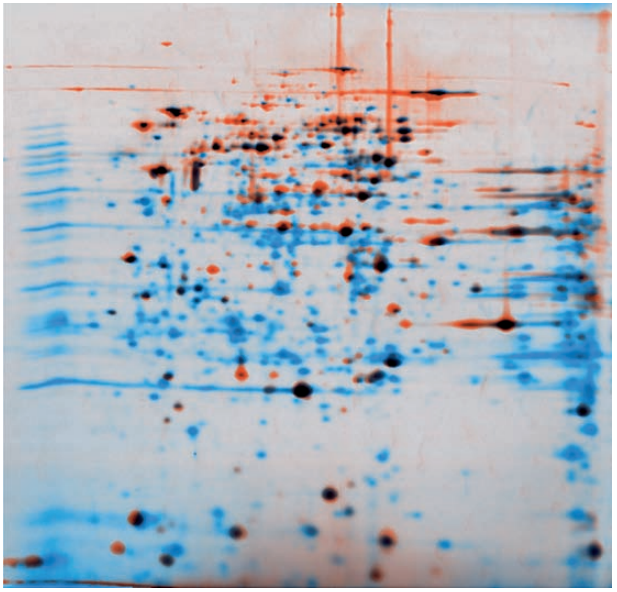


Fig. 9. Two-dimensional (2D) electrophoresis of purified yeast mitochondria compared to unprocessed sample with 2D-Image Analysis revealed the removal of degraded proteins:. blue spots, raw mitochondria; black spots, overlapping spots of same or similar intensity.

3.4. Zone Electrophoretic Enrichment of Yeast Mitochondria (see Fig. 7)

3.4.1. Electrophoretic Conditions and Data Analysis

Electrophoresis was performed in horizontal mode at 5 °C with a total flow rate of 280 mL/h within the separation chamber at a voltage of 750 V (135 mA). The samples were applied to the separation chamber with a flow rate of 0.5 mL/h via the cathodic inlet. Fractions were collected in 96-well plates and the distribution of separated particles was monitored at a wavelength of 420 nm with a Sunrise. MTP reader (Tecan). Subsequently, FFE fractions showing increased light scattering values were concentrated by centrifugation at 15 °C with 10,000 *g* for 15 min. The pellets were then snap-frozen in liquid nitrogen and used for electron microscopy (EM) or 2-DE analysis.

3.5. Conclusion

The samples of the FFE processed mitochondria were compared with unprocessed samples using 2-DE (IPG-Dalt) (*see* **Figs. 8** and **9**). Here, we gained a reduction of protein spots from 400 in the original sample to 250 in the FFE processed sample. From these 250 spots, 37% were only detectable in the FFE purified mitochondria and the nonmitochondrial proteins were reduced from 16% in the crude sample to 2% in the purified samples. Truncated proteins were also depleted from 49% to 6% in the purified mitochondria extract.

4. Notes

1. *Turbidity* of protein samples is an indication of insufficient solubility and/or protein precipitation. Protein samples should not be turbid; otherwise, the resolution of the electrophoretic separation will be poor. Turbid protein samples must be cleared by centrifugation prior to the FFE separation, whereas organelle samples are turbid by nature and must not be cleared before the FFE separation!
   The *salt concentration* of samples may not exceed 25 m*M*. If the conductivity of the sample due to the salt concentration is too high, it must be desalted or diluted to reach <25 m*M* of total salt concentration.
   Generally, the sample should be as similar to the separation media as possible with regard to the chemical and physical properties such as density, conductivity, and viscosity. Therefore, we dilute or dissolve the sample at least 1 : 3 with the separation medium.
2. The system must be *cleaned* thoroughly prior to use. Usually, the separation chamber is wiped with water, isopropanol, and petrolether and again with isopropanol and water to eliminate any organic and anorganic contamination.
   Protein sample is usually applied on the cathodic inlet. Only few samples work better when applied at the middle or anodic inlet; this can be checked for each sample. Plasma on the depletion gradient, for example, is applied in the middle. Typical sample application is between 200 µL and 750 µL per hour.

References

1. Weber, G. and Bocek, P. (1998) Recent developments in preparative free flow isoelectric focusing. *Electrophoresis* **19,** 1649–1653.
2. Zischka H, Weber G, Weber PJ, et al. (2003) Improved proteome analysis of *Saccharomyces cerevisiae* mitochondria by free-flow electrophoresis. *Proteomics* **3(6),** 906–916.
3. Hoffmann, P., Ji, H., Moritz, R. L., Connolly, L. M., et al. (2001) Continuous free-flow electrophoresis separation of cytosolic proteins from the human colon carcinoma cell line LIM 1215: a non two-dimensional gel electrophoresis-based proteome analysis strategy. *Proteomics* **1,** 807–818.
4. Obermaier, C., Jankowski, V., Schmutzler, C., et al. (2005) Free-flow isoelectric focusing of proteins remaining in cell fragments following sonication of thyroid carcinoma cells. *Electrophoresis* **26(11),** 2109–2116.

29

Microemulsion Electrokinetic Chromatography

Wolfgang W. Buchberger

Summary

Microemulsion electrokinetic chromatography (MEEKC) is an attractive capillary electrophoretic technique in which a microemulsion is used as carrier electrolyte. Analytes may partition between the aqueous phase of the microemulsion and its oil droplets, which act as a pseudostationary phase. It is well suited for the separation of neutral analytes, but can also be employed for charged analytes. A single set of separation parameters may be sufficient for separation of a wide range of analytes. Fine-tuning of the separation may be achieved by addition of organic solvents to the microemulsion or by changes in the nature of the surfactant used for stabilization of the microemulsion. In this chapter, MEEKC conditions are summarized that have proven their reliability for routine purposes. Furthermore, microemulsions can be used for on-capillary preconcentration of analytes so that the problem of poor concentration sensitivity of ultraviolet detection in capillary electrophoresis is circumvented.

Key Words: Microemulsion electrokinetic chromatography; capillary electrophoresis; pseudostationary phase; hydrophobic analytes; preconcentration.

1. Introduction

Microemulsion electrokinetic chromatography (MEEKC) is a special mode of capillary electrophoresis (CE) using a microemulsion as carrier electrolyte. Contrary to various other CE techniques, MEEKC is suited for the separation of neutral analytes. In addition, it can also be used for separation of charged species, whereby separation selectivities may be achieved which are quite different from those obtained by other CE techniques. The possibility of utilizing microemulsions in CE has been demonstrated for the first time in 1991 by Watarai ***(1)***.

From: *Methods in Molecular Biology, vol. 384: Capillary Electrophoresis*
Edited by: P. Schmitt-Kopplin © Humana Press Inc., Totowa, NJ

1.1. Fundamentals

Microemulsions are dispersions of two immiscible liquids and consist either of oil droplets suspended in water (oil-in-water [o/w] microemulsions) or of water droplets suspended in an oil phase (water-in-oil [w/o] microemulsions). Oil-in-water microemulsions are preferred for MEEKC and often consist of octane droplets dispersed in an aqueous buffer. Surfactants are added that can coat the octane droplets and lower the surface tension between the two liquids, thereby allowing the formation of a stable microemulsion. The surface tension may be further lowered by the addition of a short-chain alcohol like n-butanol, which is called a cosurfactant. The diameter of the droplets in such a microemulsion is below 10 nm. Therefore, the microemulsion is optically transparent and looks like a single-phase solvent, although it is a two-phase system.

Sodium dodecyl sulfate (SDS) is frequently used for stabilization of the microemulsion. As a result of this anionic surfactant, the oil droplets will acquire a negative charge and will exhibit an electrophoretic mobility directed towards the anode. The aqueous phase generally consists of phosphate or borate buffer of alkaline pH. In fused-silica capillaries, these buffers generate an electroosmotic flow (EOF) toward the cathode. Under alkaline conditions, the magnitude of the EOF exceeds the mobility of the oil droplets (which is directed against the EOF). Therefore, the EOF is strong enough to sweep the oil droplets to the cathode. The apparent mobility of the oil droplets is directed to the cathode and will have a magnitude that is lower than that of the EOF.

Highly water-soluble neutral analytes injected at the anodic side of the capillary will reside predominantly in the aqueous phase so that they will be transported to a detector located at the cathodic side of the separation capillary by the EOF and at its speed. The time at which they reach the detector after injection may be called t_{EOF}. Conversely, highly hydrophobic analytes will reside predominantly in the oil droplets and will be transported to the cathodic detection side according to the apparent mobility of the droplets and will reach the detector after the time t_{ME}. Other analytes of medium polarity will undergo a partitioning equilibrium between the aqueous phase and the oil phase so that they will reach the detector at a time t_r between t_{EOF} and t_{ME}. Therefore, neutral analytes can be separated according to their hydrophobicities. Obviously, this separation mechanism depends on chromatographic principles. The oil phase may be called a pseudo-stationary phase. In analogy to chromatography, one can define retention factors k for the analytes:

$$k = \frac{t_R - t_{EOF}}{t_{EOF}\left(\frac{1-t_R}{t_{ME}}\right)}.$$

In the case of a true stationary phase as encountered in liquid chromatography, the value for t_{ME} would become infinite and t_{EOF} would be the dead time, so that the equation given above would yield the result that k is the ratio of net retention time to dead time, a fact that is well known.

A schematic presentation of the MEEKC separation process is given in **Fig. 1**. Additional details on the theory of MEEKC can be found in recent reviews ***(2–4)***. It should be pointed out that the separation mechanisms in MEEKC are similar to those in micellar elektrokinetic chromatography (MEKC), which uses micelles (aggregates of surfactant molecules) as pseudostationary phase. Nevertheless, when looking for advantages of MEEKC over MEKC, two major aspects should be taken into consideration: (1) oil droplets exhibit a reduced rigidity compared to micelles so that hydrophobic analytes can more easily penetrate the surface and enter the core of the droplets, and (2) MEEKC may offer a somewhat larger separation window (the time window between t_{EOF} and t_{ME}), which may be controlled by employing mixed surfactants consisting of charged and uncharged species in different compositions. In this way, the total charge of the droplets and their mobility can be manipulated.

Acidic buffers may be used instead of basic buffers. In this case, the EOF is very low and can no longer transport a pseudostationary phase, such as droplets stabilized by anionic SDS to the cathodic detection side. In such a case, the detection end of the capillary must be the anode. Under these conditions it is also possible to achieve a considerable proconcentration effect during injection. This aspect will be discussed below.

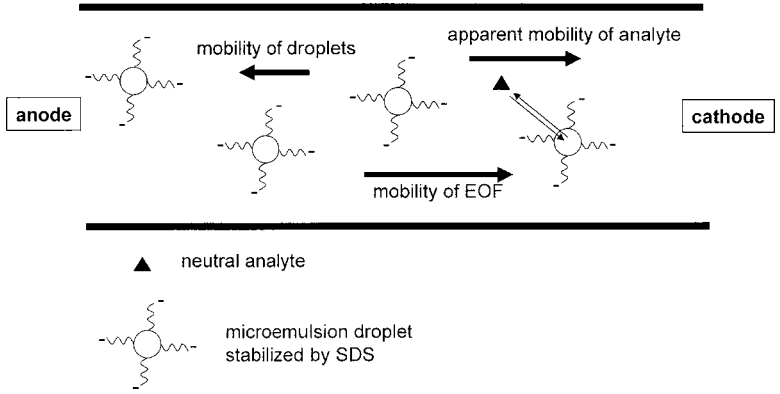


Fig. 1. Principle of the separation process in microemulsion electrokinetic chromatography for a neutral analyte in an alkaline microemulsion stabilized by negatively charged sodium dodecyl sulfate.

MEEKC separations of ionic analytes are governed by their electrophoretic mobility as well as by their interactions with the pseudostationary phase.

1.2. Optimization of the Separation of Neutral Analytes

Detailed investigatons have been reported in the literature regarding the manipulation of separation selectivity (migration order) of neutral analytes ***(5)***. Variables to be optimized include the kind of oil phase, the kind of surfactant and cosurfactant, and the addition of water-miscible organic solvents.

A wide range of water-immiscible solvents have been tested with respect to their suitability to act as pseudostationary phase, such as alkanes, alcohols, ketones, ethers, esters, or chlorinated alkanes. From the results reported in the literature, one gets the impression that the nature of the oil phase plays just a minor role for manipulation of separation selectivity. Small variations in the separation of critical peak pairs may occur, but major changes in migration order have not been observed. Another aspect connected with the type of oil phase is analysis time. Generally, a higher field strength will decrease the analysis time, but at the same time will increase the electric current. Therefore, carrier electrolytes of low ionic strength are advantageous. The ionic strength of standard-type microemulsions is quite high as a result of the presence of SDS. Oil phases of lower surface tension will require lower amounts of surfactant so that the applied voltage can be increased to speed up the separation. This approach has been used by Mahuzier et al. ***(6)***, who selected ethyl acetate or di-n-butyl tartrate as oil phases.

Variations in nature and concentration of the cosurfactant lead to considerably more pronounced effects on separation selectivity than the nature of the oil phase. A typical cosurfactant is 1-butanol (6.6 % w/w in the carrier electrolyte). Hansen et al. ***(7,8)*** have performed detailed studies using different alcohols or tetrahydrofuran at different concentrations as cosurfactants. Generally, a suitable cosurfactant is characterized by a somewhat lower hydrophobicity than the oil phase. Unfortunately, it seems that there are no general rules as to how to predict the effect of cosurfactants on a specific separation problem.

Different surfactants for stabilization of the microemulsion may also have a significant effect on the separation. Using mixtures of SDS and a neutral surfactant instead of neat SDS leads to a decrease of the charge density on the droplet and thereby to a general decrease of migration times. In addition, some changes in migration order may be observed because the hydrophobicity of the mixed surfactant is different than that of neat SDS ***(5)***. Substitution of SDS by other anionic surfactants like bile salts or phosphatidylcholine is another way to optimize separation selectivity ***(9)***. Instead of negatively charged surfactants,

one can also use cationic surfactants such as cetyltrimethylammonium bromide (CTAB) ***(10)***. This surfactant also generates a positively charged inner surface of the fused-silica capillary so that the EOF direction is reversed. Therefore, the detector must be positioned at the anodic end of the capillary when working with CTAB.

Finally, water-miscible organic solvents may be added to the carrier electrolyte. In this way, the partitioning equilibria of the analytes between the two phases can be manipulated. This aspect is of major importance when water-insoluble analytes are separated, as these would not partition at all into a purely aqueous phase and would therefore reach the detector after the time t_{ME}. This approach has been successfully applied to the analysis of hydrophobic polymer additives ***(11)***. Depending on the type of water-miscible organic solvent, there are different upper limits for use in MEEKC. Exceeding these limits results in an disintegration of the microemulsion. It has been reported that methanol may be used up to 8% (v/v), acetonitrile up to 12 %, whereas 2-propanol can be used at considerably higher concentration ***(12)***. In this context, one should not forget the well known effect of organic solvents on the magnitude of the EOF, which depends on the dielectric constant of the liquid phase, on the viscosity, and on the zeta potential of the capillary wall (all these parameters are directly influenced by amount and type of organic solvent in the aqueous phase of the carrier electrolyte).

1.3. Optimization of the Separation of Ionic Analytes

The use of MEEKC for the analysis of ionic analytes will result in a separation based on both the electrophoretic behavior and the partitioning of the analytes. The partitioning equilibrium of ionic species will be affected by the charge of the droplets. When SDS is employed as surfactant, anionic analytes will undergo repulsion from the negatively charged droplets and separation may be dominated by the electrophoretic mobility of the analytes. Cationic analytes may—besides partitioning between the aqueous and the oil phase—undergo additional ion-pairing interactions either with the negatively charged droplets or with SDS in the aqueous phase. The latter ion-pairing reaction may favor the partitioning reaction into the oil droplet ***(13)***.

The use of cationic surfactants (CTAB) leads to a repulsion of cationic analytes and to additional interactions with anionic analytes in a manner analogous to that mentioned above. Alternatively, separation of ionic analytes can be done in microemulsions containing oil droplets stabilized by a neutral surfactant. Typically, polyoxyethylene fatty ethers like Brij 35 (polyoxyethylene(23) monolaurylether) or Triton X-100 are used.

The separation of ionic analytes by MEEKC will strongly depend on the pH if the analytes undergo pH-dependent protonation/deprotonation reactions. In

such cases, both electrophoretic mobility and partitioning will depend on the pH of the aqueous phase of the microemulsion.

1.4. Sample Preconcentration by Sweeping

Sweeping preconcentration techniques have been developed by Terabe and coworkers (a review can be found in **ref. *14***) for trace analysis in CE. Sweeping is defined as the picking and accumulating of analytes by a charged pseudostationary phase that penetrates the sample zone during application of a voltage. Although most work on sweeping has been done using micelles as pseudostationary phase, the same principles work for microemulsions. Efficient preconcentration can be achieved with an oil phase stabilized by a negatively charged surfactant and an aqueous phase of low pH. The sample solution that does not contain the pseudostationary phase is injected hydrodynamically at the cathodic end of the capillary. After injection, the anionic pseudostationary phase will migrate from the cathodic carrier electrolyte vial into the capillary and into the sample zone (because of the low pH, the EOF can be neglected). In the sample zone, neutral analytes undergo partitioning and are focused into a narrow zone. As a result of the focussing effect, quite high volumes of sample may be injected without peak broadening. A more than 1000-fold increase in sensitivity is possible by sweeping techniques.

1.5. Water-in-Oil Microemulsions

As mentioned above, MEEKC separations are almost exclusively carried out in oil-in-water microemulsions. Nevertheless, more recent work has demonstrated that even water-in-oil microemulsions may be used ***(15)***. A typical water-in-oil microemulsion consists of 10% SDS, 80% butanol and 10% aqueous buffer. Despite some promising results, at the moment the impact of water-in-oil microemulsions on the further development of MEEKC cannot be fully anticipated.

1.6. Applications

The following discussion cannot give an exhaustive compilation of applications reported so far but intends to give an idea of the broad variety of classes of analytes that can be separated by MEEKC. These applications range from pharmaceutical drugs to vitamins, agrochemicals, polycyclic hydrocarbons, natural products, derivatized sugars, proteins, fatty acids, nucleosides, and chiral compounds. It is possible to use a single set of operating conditions for different applications. A microemulsion consisting of 0.8% (w/w) octane, 6.6% (w/w) 1-butanol, 3.3% (w/w) SDS, and 89.3% (w/w) 10 m*M* sodium

tetraborate buffer is suitable for a wide range of pharmaceutical compounds ***(16–18)***. In cases where this composition does not lead to satisfactory results, fine-tuning is possible by variation of the components of the microemulsion according to the principles discussed above.

Chiral MEEKC separations have become possible by the use of a chiral oil such as (2R,3R)-di-n-butyl tartrate ***(19)*** or a chiral surfactant such as dodecoxycarbonlyvaline ***(20)***. **Table 1** summarizes various applications from different fields of analysis.

Table 1
Applications of Microemulsion Electrokinetic Chromatography

Analytes	Carrier electrolyte	*Ref,*
Fat-soluble vitamins	0.8% n-octane/6.6% 1-butanol/6.0% SDS/20.0% 2-propanol/66.6% 25 m*M* phosphate buffer pH 2.5	***21***
Water- and fat-soluble vitamins	0.81% n-octane/6.61% 1-butanol/3.31% SDS/89.27% 10 m*M* sodium tetraborate	***18***
Hyydroxybenzoate preservatives	0.81% n-octane/6.61% 1-butanol/3.31% SDS/89.27% 50 m*M* phosphate buffer pH 2.1	***22***
Preservatives in food	0.8% n-octane/6.6% 1-butanol/3.3% SDS/89.3% borate buffer pH 9.5	***23***
Phenolic antioxidants	0.8% n-octane/6.6% 1-butanol/2.25% SDS/0.75% Brij35/25% 2-propanol/64.6% 10 m*M* borate buffer pH 9.2	***11***
Lignin degradation products	0.91% n-heptane/6.61% 1-butanol/1.66% SDS/90.92% 20 m*M* sodium tetraborate	***24***
Methylquinolines	0.82% n-heptane/6.62% 1-butanol/3.32% SDS/89.2% borate buffer pH 9.4; 0.82% n-octane/6.62% 1-butanol/3.32% Brij35/89.2% acetate buffer pH 4.0	***25***
Sun protection agents	0.8% n-octane/6.6% 1-butanol/2.25% SDS/0.75% Brij35/17.5% 2-propanol/72.1% 10 m*M* borate buffer pH 9.2	***26***
Polycyclic aromatic hydrocarbons	90% (v/v) [0.81% n-octane/6.61% 1-butanol/3.31% SDS/89.27% 10 m*M* sodium tatraborate], 10% (v/v) ethanol	***2***
Derivatized sugars	0.81% n-octanol/6.61% 1-butanol/3.31% SDS/89.27% 5 mM borate buffer pH 8.0	***27***
Derivatized fatty acids	0.66% n-heptane/6.55% 1-butanol/4.87% cholate/87.93% 10 mM borate buffer pH 10.2	***28***

(Continued)

Table 1
(Continued)

Analytes	Carrier electrolyte	*Ref,*
Derivatized amino acids	0.52% heptane/4.23% butanol/2.12% SDS/93.13% sodium tetraborate	***29***
Sulfated disaccharides	0.81% n-octane/6.61% 1-butanol/3.31% SDS/89.27% 10 m*M* sodium tatraborate	***30***
Green tea catechins	1.36% n-heptane/7.66% cyclohexanol/2.89% SDS/88.09% 50 m*M* sodium phosphate pH 2.5	***31***
Cardiac glycosides	0.81% n-heptane/6.61% 1-butanol/1.66% SDS/90.92% 50 m*M* sodium tetraborate	***32***
Steroids	0.81% hexanol/6.61% 1-butanol/3.31% SDS/89.27% 20 m*M* phosphate buffer pH 10.0	***33***
Steroids	0.81% n-octane/6.61% 1-butanol/3.31% SDS/89.27% 10 m*M* sodium tetraborate	***18***
Antibiotics	0.81% n-octane/6.61% 1-butanol/3.31% SDS/89.27% 10 m*M* sodium tetraborate	***18***
Cephalosporins	0.82% n-heptane/6.49% 1-butanol/1.44% glycodeoxycholic acid/5.69% Tween/86.56% 10 m*M* phosphate buffer pH 7.0	***34***
Diuretics	1.0% n-octane/7.5% 1-butanol/3.3% SDS/78.2% 10 m*M* borate buffer pH 9.5	***35***
Antiepileptic drugs and metabolites	0.48% n-octane/3.96% 1-butanol/1.98% SDS/93.6% 10 m*M* borate buffer pH 9.7	***36***
Steroids, benzodiazepines, antidepressants, antipsychotic drugs, antiepileptic drugs	0.8% n-octane/6.6% 1-butanol/6.0% SDS/20.0% 2-propanol/66.6% 25 m*M* phosphate buffer pH 2.5	***37***
Various basic and acidic drugs	0.81% n-octane/6.61% 1-butanol/3.31% SDS/89.27% 10 m*M* sodium tetraborate	***18***
Endocrine disrupting compounds	25 m*M* phosphate buffer pH 2, 80 m*M* octane, 900 m*M* butanol, 200 m*M* SDS, with 20% propanol	***38***
Food colorants	0.81% n-octane/6.61% 1-butanol/3.31% SDS/10% acetonitrile/79,27% 50 m*M* phosphate buffer pH 2.0	***39***
Rhubarb anthraquinones and bianthrones	0.5% di-n-butyl tartrate/1.2 % 1-butanol/0.6% SDS/97.7% 10 m*M* borate buffer pH 9.2	***40***

Besides its benefits for analytical chemistry, MEEKC is also a simple tool for assessments of hydrophobicity (octanol-water partition coefficient $P_{o/w}$) of neutral solutes. A linear relationship exists between log $P_{o/w}$ and log k (k being the retention factor as mentioned above). Slope and intercept of the linear calibration line can be obtained from experiments with solutes of known octanol-water partition coefficients (***41–43***).

2. Materials

1. *Microemulsion for general applications using a negatively charged oil phase*: mix 3.3 g SDS and 6.6 g 1-butanol, and then add 0.8 g n-octane and 89.3 g 10 m*M* borate buffer pH 9.4 (prepared from a 10 m*M* boric acid adjusted to pH 9.4 with NaOH). The mixture is placed in an ultrasonic bath for 30 min to obtain a clear solution. Afterward, the microemulsion is filtered through a 0.45-μm membrane filter.
2. *Microemulsion for highly hydrophobic analytes using a negatively charged oil phase*: mix 2.25 g SDS, 0.75 g Brij 35 (*see* **Note 1**), and 6.6 g 1-butanol, and then add 0.8 g n-octane, 25 g 2-propanol, and 64.6 g 10 m*M* borate buffer pH 9.4 (prepared from a 10 m*M* boric acid adjusted to pH 9.4 with NaOH). The mixture is placed in an ultrasonic bath for 30 min to obtain a clear solution. Afterwards, the microemulsion is filtered through a 0.45-μm membrane filter.
3. *Microemulsion for general applications using a neutral oil phase*: mix 3.32 g Brij 35 and 6.62 g 1-butanol, and then add 0.82 g n-heptane and 89.2 g 25 m*M* acetate buffer pH 4.0 (prepared from a 25 m*M* acetic acid adjusted to pH 4.0 with NaOH). The mixture is placed in an ultrasonic bath for 30 min to obtain a clear solution. Afterwards, the microemulsion is filtered through a 0.45-μm membrane filter (*see* **Note 2**).
4. *Microemulsion for on-capillary preconcentration by sweeping using a negatively charged oil phase*: mix 3.3 g SDS and 6.6g 1-butanol, and then add 0.8 g n-octane and 89.3 g 50 mM phosphoric acid pH 2.0. The mixture is placed in an ultrasonic bath for 30 min to obtain a clear solution. Afterwards the microemulsion is filtered through a 0.45-μm membrane filter.
5. CE instrument HP 3D (Agilent, Waldbronn, Germany), or equivalent, equipped with an ultraviolet (UV) absorbance detector, high voltage supply up to ±30 kV, and autosampler for both hydrodynamic and electrokinetic injection.
6. Fused-silica capillaries (Polymicro Technologies, Phoenix, AZ) with inner and outer diameter of 50 and 360 μm, respectively, a length from inlet to detector of 51.5 cm, and a length from inlet to outlet of 60 cm (*see* **Note 3**).
7. Sample vials for autosampler of CE instrument.

3. Methods

3.1. General Procedure for Conditioning New Fused Silica Capillaries

1. Four vials are filled with 1 *M* NaOH, water, 0.1 *M* NaOH, and 0.2 *M* HCl, respectively.

2. The vials are placed into appropriate positions of the autosampler for rinsing the capillary.
3. The capillary is rinsed with 1 *M* NaOH for 10 min, with water for 5 min, with 0.2 *M* HCl for 10 min, with water for 1 min, with 0.1 *M* NaOH for 10 min, and with water for 10 min.

3.2. Separation of Neutral Analytes Using a Negatively Charged Oil Phase

1. Two vials are filled with 0.1 *M* NaOH and microemulsion, respectively, for rinsing the capillary (the microemulsion is prepared according to the procedure given under **Subheading 2, item 1.**).
2. Two carrier electrolyte vials (for inlet and outlet side) are filled with the microemulsion.
3. Sample solutions and calibration solutions are filled into vials (*see* **Note 4**).
4. All vials are put into the appropriate positions of the autosampler.
5. The capillary is rinsed with 0.1 *M* NaOH for 5 min and with microemulsion for 5 min.
6. The first sample or calibration solution is injected using hydrodynamic injection at a pressure of 50 mbar for 5 s (*see* **Note 5**), and the separation is started by applying a voltage of +25 kV (*see* **Note 6**).
7. The capillary is rinsed with 0.1 *M* NaOH for 1 min and with microemulsion for 1 min.
8. **Steps 6** and **7** are repeated for the next sample or calibration solution.

A typical application is given in **Fig. 2**, which shows the separation of closely related methyl derivatives of quinoline, which are used as raw materials for industrial production of agro chemicals and pharmaceuticals ***(25)***. At the pH 9.4 of the carrier electrolyte, these analytes are neutral and the separation process is governed by the partitioning between the aqueous phase and the negatively charged oil droplets.

3.3. Separation of Highly Hydrophobic Analytes Using a Negatively Charged Oil Phase

1. Two vials are filled with 0.1 *M* NaOH and microemulsion, respectively, for rinsing the capillary (the microemulsion is prepared according to the procedure given under **Subheading 2, item 2**).
2. Two carrier electrolyte vials (for inlet and outlet side) are filled with the microemulsion.
3. Fill vials with sample solutions and calibration solutions prepared in the microemulsion as solvent.
4. All vials are put into the appropriate positions of the autosampler.
5. The capillary is rinsed with 0.1 *M* NaOH for 5 min and with microemulsion for 5 min.
6. The first sample or calibration solution is injected using hydrodynamic injection at a pressure of 50 mbar for 3 s, and the separation is started by applying a voltage of +30 kV.

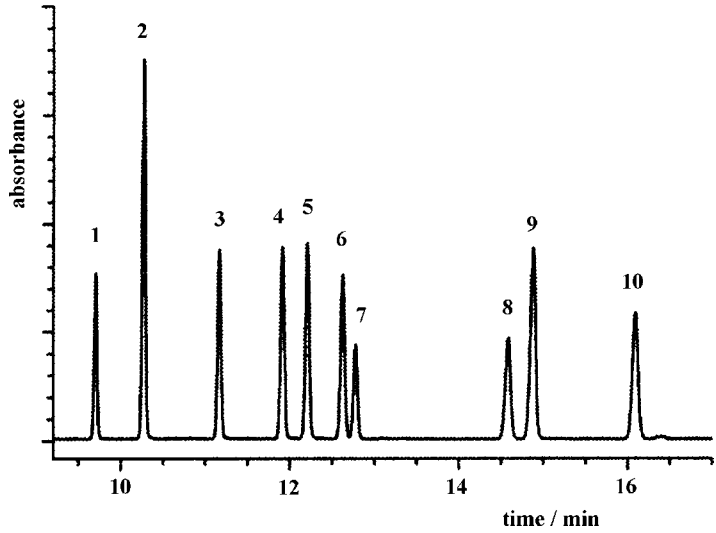


Fig. 2. Microemulsion electrokinetic chromatography separation of methylquinolines at pH 9.4 using a negatively charged oil phase. Separation conditions, *see* **Subheading 3.2.** Peaks: 1 = quinoline, 2 = isoquinoline, 3 = 2-methylquinoline, 4 = 4-methylquinoline, 5 = 3-methylquinoline, 6 = 6-methylquinoline, 7 = 8-methylquinoline, 8 = 4,8-dimethylquinoline, 9 = 2, 8-dimethylquinoline, 10 = 2, 4, 8-trimethylquinoline. Ultraviolet detection at 214 nm. Adapted from **ref. *25***.

7. The capillary is rinsed with 0.1 *M* NaOH for 1 min and with microemulsion for 1 min.
8. **Steps 6** and **7** are repeated for the next sample or calibration solution.

As an example, **Fig. 3** shows the separation of highly hydrophobic phenolic antioxidants used as additives in the production of polypropylene and similar polymers ***(11)***.

3.4. Separation of Positively Charged Analytes Using a Neutral Oil Phase

1. Two vials are filled with 0.1 *M* NaOH and microemulsion, respectively, for rinsing the capillary (the microemulsion is prepared according to the procedure given under **Subheading 2, item 3**).
2. Two carrier electrolyte vials (for inlet and outlet side) are filled with the microemulsion.
3. Vials are filled with sample solutions and calibration solutions.
4. All vials are put into the appropriate positions of the autosampler.
5. The capillary is rinsed with 0.1 *M* NaOH for 5 min and with microemulsion for 5 min.
6. The first sample or calibration solution is injected using hydrodynamic injection at a pressure of 50 mbar for 5 s (*see* **Note 5**), and the separation is started by applying a voltage of +25 kV (*see* **Notes 6** and **7**).

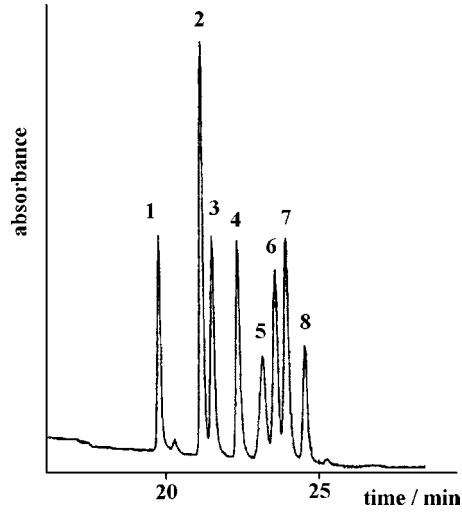


Fig. 3. Microemulsion electrokinetic chromatography separation of highly hydrophobic phenolic polymer additives. Separation conditions, *see* **Subheading 3.3.** Peaks: 1 = Irganox 1024, 2 = 2, 6-di-*tert*.-butyl-4-methylphenol, 3 = Irganox 1035, 4 = Irgafos 38, 5 = Irgafos 168, 6 = Irganox 1010, 7 = Irganox 1330, 8 = Irganox 1076. Ultraviolet detection at 214 nm. Adapted from **ref. *11***.

7. The capillary is rinsed with 0.1 *M* NaOH for 1 min and with microemulsion for 1 min.
8. **Steps 6** and **7** are repeated for the next sample or calibration solution.

A typical application is given in **Fig. 4**. The analytes include the same set of methylquinolines as in **Fig. 2**. At the pH 4.0 of the carrier electrolyte, the analytes are positively charged. Therefore, separation is governed by both the electrophoretic behavior and the partitioning between the aqueous phase and the oil phase. The use of a carrier electrolyte without the oil phase (capillary zone electrophoretic mode) would not lead to a satisfactory separation. A comparison between **Figs. 2** and **4** clearly demonstrates that completely different separation selectivities can be achieved.

3.5. Separation of Neutral Analytes with On-Capillary Preconcentration by Sweeping

1. Two vials are filled with 0.1 *M* NaOH and microemulsion, respectively, for rinsing the capillary (the microemulsion is prepared according to the procedure given under **Subheading 2, item 4**).
2. Two carrier electrolyte vials (for inlet and outlet side) are filled with the microemulsion.

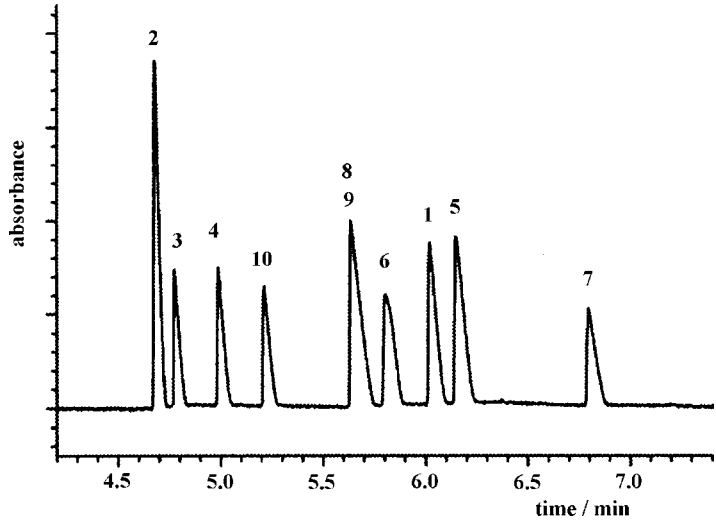


Fig. 4. Microemulsion electrokinetic chromatography separation of methylquinolines at pH 4.0 using a neutral oil phase. Separation conditions, *see* **Subheading 3.4.** Peak numbering identical to **Fig. 2**. Ultraviolet detection at 214 nm. Adapted from **ref. *25***.

3. Vials are filled with sample solutions and spiked sample solutions.
4. All vials are put into the appropriate positions of the autosampler.
5. The capillary is rinsed with 0.1 *M* NaOH for 5 min and with microemulsion for 5 min.
6. The first sample solution is injected using hydrodynamic injection at a pressure of 100 mbar for 150 s (*see* **Note 8**), and the separation is started by applying a voltage of −20 kV (*see* **Note 6**).
7. The capillary is rinsed with 0.1 *M* NaOH for 1 min and with microemulsion for 1 min.
8. **Steps 6** and **7** are repeated for the next sample or spiked sample solution (*see* **Note 9**).

4. Notes

1. The partial substitution of SDS by Brij 35 results in a lower charge of the oil droplet and therefore in a lower velocity. This leads to a decrease of the analysis time. For a specific separation, one can try to vary the ratio SDS/Brij 35 to achieve optimal analysis time.
2. This microemulsion prepared in a pH-4.0 buffer is suited for the separation of analytes that undergo protonation or deprotonation reactions at this pH, so that positively or negatively charged compounds are formed to some extent. The pH can be changed if necessary.

3. Shorter or longer capillaries can be used if necessary to optimize separation and analysis time.
4. If the analytes are not easily soluble in water, the sample and calibration solutions can be prepared in the microemulsion as the solvents. One should avoid pure organic solvents for the samples and calibration solutions, because these can disrupt the microemulsion adjacent to the zone of injected sample, leading to distorted peak shapes. It is recommended that an internal standard be added to both the sample and the calibration solutions.
5. Somewhat longer injection times can be used to achieve lower detection limits. Peak distortion will occur at too long injection times.
6. It may be advantageous to use somewhat lower or higher separation voltages depending on the length of the capillary.
7. The positive voltage applied is suited for cationic analytes. In the case of anionic analytes, it may be necessary to use a negative voltage (depending on the electrophoretic mobility of the analyte in relation to the electroosmotic mobility).
8. Depending on the analytes, this injection time may need to be decreased in order to avoid deterioration of peak shapes.
9. The incorporation of the on-line preconcentration effect makes quantitation by standard addition instead of external standards preferable.

References

1. Watarai, H. (1991) Microemulsion capillary electrophoresis. *Chem. Lett*. 391–394.
2. Altria, K. D. (2000) Background theory and applications of microemulsion electrokinetic chromatography. *J. Chromatogr*. **892,** 171–186.
3. Altria, K. D., Mahuzier, P. -E., and Clark, B. J. (2003) Background and operating parameters in microemulsion electrokinetic chromatography. *Electrophoresis* **24,** 315–324.
4. Klampfl, C. W. (2003) Solvent effects in microemulsion electrokinetic chromatography. *Electrophoresis* **24,** 1537–1543.
5. Gabel-Jensen, C., Hansen, S. H., and Pedersen-Bjergaard, S. (2001) Separation of neutral compounds by microemulsion electrokinetic chromatography: fundamental studies on selectivity. *Electrophoresis* **22,** 1330–1336.
6. Mahuzier, P. -E., Clark, B. J., Bryant, S. M., and Altria, K. D. (2001) High-speed microemulsion electrokinetic chromatography. *Electrophoresis* **22,** 3819–3823.
7. Hansen, S. H., Gabel-Jensen, C., and El-Sherbiny, D. T. M. (2001) Microemulsion electrokinetic chromatography–or solvent-modified micellar electrokinetic chromatography? *Trends Anal.Chem*. **20,** 614–619.
8. Hansen, S. H., Gabel-Jensen, C., and Pedersen-Bjergaard, S. (2001) Comparison of microemulsion electrokinetic chromatography and solvent-modified micellar electrokinetic chromatography. *J. Sep. Sci*. **24,** 643–650.
9. Lucangioli, S. E., Kenndler, E., Carlucci, A., Tripodi, V. P., Scioscia, S. L., and Carducci, C. N. (2003) Relation between retention factors of immunosuppressive drugs in microemulsion electrokinetic chromatography with biosurfactants and octanol-water partition coefficients. *J. Pharm. Biomed. Anal*. **33,** 871–878.

10. Boso, R. L., Bellini, M. S., Miksik, I., and Deyl, Z. (1995) Microemulsion electrokinetic chromatography with different organic modifiers: separation of water- and lipid-soluble vitamins. *J. Chromatogr. A*. **709,** 11–19.
11. Hilder, E. F., Klampfl, C. W., Buchberger, W., and Haddad, P. R. (2001) Separation of hydrophobic polymer additives by microemulsion electrokinetic chromatography. *J. Chromatogr. A*. **922,** 293–302.
12. Altria, K. D., Clark, B. J., and Mahuzier, P. -E. (2000) The effect of operating variables in microemulsion electrokinetic capillary chromatography. *Chromatographia* **52,** 758–768.
13. Pedersen-Bjergaard, S., Gabel-Jensen, C., and Hansen, S. H. (2000) Selectivity in microemulsion electrokinetic chromatography. *J. Chromatogr. A*. **897,** 375–381.
14. Quirino, J. P., Kim, J. -B., and Terabe, S. (2002) Sweeping: concentration mechanism and applications to high-sensitivity analysis in capillary electrophoresis. *J. Chromatogr. A*. **965,** 357–373.
15. Altria, K. D., Broderick, M. F., Donegan, S., and Power, J. (2004) The use of novel water-in-oil microemulsions in microemulsion electrokinetic chromatography. *Electrophoresis* **25,** 645–652.
16. Miola, M. F., Snowden, M. J., and Altria, K. D. (1998) The use of microemulsion electrokinetic chromatography in pharmaceutical analysis. *J. Pharm. Biomed. Anal*. **18,** 785–797.
17. Altria, K. D. (1999) Highly efficient and selective separations of a wide range of analytes obtained by an optimised microemulsion electrokinetic chromatography method. *Chromatographia* **49,** 457–464.
18. Altria, K. D. (1999) Application of microemulsion electrokinetic chromatography to the analysis of a wide range of pharmaceuticals and excipients. *J. Chromatogr. A*. **844,** 371–386.
19. Aiken, J. H. and Huie, C. W. (1993) Use of a microemulsion system to incorporate a lipophilic chiral selector in electrokinetic capillary chromatography. *Chromatographia* **35,** 448–450.
20. Mertzman, M. D. and Foley, J. P. (2004) Effect of substitution in chiral microemulsion electrokinetic chromatography. *Electrophoresis* **25,** 723–732.
21. Pedersen-Bjergaard, S., Naess, O., Moestue, S., and Rasmussen, K. E. (2000) Microemulsion electrokinetic chromatography in suppressed electroosmotic flow environment. Separation of fat-soluble vitamins. *J. Chromatogr. A*. **876,** 201–211.
22. Mahuzier, P. -E., Altria, K. D., and Clark, B. J. (2001) Selective and quantitative analysis of 4-hydroxybenzoate preservatives by microemulsion electrokinetic chromatography. *J. Chromatogr. A*. **924,** 465–470.
23. Huang, H. -Y., Chuang, C. -L., Chiu, C. W., and Yeh, J. M. (2005) Application of microemulsion electrokinetic chromatography for the detection of preservatives in foods. *Food Chem*. **89,** 315–322.
24. Javor, T., Buchberger, W., and Tanzcos, I. (2000) Determination of low-molecular-mass phenolic and non-phenolic lignin degradation compounds in wood digestion solutions by capillary electrophoresis. *Mikrochim. Acta* **135,** 45–53.

25. Schöftner, R. and Buchberger, W. (2003) Systematic investigations of different capillary electrophoretic techniques for separation of methylquinolines. *J. Sep. Sci*. **26,** 1247–1252.
26. Klampfl, C. W. and Leitner, T. (2003) Quantitative determination of UV filters in sunscreen lotions using microemulsion electrokinetic chromatography. *J. Sep. Sci*. **26,** 1259–1262.
27. Miksik, I., Gabriel, J., and Deyl, Z. (1997) Microemulsion electrokinetic chromatography of diphenylhydrazones of dicarbonyl sugars. *J. Chrmatogr. A*. **772,** 297–303.
28. Miksik, I. and Deyl, Z. (1998) Microemulsion electrokinetic chromatography of fatty acids as phenacyl esters. *J. Chromatogr. A*. **807,** 111–119.
29. Jianping, X., Jiyou, Z., Huanxiang L., et al. (2004) Microemulsion electrokinetic chromatography with laser-induced fluorescence detection: as tested with amino acid derivatives. *Biomed. Chromatogr*. **18,** 600–607.
30. Mastrogianni, O., Lamari, F., Syrokou, A., Militsopoulou, M., Hjerpe, A., and Karamanos, N. K. (2001) Microemulsion electrokinetic capillary chromatography of sulphated disaccharides derived from glycosaminoglycans. *Electrophoresis* **22,** 2743–2745.
31. Pomponio R., Gotti, R., Luppi, B., and Cavrini, V. (2003) Microemulsion electrokinetic chromatography for the analysis of green tea catechins: Effect of the cosurfactant on the separation selectivity. *Electrophoresis* **24,** 1658–1667.
32. Dobusschere, L., Demesmay C., Rocca, J. L., Lachatre, G., and Lofti, H. (1997) Separation of cardiac glycosides by micellar electrokinetic chromatography and microemulsion electrokinetic chromatography. *J. Chromatogr. A*. **779,** 227–233.
33. Vomastova, L., Miksik, I., and Deyl, Z. (1996) Microemulsion electrokinetic chromatography of steroids. *J. Chromatogr. B*. **681,** 107–113.
34. Mrestani, Y., El-Mokdad, N., Rüttinger, H. H., and Neubert, R. (1998) Characterization of partitioning behavior of cephalosporins using microemulsion and micellar electrokinetic chromatography. *Electrophoresis* **19,** 2895–2899.
35. Siren, H., and Karttunen, A. (2003) Microemulsion electrokinetic chromatographic analysis of some polar compounds. *J. Chromatogr. B*. **783,** 113–124.
36. Ivanova, M., Marziali, E., Raggi, M. A., and Kenndler, E. (2002) Microemulsion electrokinetic chromatography for the separation of carbamazepine, oxcarbazepine, and their metabolites. *J. Sep. Sci*. **25,** 863–871.
37. Pedersen-Bjergaard, S., and Gronhaug Halvorsen, T. (2000) Analysis of pharmaceuticals by microemulsion electrokinetic chromatography in a suppressed electroosmotic flow environment. *Chromatographia* **52,** 593–598.
38. Fogarty, B., Dempsey, E., and Regan, F. (2003) Potential for microemulsion electrokinetic chromatography for the separation of priority endocrine disrupting compounds. *J. Chromatogr. A*. **1014,** 129–139.
39. Huang, H. -Y., Chuang, C. -L., Chiu, C. -W., and Chung, M. -C. (2005) Determination of food colorants by microemulsion electrokinetic chromatography. *Electrophoresis* **26,** 867–877.

40. Sun, S. -W., and Yeh, P. -C. (2005) Analysis of rhubarb anthraquinones and bianthrones by microemulsion electrokinetic chromatography. *J. Pharm. Biomed. Anal*. **36,** 995–1001.
41. Gluck, S. J., Benkö, M. H., Hallberg, R. K., and Steele, K. P. (1996) Indirect determination of octanol-water partition coefficients by microemulsion electrokinetic chromatography. *J. Chromatogr. A*. **744,** 141–146.
42. Poole, S. K., Durham, D., and Kibbey, C. (2000) Rapid method for estimating the octanol-water partition coefficient by microemulsion electrokinetic chromatography. *J. Chromatogr. B*. **745,** 117–126.
43. Klotz, W. L., Schure, M. R., and Foley, J. P. (2001) Determination of octanol-water partition coefficients of pesticides by microemulsion electrokinetic chromatography. *J. Chromatogr. A*. **930,** 145–154.

30

Micellar Electrokinetic Chromatography of Aminoglycosides

Ulrike Holzgrabe, Stefanie Laug, and Frank Wienen

Summary

The components of the aminoglycosides, e.g., gentamicin, sisomicin, netilmicin, kanamycin, amikacin, and tobramycin, and related impurities of these antibiotics can be separated by means of micellar electrokinetic chromatography (MEKC). Derivatization with *o*-phthaldialdehyde and thioglycolic acid is found to be appropriate for all antibiotics. The background electrolyte was composed of sodium tetraborate (100 m*M*), sodium deoxycholate (20 m*M*), and β-cyclodextrin (15 m*M*) and has a pH value of 10.0. This method is valid for evaluation of gentamicin, kanamycin, and tobramycin. It has yet to be adopted for amikacin, paramomycin, neomycin, and netilmicin.

Key Words: MEKC; bile salts; background electrolyte; cyclodextrins; aminoglycosides; gentamicin; kanamycin; tobramycin.

1. Introduction

Micellar electrokinetic chromatography, denoted as MEKC and often called micellar electrokinetic capillary chromatography (MECC), was originally developed by Terabe ***(1)*** for separation of neutral compounds which cannot be achieved by capillary zone electrophoresis (CZE). Applying an ionic surfactant such as sodium dodecyl sulfate in a concentration higher than the critical micelle concentration and a high pH value makes a separation possible based on the differential partition of the analytes between the running buffer and the surfactant micelles.

The micelles form a pseudostationary phase moving with the migration velocity and in a direction that is different from that of the background electrolyte (BGE). Hence, the MEKC can be regarded as a hybrid of chromatography

From: *Methods in Molecular Biology, vol. 384: Capillary Electrophoresis*
Edited by: P. Schmitt-Kopplin © Humana Press Inc., Totowa, NJ

and capillary electrophoresis, and terms such as electrolyte solution and mobile phase, migration time and retention time, and elution and migration are equally used.

The separation of the analytes is possible between the migration velocity of the electrolyte solution, which is, at high pH values, identical to the electroosmotic flow (EOF), and the effective migration velocity of the surfactant micelles. Thus, analytes that remain only in the electrolyte solution cannot be separated. They migrate with the EOF at the time t_{eo}. Analytes residing exclusively in the micelles are also not separable and elute from the capillary at the migration time of the micelles t_{mc}. In the case that complexation constants between the various analytes and the micelles are different, a separation can be achieved within a characteristic migration t_a, in which $t_{eo} < t_a < t_{mc}$ (*see* **Fig. 1,** adapted from **ref. *2***). The migration order of neutral analytes is mostly related to their hydrophobicity; as a result of the hydrophobicity of the micelle core, the more hydrophobic analytes migrate more slowly than less hydrophobic analytes. For details of the physicochemical background, see the excellent introduction by Pyell ***(3)***.

For neutral analytes, the selectivity of the separation is sensitive to the differences in distribution constants between the electrolyte solution and the micelles, and in the case of ionized analytes, to the differences in distribution

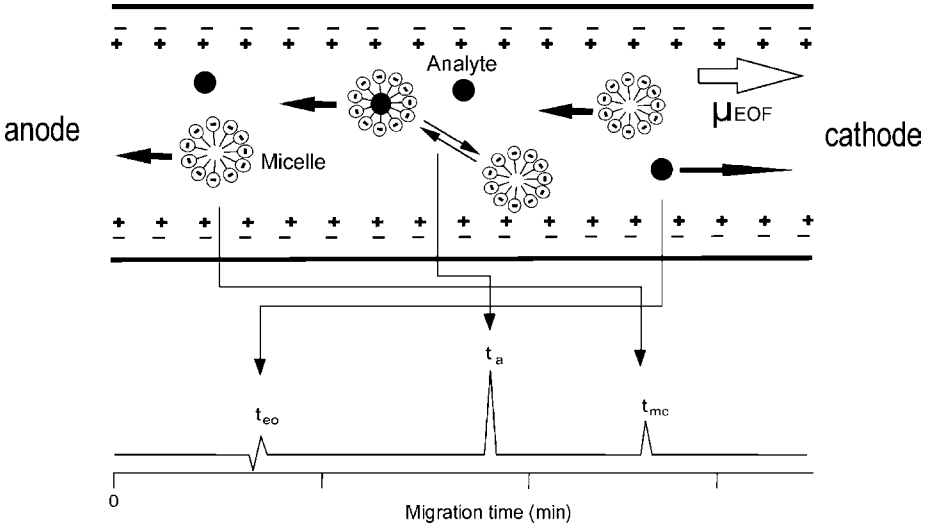


Fig. 1. Schematic representation of the separation mechanism of micellar electrokinetic chromatography (MEKC) using anionic micelles. t_{eo} = migration time of a neutral "unretained" analyte, t_a = "retention" time in MEKC, t_{mc} = migration time of a micelle.

constants between both phase and the effectively electrophoretic mobility. Favorable kinetic properties result in high efficiency and a reasonable peak capacity, especially for systems with a narrow migration window. Therefore, the choice of the surfactant system is of high importance for a satisfying separation. Separations can be further optimized by varying the pseudostationary phase/mobile phase ratio and by adding different concentrations of modifiers such as organic solvents, urea, complexing agents, e.g. cyclodextrins, etc., to the system. The modifier often reduces the distribution constant and widens the migration window. In addition, the buffer concentration, the ionic strength, and the pH may help to further widen the migration window for a better separation.

1.1. Micelle-Forming Agents

The surfactants are the selectivity determining factor. They can be categorized as anionic surfactants such as sulfates, sulfonates or carboxylates, bile salts, cationic surfactants containing quaternary ammonium head groups, and nonionic surfactants. Neutral and zwitterionic surfactants are employed as mixed-surfactant micelles by adding ionic surfactants. Otherwise, their mobility is identical to the electroosmotic mobility ***(4)***. **Table 1** gives an overview of the often-used micelle-forming agents. The surfactants used in MEKC should have a low critical micelle concentration, because high surfactant concentration would create an excessive current and high solution viscosity. The surfactant concentrations appropriate for MEKC are 10–200 m*M*. The surfactants must be available in a pure form, should have a good solubility, and a low ultraviolet (UV) absorbance and should be stable over the pH range necessary for the electroosmotic flow, i.e., pH 6.0 to 9.0.

As a result of the small detection cell volume, the detection limits are always low in comparison to high performance liquid chromatography (HPLC). The sensitivity can be enhanced by sample stacking, which is based on differences in the electric conductivity of bordering zones. As the ions move across the boundary separating regions of different electric field strength, they will be focused in a narrower zone than injected initially. In addition, sweeping can be applied, which is the "picking and accumulation of analyte molecules by the pseudostationary phase that penetrates the sample zone" ***(5)***. This also results in a focusing of the sample and, thus, in an increase in sensitivity.

1.2. Gentamicin

MEKC has been shown to be highly suitable for the separation of very complex mixtures of analytes with similar electrophoretic mobility of the components, which are often neutral, but can be also ionic. Thus, MEKC

Table 1
Surfactant Employed in Micellar Electrokinetic Chromatography and Their Critical Micelle Concentration in Distilled Water at Room Temperature

Surfactant	CMC (m*M*)
Anionic surfactants	
Sodium dodecyl sulphate (SDS)	8.1
Sodium dodecyl sulfonate	7.2
Sodium hexadecyl sulfate	2.1
Sodium *N*-lauryl-*N*-methyl-β-alaninate (ALE)	9.8 (40 °C)
Sodium *N*-lauryl-*N*-methyltaurate (LMT)	8.7 (35 °C)
Lithium perfluorooctanesulfonate (LIPFOS)	6.7
Bile salts	
Sodium cholate (Chol)	13–15
Sodium deoxycholate (DChol)	4–6
Sodium taurocholate (TC)	10–15
Sodium taurodeoxycholate (TDChol)	6
Cationic surfactants	
Tetradecyltrimethylammonium bromide (TTAB)	3.5
Cetyltrimethylammonium bromide (CTAB)	0.92
Zwitterionic surfactants	
N-Dodecyl-N,N-dimethylammonio-3-propanesulfonate	3.3
3-[(3-Cholamidopropyl)dimethylammonio-3-propanesulfonate (CHAPS)	8
Non-ionic surfactant	
Polyoxyethylene[23]dodecanol (Brij 35)	0.09
Polyoxyethylene[20]sorbitanmonolaurate	0.95

is appropriate to separate the components and impurities of aminoglycosides, e.g., gentamicin. Whereas the aminoglycosides kanamycin, neomycin, and paromomycin are characterized by one main component accompanied by some minor components of less than 5% content, gentamicin consists of four major components, i.e., GM C1, C1a, C2, and C2a, and some minor components such as GM C2b, 2-deoxystreptamine (DSA), garamine (GA), sisomicin, and netilmicin, the latter two being antibiotics on their own. In addition, impurities at a level often higher than 0.1%, which is the limit allowed for a small-molecule drugs, must be expected and evaluated.

As a result of the close structural relationship and the missing chromophor of the aminoglycosides, the evaluation of the composition and related substances is still a challenge for both HPLC ***(6–10)*** and CZE ***(11–13)*** applying

pre-capillary or pre-column derivatization, evaporative light-scattering detection, pulsed electrochemical detection, and thermospray mass detection. Recently, an MEKC method was developed ***(14)*** that is capable of separating and quantifying both the components of gentamicin and the impurities after a derivatization utilizing the o-phthaldialdehyde (OPA)/thioglycolic acid system, which was formerly used in the European Pharmacopoeia (EP) and which can be easily validated. The method is characterized by high selectivity and efficiency.

2. Materials

2.1. Apparatus

CE experiments were carried out on a HP^{3D}-CE (Agilent Technologies, Waldbronn, Germany) equipped with a DAD detector. The capillaries were purchased from Polymicro (BGB Analytik, Schloßböckelheim, Germany). The fused-silica capillaries were of 50 μm internal diameter and effective length of 24.5 cm. The samples were loaded by pressure injection applying 50 mbar for 5 s on the anode side and detection at 340 nm was performed at the cathode side. Electrophoresis was carried out at 25 °C and a voltage of 12 kV (*see* **Note 1**).

2.2. Reagents and Chemicals

1. Chemicals used were of analytical grade.
2. Gentamicin sulfate, netilmicin sulfate, and sisomicin (CRS) were purchased from Promochem (Wesel, Germany), DSA, and GA were gifts from Merck (Darmstadt, Germany); gentamicin C2b sulfate (also as known as sagamicin and micronomicin) was purchased from Pharm Chemical (Shanghai Lansheng Corporation, China).
3. The GM components C1, C1a, and C2/C2a were separated from a commercial sample of GM by column chromatography and analyzed by TLC, CE, and ^{1}H NMR ***(10)*** (*see* **Note 2**).
4. OPA (for fluorescence, ≥99%), DChol (MicroSelect ≥99%), picric acid, sodium tetraborate decahydrate (TB, 99.5%), and boric acid were purchased from Fluka/Riedel de Haen (Seelze, Germany), TGA (Reag. Ph. Eur., ≥99.0%), methanol (HPLC grade), and isopropanol from Merck (VWR-International, Darmstadt, Germany), and acetonitrile (HPLC grade) from Carl Roth (Karlsruhe, Germany). β-CD was a gift from the Consortium für Elektrochemische Industrie (München, Germany).

2.3. Buffers

1. All BGE solutions were prepared using ultrapure Milli-Q water and filtered with a 0.22-μm polyvinylidenefluoride filter (both Millipore, Milford, MA).

2. In order to prepare the BGE, adequate amounts of TB, DChol, and β-CD were weighed in a flask, 80% of the water needed was added, and the components were dissolved using an ultrasonic bath.
3. The required pH value was adjusted with NaOH solution (1.0 *M*). After the water was added, pH value was checked and adapted, if necessary.

2.4. Derivatization Reagent

1. The samples were dissolved in high-purity water solution (2.0 mg/mL) containing picric acid (IS, 7 mg/mL).
2. OPA reagent: 650 mg of OPA were dissolved in 2.0 mL of methanol and approx 15 mL of boric acid solution (pH 10.4, 30 m*M*). After ultrasonification, the solution was adjusted to pH 10.4 using potassium hydroxide solution (8 *M*). Thioglycolic acid (1.3 mL) was added and pH was adjusted again to 10.4 with potassium hydroxide solution (8 *M*).
3. This solution was diluted to 25.0 mL with boric acid solution (pH 10.4, 30 m*M*).
4. The solution can be stored at 4 °C for at least 48 h.

3. Methods

The European Pharmacopoeia (EP 5) ***(16)*** tries to limit the impurities of gentamicin by an HPLC method utilizing a styrene-divinylbenzene copolymer column and a pulsed amperometric detector. However, this method suffers from several drawbacks, e.g., the pulsed amperometric detection is not very robust, the run time of a chromatogram is longer than 70 min, and the main components of gentamicin elute partially more than 10 min. Thus, a CZE method developed by Kaale et al. ***(13)*** was a good starting point for the development of the MEKC method presented here.

Because the aminoglycosides lack any chromophores or fluorophores and all direct detection methods turned out to be not very robust, a derivatization using o-phthaldialdehyde and thioglycolic acid was chosen. This method was previously used in the PhEur and can be easily validated. Kaale et al. have also developed a corresponding in-capillary derivatization ***(17)***.

Having derivatized gentamicin, the obtained molecules are neutral and, thus, suitable for separation by MEKC. Applying the optimized CZE conditions (30 m*M* tetraborate buffer, 7.0 m*M* β-CD, 12.5% methanol), several micelle-forming agents, i.e., SDS, SChol, SDChol, STC, Brij35, CTAB, and TAB, were checked each at a concentration of 25 m*M* (*see* **Note 3**). The sodium cholic acids and, especially, the SDChol revealed the best separation. Variation of the BGE concentration between 10 and 125 m*M* tetraborate (TB) resulted in the best resolution of all components at 100 m*M*. In previous experiments, the kind and concentration of the cyclodextrins (CDs) (various neutral and negatively charged CDs) was varied and the cheap β-CD found to be appropriate. Applying increasing concentrations of β-CD lowered the run time and

gave a very good peak shape. Thus, the highest possible β-CD concentration was chosen (15 m*M*). Finally, the pH of the BGE was adapted. In a range of 9.5 to 10.5, the pH of 10.0 gave the best separation. Organic modifiers such as methanol, isopropanol, or acetonitrile did not improve the separation. For quantification purposes, an internal standard must be used. Picric acid was already successfully applied ***(11,13)*** and was also suitable for the MEKC method.

In order to assign the peaks of the electropherogram, the peaks must be spiked with reference substances. Although the method was found to be precise and robust with regard to the migration time (*see* **Fig. 2**), additional impurities may change the electropherogram in such a way that the assignment fails.

The method was applied to various lots of gentamicin collected form the European and American market. As can be seen from a comparison of **Fig. 2**, which displays a pure sample, and **Fig. 3**, which shows a sample with large number of impurities of high concentration, the methods is appropriate for evaluating the quality of a drug.

The method developed here is also appropriate for other aminoglycosides such as kanamycin and tobramycin and, with slight variation of the conditions, for amikacin, paramomycin, neomycin, and netilmicin ***(14)***.

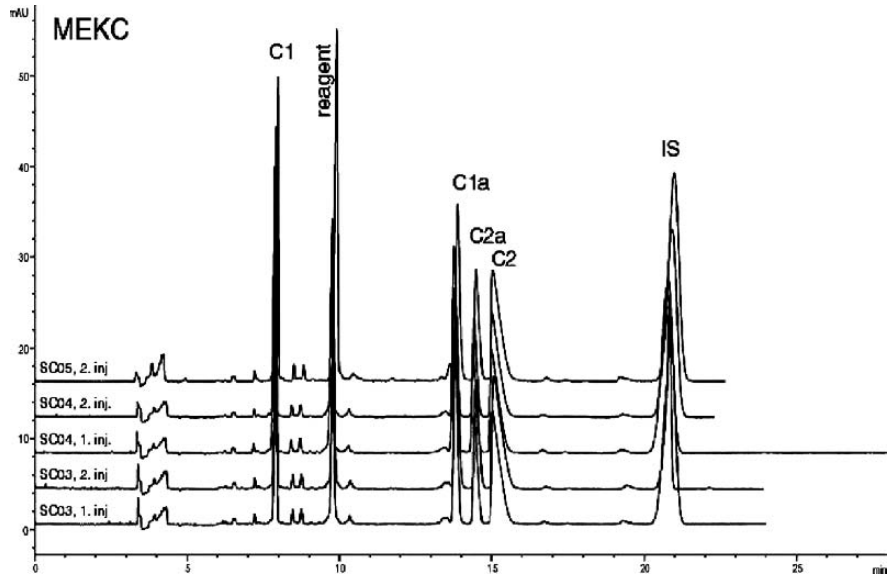


Fig. 2. Electropherograms of the same sample, but different derivatization reactions (SCO 3, 4, and 5), injected once or twice.

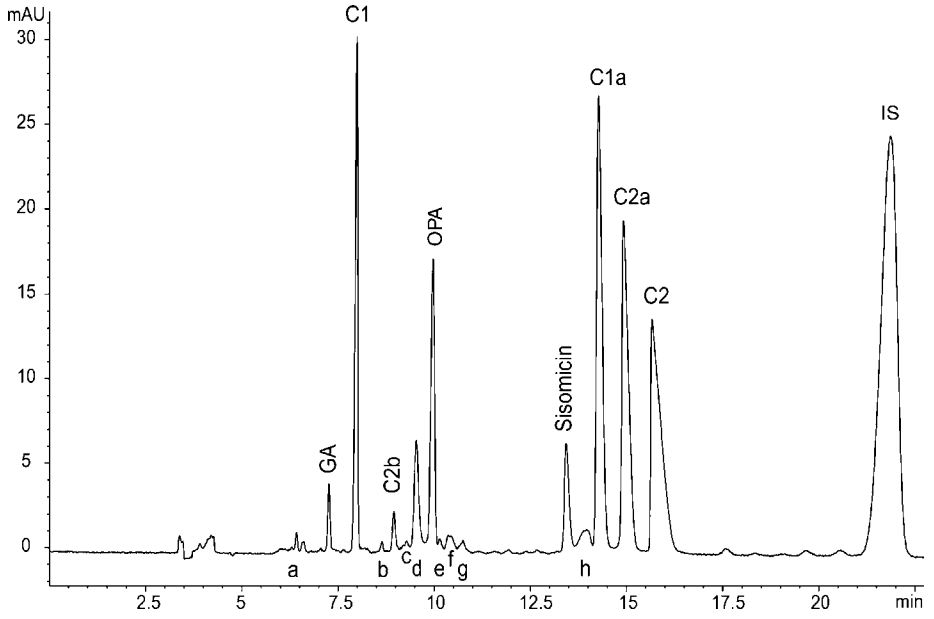


Fig. 3. Electropherogram of a sample of low purity showing sisomicin in addition to additional unknown impurities a–h.

3.1. Derivatization

The derivatization with OPA and thioglycolic acid described above was already optimized by Kaale et al. ***(11)***. The reaction can be performed either in methanol or isopropanol.

A volume of 0.45 mL of the sample solution was mixed with 0.25 mL of methanol and 0.16 mL of the OPA reagent (*see* **Note 4**). This solution was vortexed and heated in a water bath at 60 °C for exactly 4 min (*see* **Note 5**), and diluted to 1.0 mL with methanol. After cooling to room temperature, the solution was poured in a vial appropriate for CE. The measurement should start immediately.

3.2. Running Buffer

Optimized separation conditions for CE are the following:

1. The BGE was composed of a TB (100 m*M*, pH 10.0), DChol (20 m*M*) and β-CD (15 m*M*) (*see* **Notes 6** and **7**).
2. The pH value must be adapted to 10.0 (*see* **Note 8**).

3. The samples were loaded by pressure injection applying 50 mbar (= 0.0145 psi) for 5 s on the anode side and detection at 340 nm (*see* **Note 9**) was performed at the cathode side.
4. The electrophoresis was carried out at 25 °C and a voltage 12 kV.
5. In order to prove the absence or presence of netilmicin, the voltage must be increased (*see* **Note 1**).

3.3. Rinsing Procedure

In order to avoid crystallization of the components of running buffer, derivatization reagent, and the derivatized samples, and in order to increase the reproducibility, the capillary must be rinsed carefully. Thus, between two runs, the capillary was rinsed with water for 2 min (8 bar; = post-conditioning) and with NaOH solution (0.1 *M*) and water for 1.5 min (5 bar), respectively, and with HCl solution (1.0 *M*) and water for 2.0 min (5 bar), respectively, and with the BGE for 3 min (8 bar; = pre-conditioning) (*see* **Note 10**).

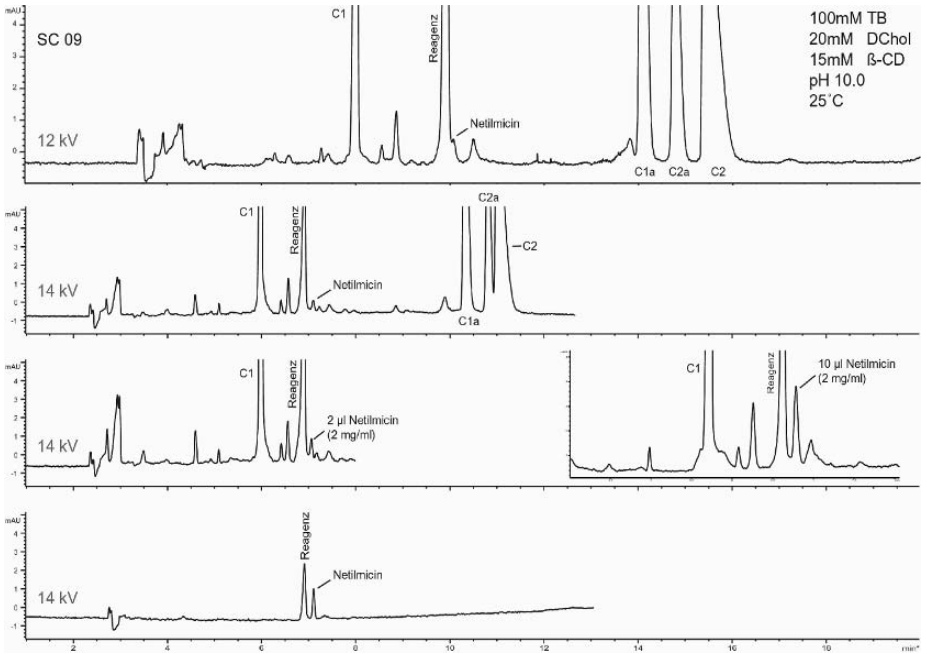


Fig. 4. **(A)** Electropherogram of a sample spiked with netilmicin; voltage 12 kV; **(B)** electropherogram of a sample spiked with netilmicin; voltage 14 kV; **(C)** electropherogram of a sample spiked with increasing amounts of netilmicin; voltage 14 kV; **(D)** electropherogram of netilmicin.

4. Notes

1. Variation of the voltage results in a change of the electropherogram. For evaluation, 12 kV was chosen. Applying 14 V netilmicin can be quantified, because a baseline separation from the reagent peak can be achieved (*see* **Fig. 4**). However, netilmicin is not expected to be found in gentamicin drug substance and was not found in any of the samples studied.
2. Because gentamicin is composed of many components, peak identification by reference substances is necessary.
3. As can be seen from **Fig. 5**, the choice of micelle forming acids determines fundamentally the separation.
4. The OPA reagents can be stored at 4 °C for 48 to 72 h to prevent additional peaks in the electropherograms that are not coming from gentamicin components ***(14)***.
5. The reaction is completed after 4 to 5 min at 60 °C. The reaction time and temperature must be checked carefully.

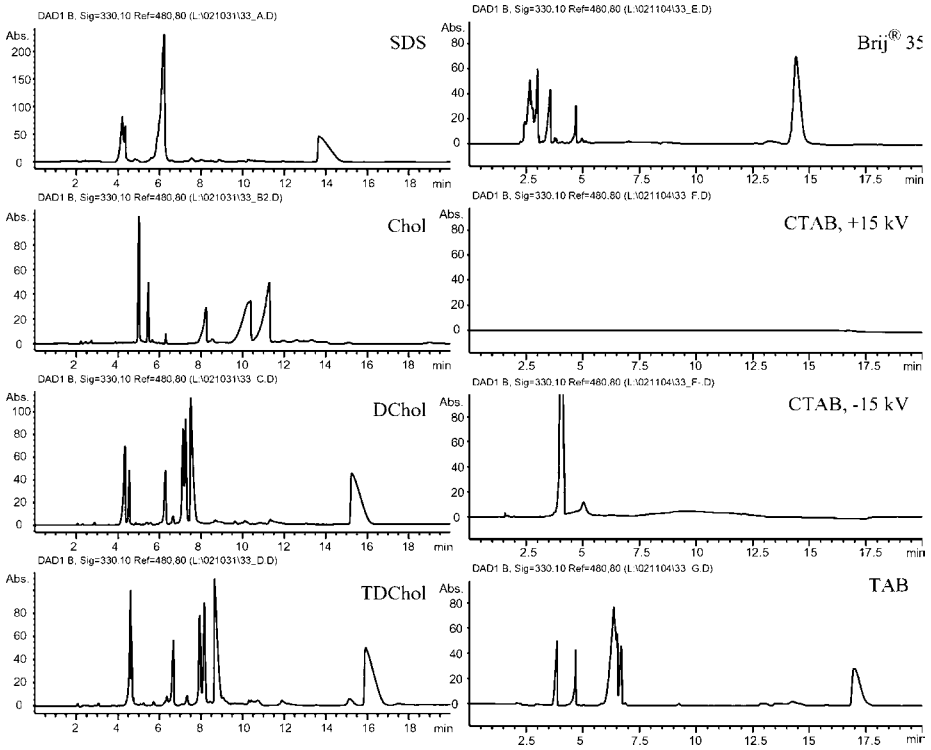


Fig. 5. Electropherograms obtained with various surfactants using the same conditions: 30 m*M* TB, 25 m*M* surfactant, pH 10.0, voltage 15 kV. Abbreviations of the surfactant can be found in **Table 1**; TAB = tetramethylammonium bromide.

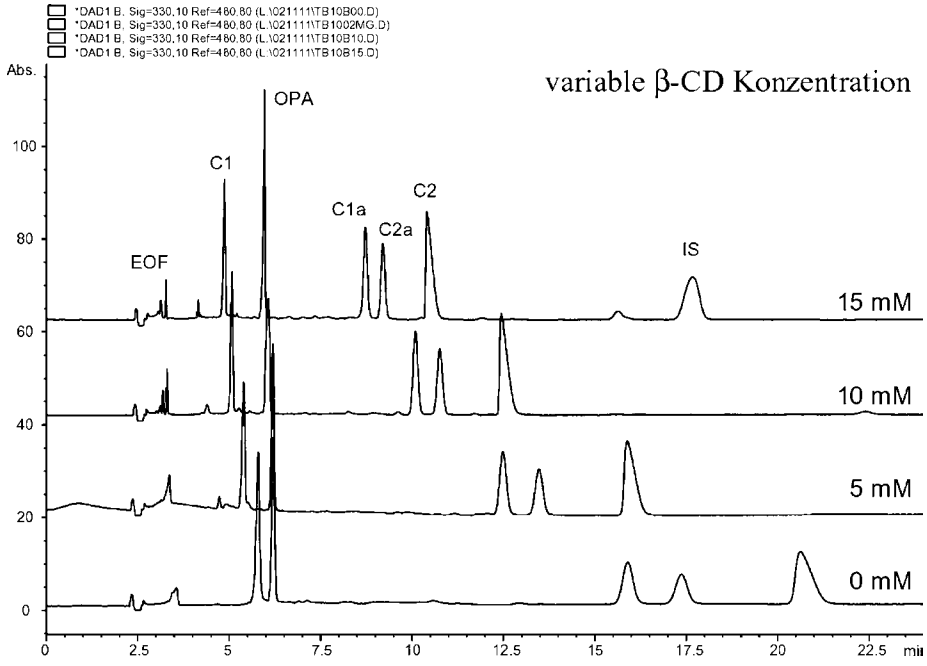


Fig. 6. Electropherogram obtained with increasing amounts of β-cyclodextrin under the same conditions 100 m*M* TB, 25 m*M* TDChol, pH 10.0, voltage 15 kV, temperature 20 °C.

6. Best separations were achieved when using 125 m*M* of TB. However, the current is very high at the TB concentration, and often the buffer reagent precipitates during the course of measurements. Therefore, a buffer concentration of 100 m*M* was finally chosen.
7. Higher β-CD concentration results in a shorter migration time and a rather sharp peak shape, which can be seen clearly in **Fig. 6**. Because the solubility of β-CD in water is limited, the concentration of β-CD was set to 15 m*M*.
8. Whereas at pH 9.5, the internal standard co-migrates with some components of gentamicin and the separation of all peaks is poor, at pH 10.5 the migration time increased substantially and the peaks became very broad (*see* **Fig. 7** = 1.1–10), Thus, pH 10.0 turned out to be a good compromise with regard to migration time and peak sharpness.
9. It is important to find a suitable detection wave length. On the one hand, the OPA reagent peak should be as small as possible to avoid covering of the substance peaks by the reagent peak. On the other hand, the substance peaks should be as large as possible in order to increase the sensitivity. As can be seen in **Fig. 8**, at 340 nm, the reagent peak has relatively low intensity and the sample peaks are of high intensity. In addition, all electropherograms were registered at the

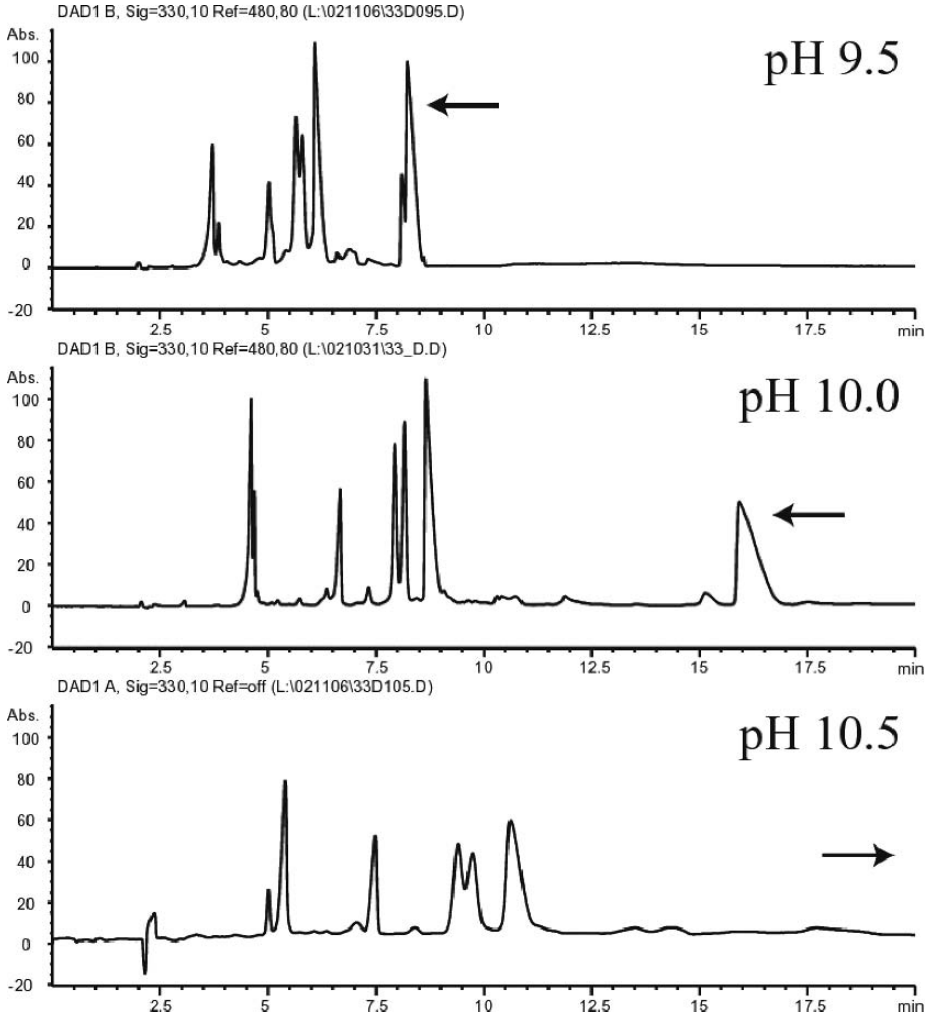


Fig. 7. Electropherogram obtained at different pH value under the same conditions: 100 m*M* TB, 25 m*M* TDChol, voltage 15 kV, temperature 20 °C.

reference wavelength of 450 nm in order to visualize artefacts of the separation, which may be caused by the instrument and are found in the entire UV spectrum. The artefacts are filtered off automatically.

10. Other rinsing procedures using SDS/acetonitrile mixtures, which are often described in the literature ***(18)***, turned out to be insufficient with respect to reproducibility.

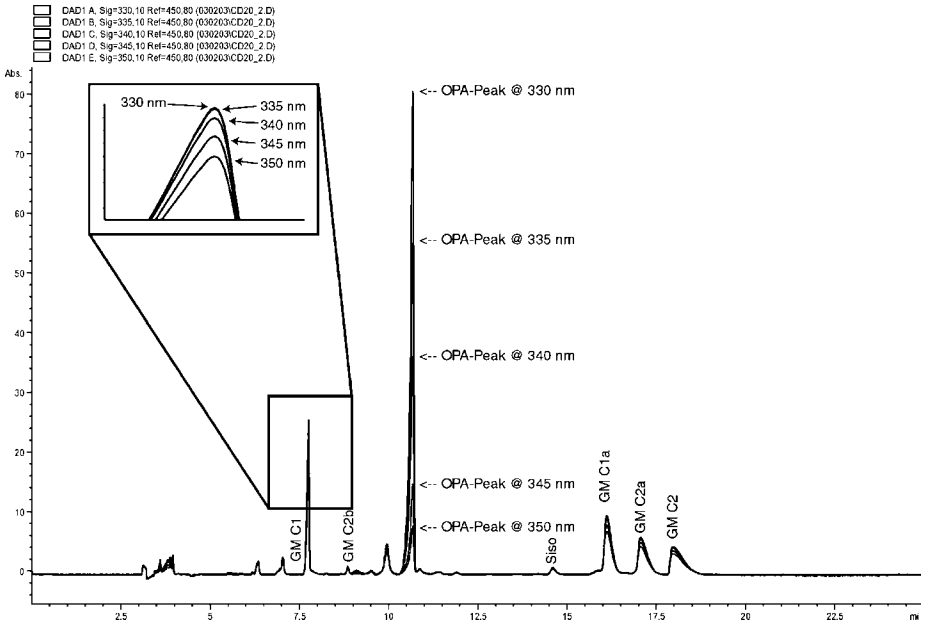
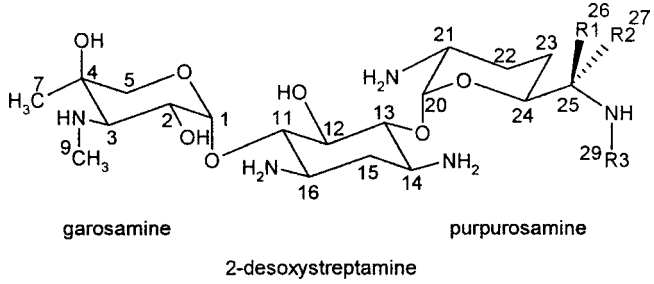


Fig. 8. Variation of the diction wavlength between 330 to 350 nm.



Scheme 1. Gentamicin (R^1, R^2, $R^3 = H$ or CH_3).

Acknowledgments

Thanks are due to the Federal Institute of Drugs and Medical Devices, Bonn, Germany, for financial support. Furthermore thanks to Dr. A. Kirsch, Merck, Darmstadt, Germany, for providing the impurities GA and DSA and samples.

References

1. Terabe, S., Otsuka, K., and Ando, T. (1985) Electrokinetic chromatography with micellar solution and open-tubular capillary. *Anal. Chem*. **57,** 834–841.
2. Watanabe, T. and Terabe, S. (2000) Analysis of natural food pigments by capillary electrophoresis. *J. Chromatogr. A*.. **880,** 311–322.
3. Pyell, U. (2000) Micellar electrokinetic chromatography, in *Encyclopedia of Analytical Chemistry*, Vol. 13 (Meyers, E.A. ed.), Wiley, Chichester, UK: pp. 11,383–11,042.
4. Poole, C. F. (2003) *The Essence of Chromatography*. Elsevier, Amsterdam: pp. 644.
5. Quirino, J. P. and Terabe, S. (1999) Sweeping of the analyte zones in electrokinetic chromatography. *Anal. Chem*. **71,** 1638–1644.
6. Seidl, G. and Nerad H. P. (1988) Gentamicin C: separation of C1, C1a, C2, C2a and C2b components by HPLC using isocratic ion-exchange chromatography and post column derivatization. *Chromatographia* **25,** 169–171.
7. Kaine, L. A. and Wolnik, K. A. (1994) Forensic investigation of gentamicin sulfates by anion-exchange ion chromatography with pulsed electrochemical detection. *J. Chromatogr. A*. **674,** 261.
8. Getek, T. A. and Vestal, M. L. (1991) Analysis of gentamicin sulfate by high-performance liquid chromatography combined with thermospray mass spectrometry. *J. Chromatogr*. **554,** 191–203.
9. Adams, E., Roelants, W., De Paepe, R., Roets, E., and Hoogmartens, J. (1998) Analysis of gentamicin by liquid chromatography with pulsed electrochemical detection. *J. Pharm. Biomed. Anal*. **18,** 689–698.
10. Clarot, I., Chaimbault, P., Hasdebteufel, F., Netter, P., and Nicolas, A. (2004) Determination of gentamicin sulfate and related compounds by high-performance liquid chromatography with evaporative light scattering detection. *J. Chromatogr. A*. **1031,** 281–287.
11. Kaale, E., Leonard, S., Van Schepdael, A., Roets, E., and Hoogmartens, J. (2000) Capillary electrophoresis analysis of gentamicin sulfate with UV detection after pre-capillary derivatization with 1,2-phthalic dicarboxaldehyde and mercapto acid. *J. Chromatogr. A*. **895,** 67–79.
12. Wienen, F., Deubner, R., and Holzgrabe, U. (2003) Composition and impurity profile of multisource raw material of gentamicin–a comparison. *Pharmeuropa* **15,** 273–279.
13. Kaale, E., Van Schepdael, A., Roets, E., and Hoogmartens, J. (2001) Development and validation of a simple capillary zone electrophoresis method for the analysis of kanamycin sulfate with UV detection after pre-capillary derivatization. *J. Chromatogr. A*. **924,** 451–458.
14. Wienen, F., and Holzgrabe, U. (2003) A new micellar electrokinetic capillary chromatography method for separating of the components of the aminoglycoside antibiotics. *Electrophoresis* **24,** 2948–2957.
15. Deubner, R., Wienen, F., and Holzgrabe, U. (2003) Assignment of the major and minor components of gentamicin for evaluation of batches. *Magn. Reson. Chem*. **41,** 589–598.

16. European Pharmacopoeia, 5th edition, European Directorate for Quality of Medicines, Strasbourg, France, 2004
17. Kaale, E., Van Goidsenhoven, E., Van Schapdael, A., Roets, E., and Hoogmartens, J. (2001) Electrophoretically mediated microanalysis of gentamicin with in-capillary derivatization and UV detection. *Electrophoresis* **22,** 2746–2754.
18. Kunkel, A. and Wätzig. H. (1999) Micellar electrokinetic capillary chromatography as a powerful tool for pharmacological investigations without sample pretreatment: a precise technique providing cost advantages and limits of detection to the low nanomolar range. *Electrophoresis* **20,** 2379–2389

31

Capillary Electrochromatography and On-Line Concentration

Guichen Ping, Philippe Schmitt-Kopplin, Yukui Zhang, and Yoshinobu Baba

Summary

Capillary electrochromatography (CEC) is a micro-separation technique that combines the advantages of capillary zone electrophoresis with those of high-performance liquid chromatography. Accordingly, it has attracted extensive attention over the last decade. Among the stationary phases for CEC, monolithic stationary phase has been regarded as the most suitable stationary phase for CEC because of its simple preparation, the elimination of frits, and its excellent performance. In this chapter, procedures for preparing CEC monolithic columns with an improved configuration, in which there are stationary phases at both sides of detection window and no stationary phase at detection window, are presented. The separation of acidic and basic compounds on such monolithic columns is used as an example to demonstrate CEC separation protocol. Additionally, an on-line concentration technique in CEC is presented. As a result of the coexistence of stationary phase and electric field in a CEC column, it is possible to employ chromatographic zone sharpening and field-amplified sample stacking effects simultaneously to improve CEC detection sensitivity.

Key Words: Capillary electrochromatography; separation mode; mobile phase; stationary phase; monolithic column; electroseparation; electroosmotic flow; one-line concentration; chromatographic zone sharpening effect; field amplified sample stacking effect.

1. Introduction

Capillary electrochromatography (CEC), a hybrid of high-performance of liquid chromatography (HPLC) and capillary electrophoresis (CE), features high selectivity of HPLC, high efficiency, and high speed as well as low sample

From: *Methods in Molecular Biology, vol. 384: Capillary Electrophoresis*
Edited by: P. Schmitt-Kopplin © Humana Press Inc., Totowa, NJ

and solvent consumption of CE. It has rapidly gained its popularity since it was introduced in 1974 ***(1)***, and its high-efficiency separation capability was demonstrated in 1981 ***(2)***. CEC uses an electrically driven flow to transport solutes through a capillary packed with stationary phase material. Separation can be achieved by differential partition between a stationary and a mobile phase, differential electromigration, or a combination of these two ***(3–5)***. Unlike capillary zone electrophoresis (CZE), both charged and uncharged species can be resolved in CEC. Separation of uncharged solutes is realized by differential interactions of the solute between the mobile and stationary phases. Charged species, on the other hand, can be influenced by their own electrophoretic mobility and by the interaction with the stationary phase.

CEC columns, in which all separation processes occur, play a critical role in a separation. In general, CEC columns can be classified into open-tubular ***(6–12)***, packed ***(13–24)***, and monolithic columns ***(25,26)***. The open-tubular column is a capillary bonded with a wall-supported stationary phase that can be a coated polymer, a bonded molecular monolayer, or a synthesized porous layer network. Although high efficiency can be achieved with the open-tubular column, it usually suffers from low sample capacity, retention factor, and detection sensitivity as a result of low phase ratio. The packed column is usually fabricated by delivering packing material into a capillary by various methods, including slurry pressure packing ***(13–15)***, electrokinetic packing ***(16–20)***, and packing with supercritical CO_2 ***(21,22)***, centripetal forces ***(23)***, and gravity ***(24)***. In packed columns, the stationary phase is retained in a capillary between inlet and outlet frits. The most common approach to the fabrication of frits involves sintering the stationary phase using a heating element or a fiber optic splicer ***(27–30)***. During the process of frit fabrication, both the bonded stationary phase and polyimide coating of the capillary are partially destroyed. As a consequence, the capillary is susceptible to breakage. In addition, as a result of the differences in the surface chemistries between the stationary phase and the frit, the frit is usually regarded as the main contributor to bubble formation, which results in unstable current, noisy baseline, and even the failure of a run. To overcome the limitation of the frit of the packed column, a fritless column, which is also called a monolithic column, has been introduced in recent years. The monolithic column is fabricated by *in situ* polymerization or by sol-gel technique in a capillary ***(25,26,31)***. Up to now, silica-based ***(31)***, acrylamide-based ***(32)***, methacrylate-based ***(25)***, polystyrene-based ***(33)*** and organic-inorganic hybrid ***(34)*** monolithic columns have been reported in the literature. Because the monolithic stationary phase can be covalently bound to the capillary inner wall, the frit in the conventional packed column and its corresponding problems are eliminated. The monolithic stationary phase has attracted considerable attention over the last decade as a result of its

simple preparation procedure and excellent performance. Hence, it has been considered a more suitable stationary phase for CEC than the packed column.

As a result of the free choice of stationary phases and emergence of specifically designed stationary phase for CEC, various separation modes can be utilized in CEC, such as reversed-phase ***(14,35)***, normal phase ***(36,37)***, ion-exchange ***(38,39)***, affinity ***(40,41)***, size exclusion ***(42,43)***, ion pair ***(44)***, hydrophilic interaction ***(45,46)***, and mixed mode ***(47,48)***. It provides great flexibility in optimizing conditions for a given separation. A number of applications from small ions to biomolecules have been reported in the literature, e.g., amino acids ***(49,50)***, amines ***(35,51)***, peptides ***(39,52,56)***, hydrocarbons ***(43,57)***, steroids ***(58,59)***, hormones ***(60)***, bile acids ***(61)***, humic degradation compounds ***(62)***, pesticides and herbicides ***(63,64)***, pharmaceuticals ***(29,65)***, cholesterol and its ester derivatives ***(66)***, nucleotides ***(67)***, nucleosides ***(68,69)***, and proteins ***(70)***.

A major challenge in CEC is the detection of samples containing analytes at low concentrations. The lack of sensitivity at low concentration originates from small sample volume and short optical length for on-line detection. One strategy for overcoming low concentration detection sensitivity is employing a detector with high sensitivity. Many detectors have been coupled to CEC, such as ultraviolet absorbance detectors ***(14,35)***, amperometric detectors ***(71)***, conductivity detectors ***(44)***, nuclear magnetic resonance spectrometry detectors ***(72)***, laser induced fluorescence detectors ***(19)***, and various mass spectrometry detectors ***(73–75)*** The use of fluorescence, electrochemical, and mass spectroscopic detectors can provide improved sensitivity in comparison to the conventional ultraviolet (UV) absorbance detector, but these detectors often can be too selective for universal use or are expensive. Another strategy for improving detection sensitivity is to use extended optical path length cells such as a bubble or Z-type cells, which can increase sensitivity 3- to 10-fold at the expense of resolution and separation efficiency. A more promising choice for increasing concentration sensitivity is on-line concentration, in which a sample plug is usually longer than normal. Both the field-amplified sample stacking (FASS) effect and the chromatographic zone sharpening effect (CZSE) have been employed to increase the amount of analytes injected without impairing peak shape or resolution ***(76–77)***. FASS consists of dissolving the sample in a buffer having a lower conductivity than separation electrolyte. Because the electric field is higher in the low-conductivity zone, the analytes move at a high velocity. The velocity drops sharply when the analytes enter the high-conductivity zone, where the electric field is lower. The preconcentrating effect should theoretically be proportional to the conductivity ratio between the separation electrolyte and the sample, but the stacking efficiency is usually lower than expected, as it is counteracted by differences in electroosmotic

flow (EOF) in the different zones *(77)*. CZSE consists of dissolving a solute in a solution of lower elution strength than mobile phase, and then eluting the solute with a mobile phase of higher elution strength; after injection, the sample zone is sharpened. Unlike with CZE, there are both a stationary phase and an electric field in a CEC column. FASS and CZSE can, therefore, be utilized simultaneously to improve the detection sensitivity of CEC.

Because of the obvious advantages of the monolithic column over the conventional packed column and its more promising future, we will focus on the research work on monolithic columns in this chapter and introduce the fabrication of CEC monolithic columns with an improved configuration, basic separation protocol on such columns, and on-line concentration in CEC.

2. Materials

1. Chemicals for column preparation including ethylene dimethacrylate (EDMA) and butyl methacrylate (MBA) are distilled *in vacuo* to remove inhibitors prior to use. Azobisisobutyronitrile (AIBN) is purified by recrystallization. Other chemicals such as 3-(trimethoxysilyl) propyl methacrylate, acetone, 2-acryloylamido-2-methylpropanesulfonic acid (AMPS), 1-propanol and 1,4-butanediol are used directly without any purification. All these chemicals are obtained from Fluka (Steinheim, Germany).
2. Unless stated otherwise, all of the model solutes in this chapter are of analytical grade.
3. Mobile phases are prepared by adjusting buffers to desired pH values, then mixing with the appropriate amount of organic modifier. The mobile phase is degassed in an ultrasonic bath for 15 min. The pH value mentioned here is that of sock buffer solution. Ultrapure water is utilized to prepare buffer and sample solutions.
4. Fused-silica capillaries (100 μm inner diameter [I.D.] × 365 μm outer diameter [O.D.]) are purchased from Yongnian Optic Fiber Plant (Hebei, China)
5. An HPLC pump is used to flush monolithic columns with mobile phase for conditioning. A manual pump is utilized (Unimicro Technologies, Pleasanton, CA) to dispel bubbles from the column when, occasionally, they form in the capillaries.
6. All experiments are performed on a P/ACE 5010 (Beckman, Fullerton, CA) equipped with Gold software (version 8.10) for data acquisition.

3. Methods

3.1. Column Preparation

3.1.1. Pretreatment of the Inner Wall of Capillaries

1. Capillaries are washed with 1 mol/L NaOH for 2 h so that siloxane groups at the inner surface of raw fused-silica capillaries can hydrolyze to increase the density of silanol groups serving as anchors for subsequent silanization.
2. The capillaries are washed with approx 50 column volumes of deionized water and acetone, respectively.

3. The capillaries are purged with nitrogen gas at ambient temperature for 5 h.
4. A solution of 30% (v/v) 3-(trimethoxysilyl) propyl methacrylate in acetone is injected into the capillaries by means of a syringe.
5. With both ends sealed with silicone septums, the capillaries are left at ambient temperature overnight, then washed by approx 50 column volumes of acetone.
6. Finally, the capillaries are purged with nitrogen gas for 5 h. By this means, methoxy groups of this compound react readily with silanol groups at the surface of capillary wall, leaving the methacryloyl end to react later with the methacrylic groups present in the monomers, so that the stationary phase becomes covalently bound to the capillary inner wall.

3.1.2. Formation of the Stationary Phase

1. Polymerization reaction solution consisting of 400 mg of the mixture of 40% (w/w) EDTA, 59.4% (w/w) of BMA and 0.6% (w/w) AMPS, 600 mg of ternary porogen composed of 10% (w/w) water, 64% (w/w) 1-propanol and 26% (w/w) 1,4-butanediol, and 6 mg of AIBN is prepared. Mixing sequence is not critical.
2. The reaction solution above is injected into pretreated capillaries.
3. The capillaries are put into a gas chromatography oven and kept at 60 °C for 20 h with both ends sealed with silicone septums.

3.1.3. Fabrication of Monolithic Columns With an Improved Configuration

Most CEC columns are composed of a segment with a given stationary phase and another part that is empty. As a result, there are discontinuities of electrochromatographic parameters such as EOF velocity, electric field strength, and conductivity in such columns. Obviously, this complicates the electrochromatographic process and makes the accurate measurement of the above-mentioned parameters difficult. We use two methods, i.e., heating and physical methods, to prepare polymer monolithic columns with the improved configuration. In contrast to partially packed CEC columns, there are stationary phases on both sides of detection window and no stationary phase at detection window in such columns. Because the length of detection window is very short, usually about 5 mm, the effect of such a small length on the above-mentioned electrochromatographic parameters could be negligible compared with the total length of a CEC column. Therefore, in these columns, the discontinuities of the electrochromatographic parameters are eliminated while no loss in detection sensitivity occurs in comparison with fully packed CEC columns.

3.1.3.1. Heating Method

1. Polymerization reaction here is reversible. The polymerization reaction occurs at moderate temperature, while the polymer decomposes into monomers at a relatively high temperature.

2. The detection window for on-column detection is made in polymer-filled capillary by burning off a 3- to 4-mm section of the polymer with an electrical filament, to whose ends voltage is applied. The length of the electrical filament is 20 cm with O.D. 0.3 mm. Applied voltage is 25 V.
3. Heating time is kept to 5 s.

3.1.3.2. Physical Method

1. The reaction mixture is injected into the capillary for a length of 10 cm.
2. The capillary is then purged with nitrogen gas for 5 mm length.
3. Subsequently, the reaction mixture is injected into the capillary again for 25 cm length.
4. After polymerization, the detection window is made right after the first segment of stationary phase by removing polyimide coating.
5. **Figure 1** shows alkylbenzene separation on both columns made by these two methods. As can be seen from **Fig. 1**, the performance of the columns is comparable. However the column, whose detection window made by heating method, bears higher column efficiency.

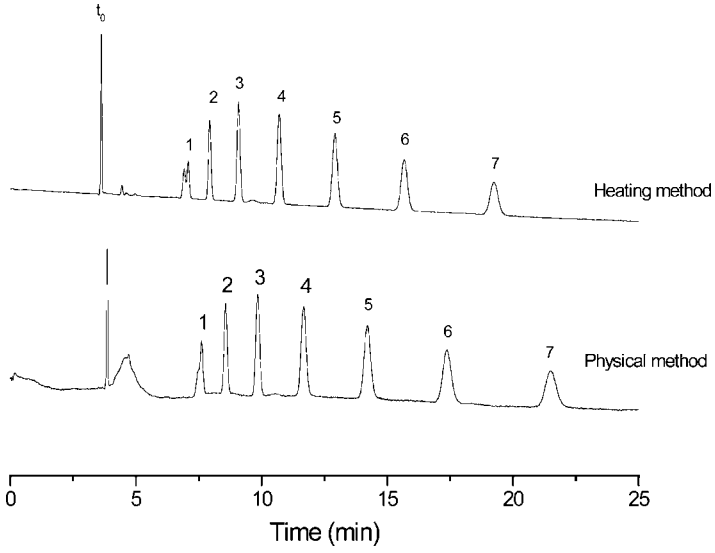


Fig. 1. Alkylbenzene separation on the monolithic columns with detection window made by heating and physical methods. Stationary phase as shown in this figure; mobile phase, 70 % acetonitrile in 2 m*M* phosphate, pH 7.0; applied voltage, 12 kV; peaks, alkylbenzenes ($C_nH_{2n+1}C_6H_5$, $n = 1$–7).

3.2. Separation of Acidic and Basic Compounds

Octadecyl silica (ODS) columns are frequently used in reversed-phase (RP)-CEC, because the well established knowledge of ODS for HPLC can be transferred to CEC directly. However, these columns still remains problematic for the separations of acidic and basic compounds in CEC. As we know, EOF originates from the negatively charged packing surface in RP-CEC as a result of the dissociation of silanol groups. Its direction is, therefore, from anode to cathode. Meanwhile, the electrophoretic flow of acidic compounds goes against the EOF, resulting in a rather long analysis time or even no peaks when the electrophoretic flow velocity is higher than the EOF velocity. The retention behavior of acidic compounds at high pH has been investigated in the literature *(79)*. However, some acidic species with higher electrophoretic mobility than that of EOF cannot be electrokinetically injected into CEC columns. Therefore, we recommend an ion-suppressed mode, where a low pH electrolyte is used as an eluent *(80)* and EOF is rather low, as EOF is a function of pH value. Additionally, the stationary phase may degrade if the pH of the mobile phase is lower than 2.5, which leads to the gradual deterioration of column performance. The analysis of basic compounds on ODS columns often suffers from broadening peaks and serious tailing, which stems from the secondary interaction between basic solutes and residual silanol groups. Addition of competing amines into running mobile phase can significantly minimize peak tailing. However, this will reduce or even reverse EOF velocity.

The polymethacrylate-based monolithic columns presented in this chapter bear sulfonic groups on the surface of the stationary phase. The pKa of sulfonic acids is much smaller than that of silanol. Hence, the stationary phase could show high EOF velocity even in ion-suppressed mode. As a result of high stability of polymer monolithic columns over the range of pH 2.0–12.0, some aromatic amines are used as model solutes and separated at pH 12.0. Under such conditions, all of these basic compounds are neutral, and the inherent reason for tailing is, therefore, eliminated.

1. Pure compound standards are dissolved into an acetonitrile-water (50:50, v/v) solution to obtain 1 m*M* stock solution, and then the stock solution is diluted with mobile phases. The concentration of each component is approx 0.1 mg/mL. Electrokinetic injection is performed at 3 kV for 3 s.
2. For aromatic acid separation, acetate is selected as a buffer and pH is 2.32. As demonstrated in **Fig. 2**, EOF mobility is found to be high enough to achieve the fast separation of acidic compounds even in ion-suppressed mode. In addition, the uncharged solutes yield symmetrical peaks with high efficiency (up to 177,000 plates/m).

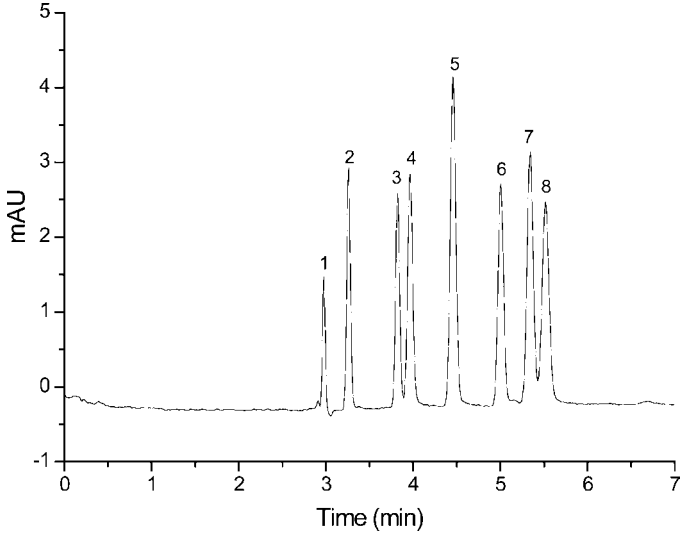


Fig. 2. Electrochromatogram of acidic compounds. Mobile phase, acetonitrile-5 mmol/L phosphate (pH 2.32) (55:45). Electrokinetic injection, 3 kV × 3s. Applied voltage, 16 kV. Peaks: 1, thiourea; 2, *p*-hydroxybenzoic acid; 3, *p*-methoxybenzoic acid; 4, *o*-aminobenzoic acid; 5, *o*-toluic acid; 6, *p*-chlorobenzoic acid; 7, *p*-bromobenzoic acid; 8, *m*-bromobenzoic. (From **ref. *32***, with permission.)

3. **Figure 3** shows the basic compound separation at pH 12.0. The baseline separation of all these basic compounds are readily achieved with symmetric peaks and column efficiency up to 114,000 plates/m without addition of any competing amines in the mobile phase. As can be seen from **Fig. 4**, the positional isomers of aromatic amines can be well separated under the identical condition.
4. It should be noted that such extreme pH conditions cannot be employed with typical silica-base packing. Otherwise, the hydrolysis of silica-based support is severe, which will undermine column efficiency. Therefore, high pH stability of monolithic polymer provides great versatility in method optimization. The columns could be used continuously for approx 2 wk and there is no significant loss in column efficiency at either high or low pH. The results here indicate that these polymer monolithic columns are more suitable for the separation of acidic and basic compounds than conventional silica-based columns.

3.3. On-Line Concentration to Improve Detection Sensitivity of CEC

Concentration effects are mainly based on the difference between sample solution and mobile phase. In order to achieve a high concentration factor, a significant amount of difference between them is preferred. However, bubble

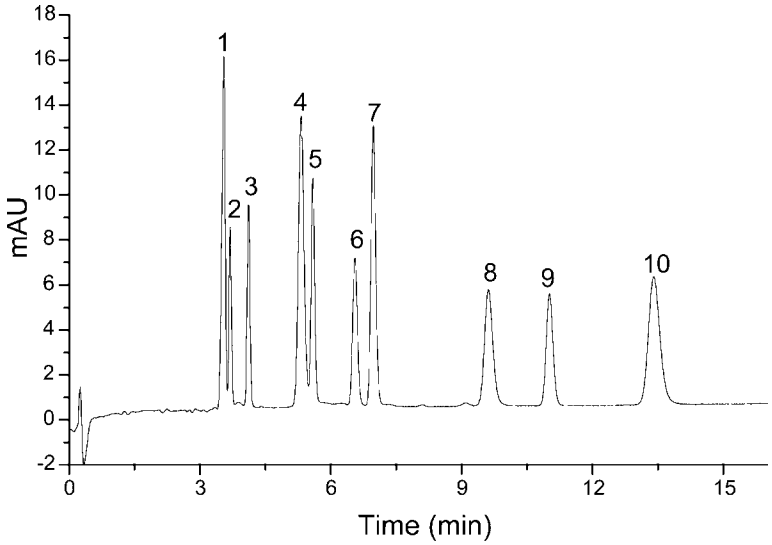


Fig. 3. Electrochromatogram of basic compounds. Mobile phase, acetonitrile-10 m*M* sodium hydroxide (pH 12.0) (55:45, v/v); electrokinetic injection, 3 kV × 3 s; applied voltage, 12 kV; peaks, 1, thiourea, 2, *o*-phenylene diamine, 3, *p*-phenylene diamine, 4, 4,4′-methylenedianiline, 5, aniline, 6, 3,4-dimethylaniline, 7, *m*-nitroaniline, 8, naphthylamine, 9, dimethylaniline, 10, 2,6-dichloro-4-nitroaniline. (From **ref. *32***, with permission.)

formation might become significant especially in a packed column. As a result of the excellent stability and elimination of frits, higher concentration effect could be obtained on such a monolithic column.

1. In order to investigate of the effect of injection time on concentration factor, benzoin, a model solute, is dissolved in 30% acetonitrile, 5 mmol/L Tris, pH 8.7 to the concentration of 18 μg/mL and injected into the CEC column with the gradual increase of injection time. As indicated in **Fig. 5**, the $W_{1/2}$ of benzoin does not increase significantly with injection time within the investigated range; moreover, the concentration factor of benzoin increases linearly with the injection time, demonstrating that the increase of injection time makes benzoin concentration linearly increase in the sample zone instead of making the sample zone broaden.
2. Benzoin is dissolved into a series of sample solutions with various acetonitrile concentrations including 20%, 30%, 40%, 50%, 60%, and 70%. The above sample solutions are injected into the column under the identical condition, i.e., 10 kV × 120 s. In RP-CEC, a linear relationship exists between log k and the volume fraction of organic modifier, where k is retention factor of a given solute ***(14)***.

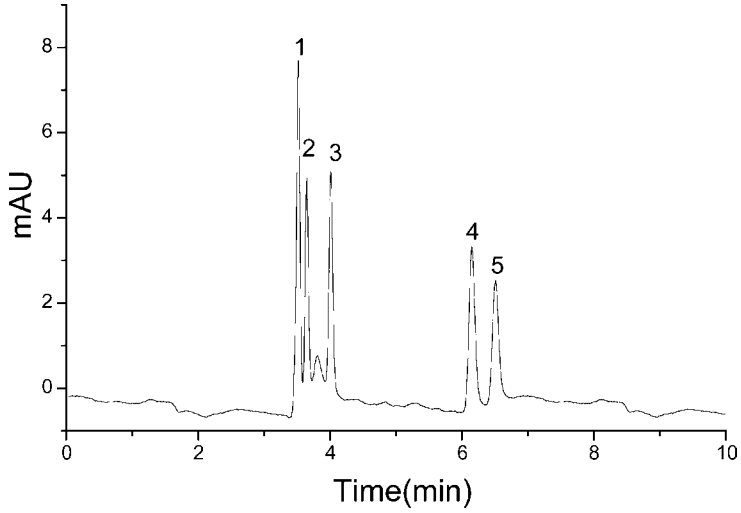


Fig. 4. Separation of positional isomers. Mobile phase, 60% acetonitrile in 10 mmol/L sodium hydroxide (pH 12.0); injection, 3 kV × 3 s; applied voltage, 12 kV; peaks, 1, thiourea, 2, *o*-phenylene diamine, 3, *p*-phenylene diamine, 4, *m*-nitroaniline, 5, *o*-nitroaniline. (From **ref. *32***, with permission.)

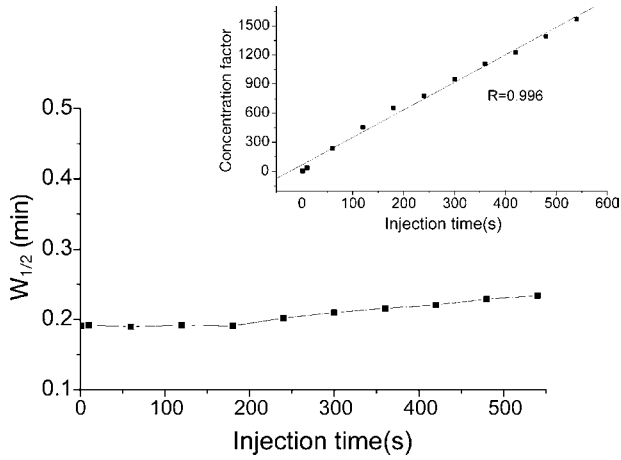


Fig. 5. Effect of injection time on peak height at half height of benzoin. Sample solution is 30% acetonitrile in 5 m*M* Tris, pH 8.7; mobile phase, 80% acetonitrile in 5 mmol/L Tris, pH 8.7; both injection and separation voltages are 10 kV. The inset is the plot of concentration factor versus injection time. (From **ref. *74***, with permission.)

Hence, a slight change in the organic modifier concentration has a significant effect on the retention factor and the migration velocity of the solute. If the organic modifier content in sample solution is lower than that in the mobile phase, the sample zone could be sharpened when the sample is eluted with the mobile phase with higher elution strength. **Figure 6** shows that the lower the organic modifier content in the sample solution, the narrower the sample zone. However, it is worthwhile to mention that the greater the difference between the organic modifier concentration in the sample solution and that in mobile phase, the higher likelihood of bubble formation in the column.

3. The absence of frits and good stability of monolithic columns allows to highly flexibly adjust organic modifier content, therefore a higher concentration factor could be achieved. Inset of **Fig. 7** demonstrates the electrochromatogram of benzoin under normal condition, i.e. the mobile phase is the same as sample solution. **Figure 7** illustrates elution curve after 60 min injection at 10 kV. Apparent concentration factor, η, is calculated with the following equation,

$$\eta = \frac{h/C}{h_0/C_0}$$

where h and h_0 are the peak height of the solute under the normal and concentration conditions, and C and C_0 are the solute concentrations under two above conditions, respectively. By virtue of CZSE alone, the concentration sensitivity could be improved by a factor of 22 000, indicating the advantages of such technique.

4. Besides mobile and stationary phases, an electric field also exists in CEC. Consequently, FASS could additionally be utilized to improve detection sensitivity of charged samples. If the electrolyte concentration in the sample solution is lower

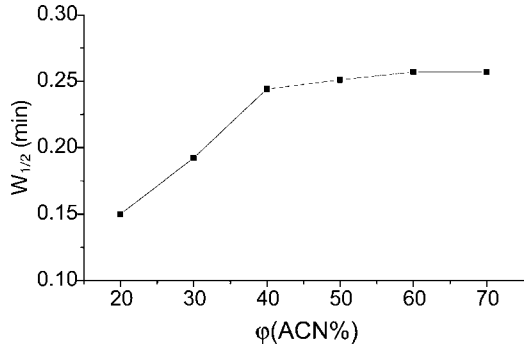


Fig. 6. Effect of the volume fraction of acetonitrile in sample solution on the peak width at half-height of benzoin. Conditions: mobile phase, 80% acetonitrile in 5 mmol/L Tris, pH, 8.7; applied voltage, 10 kV; electrokinetic injection, 10 kV × 120 s. (From **ref. *74***, with permission.)

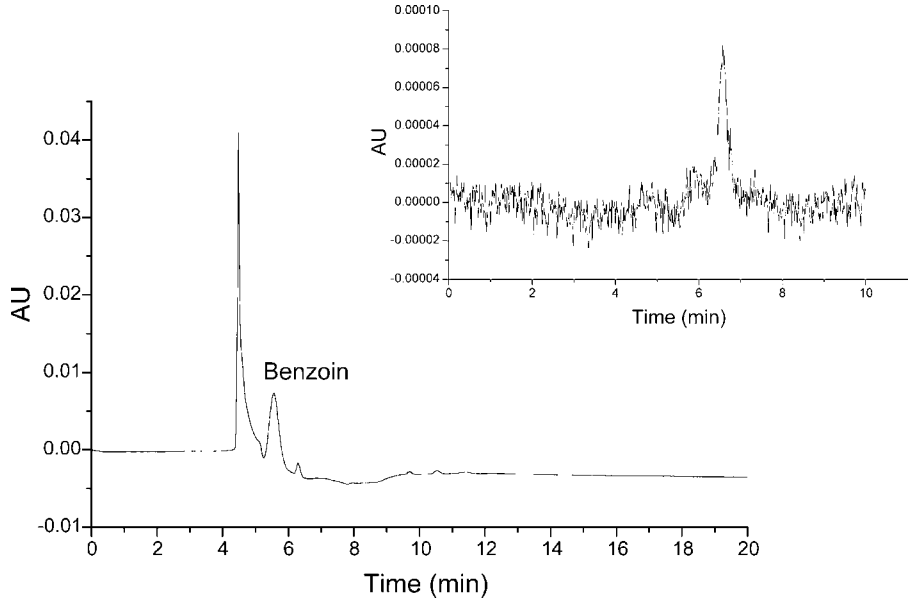


Fig. 7. Electrochromatograms of benzoin with normal injection (inset) and on-line concentration by chromatographic zone sharpening effect. Conditions: mobile phase, 80% acetonitrile in 5 mmol/L Tris, pH, 8.7, inset, sample solution, same as mible phase, pH, 8.7, sample concentration, 18 μg/mL, injection, 1 kV × 1 s; on line concentration, sample solution, 20% acetonitrile in 5 mmol/L Tris, pH, 8.7, sample concentration, 0.18 μg/mL, injection, 10 kV × 60 min. Separation voltage, 10 kV. (From **ref. *74***, with permission.)

than that in the mobile phase, the electric field strength in the sample plug is higher than that in the mobile phase zone. Therefore, the charged analytes move faster in the sample plug. Once the analytes move into the mobile phase zone, the migration velocity of the analytes decreases, and hence they are condensed at the boundary of the sample and the mobile phase. In this experiment **(Fig. 8)**, caffeine is used as the solute. Sample solution is made by dissolving an appropriate amount of caffeine into the solution containing 10% acetonitrile and 1 mmol/L sodium acetate (pH 3.7). Under this condition, caffeine is positively charged because its p*K*a is 10.4. Because both the electrolyte and organic modifier concentration in the sample solution are lower than those in the mobile phase, CZSE and FASS can be used simultaneously to improve detection sensitivity. After an injection of 300 s at 10 kV, the detection sensitivity of caffeine is improved by a factor of 24,000 in terms of peak height and sample concentration. The on-line concentration technique could aid in extending the application of CEC to the analysis of trace components in real samples.

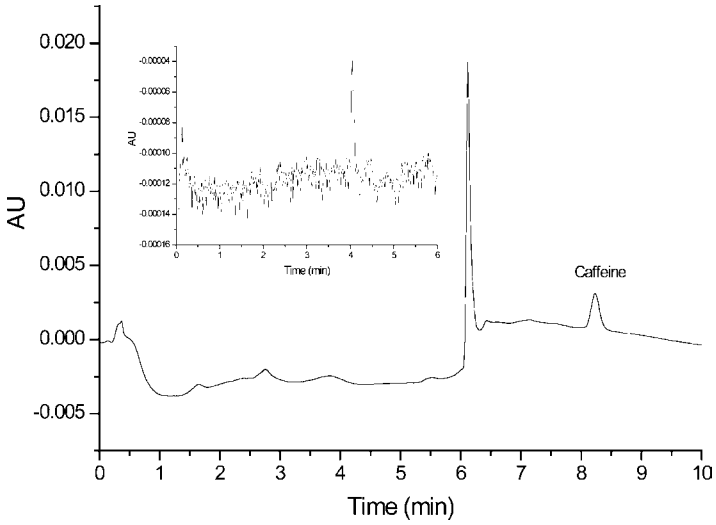


Fig. 8. Electrochromatograms of caffeine under normal injection (inset) and on-line concentration with the combination of field-amplified sample stacking and chromatographic zone sharpening effect. Conditions: mobile phase, 80% acetonitrile in 5 mmol/L NaAc, pH 3.7; inset: sample solution, same as the mobile phase, sample solution, 10 μg/mL, injection, 2 kV × 1 s; on-line concentraiton, sample solution, 10% acetonitrile in 1 mmol/L NaAc, pH, 3.7; sample concentration, 0.1 μg/mL, injection, 10 kV × 300 s. (From **ref. *74***, with permission.)

4. Notes

1. Polymer solution is sensitive to UV light; the polymerization reaction can be initiated by UV light. Therefore, the reaction solution should be protected from exposure to UV and sunlight.
2. For economy, the stock reaction solution can be stored in a refrigerator until further use. It be can be reused within 1 mo if it is stored properly.
3. Before the detection window is madthe e by heating method, the polyimide coating at detection window is removed in order to decrease the required temperature for window making. It can diminish the damage of the adjacent monolithc stationary phase.
4. During the detection-window making, it is important to wash the monolithic capillary with cold water to avoid decomposition of the adjacent bed and to take the decomposition products out of the capillary in time.
5. Prior to experiments, monolithic capillaries are flushed with mobile phase for 1 h to remove the porogen and unreacted crosslinking reagent and the monomers. The capillaries are then conditioned with the mobile phase for anther 1 h on the instrument. The applied voltage is ramped from 0 to 15 kV, and any abrupt changes in applied voltage should be carefully avoided to minimize the likelihood of bubble formation in the capillaries.
6. The capillaries are equilibrated for approx 30 min in the case of mobile phase change.

7. Unless stated otherwise, the total and effective length of separation capillaries are 20 and 27 cm, respectively. The separation capillaries are thermostatted at 25 °C, and detection wavelength is set at 214 nm.
8. The tips of the monolithic column should be stored in water after experiments. The polyimide coating swells in a solution with organic solvents, which makes the monolithic column fragile. Storing the tips of the monolithic column in water can alleviate this problem.
9. Prepare an additional reservoir vial of mobile phase. After each sample injection, dip the inlet tip of the monolithic column into this vial, then start measurements. This can minimize carry over effect, which usually leads to peak distortion and tailing.

Acknowledgments

The present work is partially supported by National Natural Science Foundation of China (No. 20105006) and 973 Project of the Ministry of Science and Technology of China (No. 001CB510202), a grant form the New Energy and Industrial Technology Development Organization of the Ministry of Economy, Trade and Industry, the CREST program of the Japan Science and Technology Corporation, a Grant-in-Aid for Scientific Research from the Ministry of Health and Welfare, a Grant-in-Aid for Scientific Research from the Ministry of Education, Science and Technology, and a Grant-in-aid of the 21st Century COE program from the Ministry of Education, Science and Technology, Japan.

References

1. Pretorius, V., Hopkins, B. J., and Schieke, J. D. (1974) Electro-osmosis: a new concept for high-speed liquid chromatography. *J. Chromatogr.* **99,** 23–30.
2. Jorgenson, J. W. and Lukacs, K. D. (1981) High-resolution separations based on electrophoresis and electroosmosis. *J. Chromatogr.* **218,** 209–216.
3. Knox, J. H., and Grant. I. H. (1987) Miniaturisation in pressure and electroendosmotically driven liquid chromatography with electroosmotic flow. *Chromatographia* **24,** 135–143.
4. Knox, J. H. (1988) Thermal effects and band spreading in capillary electroseparation. *Chromatographia* **26,** 329–337.
5. Knox, J. H. (1980) Terminology and nomenclature in capillary electroseparation systems. *J. Chromatogr. A*. **680,** 3–13.
6. Breadmore, M. C., Macka, M., Avdalovic, N., and Haddad, P. R. (2001) On-capillary ion-exchange preconcentration of inorganic anions in open-tubular capillary electrochromatography with elution using transient-isotachophoretic gradients. 2. Characterization of the isotachophoretic gradient. *Anal. Chem.* **73,** 820–828.
7. Matyska, M. T., Pesek, J. J., Boysen, R. I., and Hearn, M. T. W. (2001) Characterization of open tubular capillary electrochromatography columns for the analysis of synthetic peptides using isocratic conditions. *Anal. Chem.* **73,** 5116–5125.

8. Kapnissi, C. P., Valle, B. C., and Warner, I. M. (2003) Chiral separations using polymeric surfactants and polyelectrolyte multilayers in open-tubular capillary electrochromatography. *Anal. Chem.* **75,** 6097–6104.
9. Breadmore, M. C., Macka M., Avdalovic, N., and Haddad, P. R. (2000) Open-tubular ion-exchange capillary electrochromatography of inorganic anions. *Analyst* **125,** 1235–1241.
10. Breadmore, M. C., Boyce, M., Macka, M., Avdalovic, N., and Haddad, P. R. (2000), Peak shapes in open tubular ion-exchange capillary electrochromatography of inorganic anions. *J. Chromatogr. A*. **892,** 301–313.
11. Kapnissi-Christodoulou, C. P., Zhu, X., and Warner, I. M. (2003) Analytical separations in open-tubular capillary electrochromatography. *Electrophoresis* **24,** 3917–3934.
12. Hu, X., Kamande, M. W., Thiam, S., Kapnissi, C. P., Mwongela, S. M., and Warner, I. M. (2004) Open-tubular capillary electrochromatography/electrospray ionization-mass spectrometry using polymeric surfactant as a stationary phase coating. *Electrophoresis* **25,** 562–568.
13. Ye, M., Zou, H., Liu, Z., Ni, J., and Zhang, Y. (2000) Capillary electrochromatography using a strong cation exchange column with a dynamic modified cationic surfactant. *Anal. Chem.* **72,** 616–621.
14. Zhang, Y., Shi, W., Zhang, L., and Zou, H. (1998) Some aspects of chromatographic behavior in capillary electrochromatography. *J. Chromatogr. A*. **802,** 59–71.
15. Angus, P. D. A., Demarest, C. W., Catalano, T., and Stobaugh, J. F. (2000) Aspects of column fabrication for packed capillary electrochromatography. *J. Chromatogr. A*. **887,** 347–365.
16. Yan. C. (1995) Electrokinetic packing of capillary columns. US Patent no. 5 453 163.
17. Bailey, C. G. and Yan, C. (1998) Separation of explosives using capillary electrochromatography. *Anal. Chem.* **70,** 3275–3279.
18. Yan, C., Dadoo, R., Zare, R. N., Rakestraw, D. J., and Anex, D. S. (1996) Gradient elution in capillary electrochromatography. *Anal. Chem*. **68,** 2726–2730.
19. Dadoo, R., Zare, R. N., Yan, C., and Anex, D. S. (1998) Advances in capillary electrochromatography: rapid and high-efficiency separation of PAHs. *Anal. Chem*. **70,** 4787–4792.
20. Yan, C., Dadoo, R., Zhao, H., Zare, R. N., and Rakestraw, D. J. (1995) Capillary electrochromatography: analysis of polycyclic aromatic hydrocarbons. *Anal. Chem*. **67,** 2062–2029.
21. Healy, L. O., Owens, V. P., O'Mahony, T., et al. (2003) Supercritical fluid generated stationary phases for liquid chromatography and capillary electrochromatography. *Anal. Chem*. **75,** 5860–5869.
22. Roulin, S., Dmoch, R., Carney, R., et al. (2000) Comparison of different packing methods for capillary electrochromatography columns. *J. Chromatogr. A*. **887,** 307–312.
23. Fermier, A. M. and Colón, L. A. (1998) Capillary electrochromatography in columns packed by centripetal forces. *J. Microcol. Sep*. **10,** 439–447.

24. Reynolds, K. J., Maloney, T. D., Fermier, A. M., and Colón, L. A. (1998) Capillary electrochromatography in columns packed by gravity, preliminary study. *Analyst* **123,** 1493–1495.
25. Zou, H., Huang, X., Ye, M., and Luo, Q. (2002) Monolithic stationary phases for liquid chromatography and capillary electrochromatography, *J. Chromatogr. A*. **954,** 5–32.
26. Hilder, E. F., Svec, F., and Fréchet, J. M. J. (2004) Development and application of polymeric monolithic stationary phases for capillary electrochromatography. *J. Chromatogr. A*. **1044,** 3–22.
27. Zimina, T. M, Smith, R. M., and Myers, P. (1997) Comparison of ODS-modified silica gels as stationary phases for electrochromatography in packed capillaries. *J. Chromatogr. A*. **758,** 191–197.
28. Augus, P. D. A., Demarest, C. W., Catalano, T., and Stobaugh, J. F. (2000) Aspects of column fabrication for packed capillary electrochromatography. *J. Chromatogr. A*. **887,** 347–365.
29. Angus, P. D. A., Demarest, C. W., Catalano, T., and Stobaugh, J. F. (1999) Evaluation of 1.5 μm reversed phase nonporous silica in packed capillary electrochromatography and application in pharmaceutical analysis. *Electrophoresis* **20,** 2349–2359.
30. Chen, Y., Gerhardt, G., and Cassidy, R. (2000) Silicate polymerization for the preparation of bed-retention frits in capillary electrochromatography. *Anal. Chem*. **72,** 610–615.
31. Ishizuka, N., Minakuchi, H., Nakanishi, K., et al. (2000) Performance of a monolithic silica column in a capillary under pressure-driven and electrodriven conditions. *Anal. Chem*. **72,** 1275–1280.
32. Palm, A. and Novotny, M. V. (1997) Macroporous polyacrylamide/poly(ethylene glycol) matrices as stationary phases in capillary electrochromatography. *Anal. Chem*. **69,** 4499–4507.
33. Gusev, I., Huang, X., and Horváth, C. (1999) Capillary columns with in situ formed porous monolithic packing for micro high-performance liquid chromatography and capillary eletrochromatography. *J. Chromatogr. A*. **855,** 273–290.
34. Yan, L., Zhang, Q., Zhang, J., et al. (2004) Hybrid organic–inorganic monolithic stationary phase for acidic compounds separation by capillary electrochromatography. *J. Chromatogr. A*. **1046,** 255–261.
35. Ping, G., Zhang, L., Zhang, L., et al. (2004) Separation of acidic and basic compounds in capillary electrochromatography with polymethacrylate-based monolithic columns. *J. Chromatogr. A*. **1035,** 265–270.
36. Lai, E. P. C. and Dabek-Zlotorzynska, E. (1999) Separation of theophylline, caffeine and related drugs by normal-phase capillary electrochromatography, *Electrophoresis* **12,** 2366–2372.
37. Vickers, P. J. and Smith, N. W. (2002) Normal-phase chiral separations by pressure assisted capillary electrochromatography using the Pirkle type stationary phase Whelk-O 1. *J. Sep. Sci*. **25,** 1284–1290.

38. Scherer, B. and Steiner, F. (2001) Application of hydrophobic anion-exchange phases in capillary electrochromatography. *J. Chromatogr. A*. **924,** 197–209.
39. Ye, M., Zou, H., Liu, Z., and Ni, J. (2000) Separation of peptides by strong cation-exchange capillary electrochromatography. *J. Chromatogr. A*. **869,** 385–394.
40. Manetto, G., Bellini, M. S., and Deyl, Z. (2003) Affinity electrochromatography of acidic drugs using a liposome-modified capillary. J. Chromatogr. A. **990,** 281–289.
41. Ye, M., Zou, H., Liu, Z., Wu, R., Lei, Z., and Ni, J. (2002) Study of competitive binding of enantiomers to protein by affinity capillary electrochromatography. *J. Pharm. Biomed. Anal*. **27,** 651–660.
42. Kok, W. Th. (2004) Capillary electrochromatography in the size-exclusion mode. *J. Chromatogr. A*. **1044,** 145–151.
43. Mistry, K., Krull, I., and Grinberg, N. (2003) Size-exclusion capillary electrochromatographic separation of polysaccharides using polymeric stationary phases. *Electrophoresis* **24,** 1753–1763.
44. Galloway, M. and Soper, S. A. (2002) Contact conductivity detection of polymerase chain reaction products analyzed by reverse-phase ion pair microcapillary electrochromatography. *Electrophoresis* **23,** 3760–3768.
45. Fu, H., Jin, W., Xiao, H., Huang, H., and Zou, H. (2003) Peptide separation in hydrophilic interaction capillary electrochromatography. *Electrophoresis* **24,** 2084–2091.
46. Ye, M., Zou, H., Kong, L., Lei, Z., Wu, R., and Ni, J. (2001) Hydrophilic interaction capillary electrochromatography for the separation of polar compounds. *LCGC* **19,** 1076–1086.
47. Spikmans, V., Lane, S. J., Tjaden, U. R., and Greef, J. van der, (1999) Automated capillary electrochromatography tandem mass spectrometry using mixed mode reversed-phase ion-exchange chromatography columns. *Rapid Commun. Mass Spectrom*. **13,** 141–149.
48. Wu, R., Zou, H., Fu, H., Jin, W., and Ye, M. (2002) Separation of peptides on mixed mode of reversed-phase and ion-exchange capillary electrochromatography with a monolithic column. *Electrophoresis* **23,** 1239–1245.
49. Charvátová, J., Král, V., and Deyl, Z. (2002) Capillary electrochromatographic separation of aromatic acids possessing peptides using porphyrin derivatives as the inner wall modifiers. *J. Chromatogr. B*. **770,** 155–163.
50. Chen, Z. and Hobo, T. (2001) Chemically L-prolinamide-modified monolithic silica column for enantiomeric separation of dansyl amino acids and hydroxy acids by capillary electrochromatography and μ-high performance liquid chromatography. *Electrophoresis* **22,** 3339–3346.
51. Oguri, S., Yoneya, Y., Mizunuma, M., Fujiki, Y., Otsuka, K., and Terabe, S. (2002) Selective detection of biogenic amines using capillary electrochromatography with an on-column derivatization technique. *Anal. Chem*. **74,** 3463–3469.
52. Wu, R., Zou, H., Ye, M., Lei, Z., and Ni, J. (2001) Capillary electrochromatography for separation of peptides driven with electrophoretic mobility on monolithic column. *Anal. Chem*. **73,** 4918–4923.

53. Matyska, M. T., Pesek, J. J., Boysen, R. I., and Hearn, M. T. W. (2001) Characterization of open tubular capillary electrochromatography columns for the analysis of synthetic peptides using isocratic conditions. *Anal. Chem.* **73,** 5116–5125.
54. Walhagen, K., Unger, K. K., and Hearn, M. T. W. (2001) Capillary electrochromatography analysis of hormonal cyclic and linear peptides. *Anal. Chem.* **73,** 4924–4936.
55. Pesek, J. J., Matyska, M. T., Dawson, G. B., Chen, J. I. -C., Boysen, R. I., and Hearn, M. T. W. (2004) Open tubular capillary electrochromatography of synthetic peptides on etched chemically modified columns. *Anal. Chem.* **76,** 23–30.
56. Zhang, K., Jiang, Z., Yao, C., Zhang, Z., Wang, Q., Gao, R., and Yan, C. (2003) Separation of peptides by pressurized capillary electrochromatography. *J. Chromatogr. A*. **987,** *4*53–458.
57. Que, A. H., Mechref, Y., Huang, Y., Taraszka, J. A., Clemmer, D. E., and Novotny, M. V. (2003) Coupling capillary electrochromatography with electrospray Fourier transform mass spectrometry for characterizing complex oligosaccharide pools. *Anal. Chem.* **75,** 1684–1690.
58. Que, A. H., Palm, A., Baker, A. G., and Novotny, M. V. (2000) Steroid profiles determined by capillary electrochromatography, laser-induced fluorescence detection and electrospray–mass spectrometry. *J. Chromatogr. A*. **887,** 379–391.
59. Jiskra, J., Claessens, H. A., and Cramers, C. A. (2002) Method development for the separation of steroids by capillary electrochromatography. *J. Sep. Sci*. **25,** 1337–1345.
60. Jin, W., Fu, H., Huang, X., Xiao, H., and Zou, H. (2003) Optimized preparation of poly(styrene-co-divinylbenzene-co-methacrylic acid) monolithic capillary column for capillary electrochromatography. *Electrophoresis* **24,** 3172–3180.
61. Que, A. H., Konse, T., Baker, A. G., and Novotny, M. V. (2000) Analysis of bile acids and their conjugates by capillary electrochromatography/electrospray ion trap mass spectrometry. *Anal. Chem.* **72,** 2703–2710.
62. Ping, G., Schmitt-Kopplin, P., Hertkorn, N., Zhang, W., and Kettrup, A. (2004) Separation of selected humic degradation compounds by capillary electrochromatography with monolithic and packed columns. *Electrophoresis* **24,** 958–969.
63. Starkey, J. A., Abrantes, S., Mechref, Y., and Novotny, M. V. (2003) Sensitive analyses of agricultural chemicals by capillary electrochromatography. *J. Sep. Sci*. **26,** 1635–1642.
64. Bedair, M. and El Rassi, Z. (2002) Capillary electrochromatography with monolithic stationary phases: 1. preparation of sulfonated stearyl acrylate monoliths and their electrochromatographic characterization with neutral and charged solutes. *Electrophoresis* **23,** 2938–2948.
65. Mangelings, D., Hardies, N., Maftouh, M., Suteu, C., Massart, D. L., and Heyden, Y. V. (2003) Enantioseparations of basic and bifunctional pharmaceuticals by capillary electrochromatography using polysaccharide stationary phases. *Electrophoresis* **24,** 2567–2576.
66. Thiam, S., Shamsi, S. A., Henry, C. W., Robinson, J. W., and Warner, I. M. (2000) Capillary electrochromatography of cholesterol and its ester derivatives. *Anal. Chem.* **72,** 2541–2564.

67. Ping, G., Zhang, W., Zhang, L., Schmitt-Kopplin, P., Zhang, Y., and Kettrup, A. (2003) Rapid separation of nucleosides by capillary electrochromatography with a methacrylate-based monolithic stationary phase. *Chromatographia* **57,** 629–633.
68. Charles, J. A. M. and McGown, L. B. (2003) Separation of Trp-Arg and Arg-Trp using G-quartet-forming DNA oligonucleotides in open-tubular capillary electrochromatography. *Electrophoresis* **23,** 1599–1604.
69. Huang, Y. C., Lin, C. C., and Liu, C. Y. (2004) Preparation and evaluation of molecularly imprinted polymers based on 9-ethyladenine for the recognition of nucleotide bases in capillary electrochromatography. *Electrophoresis* **25,** 554–561.
70. Zhang, J., Huang, X., Zhang, S., and Horváth, C. (2000) Capillary electrochromatography of proteins on an anion-exchange column. *Anal. Chem.* **72,** 3022–3029.
71. Hilmi, A. and Luong, J. H. T. (2000) In-line coupling capillary electrochromatography with amperometric detection for analysis of explosive compounds. *Electrophoresis* **21,** 1395–1404.
72. Gfrorer, P., Tseng, L. H., Rapp, E., Albert, K., and Bayer, E. (2001) Influence of pressure upon coupling pressurized capillary electrochromatography with nuclear magnetic resonance spectrometry. *Anal. Chem.* **73,** 3234–3239.
73. Barceló-Barrachina, E., Moyano, E., and Galceran, M. T. (2004) State-of-the-art of the hyphenation of capillary electrochromatography with mass spectrometry. *Electrophoresis* **25,** 1927–1948.
74. Klampfl, C. W. (2004) Review coupling of capillary electrochromatography to mass spectrometry. *J. Chromatogr. A*. **1044,** 131–144.
75. Schmitt-Kopplin, P. and Frommberger, M. (2003) Capillary electrophoresis-mass spectrometry: 15 years of developments and applications. *Electrophoresis* **24,** 3837–3867.
76. Zhang, Y., Zhu, J., Zhang, L., and Zhang, W. (2000) High-efficiency on-line concentration technique of capillary electrochromatography. *Anal. Chem.* **72,** 5744–5747.
77. Ping, G., Zhang, Y., Zhang, W., et al. (2004) On-line concentration of neutral and charged species in capillary electrochromatography with a methacrylate-based monolithic stationary phase. *Electrophoresis* **25,** 421–427.
78. Burgi, D. S. and Chien, R. L. (1991) Optimization in sample stacking for high-performance capillary electrophoresis. *Anal. Chem*. **63,** 2042–2047.
79. Moffatt, F., Copper, P. A., and Jessop, K. M. (1999) Capillary electrochromatography. abnormally high efficiencies for Neutral-anionic compounds under reversed-phase conditions. *Anal. Chem*. **71,** 1119–1124.
80. Altria, K. D., Smith, N. W., and Turnbull, C. H. (1998) Analysis of acidic compounds using capillary electrochromatography. *J. Chromatogr. B*. **717,** 341–353.

32

Analysis of Alkaloids in Single Plant Cells by Capillary Electrophoresis

Katrin Wieland, Björn Thiele, and Uli Schurr

Summary

In this chapter, capillary electrophoresis (CE) is demonstrated to be a useful technique for the determination of alkaloids in microsamples of single plant cells. A single cell sampling technique with microcapillaries that includes extraction of sample volumes in the pl range from single cells, division into aliquots, addition of internal standard, and injection into the CE capillary is described. The danger of contamination and evaporation of such low sample volumes has been avoided by handling them under an inert protective layer of silicone oil. For the determination of alkaloids in cell samples, CE with direct ultraviolet detection using a high concentration of citric acid as background electrolyte provides sufficient sensitivity.

Key Words: Capillary electrophoresis, single cell analysis, alkaloids

1. Introduction

Alkaloids of tobacco such as nicotine are increasingly allocated in leaves upon leaf damage ***(1–3)***, which protects the plant from tobacco herbivores ***(3)***. The mechanisms of this inducible defense system were intensively studied during the last two decades ***(4)***. The predominant site of nicotine synthesis is the roots ***(5)*** from where nicotine is transported to the shoots in the xylem stream ***(6–8)***. The high spatial separation of the site of synthesis (roots) and the site of herbivore attack (leaves) affords a long-distance signal transduction pathway. Jasmonic acid has been demonstrated to be an essential compound of the signal transduction cascade. After leaf damage, jasmonic acid concentrations rapidly increased in damaged leaves within 90 min and more slowly in the roots, reaching maximum levels 180 min after wounding ***(9)***. As a consequence

From: *Methods in Molecular Biology, vol. 384: Capillary Electrophoresis*
Edited by: P. Schmitt-Kopplin © Humana Press Inc., Totowa, NJ

thereof, *de novo* rates of nicotine synthesis increased in the roots, leading to a significant increase in whole plant nicotine accumulation after 5 d ***(10)***.

Limited resources constrain plants to trade-offs among growth, defense, and reproduction, which are the basis of most plant defense theories. The optimal defense theory holds that plant tissues contributing more to plant fitness and those more likely to encounter herbivore attack should be better defended than other plant tissues. As a consequence, young leaves, stems, and reproductive parts should have allocated higher levels of defence metabolites than old leaves and roots ***(4)***. In fact, Baldwin et al. found that the jasmonic acid concentrations were higher in younger than in older leaves of *Nicotiana sylvestris* upon wounding of the leaves ***(11)*** and that leaf damage in *Nicotiana attenuata* dramatically increased the allocation of nicotine in capsules indicating the importance of reproductive parts to plant's fitness ***(12)***. First investigations have shown that the preferential allocation of defense metabolites continues even on the cellular level. Single cell samples of epidermis cells at the leaf tip had considerably higher concentrations of nicotine than epidermis cells at the leaf base ***(13)***.

Classical analytical approaches use bulk plant extracts, but the obtained results represent only an average of all tissues present in the sample. Because physiological processes are often restricted to specific tissues, a high-resolution analysis on the cellular level would lead to a better understanding of biological processes, such as intercellular communication, signal transduction, or wound response. One available method for sampling and handling of single cells is the use of glass microcapillaries, which enable sampling the contents of individual plant cells *in situ* in living plants ***(14,15)***. A major problem is the very small sample volume in the pl range, which can spontaneously evaporate by exposure to air. But microanalytical tools and preventive measures to avoid evaporation and contamination of the samples as well as a number of suitable analytical methods overcome this problem. For example inorganic ions can be analyzed by energy dispersive X-ray (EDX) microanalysis ***(16)*** or ion selective microelectrodes ***(17)***. Nitrate and organic solutes such as malate and sugars were determined by use of micro-fluorometric enzymatic assays ***(18–20)***. Capillary electrophoresis (CE) has been developed to an important separation technique as a result of its compatibility with biological matrices and small sample volumes. It already has been successfully applied for the analysis of single animal and human cells ***(21)***. Recently, results of applications of CE for analysis of single plant cells were published. Bächmann et al. determined inorganic anions and cations in single wheat cells using a pyromellitic acid electrolyte and imidazolesulphate electrolyte, respectively, with indirect ultraviolet (UV) detection ***(22)***. The analysis of sugars was enabled by on-column chelation with Cu(II) and direct UV detection ***(23,24)***. The measurement of amino acids

was performed by on-column derivatization with o-phthaldialdehyde (OPA)/2-mercaptoethanol and application of micellar electrokinetic chromatography (MEKC) with fluorescence detection ***(24)***. Use of a laser-induced fluorescence (LIF) detector even improved the sensitivity of amino acid analysis of single cell samples by CE ***(25)***. Finally, alkaloids were analysed in single leaf cells of tobacco plants with direct UV detection ***(13)***.

In this chapter, a protocol for sampling and aliquotation of single cell samples as well as CE analysis of alkaloids in these small volume samples will be reported.

2. Materials

2.1. Chemicals

1. Plant cultivation: all nutrient salts (**Tables 1** and **2**) were purchased from Merck (Darmstadt, Germany).
2. Sampling: silicone oil (Fluka, Taufkirchen, Germany), trimethylchlorosilane (Fluka), hydrochloric acid (p.a., Merck).
3. Alkaloid standard: 4-aminopyridine (Merck, Darmstadt, Germany), nicotine (Merck), nornicotine (Fluka, Taufkirchen, Germany), anabasine (Aldrich, Taufkirchen, Germany).
4. CE buffer: 150 m*M* citric acid (Merck), adjusted with 1 *M* NaOH (Merck) to pH 3.6.

2.2. Equipment

2.2.1. Sampling

1. Stereo microscope MZ10 (Leica, Wetzlar, Germany).
2. Microscope illumination system FO-150 (World Precision Instruments, Berlin, Germany).
3. Cold light source FLQ 85E (Olympus, Hamburg, Germany).
4. Micromanipulator (Leitz, Wetzlar, Germany).

Table 1
Stock Solution A of the Nutrient Solution

Salt	Molecular weight (g/mol)	Mass (g) for 2 L solution	Concentration (mmol/L)
K_2SO_4	174.27	48.97	141.0
K_2HPO_4	174.19	38.67	82.3
KH_2PO_4	136.09	35.66	131.0
KNO_3	101.11	39.94	97.5
NH_4NO_3	80.05	217.74	1360.0

Table 2
Stock Solution B of the Nutrient Solution

Salt	Molecular weight (g/mol)	Mass (g) for 2 L solution	Concentration (mmol/L)
$Ca(NO_3)_2 \cdot 4\ H_2O$	236.16	59.04	125.0
$Mg(NO_3)_2 \cdot 6\ H_2O$	256.43	94.88	185.0
$Fe(NO_3)_3 \cdot 9\ H_2O$	404.0	5.064	6.27
$Mn(NO_3)_2 \cdot 2\ H_2O$	251.01	1.828	3.64
$Zn(NO_3)_2 \cdot 4\ H_2O$	261.44	0.24	0.46
$CuCl_2 \cdot 2\ H_2O$	170.49	0.0805	0.24
$Na_2MoO_4 \cdot 2\ H_2O$	241.95	0.0177	0.04
H_3BO_3	61.83	1.144	9.25
HNO_3	63.02	6.094	48.35

5. Pipette puller DMZ (Zeitz Instrumente, Munich, Germany).
6. Borosilicate glass capillaries with filament (F.D. 0.2 mm), 1.5 mm outer diameter (O.D.), 0.87 mm inner diameter (I.D.) (Hilgenberg, Malsfeld, Germany).
7. Microforge for preparation of constriction capillaries (Singer Instrument, Somerset, UK)
8. Petri dishes: cell culture dish, 2 mm grid, 35 × 10 mm, polystyrol (Nalge Nunc International, Rochester, NY).

2.2.2. Capillary Electrophoresis System

1. Self-built plastic housing containing the buffer vials and electrodes ***(22)***.
2. High voltage power supply type HCN 6 M-30000 from FUG (Rosenheim, Germany).
3. UV-detector Lambda 1000 (Bischoff, Leonberg, Germany).
4. Fused-silica column (Chromatograhie Service, Langerwehe, Germany); total length: 80 cm; effective length: 59 cm; I.D.: 50 μm.
5. Data acquisition with McDAcq software (Bischoff, Leonberg, Germany).
6. Stereo microscope SMZ-1B (Nikon, Düsseldorf, Germany)
7. Micromanipulator (World Precision Instruments, Berlin, Germany).

3. Methods

3.1. Plant Cultivation

1. Preparation of the Ingestad nutrient solution: the Ingestad nutrient solution system consists of 2 stock solutions ***(26,27)***. Basically, stock solution A contains the macro nutrients **(Table 1)** and stock solution B the micro nutrients **(Table 2)**. At preparation of the nutrient solution, it is important to provide deionized water in the graduated flask in order to prevent the precipitation of insoluble salts upon

mixing both stock solutions. After that, the pH must be adjusted to 5.5 with HCl or KOH.

2. Seeds of tobacco (*Nicotiana tabacum* cv. Samsun) are germinated on sand and supplied with nutrient solution (N concentration: 1 m*M*) for 10 d. Then the seedlings are piqued and grown for an additional 2 wk with supply of nutrient solution (N concentration: 1 m*M*). After that, the plants are planted in 9 × 9 cm pots containing quartz sand (grain size distribution: 2000 µm [3.94%], 630 µm [86.69%], 200 µm [8.20%], 63 µm [0.27%]). Pots are watered every day with nutrient solution (N concentration: 5 *mM*) until water runs out of their bottoms. Tobacco plants under N-deficiency are supplied with 5 m*M* N nutrient solution until the stem has a length of 5 cm. Then nutrient supply is continued without nitrate. The pots are placed in a growth room with a light period of 12 h, 200 lx, 20 °C temperature, and 40% RH.

3.2. Sampling of Single Plant Cells

1. For sample storage silicone oil is used. It is ultrasonically extracted 20 times with Milli-Q water to remove the ionic impurities.
2. Microcapillaries for the extraction of cell contents are produced by pulling borosilicate glass capillaries on a pipet puller **(Fig. 1A)**. After pulling, the tips of the microcapillaries are too narrow to allow entry of cell sap, and therefore must be removed by gently brushing them against the surface of a solid object under the microscope. The resulting tip apertures are approx 1 µm. The permeabilities of the microcapillaries are tested under a microscope by immerging them in Milli-Q water and applying pressure to their back end. Before use microcapillaries are silanized with trimethylchlorosilane at 50 °C for 4 h.

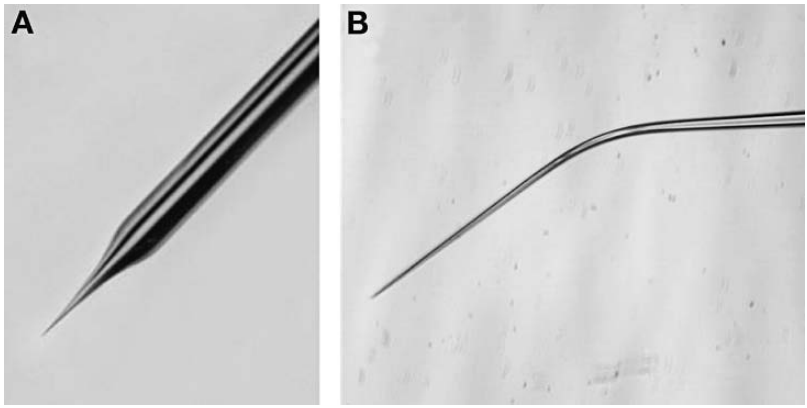


Fig. 1. Microcapillary for sampling single plant cells **(A)**. Constriction capillary for aliquotation of the sample into subsamples and internal standardization **(B)**.

3. Constriction capillaries are prepared from the normal microcapillaries with a microforge (**Fig. 1B**). After mounting the microcapillary into the microforge the barrel of the tip is brought to the heating wire. While switching on the current through the wire for 2–3 s, the constriction is formed. The bore inside the constriction must be visible under the microscope, otherwise flow of solution will be restricted. Before use, constriction capillaries are silanized with trimethylchlorosilane at 50 °C for 4 h.
4. **Figure 2** shows the experimental setup for sampling single plant cells. Pneumatic control of the microcapillary is performed with a 50-mL plastic syringe, silicone tubing, and a tube loop, which operates as a valve. During sampling, the operator holds the tube loop in his or her mouth and closes it by clenching his or her teeth. After mounting the microcapillary on a micromanipulator and its attachment to the silicone tubing, the microcapillary is filled with water-saturated silicone oil. A leaf, still attached to the intact plant, is fixed on a microscope slide with an angle of 45° to the principal axis of the microscope. The microcapillary now is brought to the leaf with an angle of 90° to the principal axis of the microscope and inserted into a surface cell (*see* **Note 1**). The cell turgor leads to a rapid entry of the vacuolar sap into the capillary tip. Because the loss of turgor will draw water from surrounding tissues into the cell by osmosis with a subsequent dilution of the sample, the capillary must be withdrawn from the cell as rapidly as possible (<1 s).
5. All subsequent steps of sample handling are illustrated in **Fig. 3**. First, the sample droplet is ejected onto the bottom of a silicone oil-filled Petri dish, thus avoiding evaporation of the droplet. Several 50-nL acidified water droplets as well as a

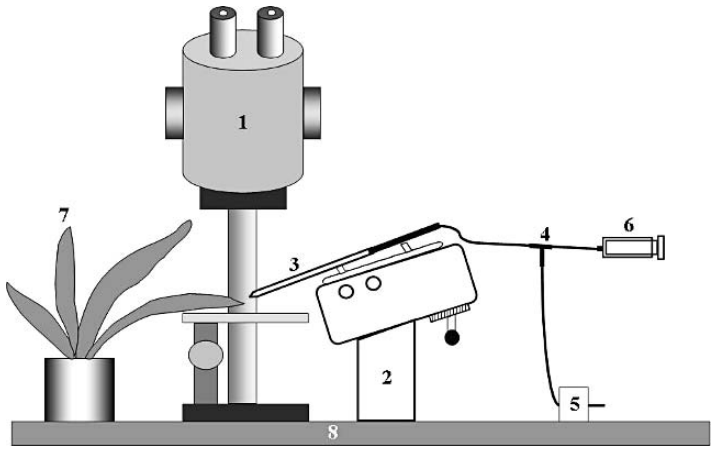


Fig. 2. Experimental setup for sampling single cells: 1, microscope; 2, micromanipulator; 3, microcapillary; 4, tubing; 5, valve; 6, syringe; 7, plant; 8, vibration damped table. (Reproduced from **ref. *22***, with permission from Elsevier B. V.)

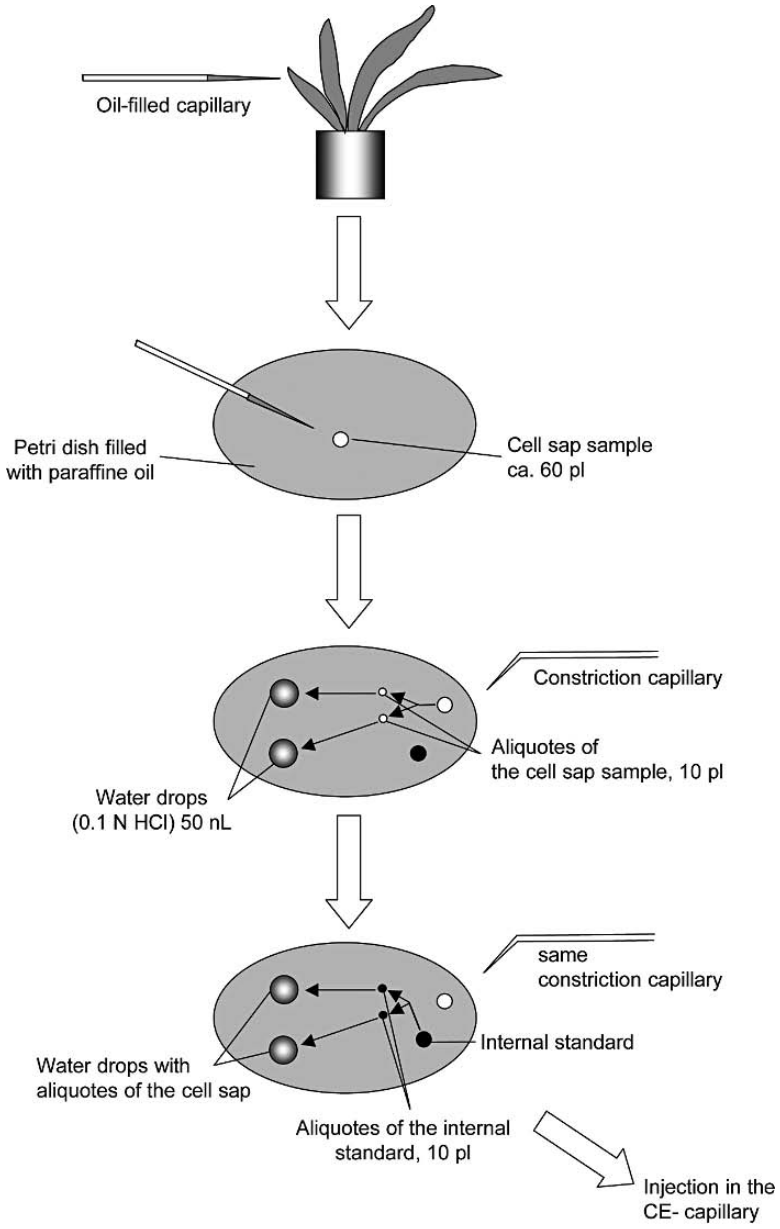


Fig. 3. Schematic of the sample handling procedure including extraction of a plant cell, depositing the sample droplet in a Petri dish, creating subsamples, and internal standardization. (Reproduced from **ref**. ***28***, with permission from ACS Publications.)

droplet of 10 m*M* 4-aminopyridine as internal standard have been positioned in the same Petri dish. The grid pattern on the bottom of the Petri dish allows unambiguous attribution of the different droplets. Then, a constriction capillary is used to create identical aliquots (~10 pl) of the sample and the internal standard. For this purpose, the constriction capillary is filled with silicone oil and by application of a slight vacuum with the syringe at closed valve, the sample is sucked in up to the constriction. The tip is moved out of the sample droplet and a small zone of silicone oil is sucked in. This procedure is repeated with the same sample droplet until several aliquots are in the constriction capillary, each separated from the others by a zone of silicone oil. Each aliquot is expelled into one of the 50-nL acidified water droplets. The intention of acidification is to avoid diffusion of alkaloids into the silicone oil due to formation of positively charged ammonium salts. After this, the constriction capillary is washed with water and filled with the internal standard of the same volume as the sample following the procedure described above. The internal standard is also expelled in the water droplets containing the samples, thus enabling the quantitative determination of the alkaloid concentrations in relation to the internal standard (*see* **Note 2**). The whole procedure is performed under a stereo microscope.

3.3. CE Analysis of Micro Droplets

1. After preparation of the samples, the injection of the water droplets containing sample and internal standard into the CE capillary is followed. **Figure 4** shows the experimental setup of the CE system. For injection, the CE capillary is mounted on

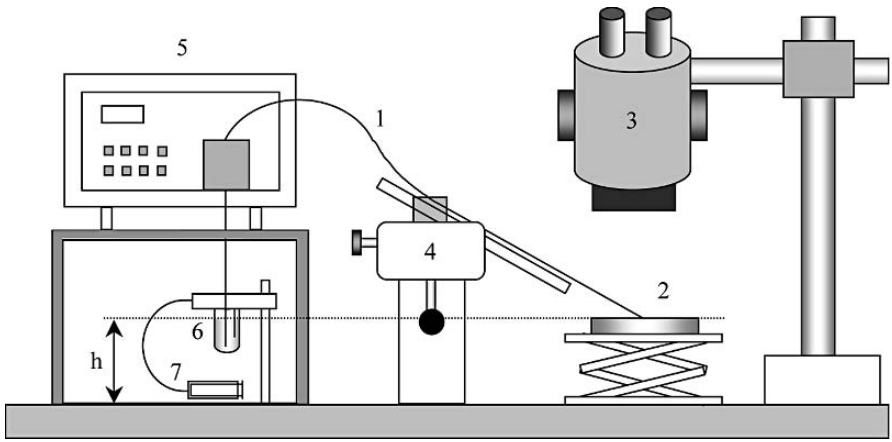


Fig. 4. Setup for injection of sample aliquots into the CE. 1, CE capillary; 2, Petri dish with sample aliquots; 3, microscope; 4, micromanipulator; 5, UV detector; 6, outlet buffer vial; 7, syringe; h, difference of level between the outlet buffer vial and the alkaloid standard vial for injection of the standard. (Reproduced from **ref. *22***, with permission from Elsevier B. V.).

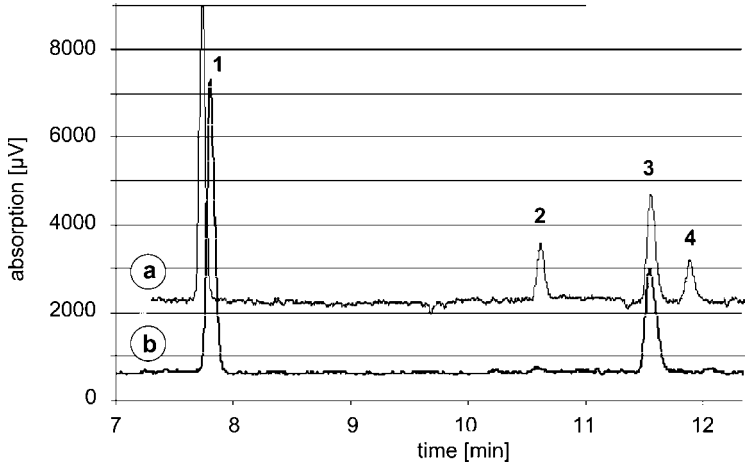


Fig. 5. Electropherograms of tobacco alkaloids in a standard mixture **(A)** and a single epidermis cell **(B)**: 1, 4-aminopyridine as internal standard; 2, nornicotine; 3, nicotine; 4, anabasine. Electrolyte: 150 m*M* citric acid (pH 3.6); capillary: 80 cm (effective length: 59 cm) × 50 µm inner diameter; CE conditions: voltage, 23 kV; detection, ultraviolet, 260 nm (at cathode); temperature, 20 °C.

a micromanipulator by which it is moved towards a water droplet. By generation of vacuum from the opposite side of the CE capillary with a syringe, the water droplet is completely sucked into the capillary. In order to facilitate the injection, the CE capillary has been conically reduced by grinding on abrasive paper. After exchange of the Petri dish against an electrolyte vial, CE separation is started.
CE conditions: voltage, 23 kV; detection, 260 nm (at cathode); temperature, 20 °C; buffer, 150 m*M* citric acid (pH 3.6).

For calibration, a 10 m*M* stock solution of nicotine, nornicotine, anabasine, and 4-aminopyridine is prepared in water and used after appropriate dilution. The alkaloid standards are hydrostatically injected at a level difference of 5 cm between the standard and the electrolyte vial for 60 s.
A new capillary is conditioned with 1 *M* NaOH, water and electrolyte each for 10 min and washed with electrolyte after every run under vacuum for 3 min.

2. **Figure 5** shows the CE analysis of alkaloids in a standard mixture and nicotine in an epidermal cell of a tobacco plant leaf. 4-Aminopyridine is used as internal standard.

4. Notes

1. Sampling from deeper cells like mesophyll cells is performed by application of a positive pressure to the end of the microcapillary. Then, contaminations from neighboring cells during the pass of the capillary through surface tissue are

avoided. After impalement of the microcapillary into a target mesophyll cell, the pressure is released to let cell sap enter the tip.
2. At this stage also storage of the prepared samples is possible for several weeks by freezing the closed Petri dishes at −20 °C.

Acknowledgments

We gratefully thank Prof. Dr.-Ing. Knut Bächmann (Emeritus) and his research group (Department of Chemistry, Darmstadt University of Technology, Germany) for teaching the technique of single cell analysis. The work was funded by the Deutsche Forschungsgemeinschaft (DFG) in project S 684 452.

References

1. Baldwin, I. T. (1988) The alkaloidal responses of wild tobacco to real and simulated herbivory. *Oecologia* **77,** 378–381.
2. Baldwin, I. T. (1988) Damage-induced alkaloids in tobacco - pot-bound plants are not inducible. *J. Chem. Ecol*. **14,** 1113–1120.
3. Baldwin, I. T. (1988) Short-term damage-induced increases in tobacco alkaloids protect plants. *Oecologia* **75,** 367–370.
4. Baldwin, I. T. (1999) Inducible nicotine production in native Nicotiana as an example of adaptive phenotypic plasticity. *J. Chem. Ecol*. **25,** 3–30.
5. Mizusaki, S., Tanabe, Y., Roguchi, M., and Tamaki, E. (1973) Changes in the activities of ornithine decarboxylase, putrescine N-methyltransferase and N-methylputrescine oxidase in tobacco roots in relation to nicotine biosynthesis. *Plant Cell Physiol*. **14,** 103–110.
6. Dawson, R. F. (1942) Accumulation of nicotine in reciprocal grafts of tomato and tobacco. *Am. J. Bot*. **29,** 66–71.
7. Baldwin, I. T. (1989) Mechanism of damage-induced alkaloid production in wild tobacco. *J. Chem. Ecol*. **15,** 1661–1680.
8. Baldwin, I. T., Oesch, R. C., Merhige, P. M., and Hayes, K. (1993) Damage-induced root nitrogen-metabolism in Nicotiana-sylvestris - testing C/N predictions for alkaloid production. *J. Chem. Ecol*. **19,** 3029–3043.
9. Baldwin, I. T., Zhang, Z. P., Diab, N., et al. (1997) Quantification, correlations and manipulations of wound-induced changes in jasmonic acid and nicotine in Nicotiana sylvestris. *Planta* **201,** 397–404.
10. Baldwin, I. T., Karb, M. J., and Ohnmeiss, T. E. (1994) Allocation of N-15 from nitrate to nicotine - production and turnover of a damage-induced mobile defense. *Ecology* **75,** 1703–1713.
11. Ohnmeiss, T. E., McCloud, E. S., Lynds, G. Y., and Baldwin, I. T. (1997) Within-plant relationships among wounding, jasmonic acid, and nicotine: implications for defence in Nicotiana sylvestris. *New Phytol*. **137,** 441–452.
12. Baldwin, I. T. and Karb, M. J. (1995) Plasticity in allocation of nicotine to reproductive parts in Nicotiana-attenuata. *J. Chem. Ecol*. **21,** 897–909.

13. Lochmann, H., Bazzanella, A., Kropsch, S., and Bächmann, K. (2001) Determination of tobacco alkaloids in single plant cells by capillary electrophoresis. *J. Chromatogr. A*. **917,** 311–317.
14. Tomos, A. D. and Leigh, R. A. (1999) The pressure probe: a versatile tool in plant cell physiology. *Annu. Rev. Plant Physiol. Plant Mol. Biol*. **50,** 447–472.
15. Tomos, A. D., Hinde, P., Richardson, P., Pritchard, J., and Fricke, W. (1994) Microsampling and measurements of solutes in single cells, in *Plant cell biology* (Harris, N. and Oparka, K. J., eds.), Oxford University Press, New York:, pp. 297–314.
16. Malone, M., Leigh, R. A., and Tomos, A. D. (1991) Concentrations of vacuolar inorganic-ions in individual cells of intact wheat leaf epidermis. *J. Exp. Bot*. **42,** 305–309.
17. Zhen, R. G., Koyro, H. W., Leigh, R. A., Tomos, A. D., and Miller, A. J. (1991) Compartmental nitrate concentrations in barley root-cells measured with nitrate-selective microelectrodes and by single-cell sap sampling. *Planta* **185,** 356–361.
18. Fricke, W., Leigh, R. A., and Tomos, A. D. (1994) Concentrations of inorganic and organic solutes in extracts from individual epidermal, mesophyll and nundle-sheath cells of barley leaves. *Planta* **192,** 310–316.
19. Fricke, W., Hinde, P. S., Leigh, R. A., and Tomos, A. D. (1995) Vacuolar solutes in the upper epidermis of barley leaves - intercellular differences follow patterns. *Planta* **196,** 40–49.
20. Kehr, J., Wagner, C., Willmitzer, L., and Fisahn, J. (1999) Effect of modified carbon allocation on turgor, osmolality, sugar and potassium content, and membrane potential in the epidermis of transgenic potato (Solanum tuberosum L.) plants. *J. Exp. Bot*. **50,** 565–571.
21. Yeung, E. S. (1999) Study of single cells by using capillary electrophoresis and native fluorescence detection. *J. Chromatogr. A*. **830,** 243–262.
22. Bazzanella, A., Lochmann, H., Tomos, A. D., and Bächmann, K. (1998) Determination of inorganic cations and anions in single plant cells by capillary zone electrophoresis. *J. Chromatogr. A*. **809,** 231–239.
23. Bazzanella, A. and Bächmann, K. (1998) Separation and direct UV detection of sugars by capillary electrophoresis using chelation of copper(II). *J. Chromatogr. A*. **799,** 283–288.
24. Lochmann, H., Bazzanella, A., and Bächmann, K. (1998) Analysis of solutes and metabolites in single plant cell vacuoles by capillary electrophoresis. *J. Chromatogr. A*. **817,** 337–343.
25. Arlt, K., Brandt, S., and Kehr, J. (2001) Amino acid analysis in five pooled single plant cell samples using capillary electrophoresis coupled to laser-induced fluorescence detection. *J. Chromatogr. A*. **926,** 319–325.
26. Ingestad, T. (1982) Relative addition rate and external concentration; driving variables used in plant nutrition research. *Plant Cell Environ*. **5,** 443–453.

27. Walter, A. and Schurr, U. (1999) The modular character of growth in Nicotiana tabacum plants under steady state nutrition. *J. Exp. Bot*. **50,** 1169–1177.
28. Bächmann, K., Lochmann, H., Bazzanella, A. (1998) Microscale processes in single plant cells. *Anal. Chem*. **70,** 645A–649A.

33

Multi-Dimensional Capillary Electrophoresis and Chromatography for Proteomic Analysis

Mingxia Gao and Xiangmin Zhang

Summary

Comprehensive two-dimensional liquid chromatography-capillary electrophoresis systems are summarized in this chapter. A variety of combinations of capillary electrophoresis and liquid chromatography modes as well as interfaces and detection technologies are discussed. A typical, comprehensive two-dimensional system coupled with reverse-phase liquid chromatography with fast capillary electrophoresis and hyphenated to mass spectrometry was demonstrated for proteomic analysis. A two-dimensional capillary electrophoresis system of coupling capillary sieving electrophoresis with micellar electrokinetic chromatography and its application in single cell analysis for protein expression profiling are presented.

Key Words: Multi-dimensional capillary electrophoresis; capillary reverse phase liquid chromatography; proteomic analysis; single cell.

1. Introduction

Multi-dimensional electrophoresis/chromatography is a powerful separation technique. Giddings ***(1)*** has shown that the peak capacity of a multidimensional separation system is the product of the peak capacities of its component individual dimensional method. If the component separation methods are orthogonal in separating mechanism, the total peak capacity of a multidimensional system is the multiple result of each dimension's. A variety of capillary electrophoresis modes, capillary zone electrophoresis (CZE), micellar electrokinetic chromatography (MEKC), capillary isoelectric focusing (CIEF), and capillary sieving electrophoresis (CSE), etc., combined with chromatography, reverse-phase

From: *Methods in Molecular Biology, vol. 384: Capillary Electrophoresis*
Edited by: P. Schmitt-Kopplin © Humana Press Inc., Totowa, NJ

liquid chromatography (RPLC), ion-exchange chromatography (IEC), and size-exclusion chromatography (SEC), etc., has been successfully applied to various multidimensional separation systems. This chapter will demonstrate the developments and applications of multidimensional capillary electrophoresis (CE) technologies.

1.1. Comprehensive Two-Dimensional Liquid Chromatography and Capillary Electrophoresis

CE is a high-speed and a high-efficiency separation technique. It is ideal as the last dimensional separation in multidimensional systems. RPLC coupled with CZE as a two-dimensional (2D) system is frequently used because of its many advantages. RPLC and CZE are orthogonal in separation mechanism. RPLC separates analytes based on hydrophobicity differences. CZE separates analytes, however, mainly on the basis of the solutes' mobility. Additionally, solvents in HPLC and buffers of CE are quite compatible in solubility.

Some pioneering work on comprehensive 2D RPLC-CZE separations has been done by Jorgenson and coworkers. In coupling RPLC to the CZE system using a computer-controlled, six-port valve loop, interface was first developed ***(2)***. After effluent from the RPLC column filled the loop, the second pump flushed the loop over the CZE capillary at specific intervals. Electromigration injection was performed on the CZE system from a RPLC flowing stream. Highly sensitive laser-induced fluorescence detection (LIFD) was used in CZE analysis of tryptic digest of ovalbumin labeling by fluorescence. A comprehensive 2D system was demonstrated by coupling SEC with CZE ***(3)***. The system was further improved ***(4)*** by using a clear polycarbonate polymer, Lexan, as the interface fabricating material. This allowed observation of the transfer of samples from LC to CZE directly. Coupling the 2D system of RPLC-CZE with mass spectrometry (MS) was also studied ***(5)***. Standard peptides and tryptic digests of ribonuclease B were analyzed by using electro-spray ionization (ESI) MS.

A "fast-CZE" technique using an optical-gating injection system was developed by Jorgenson and coworkers ***(6)***. The optical-gating interface performed analysis based on continuous photodecomposition of fluorescein isothiocyanate (FITC) using an argon-ion laser beam. A fast injection was carried out by milliseconds stop of laser radiation. A new, comprehensive 2D system was developed ***(7)*** and a three-dimensional separation system, SEC-RPLC-CZE, was also devised by using SEC as the additional dimension ***(8)***.

An off-line RPLC-CZE system was described by Issaq et al. ***(9)*** Fractions from RPLC were collected every 30 s, concentrated under vacuum, and

analyzed simultaneously by 96-array CE with LIFD. Stroink et al. ***(10)*** developed a 2D system of on-line coupling of SEC and CZE *via* a reverse-phase C18 trapping column for the analysis of structurally related enkephalins in cerebrospinal fluid.

A series of studies on multidimensional LC-CE systems have been developed in our lab. Optimized fast MEKC has been used in the 2D systems of separating neutral components in traditional Chinese medicines ***(11,12)***. A dynamic interface with pulse-contact was designed and applied for comprehensive 2D system in combining RPLC with fast MEKC. Also, a novel gas-driving device was applied to drive the capillary RPLC column back and forth. A fraction of RPLC effluent was stacked in a chamber and ejected into the CE capillary ***(12)***. The 2D switching relative standard deviations of peak heights and migration times of 100 consecutive runs were 3.3% and 2.2%, respectively. The high efficiency of this system was verified by separating hundreds of components in typical traditional Chinese medicines. Total peak capacity of the comprehensive 2D system could be over 2000.

A comprehensive 2D capillary liquid chromatography and CZE system coupled with a tandem time-of-flight (TOF-TOF) MS with matrix-assisted laser desorption/ionization (MALDI) was also investigated in our laboratory for proteomics analysis ***(13)***. The most important part of setting up such a 2D system is the fabrication of the interfaces. First of all, the interface between RPLC and CZE of the 2D system was able to tolerate high voltage switching in CE separations. Both the RPLC and MALDI-MS depositing system were unable to withstand such high voltages. So, a novel hydrodynamic injection interface was developed successfully to solve this problem. Second, a very stable nanoflow of CE effluent should be mixed with matrix of MALDI-MS and transferred onto the MALDI plates. A novel CE-MALDI interface was designed and applied to in this system. The CZE effluents were mixed with a-cyano-4-hydroxycinnamic acid (CHCA) matrix sheath flow through this interface, and deposited on the MALDI target at a 3-s time interval for further MS analysis. This system was applied to the analysis of proteins in liver cancer tissue, D20 (human hepatocellular carcinoma model in nude mice with high metastatic potential). More than 300 proteins were identified, which proved the potential application for high-throughput analysis in proteomics.

Yang et al. of our group ***(14)*** developed a comprehensive 2D system in coupling capillary RPLC with microchip electrophoresis. A valve-free gating interface was devised simply by inserting the outlet end of an LC column into the cross-channel on a chip. An LIFD was devised and used to perform on-chip, highly sensitive detection. The RPLC effluents were continuously delivered to the chip, and pinched injections of the effluents every 20 s were employed for chip CE separation. The relative standard deviations for migration time and

peak height of rhodamine B in 150 sample transfers were 3.2% and 9.8%, respectively. The effectiveness of this system was demonstrated by separating peptides of the fluorescein isothiocyanate (FITC)-labeled tryptic digests of bovine serum albumin.

Mao et al. of our group ***(15)*** also demonstrated a 2D system by using RPLC as the first dimension and CIEF as the second dimension. The focusing effect of CIEF could be not only to achieve a high resolution but also to permit low-abundance protein concentration of hundreds of times. In the comprehensive 2D RPLC-CIEF system, a peak capacity of more than 10,000 had been achieved. An electrically neutral thiol reactive dye, BODIPY maleimide with LIFD, was applied for highly sensitive detection with fmol level of proteins.

Chen et al ***(16)*** developed a 2D system coupling CIEF with capillary RPLC using CIEF as the first dimension. Focused peptides were hydrodynamically mobilized into the injection loop of a micro switching valve under the loading position, followed by subsequent injection into capillary RPLC. The resolving power of the combined CIEF-RPLC system was demonstrated using the soluble fraction of *Drosophila* salivary glands. The overall peak capacity is estimated to be around 1800 over a run time of less than 8 h.

The Tragas group ***(17)*** adopted a microdialysis hollow-fiber member to combine a gel filtration chromatography (GFC) with CIEF. Each eluted protein was directed to the microdialysis hollow-fiber member, where the simultaneous desalting and mixing of the carrier ampholyte occurred. Then, the sample was driven to a CIEF column by a pump for separation. Sample transfer and CIEF were completed in 5 min for each of the eluted fraction. Total analysis time was about 24 min.

1.2. Comprehensive 2D CE-CE Systems

2D CE-CE has been proven to be a great potential technique for the separation of proteins and peptides in biological proteomics analysis. Dovichi and coworkers ***(18)*** reported fully automated 2D MEKC-MEKC for protein analysis. In the system, proteins were labeled with the fluorogenic reagent, 3-(2-furoyl)-quinoline- 2-carboxaldehyde (FQ), which reacted with lysine residues and created highly fluorescent products. These labeled proteins were analyzed by submicellar CE at pH 7.5 to perform a first-dimension separation. Once the first components migrated from the capillary, a fraction was transferred into the second-dimension capillary, where electrophoresis was performed at pH 11.1 for further separations. Detection limits of a few zeptomoles of labeled protein were achieved. Similar work coupling capillary sieving electrophoresis (CSE) with MEKC has been demonstrated ***(19)***. This technology was applied to separate more than 150 components of fluorescence-labeled bacterium proteins.

A protein expression profile of single cells was presented by using the CSE-MEKC technology ***(20)***. Single cells of native MC3T3-E1 osteoprogenitor, MC3T3-E1 cells transfected with the human transcription regulator TWIST, and MCF-7 breast cancer cells were separated as protein expression fingerprints.

Mohan et al ***(21)*** developed a 2D system coupling CIEF with transient isotachophoresis-zone electrophoresis (CITP-CZE). In this system, carrier ampholytes, employed for the creation of pH gradient during focusing, are further used as the leading electrolyte in the second separation dimension. Separation of proteolytic peptides was demonstrated. The maximum peak capacity is estimated to be around 1600.

Pawliszyn and coworkers developed a 2D system in coupling MEKC to CIEF by using a 10-port valve with a device having two conditioning loops ***(22)***. In the loop, carrier ampholytes were added, and salts and other unwanted effluent components of the first dimension were eliminated by dialysis. Whole-column imaging detection was applied in this system.

Zhang and coworkers ***(23)*** combined CIEF with capillary gel eletrophoresis (CGE) by mounting a hollow fiber on a methacrylate resin plate. The two dimensions of capillaries with three electrodes shared one high-voltage source and one cathode fixed in a reservoir on a methacrylate plate. With the dialysis interface, small molecules of sodium dodecyl sulfate (SDS) can be mixed with analytes followed by CGE separation. Chemical mobilization was utilized to drive the sample zones of the first dimension to the second dimension. A 2D system of coupling CIEF with CZE was further developed using similar dialysis technology ***(24)***. In the first dimension of the system, focused zones were driven into the dialysis interface by electroosmotic flow (EOF). In the second dimension, each zone was separated by inverted EOF generated from the charged layer of cationic surfactant adsorbed onto the inner wall of the capillary. A 2D system of coupling CIEF with capillary none gel sieving electrophoresis for proteins separation was also presented ***(25)***.

Microfabricated chips for electrophoretic separations have attracted more interest in recent years. Microchannels and microreactors with different geometries and functions can be integrated to perform a total analysis or a parallel analysis. For multidimensional separations, sample injection, separations, and interfaces are capable of being integrated on a single chip. Recently, on-chip 2D CE systems were fabricated by Ramsey and coworkers. A comprehensive 2D MEKC-CZE system ***(26)*** and RPLC-CZE system ***(27)*** were developed using cross-channel interfaces on glass chips. The performance of microchip devices for 2D separations was improved ***(28)*** in analysis times and separation

Table 1
Two-Dimensional (2D) Capillary Electrophoresis (CE) Systems

	2D mode	Detector	Interface	Sample	Ref.
LC-CE	RPLC-CZE	MS	Valve-free hydrodynamic sampling device	Liver cancer tissue	***13***
	RPLC-MEKC	UV	Dynamic interface with pulse contact	Traditional Chinese medicine	***11,12***
	RPLC-CIEF	LIF	Fractionation	Yeast cell cytosol	***15***
	RPLC-chip CZE	LIF	Valve-free gating interface	BSA	***14***
	RPLC-CZE	LIF	Six-port valve interface	Ovalbumin	***2***
	SEC-CZE,	UV	Transverse flow-gated interface	Thyroglobulin, BSA, chicken egg albumin, myoglobin	***3***
	RPLC-CZE	LIF	Transverse flow-gated interface	A mixture of phenylalanine and glutamic	***4***
	RPLC-CZE-MS	ESI-MS	Transverse flow-gated interface	Glycosylated peptide mixtures	***5***
	RPLC-CZE SEC-RPLC-CZE	LIF	Optical-gated interface	Horse heart cytochrome c	***7,8***
	RPLC-CZE	LIF	Off-line	Cytochrome *c*, myoglobin	***9***
	SEC-CZE	UV	C18 trapping column	Enkephalins in cerebrospinal fluid	***10***
	CIEF-RPLC	UV	Microinjector	Soluble fraction of drosophila salivary glands	***16***
	GFC-CIEF	Column imaging	Microdialysis interface	Myoglobin, bovine serum albumin	***17***

CE-CE	MEKC(7.5)-MEKC(11.1)	LIF	Flow-gated interface	HT29 human adenocarcinoma cell	***18***
	CSE-MEKC	LIF	Flow-gated interface	Bacterium deinococcus radiodurans, MC3T3-E1 osteoprogenitor cells, MCF-7 breast cancer cells	***19,20***
	CITP-CZE	UV	Microdialysis interface	Cytochrome *c*, ribonuclease A, and carbonic anhydrase	***21***
	MEKC-CIEF	Column imaging	10-port valve with two dialysis loops	Myoglobin, ovalbumin, carbonic anhydrase, cytochrome c	***22***
	CIEF-CGE	UV/Vis	Dialysis interface	Hemoglobin (Hb)	***23***

(*Continued*)

Table 1
(Continued)

2D mode	Detector	Interface	Sample	Ref.
CIEF-CE	UV/Vis	Dialysis interface	Ribonuclease	***24***
CIEF- CN GE	UV/Vis	Hollow fiber interface	Hemoglobin	***25***
MEKC-CE,OCEC-CE (on chip)	LIF	Flow-gated interface	Cytochrome c,β-casein, ovalbumin	***26***,***27***,***28***
ITP-CZE(on chip)	LIF	Cross-channel injector design	eTag reporter 1, 2	***29***
IEF-SDS gel electrophoresis (on chip)	Fluorescence	Plastic microfluidic network.	Parvalbumin, trypsin inhibitor, BSA, actin	***30***

LC, liquid chromatography; RPLC, reverse-phase liquid chromatography; CZE, capillary zone electrophoresis; MS, mass spectrometry; MEKC, micellar electrokinetic chromatography; UV, ultraviolet; CIEF, capillary isoelectric focusing; LIF, laser-induced fluorescence; BSA, bovine serum albumin; SEC, size-exclusion chromatography; ESI, electrospray ionization; GFC, gel filtration chromatography; CSE, capillary sieving electrophoresis; CITP, CIEF with transient isotachophoresis; CGE, capillary gel electrophoresis; OCEC, open-channel electrochromatography; ITP, isotachophoresis; SDS, sodium dodecyl sulfate.

efficiency. Such a 2D chip system achieved 4200 peak capacity for resolution of tryptic digests of bovine serum albumin.

Coupling isotachophoresis (ITP) with CZE was demonstrated by Vreeland et al ***(29)***. The ITP-CZE system was able to produce 50-fold concentrations of solutes in comparison with pure CZE separations. Isoelectric focusing (IEF) combined with SDS gel electrophoresis on a polymer microfluidic chip was also investigated ***(30)***. Similarly to 2D gel electrophoresis, after IEF of proteins in the first dimension, the focused proteins were electrokinetically transferred into an array of orthogonal microchannels and further resolved by SDS gel electrophoresis in a parallel.

Table 1 is a list of the above works on 2D CE and related separation techniques.

2. Materials

2.1. Comprehensive 2D RPLC-CZE and MALDI-MS System

1. Samples: peptides digested from proteins in liver cancer tissue of D20. Lysis buffer of the liver cancer tissue contained 9 mol/L urea, 2% CHAPS, 50 mmol/L dithiothreitol (DTT), 0.14g/mL phenylmethylsulfonyl fluoride (PMSF). Sequencing-grade trypsin was used to digest proteins. Peptides were labeled by FITC. Myoglobin and cytochrome *c* act as standard proteins to optimize the separation conditions (all reagents from Sigma, St. Louis, MO).
2. Mobile phase: acetonitrile (ACN), HPLC-grade, trifluoroacetic acid (TFA) (from Sigma, St. Louis, MO).
3. CE buffer: triethylamine (TEA) (from Merck, Darmstadt, Germany).
4. Packing materials of capillary HPLC column: C8 particles, 5 μm Zorbax 300SB (from Agilent Technologies, Waldbronn, Germany), and spherical silica gel, Zorbax BP-SIL from (DuPont, Wilmington, DE).
5. Standard compounds used to evaluate the performance of the interfaces: benzyl alcohol, 2,6-dichlorophenol, and naphthyl alcohol (from Aldrich Chemical, Milwaukee, WI).
6. Electricity-conductive membrane on the CE capillary: 5% w/v agarose solution.
7. MALDI matrix: α-Cyano-4-hydroxycinnamic acid (CHCA) (from Aldrich Chemical, Milwaukee, WI).

2.2. Comprehensive 2D CE-CE System (CSE-MEKC System)

1. Samples: MCF-7 human breast cancer cells.
2. Reagents for derivatization: FQ was used as fluorescence reagent to react with the ε-amine of lysine residues of proteins.
3. CE buffer: the buffer of the first-dimensional CSE was 0.1 *M* Tris, 0.1 *M* CHES, 6% pullulan, and 0.1% SDS (pH 8.6). The pullulan acted as a sieving matrix in a CSE separation. The second-dimensional MEKC buffer was 0.1 *M* Tris, 0.1 *M* CHES, and 20 m*M* SDS (pH 8.6).

2.3. Equipment

1. Comprehensive 2D RPLC-CZE and MALDI-MS system:

   a. An HPLC capillary pump (Agilent).
   b. Fused-silica capillaries with 250 μm inner diameter (I.D.), 380 μm outer diameter (O.D.), and 30 cm length were used to pack capillary HPLC columns. A capillary of 75 μm I.D. and 380 μm O.D. was used for CE, total length: 30 cm, effective length: 28 cm.
   c. Mass spectrometer detection: MALDI-TOF-TOF-MS spectrometer (Applied Biosystems).

2. Comprehensive 2D CE-CE system (CSE-MEKC system)

   a. Fused-silica capillaries with 50 μm I.D. and 138 μm O.D. were used for CE. Both capillaries, the first-dimension and the second-dimension, were 30 cm long and coated with linear polyacrylamide to reduce electroosmosis for separation of a single MCF-7 cell.
   b. LIFD with a sheath-flow cuvet was used to monitor the labeled proteins. A 12-mW, 488-nm argon ion laser beam provided excitation. Fluorescence was collected with a 60×, 0.7 NA microscope objective, filtered with an Omega 630DF30 band-pass filter, and then detected with a Hamamatsu 1477 photomultiplier tube, which was biased at 1000 V.

3. Methods

3.1. Comprehensive 2D RPLC-CZE System Coupled with MALDI-MS

1. Sample preparation. The liver tissue of D20 was lysed in lysis buffer and protein was extracted after centrifugation. Proteins of 10 mg/mL concentration were attained and measured by a Bio-Rad assay. A 20-μg sample of trypsin was added to 1 mg of the protein sample in order to digest the proteins at 37°C overnight. 1 *M* $MgCl_2$ and glacial acetic acid was added to the peptide digests at volume ratio of 1:1 and 1:10, and mixed by light vortexing over 5 min. The insoluble RNA fraction was pelleted by centrifugation.
2. The construct of comprehensive 2D RPLC-CZE system coupled with MALDI-MS. **Figure 1** is a typical comprehensive 2D LC-CE system coupling with MALDI-MS. Such a system composed of a capillary HPLC system and a fast CE system as well as two interfaces hyphenated LC-CE columns and CE-MALDI deposition system.
3. The sample was first separated through capillary RPLC. Effluent from RPLC was continuously transferred into CZE through a hydrodynamic sampling interface. The CZE effluent was mixed with matrix sheath flow *via* CE-MALDI interface, and then directly deposited on the MALDI target for MS identifications.
4. The optimized separation conditions of the LC and CE were as follows. The binary mobile phases of the first dimension: A, 95% water/5% acetonitrile/0.1% TFA; B, 5% water/95% acetonitrile/0.1% TFA. The gradient of elution: 0%B increased to 20%B in 25 min, then ramped to 80%B in 45 min, at 71 min increased to 100%B

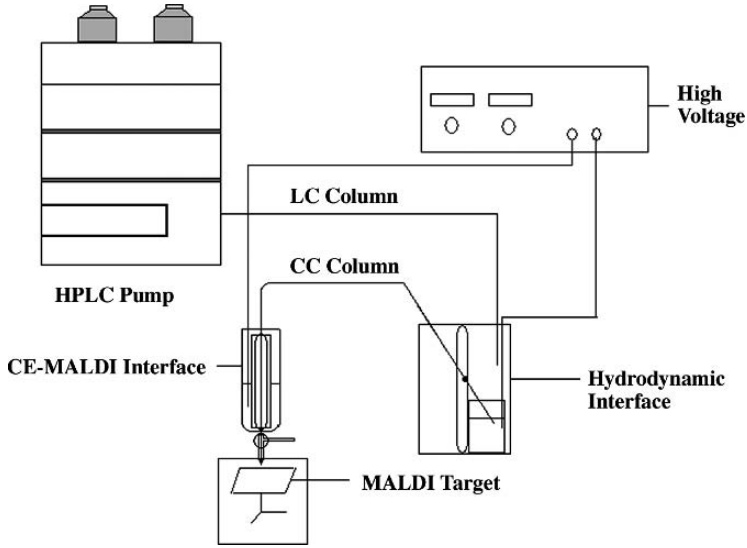


Fig. 1. Schematic configuration of the comprehensive reverse-phase liquid chromatography-capillary electrophoresis system with two interfaces. (Reproduced from **ref. *13***, with permission from John Wiley.)

and maintained for 5 min, in 10 min back to 0% B. In the second dimension, the optimized separation conditions were: 50 m*M* TEA running buffer, positive high voltage 23 kV with an EOF of 40 s.

5. Interfaces of the RPLC-CE-MALDI-MS system. The principle of the hydrodynamic interface was as shown in **Fig. 2**. A slide bar driven by a step-motor was used to move up and down for injection. The CE capillary was positioned at the "analysis position," and the inlet end of the capillary was dipped into the buffer under 3 mm depth of the liquid surface in the reservoir. Hydrodynamic injection was performed by elevating the slide bar to a position where the inlet end of the CE capillary contacted with the LC column outlet end. Once the inlet end of CE touched the LC outlet end, the inlet end was immediately surrounded by the effluent from the LC column. Because the inlet end of CE was 8 cm higher than the outlet end of CE, hydrodynamically, a part of the LC effluent was injected into CE. Injection volumes could be controlled by varying the contact time of the two columns and the elevated height of the CE inlet end. After injection, the CE column was moved back to the "analysis position" subsequently separated. During the injection process, the high voltage of the CE system was stopped before the capillary tip went up and applied again after the capillary tip moved back into the buffer reservoir. The CE-MALDI interface was fabricated as in **Fig. 3**. A stainless steel three-way tube was used to deliver the CHCA matrix solution from the syringe pump at end of the

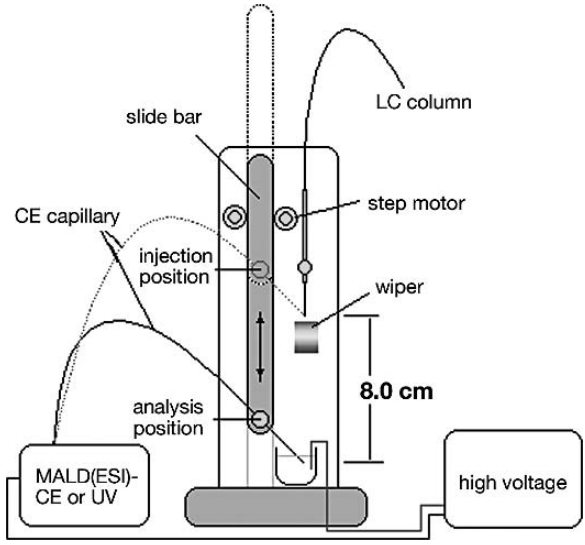


Fig. 2. Schematic diagram of hydrodynamic interface. (Reproduced from **ref. *13***, with permission from John Wiley.)

CE capillary. A membrane film was formed on the fracture of the outlet end of the CE capillary by 5% w/v agarose solution.

6. Mass spectrometer detection. After injection of the digested protein, peptides were separated by LC-CE system and effluents of CE were deposited on MALDI plates

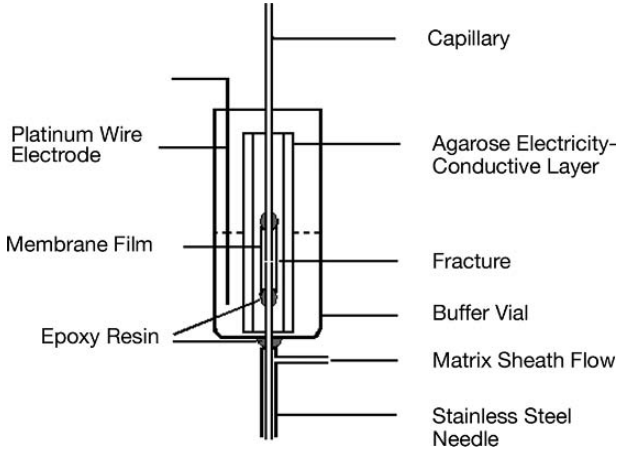


Fig. 3. Schematic diagram of the capillary electrophoresis-matrix-assisted laser desorption/ionization interface. (Reproduced from **ref. *13***, with permission from John Wiley.)

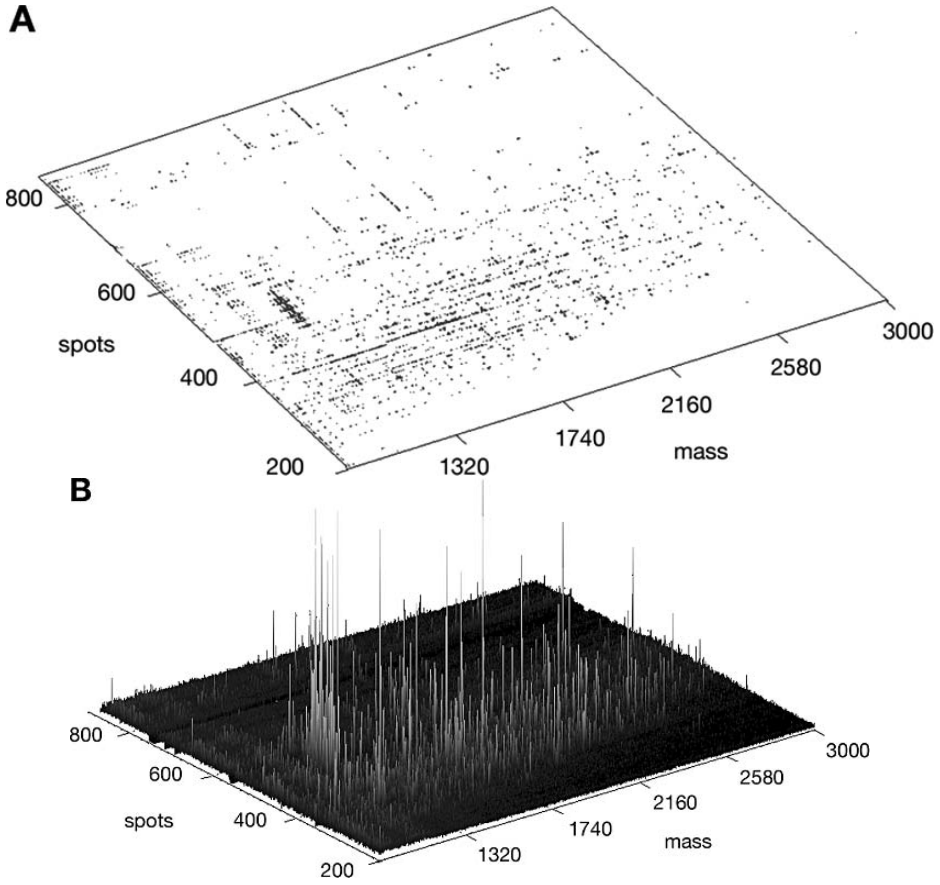


Fig. 4. Contour-mapping and three-dimensional plot of two-dimensional separation for protein tryptic peptides from liver cancer tissue. (Reproduced from **ref. *13***, with permission from John Wiley.)

at a time interval of 3 s. A total of 1800 spots was deposited in 90 min, and this was followed by MS analysis, whereby 388 proteins were identified. **Figure 4** is the contour-mapping of the proteomic peptides' separation result in 3D plot.

3.2. Comprehensive 2D CE-CE system (CSE-MEKC)

1. The construct of 2-D CE instrument and operating condition. **Figure 5** is configuration of the 2D CE system for single cells analysis. The first- dimension capillary contains an SDS-pullulan buffer system to perform CSE and the second-dimension capillary contains an SDS buffer for micellar electrokinetic capillary chromatography. Two high voltages were used to control system running. A typical operating

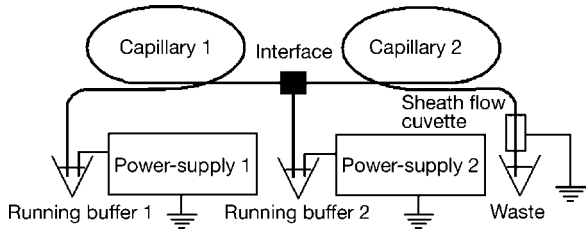


Fig. 5. Schematic configuration of the two-dimensional CE-CE system. (Reproduced from **ref**. 19, with permission from American Chemical Society.)

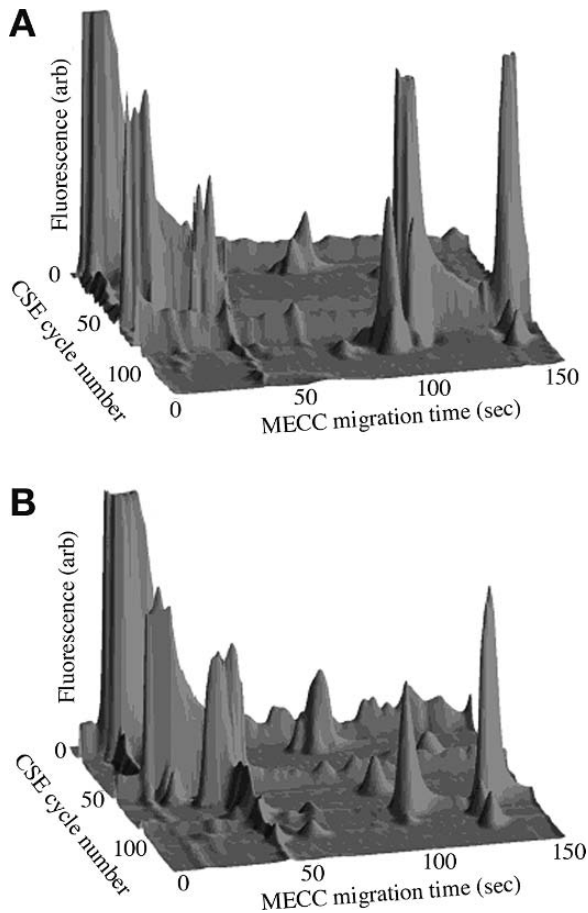


Fig. 6. Protein fingerprints from single MCF-7 breast cancer cells. **(A)** A normally cultured cell and **(B)** a cell treated for 48 h with sodium butyrate. (Reproduced from **ref**. ***20***, with permission from American Chemical Society.)

condition is as follows: Power-supply2 set at 10 kV for 5 s of sample injection on capillary 1, then ramped up to 15 kV for 660 s preseparation; afterward decreased to 12 kV. Power-supply 1 immediately increased to 12 kV after the preseparation. Capillary 1 stopped separation as a result of both power supplies maintaining 12 kV. Capillary 2 started 150 s of separation. After the first cycle of separation, power-supply1 decreased down to 0 kV for 8 s and an eluted fraction of the capillary 1 injected into the capillary 2. Then, power-supply1 was restored to 12 kV for the next 150-s cycle of separation. Hundreds of the cycles of separations were carried out to obtain a protein fingerprint.

2. Sample preparation. MCF-7 human breast cancer cells were cultured and maintained in 10% fetal bovine serum, 100 UI/mL streptomycin, 100 Ìg/mL penicillin, and 50 Ìg/mL gentamycin. Before analysis, cells were thoroughly washed with phosphate-buffered saline (PBS) three times to remove the medium. MCF-7 cells were treated with 2.5 m*M* sodium butyrate for 48 h to induce apoptosis. KCN was added to the cell suspension to give a concentration of 2 m*M*.
3. Labeling reaction and injection of a single cell. A plug of solution of 10 m*M* FQ with 0.5% SDS (W/V) was injected into the capillary by negative pressure. The capillary tip was then centered over a cell. The cell was injected into the capillary by applying negative pressure. Then, a plug of the FQ solution was injected again. The capillary tip was then placed in a vial containing buffer that had been heated to 95 °C to denature and label the proteins.
4. After the labeling reaction, the capillary tip was moved to a fresh vial of running buffer and followed by 2D separation. LIFD with a sheath-flow cuvet was used to monitor the labeled proteins.
5. **Figure 6** presents the protein mapping of single cells. **Figure 6A** is a 2D mapping generated from a cell grown under normal conditions. **Figure 6B** is from a cell that had been treated with 2.5 m*M* sodium butyrate for 48 h to induce apoptosis. The result demonstrates that comprehensive 2D CE and highly sensitivity detection would be powerful in single cell proteomic analysis.

4. Notes

1. To set up a 2D LC-CE system, several aspects should be taken into account. RPLC is used as the first dimension because solvents in RPLC are fairly compatible with CE buffer in terms of solubility. A capillary LC column is selected to match CE for sampling sizes. Analysis time matching of the HPLC and CE is also very important in a comprehensive 2D system. CZE, in contrast with capillary HPLC, is able to perform a very fast separation by using a short column and applied a high voltage. CE should be used as the second dimension of the system so that analysis time is short enough to complete hundreds of analyses in one LC run. If fast CE analysis time is 1 min, 100 times of CE analyses could be finished within 100 min LC elution.

   TEA was an excellent CE running buffer for several reasons. TEA is a volatile compound that easily escapes after deposition on MALDI target plates. Existence of TEA might suppress the sample ionization in MALDI-MS analysis. TEA buffer

with a high pH value could generate high EOF during CE separations. Also, TEA could be adsorbed on capillary wall to form a dynamic coating and to prevent proteins/peptides from adsorption.

2. The sample transfer efficiency between two dimensions is important in multidimensional system. Several aspects should be noticed in LC-CE interface fabrications. First, a good contact must be ensured because the inlet point of the CE capillary could immerse in the LC effluent. The two columns must make contact with each other at a certain angle; a variation of 30°#–#60° could be used for good performance. Second, the inlet end of the CE column should be at a level higher than that of the outlet end of CE, so that hydrodynamic injection occurs as a result of gravitation force. Third, in this system, a special "wiper" was designed to get rid of unused sample and to remove excess buffer from the reservoir. In addition, the wiper was grounded to release accumulated static, which might result in unstable LC effluent droplet.
3. In this system, ESI was not adopted because of several technical problems. ESI was run in acid sheath liquids to obtain positively charged ionizations, but CE ran in basic buffer liquid. Mixing sheath liquid with CE buffer could result in considerably unstable signals. CE effluents with TEA could suppress the ionization of peptides and lead to sensitivity loss. Another technical problem was that fast CE elution peaks were not matched with the slow MS scanning rate in ion-trap MS or Q-TOF-MS. Especially in peptide mapping using the tandem MS mode, minutes of scan time were necessary to obtain qualified MS/MS spectra. A fast CE elution peak finished in 1 or 2 s usually was too fast for ESI-MS/MS analysis. Therefore, a 2D LC-CE system with MALDI mass spectrometry was employed.
4. In-capillary cell labeling with fluorescence, FQ, was used by Dovichi and coworkers. A microscope should be used to observe the whole operation process. The applied negative pressure and injection time should be controlled accurately in order to aspirate a single cell and plug of solution.
5. Safety shields were used to protect the operator from high voltages. The detector was held at ground potential for safety.

   The detection sensitivity of this technology is the key to performing ultrasensitive protein analysis and providing high dynamic range for the multidimensional analysis of the minute amount of protein present in a single cell. LIFD with a sheath-flow cuvet was used to monitor the labeled proteins and achieve such a low detection limit.

References

1. Giddings, J. C. (1987) Concepts and comparisons in multidimensional separation. *J. High Resolut. Chromatogr. Chromatogr. Commun*. **10,** 319–323.
2. Bushey, M. M. and Jorgenson J. W. (1990) Automated instrumentation for comprehensive two-dimensional high-performance liquid chromatography/capillary zone electrophoresis. *Anal. Chem*. **62,** 978–984.

3. Lemmo, A. V. and Jorgenson, J. W. (1993) Transverse flow gating interface for the coupling of microcolumn LC with CZE in a comprehensive two-dimensional system. *Anal. Chem*. **65,** 1576–1581.
4. Hooker, T. F. and Jorgenson, J. W. (1997) A Transparent flow gating interface for the coupling of microcolumn LC with CZE in a comprehensive two-dimensional system. *Anal. Chem*. **69,** 4134–4142.
5. Lewis, K. C., Opiteck, G. J., Jorgenson, J. W., and Sheeley, D. M. (1997) Comprehensive on-line RPLC-CZE-MS of peptides. *J. Am. Soc. Mass Spectrom*. **8,** 495–500.
6. Monnig, C. A. and Jorgenson, J. W. (1991) On-column sample gating for high-speed capillary zone electrophoresis. *Anal. Chem*. **63,** 802–807.
7. Moore, A. W. and Jorgenson, J. W. (1995) Rapid comprehensive two-dimensional separations of peptides via RPLC-Optically gated capillary zone electrophoresis *Anal. Chem*. **67,** 3448–3455.
8. Moore, A. W. and Jorgenson, J. W. (1995) Comprehensive three-dimensional separation of peptides using size exclusion chromatography/reversed phase liquid chromatography/optically gated capillary zone electrophoresis. *Anal. Chem*. **67,** 3456–3463.
9. Issaq, H. J., Chan, K. C., Liu, C. S., and Li, Q. B. (2001) Multidimensional high performance liquid chromatography–capillary electrophoresis separation of a protein digest: an update. *Electrophoresis* **22,** 1133–1135.
10. Stroink, T., Wiese, G., Teeuwsen, J. (2003) On-line coupling of size exclusion and capillary zone electrophoresis *via* a reversed-phase C18 trapping column for the analysis of structurally related enkephalins in cerebrospinal fluid. *Electrophoresis* **24,** 897–903.
11. Huang, S., Xu, S. Y., Zhang, X. M. (2000) Optimization of the interface for coupling capillary high performance liquid chromatography with capillary electrophoresis in comprehensive two-dimensional system. *Chin. J. Anal. Chem*. **28,** 1467–1471.
12. Zhang, X. M, Hu, H. L., Xu, S. Y., Yang, X. H., and Zhang, J. (2001) Comprehensive two-dimensional capillary LC and CE for resolution of neutral components in traditional Chinese medicines. *J. Sep. Sci*. **24,** 385–391.
13. Zhang, J., Hu, H. L., Gao, M. X., Yang, P. Y., and Zhang, X. M. (2004) Comprehensive two-dimensional chromatography and capillary electrophoresis coupled with tandem time-of-flight mass spectrometry for high-speed proteome analysis. *Electrophoresis* **25,** 2374–2383.
14. Yang, X. H., Zhang, X. M., Li, A. Z., Zhu, S. Y., and Huang, Y. P. (2003) Comprehensive two-dimensional separations based on capillary high-performance liquid chromatography and microchip electrophoresis *Electrophoresis* **24,** 1451–1457.
15. Mao, Y. and Zhang, X. M. (2003) Comprehensive two-dimensional separation system by coupling capillary reverse-phase liquid chromatography to capillary isoelectric focusing for peptide and protein mapping with laser-induced fluorescence detection. *Electrophoresis* **24,** 3289–3295.

16. Chen, J. Z., Lee, C. S., Shen, Y. F., Smith, R. D., and Baehrecke, E. H. (2002) Integration of capillary isoelectric focusing with capillary reversed-phase liquid chromatography for two-dimensional proteomics separation. *Electrophoresis* **23,** 3143–3148.
17. Tragas, C. and Pawliszyn, J. (2000) On-line coupling of high performance gel filtration chromatography with imaged capillary isoelectric focusing using a membrane interface. *Electrophoresis* **21,** 227–237.
18. Michels, D. A., Hu, S., Schoenherr, R. M., Eggertson, M. J., and Dovichi, N. J. (2002) Fully automated two-dimensional capillary electrophoresis for high sensitivity protein analysis. *Mol. Cell. Proteomics* **1,** 69–74.
19. Michels, D. A., Hu, S., Dambrowitz, K. A., Eggertson, M. J., Lauterbach, K., and Dovichi, N. J. (2004) Capillary sieving electrophoresis-micellar electrokinetic chromatography fully automated two-dimensional capillary electrophoresis analysis of *Deinococcus radiodurans* protein homogenate. *Electrophoresis* **25,** 3098–3105.
20. Hu, S., Michels, D. A., Fazal, M. A., Ratisoontorn, C., Cunningham, M. L., and Dovichi, N. J. (2004) Capillary sieving electrophoresis/micellar electrokinetic capillary chromatography for two-dimensional protein fingerprinting of single mammalian cells. *Anal. Chem*. **76,** 4044–4049.
21. Mohan, D. and Lee, C. S. (2002) On-line coupling of capillary isoelectric focusing with transient isotachophoresis-zone electrophoresis: a two-dimensional separation system for proteomics *Electrophoresis* **23,** 3160–3167.
22. Sheng, L. and Pawliszyn, J. (2002) Comprehensive two dimensional separation based on coupling micellar electrokinetic chromatography with capillary isoelectric focusing. *Analyst* **127,** 1159–1163.
23. Yang, C., Liu, H. C., Zhang, W. B., and Zhang, Y. K. (2003) On-line hyphenation of capillary isoelectric focusing and capillary gel electrophoresis by a dialysis interface. *Anal. Chem*. **75,** 215–218.
24. Yang, C., Zhang, L. Y., Liu, H. C., Zhang, W. B., and Zhang, Y. K. (2003) Two-dimensional capillary electrophoresis involving capillary isoelectric focusing and capillary zone electrophoresis. *J. Chromatogr. A*. **1018,** 97–103.
25. Liu, H. C., Yang C., Yang Q., Zhang, W. B., and Zhang, Y. K. (2004) Construction of two-dimensional separation platform of coupl ing capillary isoelectric focusing with capillary non-gel sieving electrophoresis for proteins. *Chin. J. Anal. Chem*. **32,** 273–277.
26. Rocklin, R. D., Ramsey, R. S., and Ramsey, J. M. (2000) A microfabricated fluidic device for performing two-dimensional liquid-phase separations. *Anal. Chem*. **72,** 5244–5249.
27. Gottschlich, N., Jacobson, S. C., Culbertson, C. T., and Ramsey, J. M. (2001) Two-dimensional electrochromatography/capillary electrophoresis on a microchip. *Anal. Chem*. **73,** 2669–2674.
28. Ramsey, J. D., Jacobson, S. C., Culbertson, C. T., and Ramsey, J. M. (2003) High-efficiency, two-dimensional separations of protein digests on microfluidic devices. *Anal. Chem*. **75,** 3758–3764.

29. Vreeland, W. N., Williams, S. J., Barron, A.E., and Sassi, A. P. (2003) Tandem isotachophoresis-zone electrophoresis via base-mediated destacking for increased detection sensitivity in microfluidic systems. *Anal. Chem.* **75,** 3059–3065.
30. Li, Y., Buch, J. S., Rosenberger, F., DeVoe, D. L., and Lee, C. S. (2004) Integration of isoelectric focusing with parallel sodium dodecyl sulfate gel electrophoresis for multidimensional protein separations in a plastic microfludic network. *Anal. Chem.* **76,** 742–748.

Index

1-methylbuthylamine 82
1,2,3-propanetriol trinitrate (nitroglycerin) 102
1,3-dinitrobenzene 102
1,3,5-trinitro-1,3,5-triazacyclohexane 102
1,3,5-trinitrobenzene 102
1,3,5,7-tetranitro-N-methylaniline 102
17ß-oestradiol 99
18-crown-6 40
2-CIPAA 687
2-methylquinoline 727
2-nitrotoluole 102
2,4-D 7, 684, 687
2,4-dinitrotoluene 102
2,4,6-N-tetranitro-N-methylaniline 102
2,4,6-T 687
2,4,6-TCP 687
2,4,6-trichlorophenol 688
2,4,6-trichlorophenoxy acetic acid 688
2,4,8-trimethylquinoline 727
2,4-DCP 687
2,4-dichlorophenol 688
2,6-naphthalendicarboxylic acid (NDC) 51
2,6-pyridinedicarboxylic acid (PDA) 51
2,6-D 687
2,6-DCP 687
2,6-di-tert-butyl-4-methylphenol 728
2,6-dichloro-4-nitroaniline 759
2,6-dichlorophenol 688
2,6-dichlorophenoxy acetic acid 688
2,6-dinitrotoluene 102
2,8-dimethylquinoline 727
2-chlorophenoxy acetic acid (2–CIPAA) 688
3-methylquinoline 727
3-nitrotoluole 102
3,4-dimethylaniline 759
4-aminobenzonitrile 286
4-aminofluorescein 54
4-aminopyridine 779
4-chlorophenoxy acetic acid (4-CIPAA) 688
4-CIPAA 687
4-methylquinoline 727
4-nitrotoluole 102
4-(2-thiazolylazo) resorcinol 27
4,4'-methylenedianiline 759
4,8-dimethylquinoline 727
6-methylquinoline 727
6-ß-hydroxy hyoscyamine 184
8-methylquinoline 727

Acetate 14
Acid-hydrolyzed 382
Actinides 21
Affinity capillary electrophoresis 569, 647
Affinity complexes between virus and ligands 577
Aggregates 569
Airborne particulate matter 51
Albumin 522
Alditols 247
Alginate oligomers 345
Alkali and alkaline earth metal ion 25
Alkaloids 171, 771
Alkylbenzene 756
Alphatic acids 604
Ambient air 43
Amines 65
Amino acid 218, 457
Aminoalcohols 593, 606
Aminoglycosides 735
Ammonium 14
Anabasine 779
Analysis 569
Aniline 759
Anion selective exhaustive injection-sweeping 661
Anionic micelles 736
Anions 10
Anomeric forms of O-and C-allylglycosides 287
Anthracene 95
Apoatropine 184
Aration 171
ASP toxins 101
Assay 205
Atmospheric air sample 55
Atropine 183
Atropine enantiomers 184

Background electrolyte 541, 735
Bacteria 426, 569
Bacteria Aggregates 576
Benserazide 215

Bento[a]pyrene 95
Benzathine 221
Benzoin 760, 762
Benzylpenicillin 221
Bidimensional seperations of polyelectrolytes 560
Bile salts 735
Binding constants 647
Biogenic amines 65
Biomedical applications 457
Bisphenol-A 99
Blood samples 470
Borate-based seperation buffers 287
Bromochloroacetic acid (BCAA) 157, 160
Butylamine 83

C-allyl-galactopyranosides 293
C-allyl-glucopyranosides 293
Ca++ 27
Cadaverine 82, 83
Caffeine 763
Calcium 14
Calibration curves 626
Cancer patients 435
Capillary Coating 636
Capillary Electrochromatography 751
Capillary electrophoresis-matrix-assisted laser desorption/ionization interface 794
Capillary Electrophoresis/Mass Spectrometry 631
Capillary isoelectric focusing 569, 575
Capillary reverse phase liquid chromatography 783
Capillary-to-capillary reproducibility 622
Capilllary chromatography 10
Carbonate 14
Carboxylated sugars 307
Carboxymethyl-β-cyclodextrin (CM-β-CD) 688
Cation selective exhaustive injection 682
Cation selective exhaustive injection-sweeping 661
Cationic coating 631
Cations 7
CDCE 442
CE-ESI-MS 472
CE-laser-induced fluorescence 185
CE-LIF 472
CE-SSCP 425
CE way of thinking 611
CE/MS 135
CElixir TM 218
Cephalexin 231
Charged polysaccharides 357
Chemical composition 541
Chiral pesticides 157
Chiral separation 205, 457
Chitosan 635
Chloride 14
Chlorophenols 671, 691
Chlorophenoxy acetic acids 661, 671, 690
Chromate 55
Chromate-based BGE method 50
Chromatographic zone sharpening effect 751
Chrysene 95
Cigarette Paper 14
Clemizole 221
Clinical applicatons 457
Cobalt 26
CombiSep 96–capillary array 231
Complexing agents 21
Comprehensive 2D CE-CE Systems 786, 791
Comprehensive 2D RPLC-CZE 791
Compton's equations 597
Constant denaturant capillary electrophoresis 442
Contactless conductivity detection 3
Contour-mapping 795
Copolymers 541
Copper-based BGE 75
Corn flakes 582
Cr(III) 26
Crown ethers 75
CSE-MEKC 791
Cu 26
Cu(II) 26
Cyclodextrin 157, 735
ß-cyclodextrins 190
β-cyclodextrin (β-CD) 688
CZE-ESI-MS 405
CZSE 762

Day-to-day 622
Demissidine 185
Denatured DNA 420
Derivatization 65
Derivatized amines 78
Desisopropylatrazine 145
Detection modes 507
Detonating cord extract 113
Dextran trisaccharide 289
Diabetic nephropathy 436
Dichloroprop 96, 157
Dichlorphenol 99
Dicyclohexylcarbodiimide (DCC) 54
Dieldrin 99
Diethylamine 83, 84
Diethylstilbestrol 99
Dimethyl-β-cyclodextrin (DM-β-CD) 688
Dimethylamine 83, 84, 125

Dimethylaniline 759
Dipropylamine 84
Dithane M 45, 96
Dithiocarbamate pesticides 96
DMA-EpyM 635
DNA 415
DNA methylation 441
DNA seperation and detection 426
DNB-based BGE method 51
Domoic acid 101
Dopa enantiomers 215
DQ 682
Dye tracers 124
Dynamic capillary coating 205
Dynamic pH junction 433

EDTA 34
Electrochemical detection 431
Electroosmotic flow 614, 751
Electroosmotic flow effective mobility 611
Electrophoretic mobility 357
Electrospray ionization (ESI) interfaces 139
Electrospray ionization 135
Electrospray ionization ion source 137
Electrospray mass spectrometry 401
Enantiomer 157
Enantiomer seperation 210
Enantiosep 171
Endocrine disruptors 93
Entangled polymer solution 541
Entangled polymer solution capillary electrophoresis 559
Enterobacter aerogenes 574
Enterococcus faecium 575
Environmental samples 661
EOF-correction 619
Eosin 124
Escherichia coli 575
ESI-MS 188
Ethanolamine 82, 83
Ethynyloestradiol 99
European Pharmacopoeia (EP 5) 740
Explosives 93

FASS 761
Fe 26
Fe(III) 26
Fenoprop 96
FFE 703
Field-amplified sample injection 676
Field amplified sample stacking effect 751
Flow profiles 616
Fluoranthene 95
Fluorene 95
Fluorescein 124
Fluorescein isoth-iocyanate isomer 1 (FTTC) 78
Fluorescence 415
Foods 65
Forensic genotyping 421
Formaldehyde releasers 593, 606
Formiate 14
Free-flow electrophoresis 703
Free flow isoelectric focusing 704
Free solution CE 205
Frictional coefficient 595
Fructose 292
FTC-amines 79

Galactose 291, 292
Galactosylamine 292
Galactosylcarbamate 292
Galacturonic acid 292
Gene mutation 441
Genotyping 415
Gentamicin 735, 747
Glcosides 247
Gluco-oligosaccharides 286
Glucose 289, 291, 292
Glucosylamine 292
Glucosylcarbamate 292
Glycoalkaloids 171
Glycoconjugates 357, 384
Glycosaminoglycans 307
Glycosylamines 247
Green tea 38
Grossman's equations 596

HCB 682
Histamine 82
Homatropine 183, 184
Homopolysaccharide 382
HP-ß-CD 187
Human cerebrospinal fluid 522
Human serum albumin 705
Hyaluronan 357
Hyaluronic acid 383
Hyaluronic acid butyric ester 385
Hydrodynamic injection 611
Hydrodynamic interface 794
Hydrophobic analytes 717
Hydrophobicity (LogP) 599
Hydroxy-S-triazines 603
Hydroxyatrazine 145
Hydroxydesethylatrazine 145

Hydroxyleted polynuclear aromatics 124
Hydroxyterbutylazine 145
Hyoscyamine 183, 184

IEF 703
IgG 357
Imidazol-based BGE methods 77
Indirect UV 65
Injection mode 612
Inorganis ions 3
Ionic analytes 721
Irgafos38 728
Irgafos168 728
Irganox 1010 728
Irganox 1024 728
Irganox 1035 728
Irganox 1076 728
Irganox 1330 728
Iridium(III) 25
Isoamylamine 82
Isoelectric focusing 703
Isoforms 704
Isomaltose 289
Isomeric tripeptides 496
Isopropylamine 82
Isoquinoline 727
Isotachophoresis 171, 681, 703
Isotachophoresis stacking 683
ITP of α-chaconine 185

Juice samples 582

Kalium 27
Kanamycin 735

Lactobacillus plantaru 575
Lactose 291, 292
Lactosylamine 292
Lactosylcarbamate 292
Lactulose 292
Lanthanides 21
Large volume sample stacking 661
Large volume sample stacking with polarity switching 673, 675
Laser-induced fluoresence 65, 119
Leuconostoc mesenteroides 575
LIF 54
LIF detection 449
Lindane 99
Listeria monocitogenes 575
Littorine 184
Liver cancer tissue 795
Living polymer 557
LMW carboxylic acids 51
Log P determination 205
Low-molecular-weight (LMW) aliphatic amines 65
Low-molecular-weight carboxylic acids 43

M-nitroaniline 759, 760
Magnesium 14
Malate 14
MALDI-MS 791
Maltose 289
Maneb 96, 106
Mass spectrometry 135
McGovan hydration increments 597
MCPA 96
MCPB 96
Mecoprop 96
MEEKC 717
MEKC 125, 157, 184, 382, 735
Mesophyll cells 779
Metal analysis 21
Metal ions 21
Metal ligand interactions 21
Metalworking fluid (MWF) 621
Metham 96, 106
Methylamine 82, 83, 84
Methylation analysis 442
Mg ++ 27
Micellar electrokinetic chromatography 171, 205, 457, 499, 680, 735
Micro droplets 778
Microcapillary 775
Micrococcus luteus 574
Microdialysis 470
Microemulsion electrokinetic chromatography 205, 717
Microorganisms 569
Microsatellite analysis 442
Microsatellite instability 441
Migration time fluctuations 619
Mobility equation 596
Mobility prediction from structural data 596
Mobility scale 611
Mobility-scale transformations 616, 617
Mobility simulation 593
Molar mass distribution 357
Mono-,di-, and tricarboxylated benzenes 621
Monocarboxylic acids 55
Monolithic column 751
Monosaccharides 247
Morpholine 84

Multi-dimensional Capillary Electrophoresis 783
Multi-element seperation 25
Mutation pattern 450
MWF emulsion 625

N-acylhomoserine lactones 135, 149
N-acylhomoserines 157
N-fluorenyl-methiloxycarbonyl (Fmoc) 287
Na+ 27
NACE-electrospray ionization ESI-mass spectrometry 196
Naphthylamine 759
NCD-based BGE method 51
Netilmicin 743
Neutral sugars 247
Ni 26
Nicotiana tabacum 775
Nicotine 771, 779
Nitrobenzene 102
Nonaqueous capillary electrophoresis 171, 541
Nonaqueous CE 184, 205
Nonylphenol 99
Nor-(-) scopolamine 183
Nornicotine 779

O-aminobenzoic acid 758
O-nitroaniline 760
O-phenylene diamine 759, 760
O-toluic acid 758
Octadecyl silica (ODS) 757
Octylphenol 99
Oestriol 99
Offord model 607
Offords aquations 596
Oil droplets 718
Oil-in-water microemulsions 718
Oligomers 541
Oligonucleotides 401
Oligosaccharides 247, 307
On-capillary derivatization techniques 81
On-column ligand/receptor derivatization 647
On-column synthesis 649
On-line concentration 661, 751
On-line sample stacking 404
Organelle separation 703
Organic acid 3
Organic pollutants 93
Osmium(VI) 25
Oxalate 14
Oxidative DNA damage 431

P-bromobenzoic acid 758
P-chlorobenzoic acid 758
P-hydroxybenzoic acid 758
P-methoxybenzoic acid 758
P-phenylene diamine 759, 760
Paralytic shellfish-poisoning (PSP) 100
Paraquat and diquat 93, 97
Partial-filling affinity capillary electrophoresis 650
Pb(II) 26
PCR 415
Pd(II) 25
PDA-based BGE method 51
PDADMAC 635
PEEK capillaries 7
PEI 635
Pentachlorphenol 99
Pentaerythritol tetranitrate 102
Peptides 483
Performance characteristics 624
Pesticides 157
Pharmaceuticals 205
Pharmaceutical analysis 205
Phenanthrene 95
Phenethylamine 82
Phenolic acids 604
Phenomenological CZE-behavior model 598
Phenoxy acids 93, 95
Phenylisothiocyanate (PITC) 475
Piperidine 84
PK-simulation 597
PKa determination 205
Plant extracts 171
Pollutants 119, 157
Poly(vinylpyrrolidone) 418
Polyarginine 635
Polycyclic aromatic hydrocarbons 95
PolyE-323 635
Polyelectrolytes 541
Polymer coatings 631
Polymer synthesis 636
Polymerase chain reaction 422
Polymethacrylate-based monolithic 757
Polypeptides 541
Polystyrensulfonates 541
Potassium 14
Potato tubers 197
Pottassium o-ethylxanthate 106
PQ 682
Prealbumin 522
Precapillary complexation 25
Precapillary derivatization 79
Preconcentration 717

Procaine 221
Propylamine 83
Protein fingerprints 796
Protein hydrolysates 470
Proteins 507, 631
Proteomic analysis 783
Proteomics 703
Pseudomonas fluorescens 574
Pseudostationary phase 717
PSP toxins 102
PTC-amino acid 475
Pullulan trisaccharide 289
Putrescine 82, 83
Pyrene 95
Pyrrolidine 84

Q-agarose 635
Quantification 621
Quinine sulfate-based BGE methods 77
Quinoline 727

Ranitidine 225
Rare earth elements 23
Receptor-ligand interactions 647
Recombinant adenovirus 576
Red wine 85
Reductive amination 247, 286
REE synthetic geochemical standards 24
Relaxation effects 596
Rhodamines 124
Rhodium(III) 25
Ristocetin 647
River water 34
RP-CEC 757
Ruelene 157
Ruthenium(III) 25

S-triazines 593
Salbutamol 218
Salmonella enteriditis 575
Sample concentration 661
Sample focusing method 433
Sample preconcentration 722
Sample pretreatment 507
Sample stacking 669
Sampling single plant cells 775
Saxitoxing 100
Scatchard plot 647, 657
Schematic representation of capillary electrophoresis 612
Scopolamine 183
Scopolamine derivates 183
Selected ion monitoring 196
Selective exhaustive injection sweeping 679
Semi-empiric model 593, 597
Separation optimization 593
Sheat liquids 139
Sheatless 139
Sialic acids 307
Silanization 633
Single cell 783
Single plant cells 771
Single-strand conformation polymorphismus (SSCP) 423, 441
Sisomicin 742
Size-based separation 541
Smokers 437
SNaOshot analysis 442
Sodium 14
Sodium diethyldithiocarbamate 106
Sodium dodecyl sulfate (SDS) 718
Soil 105
Solanidine 185
Solution-phase immunoassay 185
Special electrophoretic modes 507
Speciation 21
Spermidine 82, 83
Spiked river water sample 109
SSCP 415
SSCP-CE 441
Staphylococcus aureus 575
Stokes equation 595
Sugar acids 307
Sugar phosphates 307
Sulfate 14
Sulfated ß-CDs 190
Sulfated sugars 307
Sulfonated polystyrensulfonate standard 554
Surface properties 631
Sweeping 677, 722
Sweeping-micellar electrokinetic capillary electrophoresis 661
Synthetic (Co) polymers 541
Synthetic peptides 497
Synthetic polymers 541

Tannery sample 37
Teicoplanin 647
Tetradecylmethylammoniumbromide 51
Tetrytol extract 116
Theoretical mobility 604
Thiourea 758, 759, 760
Three-dimensional plot 795

Tinopal 124
Tobacco 14, 771
Tobramycin 735
Tomatidine 185
Toxins 93
Trace amino acids neurotransmitters 470
Transition metal ions 21, 27
Triazine 135
Trichlorophenol 99
Trimethyl-β-cyclodextrin (TM-β-CD) 688
Trinitro toluene (TNT) 102, 427
Tropane alkaloids 171
Tropic acid 183
Tryptic peptides 795
TTBA 37
Two-dimensional (2D) electrophoresis 714
Two-dimensional capillary electrophoresis 561
Two-dimensional separation 795
Tyramine 82

Underivatized neutral sugars 287
Uranium (VI) 27
Urinary 8-hydroxy-2-deoxyguanosine (8OHdG) 431
Urine 34
Urine samples 432
Uronic acids 307
UV detection 93

Vancomcyin 647
Vehicle emission 43
Virus 569
Volatile aliphatic amines 65

Wall interaction 507

Y-globulin 522
Yeast Mitochondria 705
Yersinia enterolitica 575
YO-PRO-1 dye 418

Zn 26
Zone electrophoresis 703